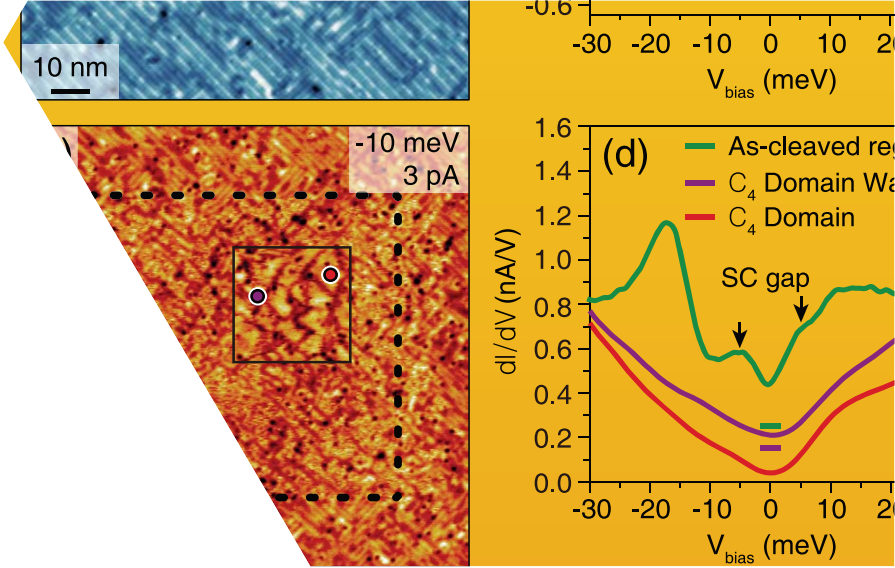


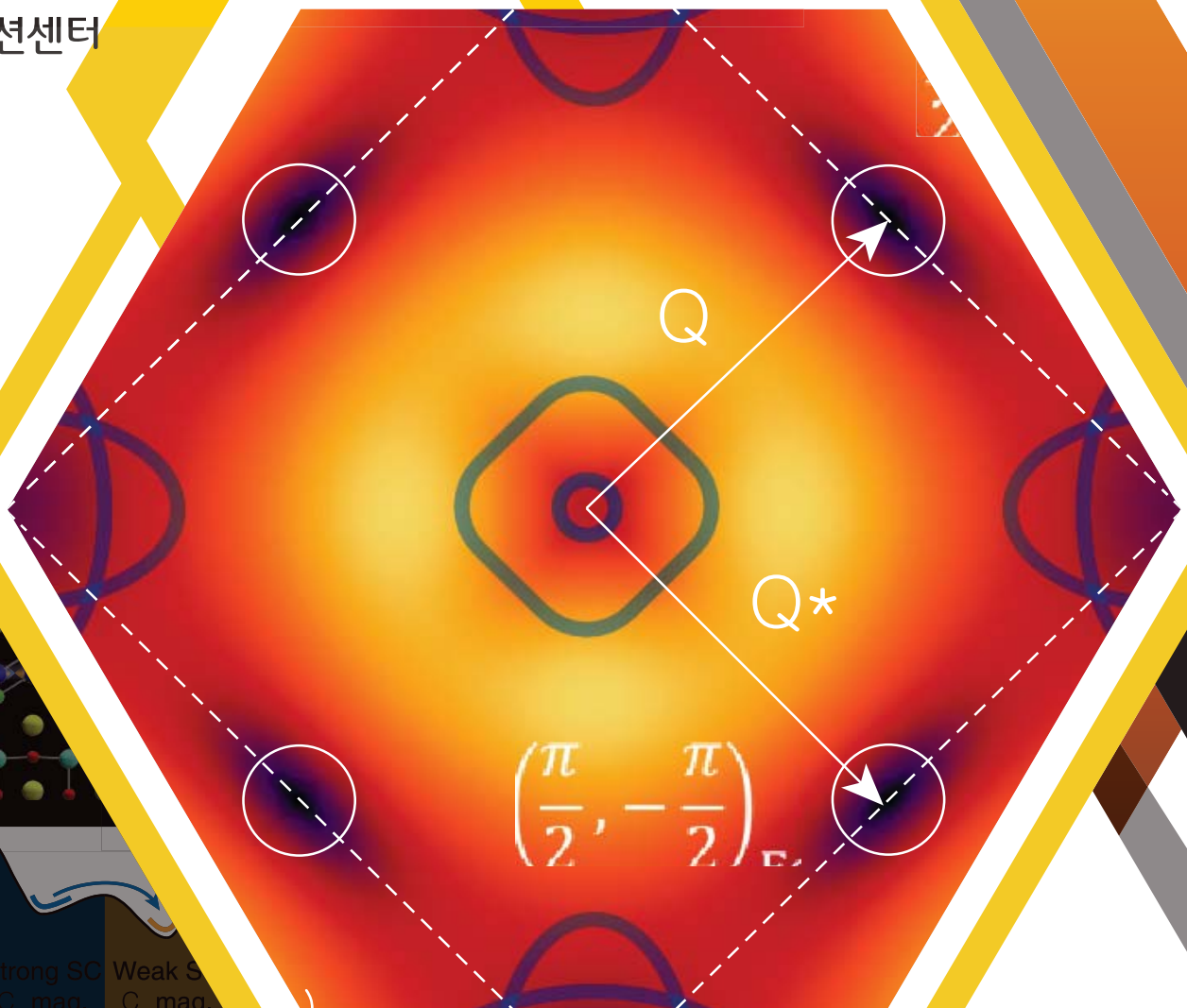
# 한국물리학회 초록집



2018년 봄 학술논문발표회  
및 제94회 정기총회

2018 KPS Spring Meeting

2018년 4월 25일(수) - 27일(금)  
대전컨벤션센터



# 구두발표논문

Oral session abstracts

## Prospects for New Pentaquark Searches

안정근\*<sup>1</sup>

<sup>1</sup>고려대학교 물리학과  
ahnjk@korea.ac.kr

### Abstract:

I would like to review experimental searches for  $\Theta^+$  and  $P_c$  pentaquark states. The  $\Theta^+$  has been searched for in multi-particle final states including either a pair of  $K+n$  or  $K^0p$ , where  $\phi$  and  $\Lambda(1520)$  states could interfere with  $\Theta^+$ . I would like to first propose a new experiment to bring a definite conclusion on the existence of  $\Theta^+$  using a low-energy  $K^+$  beam at J-PARC. A high-intensity  $K^+$  beam will slow down in a degrader before impinging on a LD2 target located in the Hyperon Spectrometer. The charge-exchange process  $K+n \rightarrow K^0p$  will be uniquely identified without Fermi-motion correction. This new experiment will end a long debate on the existence of  $\Theta^+$ . The  $P_c$  states have also been reported by the LHCb collaboration to appear in  $J/\psi p K^-$  states, where  $pK^-$  could interfere with the  $J/\psi p$  channel. However, the GlueX collaboration reports their preliminary results on  $J/\psi$  photoproduction cross sections near threshold, which indicates no significant peak structure on the  $P_c$  mass. To reconfirm  $P_c$  states, further attempts should involve a different combination of final state particles with  $J/\psi p$ . The Belle-II experiment could be the best place to confirm the  $P_c$  states in the  $J/\psi p \bar{p}$  states from  $Y$  decays. I would like to discuss some prospects for  $P_c$  searches at Belle-II.

### Keywords:

Pentaquark, J-PARC, Belle-II

## Theoretical and experimental studies for Delta(1232) photoproduction

남승일\*<sup>1</sup>, KORI Hideki<sup>2</sup>, 유병길<sup>3</sup>

<sup>1</sup>부경대학교 물리학과, <sup>2</sup>RCNP, 오사카대학, <sup>3</sup>한국항공대학교  
sinam@pknu.ac.kr

### Abstract:

In this talk, we present the theoretical and experimental studies for Delta(1232) photoproduction, using the effective Lagrangian approach at tree level. By comparing the theoretical results with the recent LEPS/SPring-8 data, we observe that the effects of the higher spin and mass mesons are crucial to describe the data as shown in the photon-beam asymmetry. The role of the nucleon resonances is investigated as well.

### Keywords:

Delta(1232) photoproduction, photon-beam asymmetry, higher spin and mass mesons.

## Charmonium states including instanton effects

YAKHSHIEV Ulugbek\*<sup>1</sup>, KIM Hyun-Chul<sup>1</sup>, HIYAMA Emiko<sup>2</sup>

<sup>1</sup>인하대학교 물리학과, <sup>2</sup>RIKEN, Strangeness Physics Laboratory  
yakhshiev@yahoo.com

### Abstract:

The heavy-quarkonium spectra is studied considering the effects from nonperturbative region. We discuss several instanton potentials with the different parameters and their affect to the charmonium states. We present also the parametrized instanton potential which can useful in practical calculations

### Keywords:

Quarkonium, instanton, heavy-quark potential

## Eta photoproduction in an effective Lagrangian approach

김현철\*<sup>1</sup>, 김상호\*<sup>2</sup>, 서정민<sup>1</sup>  
<sup>1</sup>인하대학교 물리학과, <sup>2</sup>APCTP  
hchkim@inha.ac.kr, sangho.kim.apctp.org

### Abstract:

We investigate photoproduction of the  $\eta$  meson off the neutron, employing the effective Lagrangian method and the Regge approach. We study the effects of  $N^*$  resonances near the threshold 1487 MeV, i.e.  $N^*(1520)$ ,  $N^*(1535)$ ,  $N^*(1650)$ ,  $N^*(1675)$ ,  $N^*(1680)$ ,  $N^*(1685)$ ,  $N^*(1700)$ ,  $N^*(1710)$  and  $N^*(1720)$ . The numerical results of the total and differential cross section are in good agreement with the experimental data from the A2 Collaboration.

### Keywords:

eta photoproduction, effective Lagrangian approach

## Decay-width broadening of Lambda(1405) in $\pi^- p \rightarrow K^0 \pi$ Sigma in terms of its two-pole structure

남승일\*<sup>1</sup>

<sup>1</sup>부경대학교 물리학과  
sinam@pknu.ac.kr

### Abstract:

In this talk, we present the recent work on the full-decay-width broadening of Lambda(1405) in  $\pi^- p \rightarrow K^0 \pi$  Sigma in terms of its two-pole structure. We employ the effective Lagrangian approach, using a four-point loop diagram and taking into account the negligible  $K^*-N$ -Lambda(1405) coupling strength. It turns out that the experimentally measured width for Lambda(1405) is broadened due to the nontrivial interference between the two poles.

### Keywords:

Lambda(1405), pion beam, J-PARC, Decay-width broadening.

## In-medium properties of SU(3) baryons

홍기훈<sup>1</sup>, 김현철<sup>\*1</sup>, YAKHSHIEV Ulugbek<sup>\*1</sup>

<sup>1</sup>인하대학교 물리학과

hchkim@inha.ac.kr, yakhshiev@inha.ac.kr

### Abstract:

In this talk, we present a recent investigation on the modification of the lowest-lying hyperons within the framework of the SU(3) Skyrme model. Employing the in-medium changes of dynamical parameters in the model, we evaluate the masses of the hyperons in nuclear matter. We discuss how each hyperon undergoes in nuclear environment. While the mass of the nucleon becomes smaller in nuclear matter, those of the hyperons start to increase, as the density of nuclear matter increases.

### Keywords:

SU(3) Skyrme model, nuclear matter

## Medium modification of Delta isobar states in isospin asymmetric matter

정기삼\*<sup>1</sup>, MARQUES LEAL JUNIOR Jesuel<sup>2, 3</sup>, 이수형<sup>2</sup>

<sup>1</sup>아시아 태평양 이론물리센터 YST research fellow, <sup>2</sup>연세대학교 물리학과, <sup>3</sup>IFT-UNESP  
key.s.jeong@gmail.com

### Abstract:

The role of  $\Delta$  isobar could be important in the isospin asymmetric dense nuclear matter due to its main decay channel into the nucleon and pion. The equation of state can be determined as soft/hard by early onset of the  $\Delta$  isobar state.

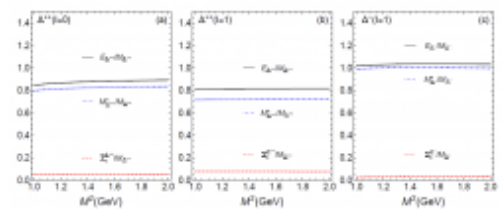
According to the relativistic mean field (RMF) type phenomenological study [1], the quasi- $\Delta$  state in the matter receives strong contribution from iso-vector meson exchange channel. In the other hand, if one assumes the fundamental quark basis in non-abelian gauge to represent the baryonic degree of freedom, the quantum number of in-medium  $\Delta$  isobar state can be calculated by operator product expansion (OPE) in QCD sector. Regarding the in-medium  $\Delta$  self-energies calculated by OPE as the averaged potentials from meson exchange channel, the density behavior of the  $\Delta$  isobar in the dense matter such as neutron star can be understood in terms of chiral symmetry breaking and non-perturbative QCD condensates.

In this study, authors calculated the in-medium self-energies of  $\Delta$  isobar and its modification in the various density and isospin condition. The one of apparent feature of the result is the strong isospin dependence of scalar self-energy and the weak vector self energy, which leads to strong reduction of the quasi- $\Delta$  energy and enhances the possibility of early onset of the  $\Delta$  isobar quantum number in the dense matter.

[1] Physical Review C92, 015802 (2015), Bao-jun Cai et al.

### Keywords:

QCD sum rules, Neutron star, Isospin asymmetry,  $\Delta$  isobar



## Resonant states of alpha-nucleon scattering in SS-HORSE approach

신익재\*<sup>1</sup>, MAZUR A.I.<sup>2</sup>, SHIROKOV A.M.<sup>2, 3, 4</sup>, MAZUR I.A.<sup>2</sup>, 김영만<sup>1</sup>, BLOKHINTSEV L.D.<sup>2, 3</sup>, VARY J.P.<sup>4</sup>, MAZUR E.A.<sup>2</sup>

<sup>1</sup>기초과학연구원, <sup>2</sup>Department of Physics, Pacific National University, <sup>3</sup>Skobeltsyn Institute of Nuclear Physics, Lomonosov Moscow State University, <sup>4</sup>Department of Physics and Astronomy, Iowa State University  
geniean@ibs.re.kr

### Abstract:

The SS-HORSE method has been suggested as a tool to describe scattering phase shifts and resonances with less efforts. Here we study resonant state in  $^5\text{He}$  and/or  $^5\text{Li}$  and also non-resonant scatterings within no core shell model using JISP16 and Daejeon16 potentials.

### Keywords:

resonances, scattering amplitude

## Artificial synapses using organic and organic-inorganic hybrid perovskite materials

XU Wentao<sup>1</sup>, MIN Sung-Yong<sup>4</sup>, CHO Himchan<sup>1, 3</sup>, KIM Young-Hoon<sup>1, 2, 3</sup>, LEE Yeongjun<sup>1, 2</sup>, HWANG Hyunsang<sup>4</sup>, 이태우\*<sup>1, 2, 3</sup>

<sup>1</sup>서울대학교 재료공학부, <sup>2</sup>서울대학교 신소재공동연구소, <sup>3</sup>서울대학교 BK21 플러스 서울대학교 창의인재양성 재료사업단, <sup>4</sup>포항공과대학교 신소재공학과  
twlees@snu.ac.kr

### Abstract:

Here we report our recent progress in developing synapse-emulating electronic devices using organic materials and organic-inorganic hybrid materials. Important working principles of a biological synapse have emulated, such as excitatory post-synaptic current (EPSC), inhibitory post-synaptic current (IPSC), paired-pulse facilitation (PPF), short-term plasticity (STP), long-term plasticity (LTP) and spike-timing dependent plasticity (STDP). Either two-terminal or three terminal architecture was fabricated. Digitally aligned semiconducting nanofibers with nano feature size were produced using our home-built electrohydrodynamic nanowire (e-NW) printer, which allow fabrication of three-terminal synaptic transistor arrays. High-quality organic-inorganic hybrid perovskite thin film facilitated the fabrication of two-terminal artificial synapses, which is essential for high-density cross-bar electrode architectures. These properties are essential for brain-inspired computation and memory, and the devices would serve as building blocks of future neuromorphic systems.

### Keywords:

neuromorphic, organic-inorganic hybrid materials, synapse, perovskite, brain-inspired computation, memory

## Fluorine Functionalized Graphene Nano Platelets for Highly Stable Inverted Perovskite Solar Cells

김진영\*<sup>1</sup>, 김기환<sup>1</sup>

<sup>1</sup>울산과학기술원 에너지및화학공학부  
jykim@unist.ac.kr

### Abstract:

Edged-selectively fluorine (F) functionalized graphene nanoplatelets (EFGnPs-F) with p-i-n structure of perovskite solar cells achieved 82% stability relative to initial performance over 30 days of air exposure without encapsulation. The enhanced stability stems from F-substitution on EFGnPs; fluorocarbons such as polytetrafluoroethylene are well known for their super-hydrophobic properties and being impervious to chemical degradation. These hydrophobic moieties tightly protect perovskite layers from air degradation. To directly compare the effect of similar hydrophilic graphene layers, edge-selectively hydrogen functionalized graphene nanoplatelet (EFGnPs-H) treated devices were tested under the same conditions. Like the pristine MAPbI<sub>3</sub> perovskite devices, EFGnPs-H treated devices were completely degraded after 10 days. The hydrophobic properties of EFGnPs-F were characterized by contact angle measurement. The test results showed great water repellency compared to pristine perovskite films or EFGnPs-H coated films. This resulted in highly air-stable p-i-n perovskite solar cells.

### Keywords:

Perovskite solar cells, p-i-n, stability, graphene, functionalized graphene, hydrophobic

## Interaction between CuSCN dopant and dimethyl sulfoxide derived intermediate phase in $\text{CH}_3\text{NH}_3\text{PbI}_3$ perovskite solar cell

강동희<sup>1</sup>, 신동근<sup>1</sup>, 정준경<sup>1</sup>, 유지수<sup>1</sup>, 김기웅<sup>1</sup>, 이현복\*<sup>2</sup>, 이연진\*<sup>1</sup>

<sup>1</sup>Institute of Physics and Applied Physics and van der Waals Materials Research Center, Yonsei University, <sup>2</sup>Department of physics, Kangwon National University  
hyunbok@kangwon.ac.kr, yeonjin@yonsei.ac.kr

### Abstract:

Organic-inorganic hybrid perovskite is attracting much attention due to its great potential for optoelectronic applications such as a solar cell. For the highly efficient solar cells, high quality perovskite film and good charge transfer from the perovskite layer to the adjacent layer should be achieved. In order to produce high quality films, dimethyl sulfoxide (DMSO) was introduced as an additive in precursor solution. In the  $\text{CH}_3\text{NH}_3(\text{MA})\text{PbI}_3$  perovskite, DMSO has been known to form intermediate phase such as  $\text{MA}_2\text{Pb}_3\text{I}_8(\text{DMSO})_2$ . This intermediate phase releases DMSO slowly during the thermal annealing, which is known to form high quality  $\text{MAPbI}_3$  film. For good charge transfer, p-type transition metal halide has been introduced to control the band position. Among them, copper thiocyanate (CuSCN) is known as a good p-dopant for  $\text{MAPbI}_3$ . However, there have been few reports on applying DMSO and CuSCN dopant at the same time. In order to fabricate a high-quality film by using the intermediate phase and to adjust the band position with doping, it is necessary to understand the interaction between the intermediate phase and dopant. In this study, the effect of CuSCN on the intermediate phase will be presented by adding DMSO and CuSCN dopant to the perovskite precursor at the same time.

[This research was supported by the MOTIE (Ministry of Trade, Industry & Energy (10079558)) and Development of materials and core-technology for future display support program.]

### Keywords:

organic-inorganic hybrid perovskite, perovskite solar cell, copper thiocyanate, ultraviolet photoelectron spectroscopy

## Electronic structure at Au/CH<sub>3</sub>NH<sub>3</sub>PbI<sub>3</sub> interface

차명주\*<sup>1</sup>, 박유정<sup>1</sup>, 강주환<sup>1</sup>, 서정화<sup>1</sup>  
<sup>1</sup>동아대학교 물리학과  
cmjzhang@gmail.com

### Abstract:

The electronic properties of the interface formed between Au and organometallic triiodide perovskite (CH<sub>3</sub>NH<sub>3</sub>PbI<sub>3</sub>) were investigated using ultraviolet photoelectron spectroscopy (UPS) and X-ray photoemission spectroscopy (XPS). The CH<sub>3</sub>NH<sub>3</sub>PbI<sub>3</sub> films were prepared onto the Au surfaces by spin casting with various solution concentrations to control the film thickness and their morphology was examined using atomic force microscopy (AFM). The CH<sub>3</sub>NH<sub>3</sub>PbI<sub>3</sub> film exhibited a band gap of 1.70 eV and the maximum valence band edge of 6.31 eV. The energy levels shift downward by 0.26 eV with a perovskite coverage of 50 wt% upon it, indicating the band bending at the interface. The observed energy level shift means the presence of the interface dipole exists at the Au/CH<sub>3</sub>NH<sub>3</sub>PbI<sub>3</sub> interface. These findings are important for understanding how the perovskite materials function in electronic devices, and the design of new materials for use in perovskite-based optoelectronic devices.

### Keywords:

UPS, XPS, perovskite, electronic properties

## Two-terminal organolead halide perovskite (OHP) synaptic device for neuromorphic device applications

HAM Seong-Gil<sup>1</sup>, CHOI Sanghyeon<sup>1</sup>, JHO Haein<sup>1</sup>, 왕건욱\*<sup>1</sup>

<sup>1</sup>KU-KIST Graduate School of Converging Science & Technology, Korea University, 145, Anam-ro, Seongbuk-gu, Seoul 136-701, Republic of Korea.  
gunukwang@korea.ac.kr

### Abstract:

The field of neuromorphic electronics that can mimic diverse functionalities of biological synapse that are the foundation of higher-level brain activities has recently emerged as a promising approach toward energy- and time-efficient computing technology [1]. Here, we fabricated an organolead halide perovskite (OHP) memristive device in two-terminal structure and utilized it as an artificial synapse. The OHP synaptic device consists of the spin-coated  $\text{CH}_3\text{NH}_3\text{PbI}_3$  film sandwiched between Ag top and ITO bottom electrode. It is believed that the switching feature for two-terminal OHP memristor is originated from the presence of the conductive filament by iodine-vacancy mediator, whose the switching states can be controlled by the electric-field domination. Using diverse electrical stimuli and relative timing between the input pulses, the essential synaptic functionalities such as short-term plasticity (STP), long-term potentiation (LTP), and long-term depression (LTD) are successfully demonstrated. Interestingly, we observed that the synaptic connectivity, namely the post-synaptic current (PSC) of the OHP synaptic device, can be further enhanced when the light illuminated the device. We believe that the photo-generated electric field could accelerate the formation of the switching filament, resulting in the increasing dynamic range of the PSC. Utilizing light-driven switching filament, we can change from STP to LTP even under the small input pulse. To identify the potential of the OHP device as an artificial synapse, we performed the pattern recognition simulation based on the experimental synaptic parameters such as the dynamic range of synaptic conductance ( $G_{\max}$  and  $G_{\min}$ ), and synaptic weight ( $G^+G^-$ ). We found the recognition rate was 81 %. These results could provide an important step toward developing the light-driven neuromorphic electronic device.

**Acknowledgments** This work was accomplished with financial support from the National Research Foundation of Korea, the KU-KIST research fund, SAMSUNG, and the Korea University Future Research Grant,

**References** [1] Jo, S. H.; Chang, T.; Ebong, I.; Bhadviya, B. B.; Mazumder, P.; Lu, W. Nanoscale Memristor Device as Synapse in Neuromorphic Systems. *Nano Lett.* 2010, 10, 1297-1301

### Keywords:

organolead halide perovskite, synaptic device, neuromorphic device applications,

## Temperature-dependent electron spin resonance and photocurrent measurements on perovskite solar cells

전남중<sup>2</sup>, 서장원<sup>2</sup>, 장정재<sup>1</sup>, 이정근\*<sup>1</sup>

<sup>1</sup>전북대학교 물리학과, <sup>2</sup>Division of Advanced Materials, Korea Research Institute of Chemical Technology, Daejeon 305-600, South Korea.  
jklee@jbnu.ac.kr

### Abstract:

Light-induced electron spin resonance (LESR) and photocurrent measurements of PCBM/perovskite(FAPbI<sub>3</sub>:MAPbI<sub>3</sub>)/PTAA solar cell structure are reported.

The photo-generated charge carriers detected by ESR upon the light irradiation showed the increase and decrease in the spin density (Ns) due to the hole transfer and recombination at the perovskite/PTAA interface. The doped poly(triaryl)amine (PTAA) thin films didn't react to light.

Temperature-dependent LESR results showed a thermal activation behavior and suggested a phase transition of the perovskite at low temperatures less than ~160 K.

Temperature-dependent photocurrent measurements on the PCBM/perovskite/PTAA solar cells also showed the same temperature dependency.

Our LESR and photocurrent results suggested the existence of interfacial barrier of ~125 meV between the perovskite and the hole transport layer.

### Keywords:

perovskite, electron spin resonance, photocurrent

## Terahertz devices based on planar plasmonic metamaterials

이중욱\*<sup>1</sup>

<sup>1</sup>전남대학교 물리학과  
leejujc@gmail.com

### Abstract:

플라즈몬 금속 구조를 이용하여 만들어진 평면 메타물질은 전자기파의 다양한 파장 영역에서 소자 개발 및 활용의 가능성으로 인해 크게 주목받고 있으며 활발한 연구가 진행되고 있다. 특히 테라헤르츠파 영역에서 평면메타물질을 이용하여 다양한 소자가 개발되고 있다. 본 연구에서는 슬롯 애퍼처 구조를 기반으로 한 다양한 메타물질 구조를 활용하여 모노폴 공진기(monopole resonator), 삼차원 파장이하 집적을 이용한 다중 핫스팟 플랫폼, 유효 고굴절 메타표면, 비등방 메타 구조를 이용한 광학등방성 등의 독창적인 광학 특성 및 그에 기반한 광소자를 구현하였다. 여기에서 제시된 기본 개념을 활용하면 적외선, 마이크로파와 같은 다양한 파장 영역에서 작동하는 새로운 개념의 광소자를 개발할 수 있을 것이며, 테라헤르츠파 센싱 및 이미징 시스템의 효율성을 향상시킬 수 있을 것이다.

### Keywords:

terahertz, metamaterial, device

## Active control of optical properties with gated-graphene metamaterials.

김튼튼\*<sup>1</sup>

<sup>1</sup>IBS, 성균관대학교 나노구조물리연구단  
t.kim@skku.edu

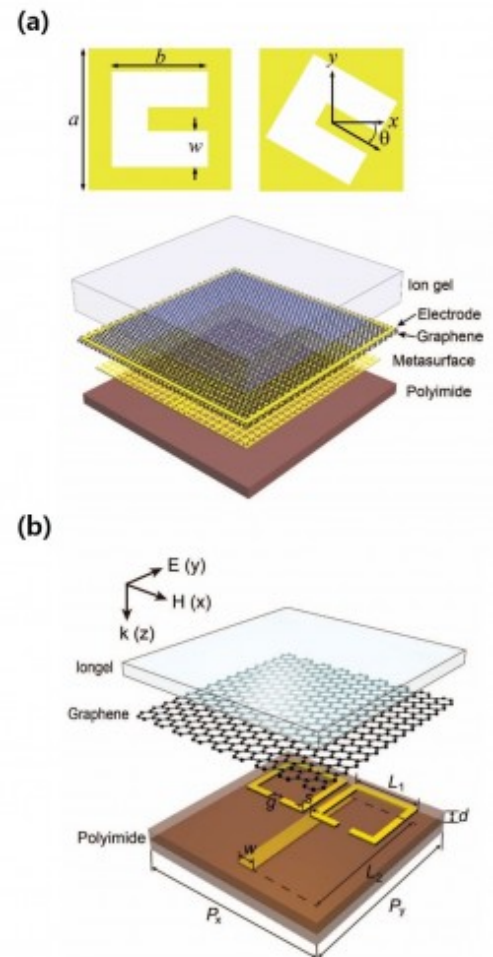
### Abstract:

Recently, progress has been made over a class of new ultrathin structured surfaces - so-called metasurfaces, which can control the wavefront of the transmitted or reflected beam, and thus tailor the wave propagation in a customer-defined manner. A metasurface consists of arrays of artificial atoms with individually engineered optical properties. Unfortunately, however, very feature that makes these devices so useful, structurally dependent optical properties, also limits their potential for dynamically manipulating electromagnetic waves as micro/nano objects are difficult to modify post-fabrication.

We present our recent progress in developing active metasurfaces which can control optical properties such as polarization, anomalous refraction, focusing, and group delay by integrating graphene layer onto metamaterials with different functional unit cells. Benefitting from the electrically controllable optical properties, the developed graphene-based meta-devices are expected to provide a myriad of important applications such as polarization controllers, ultrathin lenses and compact slow light devices.

### Keywords:

Metamaterials, graphene, terahertz, metasurfaces, slow light



## Topologically-protected waveguiding in ring resonator lattices

LEYKAM Daniel\*<sup>1</sup>

<sup>1</sup>기초과학연구원 복잡계 이론물리 연구단  
dleykam@ibs.re.kr

### Abstract:

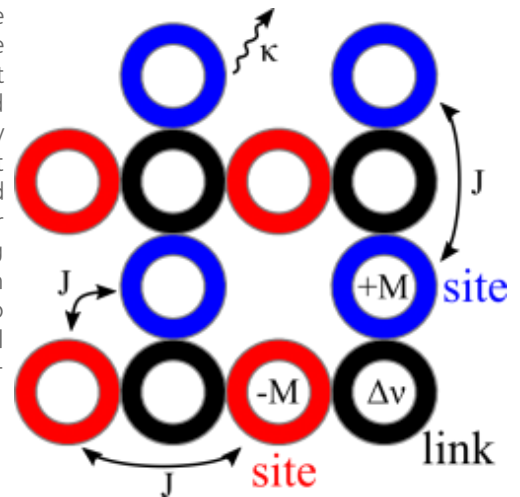
Lattices of coupled microring resonators can be used to emulate topological band structure effects and observe quantum Hall-like edge states of light. Such edge states are unidirectional and protected against disorder-induced backscattering. Existing designs for topological band structures are based on synthetic magnetic fields induced by inhomogeneous spatial or temporal modulation of the rings' resonant frequencies. I will present a simplified design for topological band structures based on resonator lattices with strong next-nearest neighbour coupling analogous to the Haldane model, which is implemented using off-resonant link rings. With this approach one can easily tune between trivial and nontrivial phases using electro-optic or nonlinear effects to switch or redirect the edge states. The reconfigurable topological waveguides enabled by this approach have potential applications for on-chip photon routing and switching at optical frequencies.

### Reference:

D. Leykam, S. Mittal, M. Hafezi, Y. D. Chong, arXiv:1802.02253

### Keywords:

topological photonics, optical devices, tight binding model



## Sub-10 nm water-filled terahertz nano-slots

김대식\*<sup>1</sup>, JEONG Jeeyoon<sup>1</sup>, LEE Kang Sup<sup>2</sup>, YUN Hyeong Seok<sup>1</sup>, KIM Zee Whan<sup>2</sup>

<sup>1</sup>Department of Physics and Astronomy, Seoul National University, <sup>2</sup>Department of Chemistry, Seoul National University  
dsk@phya.snu.ac.kr

### Abstract:

In this work we report arrays of sub-10 nm terahertz nano-slots filled with liquid water. We first fabricate sub-10 nm spacer-based nanogaps with length of 200 microns and 200 nm thickness, and then replace the spacer with water by wet-etching and diluting processes. With the extremely high aspect ratio of the nanoslots, exclusive optical detection of liquid water inside the gap is possible. The water inside the gap induces strong red-shift of the nano-slot resonance accompanied by a 700-fold increased absorption of terahertz waves, which is successfully reproduced in an analytic solution. We also demonstrate aqueous Raman spectroscopy of rhodamine 6G molecules inside the gap, confirming the full coupling of the gap with water and showing the wide applicability of this method to other molecular systems.

### Keywords:

Terahertz, Nano-optics, Water, Raman spectroscopy

## Unsaturated drift motion of carriers in graphene driven by high-field THz pulse

신희준\*<sup>1</sup>, 손주혁<sup>2</sup>, 임성주<sup>3</sup>

<sup>1</sup>한국식품연구원 식품안전연구단, <sup>2</sup>서울시립대학교 물리학과, <sup>3</sup>성균관대학교 에너지과학과, IBS Center for Integrated Nanostructure Physics (CINAP)  
sheejuns@uos.ac.kr

### Abstract:

We study that carriers in monolayer graphene can be accelerated to the Fermi velocity driven by high-power terahertz pulse  $E_{\text{THz}}$  without lattice heating at the charge-neutrality point. It is because that electron-phonon scattering rate is strongly suppressed due to the decreasing density of state near the Dirac point. Therefore the carriers can be accelerated without energy transfer to optical phonons. As a result, carriers in graphene can travel at the Fermi velocity. At the Fermi level larger than 110 meV, in contrast, excited carriers by  $E_{\text{THz}}$  heated the lattice of graphene and optical phonons are generated. The emitted optical phonons increase carrier-carrier scattering rate and drift velocity or carrier mobility can be reduced. This study indicates that the electron-optical phonon rate is affected by Fermi level in the graphene and provides insight for high-speed electronics of graphene based applications.

### Keywords:

High-field THz, Joule heating, graphene, drift velocity, optical conductivity, carrier scattering time

## 펄스 광전류 현미경을 이용한 그래핀 소자 초고속 전하수송 연구

안영환\*<sup>1</sup>, 손병희<sup>1</sup>

<sup>1</sup>아주대학교, 물리학과 및 에너지시스템학과  
ahny@ajou.ac.kr

### Abstract:

그래핀 등 2차원 나노물질과 이들에 기반한 소자에 관한 연구가 다양한 응용 분야에서 많은 관심을 받고 있으며, 특히 빠른 속도의 전자 소자로의 응용이 활발하게 연구 되고 있다. 따라서 그래핀 내부에서 일어나는 전자들의 동역학에 대한 연구가 매우 중요하다. 특히, 그래핀 내의 국소적인 포텐셜에 의한 영향은 Klein tunneling, 음의 굴절률 등 매우 흥미로운 동역학 연구 및 새로운 응용 가능성을 보여 준다. 본 연구에서는 펄스 주사 광전류 현미경을 이용하여, 국소적인 포텐셜 하의 그래핀 소자 내의 전자 동역학을 연구하였다. 우선, 한 전극에서 생성된 전하가 다른 전극으로 이동하는 시간을 측정하고, 채널길이가 1  $\mu\text{m}$  내외의 경우, THz 급 동작이 가능함을 보였다. 또한, 게이트 전압이 전자 동역학에 미치는 영향을 연구하여, 에너지에 따른 전자 속도의 분산효과를 확인하고, 이를 이용한 새로운 개념의 전기펄스 제단법을 제안한다. 본 연구는 다양한 1차원 및 2차원 나노 광/전 소자의 전자 동역학 연구에 중요한 수단으로 활용될 수 있을 것이다.

### Keywords:

그래핀, 초고속 전하수송, 펄스

## Electronic Structure Engineering of Graphene Using Patterned Dielectric Superlattices

MOON Pilkyung<sup>\*1, 2</sup>, FORSYTHE Carlos<sup>3</sup>, ZHOU Xiaodong<sup>4</sup>, TANIGUCHI Takashi<sup>5</sup>, WATANABE Kenji<sup>5</sup>,  
NARAYAN Abhay<sup>3</sup>, KOSHINO Mikito<sup>6</sup>, KIM Philip<sup>7</sup>, DEAN Cory<sup>3</sup>

<sup>1</sup>Arts and Sciences, New York University Shanghai, <sup>2</sup>NYU-ECNU Institute of Physics at NYU Shanghai,  
<sup>3</sup>Department of Physics, Columbia University, <sup>4</sup>Laboratory of Advanced Materials, Fudan University,  
<sup>5</sup>National Institute for Materials Science, <sup>6</sup>Department of Physics, Osaka University, <sup>7</sup>Department of  
Physics, Harvard University  
pilkyung.moon@nyu.edu

### Abstract:

외부 전기장을 통해 전자를 제어하는 기술은, 일반적인 격자구조의 제한을 넘어선 전자구조의 설계와 제어를 가능케한다. 최근 우리는, 그래핀을 패터닝된 유전체 초격자에 결합한, 높은 전자 이동도를 갖는 초격자 구조를 보인 바가 있다 [1]. 이 발표에서는, 이와 같은 그래핀 초격자에서 서로 다른 초격자의 대칭성이 전자와 홀 밴드의 대칭성과 전기전도도에 미치는 영향을 이론적으로 분석할 것이다. 또한, 그래핀 초격자의 자기장 속 전자에너지를 계산할 수 있는 유효모델을 보이고, 전자에너지의 프랙탈 전개 양상과 양자홀전도도의 위상수가 초격자의 대칭성을 명확히 반영함을 보일 것이다.

[1] C. Forsythe, X. Zhou, T. Taniguchi, K. Watanabe, A. Pasupathy, P. Moon, M. Koshino, P. Kim, and C. Dean, arXiv:1710.01365 (2017).

### Keywords:

그래핀; 초격자; 대칭성; 양자홀효과;

## Topological flat Wannier-Stark bands

KOLOVSKY Andrey<sup>2, 3</sup>, RAMACHANDRAN Ajith\*<sup>1</sup>, FLACH Sergej<sup>1</sup>

<sup>1</sup>IBS Center for Theoretical Physics of Complex Systems, Daejeon, South Korea, <sup>2</sup>Kirensky Institute of Physics, Krasnoyarsk, Russia, <sup>3</sup>Siberian Federal University, Krasnoyarsk, Russia  
ajithstcp@gmail.com

### Abstract:

We analyze the spectrum and eigenstates of a quantum particle in a bipartite two-dimensional tight-binding dice network. In the absence of a dc bias, it hosts a chiral flatband with compact localized eigenstates. In the presence of a dc bias, the energy spectrum consists of a periodic repetition of one-dimensional energy band multiplets, with one member in the multiplet being strictly flat. The corresponding flatband eigenstates cease to be compact, and are localized exponentially perpendicular to the dc field direction, and superexponentially along the dc field direction. The band multiplets are characterized by a topological quantized winding number (Zak phase), which changes at specific values of the varied dc field strength. These changes are induced by gap closings between the flat and dispersive bands, and reflect the number of these closings.

### Keywords:

Flat band, Wannier-Stark bands, Topology

## Negative excess shot noise by anyon braiding

이병목\*<sup>1</sup>, 한철희<sup>1</sup>, 심흥선<sup>1</sup>

<sup>1</sup>한국과학기술원 물리학과  
qudahr1222@kaist.ac.kr

### Abstract:

Fractional charges of anyons have been experimentally verified by measuring the shot noise of tunneling current at a quantum point contact (QPC) between two FQH edges. In this work, we show that the fractional statistics of Abelian anyons can be also detected by measuring shot noise in a slightly modified setup, where anyons are dilutely injected by tunneling, from an additional edge channel biased by a voltage, to the conventional fractional-charge measurement setup with a QPC in equilibrium. In the large bias voltage regime, we find that the shot noise of the tunneling current at the QPC is *reduced* from the thermal equilibrium noise by the value  $2qI$ , where  $q$  is the fractional charge of anyons and  $I$  is the tunneling current. This is opposite to the fractional-charge measurements where the noise is enhanced by the same value. The negative excess noise occurs due to a transport process in which an anyon, thermally excited at the QPC, effectively braids around another anyon dilutely injected from the additional edge to the QPC. Our finding provides an experimentally feasible way of detecting the fractional statistics.

### Keywords:

fractional statistics, anyon, shot noise

## Quantum confinement in three-dimensional Dirac semimetal $\text{Cd}_3\text{As}_2$ nanowires with magnetic tunnel barriers

JUNG Minkyung<sup>\*1</sup>, YOSHIDA Kenji<sup>2</sup>, PARK Kidong<sup>3</sup>, ZHANG Xiao-Xiao<sup>4</sup>, YESILYURT Can<sup>5</sup>, SIU Zhou Bin<sup>5</sup>, JALIL Mansoor B. A.<sup>5</sup>, PARK Jinwan<sup>6</sup>, PARK Jeunghye<sup>3</sup>, NAGAOSA Naoto<sup>4</sup>, SEO Jungpil<sup>6</sup>, HIRAKAWA Kazuhiko<sup>2</sup>

<sup>1</sup>DGIST 연구부, <sup>2</sup>IIS, University of Tokyo, <sup>3</sup>Department of Chemistry, Korea University, <sup>4</sup>Department of Applied Physics, University of Tokyo, <sup>5</sup>ECE, National University of Singapore, <sup>6</sup>EMS, DGIST  
minkyung.jung@dgist.ac.kr

### Abstract:

Three-dimensional (3D) Dirac semimetals have attracted considerable attention owing to their exotic properties, both predicted in theory and recently demonstrated experimentally. Here, we demonstrate single quantum dots confined with two p-n junctions in 3D Dirac semimetal  $\text{Cd}_3\text{As}_2$  nanowires under high magnetic fields. The device can be operated in two different regimes: (i) an n-type channel between n\*-type leads underneath the source-drain contacts, creating an open regime (n\*-n-n\* configuration); (ii) a p-type channel in the middle of the nanowire, forming a p-type quantum dot (QD) (n\*-p-n\* configuration). At zero magnetic field, the quantum confinement effect vanishes in the n\*-p-n\* QD because the Dirac fermions penetrate p-n junctions with high transmission probability (Klein tunneling). However, the high magnetic fields bend the Dirac fermion trajectories at the p-n junction due to cyclotron motion, preventing the Klein tunneling. This results in a strong confinement at p-n junctions of Dirac materials. In this regime, the device shows clean Coulomb diamonds, indicating that a single QD is formed in a Dirac semimetal nanowire.

### Keywords:

Dirac semimetal,  $\text{Cd}_3\text{As}_2$ , Klein tunneling, Nanowire, Quantum dot

## Tight-Binding Model for Quasi-One-Dimensional Topological Insulators

민흥기\*<sup>1</sup>, 유치호\*<sup>1, 2</sup>, ZHANG Fan\*<sup>2</sup>, LIU Cheng-Cheng<sup>3</sup>

<sup>1</sup>Department of Physics and Astronomy, Seoul National University, Seoul 08826, Republic of Korea,  
<sup>2</sup>Department of Physics, The University of Texas at Dallas, Richardson, Texas 75080, USA, <sup>3</sup>Beijing Key Laboratory of Nanophotonics and Ultrafine Optoelectronic Systems, School of Physics, Beijing Institute of Technology, Beijing 100081, People's Republic of China  
hmin@snu.ac.kr, yoon@snu.ac.kr, zhang@utdallas.edu

### Abstract:

Recently discovered quasi-one-dimensional topological insulators (quasi-1D TIs) are proposed as weak TI candidates in which stabilization and annihilation of surface Dirac cones are expected to be observed directly from experiments, due to the existence of multiple natural cleavage surfaces. We construct the effective low-energy model Hamiltonian for quasi-1D TIs which can describe all the sixteen  $Z_2$  topological phases. From the model calculation, not only the bulk band structure but also the topological surface states are successfully reproduced. In addition, we study thin-films of quasi-1D TIs and find surface-normal-dependent oscillating behavior of  $Z_2$  topological index as a function of the number of layers.

### Keywords:

quasi-one-dimensional material, topological insulator, topological phase of matter, thin-film material

## Magnetism in doped two-dimensional PdSe<sub>2</sub>

최형준\*<sup>1</sup>, 조요셉<sup>1</sup>

<sup>1</sup>Department of Physics, Yonsei University, Seoul 03722  
h.j.choi@yonsei.ac.kr

### Abstract:

Two-dimensional PdSe<sub>2</sub> layers have excellent air stability and a band gap that depends on the number of layers. Recently, monolayer (ML) PdSe<sub>2</sub> has been successfully exfoliated. In previously reported density functional theory (DFT) calculations, the valence bands of ML PdSe<sub>2</sub> have very large effective masses. This may imply that the system is close to instability. In our present work, we investigate energetic stability of magnetic phases in hole-doped ML PdSe<sub>2</sub> using first-principles DFT calculations. We consider both ferromagnetism and antiferromagnetism, and their effects on electronic structures. This work was supported by NRF of Korea (Grant No. 2011-0018306) and KISTI supercomputing center (Project No. KSC-2017-C3-0079)

### Keywords:

PdSe<sub>2</sub>, DFT

## Scalar Aharonov-Bohm effect without a loop in superconducting charge qubit

김영완<sup>1</sup>, 강기천\*<sup>1</sup>

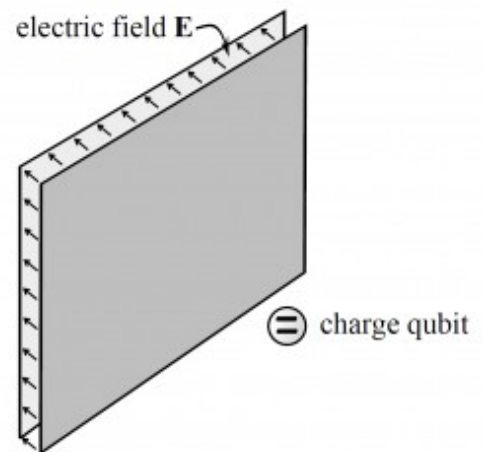
<sup>1</sup>전남대학교 물리학과  
kicheon.kang@gmail.com

### Abstract:

아라노프-보움(Aharonov-Bohm) 효과는 전하가 전자기장과 직접 중첩되지 않는 경우에도 전자기장과 원 상호작용에 의해서 발생하는 효과인 것으로 일반적으로 받아들여진다. 이같은 논지로 인 아라노프-보움 효과의 관측을 위해서는 반드시 간섭계의 닫힌 고리구조가 필수적인 것으로 이해된다. 이와는 대조적으로, 본 연구에서는 고리(loop) 구조가 아닌 초전도 전하 큐비트를 통하여 아라노프-보움 효과가 관측될 수 있음을 보인다. 서로 반대의 전하를 갖는 무한 평행판 밖에 전하 큐비트를 두어 스칼라 아라노프-보움 효과를 구현할 수 있다. 로렌츠-공변 국소 장 상호작용(Lorentz-covariant local field interaction) 이론을 적용하여, 우리는 관측 가능한 양자 위상 (quantum phase)이 발생함을 보인다. 또한 대전판에 발생하는 여기 전하 (induced charge)들은 스칼라 아라노프-보움 효과에 아무런 영향을 주지 않음을 논증한다.

### Keywords:

아라노프-보움(Aharonov-Bohm) 효과, 초전도 전하 큐비트 (superconducting charge qubit), 로렌츠-공변 국소 장 상호작용 (Lorentz-covariant local field interaction)



## Flatband Generators in One Dimension

울라이무마이마이티\*<sup>1, 2</sup>

<sup>1</sup>기초과학연구원 복잡계 이론물리 연구단, <sup>2</sup>과학기술연합대학원대학교, IBS School  
ibrahim.dulani@yahoo.com

### Abstract:

Flatband is a dispersionless energy band of a lattice, which occurs due to destructive interference. Consequently, the eigenstates of a flatband are typically compactly localized and are highly degenerate. A slight perturbation, disorder or non-linearity lift the degeneracy significantly changing properties of the lattice, making flatband an excellent testbed for unconventional physics. We introduce a systematic approach to generate flatbands in  $d=1$  lattice Hamiltonians with nearest neighbor hopping and compact localized states (CLS). Our construction relies on inverse eigenvalue problem, where we reconstruct the Hamiltonian from its CLS. Using this method we can construct flatband Hamiltonians which possess at least one flatband. This method extends naturally to arbitrary number of bands and arbitrary number of CLS size.

### Keywords:

Flatband, tight-binding, 1D system

## Charge Kondo effects in a quadruple quantum dot

최주호\*<sup>1</sup>, 유광수<sup>1</sup>, 심흥선<sup>1</sup>  
<sup>1</sup>한국과학기술원 물리학과  
jhchoi1201@kaist.ac.kr

### Abstract:

We theoretically study a charge Kondo effect in a quadruple dot, whose shape is such that three dots A,B,C are located at the three corners of a triangle respectively and the other dot D is at the center of triangle. Here, dots A and B are coupled to reservoirs via electron tunneling while the others are not. When the system has ground-state charge configurations  $(N_A=1, N_B=1, N_C=1, N_D=0)$  and  $(0,0,0,1)$ , we find that the system can show a charge Kondo effect whose properties depend on an external magnetic field and inter-dot tunneling between A and B. When an external magnetic field is applied but there is no inter-dot tunneling, a single channel Kondo effect occurs. In this case, the spin degree of freedom is suppressed, and the two charge configurations act as the pseudospin of the Kondo effect. When the inter-dot tunneling is allowed, but there is no external magnetic field, an anisotropic two channel Kondo effect can appear. In this case, electrons of dot A and B in the charge configuration  $(1,1,1,0)$  form a spin singlet state. The conductance through the system is discussed for the two cases.

### Keywords:

Mesoscopic, Charge Kondo effect, Quantum dot,

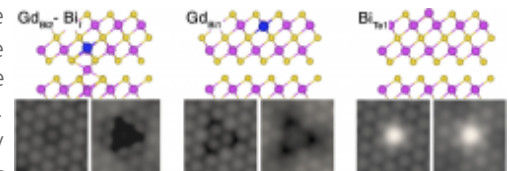
## Identification of Gd-induced and intrinsic point defects near the $\text{Bi}_2\text{Te}_3(111)$ surface

신은하<sup>1</sup>, 김진수<sup>2</sup>, 정명화<sup>2</sup>, 황찬용<sup>3</sup>, 김미영<sup>1</sup>, 김한철\*<sup>1</sup>

<sup>1</sup>숙명여자대학교 공과대학 응용물리학과, <sup>2</sup>서강대학교 자연과학부 물리학과, <sup>3</sup>한국표준과학연구원 양자기술연구소  
hanchul@sm.ac.kr

### Abstract:

$\text{Bi}_2\text{Te}_3$  is one of the representative topological insulators possessing the topologically-protected metallic surface states. In order to understand the effect of magnetic impurities on the metallic surface states, we have investigated  $\text{Bi}_2\text{Te}_3$  containing substitutional Gd which is isovalent with Bi. As-grown  $\text{Bi}_{2-x}\text{Gd}_x\text{Te}_3$  and the annealed sample show significantly different STM image features on their (111) surfaces. Using first-principles calculations based on the density functional theory, we have successfully identified the various STM image features residing near-surface both in as-grown and the annealed samples. With the identification of point defects, we are able to speculate a Gd-out-diffusion mechanism comprising the formation of (i) Te vacancy, (ii) Bi antisite, and (iii) substitutional Ga at Bi site.



This work was supported by the National Research Foundation of Korea (NRF) grant funded by the Korea government (MSIP) (No.2014R1A2A1A1105401, 2017R1A2B3007918, 2012M3C1A6035684, 2015R1A2A2A01005564, 2017R1A2B4012972, 2015M2A2A6A01045343, and 2016K1A4A4A01922028). The calculations were supported by Supercomputing Center/Korea Institute of Science and Technology Information with supercomputing resources including technical support (No. KSC-2016-C2-0059).

### Keywords:

$\text{Bi}_2\text{Te}_3$ , topological insulator, Gd defect, Scanning tunneling microscopy, first-principles calculations

## Cooperative Research of Simulations and Experiments for Structural Change of Carbon Linear Chains and MoS<sub>2</sub>.

이건도\*<sup>1</sup>

<sup>1</sup>서울대학교 재료공학부  
gdlee@snu.ac.kr

### Abstract:

The structural changes in low dimensional materials has been a long time subject of intensive investigation because the structural and electronic properties are determined by the structure. In order to study the structural changes, many state-of-art observation techniques such as transmission electron microscopy (TEM) and scanning tunneling microscopy techniques have been developed and utilized. However, since the process of structural change is finished in a very short time, it is very difficult to clarify the process and the origin of structural changes even within the state-of-the-art microscopy methods. On the other hands, various simulation methods have been developed to study and predict the property of materials. Among those methods, the density functional theory (DFT) calculation method is widely used due to the accuracy and predictability. The tight-binding molecular dynamics (TBMD) simulation method is also attempted to study the dynamics in materials. In the cooperative research of DFT calculation, TBMD simulation method, and TEM experiment, I studied successfully defects and dopants in 2D materials [1-4] as well as structural changes in nanomaterials [5,6]. In this talk, the recent results on the structural changes of carbon double linear chains and the phase transition of MoS<sub>2</sub> will be introduced. Under the electron irradiation, the carbon double linear chains are found in the graphene constriction. In the short double linear chain, the reversible aromatic ring cyclization, so-called Bergman cyclization is observed. Our TBMD simulation is exploited to explain the structural changes in carbon double linear chain. It is also found the phase transition in MoS<sub>2</sub> patch is induced by gas molecule and it improves greatly the catalyst effect. The origin of the phase transition is explained in atomic scale by using DFT calculation method.

### References

- [1] K. He et al., Nature Communications 5:3040 (2014).
- [2] A. W. Robertson et al., Nano Letters, 15 5950 (2015)
- [3] S. Wang et al., ACS Nano 10, 5419 (2016)
- [4] A. W. Robertson et al., ACS Nano 10, 10227 (2016)
- [5] D. -H Nam et al. Advanced Materials 29, 1702958 (2017)
- [6] M. S. Choi et al. Advanced Materials 29, 1703568 (2017)

### Keywords:

DFT calculation, Tight-binding, MoS<sub>2</sub>, Carbon linear chains

## First-principles design of memcapacitors for neuromorphic computation from multiferroics

이준희\*<sup>1</sup>

<sup>1</sup>울산과학기술원 에너지 및 화학공학부  
junhee@unist.ac.kr

### Abstract:

Understanding various interactions among charge, spin, and lattice in multiferroics implies endless possibilities for material engineering. And such interactions may result in various alternative multiferroic phases that have different spin-charge-lattice combinations and thus distinct dielectric properties that can be controllable by electric field. I will talk about how to design multi-level dielectrics (memcapacitors) from the alternative phases for developing neuromorphic computations with ultralow energy consumption. And some recent experiments verifying our theoretical predictions will be introduced. I will highlight the importance of first-principles design and collaboration with experiments to reveal the novel phases with multiple dielectric constants for the next-generation neuromorphic computation.

### Keywords:

memcapacitor, neuromorphic, first principles

## First-principles study on electron-phonon interactions and their spectroscopic signatures in two-dimensional crystals

손영우\*<sup>1</sup>

<sup>1</sup>고등과학원 계산과학부  
hand@kias.re.kr

### Abstract:

In this talk, I will present my recent works regarding on interplay between structural variations and electronic states in two-dimensional crystals such as graphene, bilayer graphene, and two-dimensional crystals and their spectroscopic consequences.

### Keywords:

First-principles calculations, two-dimensional crystals, spectroscopy

## 연구장비산업 및 국산연구장비개발

조영훈\*<sup>1</sup>, 이상갑<sup>1</sup>, 김진규<sup>1</sup>, 최명철<sup>1</sup>, 최연석<sup>1</sup>, 장기수<sup>1</sup>, 이한주<sup>1</sup>, 서정주<sup>1</sup>

<sup>1</sup>한국기초과학지원연구원(Korea Basic Science Institute)  
younghun@kbsi.re.kr

### Abstract:

연구시설 및 장비산업은 과학기술의 발전을 견인하고, 국가 과학기술 역량을 나타내는 지표로, 고도의 기술지식 집약적 융합산업이자 국가 경제발전에 기여하는 바가 매우 큰 분야입니다. 실제로 1901년부터 2008년까지의 과학분야 노벨상 수상자 중 26명이 분석기술·장비개발을 통하여 노벨상을 수상하였습니다. 과학선진국은 이러한 현실을 직시하여 꾸준한 투자를 통하여 과학기술 원천기술 확보와 연구장비 개발 경쟁을 심화하고 있다.

하지만, 국내 연구장비는 대부분을 수입에 의존하고 있고, 이러한 결과 국내 R&D 자본의 해외 유출이 심각한 수준이다. 2014년 기준 국내 연구장비 시장의 85%가 외산이고, 정부 R&D 구축액 상위 20개 제작사 중 국내기업은 전무한 것이 현실이다.

본 분석과학 연구장비 개발사업은 이러한 현실을 극복하고자, KBSI에서 전략적으로 육성하고 있는 사업으로, 2017년부터는 국가과학기술연구회에서 시행하는 Big Issue Group 사업으로 확대되어 수행하고 있다.

이를 통하여 연구장비산업 고부가가치화와 및 경쟁력 확보를 통한 국가 R&D 생산성 제고를 도모하고, 연구장비 제조·판매 기업의 성장 및 고급 일자리 창출에 기여할 것이다. 연구장비 제조기업이 요구하는 니즈와 대학·연구기관 등이 제공할 수 있는 시즈를 연계하여 연구장비 국산화 확대에 기여할 것이다.

또한, 본 발표를 통하여 국산 연구장비개발 필요성에 대한 인식을 확대하고, 국산 연구장비산업의 발전, 나아가 연구산업 발전에 기여하는 자리가 되었으면 한다.

### Keywords:

연구장비, 연구장비개발, 연구산업

## 전자기 물성측정장비 개발(Development of Electro-Magnetic Property Measurement System)

최연석\*<sup>1</sup>, 이계행<sup>1</sup>, 박승영<sup>1</sup>, 방준혁<sup>1</sup>, 장재영<sup>1</sup>, 황영진<sup>1</sup>, 김명수<sup>1</sup>, 조영훈<sup>1</sup>, 이해근<sup>2</sup>, 김동현<sup>3</sup>, 정상권<sup>4</sup>

<sup>1</sup>한국기초과학지원연구원, <sup>2</sup>고려대, <sup>3</sup>충북대, <sup>4</sup>KAIST  
ychoi@kbsi.re.kr

### Abstract:

전자기 물성측정장비(EMPS; Electro-Magnetic Property measurement System)는 자기장 발생 플랫폼, 프로브 및 밀폐순환 액화기를 이용하여 자기장 및 온도가변 환경에서 전기적, 자기적 물성 특성을 측정하는 장비이다. 국내 연구자들은 물질의 특성 분석을 위하여 자기적, 전기적, 열적 물성측정을 개별장비에서 수행해 왔으며, 이로 인하여 각각의 물성측정 장비를 구입해야 하는 경제적 부담이 가중되어 왔다. 이러한 연구환경 개선 및 국내 물성연구 진흥을 위해서는 물성특성 연구장비의 국산화가 필수적이며 다목적 물성특성 측정장비가 개발되어야 한다. 한국기초과학지원연구원은 다목적 물성특성 측정 장비 제작, 상용화 및 유지보수 기술 확립을 위하여 2017년부터 전자기 물성측정장비 개발사업을 진행해 오고 있다. 전자석 및 초전도자석을 이용하여 자기장 발생 플랫폼을 개발하고, JT 냉동기를 이용한 다중환경에서 물성측정 프로브 및 극저온 냉동기를 이용한 밀폐순환 액화기를 개발하여 통합하게 된다. 본 발표에서는 개발중인 전자기 물성측정장비를 소개하고, 현재까지 개발성과 및 향후 계획에 대하여 소개한다.

### Keywords:

물성측정, 전자기, 극저온, 초전도, 열전도

## 송수신부 일체형 광학적 원격시정측정장치 개발

점진상\*<sup>1</sup>, 이재용<sup>1</sup>

<sup>1</sup>한국표준과학연구원 첨단장비연구소  
jsjung@kriss.re.kr

### Abstract:

시정은 사람의 눈으로 볼 수 있는 최대 거리를 의미한다. 시정 악화는 대기 중 미세먼지와 상대 습도 그리고 안개와 밀접한 관계가 있다. 기상청에서는 1시간 간격으로 시정을 측정하여 실시간으로 공개하고 있다. 일반적으로 시정은 숙련된 전문 인력이 시정목표도를 이용하여 목측으로 측정한다. 하지만 이러한 목측은 유지관리에 많은 비용이 들고 측정값이 부정확하다는 단점이 있다. 이를 보완하기 위해서 기상청에서는 안개 시 시정을 측정하는 전방산란식 시정측정기를 병행하여 사용하고 있다. 전방산란식 시정계의 경우 사용되는 파장이 적외선 영역이라 실제 보는 행위가 일어나는 가시광선 영역을 대표할 수 없다. 또한 전방산란식의 경우 빔흡수 특성은 반영하지 못하기 때문에 도심지역에서 시정을 측정하기에 적합하지 않다는 단점이 있다. 본 연구에서는 송수신부 일체형으로 광학계와 반사경을 이용하여 광투과도를 측정하여 시정을 산출하는 광학적 원격시정계를 개발하였다. 530 nm의 파장을 사용하여 가시광선 영역을 대표할 수 있도록 하였고, 레트로타입의 반사경을 도입하여 현장 설치를 용이하게 하고 광경로를 자유롭게 조절할 수 있게 구성하였다. 개발된 시정계 본체는 야외설치용 하우징에 거치하였다. 하우징의 윈도우는 압축공기와 브러쉬를 이용하여 주기적으로 청소를 하여 윈도우 오염으로 인한 측정값 오차가 발생하는 것을 방지하였다. 개발된 시정계를 야외에 설치한 후 기존의 전방산란식 시정계와 광투과방식의 시정계와 비교 측정을 수행하였다. 장기간의 비교평가 결과 개발된 광투과방식 시정계가 악시정을 잘 모사하는 것으로 나타났다.

### Keywords:

시정측정장치, 원격시정계, 광투과방식, 전방산란식

## 가스클러스터 이온빔 및 비행시간형 이차이온 질량분석기 개발

최명철\*<sup>1</sup>, 이상주<sup>1</sup>, 최창민<sup>1</sup>, 백지영<sup>1</sup>, 김일희<sup>1</sup>, 민부기<sup>1</sup>, 김정진<sup>1</sup>, 어재영<sup>1</sup>

<sup>1</sup>한국기초과학지원연구원  
cmc@kbsi.re.kr

### Abstract:

클러스터이온빔을 사용하는 비행시간형 질량분석기(cluster ion beam TOF SIMS)는 시료의 표면에 존재하는 미량의 다양한 시료를 복잡한 전처리 없이 직접 그 화학적 조성을 분석할 수 있는 장비이다. 특히 최근 클러스터 이온빔이 장비에 도입 되면서 기존에는 분석이 어려웠던 분자구조를 파괴하지 않고 검출할 수 있는 길이 열리고 있다. 즉, 분자와 같이 보다 큰 형태의 이온을 직접 검출할 수 있다는 것이다. 이러한 기능은 산업에 널리 사용되고 있는 다양한 폴리머, 각종 유기물 특히, 디스플레이 분야에 중요한 OLED패널의 분석에 적합한 특징을 가지고 있다. 국내 산업체가 세계적인 경쟁력을 가지고 있는 분야에서 사용되는 분석장비, 특히, 질량분석장비분야는 모두 외국의 제품에 의존하여 분석하고 있는 실정이다. 이러한 국내 분석장비 산업의 문제점을 해결하기 위하여 KBSI에서는 그 동안 이온빔 및 다양한 질량분석기를 개발해오고 있으며 이를 결합하여 효과적인 국산 분석장비로 개발해나가고 있다.

본 발표에서는 20 kV급 가스 클러스터이온빔 원을 개발하였으며 이를 이용하는 비행시간형 질량분석기와 기능들을 개발 진행하고 있으며, 전량 외산 장비에 의존하고 있는 클러스터 이온빔 비행시간형 질량분석기의 국산화 개발과 함께 핵심 요소기술인 다양한 이온빔 개발을 통한 새로운 분석장비 및 기능 구현을 위한 연구결과들 및 향후 분석장비 개발 계획에 대하여 발표할 것이다.

### Keywords:

이온빔원, 클러스터이온빔, 비행시간형 질량분석기, 이차이온 질량분석기, 이차이온, 질량분석

## 나노박막 광물성 분석을 위한 3-편광자 분광타원계측기 개발

제갈원\*<sup>1</sup>, 조용재<sup>1</sup>, 조현모<sup>1</sup>, 김동형<sup>1</sup>

<sup>1</sup>한국표준과학연구원 첨단측정장비 연구소  
wchegal@kriss.re.kr

### Abstract:

분광타원계측기(spectroscopic ellipsometer; SE)는 시편에 의한 편광상태 변화량(예: Y와 D 스펙트럼)을 측정하고, 측정 데이터로부터 박막의 두께와 굴절률 등을 이론적 분석을 통하여 얻어내는 기술이다. SE는 초고속으로 대면적을 매우 정밀하게 측정할 수 있는 장점 때문에 박막 관련 다양한 분야의 연구개발에 활용되고 있다. 그러나 기존 분광타원계측기들은 등방성 물성만을 측정할 수 있는 반면에 반도체 소자의 비대칭 나노 패턴형상, OLED 유기박막의 복굴절, 편광부품 광물성 등의 비등방 물성 측정에 관련된 연구개발 분야가 최근 급증하고 있다. 본 발표에서는 무색수차를 갖는 3개의 편광자들로만 구성된 새로운 편광 광학계를 사용하여 시편의 물리 행렬의 비등방 성분들을 측정할 수 있는 물리 행렬 분광타원계측기 개발 관련 기술을 소개하고자 한다.

### Keywords:

분광타원계측기, 대면적 광학계, 비등방 물리 행렬, 박막측정

## Complex adaptive systems: from the brain to society

민병준\*<sup>1</sup>

<sup>1</sup>충북대학교 물리학과  
min.byungjoon@gmail.com

### Abstract:

Complex systems are often adaptive in that they mutate corresponding to a changing environment. Ecosystems, social systems, and neural systems are prominent examples of complex adaptive systems showing complexity and the ability to change to promote survival in a fluctuating environment. We here explore the origins, models, and consequences of adaptation in complex systems focusing on neural plasticity and fragmentation in society. We propose a theory for identifying the influential areas in the brain plasticity and examine the role of nonlinearity in a model of social fragmentation.

### Keywords:

Complex Systems, Adaptation, Plasticity, Fragmentation

## Synchronization of chaotic oscillators and Kuramoto oscillators

조영설\*<sup>1</sup>

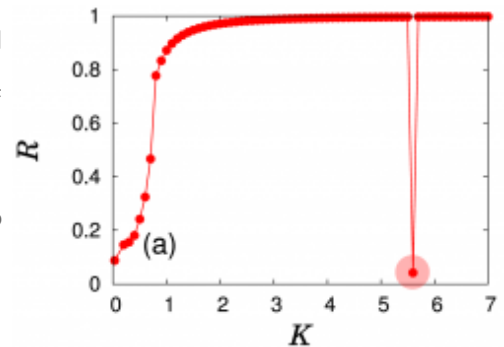
<sup>1</sup>전북대학교 물리학과  
yscho@jbnu.ac.kr

### Abstract:

We consider two types of spontaneous synchronization. The first type is the synchronization of identical chaotic oscillators induced by structural symmetry of the given network. The second type is the synchronization of the oscillators of heterogeneous natural frequency distribution driven by diffusive coupling in Kuramoto system. In this presentation, we briefly introduce our recent study on these two topics.

### Keywords:

synchronization, chaotic oscillator



## Higher-order correlations in bursty dynamics

조한현\*<sup>1</sup>

<sup>1</sup>아시아 태평양 이론물리센터 -  
hang-hyun.jo@apctp.org

### Abstract:

Characterizing inhomogeneous temporal patterns in natural and social phenomena is important to understand underlying mechanisms behind such complex systems. Temporal inhomogeneities in event sequences have been described in terms of bursts that are rapidly occurring events in short time periods alternating with long inactive periods. The inhomogeneities of inter-event times have been extensively studied, while the correlations between inter-event times, often called correlated bursts (CB), are largely unexplored. Therefore, we study the correlated bursts (i) by modeling CB by the bursty-get-burstier mechanism, (ii) by investigating the limits of memory coefficient in measuring CB, and (iii) by detecting the hierarchical burst structure. We also discuss some ongoing and future works.

### Keywords:

bursty dynamics, power-law distribution, inter-event time, correlations between inter-event times

## Anomalous single-molecule dynamics in living matters: at the intersection of biophysics and statistical physics

JEON Jae-Hyung<sup>\*1</sup>

<sup>1</sup>Department of Physics, POSTECH  
jeonjh@gmail.com

### Abstract:

Recent advance of single-particle tracking (SPT) technique has significantly elevated the understanding of single-molecule dynamics in living and soft-matter complex systems. Without in priori assumption on the underlying dynamics, the SPT tools make it possible to access the information on transport and/or conformational dynamics of individual molecules and, further, to obtain physical observables in a single-molecule level, without ensemble-averaging. It has been found that the viscoelastic and active (nonequilibrium) nature of the intracellular environment often induce, so called, “strange kinetics”. Currently this field, often dubbed anomalous diffusion, is rapidly growing at the intersection of biophysics and statistical physics. In this talk, I will introduce the field of anomalous diffusion, with a few research topics undertaken in my group including the transport dynamics of neuronal mRNP, the resetting dynamics of fractional Brownian motion, and the molecular diffusion in a nucleus.

### Keywords:

Anomalous diffusion, single-particle tracking, active matter, resetting, first-passage, human chromosome

## Vertically aligned MIM structure and its application for Biosensor

유흥삼\*<sup>1</sup>, 유의상<sup>1</sup>

<sup>1</sup>한국과학기술연구원(KIST) 국가기반기술본부, 센서시스템연구센터  
ysryu82@kist.re.kr

### Abstract:

The nanoscaled to microscaled biological units and their assemblies such as virus, exosomes which generally have diameters less than 100 nm, which makes it difficult to isolate pure populations by traditional methods. Here we show that dielectrophoresis (DEP) can be used to collect and sort sub-100 nm small unilamellar vesicles (SUVs), a model of exosomes. Furthermore newly designed DEP platform enables to trap and isolate the specific biomaterials depending on their physico-chemical properties by varying DEP frequency and Field intensities.

### Keywords:

Dielectrophoresis, nanovesicle, small unilamellar vesicle, nanogap, sorting.

## Physical manipulation and characterization of living brain cells

LEE Ga-Young<sup>1</sup>, JANG You-Na<sup>2</sup>, LEE Kea Joo<sup>2</sup>, KIM Kipom\*<sup>1</sup>

<sup>1</sup>Research Equipment Core Facility Team, Korea Brain Research Institute, <sup>2</sup>Department of Structure & Function of Neural Network, Korea Brain Research Institute  
kpkim@kbri.re.kr

### Abstract:

Living cells are composed of active, delicate, and elastic materials with different physical properties. Recent studies have shown how physical stresses are integrated into a coherent biological response of molecules inside living cells. Indeed, brain cells exhibit distinct physical behaviors depending on their types, microcompartments, and alterations in the internal and external environments. To study the diverse physical properties of living brain cells, we have been developing an optical microscopy combined with optical manipulation tools in which mechanical force is delivered to the local surface sites of cells. Basically the optical microscopy is used to watch the living cells and observe biological processes inside living cell in real time. Simultaneously, optical manipulation tools enable us to physically manipulate individual cells and to characterize physical properties of microcompartments of the cell. Here we present the operating principles of the optical force microscopy, some preliminary results, and future applications. We expect that this study would contribute to a better understanding of the biological response of brain cells under various changes in physical environments.

### Keywords:

cell mechanics, optical tweezers

## Investigation on the deterministic mechanism of cell motility in a cancer

이현균<sup>1</sup>, 이경진\*<sup>1</sup>  
<sup>1</sup>고려대학교 물리학과  
kyoung@korea.ac.kr

### Abstract:

Revealing deterministic mechanism of a cell's motility has a major significance not only in biology but also in physics. Late investigations on various types of cells including microglia and dendritic cells have elucidated the intracellular machinery that drives distinct behaviors of these cells. For example, a periodic migration pattern emerges due to continual redistribution of motor proteins within a dendritic cell, a type of immune cell. On the other hand, our investigation on a 'malignant' breast cancer cell line has been led to focus on an extracellular source of deterministic migration pattern of this particular cell type, which is the cell-to-cell contact. The simplest example is the persistent rotation between a pair of cells in contact. This is in clear contrast with the highly stochastic behavior observed from an isolated breast cancer cell; it suggests contact-based interaction as a prevailing deterministic factor over any intracellular machinery. As expected, the behavioral pattern becomes more complicated as the cell-cluster grows in size, and culminates in a super-diffusive motion in a dense (or 'confluent') population. In this presentation, we show our progress in the investigation on origins of the super-diffusivity by looking at how time-constants associated with directional persistence evolves with the number of neighbors. We also present our simulation result to recapitulate the observation.

### Keywords:

cell motility, cancer, cell-to-cell, contact

## Identifying chromosome domains at multiple scales and their hierarchy

현창봉\*<sup>1</sup>, 김민혁<sup>1</sup>, 박지현<sup>1</sup>

<sup>1</sup>고등과학원 계산과학부  
hyeoncb@kias.re.kr

### Abstract:

The spatial organization of the genome has a fundamental implication on the life of the cell. With the advent of chromosome conformation capture technique and genome sequencing, the problem of identifying domain structures from the pairwise interactions in the genome has received much attention over the past decade. However, existing methods rely on differently prepared data and algorithms to find domains at specific scales. Here we develop a unified method for finding the domain solutions at multiple scales. The scale of the domains is tuned by a single parameter, which controls the model's prior preference to a less fragmented domain solution. We find a family of domain solutions at varying scales, revealing an interesting structure of hierarchy between the domains at small and large scales. We successfully validate the domain solutions by comparing to appropriate bio-markers, and furthermore show that our method work as well as each of the previous methods at the corresponding scale.

### Keywords:

Chromosome organization, Markov Chain Monte Carlo

## Deformability-dependent inertial focusing in a triangular channel

이원희\*<sup>1, 2</sup>, 최요한<sup>1</sup>, 김정아<sup>1</sup>

<sup>1</sup>한국과학기술원, 나노과학기술대학원, <sup>2</sup>한국과학기술원, 물리학과  
whlee153@kaist.ac.kr

### Abstract:

In a variety of diseases, such as cancer, blood disease, inflammation, infected cells have different mechanical phenotypes from normal cells. Cell deformability is recognized as a new biomarker that determines invasiveness of cancer cell and the methods to differentiate cancer cells based on deformability are studied.

Inertial microfluidic is an effective and high-throughput method to separate and enrich the target micro particles or cells. Particles flowing through the micro-channel are concentrated at a specific equilibrium position due to the inertial lift forces. The inertial lift forces, therefore the equilibrium positions, are affected by particle size, shape, deformability, channel shape, and fluid flow rate, which allows particle separations.

The inertial focusing in the microchannels with triangular cross-section shows interesting size and Reynolds number dependence. We investigated focusing position changes depending on deformability of particles in the channels with cross-section shape of right isosceles triangle. PDMS particles synthesized at various ratios and various viscous silicon oils were prepared as particles/drops of different deformability. The focusing positions of the particles and droplets vary with their deformability, which significantly differs from the focusing positions of solid particles. Under the same Re conditions, the equilibrium position of a particle with a small deformability is closer to the wall. For silicon oil droplets, additional corner focusing positions are found under low Re condition. This deformability dependent particle focusing can be applied to separations of the more deformable cells such as metastatic cancer cells.

### Keywords:

Inertial focusing, Deformability, Particle separation

## 기니피그 동물실험을 통한 초음파가 청력에 미치는 영향 연구

성인호<sup>1</sup>, 안강현\*<sup>1</sup>

<sup>1</sup>충남대학교 물리학과  
ahnkh@cnu.ac.kr

### Abstract:

청각 손실은 많은 경우 가청 영역 대 노이즈에 노출 되어 발생한다. 가청 영역 밖의 초음파는 들리지 않기 때문에 청각 손실이 일어나지 않는다고 상식적으로 생각해 왔다. 본 연구는 가청영역 이외의 주파수대역(초음파)에서 청력에 손실을 줄 수 있는지에 대해 알아보기 위해 동물 실험을 수행하였다. 기니피그의 가청역은 54Hz에서 49,000Hz이므로 58,000Hz의 소리는 들리지 않는 초음파 영역이다. 이 주파수를 발생하는 장치를 제작하여 기니피그를 초음파에 2시간 노출시키고 2시간 노출시키지 않음을 5번 반복하였다. 그 후 청성 뇌관 반응 검사를 실시하였는데 실험에 이용된 두 개체의 기니피그 모두 청력 손실이 발생함을 확인하였다. 기니피그의 고막 안에는 삼출이 없었지만, 청성 뇌관 반응 문턱값이 기존 문턱값에 비해 10dB 높아진 것을 확인하였다. 초음파가 물리적으로 어떻게 청각 손실을 일으킬 수 있는지 그 가능성에 관한 고찰을 하였다.

### Keywords:

청각손실, 초음파

## KOMAC의 이온빔 장치 현황

조용섭\*<sup>1</sup>

<sup>1</sup>한국원자력연구원 양성자가속기연구센터  
choys@kaeri.re.kr

### Abstract:

1980년대 DuoPIGatron 이온원을 기반으로 한 기체 이온빔 장치의 개발이 한국원자력연구원 당시 핵물리부의 주도로 시작되어 현재 까지 운영되고 있다. 이후 철, 구리 등 금속이온을 제공하기 위해 Bernas 이온원을 기반으로 한 이온빔 장치가 운영되었고, 2010년대 100 MeV 양성자가속기의 입사기로 활용된 마이크로파 이온원이 개발되어 현재까지 사용되고 있다. 2013년 이후 KOMAC (한국원자력연구원 양성자가속기연구센터)에서는 금속 증기 진공 아크 이온원, 알칼리 금속 이온원, 소형 고주파 이온원, 전자빔 이온원 등의 다양한 이온원 연구가 진행되고 있으며, 이러한 이온원에서 얻어지는 이온빔을 활용하기 위한 장치의 개발도 동시에 진행되고 있다. 이와 더불어 러더포드 후방 산란 분석법 (RBS), 양성자 유도 X선 방출 분석법 (PIXE) 등 이온빔 분석과 수 MeV의 이온빔 조사를 위해 1.7 MV 탄뎀형 가속기가 운영되고 있으며, 가속기 질량 분석 (AMS)을 위해 3.0 MV 탄뎀형 가속기의 설치가 진행되고 있다. 이번 학회에서는 KOMAC의 이온빔 장치 현황에 대해 발표하고자 한다. Acknowledgement : This work has been supported through KOMAC (Korea of Multi-purpose Accelerator Complex) operation fund of KAERI by MSIT (Ministry of Science and ICT).

### Keywords:

이온빔, 이온원, PIXE, RBS, AMS

## Monitor for Micro-bunching Instability in Free Electron Laser

강흥식\*<sup>1</sup>, 김창범<sup>1</sup>, 김규진<sup>1</sup>, 고준호<sup>2</sup>, 고인수<sup>1</sup>  
<sup>1</sup>포항공과대학교 가속기연구소, <sup>2</sup>포항공과대학교  
hskang@postech.ac.kr

### Abstract:

It is well known that the interaction between the coherent synchrotron radiation and the electron beam can generate the micro-bunching instability. The free electron laser intensity can be affected significantly by growing up of the micro-bunching instability. However, a direct measurement tool for the micro-bunching instability has not been developed yet. We installed a CCD camera in a coherent radiation monitor setup to measure the micro-bunching instability. The CCD camera successfully monitors the micro-bunching instability and provides a direct measurement tool of the micro-bunching instability in the X-ray Free Electron Laser.

### Keywords:

Micro-bunching instability, Free electron laser, PAL-XFEL

## 진공다이오드의 전자 주행시간 제한 분석

전석기<sup>1</sup>, 김재훈\*<sup>1</sup>

<sup>1</sup>한국전기연구원 전자기파응용연구센터  
jkim@keri.re.kr

### Abstract:

두개의 평행판 전극으로 구성된 진공 다이오드에서 DC와 AC 전기장에 의해 가속 또는 감속되며 운동하는 전자의 운동을 분석하면, AC 전기장의 주파수가 일정값을 넘을 경우, 음극에서 방출된 전자가 양극에 도달하지 못한다는 사실은 잘 알려져 있다. 음극에서 방출된 전자가 양극에 도달하게 하기 위해서는 AC 전기장의 한 주기보다 충분히 작은 시간 안에 전자가 음극에서 양극으로 이동하도록 다이오드를 구성하면 된다. 이와 같이 전자 주행시간을 제한하는 것은 간단한 진공다이오드는 물론 다양한 전자소자에서 전자 또는 캐리어의 운동 시간을 제한하는 것으로 나타난다. 본 연구팀은 전자 주행시간 제한에 대한 면밀한 이론적 고찰을 통해 기존 전자소자가 가지는 주파수 상한의 물리적 이해를 넓히고 주파수 상한을 크게 넘어서는 진공전자소자의 개발 가능성을 보였다.

### Keywords:

전자 주행시간 제한, 진공소자

## 가속기 기반의 의료기기와 표준

조일성\*<sup>1</sup>

<sup>1</sup>한국원자력의학원  
ischo@kirams.re.kr

### Abstract:

방사선치료와 핵 의학은 물리학과 생물학 그리고 가속기 공학과 의학이 융합된 분야이다. 방사성동위원소를 사용하는 초창기 방사선치료에서 대단위 가속기를 사용하는 현대의 방사선의학에 이르기 까지, 방사선의학은 최첨단 기술을 바탕으로 컴퓨터 제어기술과 로봇틱 기술까지 흡수하여 계속 발전하고 있다. 본 발표에서는 가속기를 기반으로 하는 의료기기가 환자에게 안전하게 사용되기 위한 요구조건을 살펴보고, 의료기기의 허가에 어떻게 적용되는지 논의하고자 한다.

### Keywords:

가속기 기반의 의료기기와 표준

## Beta-limiting instabilities and projected global MHD mode stabilization in KSTAR

PARK Y.S.\*<sup>1</sup>, SABBAGH S.A.<sup>1</sup>, BERKERY J.W.<sup>1</sup>, JIANG Y.<sup>1</sup>, AHN J.H.<sup>1</sup>, BIALEK J.M.<sup>1</sup>, KIM J.<sup>2</sup>, KO W.H.<sup>2</sup>, HAN H.S.<sup>2</sup>, HAHN S.H.<sup>2</sup>, BAK J.G.<sup>2</sup>, JEON Y.M.<sup>2</sup>, PARK B.H.<sup>2</sup>, KO J.S.<sup>2</sup>, IN Y.K.<sup>2</sup>, YOON S.W.<sup>2</sup>, WANG Z.R.<sup>3</sup>, FERRARO N.M.<sup>3</sup>, GLASSER A.H.<sup>4</sup>, YUN G.S.<sup>5</sup>, OH Y.K.<sup>2</sup>, PARK H.K.<sup>2, 6</sup>

<sup>1</sup>Department of Applied Physics, Columbia University, New York, NY, USA, <sup>2</sup>National Fusion Research Institute, Daejeon, Korea, <sup>3</sup>Princeton Plasma Physics Laboratory, Princeton, NJ, USA, <sup>4</sup>Fusion Theory and Computation Inc., Kingston, WA, USA, <sup>5</sup>Pohang University of Science and Technology, Pohang, Korea, <sup>6</sup>Ulsan National Institute of Science and Technology, Ulsan, Korea  
ypark@pppl.gov

### Abstract:

High normalized beta plasma operation in KSTAR was limited by onset of resistive tearing mode instabilities. To accurately examine stability of these plasmas, high fidelity kinetic equilibrium reconstructions have been developed. The present kinetic equilibrium reconstructions include Thomson scattering and charge exchange spectroscopy data, and allowance for fast particle pressure. In addition, up to 25 channels of motional Stark effect data are used to produce reliable evaluation of the safety factor,  $q$ , profile. The reconstructed high beta equilibria can exhibit significant variation of the reconstructed  $q$ -profile dependent upon the broadness of the bootstrap current profile as computed by TRANSP analysis. The stability of the observed  $m/n = 2/1$  tearing mode is computed by using the resistive DCON code and by the M3D-C<sup>1</sup> code with the kinetic EFIT reconstructions as input. For equilibria at high  $\beta_N > 3$ , the tearing stability index,  $\Delta'$ , at the  $q = 2$  surface is more unstable compared to that of equilibria at reduced  $\beta_N$ , indicating that stabilizing neoclassical components of tearing stability may need to be invoked to produce consistency with experiment. MISK code analysis which examines global MHD stability modified by kinetic effects shows significant passive kinetic stabilization of the RWM. In preparation for plasma operation at higher beta utilizing the second NBI system now being installed, three sets of magnetic field sensors will be used for RWM active feedback control. To accurately determine the dominant  $n$ -component produced by unstable RWMs, an algorithm has been developed that includes magnetic sensor compensation of the prompt applied field and the field from the induced current on the passive conductors. Developed mode identification using the compensated magnetic measurements well measures the toroidal phase of a slowing rotating  $n = 1$  MHD mode. This analysis on stability, transport, and control provides the required foundation for disruption prediction and avoidance research on KSTAR.

### Keywords:

MHD, magnetohydrodynamics, plasma instability, resistive wall mode, RWM, tearing mode, NTM, KSTAR, plasma control, disruption

## Rotation and LH transition studies under resonant and non-resonant non-axisymmetric magnetic fields in KSTAR\*

고(Ko)원하(Won-Ha)\*<sup>1</sup>, 인용균<sup>1, 2</sup>, 한현선<sup>1</sup>, 전준우<sup>1</sup>, 김현석<sup>1</sup>, 이종하<sup>1</sup>, 이형호<sup>1</sup>, 설재춘<sup>1</sup>, IDA K.<sup>3</sup>, 전영무<sup>1</sup>, 김재현<sup>1</sup>, 한상희<sup>1</sup>, 윤시우<sup>1</sup>, 오영국<sup>1</sup>, 박현거<sup>2</sup>

<sup>1</sup>국가핵융합연구소 KSTAR연구센터, <sup>2</sup>Ulsan National Institute of Science and Technology, <sup>3</sup>National Institute for Fusion Science  
whko@nfri.re.kr

### Abstract:

The tokamak research has been emphasizing that the plasma rotation plays an important role in determining transport which is related in rotation shear and stability affected by increased rotation [1]. Significantly low H-mode power threshold ( $P_{TH}$ ) has been observed in KSTAR in comparison with other conventional devices. Such a favorable finding is attributable to an order of magnitude lower intrinsic error field ( $\langle \delta B/B_0 \rangle_{m/n=2/1} \sim 1 \times 10^{-5}$  [2]) and toroidal field ripple ( $\delta_{TF}=0.05\%$  [3]), which has been corroborated by high pedestal rotation in KSTAR [1]. Since the L-H power threshold is known to be greatly affected by non-axisymmetric fields from numerous studies, a systematic scan has been conducted with the most influence non-axisymmetric components,  $n=1$  and  $n=2$ . Non-axisymmetric fields influence on L-H power threshold is consistent with other studies, suggesting the importance of low order intrinsic error field in future machine. Benefits of low non-axisymmetric fields on  $P_{TH}$  are confirmed in both KSTAR and DIII-D [4]. The H-mode power threshold study is very important to determine the power requirements for future devices and especially, the dependence between H-mode power threshold and non-axisymmetric field or intrinsic error field is significant in development of future machine.

\*This work was supported by the Korean Ministry of Science, ICT and Future Planning of Republic of Korea.

[1] W.H. Ko, *et. al*, Nucl. Fusion 55 083013 (2015).

[2] Y. In *et al*, Nucl. Fusion 55 043004 (2015).

[3] S.W. Yoon *et al*, IAEA-FEC (2014).

[4] P. Gohil, *et. al*, Nucl. Fusion 51 103020 (2011).

### Keywords:

Rotation, LH transition, non-axisymmetric magnetic fields

## SUSY Searches in Vector Boson Fusion Topology and mu+VBF Trigger Performance in CMS

김민석\*<sup>1</sup>, 김동희<sup>1</sup>  
<sup>1</sup>경북대학교 물리학과  
minsuk@cern.ch

### Abstract:

A review of results in SUSY searches in VBF topology is presented. A 13 TeV projection of these searches is performed with a report on the VBF+mu trigger performance using 2017 data collected by the CMS experiment.

### Keywords:

SUSY, VBF Topology, Trigger Performance, CMS

## LSP baryogenesis and neutron-antineutron oscillations from R-parity violation

CALIBBI Lorenzo<sup>1</sup>, 전응진<sup>1</sup>, 신창섭\*<sup>1</sup>  
<sup>1</sup>기초과학연구원 순수물리이론연구단  
csshin@ibs.re.kr

### Abstract:

R-parity and baryon number violating operators can be allowed in the Supersymmetric Standard Model and thus lead to interesting baryon number violating processes such as n-n oscillations and baryogenesis of the Universe via the decay of the lightest supersymmetric particle (LSP). Adopting the LSP baryogenesis mechanism realized by the late decay of the axino, we identify a single coupling  $\lambda''_{313}$  as a common origin for the matter-antimatter asymmetry of the Universe as well as potentially observable n-n oscillation rates. From this, rather strong constraints on the supersymmetry breaking masses and the axion decay constant are obtained. The favoured parameter space of  $\lambda''_{313} \sim 0.1$  and sub-TeV masses for the relevant sparticles is readily accessible by the current and future LHC searches.

### Keywords:

baryogenesis, axion, supersymmetry

## Common exotic decays of top partners

F LACKE, ThomasDieter<sup>\*1</sup>

<sup>1</sup>IBS CTPU

tom.flacke@gmail.com

### Abstract:

Many Standard Model extensions that address the hierarchy problem contain Dirac-fermion partners of the top quark, which are typically expected around the TeV scale. Searches for these vector-like quarks mostly focus on their decay into electroweak gauge bosons and Higgs plus a standard model quark. In this article, backed by models of composite Higgs, we propose a set of simplified scenarios that include more exotic decay channels, which modify the search strategies and affect the bounds. Analysing several classes of underlying models, we show that exotic decays are the norm and commonly appear with large rates. All of these models contain light new scalars that couple to top partners with charge  $5/3$ ,  $2/3$ , and  $-1/3$ . We identify the contributing particle content and novel top partner decays that occur most commonly, provide effective Lagrangians, benchmarks, and a brief discussion of phenomenological bounds and newly occurring final states. In the second part of the article, we provide details on the underlying models and underlying parameters which yield the benchmark points used in our phenomenological discussion.

### Keywords:

Beyond the Standard Model, Collider Phenomenology, Vectorlike Quarks, Composite Higgs Models

## Search for Charged Higgs Boson Decaying to W Boson and Pseudo-scalar Higgs Boson at 13TeV using CMS Detector

변지환<sup>1</sup>, 유금봉<sup>1</sup>, 양운기\*<sup>1</sup>

<sup>1</sup>서울대학교 물리학과  
ukyang@snu.ac.kr

### Abstract:

A search for charged Higgs boson decaying to W boson and pseudo-scalar Higgs boson is presented. The search is based on the dataset of proton-proton collision at center of mass energy 13TeV collected with CMS detector at LHC in 2016, where corresponding integrated luminosity is 35.9/fb. In the search trilepton events including at least 2 muons with opposite charge are used, and charged Higgs boson's mass from 100 to 160GeV, pseudo-scalar Higgs boson's mass from 15 to 35GeV is investigated.

### Keywords:

Charged Higgs, Pseudo-scalar Higgs, Top, CMS, LHC

## Search for flavor-changing neutral current interaction of the top quark and the higgs boson decaying into $b\bar{b}$ using deep learning method at $\sqrt{s} = 13$ TeV

박지원\*<sup>1</sup>, 김태경<sup>1</sup>, 고정환<sup>2</sup>, 안서현<sup>1</sup>  
<sup>1</sup>한양대학교 물리학과, <sup>2</sup>경희대학교 물리학과  
minerva1993@gmail.com

### Abstract:

In this presentation, the results of searching for Higgs-mediated flavor-changing neutral current of top decay modes are presented. In 2017, Large Hadron Collider (LHC) has accumulated proton-proton collision data corresponding to an integrated luminosity of  $41.3 \text{ fb}^{-1}$  at a center-of-mass energy of 13 TeV with the CMS detector. Using this dataset, the search is performed with the events of the final state of one lepton, 4 jets and two b jets. Several machine learning methods are used to improve discrimination power between signal and background.

### Keywords:

top quark, higgs boson, flavor-changing neutral current, fcnc

## Higgs inflation and commodity phase transition with N scalar in the post-Higgs era

BIAN Ligong\*<sup>1</sup>, CHENG Wei<sup>2</sup>

<sup>1</sup>Department of Physics, Chongqing University, <sup>2</sup>Department of Physics, Chung-Ang University  
ligongbian86@cau.ac.kr

### Abstract:

We studied the Higgs inflation with the N-scalar extended standard model of particle physics (SM). The O(N) symmetry preserved by the N-scalar can be spontaneously broken to O(N-1) with remnant N-1 Goldstones, which gains masses through non-perturbative gravity effects and can contribute to dark radiations. The number of N is strictly bounded by the current Higgs precisions and electroweak precision observables. The mixing of extra heavy Higgs with the SM Higgs confronts with severely constraints from LHC, especially CEPC, ILC, FCC-ee. The cosmological phase transition has been investigated in the Higgs inflation feasible parameter spaces, where the phase transition type can be strongly ordered through one-step or two-step paths.

### Keywords:

Higgs inflation, O(N) symmetry, cosmological phase transition, Higgs precision

## Search for high-mass resonances in dilepton final state using 13 TeV data collected by the CMS detector in 2016 and first look on 2017 performance

오민석\*<sup>1</sup>, 유휘동\*<sup>1</sup>

<sup>1</sup>서울대학교 물리학과

khaosmos93@gmail.com, hdyoo@cern.ch

### Abstract:

A search for new high-mass resonances decaying into electron or muon pairs is performed using full data obtained from 2016 proton-proton collisions at 13 TeV. The search exploits data collected by the CMS experiment at a center-of-mass energy of 13 TeV, corresponding to an integrated luminosity of 36 /fb. No significant deviations are observed from the Standard-model expectation. Upper limits on the product of a new resonance production cross section and branching fraction to dileptons are calculated in a model-independent manner. A lower mass limit is set at 95% confidence level for new spin-1 resonance arising in the sequential standard model, superstring-inspired model and spin-2 Kaluza-Klein graviton arising in the Randall-Sundrum model of extra dimensions. Also first look on the 2017 lepton channel performance is presented.

### Keywords:

CERN, LHC, CMS, New Physics, BSM, Zprime

## Search for Heavy Majorana Neutrinos in the Events with Same-Sign Lepton Pairs and Jets Using the CMS Detector in pp Collisions at $\sqrt{s} = 13$ TeV

양운기\*<sup>1</sup>, 김재성\*<sup>1</sup>, 전시현<sup>1</sup>, 오성빈<sup>1</sup>, 알몬드존<sup>1</sup>

<sup>1</sup>서울대학교 물리학과

ukyung@snu.ac.kr, jskim@cern.ch

### Abstract:

We present searches on Heavy Majorana neutrinos in the events with same-sign lepton pairs and jets, using the pp collision data collected from CMS detector at the centre-of-mass energy 13 TeV. The search range is extended to 20 GeV and 1500 GeV, lower and upper bound respectively, compared to the previous analysis using 8 TeV data. Vector boson fusion production channel is considered as well as s-channel, which improves the sensitivities for mass above several hundreds of GeV. We set upper limits on muon mixing squared, electron mixing squared, and muon-electron cross mixing.

### Keywords:

LHC, CMS, neutrino, Heavy Neutrino

## Top quark pair differential cross sections at 13 TeV in CMS

ROH YounJung\*<sup>1</sup>

<sup>1</sup>고려대학교 물리학과  
kuyoun@korea.ac.kr

### Abstract:

Differential measurements of top quark pair production cross sections are presented using data collected by CMS at 13 TeV. The differential cross sections are measured as a function of various kinematic observables. The  $t\bar{t}$  measurements are extended to the TeV range using jet substructure techniques to exploit the boosted regime. The multiplicity and kinematic distributions of the jets produced in addition to the top quark pair are also investigated. The results are confronted with precise theory calculations.

### Keywords:

Top quark, CMS, Differential cross section

## Entanglement Entropy for Open Bosonic Strings on Dp-branes

이태진\*<sup>1</sup>

<sup>1</sup>강원대학교 물리학과  
taejin@kangwon.ac.kr

### Abstract:

Choosing one of the spatial coordinates which are tangential to the hyperplane on which Dp-branes are located, we divide the hyperplane into two halves. By using the string wave function in the Fock space representation, we evaluate the entanglement entropy.

### Keywords:

entanglement entropy, bosonic string, D-branes, string field theory

## 6d strings and exceptional instantons

LEE Ki-Hong<sup>\*3</sup>, KIM Seok<sup>\*3</sup>, KIM Hee-Cheol<sup>\*1</sup>, KIM Joonho<sup>\*2</sup>, PARK Jaemo<sup>\*1</sup>

<sup>1</sup>Department of Physics, Postech, Pohang 790-784, Korea, <sup>2</sup>School of Physics, Korea Institute for Advanced Study, Seoul 130-722, Korea, <sup>3</sup>Department of Physics and Astronomy & Center for Theoretical Physics, Seoul National University, Seoul 151-747, Korea  
khlee11812@gmail.com, skim@phya.snu.ac.kr, heecheol1@gmail.com, joonhokim@kias.re.kr, jaemo@postech.ac.kr

### Abstract:

We propose new ADHM-like methods to compute the Coulomb branch instanton partition functions of 5d and 6d supersymmetric gauge theories, with certain exceptional gauge groups or exceptional matters. We study G2 theories with  $n_7 \leq 3$  matters in 7, and SO(7) theories with  $n_8 \leq 4$  matters in the spinor representation 8. We also study the elliptic genera of self-dual instanton strings of 6d SCFTs with exceptional gauge groups or matters, including all non-Higgsable atomic SCFTs with rank 2 or 3 tensor branches. Some of them are tested with topological vertex calculus. We also explore a D-branebased method to study instanton particles of 5d SO(7) and SO(8) gauge theories with matters in spinor representations, which further tests our ADHM-like proposals.

### Keywords:

Brane Dynamics in Gauge Theories, Instantons, Field Theories in Higher Dimensions,

## Gravity from Entanglement and RG Flow in a Top-down Approach

권오갑\*<sup>1</sup>, 장동민<sup>1</sup>, 김윤배\*<sup>1</sup>, TOLLA Driba<sup>1</sup>  
<sup>1</sup>성균관대학교 물리학과  
okabkwon@gmail.com, yoonbai@skku.edu

### Abstract:

We have tested the duality between the mass-deformed ABJM theory and asymptotically AdS<sub>4</sub> gravity theory, which is obtained from the Kaluza-Klein (KK) reduction of the 11-dimensional supergravity on the LLM geometry. In this talk, we extend the KK reduction procedure beyond the linear order and establish non-trivial KK maps between 4-dimensional fields and 11-dimensional fluctuations. We rely on this gauge/gravity duality to calculate the entanglement entropy by using the Ryu-Takayanagi holographic formula and the path integral method developed by Faulkner. We show that the entanglement entropies obtained using these two methods agree when the asymptotically AdS<sub>4</sub> metric satisfies the linearized Einstein equation with nonvanishing stress-energy tensor for two scalar fields.

### Keywords:

Entanglement entropy, Einstein equation, LLM geometry

## Holographic Entanglement Entropy with Momentum Relaxation

김경규\*<sup>1</sup>, 박찬용<sup>2, 3</sup>, 이정훈<sup>2</sup>, 안병준<sup>4</sup>

<sup>1</sup>세종대학교 물리학천문학과, <sup>2</sup>아시아태평양 이론물리센터, <sup>3</sup>포항공과대학교 물리학과, <sup>4</sup>연세대학교 물리학과  
kimkyungkiu@gmail.com

### Abstract:

We study the holographic entanglement entropy for the strip and sharp wedge entangling regions in momentum relaxation systems. In the case of strips, we found analytic and numerical results for the entanglement entropy and showed the effect on the minimal surface by the electric field. We also studied the entanglement entropy of wedges and we confirmed that there is a linear change in the electric field. This change is proportional to the thermoelectric coefficient that can be measured.

### Keywords:

holographic entanglement entropy, momentum relaxation, electric field

## Black hole complementarity with the generalized uncertainty principle in Gravity's Rainbow

엄화진\*<sup>1</sup>, 김원태<sup>1</sup>, 김용완<sup>1</sup>

<sup>1</sup>서강대학교 물리학과  
um16@sogang.ac.kr

### Abstract:

When gravitation is combined with quantum theory, the Heisenberg uncertainty principle could be extended to the generalized uncertainty principle accompanying a minimal length. To see how the generalized uncertainty principle works in the context of black hole complementarity, we calculate the required energy to duplicate information for the Schwarzschild black hole. It shows that the duplication of information is not allowed and black hole complementarity is still valid even assuming the generalized uncertainty principle. On the other hand, the generalized uncertainty principle with the minimal length could lead to a modification of the conventional dispersion relation in light of Gravity's Rainbow, where the minimal length is also invariant as well as the speed of light. Revisiting the gedanken experiment, we show that the no-cloning theorem for black hole complementarity can be made valid in the regime of Gravity's Rainbow on a certain combination of parameters.

### Keywords:

modified gravity, quantum black holes

## Modified Wightman function and Unruh effect on generic models in nonlocal field theory

GIM Yongwan\*<sup>1</sup>, UM Hwajin<sup>1</sup>, KIM Wontae<sup>1</sup>

<sup>1</sup>서강대학교 물리학과  
yongwan89@sogang.ac.kr

### Abstract:

We set up a generic nonlocal model having the same set of solutions as the local theory but allowing Lorentz violations. In this model, we calculate the modified Wightman function and the rate of response function. By using the Unruh-DeWitt detector method, it turns out that the Unruh effect should be corrected by the minimal length representing the nonlocality. Additionally, by taking the Lorentz-invariant limit, we show that the Wightman function and the Unruh effect remain the same as the local theory.

### Keywords:

Unruh effect, Wightman function

## Generalized Kerr-Schild Formalism in Double Field Theory and Classical Double Copy

이강훈\*<sup>1</sup>, 박상아<sup>2</sup>

<sup>1</sup>기초과학연구원 순수물리이론 연구단, <sup>2</sup>고등과학원  
kanghoon.lee1@gmail.com

### Abstract:

We present a novel solution generating technic in double field theory and 10-dimensional supergravities by generalizing Kerr-Schild formalism in general relativity. This formalism leads directly the classical double copy, which says that a class of NSNS sector solutions can be represented by a pair of solutions of linearized Yang-Mills theory.

### Keywords:

double field theory, generalized Kerr-Schild metric, classical double copy

## Mott Transition in Holography

서(Seo)윤석(Yunseok)\*<sup>1</sup>, 신(Sin)상진(Sang-Jin)<sup>2</sup>, 송(Song)근호(Geunho)<sup>2</sup>, Qi Yong-Hui<sup>2</sup>  
<sup>1</sup>광주과학기술원 GIST 대학, <sup>2</sup>한양대학교  
yseo@gist.ac.kr

### Abstract:

We investigate emergence of Fermi liquidity and gap generation in strongly interacting fermion system by using gauge gravity duality. We introduce bulk fermion mass and dipole interaction term in 4 dimensional AdS space-time and calculate fermion Green's function. We find there are many interesting phases which contains Fermi liquid, bad metal, semi-metal and gapped feature. We also find there are competition between fermi liquidity and gap generation by tuning bulk mass and dipole interaction term. We propose 'Holographic Hubbard model' in terms of phases and parameters.

### Keywords:

Holography, Spectral density, Mott transition, Psuedo-gap, strongly correlated system.

## Holographic Hubbard Model

신상진\*<sup>1</sup>, 서윤석<sup>2</sup>, Qi Yonghui<sup>1</sup>, 송근호<sup>1</sup>  
<sup>1</sup>한양대학교 물리학과, <sup>2</sup>광주과학기술원  
sangjin.sin@gmail.com

### Abstract:

Starting from a canonical holographic model of a probe fermion with bulk mass and a dipole interaction, we study the phases of holographic fermion as function of dipole coupling  $p$  and the Dirac bulk mass  $m$ . If we consider a specific embedding in the phase diagram, we can get the corresponding mapping of an Hubbard model into a holographic model, which defines a "holographic Hubbard model". This model will be useful for the interpretation of some experiments.

### Keywords:

Holography, Spectral density, Hubbard Model, Phase diagram

## 랩걸 in Korea

황정아\*<sup>1</sup>

<sup>1</sup>한국천문연구원  
sungbin@kaist.ac.kr

### Abstract:

2017년 1월 호프 자렌의 『랩걸: 나무, 과학 그리고 사랑』이 한국에 출판되면서 현재까지 과학 분야 베스트셀러 책이 되고 있다. 미국의 한 여성과학자의 자전적 에세이에 한국을 포함한 전 세계 사람들이 이토록 공감한 이유는 무엇이였을까. 이 책을 읽고 한국의 여성과학자들이 처해 있는 상황과 미국의 여성과학자들이 처한 현실이 크게 다르지 않음을 깨닫는다. 수많은 장애물에도 불구하고 어려움을 견디고 성장해서 큰 나무와 같은 과학자가 된 주인공의 과학과 삶을 대하는 태도에서 오늘날을 살아가는 많은 과학자와 과학을 공부하고 있는 학생들에게 시사하는 바가 크다. 무엇보다 '알쓸신잡2' 마지막 회에서 유시민 작가가 딸에게 추천하고 싶은 책으로 이 책을 언급하면서 일반인들에게도 많이 회자되고 있어서, 본 발표에서는 이 책의 내용을 다시 한 번 되새겨 보고자 한다.

### Keywords:

여성, 과학자

## 변화무쌍한 네트워크, 뇌

송민령\*<sup>1</sup>

<sup>1</sup>한국과학기술원  
sungbin@kaist.ac.kr

### Abstract:

뇌는 동물의 내적 상태와 주변 상황을 예측하여 적절한 움직임을 만들어냅니다. 예측하는 기계인 뇌의 중요한 특징 중 하나는 가소성입니다. 가소성이란 경험과 환경에 따라 구조와 기능이 유연하게 변하는 성질을 뜻합니다. 뇌는 주변 상황에 적응하며 평생토록 변해갑니다. 뇌의 또다른 두드러진 특징은 뇌가 신경세포들의 네트워크라는 점입니다. 뇌가 네트워크라는 사실은 오랫동안 당연하게 여겨져 왔지만, 뇌가 어떤 네트워크인지, 네트워크로서 뇌가 어떻게 동작하는지에 대해서는 최근에야 활발한 연구가 이뤄지고 있습니다. 뇌의 가소성과 네트워크로서의 특징이 어떻게 예측에 기여하는지, 이 이해가 인간에 대한 생각을 어떻게 바꿔가고 있는지 이야기해 보고자 합니다.

### Keywords:

뇌, 네트워크

## 빅뱅의 메아리 - 우주배경복사

이강환\*<sup>1</sup>

<sup>1</sup>서대문자연사박물관  
sungbin@kaist.ac.kr

### Abstract:

우주배경복사는 빅뱅 38만년 후에 우주 전체에 고루 퍼진 빛이다. 우주배경복사는 초기 우주의 흔적을 고스란히 담고 있기 때문에 우주의 역사를 연구하는데 매우 중요한 자료가 되고 있다. 우주배경복사를 발견하고 연구해 온 과정은 우주론이 발전해온 역사와 궤를 같이하고 있다. 우주배경복사는 빅뱅 우주론의 가장 강력한 근거일 뿐만 아니라 현재 우리가 알고 있는 우주의 물리량을 가장 정밀하게 구할 수 있는 자료가 되기도 한다. 그래서 우주배경복사만을 관측하기 위해 발사한 우주망원경만 해도 3대나 된다. 우주론의 역사 속에서 우주배경복사의 발견과 연구가 어떤 역할을 했는지, 우주배경복사에서 어떻게 우주의 물리량을 계산해내는지 살펴본다.

### Keywords:

우주, 배경복사, 빅뱅

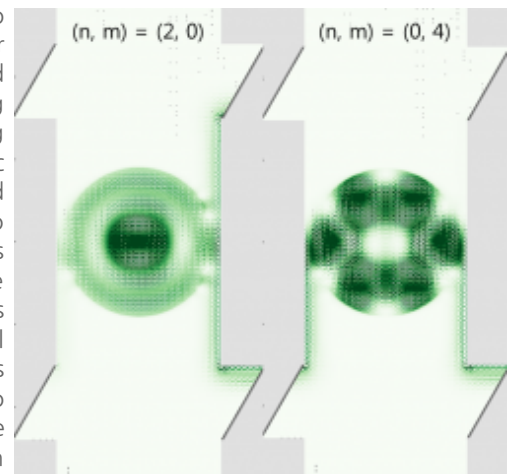
## Imaging of Fano Resonances in a Magnetic Quantum Dot in Graphene

명노준\*<sup>1</sup>

<sup>1</sup>조선대학교 물리교육과  
nmyoung@chosun.ac.kr

### Abstract:

In graphene, localization of Dirac fermions has been a challenging topic to manipulate their transport carrying charges, spins, or valleys both for potential applications and fundamental interests. With the bad confinement of Dirac fermion due to Klein tunneling, using inhomogeneous magnetic fields is one significant candidate for controlling Dirac fermion transport. Although the magnetic confinement of Dirac fermions in graphene has been believed to be a successful, it has gained relatively less attention from researchers because of the difficulty to demonstrate the magnetically localized states in practice. Therefore, in this study, we theoretically obtain imaging of the localized states in the magnetic quantum dot in graphene. We investigate how Dirac fermions propagate through the magnetic quantum dot, when a quantum Hall edge channel is strongly coupled to the magnetic quantum dot; in this case, Fano resonances are observed in the conductance spectra. At Fano resonances, current density clearly exhibits a regular profile inside the magnetic quantum dot, which corresponds to eigenfunction distribution for the analytic solutions.



### Keywords:

Graphene, Fano Resonance, Quantum Hall Effect

## Designing defect-based qubit candidates in wide-gap binary semiconductors

서호성\*<sup>1, 2, 3</sup>, MA He<sup>4</sup>, GOVONI Marco<sup>2, 3</sup>, GALLI Giulia<sup>2, 3</sup>

<sup>1</sup>Department of Physics, Ajou University, Suwon, Korea, <sup>2</sup>Institute for Molecular Engineering, University of Chicago, Chicago, IL, USA, <sup>3</sup>Materials Science Division, Argonne National Laboratory, Lemont, IL, USA, <sup>4</sup>Chemistry Department, University of Chicago, Chicago, IL, USA  
hseo2017@ajou.ac.kr

### Abstract:

The development of novel quantum bits is key to extend the scope of solid-state quantum information science and technology. Here, using first-principles calculations, we propose that large metal ion - vacancy complexes are promising qubit candidates in two binary crystals: 4H-SiC and w-AlN. In particular, we found that the formation of neutral Hf- and Zr-vacancy complexes is energetically favorable in both solids; these defects have spin-triplet ground states, with electronic structures similar to those of the diamond NV center and the SiC di-vacancy. Interestingly, they exhibit different spin-strain coupling characteristics, and the nature of heavy metal ions may allow for easy defect implantation in desired lattice locations and ensure stability against defect diffusion. In order to support the future experimental identification of the proposed defects, we report predictions of their optical zero-phonon line, zero-field splitting, and hyperfine parameters. The defect design concept identified here may be generalized to other binary semiconductors to facilitate the exploration of new solid-state qubits.

### Keywords:

Solid-state quantum bits, Diamond NV center, Wide-gap semiconductors, Defect-based qubits

## Detection of Electron Arrival Time by a Dynamical Barrier

박완기\*<sup>1</sup>, 류성근<sup>1</sup>, 심흥선<sup>1</sup>

<sup>1</sup>한국과학기술원 물리학과  
wanki@kaist.ac.kr

### Abstract:

There are recent investigations of detecting the arrival time distribution of a single-electron wave packet by measuring electron current through a time-dependent potential barrier. But how fast the barrier should rise is not fully understood. We theoretically investigate an optimal rising speed of the barrier by studying the tunneling of a single-electron wave packet through the dynamical barrier. In this tunneling problem, there are time scales: tunneling time through the barrier, temporal width of the wave packet, and a barrier-opening time during which tunneling is allowed. We find that the competitions among the time scales determine whether the barrier operates properly as an arrival time detector. Our finding suggests an optimal rising time in the arrival time detection.

### Keywords:

mesoscopic physics, electron quantum optics, arrival time detection

## Network microbiomics: roadmap for exploring complex microbial ecosystems inside human body

김판준\*<sup>1</sup>

<sup>1</sup>Hong Kong Baptist University 생물학과  
extutor@gmail.com

### Abstract:

Recent technologies have generated an enormous amount of biological data at various scales. I am interested in providing a computational framework for unraveling the collective behavior of biomolecules, cells, and organisms, aided by systematic analyses of large-scale biological datasets.

Our resident gut microbial community, or gut microbiome, provides us with a variety of biochemical capabilities not encoded in our genes. This human gut microbiome is linked not only to our health, but also to various disorders such as obesity, cancer, and diabetes. We constructed the literature-curated global interaction network of the human gut microbiome mediated by various chemicals. Using our network, we conducted a systematic analysis of the microbiomes in type 2 diabetes patients, and revealed the metabolic infrastructure of the gut ecosystem implicated in disease. Our network framework shows promise for investigating complex microbe-microbe and host-microbe chemical cross-talk, and identifying disease-associated features.

Furthermore, I will discuss my other research areas, in relation to molecular networks inside cells, such as transcriptional regulatory networks for biological rhythms.

### Keywords:

biological networks, systems biology, computational modeling

## The compaction of a polymer surrounded by the crowding particles with size distribution.

김주인\*<sup>1</sup>

<sup>1</sup>공군사관학교 기초과학과  
juinkim75@gmail.com

### Abstract:

A polymer can be compacted by the depletion effect of small particles around it. The polymer will shrink with increasing number density of the small particles(crowders). In the case that the crowding particles have variable sizes(polydisperse case), the polymer size was described as the function of the sum of weighted number density of crowders in which the weight factor is the square of the size of a crowding particle. In this study, we propose an overlap volume of depletion layers of two monomers for a crowder as the weight factor and discuss how to evaluate the overlap volume especially when the interaction between a monomer and a crowder is given as soft potential(Weeks-Chandler-Anderson(WCA) potential) in molecular dynamics simulation.

### Keywords:

polymer, compaction, depletion, crowding, molecular dynamics

## Neutron-proton Pairing Correlations and Deformation for $N = Z$ Nuclei in $pf$ -shell by the deformed BCS and HFB approach

천명기<sup>1</sup>, 하운자\*<sup>1</sup>

<sup>1</sup>승실대학교 물리학과  
eunhasky@hotmail.com

### Abstract:

We investigated neutron-proton pairing correlations effects on the shell evolution of ground state energies by the deformation for  $N = Z$  nuclei in  $pf$ -shell, such as  $^{44}\text{Ti}$ ,  $^{48}\text{Cr}$ ,  $^{52}\text{Fe}$ ,  $^{64}\text{Ge}$ ,  $^{68}\text{Se}$ , and  $^{72}\text{Kr}$ . We started from a simple shell-filling model constructed by a deformed Woods-Saxon potential with  $\beta_2$  deformation, and included pairing correlations in the residual interaction, which give rise to smearing of the Fermi surface revealing interesting evolution of the Fermi energy along the shell evolution. In this work, like-pairing and unlike-pairing correlations decomposed as isoscalar  $T=1$  and isovector  $T=0$  components are explicitly taken into account. Finally, we estimate ground state energies comprising the mean field energy, the pairing energy and the self-energy due to the pairing correlations, in terms of the deformation. The enhanced  $T=0$  pairing interaction gives oblate deformations for  $^{72}\text{Kr}$  and  $^{68}\text{Se}$ , whose feature is different from other  $pf$ -shell  $N=Z$  nuclei considered in this work.

### Keywords:

pairing correlations, BCS

## Probe of nuclear matter density distribution of ${}^6\text{He}$ via proton elastic scattering at 200 A MeV and high momentum transfers

CHEBOTARYOV Sergey<sup>1, 2</sup>, UESAKA Tomohiro<sup>2</sup>, SAKAGUCHI Satoshi<sup>3</sup>, KIM Wooyoung<sup>\*1</sup>

<sup>1</sup>경북대학교 물리학과, <sup>2</sup>RIKEN Nishina Center for Accelerator-Based Science, RIKEN, Saitama 351-0198, Japan, <sup>3</sup>Department of Physics, Kyushu University, Fukuoka 819-0395, Japan  
wooyoung@knu.ac.kr

### Abstract:

Differential cross sections and analyzing powers of  $p$ - ${}^6\text{He}$  elastic scattering were measured in inverse kinematics at the incident energy of 200 A MeV, covering high momentum transfer region of 1.7-2.7  $\text{fm}^{-1}$  at RIKEN, RIBF.

The experimental data was analyzed based on the relativistic impulse approximation (RIA) using IA2 interaction and input density matrix defined based on relativistic mean field (RMF) calculations. Sensitivity of the elastic scattering at low and high momentum transfers to the density distribution has been investigated. The data taken in the high momentum transfer region covered by the present work, shown more than an order of magnitude higher sensitivity to the inner part of  ${}^6\text{He}$  density distribution in comparison to the peripheral part. This feature makes the present data valuable to deduce the inner part of  ${}^6\text{He}$  density. RIA using IA2 interaction and RMF density matrix was applied for the proton elastic scattering data of  ${}^6\text{He}$  to deduce the inner part of its density distribution. Using two phenomenological density models, assuming alpha-like core and two-neutron halo structure of  ${}^6\text{He}$ , the radius of the distribution of the alpha-like core was determined to be 1.87 +/- 0.05 fm. The result is in agreement with the radius of point-proton distribution of  ${}^6\text{He}$  deduced from the charge radius measurement. The obtained results support the assumption that  ${}^6\text{He}$  consists of an alpha-like core and two-neutron halo.

This talk will provide overview of the experimental setup and measurements which were carried out during beamtime along with analysis of the data taken in this experiment. The deduced differential cross-section of  $p$ - ${}^6\text{He}$  elastic scattering at 200 A MeV will be presented. Results of theoretical analysis to investigate distinguishing features of the obtained differential cross sections using RIA framework will be briefly explained.

${}^6\text{He}$

### Keywords:

${}^6\text{He}$ , proton elastic scattering, nuclear matter density

## DD $\sigma$ and D\*D\* $\sigma$ coupling constants

김희진<sup>1</sup>, 김현철<sup>\*1, 2</sup>

<sup>1</sup>Department of Physics, Inha University, Incheon 22212, Republic of Korea, <sup>2</sup>School of Physics, Korea Institute for Advanced Study (KIAS), Seoul 02455, Republic of Korea  
hchkim@inha.ac.kr

### Abstract:

In this talk, we present a recent investigation on the DD $\sigma$  and D\*D\* $\sigma$  coupling constants derived by the dispersion theoretical approach. We first calculate the  $D\bar{D} \rightarrow \pi\pi$  and  $D^*\bar{D}^* \rightarrow \pi\pi$  amplitudes in the pseudo-physical region. We combine them with the  $2\pi$  amplitudes. Constructing the  $D\bar{D}$  and  $D^*\bar{D}^*$  amplitudes by means of two-body unitarity, we obtain the spectral functions of  $D\bar{D}$  and  $D^*\bar{D}^*$ . In order to obtain the DD $\sigma$  and D\*D\* $\sigma$  coupling constants, we approximate the amplitudes as the zero-width distribution functions. We discuss the results.

### Keywords:

Heavy meson

## Electromagnetic properties of the lowest-lying singly heavy baryons in a mean-field approach

김준영<sup>1</sup>, 김현철\*<sup>1</sup>  
<sup>1</sup>인하대학교 물리학과  
hchkim@inha.ac.kr

### Abstract:

When one takes the limit of the infinitely heavy-quark mass, a singly heavy baryon can be regarded as  $N_c - 1$  valence quarks bound by the meson mean fields that are produced by the valence quarks self-consistently. In this limit a heavy quark is merely considered to be a static color source. This approach was successful in describing the mass splitting of the lowest-lying singly heavy baryons.

In this talk, we present recent results of the electromagnetic form factors of the heavy baryons within this mean-field approach. Since the heavy quark inside a heavy baryon is regarded as a static color source, we assume that it is a point-like particle.

It implies that the heavy quark provides a constant contribution to the electric form factors. On the other hand, the  $Q^2$  dependence is governed by the soliton with light-quark pair. In the limit of  $m_Q \rightarrow \infty$ , the heavy quark does not affect the magnetic form factors of heavy baryons.

We discuss the results of the electric charge and magnetic densities, and the electromagnetic form factors. We find that the positive-charged heavy baryons are rather compact objects in comparison with the proton.

### Keywords:

Heavy baryons, electromagnetic form factors, pion mean fields, chiral quark-soliton model

## magnetic moments of singly heavy baryons

김현철\*<sup>1</sup>, 양길석<sup>2</sup>

<sup>1</sup>인하대학교 물리학과, <sup>2</sup>승실대학교 물리학과  
hchkim@inha.ac.kr

### Abstract:

In the limit of the infinitely heavy baryon mass, a singly heavy baryon can be viewed as a bound state of valence  $N_C - 1$  quarks in a mean-field approach. The presence of the  $N_C - 1$  valence quarks will polarize the Dirac sea, which creates the meson mean fields self-consistently, and the  $N_C - 1$  valence quarks are bound by the mean fields. This approach is called the chiral quark-soliton model and has a certain merit, since we can use all dynamical parameters fixed in the light-baryon sector to study also the heavy baryon properties. In the present talk, we present a recent investigation on the magnetic moments of the heavy baryon within the chiral quark-soliton model. The magnetic moments of the baryon sextet are derived. We determine those of the baryon sextet (both spin 1/2 and 3/2). We find that the numerical results of the magnetic moments of the baryon sextet with spin 3/2 are just 3/2 larger than those with spin 1/2. The magnetic moments of the bottom baryons are the same as those of the corresponding charmed baryons.

### Keywords:

magnetic moments of heavy baryons, meson mean fields, chiral quark-soliton model

## Search for a New $\Lambda$ Resonance with the HypTPC

양성배\*<sup>1</sup>

<sup>1</sup>고려대학교, 물리학과  
sbyang@rcnp.osaka-u.ac.jp

### Abstract:

일반적인 쿼크 모델로 설명되지 않는 새로운 람다 강입자의 실마리를 Belle 그룹과 Crystall Ball 그룹의 실험 결과에서 찾을 수 있다. Belle 실험 결과 중  $\Lambda_c^+ \rightarrow pK^+\pi^+$  붕괴 Dalitz 도표 분석에서 질량  $\sim 1.665 \text{ GeV}/c^2$  이며 얇은 두께를 가지는 공명픽을  $pK^-$ 의 불변질량 분포에서 발견 하였다 [1]. 또한 Crystall Ball 그룹의  $pK^- \rightarrow \Lambda n$  작용 반응각 분포에서 스핀 3/2인 새로운 강입자의 흔적을 이 질량 근처에서 볼 수 있다 [2-4]. 만약 두개의 독립적인 실험 결과가 같은 강입자에 의한 것이라면, 질량  $\sim 1.665 \text{ GeV}/c^2$  이며 얇은 두께와 스핀 3/2 값을 가지는 새로운 람다 강입자가 존재한다.

이 새로운 람다 강입자( $\Lambda^*$ )의 탐색이 일본 J-PARC 하드론 연구 시설에서 계획 중이다 (J-PARC P72 [5]). 액체 수소 타겟을 이용한  $pK^- \rightarrow \Lambda n$  작용을 통해  $\Lambda^*$ 의 존재를 확인하고 스핀과 페리티 등의 특징도 결정할 수 있다. 이 실험은 'H-dibaryon 탐색 (J-PARC E42 [6])'과 같이 Hyperon Time Projection Chamber (HypTPC)를 사용하는 실험들 중 하나이다. 이 실험에서 HypTPC는 p와  $\pi^-$ 로 붕괴된  $\Lambda$ 를 재구성하기 위하여 사용된다.

이 새로운 람다 강입자가 일반적인 쿼크 모델로는 설명되지 않는다는 것을 고려할 때, 이 실험을 통해 강입자에 대한 기존의 이해를 크게 바꿔 줄 것이다. 이 새로운 강입자의 실마리와 실험 준비 상황에 대한 토의가 있을 것이다.

[1] S.B. Yang et al. (Belle Collaboration), Phys. Rev. Lett. 117, 011801 (2016).

[2] A. Starostin et al. (Crystal Ball Collaboration), Phys. Rev. C 64, 055205 (2001).

[3] Bo-Chao Liu and Ju-Jun Xie, Phys. Rev. C 85, 038201 (2012).

[4] H. Kamano et al., Phys. Rev. C 92, 025205 (2015).

[5] K. Tanida et al., J-PARC P72 Proposal ('Search for a Narrow  $\Lambda^*$  Resonance using the  $p(K^-, \Lambda)n$  Reaction with the hypTPC Detector').

[6] J.K. Ahn, JPS Conf. Proc., 031004 (2017).

### Keywords:

J-PARC, Hadron, HypTPC

## Tribaryon configurations and the inevitable three nucleon repulsions at short distance

이수형\*<sup>1</sup>, 박아론<sup>1</sup>, 박우성<sup>1</sup>  
<sup>1</sup>연세대학교 물리학과  
suhoung@yonsei.ac.kr

### Abstract:

We decompose the tribaryon in terms of SU(3) flavor and spin state and analyze their color-spin-flavor wave function following Pauli principle. By comparing the color-color and color-spin interactions of compact tribaryon configuration against the lowest three nucleon threshold within a constituent quark model, we show that the three nucleon forces have to be repulsive at short distance for all possible quantum numbers and all values of the SU(3) symmetry breaking parameter. Our work identifies the origin of the repulsive nuclear three body forces including the hyperons at short distance that are called for from phenomenological considerations starting from nuclear matter to the maximum mass of a neutron star.

### Keywords:

tribaryon, constituent quark model

## Tetraquark mixing framework for light mesons and the role of spin-1 diquarks

김흥중\*<sup>1</sup>

<sup>1</sup>한국항공대학교 기초학문연구소  
hungchong@kau.ac.kr

### Abstract:

We propose a tetraquark mixing framework for light mesons with  $J^P = 0^+$  in the diquark-antidiquark model using two spin configurations,  $|J, J_{12}, J_{34}\rangle = |000\rangle, |011\rangle$ , where  $J$  is the spin of the tetraquark,  $J_{12}$  the diquark spin,  $J_{34}$  the antidiquark spin.

The two configurations,  $|000\rangle$  and  $|011\rangle$ , are found to mix strongly through the color-spin interaction and physical states can be identified with certain mixtures of the two configurations which diagonalize the hyperfine masses of the color-spin interaction. This framework is supported by the presence of two nonets in light meson systems,  $f_0(500)$ ,  $f_0(980)$ ,  $a_0(980)$ ,  $K_0^*(800)$  in light nonet,

and  $f_0(1370)$ ,  $f_0(1500)$ ,  $a_0(1450)$ ,  $K_0^*(1430)$  in heavy nonet.

We report that their mass splittings are qualitatively consistent with the hyperfine mass splittings.

Our tetraquark model also suggests that, due to the relative sign differences in the mixtures, the couplings of fall-apart decays into two pseudoscalar mesons are strongly enhanced for the light nonet while they are suppressed in the heavy nonet. Experimentally, this prediction is tested very well for the decays of the isovector resonances,  $a_0(980)$ ,  $a_0(1450)$ .

### Refs:

1. EPJC (2017) 77:173, H. Kim, M.K.Cheoun, K.S.Kim
2. EPJC (2017) 77:435, K.S. Kim, H.Kim
3. arXiv: 1711.08213, H.Kim, K.S.Kim, M.K.Cheoun, M.Oka

### Keywords:

tetraquarks, color-spin interaction

## Universal physics of two neutrons with one flavored meson

RAHA Udit<sup>2</sup>, KAMIYA Yuki<sup>3</sup>, 안도슌이치<sup>\*1</sup>, HYODO Tetsuo<sup>3</sup>

<sup>1</sup>선문대학교 정보디스플레이학과, <sup>2</sup>Department of Physics, Indian Institute of Technology Guwahati ,

<sup>3</sup>Yukawa Institute for Theoretical Physics, Kyoto University  
shungichi.ando@gmail.com

### Abstract:

We investigate the  $s$ -wave three-body system of two neutrons and one flavored meson with total spin-isospin  $J=0, I=3/2$ . The meson-neutron scattering length can become infinitely large in an unphysical region of the quark mass when extrapolated from strangeness to charm in the so-called zero coupling limit. Using a low-energy cluster effective field theory, we demonstrate that the Efimov effect is manifest in the three-body system when the meson-neutron scattering length is extrapolated to the unitary limit of the two-body interaction. We thereby discuss the consequence of universal physics in the physical  $K^{*}nn$  and  $D^{*0}nn$  systems.

### Keywords:

$K$ - $nn$ ,  $D^{*0}nn$ , universality, unphysical quark mass, unitary limit, zero coupling limit, effective field theory

## High-efficiency perovskite light-emitting diodes and investigation on their photophysical properties

이태우\*<sup>1, 2, 3</sup>, 조힘찬<sup>1, 3</sup>, 김주성<sup>1</sup>, 김영훈<sup>1, 2, 3</sup>, 정수훈<sup>1, 2</sup>, 박민호<sup>1, 2</sup>

<sup>1</sup>서울대학교 재료공학부, <sup>2</sup>서울대학교 신소재공동연구소, <sup>3</sup>서울대학교 BK21플러스 서울대학교 창의인재양성 재료사업단

twlees@snu.ac.kr

### Abstract:

Metal halide perovskites have been used as emission layers in perovskite light-emitting diodes (PeLEDs), and have many advantages such as high charge-carrier mobility, solution processability, high color purity, color tunability and low material cost. However, low electroluminescence (EL) efficiency of PeLEDs at room temperature is a challenge that must be overcome. Here, we present high-efficiency PeLEDs using various strategies to overcome the EL efficiency limitations where the perovskite emission layers are in forms of 3D bulk polycrystalline films and multi-layered (quasi-2D structure) polycrystalline films. First, we introduced a self-organized buffer hole injection layer to reduce the hole injection barrier and prevent luminescence quenching at the interface. High-efficiency methylammonium lead bromide (MAPbBr<sub>3</sub>) and CsPbBr<sub>3</sub> PeLEDs were realized based on the buffer hole injection layer and fine stoichiometry control that prevents the formation of strong luminescence quenchers (metallic Pb atoms). To investigate the origins of luminescence quenching, we observed the temperature dependence of current hysteresis and EL spectrum; current hysteresis occurred at all temperatures and increased exponentially as temperature increased, which can be ascribed to migration of Br<sup>-</sup> anions. The activation energies for EL quenching, blue-shift and linewidth broadening were obtained and the origins of changes were analyzed. Also, we suggest that the efficiency in PeLEDs can be increased by decreasing MAPbBr<sub>3</sub> grain size and consequently improving uniformity and coverage of MAPbBr<sub>3</sub> layers. Using these strategies, high-efficiency PeLEDs were demonstrated (current efficiency = 42.9 cd/A). Furthermore, by unravelling additive-based nanocrystal pinning, EL efficiency limitations were identified and effectively overcome; we achieved the highest external quantum efficiency (8.79%) among pure green organic-inorganic hybrid PeLEDs. Ideally-designed polymeric anode materials further boosted the highest EQE of MAPbBr<sub>3</sub> PeLEDs up to 10.93%. We also developed efficient quasi-2D PeLEDs that incorporate perovskite emission layers with Ruddlesden-Popper phase. The quasi-2D PeLEDs showed higher efficiency and luminance compared to pure 3D and 2D counterparts because of the advantages of quasi-2D perovskites including improved film morphology, exciton confinement and reduced trap density. Electronic disorder of perovskite polycrystalline films were investigated via temperature-dependent optical properties. Temperature-dependent UV-visible absorption measurement revealed that 3D bulk perovskite polycrystalline films fabricated by a single-step spin-coating process have low thermal and structural disorder, which was only up to ~30 meV even at room temperature.

### Keywords:

organic/inorganic hybrid perovskites, alternative emitters, large color gamut, photoluminescence, Ruddlesden-Popper phase

## New Class Semiconducting Materials of Organic - Inorganic Halides

SEO Seongrok<sup>1</sup>, JEONG Seonghwa<sup>1</sup>, SHIN Hyunjung\*<sup>1</sup>

<sup>1</sup>Department of Energy Science, Sungkyunkwan University  
hshin@skku.edu

### Abstract:

CH<sub>3</sub>NH<sub>3</sub>PbI<sub>3</sub> with perovskite crystal structure has attracted considerable interest for high power conversion efficiency. Metal oxide grown *via* ALD provides pinhole-free uniform and dense films which are suited to function as passivation layer since ALD is deposited by self-limiting sequential chemical reaction. ALD chemistry for TiO<sub>2</sub> and ZnO are well known and the process requires relatively low deposition temperature as much as ~ 100 °C, even possible at 50 °C, which is applicable to deposit onto halide perovskite. In this presentation, we report highly efficient perovskite solar cells having a long-term stability that adapts uniform and dense inorganic charge transport layer (NiO and TiO<sub>2</sub> and ZnO) grown by atomic layer deposition (ALD) at relatively low temperature. Ultra-thin un-doped NiO films were prepared by ALD with a highly precise control over the thickness. Thin enough (5 ~ 7.5 nm in thickness) NiO films with the thickness of few times of Debye length (1 ~ 2 nm for NiO) show enough conductivities achieved by overlapping space charge regions, which finally exhibited a highest PCE of 17.40 % with a negligible current-voltage hysteresis. Furthermore, highly dense inorganic electron transport layer (ETL) has been deposited onto perovskite using ALD process at relatively low temperature (100 °C). The devices shows excellent water-resistant properties and long-term stability at 85 °C under illumination compared to devices without ETL grown by ALD.

**Acknowledgments** This work was supported by Korean government through NRF-2017R1A4A1015770 (Basic Research Laboratory Program), NRF-2016M3D1A1027664 (Future Materials Discovery Program), and NRF-2017M3C1B7014335 (STEAM Research Program)

**References** [1] Shin, H., et. al., "Self-formed Grain Boundary Healing Layer for Highly Efficient CH<sub>3</sub>NH<sub>3</sub>PbI<sub>3</sub> Perovskite Solar Cells", *Nature Energy*, 1, 16081 (2016), [2] Shin, H., et. al., "An Ultra-thin, Un-doped NiO Hole Transporting Layer of Highly Efficient (16.4 %) Organic - Inorganic Hybrid Perovskite Solar Cells", *Nanoscale*, 8, 11403 - 11412 (2016), [3] Shin, H., et. al., "Origin of Hysteresis in CH<sub>3</sub>NH<sub>3</sub>PbI<sub>3</sub> Perovskite Thin Films", *Adv. Func. Mater.* 1701924 (2017), [4] Shin, H., et. al., "Preferred-oriented Grains with Low-angle Grain Boundaries in Halides Perovskite Films by Pressure-induced Re-crystallization", accepted for the publication in *Adv. Energy Mater.* (2017)

### Keywords:

Inorganic Halides

## Cesium lead halide perovskites materials for high-efficiency quantum dot light-emitting diodes

KIM Soo Young\*<sup>1</sup>

<sup>1</sup>School of Chemical Engineering and Materials Science, Chung-Ang University  
sooyoungkim@cau.ac.kr

### Abstract:

In this study, Inorganic CsPbX<sub>3</sub> perovskites with compositions including CsPbBr<sub>x</sub>Cl<sub>3-x</sub>, CsPbBr<sub>3</sub>, and CsPbBr<sub>x</sub>I<sub>3-x</sub> were synthesized, and their properties were investigated. Tauc plots calculated from the UV-vis spectra of the materials showed that the band gaps of CsPbBr<sub>x</sub>Cl<sub>3-x</sub>, CsPbBr<sub>3</sub>, and CsPbBr<sub>x</sub>I<sub>3-x</sub> were 2.7, 2.35, and 1.8 eV, respectively. The as-prepared CsPbX<sub>3</sub> nanocrystals (NCs) had a cubic structure and their crystal sizes were around 5-10 nm. The diffraction peak intensity of the (110) plane increased by adding Cl anion and reduced by adding I anion. In contrast, the peak intensity of the (200) plane reduced by the introduction of Cl<sup>-</sup> ions and increased by the introduction of I<sup>-</sup> ions, suggesting that the nature of the halide anions affects the crystal orientation of CsPbX<sub>3</sub> quantum dots. The highest occupied molecular orbital/lowest unoccupied molecular orbital levels of CsPbBr<sub>x</sub>Cl<sub>3-x</sub>, CsPbBr<sub>3</sub>, and CsPbBr<sub>x</sub>I<sub>3-x</sub> calculated from ultraviolet photoemission spectra and UV-vis spectra, were 6.5/3.8, 6.5/4.15, and 6.1/4.3 eV, respectively. The maximum luminance values measured for CsPbBr<sub>x</sub>Cl<sub>3-x</sub>, CsPbBr<sub>3</sub>, and CsPbBr<sub>x</sub>I<sub>3-x</sub>-based LEDs were 15.2, 51.7 and 21.7 cd/m<sup>2</sup>, respectively.

Furthermore, we present a study of the synthesis-temperature dependence of CsPbX<sub>3</sub> perovskite for NCs, using X-ray scattering. To this end, we synthesized CsPbX<sub>3</sub> perovskite NCs at different reaction temperatures in the form of colloids and spin-coated films, and performed small-angle and wide-angle X-ray scattering measurements to characterize the sizes and crystal structures of the NCs and their assembled structures. The synthesis temperature is that of the reaction between Cs-oleate and PbX<sub>2</sub> (X: I, Br, or Cl), and it is the reaction temperature rather than the reaction duration that determines the size of the CsPbX<sub>3</sub> NCs. We also investigated the dependence on the synthesis temperature of the performance of quantum dot LED devices fabricated with these NCs. It is expected that this research provides an overview of the energy levels and crystal structures of CsPbX<sub>3</sub> quantum dots for the design of inorganic perovskite-based LEDs with high luminance and power efficiencies.

### Keywords:

Organo/inorgano hybrid perovskite materials, Light emitting diodes, Energy band diagram, X-ray scattering

## Materials Engineering for Efficient and Stable Halide Perovskite Solar Cells

NOH Jun Hong\*<sup>1, 2</sup>

<sup>1</sup>School of Civil, Environmental and Architectural Engineering, Korea University, <sup>2</sup>Division of Advanced Materials, Korea Research Institute of Chemical Technology  
junhnoh@korea.ac.kr

### Abstract:

The perovskite solar cells have showed unprecedented progress in power conversion efficiency (PCE) reaching 22 % in last several years. This progress is attributed to developments in terms of device architecture, perovskite materials, and fabrication process based on material engineering. In particular, since it is difficult to form a desired perovskite film due to a unique self-assembly crystallization behavior of perovskite crystals, a key factor to achieve the high performance is how to make a high quality perovskite film with compact morphology and low trap density on n(p)-type semiconductor layers. In order to control such material factors of perovskite halide crystal films, we have introduced mediator which retards direct reaction between organic halide and inorganic halide and influences on crystal growth. We demonstrated that dimethyl sulfoxide (DMSO) is an excellent mediator for formation of high-quality halide thin film. The iodide management also was performed using  $I_3^-$  ions to reduce internal trap density in the halide film. In addition to PCE, recently, long-term stability of the perovskite solar cells is big challenge. The stability of PSC is not only related to halide materials themselves but also is dependent on n(p)-type oxide and organic semiconducting layers. In this talk, material engineering of perovskite halides and oxide semiconductors will be introduced for achieving efficient and stable perovskite solar cells by formation of high-quality perovskite halide crystal thin film and novel oxide semiconducting film.

### Keywords:

perovskite, solar cells, formamidinium, hybrid, halide, stability

## InAs nanorods/graphene layers/ZnO nanorods hybrid nanomaterials for broadband light-harvesting device applications

이규철\*<sup>1</sup>, 최영빈<sup>1</sup>, 조장현<sup>2</sup>, 김호성<sup>3</sup>, 박준범<sup>1</sup>, 김희훈<sup>1</sup>, 박준영<sup>1</sup>, 정건욱<sup>1</sup>, 금대명<sup>3</sup>, 송진동<sup>3</sup>, 최원준<sup>3</sup>, 신유리미<sup>4</sup>, 조성래<sup>4</sup>, 김미영<sup>2</sup>

<sup>1</sup>서울대학교 물리천문학부, <sup>2</sup>서울대학교 재료공학부, <sup>3</sup>한국과학기술연구원, <sup>4</sup>울산대학교 물리학과  
gcyi@snu.ac.kr

### Abstract:

Monolithic integration of wide and narrow bandgap semiconductors can broaden the spectral absorption range and improve the performance of light-harvesting devices. Graphene layers have recently been suggested as a universal substrate for the growth of various kinds of semiconductor nanorods, including ZnO, GaN, InAs, and GaAs nanorods. The periodic hexagonal atomic arrangement of graphene can provide various sizes of supercells for the heteroepitaxial growth of various materials with different lattice constants, thereby enabling the monolithic integration of various types of semiconductor nanorods on graphene surfaces. Additionally, Hong *et al.* recently demonstrated that both surfaces of suspended graphene can act as substrates for semiconductor nanorod growth, showing a double heterostructure as found in InAs/graphene/InAs.[1] Here, we suggest a method of monolithically integrating wide and narrow bandgap semiconductor nanorods using graphene layers.

In this work, we report the epitaxial growth of InAs and ZnO nanorods on each surface of graphene layers and our investigation of the chemical composition and crystal structure of these heterostructures using electron microscopy. The suspended graphene layers as substrates were prepared on hole-patterned SiO<sub>2</sub>/Si<sub>3</sub>N<sub>4</sub> membranes. ZnO nanorods were grown vertically on one side of suspended graphene layers by selective-area metal-organic vapor-phase epitaxy and InAs nanorods were grown vertically on the other side by catalyst-free molecular beam epitaxy. Electron microscopy images revealed that the InAs nanorods and ZnO nanorods had grown vertically on each surface of the same graphene layers, forming an InAs nanorods/graphene layers/ZnO nanorods hybrid nanomaterial. Both cross-sectional and plan-view electron microscopy images showed that the InAs nanorods/graphene layers/ZnO nanorods had grown heteroepitaxially without interfacial layers or structural defects. Furthermore, photodetectors were fabricated using these hybrid nanomaterials and their electrical and spectral response characteristics were investigated.

[1] Hong, Y. J., Yang, J. W., Lee, W. H., Ruoff, R. S., Kim, K. S., Fukui, T., *Advanced Materials* 25, 6847–6853 (2013).

### Keywords:

graphene, nanorod, semiconductor, integration, photodetector

## Study on the mechanism of photocurrent generation according to change in surface state condition of $\text{Bi}_2\text{Te}_3$ topological insulator nanowire

박담비<sup>1</sup>, 정광식<sup>1</sup>, 김다정<sup>1</sup>, 맹인희<sup>2</sup>, 강철<sup>2</sup>, 조만호\*<sup>1</sup>

<sup>1</sup>연세대학교 물리학과, <sup>2</sup>고등광기술연구소  
mh.cho@yonsei.ac.kr

### Abstract:

confirm the TI surface state effect, we prepared single-crystal  $\text{Bi}_2\text{Te}_3$  nanowires and Mn-doped  $\text{Bi}_2\text{Te}_3$  nanowires. The photocurrent in nanowires were measured under the illumination of visible (532nm) light. The obtained photoresponsivity of  $\text{Bi}_2\text{Te}_3$  nanowire for visible light is a remarkable improvement, compared to the Mn-doped  $\text{Bi}_2\text{Te}_3$  nanowires. The result indicates that the high-quality crystal structure of nanostructure and the presence of TI surface state effectively contribute to the significant improvement in photocurrent sensitivity. Also, we measured the optical pump-Thz probe spectroscopy to analysis the photocurrent generation mechanism. As a result, it was confirmed that the surface state condition of TI significantly affects the photocurrent generation.

### Keywords:

topological insulator, surface state, photocurrent generation, carrier dynamics

## Blue luminescence of graphene quantum dots from wasted coffee grounds and their application as luminescence materials for noble white LEDs.

홍우태<sup>1</sup>, 박진영<sup>2</sup>, 정종원<sup>2</sup>, 문병기<sup>3</sup>, 양현경\*<sup>1, 2</sup>

<sup>1</sup>부경대학교, LED공학협동과정, <sup>2</sup>부경대학교, 과학기술융합전문대학원, LED융합공학전공, <sup>3</sup>부경대학교, 물리학과  
hkyang@pknu.ac.kr

### Abstract:

Graphene quantum dots (GQDs) exhibit excellent potential to apply in bio-imaging, photo-catalysis and sensors. Nowadays, GQDs have become a considerable candidate as a luminescent materials, due to the quantum confinement effect, cheap prices and low toxicity. To apply the GQDs as luminescent materials, massive production and controllable properties of GQDs are demanded.

In order to control the optical properties, synthesis condition of GQDs is considerable solution. The general synthesis of GQDs is top-down method which is unsuitable for mass production owing to the use of strong acid, oxidizer, and high energy. Recently, hydrothermal method were suggested because of its simplicity, cheap fabrication prices and eco-friendly properties.

In this study, the blue emitting GQDs derived from wasted coffee powder were synthesized by using a hydrothermal process. The wasted coffee powder is favorable candidate due to the high waste quantity and low recycle ratio. Through the carbonization, hydrothermal reduction and cutting of organic component in the wasted coffee powder, the GQDs can be fabricated. of photoluminescence spectra, UV-visible absorption spectra, Fourier transform infrared spectra, transmission electron microscope and Raman spectra of the GQDs were studied to analyze Structural and luminescent properties. Also, white LEDs were fabricated by combining GQDs, phosphors and UV LEDs.

### Keywords:

graphene quantum dot, wasted coffee ground, LED

## Analysis of Hump Characteristics in ReS<sub>2</sub> Field-Effect Transistors

이상욱\*<sup>1</sup>, 최준희<sup>1</sup>, 신종목<sup>2</sup>, 장호균<sup>2</sup>, 김규태<sup>2</sup>  
<sup>1</sup>이화여자대학교, 물리학과, <sup>2</sup>고려대학교, 전기전자전파공학부  
nicesw@gmail.com

### Abstract:

Unlike group VI-TMDs, group VII-TMDs such as the rhenium-based dichalcogenides crystallize in a distorted triclinic structure due to an extra electron in the *d* orbital. Because of this structure, the interlayer coupling is weaker than other TMDs, and as a result, ReS<sub>2</sub> acts as a stack of electronically and vibrationally separated monolayers even in bulk form. Here, we demonstrated electrical characteristics of multilayer ReS<sub>2</sub> FETs with the humps in a subthreshold region. Through the I-V measurements according to the thickness of ReS<sub>2</sub> flakes, it was confirmed that the hump phenomenon was found as the thickness increased. The parallel equivalent circuit modeling of the transistor with the PSPICE simulation was well fitted with the ReS<sub>2</sub> transfer curve.

### Keywords:

ReS<sub>2</sub>, TMDs, 2D materials, Field-Effect Transistors, FETs, Electrical properties

## Gate-tunable photodetector and ambipolar transistor in graphene/semiconductor barristor with ion-gel dielectric

박배호\*<sup>1</sup>, 오광택<sup>1</sup>, 전지훈<sup>1</sup>, 이덕현<sup>1</sup>, 오다에<sup>1</sup>, 김영철<sup>2</sup>, 안영환<sup>2</sup>

<sup>1</sup>건국대학교 물리학과, <sup>2</sup>아주대학교 물리학과  
baehpark@konkuk.ac.kr

### Abstract:

실리콘 기반 반도체 소자 산업에서는 소자의 동작 속도를 높이기 위하여 전자가 움직이는 통로의 폭을 줄이는 미세화 공정이 필수적이다. 그러나 공정이 미세해질수록 전류의 누설이 심해지는 문제점들을 나타내고 있기 때문에, 실리콘 기반 반도체 소자를 대체할 물질이 필요시 되고 있다. 최근 단결정 실리콘보다 100배 이상 전자를 빠르게 이동시킬 수 있고 구리보다 100배 이상 전기가 잘 통하며 늘리거나 구부려도 전기적 성질을 잃지 않는 이차원 원자 결정소재 그래핀이 차세대 소재로 많은 주목을 받고있다. 높은 전기 전도도와 투명성, 유연성 등의 특성으로 인해 그래핀을 전극으로 활용하고자 하는 연구들이 수없이 진행되어 왔다. 그래핀은 밴드갭이 없는 전자구조의 특이성으로 인하여 온/오프 비(on/off ratio)가 작아 트랜지스터 등의 고속 소자를 직접화 하는 데에 있어 어려움을 보이고 있기 때문에, 최근에는 그래핀을 전극의 역할이 아닌 채널 소재로의 연구들이 수 없이 진행되고 있다. 이러한 연구들은 대부분 밴드갭이 없는 그래핀에 도핑, 구조 변화 등의 방법으로 밴드갭을 생성하여 반도체 소자로 사용하려는 방법들이 대부분이지만, 실리콘과 그래핀과의 접합을 통해 소자를 제작하는 방법이 소개되어 온/오프 비 문제를 극복하는 연구가 소개되었지만 그래핀 고유 특성을 잃어버리는 한계를 보여주었다.

본 연구에서는 이온겔 게이트 절연체를 포함하는 그래핀과 유기물, 이차원 단결정 소재와의 이중 접합 구조의 소자를 제작하여 기존 실리콘 기반 소자의 단점들을 극복하고 본래 그래핀의 장점인 높은 온/오프 비와 전자이동도를 가지는 소자를 구현하는 성과를 가져왔다. 또한 4%이상의 직접적인 휘어짐에도 저항변화가 거의 없으며, 90% 이상의 투명도를 가지고, 양극성 특성도 보여줌으로 인해 그래핀 기반 소자 상용화를 구현할 수 있을 것으로 기대된다.

### Keywords:

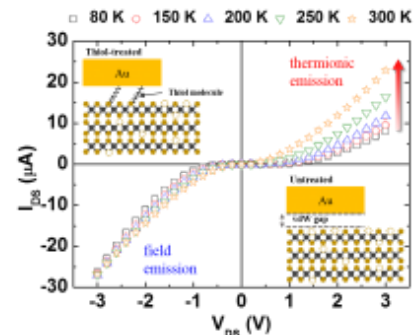
barristor, graphene, ambipolar, ion-gel, photodetector

## Carrier injection enhancement via directly deposited thiol-molecules on MoS<sub>2</sub> field-effect transistors

조경준<sup>1</sup>, 박진수<sup>1</sup>, 김재근<sup>1</sup>, 정승준<sup>2</sup>, 이택희\*<sup>1</sup>  
<sup>1</sup>서울대학교 물리학과, <sup>2</sup>KIST  
tlee@snu.ac.kr

### Abstract:

Although two-dimensional (2D) molybdenum disulfide (MoS<sub>2</sub>) has gained a great attention due to its unique physical properties, the limited electrical contact to 2D semiconductor still impedes to realize high-performance of 2D MoS<sub>2</sub>-based electronic devices. In this regard, many studies have been conducted to improve the carrier injection properties by inserting thin tunneling layers, such as hexagonal boron nitride or graphene, between semiconductor channel and electrodes.[1,2] However, the reported strategies require relatively low-yield and time-consuming transfer processes on MoS<sub>2</sub> flakes. Here, we suggest a simple contact modification method which introduces chemically adsorbed thiol-molecules as thin tunneling barriers between the metal electrodes and MoS<sub>2</sub> channels. The directly deposited thiol-molecules via the vapor-deposition process introduce additional tunneling paths at the contact regions, improving the carrier injection properties with lower activation energies in MoS<sub>2</sub> field-effect transistors. Additionally, by inserting thiol-molecules at the only one contact region, asymmetric carrier-injection was feasible depending on the temperature and gate bias.[3]



[1] J. Wang et al., Adv. Mater. 28, 8302 (2016).

[2] X. Cui et al., Nano Lett. 17, 4781 (2017).

[3] K. Cho et al., Adv. Mater. accepted (2018).

### Keywords:

MoS<sub>2</sub>, contact engineering, charge injection, thiol-molecules, electrical transport

# A programmable molecular-scale rectifier driven by the interface-engineered molecular junction consisting of the 2D semiconducting layer and the self-assembled monolayers

SHIN Jaeho<sup>1</sup>, YANG Seounghoon<sup>1</sup>, LEE Chul-Ho<sup>1</sup>, 왕건욱\*<sup>1</sup>

<sup>1</sup>KU-KIST Graduate School of Converging Science & Technology, Korea University, 145, Anam-ro, Seongbuk-gu, Seoul 02841, Republic of Korea  
gunukwang@korea.ac.kr

## Abstract:

Since Aviram and Ratner initially proposed the possibility of a molecular-scale rectifier in 1974, diverse type of molecular diodes driven by a specific molecular itself or the asymmetric interfacial engineering has been extensively suggested and demonstrated [1-4]. In this study, we propose a new class of molecular-scale rectifier based on a hybrid molecular junction system that is composed with stacked of the Au (or graphene)/the 2D material (MoS<sub>2</sub>)/the standard self-assembled monolayer (SAM) (alkyl- or conjugated molecules)/Au probe tip. The 2D material and the SAM are sandwiched between the Au probe tip and conducting electrode (graphene or Au) using conductive atomic force microscopy (CAFM) technique. In the case of the molecular junction without 2D semiconducting material, the typical tunneling behavior through molecular barrier has been observed when the tip-loading force was 1 nN. When the tip-loading force was increased from 1 to 100 nN, however, the intriguing transition of the Fowler-Nordheim tunneling regime was observed, which can be interpreted by the correlation effects of the molecular-tilt configuration and the vdW interactions on the tunneling barriers [5]. In the case of the molecular junction with the 2D MoS<sub>2</sub> material, the diode feature with rectification ratio  $> \sim 10^3$  was observed [6]. Furthermore, this ratio can be programmed according to the number of MoS<sub>2</sub> layers, molecular length, and energy-alignment between 2D/SAM. Our suggested rectifier architecture can provide potential benefit to simply implement the molecular-scale diode function and propose the idea to improve the diode performance.

**Acknowledgement :** This work was accomplished with financial support from the National Research Foundation of Korea, the KU-KIST research fund, SAMSUNG, and the Korea University Future Research Grant.

## Reference :

- [1] Aviram, A.; Ratner, M. A. *Chem. Phys. Lett.* **1974**, *29*, 277-283
- [2] Diez-Perez, I.; Hihath, J.; Lee, Y.; Yu, L.; Adamska, L.; Kozhushner, M. A.; Oleynik, I. I.; Tao, N. *Nat. Chem.* **2009**, *1*, 635-641
- [3] Dyck, C. V.; Ratner, M. A. *Nano Lett.* **2015**, *15*, 1577-1584
- [4] Yuan, L.; Breuer, R.; Jiang, L.; Schmittl, M.; Nijhuis, C. A. *Nano Lett.* **2015**, *15*, 5506-5512
- [5] Shin, J.; Gu, K.; Yang, S.; Lee, C.-H.; Lee, T.; Jang, Y. H.; Wang, G. \* Submitted (2018)
- [6] Shin, J.; Yang, S.; Lee, C.-H.; Wang, G. \* in preparation (2018)

## Keywords:

Molecular electronics, 2D semiconducting materials, molecular-scale diode

## Negative Fermi-level Pinning Effect Observed in Metal/GaAs Junction with Graphene Insertion Layer

박기복\*<sup>1, 2</sup>, YOON Hoon Hahn<sup>1</sup>, SONG Wonho<sup>1</sup>, JUNG Sungchul<sup>1</sup>, KIM Junhyung<sup>2</sup>, MO Kyuhung<sup>1</sup>,  
JEONG Hu Young<sup>3</sup>, LEE Jong Hoon<sup>3</sup>

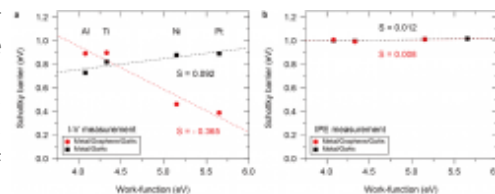
<sup>1</sup>Department of Physics, Ulsan National Institute of Science and Technology, <sup>2</sup>School of Electrical and Computer Engineering, Ulsan National Institute of Science and Technology, <sup>3</sup>UNIST Central Research Facilities, Ulsan National Institute of Science and Technology  
kibogpark@unist.ac.kr

### Abstract:

We report the direct observation revealing that the electric dipole layer due to the chemical interaction of metal/graphene contact can induce the negative Fermi-level pinning effect in metal/graphene/n-GaAs(001) junction, supported by the Schottky barrier decreasing as metal work-function increasing. The chemical interaction dipole layer and the work-function difference between metal and graphene determine the change of electrostatic potential across metal/graphene interface combinedly. In particular, this combined effect is influential to the local Schottky barrier formed on the region of GaAs surface with low interface-trap. The graphene insertion layer takes a role of diffusion barrier preventing the atomic intermixing at interface and preserving the low interface-trap density region. The electron transport through metal/graphene/n-GaAs(001) junction is dominated by the low Schottky barrier patches which will be the low interface-trap density region for metals with large work functions. Our work provides an experimental method to form Schottky (metal/GaAs) and Ohmic (metal/graphene/GaAs) contacts simultaneously on a GaAs substrate covered partially with graphene by using identical metal electrodes.

### Keywords:

Schottky Contact, Gallium Arsenide, Fermi-Level Pinning, Graphene, Diffusion Barrier, Interface Dipole Layer



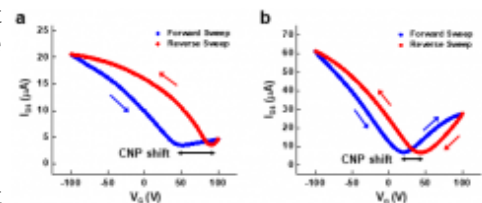
## Minimization of Water Molecule Trapping at Graphene/Substrate Interface Using Dry Transfer with Flexible Supporting Layer

JUNG Sungchul<sup>1</sup>, YOON Hoon Hahn<sup>1</sup>, JIN Hanbyul<sup>2</sup>, MO Kyuhung<sup>1</sup>, CHOI Gahyun<sup>1</sup>, LEE Junghyun<sup>3</sup>,  
PARK Hyesung<sup>3</sup>, 박기복\*<sup>1, 2</sup>

<sup>1</sup>Department of Physics, Ulsan National Institute of Science and Technology, <sup>2</sup>School of Electrical and Computer Engineering, Ulsan National Institute of Science and Technology, <sup>3</sup>School of Energy and Chemical Engineering, Ulsan National Institute of Science and Technology  
kibogpark@unist.ac.kr

### Abstract:

CVD graphene has been usually transferred by using PMMA-assisted wet transfer method relying on its simplicity and good coverage. During the wet transfer process, however, water molecules can be trapped between the substrate and graphene layer. Generally, the CVD graphene transferred on SiO<sub>2</sub> substrate is p-doped and the trapped water molecules enhance the p-doping of graphene. Moreover, the trapped water molecules also cause the unwanted hysteric current-voltage behaviors of the field effect transistor (FET) based on the transferred graphene. In this work, a simple but quite efficient dry transfer method adopting an additional flexible supporting layer attached to the PMMA-graphene stack is demonstrated. A commercial Kapton tape is used as the flexible supporting layer. N<sub>2</sub> blowing and heating processes are preceded before transferring graphene on the substrate. The dry-transferred graphene is found to have much smaller doping and hysteric behavior compared to the conventional wet-transferred graphene. Furthermore, the carrier mobility is also found to be improved noticeably from the operational performances of fabricated FETs. Our dry transfer method is readily applicable for transferring graphene onto large-scale substrate with both minimized water-molecule-trapping at interface and good coverage throughout the entire substrate.



### Keywords:

Graphene, Dry Transfer, Water Molecule Trapping, Charge Neutrality Point, Flexible Supporting Layer, Field Effect Transistor

## Highly Effective Organic Light-Emitting Diodes System Based on Thermally Activated Delayed Fluorescence Materials

LEE Sae Youn\*<sup>1</sup>

<sup>1</sup>Department of Energy and Materials Engineering, Dongguk University  
saeyounlee@dongguk.edu

### Abstract:

High-efficiency organic light-emitting diodes (OLEDs) are being developed intensively for next-generation flat-panel displays and general lighting applications<sup>1</sup> owing to their advantages of wide view angles, light weight, flexibility, as well as improved brightness. In the past decade, nearly 100% internal electroluminescence (EL) quantum efficiency ( $\eta_{int}$ ) has been achieved by employing transition metal-centered phosphorescent emitters such as iridium(III) and platinum(II) organometallic complexes that can harvest both singlet and triplet excitons by fast intersystem crossing (ISC) for phosphorescence emission. However, these phosphorescent materials suffer from instability in practical applications, especially for blue and white emission. The expense and rarity of precious-metal complexes also limits their cost effectiveness and long-term mass production. Realizing high-efficiency electroluminescence (EL) through a simple organic system while aiming to reduce production costs and simplify manufacturing processes is pivotal for next-generation OLED technology.

We recently explored an alternative approach to harvest excited triplet energy through up-conversion by thermal activation, giving rise to thermally activated delayed fluorescence (TADF) without using precious metal complexes.[1-3] In this lecture, we introduce molecular design strategy, photophysical analysis method, and various application of TADF materials based on our previous research.

[1] S.Y. Lee et.al., *Angew. Chem. Int. Ed.*, **126**, 6520 (2014)

[2] S. Y. Lee et.al., *Adv. Mater.*, **28**, 4626 (2016)

[3] S. Y. Lee et.al., *Adv. Mater.*, **28**, 4019 (2016)

### Keywords:

Organic light-emitting diodes

## Interface engineering for high-performance all-inkjet-printed organic thin-film transistors

CHUNG Seungjun\*<sup>1</sup>

<sup>1</sup>Photoelectronic Hybrids Research Center, Korea Institute of Science and Technology (KIST)  
seungjun@kist.re.kr

### Abstract:

Printing technologies is one of the most promising candidates to realize solution-processed organic thin-film transistors (OTFTs) which can be potential driving components for flexible and large-area electronic applications.[1-2] However, owing to the poor solvent and thermal resistance of the printed organic semiconductors, bottom-contact OTFTs have been typically adopted instead of top-contact ones; therefore, solution-printing of organic semiconductors onto bottom source/drain electrodes and gate dielectrics results in a high contact resistance as well as unfavorable crystal structures of  $\pi$ -conjugated semiconductors during solvent drying, yielding poor electrical performance. Moreover, a large mismatch in the surface energy between the bottom source/drain electrode and gate dielectric materials develops an undesired and inhomogeneous solution-processed semiconducting layer. Although the introduction of self-assembled monolayers (SAM) to gate dielectrics has been intensively studied to result highly ordered crystals of  $\pi$ -conjugated organic semiconductors and deactivate the interface polar moieties, however, typical SAM treatments have been used only for either gate dielectric or bottom electrodes. Furthermore, those methods require a sufficient coupling reaction time under inert conditions, as well as complicated procedures. Therefore, a more compatible surface treatment to high-speed and facile printing methodology is highly required. [3]

In this presentation, we report single-step interface engineering which can be employed on both electrodes and gate dielectric for all-inkjet-printed, transparent, flexible OTFTs and inverters simultaneously. By introducing end-functionalized polystyrene interlayer, organic-compatible and hydroxyl-free interfaces drastically reduce the interfacial trap and contact resistance resulting significantly enhanced the charge injection from the electrode to the semiconductor layer, but the charge-carrier transport along the  $\pi$ -overlapped semiconducting domains. This strategy provide an attractive pathway toward the realization of high-performance flexible organic electronics with a low-temperature and low-cost printing process.

[1] S. Chung et al., Adv. Mater. 25, 4773 (2013).

[2] J. Ha et al., ACS Appl. Mater. Interfaces 9, 8819 (2017).

[3] T.-Y. Kim et al., ACS Nano 10, 10273 (2017)

### Keywords:

organic thin-film transistors

## Impact of self-assembled monolayer on carrier mechanism of organic 6,13-Bis(triisopropylsilylethynyl) pentacene device

복문정<sup>1, 2</sup>, 정준호<sup>\*2</sup>, 임은주<sup>\*1</sup>

<sup>1</sup>단국대학교, 과학교육과, <sup>2</sup>한국기계연구원, 나노공정  
jhjeong@kimm.re.kr, elim@dankook.ac.kr

### Abstract:

Using two kinds of organic molecules as self-assembled monolayers (SAMs), we showed that SAM layer gives a significant impact on the carrier injection of organic device. PFBT and MPTMS molecules were selected as SAM molecules, which were treated on the Au electrode substrate. MPTMS is used to induce Si reaction with 6,13-Bis(triisopropylsilylethynyl) pentacene (TIPS) material. After the SAM treatment, TIPS film was prepared and evaluated by the AFM, visible absorption spectra with contact angle measurement. To verify the chemical binding reaction of MPTMS with TIPS, XPS was also measured. The electrical measurements were also carried out to observe the changes of carrier injection in charge behavior of the organic device with the treated SAM monolayer. Results indicate that the chemical interaction of the monolayer improves the intrinsic carrier concentration and decreases the carrier transit time. We believe that our findings will greatly contribute to the interface engineering between the organic semiconductor layer and electrode in organic devices.

### Keywords:

TIPS-pentacene, MPTMS, PFBT, SAM, Organic Semiconductor

## Time dependent current behavior of unipolar organic resistive memory devices under a constant voltage stress

이우철<sup>1</sup>, 김영록<sup>1</sup>, 송영걸<sup>1</sup>, 유대경<sup>1</sup>, 강기훈<sup>1</sup>, 이택희\*<sup>1</sup>

<sup>1</sup>서울대학교 물리학과  
tlee@snu.ac.kr

### Abstract:

Organic resistive memory is one of the promising next-generation data storage technologies due to several advantages such as versatility of organic materials, low-cost device fabrication, and application on printable and flexible devices. However, the mechanism of the resistive switching phenomenon in organic resistive memory devices has not been clearly understood [1]. In this study, we investigated the time-dependent current behavior of unipolar-type organic memory devices under a constant voltage stress. In this measurement, the current abruptly increased several times and reached ON state even when the applied stress voltage was below the threshold voltage. The distribution of the time required to reach ON state (denoted as turn-on time) was described with Weibull distribution which has often been used for time-dependent gate dielectric breakdown in transistors [2]. Through statistical analysis of the turn-on times, we found that the abrupt increase of current follows a specific probability law. The probability of current increase over time is found to be constant during current increasing under the same voltage stress. The probability exponentially increases as the stress voltage bias increases. It was also found that the lower the temperature, the lower the probability. Our measurement results suggest that percolation networks of the conducting paths were generated during the turn-on process of unipolar organic memory devices.

### Keywords:

Organic memory devices, unipolar memory devices, Weibull distribution

## Amplified spontaneous emission from dye-doped submicron silica beads with gold nanoparticles

LEE Chang-Won\*<sup>1</sup>

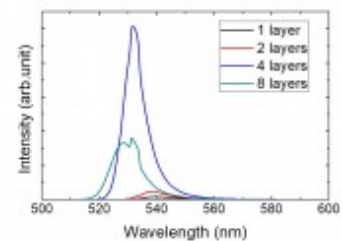
<sup>1</sup>School of Basic Sciences, Hanbat National University  
cwlee42@hanbat.ac.kr

### Abstract:

We study the emission properties of self-assembled dye-doped submicron silica beads with gold nanoparticle coating. With increasing number of layers of the spheres, the spontaneous emission from dye molecules blue-shifts and becomes narrow indicating transition to amplified spontaneous emission. We attribute the lattice formed by the spheres, which is fcc closed packing, may lead to external cavity effect on the emission from the dyes.

### Keywords:

amplified spontaneous emission, external cavity, pseudolasing



## Enhancing light absorption in a ultrathin semiconductor metafilm

김수진\*<sup>1</sup>

<sup>1</sup>고려대학교 전기전자공학부  
kimsjku@korea.ac.kr

### Abstract:

Light absorption in an ultrathin film is of great interest for the last decade due to the potential applications in diverse optoelectronics. In this presentation, we show the near unity light absorption for target wavelengths in a thin semiconductor film when the nanostructured elements are arranged in deep subwavelength scale. Furthermore, we theoretically and experimentally demonstrate the efficient photon sorting in a lateral direction of metafilm based on the anti-hermitian coupling between resonant meta-atoms. Subsequently, we show the useful extraction of photocurrent from the metafilms for the diverse device applications such as a filterless photodetector.

### Keywords:

metasurface, semiconductor metafilm, light absorption, photon sorting

## Amplifying or suppressing scattering of visible light

김선경\*<sup>1</sup>, 김상우<sup>1</sup>, 문윤종<sup>1</sup>

<sup>1</sup>경희대학교 응용물리학과  
sunkim@khu.ac.kr

### Abstract:

빛의 파장과 유사한 크기를 가진 광학 구조는 특정 주파수에서 강한 Mie 산란 특성을 나타낸다. 이 발표에서는 버금파장 구조의 산란 강도를 증폭하거나 억제하는 광학 설계 법칙 및 실험 결과를 토의하고, 산란 증폭과 억제를 이용한 응용 분야를 각각 소개한다.

### Keywords:

Light scattering, Optical antenna, Invisibility cloak

## Large area aberration correction for laser scanning microscopy by 'closed-loop accumulation of single scattering' (CLASS) algorithm

JUNG Yookyung\*<sup>1, 3</sup>, KANG Pilsung<sup>1, 2</sup>, KWON Yongwoo<sup>1, 2</sup>, HONG Jin Hee<sup>1, 2</sup>, CHOI Wonshik<sup>1, 2</sup>

<sup>1</sup>Center for Molecular Spectroscopy and Dynamics, Institute for Basic Science (IBS), Seoul 02841, Republic of Korea, <sup>2</sup>Department of Physics, Korea University, Seoul 02841, Republic of Korea, <sup>3</sup>Center for Systems Biology and Wellman Center for Photomedicine, Massachusetts General Hospital and Harvard Medical School, Boston, MA 02114, USA

omeletjung@korea.ac.kr

### Abstract:

'Collective accumulation of single scattering (CASS)' and 'Closed-loop accumulation of single scattering (CLASS)' microscopy have opened new routes to deep tissue imaging by providing novel solutions to the problems of light scattering and aberration. Until now these methods demonstrated monochromatic contrast utilizing back scattered illumination light.

Here, I introduce a novel imaging method to correct aberration for the laser scanning microscopy by adopting CLASS algorithm. This method can be applied to any type of laser scanning microscopy, and it is expected that aberration correction will enhance the imaging depth and resolution while it is still providing full spectral information of regular confocal/multiphoton microscopy. The strength and challenge of the introduced method over the current adaptive optical microscopy will be also discussed.

### Keywords:

aberration, deep tissue imaging, CASS, CLASS, laser scanning microscopy, adaptive optical microscopy

## 광자결정 합금계에서 광자 띠꼬리 상태의 모드 특성 제어에 대한 연구

전현수\*<sup>1</sup>, 이명재<sup>1</sup>

<sup>1</sup>서울대학교 물리천문학부  
hsjeon@snu.ac.kr

### Abstract:

1987년에 광자결정의 개념이 제안된 직후, 무질서가 인가된 주기적 광학계에서는 결정구조에 의한 결맞음과 무작위성에 의한 다중산란 사이의 상호작용으로 광자가 공간적으로 강하게 국지화될 수 있음이 알려졌다. 이러한 광자의 국지적인 고유모드는 반도체 내의 전자 띠꼬리 상태와 유사한 분광학적, 공간적 모드 특성을 나타낼 것으로 기대되었다. 본 연구에서는 InP 기반의 다중양자우물이 내재된 박막에 2차원 광자결정 합금계를 구현하여 발진모드의 에너지와 근접장의 공간적 분포를 분석함으로써 광자 띠꼬리 상태의 존재를 실험적으로 증명하고, 그 광학적 특성을 규명하였다. 그리고 광자결정 합금계의 구조적 자유도를 활용하여 광자 띠꼬리의 모드 밀도와 에너지, 공간적 크기, 분포 형태 등의 특성을 직접적으로 제어할 수 있음을 시연하였다.

### Keywords:

빛의 제어, 구조화된 빛, 근접장 제어, 빛의 국지화, 광자 띠꼬리, 띠꼬리 레이저, 광자결정합금, 랜덤 레이저

## Focusing of light energy to the embedded target in scattering medium

최원식\*<sup>1, 2</sup>, 정승원<sup>1, 2</sup>, 이에령<sup>1, 2</sup>, 최원준<sup>1, 2</sup>, 강성삼<sup>1, 2</sup>, 홍진희<sup>1, 2</sup>, 박진성<sup>2</sup>, 임용식<sup>3</sup>, 박홍규<sup>2</sup>  
<sup>1</sup>고려대학교 IBS 분자 분광학 및 동력학 연구단, <sup>2</sup>고려대학교 물리학과, <sup>3</sup>건국대학교 나노전자기계공학부  
wonshik@korea.ac.kr

### Abstract:

In optical methodologies such as biomedical imaging, phototherapy, and optogenetics, the efficient delivery of light energy is prerequisite for in-vivo applications. However, only a small fraction of incident waves can reach the target object due to random diffusion by multiple light scattering. Here, we present a method to counteract random diffusion and to focus light energy toward the deeply embedded target in scattering media with the implementation of the reflection eigenchannels of a specific flight time. Coupling the time-gated reflection eigenchannels with large eigenvalues, we could enhance a more than 10-fold in light energy delivery in comparison with the case of random diffusion. We expect that our work will improve the working depth of imaging, sensing, and light stimulation.

### Keywords:

light energy, embedded target, time-gated reflection eigenchannels, scattering medium

## Entangled State Tunneling in Strongly Correlated Systems

홍중배\*<sup>1</sup>

<sup>1</sup>서울대학교 물리학과, <sup>2</sup>인천대학교 기초과학연구소  
jbhong@snu.ac.kr

### Abstract:

In electron tunneling from a metallic tip to a correlated system, the incoming electron encounters strong Coulomb repulsion at the site to which it hops from the tip. The only possible way to avoid the strong Coulomb repulsion is to form a Kondo singlet between a spin in the tip and the localized spin at the correlated sample, and to perform coherent co-tunneling. Therefore, one must consider all coherent spins in the tip and sample in a bunch, which I call entangled (many-body) state. This circumstance always occurs in scanning tunneling spectroscopy (STS) for correlated systems [1]. The study for tunneling conductance of correlated systems in terms of entangled state tunneling resolves various puzzles in explaining STS data. In this talk, I explain tunneling conductance of quantum impurity systems, Fe-based superconductors, and SmB<sub>6</sub>.

[1] J. Hong, Int. J. Mod. Phys[1]. B **31**, 1742009 (2017).

### Keywords:

scanning tunneling spectroscopy, quantum impurity systems, Fe-based superconductors

## Mott transition and Holography of the Hubbard Model

신상진\*<sup>1</sup>, 서윤석<sup>1</sup>, 송근호<sup>1</sup>, 채용희<sup>1</sup>

<sup>1</sup>한양대학교 물리학과  
sangjin.sin@gmail.com

### Abstract:

We show that the competition between the fermi liquidity and the gap generation, which is the physics of the Hubbard model, can be studied in a canonical holographic model of a probe fermion with bulk mass and a dipole interaction. The mass near  $1/2$  tries to protect the fermi liquidity while large dipole coupling tries to generate the mass gap so that the model reproduce the basic feature of the Mott transition in Hubbard model. In fact, the spectral density of holographic model reproduces two of the most important predictions of the dynamical mean field theory (DMFT) calculation: namely, the transfer of the degree of freedom from the quasi-particle peak to the side peak, and the narrowing of the quasi-particle peak until its disappearance with increasing on-site repulsion. The zero temperature phase diagram of our holographic model contains several phases including fermi liquid and Mott insulator and any line connecting these two phases defines a holographic Hubbard model.

### Keywords:

Mott transition, spectral density, Holography

## Electronic excitation spectra of 4d transition-metal-based honeycomb system $\alpha$ -RuCl<sub>3</sub>

김범현\*<sup>1</sup>, SHIRAKAWA Tononori<sup>1</sup>, YUNOKI Seiji<sup>1</sup>

<sup>1</sup>Computational Condensed Matter Physics Laboratory, RIKEN, Japan  
bomisu@postech.ac.kr

### Abstract:

Recently the research on 4d transition-metal-based honeycomb system  $\alpha$ -RuCl<sub>3</sub> has been drawn much attention because the mutual interplay among electronic kinetics, electron-electron interaction, and strong spin-orbit coupling (SOC) of Ru<sup>3+</sup> ions can bring about exotic electronic phases. Strong directional hopping character mediated by edge-shared Cl ligand orbitals can give rise to the quasimolecular orbital (QMO) formation at each hexagon and stabilize the band insulating feature. In contrast, both strong SOC and Coulomb repulsion suppress the hopping effect and propel the Mott insulating phase of spin-orbital entangled  $j_{\text{eff}}=1/2$  orbitals. Moreover, different electronic phases can manifest themselves in electronic excitations [1].

In the study, we have studied excitation behaviors of  $\alpha$ -RuCl<sub>3</sub> in the vicinity of spin-orbital excitation in both electronic phases. With the help of the Lanczos exact diagonalization and continued fraction methods, we have calculated theoretical excitation spectra measured with the optical conductivity, Raman spectroscopy, and resonant inelastic x-ray scattering. Based on our result, we have analyzed recent experimental observations of optical conductivity and Raman spectroscopy in  $\alpha$ -RuCl<sub>3</sub>.

[1] B. H. Kim, T. Shirakawa, and S. Yunoki, Phys. Rev. Lett. 117, 187201 (2016)

### Keywords:

$\alpha$ -RuCl<sub>3</sub>, Optical conductivity, Raman spectra, RIXS spectra

## Role of the Hund's and Spin-orbit Couplings in $\text{Sr}_2\text{RuO}_4$ at Zero Temperature

고아라\*<sup>1</sup>, 이형준<sup>2, 3</sup>, 김충현<sup>2, 3</sup>

<sup>1</sup>기초과학연구원 복잡계이론물리연구단, <sup>2</sup>기초과학연구원 강상관계물질연구단, <sup>3</sup>서울대학교 물리천문학부  
arago@ibs.re.kr

### Abstract:

$\text{Sr}_2\text{RuO}_4$  has attracted much interest as a strongly correlated multiorbital system with unconventional superconductivity at very low temperature. Its theoretical understanding, however, is still lacking in spite of the simple crystal structure. This is because of complicated correlation effects in multiorbital, particularly with the spin-orbit coupling. We focus on zero temperature behavior of the normal state of this material by using the density functional theory plus dynamical mean-field theory with the exact diagonalization impurity solver. We find that the effective total angular momentum eigenstates are suitable to describe the quasiparticles and excitations in  $\text{Sr}_2\text{RuO}_4$  although the spin-orbit coupling is relatively small. We examine how the Hund's coupling influences a correlated metal to reveal orbital-dependent correlations and freezing moments. The correlation effects on spectral properties are also discussed.

### Keywords:

strontium ruthenate, DFT+DMFT, multiorbital, correlation, spin-orbit coupling, Hund's coupling

## Transition temperature of excitonic insulator phase in a transition metal dichalcogenide 1T-TiSe<sub>2</sub>.

복(Bok)진모(Jin Mo)\*<sup>1</sup>, 최(Choi)한용(Han-Yong)<sup>1</sup>

<sup>1</sup>성균관대학교 물리학과  
bockill@skku.edu

### Abstract:

We calculated the transition temperature of excitonic insulator phase to understand the mechanism of charge density wave (CDW) state in the transition metal dichalcogenide TiSe<sub>2</sub>. The linearized CDW gap equation with statically screened coulomb interaction was employed to find transition temperature in realistic TiSe<sub>2</sub> model. For realistic TiSe<sub>2</sub> model, one hole band centered at  $\Gamma$  point and three electron bands located M points in 2D periodic hexagonal lattice were considered. The calculated transition temperature roughly agrees with actual  $T_c$  from measurements. We found that the behavior of  $T_c$  as a function of band gap and chemical potential is consistent with the experiments for pressure and Cu intercalated TiSe<sub>2</sub>. From the results, we discuss possibility of the CDW state in TiSe<sub>2</sub> originating from exciton condensation.

### Keywords:

excitonic insulator, TMDC, TiSe<sub>2</sub>

## Interaction effects on the Kane-Mele Model in the Hofstadter regime

이성빈\*<sup>1</sup>, MISHRA Archana<sup>1</sup>

<sup>1</sup>한국과학기술원 물리학과  
sungbin@kaist.ac.kr

### Abstract:

Considering interacting Kane-Mele model of honeycomb lattice in the Hofstadter regime, we realize that the orbital motion of electrons can induce versatile topological phases with spontaneously broken symmetries. In the Hofstadter regime without spin orbit coupling, the interactions lead to the breaking of translational and rotational symmetries of the system resulting in nematic and ferrielectric phases. Here, within the mean field framework, we extend the study and consider the onsite and nearest neighbor interactions in the Kane-Mele model and discuss possible phases in the absence and presence of magnetic field at each integer filling of electrons.

1. Interaction effect on Kane Mele model at zero magnetic field: At half filling, the interplay of intrinsic spin-orbit coupling and onsite interaction leads to the phase transition from quantum spin Hall insulator to an antiferromagnetic Mott insulator with magnetization in the xy-plane. At quarter filling, we study this interplay and show that the combined effect opens a wide region of ferromagnetic Chern insulating phase in between metal and normal insulator. We further discuss the experimental realization of these phases in series of transition metal trichalcogenides.

2. We extend our study to analyze the collaborative effect of magnetic field, spin orbit coupling and interactions. Focusing on  $2\pi/3$  magnetic flux per plaquette, we realize numerous interesting phases like insulator with noncoplanar magnetic ordering, ferrimagnetic Chern insulator with nematic charge order, ferrimagnetic-ferrielectric Chern insulators etc. Many of these phase transitions are also accompanied with the change in the topology of the system. Our theoretical study broadens the field of topological phases accompanied with multiferroic like properties, as a consequence of the interplay of magnetic field, spin orbit coupling and interactions.

### Keywords:

Kane Mele model, Hofstadter regime, interaction, topological transition, multiferroic

## Coexistence of strong electron-phonon coupling and flat band ferromagnetism in hole-doped boron triangular Kagome lattice

한우현\*<sup>1</sup>, 김성현<sup>2</sup>, 이인호<sup>3</sup>, 장기주<sup>1</sup>

<sup>1</sup>한국과학기술원 물리학과, <sup>2</sup>Department of Materials, Imperial College London, <sup>3</sup>Korea Research Institute of Standards and Science  
hanwooh@kaist.ac.kr

### Abstract:

Electron-phonon coupling (EPC) in solids plays an important role in electrical resistivity, carrier mobility, optical absorption, and Cooper pairs in conventional superconductors. The EPC strength is closely related to the density of states (DOS) at Fermi energy and provides an opportunity to observe unexpected physical phenomena. For example, in graphene, alkali atom adsorption, external carrier doping, and mechanical strain can increase the EPC strength due to the increase of the DOS. A Kagome lattice may be an interesting system to study the effect of the DOS on the EPC because it intrinsically exhibits a flat band due to destructive interferences on the lattices, yielding a large DOS when the Fermi energy is located near the flat band. Despite the expectation of strong EPC in the Kagome lattice, it is difficult to realize a proper material with a flat band.

Recently, we have predicted a two-dimensional boron triangular Kagome lattice on a silver substrate, termed B<sub>9</sub> Kagome lattice, based on the first-principles evolutionary materials design [1]. In this work, we study the effect of hole doping on the EPC strength in the B<sub>9</sub> Kagome lattice through first-principles density functional calculations. The B<sub>9</sub> Kagome lattice exhibits a flat band near the Fermi level and thus a half-metallic ferromagnetism. We find that hole doping greatly enhances the EPC strength in the B<sub>9</sub> Kagome lattice, maintaining the ferromagnetism, which is attributed to the high DOS as well as the Fermi surface nesting. Our results infer the possible coexistence of ferromagnetism and phonon-mediated superconductivity in hole-doped B<sub>9</sub> Kagome lattices.

[1] S. Kim, W. H. Han, I.-H. Lee, and K. J. Chang, *Scientific Reports* 7, 7279 (2017).

### Keywords:

Density functional theory, Kagome lattice, electron-phonon coupling

## Strain effect on the electronic properties of Copper doped CdSe nanoplatelet

변성재<sup>1</sup>, 김용훈\*<sup>1</sup>

<sup>1</sup>한국과학기술원 EEWS대학원  
y.h.kim@kaist.ac.kr

### Abstract:

Cadmium Selenide (CdSe) nanoplatelets(NPL) are appealing due to their anisotropic growth controlled at the atomic scale and optical properties. However, to the best of our knowledge, not much work has studied the doping of the CdSe NPL. Herein, by means of density functional theory (DFT) calculation, we investigate the geometrical and electronic properties of the copper(Cu)-doped CdSe NPL at the atomic level. In particular, we study the strain effect on the electronic properties of the 3.5 monolayer Cu-doped zinc-blend(ZB) CdSe NPL capped with oleic acid organic ligand. The strain effect is indeed shown to change the Cu mid-gap states which are located near the fermi-level. To understand the origin of Cu states shift under strain, we analyze the local density of states for Cu-doped CdSe NPL and find that Jahn-Teller distortion plays an important role. On the basis of our results, we further show that the Cu states are shifted with ligand-induced strain upon exchange of oleic acid with thiol acid.

### Keywords:

II-VI Semiconductor, Colloidal Nanoplatelets, Electronic-Structure, first-principles calculations

## Strain engineering of phonon thermal transport properties in 2H-MoTe<sub>2</sub> monolayer

신영한\*<sup>1</sup>, SHAFIQUE Aamir<sup>1</sup>

<sup>1</sup>울산대학교 물리학과  
hoPONpop@ulsan.ac.kr

### Abstract:

Strain is a very useful and effective tool to enhance the performance of the semiconducting devices. It can tune electronic, optical, and thermoelectric properties. However, the effect of tensile strain on the phonon thermal transport of two-dimensional materials is unpredictable because the flexural acoustic (ZA) mode becomes harder and transverse acoustic (TA) and longitudinal acoustic (LA) modes become softened[1, 2, 3]. The effect of strain on the phonon properties (such as phonon group velocity, phonon anharmonicity and phonon lifetime) and lattice thermal conductivity of the 2H-MoTe<sub>2</sub> monolayer is studied by solving Boltzmann transport equation based on first principles calculations. We compare phonon properties and lattice thermal conductivity of the unstrained 2H-MoTe<sub>2</sub> to those of the biaxially strained ones. One of the common features of the two dimensional materials is quadratic nature of the ZA mode that disappears by applying tensile strain. We find that lattice thermal conductivity of the monolayer 2H-MoTe<sub>2</sub> is so sensitive to tensile strain that it is reduced up to three times by applying 8% biaxial tensile strain due to the reduction in phonon group velocities and phonon lifetime. We analyzed how contribution of each mode in lattice thermal conductivity changes with tensile strain. These results highlight that tensile strain is one of key parameters in engineering phonon transport properties in monolayer 2H-MoTe<sub>2</sub>.

### References

- [1] H. Liu, G. Qin, Y. Lin, M. Hu, Nano Lett., 16, 3831-3842 (2016).
- [2] X.N. Bonini, J. Garg, N. Marzari, Nano Lett. 12, 2673-2678 (2012).
- [3] Y.D. Kuang, L. Lindsay, S.Q. Shi, G.P. Zheng, Nanoscale 8, 3760-3767 (2016).

### Keywords:

Strain, lattice thermal conductivity, monolayer 2H-MoTe<sub>2</sub>, phonon anharmonicity

## Bias dependent transport properties of passivated tilted black phosphorene nanoribbons

홍지상\*<sup>1</sup>, SUBHAN Fazle<sup>1</sup>

<sup>1</sup>부경대학교 물리학과  
hongj@pknu.ac.kr

### Abstract:

Using the density functional theory incorporated with non-equilibrium Green's function (NEGF) technique, we explore the bias dependent transport of tilted phosphorene nanoribbon (TPNRs). Here, we considered three types of nanoribbons; self-passivated (TPNR<sub>self</sub>), H-passivated (TPNR<sub>H</sub>), and O-passivated (TPNR<sub>O</sub>) systems. TPNR<sub>self</sub> showed an Indirect Gap band of 0.53 eV while TPNR<sub>H</sub> displayed a Direct Gap band of 1.32 eV. In TPNR<sub>O</sub>, we observe a spin polarized band structure with spin dependent band gap. The IV curve was dependent on the passivation effect. In TPNR<sub>self</sub> and TPNR<sub>H</sub>, the current was monotonically increased with an external bias, but the magnitude of current in the TPNR<sub>self</sub> was more than 10 times greater than in the TPNR<sub>self</sub>. Unlike the IV characteristics in TPNR<sub>self</sub> and TPNR<sub>H</sub>, the current in TPNR<sub>O</sub> almost vanished beyond an external bias of 1.7 V. Mostly, the bias dependent IV curve was interpreted based on the band structure in lead parts. However, we find that the conventional approach is not sufficient to analyze the IV curve. Indeed, we have shown that the IV curve could be calculated by taking the dependent density of states in the scattering part of the transmission channel. It was also found that the electron flow channel was dependent on the passivation effect. It was uniformly distributed over the entire nanoribbon in TPNR<sub>self</sub> and TPNR<sub>H</sub>. In contrast, the electron flow was mostly along the edge line in TPNR<sub>O</sub>. Besides, we found that an external bias could manipulate the spin in the polarization current conduction and this may suggest that the TPNR<sub>O</sub> can be utilized for spintronic application potential.

### Acknowledgments

This research was supported by the National Science Foundation of Korea (NRF) funded by the Ministry of Science, ICT and Future Planning (2016R1A2B4006406) and by the Supercomputing Center. resources including technical support (KSC-2017-C3-0031).

### Keywords:

nanoribbons, phosphorene, nonequilibrium calculations, green's function, electron transport

## First-principle study on novel group IV-V van der Waals materials

이승준<sup>1</sup>, 권영균\*<sup>1</sup>  
<sup>1</sup>경희대학교 물리학과  
ykkwon@khu.ac.kr

### Abstract:

Since the successful exfoliation of graphene from graphite, a variety of two-dimensional (2D) van der Waals (vdW) materials have also been emerged and extensively studied over the last decade. Nevertheless there have been continuing demand for new 2D vdW materials that can exhibit unusual physical properties. Here, we propose layered IV-V compounds as novel 2D vdW materials based on our first-principles calculations. Our predicted IV-V compounds are in the form of  $A_2B_2$ , where A and B are elements in group IV or 14 (C, Si, Ge, Sn) and group V or 15 (N, P, As, Sb), respectively. These structures are similar to those of layered III-VI compounds, such as GaSe or InSe. [1] Our investigation reveals that newly-discovered compounds have two distinguishable phases, M and I, which have a mirror and an inversion symmetry. To explore their structural stabilities and their phase transitions from one phase to the other, we perform geometrical optimization; evaluate their phonon dispersion relations; and estimate activation barrier of the phase transitions. We further investigate their electronic properties by calculating not only their electronic band structures, but also carrier transport properties including electron-phonon interaction.

[1] Doni, E., Girlanda, R., Grasso, V. et al. Nuov Cim B (1979) 51: 154.

### Keywords:

First-principle, two-dimensional, van der waals

## Behavior of a H<sub>2</sub>O molecule in a hybrid carbon/boron nitride heteronanotube

관우김\*<sup>1</sup>, 김건\*<sup>1</sup>

<sup>1</sup>세종대학교 물리학과

dndnwnan@gmail.com, kimgunn@gmail.com

### Abstract:

GwanWoo Kim and Gunn Kim

<sup>1</sup>*Department of Physics and Astronomy & Graphene Research Institute, Sejong University, Seoul 05006, Korea*

In this presentation, we report a first-principles study of a water molecule inside a carbon nanotube/boron nitride nanotube (CNT/BNNT) hybrid structure. We investigate structural, energetic, and electronic properties of the system using density functional theory calculations. For the van der Waals interaction, Grimme's DFT-D2 method was used. In the model structures, the (7, 7) CNT and BNNT were chosen. The equilibrium distance between a water molecule and the wall of the CNT (BNNT) was calculated to be 3.1 Å (3.0 Å). In the CNT (BNNT), the energy of the water molecule was 103 meV lower (122 meV lower) at the center of the tube, and was 226 meV lower (257 meV lower) at the equilibrium position in the tube than in vacuum. The potential profile along the tube axis shows a dramatic change around the heterojunction. We also provide the projected density of states of hydrogen and oxygen atoms in the water molecule in the tube to show whether the orbital hybridization changes between the tube wall and the H<sub>2</sub>O molecule, depending on the location of the H<sub>2</sub>O molecule.

### Keywords:

DFT, CNT, BNNT, heterojunction, water.

## On the Origin of High Hydrogen Evolution Catalytic Activity and Stability in Cobalt-Embedded C<sub>2</sub>N

김용훈\*<sup>1</sup>, 노민중<sup>1</sup>, 김효석<sup>1</sup>  
<sup>1</sup>한국과학기술원 EEWS대학원  
y.h.kim@kaist.ac.kr

### Abstract:

Transition metal-embedded two-dimensional materials have recently drawn significant research interest because they can serve as excellent catalysts in fuel cells, hydrogen production devices, etc. Especially, cobalt oxide encapsulated in C<sub>2</sub>N (Co@C<sub>2</sub>N) was recently shown to exhibit excellent catalytic performance for hydrogen evolution reaction (HER) together with high stability [1], but their precise understanding still remains elusive. Based on first-principles calculations, we herein scrutinize the mechanisms of enhanced HER performance of Co@C<sub>2</sub>N, particularly focusing on the role of C<sub>2</sub>N. We explore three plausible mechanisms that include (i) single-atom catalyst, (ii) quantum tunneling from substrate, and (iii) atomic-cluster catalyst. Among the three, we find that the atomic-cluster catalyst mechanism, in which few-atom Co cluster encapsulated within the hole region formed between two C<sub>2</sub>N layers explains the experimentally-observed high HER activity. The atomic-cluster catalyst might prove to be a general mechanism for the TM-embedded two-dimensional catalysts.

[1] Mahmood, J. *et al*, *Chem. Mater.* **27**, 4860 (2015)

### Keywords:

Density Functional Theory, Hydrogen Evolution Reaction, 2D-Materials (C<sub>2</sub>N), Metal Atomic Catalyst

## Projection orbital dependence of DFT+DMFT

최형준\*<sup>1</sup>, 한만천<sup>1</sup>, 오형주<sup>1</sup>, 이충기<sup>1</sup>

<sup>1</sup>Department of Physics, IPAP, and Center for Computational Studies of Advanced Electronic Material Properties, Yonsei University, Seoul 03722, Korea  
h.j.choi@yonsei.ac.kr

### Abstract:

Combination of the first-principles density functional theory (DFT) and the dynamical mean field theory (DMFT), which is called as DFT+DMFT, is a practical tool for investigation of correlated materials. Performing DFT+DMFT requires projection of the green's function in a solid to correlated orbitals. Because this choice of correlated orbitals crucially affects mapped dynamical mean field simulation, one has to choose these orbitals carefully. In this work, we studied projection orbital dependence of the DFT+DMFT simulation by changing size and form of correlated orbitals. We used our DFT+DMFT program, which is developed by merging the SIESTA program and our continuous-time quantum Monte Carlo impurity solver. This work was supported by NRF of Korea (Grant No. 2011-0018306) and KISTI supercomputing center (Project No. KSC-2017-C3-0079).

### Keywords:

DFT+DMFT, DMFT, CTQMC, Dynamical Mean Field Theory

## Three-dimensional Dirac semimetal in a wallpaper multilayer

김영국\*<sup>1</sup>, 오윤탁<sup>1</sup>, 민홍국<sup>1</sup>  
<sup>1</sup>성균관대학교 물리학과  
youngkuk@skku.edu

### Abstract:

We study a realization of a three-dimensional (3D) Dirac semimetal in noncentrosymmetric crystals, based on the layers of wallpaper semimetals. Wallpaper semimetals are a class of topological semimetals in two dimensions that host massless fermions formed from symmetry-enforced band degeneracies. We introduce an explicit tight-binding model for wallpaper group  $p4g$  and  $pgg$  to show that a 3D stack of the wallpaper semimetals hosts 3D Dirac points (DPs) and Weyl line nodes (WLN) with strong spin-orbit coupling and time-reversal symmetry. The DPs and WLN are reduced to Weyl points under a strain, mediating the topological phase transition between 3D time-reversal invariant topological insulator and normal insulators. The material realization based on first-principles calculations is discussed.

### Keywords:

Non-symmorphic Dirac semimetal, Nodal line semimetal, Surface state

## 자유곡면 삼차원 형상측정기술(Freeform 3D Surface Measurement using Deflectometry)

김영식\*<sup>1, 2</sup>, NGUYEN M. T.<sup>1, 2</sup>, 이혁교<sup>1, 2</sup>

<sup>1</sup>한국표준과학연구원 첨단측정장비연구소, <sup>2</sup>과학기술연합대학원대학교 측정과학과  
young.ghim@kriss.re.kr

### Abstract:

자유곡면이란 어떠한 축에 대해서도 비대칭성을 가진 임의의 면을 말하며 최근 등장한 스마트 안경과 HMD(Head Mounted Display) 등의 신개념 디스플레이의 핵심 광학부품들은 모두 자유곡면으로 이루어져 있다. 이러한 자유곡면은 기존의 구면이나 비구면으로만 이루어진 광학계의 광학적 성능의 한계를 뛰어넘을 뿐만 아니라 디자인 요소도 동시에 추구할 수 있기 때문에 전세계적으로 많은 연구가 이루어지고 있다. 한국표준과학연구원 첨단측정장비연구소에서는 지난 수년 동안 자유곡면형상측정기술을 연구해 왔고, 그 중 편향측정법을 이용한 삼차원 형상측정기술을 소개하고자 한다. 편향측정법은 측정 대상물의 국부 기울기에 따라 입사된 규칙적인 패턴의 변화를 측정하는 방식으로 측정된 국부 영역의 기울기 값으로부터 전체 형상을 복원하는 기술이다. 따라서 기존의 간섭계와 달리 별도의 기준면 없이도 측정 대상물에 대한 삼차원 형상 측정이 가능하게 되어 차세대 자유곡면형상 측정기로 각광을 받고 있다.

### Keywords:

자유곡면, 편향측정법, 삼차원 형상측정

## 차세대 극저자장 NMR/MRI 기반 분석 진단 장비 개발

김기웅\*<sup>1, 2</sup>

<sup>1</sup>한국표준과학연구원 첨단측정장비연구소 극저자장측정팀, <sup>2</sup>Dept. of Medical Physics, UST  
kwkim@kriss.re.kr

### Abstract:

Currently, micro-Tesla nuclear magnetic resonance (NMR) gets attracting interests of many researchers.  $\mu$ T-NMR is based on superconducting quantum interference device (SQUID) technology. A weak sample polarization, flux-creeping noise in a SQUID pick-up coil, and long-lasting eddy currents along the wall of a magnetically shielded room (MSR) limit the detection sensitivity of NMR signals. For solutions for those problems, we introduce dynamic nuclear polarization (DNP), superconductive magnetic hysteresis, and a new design of an MSR, respectively. These breakthrough techniques improve the performance of the NMR system and enable to widen the range of applications.

In order to develop a novel analysis instruments, we can exploit particular physical properties in a low magnetic field with the SQUID NMR technology. In this presentation, we introduce several  $\mu$ T specific applications; 2D NMR spectrum in a strongly coupled regime for material identification,  $T_1$ -enhanced contrast MRI for cancer mapping, non-field-recycling NMR with DNP, and biomagnetic resonance.

### Keywords:

핵자기공명, NMR, MRI, SQUID, Ultra low field

## 30kV 보급형 투과전자현미경 개발 현황

한철수\*<sup>1</sup>, 정종만<sup>1</sup>, 이상철<sup>1</sup>, 조복래<sup>2</sup>, 박인용<sup>2</sup>, 최기봉<sup>3</sup>, 김용주<sup>4</sup>, 김진규<sup>1</sup>  
<sup>1</sup>한국기초과학지원연구원, <sup>2</sup>한국표준과학연구원, <sup>3</sup>한국기계연구원, <sup>4</sup>코셈  
jjintta@kbsi.re.kr

### Abstract:

전자현미경은 나노 미터 수준에서 시료의 형상 또는 구조 분석이 가능한 장점 때문에 나노 및 바이오 분석 과학 분야에 있어서 필수적으로 활용되고 있는 연구장비이다. 본 발표에서는 투과전자현미경의 보급을 전량 외산 장비에 의존하고 있는 국내 환경에서 국내 기관이 자체 기술로 진행중인 연구장비 개발 프로젝트를 소개하고자 한다. 국내 자체 기술의 확보 및 이를 통해 개발 중인 투과전자현미경은 30kV급의 보급형 장비로써 바이오 분야에 활용이 가능한 성능과 장점을 가지고 있다. 성공적인 장비 개발을 위한 필수핵심 요소기술인 전계 방출형 전자총, 전자기 렌즈로 구성된 광학계, 시료 스테이지 및 영상 검출 장치 등을 다양한 전문기관들과 융합연구를 통해 개발하고 있으며, 현재 개발 중인 제작품에 대한 테스트 결과와 향후 계획에 대하여 발표할 것이다.

### Keywords:

투과전자현미경, 전계 방출 전자총, 전자 광학계, 시료 스테이지, 영상 검출 장치

## 전자현미경과 광학현미경의 융복합 장비 개발(Development of Correlative Light and Electron Microscopes)

조복래\*<sup>1, 2</sup>, 함영권<sup>2</sup>, 이광훈<sup>2</sup>, 박인용<sup>1</sup>

<sup>1</sup>한국표준과학연구원 첨단측정장비연구소, <sup>2</sup>㈜모듈사이  
blcho@kriss.re.kr

### Abstract:

현미경은 크게 가시광선을 사용하는 광학현미경과 전자빔을 사용하는 전자현미경으로 구분된다. 광학현미경은 컬러 이미지 및 3차원 정보를 볼 수 있지만 마이크로미터( $\mu\text{m}$ ) 미만의 해상도를 제공하지 않는다. 또한 전자현미경은 나노미터( $\text{nm}$ )급의 고해상도 정보를 통해 원소단위의 정보를 알 수 있지만, 이미지가 흑백이라는 단점이 있다. 한국표준과학연구원 첨단측정장비연구소 광전자융합팀에서는 개별 플랫폼인 광학현미경과 전자현미경을 하나로 통합하는 '광전자 융합현미경'을 광학과 전자 다른 두 종류의 대물렌즈를 기구적으로 융합하는 형태로 개발하였다. 연구진은 렌즈의 형태를 간섭하지 않는 형태로 재설계하여 물리적 제약을 극복했으며, 전자제어계와 소프트웨어 등의 필수요소까지 통합함으로써 분해능 700nm의 광학이미지와 분해능 3nm 이하의 전자현미경 이미지를 동시에 얻을 수 있는 현미경을 구현하였다. 광전자 융합현미경은 특히 반도체나 디스플레이 공정에서 불량품을 검출하는 데 효과적으로 사용할 수 있다. 먼저 광학 파트를 통해 마이크로 수준에서 결함이 의심되는 곳을 컬러로 파악한 후, 동시에 전자 파트로 나노 수준까지 성분을 정밀 관찰한다면 검출의 정확도를 향상시키고 소요시간을 크게 단축할 수 있다. 광전자 융합현미경은 연구원 창업기업인 (주)모듈사이를 통해 상품화가 추진되고 있다.

### Keywords:

Electron Microscope(전자현미경), Light Microscope(광학현미경)

## 국산장비신뢰성평가센터 현황

서정주\*<sup>1</sup>, 김영환<sup>1</sup>, 김민선<sup>1</sup>, 이정민<sup>1</sup>

<sup>1</sup>한국기초과학지원연구원

jjseo@kbsi.re.kr

### Abstract:

국산장비신뢰성평가센터는 분석장비의 비교/평가/진단/개선을 통해 국산장비의 신뢰도를 높여서 국산연구장비 산업을 육성, 지원하고자 설립되었다. 국산장비신뢰성평가센터는 국산장비 상시체험, 장비활용, 교육 및 홍보를 위한 활용랩을 설치 운영하고 있으며 연구 분석장비의 신뢰성평가 체계 마련을 위해 장비성능평가 표준을 구축하고 국산장비 성능평가를 진행하고 있다.

국산장비성능향상사업을 통하여 국산연구장비의 성능을 향상시키고 시장을 확장시키는 역할을 하고 있으며 국산말디질량분석기의 성능향상 사례를 발표할 예정이다.

또한 연구장비의 유지보수 전문가 육성을 통한 국내 첨단고가 연구시설 및 장비의 수명연장과 성능향상을 위한 개조·개발의 전문기술자들을 배출함으로써 연구장비 유지보수에 따른 장비 가동률 향상과 기초과학연구 활성화에 기여하고 있다.

### Keywords:

연구장비, 신뢰성 평가, 성능향상, 유지보수, 기술교육

## Theory of large intrinsic spin Hall effect in iridate semimetals

PATRI Adarsh S.<sup>1</sup>, HWANG Kyusung<sup>1, 2</sup>, LEE Hyun-Woo<sup>1, 3</sup>, KIM Yong Baek\*<sup>1</sup>

<sup>1</sup>Department of Physics and Centre for Quantum Materials, University of Toronto, <sup>2</sup>Department of Physics, The Ohio State University, <sup>3</sup>Department of Physics, Pohang University of Science and Technology  
ybkim@physics.utoronto.ca

### Abstract:

We theoretically investigate the mechanism to generate large intrinsic spin Hall effect in iridates or more broadly in 5d transition metal oxides with strong spin-orbit coupling. We demonstrate such a possibility by taking the example of orthorhombic perovskite iridate with nonsymmorphic lattice symmetry, SrIrO<sub>3</sub>, which is a three-dimensional semimetal with nodal line spectrum. It is shown that large intrinsic spin Hall effect arises in this system via the spin-Berry curvature originating from the nearly degenerate electronic spectra surrounding the nodal line. This effect exists even when the nodal line is gently gapped out, due to the persistent nearly degenerate electronic structure. The magnitude of the spin Hall conductivity is shown to be comparable to the best known example such as doped topological insulators and the biggest in any transition metal oxides. To gain further insight, we compute the intrinsic spin Hall conductivity in both bulk and thin film systems. We find that the geometric confinement in thin films leads to significant modifications of the electronic states, leading to even bigger spin Hall conductivity in certain cases. We compare our findings with the recent experimental report on the discovery of large spin Hall effect in SrIrO<sub>3</sub> thin films.

### Keywords:

Spin Hall effect, semimetals, iridate

## Spin-resolved measurements on Majorana zero modes

전(Jeon)상준(Sangjun)\*<sup>1, 2</sup>, XIE Yonglong<sup>2</sup>, LI Jian<sup>1, 3</sup>, BERNEVIG B. Andrei<sup>2</sup>, YAZDANI Ali<sup>2</sup>  
<sup>1</sup>중앙대학교 물리학과, <sup>2</sup>Department of Physics, Princeton University, <sup>3</sup>Institute for Natural Sciences,  
Westlake Institute for Advanced Study  
jsangjun@gmail.com

### Abstract:

A variety of condensed matter systems can be used to engineer topological superconductivity and MZMs. To date, evidence for MZMs has come from experiments that have detected their zero-energy excitation signature in various spectroscopic measurements when the parameters of the system make it most likely to be in a topological superconducting phase. However, the question as to whether a MZM could be distinguished from a finely tuned or accidental trivial zero-energy edge state in these experiments has been unresolved. Using spin-polarized spectroscopic measurement studied on chains of iron (Fe) atoms self-assembled on superconducting lead (Pb), we found a distinctive spin signature of MZMs that exceeds the spin-polarization of the normal-state background of iron chain. This feature, captured by a model calculations, is a direct consequence of the nonlocality of the Hilbert space of MZMs emerging from a topological band structure. This study establishes spin-polarization measurement as a diagnostic tool to distinguish topological MZMs from trivial in-gap states of a superconductor.

### Keywords:

Majorana, SPSTM

# New Fractional Quantum Hall States in Monolayer Graphene

KIM Youngwook\*<sup>1</sup>

<sup>1</sup>Max-Planck-Institut für Festkörperforschung, 70569 Stuttgart, Germany  
y.kim@fkf.mpg.de

## Abstract:

In two dimensional electron systems (2DESs) within a magnetic field, the kinetic energy of electrons is quenched and Landau levels (LL) are gradually depopulated. Clean 2DESs host various correlation-driven ground states at partially filled LL such as fractional quantum Hall effect, charge density waves (CDW), and Wigner crystallization. These correlated-phenomena strongly depend on the orbital character. For example, in GaAs fractional quantum Hall states (FQHSs) which take an odd denominator are dominant in the lowest LL of quantum number  $N = 0$ . In  $N = 2$ , however, FQHSs are absent and instead CDW phases takes over the ground state. In  $N = 1$  FQHSs and CDW phase coexist, and in addition a paired composite fermion state arises which results in an even-denominator FQHS. Recent experiments on ZnO/MgZnO and bilayer graphene have demonstrated a similar trend of ground states. In monolayer graphene, various correlated ground states have been predicted, however, only odd-denominator states have been observed and more generally experiments have focused primarily on the  $N = 0$  and  $N = 1$  LL.

Here, we present FQHSs in monolayer graphene which is encapsulated by thicker hBN layers that are additionally sandwiched between graphite. A variety of odd denominator FQHSs, as previously reported, are observed in  $N = 0$  and 1. However, surprising is that robust four-flux FQHSs are clearly resolved instead of usual two-flux FQHSs at  $N = 2$ . Also, multiple incompressible even-denominator FQHSs are observed in  $N = 3$  without any additional odd-denominator FQHSs.

## Keywords:

Fractional Quantum Hall Effect, Graphene

## Absorbing phase transition and density distribution in continuous media

LEE Sang Bub\*<sup>1</sup>

<sup>1</sup>Department of Physics, Kyungpook National University  
sblee@knu.ac.kr

### Abstract:

The nonequilibrium absorbing phase transition of interacting particles in continuous media is studied via Monte Carlo simulations. Initially  $\rho L^d$  spherical particles are distributed in a  $d$ -dimensional cubic box of side  $L$ , and those particles which overlap with other particles are considered to be active and isolated particles are inactive. The dynamics proceed in a way that active particles repel overlapped particles. If the density of particles  $\rho$  is larger than a certain critical density  $\rho_c$ , the density of active particles saturates and the system remains in an active state, whereas, if  $\rho < \rho_c$ , it decreases to 0 and the system falls into an absorbing state; thus, the system undergoes an absorbing phase transition. The critical behaviors depending on different initial distributions were discussed particularly in two dimensions in conjunction with the density distribution of particles, and the numerical results were compared with those of the continuum version of contact process. The role of impurity particles in absorbing phase transition is also discussed.

### Keywords:

absorbing phase transition, critical behavior, continuous media, Monte Carlo

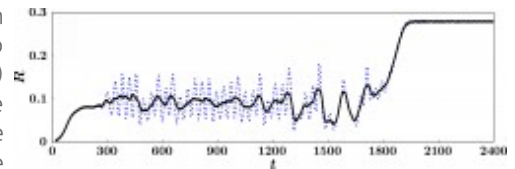
## Metastable state on the way to traveling-wave synchronization state

박진하<sup>1</sup>, 강병남\*<sup>1</sup>

<sup>1</sup>서울대학교 물리천문학부 물리학과  
kahng@phya.snu.ac.kr

### Abstract:

Presence of metastable state in synchronization transitions (STs) has been rarely highlighted. Here we consider a Kuramoto model with two competing types of oscillators, which involves a traveling-wave (TW) synchronized phase. We observe an abrupt ST from the incoherent state to the TW state through a long-lasting metastable state, similarly to the two step transitions in hybrid percolation models. Our explanation of the metastability is that the dynamic flow remains within a limited region of phase space and circulates through a few active states bounded by saddle and stable fixed points. This complex flow generates a long-lasting critical behavior, a signature of a hybrid phase transition. We show that the long-lasting period can be controlled by varying the density of inhibitory/excitatory interactions. We discuss a potential application of this transition behavior to the recovery process of human consciousness.



### Keywords:

Hybrid synchronization transition, metastability, Kuramoto model, traveling wave, consciousness recovery

## Discontinuous Percolating Transition in Growing Networks

오수민<sup>1</sup>, 손승우<sup>\*2</sup>, 강병남<sup>\*1</sup>

<sup>1</sup>서울대학교 물리학과, <sup>2</sup>한양대학교 에리카 캠퍼스 응용물리학과  
sonswoo@gmail.com, kahng@phya.snu.ac.kr

### Abstract:

We study the percolation transition of growing networks under the specific restriction rule to suppress growth of large cluster. Our network start at a single node and a new node is added every time step  $t$ . To choose two node to be linked, we select one node randomly from the set of all nodes and then randomly select the other one among the  $g$  fraction subset of nodes from the smallest clusters sorted in ascending order of cluster size  $s$ . The selected two nodes are linked with probability  $p$ . Differently from other growing network models, this restricted model not only undergoes discontinuous percolating phase transition at  $p_c$ , but also the mean cluster size starts to diverge at  $p_b$  before the percolating transition. We find the cluster size distribution  $n_s(p)$  follows a power law at  $p < p_c$  for a large cluster size  $s$ . Interestingly, for the interval of  $p_b \leq p < p_c$ , the critical exponent  $\tau$  of  $n_s(p)$  decreases from 3 to 2 continuously as  $p$  approaches from  $p_b$  to  $p_c$ . This model is reduced into a growing random networks (Callaway) model, which shows an infinite-order phase transition, when  $g$  goes to 1.

### Keywords:

percolation, discontinuous phase transition, growing networks.

## Absorbing Phase Transitions in Deterministic Fixed-Energy Sandpile Models

박수찬\*<sup>1</sup>

<sup>1</sup>가톨릭대학교 물리학과  
spark0@catholic.ac.kr

### Abstract:

We investigate the origin of the difference, which was noticed by Fey et al. [Phys. Rev. Lett. **104**, 145703 (2010)], between the steady state density of an abelian sandpile model (ASM) and the transition point of its corresponding deterministic fixed-energy sandpile model (DFES). Being deterministic, the configuration space of a DFES can be divided into two disjoint classes such that every configuration in one class should evolve to one of absorbing states, whereas no configurations in the other class can reach an absorbing state. Since the two classes are separated in terms of toppling dynamics, the system can be made to exhibit an absorbing phase transition at various points that depend on the initial probability distribution of configurations. Furthermore, we show that in general the transition point also depends on whether an infinite-size limit is taken before or after the infinite-time limit. To demonstrate, we numerically study the two-dimensional DFES with Bak-Tang-Wiesenfeld toppling rule (BTW-FES). We confirm that there are indeed many thresholds. Nonetheless, the critical phenomena at various transition points are found to be universal. We furthermore discuss a microscopic absorbing phase transition, or a so-called spreading dynamics, of the BTW-FES, to find that the phase transition in this setting is related to the dynamical isotropic percolation process rather than self-organized criticality. In particular, we argue that choosing recurrent configurations of the corresponding ASM as an initial configuration does not allow for a nontrivial APT in the DFES.

### Keywords:

fixed-energy sandpile, absorbing phase transition, Bak-Tang-Wiesenfeld

## Real-time observation of molecular dynamics during target searching and DNA cleavage by CRISPR-Cas12a

전용문<sup>1</sup>, 최유희<sup>2</sup>, 장윤수<sup>2</sup>, 구지영<sup>1</sup>, 이승환<sup>3</sup>, 정철현\*<sup>1</sup>, 이상화\*<sup>2</sup>, 배상수\*<sup>4</sup>

<sup>1</sup>한국과학기술연구원, 테라그노시스 연구단, <sup>2</sup>광주과학기술원, 고등광기술연구소, <sup>3</sup>한국생명공학연구원, 국가영장류 센터, <sup>4</sup>한양대학교, 화학과  
avecmoi@gmail.com, sanglee@gist.ac.kr, sangsubae@hanyang.ac.kr

### Abstract:

Cas12a( also called Cpf1) is a key enzyme of CRISPR-mediated immunity in prokaryotes such as the well-known Cas9 protein. As part of its essential cellular functions, the enzyme recognizes and cleaves DNA with a single guide RNA. This RNA-guided nuclease activity of Cas12a has been recently harnessed for genome editing like Cas9, but the regulation mechanism is not well understood. Using single-molecule fluorescence approach, we observed the entire dynamic processes from the target searching to the DNA cleavage by Cas12a from *Acidaminococcus sp.* (AsCas12a). Our results reveal that AsCas12a finds their target via 1D diffusion, and shows transient binding or stable binding on the target site, resulting DNA cleavage in ordered sequence. We also figured out that more than 17 bp matching of PAM-proximal region ensures the stable binding of AsCas12a which is main determinant of target recognition and cleavage. Here, based on these results, we proposed the molecular mechanism of target searching and DNA cleavage by AsCpf1 and elucidated clearly the roles of PAM in these processes.

### Keywords:

CRISPR/Cas12a, Genome editing, Single molecule tracking, Single molecule FRET

## 세포 활동에서 일어나는 분자력의 측정

KIM Byoung Choul\*<sup>1</sup>

<sup>1</sup>Major of Nano-Bioengineering, Incheon National University  
thebcklab@gmail.com

### Abstract:

보고, 듣고, 만지고, 맛보는 모든 순간에, 우리 몸에 있는 세포는 외부로부터의 자극을 인지하고, 상황에 따라 다르게 반응한다. 특히, 물리적·기계적 자극은 세포의 기능, 모양, 성장, 분화 등 다양한 세포활동에 큰 영향을 미치는 것으로 알려졌다. 이중나선 DNA를 기반으로 한 분자력 센서 (Tension Gauge Tether (TGT))는 물리적·기계적 자극이 세포 활동에 미치는 영향을 단분자 수준으로 측정할 수 있도록 고안되었다. 본 연구에서는 TGT 기술을 이용하여, 세포가 표면에 부착하고 퍼지는 과정에서 작용하는 세포막 단백질과 ECM 분자 사이의 힘의 전달 혹은 세포 신호전달체계를 활성화할 수 있었다. 그 결과 1) 세포 노화에 따른 기계적 자극에 대한 반응의 변화, 2) 세포 내TGF $\beta$ -1 혹은 Notch 신호체계 활성화에 필요한 기계적 힘의 크기를 연구할 수 있었다.

### Keywords:

Mechanobiology, Single molecule measurement

## Dynamic Control of DNA precursor synthesis in Early Embryos

송용현\*<sup>1</sup>

<sup>1</sup>고등과학원 계산과학부  
yonghyun@kias.re.kr

### Abstract:

Animal embryogenesis begins with cell divisions, which require large amounts of DNA precursors (deoxyribonucleoside triphosphates (dNTPs)). Little is understood about how embryos satisfy this demand. We examined the dNTP synthesis pathway in the early *Drosophila* embryo, in which gastrulation is preceded by 13 sequential nuclear cleavages within two hours of fertilization. Surprisingly, despite the breakneck speed at which *Drosophila* embryos synthesize DNA, maternally deposited dNTPs can generate less than half of the genomes needed to reach gastrulation. The rest of the dNTPs are synthesized “on the go”. The rate-limiting enzyme of dNTP synthesis, ribonucleotide reductase, is inhibited by endogenous levels of dATP present at fertilization and is activated as dATP is depleted via DNA polymerization. This feedback inhibition renders the concentration of dNTPs at later stages of embryogenesis robust with respect to large variations in maternal supplies, and is essential for normal progression of embryogenesis.

### Keywords:

DNA metabolism, RNR, feedback inhibition, allostery, embryogenesis

## Axonal mRNA dynamics in live hippocampal neurons

이병훈<sup>1</sup>, 방석영<sup>3</sup>, 이승렬<sup>3</sup>, 전누리<sup>3</sup>, 박혜윤\*<sup>1, 2</sup>

<sup>1</sup>Department of Physics and Astronomy, Seoul National University, Seoul, 08826, Korea, <sup>2</sup>Institute of Applied Physics, Seoul National University, Seoul, 08826, Korea, <sup>3</sup>Division of WCU (World Class University) Multiscale Mechanical Design School of Mechanical and Aerospace Engineering Institute of Advanced Machinery and Design Seoul National University, Seoul 08826, Korea  
hyeyoon.park@gmail.com

### Abstract:

Local protein synthesis has a critical role in axonal guidance and regeneration. Yet it is not clearly understood how abundantly mRNA molecules are present in axons and how the mRNA localization is regulated in axons. To address these questions, we investigated mRNA motion in live axons using a transgenic mouse that expresses fluorescently labeled endogenous  $\beta$ -actin mRNA. By culturing hippocampal neurons in a microfluidic device that allows separation of axons from dendrites, we performed single particle tracking of  $\beta$ -actin mRNA selectively in axons. We found that  $\beta$ -actin mRNAs frequently localize at the neck of filopodia which can grow as an axon collateral branch and at varicosities where synapses typically occur. Since both filopodia and varicosities are known as actin-rich areas, we investigated the dynamics of actin filaments and  $\beta$ -actin mRNAs simultaneously by using high-speed dual-color imaging. We found that axonal mRNAs likely to colocalize with actin filaments and show sub-diffusive motion within the actin-rich regions. Furthermore, we found the mRNAs that do not colocalize with actin-rich regions can show super-diffusive motion. Based on these findings, we are developing a model for the transport and localization process to understand how axonal mRNAs are targeted to the actin hot spots. The novel findings on the dynamics of  $\beta$ -actin mRNA will shed important light on the biophysical mechanisms of mRNA transport and localization in axons.

### Keywords:

Axonal mRNA,  $\beta$ -actin mRNA, Single particle tracking, Local protein synthesis

## Dynamics of transcription and transport of labeled-endogenous Arc mRNA in live neurons

박혜윤\*<sup>1, 4</sup>, 문형석<sup>1</sup>, DAS Sulagna<sup>2</sup>, SINGER Robert H.<sup>2, 3</sup>

<sup>1</sup>Department of Physics and Astronomy, Seoul National University, <sup>2</sup>Department of Anatomy and Structural Biology, Albert Einstein College of Medicine, <sup>3</sup>Howard Hughes Medical Institute, Janelia Research Campus, <sup>4</sup>The Institute of Applied Physics, Seoul National University  
hyeyoon.park@gmail.com

### Abstract:

Spatially and temporally controlled gene expression is crucial for the formation of memory. Especially, an immediate early gene Arc is known to be deeply involved in the modulation of synaptic plasticity. Upon stimulation, transcription of Arc mRNA occurs in a selected group of neurons. After transcription, Arc mRNA is transported to the desired destinations including distal parts of dendrites for local translation. These two biological phenomena, transcription and transport of Arc mRNA undoubtedly have significant roles in the memory formation. We developed Arc-PBS KI mouse for single mRNA imaging in live cells by knocking in 24 tandem arrays of PP7 binding site (PBS) in the 3' untranslated region (3' UTR) of the Arc gene. Using the Arc-PBS KI mouse, we investigated the dynamics of transcription and the transport of Arc mRNAs in live primary neuron cultures. First, we simultaneously imaged somatic  $Ca^{2+}$  activity and Arc mRNA transcription after stimulation by bicuculline. Whereas synchronized bursts of  $Ca^{2+}$  activity was induced in 100% of neurons, Arc transcription was induced only in a subpopulation of neurons during 30 min of observation after stimulation. To determine the factor governing this selection of Arc transcribing neurons, we performed immunostaining of Ser-133 residue phosphorylated transcription factor CREB and single molecule FISH of Arc mRNA together. We found that neurons with higher level of CREB phosphorylation (Ser-133) have indeed higher probability of Arc transcription. Over-expressing dominant negative form of CREB (mCREB) revealed that there is no causal effect of pCREB on Arc transcription but there could be a complex interplay between upstream signals that regulate both pCREB level and Arc transcription. We also investigated transport of Arc mRNAs along the dendrites after stimulation. Most of the Arc mRNAs were in rest phase (~88%) during one-minute observation time, and even the directed motions of Arc mRNAs were frequently interrupted by rests, similar to the previously reported behavior of  $\beta$ -actin mRNAs. The active movements of Arc mRNAs were bidirectional but slightly biased toward anterograde direction. Also contrary to the known neural activity dependent localization of Arc mRNA, inhibiting neural activity for 20 min didn't alter the moving fraction of Arc mRNA. In summary, this study presents new perspectives about the dynamics of transcription and transport of endogenous Arc mRNA, which plays important roles in synaptic plasticity at the molecular level.

### Keywords:

Single molecule imaging, memory, neuron, mRNA

## Single-molecule diffusion analysis of proteins on DNA

이종봉\*<sup>1, 2</sup>, 김대형<sup>1</sup>

<sup>1</sup>Department of Physics, POSTECH, Pohang, Korea, <sup>2</sup>School of Interdisciplinary Bioscience & Bioengineering, POSTECH, Pohang, Korea  
jblee@postech.ac.kr

### Abstract:

UV-damage to DNA can arrest DNA replication, which results in cell death. Human cells have a translesion synthesis (TLS) system that resumes the stalled DNA replication process. The interaction between p15<sup>PAF</sup> (PCNA association factor) and PCNA (proliferating cell nuclear antigen) plays an essential role at the initiation of the TLS process. The intrinsically disordered protein p15<sup>PAF</sup> regulates the DNA polymerase switching of PCNA by directly interacting with the PCNA sliding clamp for the TLS process. Interestingly, recent structure and NMR studies show that p15<sup>PAF</sup> tightly binds to the front-face of PCNA and simultaneously contacts the inside of the central hole of PCNA. To investigate the dynamic features of PCNA in the presence of p15<sup>PAF</sup>, we directly examined the thermal fluctuation-driven motion of a single PCNA and p15<sup>PAF</sup> molecule fluorescently labeled with Cy5 and Cy3 and also examined FRET changes at the DNA junction. These results strongly suggest that p15<sup>PAF</sup> may drag the movement of PCNA along the DNA to control freely diffusing PCNA. This can facilitate the switch from replicative to translesion synthesis polymerase.

### Keywords:

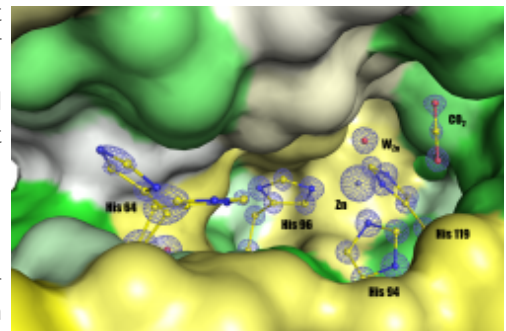
Single-molecule, fluorescent microscopy, TLS, translesion synthesis, PCNA, p15

## Tracking active-site solvents in human carbonic anhydrase II

김진균<sup>1</sup>, 김채운\*<sup>1</sup>  
<sup>1</sup>울산과학기술원  
cukim@unist.ac.kr

### Abstract:

Human carbonic anhydrase II (hCA II) is a zinc metalloenzyme that catalyzes the reversible hydration/dehydration of carbon dioxide and water to bicarbonate and a proton. In this study, ultrahigh-resolution crystallographic structures of hCA II cryocooled under various CO<sub>2</sub> internal pressures are presented. The structures reveal new intermediate solvent states of hCA II that provide crystallographic snapshots during the restoration of the proton-transfer water network in the active site. Based on these structures, a water network-restructuring mechanism is proposed. This mechanism explains how waters in the active sites are replenished, which are directly responsible for the reconnection of the proton-transfer water network. This study provides the first 'physical' glimpse of how a water reservoir flows into the hCA II active site during its catalytic activity.



### Keywords:

carbonic anhydrase II, proton transfer, intermediate states, water dynamics

## 경량유연 CIGS 박막 태양전지의 우주활용 가능성 연구

조윤애<sup>1</sup>, 곽지혜\*<sup>1</sup>, 김기환<sup>1</sup>, 안승규<sup>1</sup>, 송희은<sup>1</sup>, 김경수<sup>1</sup>, 윤재호<sup>1</sup>

<sup>1</sup>한국에너지기술연구원 태양광연구실  
bleucoeur@kier.re.kr

### Abstract:

우주자원에 대한 연구 및 활용방안은 전 세계적 관심사이며, 특히 우주 태양광발전은 위성체 등에 대한 전원공급 뿐만 아니라 에너지 부족문제를 해결할 미래기술로 연구되어 오고 있다. GaAs를 기반으로 하는 기존 우주용 태양전지인 III-V족 화합물 태양전지는 고효율의 장점을 가지나 그 제조 공정이 매우 복잡하고 고가이며 외부 충격에 약한 단점을 가지고 있다. 현재까지 국내 인공위성을 비롯한 우주비행체의 경우 위와 같은 고가의 태양전지를 전량 수입하여 사용하고 있으나 우주용 태양전지 개발 및 평가기술은 국내에 전무한 실정이다.

본 연구에서 주목하는  $\text{CuIn}_{1-x}\text{Ga}_x\text{Se}_2$  (CIGS) 화합물 박막 태양전지는 Cu, In, Ga, Se의 4원소로 이루어진 광흡수층이 갖는 높은 광흡수계수를 기반으로 22.6%의 고효율(독일 ZSW 연구소)을 보고한 바 있으며, 경량유연기판 위에 제조가 가능하고 높은 무게당 전력비와 내방사선 특성을 가지며 상대적으로 저가이므로 우주용 태양전지 활용에 매우 적합하다.

한국에너지기술연구원(KIER)에서는 1990년대 초부터 CIGS 박막 태양전지 연구를 수행해 왔으며, AM1.5 조건에서 20%의 CIGS 박막 태양전지 효율을 달성한 바 있다. 이러한 지상용 CIGS 박막 태양전지에 대한 축적된 기술과 노하우를 기반으로 경량기판 상에 CIGS 박막 태양전지를 제조하여 우주용으로 개발하고자 하는 연구가 진행 중이며, 본 발표에서는 KIER에서 제조된 CIGS 박막 태양전지에 대해 KOMAC의 양성자가속기를 활용하여 수행된 내방사선 특성 연구 결과들과 함께 관련 연구 동향을 소개하고자 한다.

### Keywords:

우주용, 화합물 박막 태양전지, 저가 경량, CIGS계 광흡수층, 우주환경 내구성

## Low Earth Orbit Space Radiation Dosimeter Onboard the NEXTSat-2

남욱원<sup>2</sup>, 문봉곤<sup>2</sup>, 박원기<sup>2</sup>, 표정현<sup>2</sup>, 손종대<sup>2</sup>, 황정아<sup>2</sup>, 이재진<sup>2</sup>, 김성환<sup>3</sup>, 류동민<sup>4</sup>, MALIMBAN Justin<sup>4</sup>, 예성준<sup>4</sup>, 김계령\*<sup>1</sup>

<sup>1</sup>한국원자력연구원 양성자가속기연구센터, <sup>2</sup>한국천문연구원, <sup>3</sup>청주대학교, <sup>4</sup>서울대학교  
kimkr@kaeri.re.kr

### Abstract:

The development of LEO-DOS (the low earth orbit space radiation dosimeter) was initiated as a scientific payload of the NEXTSat-2, which is the next generation small satellite program in Korea to be launched on 2021. The major scientific objectives of the LEO-DOS are to map the dose contribution by charged particles and neutrons in LEO, to study the space radiation and environment variations at the solar minimum activity and to verify the relative biological effectiveness (RBE) of neutrons for radiation risk assessment. The main instrument of LEO-DOS consists of the tissue equivalent proportional counter (TEPC), made of a tissue-equivalent plastic and filled with low-pressure tissue equivalent propane gas. The dos contribution by charged particles and neutrons using the anti-coincidence method in combination with a plastic detector for detecting charged particles. Therefore, the LEO-DOS is expected to provide accurate and comprehensive in-situ measurement of the local radiation environment in the low earth orbit. Also, we will discuss about some applications of LEO-DOS instrument on the ground.

### Keywords:

Space Radiation Monitor, Tissue Equivalent Proportional Counter, Neutron and Charged Particles Dose, Low Earth Orbit

## 인공위성 운영과 우주방사선 영향 분석 및 시험

고대호<sup>1</sup>, 김계령\*<sup>2</sup>

<sup>1</sup>한국항공우주연구원 탑재체광학팀, <sup>2</sup>한국원자력연구원 양성자기반공학기술개발사업단  
kimkr@kaeri.re.kr

### Abstract:

인공위성에 사용되는 전자/광학 부품은 위성이 운영되는 우주방사선 환경에 노출되어 다양한 성능 변화가 일어나게 된다. 인공위성은 한 번 발사하게 되면 수리 및 유지보수가 거의 불가능하기 때문에 이러한 성능 변화를 정확히 예상하여 이를 미연에 방지해야 한다. 이를 위하여 위성은 설계단계부터 주요 부품에 대해서 우주방사선 영향을 고려하여 다양한 분석 방법과 시험을 통하여 개발을 진행하게 된다. 본 발표에서는 실제 위성 개발에 활용되는 분석 방법 및 시험 방법과 이론적 배경을 소개하며 항공우주연구원에서 수행하였던 실험에 대해서 간략하게 소개하고자 한다.

### Keywords:

우주방사선, 인공위성

## Radiation Effect on deep sub-micron semiconductor devices

임철승\*<sup>1</sup>

<sup>1</sup>삼성전자

chul.lim@samsung.com

### Abstract:

우주 방사선 또는 반도체 패키지 내 알파 입자에 의해 반도체 메모리 소자등과 같은 기억장치 등에서 오류가 발생하며, 이를 소프트 오류라고 한다. 이러한 소프트 오류는 반도체 공정의 미세화 및 기억용량의 증가에 따라 점차 증가하는 추세이며, 이를 평가 및 감소를 위한 연구가 국내외에서 지속적으로 수행되어 왔다. 해당 세션에서는 이러한 소프트 오류에 대한 기본 개념에 대해 설명하고 이해를 높일 수 있는 시간을 마련하고자 한다.

### Keywords:

radiation effect, semiconductor devices

## 우주/자연 방사선 모사 실험을 위한 100 MeV 저선량 양성자 빔라인

김유미\*<sup>1</sup>, 윤상필<sup>1</sup>, 권혁중<sup>1</sup>, 김계령<sup>1</sup>, 조용섭<sup>1</sup>

<sup>1</sup>양성자가속기연구센터, 한국원자력연구원  
yumikim@kaeri.re.kr

### Abstract:

최근 우주/자연 산업이 성장함에 따라 우주/자연 방사선 영향에 대한 전자소자 및 물질의 관심이 증대되고 있는 추세이다. 양성자가속기연구센터에서는 우주/자연 방사선 모사 실험 등을 위한 저선량 양성자 빔을 제공할 수 있는 빔라인을 개발하여 운영 중에 있다. 저선량 빔라인은 최대 빔 에너지 100 MeV, 최대 평균 전류 10 nA 제원을 가지며, 이를 이용하여 100mm × 100mm 면적에 10% 이하의 균일도로 최소  $1.0 \times 10^5$  #/cm<sup>2</sup>의 양성자를 제공할 수 있다. 가속기에서 가속된 빔은 고출력 콜리메이터를 통과하여 빔 전류가 최소  $10^{-4}$ 로 감소하며, 이후 팔극전자석을 이용하여 균일한 빔을 제공한다. 표적실에는 빔 프로파일 및 조사선량을 측정하기 위한 이온챔버가 설치되어 있으며, 이용자의 요구조건에 따른 빔 특성을 바꾸어주기 위한 빔 이용장치가 설치되어 있다. 본 발표에서는 100 MeV 양성자가속기 기반 저선량 빔라인과 이의 초기 시험결과에 대해서 논한다.

-----  
본 연구는 미래창조과학부의 연구비 지원을 받았음.

### Keywords:

우주방사선, 자연방사선, 양성자빔, 저선량, 빔라인

## Search for the Higgs decaying to $\mu^+\mu^-$ in $t\bar{t}H$ production at CMS

LEE Sang\_Man<sup>1</sup>, 박인규\*<sup>1</sup>, 이상훈<sup>1</sup>, 강예찬<sup>1</sup>

<sup>1</sup>서울시립대학교 물리학과  
icpark@uos.ac.kr

### Abstract:

The dimuon decay mode of the Higgs bosons has a small branching ratio and currently, only an upper limit of the Higgs coupling strength to the muon has been obtained. By probing the  $t\bar{t}H$  process, in the channel where the Higgs decays into two oppositely charged muons, we aim to obtain a more precise measurement of the Higgs coupling strength to the muon while also strengthening our understanding of the Higgs coupling to the top quark. We present an optimization of the signal strength of this process by studying data obtained by the CMS detector from run 2, 13 TeV proton proton collisions at the Large Hadron Collider, utilizing all of the top pair decay channels: the full leptonic, full hadronic and semi leptonic.

### Keywords:

CMS, LHC, Higgs, Higgs Boson, muon, top

## Search for a light charged Higgs boson decaying to $c\bar{b}$ in $pp$ collisions at $\sqrt{s} = 13$ TeV

OH Byung-Hun<sup>1</sup>, YOON Inseok<sup>1</sup>, YU GeumBong<sup>1</sup>, ALMOND John Leslie<sup>1</sup>, YANG Un-ki\*<sup>1</sup>

<sup>1</sup>Seoul National University, Department of Physics  
un.ki.yang@cern.ch

### Abstract:

We present the search result of charged Higgs boson in top quark pair events using the CMS data from  $pp$  collisions at 13 TeV. In this search where charged Higgs bosons are lighter than top quark, they can appear in top quark decays as like  $t \rightarrow H + b$ . In particular, the branching ratio of charged Higgs decay into  $c\bar{b}$  can be enhanced in type-Y two Higgs doublet model.

In the lepton+jets channel of the Standard Model top pair events, the final state has one lepton, four jets (two b-jets and two light jets), and missing transverse energy. If the charged Higgs is produced from top decay, three b-jets are expected in the final state. Thus, a search for the light charged Higgs at two & three b-jets channel is performed using 36.4/fb of the data.

### Keywords:

Higgs, Light Charged Higgs, 2HDM, CMS, LHC

## Background Estimation in Same-Sign Dilepton Events Using the CMS Detector in pp Collisions at $\sqrt{s} = 13$ TeV

양운기\*<sup>1</sup>, 전시현\*<sup>1</sup>, 김재성<sup>1</sup>, 오성빈<sup>1</sup>, 알몬드준<sup>1</sup>

<sup>1</sup>서울대학교 물리학과

ukyang@snu.ac.kr, shjeon@cern.ch

### Abstract:

The same-sign dilepton channel is one of the significant features in heavy neutrino analyses due to its rare signature in the standard model. Two major backgrounds for this channel are non-prompt and charge mismeasured leptons. Non-prompt leptons are leptons that are either misidentified hadrons, leptons from heavy-flavor jets, and charge mismeasured leptons is the case when a lepton emits Bremsstrahlung radiation and is reconstructed with the wrong charge. We present the estimation methods for these two backgrounds using the pp collision data collected from CMS detector at center-of-mass energy 13 TeV.

### Keywords:

LHC, CMS, same-sign, heavy neutrino, non-prompt, charge mismeasured

## Search for high mass resonances decaying into four lepton final state at 13 TeV with the CMS detector

이준빈\*<sup>1</sup>, 유휘동<sup>1</sup>, 남경욱<sup>1</sup>

<sup>1</sup>서울대학교 물리학과  
joon.bin.lee@cern.ch

### Abstract:

A search for heavy resonances decaying into four-lepton final states in pp collisions is performed. This search is based on the data collected in CMS detector at the LHC. The full 2016 dataset corresponding to an integrated luminosity of 36 /fb at the center-of-mass energy of 13 TeV is used. Benchmark signal samples are generated using Monte Carlo simulation. Event selection takes into account the inefficiency arising from the boosted signature. Data-driven method is used to determine backgrounds with respect to fake muons. Upper limits on the cross section times branching ratio as a function of resonance mass are presented.

### Keywords:

CERN, CMS, Z', higgs, BSM, data-driven method

## Study of the differential and double differential Drell-Yan cross sections with 2016 data at 13 TeV

배달민\*<sup>1</sup>

<sup>1</sup>서울대학교 자연과학대학 물리천문학부  
dalmin.pai@cern.ch

### Abstract:

Study of the differential and double differential Drell-Yan cross sections in the dilepton channel is presented. The analysis is based on the full 2016 dataset, corresponding to an integrated luminosity of  $36 \text{ fb}^{-1}$  of proton-proton collision data collected by the CMS detector. The cross sections are studied as a function of dilepton invariant mass and rapidity. The results are corrected by taking into account difference of data and simulation. Background estimated using data-driven method and corrections including detector effects are discussed.

### Keywords:

CMS, Drell-Yan process, differential cross section, 2016, SMP

## Initial State Radiation at LHC

양운기\*<sup>1</sup>, 최준호\*<sup>1, 2</sup>, 김준호<sup>1</sup>, 서현산<sup>1</sup>, 알몬드존<sup>1</sup>, 유금봉<sup>1</sup>  
<sup>1</sup>서울대학교 물리학과, <sup>2</sup>서울대학교 기초과학연구원  
ukyung@snu.ac.kr, jhchoi@cern.ch

### Abstract:

We present a study of initial state radiations (ISR) in Drell-Yan events from pp collision at LHC with CMS data. ISR from hadron collisions plays an important role in jet physics, which has an impact on precision measurements and searches for new physics. We develop a systematic way to study the ISR effect using Drell-Yan events. The truncated mean of the dilepton transverse momentum distribution is found to have a logarithmic slope as a function of dilepton invariant mass square. This logarithmic slope can be used to control ISR effect in the SM processes and new physics processes.

### Keywords:

Standard Model, QCD, LHC, CMS

## Measurement of top quark mass using charmed meson in b-jet

박인규\*<sup>1</sup>, 김지현<sup>1</sup>, 이상훈<sup>1</sup>, 정동준<sup>1</sup>, 강다영<sup>1</sup>, 김슬기<sup>1</sup>

<sup>1</sup>서울시립대학교 물리학과  
icpark@uos.ac.kr

### Abstract:

Jet Energy uncertainty is one of the largest systematics when measuring the top quark mass. Measuring the top quark mass using charmed mesons within b-quark jet provides an alternative solution. As this method does not rely on jets when extracting the top quark mass, it reduces the systematics due to jet energy uncertainties. In this presentation, we will show the  $J/\psi$ ,  $D0$  and  $D^*$  reconstructed in the b jets. Using 2016 LHC 13 TeV data collected by the CMS detector, we measure the mass of the top quark using charm meson with an isolated lepton.

### Keywords:

LHC, CMS, Top quark mass, Charmed meson

## Measurement of $|V_{ts}|$

박인규\*<sup>1</sup>, 이상훈\*<sup>1</sup>, WATSON Ian James<sup>1</sup>, 장우진<sup>1</sup>, 전다정<sup>1</sup>

<sup>1</sup>서울시립대학교 물리학과

icpark@uos.ac.kr, jason.lee@cern.ch

### Abstract:

In the Standard Model, the strength of flavor-changing weak interactions of the quarks (e.g. from a top to a b-quark) can be described by the CKM matrix, which is required to be unitary and where the diagonal elements (describing the in-generational transitions, such as t to bW) are close to 1. In particular, the off-diagonal  $V_{ts}$  element, whose square describes the relative rate of t to sW decays, is small and has yet to be measured. Until now, only the b-quark decay of the top has been observed. We perform a measurement of the rate of the t decaying to an s-quark and W, which therefore can be interpreted as a measurement of  $|V_{ts}|$ . While  $|V_{ts}|$  is well-constrained assuming the unitarity of the CKM matrix, new physics beyond the standard model may break the unitarity condition, and therefore a direct measurement should be performed to confirm the size of  $V_{ts}$ .

### Keywords:

CKM matrix,  $V_{ts}$ , top, s quark, CMS, LHC

## Measurements of Higgs boson production and couplings using $H \rightarrow WW$ in pp collisions at 13 TeV

이상은\*1

<sup>1</sup>경북대학교 물리학부  
d4space@gmail.com

### Abstract:

Results on measurements of the standard model Higgs boson decaying to a W boson pair are reported. The event sample corresponds to an integrated luminosity of 35.9/fb, collected in pp collisions at  $\sqrt{s} = 13$  TeV by the CMS detector at the LHC during 2016.

### Keywords:

Higgs LHC CMS

## Supersymmetric gauged matrix models from dimensional reduction on a sphere

CLOSSET Cyril<sup>2</sup>, 김동욱\*<sup>1</sup>, 성락경<sup>3</sup>

<sup>1</sup>서울대학교, 물리천문학부, <sup>2</sup>TH department, CERN, <sup>3</sup>Yau Mathematical Sciences Center, Tsinghua University  
sg1841@snu.ac.kr

### Abstract:

It was recently proposed that  $N=1$  supersymmetric gauged matrix models have a duality of order four -that is, a quadrality- reminiscent of infrared dualities of SQCD theories in higher dimensions. We show that the zero-dimensional quadrality proposal can be inferred from the two-dimensional Gaiotto-Gukov-Putrov triality. We consider two-dimensional  $N=(0,2)$  SQCD compactified on a sphere with the half-topological twist. For a convenient choice of R-charge, the zero-mode sector on the sphere gives rise to a simple  $N=1$  gauged matrix model. Triality on the sphere then implies a triality relation for the supersymmetric matrix model, which can be completed to the full quadrality. While the conventional argument was mostly inspired by string theory and the geometry of Calabi-Yau manifold, this approach adds field-theoretic derivation to understanding of matrix model quadrality.

### Keywords:

gauge theory, matrix model, supersymmetry, duality, infrared duality, compactification, topological twist

## Search of heavy charged Higgs from a heavy neutral Higgs cascade decay with semileptonic final states

박성찬\*<sup>1</sup>, [KANG Dong\\_Woo](#)<sup>2</sup>, SHIN Seodong<sup>1, 3</sup>, [DERMISEK Radovan](#)<sup>4</sup>, [LUNGHI Enrico](#)<sup>4</sup>

<sup>1</sup>Department of Physics and IPAP, Yonsei University, <sup>2</sup>Department of Physics, Sungkyunkwan University,

<sup>3</sup>Enrico Fermi Institute, University of Chicago, <sup>4</sup>Physics Department, Indiana University  
seongchan.park@gmail.com

### Abstract:

We investigate the Higgs cascade decay in the extended Higgs sector. We considered the process  $pp \rightarrow H^0 \rightarrow H^\pm W^\mp \rightarrow tbW$  where  $H^0$  is heavy Higgs boson,  $H^\pm$  is charged Higgs boson. The final state is same as  $t\bar{t}$  process but the kinematic properties are different. We develop the technique using difference of kinematic properties and multivariable analysis. Our analysis technique improve the sensitivity and may give the possibility to discover the additional Higgs at the LHC or HL-LHC.

### Keywords:

Collider Physics, Heavy Higgs, Charged Higgs, LHC

## Non-thermal WIMP baryogenesis

최기영<sup>1</sup>, 강신규<sup>2</sup>, 김종국\*<sup>1</sup>

<sup>1</sup>성균관대학교, 물리학과, <sup>2</sup>서울과학기술대학교, 교양학부  
jongkukkim@skku.edu

### Abstract:

We propose a WIMP baryogenesis achieved by the annihilation of non-thermally produced WIMPs from decay of heavy particles, which can result in low reheating temperature. Dark matter (DM) can be produced non-thermally during a reheating period created by the decay of long-lived heavy particle, and subsequently re-annihilate to lighter particles even after the thermal freeze-out. The re-annihilation of DM provides the observed baryon asymmetry as well as the correct relic density of DM. We investigate how without effects can affect the generation of the baryon asymmetry and study a model suppressing them. In this scenario, we find that DM can be heavy enough and its annihilation cross section also can be larger than that adopted in the usual thermal WIMP baryogenesis.

### Keywords:

Baryogenesis dark matter early Universe

## Clockwork graviton contributions to muon $g-2$

홍덕기\*<sup>1</sup>

<sup>1</sup>부산대학교 물리학과  
deogki@gmail.com

### Abstract:

The clockwork mechanism for gravity introduces a tower of massive graviton modes, "clockwork gravitons," with a very compressed mass spectrum, whose interaction strengths are much stronger than that of massless gravitons. In this work, we compute the lowest order contributions of the clockwork gravitons to the anomalous magnetic moment,  $g-2$ , of muon in the context of extra dimensional model with a five dimensional Planck mass,  $M_5$ . We find that the total contributions are rather insensitive to the detailed model parameters, and determined mostly by the value of  $M_5$ . In order to account for the current muon  $g-2$  anomaly,  $M_5$  should be around 0.2 TeV, and the size of the extra dimension has to be quite large,  $l_5 \geq 10-7m$ . For  $M_5 \geq 1$  TeV, the clockwork graviton contributions are too small to explain the current muon  $g-2$  anomaly. We also compare the clockwork graviton contributions with other extra dimension models such as Randall-Sundrum models or large extra dimension models. We find that the leading contributions in the small curvature limit are universal, but the cutoff-independent subleading contributions vary for different background geometries and the clockwork geometry gives the smallest subleading contributions.

### Keywords:

Clockwork, graviton, muon  $g-2$ , extra dimensions

## Unitarizing SIMP scenario with dark vector resonances

최수민<sup>1</sup>, 이현민\*<sup>1</sup>, 고병원<sup>2</sup>, ALEXANDER Natale<sup>2</sup>

<sup>1</sup>중앙대학교 물리학과, <sup>2</sup>고등과학원 물리학부  
hminlee@cau.ac.kr

### Abstract:

We investigate a scenario of Strongly Interacting Massive Particles (SIMPs) where the thermal relic density of dark pion dark matter (DM) is determined by number changing  $3 \rightarrow 2$  annihilations in a strongly interacting dark sector. In this scenario, including dark vector mesons in the hidden local symmetry scheme, we find that dark vector mesons unitarize the dark chiral perturbation theory (ChPT) efficiently and extend the range of validity of the leading order calculations. In QCD-like theories with  $SU(3)_L \times SU(3)_R / SU(3)_V$  flavor symmetry, we show explicitly that the inclusion of these dark vector mesons in the  $3 \rightarrow 2$  annihilation and  $2 \rightarrow 2$  self-scattering of DM eliminates the tension between the Bullet Cluster bound and the relic density condition in a wide parameter space.

### Keywords:

Dark matter, Small-scale problems, Dark mesons

## Light inflaton completing Higgs inflation

이현민\*<sup>1</sup>

<sup>1</sup>중앙대학교 물리학과  
hminlee@cau.ac.kr

### Abstract:

We consider the extension of the Standard Model (SM) with a light inflaton where the unitarity problem in Higgs inflation is circumvented in the entire field space and the vacuum instability problem in the SM is solved at the same time. The linear non-minimal coupling of the inflaton to gravity leads to a significant kinetic mixing between the inflaton and the graviton such that perturbative unitarity is restored up to Planck scale. We show the correlation between unitarity scale and inflationary observables in this model and discuss how the effective Higgs inflation appears.

### Keywords:

Inflation, Non-minimal coupling, Higgs boson, Unitarity

## Very light dilaton and naturally light Higgs boson

홍덕기\*<sup>1</sup>

<sup>1</sup>부산대학교 물리학과  
deogki@gmail.com

### Abstract:

We study very light dilaton, arising from a scale-invariant ultraviolet theory of the Higgs sector in the standard model of particle physics. Imposing the scale symmetry below the ultraviolet scale of the Higgs sector, we alleviate the fine-tuning problem associated with the Higgs mass. When the electroweak symmetry is spontaneously broken radiatively *à la* Coleman-Weinberg, the dilaton develops a vacuum expectation value away from the origin to give an extra contribution to the Higgs potential so that the Higgs mass becomes naturally around the electroweak scale. The ultraviolet scale of the Higgs sector can be therefore much higher than the electroweak scale, as the dilaton drives the Higgs mass to the electroweak scale. We also show that the light dilaton in this scenario is a good candidate for dark matter of mass  $m_D \sim 1 \text{ eV} - 10 \text{ keV}$ , if the ultraviolet scale is about  $10 - 100 \text{ TeV}$ . Finally we propose a dilaton-assisted composite Higgs model to realize our scenario. In addition to the light dilaton the model predicts a heavy  $U(1)$  axial vector boson and two massive, oppositely charged, pseudo Nambu-Goldstone bosons, which might be accessible at LHC.

### Keywords:

light dilaton, scale symmetry, composite Higgs, naturalness problem

## Casimir scaling and Yang-Mills glueballs

홍덕기\*<sup>1</sup>, 이종완<sup>1</sup>  
<sup>1</sup>부산대학교 물리학과  
deogki@gmail.com

### Abstract:

We conjecture that in Yang-Mills theories the ratio between the ground-state glueball mass squared and the string tension is proportional to the ratio of the eigenvalues of quadratic Casimir operators in the adjoint and the fundamental representations. The proportionality constant depends on the dimension of the space-time only, and is henceforth universal. We argue that this universality, which is supported by available lattice results, is a direct consequence of area-law confinement. In order to explain this universal behaviour, we provide three analytical arguments, based respectively on a Bethe-Salpeter analysis, on the saturation of the scale anomaly by the lightest scalar glueball and on QCD sum rules, commenting on the underlying assumptions that they entail and on their physical implications.

### Keywords:

Glueballs; Yang-Mills theories; Confinement; Casimir scaling

## A recent progress in the study of in-medium quarkonium by lattice NRQCD

김세용\*<sup>1</sup>

<sup>1</sup>세종대학교 물리학과  
skim@sejong.ac.kr

### Abstract:

Quarkonium is expected to be a "thermometer" of quark-gluon plasma. Thus, in-medium properties of quarkonium is under active experimental and theoretical investigations. Over several years, we have been studying in-medium quarkonium through lattice non-relativistic QCD. It is found that the dominant systematic uncertainty in lattice NRQCD study of quarkonium centers around Bayesian reconstruction of in-medium spectral functions from quarkonium correlators. Here, we report our progress in the study of Bayesian reconstruction method and discuss our recent result on in-medium quarkonium properties from (1)highly accurate quarkonium correlator calculated by lattice NRQCD and (2)Bayesian reconstructed spectral functions of quarkonium correlators.

### Keywords:

quarkonium, quark-gluon plasma, lattice gauge theory, NRQCD

## 초중등 학생을 위한 현대물리 지도 방안 연구

박중원\*<sup>1</sup>, 조한국<sup>2</sup>

<sup>1</sup>전남대학교 물리교육과, <sup>2</sup>단국대학교 교양학부  
jwpark94@jnu.ac.kr

### Abstract:

중등학생들이 실제로는 과학수업시간에 현대물리와 관련된 내용을 배우고 싶어하고, 학생들의 일상생활이 현대물리 내용과 관련된 경우가 많으며, 첨단과학기술이 학교 물리교육에서 폭넓게 활용될 수 있다는 측면에 근거하여, 현대물리를 초중등 물리교육에 도입하기 위한 목적으로 본 연구를 수행하였다.

본 연구에서는 150명의 고등학생들을 대상으로 어떤 현대물리나 첨단과학기술 내용을 배우고 싶어하는지를 조사하고, 6명의 물리학자를 대상으로 중등물리에서 어떤 현대물리 내용이 지도될 필요가 있다고 생각하는지를 조사하였다. 그리고 2012~2017년 동안 발행된 과학잡지(과학 동아)와 2007~2017년 동안 발행된 물리교육 잡지(The Physics Teacher) 및 2013~2017년 동안 발행된 새물리에서 어떤 현대물리 내용들이 다루어져 왔는지를 조사하였다. 그리고 조사 결과를 2015 개정 물리교육과정과 비교하였다.

주요 결과는 다음과 같다. 첫째, 학생들이 배우고 싶다고 응답한 내용들 중 현대물리 내용이 24%로 약 1/4에 달하였고, 첨단과학기술 내용까지 포함하면 약 45%나 되었다. 그리고 학생들이 배우고 싶어하는 현대물리 내용들 중 약 33%가 2015 개정 교육과정에 포함되어 있었지만, 첨단과학기술 내용은 거의 없었다. 둘째, 물리학자들은 다양한 영역에서 현대물리 내용을 중등물리교육에서 필요하다고 제시하였고, 제시된 내용들 중 약 37%가 개정 교육과정에 포함되어 있었다. 셋째, 과학 동아에서는 발간호당 약 4.5개의 현대물리 내용을 주요 기사로 다루고 있었고, 그 내용들 중 약 40%가 개정교육과정에 포함되어 있었다. The Physics Teacher에서는 발간호당 약 1.3개의 기사를 현대물리 내용으로 다루고 있었고, 이들 내용 중 약 28%가 개정교육과정에 포함되어 있었다. 그러나 새물리에서는 초중등 학생을 대상으로 한 현대물리 교육 연구가 발간호당 약 0.25편에 불과하였다. 또한 위의 분석에서, 개정교육과정에 포함된 내용들은 거의 물리 I과 II에 한정되어 있어, 중학교나 고등학교 1학년 교육과정에서 다루는 내용은 거의 없었다.

마지막으로 현대물리 내용을 초중등 교육에 도입하기 위한 방안으로, 학생들에게 자연 세계에 대한 흥미와 호기심을 갖도록 하는 방식, 현대 물리 내용을 최대한 학생들의 일상적 경험과 연결짓는 방식, 그리고 현대물리 또는 첨단과학기술 내용과 관련된 다양한 시뮬레이션, 애니메이션, 동영상, 그림 자료들을 활용하는 방식을 제안하고, 구체적인 지도 자료의 예시를 제시하였다.

### Keywords:

초중등 물리교육

## 대학 일반 물리학 교수 학습의 개선 방향

정중훈\*<sup>1</sup>, 조경현<sup>2</sup>

<sup>1</sup>인하대학교 물리학과, <sup>2</sup>포항공과대학교 물리학과  
jhjung@inha.ac.kr

### Abstract:

급격한 과학기술의 발전 속에서 대학교육의 혁신을 요청하는 목소리가 더욱 높아지고 있다. 대학 일반물리학은 이공계열 대학 신입생들에게 필수적으로 요구되는 기초과학 교과목의 하나이다. 학생들에게 단편적인 물리학 지식의 전달이 아니라 과학과 기술의 융합시대를 살아가는데 필요한 살아있는 기초 물리 지식의 학습과 함께 이 과정을 통해서 비판적 사고력, 문제해결능력, 학습능력, 의사소통 능력 등의 기본 역량도 함께 기를 수 있는 교수 학습 개선 방향에 대해 논해본다.

### Keywords:

대학 일반물리학, 교수 학습 개선

## 소프트웨어를 이용한 가상 실험 및 실습

신민철\*<sup>1</sup>

<sup>1</sup>한국과학기술원 전기및전자공학과  
mshin@kaist.ac.kr

### Abstract:

계산 과학은 이론과 실험으로 양분된 기존 연구 체계에서 제3의 방법론으로 떠오른 새로운 패러다임이다. 수식으로 다루기에는 너무 난해한 문제 또는 실험하기에는 너무 비용이 많이 드는 문제에 대해서 수학적 모델링, 시뮬레이션, 가시화 등의 과정을 통하여 물리 현상에 대한 직관적 이해를 돕는 분석 도구를 제공한다. 과거 물리 교육에 사용되었던 시뮬레이션 툴은 단순한 가시화에 초점을 두었으나, 계산 과학과 접목하여 수치해석에 기반을 둔 시뮬레이션 툴은 실제 문제와 최대한 근접하게 다룸으로써 실험을 대체하거나 해석적 풀이의 한계를 뛰어넘고자 하는 목적이라는 점에서 크게 다르다. 대표적인 사례로서 미국의 nanoHUB을 들 수 있는데, 이 사이트는 전문 연구용 툴을 제공하는 것으로 출발하였으나 최근에는 전문 연구용 툴을 활용한 교육이 크게 활성화 되고 있다. 국내에서는 에디슨(edison.re.kr)를 통하여 유사한 프로젝트가 수행되었다. 에디슨 사이트는 나노 소재 및 소자에 관련한 첨단 분석 툴 뿐 만아니라 가상 실험 및 온라인 커리큘럼 등 교육에 활용할 수 있는 툴을 제공한다. 본 강연에서는 에디슨 툴에 대한 소개 및 물리 교육에 있어서의 활용에 대해서 이야기하고, 더불어 웹 기반의 실습 환경을 제공하는 Jupyter 툴에 대한 소개 및 데모를 진행할 예정이다.

### Keywords:

물리교육, 가상실험, 온라인 커리큘럼, 계산 과학

## 취업과 물리교육

정중훈\*<sup>1</sup>

<sup>1</sup>인하대학교 물리학과  
jhjung@inha.ac.kr

### Abstract:

본 발표에서는 2017년 물리학회 물리교육 위원회에서 수행한 “취업 및 자격 시험 관련 자료 수집 및 정리”과제 결과를 발표하고자 한다. 취업 시즌에 공지되는 채용 공고를 보면, 물리학과 매우 밀접한 관련이 있는 기업임에도 관련 전공에 물리학자가 명시 되지 않은 경우가 많이 있어, 전국 대학의 물리학과 학생들의 사기를 떨어뜨리고 있는 상황이다. 본 연구 발표에서는 지난 1-2년 동안 물리학과와 관련된 기업의 채용 공고 자료를 수집 정리하고, 이를 통해 물리학회 차원의 대응 방법에 대해 논의하고자 한다.

### Keywords:

취업, 자격 시험, 채용 공고

## Hodoscope Prototype Tests for J-PARC Experiments with HypTPC

정우승<sup>1, 2</sup>, 안정근<sup>\*1, 2</sup>

<sup>1</sup>고려대학교, 물리학과, <sup>2</sup>for the J-PARC E42/45 collaboration  
ahnjk@korea.ac.kr

### Abstract:

6쿼크 H-dibaryon을 찾는 J-PARC E42실험과 Missing Baryon Resonance를 연구하는 J-PARC E45실험을 위하여 초전도전자석과 TPC(HypTPC)로 구성된 Hyperon Spectrometer를 개발하였다. HypTPC는 TPC 본체와 TPC Hodoscope로 이루어져 있다. TPC Hodoscope는 트리거의 생성 및 HypTPC에서 검출된 입자들의 구별을 하는 역할을 담당한다. 따라서 HypTPC를 포용하는 넓은 수용 면적을 가져야 한다. 그렇기 때문에 TPC Hodoscope는 크기  $80^L \times 7^W \times 1^T$  cm의 32개 신틸레이터가 TPC의 옆을 둘러싸는 형태를 갖는다. 그리고 1.5 T 자기장 안에서 동작하기 위하여 Multi-Pixel-Photon-Counter(MPPC)를 사용하여 신호처리를 한다. 실제 검출기에 사용될 신틸레이터보다 짧은  $15^L \times 7^W \times 1^T$  cm 크기의 신틸레이터를 사용하여 TPC Hodoscope의 시제품을 제작하였다. 시제품의 우주선 테스트를 결과 약 170 ~ 180 ps의 시간 분해능을 얻을 수 있었다. 앞으로 실제 빔을 이용한 테스트 또한 계획하고 있다. 이번 발표에서 TPC Hodoscope 시제품의 우주선 테스트 결과와 Hyperon spectrometer의 예상 성능을 논의할 것이다.

### Keywords:

J-PARC, H-dibaryon, E42, E45, TPC, Trigger Hodoscope, MPPC

## 면적선원 표면방출을 절대측정기 개발

황상훈\*<sup>1</sup>, 박태순<sup>2</sup>, 이경범<sup>1</sup>, 이종만<sup>1</sup>, 선용근<sup>1, 3</sup>

<sup>1</sup>한국표준과학연구원 방사선표준센터, <sup>2</sup>(주)덕인, <sup>3</sup>경북대학교 물리학과  
shhwang@kriss.re.kr

### Abstract:

표면오염감시기는 방사성동위원소를 사용하는 다양한 작업장에 사용되며 6개월마다 교정이 법으로 정해져 있다. 교정 수행을 위해서는 알파 혹은 베타를 방출하는 면적선원을 이용하며 방출효율과 표면오염검사기의 계수율을 비교한다. 면적선원의 표면방출을 측정을 위해서 한국표준과학연구원(KRIS)의 표면방출을 절대측정장치 (다중선 비례계수기, MWPC)을 이용한다. 표준기로 사용중인 다중선 비례계수기는 약 30년전에 제작되었으며 Cl-36 면적선원을 이용하여 0.46%의 불확도를 보인다. 최근 남아프리카공화국의 표준원인 NMISA에서 다중선비례계수기의 제작을 요청하였으며, 본원 표준기의 교체를 위해서 새로운 다중선 비례계수기를 제작하였다. 본 발표에서는 새로운 다중선비례계수기의 소개와 Cl-36과 Am-241의 면적선원을 이용한 불확도 산출에 대한 결과를 발표할 예정이다.

### Keywords:

다중선비례계수기, 면적선원

## 20MeV 양성자 빔을 이용한 ALPIDE(ALICE Pixel Detector)의 총 이온화 선량 효과 측정가능성 연구

엄종식<sup>1</sup>, 이상현<sup>1</sup>, 유인권<sup>\*1</sup>  
<sup>1</sup>부산대학교 물리학과  
yoo@pusan.ac.kr

### Abstract:

ALPIDE(ALICE Pixel Detector)는 MAPS(Monolithic Active Pixel Sensor)를 기반으로 제작된 픽셀 검출기이다. ALICE에서는 이 ALPIDE칩을 사용하여 내부궤적장치(Inner Tracking System)의 업그레이드가 현재 진행 중이며, 이 칩의 방사선 내구성 연구는 중요한 특성 연구의 하나이다. 본 연구에서는 이 ALPIDE 칩의 방사선내구성 특성연구에 한국 경주의 양성자 가속기를 어떻게 활용할 수 있는지를 타진하였다. 이 연구를 위하여 경주 양성자 가속기의 20MeV 양성자빔(플럭스:  $10^{13}/\text{cm}^2\text{s}$ )을 사용하며 100 $\mu\text{m}$  두께의 금 박을 이용하여 빔 플럭스를 감소시켰다. 일정 흡수선량에 도달할 때까지 빔을 조사한 후에 픽셀 내부 회로의 전하 문턱값 및 이 회로를 제어하는 DAC의 선형성을 측정하였고, 목표 흡수선량까지 이를 반복하였다. 본 발표에서는 먼저 GEANT4 모의실험 및 측정값을 이용하여 계산한 흡수선량값에 대해 논의하고 측정 전/후의 회로 제어용 DAC들의 선형성 결과를 확인하여 DAC가 주는 영향을 확인한다. 그리고 흡수선량에 따른 전하 문턱값의 변화 및 시간에 따른 변화와 그 회복효과에 대해서 논의한다. 측정된 흡수선량에 따른 전하 문턱값의 변화를 기존의 측정결과와 비교하여 경주 양성자 가속기 연구소의 양성자빔을 이용한 총 이온화 효과 활용가능성을 논의한다.

### Keywords:

ALPIDE, MAPS, 방사선 내구성, 총 이온화 선량

## 단일형 활성 실리콘 픽셀 센서의 디자인에 따른 전하수집효율 및 전하수 집시간 연구

이상현<sup>1</sup>, 송지혜<sup>1</sup>, 오근수<sup>1</sup>, 유인권\*<sup>1</sup>  
<sup>1</sup>부산대학교 물리학과  
yoo@pusan.ac.kr

### Abstract:

단일형 활성 픽셀 센서 (Monolithic Active Pixel Sensor, MAPS) 기술은, 신호 처리 회로를 실리콘 센서와 결합시킨 신기술로서, 이를 이용한 실리콘 센서 (Silicon sensor)는 통과하는 입자의 뒤튐림을 최소화하면서도 뛰어난 공간 분해능과 효율을 가져 입자 충돌 실험에서의 차세대 검출기로서 기대되고 있다. 인베스티게이터 (Investigator)는, 현재 ALICE 및 STAR의 내부궤적장치 (업그레이드) 에 주로 사용된 실리콘 센서 이 후를 위하여 연구, 개발이 진행 중인 차세대 실리콘 센서이다. 인베스티게이터는 서로 다른 134개의 미니 (8×8 픽셀) 매트릭스로 구성돼 있으며, 각 미니 매트릭스는 다양한 크기 (20 $\mu$ m ~ 50 $\mu$ m)의 픽셀 및 수집 N-well (Collection N-well) 간격 (Spacing) 을 가지고 있다. 본 발표에서는 다양한 픽셀 센서 디자인에 따른 전하수집효율 (Charge Collection Efficiency) 및 전하수집시간 (Charge Collection Time) 의 측정결과가 다루어질 예정이다.

### Keywords:

단일형 활성 실리콘 픽셀 센서, 인베스티게이터, 전하수집효율, 전하수집시간

## Primary System for Measurement of the Beta Emitting Gaseous Radioactive Isotopes at KRISS

황상훈\*<sup>1</sup>, 선용근<sup>1, 2</sup>, 이종만<sup>1</sup>, 이경범<sup>1</sup>, 김우영<sup>2</sup>

<sup>1</sup>한국표준과학연구원 방사선표준센터, <sup>2</sup>경북대학교 물리학과  
shhwang@post.j-parc.jp

### Abstract:

한수원중앙연구원의 연구에 따르면 원자력발전소에서 배출되는 베타입자를 방출하는 기체상의 방사성 동위원소 (<sup>37</sup>Ar, <sup>39</sup>Ar, <sup>85</sup>Kr, <sup>127</sup>Xe, <sup>131m</sup>Xe, <sup>133</sup>Xe, <sup>3</sup>H)의 배출량은 경수로원전의 경우 2001년~2010년 사이 연평균 11.61 TBq/reactor이다. 이렇게 많은 방출량에도 국내에서는 기체상의 방사성 동위원소의 방사능을 절대측정 할 수 있는 기술이 미흡하다. 국외 표준기관 (NPL, NMIJ, PTB, LNH, NIST 등)에서 길이보상법을 이용한 내부비례계수기를 이용하여 기체상 방사능 절대측정기술을 확보하고 유지하고 있다. 이에 한국표준과학연구원(KRISS)에서 이 방법을 이용하여 primary system을 개발하였고 시운전 중에 있다. 현재의 시스템은 25 mm의 내경을 갖는 길이가 다른 스테인레스의 튜브 3개(150 mm, 200 mm and 350 mm)와 이온화된 전자를 수집하는 애노드 역할을 하는 25  $\mu$ m의 지름을 갖는 금이 입혀진 텅스텐와이어로 구성되어있다. 이 3개의 튜브는 지름이 600mm인 하나의 큰 진공챔버안에 위치해 있다. 방사성 가스로 9:1의 비로 아르곤과 메탄이 섞여있는 P-10가스를 이용한다. 카운터에 인가하는 전압과 챔버안의 적절한 가스 압력을 정하고 문턱 에너지 레벨을 알기위해서 X-ray 선원인 Fe-55를 각 카운터에 설치하였다. Kr-85 선원을 이용하여 시운전하였다. 이 발표에서 Kr-85의 방사능과 불확도에 대한 예비 결과를 논의할 것 입니다.

### Keywords:

Primary System, proportional counter, Length-compensation, Gaseous Radioactive Isotopes, 원자력발전, 기체상 방사능, 내부비례계수기, 절대측정, 국가표준

## Production of Hyperpolarized $^{129}\text{Xe}$ with Optical Pumping and Spin Exchange

KAVTANYUK Vladimir<sup>1</sup>, STEPANYAN Samuel<sup>1</sup>, CHEBOTARYOV Sergey<sup>1</sup>, TAN Joshua Artem<sup>1</sup>, 박형우<sup>1</sup>,  
선용근<sup>1</sup>, ANDO Yu<sup>1</sup>, 배영철<sup>1</sup>, 김우영\*<sup>1</sup>  
<sup>1</sup>경북대학교 물리학과  
wooyoung@knu.ac.kr

### Abstract:

Hyperpolarized  $^{129}\text{Xe}$  was successfully obtained with a highest output of  $55\pm 2\%$  using spin-exchange via optical pumping (SEOP) method. SEOP is based on polarizing the valence electron of the alkali metal ( $^{85}\text{Rb}$ ) by the resonant absorption of a laser light, enhancing a single state of the ground level. The polarization of  $^{129}\text{Xe}$  happens due to collisions with polarized Rb vapor by the spin-exchange process. The experiment performed at a total pressure 600 Torr, under a 30 Gauss magnetic field, and using a 60 W circularly polarized laser light with a wavelength tuned to 794.7 nm.  $\text{N}_2$  and  $^4\text{He}$  were used as buffer gases. Polarization measurements were done using a  $216\pm 1$  G permanent magnet. Depolarization time  $T_1$  of the hyperpolarized  $^{129}\text{Xe}$  was measured to be about 2 hours. Nuclear magnetic resonance (NMR) Apollo LF-1 apparatus was responsible for data acquisition.

### Keywords:

Polarization,  $^{129}\text{Xe}$ , Spin Exchange, Optical Pumping

## 2D Semiconductor Monolayers and Heterostructures

CHANG Wen-Hao\*<sup>1</sup>

<sup>1</sup>Department of Electrophysics, National Chiao Tung University, Hsinchu, Taiwan  
whchang@mail.nctu.edu.tw

### Abstract:

Semiconductor heterojunctions (HJs) have played a central role in both fundamental physics and modern device applications. Recent advances in HJs formed by vertically stacked or laterally stitched 2D semiconductors, such as transition metal dichalcogenide (TMD) monolayers, further push semiconductor HJs down to atomically-thin thickness with atomically sharp interface, providing new opportunity for novel device applications. TMD HJs also feature their type-II band alignment, which can separate photoexcited electrons and holes in different materials through efficient interlayer charge transfer, making them very promising for photovoltaic applications. In this talk, I will present our recent endeavors on the material synthesis and fundamental study of 2D TMDs. Firstly, I shall demonstrate the growth of various TMD monolayers and HJs by chemical vapor deposition (CVD). The valley dynamics of monolayer TMD will be discussed. I will also demonstrate the manipulation of light-matter coupling in 2D TMDs using photonic and plasmonic structures. Finally, I will show new coupled spin-valley physics in TMD vertical HJs caused by the interlayer quantum interference.

### Reference

- [1] W.-T. Hsu *et al.*, to appear in Nature Comm. (2018).
- [2] W.-T. Hsu *et al.*, Nature Comm. **8**, 929 (2017).
- [3] W.-T. Hsu *et al.*, Nature Comm. **6**, 8963 (2015).
- [4] M.-Y. Li *et al.*, Science **349**, 524-528 (2015).
- [5] W.-T. Hsu *et al.*, ACS Nano **8**, 2951 (2014).

### Keywords:

transition metal dichalcogenide, Semiconductor heterojunctions

## Two-dimensional heterostructure electronic devices

LEE Gwan-Hyoung\*<sup>1</sup>

<sup>1</sup>Materials Science and Engineering, Yonsei University  
gwanlee@yonsei.ac.kr

### Abstract:

Two-dimensional (2D) materials have brought a great deal of excitement to nanoscience community with their attractive and unique properties. Such excellent characteristics have triggered highly active researches on 2D material-based electronic devices. New physics observed only in 2D semiconductors allow for development of new-concept devices. However, there are several obstacles to be overcome for practical application of 2D materials and their devices. In this talk, I will show novel approach to fabricate high performance 2D electronic devices by utilizing van der Waals heterostructures, which have been achieved by putting a 2D material onto another. This enables us to investigate intrinsic physical properties of atomically-sharp heterostructure interfaces and fabricate high performance optoelectronic devices for advanced applications. I used unique band structures of 2D materials and their heterostructures to reduce Schottky barrier between 2D semiconductor and contact and eliminate scattering from charged impurities.

### Keywords:

Two-dimensional heterostructure electronic devices

# Excitonic Fine Structures of Semiconducting Low-dimensional Nano-materials

CHENG Shun-Jen\*<sup>1</sup>

<sup>1</sup>Department of Electrophysics, National Chiao Tung University, Hsinchu, Taiwan  
sjcheng@mail.nctu.edu.tw

## Abstract:

Owing to inherent or extrinsic symmetry breakings, the excitonic spectra of semiconductors under photo-excitation usually cannot sustain the multi-fold spin- or pseudospin-degeneracy of the ground states, and are featured by fine structure splittings (FSSs) caused by Coulomb interactions. The excitonic fine structures (FS's) of low-dimensional semiconductors have been well recognized as an intriguing feature involved in rich physics phenomena, including bright-dark exciton conversion, exciton dynamics, thermalization-induced decoherence, and entanglement of emitted photon pairs. In this talk, I will present our recent theoretical and computational investigations of the excitonic fine structures of low-dimensional semiconductors, including the quasi-0D self-assembled semiconductor quantum dots [1] and 2D transitional metal dichalcogenide (TMD) monolayers.[2] In the former, we conduct group theory analysis and numerical computations for the exciton spectra of GaAs droplet epitaxial QDs in the multi-band theory. We show that the FSSs of asymmetric QDs can be well tuned and even fully eliminated by the application of external stresses. The predicted stress-elimination of the FSSs of photo-excited QDs is a desirable feature for realizing QD-based "on-demand" entangled photon-pair emitters.[1] In the studies of 2D TMD monolayers, we solve the Bethe-Salpeter equation for strongly bound exciton subjected to strong direct Coulomb interactions and spin- and valley-associated e-h exchange ones, based on the DFT-based tight binding theory. The computational results present rich spectral features of the exciton fine structures in the 2D materials, composed of the states of bright exciton, spin-forbidden dark exciton, and momentum-forbidden indirect exciton. It is shown that the scatterings between the bright exciton states and the valley indirect exciton ones could be significant via long-wavelength phonons at finite temperatures, and the emergence of the valley indirect exciton in the fine structures essentially affect the optical behavior of the 2D material under thermalization.[3]

## References

- [1] O. Benson, C. Santori, M. Pelton, and Y. Yamamoto, Phys. Rev. Lett. **84**, 2513 (2000).
- [2] K. F. Mak, *et al.*, Phys. Rev. Lett. **105**, 136805 (2010).
- [3] M. Selig *et al.*, Nature Comm. **7**, 13279 (2016).

## Keywords:

Exciton, 2D materials

## 2D materials-based gas sensors

YANG Woochul\*<sup>1</sup>, ZHANG Shaolin<sup>1</sup>, HANG Nguyen Thuy<sup>1</sup>

<sup>1</sup>Department of Physics, Dongguk University  
wyang@dongguk.edu

### Abstract:

Gas sensors able to identify or quantify specific gases and vapors have been applied in many fields such as industry and agriculture production, indoor and outdoor environmental monitoring, and medical diagnosis. Metal oxides, as mostly applied conventional sensor materials, have been widely utilized for gas sensing for their low costs and high sensitivities. However, their high operating temperature and consequent large power consumption, as well as low selectivity make them not applicable for next generation wearable sensor application. It is necessary to explore high-performance gas sensing materials with room or low operating temperature.

Recently raised two-dimensional (2D) materials, represented by graphene and its layered inorganic analogues, have presented great potential in room-temperature gas sensor application owing to their large surface-to-volume ratio and strong surface activities, which would be excellent substitutes of metal oxides for developing next generation gas sensor. In this study, we present our recent works related to the 2D materials-based gas sensors. Graphene, graphene-like carbon nitride ( $g\text{-C}_3\text{N}_4$ ), and transition metal dichalcogenides (TMDs) nanosheets, including  $\text{MoS}_2$  and  $\text{MoSe}_2$ , were fabricated in large-scale by optimized liquid-phase exfoliation methods, and applied to detect volatile organic compounds (VOCs) and humidity vapors. Systematic and comparative studies have been conducted to investigate the sensing properties of pure and composited 2D materials. The gas sensing mechanisms have been revealed. These results are expected to be of instructive significance to the future design of 2D materials-based gas sensors.

### Keywords:

2D materials; gas sensor;  $g\text{-C}_3\text{N}_4$ ;  $\text{MoS}_2$ ; VOC gas

## Tunneling photocurrent assisted by interlayer excitons in staggered van der Waals heterobilayers

이현석\*<sup>1, 2</sup>

<sup>1</sup>충북대학교 물리학과, <sup>2</sup>기초과학연구원 나노구조물리연구단  
hsl@chungbuk.ac.kr

### Abstract:

Vertically stacked van der Waals (vdW) heterostructures have been suggested as a robust platform for studying interfacial phenomena and related electric/optoelectronic devices. While interlayer Coulomb interaction mediated by vdW coupling has been extensively studied for carrier recombination processes in diode transport, its correlation with interlayer tunneling transport has not been elucidated. Here, we report a contrast between tunneling and drift photocurrents tailored by the interlayer coupling strength in MoSe<sub>2</sub>/MoS<sub>2</sub> heterobilayers (HBs).

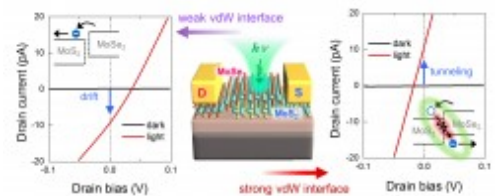
Interfacial coupling modulated by thermal annealing was identified by interlayer phonon coupling in Raman spectra and the emerging interlayer exciton peak in photoluminescence spectra. In strongly coupled HBs, positive photocurrent was observed owing to inelastic band-to-band tunneling assisted by interlayer excitons that prevailed over exciton recombination. By contrast, weakly coupled HBs exhibited a negative photovoltaic diode behavior, manifested as a drift current without interlayer excitonic emission. Our study sheds light on tailoring tunneling transport for numerous optoelectronic HB devices [1].

### References:

[1] D. H. Liang *et al.*, *Adv. Mater.* 29,1701512 (2017)

### Keywords:

transition metal dichalcogenides, van der Waals heterobilayers, tunneling, photovoltaics, interlayer excitons



## Investigation of thickness-dependent avalanche breakdown phenomena in MoS<sub>2</sub> field-effect transistors

박진수<sup>1</sup>, 이택희\*<sup>1</sup>, 장연식<sup>1</sup>, 김재근<sup>1</sup>, 조경준<sup>1</sup>, 신지원<sup>1</sup>, 정승준<sup>1</sup>

<sup>1</sup>서울대학교 물리학과  
tlee@snu.ac.kr

### Abstract:

Recently, two-dimensional (2D) molybdenum disulfide (MoS<sub>2</sub>) has been widely investigated to realize field-effect transistor (FET) applications.[1] Although their electrical characteristics have been extensively studied, there is no report on the electrical properties of MoS<sub>2</sub> FETs under a high electric field due to their limited efficiency of energy dissipation from atomically-thin thickness. Here, we report our study of the avalanche breakdown in MoS<sub>2</sub> FETs under high electric fields. The critical electric field ( $E_{CR}$ ) and impact ionization rate ( $\alpha$ ) were carefully investigated. The measured results indicated that the values of  $E_{CR}$  and  $\alpha$  had a strong dependence on the layer thickness of MoS<sub>2</sub>, which is closely related to its quantum confinement effect in the unique 2D systems. Furthermore, we systemically investigated avalanche breakdown phenomena in MoS<sub>2</sub> FETs with various channel lengths corresponding to electrical fields under different gate bias and temperature conditions.

### References

[1] B. Radisavljevic et al., *Nature Nanotechnology*, **6**, 147 (2011).

### Keywords:

mos2, field-effect transistors, avalanche breakdown

## Broadband Omnidirectional Absorption Enhancement of MoS<sub>2</sub> on Sub-100-nm SiO<sub>2</sub>/Si

KIM Dong-Wook\*<sup>1</sup>, [KIM Eunah](#)<sup>1</sup>, CHO Jin-Woo<sup>2</sup>, NGUYEN Trang Thi Thu<sup>1</sup>, KIM Sun-Kyung<sup>2</sup>, YOON Seokhyun<sup>1</sup>

<sup>1</sup>Department of Physics, Ewha Womans University, <sup>2</sup>Department of Applied Physics, Kyung Hee University  
dwkim@ewha.ac.kr

### Abstract:

MoS<sub>2</sub>, one of the most representative 2D atomically thin semiconductors, has attracted great research interest due to its unique optical, electrical, and mechanical properties. Optical spectra of MoS<sub>2</sub> allow us to identify the layer thickness, estimate the bandgap energy, and characterize the structural phase. In this regard, enhanced light-matter interaction in the MoS<sub>2</sub> layers is crucial for the material characterization as well as its optoelectronic device applications. To boost the optical absorption, researchers have used photonic nanostructures, Fabry-Perot-type cavities, and plasmonic metal nanostructures. In this work, we investigated optical characteristics of the MoS<sub>2</sub> monolayers on SiO<sub>2</sub>/Si substrates with very thin SiO<sub>2</sub> layers (thickness of SiO<sub>2</sub> = 40 ~ 130 nm). The propagation of light in the sub-100 nm SiO<sub>2</sub> layer results in the phase change of light but it is not enough to induce the Fabry-Perot resonance. It should be noted that the incident light undergoes phase changes upon reflection and transmission at the MoS<sub>2</sub>/SiO<sub>2</sub> and MoS<sub>2</sub>/air interfaces due to the large extinction coefficient of MoS<sub>2</sub>. The interface phase change is insensitive to the wavelength and incident angle of the light. The measured Raman and optical reflection spectra of the samples clearly showed that the MoS<sub>2</sub> monolayers on sub-100 nm SiO<sub>2</sub>/Si substrates exhibited broadband omnidirectional absorption enhancement. This work showed that the use of sub-100-nm-thick SiO<sub>2</sub>/Si substrates could provide us a very useful means to tune the optical spectral responses of 2D semiconductors.

### Keywords:

broadband, omnidirectional, absorption, MoS<sub>2</sub>, SiO<sub>2</sub>

## Polarized Raman Study of Group IV Monochalcogenides: SnS and SnSe

정현식\*<sup>1</sup>, SRIV Tharith<sup>1</sup>  
<sup>1</sup>서강대학교 물리학과  
hcheong@sogang.ac.kr

### Abstract:

Tin sulfide (SnS) and tin selenide (SnSe) are group IV monochalcogenides of orthorhombic structure and belong to the space group  $D_{2h}^{16}$  (Pnma), which have eight atoms per unit cell. These two materials show different electrical and optical properties, which are useful in thermoelectric devices and photovoltaic applications [1-3]. The different perspective views of these group IV monochalcogenides along the  $a$ -,  $b$ - and  $c$ -axial directions result in interesting anisotropic nature [4]. Polarized Raman spectroscopy can effectively be used to study the anisotropic properties of thin materials such as black phosphorous and tungsten diselenide (WSe<sub>2</sub>) [5-7]. Additionally, this technique was employed to study the anisotropic properties of SnS and SnSe single crystals [8] using 647.1 nm laser. Recently, similar study was done to reveal the anisotropy and thickness dependence of thin SnS flake synthesized by physical vapor deposition (PVD) method using 514.5 and 632.8 nm lasers [9]. Similarly, polarized-Raman measurements were performed on SnSe nanosheets and nanoplate that were grown using chemical vapor deposition (CVD) and PVD, respectively [10-11], to find their properties. However, no systematic studies on mechanically exfoliated thin SnS and SnSe samples were done. In our study, we performed polarization-angle dependence of the Raman modes of mechanically-exfoliated thin SnS and SnSe samples of different thickness by using 632.8, 514.4 and 441.6 nm excitation wavelengths. Laser power was kept below 100 uW to avoid local heating. Our results show strong thickness, polarization angle and excitation energy dependences of A<sub>g</sub> and B<sub>3g</sub> modes of mechanically-exfoliated thin SnS and SnSe samples.

### References

- [1]. M. Kul, *Vacuum* 107, p. 213 (2014).
- [2]. E. Barrios-Salgado, M. T. S. Nair, and P. K. Nair, *J. Solid State Science & Technology* 3, p. 169 (2014).
- [3]. L.-D Zhao et al., *Nature* 508, p. 373 (2014).
- [4]. W. Shi et al., *Adv. Sci.*, pp. 1-18 (2018).
- [5]. A.-L Phaneuf-L'Heureux et al., *Nano Lett.* 16, pp. 7761-7767 (2016).
- [6]. J. Wu, N. Mao, L. Xie, H. Xu and J. Zhang, *Angew. Chem.* 127, pp. 2396-2399 (2015).
- [7]. S. Kim, K. Kim, J.-U Lee and H. Cheong, *2D Materials* 4, p.\_\_\_\_ (2017).
- [8]. H. R. Chandrasekhar, R. G. Humphreys, U. Zwick, and M. Cardona, *Phys. Rev. B* 15, p. 2177 (1977).
- [9]. M. Li et al., *RSC Adv.* 7, pp. 8759-48765 (2017).
- [10]. T. Pei et al., *Adv. Electron. Mater.* 2, pp. 1-7 (2016).
- [11]. X.-Z. Li et al., *Nanoscale* 9, p. 14558 (2017).

### Keywords:

Tin sulfide (SnS), tin selenide (SnSe), polarized Raman spectroscopy, AFM

## Resonance behaviours of graphene mechanical resonators with a porous structure

이상욱\*<sup>1</sup>, 권민희<sup>1</sup>, 윤주희<sup>1</sup>, 신동훈<sup>1</sup>, 최준희<sup>1</sup>

<sup>1</sup>이화여자대학교 물리학과  
nicesw@gmail.com

### Abstract:

In the present work, we studied the resonance behaviours of holey graphene drums with various periodic patterns. Finite element modeling simulation results suggest that the resonance frequency of the graphene drum gradually increases and then drops as the number of pores of the graphene increases from 0 to 100. The porous graphene resonator devices were also realized by transferring a porous graphene membrane on to a SiN window, and their resonance behaviours were experimentally characterized and compared with simulation results. In this presentation, we discuss the simulation and experimental results in detail.

### Keywords:

nanoelectromechanical systems, mechanical resonator, graphene

## Sunlight Photocatalytic Activity of Graphene-V<sub>2</sub>O<sub>5</sub> Micro/Nano spheres

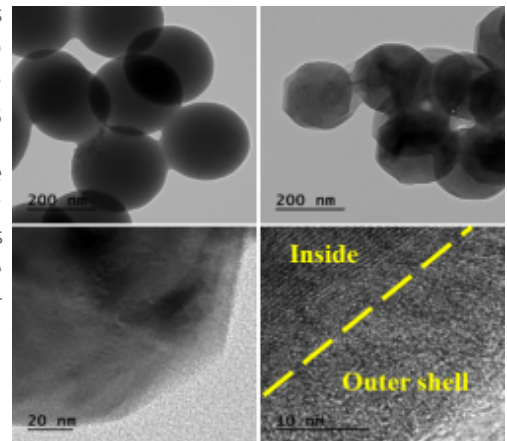
김석원\*<sup>1</sup>, LE Top Khac<sup>1</sup>, 강만일<sup>1</sup>  
<sup>1</sup>울산대학교 물리학과  
sokkim@ulsan.ac.kr

### Abstract:

Pure V<sub>2</sub>O<sub>5</sub> micro/nano spheres and graphene-V<sub>2</sub>O<sub>5</sub> micro/nano spheres (G-V<sub>2</sub>O<sub>5</sub>) with different diameters of V<sub>2</sub>O<sub>5</sub> spheres were prepared by two steps combined chemical reaction and hydrothermal methods. The morphologies and crystal structure of the pure V<sub>2</sub>O<sub>5</sub> and G-V<sub>2</sub>O<sub>5</sub> micro/nano spheres were investigated by SEM, TEM, XRD, and Raman measurements. The decreased emission intensity in the photoluminescence spectra and the increased photoconductivity of G-V<sub>2</sub>O<sub>5</sub> show that charge-carriers facile transfer from V<sub>2</sub>O<sub>5</sub> to graphene. The photocatalytic activities of pure V<sub>2</sub>O<sub>5</sub> and G-V<sub>2</sub>O<sub>5</sub> micro/nano spheres with methylene blue dye under direct sunlight irradiation show that G-V<sub>2</sub>O<sub>5</sub> exhibits higher photodegradation efficiency than that of the pure V<sub>2</sub>O<sub>5</sub>.

### Keywords:

V<sub>2</sub>O<sub>5</sub> micro/nano spheres, graphene-V<sub>2</sub>O<sub>5</sub> micro/nano spheres, photocatalyt



## Local chemical modification of MoS<sub>2</sub> layer using AFM lithography

박배호\*<sup>1</sup>, 오다예<sup>1</sup>, 이덕현<sup>1</sup>, 오광택<sup>1</sup>, 전지훈<sup>1</sup>  
<sup>1</sup>건국대학교 물리학과  
baehpark@konkuk.ac.kr

### Abstract:

Van Waals Force로 layer 구조를 이루고 있는 TMD(Transition metal dichalcogenide) 물질들은 Semiconductor의 특징을 지님과 동시에 Transition metal에 따라 서로 다른 물성을 보여주기 때문에 여러 방면으로 다양한 연구가 진행되고 있다. 그 중 MoS<sub>2</sub> 물질은 phase에 따라 Semiconductor 또는 Metal 특성을 보여주기도 하며, Hydrogenation이나 Proton irradiation을 통해 magnetic적 특성이 변하는 등 기초 물성에 대한 연구가 소자응용연구와 함께 활발히 진행되고 있다.

본 연구에서는 AFM lithography를 통해 graphene 표면의 C-OH, C-O-C, C-O 결합을 조절하였던 선행연구를 바탕으로 MoS<sub>2</sub>의 표면을 국소적으로 Oxidation 또는 Hydrogenation을 하여 그에 따른 전기적 또는 자기적 변화에 대한 연구를 진행하였다. Raman 측정을 통해 lithography 환경에 따른 Phase transition를 확인, Magnetic force microscopy(MFM) 측정을 통해 lithography 조건에 따른 MoS<sub>2</sub>의 Magnetic 변화를 측정하였다. 본 연구결과는 국소적인 Oxidation 또는 Hydrogenation 된 MoS<sub>2</sub>가 차세대 Magneto-electronic 소자 연구에 응용될 것으로 기대된다.

### Keywords:

MoS<sub>2</sub>, TMD, MFM, Lithography

## X-ray Generation Based on Carbon Nanotube Field Emitter

GUPTA Amar Prasad<sup>1</sup>, 김우섭<sup>1</sup>, 임종민<sup>1</sup>, 박준영<sup>1</sup>, 안정선\*<sup>1</sup>, 여승준<sup>1</sup>, 류제황<sup>1</sup>

<sup>1</sup>경희대학교 물리학과  
johnsonahn@khu.ac.kr

### Abstract:

Since the discovery of x-rays more than 100 years ago, a little has been changed to the technology used for producing it. Due to relatively cheaper and easier way to produce x-rays through thermionic emission by filament, this technique has dominated since its conception. X-ray technology is currently used intensively not just in the medical field but also in industrial and security fields. However, there is a growing concern for modifying this analogue based technology because of its inefficient way to produce x-rays and x-rays system being relatively larger. Researchers around the world has come up with the idea to solve these problems related with thermionic emission by replacing it with digital based field emission cold cathode x-rays. Moreover, integrating the field emission technology with promising nanotechnology could be a better choice to develop nanomaterial based next generation x-rays system. Carbon Nanotube as a nanomaterial and field emission emitter has qualitatively and quantitatively more advantages than other materials in respect to low turn on voltage and high current density. This presentation deals with PECVD fabrication techniques of Carbon Nanotube on stainless steel and Si substrate for developing a high performing electron field emitter that can be used for promising next-generation x-ray sources.

### Keywords:

Carbon nanotubes, Field emitter, X-rays, PECVD

## “Peel and Stack” Technique for Large-area Graphene with Pristine Interfaces

양성준<sup>1</sup>, 최신영<sup>1</sup>, 이승민<sup>1</sup>, 김철주\*<sup>1</sup>

<sup>1</sup>포항공과대학교 화학공학과  
kimcj@postech.ac.kr

### Abstract:

In this study, we present a new process to form pristine interfaces between graphene and other materials on a large scale, which we named “*Peel and Stack*” technique. Graphene can be transferred onto arbitrary materials, resulting in various hetero-interfaces. In particular, pristine interfaces with low impurities enable various novel devices such as transistors, photodetectors and tunneling diodes. However, the current transfer techniques require chemical etching of graphene growth substrates to separate the film from the surface, leaving many impurities at the final interfaces. In order to address the issue, we use germanium as a growth substrate, which has a much weaker attraction with graphene than conventional metallic substrates, so we can physically separate the films. After optimization of graphene growth, we deposit boron nitride films on the as-grown samples, and efficiently peel off the whole film and transfer it onto arbitrary substrates. Using many spectroscopy and imaging techniques such as Raman, X-ray photoelectron spectroscopy, and transmission electron microscopy, we confirm that our process doesn't lead to additional atomic defects or contaminations in the graphene film. Also, the doping level and uniformity of the final film is found to be within  $10^{12} \text{ cm}^{-2}$ , which is an order of magnitude lower than the case of film transferred by conventional techniques including chemical etchings.

### Keywords:

Graphene, Transfer, Interfaces, Heterostructures

## Interaction between electron and charge density wave instability in quasi 1D material

김용관\*<sup>1</sup>

<sup>1</sup>한국과학기술원, 나노과학기술대학원  
yeongkwan@kaist.ac.kr

### Abstract:

Electron-bosonic mode interaction is one of the key ingredients of the light-matter interaction and can manifest many exotic phenomena in solid such as superconductivity. One possible bosonic mode that can interact with the electron is a collective excitation mode of charge density wave (CDW). As CDW is the spatial modulation of electron density, its collective excitation modes closely mimic the phonon modes thus similar interaction is expected. However, this new possible interaction is only rarely studied so far.

In this presentation, the signature of interaction between the electron and CDW instability will be presented captured by angle-resolved photoemission spectroscopy in quasi-1D CDW system NbSe<sub>3</sub>. A kink, the representative feature of electron-bosonic mode coupling was observed in the electronic structure only when CDW phase present in the system. As the CDW is suppressed via Ta doping, the kink disappeared, implying that the observed kink is the result of interaction between the electron and collective excitation mode of CDW.

### Keywords:

charge density wave, angle-resolved photoemission spectroscopy, NbSe<sub>3</sub>

## Chiral Atomically Thin Films

KIM Cheol-Joo\*<sup>1</sup>

<sup>1</sup>Department of Chemical Engineering, Pohang University of Science and Technology  
kimcj@postech.ac.kr

### Abstract:

Here, we present a novel approach for programming optical properties of atomically thin films, namely chiral stacking, where atomically thin crystalline films are stacked one-by-one with precise control of the interlayer rotation ( $\theta$ ) and polarity. Based on the approach, we produced chiral bilayer graphene film, which has left- and right- handed counter parts, connected by mirror symmetry.[1] The film displays one of the highest intrinsic ellipticity values ( $6.5 \text{ deg } \mu\text{m}^{-1}$ ) ever reported, and a remarkably strong circular dichroism (CD) with the peak energy and sign tuned by  $\theta$  and polarity. We show that these chiral properties originate from the large in-plane magnetic moment associated with the interlayer optical transition. Furthermore, we show that we can program the chiral properties of atomically thin films layer-by-layer by producing three-layer graphene films with structurally controlled CD spectra. Our fabrication process and tunable chiral properties can be extended from graphene to other two-dimensional layered materials to form chiral atomically thin films. This would allow the realization of chiral properties with diverse electrical and optical features.

[1] CJ Kim, A. Sánchez-Castillo, Z. Ziegler, Y. Ogawa, C. Noguez and J. Park, "Chiral Atomically Thin Films", *Nat. Nanotechnol.* 11, 520-524 (2016)

### Keywords:

Chirality, Graphene, Circular Dichroism

## Room-temperature single photon emission from defects in gallium nitride

JEONG Kwang-yong\*<sup>1</sup>

<sup>1</sup>Department of Nano Science and Technology, Gachon University  
kyjeong@gachon.ac.kr

### Abstract:

Realization of solid state quantum photonic technologies require bright single photon emitters[1,2]. So far, such emitters have been identified in diamond[3,4], hexagonal silicon carbide[5] and hexagonal boron nitride[6]. Unfortunately, these materials are not amenable to standard nanofabrication processes and cannot be easily grown on a wafer scale, therefore, impeding the scalability of integrated quantum photonics on a single chip. Hence, there is great interest to identify quantum emitters in technologically mature semiconductors. Here, we demonstrate robust single photon emitters based on defects in gallium nitride (GaN). We show their excellent photophysical properties including bright emission of up to 500,000 counts/s and a short lifetime (~ 2 ns). The emitters have strong and narrow, linearly polarized single photon fluorescence at room temperature. We further show that the emitters can be found in a variety of GaN wafers, thus offering reliable and scalable platform for further technological development. Our result paves the way for scalable integrated photonics on a single chip.

- [1] M. G. Thompson, A. Politi, J. C. Matthews, J. L. O'Brien, IET circuits, devices & systems 2011, 5, 94.
- [2] O. Gazzano, S. M. de Vasconcellos, C. Arnold, A. Nowak, E. Galopin, I. Sagnes, L. Lanco, A. Lemaître, P. Senellart, Nature communications 2013, 4, 1425.
- [3] A. Batalov, C. Zierl, T. Gaebel, P. Neumann, I. Y. Chan, G. Balasubramanian, P. R. Hemmer, F. Jelezko, J. Wrachtrup, Phys Rev Lett 2008, 100, 077401.
- [4] A. Batalov, V. Jacques, F. Kaiser, P. Siyushev, P. Neumann, L. J. Rogers, R. L. McMurtrie, N. B. Manson, F. Jelezko, J. Wrachtrup, Phys Rev Lett 2009, 102, 195506.
- [5] S. Castelletto, B. C. Johnson, V. Ivády, N. Stavrias, T. Umeda, A. Gali, T. Ohshima, Nat Mater 2014, 13, 151.
- [6] T. T. Tran, K. Bray, M. J. Ford, M. Toth, I. Aharonovich, Nature nanotechnology 2016, 11, 37.

### Keywords:

Single photon source, gallium nitride, quantum defect

## Multiresonant Nanoplasmonics by Out-of-plane Engineering

ZHOU Wei<sup>\*1</sup>

<sup>1</sup>Department of Electrical and Computer Engineering, Virginia Tech  
wzh@vt.edu

### Abstract:

A core goal of information technology is to alleviate the bottleneck between fiber-based optical networks for telecommunication and semiconductor-based devices for data generation, processing, routing, and storage. Accomplishing this will require the accelerated development of low-cost, compact, energy-efficient optoelectronic and nonlinear-optical devices for faster information handling and transfer. Plasmonic nanoresonators and nanoantennas can control light flows and enhance light-matter interactions at subwavelength scale, and thus can potentially be used as nanoscale components in integrated optics systems either for passive optical coupling, or for active optical modulation and emission. Here we investigated a new type of multilayered metal-insulator optical nanocavities that can support multiple localized plasmon resonances with ultra-small mode volumes. The total number of resonance peaks and their resonance wavelengths can be controlled by simple geometric design rules. Multi-resonant plasmonic nanocavities can serve as broadband nanoantennas to convert electromagnetic energy between near-field and far-field regions. Furthermore, radiation decay rates and thus modulation speeds of light emitting devices can be increased at multiple wavelength ranges by such multi-resonant optical nanocavities through Purcell effects.

### Keywords:

plasmonics, resonators, antennas

## Tunneling rectification in two dimensional quantum barriers

KIM Dai-Sik\*<sup>1</sup>

<sup>1</sup>Centre for Angstrom Scale Electromagnetism, Department of Physics and Astronomy, Seoul National University, Seoul 151-747, Korea  
dsk@phya.snu.ac.kr

### Abstract:

We take advantage of recent advances in nano technology to study quantum scale light matter interaction. Terahertz waves are squeezed into extreme aspect ratio slot antennas. In the middle of a nano slot antennas, the electric field intensity can be a million times stronger than the incident one. Thereby, cross sections of molecules can be hugely enhanced and the probing depth decreases. Quantum tunneling of electrons through nanometer and Angstrom sized gaps are inevitable, rendering different dielectric constants. These efforts originated from nearly perfect transmission through terahertz slot antennas with tens of microns of feature sizes, together with its nanometer sized counterparts. We will discuss our recent results on tunneling through closed, macroscopic rings of quantum barriers. Surface current driven tunneling provides a new paradigm compared with the conventional voltage driven tunneling, being ultrasensitive to the global geometry and symmetry of the planar geometry. Macroscopic geometries can be used to govern total tunneling currents.

### Keywords:

terahertz, tunneling, rectification, nano

## Electronic interactions and vibrations of small metallic clusters

MEDEGHINI F.<sup>1</sup>, MAIOLI P.<sup>1</sup>, CRUT A.<sup>1</sup>, DEL FATTI N.<sup>1</sup>, VALLÉ Fabrice\*<sup>1</sup>

<sup>1</sup>FemtoNanoOptics Group, LASIM, CNRS and Université de Lyon, France  
fabrice.vallee@univ-lyon1.fr

### Abstract:

Reduction of the size of a material to the nanometric range drastically modifies many of its physical and chemical properties. For metal nano-objects with size down to a few nanometers, these modifications mainly originate from classical effects, while for smaller sizes below about 2 nm (less than about 250 atoms), quantization plays an important role. Though the impact of quantization on static properties (ionization threshold, melting temperature, optical absorption, ...) of free clusters has been extensively investigated, the induced changes of the electronic interactions (i.e., electron-electron and electron-phonon interactions within the confined system) and of their vibrational response have been much less studied.

Using high-sensitivity ultrafast pump-probe spectroscopy, we investigate the electronic and vibrational kinetics of metal nanoparticles formed by few hundred to few atoms. More precisely, the relaxation process of photoexcited nonequilibrium electron is followed in the time-domain, yielding information on the electron-electron and electron-vibration energy exchange processes. Investigations have been performed both in surfactant-free glass-embedded silver clusters to limit surface effects, and in chemically synthesized gold cluster stabilized with thiols. The efficiency of the electronic interactions is observed to increase with size reduction down to about 2 nm, consistently with previous results in larger size particles. It is shown to decrease for smaller sizes, an effect ascribed to quantization of the electronic states. Size dependence of the acoustics vibrational response of silver and gold clusters in this size range will also be discussed in the context of transition from an elastic body (macroscopic elastic model) to a molecular type of description of the vibrational modes of nano-objects.

### Keywords:

Metal clusters, electronic interactions, Vibrations, Femtosecond spectroscopy

## Coherent exciton dynamics in ReS<sub>2</sub>: optical Stark effect and quantum beats

SIM Sangwan<sup>1, 2</sup>, LEE Daeon<sup>1</sup>, TRIFONOV Artur V.<sup>3</sup>, KIM Taeyoung<sup>1</sup>, NOH Minji<sup>1</sup>, CHA Soonyoung<sup>1</sup>, SOH Chan Ho<sup>1</sup>, SUNG Ji Ho<sup>2, 4</sup>, CHO Sungjun<sup>5</sup>, SHIM Wooyoung<sup>5</sup>, JO Moon-Ho<sup>2, 4, 6</sup>, CHOI Hyunyoung<sup>\*1</sup>

<sup>1</sup>School of Electrical and Electronic Engineering, Yonsei University, Seoul 03722, Korea, <sup>2</sup>Center for Artificial Low Dimensional Electronic Systems, Institute for Basic Science, Pohang 37673, Korea, <sup>3</sup>Spin Optics Laboratory, St. Petersburg state University, St. Petersburg 198504, Russia, <sup>4</sup>Division of Advanced Materials Science and <sup>5</sup>Department of Materials Science and Engineering, Pohang University of Science and Technology, Pohang 37673, Korea, <sup>6</sup>Department of Materials Science and Engineering, Yonsei University, Seoul 03722, Korea, <sup>6</sup>Department of Materials Science and Engineering, Pohang University of Science and Technology, Pohang 37673, Korea  
hychoi@yonsei.ac.kr

### Abstract:

In the past few years, two-dimensional (2D) transition metal dichalcogenides (TMDs) have received intensive attention. Among the TMD materials, rhenium disulfide (ReS<sub>2</sub>) is a recently studied group VII 2D TMD material which exhibits in-plane reduced crystal symmetry compared to the molybdenum or tungsten dichalcogenides. Interestingly, this reduced symmetry gives rise to strongly anisotropic excitons which have different orientations and optical selection rules. However, the coherent nature of such anisotropic exciton dynamics in ReS<sub>2</sub> are barely unknown and rarely performed. Here, we report the ultrafast coherent dynamics of anisotropic excitons. In this presentation, we discuss two representative examples of optical Stark effect and quantum beat in a few layer ReS<sub>2</sub>. Optical Stark effect is a coherent light-matter interaction, by which the quantum exciton state can be changed by non-resonant light illumination. We found that the optical Stark effect can manipulate the two anisotropic exciton states by applying a linear polarized light to few-layer ReS<sub>2</sub>. Furthermore, we can selectively tune the stark shift of exciton states by manipulating the light polarization. For the exciton quantum beat, it is another coherent dynamics, not thoroughly studied in semiconductor, though. Significantly, the transient periodic oscillations induced by the quantum coherent superposition is rarely reported in 2D TMDs. Here, we report a pure quantum phenomenon, namely quantum beats of anisotropic excitons in a few layer ReS<sub>2</sub>. To observe the exciton quantum beat signal, we equally balance the population of the two excitons by manipulation the angle of the linearly polarized light. Our finding gives a new route for polarization-controlled exciton states in 2D materials.

### Keywords:

exciton, two-dimensional materials, ultrafast spectroscopy, optical spectroscopy



## Coherent control of correlated materials via coherent lattice vibrations

KIM Kyungwan\*<sup>1</sup>

<sup>1</sup>Department of Physics, Chungbuk National University, Korea  
kyungwan@chunbguk.ac.kr

### Abstract:

Understanding light matter interactions is a key to ultrafast control of material properties. One of promising approaches for the ultrafast control is to utilize coherent lattice vibrations. Strong electron phonon coupling gives rise to oscillations of lattice upon photon pumping. The in-phase motion of ions has been suggested to modify various properties of materials such as a magnetic order, a ferroelectric order as well as a superconducting order.

In this talk, I will discuss recent progress of ultrafast control of correlated material properties utilizing coherent phonon oscillations. In the case of Fe-based superconductors, pronounced coherent oscillations of As ions upon near infrared pumping strongly modulate the electronic and magnetic properties almost instantaneously. We found that the effect is huge enough to transiently generate a magnetic order in the normal state by modulating the band structure. A combined study of the lattice and the band structure by an X-ray free electron laser and time resolved ARPES, respectively, allows us to determine the deformation potential experimentally for the first time. Such ultrafast studies provide a new insight to better understand material properties and also pave a way to the ultrafast control of material properties.

### Keywords:

ultrafast control, coherent oscillations, Fe-based superconductors

## 강유전체 터널 접합구조에서의 양이온 이동을 이용한 시냅스 모방 멤리스터 소자

박배호\*<sup>1</sup>, 윤찬수<sup>1</sup>, 이지혜<sup>1</sup>, 이상익<sup>1</sup>, 전지훈<sup>1</sup>, 장준태<sup>2</sup>, 김대환<sup>2</sup>, 김영현<sup>3</sup>

<sup>1</sup>건국대학교 물리학과, <sup>2</sup>국민대학교 전자공학부, <sup>3</sup>한국표준과학연구원  
baehpark@konkuk.ac.kr

### Abstract:

시냅스는 인접한 두 뉴런 사이의 시냅스 가소성을 조절함으로써 뉴로모픽 컴퓨팅 시스템에서 핵심적인 역할을 담당한다. 뇌 기억 능력의 기반이 되는 신경가소성은 short-term plasticity(STP)와 long-term potentiation(LTP)로 분류할 수 있는데, 이는 각각 시냅스 연결의 순간적, 영구적 강화에 의해 달성된다. 점진적으로 변화하는 컨덕턴스를 가지는 memristor는 생물학적 시냅스가 수행하는 뉴로모픽 컴퓨팅을 모방하는데 적용될 수 있다. 인간의 뇌에는  $10^{15}$ 개의 시냅스가 존재하면서도 약 10 W 정도의 전력만 소비하기 때문에 시냅스를 모방하는 memristor 소자는 낮은 에너지 소모와 초미세 구조를 가져야만 한다. 또한, 뉴런에서의 시냅스 가소성은 성장세포에 의해서 선택적으로 조절되기 때문에 뉴런 사이의 회로를 재구성할 수 있다.

본 발표에서는 두께가 약 4 nm인  $\text{PbZr}_{0.52}\text{Ti}_{0.48}\text{O}_3$ (PZT) 초박막을 가지는  $\text{Ag/PZT/La}_{0.8}\text{Sr}_{0.2}\text{MnO}_3$ (LSMO) 강유전 터널 접합을 이용해 구현한 시냅스 소자를 소개하고자 한다. 매우 얇은 강유전 터널 접합 구조에서 유도되는 Ag 이온의 이동은 큰 on/off 비율( $10^7$ )과 낮은 에너지 소모(potential 에너지 소모 = ~22 aJ, depression 에너지 소모 = ~2.5 pJ)를 가능하게 한다. 또한, PZT 박막 내부에서의 유전 분극을 아래쪽으로 정렬하는 간단한 동작에 의해서 강유전 터널 접합에서 STP-LTP 전환과 같은 시냅스 가소성을 선택적으로 조절할 수 있다. 따라서, Ag/PZT/LSMO 강유전 터널 접합에서의 Ag 이온 이동을 이용하는 시냅스 소자는 생물학적 시스템에서의 재구성 학습 및 기억 기능을 모사하는 회로에 사용될 수 있다.

### Keywords:

강유전체 터널 접합 구조, 양이온 이동, 시냅스, 멤리스터

## Ferroelectrically tunable magnetic skyrmions in ultrathin oxide heterostructures

노태원\*<sup>1</sup>, WANG Lingfei\*<sup>1</sup>

<sup>1</sup>Center for Correlated Electron Systems, Institute for Basic Science  
twnoh@snu.ac.kr, lingfei.wang@snu.ac.kr

### Abstract:

Magnetic skyrmion is a topologically protected whirling spin texture in nanoscale. Its small size, topologically-protected stability, and solitonic characteristics can hold great promise for future spintronics. To translate these compelling advantages into real logic or memory devices, a key challenge is effectively manipulating the skyrmion properties, including spatial distribution, density, size and thermodynamic stability. Here we reported a ferroelectrically stabilized and highly tunable skyrmion platform, BaTiO<sub>3</sub>/SrRuO<sub>3</sub> ultrathin bilayer heterostructure. The ferroelectric proximity effect at the heterointerface can induce a pronounced Dzyaloshinskii-Moriya interaction in ultrathin SrRuO<sub>3</sub> films. The resultant magnetic skyrmions were demonstrated through both transport measurements and magnetic force microscopy. Moreover, by manipulating the ferroelectric polarization of BaTiO<sub>3</sub>, we achieved a local, nonvolatile and switchable control of skyrmion density and stability. Our discovery of ferroelectrically-tunable skyrmions can pave a new way to improve the configurability and addressability of skyrmion-based functional devices.

### Keywords:

Magnetic skyrmion, ferroelectric, oxide thin film

## Phase Nanopillars, Aeroelastic Flutters, and Gore-Tex fabrics for Piezoelectric and Triboelectric Nanogenerator Applications

SHIN Dong Myeong<sup>1</sup>, OH Jinwoo<sup>1, 3</sup>, HONG Suck Won<sup>2</sup>, KIM Hyung Kook<sup>1, 3</sup>, [HWANG Yoon-Hwae](mailto:yhwang@pusan.ac.kr)<sup>\*1, 3</sup>

<sup>1</sup>Department of Nanofusion Technology, Pusan National University, Busan 46241, South Korea,  
<sup>2</sup>Department of Cogno-Mechatronics Engineering, Pusan National University, Busan 46241, South Korea,  
<sup>3</sup>Department of Nanoenergy Engineering, Pusan National University, Busan 46241, South Korea  
[yhwang@pusan.ac.kr](mailto:yhwang@pusan.ac.kr)

### Abstract:

We present bioinspired nanogenerators based on vertically aligned phage nanopillars. Vertically aligned phage nanopillars enable not only a high piezoelectric response but also a tuneable piezoelectricity. Piezoelectricity is also modulated by tuning of the protein's dipoles in each phage. The sufficient electrical power from phage nanopillars thus holds promise for the development of self-powered implantable and wearable electronics [1].

We also present that aerodynamic and aeroelastic flutter membrane triboelectric nanogenerators(FM-TENG) were successfully used to harvest broadband airflow energy. The unit component of the flutter membrane consists of thin, free-standing Al foil electrodes covered on both sides with electrospun poly(vinyl chloride) nanofiber-structured mats, which provide advantageous tribo-surfaces specifically to increase the friction area. The aerodynamic and aeroelastic FM-TENG have great potential to be used in numerous areas of self-powered electronic systems and in-situ wireless sensor applications for automobiles or aircraft[2].

Lastly, we present another type of triboelectric nanogenerators with gold nanodots on Gore-Tex lining surface. We could successfully harvest electrostatic energy by sliding Gore-Tex lining surface with a human skin and several clothes and by an airflow-driven flutter. This study develops an efficient path for harvesting human body energy and promoting the development of wearable electronics and smart clothes.

1] D. M. Shin et. Al, *Bioinspired piezoelectric nanogenerators based on vertically aligned phage nanopillars*, Energy and Environmental Science (2015) 8, 3198.

2] H. Phan et. Al, *Aerodynamic and aeroelastic flutters driven triboelectric nanogenerators for harvesting broadband airflow energy*, Nano Energy (2017) 33, 476-484

### Keywords:

Piezoelectric, Triboelectric, Nanogenerator, M13 bacteria phase, Flutters, Gore-Tex Fabric

## Microwave Tunable Devices based on Ferroelectric Materials

MOON Seung Eon<sup>\*1, 2</sup>, LEE Jaewoo<sup>1</sup>, IM Jong Pil<sup>1</sup>, KIM Jeong Hun<sup>1</sup>, IM Sol Yee<sup>1</sup>, LEE Seung Min<sup>1</sup>  
<sup>1</sup>ETRI ICT Materials & Components Research Lab. ICT Materials Research Group, <sup>2</sup>UST Advanced Device Technology  
semoon@etri.re.kr

### Abstract:

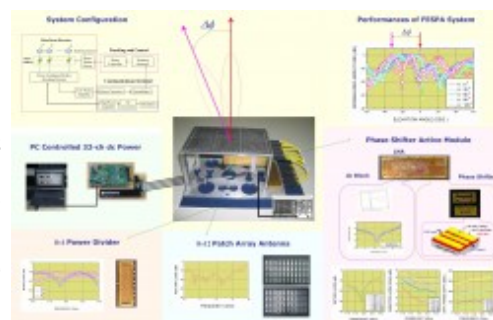
Due to its small size, simple process for making the device, low power consumption, low production cost, high transmission power capability, fast response time, and possibility for electric tuning because of the feasibility to change the dielectric constant, ferroelectric material is one of the promising candidates for a microwave tunable device, as well as in other application fields such as dynamic random access memory (DRAM), non-volatile ferroelectric random access memory (FRAM), piezoelectric devices, and pyroelectric devices. Moreover, analog or digital control is possible for a ferroelectric phase shifter due to the possibility of electric continuous tuning.

Moreover, depending on the type of electronic control medium or mechanism adopted, these phase shifters can be categorized as ferrite, semiconductor, and ferroelectric phase shifters. For a ferromagnetic phase shifter, it is hard to control speedy beam scanning because of the slow response time, and a bulky element size and high power consumption are other weak points. For a semiconductor phase shifter, large loss in the high frequency range and a low transmission power capability are shortcoming points.

In this talk, we will discuss the required characteristics for ferroelectric thin film and report our designs and performances of the ferroelectric phase shifters. Using the above ferroelectric phase shifters, power divider, bias tee, and micro-strip patch antenna, the prototype phased array antenna was assembled and the measured performance of the system will be presented.

### Keywords:

Microwave, Tunable Device, Phase Shifter, Ferroelectric



## Charge density functional plus U theory of LaMnO<sub>3</sub>: Phase diagram, electronic structure, and magnetic interaction

장승우<sup>1</sup>, 이시현<sup>1</sup>, 윤희기<sup>1</sup>, 한명준\*<sup>1</sup>

<sup>1</sup>한국과학기술원 물리학과  
mj.han@kaist.ac.kr

### Abstract:

We perform charge density functional theory plus U calculation of LaMnO<sub>3</sub>. While all the previous calculations were based on spin density functionals, our result and analysis show that the use of spin-unpolarized charge-only density is crucial to correctly describe the phase diagram, electronic structure and magnetic property. Using magnetic force linear response calculation, a long-standing issue is clarified regarding the second neighbor out-of-plane interaction strength. We also estimate the orbital-resolved magnetic couplings. Remarkably, the inter-orbital  $e_g$ - $t_{2g}$  interaction is quite significant due to the Jahn-Teller distortion and orbital ordering.

### Keywords:

DFT+U, LaMnO<sub>3</sub>, constrained random phase approximation (cRPA), magnetic force linear response theory (MFT)

## Analytic continuation via “domain-knowledge free” machine learning

윤(Yoon)홍기(Hongkee)<sup>1</sup>, 심(Sim)재훈(Jea-Hoon)<sup>1</sup>, 한명준\*<sup>1</sup>

<sup>1</sup>한국과학기술원 물리학과  
mj.han@kaist.ac.kr

### Abstract:

Hongkee Yoon<sup>1</sup>, Jea-Hoon Sim<sup>1</sup>, and Myung Joon Han<sup>1</sup>

<sup>1</sup>Department of Physics, KAIST, 291 Daehak-ro, Yuseong-gu, Daejeon 34141, Republic of Korea

We present a machine learning (ML) approach to the analytic continuation which is the notorious problem in quantum many-body physics. Especially the analytic continuation is applied to obtain spectral function from imaginary time Green's function calculated from quantum Monte Carlo (QMC). However, the analytic continuation is an ill-conditioned problem, therefore, many numerical approaches exist; such as maximum entropy method [1,2], stochastic method [3], and Padé approximation [4]. Here we show that by using modern machine learning techniques [5-6], such as convolutional neural network and stochastic gradient descent based optimizers, ML-based Green's function to DOS kernel can be realized without detailed “domain-knowledge” about previous analytic continuation approaches. Furthermore, the ML-based kernel is faster than conventional analytic continuation algorithms and more robust to noise from Green's function. Our approach to tackling ill-posed problems by data-based ML shows the applicability of ML in other ill-posed physics problems.

[1] Jarrell, M. & Gubernatis, J. E. Bayesian inference and the analytic continuation of imaginary-time quantum Monte Carlo data. *Physics Reports* **269**, 133-195 (1996).

[2] Bergeron, D. & Tremblay, A.-M. S. Algorithms for optimized maximum entropy and diagnostic tool for analytic continuation. *Phys. Rev. E* **94**, 023303 (2016).

[3] Sandvik, A. W. Stochastic method for analytic continuation of quantum Monte Carlo data. *Phys. Rev. B* **57**, 10287 (1998).

[4] Vidberg, H. J. & Serene, J. W. Solving the Eliashberg equations by means of N-point Padé approximants. *J. Low Temp. Phys.* **29**, 179 (1977).

[5] LeCun, Y., Bengio, Y. & Hinton, G. Deep learning. *Nature* **521**, 436-444 (2015).

[6] Szegedy, C. *et al.* Going Deeper with Convolutions. *arXiv:1409.4842 [cs]* (2014).

### Keywords:

Analytic continuation, Machine learning, quantum Monte Carlo (QMC)

## Matrix-valued maximum entropy method: basis-independent formalism

한명준\*<sup>1</sup>, 심재훈<sup>1</sup>

<sup>1</sup>한국과학기술원 물리학과  
mj.han@kaist.ac.kr

### Abstract:

Analytic continuation of the quantum Monte Carlo (QMC) data written in the imaginary frequency to the real axis is one of the difficult numeric problems mainly due to the tiny noise of QMC data has a serious impact on the resulting real frequency spectra. While the maximum entropy method (MEM) is one of the most suitable choices to gain information from the noisy input data, its applications are limited by the non-negative condition of the output spectral function. Here we have extended the MEM to the matrix-valued function, introducing quantum relative entropy as a regularization function. As a true matrix-valued method, our approach is invariant under the arbitrary unitary transformation of the input matrix. Without introducing further ambiguity, Bayesian probabilistic interpretation of the ordinary MEM can be applied [1]. The application of the generalized method to DFT + DMFT results [2] for real materials shows that it provides a reasonable band structure without introducing a material specific base set.

[1] M. Jarrell and J. E. Gubernatis, *Physics Reports* **269**, 133 (1996).

[2] <http://www.openmx-square.org/>

### Keywords:

DMFT, QMC, Analytic continuation

## Long-range Coulomb Interaction effects on Topological Phase Transitions between Semi-metals and Insulators

문은국\*<sup>1</sup>, 한상은<sup>1</sup>

<sup>1</sup>한국과학기술원 물리학과  
egmoon@kaist.ac.kr

### Abstract:

Topological states may be protected by a lattice symmetry in a class of topological semi-metals. In three spatial dimensions, the Berry flux around gapless excitations in momentum space defines a chirality concretely, so a protecting symmetry may be referred to as a chiral symmetry. Prime examples include Dirac semi-metal (DSM) in a distorted spinel, BiZnSiO<sub>4</sub>, protected by a mirror symmetry and DSM in Na<sub>3</sub>Bi, protected by a rotational symmetry. In these states, topology and a chiral symmetry are intrinsically tied. In this work, we investigate characteristics interplay between a chiral symmetry order parameter and instantaneous long-range Coulomb interaction with the standard renormalization group method. We show that a topological transition associated with a chiral symmetry is stable under the presence of the Coulomb interaction and the electron velocity always becomes faster than one of a chiral symmetry order parameter. Thus, the transition *must not* be relativistic, which implies a supersymmetry is intrinsically forbidden by the long-range Coulomb interaction. Asymptotically exact universal ratios of physical quantities such as energy gap ratio are obtained, and connections with experiments and recent theoretical proposals are also discussed.

### Keywords:

Long-range Coulomb Interaction effects, topological phase transition, topological semi-metal, dirac semi-metals, chiral symmetry

## Topological and transport properties in intermetallic $\text{PbPd}_3$

AHN Kyo-Hoon<sup>1</sup>, LEE K.-W.\*<sup>1, 2</sup>

<sup>1</sup>Department of Applied Physics, Graduate School, Korea University, Sejong, <sup>2</sup>Division of Display and Semiconductor Physics, Korea University, Sejong  
mckwan@korea.ac.kr

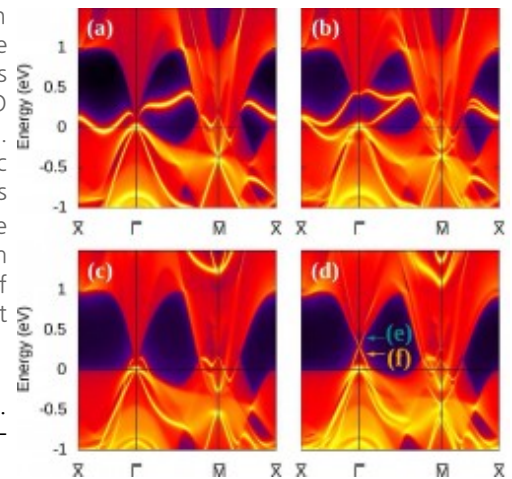
### Abstract:

Discoveries of graphene and topological insulators have boosted research of novel quantum matter. Topological Dirac semimetals (TDSs) are interesting as a "3D counterpart of graphene". The realization of TDSs remains limited, since the chemical composition is hard to control in 3D materials and the spin-orbital coupling (SOC) leads to complicated effects. Here, using ab initio calculations, we propose a new TDS in the cubic  $\text{PbPd}_3$ , which shows several remarkable topological characters such as Dirac cones, Fermi arcs, and triple degenerate points. In addition to the interesting topological characters, a dispersionless band, originating from the lack of  $dd\delta$  hopping, appears along the  $\Gamma$ -X line within a few meV of the Fermi level. We investigated the effects of the flat band on transport and optical properties by varying the doping concentration.

[Acknowledgements] The research has been collaborated with W. E. Pickett. We supported by NRF of Korea under Grant. No. NRF-2016R1A2B4009579.

### Keywords:

first principles, topological materials, transport properties



## Spin state transition in FeO<sub>2</sub> under pressure

심지훈\*<sup>1, 3, 4</sup>, 장보규<sup>1</sup>, 김덕영<sup>2</sup>

<sup>1</sup>포항공과대학교 화학과, <sup>2</sup>Center for High Pressure Science and Technology Advanced Research (HPSTAR), <sup>3</sup>포항공과대학교 물리학과, <sup>4</sup>포항공과대학교 첨단원자력공학부  
jhshim@postech.ac.kr

### Abstract:

Iron oxide is a key compound to understand the state of the deep Earth. It has been believed that previously known oxides such as FeO and Fe<sub>2</sub>O<sub>3</sub> will be dominant at the mantle conditions. However, the recent observation of FeO<sub>2</sub> shed another light to the composition of the deep lower mantle (DLM) and thus understanding of the physical properties of FeO<sub>2</sub> will be critical to model DLM [1]. Nevertheless, the electronic structure and magnetic properties of FeO<sub>2</sub> under high pressure are still poorly understood. Also there is controversy about oxidation state of Fe in FeO<sub>2</sub> [2, 3].

Here, we investigate the spin state transition of FeO<sub>2</sub> under high pressure by using both experimental and first-principles approach. The abrupt volume collapsing and the disappearance of the low-energy satellite in the Fe K  $\beta$  emission spectrum indicate the existence of spin state transition in FeO<sub>2</sub>. The electronic structures are investigated by using density functional theory (DFT) and its combination with dynamical mean field theory (DMFT). The calculated phase diagram of FeO<sub>2</sub> is sensitively affected by the O<sub>2</sub> dimer bond length which is related to oxidation state. Our results indicate that the spin state transition of FeO<sub>2</sub> is originated from Fe (II) with peroxide O<sub>2</sub><sup>2-</sup> state.

- [1] Q. Hu, D. Y. Kim, W. Yang, L. Yang, Y. Meng, L. Zhang, and H.-K. Mao, *Nature (London)* 534, 241 (2016).  
[2] B. G. Jang, D. Y. Kim, and J. H. Shim, *Phys. Rev. B* 95, 075144 (2017).  
[3] S.V. Streltsov, A.O. Shorikov, S.L. Skornyakov, A.I. Poteryaev, D.I. Khomskii, *Sci. Rep.* 7, 13005 (2017).

### Keywords:

Spin state transition, Mott insulator, Iron oxides

## Entanglement negativity in the Anderson impurity model at finite temperature

SHIM Jeongmin<sup>1</sup>, SIM H.-S.\*<sup>1</sup>, LEE Seung-Sup\*<sup>2</sup>

<sup>1</sup>Department of Physics, Korea Advanced Institute of Science and Technology, <sup>2</sup>Arnold Sommerfeld Center for Theoretical Physics, Ludwig-Maximilians-University Munich  
hssim@kaist.ac.kr, s.lee@lmu.de

### Abstract:

Entanglement is useful to characterize many-body ground states. It will be also interesting to study entanglement in many-body thermal states. We compute the entanglement negativity between the impurity and the bath for the single-impurity Kondo model and for the single-impurity Anderson model at finite temperature [1], using the numerical renormalization group method. For the Kondo model, the negativity detects the features of the low-energy Fermi-Liquid quasiparticles, such as universal power-law thermal suppression of the entanglement. For the Anderson model, the negativity shows the temperature dependence which reflects the renormalization group flow of the model.

[1] J. Shim, H.-S. Sim, and S.-S. B. Lee, submitted to Phys. Rev. B

### Keywords:

Quantum Entanglement, Quantum impurity systems, Numerical renormalization group

## van der Waals epitaxial growth of $\alpha$ -MoO<sub>3</sub> nanosheets on various 2D substrates

이관형\*<sup>1</sup>, [KIM Jong\\_Hun](#)<sup>1</sup>, DASH Jatis Kumar<sup>3</sup>, KWON Jun-Young<sup>1</sup>, HYUN Changbae<sup>2</sup>

<sup>1</sup>. Department of Materials Science and Engineering, Yonsei University, Seoul, Korea, <sup>2</sup>. Department of Materials Science and Engineering, Yonsei University, Seoul, Korea, <sup>3</sup>Department of Physics, SRM University, India  
gwanlee@yonsei.ac.kr

### Abstract:

Since the successful isolation of graphene with one-atom layer, two dimensional (2D) materials have been investigated explosively. Nevertheless, 2D transition metal oxides (TMOs) have been less explored due to lack of synthesis methods for them. However, it is expected that the TMOs would be essential elements for future electronic/optoelectronic applications due to remarkable properties, such as large bandgap, high dielectric constant, and small leakage current. They can be used as fundamental blocks for van der Waals (vdW) heterostructures, stacked structures of 2D layers. Here we demonstrate epitaxial growth of a representative TMO,  $\alpha$ -MoO<sub>3</sub> nanosheet, on other 2D crystals, such as graphene, hBN, transitional metal dichalcogenides (TMDs), and mica. The synthesized  $\alpha$ -MoO<sub>3</sub> has a layered structure with high crystallinity. Our electrical measurements and band structure analyses shows that  $\alpha$ -MoO<sub>3</sub> has large band gap (~ 3 eV) and low work function, which means that  $\alpha$ -MoO<sub>3</sub> can be used as a tunnel barrier, dielectric, and doping agent. More interestingly, we can transform  $\alpha$ -MoO<sub>3</sub> to MoS<sub>2</sub> through post sulfurization process. Our work shows a promising way to produce high quality 2D oxides with epitaxial relation and great potential of MoO<sub>3</sub> as 2D dielectric and insulating material.

### Keywords:

2D-materials, transition metal oxide, MoO<sub>3</sub>, molybdenum trioxide

## Effect of epitaxially grown MoO<sub>3</sub> on characteristics of graphene

이관형\*<sup>1</sup>, 김한결<sup>1</sup>, 김종훈<sup>1</sup>, DASH Jatis Kumar<sup>2</sup>

<sup>1</sup>연세대학교 신소재공학과, <sup>2</sup>Department of Physics, SRM University  
gwanlee@yonsei.ac.kr

### Abstract:

In recent years, two-dimensional (2D) materials have attracted great attention due to their unique properties. Among them, graphene has attractive properties, such as high carrier mobility, flexibility, and transparency, which make graphene an emerging candidate for next-generation device material. Despite explosive researches of 2D materials, 2D oxides have not been studied actively. Molybdenum trioxide ( $\alpha$ -MoO<sub>3</sub>) is a layered material stacked along b-axis direction with weak van der Waals force.

We already demonstrated epitaxial growth of MoO<sub>3</sub> on graphite by evaporating Mo film in ambient condition. Interaction between graphene and the grown MoO<sub>3</sub> is highly interesting because graphene/MoO<sub>3</sub> interface is highly crystalline heterointerface. Here we report effect of MoO<sub>3</sub> formation on hole doping and strain in graphene covered by MoO<sub>3</sub>. Due to large lattice mismatch between graphene and MoO<sub>3</sub> and hole doping effect of MoO<sub>3</sub>, graphene, on which MoO<sub>3</sub> is grown, shows compressive strain and hole doping of 0.2% and  $2.0 \times 10^{23} \text{ cm}^{-2}$ , respectively. Interestingly, bilayer graphene shows decoupled between layers. This results from asymmetry in hole injection and strain of top and bottom graphene layers. Our work suggests high possibility of carrier doping and strain engineering of 2D materials using van der Waals epitaxial growth of MoO<sub>3</sub>.

### Keywords:

two-dimensional material, van der Waals heterostructure, graphene, molybdenum trioxide

## Controlled Synthesis of High-quality 2D Semiconductor Film

이관형\*<sup>1</sup>, 정연준<sup>1</sup>

<sup>1</sup>Department of Materials Science and Engineering, Yonsei University  
gwanlee@yonsei.ac.kr

### Abstract:

Two-dimensional (2D) materials have promising properties due to the quantum confinement effect, which is based on the unique thin thickness. Therefore, it has been expected that 2D materials can be used as templates for next-generation nano-optoelectronic devices. Various techniques to produce large-area 2D materials, such as chemical vapor deposition (CVD), atomic layer deposition (ALD), and physical vapor deposition (PVD), have been proposed for practical application of 2D materials in industry because widely used mechanical exfoliation is not appropriate for mass production. However, there are a number of factors to influence quality of the grown 2D materials. We are still lack of understanding of growth mechanism. Therefore, it is important to systematically investigate synthesis factors that dominantly affect quality of the grown films. Here we conducted growth of 2D semiconductor films under various conditions by modulation of synthesis factors: 1) gas flow, 2) growth temperature, 3) promoter, and 4) substrate. Optimization of gas flow and temperature results in improved quality of 2D semiconductor, MoS<sub>2</sub>, compared to the exfoliated MoS<sub>2</sub>. In addition, use of appropriate promotor allows for control of grain size. Our results shows a significant step forward realization of large-area 2D semiconductor film, which can be expanded to practical applications.

### Keywords:

2D materials, Chemical Vapor Deposition, MoS<sub>2</sub>, Transition Metal Dichalcogenides

## Characterizations of MoS<sub>2</sub>/Si Photodiodes Fabricated by High-Working Pressure Plasma-Enhanced Chemical Vapor Deposition

KIM Dong-Wook\*<sup>1</sup>, KWON Soyeong<sup>1</sup>, SONG Jungeun<sup>1</sup>, CHOI Dongrye<sup>1</sup>, KIM Yonghun<sup>2</sup>, CHO Byungjin<sup>3</sup>

<sup>1</sup>Department of Physics, Ewha Womans University, <sup>2</sup>Korea Institute of Materials Science, <sup>3</sup>Department of Advanced Materials Engineering, Chungbuk National University  
dwkim@ewha.ac.kr

### Abstract:

2D semiconductor MoS<sub>2</sub> has sizable band gap (1.2 ~ 1.8 eV) and large absorption coefficients at visible wavelength range. For 3D semiconductors, such as Si, GaAs, and GaN, well-established fabrication techniques for various device applications are available. 2D-3D hybrid semiconductor heterojunctions have attracted great attention since they can take advantages of both 2D and 3D semiconductors. In this work, we fabricated trilayer-MoS<sub>2</sub>/p-type Si heterojunctions at 100 °C using a high-working pressure plasma-enhanced chemical vapor deposition technique. Dark current-voltage (*I*-*V*) characteristics of the MoS<sub>2</sub>/Si heterojunctions showed rectifying behaviors. The temperature dependent transport data were analyzed based on 3D conventional diode models, which helped us to understand the dominant recombination processes of the MoS<sub>2</sub>/Si heterojunctions. Under illumination of a green light (wavelength: 532 nm), the heterojunction exhibited negligible and large photocurrent (*I*<sub>ph</sub>) in forward and reverse bias, respectively. The measured *I*<sub>ph</sub> was linearly proportional to the laser power, indicating very efficient carrier collection. This suggested that the interface defect states did not cause serious recombination loss in our heterojunctions. Increase of the operation frequency from 100 to 3900 Hz reduced the *I*<sub>ph</sub> only about 30%. All these results showed that our low-temperature synthesis could produce high quality MoS<sub>2</sub>/Si heterojunctions for optoelectronic applications. This fabrication process could be useful for other 2D materials, such as MoSe<sub>2</sub>, WS<sub>2</sub>, and WSe<sub>2</sub>.

### Keywords:

MoS<sub>2</sub>, Si, heterojunction, photodiode

## Synthesis and upconversion emission properties of $\text{Y}_2\text{Mo}_4\text{O}_{15}:\text{Er}^{3+}/\text{Yb}^{3+}$ green-emitting phosphors for various applications

유재수\*<sup>1</sup>, DU Peng<sup>1</sup>  
<sup>1</sup>경희대학교 전자공학과  
jsyu@khu.ac.kr

### Abstract:

Temperature is a basic constant in many fields, such as medical science, industry and daily life, so its accurate measurement and monitoring is very important. Currently, the optical temperature sensor based on upconversion (UC) emission of the rare-earth doped nanocrystals by the fluorescence intensity ratio (FIR) technique has drawn much attention owing to its advantages of real-time detection, high sensitivity and high spatial resolution. Although some admirable achievements have been obtained in optical thermometry, more efforts still are needed to further improve their sensor sensitivities. Thus, in this presentation, the  $\text{Y}_2\text{Mo}_4\text{O}_{15}$  was selected as the luminescent host and a series of  $\text{Er}^{3+}/\text{Yb}^{3+}$ -codoped  $\text{Y}_2\text{Mo}_4\text{O}_{15}$  green-emitting phosphors were prepared by a simple sol-gel method. The studied samples were characterized by X-ray diffraction, field-emission scanning electron microscope image and UC emission spectra. Furthermore, with the help of the FIR technique, the optical thermometric properties of the resultant compounds were studied by analyzing the temperature-dependent UC emission spectra. Besides, the effect of doping concentration on the sensor sensitivities of the final products was also investigated. Ultimately, the internal heating performance of the synthesized phosphors induced by the laser pump power was systematically studied.

### Keywords:

Upconversion, Rare-earth, Phosphors

## Size-dependent energy spacing and lifetime in colloidal CdSe quantum dots

KIM Sung Hun<sup>1</sup>, MAN Minh Tan<sup>1</sup>, LEE Hong Seok\*<sup>1</sup>

<sup>1</sup>Department of Physics, Chonbuk National University  
hslee1@jbnu.ac.kr

### Abstract:

Colloidal semiconductor quantum dots (QDs) have attracted considerable attention in various disciplines due to their unique size- and shape-dependent optical and electronic properties. In particular, light-emitting characteristics of CdSe QDs in a wide range of wavelengths make them a new class of emitter for various technological applications such as light-emitting diodes, solar cells and biomedical imaging. However, despite the recent efforts to synthesize high-quality CdSe QDs, reliable protocols are still required for realizing their reproducible size control, and narrow size distributions. In this work, we used the hot-injection technique which is a size-controlled synthesis of monodisperse CdSe QDs. Understanding and exploiting the optical properties of CdSe QDs, we can calculate size-dependent energy spacing by absorption and fluorescence peak position and estimate the size of CdSe QDs as compared transmission electron microscopy which is carried out to the size-dependent CdSe QDs. Time-resolved photoluminescence is involved in the confinement energies and electron-hole exchange interaction.

### Keywords:

Colloidal quantum dots, Optical properties, Energy spacing, Lifetime, Surface states

## Uncooled Active SWIR Photodetectors based on PbS Quantum Dots

강신원\*<sup>1</sup>, 박철언<sup>1</sup>, 권진범<sup>1</sup>, 김세완<sup>1</sup>, 쉬빈루에이<sup>1</sup>

<sup>1</sup>School of Electronics Engineering College of IT engineering, Kyungpook National University, Sankyuk-dong Bukgu 702-710 Daegu, Rep. Korea  
swkang@knu.ac.kr

### Abstract:

Recently, short wave infrared (SWIR) photodetectors have been used in various fields such as military products and medical products to overcome limits of human's eyes. SWIR photodetectors based on various types of materials are currently being developed by many researchers. Among these materials, PbS quantum dots are widely used in SWIR photodetectors because the absorbed wavelength band of PbS quantum dots can be easily controlled by adjusting their synthesis time and temperature. However, most developed SWIR photodetectors based on PbS quantum dots require additional cooling system because they have to be operated in low temperature. In this study, we developed the non-cooling active SWIR photodetector based on PbS quantum dots operated in room temperature and measured I-V characteristics of it according to IR light.

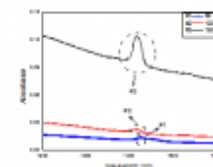


Figure 1. PbS quantum dots absorption spectrophotometry according to reaction temperature.

### Acknowledgement

This work was supported by a National Research Foundation of Korea (NRF) grant funded by the Korea Government (MSIP) (No. NRF 2017R1D1A3B03032042) and the BK21 Plus project funded by the Ministry of Education, Korea (21A20131600011)

This research was supported by the KIAT(Korea Institute for Advancement of Technology) grant funded by the Korea Government(MOTIE : Ministry of Trade Industry and Energy). (No. P0001018 HRD program for 00000)

### REFERENCES

- [1] Haiguang Zhao, "Towards controlled synthesis and better understanding of highly luminescent PbS/CdS core/shell quantum dots", J. Mater. Chem., 1-7(2011)
- [2] Emre Heves, "PbS colloidal quantum dot photodiodes for SWIR detection", Procedia Engineering., 1-4(2012)

### Keywords:

Photodetectors; PbS quantum dots(QDs), SWIR

## Droplet 에피택시 법으로 성장된 InSb/GaSb 양자점의 광학적 특성에 관한 연구

김종수\*<sup>1</sup>, 소모근<sup>1</sup>, 조현준<sup>1</sup>, 김민석<sup>1</sup>, 이상준<sup>2</sup>, 김준오<sup>2</sup>, DAHIYA Vinita<sup>3</sup>, KRISHNA Sanjay<sup>3</sup>

<sup>1</sup>영남대학교, 물리학과, <sup>2</sup>한국표준과학연구원, <sup>3</sup>Department of Electrical and Computer Engineering, Ohio State University

jongsukim@ynu.ac.kr

### Abstract:

본 연구에서는 격자부정합(lattice mismatch) 화합물반도체 물질계에서 양자점 형성에 적용되는 Stranski-Krastanov (S-K) 방법을 대체하여 droplet 에피택시(DE) 방법으로 InSb/GaSb 양자점을 형성하고 그 광학적 특성을 광발광(Photoluminescence; PL) 및 반사 변조 분광학(Photoreflectance; PR) 실험으로 분석하였다. 양자점 시료의 성장은 GaSb (100) 기판 위에 기판온도 500 °C에서 200 nm 두께의 GaSb 완충 층을 성장하고 기판온도를 50 °C로 낮춘 후 2.0 ML

의 In droplet을 조사하여 형성하였다. 양자점 성장을 Reflection high-energy electron diffraction (RHEED)로 확인한 후 200 nm의 GaSb 덮개 층을 성장하였다. 양자점의 전자와 정공의 구속에 의한 에너지 준위를 측정하기 위해 저온 PL 측정을 수행 하였다. Fig. 1은 13 K에서 관측한 InSb/GaSb 양자점 및 GaSb 완충층의 PL 신호이다. InSb 양자점은 0.69 eV에서 강한 발광을 보였다. 온도 의존성 PL 실험에서 InSb 양자점의 활성화 에너지(activation energy) 값으로부터 저온 성장 DE에서 양자점 형성이 가능함을 확인 하였다. Fig. 2는 GaSb 완충층 및 InSb 양자점의 온도에 따른 PL 세기를 온도 (T)의 역함수 (1/kT)로 나타내었다. 고온 영역에서 선형 부분의 기울기로부터 구해진 GaSb 완충층 및 InSb/GaSb 양자점의 활성화 에너지는 각각 약 18.5와 39.8 meV 이다. 이 결과는 기존에 보고된 S-K InSb 양자점과 GaSb 완충층의 활성화 에너지와 유사하였다 [1, 2]. 아울러 DE로 형성된 InSb 양자점이 GaSb 완충층에 미치는 영향을 연구하기 위하여, PR 측정을 통해 GaSb 완충층의 전기장 변화를 관찰하였다. InSb 양자점이 삽입된 GaSb 완충층의 전기장 세기는 양자점이 삽입되지 않은 GaSb 완충층의 전기장 세기보다 감소함을 보였다. 이는 InSb 양자점의 양자구속 효과와 저온 성장된 GaSb 층에 생성된 결함으로 인한 것으로 사료된다. 아울러 결함이 광학적 특성에 미치는 영향을 자세히 연구하기 위하여, 온도 및 광 세기 의존성 PR 실험을 수행하였다.

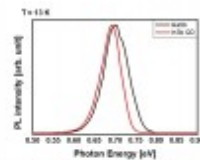


Fig. 1. Low temperature PL spectrum of InSb/GaSb and GaSb buffer layer.

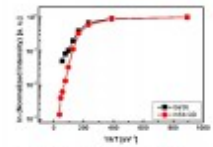


Fig. 2. PL intensities of GaSb buffer layer and InSb/GaSb QD as a function of reciprocal temperatures.

### Keywords:

InSb quantum dot, droplet epitaxy, photoluminescence, photoreflectance

## Nematic order in iron-based superconductors - who is responsible and how we know?

CHUBUKOV Andrey\*<sup>1</sup>

<sup>1</sup>University of Minnesota  
achubuko@umn.edu

### Abstract:

The phase diagram of several families of Fe-based materials shows not only superconductivity at elevated temperatures, but also unconventional non-superconducting states. In this talk, I will discuss the origin of one of them – the nematic phase in which the system spontaneously breaks lattice rotational symmetry. The nematic order was initially thought to be associated with magnetism because in most of Fe-based superconductors it emerges right before the magnetic order. However, in FeSe and related materials, which has been extensively studied over the last few years, the regions of nematic and magnetic order are well separated. This fueled speculations that, at least in FeSe, the nematic order emerges as a spontaneous orbital order. I will show the results of RG-based studies, which treat magnetic and orbital fluctuations on equal footings, and discuss whether the two scenarios can be distinguished in Raman measurements, which probe d-wave charge susceptibility. Along these lines, I will also discuss new theoretical ideas about the uniform dynamical susceptibility for a non-conserving order parameter. Finally, I will discuss some novel properties of a superconducting state, emerging out of a nematic phase, and compare theoretical results with recent STM measurements.

### Keywords:

Fe-based superconductivity, emergent orbital order

## BCS-BEC crossover in $\text{FeSe}_{1-x}\text{S}_x$ superconductors.

SHIBAUCHI Takasada\*<sup>1</sup>

<sup>1</sup>University of Tokyo  
shibauchi@k.u-tokyo.ac.jp

### Abstract:

Among iron-based superconductors, FeSe has the simplest crystal structure but it exhibits arguably the richest physics. Unlike other iron-based materials, the bulk FeSe samples do not show magnetic order below the structural (nematic) transition at 90 K. The electronic structure is quite unusual, having very small and anisotropic hole and electron pockets with the very low Fermi energies [1]. This put the system deep inside the BCS-BEC crossover regime, and we find giant superconducting fluctuations above  $T_C$  consistent with the preformed pairs [2]. By substituting Se with isoelectric S, the structural transition temperature can be completely suppressed, which allows us to tune into a nonmagnetic nematic quantum critical point [3]. In the non-nematic (tetragonal) phase, the temperature dependence of specific heat shows quite unusual behaviors, suggesting an unexpected evolution of superconducting fluctuations with S substitutions.

[1] S. Kasahara *et al.*, PNAS **111**, 16309 (2014).

[2] S. Kasahara *et al.*, Nat. Commun. **7**, 12843 (2016).

[3] S. Hosoi *et al.*, PNAS **113**, 8139 (2016).

### Keywords:

Fe-based superconductivity, emergent nematic order

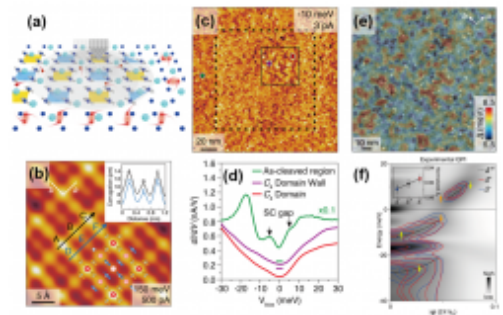
# Controlling iron-based superconductivity with spin currents

LEE Jhinhwan\*<sup>1</sup>

<sup>1</sup>Department of Physics, Korea Advanced Institute of Science and Technology  
jhinhwan@gmail.com

## Abstract:

We have explored a new mechanism for switching magnetism and superconductivity in a magnetically frustrated iron-based superconductor using spin-polarized scanning tunneling microscopy (SPSTM) [1,2]. Our SPSTM study on single crystal  $\text{Sr}_2\text{VO}_3\text{FeAs}$  made of alternating self-assembled FeAs monolayer and  $\text{Sr}_2\text{VO}_3$  bilayers shows that a spin-polarized tunneling current can switch the FeAs-layer magnetism into a non-trivial  $C_4$  ( $2\times 2$ ) order, which cannot be achieved by thermal excitation with unpolarized current. Our tunneling spectroscopy study shows that the induced  $C_4$  ( $2\times 2$ ) order has characteristics of plaquette antiferromagnetic order in the Fe layer and strongly suppresses superconductivity. Also, thermal agitation beyond the bulk Fe spin ordering temperature erases the  $C_4$  state. These results suggest a new possibility of switching local superconductivity by changing the symmetry of magnetic order with spin-polarized and unpolarized tunneling currents in iron-based superconductors [3,4]. We also performed high-resolution quasiparticle interference (QPI) measurements, self-consistent BCS-theory-based QPI simulations and a detailed e-ph coupling analysis to provide direct atomic-scale proofs of enhancement of iron-based superconductivity due to the BCS mechanism based on forward-scattering interfacial phonons [5].



- [1] Jin-Oh Jung *et al.*, Rev. Sci. Instrum. **88**, 103702 (2017)
- [2] Jhinhwan Lee, Rev. Sci. Instrum. **88**, 085104 (2017)
- [3] Seokhwan Choi *et al.*, Phys. Rev. Lett. **119**, 227001 (2017)
- [4] Dirk van der Marel, Physics **10**, 127 (2017)
- [5] Seokhwan Choi *et al.*, Phys. Rev. Lett. **119**, 107003 (2017)

## Keywords:

Magnetism, Superconductivity, Spin-polarized STM, Heterostructure, Iron-based Superconductor

## Probing Hidden Quantum Critical Point in Unconventional Superconductors

PARK Tuson\*<sup>1</sup>

<sup>1</sup>Department of Physics, Sungkyunkwan University  
tp8701@skku.edu

### Abstract:

Heavy fermion compounds belong to the family of the high- $T_c$  superconductors in which the superconducting (SC) gap is unconventional and the ratio of  $T_c$  to Fermi energy is unusually large. The tunable competing energy scales ( $\sim$  meV) of heavy fermions lead to unique opportunity to control their quantum states via non-intrusive perturbations such as pressure. In this presentation, we discuss evidences for the interplay between unconventional superconductivity and a quantum critical point (QCP) that is inherently obscured by a pressure-induced dome of superconductivity in quantum critical metals. A sharp peak in the pressure dependence of the critical current density coincides with a hidden QCP in both pure and 4.4% Sn doped CeRhIn<sub>5</sub>, implying that the superconducting (SC) coupling strength is strongly enhanced where SC pair breaking is expected to be the strongest. These results underline that the ubiquitous quantum critical point (QCP) is directly linked to unconventional superconductivity in strongly correlated materials [1].

[1] S.-G. Jung et al., Nat. Commun. 9, 434 (2018)

### Keywords:

unconventional superconductivity, quantum critical point, critical current, pressure

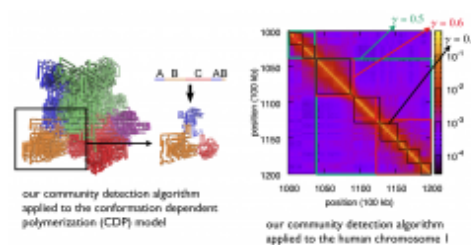
## Finding higher-order interactions in human chromosomes

이상훈\*<sup>1, 2</sup>, 김영훈<sup>3</sup>, 이성민<sup>4</sup>, DURANG Xavier<sup>5</sup>, 전재형<sup>3</sup>, LIZANA Ludvig<sup>6</sup>, STENBERG Per<sup>7</sup>

<sup>1</sup>고등과학원 물리학부, <sup>2</sup>경남과학기술대학교 교양학부, <sup>3</sup>POSTECH 물리학과, <sup>4</sup>고려대학교 물리학과, <sup>5</sup>서울시립대학교 물리학과, <sup>6</sup>Department of Physics, Umeå University, <sup>7</sup>Department of Molecular Biology, Umeå University  
lshlj82@gmail.com

### Abstract:

In this post-genome sequence era, the investigation of the genomic interactions on top of the identified sequence is of great importance. There exist nontrivial structural properties in the interactions, despite the fact that the sequence itself is a topologically simple one-dimensional structure. In particular, the group or modular structures are crucial substructures of chromosome interactions. As the weighted network structures effectively capture the genomic interactions, the identification of such substructures naturally corresponds to finding the modular or community structures in the genomic interaction network. In this work, we suggest a systematic way to identify functionally associated communities composed of possibly noncontiguous subsets of the sequence, using a network community identification algorithm. First, we apply our algorithm to the simulated chromosome structures with fractal scaling based on a polymer model, and find that it indeed captures compact substructures in a sequence. As the real data, we take a representative genomic interaction data called the Hi-C map and apply algorithms for network community detection, in particular, with the tunable resolutions parameter that enables us to find communities with various resolutions. For validity of our method, we compare several known biological markers for the community boundary, such as the enrichment of transcriptional repressor CTCF and RNA expression levels, with our systematically identified communities.



### Keywords:

biological network, network community structure, chromatin interaction, human chromosome

## Origin of the controversy of golden time scaling in disease and failure propagation models on random networks

강병남\*<sup>1</sup>, 최원준<sup>1</sup>, 이덕재<sup>1</sup>  
<sup>1</sup>서울대학교 물리학과  
kahng@phya.snu.ac.kr

### Abstract:

A few years ago, there happened a big controversy on the scaling behavior of the golden time required to reach a pandemic outbreak on inter-dependent (ID) networks. When a certain number of nodes are removed randomly in a giant cluster on ID networks, those damages induce another failure successively, eventually leading to a cascading failure of the entire system. Interestingly, during the cascading process, the size of a giant cluster sustains for a long time, which is called golden time, then collapses suddenly to zero at a transition point. The golden time  $t_c$  scales with the system size  $N$  as  $t_c \sim N^{\beta}$ . The exponent  $\beta$  was a controversial issue. It was argued in Ref.1 that depending on considering sample to sample fluctuation of transition points,  $\beta=1/3$  or  $1/4$ . On the other hand, in Ref. 2, it was argued that the exponent value  $1/4$  is incorrect, but rather  $0.280$  after extensive simulations on a surface growth model. Resolution or even finding the origin of this discrepancy seemed to be difficult thus far.

Here we use a two-step contagion model, which also exhibits rapid cascading after long plateau stage during the spreading process, and find some origin underlying this discrepancy. We consider the effect of stochastic fluctuation in the evolution equation. When the damage size is of  $O(N)$ , the noise term fluctuates over samples and the functional form of the distribution of the noise term changes as the system size is increased. It is uncertain yet within our simulation range  $N \sim O(10^9)$  if the shape of the distribution function reduces to the Gaussian distribution. Thus the Gaussian approximation breaks down within our simulation limit, which makes the exponent  $\beta$  larger than  $1/4$ . If it is reduced to the Gaussian with the standard deviation  $\sigma \sim N^{1/2}$  in the thermodynamic limit, then the golden time would behave as  $N^{1/4}$ . Further studies on other models are needed.

### References:

1. D. Zhou, et al, PRE 90, 012803, (2014).
2. P. Grassberger, Phys. Rev. E 91, 062806 (2015).

### Keywords:

Epidemics, avalanche time, noise distribution

## The majority-vote model on multiplex networks

고광일\*<sup>1</sup>, 최지혜<sup>1</sup>  
<sup>1</sup>고려대학교 물리학과  
kgoh@korea.ac.kr

### Abstract:

Majority-vote model is a much-studied model for social opinion dynamics of two competing opinions. With the recent appreciation that our social network comprises a variety of different "layers" forming a multiplex network, a natural question arises on how such multiplex interactions affect the social opinion dynamics and consensus formation. Here, the majority-vote model will be studied on multiplex networks to understand the effect of multiplexity on opinion dynamics. We will discuss how global consensus is reached by different types of voters: AND- and OR-rule voters on multiplex system and voters on single network system. The AND-model reaches the largest consensus below  $q_c$ . However, it needs much longer time to reach consensus than other models and the consensus collapses abruptly in the vicinity of the critical point. The OR-model has smaller level of consensus than AND-rule but it reaches the consensus more quickly thanks to weak endurances. The OR-model exhibits more active dynamics with more opinion flips as well as more disagreements than the AND-model, which render its consensus transition continuous at the critical point. The numerical simulation results are supported by analytical calculations based on approximate master equation.

### Keywords:

Majority-vote model, Multiplex networks

## Spreading in systems with correlated bursts

HIRAOKA Takayuki\*<sup>1</sup>, JO Hang-Hyun<sup>1</sup>

<sup>1</sup>Asia Pacific Center for Theoretical Physics  
takayuki.hiraoka@apctp.org

### Abstract:

Bursty dynamics, which is commonly observed in various human activities, is associated with two key characteristics: heavy-tailed inter-event time (IET) distributions and correlations between the IETs. By studying simple epidemic models, previous studies show how the non-Poissonian character represented by the shape of IET distribution affects the spreading behavior in temporal networks. The effect of the correlations between IETs on spreading, however, is not fully understood although it is significant if one employs more realistic models in which transmission of infection involves more than one contact between two individuals. We analytically show that the average relay time for transmission increases for a time series with higher IET correlations in the cases of two-step contagion and probabilistic contagion. We also demonstrate by means of numerical simulations that positive correlation between IETs leads to slow spreading in regular tree graphs and in regular random graphs.

### Keywords:

temporal network, spreading, bursty dynamics, temporal correlation

## Stochastic causality inference with limited data

조정호\*<sup>1</sup>

<sup>1</sup>고등과학원 계산과학부  
jojunghyo@kias.re.kr

### Abstract:

Inferring causal relations between variables given their time series is a general problem in many scientific areas. When system dynamics is stochastic and available data is limited, the inference problem becomes more challenging. We have recently developed a new method based on statistical physics. In this presentation, I will introduce our inference method, and demonstrate that it outperforms previous approaches for solving the inverse Ising model. Furthermore, I will show its applicability for reconstructing neural networks from the time series data of neuronal firing, and currency networks from the time series data of currency exchange rates between countries.

### Keywords:

Network reconstruction, Time series, Kinetic Ising model, Neural network, Currency exchange

## Effect of dismantling algorithms and fractality of network

강병남\*<sup>1</sup>, 임윤석<sup>1</sup>  
<sup>1</sup>서울대학교 물리학과  
kahng@phya.snu.ac.kr

### Abstract:

Optimal percolation problem, finding a minimal set of nodes to be removed to disentangle the giant connected component of a network, is not scalable if we require the exact solution. To deal with large networks, only approximations obtained by heuristic algorithms can be expected. Recently, many heuristic algorithms have been proposed, and most of them assume that the target network is locally treelike. However, those algorithms are known to be also effective on real-world networks, which contain many local loops. In this study, we investigate the behavior of CI algorithm, one of the best algorithm based on centrality measure, and BPD algorithm, based on the Belief Propagation method, on the networks equipped with many local loops. Their typical behavior is studied by applying them on some real-world networks. Loop characteristics can be controlled systemically by modifying fractality of networks. Using Fractal Network Model, it is shown that BPD algorithm is better on every graph instance, and the gap between them is larger especially on fractal networks. We analyze the effect of the algorithms on networks in detail by investigating the change in graphical representation, global network measures and local measure distributions.

### Keywords:

network dismantling, optimal percolation, fractality

## Threshold cascade model on signed networks

고광일\*<sup>1</sup>, 이성민<sup>1</sup>, 이규민<sup>2</sup>, 김재우<sup>1</sup>  
<sup>1</sup>고려대학교 물리학과, <sup>2</sup>KAIST 문술미래전략대학원  
kgoh@korea.ac.kr

### Abstract:

We study a threshold cascade dynamics on signed networks, in which there are two types of links, positive and negative links. Depending on negative link density, the suppressive effect on global cascade is found. Interestingly, the existence of negative interactions introduces additional source of complexity leading to degeneracy, and thereby decreased predictability of cascade outcomes. We investigate such complexity under various conditions. We further show that the positive-negative degree correlation widespread in real-world signed networks has observable impact on cascade outcomes: The positive correlations between positive and negative degrees suppresses the global cascades compared to its uncorrelated counterparts, while the negative correlations tend to promote the global cascades.

### Keywords:

signed network, cascade dynamics

## Cutoff-dependent finite-size scaling in scale-free networks

HA Meesoon\*<sup>1</sup>, BAEK Yongjoo<sup>2</sup>, CHUNG Kihong<sup>3</sup>

<sup>1</sup>Department of Physics Education, Chosun University, <sup>2</sup>Department of Physics, University of Cambridge, UK, <sup>3</sup>KAIST  
msha@chosun.ac.kr

### Abstract:

We revisit the cutoff-dependent finite-size scaling (FSS) in scale-free networks, where we employ the susceptible-infected-recovered (SIR) model and the generalized epidemic process (GEP). In particular, we consider the strong, natural, and weak cutoff regimes. The SIR model yields the criticality of the ordinary bond percolation phase transition, while the GEP does the tricriticality and the criticality. Based on numerical testes and scaling arguments, we propose the extended FSS theory, together with the degree-cutoff scaling and crossover scaling, to speculate several length competitions. Finally, we present the universal scaling properties of dynamic phase transitions, which competes with the combined effects of structural heterogeneity and cutoff scaling.

### Keywords:

cutoff-dependent finite-size scaling; scale-free networks; bond percolation; directed percolation; criticality; tricriticality; crossover scaling;

## Epigenetically controlled phase separation of DNA revealed by multi-scale simulations and experiments

유제중\*<sup>1</sup>, 김하진<sup>2</sup>, 하택집<sup>3</sup>, AKSIMENTIEV Aleksei<sup>4</sup>

<sup>1</sup>기초과학연구원, 복잡계자기조립연구단, <sup>2</sup>Department of Physics, UNIST, <sup>3</sup>Department of Biophysics and Biophysical Chemistry, Johns Hopkins University, <sup>4</sup>Department of Physics, University of Illinois at Urbana-Champaign  
jejoong@gmail.com

### Abstract:

Recent experiments clearly showed that human chromosomal DNA forms not a random polymeric mixture but a highly ordered structure, in which the pair-wise contacts between specific loci separated by hundreds of millions base pairs are well preserved. Consequently, a rapidly emerging question in biology is what are the key factors that determine the structure of DNA and what are the underlying driving forces. Although the question remains largely unanswered, it is generally believed that there should exist unknown proteins that mediate such a long-ranged contact between loci. Here, against the belief, we propose a physics-based (i.e., protein-free) model that is simply based on the physics of polycation-mediated condensation of DNA. At a short DNA level, our all-atom molecular dynamics (MD) simulations and various experimental assays unanimously show that the AT content of DNA sequence and methylations of either DNA or the histone tails directly control the strength of inter-DNA forces. Then, using a novel coarse-grained model, we show that a long DNA or many short DNA fragments undergo a large-scale phase separation based on their sequences and epigenetic states. Overall, our findings suggest a novel epigenetic mechanism that can contribute to the mechanical regulation of nucleus-scale organization of chromosomes.

### Keywords:

DNA, phase separation, molecular dynamics simulation

## Study on the conformational transition between the inactive and active form of c-Src tyrosine kinase: transition pathway based on free energy sampling

WU Sangwook\*<sup>1</sup>, YOON Hyun Jung<sup>1</sup>, MYOUNG Hunjoo<sup>2</sup>, LEE Sungmin<sup>3</sup>, PARK Sun Joo<sup>4</sup>

<sup>1</sup>Department of Physics, Pukyong National University, <sup>2</sup>Korea Institute of Science and Technology Information, <sup>3</sup>Department of Physics and Institute of Basic Science, Korea University, <sup>4</sup>Department of Chemistry, Pukyong National University  
sangwoow@pknu.ac.kr

### Abstract:

Non-receptor tyrosine kinase c-Src plays a critical role in numerous cellular signalling pathways. Activation of c-Src from its inactive to the active state involves large-scale conformational changes, and is controlled by the phosphorylation state of two major phosphorylation sites, Tyr416 and Tyr527. A detailed mechanism for the entire conformational transition of c-Src via phosphorylation control of Tyr416 and Tyr527 is still elusive. In this study, we investigated the inactive-to-active conformational change of c-Src using free energy sampling. Based on the free energy sampling, we propose a transition pathway for the activation process of the c-Src tyrosine kinase.

### Keywords:

MD simulation

## New interpretation of supercritical fluid

조용석\*<sup>1</sup>, 이원보\*<sup>2</sup>

<sup>1</sup>경상대학교 물리학과, <sup>2</sup>서울대학교 생명화학공학과  
yongseokjho@gmail.com, wblee@snu.ac.kr

### Abstract:

Although the macroscopic phase over critical point falls into a single supercritical fluid phase (SCF), interesting inhomogeneity in response functions have been observed. In this work, we show that this macroscopic change is originated from the microscopic configuration changes by using machine learning technique, which eventually classifies SCF into two local states: gas-like and liquid-like states. In this view point, the SCF is actually a mixture of inhomogeneous local states. And the abrupt divergence along the phase transition line broadened into finite and triangular area in SCF, like a river flowing into delta at sea (we call it "Widom delta"). According to this argument, we show that the Widom line can be interpreted as a part of Widom delta satisfying a particular condition.

### Keywords:

supercritical fluid, machine learning, phase transition, phase coexistence, widom line

## A Theoretical Model of a Nanofluidic Device for Continuous Separation of Biomolecules

PARK Pyeong Jun\*<sup>1</sup>

<sup>1</sup>Korea National University of Transportation  
pjpark@ut.ac.kr

### Abstract:

We develop a nano-structure device under a constant electric field and perform a continuous separation of DNAs with their sizes ranging from 50bps to 766bps. In our device, DNAs have distinct deflection angles according to their sizes, and continuous separation of DNAs become possible. To get an insight on the working principles of the device, we introduce a stochastic model of a DNA in the nanofilter with periodic structure, and analyze the dynamics of DNAs as well as the resolution of the device in the separation of DNAs with particular sizes. We obtain the trajectory and dispersion of the DNAs in a closed form, and illucidate the physical principles of the separation mechanism in our device. Based on our theoretical analysis, we provide the design principles of the nanofilter device with a specific target resolution in the continuous separation of DNAs and other biomolecules.

### Keywords:

Stochastic Dynamics, DNA Separation, Nanofilter, Electrophoresis

## 반도체/디스플레이 플라즈마 공정에서 플라즈마 변수에 대한 RF bias 의 영향

이호창\*<sup>1</sup>

<sup>1</sup>한국표준과학연구원 첨단측정장비연구소  
lhc@kriss.re.kr

### Abstract:

RF bias가 인가되는 플라즈마 공정 장비는 반도체/디스플레이 산업에서 널리 사용되고 있지만, 대부분의 연구는 자기 바이어스 효과에 의한 이온에너지 제어에만 한정되어 있으며, 공정 결과와 소자 품질에 결정적인 역할을 하는 플라즈마 물성 상관관계에 대한 이해는 많이 부족한 실정이다. 본 발표에서는 RF bias에 의한 플라즈마 밀도, 전자 온도, 전자에너지분포, 전자 가열 물성, 플라즈마 균일도 변화에 대한 연구 결과를 발표할 것이다 [1-7]. 이러한 RF bias와 플라즈마 변수의 상관관계에 대한 연구는 방전 특성의 물리적 이해뿐만 아니라, 반도체/디스플레이 공정 최적화와 차세대 플라즈마 공정 장비 개발에 큰 도움을 주리라 예상된다.

[1] H.C. Lee et al., Applied Physics Letters, 96, 071501 (2010).

[2] H.C. Lee et al., Physical Review E 81, 046402 (2010).

[3] H.C. Lee et al., Applied Physics Letters, 101, 244104 (2012).

[4] H.C. Lee et al., Plasma Sources Science and Technology 21 035003 (2012).

[5] H.C. Lee et al., Plasma Sources Science and Technology 22 032002 (2013).

[6] H.C. Lee et al., Plasma Sources Science and Technology 24 0240 (2015).

[7] H.C. Lee, Applied Physics Reviews, "Review of Inductively Coupled Plasmas: Nano-Applications and Bistable Hysteresis Physics", (2018).

e-mail: LHC@kriss.re.kr

### Keywords:

반도체/디스플레이 플라즈마 공정, 플라즈마 변수, RF bias

## Numerical Plasma Simulations for Materials Processing

이해준\*<sup>1</sup>

<sup>1</sup>부산대학교 전기컴퓨터공학부  
haejune@pusan.ac.kr

### Abstract:

저온 비평형 플라즈마는 전자 온도가 수 만도에 이르지만 이온과 중성기체의 온도는 상온과 유사한 값을 지니는 플라즈마를 의미하며 이러한 비평형 플라즈마를 이용한 물질 가공은 반도체 산업에서 중요하게 다뤄지는 식각 및 증착 공정에서부터 플라스틱 및 고분자 재료의 처리, 나노 물질 합성, 나아가 생체 재료 및 세포에 이르기 까지 광범위한 내용을 포함한다. 본 발표에서는 플라즈마의 특성으로부터 물리적 화학적 반응을 선택적으로 구현하는 원리에 이르기까지의 내용을 플라즈마 물리 및 컴퓨터 시뮬레이션의 관점에서 설명한다. 반도체 공정용 Plasma Etching, Plasma Enhanced Chemical Vapor Deposition (PECVD) 장비의 증착 공정, 플라즈마 토치를 이용한 나노 입자 생성, 그리고 나아가 플라즈마와 세포와의 상호작용에 이르기까지 다양한 압력 및 인가 전압의 영역에서 저온 플라즈마를 이용한 물질의 표면처리 처리 반응에 대해서 설명하고 이를 컴퓨터 시뮬레이션으로 구현한 해석 사례를 소개한다.

### Keywords:

플라즈마 시뮬레이션, 플라즈마 물질 가공

## 열플라즈마를 이용한 봉화금속 나노입자의 합성과 이를 함유한 하이드로젤의 감마선 차폐 특성

오정환<sup>1</sup>, 권석현<sup>2</sup>, 김민석<sup>1</sup>, 선정운<sup>2</sup>, 최수석<sup>\*1</sup>  
<sup>1</sup>제주대학교 에너지공학과, <sup>2</sup>서울대학교 재료공학부  
sooseok@jejunu.ac.kr

### Abstract:

원자력 산업에서 납과 같이 원자번호가 크고 밀도가 높은 금속은 감마선의 차폐를 위해 사용되며, 붕소 및 카드뮴과 같은 물질은 중성자의 흡수를 위해 사용된다. 특히 붕소는 높은 용융점 및 기화점을 가지고 있으므로 기상법을 이용한 붕소계열 나노물질의 합성을 위해서는 매우 높은 온도가 요구된다. 본 연구에서는 고온의 열플라즈마를 이용하여 원료물질을 기화시켜 급냉함으로써 봉화금속 나노입자를 합성하였다. 전산해석을 통하여 나노물질 합성을 위한 설계 및 운전변수를 연구하였으며, 수십 마이크로미터 크기의 붕소와 금속 원료분말이 기화하기에 충분한 5,000 K 이상의 고온이 플라즈마 제트에 잘 형성됨을 확인하였다. 또한, 반응기에서는  $10^4$  K/s 이상의 급냉 환경이 조성되어 포화된 원료물질이 포화 및 응축되어 나노물질이 만들어질 수 있음을 전산해석을 통해 예측하였다. 실험에서 합성된 나노입자의 평균크기는 약 50 nm 내외로 확인되었으며, 이들 나노입자 및 수십 마이크로미터 크기의 원료물질을 하이드로젤에 함유시켜 연성의 방사선 차폐재료를 제작하여 감마선 차폐 특성을 연구하였다. 연성재료는 0.662 MeV의 감마선을 방출하는  $^{137}\text{Cs}$ 와 1.17 MeV와 1.33 MeV의 감마선을 방출하는  $^{60}\text{Co}$ 에 대하여 두께별로 조사함으로써 감쇠계수를 도출하였다.  $^{137}\text{Cs}$  선원에 대해서는 0.014 Sv의 비교적 약한 감마선을 조사하여 최대  $0.46\text{ cm}^{-1}$ 의 감쇠계수를 측정하였으며,  $^{60}\text{Co}$  선원에 대해서는 6.0 Sv의 비교적 강한 감마선을 조사하여 방사선 조사 이후에도 재료의 연성이 잘 유지됨을 확인하였다.

### Keywords:

열플라즈마, 나노입자, 봉화금속, 하이드로젤, 감마선, 감쇠계수

## Recent progress of cut-off probe research

YOU ShinJae\*<sup>1</sup>

<sup>1</sup>Dept. Physics, Chungnam National University  
sjyou@cnu.ac.kr

### Abstract:

In this paper, we present the recent progress of the cutoff probe research which has been performed for last decade. This paper shows the whole progress for the cutoff probe including how to start to develop the cutoff probe in the initial period, what idea has been included during the development, how to evolve the probe during ten years.

The cutoff probe was made by simple intuition for the cutoff phenomenon of the plasma wave. However, the unexpected complicated S21 spectrum gave big confusion for the cutoff frequency. At that time, just compared the cutoff probe result with the other probe result such as Langmuir probe and oscillation probe, the cutoff frequency could be determined. Later, EM waver simulation supported the validation for the cutoff frequency determination. Recently, by supposing the circuit modeling, the physics behind for the cut off probe spectrum (S21) was revealed and the accuracy and the application window of the probe were established. In addition to them, By cooperating with the accuracy measurement of the cutoff probe reactance, the e-n collision frequency as well as the electron density were calculated with good precision. The fast measurement cutoff probe "named fourier cutoff probe" which can applied to the rapid change environment of plasma has been also developed.

Based on recent developments we also introduce a novel methodology to interpret the probe spectrum that eliminates the sheath and collisional effects and enables the use of this precise diagnostic technique in a broad range of practical processing conditions.

### References

- [1] J.-H. Kim, et al. Metrologia 48, pp. 306, 2011.
- [2] D. W. Kim, et al. Appl. Phys. Lett. 99, pp. 131502, 2011.
- [3] J. H. Kwon et al. J. Appl. Phys. 110, p. 023304, 2011.
- [4] J. H. Kwon et al. Appl. Phys. Lett. 96, p. 081502, 2010.

### Keywords:

Recent progress of cut-off probe research

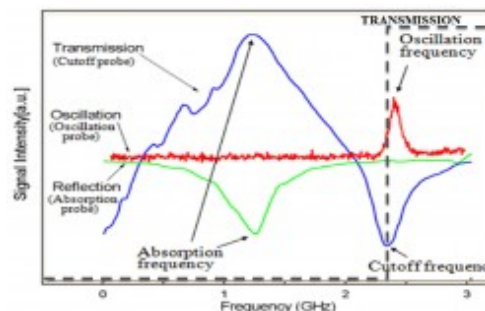


Fig. 1: Transmission spectrum of the original cutoff probe (blue line), Oscillation probe spectrum (red line), Absorption spectrum (green line)

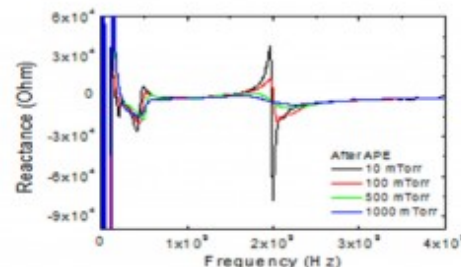


Fig. 2: Reactance spectrum of the cutoff probe at various gas pressures, which is obtained by APE (Auto Port Extension)

## The CMS RPC Detector Status and Operation

고정환\*<sup>1, 2</sup>, 김태정<sup>2</sup>

<sup>1</sup>경희대학교 물리학과, <sup>2</sup>한양대학교 물리학과  
jhgoh@khu.ac.kr

### Abstract:

The CMS experiment at the CERN LHC is composed of three different muon detector systems: Drift Tubes (DT), Cathode Strip Chambers (CSC) and Resistive Plate Chambers (RPC). The CMS RPC system covers  $|\eta| < 2.1$  contributing muon triggering and reconstruction. The CMS RPC collaboration has exploited data samples collected during 2017 at 13 TeV for detector and trigger performance studies. In this talk, the overall performance results at 13 TeV, plans for the consolidation of the CMS RPC system, in view of the increased luminosity expected in HL-LHC, development status about new RPC data automation utility for the fast and efficient withdrawal of RPC condition data are reported.

### Keywords:

CMS experiment, RPC detector, operation

## Jet Discrimination with Weakly Supervised Learning

박인규\*<sup>1</sup>, 이상훈\*<sup>1</sup>, WATSON Ian James\*<sup>1</sup>, 이유재\*<sup>1</sup>

<sup>1</sup>서울시립대학교 물리학과

icpark@uos.ac.kr, jason.lee@uos.ac.kr, ian.james.watson@cern.ch, gkftthddk@gmail.com

### Abstract:

An enormous quantity of data has been collected from particle detectors, such as the CMS at the LHC, and deep learning techniques are being proposed to analyze these large datasets. However, common deep learning techniques are not ideal for such data because fully supervised learning needs true label for training data, while only imperfect simulation can be used for labelling for the LHC. Instead, imperfectly labeled data can be analysed using weakly supervised learning, in which we do not know the true label for experimental data but we know the approximate probability of the categories. We apply weakly-supervised learning to the case of quark-gluon jet classification, where the dijet production process will produce a greater proportion of gluon jets, and Z boson associated jet production produces a greater proportion of quark jets.

### Keywords:

Particle Physics, Jet discrimination, Machine Learning, Deep learning, Weakly supervised Learning

## Quark Gluon classification with deep learning

박인규\*<sup>1</sup>, 이상훈\*<sup>1</sup>, WATSON Ian James\*<sup>1</sup>, 이윤재\*<sup>1</sup>, 장우진\*<sup>1</sup>, 양승진<sup>1</sup>

<sup>1</sup>서울시립대학교 물리학과

icpark@uos.ac.kr, Jason.Lee@cern.ch, ian.james.watson@cern.ch, gkftthddk@gmail.com,  
jang00777@naver.com

### Abstract:

In many searches for new physics signals at the LHC, jets are initiated by light-flavour quarks, while the jets in Standard Model background processes are initiated by gluons. An effective quark/gluon jet discrimination algorithm would, therefore, be an important tool for beyond the Standard Model searches. Current methods for quark/gluon jet discrimination based on traditional machine learning techniques, however, have only marginal discrimination ability. Recent breakthroughs in image classification, in particular a class of techniques training deep neural networks, have revolutionized machine learning in recent years. These techniques can be applied to quark/gluon discrimination by transforming jets into images based on energy deposition. In this study, we train deep learning models on jet images and evaluate their performance for quark/gluon discrimination using simulated data of the CMS detector at the LHC.

### Keywords:

LHC, CMS, Jet Physics, Deep Learning

## Status report of the RPC upgrade for the PHASE-2 CMS

LEE Kyong Sei<sup>\*1</sup>, CHOI Suyong<sup>1</sup>, KANG Minho<sup>1</sup>, JO Youngmin<sup>1</sup>

<sup>1</sup>고려대학교 기초과학연구원 물리학과  
kslee0421@korea.ac.kr

### Abstract:

In the future PHASE-2 high luminosity runs, the LHC will be operated with an instantaneous luminosity of maximum  $7 \times 10^{34} \text{ cm}^{-2} \text{ s}^{-1}$ . The CMS muon system in the PHASE-2 LHC runs will be extended up to  $\eta$  region of 2.4 where only the cathode strip chambers are currently present for the muon measurement. In view of the high background conditions in the HL-LHC runs, we have studied high-sensitive double-gap resistive plate chambers to improve the rate capability and to enhance the detector longevity. A series of intensive and systematic R&Ds with muon beams and gamma-ray sources indicates the choice of the detector technology for the extension of the RPC system is a thin phenolic double-gap model. The RPC detector upgrade for the PHASE-2 will be completed with the installation of the chambers during the Technical Stops at the end of 2022 and 2023.

### Keywords:

Resistive Plate Chambers, Compact Muon Solenoid, Large Hadron Collider

## Background simulation for triple GEM detector

박인규\*<sup>1</sup>, 이상훈<sup>1</sup>, 강예찬<sup>1</sup>

<sup>1</sup>서울시립대학교 물리학과  
icpark@uos.ac.kr

### Abstract:

During the upcoming Long Shutdown 2 of LHC at CERN, the triple GEM detector, called GE 1/1, will be installed in CMS endcap. As this area is in heavy radiation environments coming from the collision. We need to know how this environment will affect on detector's performance. So we simulated response of GE 1/1 to background particle like neutrons and photons with using Geant4. Through this work, we estimate the effect of background particles in the detector and extract relevant information to be used for aging studies.

### Keywords:

CMS, GEM, Simulation, Geant4

## Muon ID and Isolation for LHC phase2

박인규\*<sup>1</sup>, 이상훈\*<sup>1</sup>, 전다정<sup>1</sup>, 윤예빈<sup>1</sup>  
<sup>1</sup>서울시립대학교 물리학과  
icpark@uos.ac.kr, jason.lee@cern.ch

### Abstract:

The Large Hadron Collider (LHC) has planned upgrades during the second and the third Long Shutdown (LS), which will increase the LHC luminosity to  $5 \times 10^{34} \text{ cm}^{-2}\text{s}^{-1}$ . Together with ageing and the expected high pile-up conditions, the performance of the CMS muon system is expected to significantly degrade. The muon system will be upgraded to improve the trigger and reconstruction performance and we present the expected muon identification and isolation performance. To further improve the expected identification performance, we also include, for the first time, muon isolation information as part of the selection criteria.

### Keywords:

Muon ID, Isolation, phase2

## Track isolation studies for level-1 pixel detector

이중호<sup>1</sup>, 문창성\*<sup>1</sup>, 홍지은<sup>1</sup>

<sup>1</sup>경북대학교 물리학과  
csmoon@knu.ac.kr

### Abstract:

We present the track isolation studies for the CMS phase2 upgrade to improve a level-1 pixel-based track trigger performance for the electron identification. Track isolation algorithm for the level-1 pixel trigger uses the topological difference between prompt electrons from the primary vertex and semi-leptonic decay electrons from the jet because prompt electrons are more isolated than semi-leptonic decay electrons. The track isolation information can help the level-1 pixel trigger for the electron identification performance to reject the background from semi-leptonic decay while keeping signal selection efficiency. We develop a primary vertex finding algorithm using level-1 pixel clusters in order to remove the pixel tracks from pile-up interactions. Several kinematic parameters are employed for the track isolation algorithm. The signal efficiency and the background rejection factor are measured using the track isolation algorithm.

### Keywords:

LHC CMS Phase-II L1 Pixel, L1Track, L1Trigger Upgrade, Track isolation, Primary vertex

## L1 pixel track update for the phase-II L1 track trigger

YU Geum Bong\*<sup>1</sup>, MOON Chang-Seong<sup>2</sup>, KIM Junho<sup>1</sup>, SAVOY-NAVARRO Aurore<sup>3</sup>, YANG Un-Ki<sup>1</sup>  
<sup>1</sup>서울대학교 물리학과, <sup>2</sup>경북대학교 물리학과, <sup>3</sup>FNAL and CNRS/IN2P3  
gbyu@snu.ac.kr

### Abstract:

The biggest challenge in the high luminosity LHC operation starting from 2025 is the trigger. In order to keep interesting events with similar efficiency of LHC run2 with same pt threshold, plenty of efforts are put in to develop the first level trigger. In particular, the upgraded tracker in phase-II can provide self-seeded L1 track in a real time. Interpolating the L1 track into pixel detector provides an excellent opportunity to enhance the signal efficiency and reduce fake rates in early stage. This talk presents improvements of the L1 pixel track which is the refitted L1 track with pixel hits using updated tracker design and CMS software.

### Keywords:

LHC CMS Phase-II L1 Pixel L1Track L1Trigger Upgrade

## On the limits of the hadronic energy resolution of calorimeters

이세욱\*<sup>1</sup>

<sup>1</sup>경북대학교 물리학과  
sehwook.lee@knu.ac.kr

### Abstract:

In particle physics experiments, the quality of calorimetric particle detection is typically considerably worse for hadrons than for electromagnetic showers. In this paper, we investigate the root causes of this problem and evaluate two different methods that have been exploited to remedy this situation: compensation and dual readout. It turns out that the latter approach is more promising, as evidenced by experimental results.

### Keywords:

Calorimetry, Dual-Readout, Compensation

## Gravitational waves from first-order phase transitions: an analytic approach to reveal the spectrum structure

JINNO Ryusuke\*<sup>1</sup>, TAKIMOTO Masahiro<sup>1</sup>

<sup>1</sup>IBS-CTPU

jinno@ibs.re.kr

### Abstract:

Gravitational waves (GWs) from first-order phase transitions, if observed, will give us an important clue to unknown high-energy physics. Now GWs from astrophysical sources have been detected by ground interferometers, and in the future we expect more sensitive space interferometers. Nevertheless, we still have limited knowledge on what kind of structures are hidden in the GW spectrum resulting from such transitions. In this talk I will introduce a recent analytic approach to reveal the structures hidden in the GW spectrum. This approach will help to make more reliable estimate on the detection prospect, and/or to see whether GWs really came from a first-order phase transition once they are detected.

(This talk is based on arXiv:1703.09020)

### Keywords:

Gravitational waves

## Gravitational-Wave Fringes at LIGO: Detecting Gravitational Lensing by Compact Dark Matter

JUNG Sunghoon\*<sup>1</sup>, SHIN Chang Sub<sup>1</sup>

<sup>1</sup>Seoul National University  
sunghoonj@snu.ac.kr

### Abstract:

Utilizing gravitational-wave (GW) lensing opens a new way to understand the history and structure of the universe. In spite of coarse angular resolution and short duration of observation, we show that LIGO can detect the GW lensing induced by small structures, in particular by compact dark matter (DM) of  $(10 - 10^5) M_{\text{sun}}$ , which remains an interesting DM candidate. The lensing is detected through GW frequency chirping, creating the natural and rapid change of lensing patterns: frequency-dependent amplification and modulation of waveforms. As a highest-frequency GW detector, LIGO is a unique GW lab to probe such light compact DM. With design sensitivity of Advanced LIGO, one-year observation can detect as many as 1000 lensed GWs and constrain compact DM fraction as small as  $f_{\text{DM}} > 10^{-3}$ .

### Keywords:

LIGO

## Hearing the echoes of dark matter and the early universe

HUANG Fa Peng\*<sup>1</sup>

<sup>1</sup>IBS-CTPU

huangfp@ibs.re.kr

### Abstract:

We how to hear the echoes of the early universe, especially the dark matter and baryogenesis by new approaches beyond the particle colliders, such as the pulsar timing array experiments (such as SKA) and Laser Interferometer experiments (such as LISA).

### Keywords:

dark matter

## Growth and characterization of $Tl_2ZrCl_6$ scintillator crystal for X- and $\gamma$ -ray detection

PHAN Vuong Quoc<sup>1</sup>, 김홍주\*<sup>1</sup>, ROOH Gul<sup>2</sup>, KIM S.H.<sup>3</sup>

<sup>1</sup>경북대학교 물리학과, <sup>2</sup>Department of Physics, Abdul Wali Khan University, Mardan, 23200, Pakistan ,

<sup>3</sup>Department of Radiological Science, Cheongju University, Cheongju 41566, Korea  
hongjoo@knu.ac.kr

### Abstract:

Thallium zirconium chloride ( $Tl_2ZrCl_6$ ) is a promising candidate for X- and  $\gamma$ -ray detection.  $Tl_2ZrCl_6$  crystal has excellent scintillating properties among intrinsic scintillators and high effective atomic number ( $Z=69$ ). It has the cubic structure of the  $K_2PtCl_6$  crystal, which is a desirable property for a large-size-crystal growth. In this study, the crystal is grown by two zones vertical Bridgman technique. The luminescence and scintillation properties of the  $Tl_2ZrCl_6$  crystal were studied under X- and  $\gamma$ -ray excitation. A broad emission band centered at 460 nm was obtained under X-ray excitation. The light yield and energy resolution are estimated to be 47,000 photons/MeV and 4.3% (full-width-at-half-maximum), respectively, obtained from the pulse-height spectra under a  $^{137}Cs$  662-keV  $\gamma$ -ray excitation. Two decay components with constants of 870 ns (9.3%) and 2.7  $\mu s$  (97.7%) were observed.

### Keywords:

Scintillator, X-ray, Decay time, Light yield, Energy resolution

## NSCL LANA 중성자 검출기를 이용한 LAMPS 중성자 검출기 FADC 전자 장비의 시운전과 물리데이터 측정

이종원\*<sup>1</sup>, 김영진<sup>2</sup>, 남선호<sup>1</sup>, 박정혁<sup>1</sup>, 안정근<sup>1</sup>, 이정우<sup>1</sup>, 이효상<sup>2</sup>, 홍병식<sup>1</sup>, 김상렬<sup>3</sup>  
<sup>1</sup>고려대학교, <sup>2</sup>기초과학연구원 중이온가속기 구축사업단, <sup>3</sup>노티스코리아  
laerad84@gmail.com

### Abstract:

LAMPS 실험그룹에서는 LAMPS 중성자 검출기용으로 개발한 FADC 신호처리회로를 미국 Michigan State University의 National Superconducting Cyclotron Laboratory (NSCL)에서 실시된 e14030, e15190 실험에서 Large Area Neutron Array (LANA) 중성자 검출기에 연결하여 성능을 테스트 하였다. 실험은 2018년 2월부터 3월에 걸쳐 진행되었으며, Ca-40/Ca-48 140 MeV/u, 1 nA 빔과 Ni-58/Sn-112 표적충돌에서 발생한 핵자 및 파편핵의 데이터를 측정하였다. 본 연구진은 본 실험과 이전에 진행되었던 실험들을 통해 도출된 결과를 종합하여 LAMPS FADC의 성능을 연구하였으며, 운용법에 대하여 정리하였다. 그리고 FADC에서 취득한 파형데이터의 해석방법을 연구하였다.

본 발표에서는 데이터 처리량에 따른 LAMPS FADC DAQ의 운용법 및 파형데이터 해석방법 및 특징에 대하여 발표할 것이다.

### Keywords:

FADC, LAMPS, 중성자검출기, 중이온가속기

## Performance test of a position-sensitive ionization chamber for KoBRA recoil spectrometer at RAON

KWAG Minsik\*<sup>1</sup>, CHAE Kyungyuk<sup>1</sup>, AKERS Charles<sup>2</sup>, CHA Soomi<sup>1</sup>, IRIBE Kotaro<sup>3</sup>, KIM Duhyun<sup>1</sup>, KIM Minju<sup>1</sup>, LEE Kwangbok<sup>2</sup>, OKA Syohei<sup>3</sup>, TERANISHI Takashi<sup>3</sup>, UENO Yuki<sup>3</sup>, YOSHIDA Hiroya<sup>3</sup>

<sup>1</sup>Department of Physics, Sungkyunkwan University, <sup>2</sup>Rare Isotope Science Project, Institute for Basic Science, <sup>3</sup>Department of Physics, Kyushu University  
gwakpd@gmail.com

### Abstract:

Beam current monitoring and particle identification of beam and beam-like heavy recoils are important for cross section measurement in nuclear physics experiment. A gas-filled ionization chamber is suitable device for this purpose because of its sturdiness against radiation damage and relatively good energy resolution. A new design of fast response ionization chamber with multi-wire electrodes has been developed at the Sungkyunkwan University in order to overcome the limit in maximum counting rate (~100,000 pps) of conventional design. The ionization chamber was tested and commissioned by using 36 MeV  $^{12}\text{C}$  and  $^{16}\text{O}$  beams delivered from 8 MV tandem accelerator at Kyushu University. The maximum counting rate of about 800,000 pps was achieved. This ionization chamber will be used for the experiment at the KoBRA (Korea Broad acceptance Recoil spectrometer and Apparatus) at RAON. The experimental setup and results of beam test will be presented.

### Keywords:

Position-sensitive ionization chamber, Fast response time

## Crystal growth, optical and luminescence properties of $\text{Na}_6\text{Mo}_{11}\text{O}_{36}$ single crystal

김홍주\*<sup>1</sup>, PANDEY Indra Raj<sup>1</sup>, LEE Moo Hyun<sup>2</sup>

<sup>1</sup>Department of Physics, Kyungpook National University, <sup>2</sup>Center for Underground Physics, Institute for Basic Science  
hongjoo@knu.ac.kr

### Abstract:

The inorganic materials of  $\text{Na}_6\text{Mo}_{11}\text{O}_{36}$  was synthesized by solid state reaction and the single crystal was grown by using the Czochralski technique. The crystal structure of the compound was confirmed by X-Ray Diffraction (XRD) analysis. The XRD analysis reveals that;  $\text{Na}_6\text{Mo}_{11}\text{O}_{36}$  compound has single phase. The phase structure of this compound is very closely related with  $\text{Na}_2\text{Mo}_4\text{O}_{13}$  phase. But, crystal growth with Czochralski technique was only possible for  $\text{Na}_6\text{Mo}_{11}\text{O}_{36}$  compound. The luminescence light yield and fluorescence decay time of the crystal was studied at room temperature to 10 K by using 280 nm light emitting diode (LED) source. The crystal has no luminescence at room temperature but luminescence below 150 K. Transmittance spectrum measurement was carried out to study the optical quality of the crystal. The luminescence light yield of  $\text{Na}_6\text{Mo}_{11}\text{O}_{36}$  was compared with the  $\text{Li}_2\text{MoO}_4$  crystal at 10 K, and it is higher than that of  $\text{Li}_2\text{MoO}_4$  crystal. Since, there is a possibility of growing single crystal of  $\text{Na}_6\text{Mo}_{11}\text{O}_{36}$  compound and has significant luminescence light yield at 10 K and has no heavy elements, it might be the possible candidate crystal for rare event search experiment such as  $0\nu\beta\beta$  decay at cryogenic temperature.

### Keywords:

Inorganic materials; Single Crystal; Czochralski technique, Crystal structure; Optical quality

## Crystal growth and scintillation properties of $\text{TlSr}_2\text{I}_5$ : a novel scintillator for radiation detection

KHAN Arshad<sup>1</sup>, ROOH Gul<sup>2</sup>, 김홍주\*<sup>1</sup>, KIM Sunghwan<sup>3</sup>

<sup>1</sup>경북대학교 물리학과, <sup>2</sup>Department of Physics, Abdul Wali Khan University, Mardan, 23200, Pakistan,

<sup>3</sup>Department of Radiological Science, Cheongju University, Cheongju 41566, Korea  
hongjoo@knu.ac.kr

### Abstract:

Scintillators with high effective atomic number ( $Z_{\text{eff}}$ ) and density are required for the efficient detection of ionizing radiations. Due to presence of high Z-number and density of thallium ion in the host material enhances the density and  $Z_{\text{eff}}$  of the crystal. Our group recently discovered new thallium based  $\text{TlSr}_2\text{I}_5$  scintillator which show promising scintillation properties for X and  $\gamma$ -rays spectroscopy applications. This crystal is grown by two zones vertical Bridgman technique. The room temperature X-ray induced emission spectra of pure and  $\text{Eu}^{2+}$  doped crystals contained broad emission bands between 445-670 nm peaking at 528 nm and 430-600 nm peaking at 463 nm, respectively. Energy resolution of 4.2 % (FWHM) with a light output of 70,000 ph/MeV are obtained for 3 mol%  $\text{Eu}^{2+}$  doped crystal under 662 keV  $\gamma$ -rays excitation. More than two decay constants are observed for the pure and  $\text{Eu}^{2+}$  doped samples, at room temperature. Effective Z-number and density are found to be 61 and 5.30 g/cm<sup>3</sup>, respectively. The excellent scintillation performance of this crystal reveals its potential for the detection of ionizing radiations in various applications.

### Keywords:

Crystal growth, Scintillator, X-ray, Bridgman technique

## Induced-photon imaging of raster-scan-mode proton beams

이경세\*<sup>1</sup>, 강민호<sup>1</sup>, 조영민<sup>1</sup>, 박성근<sup>1</sup>  
<sup>1</sup>고려대학교 기초과학연구원 물리학과  
kslee0421@korea.ac.kr

### Abstract:

We report R&D results on multi-layered resistive plate chamber for verification of therapeutic hadron beams. In the present research, a multi-layered glass RPC was constructed with floating glass and tested with 140-MeV raster-scan-mode proton beams provided by a therapeutic cyclotron at the Samsung Proton Therapy Center. The two-dimensional images of the beam-induced prompt and delayed gammas were obtained in a condition of 'beam on' by using a 5-cm-thick lead collimator with 10-mm-pitch 4-mm-diameter holes. The gamma images of the beam-activated area formed in an acrylic phantom agree well with data predicted using GEANT4 simulations.

### Keywords:

Verification of hadron beam, Particle therapy, Multi-layered RPCs, Beam-induced gammas

# Ultrastrong Photoinduced Modulation Doping on 2D/Heterostructures for Photonics and Photo-to-Energy Conversions

CHEN Chun-Wei\*<sup>1</sup>

<sup>1</sup>Department of Materials Science and Engineering, National Taiwan University, Taipei, Taiwan  
chunwei@ntu.edu.tw

## Abstract:

In this talk, I would like to present the strong light-matter interactions at 2D/heterostructure for photonics and photovoltaics. I would like to introduce precisely controlled ultrastrong photoinduced modulation doping based on graphene/TiOx heterostructure, where trap-state-mediated photoinduced charge transfer from the remote bulk TiOx ultrathin film to graphene resulted in a strikingly high n-type doping level ( $>10^{13} \text{ cm}^{-2}$ ), showing both unique advantages of using the conventional chemical doping (high doping concentrations) and photoinduced doping (reversible and controllable).[1] A novel approach to precisely control the band gap opening of a bilayer graphene/TiOx heterostructure by optical modulation will be addressed. In addition, I would like to demonstrate interesting optically controllable graphene electronics due to strong light-matter interactions at graphene heterostructure. For example, the *dual* carrier-typed transport behavior of a graphene transistor by wavelength-selective illumination will be demonstrated [2]. A new concept of photoactive graphene/TiOx heterostructure transparent electrode for photovoltaic application will be also shown [3]. The precisely controllable photoinduced charge transfer can be also applied to a MoS2 and black phosphorus and FETs to achieve a tunable carrier transport by light illumination. [4] In addition, the role of surface oxides on high mobility InSe FET will be also present [5,6]. Finally, I would like to present our recent discovery on low threshold lasing from 2D organic-inorganic perovskite single crystals if the time is allowed.[7]

## Reference:

- [1]. *Advanced Materials*, Vol.27, 7809, (2015)
- [2]. *Advanced Materials*, Vol.27, 282, (2015)
- [3]. *Energy & Environmental Science*, 8, 2085, (2015)
- [4]. *ACS Photonics*, 3, 1102, (2016)
- [5]. *ACS Photonics*, 4, 2930, (2017)
- [6]. *ACS Nano*, 11, 7362, (2017)
- [7]. *Nano Letters*, (under revision)

## Keywords:

2D/Heterostructures, Photo-to-Energy Conversions

## Charge Transport in Graphene-Based Devices

LIANG Chi-Te\*<sup>1</sup>

<sup>1</sup>Department of Physics, National Taiwan University, Taipei, Taiwan  
ctliang@phys.ntu.edu.tw

### Abstract:

In this talk, I shall present our recent experimental results on graphene-based devices. In particular, renormalization-group (RG) studies of monolayer graphene grown on SiC will be described [1, 2]. Both semi-circle [1] and cusp-like RG flow [2] can be observed in highly disordered monolayer graphene. Moreover, I shall discuss our recent experimental results on the fractional quantum Hall effect in the  $N=2$  Landau level in bilayer graphene [3] which may well open a new research area. Finally I am going to present results Shubnikov-de Haas oscillations obtained on moderate disordered graphene which can be used to study the temperature dependence of the carrier density [4] and the crossover from "ordinary metal" to disordered graphene [5].

### References

- [1] L.-I. Huang *et al.*, RSC Adv. 6, 71977 (2016).
- [2] L.-I. Huang *et al.*, RSC Adv. 7, 31333 (2017).
- [3] G. Diankov *et al.*, Nat. Commun. 7, 13908 (2016).
- [4] C.-W. Liu *et al.*, 2D Mater. 4, 025007 (2017).
- [5] C. Chuang *et al.*, Nanoscale 9, 11537 (2017).

### Keywords:

Graphene, Fractional quantum Hall effect, Electron-electron interactions, Shubnikov-de Haas oscillations

## Investigation for formation mechanism of InAs nanostructures on GaSb (100) surface

KIM Jong\_Su\*<sup>1</sup>, DAHIYA Vinita<sup>2</sup>, ZAMIRI Marziyeh<sup>3</sup>, KRISHNA Sanjay<sup>2</sup>, LEE Sang Jun<sup>4</sup>, KIM Jun Oh<sup>4</sup>, SO Mo Geun<sup>1</sup>

<sup>1</sup>Department of Physics, Yeungnam University, <sup>2</sup>Department of Electrical and Computer Engineering, Ohio State University, <sup>3</sup>University of Wisconsin; Madison, <sup>4</sup>Korea Research Institute of Standards and Science

jongsukim@ynu.ac.kr

### Abstract:

In this work, we investigated the formation mechanism of InAs nanostructures on GaSb (100) surface during the droplet epitaxy (DE). The surface reconstructions were observed by using the reflection high-energy electron diffraction (RHEED). Indium (In) migration behavior on GaSb (1x3) and (2x5) surfaces were discussed. The structural properties of In-droplet were investigated with atomic force microscopy (AFM) and scanning electron microscopy (SEM).

After In-droplets formation, the In-droplets were crystallized with As-supply. To investigate the shape transition of InAs nanostructures, we controlled various growth parameters such as substrate temperature and As-flux during crystallization process.

In addition, the optical properties from the InAs/GaSb hetero-interface were investigated by photoreflectance (PR) spectroscopy.

### Keywords:

Droplet epitaxy, InAs, GaSb, InAs/GaSb hetero-interface

## Atomically Resolved Local Electronic Structure of Halide Perovskites

CHIU Ya-Ping\*<sup>1</sup>

<sup>1</sup>Department of Physics, National Taiwan University, Taipei 106, Taiwan  
ypchiu@phys.ntu.edu.tw

### Abstract:

We conduct scanning tunneling microscopy and spectroscopy (STM/S) to investigate the atomic-scale local electronic structure in the halide perovskite  $\text{CH}_3\text{NH}_3\text{PbBr}_3$  (MAPbBr<sub>3</sub>). In STM results, the cleaved surface of MAPbBr<sub>3</sub> shows a stable co-existence of dimer and zigzag phases, whose unit cells only differed in a minute displacement  $\sim 2\text{\AA}$  between the central Br atoms. The structural discrepancy in these two phases is related to the rotatable dipoles of the MA cations which have electrostatic interactions with the neighboring Br atoms. The rotational and positional change of the MA cations and Br ions result in the stable configuration in the dimer and zigzag phase is ferroelectric and anti-ferroelectric, respectively. In STS measurements, the local density of states are acquired at different sites of these two phases to demonstrate their individual local electronic structure near the Fermi level. The atomically resolved electronic result shows that the anti-ferroelectric structure is  $\sim 0.5$  eV lower in energy than the ferroelectric one.

### Keywords:

halide perovskite, scanning tunneling microscopy

## Kinetic Carrier Transfer and Diamagnetic Shift in InP-GaP Lateral Nanowire under Pulsed Magnetic Fields

KIM Yongmin\*<sup>1</sup>, SONG J. D.<sup>2</sup>, SHIN Y. H.<sup>1</sup>

<sup>1</sup>Department of Physics, Dankook University, <sup>2</sup>KIST  
yongmin@dankook.ac.kr

### Abstract:

Linearly polarized photoluminescence (PL) measurements were carried out on InP-GaP lateral nanowires grown using a lateral composition modulation method in pulsed magnetic fields up to  $\sim 50$  T. Two prominent PL peaks were observed at 5 K from each cross-polarization direction (the P//[110] and P//[1 $\bar{1}$ 0] crystal directions). By varying the excitation laser power, the higher- and lower-energy peaks were identified as the transitions from the InGaP bulk layers and from the nanowire structure, respectively. For the nanowire transitions, the polarization directions parallel to the [1 $\bar{1}$ 0] and [110] directions are recognized as recombination from the InP conduction band to the InP (type I) and GaP (type II) valence band, respectively. The transitions from the InGaP bulk exhibit a free-to-bound exciton transition below 60 K. These two different PL peaks exhibit anomalous energy shifts with respect to the direction of the magnetic field due to the variation of the confined energy in the exciton center of mass potential.

### Keywords:

photoluminescence, Diamagnetic Shift, Kinetic Carrier Transfer

## High-power generable Triboelectric Nanogenerator for Self-powered system

BAIK Jeong Min\*<sup>1</sup>

<sup>1</sup>School of Materials Science and Engineering, KIST-UNIST-Ulsan Center for Convergent Materials, Ulsan National Institute of Science and Technology (UNIST)  
jbaik@unist.ac.kr

### Abstract:

For existing triboelectric nanogenerators, it is important to explore unique methods to further enhance the electric output power under realistic environments in order to speed up its commercialization. Here, we report a triboelectric nanogenerator which can generate high-output energy of 3 mJ/s under low frequency of 3 Hz, corresponding to the energy required to operate various healthcare sensors. It is based on the three-layered TENG, consisting of a top layer with polymer film on the top electrode, a middle layer and a bottom layer with metallic film. The polyvinylidene fluoride grafted with tert-Butyl acrylate of 18 % mole percent was synthesized, used as a polymer instead of polytetrafluoroethylene. Silver nanowires-embedded PDMS decorated by Au nanoparticles capped with 4-Dimethylaminopyridine was fabricated, adopted to enhance the electron donor characteristics in middle and bottom layers. The spring constants are also optimized based on spring mass system. Finally, by means of increasing working frequency through a gear-cam system, the charging time to energy storage systems such as capacitor and battery is significantly decreased from several hours to several minutes. Based on these results, three portable power-supplying systems, which provides enough DC power for charging a battery of smart watch/calculator/healthcare sensor are successfully developed.

### Keywords:

High-power generable Triboelectric Nanogenerator

## 유연 단백질 필름을 이용한 전자피부 구현

김성환\*<sup>1, 2</sup>, 민경택<sup>2</sup>, 조민식<sup>2</sup>, UMAR Muhammad<sup>2</sup>  
<sup>1</sup>아주대학교, 물리학과, <sup>2</sup>아주대학교, 에너지시스템학과  
sunghwankim@ajou.ac.kr

### Abstract:

외부 자극을 전자신호로 변환할 수 있는 감각기관들을 다수 포함하고 있는 피부조직을 인공적으로 모사하려는 연구들이 활발하게 벌어지고 있다. 통칭 전자피부라 불리는 이들 인공소자들은 유연한 고분자 필름에 전극과 다양한 전자소자들을 집적하여 온도, 습도, 늘림 등 외부자극을 전기신호로 변환하여 측정하는 기능을 담고 있으며, 차세대 헬스케어 소자로 많은 관심을 받고 있다. 그러나 기존 합성 고분자들은 부족한 생체적합성과 낮은 투습성으로 실제 생체조직을 모방하기에는 부족함이 있다. 본 연구에서는 실크 단백질로 유연하고 늘림이 가능한 필름을 형성하고 여기에 은 나노와이어 전극을 형성한 전자소자들을 구현한 결과들을 보고하고자 한다. 높은 투습성과 역학적 안정성을 지닌 소자의 구현이 가능하였고, 이를 바탕으로 심전도 측정, 도파민 센서, 그리고 RF 안테나 등 다양한 소자들을 구현할 수 있었다.

### Keywords:

실크 단백질, 전자피부, 수화젤

## Soft curved image sensor array using MoS<sub>2</sub> and graphene

KIM Dae-Hyeong\*<sup>1</sup>

<sup>1</sup>Center for Nanoparticle Research, Institute for Basic Science / School of Chemical and Biological Engineering, Seoul National University  
dkim98@snu.ac.kr

### Abstract:

Although recent efforts in device designs and fabrication strategies have resulted in meaningful progresses to the goal of soft optoelectronics, significant challenges still remain in fabricating a soft form of the image sensor array. In this presentation, we report our recent achievement in a high-density soft curved image sensor (CurvIS) array by using a heterostructure of inherently soft 2D materials (MoS<sub>2</sub> and graphene), by employing an ultrathin device structure, and by applying strain-isolating/-releasing array designs. This high-density soft CurvIS array with the single-lens optics successfully acquires pixelated images without optical aberration and infrared noises. We also present a human-eye-inspired soft implantable optoelectronic device based on the developed CurvIS array. Theoretical analysis in conjunction with supporting experiments corroborates the validity of the proposed soft materials and device designs.

### Keywords:

MoS<sub>2</sub>, graphene

## Mechanically tunable metasurfaces on stretchable substrates: optical zoom lens and switchable holograms

EE Ho-Seok<sup>\*1, 2</sup>, AGARWAL Ritesh<sup>2</sup>, MALEK Stephanie C.<sup>2</sup>

<sup>1</sup>Department of Physics, Kongju National University, <sup>2</sup>Department of Materials Science and Engineering,  
University of Pennsylvania  
hoseok.ee@gmail.com

### Abstract:

Metasurfaces are ultrathin flat surfaces that produce abrupt changes in a light beam over a sub-wavelength length-scale. The 2D metasurface also enables the fabrication of tunable optical elements, making them attractive for the design of reconfigurable photonic devices. To demonstrate the concept of a tunable metasurface, we have developed several mechanically tunable Berry-phase metasurfaces operating in the visible frequency regime using a stretchable polydimethylsiloxane (PDMS) substrate. We first demonstrate that the anomalous refraction angle and therefore the optical wavefront can be continuously tuned by mechanical stretching of the substrate. We then demonstrate proof-of-concept prototypes of tunable metasurfaces with potential real-world applications: a 1.7 $\times$  ultrathin flat optical zoom lens and a switchable metasurface hologram.

The tunable metasurface structures composed of an array of Au nanoantennas with different orientation angles are designed and optimized using finite-difference time-domain simulations. The designed metasurfaces are first fabricated on a Si substrate using HSQ/PMMA bilayer e-beam lithography and e-beam evaporation of Au and then are transferred to a PDMS film. The fabricated metasurfaces are optically characterized for various stretch ratios. In a tunable metasurface with a constant phase gradient, measured anomalous refraction angles agreed well with calculations using the generalized law of refraction and successfully demonstrated that the refraction angle of the metasurface can be tuned from 11.4 $^\circ$  to 14.9 $^\circ$  by changing the stretch ratio of the substrate.

We designed, fabricated, and optically characterized the first ultrathin flat stretchable metasurface zoom lens, proving that our tunable metasurfaces can control an optical wavefront for practical applications. By reconstructing captured light intensity profiles of the transmitted beam with the opposite circular polarization, longitudinal beam profiles are obtained. The results showed that the focal length of the lens increases from 150 to 250  $\mu\text{m}$  as the stretch ratio changes from 100% to 130% successfully demonstrating the optical zoom function of the flat lens.

We will also discuss our efforts to design a mechanically switchable hologram as another example of tunable metasurface operating in the visible region. To obtain the phase profiles required for the switchable hologram, a phase-only computer generated hologram was designed with a multi-plane hologram generation technique and a metasurface that produced the obtained phase profile was fabricated and transferred to a PDMS film. Experimentally, the metasurface hologram switches the image when the PDMS film is stretched or relaxed by a certain amount.

Tunable metasurfaces demonstrated in this work will be useful for a variety of applications in information technology, biomedical sciences, integrated optics, optical communications, imaging, flat displays, and wearable consumer electronics.

### Keywords:

Metasurfaces

## Novel nanophotonic devices: graphene-based nanolasers & photon-triggered nanowire transistors

박홍균\*<sup>1</sup>

<sup>1</sup>고려대학교 물리학과  
hgpark@korea.ac.kr

### Abstract:

In this talk, I will present graphene-based nanolasers and photon-triggered nanowire transistors. First, I'll talk about the demonstration of coupled photonic-crystal nanolasers with asymmetric optical gains. We observed the phase transition of lasing modes at exceptional points through tuning of the area of graphene cover on one photonic-crystal cavity and systematic scanning photoluminescence measurements. As the gain contrast between the two identical photonic-crystal cavities exceeds the intercavity coupling, the phase transition occurs from the bonding/anti-bonding lasing modes to the single-amplifying lasing mode, which is confirmed by the experimental measurement of the mode images and the theoretical modeling of coupled cavities with asymmetric gains. In addition, we demonstrated active tuning of exceptional points by controlling the optical loss of graphene through electrical gating.

Second, I'll show photon-triggered nanowire transistors, photon-triggered nanowire logic gates and a single nanowire photodetection system. Nanowires are synthesized with long crystalline Si segments connected by short porous Si segments. Exposing the porous Si segment to light triggers a current in the nanowire with a high on/off ratio of  $>8 \times 10^6$ . A device that contains two porous Si segments along the nanowire can be triggered using two independent optical input signals. Using localized pump lasers, we demonstrated photon-triggered logic gates including AND, OR and NAND gates. Furthermore, we take advantage of the high photosensitivity and fabricate a submicrometer-resolution photodetection system. We believe that photon-triggered transistors offer a new venue towards multifunctional device applications such as programmable logic elements and ultrasensitive photodetectors.

### Keywords:

graphene, nanolaser, nanowire, transistor

## Real-space Mapping of Surface Photovoltage in Semiconductor Nanostructures

KIM Dong-Wook\*<sup>1</sup>, KIM Eunah<sup>1</sup>, KWON Soyeong<sup>1</sup>

<sup>1</sup>Department of Physics, Ewha Womans University  
dwkim@ewha.ac.kr

### Abstract:

Semiconductor nanostructures exhibit unique optical properties, including enhanced absorption/scattering cross-sections and strong light confinement near the surface. In order to take advantages of these optical benefits, there have been intensive research efforts to realize nanostructure-based optoelectronic devices. For such purposes, it is very important to understand and control the creation and transport of charge carriers in the semiconductor nanostructures under light illumination. Surface photovoltage (SPV) - surface potential change by a light source - measurements have been used to study the behaviors of photo-generated charge carriers in semiconductors. The magnitude and sign of SPV are determined by the number of the photo-carriers and band profiles near the sample surface. SPV mapping with nanoscopic spatial resolution can be obtained using Kelvin probe force microscopy. In this talk, I will introduce some of the recent research activities in my group, relevant to real-space mapping of SPV in various semiconductor nanostructures, such as ZnO/Ag nanogratings, P3HT-coated Si-nanopillar arrays, and P3HT layers with embedded photon upconversion nanorods. These works show that the SPV mapping could successfully reveal interplay among photons, surface plasmons, and charges in semiconductor nanostructures.

### Keywords:

Semiconductor nanostructures, optical properties, Surface photovoltage

## Plasmonic Hot Electrons Doping of 2D Materials

FANG Zheyu\*<sup>1</sup>

<sup>1</sup>School of Physics, State Key Laboratory for Mesoscopic Physics, Peking University, Beijing 100871  
China  
zhyfang@pku.edu.cn

### Abstract:

Plasmonics deals with the phenomena of collective vibration of electrons in the interface between metallic and dielectric media. With the advanced nanofabrication techniques, a broad variety of nanostructures can be designed and fabricated for plasmonic investigations at nanoscale. In this presentation, we will demonstrate our latest results of the design of new plasmonic nanostructures and the characterization of surface plasmon nanostructures with 2D materials by using Scanning Near-field Optical Microscopy (SNOM), which is one of the unique characterization tools for nano-optical detection, and other techniques, and discuss some fundamental properties for both localized surface plasmons and surface plasmon polaritons arise a new insight and understanding for the electro-optical devices, such as plasmonic PL control, active plasmonic modulator and detectors for energy harvesting.

### Keywords:

Plasmonics, Hot electrons, 2D materials

## Quantitative Metal Nanogap Plasmonics

NAM Jwa-Min\*<sup>1</sup>

<sup>1</sup>Department of Chemistry, Seoul National University  
jmnam@snu.ac.kr

### Abstract:

Designing, synthesizing and controlling plasmonic metal nanostructures with high precision and high yield are of paramount importance in optics, nanoscience, chemistry, materials science, energy and biotechnology. In particular, synthesizing and utilizing plasmonic nanostructures with ultrastrong, controllable and quantifiable signals is key to the wide and practical use of plasmonic enhancement-based spectroscopies including surface-enhanced Raman scattering (SERS), but highly challenging. Here, I will introduce the design and synthetic strategies for molecularly tunable and structurally reproducible plasmonic nanogap structures with strong, controllable and quantifiable SERS signals [1-10]. I will also show their potentials in addressing some of important challenges in science, and discuss how these new plasmonic nanogap materials can lead us to new breakthroughs in biotechnologies including biosensing, bioimaging and theranostic applications [11-14].

### References

- [1] J.-M. Nam\* et al, Nanogap-Engineerable, Raman-Active Nanodumbbells for Single-Molecule Detection, *Nature Materials* **9**, 50 (2010).
- [2] J.-M. Nam\* et al, Highly Uniform and Reproducible Surface-Enhanced Raman Scattering from DNA-Tailorable Nanoparticles with 1-nm Interior Gap, *Nature Nanotechnology* **6**, 452 (2011).
- [3] J.-M. Nam\* et al, Directional Synthesis and Assembly of Bimetallic Nanosnowmen with DNA, *J. Am. Chem. Soc.* **134**, 5456 (2012).
- [4] J.-M. Nam\* et al, Tuning and maximizing the single-molecule surface-enhanced Raman scattering from DNA-tethered Nanodumbbells, *ACS Nano* **6**, 9574 (2012).
- [5] J.-M. Nam\* et al, Single-Molecule and Single-Particle-Based Correlation Studies between Localized Surface Plasmons of Dimeric Nanostructures with ~1-nm Gap and Surface-Enhanced Raman Scattering, *Nano Letters* **13**, 6113 (2013).
- [6] J.-M. Nam\* et al, Plasmonic Nanosnowmen with a Conductive Junction as Highly Tunable Nanoantenna Structures and Sensitive, Quantitative and Multiplexable Surface-Enhanced Raman Scattering Probes, *Nano Letters* **14**, 6217 (2014).
- [7] J.-M. Nam\* et al, Thiolated DNA-Based Chemistry and Control in the Structure and Optical Properties of Plasmonic Nanoparticles with Ultrasmall Interior Nanogap, *J. Am. Chem. Soc.* **136**, 14052 (2014).
- [8] J.-M. Nam\* et al, Quantitative Plasmon Mode and Surface-Enhanced Raman Scattering Analyses of Strongly Coupled Plasmonic Nanotrimers with Diverse Geometries, *Nano Letters* **15**, 4628 (2015).
- [9] J.-M. Nam\* et al, Transformative Heterointerface Evolution and Plasmonic Tuning of Anisotropic Trimetallic Nanoparticles, *J. Am. Chem. Soc.* **139**, 10180 (2017).
- [10] J.-M. Nam\* et al, Plasmonic Nanogap-Enhanced Raman Scattering with Nanoparticles, *Accounts of Chemical Research* **49**, 2746 (2016).
- [11] J.-M. Nam\* et al, Oxidative Nanopeeling Chemistry-Based Synthesis and Photodynamic and Photothermal Therapeutic Applications of Plasmonic Core-Petal Nanostructures, *J. Am. Chem. Soc.* **136**, 16317 (2014).
- [12] J.-M. Nam\* et al, Plasmonically Engineered Nanoprobes for Biomedical Applications, *J. Am. Chem. Soc.* **138**, 14509 (2016).
- [13] J.-M. Nam\* et al, Synthesis, Optical Properties and Multiplexed Raman Bio-Imaging of Surface Roughness-Controlled Nanobridged Nanogap Particles, *Small* **12**, 4726 (2016)
- [14] J.-M. Nam\* et al, Dealloyed Intra-Nanogap Particles with Highly Robust, Quantifiable Surface-Enhanced Raman Scattering Signals for Biosensing and Bioimaging Applications, *ACS Central Science*, **4**, 277, (2018)

### Keywords:



## Toward Room-Temperature Quantum Photonics Based on Group III-Nitride Semiconductor Nanostructures

CHO Yong-Hoon\*<sup>1</sup>

<sup>1</sup>Department of Physics and KI for the NanoCentury, Korea Advanced Institute of Science and Technology (KAIST), Daejeon, Republic of Korea  
yhc@kaist.ac.kr

### Abstract:

Group III-nitride semiconductor nanostructures have attracted a lot of attention since they provide unique platform for versatile classical and quantum photonic applications. Here, we present effective single photon generation and exciton-polariton condensates at room temperature based on group III-nitride quantum structures grown on various nano- and micro-structures. First, we demonstrated the self-aligned deterministic coupling of single quantum dot (QD) to nanofocused plasmonic modes, showing strong spontaneous emission enhancement of QDs over a wide spectral range. We also found that the majority of the extracted light from single QD was guided toward the bottom of the pyramid with high directionality. Nano-pyramidal structures were detached from a substrate and the far-field radiation pattern was measured using Fourier microscopy. Second, we demonstrated the room-temperature exciton-polariton condensates from single hexagonal GaN core and GaN/InGaN core-shell microwires. Exciton-polaritons are bosonic quasi-particles providing a unique semiconductor-state system for studying interacting condensate. The temperature upper limit for GaN is expected to be above room temperature owing to large exciton binding energy and oscillator strength. The single microwire structure with the manipulation of this local excitation provide a versatile method to control the extended state at room temperature. These approaches overcome the major hurdles in the implementation of practical solid-state quantum devices and shows great promise for versatile quantum photonic applications.

### Keywords:

quantum dots, single photon generation, exciton-polariton condensates

## Ultrasensitive Terahertz Detection of Light-induced Conformational Change in Rhodopsin Nanovesicles

SEO Minah\*<sup>1</sup>

<sup>1</sup>Korea Institute of Science and Technology (KIST), Seoul 02792, Korea  
mse0@kist.re.kr

### Abstract:

To understand photo-reaction process in vision, elucidating molecular mechanisms of signal transduction in rhodopsin including a conformational change of retinal is very crucial, because a conformational change from 11-cis to all-trans configuration of retinal, specifically, initiates a chain reaction for further vision process. In this study, we developed an ultrasensitive terahertz (THz) molecule-specific sensing platform using nanoscale aperture resonance that allows us to detect the light-induced conformational change of retinal embedded in photoreceptor-nanovesicles. Terahertz electromagnetic waves have shown substantial promise for optical sensing and detecting of such small molecules, based on their intrinsic vibrational and rotational modes at THz frequency regime. In order to increase sensitivity and selectivity for small molecules, subwavelength metal structures in the order of  $\lambda/10 \sim \lambda/10,000$  have been suggested that can induce huge enhancement in field transmission/reflection and, in turn, colossal absorption cross section increase of the target molecules. Furthermore, to get more dramatic increase of sensing efficiency and accuracy, various sample capturing techniques such as netting or physical sweeping of target samples into sensing hot-spot have been shown. Our approach will provide a complete reinterpretation in improving ultrasensitive THz molecule-specific sensors.

### Keywords:

Molecule sensor, Terahertz spectroscopy, Near-field enhancement, Subwavelength optics

## Nanoscale electrostatic and electrochemical transistors in Vanadium dioxide

TANAKA Hidekazu<sup>\*2, 3</sup>, WEI TingTing<sup>2</sup>, SASAKI Tsubasa<sup>2</sup>, KANKI Teruo<sup>2</sup>

<sup>1</sup>충남대학교 물리학과, <sup>2</sup>Institute of Scientific and Industrial Research, Osaka University, <sup>3</sup>Center for Spintronics Research Network (CSRN), Graduate School of Engineering Science, Osaka University  
h-tanaka@sanken.osaka-u.ac.jp

### Abstract:

Vanadium dioxide ( $\text{VO}_2$ ) is the prototypical material, possessing a dramatic resistance changes between a metallic state and an insulating state around room temperature. Controlling of this MIT by an electric field is expected toward the realization of Mott transistor. We report  $\text{VO}_2$  nanowire channel based field effect-transistors with a side-gate-type, bilayer insulating gates, air-gap side gate type, respectively. The planer side-gate-type-FET with epitaxial  $\text{VO}_2$  channels width of 300 nm exhibited electrostatic channel resistance modulation of 4.5% at gate bias of 30 V in dry  $\text{N}_2$  atmosphere, and their modulation rate depends on channel wire width.  $\text{VO}_2$  nanowire-based FETs with high- $k$  inorganics  $\text{Ta}_2\text{O}_5$ /organic polymer parylene-C hybrid solid gate insulator were prepared to enhance induced carrier density, and the maximum value of resistance modulation is up to 8.6% for  $V_G = \pm 30$  V, near the phase transition temperature. As further investigation, dramatic transport changes were demonstrated by electric field-induced hydrogenation at room temperature in the  $\text{VO}_2$  nano channel FET through the nanogaps separated by humid air in a field-effect transistor with planar-type gates. We will discuss their modulation mechanism in nanoscale electrostatic and electrochemical transistors in correlated oxides.

### Keywords:

Vanadium Oxide, Nanoscale Devices, Transistor, Nanowire, FET

# Stabilization of 2-Dimensional Electron Gas and Interplay between Superconductivity and Magnetism in SrTiO<sub>3</sub> Capped LaAlO<sub>3</sub>/SrTiO<sub>3</sub>

송중현\*<sup>1</sup>, 김진희<sup>2</sup>

<sup>1</sup>충남대학교 물리학과, <sup>2</sup>표준과학연구원  
songjonghyun@cnu.ac.kr

## Abstract:

The LaAlO<sub>3</sub>/SrTiO<sub>3</sub> heterointerface exhibits various intriguing phenomena such as ferromagnetism and superconductivity. It has been widely studied for being a low-dimensional ferromagnetic oxide superconducting system with a strong gate-tunable spin-orbit interaction. However, its lack of stability and environmental susceptiveness have been an obstacle to its further experimental investigations and applications. We demonstrate that capping the bilayer with SrTiO<sub>3</sub> relieves this thickness limit, while enhancing the stability and controllability of the interface. In addition, the SrTiO<sub>3</sub>-capped LaAlO<sub>3</sub> exhibits unconventional superconductivity; the critical current dramatically increases under a parallel magnetic field, and shows a reversed hysteresis contrary to the conventional hysteresis of magnetoresistance. The oxide trilayer could be a robust platform for studying the extraordinary interplay of superconductivity and ferromagnetism at the interface electron system between LaAlO<sub>3</sub> and SrTiO<sub>3</sub>.

## Keywords:

2-Dimensional Electron Gas, Magnetism, Superconductivity, LaAlO<sub>3</sub>/SrTiO<sub>3</sub>

## Revealing of the Mott transition and perspective of its application in the VO<sub>2</sub> films

SLUSAR Tetiana\*<sup>1</sup>, CHO Jin-Cheol<sup>1, 2</sup>, LEE Hyang-Rok<sup>3</sup>, YEE Ki-Ju<sup>3</sup>, KIM Hyun-Tak<sup>1, 2</sup>

<sup>1</sup>MIT Lab, ETRI, <sup>2</sup>Department of Advanced Device Technology, UST, <sup>3</sup>Department of Physics, CNU  
tslusar@etri.re.kr

### Abstract:

In 1959 Morin discovered a reversible phase changing from insulator to metal (IM transition or IMT) in a bulk VO<sub>2</sub> single-crystal, occurred on heating-cooling cycles at a critical temperature ( $T_{IMT}$ ) of ~ 340 K. Along with the “jump” in electrical properties, the IMT is associated with a structural transition and IR optical switching. These property-changing features make VO<sub>2</sub> an attractive material for various applications (sensors, smart windows, memory devices, transistors etc.).

To meet the industrial requirements leading to the widespread VO<sub>2</sub>-based devices implementation, the following challenges should be overcome:

Dimensionality reduction of the samples (bulk crystals → thin films → nanowires → nanoparticles) while maintaining their excellent properties;

Effective integration of VO<sub>2</sub> with existing Si-based technology;

Fabrication of the samples with controllable  $T_{IMT}$  values;

Realization of the ultrafast electronic switching within the same crystalline structure (Mott transition);

Understanding of the physics of the phase transition in VO<sub>2</sub>.

In the talk, using the VO<sub>2</sub> thin films (the most adequate dimensionality for the application purposes) on AlN/Si substrate, we prove the excellence of the properties of VO<sub>2</sub> joined with silicon, reveal the Mott transition pathway and perspective of the VO<sub>2</sub> application.

### Keywords:

Mott Transition, transition metal oxide, VO<sub>2</sub>, thin films, 2D heterostructure

## Self-interaction correction calculations of band edges and alignments in transition metal dichalcogenides and their heterostructures

김용훈\*<sup>1</sup>, 김효석<sup>1</sup>

<sup>1</sup>한국과학기술원 EEWS대학원  
y.h.kim@kaist.ac.kr

### Abstract:

In view of realizing advanced devices based on newly emerging low-dimensional materials and their heterostructures, prediction of band edges and their alignment is currently a primary target of first-principles calculations. Because of the well-known self-interaction error, the conventional local density and generalized gradient approximations within density functional theory (DFT) perform poorly in predicting band lineup and defect states. Although adopting hybrid DFT functionals or the many-body GW method could be in principle a solution, their computational cost is often too high to be routinely employed. Self-interaction correction approaches could provide a practical solution for this problem [1], and in this work we particularly consider the atomic self-interaction correction (ASIC) method [2]. While previous ASIC studies typically used a globally fixed ASIC parameter, we recently showed that selecting different ASIC parameters according to atomic species could provide more reliable defect level locations for transition metal dichalcogenide (TMDC)/graphene interfaces [3]. Here, we extend the study and apply the method to various TMDC/TMDC and TMDC/graphene heterostructures with or without defects. Comparison with available experimental results show that our approach can accurately and efficiently predict band alignment and defect states in TMDC and heterostructures based on them [4].

[1] J. P. Perdew and A. Zunger, Phys. Rev. B **23**, 5048 (1981).

[2] C. D. Pemmaraju, T. Archer, D. Sánchez-Portal, and S. Sanvito, Phys. Rev. B **75**, 045101 (2007).

[3] J. Shim, *et al.* Adv. Mater. **28**, 5293 (2016).

[4] H. S. Kim, S. Sanvito, and Y.-H. Kim (in preparation).

### Keywords:

ASIC, TMDC

## *Ab initio* Study of Uniaxial Stress Applied GeTe, a Phase Transition Material for Non-thermal Phase Transition Mechanism

박한진<sup>1</sup>, 양원준<sup>2</sup>, 김다솔<sup>2</sup>, 박승종<sup>2</sup>, 조만호<sup>2</sup>, 권영균\*<sup>1</sup>

<sup>1</sup>경희대학교 물리학과, <sup>2</sup>연세대학교 물리학과  
ykkwon@khu.ac.kr

### Abstract:

Recently, phase change materials (PCM) have attracted attention as candidate for next generation memory device elements. But it has several problems in power consumption, information storage capacity, energy efficiency, and so on. We use *ab initio* density functional theory to investigate *non thermal* phase transition of a prototypical phase change material, GeTe, induced by uniaxial strain. We focus on the rhombohedral structure which can be interpreted as a layered structure, in which layers are separated by long bonds. It is found that GeTe layered structure experiences a phase transition from one crystalline phase to the other crystalline one under external uniaxial tensile stress. We identify that the latter phase is essentially regarded as another layered structure rotated from the former phase through the exchange mechanism between short and long bonds. Our electronic transport calculation also shows that the conductance changes significantly during such phase transition, implying that uniaxial strain may induce non-thermal phase transition in GeTe.

### Keywords:

PCM, PCRAM, Phase transition

## First principles calculations on Electronic structures and Polar properties in ( $\kappa$ , $\epsilon$ )-Ga<sub>2</sub>O<sub>3</sub>

김복기\*<sup>1</sup>, 김주영<sup>1</sup>  
<sup>1</sup>부산대학교 물리학과  
boggikim@pusan.ac.kr

### Abstract:

Recently, Ga<sub>2</sub>O<sub>3</sub> has been attracted lots of research interest because of its fascinating properties as well as potential applications. The polar polymorphic structure of Ga<sub>2</sub>O<sub>3</sub>,  $\kappa$ -Ga<sub>2</sub>O<sub>3</sub> and  $\epsilon$ -Ga<sub>2</sub>O<sub>3</sub>, was the main research theme, however, there are quite inconsistent reports. By first-principles calculations, we have investigated the electronic structure and polar properties of  $\kappa$ - and  $\epsilon$ -Ga<sub>2</sub>O<sub>3</sub>. We have analyzed the polarization value for the  $\kappa$ - and  $\epsilon$ -Ga<sub>2</sub>O<sub>3</sub> by layer analysis to confirm the ferroelectric alignment of the polarization in the different layers. Moreover, the bandgap of materials is estimated with two different functional methods, which are the hybrid functional method and PBEsol functional. Our works not only show that the clear explanation of inconsistency in previous studies, but also play important roles for future study on the technological breakthrough using polar Ga<sub>2</sub>O<sub>3</sub>.

### Keywords:

Ga<sub>2</sub>O<sub>3</sub>, First principle calculation, polarization

## Reentrant Quantum Spin Hall States in Charge Density Wave Phase of Doped Single-Layer Transition Metal Dichalcogenides

이준호<sup>1</sup>, 손영우\*<sup>1</sup>  
<sup>1</sup>고등과학원 계산과학부  
hand@kias.re.kr

### Abstract:

Using first-principles calculation methods, we reveal a series of phase transitions as a function of electron doping in single-layer 1T'-MoTe<sub>2</sub> and 1T'-WTe<sub>2</sub> exhibiting quantum spin Hall (QSH) edge states without doping. As increasing doping, we show that a phonon mediated superconducting phase first realizes and is followed by a charge density wave (CDW) phase with a nonsymmorphic lattice symmetry. The newly found CDW phase exhibits Dirac or Weyl energy bands with a spin-orbit coupling in case of a fractional band filling and re-enters into topological insulating phase with fully filled bands. The robust resurgence of QSH state coexisting with the CDW phase is shown to originate from band inversions induced by the nonsymmorphic lattice distortion through the strong electron-phonon interaction, thus suggesting a realization of various interfacial states between superconducting, density wave and topological states on a two-dimensional crystal only by doping.

### Keywords:

Quantum spin Hall state, charge-density wave, monolayer 1T'-TMDCs

## Vacancy distribution and structural distortion in Ge-Sb-Te phase change materials

송영선<sup>1</sup>, 지승훈\*<sup>1</sup>

<sup>1</sup>포항공과대학교 물리학과  
seunghoonjhi@gmail.com

### Abstract:

Chalcogenide ternary compounds  $\text{Ge}_2\text{Sb}_2\text{Te}_5$  (GST) are well-known phase-change materials that exhibit fast structural transition between amorphous and crystalline phases. Metastable m-GST, its crystalline phase, is a distorted NaCl structure with 4(b) sites occupied by 40% Ge, 40% Sb, and 20% vacancies. Atomic configuration of 4(b) sites, especially the distribution of vacancy, is known to be crucial not only for phase-change process but also to the electrical transition such as Anderson localization. Despite its significance, consensus on the 4(b)-site configuration is yet to be established. In this talk, we present the effect of vacancy ordering in m-GST on material properties, in terms of resonant bonding. We established a simple tight binding model which enables us to analyze the total system as a set of linear atomic chains. We then calculated the energy and the delocalization properties of the linear chains using the tight binding model and ab initio calculations. We found that the vacancy distribution determines the geometry of linear chains and ultimately energetics and resonance of the system. We also found that disorder in vacancy distribution leads to dynamic instability of the system that induces a Peierls-type dimerization. Further calculations revealed that such structural distortions ultimately affect the electrical conductivity and the dielectric function. We expect that this work will deepen our understanding of resonant p-bonds in GST system and the relationship between vacancy ordering and material properties.

### Keywords:

Phase change materials,  $\text{Ge}_2\text{Sb}_2\text{Te}_5$ , Vacancy ordering, Resonant bond, Density Functional Theory, Tight binding model

## MoS<sub>2</sub> @VS<sub>2</sub> nanocomposite as a superior hybrid anode material for Li/Na ion batteries

신영한\*<sup>1</sup>, SAMAD ABDUS<sup>1</sup>

<sup>1</sup>울산대학교 물리학과  
hoPONPOP@ulsan.ac.kr

### Abstract:

Pristine monolayer MoS<sub>2</sub> is almost noble to the Li/Na adsorption. It also has a high band gap which can reduce the Li/Na reversibility. On the other hand monolayer VS<sub>2</sub> is metallic and binds the Li/Na ions strongly however it has not been prepared experimentally to date. Using density functional theory calculations we show that the monolayer VS<sub>2</sub> can be stabilized by using monolayer MoS<sub>2</sub> as a substrate. The monolayer VS<sub>2</sub> is stabilized because of the high energy released in the formation of the MoS<sub>2</sub> @VS<sub>2</sub> nanocomposite and interfacial charge accumulation. It also boosts the Li/Na adsorption capacity and electronic conductivity of the anode. The Li/Na storage capacity of the nanocomposite reaches to 584 mAh/g. The Li/Na diffusion barriers at the MoS<sub>2</sub> and VS<sub>2</sub> surfaces of the nanocomposite are comparable to those on their corresponding monolayers. The Li/Na diffusion barriers at the interface of the nanocomposite are comparable to those in the bulk MoS<sub>2</sub>. Capping monolayer MoS<sub>2</sub> with monolayer VS<sub>2</sub> can cover the weakness of the two material as an anode for Li/Na ion batteries.

### Keywords:

Li/Na ion batteries, MoS<sub>2</sub>@VS<sub>2</sub> nanocomposite, Specific capacity, Diffusion barrier

## How & Why does the time-evolving Kohn-Sham wavefunctions observe the Berry curvature of a solid?

박노경\*<sup>1</sup>, 신동빈<sup>1</sup>

<sup>1</sup>울산과학기술원 자연과학부  
noejung@unist.ac.kr

### Abstract:

In recent decade, topological numbers have become an important index to characterize the quantum mechanical behavior of Bloch electrons. Besides heuristic simplified model, actual calculations of Chern numbers and Berry curvatures have been achieved through the linear responses of the ground state electronic structure. Here we explore an alternative way of computation using the real-time propagation time dependent density functional theory (rt-TDDFT). By adding a mild dc-bias field through the vector potential, the real-time scheme can make the Bloch vector run adiabatically around the whole Brillouin zone, which produces the band Chern number or Berry phase in the response of Hall current. We discuss that, while our results are consistent with the values obtained from the linear response, and this real-time scheme can naturally be extended to a non-linear regime. Our examples include valley Hall, quantum spin Hall, and quantum anomalous Hall system. We further investigate the non-equilibrium charge and spin accumulation on edge of nano-ribbon in valley Hall and spin valley Hall system.

### Keywords:

DFT, TDDFT, Berry curvature

## Electronic properties of periodically oxygen-terminated phosphorus graphene

CHAE Jinwoong<sup>1</sup>, KIM Gunn\*<sup>1</sup>

<sup>1</sup>Department of Physics and Astronomy & Graphene Research Institute, Sejong University  
kingunn@gmail.com

### Abstract:

Using ab initio calculations based on density functional theory, we have investigated geometric and electronic properties of the oxygen-terminated polyphenylene superhoneycomb network (O-PSN) and compared them with those of the hydrogen-terminated PSN. In our study, the energy cutoff was 600 eV, and the wave functions were expanded, using a plane wave basis set. According to our band structure calculations, the band gap of PSN (O-PSN) is 2.40 eV (0.91 eV). Interestingly, PSN has a direct band gap whereas O-PSN has an indirect band gap. We will also compare the detailed projected densities of states of the two systems.

### Keywords:

DFT, Phosphorus graphene

## Ferromagnetism and magnetic nodal lines in a hexagonal InC sheet

김영국\*<sup>1, 2, 3</sup>, 전수남<sup>2, 3</sup>, 오윤탁<sup>1</sup>

<sup>1</sup>성균관대학교 물리학과, <sup>2</sup>성균관대학교 에너지과학과, <sup>3</sup>Center for Integrated Nanostructure Physics (CINAP), Institute for Basic Science (IBS)  
youngkuk@skku.edu

### Abstract:

Based on first-principles calculations, we design a novel two-dimensional (2D) ferromagnetic system hosting symmetry-protected magnetic nodal lines in momentum space. We show that a hexagonal InC sheet is stabilized by a ferromagnetic order, characterizing one-dimensional line nodes protected by mirror symmetry without time-reversal symmetry. Both type-I and type-II-like nodal lines occur near the Fermi level with an alternating chain of electron and hole pockets, originated from trigonal warping. We argue that type-I and type-II nodal lines hosted in a generic 2D system can be qualitatively distinguished by the chain of electron and hole pockets. The symmetry protection of the line nodes is rationalized based on our tight-binding model.

Our finding suggests that the hexagonal InC may provide a new venue for carbon-based 2D ferromagnetism and spin-related phenomena.

### Keywords:

Two dimension, nodal lines, ferromagnetism

## Quantum dot excitons coupled to a hyperbolic metamaterial

이동환\*<sup>1</sup>, 장유동<sup>1</sup>, DEVARAJ Vasanthan<sup>1</sup>, 김문덕<sup>1</sup>

<sup>1</sup>충남대학교 물리학과  
dlee@cnu.ac.kr

### Abstract:

Hyperbolic metamaterial (HMM) has anisotropic dielectric constants, negative in one direction and positive in other directions. As a result, its isofrequency curve is hyperboloidal, supporting infinite wavevectors ( $k$ ) at a given frequency and, as a result, allowing propagation of high- $k$  modes, evanescent waves, in the HMM medium. Since HMM has a large photonic density of states (PDOS) due to abundant high- $k$  states coming from the hyperbolic dispersion curve and the spontaneous emission rate of an emitter increases proportionally with PDOS, an emitter placed close to HMM is expected to experience the strong rate enhancement.

Enhancement of the emission rate using HMM has been reported with dye molecules or colloidal quantum dots, but only qualitatively. We demonstrate quantitatively the role of HMM in the emission rate enhancement by coupling excitons in epitaxial quantum dots to the HMM, utilizing ideal characteristics of the quantum dots: the precisely defined distance between emitters and HMM, the same dipole direction for all emitters, single-exponential PL decay, and isolation of metal-related effects.

### Keywords:

quantum dot, exciton, metamaterial

## Quantum photonics based on solid-state quantum system

김제형\*<sup>1, 2</sup>, WAKS Edo<sup>2</sup>

<sup>1</sup>울산과학기술원 물리학과, <sup>2</sup>Department of Electrical and Computer Engineering and Institute for Research in Electronics and Applied Physics, University of Maryland  
jehyungkim@unist.ac.kr

### Abstract:

Excitons in nano-sized semiconductors show interesting optical and electrical properties. Especially when they are in three-dimensionally confined quantum structures, i.e, quantum dots, they behave like artificial atoms. Single excitons in solid-state quantum structures can provide a source of single photons, and the multiple exciton complex such as biexciton or charged exciton are useful to realize entangled photon pairs and spin qubits. Recently there have been a number of studies that integrate these solid-state quantum emitters to various photonic structures and demonstrate bright single photon sources, cavity quantum electrodynamics, non-linear quantum switch, and quantum simulators. Although the semiconductor quantum dots have a strong potential for the applications in quantum information science, the randomness in their frequency and position, and strong interaction with the environment which limits them to be used for practical applications since the most quantum information processing require multiple qubits with long coherence time. Here, I present recent research on quantum dots in a photonic crystal structure for quantum photonics applications. Quantum dots, engineered electronic band structures, are able to generate quantum light, and the photonic crystal, engineered photonic band structures can enhance the brightness and spontaneous emission rate of the coupled emitters. To overcome randomness we developed a local engineering technique that enables multiple, identical quantum dots on-a-chip. As a result, we successfully demonstrate two-photon interference measurements between single photons from separated quantum dots and super-radiant emission between two quantum dots on a waveguide. Our approaches, therefore, pave the way for the scalable, controllable quantum devices involving multiple, identical quantum emitters on a chip.

### References:

- [1] J.-H. Kim et al., Two-photon interference from the far-field emission of chip-integrated cavity-coupled emitters, *Nano Letters*, 16, 7061 (2016)
- [2] J.-H. Kim et al., Hybrid integration of solid-state quantum emitters on a silicon photonic chip, *Nano Letters*, 17, 7394 (2017)

### Keywords:

quantum dots, photonic crystals, quantum photonics, single photon, excitons

## 그래핀에서의 2차원 엑시톤 광발광 특성

박영신\*<sup>1</sup>, 명창우<sup>1</sup>, 황찬국<sup>2</sup>

<sup>1</sup>울산과학기술원 자연과학부, <sup>2</sup>포항가속기 연구소 빔라인부  
ysinpark@unist.ac.kr

### Abstract:

2004년 그래파이트로부터 단일 층의 그래핀을 박리하는데 성공함으로써 지난 십 수년간 그래핀에 대한 수없이 많은 연구가 이루어졌다. 이는 그래핀이 가지는 고유한 특성이 볼루리언 영역의 K 점에서 전도대와 가전자대가 만나 선형적인 디랙콘을 형성함으로써 우수한 전기적인 특성을 나타내어 차세대 전자소자의 소재로서 각광을 받아왔다. 그러나 에너지 갭이 0이라는 점은 오히려 전자소자의 개발에는 제한을 초래하고, 광학소자로는 이용할 수 없는 단점이 있다. 따라서 본 연구에서는, 그래핀을 Cu 기판 위에 성장함으로써 그래핀의 카본과 Cu 표면의 하이브리드에 의하여 그래핀에 새로운 밴드를 형성함으로써 2차원의 엑시톤 천이 과정을 측정하였고, 그 결과 3.16 eV 근처에서 3 meV 정도의 반치폭을 가지는 아주 강한 엑시톤을 관측을 하였다. 밀도 함수론 계산을 통하여 이들 에너지가 그래핀의  $\pi$ 와 Cu의 d 궤도의 하이브리드에 의해서 형성된 새로운 밴드임을 확인 하였고, 이들 결과로부터 그래핀을 광학적인 소자로서의 응용 가능성을 제시한다.

본 연구는 한국 연구 재단의 기초연구과제 (2015R1D1A1A01058332) 및 토포로지 물질연구센터 (No. 2011-0030787)를 통하여 지원 받았음.

### Keywords:

2차원의 photoluminescence, 그래핀, 하이브리드

## Resonantly enhanced second harmonic generation at exciton levels in transition metal dichalcogenide nanostructures

장 (Jang)준익 (Joon Ik)\*<sup>1</sup>, 임 (Rhim)성현 (Sonny)<sup>2</sup>, 김 (Kim)용수 (Yong Soo)<sup>2</sup>  
<sup>1</sup>서강대학교 물리학과, <sup>2</sup>울산대학교 물리학과  
jjcoupling@sogang.ac.kr

### Abstract:

Every nonlinear optical (NLO) phenomenon occurs as a consequence of the change in optical properties of a host material in the presence of strong electromagnetic perturbation, which in turn induces the modification of the light field itself. Noncentrosymmetrically engineered nanostructures derived from transition metal dichalcogenides (TMDs) provide an ideal platform for studying atomic-scale NLO effects, especially second harmonic generation (SHG). In this focus session, we will talk about wavelength-dependent SHG response observed from the artificially stacked TMD nanostructures, consisting of  $\text{MoS}_2\text{xSe}_2(\text{x}-1)$  monolayers with different energy gaps. Our proof-of-concept study indicates that the spectral range for efficient SHG can be manipulated by controlling the Se concentration of each layer, which in turn tunes the energy levels of the spin-orbit-split A exciton and B exciton of each layer. The strengthening and widening effects of SHG are interpreted as the superposition of resonant SHG across the A exciton and B exciton levels of the constituent layers. Our results demonstrate the feasibility of two-dimensional scaffolds in which highly efficient SHG can be harnessed over a broad spectral range.

### Keywords:

transition metal dichalcogenide, second harmonic generation, excitons, resonance, vertical heterostructure

## A phenomenological theory of the anomalous pseudogap phase in underdoped cuprates

ZHANG Fuchun\*<sup>1</sup>

<sup>1</sup>Kavli Institute for Theoretical Sciences (UCAS)  
fuchun@ucas.ac.cn

### Abstract:

Underdoped cuprates show anomalous pseudogap phase, which is challenging to describe in the conventional Landau Fermi liquid theory. In this talk, I shall present a phenomenological theory proposed by Yang, Rice and myself, based on an ansatz analogies to the approach to Mott localization at weak coupling in lower dimensional systems. I will describe the motivation underlying this ansatz and make comparison with a range of experiments.

### Keywords:

high temperature superconductivity, underdoped cuprates

## Electron Number-Based Phase Diagram of $\text{Pr}_{1-x}\text{LaCe}_x\text{CuO}_{4-\delta}$ and Possible Absence of Disparity between Electron- and Hole-Doped Cuprate Phase Diagrams

김창영\*<sup>1</sup>

<sup>1</sup>서울대학교 물리천문학부  
changyoung@snu.ac.kr

### Abstract:

We performed annealing and angle resolved photoemission spectroscopy studies on electron-doped cuprate of  $\text{Pr}_{1-x}\text{LaCe}_x\text{CuO}_{4-\delta}$  (PLCCO). It is found that the optimal annealing condition is dependent on the Ce content  $x$ . The electron number ( $n$ ) is estimated from the experimentally obtained Fermi surface volume for  $x=0.10$ , 0.15 and 0.18 samples. It clearly shows a significant and annealing dependent deviation from the nominal  $x$ . In addition, we observe that the pseudo-gap at hot spots is also closely correlated with  $n$ ; the pseudogap gradually closes as  $n$  increases. We established a new phase diagram of PLCCO as a function of  $n$ . Different from the  $x$ -based one, the new phase diagram shows similar antiferromagnetic and superconducting phases to those of hole doped ones. Our results raise a possibility for absence of disparity between the phase diagrams of electron- and hole-doped cuprates.

### Keywords:

Superconductivity, ARPES, Cuprate

## Dirac magnons and nodal line magnons: theory and experiment

FANG Chen\*<sup>1</sup>

<sup>1</sup>Institute of Physics, Chinese Academy of Sciences  
cfang@iphy.ac.cn

### Abstract:

We study the topological properties of magnon excitations in three-dimensional antiferromagnets, where the ground state configuration is invariant under time-reversal followed by space-inversion (PT-symmetry). We prove that Dirac points and nodal lines, the former being the limiting case of the latter, are the generic forms of symmetry-protected band crossings between magnon branches. As a concrete example, we study a Heisenberg spin model for a "spin-web" compound, Cu<sub>3</sub>TeO<sub>6</sub>, and show the presence of the magnon Dirac points assuming a collinear magnetic structure. Upon turning on symmetry-allowed Dzyaloshinsky-Moriya interactions, which introduce a small non-collinearity in the ground state configuration, we find that the Dirac points expand into nodal lines with nontrivial Z<sub>2</sub>-topological charge, a new type of nodal lines unpredicted in any materials so far. As a follow up on the theory, we use inelastic neutron scattering to reveal the presence of topological spin excitations (magnons) in Cu<sub>3</sub>TeO<sub>6</sub>, which features a unique lattice of magnetic spin-1/2 Cu<sup>2+</sup> ions. Using highly accurate measurement and calculation, we visualize two magnon bands that cross at Dirac points protected by (approximate) U(1) spin-rotation symmetry. Being the limiting case of topological nodal lines with Z<sub>2</sub>-monopole charges, these Dirac points are new to the family of experimentally confirmed topological band structures. Our results render magnon systems a fertile ground for exploring novel band topology with neutron scattering, along with distinct observables in other related experiments.

### Keywords:

Exotic magnetism, Dirac Magnons

## Higgs Mode and its Decay in the Two-Dimensional Antiferromagnet $\text{Ca}_2\text{RuO}_4$

김범준\*<sup>1</sup>

<sup>1</sup>포항공과대학교 물리학과  
bjkim6@gmail.com

### Abstract:

Condensed-matter analogs of the Higgs boson in particle physics allow insights into its behavior in different symmetries and dimensionalities. Evidence for the Higgs mode has been reported in a number of different settings, including ultracold atomic gases, disordered superconductors, and dimerized quantum magnets. However, decay processes of the Higgs mode (which are eminently important in particle physics) have not yet been studied in condensed matter due to the lack of a suitable material system coupled to a direct experimental probe. A quantitative understanding of these processes is particularly important for low-dimensional systems where the Higgs mode decays rapidly and has remained elusive to most experimental probes. In this talk, I will discuss on our recent discovery of a Higgs mode in a two-dimensional antiferromagnet, which we study using spin-polarized inelastic neutron scattering. Our spin-wave spectra of  $\text{Ca}_2\text{RuO}_4$  directly reveal a well-defined, dispersive Higgs mode, which quickly decays into transverse Goldstone modes at the antiferromagnetic ordering wavevector. Through a complete mapping of the transverse modes in the reciprocal space, we uniquely specify the minimal model Hamiltonian and describe the decay process. We thus establish a novel condensed matter platform for research on the dynamics of the Higgs mode.

### Keywords:

higgs mode, quantum magnet

## Self-organizing behavior in coupled oscillators that sync and swarm

홍현숙\*<sup>1</sup>

<sup>1</sup>전북대학교 자연과학대학, 물리학과  
hhong@jbnu.ac.kr

### Abstract:

Synchronization phenomena have been widely observed in various systems in nature, where the individual component in the system coordinate the timing of their oscillatory behavior, but they do not move through space. Another form of the self-organization has been observed in flocking birds and schooling fish etc., but with no substantial changing their internal states. We here explore systems in which both coordinating timing and swarming of the components occur together. In particular, we consider coupled oscillators that can swarm and synchronize via the interplay between the spatial dynamics and the state ones. We model a system that shows such dual character, and find that the system exhibits collective states that may be observable in some real biological and physical systems.

Ref: "Oscillators that sync and swarm", Kevin P. O'Keefe, Hyunsuk Hong, and Steven H. Strogatz, Nature Communications 8, 1504 (2017).

### Keywords:

swarming oscillators, self-organization, coupled oscillators, collective behavior

## Nonlinear Disordered Discrete Time Quantum Walks

세르게이플라흐\*<sup>1</sup>

<sup>1</sup>기초과학연구원 복잡계 이론물리 연구단  
sflach@ibs.re.kr

### Abstract:

Discrete quantum walks (DQW) are a main tool in quantum computing research. At the same time, they are fascinating mathematical models on lattices with unitary operators involving only nearest neighbor coupling, and thus with a speedup in certain computations up to two orders of magnitude as compared to Hamiltonian based dynamics. I will introduce the translationally invariant DQW and its massive Dirac two-band structure. I will then introduce disorder and demonstrate the existence of, and control over Anderson localization [1]. Finally I will generalize the disordered DQW by adding nonlinear terms to the unitary operations. As a result, wave packet dynamics is characterized by a slow sub-diffusive destruction of Anderson localization [2]. I will show that we can drive this process to unprecedented times as compared to previous studies. This will allow us to surpass the current computational horizon by a factor of up to  $10^3$  and check whether the never-ending sub-diffusion IS keeping its universality beyond the hold horizons, or whether a slowing down effect will be seen as claimed in some publications.

[1] I. Vakulchyk, M. V. Fistul, P. Qin and S. Flach, Phys. Rev. B 96, 144204 (2017)

[2] I. Vakuchyk, M.V. Fistul and S. Flach, in preparation.

### Keywords:

discrete time quantum walks, disorder, Anderson localization, nonlinearities, wave packet spreading, subdiffusion

## Weakly nonergodic dynamics in the Gross-Pitaevskii lattice

THUDIYANGAL Mithun\*<sup>1</sup>, KATI Yagmur<sup>1</sup>, DANIELI Carlo<sup>1</sup>, FLACH Sergej<sup>1</sup>

<sup>1</sup>Center for Theoretical Physics of Complex Systems, Institute for Basic Science, Daejeon 34126, Korea  
mithunnairt@gmail.com

### Abstract:

The microcanonical Gross-Pitaevskii (aka semiclassical Bose-Hubbard) lattice model dynamics is characterized by a pair of energy and norm densities. The grand canonical Gibbs distribution fails to describe a part of the density space, due to the boundedness of its kinetic energy spectrum. We define Poincare equilibrium manifolds and compute the statistics of microcanonical excursion times off them. The distribution function tails quantify the proximity of the many-body dynamics to a weakly-nonergodic phases, which occurs when the average excursion time is infinite. We find that a crossover to weakly-nonergodic dynamics takes place inside the nonGibbs phase, being unnoticed by the largest Lyapunov exponent.

### Keywords:

Nonergodic dynamics, Gibbs distribution

# Intermittent Dynamics and Weak Non-Ergodicity in Many-Body Systems

DANIELI Carlo\*<sup>1</sup>, FLACH Sergej<sup>1</sup>

<sup>1</sup>Center for Theoretical Physics of Complex Systems, Institute for Basic Science, Daejeon, Korea  
peldicarotadaywalker@gmail.com

## Abstract:

Integrable models are characterized by a set of preserved actions. Close to the limits, the nonintegrable perturbations span a coupling network in action space which can be short or long ranged. The equilibrium dynamics of a system close to such limits is sensitive to the network type. Long range networks enforce ergodicity with large but finite relaxation time scales at a finite distance to the integrable limit. Short range networks lead to a loss of ergodicity at a finite distance from the limit. We demonstrate this by choosing observables which turn conserved actions at the limit. Off the limit, and fixing their value to the proper statistical average, they define manifolds in the phase space of an ergodic and equipartitioned many-body system. A typical trajectory pierces such manifolds infinitely often as time goes to infinity. Close to the integrable limit, the dynamics yields a power-law distribution of the excursion times off the manifolds. The exponent is used as a measure of distance from a weakly nonergodic regime. We analyse several cases: the Fermi Pasta Ulam chain in the limit of small energies (long range network), and the Klein-Gordon, Discrete Gross Pitaevskii and coupled rotor lattices in the limit of large energies (short range network).

## Keywords:

Nonlinear dynamics, Ergodicity, Integrability

## Signatures of many-body localization in steady states of open quantum systems

VAKULCHYK Ihor<sup>\*1, 2</sup>, YUSIPOV Igor<sup>3</sup>, IVANCHENKO Mikhail<sup>3</sup>, FLACH Sergej<sup>1</sup>, DENISOV Sergey<sup>3, 4</sup>  
<sup>1</sup>Center for Theoretical Physics of Complex Systems, IBS, <sup>2</sup>Korea University of Science and Technology,  
<sup>3</sup>Lobachevsky University, <sup>4</sup>University of Augsburg  
igrvak@gmail.com

### Abstract:

Many-body localization (MBL) is a result of the balance between interference-based Anderson localization and many-body interactions in an ultra-high dimensional Fock space. It is usually expected that dissipation is blurring interference and destroying that balance so that the asymptotic state of a system with an MBL Hamiltonian does not bear localization signatures. We demonstrate, within the framework of the Lindblad formalism, that the system can be brought into a steady state with non-vanishing MBL signatures. We use a set of dissipative operators acting on pairs of connected sites (or spins), and show that the difference between ergodic and MBL Hamiltonians is encoded in the imbalance, entanglement entropy, and level spacing characteristics of the density operator. An MBL system which is exposed to the combined impact of local dephasing and pairwise dissipation evinces localization signatures hitherto absent in the dephasing-outshped steady state.

### Keywords:

many-body localization (MBL), open systems, Lindblad, dissipation

## Excitation of localized states in the flat band of exciton-polariton Lieb lattice

SUN Meng<sup>\*1, 2</sup>, SAVENKO Ivan<sup>1</sup>, RUBO Yuri<sup>1, 3</sup>, FLACH Sergej<sup>1</sup>

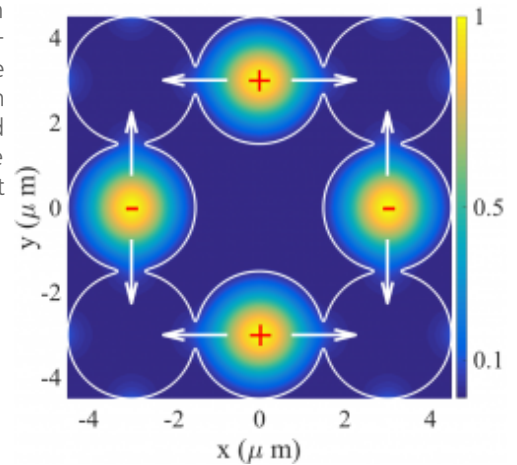
<sup>1</sup>Center for Theoretical Physics of Complex Systems, Institute for Basic Science (IBS), Daejeon 34051, Republic of Korea, <sup>2</sup>Basic Science Program, Korea University of Science and Technology (UST), Daejeon 34113, Republic of Korea, <sup>3</sup>Instituto de Energias Renovables, Universidad Nacional Autonoma de Mexico, Temixco, Morelos, 62580, Mexico  
sunmeg.89@gmail.com

### Abstract:

We demonstrate the possibility to excite the compact localized states in the flat band of exciton-polariton Lieb lattice by the short Laguerre-Gaussian pulse and investigate the stability of these states in the presence of distributed losses in the lattice and repulsive interaction between polaritons. We show how the graphs of the localized states are extended in time in the presence of additional incoherent pumping, which paves the way for analogue computations with exciton-polariton condensates in flat bands.

### Keywords:

Exciton-Polariton; Flat Band;



## Evolution of carrying capacity induced from mutation and extinction of populations in a stochastic system

박혜진\*<sup>1</sup>, PICHUGIN Yuriy<sup>1</sup>, HUANG Weini<sup>2</sup>, TRAUlsen1 Arne<sup>1</sup>

<sup>1</sup>Max Planck Institute for Evolutionary Biology Theory Department, <sup>2</sup>Centre for Tumour Biology, Barts Cancer Institute  
phj.hyejin@gmail.com

### Abstract:

Once a mutant emerges in the population, new interactions are drawn between types, which may lead to changes in the population size. Using the game theory, we implement this population dynamics in a stochastic system. Since interactions between types are described by a game payoff matrix, the emergence of a mutant is interpreted as extending the payoff matrix. New equilibria can emerge by the change of the payoff matrix. If the population settles to a new equilibrium state, the population size changes. We examine the change of population size in time and quantify the extinction risk by the mean time to extinction.

### Keywords:

Evolutionary dynamics, Population dynamics, Stochastic process, Extinction phenomenon

## High-speed FRET-PAINT for tissue imaging

홍성철\*<sup>1</sup>

<sup>1</sup>서울대학교 물리.천문학부  
shohng@snu.ac.kr

### Abstract:

Superresolution fluorescence microscopy can generate molecule-specific three-dimensional images with tens of nanometer resolution. Unfortunately, current superresolution fluorescence microscopy techniques cannot operate at thick tissue samples due to huge background generated from samples and photobleaching of fluorescent probes. We developed multi-colored superresolution fluorescence microscopy that provides 3D images of thick samples by combining the line-illumination confocal microscopy (LICM) with the DNA-PAINT technique. Good optical sectioning capability of LICM allowed clear 3D images by suppressing excessive fluorescence background of the DNA-PAINT approach, which normally prevented thick sample imaging. On the other hand, DNA PAINT freed us from the photobleaching problem of STORM probes, and we could obtain super-resolution 3D images of whole cells. The imaging speed of DNA-PAINT (1-3 frames per hour), however, is extremely slow compared to those of other super-resolution fluorescence microscopy techniques. To overcome the problem, we developed an accelerated super-resolution fluorescence microscopy named FRET-PAINT. Compared to conventional DNA-PAINT, the imaging speed of the microscopy was increased up to 55-fold.

### Keywords:

Superresolution Fluorescence Microscopy, DNA-PAINT, FRET

## Breaking the Photobleaching and Labeling Limits of Super-resolution Optical Microscopy

심상희\*<sup>1</sup>

<sup>1</sup>고려대학교 화학과  
sangheeshim@korea.ac.kr

### Abstract:

Super-resolution fluorescence microscopy opens new windows for visualizing ultrastructural dynamics. When applied to living cells, super-resolution fluorescence microscopy suffers from the limited length of time-lapse series due to high intensities of illumination and photobleaching of fluorophores. In addition, the large sizes of fluorophores and/or tagging molecules (e.g. antibodies, self-labeling proteins, etc) can perturb the system of interest, resulting in artifacts in the structure and/or dynamics. Here, I introduce two examples of our efforts to overcome these challenges in photobleaching and labeling.

First, we use a fluorogen-binding protein, UnaG for overcoming the photobleaching limit by controlling the switching kinetics and by supplying a large excess of fluorogenes. UnaG fluorescence can be switched off by blue light and then, recovered by replacing the damaged fluorogen with a fresh one in solution for hundreds of cycles. These switching properties enabled long-term super-resolution imaging based on single-molecule localization, with significant improvement (about 10-fold) in the number of independent super-resolution snapshots.

Second, we develop label-free super-resolution optical microscopy based on stimulated Raman scattering (SRS), which amplifies the minute signal of Raman scattering with minimal non-resonant background and well-defined point spread function. We devised a way to selectively deplete SRS signal by another competing SRS for super-resolution SRS microscope in a confocal geometry like stimulated emission depletion (STED) fluorescence microscopy. We provide theoretical description and experimental evidence that the selective suppression behavior is due to the limited number of pump photons used for both two SRS processes when an intense depletion beam induces one SRS process.

### Keywords:

Super-resolution optical microscopy, Fluorescence, Stimulated Raman Scattering

## Single-molecule Study of Spiropyran Molecules by using Spectrally Resolved Super-Resolution Microscopy

김두리\*<sup>1</sup>

<sup>1</sup>한양대학교 화학과  
dooldoory@gmail.com

### Abstract:

The potentially rich dimension of spectrally resolved single-molecule fluorescence, an important factor in the development of super-resolution microscopy, remains largely unexplored for single-molecule reactions. Conventional approaches for single-molecule spectral measurement rely on locally confined, single-location illumination and detection, thus necessitating sample scanning to measure different molecules and are limited in throughput and spatial resolution. Moreover, for fluorogenic reactions, as one cannot predict a priori at what location a single, non-fluorescent (thus undetectable) reactant molecule would react to generate a fluorescent product molecule, it is difficult to follow the reaction dynamics of individual molecules through single location spectral measurements.

We attempted to overcome this issue here by demonstrating that the capability to resolve in situ the fluorescence emission spectra of single product molecules of a fluorogenic reaction can help unveil rich, multipath reaction pathways. This was achieved through a wide-field single-molecule spectroscopy and super-resolution method we recently developed, namely spectrally resolved stochastic optical reconstruction microscopy (SR-STORM).

In this work, we generalize SR-STORM to single-molecule fluorogenic reactions by studying the isomerization of 6-nitro BIPS, a representative photochromic spiropyran. By recording both the images and emission spectra of thousands of single fluorescent molecules stochastically generated from the ring-opening reaction of a spiropyran, we provide mechanistic insights into its multipath reaction pathways.

### Keywords:

Super-Resolution Microscopy, single-molecule spectroscopy, photochromism

## Background-free STED nanoscopy using light polarization switching

LEE Jong-Chan\*<sup>1, 2</sup>, MA Ye<sup>4</sup>, HAN Kyu Young<sup>3</sup>, HA Taekjip\*<sup>2, 4, 5</sup>

<sup>1</sup>대구경북과학기술원 뉴바이올로지, <sup>2</sup>Department of Biophysics and Biophysical Chemistry, Johns Hopkins University / School of Medicine, <sup>3</sup>CREOL, The College of Optics and Photonics, University of Central Florida, <sup>4</sup>Department of Biomedical Engineering, Johns Hopkins University / School of Medicine, <sup>5</sup>Howard Hughes Medical Institute  
spiritljc@gmail.com, tjha@jhu.edu

### Abstract:

Stimulated emission depletion (STED) super-resolution microscopy (or nanoscopy) offers significant enhancement of optical resolution compared to conventional microscopy. To achieve resolution beyond the diffraction-limit, STED nanoscopy uses orders of magnitude (roughly  $\sim 10^5$ ) more photons than the conventional confocal microscopy. Those additional 'STED' photons, at the red-shifted tail of fluorophore spectrum, are designed to deplete the fluorescence of a fluorophore at the periphery of focus instead of exciting it to achieve diffraction unlimited resolution. However, because of strong intensity, STED photons can induce unintended results such as increased background noise, photobleaching and phototoxicity. In particular, increased background noise can decrease the signal-to-background ratio (SBR) and deteriorates the image quality. In other words, the low spatial frequency fluorescence background can mask the high spatial frequency, super-resolution, fluorescence signal.

Here, we will first review the principle of STED nanoscopy technique and argue that the background noise problem is one of the biggest bottleneck of current state-of-the-art STED nanoscopy. Then, we report a simple and easy-to-implement method, which we call polarization switching STED (psSTED), that can efficiently suppress the low spatial frequency background appearing in STED images. In psSTED, we switch the STED beam polarization between two different circularly polarized states to record a regular STED image and a background noise image. A simple, unambiguous subtraction process between these two images provides us with a background-free super-resolved image. With both simulation and experimentation, we demonstrate psSTED for both the high STED power case where the STED excitation-related background is strong, and the low STED power case where the background noise is mostly due to incomplete depletion. Finally, we compare the performance of psSTED with other state-of-the-art background subtraction methods and highlight its capability of efficient background suppression with a much simpler hardware implementation.

### Keywords:

Super-resolution microscopy, STED, Nanoscopy

# Analysis of Key Technologies for Development of MHD Direct-Power Generation System

장두희\*<sup>1</sup>, 진형곤<sup>1</sup>

<sup>1</sup>한국원자력연구원 핵융합기술개발부  
doochang@kaeri.re.kr

## Abstract:

Magneto-hydro-dynamic (MHD, magneto-fluid-dynamics or hydro-magnetics) direct-power generation is based on the Faraday-law of electromagnetic induction. Plasma (partially ionized gas) or liquid metal are working fluids in the MHD system, similar to the mechanism for the magnetosphere of earth's atmosphere. The fluid density and pressure of controllable MHD process should be increased to meet a maximum efficiency in the generated power. Critical problems are initiated from the low conductivity characteristics in the gas at high temperature. High temperature gaseous conductor with a high velocity is passed through a strong magnetic field, and a current is generated and extracted by the electrodes inside the gas stream. And then, the thermal energy of gas is converted directly into the electrical energy. MHD power generation is a unique and highly efficient method of power generation with nearly zero environmental pollution. Efficiency evaluations are the most important factor for establishing a commercial power plant. MHD power plants have an overall efficiency of 55-60%, however it can be boosted up to 80% or more by using superconducting magnets in this process. Whereas the other non-conventional methods of power generation such as solar, wind, geothermal, tidal have a highest efficiency not more than 35%. By using the MHD power generation method separately or by combined operation with conventionally thermal or nuclear plants, it is hope to increase dramatically the plant efficiency in near future. The present status of MHD power generation technologies are reviewed in this presentation, and the key technologies of MHD power generation system is analyzed for the development of future green-energy power generation system.

## Keywords:

MHD power generation, working fluid, power efficiency, conductivity, flow velocity, strong magnetic field

## Influence of pre-breakdown process and streamer structure on shock wave development by underwater pulsed spark discharges

정경재\*<sup>1</sup>, 이건<sup>1</sup>, 황용석<sup>1</sup>

<sup>1</sup>서울대학교 원자핵공학과  
jkjsh1@snu.ac.kr

### Abstract:

In this paper, we address an importance of pre-breakdown process in shock wave development by underwater pulsed spark discharges. In addition to the duration of pre-breakdown process, it has been experimentally demonstrated that the morphology of the underwater streamer contributes significantly to the enhancement of shock waves in the surrounding water. Based on this observation, we propose a preconditioning treatment on the water gap by electrolysis which is much more advantageous than conventional gas injection methods. Combining this treatment with negatively enhanced electrode structure, the negative (anode-directed) subsonic streamers are successfully produced with the initiation time comparable to that of the conventional positive (cathode-directed) streamers in the existing device. It is clearly shown that the acceleration of pre-breakdown process using electrolysis overcomes the biggest drawback of negative subsonic discharges, i.e. the slow vapor bubble formation due to screening effect, and thus provides a way to improve the efficiency of shock wave generation by pulsed spark discharges in water. This result is consistent with our previous studies indicating that the initial state of the spark channel is one of the most important factors in determining the strength of underwater shock wave.

### Acknowledgement:

This research was partly supported by Technology development program of MSS (No. S2544022) and the Basic Science Research Program through the National Research Foundation of Korea (NRF) funded by MSIT (No. NRF-2017R1A2B4007122). The Brain Korea 21 Plus Program (No.21A20130012821) also partly supported this work.

### Keywords:

Underwater pulsed spark discharge, shock wave, pre-breakdown process, subsonic streamer

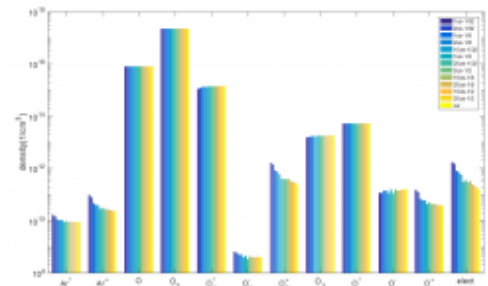
# 0-D Global Simulation of Reactive Species Generation in Atmospheric Argon/Oxygen Plasma with Pulsed Power Source.

정석용<sup>1</sup>, 남우진<sup>1</sup>, 윤건수\*<sup>1, 2</sup>, 이재구<sup>2</sup>

<sup>1</sup>포항공과대학교 물리학과, <sup>2</sup>포항공과대학교 첨단원자력공학부  
gunsu@postech.ac.kr

## Abstract:

0-D global simulation of atmospheric pressure Argon / O<sub>2</sub> plasma with pulsed power was performed. The densities of reactive species were investigated for varying pulse periods and duty cycles with fixed time-averaged power and constant plasma volume. We found that the time-average density of each species increases or decreases monotonically with increasing pulse width. For the case with the same pulse width, it was confirmed that the density of the reactive species is almost the same for different pulse periods under the condition of the same time-averaged power. The time- average electron density is proportional to the power as expected. The temporal variation of the electron temperature during the pulse rise is identical regardless of the power condition. We also studied a pulsed microwave plasma jet experiment with open boundary using a similar simulation scheme. Considering the variation of the length of the plasma observed in the actual experiment [4], the change of the power coupling according to the length change [3] is considered. Since the power efficiency is better when the volume of the plasma is smaller, the power efficiency is maximum before pulse-on, and then slowly decreases as the plasma jet extends. Therefore, on average, the power delivered to the plasma is greater than the case of continuous wave, and more reactive species can be generated for the same input power. This study is expected to help control the generation of active species in plasma devices using pulse power. This research was supported by the National Research Foundation of Korea under BK21 + program, grant No. 2015R1D1A1A01061556 (Ministry of Education), and grant Nos. 2015M3A9E2066986 and grant No. 2016K1A4A4A01922028 (the Ministry of Science and ICT). This work was also partially supported by Asia-Pacific Center for Theoretical Physics.



## References:

- [1] G.Y Park et al, Plasma Process. "Global Model of He/O<sub>2</sub> and Ar/O<sub>2</sub> Atmospheric Pressure Glow Discharges", Polym. 5, 569-576 (2008)
- [2] E.G Thorsteinsson et al, "A global (volume averaged) model of a chlorine discharge", Plasma Sources Sci. Technol. 19, 015001, 15pp (2010)
- [3] Y.J Nam et al, "Asymmetric frequency dependence of plasma jet formation in resonator electrode", Eur. Phys. J. D (2017) 71: 134
- [4] Y.J Nam et al. "Intensification of Atomic and Continuum Emissions in Pulsed Microwave Plasmas at Atmospheric Pressure" submitted

## Keywords:

pulsed microwave, atmospheric pressure plasma, global simulation,

## Intensification of Atomic and Continuum Emissions in Pulsed Microwave Plasmas at Atmospheric Pressure

남우진<sup>1</sup>, 정석용<sup>1</sup>, 이재구<sup>1, 2</sup>, 윤건수\*<sup>1, 2</sup>

<sup>1</sup>포항공과대학교 물리학과, <sup>2</sup>포항공과대학교 첨단원자력공학부  
gunsu@postech.ac.kr

### Abstract:

Physical properties of atmospheric pressure argon plasma driven by pulsed microwave are investigated. Time-resolved optical emission measurements of argon emission line, electron continuum emission and hydroxyl molecular emission line are used to analysis the dynamics of pulsed microwave plasma. Spectroscopic measurements reveal an initial burst of light emission from the igniting argon plasma at the microwave pulse rise. The emission overshoot can be interpreted as a transient increase in electron temperature supported by a simple global model simulation. Interestingly, another emission overshoot is observed hundreds nanoseconds after pulse off. This may be due to a sudden drop in electron temperature causing a non-equilibrium state between the loss and production of each species in the plasma. In particular, the recombination rate of argon ion increases at the moment of pulse off, triggering the increase in the population of excited argon which then leads to intensification of the plasma emission. Time-resolved emission intensity measurements suggest that pulsed microwaves can be used to manipulate the number density of specific molecules in the plasma, such as OH, NO etc.

\*This research was supported by the National Research Foundation of Korea under BK21+program, grant No.2015R1D1A1A01061556 (Ministry of Education), and grant Nos. 2015M3A9E2066986 and 2016K1A4A4A01922028 (Ministry of Science and ICT). This work was also partially supported by Asia-Pacific Center for Theoretical Physics.

### Keywords:

microwave plasma, pulsed microwave, optical emission spectroscopy, global model simulation

## Modeling of atomic processes in dense plasmas

CHUNG Hyun-Kyung\*<sup>1</sup>, CHO Min-Sang<sup>1</sup>, CHO Byoung-Ick<sup>1</sup>

<sup>1</sup>광주과학기술원 물리 광학과  
hchung.hedp@gist.ac.kr

### Abstract:

Recent developments in large plasma generation devices such as NIF (National Ignition Facility), high power short pulse lasers, X-ray free electron lasers (XFEL) and Z machines have made it possible to create and study the state of matter under extreme conditions. Particularly, solid density targets interact with high power lasers and produce a state of dense plasmas at finite temperatures. The new state of matter created in the laboratories requires novel theories and modelling capabilities to understand the physics of the exotic states.

Spectroscopic methods have been successfully used to understand transient states of matter and diagnose plasma thermodynamic conditions. For analysis of observed spectral data, one needs to apply a theoretical model to simulate atomic processes in dense plasmas and hence to predict spectroscopic observables. In the last decade, a generalized collisional-radiative model called FLYCHK has been available publicly (<http://nlte.nist.gov/FLY>) to approximately 1000 plasma scientists and applied to a wide range of plasma conditions relevant to long or short-pulse laser-produced plasmas, tokamak plasmas, or astrophysical plasmas. Recently, the model is extended and applied to solid density plasmas created by X-ray free electron lasers. An overview of atomic processes in dense plasmas and the simulations of XFEL produced plasmas are given in this presentation.

### Keywords:

collisional-radiative model, plasma spectroscopy, laser-matter interaction, spectroscopic diagnostics, atomic processes in plasmas

## Investigation of the effect of amplified spontaneous emission (ASE) on the formation of a preplasma on a thin foil target

PHUNG VANESSA LING JEN<sup>1</sup>, KIM JINJU<sup>1</sup>, KIM MINSEOK<sup>1</sup>, 석희용\*<sup>1</sup>

<sup>1</sup>광주과학기술원 물리광학과  
hysuk@gist.ac.kr

### Abstract:

With the current state-of-the art of laser technology, the existence of amplified spontaneous emission (ASE) and prepulse can be limited but still inevitable. As the laser intensity increases, the ASE and prepulse effects become significant in interaction of the intense laser pulse and a thin foil target before main pulse arrives. When the ASE level exceeds the ionization and damage thresholds of the target materials, formation of the preplasma on the target surface due to the ASE will lead to destruction of the thin foil target. This early interaction may be very important in ion acceleration using a high power laser and a thin foil. So far, there have not been much studies on the formation and dynamics of the preplasma. In this work, we used a small mJ-scale laser system for this study and investigated the expanding preplasma by using the pump and probe method. Some detailed results will be shown in this presentation.

### Keywords:

ASE, preplasma, thin foil, pump-probe technique

## Intensity dependent XFEL transmission in solid-density plasmas

CHO Min Sang<sup>1, 2</sup>, CHUNG Hyun-Kyung<sup>1</sup>, 조병익\*<sup>1, 2</sup>

<sup>1</sup>Gwangju Institute of Science and Technology, <sup>2</sup>Center for Relativistic Laser Science, Institute of Basic Science

bicho@gist.ac.kr

### Abstract:

The possibility of generating solid-density plasmas isochorically heated by X-ray free electron laser (XFEL) provides unique opportunities in the experimental study of dense plasmas. A study of the x-ray transmission penetrated from the solid-density plasmas allows us to have significant insight into x-ray absorption mechanism. Here, we use the collisional-radiative population kinetic calculations to present the intensity dependent x-ray absorption in different solid targets, such as aluminum, silicon, and magnesium. X-ray photons with high peak intensity of XFEL pulses create excited states where absorption is larger than the ground state absorption. At the resonant energy of neutral atom, different x-ray absorption in the intensity range near  $10^{17}$  W/cm<sup>2</sup> has been observed. Detailed population kinetics of charge states relevant to the absorption of x-ray photons will be discussed.

This work was supported by Institute of Basic Science (IBS-R012-D1) and National Research Foundation of Korea (No. 2015R1A5A1009962 and 2016R1A2B4009631)

### Keywords:

solid-density plasma, XFEL, x-ray absorption, intensity dependent absorption

## 레이저 유도 이온 가속 과정에서 발생하는 레이저 스펙트럼의 파장 변이

이성근<sup>1, 2</sup>, 전천하<sup>2</sup>, 김승연<sup>2</sup>, 김태윤<sup>3</sup>, 이황운<sup>2</sup>, 윤진우<sup>3</sup>, 성재희<sup>2, 3</sup>, 이성구<sup>2, 3</sup>, 최일우<sup>2, 3</sup>, 남창희\*<sup>1, 2</sup>

<sup>1</sup>광주과학기술원 물리광학과, <sup>2</sup>기초과학연구원 초강력레이저과학연구단, <sup>3</sup>광주과학기술원 고등광기술연구소  
chnam@gist.ac.kr

### Abstract:

처프 펄스 증폭(Chirped Pulse Amplification, CPA)을 이용한 초고출력 레이저 펄스를 만드는 기술이 개발된 이래, 펨토초 수준의 짧은 펄스폭을 가진 고출력 레이저 펄스를 이용한 입자가속 기술이 대두되어 왔다. 고체 표적에 고강도 펨토초 레이저 펄스를 집속하면 표적 내부의 이온을 가속시킬 수 있다. 특히 나노미터 수준의 얇은 고체 표적에  $10^{20}$  W/cm<sup>2</sup> 이상의 강한 펄스가 집속될 경우 광압 가속(Radiation Pressure Acceleration, RPA)을 통해 전자가 먼저 가속된 후, 쿨롱 힘에 의해 표적 내부의 이온들이 가속될 수 있다. 광압 가속이 발생했을 경우 레이저 펄스의 광압에 의해 가속되는 전자 막이 형성되는데, 이 전자 막에서 레이저가 반사될 경우 도플러 전이를 통해 빛의 파장이 변하며 그 양은 전자 막의 속도에 의존한다. 따라서 움직이는 전자 막에 의해 반사된 빛의 도플러 전이를 측정하여 전자 막의 속도를 추정할 수 있다. 본 연구에서는 초강력레이저과학연구단에서 개발한 4PW 레이저 펄스를 이용하여 얇은 표적에서의 이온 가속 실험을 진행하고, 그 실험에서 발생한 스펙트럼을 분석하였다. 표적에 집속한 레이저 펄스는 표적에서 반사되거나 상대론적 투과도(Relativistic Transparency)에 의해 표적을 투과하기 때문에 이 두 위치에서 스펙트럼을 측정하였다. 그 뒤 측정된 스펙트럼의 형태를 분석하여 스펙트럼 내 도플러 전이와 가속된 이온들과의 관계 및 이온 가속 과정에서 발생하는 레이저-물질 상호작용을 조사하였다.

### Keywords:

이온 가속, 도플러 전이, 스펙트럼, 짧은 펄스 레이저

## Evolution of Plasma Wave in Laser Plasma Acceleration

남창희\*<sup>1</sup>, CHO Myung Hoon<sup>2</sup>, KIM Chul Min<sup>1, 2</sup>, RYU Chang-Mo<sup>2</sup>

<sup>1</sup>광주과학기술원 물리광학과, <sup>2</sup>Center for Relativistic Laser Science, Institute for Basic Science  
chnam@gist.ac.kr

### Abstract:

Laser wakefield acceleration is a compact electron acceleration scheme due to its high accelerating field. This high accelerating field is generated in plasma waves and normally has higher amplitude with higher laser intensity in a given plasma. As the intensity of the laser increases, the electrons of the plasma are largely pushed out, and an ion cavity so called 'bubble' is formed. Previous models to describe the electron acceleration and electron injection in LWFA have developed based on a non-evolving 'bubble'. In this talk, we suggest a phenomenological model of an evolving bubble. The evolution of bubble can be expressed from the energy transition from a laser pulse to plasma. We show clear evidences that the energy loss rate of laser pulse highly relates to the size of bubble. Our model is developed from the laser pulse equation in assumptions of local pulse depletion, which can occur at an intense laser pulse. We could also show the analytic condition of laser pulse compression in the plasma from the derived laser pulse equation. The model is tested with 1D, 2D, and 3D PIC simulations by evaluating the energy loss rate of laser pulse, the evolution of bubble size, and the time duration of electron injection. The model well-predicts the phenomenon of continuous electron injection, which indicates the self-injection of LWFA is not the uncontrollable thing.

### Keywords:

LWFA, pulse compression, laser depletion, plasma wave

## Studies of initial state radiations in Drell-Yan events from ppbar collision at 1.96TeV

양운기\*<sup>1</sup>, 서현산\*<sup>1</sup>, 최준호<sup>1, 2</sup>, 김준호<sup>1</sup>, 유금봉<sup>1</sup>  
<sup>1</sup>서울대학교 물리학과, <sup>2</sup>서울대학교 기초과학연구원  
ukyang@snu.ac.kr, hyon.san.seo@cern.ch

### Abstract:

We present the studies of initial state radiations (ISR) in Drell-Yan events from ppbar collision at 1.96TeV with CDF Run II data. ISR from hadron collisions plays an important role in jet physics, which has an impact on precision measurements and searches for new physics. We develop a systematic way to study the ISR effect using Drell-Yan events. The truncated mean of the dilepton transverse momentum distribution is found to have a logarithmic slope as a function of dilepton invariant mass square. This logarithmic slope can be used to control ISR effect in the SM processes and new physics processes.

### Keywords:

CDF, Tevatron, Standard Model, QCD

## Present Status of KOTO

김준이\*<sup>1</sup>, 김은주<sup>1</sup>, 안정근<sup>2</sup>, 임계엽<sup>3</sup>  
<sup>1</sup>전북대학교 물리교육학과, <sup>2</sup>고려대학교 물리학과, <sup>3</sup>KEK  
jjkim1290@gmail.com

### Abstract:

The KOTO experiment at J-PARC is searching for KL pi0nunu-bar decay mode whose branching ratio is estimated as  $3.0 \times 10^{-11}$  in SM. In this talk, present status of data analysis including January 2018 data will be explained. Subsystem upgrade starting in summer 2018 to address some background rejection issues will be also discussed.

### Keywords:

E14 KOTO J-PARC KL pi0nunu-bar

## Current Status of the JSNS<sup>2</sup> Experiment

PAC M. Y.\*<sup>1</sup>, JANG H. I.<sup>6</sup>, KIM S. B.<sup>6</sup>, KWON E.<sup>6</sup>, SEO H.<sup>6</sup>, SEO S. H.<sup>6</sup>, KIM J. Y.<sup>2</sup>, JOO K. K.<sup>2</sup>, LIM I. T.<sup>3</sup>, MOON D. H.<sup>2</sup>, SHIN C. D.<sup>2</sup>, KIM W.<sup>5</sup>, CHEOUN M. K.<sup>9</sup>, JEON H. K.<sup>10</sup>, JEON S. H.<sup>10</sup>, ROTT C.<sup>10</sup>, YU I.<sup>10</sup>, CHOI J. H.<sup>1</sup>, KIM E. J.<sup>4</sup>, JANG J. S.<sup>11</sup>, KANG S. K.<sup>8</sup>

<sup>1</sup>Department of Radiology, Dongshin University, <sup>2</sup>Department of Physics, Chonnam National University, <sup>3</sup>Department of Physics Education, Chonnam National University, <sup>4</sup>Division of Science Education, Chonbuk National University, <sup>5</sup>Department of Physics, Kyungpook National University, <sup>6</sup>Department of Fire Safety, Seoyoung University, <sup>7</sup>Department of Physics and Astronomy, Seoul National University, <sup>8</sup>School of Liberal Arts, Seoul National University of Science and Technology, <sup>9</sup>Department of Physics, Soongsil University, <sup>10</sup>Department of Physics, Sungkyunkwan University, <sup>11</sup>Gwangju Institute of Science and Technology  
pac@dsu.ac.kr

### Abstract:

The hunting for sterile neutrinos is one of the most interesting topics in neutrino physics. Using muon antineutrinos produced from muon decay at rest, the JSNS<sup>2</sup> experiment is aimed to search for the existence of neutrino oscillation with  $\Delta m^2$  near  $eV^2$  based on electron antineutrinos appearance at the J-PARC Materials and Life Science Experimental Facility (MLF). The JSNS<sup>2</sup> expects an ultimate direct test of the LSND results at lower backgrounds utilizing a pulsed neutron beam and a better neutrino detector with gadolinium loaded liquid scintillator.

The detector is under construction and additional efforts are going on. The JSNS<sup>2</sup> anticipates that that we can start dry run at the end of this year.

We report the current status of the JSNS<sup>2</sup> experiment

### Keywords:

sterile neutrino, JSNS2



## Progress Status of the SHiP Experiment

윤천실\*<sup>1</sup>, 고재우<sup>1</sup>, 김성현<sup>1</sup>, 박병도<sup>1</sup>, 손종윤<sup>1</sup>, 이강영<sup>1</sup>, 박성근<sup>2</sup>, 이경세<sup>2</sup>, 김영균<sup>3</sup>, 최기영<sup>4</sup>, 우종관<sup>5</sup>  
<sup>1</sup>경상대학교 물리교육과 & 기초과학연구소, <sup>2</sup>고려대학교 물리학과, <sup>3</sup>광주교육대학교 과학교육과, <sup>4</sup>성균관대학교  
물리학과, <sup>5</sup>제주대학교 물리학과  
chunsil.yoon@ymail.com

### Abstract:

The SHiP (Search for Hidden Particles) is a multipurpose fixed-target experiment at CERN SPS that will search for light long-lived exotic particles whose mass ranges are from sub-GeV up to  $O(10)$  GeV/ $c^2$  with superweak coupling down to  $10^{-10}$ . Two main aims of the SHiP experiment are the observation of hidden particles predicted by a large number of recently elaborated models of hidden sectors beyond the standard model, and also high-statistics study of tau neutrino events. A major concern for the experimental design is the precise knowledge of the muon flux and the associated charm production cross section. To get this information, a test experiment with SHiP target replica will be carried out using CERN SPS 400 GeV/c proton beam at H4 area in July 2018. We will present the preparation status of the test experiment and our contributions to the Nuclear emulsion target and the muon trigger system composed of five resistive plate chambers (RPCs).

### Keywords:

SHiP, Hidden particles, Tau neutrino, Nuclear emulsion, RPC, CERN SPS

## Search for Axino in the SHiP Experiment

고재우\*<sup>1</sup>, 김성현<sup>1</sup>, 박병도<sup>1</sup>, 손종윤<sup>1</sup>, 윤천실\*<sup>1</sup>, 이강영<sup>1</sup>, 최기영\*<sup>2</sup>, 박성근<sup>3</sup>, 이경세<sup>3</sup>, 김영균<sup>4</sup>, 우종관<sup>5</sup>  
<sup>1</sup>경상대학교 물리교육과 & 기초과학연구소, <sup>2</sup>성균관대학교 물리학과, <sup>3</sup>고려대학교 물리학과, <sup>4</sup>광주교육대학교 과  
학교육과, <sup>5</sup>제주대학교 물리학과  
amusejw88@gnu.ac.kr, chunsil.yoon@ymail.com, ckysky@gmail.com

### Abstract:

The SHiP experiment is searching for hidden particles with mass of less than  $O(10)$  GeV. One of the candidates is the light axino dark matter and neutralino as the next lightest supersymmetric particle. A main feature of this model is the decay of the neutralino into axino and a photon or charged leptons. In this talk, we report the status of the Monte-Carlo simulation of axino search in the SHiP experiment.

### Keywords:

SHiP, Hidden particles, Axino

## Dark matter research with deep learning

CHO Kihyeon\*<sup>1</sup>, YEO Insung<sup>1</sup>

<sup>1</sup>Korea Institute of Science and Technology Information  
cho@kisti.re.kr

### Abstract:

Theoretical and experimental studies have been consistently performed to find dark matter. The project of dark matter research cluster supported by National Research Council of Science and Technology in Korea has done successfully to collaborate between astronomical (indirect) search and accelerator search with helps of theorists. Therefore, dark matter research cluster has been again approved to expand current cluster to Information and Communication Technology (ICT) based on deep learning. We have been in the process of forming so-called dark matter research cluster season 2 to expand the foundation for cooperative research since last December.

Through this, we propose to research and develop intellectual information platform and provide a theoretical template to identify the foundation of dark matters. We also propose to perform astronomical/particle experiment-theory-simulation data utilizing integral research. We also would like to develop a deep-learning software algorithm on dark matter research and process PB-level data.

This could enable us to research and develop an intelligent information platform that combines deep-learning-based astronomical/particle experimental data. It could lead in developing ICT that makes efficient research to search for dark matter.

### Keywords:

Dark matter, Deep Learning, Particle Physics, Beyond the Standard Model

## 중력파 검출의 새로운 방법

박일홍\*<sup>1</sup>

<sup>1</sup>성균관대학교 물리학과  
ilpark@skku.edu

### Abstract:

2017년 LIGO 그룹을 비롯한 세계의 70여개 관측소는, 중력파 GW170817에서 중력파는 물론 다양한 전자기파도 함께 검출함으로써 multi-messenger science의 시대를 열고 있습니다. 앞으로 뉴트리노를 포함한 우주입자의 동시 검출과 아울러, 여러 band에서의 중력파 검출이 가장 중요한 이슈가 될 것입니다. 특히 초기우주 연구를 위하여는 낮은 주파수의 중력파 검출이 필요하며, CMB와 Pulsar Timing Array와 같은 방법이 진행 중입니다. 우리는 낮은 주파수는 물론 wide band 중력파를 검출할 수 있는 우주에서의 중력파 검출의 새로운 아이디어와 방법을 제시하며 소개하고자 합니다.

### Keywords:

중력파 관측, 전자기파 관측, 입자천문학, multi-messenger science

## 새로운 방법의 중력파 검출을 위한 이론적 계산

김동훈\*<sup>1</sup>, 박일홍<sup>2</sup>

<sup>1</sup>서울대학교 물리천문학부, <sup>2</sup>성균관대학교 물리학과  
ki1313@yahoo.com

### Abstract:

최근 LIGO에 의한 중력파 GW170817의 검출과 더불어 동시에 감마선, X선, 가시광선을 통한 중력파 천체의 포착은 이른바 multi-messenger astronomy라는 새로운 천체물리학의 장을 열었다. 이러한 조류에 발맞춰, broad band의 중력파 검출 및 전자기파 동시 관측을 위한 새로운 형태의 우주 실험 장치의 설계가 현재 구상 중인데, 이에 대비한 이론적 예측 및 계산을 보이고자 한다.

### Keywords:

중력파, multi-messenger astronomy

## Distribution of primordial black holes and small-scale constraints

공진욱\*<sup>1</sup>

<sup>1</sup>한국천문연구원 이론천문연구센터  
jinn.ouk.gong@gmail.com

### Abstract:

We show that the number of primordial black holes (PBHs) which is originated from primordial density perturbations with moderately-tilted power spectrum fluctuates following the log-normal distribution, while it follows the Poisson distribution if the spectrum is steeply blue. The log-normal PBH number fluctuation behaves as an isocurvature mode and affects the matter power spectrum and the halo mass function in a different way from those for the Poisson case. The future 21cm observation can put a stronger constraint on the PBH fraction than the current one in a wide mass range,  $10^{-6}M_{\text{sun}} \sim 100M_{\text{sun}}$ .

### Keywords:

primordial black holes

## Inflaton fragmentation in E-models of cosmological $\alpha$ -attractors

HASEGAWA Fuminori<sup>1</sup>, HONG Jeong-Pyeong<sup>\*1</sup>

<sup>1</sup>The University of Tokyo, Japan  
jhp0731ic@gmail.com

### Abstract:

Cosmological  $\alpha$ -attractors are observationally favored due to the asymptotic flatness of the potential. Since its flatness induces the negative pressure, the coherent oscillation of the inflaton field could fragment into quasi-stable localized objects called oscillons. We investigated the possibility of oscillon formation in E-models of  $\alpha$ -attractors. Using the linear analysis and the lattice simulations, we found that the instability sufficiently grows against the cosmic expansion and the inflaton actually fragments into the oscillons for  $\alpha \lesssim 10^{-3}$ .

### Keywords:

Inflaton fragmentation

## KK Towers in the Early Universe: Phase Transitions, Relic Abundances, and Applications to Axion Cosmology

DIENES Keith<sup>2</sup>, KOST\_Jeff\*<sup>1</sup>, THOMAS Brooks<sup>3</sup>

<sup>1</sup>IBS-CTPU, <sup>2</sup>University of Arizona, <sup>3</sup>Lafayette College  
jeffkost@ibs.re.kr

### Abstract:

We discuss the early-universe cosmology of a Kaluza-Klein (KK) tower of scalar fields in the presence of a mass-generating phase transition, focusing on the time-development of the total tower energy density as well as its distribution across the different KK modes. We find that both of these features are extremely sensitive to the details of the phase transition and can behave in a variety of ways significant for late-time cosmology. In particular, the interplay between the temporal properties of the phase transition and the mixing it generates are responsible for both enhancements and suppressions in the late-time abundances, sometimes by orders of magnitude. We map out the complete model parameter space and determine where traditional analytical approximations are valid and where they fail. Finally, we apply this machinery to the example of an axion-like field in the bulk, mapping these phenomena over an enlarged axion parameter space that extends beyond those accessible to standard treatments.

### Keywords:

scalar, axion, extra dimensions, cosmology, phase transition, mass generation

## Type Ib/Ic Supernovae: Effects of Nickel Mixing on the Early-time Evolution and Implications for the Progenitors

YOON Sung-Chul\*<sup>1</sup>

<sup>1</sup>Seoul National University  
yoon@astro.snu.ac.kr

### Abstract:

Type Ib/Ic supernovae (SNeIb/Ic) are characterized by the lack of hydrogen lines in their spectra, implying stripped-envelope progenitors. The observed properties of SNeIb/Ic including the ejecta mass and light curve shape implies that most of SNeIb/Ic originate from massive binary stars but we still do not understand well what distinguishes SN Ib progenitors from those of SN Ic. Given that non-thermal processes resulting from radioactive decay of nickel play a crucial role in the formation of helium lines that are found in SN Ib spectra, constraining nickel mixing by SN observations would provide invaluable information on the nature of SN Ib/Ic progenitors. Here we argue that the early-time evolution of SN Ib/Ic light curves and color can be a powerful probe of nickel mixing in the SN ejecta, based on radiation-hydrodynamics simulations of multi-color SN light curves. Our result also implies that SN Ib and Ic progenitors are distinctively different from each other in terms of helium contents, rather than they form a continuous sequence.

### Keywords:

Type Ib/Ic Supernovae

## Mechanism of Core-Collapse Supernovae and Expected Neutrino and Gravitational Wave Signals

TAKIWAKI Tomoya<sup>\*1</sup>

<sup>1</sup>National Astronomical Observatory of Japan  
takiwaki.tomoya@nao.ac.jp

### Abstract:

Three-dimensional simulations of collapse-driven supernovae become feasible recently. These simulations partially solved the long lasting mystery of the explosion mechanism of the supernovae: the shock stalls in one-dimensional spherical symmetric simulations and revives in three-dimensional simulations by enhancing the efficiency of the neutrino heating via the convection and standing accretion shock instability. Comparison between the simulations and the future observation would be the next urgent task. Especially the neutrino observation of twin Hyper-Kamiokandes in Japan and Korea is crucial to complete understanding of the phenomena. In this talk, I will review recent issues on the mechanism of core-collapse supernovae and expected neutrino and gravitational wave signals that should be detected in the future observations.

### Keywords:

Core-Collapse Supernovae

## Survey of Supernovae and Variable Objects Using the KMTNet Telescopes

KIM Sang Chul\*<sup>1</sup>

<sup>1</sup>Korea Astronomy and Space Science Institute  
sckim@kasi.re.kr

### Abstract:

The Korea Microlensing Telescope Network (KMTNet) is composed of three 1.6-m telescopes equipped with large field-of-view (2 deg X 2 deg) CCDs and are located in three southern-hemisphere sites (Chile, South Africa, and Australia) making it possible to monitor celestial objects 24 hours continuously. We initiated a program to search for supernovae and variable objects using about 17% time of this system with as much short cadence as possible by taking advantage of the 24 hour sky coverage. We mainly use B, V, and I-band broadband optical filters and the pixel scale of the e2V 18K X 18K pixels CCD is 0.40" per pixel. We will show the status and results obtained using this system on Galactic variable stars, external galaxies, novae, supernovae and transient objects.

### Keywords:

Supernovae, KMTNet Telescopes

## Overview of Korean Neutrino Observatory

SEO Seon-Hee\*<sup>1</sup>

<sup>1</sup>Seoul National University  
sunny.seo@snu.ac.kr

### Abstract:

Hyper-Kamiokande (Hyper-K) succeeds the very successful Super-K experiment and will consist of two identical detectors, each filled with 260 kton water and equipped with 40% photo-coverage. Physics program of Hyper-K is broad, covering from particle physics to Astrophysics. The 1st detector will be built in Japan, and the 2nd detector is considered to be built in Korea because locating the 2nd detector in Korea improves physics sensitivities in most cases thanks to the longer baseline (~1,100 km) and larger overburden (~1000 m) for Korean candidate sites. The 2nd Hyper-K detector in Korea is also called Korean Neutrino Observatory (KNO). In this talk, we present introduction, physics and astronomy potentials, and status of KNO.

### Keywords:

Korean Neutrino Observatory

## Phase controlled laser-combined STM

SHIGEKAWA Hidemi\*<sup>1</sup>

<sup>1</sup>Faculty of pure and applied sciences, University of Tsukuba, Tennodai 1-1-1, Tsukuba, 305-8573,  
Japan  
hidemi@ims.tsukuba.ac.jp

### Abstract:

Since the invention of scanning tunneling microscopy (STM), the addition of high time-resolution to STM has been one of the most challenging issues, and various time-resolved STMs have been considered [1]. The most successful approach among them is to combine STM with electric and optical pump-probe (OPP) techniques [2-5]. In OPP-STM which we have been developing, the sample surface below STM tip is excited by a train of pulse pairs, similarly to the case of the OPP method, and tunneling current is measured as a function of delay time. Using circularly polarized light, nanomagnetism can be explored. For example, we have succeeded in observing the relaxation of spins oriented in a single quantum well. By applying an external magnetic field, spin precession was also observed by STM.

In addition to the use of absorption bleaching mechanism, a new technique is to use THz pulses. Although it is difficult to apply a high bias voltage between the STM tip and sample in general, the tip-enhanced THz monocycle pulses enable it and taking a snapshot of ultrafast dynamics becomes possible [6,7]. Furthermore, control of the carrier envelope phases (CEP) in pump and probe pulses paves the way for the development of new time-resolved analyses. The physics and chemistry of nanoscience, such as the molecular dynamics, chemical reactions, phase transitions, and carrier dynamics in functional materials can be explored. To establish the new spectroscopy, we have developed a technique to probe the phase of tip-enhanced electric field.

Details will be discussed at the conference with recent results.

- [1] Terada, Y.; Yoshida, S.; Takeuchi, O.; and Shigekawa, H., *J. Phys. Condens. Matter.*, **22**, 264008-264015 (2010) and references therein.
- [2] Loth, S.; Etzkorn, M.; Lutz, C.P.; Eigler, D.M; and Heinrich, A.J., *Science*, **329**, 1628-1630 (2010).
- [3] Terada, Y.; Yoshida, S.; Takeuchi, O.; and Shigekawa, H., *Nature Photonics*, **4**, 869-874 (2010).
- [4] Cocker, T. L.; and Hegmann, F. A. et al., *Nature Photonics*, **7**, 620-625 (2013).
- [5] Yoshida, S.; and Shigekawa, H. et al., *Nature Nanotechnology*, **9**, 588-593 (2014).
- [6] Yoshioka, K.; Katayama, I.; Minami, Y.; Kitajima, M.; Yoshida, S.; Shigekawa, H.; and Takeda, J., *Nature Photonics*, **10**, 762-765 (2016).
- [7] Cocker T.; Peller D.; Yu P.; Repp J.; and Huber R., *Nature* 539, 263-267 (2016).

### Keywords:

time-resolved STM, THz-STM, ultrashort-pulse laser, ultrafast dynamics, carrier envelope phase

## Energy conversion and transfer at a single molecule

KIM Yousoo\*<sup>1</sup>

<sup>1</sup>Surface and Interface Science Laboratory, RIKEN,  
ykim@riken.jp

### Abstract:

Excitation of molecules by light irradiation triggers various important energy conversion processes, such as luminescence, photochemical reactions, and photovoltaics. Detailed understanding of the molecular excited states is crucial to improve and develop organic energy conversion devices based on opto-electronic/opto-chemical processes.

In this talk, I will discuss two issues focusing on the interaction between a single molecule and localized surface plasmon to describe fundamental aspects of energetics on the solid surfaces.

Absorption spectroscopy is a powerful tool to describe the molecular excitations and the combination with emission (luminescence) spectroscopy which deals with deexcitation processes is effective to investigate the excited states. Single-molecule luminescence detection has progressed rapidly and become indispensable in quantum physics, physical chemistry, and biophysics. However, despite considerable effort and progress, absorption spectroscopy is far behind; number of molecules are still necessary to obtain an absorption spectrum. A difficulty lies in the difference between the diffraction limit of excitation light and absorption cross section of a single molecule. Here I introduce our recent progress in measurement of the single molecule luminescence and absorption spectra of a single molecule using a scanning tunneling microscope (STM) equipped with optical detection facilities, which is applied to the real-space investigation of energy transfer between two molecules.

Localized surface plasmon (LSP) induced chemical reactions of molecules adsorbed on metal nanostructures are attracting increased attention as novel photocatalytic reactions. Most of previous papers explained that the reactions occur through the indirect hot-electron transfer mechanism. However, the proposed indirect mechanism has been discussed on the basis of ensemble observations of the local reactions and is, therefore, still controversial. Here, I propose a novel reaction mechanism on the basis of real-time and real-space observation of single-molecule chemical reaction induced by a LSP. This is achieved by optically exciting the LSP in the gap between a plasmonic Ag tip of an STM and a metal substrate. The LSP-induced reaction will be explained in detail by comparing with visible-light-induced photoreaction of the molecule.

### Keywords:

Scanning tunneling microscopy, single-molecule absorption, single-molecule photoreaction, localized surface plasmon

## Magnetic quantum sensing using nitrogen-vacancy center in diamond

이동현\*<sup>1</sup>

<sup>1</sup>고려대학교 물리학과  
donghun@korea.ac.kr

### Abstract:

Quantum sensors utilize non-classical nature of quantum systems to realize unprecedented levels of sensitivity. Among various quantum sensors such as superconducting devices and atomic vapor cells, nitrogen-vacancy (NV) centers in diamond has gotten rapidly growing interests in the field of scanning magnetometry. The diamond NV center has promising potential for nanometer and nanotesla magnetic sensing and imaging due to its atomic-scale size, long spin coherence times and high magnetic field sensitivity (e.g.  $< \text{nT/Hz}^{1/2}$ ). By incorporating a NV center at the tip of scanning probe microscope, one can realize a novel scanning magnetometer with high spatial resolution and sensitivity. In this talk, I will introduce the basic working principles, experimental methods, and sensing/imaging examples of solid-state magnetic materials including hard disk drive, magnetic nanowires and room temperature skyrmions.

### Keywords:

quantum sensor, diamond NV center, scanning magnetometer

## PLGA-Nanofiber Scaffolds as a platform carrying Tumor Antigen-Specific Cytotoxic T Lymphocytes in vivo

JIIA Global Research Laboratory, Department of Biochemistry and Molecular Biology, Korea University College of Medicine<sup>1</sup>, KIM JungWon<sup>1</sup>, JEON SeungHyun<sup>1</sup>, LEE Kyung-Mi\*<sup>1</sup>

<sup>1</sup>Global Research Laboratory, Department of Biochemistry and Molecular Biology, Korea University College of Medicine  
kml60637@gmail.com

### Abstract:

One of recent approaches for cancer treatment is adoptive cell therapy (ACT) of injecting effector cells expanded in vitro. However, low numbers of effector cells and insufficient persistence have been in the way of successful ACT in clinical settings. These limitations could be overcome through using biocompatible poly (lactide-co-glycolide) (PLGA) nanofiber and thereby efficiently delivering human tumor antigen-specific cytotoxic T lymphocytes (CTLs) directly to the tumor site from the platform. In addition, PLGA nanofiber scaffolds were modified with monoclonal antibodies (anti-CD8 and anti-CD28 Abs) providing CTLs with adhesion and co-stimulatory signals, with them gradually releasing attached CTLs. Compared to CTLs in conventional rapid expansion protocol (REP), the nanofiber originated ones are more activated with higher CD28 expression higher cytotoxicity. Thus, these results demonstrated that anti-CD8/anti-CD28 Ab-conjugated PLGA nanofiber scaffolds can bind CTL clones, resulting in improving their anti-tumor activities and then gradually releasing them with their functions performed. Thus, the combination therapy of tumor antigen-specific CTLs and nanofiber presented here may be more effective than traditional methods as novel cell therapy strategy.

### Keywords:

PLGA, Nanofiber, Cytotoxic T Lymphocyte

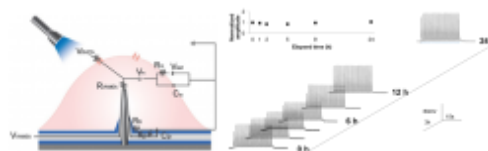
## Nanowire Devices for Neural Interfaces

KWON Juyoung<sup>1</sup>, YOO Jisoo<sup>1</sup>, LEE Hyo Jung<sup>1</sup>, NA Jukwan<sup>1</sup>, CHOI Heon-Jin<sup>\*1</sup>

<sup>1</sup>Department of Materials Science and Engineering, Yonsei University  
hjc@yonsei.ac.kr

### Abstract:

Recent advances in the field of neural interfaces have been developed to improve the precision with high resolution of recording and specificity of stimulation to the level of individual cells. To measure the accurate neural signal and activate neurons with enhanced selectivity, the efficient coupling between the cell membrane and the measuring electrodes is required. Here, we demonstrate a vertical nanowire multi-electrode array (VNMEA) with feature sizes and densities comparable to neural circuits which enable the long-term intracellular recording and stimulation by forming tight junctions with cell membranes. The vertical nanowire electrodes pierced the cell membrane without compromising cell viability, and precisely monitor and control neural activity, excluding the cell membrane resistivity and capacitance as factors for improved resolution and specificity. We show that vertical nanowire electrodes can record both extracellular and intracellular recording over a long period time with the amplitude and shape of the action potential recorded with high signal-to noise ratios. A tight seal between the cell membrane and the nanowire electrodes minimizes signal loss to the bath medium and achieves low impedance across the cell-electrode interface. Also, intracellular stimulation through the NW electrodes enhances cellular differentiation at high efficiency relative to extracellular stimulation under the same conditions because of efficient coupling between the cell membrane and NW electrodes. We further develop this intracellular recording and stimulation platform for 'electroceutical' devices which designed to achieve targeted and efficient neural excitation involved in disease process. With the advantages of long-term recording, high efficient stimulation, and minimal invasiveness, VNMEA could pave way in neuroprosthetics and in basic physiology research and also provides a good platform for the development in chronic neural applications.



### Keywords:

Neural interfaces, Vertical nanowire multi-electrodes array (VNMEA), Intracellular recording, Intracellular stimulation, Electroceuticals

## High capture and release efficiency of cancer cells using microfluidics channel-coupled 3D quartz nanohole arrays

이상권\*<sup>1</sup>, 임정택<sup>1</sup>, 윤요섭<sup>1</sup>, 이원용<sup>1</sup>, 김길성<sup>1</sup>

<sup>1</sup>중앙대학교 물리학과  
sangkwonlee@cau.ac.kr

### Abstract:

Nanostructured materials, such as silicon nanowires, quartz nanostructures, and polymer-modified nanostructures, are a promising new class of materials for the capture and enumeration of very rare tumor cells, including circulating tumor cells (CTCs), to examine their biological characteristics in whole blood of cancer patients. These cells can then be applied towards transplantation, anti-tumor cell therapy, and cell-secreted protein studies. It is believed that 3-dimensional (3D) nanostructured substrates efficiently enhance cell capture yields due to the increased local contacts between the 3D nanostructures and extracellular extensions of the tumor cells. Recent studies have been performed with enhanced cell capture yields thanks to various nanostructured platforms; however, there remains an urgent need both to capture and release viable rare tumor cells for further molecular (i.e., protein) analysis and to develop patient-specific drugs. Here, we first demonstrate that our 3D quartz nanohole arrays (QNHA) tumor cell capture and release system allows us to not only selectively capture rare tumor cells, but also to release the cells with high capture and release rates. This system was developed with streptavidin (STR)-functionalized QNHA (STR-QNHA) with a microfluidics channel. Our system has ideal cell-separation yields of as high as 85-91% and high release rates of >90% for BT20 cell line. We suggest that use of microfluidics channel technique coupled with STR-QNHA cell capture and release chip (STR-QNHA cell chip) would be a powerful and simple process to evaluate the capture, enumeration, and release of CTCs from patient whole blood for studying further cell therapy and tumor-cell-secreted molecules.

### Keywords:

Circulating tumor cells, Nanohole array, Microfluidics, BT20 cancer cells

## 상관된 광자의 생성 및 양자간섭

김현오\*<sup>1</sup>

<sup>1</sup>부산대학교 물리학과  
quantum@pusan.ac.kr

### Abstract:

1980년대 중반부터 시작된 상관된 광자 (correlated photon pairs)의 생성 및 이들의 양자 간섭 현상에 관한 연구는 양자역학의 근본적인 특성을 이해하고 규명하기 위한 순수학문적인 연구와 더불어 최근까지 활발한 연구가 진행되고 있는 양자정보통신 기술 분야의 개념적 기반이 되고 있다. 현재까지 다양한 형태로 개발되고 있는 상관된 광자쌍 및 얽힘 광자 (entangled photons)는 양자정보통신 및 양자 기술 분야에서 핵심적인 광원으로서의 중요성 및 활용성이 증가되고 있다. 상관된 광자가 갖는 편광, 진동수, 공간모드 등의 특성들은 다양한 형태의 간섭계를 통해서 특별한 형태의 중첩 상태 또는 얽힘 상태를 형성할 수 있고, 이는 양자적 중첩 상태의 본질에 대한 이해와 이를 바탕으로 양자정보통신 분야에서 핵심적인 광원으로 활용되고 있다. 본 발표에서는 비선형 매질에서 자발적 매개하향변환 (spontaneous parametric down-conversion)에 의한 상관된 광자의 생성과 측정, 얽힘 상태의 생성, 그리고 이를 이용한 다양한 간섭계에서 나타나는 양자 간섭 현상에 관한 실험적인 내용들을 최근까지 수행된 연구 내용을 통해서 소개할 것이다.

### Keywords:

상관된 광자, 양자정보, 양자간섭

## Broadband Second-Harmonic-Generation metasurfaces based on Stark-tunable intersubband nonlinearities

이종원\*<sup>1</sup>, 유재연<sup>1</sup>

<sup>1</sup>울산과학기술원 전기전자컴퓨터공학부  
jongwonlee@unist.ac.kr

### Abstract:

Nonlinear response from optical metasurfaces have opened a new direction in research, with interesting applications such as super-resolution imaging and efficient frequency conversion in subwavelength thin-film with greatly-relaxed phase-matching constraints [1,2]. Recently, nonlinear metasurfaces with record second-order nonlinearities up to 4-5 orders of magnitude larger than in traditional bulk nonlinear materials based on coupling of electromagnetic modes with intersubband nonlinearities in multiple-quantum-well structure have been demonstrated [2,3]. However, efficient SHG from the metasurface is only possible near the intersubband resonant frequency due to the resonant characteristics of the intersubband nonlinearities, and thus the operating wavelength for the SHG (SHG bandwidth) is very limited.

In this work, we demonstrate active nonlinear metasurfaces for broadband SHG based on Stark-tunable intersubband nonlinearities in which the intersubband transition energies in the MQW are modulated from bias voltages applied to the MQW layer. We designed plasmonic resonators to achieve the maximum SHG conversion efficiencies at each bias voltages. The maximum SHG conversion efficiencies and the spectral response of SH power with input pump wavelength range from  $\lambda_{FF}=7$  to  $13\mu\text{m}$  were calculated for the bias voltages from -4V to 4V with 1V step. From the theoretical calculations, we obtained conversion efficiencies over 0.1% for the bias voltages and 5 times broader SHG operation wavelength compared to the passive device (0V). The active nonlinear metasurfaces proposed in this work may have significant practical impact on variety of applications, including broadband frequency up- and down-conversion, spectroscopy and imaging systems requiring broadband operation.

**Acknowledgements** This work has been supported by the Basic Science Research Programs through the NRF grant No. 2016R1C1B2009604.

### References

- [1] J. B. Pendry, *Science*, **322**, 71-73 (2008).
- [2] J. Lee et. al., *Nature*, **511**, 65-69 (2014).
- [3] J. Lee et. al., *Adv. Opt. Mat.*, **4**, 664-670 (2016).

### Keywords:

Metasurface, Nonlinear Optics, Intersubband Transitions, Second Harmonic Generation

## Shape ellipticity dependence of exciton ne levels and optical nonlinearities in CdSe and CdTe nanocrystal quantum dots

김광석\*<sup>1</sup>, 양하늬\*<sup>1</sup>

<sup>1</sup>부산대학교 물리교육과/광메카트로닉스공학과/인지메카트로닉스공학과 대학원  
kskyhm@pusan.ac.kr, chickeny@nate.com

### Abstract:

Shape ellipticity dependence of the exciton fine energy levels in CdTe and CdSe nanocrystal quantum dots were compared by considering the crystal structure and the Coulomb interaction of an electron and a hole. While quantum dot ellipticity changes from an oblate to prolate via spherical shape, both the fine energy levels and the dipole moment in the wurtzite structure of a CdSe quantum dot change linearly for ellipticity. In contrast, CdTe quantum dots were found to show a level crossing between the bright and dark exciton states with a significant change of the dipole moment due to the cubic structure. Shape ellipticity dependence of the optical nonlinearities in CdTe and CdSe nanocrystal quantum dots was also considered by using semiconductor Bloch equations. For a spherical shape quantum dot, only 1L dominates the optical nonlinearities in a CdSe quantum dot, but both 1U and 0U contribute in a CdTe quantum dot. As excitation pulse area becomes strong, the optical nonlinearities of both CdSe and CdTe quantum dots are mainly governed by absorption saturation. However, in the case of an oblate CdTe quantum dot, the real part of nonlinear refractive index becomes relatively significant.

### Keywords:

quantum dot, exciton, absorption

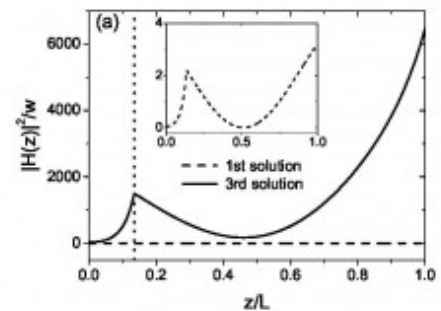
# Giant enhancement of reflectance due to the interplay between surface confined wave modes and nonlinear gain in dielectric media

KIM Kihong\*<sup>1</sup>, KIM Sangbum<sup>1</sup>

<sup>1</sup>Department of Energy Ssystems Research and Department of Physics  
khkim@ajou.ac.kr

## Abstract:

We present a numerical study of the interplay between the surface confined wave modes (surface plasmons or waveguide modes) excited by obliquely incident p waves and the linear and nonlinear gain of the dielectric layer in the Otto configuration. In the purely linear case, the interplay between linear gain and surface plasmons generates a large reflectance peak with its value much greater than 1. As the linear gain increases, the peak appears at smaller incident angles, and the associated modes become waveguide modes. When the nonlinear gain is turned on, the reflectance shows very strong multistability near the incident angles associated with surface confined wave modes. As the nonlinear gain parameter is varied, the reflectance curve undergoes complicated topological changes. It is observed that a giant amplification of the reflectance by three orders of magnitude occurs near the incident angle associated with a waveguide mode for a very small nonlinear gain. Also, there exists a range of the incident angle where the wave is dissipated rather than amplified even in the presence of gain. We suggest that this can provide the basis for a possible new technology for thermal control in the subwavelength scale.



## Keywords:

nonlinear gain, surface plasmon, waveguide mode

## Topological phases of non-symmorphic crystals: 1/4 filled Shastry-Sutherland lattice.

이성빈\*<sup>1</sup>, 양현준<sup>1</sup>

<sup>1</sup>한국과학기술원 물리학과  
sungbin@kaist.ac.kr

### Abstract:

Shastry-Sutherland lattice at quarter filling is studied to investigate a possible time-reversal invariant topological insulator. With additional spin-orbit (SO) coupling, the tight-binding model is simplified to preserve time-reversal and inversion symmetries but break non-symmorphic symmetries which protect line degeneracies in Brillouin zone. To determine Z<sub>2</sub> invariants, time-reversal invariant momentum (TRIM) points are examined. Furthermore, the reason that the degeneracy at M point is robust under breaking symmetries is argued and it is confirmed that Dirac cones appear when the Z<sub>2</sub> invariant is -1 in the absence of SO coupling. Also the effects of long-range hoppings that respect the model's symmetries are studied. Finally, the edge spectrum for the nontrivial phase is presented.

### Keywords:

Non-symmorphic symmetry, Topological insulators

## Topological magnon bands in the zigzag and stripy phases of antiferromagnetic honeycomb lattice

이기훈\*<sup>1, 2</sup>, 정석범\*<sup>1, 2, 3</sup>, 박기수<sup>1, 2</sup>, 박제근<sup>1, 2</sup>

<sup>1</sup>기초과학연구원 강상관계 물질 연구단, <sup>2</sup>서울대학교, 자연과학대학 물리천문학부, <sup>3</sup>서울시립대학교 물리학과  
kihoonlee@snu.ac.kr, chung.sukbum@gmail.com

### Abstract:

We investigated the topological property of magnon bands in the collinear magnetic orders of zigzag and stripy phases for the antiferromagnetic honeycomb lattice and identified Berry curvature and symmetry constraints on the magnon band structure. Different symmetries of both zigzag and stripy phases lead to different topological properties, in particular, the magnon bands of the stripy phase being disentangled with a finite Dzyaloshinskii-Moriya (DM) term with non-zero spin Chern number. This is corroborated by calculating the spin Nernst effect. Our study establishes the existence of the non-trivial magnon band topology for all observed collinear antiferromagnetic honeycomb lattice in the presence of the DM term.

### Keywords:

antiferromagnetism, topological insulator, magnon, spin waves, spin current, thermomagnetic effects

## Superconductivity in two-dimensional ferromagnetic MnB

홍지상\*<sup>1</sup>, FAROOQ Muhammad Umar<sup>1</sup>, KHAN Imran<sup>1</sup>, SON Jicheol<sup>1</sup>

<sup>1</sup>부경대학교 물리학과  
hongj@pknu.ac.kr

### Abstract:

Using the universal structure predictor algorithm, we proposed that two-dimensional MnB structures with p4mmm ( $\alpha$ -MnB) and pmma(?) ( $\beta$ -MnB) symmetries could be synthesized. This finding was verified by dynamical stability, molecular dynamics, and mechanical properties. The  $\alpha$ -MnB has an in-plane stiffness  $Y_x (= Y_y)$  around 100 N / m while the  $\beta$ -MnB is an asymmetric mechanical stiffness of  $Y_x = 186$  N / m and  $Y_y = 139$  N / m. Both systems show a ferromagnetic ground state with metallic band structures. The calculated magnetic moments were 2.14 and 2.34  $\mu_B$  per Mn-B pair in the  $\alpha$ -MnB and  $\beta$ -MnB. Furthermore, we investigated the potential superconductivity. In the  $\alpha$ -MnB, we found the unique feature of Kohn anomaly at  $q \sim 2k_F$  in the diagonal direction of the Brillouin zone. The  $\beta$ -MnB phonon spectra showed a valley of degenerated localized softening vibration modes at the edge of the Brillouin zone. The ZA and the LA phonon branches in this valley induced the largest contribution to electron-phonon coupling strength. The calculated total electron-phonon coupling parameters were 1.20 and 0.89 in  $\alpha$ -MnB and  $\beta$ -MnB systems. And therefore the overall, we predict that the  $\alpha$ -MnB and  $\beta$ -MnB systems are 2D superconducting states ferromagnetic with  $T_c \approx 10-13$  K.

### Acknowledgments

This research was supported by the National Science Foundation of Korea (NRF) funded by the Ministry of Science, ICT and Future Planning (2016R1A2B4006406) and by the Supercomputing Center / Korea Institute of Science and Technology Information with supercomputing resources including technical support (KSC-2017-C3-0031).

### Keywords:

two-dimensional materials, Superconductivity, ferromagnetic

## Resonant frequencies and spatial correlations in frustrated arrays of Josephson type nonlinear oscillators

알렉시 안드리아노브\*<sup>1</sup>, FISTUL Mikhail<sup>1, 2</sup>

<sup>1</sup>Center for Theoretical Physics of Complex Systems, Institute for Basic Science (IBS), Daejeon 34051, Republic of Korea, <sup>2</sup>Russian Quantum Center, National University of Science and Technology "MISIS", 119049 Moscow, Russia  
alexei@pcs.ibs.re.kr

### Abstract:

We present a theoretical study of resonant frequencies and spatial correlations of Josephson phases in frustrated arrays of Josephson junctions. Two types of one-dimensional arrays, namely, the diamond and sawtooth chains, are discussed. For these arrays in the linear regime the Josephson phase dynamics is characterized by multiband dispersion relation  $\omega(k)$ , and the lowest band becomes completely at a critical value of frustration,  $f = f_c$ . In a strongly nonlinear regime such critical value of frustration determines the crossover from non-frustrated ( $0 < f < f_c$ ) to frustrated ( $f_c < f < 1$ ) regimes. The crossover is characterized by the thermodynamic spatial correlation functions of phases on vertices,  $\phi_i$ , i.e.  $C_p(i - j) = \langle \cos[p(\phi_i - \phi_j)] \rangle$  displaying the transition from long- to short-range spatial correlations. We find that higher-order correlations functions, e.g.  $p = 2$  and  $p = 3$ , restore the long-range behavior deeply in the frustrated regime,  $f \simeq 1$ . Monte-Carlo simulations of the thermodynamics of frustrated arrays of Josephson junctions are in good agreement with analytical results.

### Keywords:

josephson junctions, frustration

## Spin-lattice Coupling in U(1) Quantum Spin Liquids

문은국\*<sup>1</sup>, 이상진<sup>1</sup>

<sup>1</sup>한국과학기술원 물리학과  
egmoon@kaist.ac.kr

### Abstract:

Quantum spin liquids (QSLs) are exotic phases with intrinsic massive entanglements. Instead of microscopic spins, fractionalized particles and gauge fluctuations are emergent, revealing QSLs' exotic natures. Quantum spins with strong spin-orbit coupling on a pyrochlore lattice, for example  $\text{Pr}_2\text{Zr}_2\text{O}_7$ , are suggested to host a U(1) QSL with emergent photons, gapless excitations without breaking any symmetries, as well as emergent monopoles. One of the key issues in QSLs is an interplay between emergent degrees of freedom of QSLs and conventional degrees of freedom, and we investigate the interplay by constructing a general theory of spin-lattice coupling in U(1) QSLs. We find that the coupling induces characteristic interplay between phonons and photons. For example, photons become qualitatively more stable than phonons at low temperature. We also propose mechanisms to detect emergent photons in experiments such as sound attenuation and thermal transport relying on spin-lattice coupling in U(1) QSLs.

### Keywords:

U(1) Spin Liquid, Spin ice

## Spin-1 bilinear-biquadratic model on star lattice

이현용\*<sup>1</sup>, NAOKI Kawashima<sup>1</sup>

<sup>1</sup>The University of Tokyo Institute for Solid State Physics  
hyunyong.rhee@gmail.com

### Abstract:

We study the ground-state phase diagram of the  $S=1$  bilinear-biquadratic model (BLBQ) on the star lattice with the state-of-art tensor network algorithms. The system has five phases: the ferromagnetic, anti-ferromagnetic, ferroquadrupolar, and spin-liquid phases. The phases and their phase boundaries are determined by examining various local observables, correlation functions and transfer matrices exhaustively. The spin liquid phase, which is the first quantum disordered phase found in two-dimensional BLBQ model, is gapped and devoid of any conventional long-range order. It is also characterized by fixed-parity virtual bonds in the tensor network formalism, analogous to the Haldane phase, while the parity varies depending on the location of the bond.

### Keywords:

Quantum spin liquid, Classical statistical mechanics, Frustrated quantum magnet

## Correlation between Compensation Temperatures of Magnetization and Angular Momentum in GdFeCo Ferrimagnets

KIM Duck-Ho\*<sup>1</sup>, HIRATA Yuushou<sup>1</sup>, OKUNO Takaya<sup>1</sup>, NISHIMURA Tomoe<sup>1</sup>, KIM Dae-Yun<sup>2</sup>, FUTAKAWA Yasuhiro<sup>3</sup>, YOSHIKAWA Hiroki<sup>3</sup>, TSUKAMOTO Arata<sup>3</sup>, KIM Kab-Jin<sup>4</sup>, CHOE Sug-Bong<sup>2</sup>, ONO Teruo<sup>1</sup>

<sup>1</sup>Institute for Chemical Research, Kyoto University, <sup>2</sup>Department of Physics, Seoul National University,

<sup>3</sup>College of Science and Technology, Nihon University, <sup>4</sup>Department of Physics, Korea Advanced

Institute of Science and Technology

kim.duckho.23z@st.kyoto-u.ac.jp

### Abstract:

Recently, magnetic field-controlled antiferromagnetic spin dynamics has been achieved using ferrimagnets [1]. This observation reveals that ferrimagnets exhibit the antiferromagnetic dynamics because of the zero net angular momentum at the compensation temperature of the angular momentum. Although remarkable efforts have been made theoretically and experimentally [1, 2, 3] in understanding the role of angular momentum compensation in DW dynamics, it is difficult to determine the angular momentum compensation temperature because of the methodological complexities. Here, we propose a way to estimate the angular momentum compensation temperature of ferrimagnets. We find a linear relation between the compensation temperatures of the magnetization and angular momentum in GdFeCo ferrimagnetic materials, which is proved by theoretically as well as experimentally. The linearity comes from the power-law criticality and is governed by the Curie temperature and the Landé g factors of the elements composing the ferrimagnets. Therefore, measuring the magnetization compensation temperature and the Curie temperature, which are easily assessable experimentally, enables to estimate the angular momentum compensation temperature of ferrimagnets. Our study provides efficient avenues into an exciting world of ferrimagnetic spintronics.

### References

- [1] K.-J. Kim et al., Nat. Mater. doi:10.1038/nmat4990 (2017).
- [2] C. D. Stanciu et al., Phys. Rev. B 73, 220402(R) (2006).
- [3] C. Kaiser, A. F. Panchula, and S. S. P. Parkin, Phys. Rev. Lett. 95, 047202 (2005).

### Keywords:

Ferrimagnet, Angular momentum compensation temperature, Domain-wall motion

## Search for Room Temperature Compensated Half-metals in Inverse-Heusler Compounds $\text{Cr}_2\text{CoZ}$ ( $Z=\text{Al}, \text{Ga}, \text{In}$ )

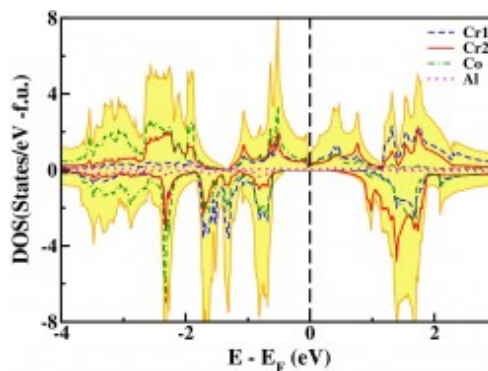
JIN Hyo-Sun<sup>2</sup>, LEE K.-W.\*<sup>1, 2</sup>

<sup>1</sup>Division of Display and Semiconductor Physics, Korea University, Sejong , <sup>2</sup>Department of Applied Physics, Graduate School, Korea University, Sejong  
mckwan@korea.ac.kr

### Abstract:

The compensated half-metal (CHM), which is anticipated as a promising candidate for spintronic applications, is a half-metal with the exactly compensated net moment. However, the realization of CHMs is very limited.

Using three correlated band theory approaches of the GGA+U, the Tran and Blaha modified Becke-Johnson functional (mBJ), and the hybrid functional, we have revisited several Cr-based ferrimagnetic inverse-Heusler compounds, which were suggested to have a small net moment.  $\text{Cr}_2\text{CoAl}$  shows an exact CHM, whereas  $\text{Cr}_2\text{CoGa}$  and  $\text{Cr}_2\text{CoIn}$  are ferrimagnets with a small moment. This is also confirmed by the fixed spin moment calculation. Additionally, change in volume of  $\text{Cr}_2\text{CoAl}$  by  $\pm 5\%$  does not alter the CHM state. Therefore, considering the observed high Curie temperature of  $T_C \sim 750\text{K}$ , our results suggest that  $\text{Cr}_2\text{CoAl}$  is an exact room temperature CHM.



**Acknowledgements:** This research was supported by NRF-2016R1A2B4009579.

### Keywords:

first principles calculations, compensated half-metals, inverse Heusler, spintronics

## Design of Co<sub>2</sub>Y-type hexaferrite single crystals by adjusting the spin anisotropy and phase competition to enhance the magnetoelectric coupling in the wide temperature range

김기훈\*<sup>1</sup>, 박창배<sup>1</sup>

<sup>1</sup>서울대학교 물리천문학부

khkim@phya.snu.ac.kr

### Abstract:

Even though the Co<sub>2</sub>Y-type hexaferrites have a great potential for realizing the huge magnetoelectric (ME) coupling at room temperature, there are few researches to optimize the ME coupling in the Co<sub>2</sub>Y-type hexaferrites. To not only maximize the ME coupling, but also investigate the physical origin of the enhancement, we have grown Co<sub>2</sub>Y-type hexaferrites single crystal series Ba<sub>2-x</sub>Sr<sub>x</sub>Co<sub>2</sub>(Fe<sub>1-y</sub>Al<sub>y</sub>)<sub>12</sub>O<sub>22</sub> ( $1.0 \leq x \leq 1.9$ ,  $0.00 \leq y \leq 0.08$ ) with self-flux method. We have observed that, among the grown crystals, the nominal composition with  $x = 1.8$  and  $y = 0.04$  has the largest ME coupling coefficient,  $dP/dH$ , and magnetic controllable electric polarization,  $\Delta P_{\max}$ , in the various temperature range ( $dP/dH = 25000$  ps/m and  $\Delta P_{\max} = 430$   $\mu\text{C}/\text{m}^2$  at 10 K and  $dP/dH = 1000$  ps/m and  $\Delta P_{\max} = 60$   $\mu\text{C}/\text{m}^2$  at 300 K each). They are the largest values in the known Co<sub>2</sub>Y-type hexaferrites so far. Moreover, electric phase diagram and magnetic structure as Al substitution are demonstrated by bulk magnetization, dielectric constant and neutron scattering studies. In conclusion, we suggest that optimization of spin anisotropy and phase competition between transverse cone and alternating longitudinal cone, which are driven by Sr and Al substitution, result in the ME coupling optimization in the  $x = 1.8$  and  $y = 0.04$  composition. The role of Sr, Co and Al ions in the spin frustration and magnetic anisotropy will be also discussed.

### Keywords:

Multiferroics, Magnetoelectric coupling, Hexaferrites, Spin frustration

## Short-ballistic Josephson coupling in vertical and planar graphene heterojunctions

LEE Hu-Jong\*<sup>1</sup>

<sup>1</sup>포항공과대학교 물리학과  
hjlee@postech.ac.kr

### Abstract:

Realization of strong proximity coupling in Josephson junctions (JJs), incorporating various two-dimensional (2D) van der Waals (vdW) materials including graphene, has recently attracted much research interest. In this study, we realized the short-ballistic strong Josephson coupling in vertical [1,2] and planar [3] proximity Josephson junctions with mono-layer graphene as the thin normal-conducting spacer. For vertical graphene Josephson junctions (GJJs), the strong proximity coupling is realized by shortening the channel length down to an atomic scale, *i.e.*, across the thickness of mono-layer graphene between two superconducting-layer electrodes with clean interfaces. For planar GJJs, two superconducting electrodes are arranged close to each other within a few-hundred-nm spacing along the plane of a graphene layer. Here, the strong coupling is realized via the ballistic conducting channels of a boron-nitride(BN)-protected graphene layer together with highly transparent edge superconducting contacts. The strong Josephson coupling and the easy gate tunability of the coupling strength can be conveniently utilized for unit components of quantum devices with highly robust coherence. If time allows, I will also briefly discuss how the Josephson effect is adopted to explore fundamental material properties such as the robust surface conduction in a topological insulator.

[1] Gil-Ho Lee *et al.*, Nature Communications 6:6181 DOI: 10.1038/ncomms7181 (2015).

[2] Minsoo Kim *et al.*, Nano Letters 17, 6125 (2017).

[3] Jinho Park *et al.*, Physical Review Letters 120, 077701 (2018).

### Keywords:

proximity Josephson junction, graphene Josephson junction, short-ballistic Josephson coupling

## Violation of Ohm's law as a hallmark of the three-dimensional Weyl metal

김현정\*<sup>1, 2</sup>

<sup>1</sup>대구대학교 물리학과, <sup>2</sup>대구대학교 신소재에너지공학과  
hjkim76@daegu.ac.kr

### Abstract:

As an exotic metallic state, the Weyl metal has pairs of Weyl nodes in the  $k$  space and shows topological surface state known as Fermi arc and anomalous electrical transport originating from chiral anomaly. Ever since observed in  $\text{Bi}_{0.96}\text{Sb}_{0.04}$ , which becomes a three-dimensional (3D) Weyl metal in parallel electric ( $E$ ) and magnetic ( $B$ ) fields, the negative longitudinal magnetoresistance has been the only transport signature of 3D Weyl metals, such as TaAs,  $\text{Na}_3\text{Bi}$ ,  $\text{Cd}_3\text{As}_2$  and so on. Here as an indisputable fingerprint for existence of chiral anomaly, we present violation of Ohm's law in  $\text{Bi}_{0.96}\text{Sb}_{0.04}$ , which occurs only in the longitudinal configuration ( $E//B$ ). Instead of constant conductivity, nonlinear conductivity components proportional to  $E^2$  are observed. This nonlinear conductivity in the longitudinal configuration is described by Boltzmann transport theory that incorporates chiral anomaly and resultant charge pumping phenomenon. As the Boltzmann transport theory suggests, the nonlinear conductivity components at different  $E$  and  $B$  are scaled into a single universal function. As a hallmark of the Weyl metal, the nonlinear conductivity of the Weyl metal opens the door to a novel nonlinear electronic component at low frequency.

### Keywords:

Weyl metal, chiral anomaly, Violation of Ohm's law

## Deformation and interface states of bipolar quantum Hall graphene

명노준<sup>1</sup>, 박희철\*<sup>2</sup>

<sup>1</sup>조선대학교 물리교육학과, <sup>2</sup>기초과학연구원 복잡계이론물리 연구단  
hcpark@ibs.re.kr

### Abstract:

We have studied deformation effect on the interface states generated by bipolar junction on the quantum Hall graphene. Coherent transport across the junction exhibits two mesoscopic features: valley-isospin dependence of the quantum Hall conductance, the Aharonov-Bohm (AB) effects with the interface channels, and Fano resonance between interface state and the localized state due to the gauge field induced by deformation. We demonstrate that the valley-isospin dependences can be measured in a graphene sample with perfect edge terminations, resulting in conductance oscillation and Fano resonance for the smallest Chern number case. Especially, the localized states are characterized by different valleys and scatter the valley-isospinors. For larger Chern numbers, on the other hand, the conductance exhibits an oscillatory behavior of which period is relatively longer than the valley-isospin dependent oscillation. This conductance oscillation is ascribed to the AB effect, which is implicitly created by the split metallic channels near the junction interface.

### Keywords:

quantum Hall graphene, interface states, pseudo gauge field

## 모두가 참여하고 모두가 누리는 4차 산업혁명 구현

서은경\*<sup>1</sup>

<sup>1</sup>전북대학교 반도체과학기술학과  
eksuh@jbnu.ac.kr

### Abstract:

우리는 지금 4차 산업혁명의 시대를 맞고 있다. 디지털과 아날로그의 융합혁명으로 시작하여 현실과 가상이 인간을 중심으로 융합하는 혁명이라 할 수 있다. 4차 산업혁명은 IoT, 빅데이터/클라우드, 인공 지능 등 O2O 융합 기술로 생산 혁명을 가져올 것이며, 기술 융합을 넘어서 경제사회의 분배 혁명과 인간의 행복을 최적화 하는 소비 혁명을 가져올 것으로 예측되고 있다. 우리는 능동적으로 변화를 하던가, 아니면 변화를 강요받던가 하는 기로에 서 있으며, 따라서 4차 산업혁명은 위기이자 경제·사회 구조적 과제를 동시에 해결하는 새로운 성장의 기회라 할 수 있다. 정부는 혁신 성장을 위한, 사람 중심의 4차 산업혁명 추진을 위해 큰 그림을 그리고 동시에 구체적인 실행의 균형과 민관 팀플레이를 통한 혁명을 추구하고 있으며, 이를 위해 민관이 공동 참여하는 4차산업혁명위원회를 운영하고 있다. 본 강연에서는 현재 진행되고 있는 4차산업혁명위원회의 활동과 국가의 대응전략을 간단히 소개하고 여성과학기술인의 역할과 리더십에 대해 이야기를 나누고자 한다.

### Keywords:

4차 산업혁명, 여성과학기술인

## 물리학과 여성, 미래 여성들의 역할

조향숙\*<sup>1</sup>

<sup>1</sup>한국과학창의재단  
jung.ranju@gmail.com

### Abstract:

물리학에서 다루는 역학, 전자기학, 장론과 인간사회에서 작용하는 원리를 비교한다. 과학창의재단이 하는 일을 소개한다. 여성과 남성의 비율이 5:5인데 일터와 조직에서 일하는 여성의 수는 상대적으로 적고, 물리학 분야는 더 적다. 페이스북 최고운영책임자 쉐릴 샌드버그가 쓴 '린인'과 세계 최고의 광고회사 맥켄 에릭슨의 최초의 여성 CEO인 니나 디세사의 '유혹과 조종의 기술'에 나오는 업무현장에서 남녀의 특징을 소개한다. 말과 시험에서 우세하던 여학생들이 조직의 상부로 올라갈수록 줄어드는 현상을 조직문화와 연결해 살펴보고자 한다.

### Keywords:

여성

## Emergent Spacetime Supersymmetry at Superconducting Quantum Criticality of a Single Dirac Cone

YAO Hong<sup>\*1</sup>

<sup>1</sup>Institute for Advanced Study, Tsinghua University  
yaohong@tsinghua.edu.cn

### Abstract:

No definitive evidence of spacetime supersymmetry (SUSY) that transmutes fermions into bosons and vice versa has been revealed in nature so far. Moreover, whether spacetime SUSY in 2+1 and higher dimensions can occur or emerge in generic microscopic models remains open. Here, we introduce a lattice realization of a single Dirac fermion with attractive Hubbard interactions that preserves both time-reversal and chiral symmetries. By performing numerically-exact sign-problem-free determinant quantum Monte Carlo simulations, we show that the interacting single Dirac fermion in 2+1 dimensions features a superconducting quantum critical point (QCP). More remarkably, we demonstrate that the N=2 spacetime SUSY in 2+1D emerges at the superconducting QCP by showing that the fermions and bosons have identical anomalous dimensions 1/3, a hallmark of the emergent SUSY. To the best of our knowledge, this is the first observation of emergent 2+1D spacetime SUSY in quantum microscopic models. We further discuss some experimental signatures which can be measured to test such emergent SUSY in candidate systems such as the surface of 3D topological insulators.

[1] Zi-Xiang Li, Abolhassan Vaezi, Christian B. Mendl, and Hong Yao, arXiv:1711.04772

### Keywords:

supersymmetry, quantum Monte Carlo, quantum criticality

## Numerical Investigation of trimer correlations in two and one dimensions

한정훈\*<sup>1</sup>

<sup>1</sup>성균관대학교 물리학과  
hanjemme@gmail.com

### Abstract:

For the past several years our group (myself, Dr. Hyunyong Lee, Yuntak Oh) and professor Katsura at the University of Tokyo has been investigating various models with an eye to generalize the famous dimer spin liquid picture to that of trimers. A trimer is, roughly speaking, a singlet object made up of three local spins and can arise, in principle, in spin-1 models when appropriate interactions are given. In this talk, we give a survey of our efforts starting with the tensor-network type of construction of featureless insulator in spin-1 square lattice, where the first hint of trimer correlation in certain kinds of spin liquid variational wave function was noticed. This observation was subsequently examined in the setting of a classical trimer model in collaboration with prof. Katsura. Both the counting problem of the number of available trimer configurations and the calculation of trimer-trimer correlation functions were solved successfully with a little adaptation of the numerical techniques for doing tensor network calculations. In our final project, a microscopic spin-1 model Hamiltonian in one dimension was written down and its ground state properties were uncovered by the density matrix renormalization group method. Interestingly, the model we wrote down, while superficially consisting of rather different interactions, gave rise to a quantum phase diagram almost identical to that of the bilinear-biquadratic spin-1 chain Hamiltonian studied thoroughly a decade ago. It is hoped that our presentation can be a spur to those working in quantum magnetism to look for interesting correlations in spin-1 materials.

### Keywords:

trimer correlation, tensor network, DMRG

## Revealing fermionic quantum criticality from new Monte Carlo techniques

MENG Zi Yang\*<sup>1</sup>

<sup>1</sup>Institute of Physics, Chinese Academy of Sciences  
zymeng@iphy.ac.cn

### Abstract:

In this talk, I will present recent developments in the numerical investigation of fermionic quantum criticality in the form of Fermi surfaces coupled to various critical bosonic fluctuations. The thence obtain itinerant quantum critical points reveal rich and fundamental physics that has immediate impact on both theoretical and experimental investigations in the correlated electrons systems such as Cu- and Ir-based superconductors, heavy-fermion systems as well as the interacting topological state of matter and phase transitions. These developments are made possible due to the insightful model design as well as the algorithmic developments in the Monte Carlo techniques, which I will also cover within this talk.

### Keywords:

quantum Monte Carlo, quantum criticality

## Role of Hund's coupling in spin-orbit entangled ground states

GO Ara<sup>\*1</sup>

<sup>1</sup>Center for Theoretical Physics of Complex Systems, Institute for Basic Science  
arago@ibs.re.kr

### Abstract:

We investigate the role of the Hund's coupling in single-particle excitation spectra of spin-orbit entangled ground states. The Hund's coupling has been often neglected in theoretical interpretations of spin-orbit coupled systems, simply because it is relatively small in materials with strong spin-orbit coupling. However, the multiplet structure controlled by the Hund's coupling makes it an essential ingredient for understanding the spectral properties of the spin-orbit entangled systems. Here we examine how the Hund's coupling plays a key role in single-particle excitation spectra by analyzing atomic  $t_{2g}$  model Hamiltonian, then conduct dynamical mean-field theory calculations to further clarify the analysis under various circumstances.

### Keywords:

Hund's coupling, spin-orbit entangled states, dynamical mean-field theory

## Theory for selective cargo transport through the nuclear pore complex: Interactive diffusion over fluctuating polymer barrier

김용운\*<sup>1</sup>

<sup>1</sup>한국과학기술원 나노과학기술대학원  
y.w.kim@kaist.ac.kr

### Abstract:

Macromolecular transport through the nuclear pore complex (NPC) is of vital importance in eukaryotic cells. However, there is still uncertainty regarding how the structure and dynamics of the FG nucleoporin proteins (FG-nups) lining the pore and their interactions with transport factors (TF) and enzymes (RanGTP) all come together functionally to regulate transport. Here, we develop a self-contained theory that, starting with sequence information, predicts the polymer conformations of FG-nups, calculates the resulting free energy barrier for cargo transport, and uncovers different transport regimes of current and transit time based on cargo size, transport factor affinity and RanGTP concentration. Our results point to co-operativity between TFs and RanGTP as a key determinant of size-selective permeability and rapid transport across NPC.

### Keywords:

nucleocytoplasmic transport, conformational fluctuations, transport barrier, barrier crossing dynamics, cooperativity

## Fast sparsely synchronized rhythms in a small-world neuronal network with inhibitory spike-timing-dependent plasticity

KIM Sang-Yoon<sup>1</sup>, LIM Woochang\*<sup>1</sup>

<sup>1</sup>Institute for Computational Neuroscience and Department of Science Education, Daegu National University of Education  
wclim@icn.re.kr

### Abstract:

We consider the Watts-Strogatz small-world network (SWN) consisting of inhibitory fast spiking Izhikevich interneurons. This inhibitory neuronal population has adaptive dynamic synaptic strengths governed by the inhibitory spike-timing-dependent plasticity (iSTDP). In previous works without iSTDP, fast sparsely synchronized rhythms, associated with diverse cognitive functions, were found to appear in a range of large noise intensities for fixed strong synaptic inhibition strengths. Here, we investigate the effect of iSTDP on fast sparse synchronization (FSS) by varying the noise intensity  $D$ . We employ an asymmetric anti-Hebbian time window for the iSTDP update rule [which is in contrast to the Hebbian time window for the excitatory STDP (eSTDP)]. Depending on values of  $D$ , population-averaged values of saturated synaptic inhibition strengths are potentiated [long-term potentiation (LTP)] or depressed [long-term depression (LTD)] in comparison with the initial mean value, and dispersions from the mean values of LTP/LTD are much increased when compared with the initial dispersion, independently of  $D$ . In most cases of LTD where the effect of mean LTD is dominant in comparison with the effect of dispersion, good FSS (with higher spiking measure) is found to get better via LTD, while bad FSS (with lower spiking measure) is found to get worse via LTP. This kind of Matthew effect in inhibitory synaptic plasticity is in contrast to that in excitatory synaptic plasticity where good (bad) synchronization gets better (worse) via LTP (LTD). Emergences of LTD and LTP of synaptic inhibition strengths are intensively investigated via a microscopic method based on the distributions of time delays between the pre- and the post-synaptic spike times. Furthermore, we also investigate the effects of network architecture on FSS by changing the rewiring probability  $p$  of the SWN in the presence of iSTDP.

### Keywords:

Inhibitory spike-timing-dependent plasticity, Fast sparsely synchronized rhythm, Watts-Strogatz small-world network

## Encoding information into autonomously bursting neural network with pairs of two time-delayed pulses

이경진\*<sup>1</sup>, 김준환<sup>1</sup>, 이호준<sup>1</sup>

<sup>1</sup>고려대학교 물리학과  
kyoung@korea.ac.kr

### Abstract:

Biological neural networks with many plastic synaptic connections can store external input information in the map of synaptic weights as a form of unsupervised learning. However, the same neural network often produces dramatic reverberating events in which many neurons fire almost simultaneously - a phenomenon coined as 'population burst.' The autonomous bursting activity is a consequence of the delicate balance between recurrent excitation and self-inhibition; as such, any periodic sequences of burst-generating stimuli delivered even at a low frequency ( $\sim 1$  Hz) can easily suppress the entire network connectivity. Here we demonstrate that ' $\Delta t$  paired-pulse stimulation,' can be a novel way for encoding spatially-distributed high-frequency ( $\sim 10$  Hz) information into such a system without causing a complete suppression. The encoded memory can be probed simply by delivering multiple probing pulses and estimating the precision of the arrival times of the subsequent evoked recurrent bursts. This model study also nicely explains the biophysical mechanism responsible for the experimental observations that we reported earlier in [Choi et al., Phys. Rev. Lett. 108, 138103 (2012)].

### Keywords:

neuronal population bursts, neuronal oscillations, learning and memory, synaptic encoding

## How the nose is optimized: statistical design principles of human olfactory receptors

BAK Ji Hyun\*<sup>1</sup>

<sup>1</sup>School of Computational Sciences, KIAS  
jhbak@kias.re.kr

### Abstract:

The primary computational task of olfactory sensing is the discrimination of different odors. An odor captures the chemical state of the environment in a mixture of smell molecules, called odorants. Olfactory sensing is realized by the selective binding of odorants to a set of olfactory receptors (ORs), which in turn activates the corresponding olfactory sensory neurons, constructing the brain's first representation of the odor. Despite the high-dimensional nature of olfactory sensing, recent measurements with human ORs suggest that the odorant-receptor interaction is sparse; only a small fraction of all available pairs interact. Why did the OR system evolve this way? More generally, what are the optimal interaction structures for effective olfactory discrimination? We investigate these questions by combining studies of model systems and analyses of experimental data. We show that optimization depends on the statistical properties of the olfactory environment, and furthermore suggest that the human OR system is adapted to the natural odor statistics.

### Keywords:

biological sensing; olfactory receptors; odor coding; information optimization; natural statistics

## 자기조직화하여 민감도를 증강시키는 청각 유모세포 시냅스 소포

안강현\*<sup>1</sup>

<sup>1</sup>충남대학교 물리학과  
ahnkh@cnu.ac.kr

### Abstract:

청각유모세포에 소리 신호가 들어 올 때 시냅스를 통해 소포들이 신경전달 물질을 방출한다. 청각의 특징 중 하나는 이때 방출하는 시각의 정확성이 놀라울 정도로 높다는 것이다. 본 연구에서 청각 유모 세포의 소포가 글루타마이트 등의 신경 전달 물질을 방출하는 과정에 관한 회로이론을 제안한다. 이 이론을 통해서 보면 소포는 스스로 자기조직화 해서 외부 전기 자극에 매우 민감한 상태에 이르고 이를 통해 외부 신호에 매우 정확한 시간에 반응 할 수 있는 상태가 될 수 있다. 칼슘을 통해서 신경 전달물질을 방출하는 과정 뿐 아니라 전기 신호에 의해 직접적으로 자극을 받아서 신호 전달이 이루어지는 과정을 제안한 이론이다.

### Keywords:

소포, 시냅스, 자기조직화

## Neural field theory of Parkinson's disease and generalized epilepsies

김종원\*<sup>1</sup>

<sup>1</sup>인제대학교 헬스케어 IT  
jongwonkim@inje.ac.kr

### Abstract:

The mechanisms underlying neural oscillations in Parkinson's disease (PD) and generalized epilepsies are explored via a neural field model of the corticothalamic-basal ganglia (CTBG) system. In addition to normal EEG rhythms, enhanced activity around 4 Hz and 20 Hz exists in the model, consistent with the characteristic frequencies observed in PD. These rhythms result from resonances in loops formed between the BG and CT populations, analogous to those that underlie epileptic oscillations in a previous CT model. Dopamine depletion is argued to weaken the dampening of these loop resonances in PD, and network connections then explain the significant coherence observed between BG, thalamic, and cortical population activity around 4-8 Hz and 20 Hz. Furthermore, the model predicts an increased likelihood of absence (petit mal) seizure resulting from pathologically low dopamine levels in accordance with experimental observations. Suppression of absence seizure activity is demonstrated when afferent and efferent BG connections to the CT system are strengthened. Overall, the findings demonstrate strong parallels between coherent oscillations in generalized epilepsies and PD, and provide insights into possible comorbidities.

### Keywords:

Neural field theory, Parkinson's disease, Epilepsy

## How randomly distributed attractive particles evolve in 1D: Defects of liquid crystals in capillaries

ALMUKAMBETOVA Madina<sup>1</sup>, JAVADI Arman<sup>1</sup>, JEONG Joonwoo<sup>\*1</sup>

<sup>1</sup>Department of Physics, UNIST  
jjeong@unist.ac.kr

### Abstract:

Symmetry-breaking phase transitions often lead to the formation of topological defects. Examples range from vortices in superfluids to cosmic domains and strings in the early universe. Nematic liquid crystals as the simplest partially ordered matter have been a useful model system to study a variety of topological defects. Here we introduce another simple liquid crystal-based system to investigate the defect formation and the defect annihilation dynamics. Lyotropic cholesteric liquid crystal confined in capillary tubes exhibits spontaneous chiral symmetry breaking. Domains of two different handednesses coexist in with domain-wall-like defects between them. We experimentally measured the positions of each defect, the defect-to-defect distances, and their time evolution. Our investigation on the statistical distribution of the distances reveals that the system is almost equivalent to the annihilation dynamics of randomly distributed particles in 1D with an attractive power-law pair potential.

### Keywords:

Topological defects, Liquid crystals, Confinement

## 자연계열 전공자 노동시장 이행 성과 및 경쟁력 확보 방안

심정민\*<sup>1</sup>

<sup>1</sup>한국과학기술기획평가원  
sjmin1@kistep.re.kr

### Abstract:

과학기술의 원천이자 기초적인 토대를 형성하고 있는 자연과학분야는 불확실한 환경 하에서 지속가능한 경제발전 및 국가경쟁력을 견인하는 핵심요소로 인식되고 있다. 하지만 이런 사회적 인식과는 달리 자연과학분야 전공학생의 노동시장 이행은 원활하지 않는 편이며, 그 간의 이공계인력 정책 역시 전공별 특성을 고려하지 않고 추진되고 있다. 이에, 물리학을 포함한 자연계열 학생의 노동시장 이행 성과를 살펴보고 지속적으로 자연계열 인력이 노동시장에서 경쟁력을 확보하기 위한 정책적 방안을 고민해보고자 한다.

### Keywords:

이공계 인력정책, 자연계 경쟁력

## 암치료기용 레이저 플라즈마 가속 전자빔 발생 연구 현황

김경남<sup>1</sup>, 김재훈\*<sup>1</sup>, 황보용훈<sup>1</sup>, 전석기<sup>1</sup>, 김금배<sup>2</sup>, 한수림<sup>2</sup>  
<sup>1</sup>한국전기연구원 첨단의료기기연구본부, <sup>2</sup>한국원자력의학원 방사선기기부  
jkim@keri.re.kr

### Abstract:

레이저 웨이크 필드 가속의 안정성과 재현성의 증가로 인해 레이저 기반 암 치료 장치 적용에 가능성이 증가하고 있다. 일반적으로 다른 입자빔과 비교하여 고 에너지 전자빔은 정상세포의 손상을 최소화 하며 인체 깊은 곳까지 투과가 가능하다는 특징이 있다. 이러한 특징을 이용하여 여러방향에서 동시에 암세포 위치에 조사한다면 적은 손상으로 효율적인 치료가 가능하다. 본 연구에서는 레이저 웨이크 필드 가속의 안정성과 재현성 개선을 위해 헬륨, 질소 및 혼합가스를 타깃을 이용한 전자빔 특성을 연구하였다. 또한 밀도 선형 증가 구조를 적용한 가스 타깃에 레이저를 조사하여 30 pC이상의 전하량을 갖는 200 MeV 이상의 고에너지 전자빔을 얻었으며 이때 전자빔 에너지 재현율은 60% 이상이고 전자 가속율은 100%였다.

### Keywords:

레이저 플라즈마, 전자빔 가속, 입자빔 가속

## High-vacuum Laser Electron Acceleration using a metal target for a compact light source

박성희\*<sup>1</sup>

<sup>1</sup>고려대학교 가속기과학과  
shparkblue7@gmail.com

### Abstract:

As developed technologies in laser acceleration, applications, such as a light source or an injector, have come to the fore. Among the issues in stability, quality, duty factor, and so on, maintaining high vacuum is the one of issues to solve. Especially, the injection of electron beams to a storage ring requires to maintain high vacuum for longer lifetime. It was demonstrated laser electron accelerations using laser-ionized metallic plasma as a pre-plasma. Unlike gas targets, the amount of evaporated metallic gas is little to affect the vacuum in experimental chamber. Since it is determined by ns or ps lasers used for laser-induced ionization of metal surface, it will be good for high repetition and high vacuum operation. The experimental results and the issues for a compact light source will be presented.

### Keywords:

Laser electron acceleration, light sources, Synchrotron radiation, metallic plasma

## Particle-in-cell simulations for laser plasma accelerator study

배기훈\*<sup>1, 2</sup>, 남창희<sup>1, 3</sup>

<sup>1</sup>기초과학연구원, 초강력 레이저과학 연구단, <sup>2</sup>광주과학기술원, 고등광기술연구소, <sup>3</sup>광주과학기술원, 물리광학과  
khpae1@gist.ac.kr

### Abstract:

Particle-in-cell (PIC) simulations have played an important role in the development of laser-plasma based accelerators (LPAs), from the beginning of the laser wakefield accelerator concept, from the electron acceleration, proton and ion acceleration to the photon acceleration. In the LPA, large number of charged particles interact with strong laser field resulting in multi-species, multi-temperature, locally non-neutral, structured plasmas, which could have been well modeled with PIC simulations. With the progress of LPA research, large scale experiments are being performed and sophisticated theories are developed. In accordance with this trend, the scale of PIC simulations is growing and simulation schemes are improved or newly developed in the massively parallel computing environments. Recently, the development of laser technology enabled a focused intensity of  $10^{22}$  W / cm<sup>2</sup> extending the LPA research interest to the strong field quantum electrodynamics regime, where PIC simulations are playing a pioneering role. In this talk, the review will be given on the PIC method for the LPA study and the challenges will be discussed.

### Keywords:

Particle-in-cell; Laser-plasma accelerator

## 이온층이 강화된 이중층 타겟을 이용한 레이저-플라즈마 가속 이온빔의 에너지 스펙트럼 측정 및 특성분석

김하남<sup>1, 2</sup>, 이기태\*<sup>2</sup>, KUMAR Manoj<sup>2</sup>, 류우제<sup>2, 3</sup>, 김경남<sup>4</sup>, 박성희<sup>5</sup>, 전민용<sup>1</sup>, 정영욱<sup>2</sup>, 최일우<sup>6, 7</sup>, 이성근<sup>6, 8</sup>, 강승우<sup>6, 7</sup>, 윤현호<sup>6</sup>, 전천하<sup>6</sup>, 장용희<sup>6</sup>, 성재희<sup>6, 7</sup>, 이성구<sup>6, 7</sup>, 남창희<sup>6, 8</sup>

<sup>1</sup>충남대학교 물리학과, <sup>2</sup>한국원자력연구원 초고속방사선연구실, <sup>3</sup>한남대학교 물리학과, <sup>4</sup>한국전기연구원 전자기파 응용센터, <sup>5</sup>고려대학교 가속기학과, <sup>6</sup>기초과학연구원 초강력레이저과학연구단, <sup>7</sup>광주과학기술원 고등광기술연구소, <sup>8</sup>광주과학기술원 물리광학과  
klee@kaeri.re.kr

### Abstract:

레이저-플라즈마 상호작용에 의한 이온빔 가속연구는 수  $\mu\text{m}$ 의 짧은 영역에서 100 GV/m에 해당하는 높은 가속전기장을 얻을 수 있고 다양한 분야로의 응용가능성을 가지고 있어 지난 20년 간 많은 연구들이 수행되었다. 하지만 아직까지도 이온빔의 가속원리를 정확히 규명하기 위해서 이론과 실험을 통해 많은 부분들을 연구하고 이해할 필요가 있다. 대표적인 이온가속 원리 중에 하나인 target normal sheath-field acceleration (TNSA)은 고강도의 레이저를 필름형태의 타겟에 집속하였을 때 발생하는 열전자 (hot electrons)에 의해 타겟에 수직인 방향으로 가속전기장이 형성되고 이로 인해 이온빔이 가속되는 것이다. 가속전기장은 플라즈마 외부, 즉 타겟의 후면 (rare side)에 형성되는데 이온빔 가속은 주로 이 표면에 형성된 전기장을 이용한다. 하지만 시간이 지남에 따라 플라즈마 내부로도 정전기장이 확산되어간다. 한국원자력연구원에서는 이와같이 플라즈마 내부로 확산된 정전기장에 의해 이온빔 가속이 가능한 타겟 구조를 고안하였다.

본 연구에서는 이온층이 강화된 금속-플라스틱 구조의 이중층 타겟에서 30 TW와 150 TW 레이저 시스템을 사용하여 발생한 양성자 빔과  $\text{C}^{6+}$ 이온빔의 에너지 스펙트럼을 측정하고 그 특성을 분석하였다. 단일층 타겟을 사용하였을 때 열적인 분포의 에너지 스펙트럼이 관측된 것에 비해 이중층의 경우, 높은 에너지 영역에서 더 많은 이온빔이 가속된 에너지 스펙트럼을 얻었다. 또한 에너지 폭이 좁은 이온빔도 관측하였다.

### Keywords:

레이저-플라즈마 가속, 이온빔 가속, 양성자 가속, TNSA, 이중층 타겟

## Hybrid Laser Wakefield Acceleration: Transition from LWFA to PWFA

PATHAK Vishwa Bandhu\*<sup>1</sup>, KIM Hyung Taek<sup>2</sup>, KIM Chul Min<sup>2</sup>, NAM Chang Hee<sup>1, 3</sup>

<sup>1</sup>Center for Relativistic Laser Science, Institute for Basic Science (IBS), Gwangju, Republic of Korea,,

<sup>2</sup>Advanced Photonics Research Institute, GIST, Gwangju, Republic of Korea,, <sup>3</sup>Dept of Physics and Photon Science, GIST, Gwangju, Republic of Korea  
vishwabandhu@ibs.re.kr

### Abstract:

Plasma based accelerators are compact and table-top unconventional accelerators due to high energy gradients of  $\sim 100$  GeV / m that can be sustained in accelerating nonlinear plasma wave-structures. Drivers like a short-intense laser pulse or an ultra-relativistic charged beam can excite these nonlinear plasma waves behind it, so their accelerating field structures are also called wakefield. Laser wakefield acceleration (LWFA) and plasma wakefield acceleration (PWFA) have been demonstrated and studied independently. However, there is a strong possibility that these processes can be transitioned from LWFA to PWFA. Here is the full-scale 3D PIC OSIRIS simulations we show the transition of LWFA to PWFA to further enhance and control the energies of the accelerated electron bunches. In such a hybrid acceleration process, the electron bunch is accelerated by a short and intense laser pulse, then its own wake after the depletion of the laser pulse. If the wakefield excited by the electron bunch is strong enough, it can trap the low energy energies of the electron bunch and accelerate them to higher energies. We show that the particle energies can be doubled in the LWFA assisted PWFA, as compare to the single LWFA stage. The coupling between the two processes is strongly dependent on the laser and plasma parameters, and we demonstrate that by controlling these parameters we can control the accelerated beam quality. it can trap the low energy tail of the electron bunch and accelerate them to higher energies. We show that the particle energies can be doubled in the LWFA assisted PWFA, as compare to the single LWFA stage. The coupling between the two processes is strongly dependent on the laser and plasma parameters, and we demonstrate that by controlling these parameters we can control the accelerated beam quality. it can trap the low energy tail of the electron bunch and accelerate them to higher energies. We show that the particle energies can be doubled in the LWFA assisted PWFA, as compare to the single LWFA stage. The coupling between the two processes is strongly dependent on the laser and plasma parameters, and we demonstrate that by controlling these parameters we can control the accelerated beam quality.

### Keywords:

Laser wakefield acceleration, Plasma based accelerator, Plasma wakefield acceleration

## Characterization of laser wakefield accelerated GeV electron beams using a multi-screen method

HOJBOTA Calin Ioan<sup>\*1, 2</sup>, KIM Hyung Taek<sup>\*2, 3</sup>, SHIN Junghun<sup>2</sup>, ANICULAESEI Constantin<sup>2</sup>, RAO Bobbili Sanyasi<sup>2</sup>, HEGELICH Bjorn Manuel<sup>1, 2</sup>, NAM Chang Hee<sup>1, 2</sup>

<sup>1</sup>광주과학기술원, <sup>2</sup>Center for Relativistic Laser Science, IBS, Gwangju, Republic of Korea, <sup>3</sup>Advanced Photonics Research Institute, GIST, Gwangju, Republic of Korea  
calinhojbota@gist.ac.kr, htkim@gist.ac.kr

### Abstract:

During laser wakefield electron acceleration (LWFA), a high intensity laser pulse [1] propagating in a plasma drives a nonlinear wave, which can then be used to accelerate particles to high energies [2,3]. Despite significant progress during the past decades, current electron beams obtained from LWFA are still prone to a significant energy spread, pointing instability and divergence. Shot-to-shot fluctuations in the aforementioned quantities make the characterization of electron beams difficult if conventional methods are used. Novel diagnostic is therefore required in order to draw precise conclusions on the beam parameters.

Our work proposes a new approach for characterizing electron beams obtained from LWFA. We present a setup in which we combine a dipole magnet and multiple scintillating screens. This method, combined with an iterative algorithm, can measure the beam pointing and energy distribution within a single shot. We apply this technique to experimental data obtained at CoReLS, where multi-GeV electron beams are generated from the propagation of a petawatt laser pulse through a cm-scale gas cell. The results obtained show that the proposed method can be used to accurately characterize electron beams from LWFA and significantly improve the single-shot diagnostic used in laser-plasma interactions.

J. H. Sung et al., "4.2 PW, 20 fs Ti:Sapphire laser at 0.1 Hz", *Opt. Lett.*, **42**, 2058 (2017)

H.T. Kim et al., "Stable multi-GeV electron accelerator driven by waveform-controlled PW laser pulses", *Scientific Reports*, **7**, 10203 (2017)

H.T. Kim et al, "Enhancement of Electron Energy to the Multi-GeV Regime by a Dual-Stage Laser-Wakefield Accelerator Pumped by Petawatt Laser Pulses", *Phys. Rev. Lett.*, **111**, 165002 (2013)

### Keywords:

laser wakefield acceleration, electron beam, diagnostic, electron spectrometer

## First limits on the WIMP scattering cross section from the COSINE-100 experiment's first three months of data

하창현\*<sup>1</sup>

<sup>1</sup>기초과학연구원 지하실험연구단  
changhyon.ha@gmail.com

### Abstract:

The COSINE-100 experiment searches for dark-matter interactions using an array of scintillating NaI(Tl) crystals that serve both as a WIMP-interaction target and a nuclear-recoil detector in the low-background environment of the Yangyang underground laboratory. Using the first three months of COSINE-100 data, we performed fits for a possible WIMP signal to energy spectra between 2 and 6 keV with typical background levels of 3~counts/day/kg/keV. Preliminary limits on the WIMP-nucleon cross section based on these fits will be presented.

### Keywords:

Dark Matter, NaI(Tl) scintillator

## The status of AMoRE experiment

김승천\*<sup>1</sup>

<sup>1</sup>기초과학연구원 지하물리실험단  
sckim@ibs.re.kr

### Abstract:

The AMoRE (Advanced Mo based Rare process Experiment) collaboration has been carrying out an experimental search for neutrinoless double beta decay of Mo-100. A pilot version of the project is currently operating with six CaMoO<sub>4</sub> crystals that have a total mass of 1.9 kg and are comprised of enriched Mo-100 and depleted Ca-48 nuclides. Each crystal is equipped with two MMC-based low temperature sensors; one to measure heat and the other light signals. The six crystal modules are installed in a dilution refrigerator that operates at 10 mK at the YangYang underground laboratory. A thorough investigation of the backgrounds is underway and the sources of the main background components have been tentatively identified. AMoRE will continue to operate in the pilot mode and preparations for the next data taking run are nearly complete. A description of the experimental arrangement and its current status will be presented.

### Keywords:

double beta decay, CaMoO<sub>4</sub>, Mo-100, MMC

## The first axion search results in the frequency range between 2.45 and 2.75 GHz

정우현\*<sup>1</sup>, 권오준<sup>1</sup>, 이도유<sup>2</sup>, 김진수<sup>2</sup>, 안단호<sup>2</sup>, KUTLU Caglar<sup>2</sup>, SEMERTZIDIS Yannis<sup>1, 2</sup>  
<sup>1</sup>기초과학연구원 액시온단, <sup>2</sup>한국 과학 기술 연구원  
gnuhcw@ibs.re.kr

### Abstract:

The axion is an excellent dark matter candidate motivated by the Peccei-Quinn solution to the strong-CP problem. The IBS Center for Axion and Precision Physics Research (IBS/CAPP) in Korea has built an infrastructure to search for dark matter axions using the so called “haloscope” method by Sikivie, which measures the excess radiation deposited in a cavity from the conversion of a dark matter axion into a microwave photon in a strong magnetic field. The CAPP’s pilot axion experiment (CAPP-PACE) aiming at the frequency range around 2.5 GHz has already started taking data since the end of 2017 and plans to continue to scan more frequency ranges up to 2.75 GHz, which have not been experimentally explored. I will present the first axion data of CAPP-PACE with an emphasis on the signal processing and R&D for improving the sensitivity.

### Keywords:

axion;cavity;

## A dark matter search with NaI(Tl) crystals by using a pulse shape discrimination analysis

김경원\*<sup>1</sup>

<sup>1</sup>기초과학연구원 지하실험연구단  
kwkim@ibs.re.kr

### Abstract:

The KIMS-NaI is an experiment directly detecting Weakly Interacting Massive Particles (WIMPs) via their weak interactions with nuclei in low-background NaI(Tl) crystals. Underground data for the WIMP search were obtained in the Yangyang underground laboratory, with two NaI(Tl) crystals having high light-outputs. Since scintillation characteristics of nuclear recoil from the WIMP interaction and electron recoil backgrounds are different, it is possible to distinguish the two event types by using a pulse shape discrimination (PSD) method. We measured the pulse shapes produced by neutrons and gamma rays in a test NaI(Tl) crystal that was exposed to a neutron beam from a deuteron-based generator and a gamma-source. Surface nuclear recoil which can be misidentified as a nuclear recoil WIMP candidate event was also investigated and taken into account in the analysis. Preliminary results based on the PSD analysis by using 2967 kg\*days data will be presented in this talk.

### Keywords:

dark matter, WIMP, PSD

## Search for the axion dark matter in the CAPP8TB experiment at IBS/CAPP

AHN Saebyeok\*<sup>1</sup>, CHOI Jihoon<sup>2</sup>, KIM Jongkuk<sup>1</sup>, KO Byeongrok<sup>2</sup>, LEE Soohyng<sup>2</sup>

<sup>1</sup>Department of Physics, Korea Institute of Science and Technology (KAIST), <sup>2</sup>Center for Axion and Precision Physics Research (CAPP), Institute for Basic Science (IBS)  
asb5229@kaist.ac.kr

### Abstract:

The strong CP problem related to the conflicting experimental results on the neutron EDM could be solved by the Peccei-Quinn mechanism. This mechanism invokes a new U(1) symmetry, the breakdown of which creates the axion field. If the axion mass range is below 1 meV, the hypothetical particle can also be a cold dark matter candidate. Its interaction with ordinary matter, other than gravitationally, is extremely weak. Among a variety of methods developed to detect the invisible axion, a microwave haloscope utilizes the Primakoff effect proposed by Sikivie. CAPP8TB is an axion haloscope search experiment with various state-of-the-art techniques such as low noise cryogenic amplifiers and strong magnetic fields that maximize the sensitivity. In this presentation, the axion search experiment dedicated to the axion mass range of 6.62-7.0303  $\mu\text{eV}$  (1.6-1.7 GHz) is described, where the experimental key parameters include a magnetic field of 8 T, a cavity volume of about 3.5 L and a HEMT based system noise temperature of below 2 K. An upgrade plan with quantum-noise-limited superconducting amplifiers is also discussed

### Keywords:

Axion, dark matter

## Searching high mass regions for axion dark matter at IBS/CAPP

정준우<sup>1</sup>, 윤성우\*<sup>2</sup>, 김동락<sup>2</sup>, 김종국<sup>1</sup>, 김진근<sup>2</sup>, 박희준<sup>2</sup>, 유종희<sup>1, 2</sup>, SEMERTZIDIS Yannis K.<sup>1, 2</sup>  
<sup>1</sup>한국과학기술원, 물리학과, <sup>2</sup>기초과학연구원, 액시온 및 극한 상호작용 연구단  
swyoun@ibs.re.kr

### Abstract:

The Center for Axion and Precision Physics Research (CAPP) of the Institute for Basic Science (IBS) has completed the construction of the infrastructure for axion dark matter search experiments. An experiment utilizing a 9 T superconducting magnet with a 127 mm bore placed in a He-3 cryogenic system is currently under preparation. This experiment will explore relatively high mass regions up to 30  $\mu\text{eV}$  by employing a new cavity design known as multiple-cell cavity. We present the status of the experiment and discuss the future prospects.

### Keywords:

axion, dark matter, haloscope, multiple-cell cavity

## First New Physics Probe at the ProtoDUNE Detectors

박종철\*<sup>1</sup>

<sup>1</sup>충남대학교 물리학부  
log1079@gmail.com

### Abstract:

We propose, for the first time, the potential of new physics opportunities at the ProtoDUNE detectors in the context of dark matter physics. More specifically, we explore various experimental signatures at the cosmic frontier, arising in boosted dark matter scenarios, i.e., relativistic, inelastic scattering of boosted dark matter often created by the annihilation of its heavier component which usually comprises of the dominant relic abundance. Although signal features are unique enough to isolate signal events from potential backgrounds, vetoing a vast amount of cosmic background is rather challenging as the detectors are located on the ground. We argue, with a careful estimate, that such backgrounds nevertheless can be well under control via performing dedicated analyses after data acquisition. We then discuss some phenomenological studies which can be achieved with ProtoDUNE, employing a dark photon scenario as our benchmark dark-sector model.

### Keywords:

Dark matter, ProtoDUNE, Boosted dark matter, Cosmic background

## Search for PeV-scale dark matter from the High-energy neutrino and gamma-ray observation

박성찬\*<sup>1</sup>, 조용수<sup>1</sup>

<sup>1</sup>연세대학교 물리학과  
seongchan.park@gmail.com

### Abstract:

We explore the essential features from the decay of PeV-scale dark matter. From the observation of PeV neutrinos in the IceCube and the gamma-ray constraints from the Fermi-LAT observation, the heavy dark matter might be neutrino-phillic and hadro-phobic in its decay. We investigate the detail by using a seesaw-inspired RH-neutrino portal model as an example of the five-dimensional operator and the generic effective field theory approach in other higher-dimensional operators. The future prospects of the detection at the IceCube-Gen2 and HAWC, CTA gamma-ray observatories are also discussed.

### Keywords:

PeV-scale dark matter, Superheavy dark matter, PeV neutrinos, IceCube, Fermi-LAT, HAWC, CTA, seesaw model, neutrino portal, effective field theory

## Dark Matter Direct Detection with Spin-2 Mediators

이현민\*<sup>1</sup>, 강유진<sup>1</sup>, 박명훈<sup>2</sup>, CARRILLO-MONTEVERDE Alba<sup>3</sup>, SANZ Veronica<sup>3</sup>  
<sup>1</sup>중앙대학교 물리학과, <sup>2</sup>서울과학기술대학교 기초교육학부, <sup>3</sup>Department of Physics and Astronomy,  
University of Sussex  
hminlee@cau.ac.kr

### Abstract:

We consider a massive spin-2 mediator that couples to dark matter and the SM particles through the energy-momentum tensor. We identify the effective interactions between dark matter and the SM quarks with mediator integrated out and match them to the gravitational form factors for nucleons. Then, we show the non-relativistic operators between dark matter and nucleons. Finally, we discuss the interplay between relic density conditions, direct detection bounds and dijet resonance searches for the spin-2 mediator.

### Keywords:

dark matter, spin-2 mediator, direct detection

## Tension-free $H_0$ from evanescent dark energy

VAN PUTTEN Maurice\*<sup>1</sup>

<sup>1</sup>Physics and Astronomy, Sejong University  
mvp@sejong.ac.kr

### Abstract:

We derive a stress-energy tensor for dark energy and dark matter in the cosmological vacuum from evanescence across the cosmological horizon. A detailed confrontation with data on the Hubble parameter  $H(z)$  over an extended range of redshift  $z$  gives  $H_0=74.26$  (pm 2.6), consistent with Anderson & Riess (2017) and Guidorzi et al.(2017) from GW170817. It derives from  $\Lambda = \omega_0^2$ , where  $\omega_0 = (1-q)^{(1/2)}H$  is the fundamental frequency of the cosmological horizon, where  $q$  is the deceleration parameter. Further observational consequences of the cosmological horizon are found in CO galaxy dynamics, in a confrontation of numerical galaxy models in  $\Lambda$ CDM and SPARC data. (Based on van Putten, 2017, ApJ, 848, 28; ApJ 837, 22.)

### Keywords:

Dark energy, galaxy dynamics

## f(R) inflation models

이석천\*<sup>1</sup>

<sup>1</sup>경상대학교 기초과학연구소  
skylee2@gmail.com

### Abstract:

After we briefly overview the Starobinsky inflation model, we also review the several modifications of that model based on both theoretical and observational reason. These modification are known to be very limited in order to be consistent with observations. We investigate possible extension of model from phenomenological aspects.

### Keywords:

f(R)-gravity, inflation.

## Small-scale Features of Thermal Inflation: CMB Distortion, Substructure Abundance, and 21cm Power Spectrum

홍성욱\*<sup>1</sup>, 조희승<sup>2</sup>, 안경진<sup>3</sup>, STEWART Ewan<sup>4</sup>

<sup>1</sup>한국천문연구원 대형망원경사업단 과학연구그룹, <sup>2</sup>대구경북과학기술원 융복합대학기초학부, <sup>3</sup>조선대학교 지구과학교육과, <sup>4</sup>한국과학기술원 물리학과  
swhong@kasi.re.kr

### Abstract:

Thermal inflation is an additional inflationary mechanism before the big bang nucleosynthesis, which solves the moduli problem and naturally provides a plausible dark matter candidate. Thermal inflation leaves a slight enhancement followed by huge suppression of a factor of  $\sim 50$  in the curvature and matter power spectrum, which can be expressed in terms of a single characteristic scale  $k_b$ . Here we describe the observability from various observations, such as CMB distortion, satellite galaxy abundance in the Milky-Way-sized galaxies, and 21-cm power spectrum before the epoch of reionization.

### Keywords:

Thermal Inflation, CMB Distortion, Satellite Galaxy Abundance, 21cm Power Spectrum

## Cosmological Horizons and Particle Horizons for Wormhole Cosmology

김성원\*<sup>1</sup>

<sup>1</sup>이화여자대학교 과학교육과  
sungwon@ewha.ac.kr

### Abstract:

Recently we got the exact solution of the cosmological model from the isotropic form of the Morris-Thorne type wormhole. By solving the Einstein's field equation, we found the exact solution of a wormhole in expanding Friedmann-Lemaître-Robertson-Walker universe. In this paper we examine the dynamic properties of apparent horizons depending on the distribution of cosmic matter. The matter-, radiation-, and lambda-dominated universes are considered for single component universe. For the multi-component universe case, we adopt the universe with matter and lambda. Two apparent horizons exist at late times in matter-dominated universe and radiation-dominated universe, while they exist only at very early times in lambda-dominated universe. When we consider the matter- and lambda-dominated universe, the apparent horizons coincide at a certain time. The particle horizon is also discussed on what is happening for the case of with wormhole.

The particle horizon with wormhole shows the elimination of wormhole region and that without wormhole starts later than that with wormhole in proper distance coordinate. The past light cones with or without wormhole shows the similar natures to the particle horizon.

### Keywords:

wormhole, cosmology, cosmological horizon, particle horizon

## Negative Mass in AdS Space

김경규\*<sup>1</sup>

<sup>1</sup>세종대학교 물리학과  
kimkyungkiu@gmail.com

### Abstract:

We consider black brane solutions with negative mass in AdS spacetime. These can be dual geometries to a hydrodynamics with effective negative mass. We discuss thermodynamics and fluid/gravity correspondence for the black branes.

### Keywords:

Negative Mass in Gravity, Black hole, Gauge/gravity correspondence

## Primordial Gravitational Waves in Gauss-Bonnet inflation

고석태\*<sup>1</sup>, GANSUKH Tumurtushaa<sup>2</sup>

<sup>1</sup>제주대학교 과학교육학부 물리교육전공, <sup>2</sup>CTPU, IBS  
kundol.koh@jejunu.ac.kr

### Abstract:

We investigate the primordial gravitational wave in a single field driven inflationary model in which a scalar field is coupled to Gauss-Bonnet term. Gauss-Bonnet inflation is classified into two types based on their predictions of the inflationary tensor power spectrum: blue-tilted ( $n_T > 0$ ) or red-tilted ( $n_T < 0$ ) type, respectively. The energy spectra of the primordial gravitational waves are calculated for both types and the distinctive features are shown in the frequency ranges of 0.1 ~ 1 Hz for the blue-tilted type models.

### Keywords:

Primordial Gravitational waves, Gauss-Bonnet, inflation, reheating

## Exact Amplitudes for Six Polarization Modes of Massive Gravitational Waves

현영환\*<sup>1</sup>, 김윤배<sup>1</sup>, 이석천<sup>2</sup>

<sup>1</sup>성균관대학교 물리학과, <sup>2</sup>경상대학교 기초과학연구소  
yhhyun@skku.edu

### Abstract:

The six polarization modes were investigated by Eardley et al. in 1973. In the first classification of the extended general relativity theories based on these polarization modes was based on the Newman-Penrose formalism and the weak, plane, and null propagating assumptions. Recently, it is suggested that the calculation of the polarization amplitude for the massive propagations in terms of the Newman-Penrose scalars is not exact. In this work, we calculate the exact amplitude for the gravitational waves which propagate along the non-null geodesic.

### Keywords:

polarization mode, gravitational wave

## Determining Unsafety Channels in Interferometric Gravitational-Wave Telescope

정필중\*<sup>1</sup>

<sup>1</sup>광주과학기술원 물리광학과  
scilavinka.pj@gist.ac.kr

### Abstract:

The two black holes create a vivacious tone, the accent of a supernova explosion and the pulsation of a new neutron star at the center. Spreading calmly into the universe through space-time, Humanity can now hear a huge symphony of the cosmos. New ears to hear this symphony are laser interferometer gravitational-wave telescopes such as LIGO, Virgo, GEO, and KAGRA. However, since the signal of gravitational-wave is very weak, these telescopes cannot detect purely gravitational-wave signals. Because the mechanical defects that the equipment has, the artificial noises outside and the effects of the noises of the earth are all observed. Therefore, it is important to identify and distinguish the causes of these noises and determine the actual gravitational-wave signal. Among them, the preceding task is to determine the unsafety channels among the many auxiliary channels in the interferometer. unsafety channel study is to diagnose the safety of channels by analyzing the correlation between the gravitational-wave channel and the auxiliary channels. In this way, a standard method called hierarchical-veto (hveto) is used. In this report, the reason and the specific methodology for determining unsafety channels in the laser interferometer gravitational-wave telescope will be reviewed.

### Keywords:

Gravitational Wave, Data Analysis, hierarchical-veto, Channel Safety Study

## Impact of Neutron Star Merger vs. Supernova on Explosive Nucleosynthesis and Neutrino Oscillation

KAJINO Toshitaka\*<sup>1</sup>

<sup>1</sup>National Astronomical Observatory of Japan, The University of Tokyo, Beihang University, International Research Center for Big-Bang Cosmology and Element Genesis  
kajino@nao.ac.jp

### Abstract:

GW170817 was an event of the century that has opened the window to the frontier of multi-messenger astronomy and astrophysics. Gravitational waves from most likely the merging neutron stars were detected by LIGO-Virgo collaboration, and GRB was observed in Fermi-GBM. Although none the emission line from specific r-process elements were detected, total energy in observed optical and near-infrared emissions is consistent with radiative decays of r-process nuclei which are predicted theoretically. Neutrinos were not detected because of their too low flux from GW170817 that occurred at a distance 0.13 Gly away. We now await a nearby GW event (probably once per ten thousand years in our Milky Way) for spectroscopic observation of still unidentified r-process elements from neutron star mergers (NSMs). Core-collapse supernovae (of both magneto-hydrodynamic jet supernovae; MHD Jet-SNe, and neutrino-driven wind supernovae; v-SNe) are viable candidates for the r-process sites. NSMs could not contribute to the early Galaxy for cosmologically long merging time-scale for slow GW radiation, while MHD Jet-SNe can explain the "universality" in the observed abundance pattern in metal poor stars. Nevertheless, NSM like GW170817 is a possible nucleosynthetic site for the solar-system r-process abundance. We would like to propose a novel solution to this twisted problem by carrying out both NSM and SN r-process nucleosynthesis calculations and SPH N-body numerical simulation of Galactic chemo-dynamical evolution. We will also discuss the impact of the SN nucleosynthesis on the physics of neutrino oscillations including MSW matter effect and self-interacting collective and oscillations.

### Keywords:

Neutron Star Merger, Supernova

## Production of Nuclei in Type II Supernova via Neutrino-process

KUSAKABE Motohiko\*<sup>1</sup>

<sup>1</sup>Beihang University, International Research Center for Big-Bang Cosmology and Element Genesis, Japan  
kusakabe@buaa.edu.cn

### Abstract:

Several stable nuclei in the Solar system partially originate from supernova (SN) nucleosynthesis. They include light nuclei,  ${}^7\text{Li}$  and  ${}^{11}\text{B}$ , and heavy p-nuclei,  ${}^{138}\text{La}$  and  ${}^{180}\text{Ta}$ . Also, neutrino reactions on the s-nuclei during SNe produce short-lived nuclei the existence of which can be kept in primitive meteorites. It has been pointed out that the ratio of yields,  ${}^7\text{Li}/{}^{11}\text{B}$ , depends upon the hierarchy type of neutrino mass. The neutrino oscillation in SNe is affected by electrons and neutrinos. Therefore, yields of the neutrino process can depend on stellar and explosion models as well as initial neutrino spectra at the neutrino sphere. In this talk, we show results for calculations of SN nucleosynthesis with the oscillation and reactions of neutrinos taken into account. New initial abundances for s-nuclei are adopted, and their impacts are analyzed.

### Keywords:

Type II Supernova, Neutrino-process

## Constraining Nuclear Equation of State with Coalescing Neutron Stars

HYUN Chang Ho\*<sup>1</sup>

<sup>1</sup>Daegu University  
hch@daegu.ac.kr

### Abstract:

Measurement of gravitational wave (GW170817), gamma-ray burst (GRB 170817A), and subsequent electromagnetic signals (AT2017gfo) identified the observation of two neutron star merge for the first time in human history. Analysis of phase evolution of gravitational waves and simulation of post-merge remnants with UV/optical/IR information from observation provide a range for the dimensionless tidal deformability  $400 \leq \tilde{\Lambda} \leq 800$ . The range establishes strong constraints to the nuclear equation of state that is applicable at supra-saturation densities. In order to obtain a theoretical prediction for the range of  $\tilde{\Lambda}$ , we perform calculations with nuclear energy density functionals that are constrained by available data of nuclei, nuclear matter around the saturation, and the maximum mass of neutron stars. We obtain a range of  $370 \leq \tilde{\Lambda} \leq 700$  for the tidal deformability, and  $11.8 \text{ km} \leq R \leq 12.8 \text{ km}$  for the radius of a  $1.4 M_{\odot}$  neutron star.

### Keywords:

Constraining Nuclear Equation of State with Coalescing Neutron Stars

## Ultrafast optical studies of valley pseudospin in transition metal dichalcogenide heterostructures

김종환\*<sup>1</sup>

<sup>1</sup>포항공과대학교 신소재공학과  
jonghwankim@postech.ac.kr

### Abstract:

The valley degree of freedom in 2D transition metal dichalcogenides (TMD) recently emerged as a novel information carrier in addition to spin and charge. In particular, the intrinsic valley lifetime of holes is expected to be remarkably long due to the unique spin-valley locking behavior. However, the formation of exciton in monolayers under the light illumination drastically limits valley lifetime via exchange interaction. Here, we demonstrate that van der Waals heterostructures of TMD provides an excellent valley electronics platform where valley polarization of holes exhibits long lifetime and large magnitude. Ultrafast charge transfer process in heterostructures breaks intralayer excitons and effectively disables its exchange interaction. Pump-probe spectroscopy reveals more than microsecond and near-unity valley polarization of holes in TMD heterostructures. Furthermore, spin and valley current can generate and propagate more than 20  $\mu\text{m}$  for the hole doping case. Our ultrafast optical studies reveal promising potential of valley electronic states in TMD monolayers for novel valleytronics and spintronics applications.

### Keywords:

Valley pseudospin, TMD, 2D materials, valley electronics

## Room-temperature manipulation of valley-locked spin-photocurrent in $WSe_2$ -graphene-topological insulator heterostructures

최현용\*<sup>1</sup>, 차순영<sup>1</sup>, 노민지<sup>1</sup>, 김제현<sup>2</sup>, 손장엽<sup>2, 3</sup>, 배혜민<sup>1</sup>, 이도연<sup>1</sup>, 김호일<sup>4, 5</sup>, 이제관<sup>1</sup>, 심상완<sup>1</sup>, 신호승<sup>1</sup>, 양승훈<sup>6</sup>, 이철호<sup>6</sup>, 조문호<sup>5, 7</sup>, 김성준<sup>4, 5</sup>, 김도현<sup>2</sup>

<sup>1</sup>School of Electrical and Electronic Engineering, Yonsei University, <sup>2</sup>Department of Physics and Astronomy, Seoul National University, <sup>3</sup>Department of Mechanical Science and Engineering, University of Illinois at Urbana-Champaign, <sup>4</sup>Department of Physics, Pohang University of Science and Technology (POSTECH), <sup>5</sup>Center for Artificial Low Dimensional Electronic Systems, Institute for Basic Science (IBS), <sup>6</sup>KU-KIST Graduate School of Converging Science and Technology, Korea University, <sup>7</sup>Department of Materials Science and Engineering, Pohang University of Science and Technology (POSTECH)  
hychoi@yonsei.ac.kr

### Abstract:

Manipulating multiple degree of freedom (DoF) in condensed matter systems is at the heart of growing fields in modern information technology. Other than charge DoF, recent attentions on spin and valley DoF in atomically thin two-dimensional materials have shown great potentials in using the two DoFs for novel device applications; yet numerous researches have confirmed that selective manipulation of the two DoF is very challenging due to the inherent valley-spin coupling. Here, we report the optoelectronic manipulation and selective detection of valley-locked spin-polarized electrons using lateral heterostructure devices of  $WSe_2$ -graphene-topological insulator. Our approach is first to optically generate the valley-spin coupled DoF at electrically modulated  $WSe_2$  transistors. To achieve complete electronic-transport functionality, we use graphene as a spin diffusion channel. After the valley-locked spin-polarized electrons diffuse along the graphene, the characteristic spin-momentum locking of topological insulator is used as an electrical readout of the spin DoF, exclusively. Our *non-local* optoelectronic measurement quantitatively determines the spin polarizability over the entire lateral direction, reaching over 50 % even without using spin-tunneling barriers. Operating at room temperature, our device may open up a new research arena toward practical "opto-spin-valleytronic" device applications.

### Keywords:

Valleytronics, transition metal dichalcogenides, topological insulator, spintronics



## Electrical and mechanical control of valley polarization in MoS<sub>2</sub>

이지은\*<sup>1</sup>

<sup>1</sup>아주대학교 물리학과  
jieuntb@gmail.com

### Abstract:

Two-dimensional honeycomb lattices with broken inversion symmetry exhibit unique valley degree of freedom (DOF) of electrons as recently shown in gapped graphene and transition metal dichalcogenides. The electrical control of valley DOF in these materials allows fast and local manipulation of valley polarization necessary for the development of valleytronic devices on chip. In this talk, we describe methods to electrically control valley polarization in MoS<sub>2</sub> including the valley Hall effect and valley magnetoelectricity. We also present our recent results on mechanical control of valley polarization in flexible MoS<sub>2</sub> transistors driven by Berry curvature effects.

### Keywords:

Valley, Electrical control, Flexible device, Transition metal dichalcogenides

## Charge and Spin-Valley Transfer in Transition Metal Dichalcogenides Heterostructure

KIM Suk Hyun\*<sup>1</sup>

<sup>1</sup>Stanford University  
skim17@stanford.edu

### Abstract:

Monolayer transition metal dichalcogenides (TMDC) offer new avenues to control valley and spin polarization based on their valley circular dichroism and spin-valley locking. In this context, interesting issues arise when two TMDC layers are stacked in a vertical heterostructure and interlayer charge transfer processes become possible.

Recently there was a report that a charge transfer in MoSe<sub>2</sub>-WSe<sub>2</sub> heterostructure is carrying not only charge itself but also spin valley information over the layers, observed by polarization sensitive CW laser pump probe spectroscopy at the temperature 30 K. However the experiments were bound to steady state observation and giving access only to the lower spin conduction band of electron receptor material MoSe<sub>2</sub>, required testing a number of heterobilayer samples with different relative crystallographic orientations to compare the degree of information conservation in spin and valley.

In our study, we investigate the spin-valley characteristics of charge transfer in MoS<sub>2</sub>-WSe<sub>2</sub> heterostructure with similar technique as previous study, utilizing ultrafast pump probe spectroscopy in room temperature. In particular, when we excite the A exciton in WSe<sub>2</sub> with circularly polarized ultrafast pump radiation, we observed circular dichroism of probe pulse for both the A and B excitonic transitions in MoS<sub>2</sub>. We confirmed that spin valley transfer happens even in room temperature as well, decays in few picosecond time scale. By comparing the A and B excitonic signal, we could conclude that spin information is only conserved while valley is lost.

### Keywords:

Valleytronics, TMDC, MoS<sub>2</sub>, WSe<sub>2</sub>, Heterostructure

## 화합물 반도체 (30+30)년 - 우리나라 반도체의 역사, 故정중현 선생을 회고하며

노삼균\*<sup>1</sup>

<sup>1</sup>동국대학교 물리반도체과학부  
samkyunoh52@gmail.com

### Abstract:

제3·4차 산업혁명의 원동력인 반도체는 '기술'과 '물리학'이라는 2개의 상호보완적 축을 가지고 발전해 왔으며, 크게 실리콘(silicon, Si) 계와 비실리콘(non-Si) 계로 나눌 수 있다. Si 계가 원시 트랜지스터에서 출발하여 현대 초고집적-초미세 소자에 이르기까지 반도체의 '기술을 주도 (technology-drive)'해 온 반면, non-Si 계의 대명사인 화합물반도체는 이종접합에서 발견된 저차원계 고유의 물리현상의 탐구와 이에 기초한 양자소자의 구현을 통하여 반도체의 '물리학을 선도 (physics-drive)'해 왔다. 즉, Si이 반도체 기반의 현대 기술산업을 창출한 주역이라면, 화합물반도체는 새로운 물리학 분야를 선도한 개척자로 평가할 수 있다.

Si 기반의 반도체 기술과 산업이 그 거대한 몸통을 드러낸 때는 집적회로(IC)의 고밀도화 전쟁이 시작된 1970년 초인데, 우리나라가 반도체 산업에 본격적으로 뛰어든 때는 35년 전 삼성반도체통신(삼성전자의 전신)이 64-kb DRAM 개발을 시작한 1983년이다. 한편, non-Si 반도체를 대표하는 III-V족 화합물반도체 (GaAs, InP 등) 연구개발은 1970-80년대에 비약적으로 발전한 반도체 에피텍셀 성장기술과 그 맥을 같이 하는데, 1970년대는 발광소자 (LED, LD)의 성공과 함께 양자우물(QW), 초격자(SL) 등 이종구조가 실현된 시기이고, 1980년대는 LD 광원과 광섬유의 실용화로 현재의 초고속 인터넷을 가능하게 한 광통신시스템이 그 모습을 드러내기 시작한 때이다. 특히, 1990년대 전후에 고조된 화합물 반도체 기반의 QW/SL 및 양자선/양자점(QWi/QD) 저차원구조 연구는 CNT와 Graphene과 같은 새로운 1D/2D 물질계의 발견을 촉발시켰으며, 응집물질 분야뿐만 아니라 생명과학 분야에까지 '나노nano'로 대변되는 저차원 개념을 확산시키는 선구자적 역할을 하였다.

1980년경부터 전성기를 맞이했던 "화합물 반도체 30년"은 초기 기억/연산 IC가 컴퓨터·광통신-핸드폰·인터넷으로 발전한 '격변의 과학기술 시대'와 일치하는데, 오늘 강연에서는 한국물리학회 반도체물리학회 창립 4반세기 (1993년 응집물질물리학회에서 분립)에 즈음하여 우리나라 반도체 제1세대를 대표하는 故정중현선생 (초대 분과회장, 2016년 12월 향년 91세로 타계)의 초창기 30년간의 발자취를 돌아보고, 이후 최근 30년간 필자가 수행한 화합물반도체 관련 연구개발 주제를 간략히 소개하고자 한다.

### Keywords:

화합물반도체, 저차원계, 양자우물, 초격자, 양자선, 양자점

## Mitigating charge noise in exchange gate operations between spin qubits

SHIM Yun-Pil\*<sup>1, 2</sup>

<sup>1</sup>Laboratory for Physical Sciences, College Park, <sup>2</sup>University of Maryland, College Park  
ypshim@lps.umd.edu

### Abstract:

Spin qubits in semiconductor quantum dots (QDs) are one of the leading candidates for implementation of quantum computing devices, mainly due to their long coherence times, scalability, and compatibility with existing semiconductor technology. Exchange interactions between spins provide a fast and efficient way of controlling spin-spin interactions and two-qubit gate operations. While electrical control of the spin degree of freedom is promising, the exchange interaction reintroduces charge noise to the spin system.

Recent experiments showed that optimizing the control of exchange interaction can significantly improve the coherence of the operations; they make use of the symmetric operation, which directly controls the tunnel barrier at a sweet spot where the exchange interaction is insensitive to fluctuations in the detuning between QD energy levels up to the first order. This is in contrast to the conventional method of exchange control by tilting the QD energy levels in the detuning regime.

We provide a theoretical study on these two different types of exchange control operations between localized spins - barrier or tilt control. We use two different theoretical models: Hubbard model and confining potential model. The Hubbard model is a very simple and intuitive model with parameters for the QD orbital energies, tunneling, and direct Coulomb interactions. But it is not clear a priori how the parameters in the Hubbard model are affected by charge noise, and it is not straightforward to connect parameters of the Hubbard model with experimental voltage controls on metallic gates used for defining QDs and control electric signals.

A more general theoretical framework is necessary and for this we use a microscopic confining-potential model where each QD is defined by its confining potential and the barrier potential between QDs. Particularly, barrier vs tilt control of the exchange interaction are systematically studied showing that the insensitivity on the gate charge noise for barrier control in symmetric regime can potentially lead to efficient implementation of quantum gates with higher fidelities than the conventional tilting gates in the detuning regime.

### Keywords:

Quantum dot, spin qubit, charge noise, exchange interaction, quantum computing, quantum gate

## Realization of a universal quantum gate set and demonstration of a simple algorithm in two superconducting transmon circuit QED system

CHONG Yunuk\*<sup>1</sup>, NOH Taewan<sup>1</sup>

<sup>1</sup>Korea Research Institute of Standards and Science  
yonuk@kriss.re.kr

### Abstract:

We present a realization of the controlled-NOT (cNOT) gate in two transmon circuit QED system based on all-microwave controlled entangling gate. We adopted the microwave-activated phase (MAP) gate for entanglement generation and the Z-axis phase gate based on hyperbolic secant microwave pulse to compensate accumulated unwanted phases. We performed quantum process tomography (QPT) to estimate the process fidelity and will show the results. Having a universal set of quantum gates, we present a demonstration of Deutsch-Josza algorithm in our two-qubit system. This research was supported by the R&D Convergence Program of NST (National Research Council of Science and Technology) of Republic of Korea (Grant No. CAP-15-08-KRISS).

### Keywords:

superconducting qubit, circuit QED, cNOT gate, Deutsch-Josza algorithm

## Coherent quantum control and magnetism on atoms on surfaces

최 (Choi)태영 (Taeyoung)\*<sup>1, 2</sup>

<sup>1</sup>양자나노과학연구소 (Quantum Nanoscience), 기초과학연구원 (IBS), <sup>2</sup>이화여자대학교 (Ewha Womans University), 물리학과 (Department of Physics)  
tchoi@ewha.ac.kr

### Abstract:

Magnetometry having both high magnetic field sensitivity (energy resolution) and nanoscale spatial resolution has been of great interest and an important goal for applications in diverse fields covering physics, chemistry, material science, and biomedical science. The scanning tunneling microscope (STM) has been one of the most versatile tools for atomic-scale imaging, manipulation, and tunneling spectroscopy.

Here, we successfully combine electron spin resonance (ESR) and STM, coherently driving spin resonance of individual iron (Fe) atoms on surfaces (MgO/Ag(100)). A radio-frequency electric field (~20 GHz), applied at the tunneling junction, modulates the spin state of the Fe atoms. The spin resonance signal is detected by a spin-polarized tunneling current. The ESR signals from individual Fe atoms differ by a few GHz (~10  $\mu$ eV) while the ESR linewidth is in the range of only a few MHz (~10 neV). Such a high energy resolution enables us to distinguish spin distributions down to single-atom level and to investigate weak magnetic interactions.

When we placed two Fe atoms close together with controlled atom manipulation, we found that the ESR signal from each Fe atom splits into doublet, of which separation depends on the distance between two atoms. Our measurements show  $r^{-3.024 \pm 0.026}$  distance-dependent splitting, in excellent agreement of magnetic dipole-dipole interaction. We utilized this precisely measured dipolar interaction to determine the location and magnetic moment of unknown spin centers with sub-angstrom and one hundredth of Bohr magneton precision.

Our ESR-STM may promise the STM as a new and unique platform for a quantum sensor, investigating spin-labeled molecular structures and a quantum information processor, modeling quantum magnetism.

### Keywords:

Scanning tunneling microscopy, spectroscopy, electron spin resonance, magnetic dipolar interaction, quantum sensing

## Spin dynamics of Ho single atom magnets

DONATI Fabio\*<sup>1, 2</sup>

<sup>1</sup>양자나노과학연구소 (Quantum Nanoscience), 기초과학연구원 (IBS), <sup>2</sup>이화여자대학교 (Ewha Womans University), 물리학과 (Department of Physics)  
donati.fabio@qns.science

### Abstract:

Atomic-scale magnets with long magnetic lifetimes represent the smallest unit of matter that can be used to store and manipulate information. Understanding their properties is the key to reach the ultimate downscaling of magnetic memories. The main requirement of a magnetic bit is to retain a net magnetization in absence of magnetic field on a long timescale. The fingerprint of this feature is the remanence in magnetic hysteresis loops.

Electron spins in single atoms on surfaces can be addressed both with ensemble-averaging X-ray spectroscopies and with scanning probe techniques. The latter allows the control and manipulation of individual spins with atomic precision. These techniques have been used to pioneer the magnetism of single rare earth atoms on surfaces [Myamachi et al., Nature **503**, 242 (2013); Donati et al., Phys. Rev. Lett. **113**, 237201 (2014)]. Due to the strong localization of the 4f electrons, the spins of these atoms weakly interact with the environment and can have magnetic lifetimes of the order of thousands of seconds at 2.5 K [Donati et al, Science **352**, 318 (2016); Baltic et al, Nano Lett. **16**, 7610 (2016)]. The possibility of reading and writing their magnetic states at the atomic scale demonstrated the potential of these atoms as magnetic bits [Natterer et al., Nature **543**, 226 (2017)].

In this presentation, I will describe the recent advances in the field that led to the discovery of magnetic remanence in Ho atoms on MgO/Ag(100). Using X-ray magnetic circular dichroism, we demonstrated that these atoms exhibit magnetic lifetimes on the timescale of thousands of seconds at 2.5 K. These features qualify them as the first single atom magnets. Remarkably, they exhibit an exceptional magnetic stability up to 30 K [Donati et al, Science **352**, 318 (2016)]. Using scanning tunneling microscopy in high magnetic fields, we identify the threshold of their spontaneous magnetic relaxation at about 45 K, where we observe spin fluctuations on the time scale of tens of seconds [Natterer et al, arXiv:1712.07871]. Finally, I will discuss the present understanding about the magnetic behavior of Ho atoms and the general principles for designing novel single atom magnets with magnetic stability at even higher temperatures.

### Keywords:

X-ray absorption spectroscopy, X-ray magnetic circular dichroism, scanning tunneling microscopy, single atom magnets, magnetic lifetimes, rare earth atoms.

## A Study on the Radiation Damage of Tumor Cell in BNCT

LIU Dong\*<sup>1</sup>, WOO Jong-Kwan\*<sup>1</sup>

<sup>1</sup>제주대학교 물리학과

LIUDONGCN@jejunu.ac.kr, w00jk@jejunu.ac.kr

### Abstract:

The dose distribution of emitters in subcellular level is one of the most important influences to evaluate the treatment effects and side effects in Boron Neutron Capture Therapy (BNCT). In order to analyze and evaluate the characteristics of dose distribution and influence factors that affect the dose distribution in tumor cell, in this study we defined an improved tumor cell model and summarized 6 interaction models for emitters and tumor cellular materials. The interaction processes are simulated using two kinds of Monte Carlo programs, SRIM and GEANT4. By analyzing the simulation results, we concluded the distribution of ionizing energy in the nucleus region of tumor cells is effected by the type of reactions, the type of emitted ions and the microdistribution of boron atoms. Finally, we found that the microdistribution of boron atoms is a potentially manageable factor that influences the distribution of ionizing energy in tumor cell. Therefore, the results are beneficial to describe the distribution characteristics of emitted ions, and have potentially guiding significant for the development of boron delivery agents.

### Keywords:

Boron Neutron Capture Therapy (BNCT), Radiation Damage, Monte Carlo simulation

## High-sensitivity chip calorimeter based on parylene microfluidics for measurements of cellular metabolic rate

김지혜<sup>1</sup>, 남성민<sup>1</sup>, 김종현<sup>1</sup>, 서수민<sup>1</sup>, 이원희\*<sup>1, 2</sup>

<sup>1</sup>한국과학기술원 나노과학기술대학원, <sup>2</sup>한국과학기술원 물리학과  
whlee153@kaist.ac.kr

### Abstract:

Calorimetry can provide universal cell-based assay methods by measuring the heat flux, which is proportional to cellular metabolic rate that is an excellent indicator of physiological state and its changes. Any changes in the environment, nutrient states or external stimuli are reflected in the metabolic status of the living cells, which is directly monitored by the calorimetric assay. A chip calorimeter is a promising tool for measuring cellular metabolic rate in a high-throughput manner. However, it was difficult to achieve both high sensitivity and capability of handling cells on a chip. We developed a highly sensitive chip calorimeter for measurement of cellular metabolic rate changes; the thin film parylene microfluidics (~ 10  $\mu\text{m}$  thickness) providing minimal device heat capacity and the on-chip vacuum chamber for the best possible insulation.

The developed parylene-based microfluidic chip calorimeter has two major improvements: vanadium pentoxide thermistor with a high temperature coefficient (~ - 3 %/K) is integrated, and parylene microfluidics is enabled by newly developed molding and bonding technique. Bonding of parylene layers with the nano-adhesive layer deposited by initiated-CVD allowed fast fabrication of parylene microfluidics with minimal limitations in channel design such as channel length and height, which provided better thermal insulation and on-chip control of fluids and cells. The chip calorimeter has an excellent power resolution of a few nW and a temperature resolution better than  $10^{-4}$  K. We demonstrated cellular metabolic rate measurements by monitoring the changes of heat production from a-few-hundred cells responding to controlled stimuli. The developed chip calorimeter is expected to provide unique tools for cell based assay in the fields such as drug discovery and cellular toxicity tests.

### Keywords:

Microfluidic chip calorimeter, Parylene microfluidics, Vanadium oxide, Metabolic rate

## Inertial focusing in triangular channel under various parameters

김정아<sup>1</sup>, 이재령<sup>3</sup>, 전은채<sup>3</sup>, 이원희\*<sup>1, 2</sup>

<sup>1</sup>한국과학기술원 나노과학기술대학원, <sup>2</sup>한국과학기술원 물리학과, <sup>3</sup>한국기계연구원 나노융합기계연구본부  
whlee153@kaist.ac.kr

### Abstract:

Microchannel flows of particle suspension with finite-Reynolds number display inertial focusing, that is, particles focus at equilibrium positions by the balance of the inertial lift forces. Inertial focusing provides passive and high-throughput manipulation methods of cells or particles in a microchannel. In previous studies, we investigated inertial focusing in triangular channels and observed various unique phenomena which could not be found in typical rectangular channels, including shift of top focusing positions and alteration of focusing configuration in accordance with  $Re$  and  $a/H$  ( $a$  = particle diameter,  $H$  = hydraulic diameter). We studied inertial focusing in triangular channels more in detail by varying channel cross-sectional shapes: vertex angle ( $45^\circ$ ,  $60^\circ$ ,  $90^\circ$ ,  $120^\circ$ ), dimension (channel height 20-130  $\mu\text{m}$ ) were changed while regulating  $Re$  from 20 to 120. Equilateral triangular channels do not show large transition depending on changes of parameters because of  $120^\circ$  rotational symmetry. In case of acute triangular channels, two focusing positions which are located near each side wall (similar with high-aspect ratio rectangular channel) become three focusing positions as  $Re$  is increased or  $a/H$  is decreased. In case of obtuse triangular channels, two focusing positions that are located in top and bottom of the channel become three as  $Re$  is increased or  $a/H$  is decreased. The total number of focusing positions in  $120^\circ$  triangular channels increases up to five when  $Re$  is increased and  $a/H$  is decreased. In addition to transition of focusing configuration, the acute triangular and obtuse triangular channels show opposite direction of top focusing position shift as  $Re$  is increased.

### Keywords:

Inertial focusing, Triangular microchannel, Hydrodynamic Particle manipulation

## 중학교 영재학생들의 여러 가지 운동 상황에 대한 그래프 변환활동에서 나타나는 오류

김성원\*<sup>1</sup>, 최연정<sup>2</sup>

<sup>1</sup>이화여자대학교 과학교육과, <sup>2</sup>풍산고등학교  
sungwon@ewha.ac.kr

### Abstract:

본 연구에서는 학생들이 그래프 전환 과정에서 경험하는 오류의 유형을 확인하기 위하여 경기도 소재 중학교 2학년 영재학급 20명을 대상으로 하여 10차시 수업을 통하여 그래프 작성 및 해석 활동을 진행하였다. 학생 활동은 교과서 분석에 활용된 여러 가지 운동과 관련된 활동으로 1차 그래프 변환 활동과 2차 그래프 변환 활동으로 구성되어 있다. 각 활동에 활용된 활동지와 질문지를 수집하였고 필요한 경우 활동지에 대한 심층 면담을 진행하였다.

연구 결과, 첫째, 교과서 분석에서 나타난 그래프 작성 및 해석활동은 그래프의 해석 활동이 비교적 더 많은 비중을 차지하고 있으며 그래프 활동 수준에 있어서는 축의 눈금까지 안내하는 경우가 가장 많았다. 또한 그래프 해석에서는 2개 이상의 그래프의 변수 간 관계들을 해석하는 활동보다 1개 그래프를 해석하는 활동이 더 많이 제시됨을 확인하였다. 둘째, 학생들의 그래프 전환에서 나타나는 어려움과 다양한 오류의 유형을 분석한 결과 추가적인 표상인 표를 제공하였을 때 학습자들이 그래프 전환에서 정확한 수치를 확인하고 이를 반영하여 수치적으로 보다 정확한 그래프를 그리는 것을 확인하였으나 일부 학생들의 경우 표가 없을 때 보이지 않던 그래프 상의 오류를 보여주기도 하였다. 여러 가지 운동 상황을 글과 그림으로 표현하고 그래프로 전환하는 활동에서 학습자는 물체의 운동 위치와 그래프를 혼동하여 운동궤적을 그래프 상에 그대로 표현하거나 위치, 이동거리, 상대속도, 등속도와 같은 물리 개념에 대한 이해가 부족함을 확인할 수 있었다. 물리 개념에 대한 이해가 정확한 경우에도 이를 그래프 상에 어떻게 표현하는지를 알지 못하는 경우가 있고, 그래프의 축의 의미 및 변수 설정, 눈금 설정과 같은 기본적인 그래프 표현에서 어려움을 나타내는 경우도 볼 수 있었다.

### Keywords:

중학교 영재, 여러가지 운동, 그래프 변환활동

## 해저케이블 건설, 전기장 개념 형성, 그리고 중등교과서에서 정착: 19세기 말 영국 중등 물리 교과서를 중심으로

김유진<sup>1</sup>, 김지나<sup>\*1</sup>

<sup>1</sup>부산대학교 물리교육과  
mailto:jina@pusan.ac.kr

### Abstract:

물리 교과서는 물리학 외적인 부분과 완전히 분리되어 독립적으로 구성되어 있다. 정상과학의 패러다임 안에서 물리 개념은 그 자체로 설명이 되기 때문에, 개념의 기원과 발전 과정에 대한 언급을 하지 않는 것이 일반적인 물리 교과서 서술 방식이다. 물리 교과서의 일부는 자동차나 핸드폰의 원리를 통해서 생활 속의 물리학을 설명하고 있지만, 이것은 물리가 응용되는 예시를 보여줄 뿐이다. 힘, 에너지, 전기장과 같은 핵심적인 물리 개념들은 이론 체계 속에서 스스로 존재하는 것으로 설명되고, 그 기원에 대한 설명은 찾기 힘들다. 그러나 정상과학이 교육의 내용이라고 해서, 교육의 방법이 반드시 물역사적으로 이루어져야 하는 것은 아니다. 이론 외적인 요소를 배제한 교과서 구성은 학생의 흥미를 고취하기에도 어려울 뿐만 아니라, 실제로 물리 개념이 발전하고 정착한 과정과도 다르다.

이 연구에서는 물리교과서에 수록된 이론과 패러다임이 발생하고 정착하는 과정에서 그 이론의 토대가 되었던 시대적 요구나 현상을 밝혀내고자 한다. 물리학의 유구한 역사에서 이러한 예시는 여러 가지가 있는데, 그 중에서 '전기장' 개념의 형성과 정착 과정을 분석할 것이다. 1800년에 볼타의 논문이 발표된 이후에 많은 과학자들이 손쉽게 전기를 생성하고 보관할 수 있게 되었고, 전기에 대한 연구가 활발하게 진행이 되었다. 이후에 전자기 유도 현상이 보고되고 발전기가 만들어지면서 대용량의 전기를 생성하고 전달할 수 있었기 때문에, 19세기 후반부에 전기 관련 산업은 크게 발전하였다. 이러한 발전의 과정에서 전기에 대한 연구는 더욱 깊게 진행되었고, 과학기술과 사회는 더 밀접하게 상호영향을 주고받았다. 이 때 전기 관련 산업이 가장 발달한 나라 중 하나인 영국에서 '전기장' 개념이 완성되었다. 이 논문에서는 과학외적 문제가 과학에 요구한 해결책으로써 전기장 개념이 등장하고 인정받았던 과정을 살펴보고, 그러한 개념의 교과서 정착 과정을 19세기 후반의 영미권 교과서를 중심으로 살펴 볼 것이다.

### Keywords:

물리교육, 교과서, 전기장, 해저케이블, 자체유도, 지연

## 2015 개정 교육과정 물리 I 교과서 내 탐구활동과 과학과 핵심역량과의 연계성 분석

유준희\*<sup>1</sup>, 홍진수<sup>1</sup>

<sup>1</sup>서울대학교 사범대학 물리교육과  
yoo@snu.ac.kr

### Abstract:

2015 개정 과학과 교육과정에서는 미래 사회를 살아가기 위해 필요한 핵심역량을 정의하고 이를 강조하고 있다. 한편 미국에서는 미국 국립 연구회(NRC, 2012)의 차세대 과학기준(NGSS)을 만들고 과학적 실천요소를 제시하였다. 이에 본 연구에서는 과학과 핵심역량과 NGSS에서 제시한 과학적 실천요소의 연계성을 찾고 기존 연구를 바탕으로 물리 교과서에서 핵심역량을 어떻게 반영하는지 밝히 고자 하였다. 이를 위해 2015 개정 물리 I 교과서 5종 내 탐구활동을 핵심역량 틀에서 분석하였다.

### Keywords:

교과서, 탐구활동, 핵심역량, 차세대과학기준(NGSS)

## 일반계 고등학생의 불확정성원리에 대한 이해 및 인식

유준희\*<sup>1</sup>, 민경모<sup>1</sup>

<sup>1</sup>서울대학교 사범대학 물리교육과  
yoo@snu.ac.kr

### Abstract:

Ozawa(2003)는 하이젠베르크의 불확정성 원리를 개선한 '보편적으로 타당한 불확정성 원리'를 발표하여 '불확정성'을 오차, 교란, 표준편차로 구분하였다. 실제로 2009 개정 교육과정 물리II 교과서는 '불확정성'이라는 용어의 물리적 의미를 제대로 표현하기 않았고, 수업을 하더라도 학생이 상당히 모호한 개념으로 이해할 가능성이 있다(박송이, 2014). 본 연구의 목적은 일반계 고등학교 물리II 과목에서 불확정성원리를 학습한 학생들의 이해를 인식론적 측면과 관련된 지식 측면에서 탐색하는 것이다. 설문지는 Ozawa(2003)의 분류를 이용한 '불확정성' 용어 정의의 이해와 교과적 맥락 속에서 불확정성 원리에 대해 어떤 지식적 측면을 알아볼 수 있도록 구성하였다. 이후 일반계 고등학교 학생 12명을 대상으로 자료를 수집하였다. 연구 결과 첫째, 학생 중 상당수가 '불확정성' 용어의 정의를 측정 행위로 나타나는 자연에 내재된 오차 및 교란으로 이해하였다. 일부 학생은 이를 측정 기기의 한계로 생각하거나 표준편차로 이해하는 경우도 있었다. 둘째, 불확정성원리에 대한 지식으로는 '컵에 반 즙음 담긴 물'이나 '어떤 물체의 위치와 운동 상태를 동시에 측정할 수 없다'와 같이 교과서에 서술된 내용을 그대로 언급하였다. 일부 학생은 교과서에 없는 '확률적인 것' 또는 '결정론적 세계관을 바꾸는 계기'로 설명하였다. 명확히 정의되지 않은 '불확정성' 용어가 다양한 인식과 이해를 나타나게 할 것 같다고 볼 수 있어 추후 '불확정성' 용어와 학생의 인식 사이의 관계에 관한 연구를 할 필요가 있다.

### Keywords:

일반고, 고등학생, 불확정성, 불확정성원리

## 자생적 온라인 교사 공동체의 질문 분석을 통한 초등교사의 광학교수관련 교사지식 수요 파악

유준희\*<sup>1</sup>, 김윤희<sup>1</sup>

<sup>1</sup>서울대학교 사범대학 물리교육과  
yoo@snu.ac.kr

### Abstract:

이 연구의 목적은 초등교사를 위한 자생적 온라인 교사 공동체 '인디스쿨'에서 광학과 관련된 단원의 수업을 위해 공유되는 질문 게시글을 분석함으로써 현장교사들이 요구하는 교사지식을 파악하는 것이다. 이를 위해 '인디스쿨'이 설립된 2000년부터의 광학 관련 단원에 대한 질문 119개를 분석하였다. 질문은 Grossman(1990)이 개발한 교사지식(Teacher knowledge)의 개념틀을 바탕으로 Magnusson et al.(1999)이 과학 교과교육학지식(PCK for science teaching)을 추가해 발전시킨 Abell(2008)의 교사지식모델을 사용하였다. 분석 결과, 초등교사들은 교과내용지식(SMK)적 측면의 질문을 많이 하였으며, 그중 볼록렌즈로 상이 보이는 원리에 대한 질문이 다수를 차지했다. 교과교육학지식(PCK)적 측면의 질문으로는 학생 안전과 관련된 수업설계, 교과서 대체 실험 등에 대한 질문이 주를 이뤘다. 이러한 자생적 온라인 커뮤니티의 질문 게시글 분석을 통해 파악한 교사의 요구사항은 교사용 지도서 편찬, 교사 연수 과정 개발 등에 반영되어야 할 것이다.

### Keywords:

자생적 온라인 교사 공동체, 인디스쿨, 광학, 교사지식

## “새물리”에 수록된 물리교육 논문의 서론 서술 특징

조광희\*<sup>1</sup>

<sup>1</sup>조선대학교 물리교육과  
khjo@chosun.ac.kr

### Abstract:

본 연구 발표에서는 “새물리” 학술지에 실린 물리교육 논문의 서론 서술 단계를 탐색적으로 분석하여, 물리교육 논문의 특징을 파악하고자 한다. 학술지 논문의 서론은 연구자들에게 상대적으로 작성하기 어려운 부분 중의 하나로 알려져 있다. 그리고 논문의 서론은 학문의 성격에 따라 고유한 특징이 있다. 물리교육 분야는 전통적인 관점에서 자연과학을 대표하는 물리학과 사회과학에 해당하는 교육학의 사이에서, 복합적이고 간학문적 특성을 지닌다. 이러한 점들을 고려하여, 물리교육에 관한 대표적인 국문 학술지인 새물리의 학술 논문을 분석하고 물리교육 논문의 성격을 파악하여 물리교육 논문의 서론 작성을 위한 시사점을 얻고자 한다.

### Keywords:

새물리, 물리교육 논문, 서론 서술 단계

## Inconsistencies between students' understandings in ray tracing methods and formulae of image formation

유준희\*<sup>1</sup>, TADEO Danilo Jr Austria<sup>1</sup>

<sup>1</sup>서울대학교 사범대학 물리교육과  
yoo@snu.ac.kr

### Abstract:

The meaningful understanding of physics topics can happen when students are able develop and attain both the mathematical and the conceptual understandings. This study investigated on the Filipino high school students' understanding of image formation using ray tracing and formulae. 292 Filipino high school students have participated in 20-item paralleled pre-and-post tests. The gains were 0.20 for image formation of plane and curved mirrors, 0.22 for image formation of plane and curved lenses, and 0.10 for mirror equation. However, inconsistencies with the students' drawn models of light reflection on mirrors and refraction on lenses were observed. Specifically, students had difficulties on representing how light rays hitting either the mirror or lens at angle will reflect or refract respectively. The correctness of these ray models were only 0.25 for plane mirror, and 0.22 for plane lens. Thus, attending to these issues will be needed.

### Keywords:

reflection, refraction, ray diagrams, mirror or lens equation

## 국립 대구 과학관을 활용한 과학과 예술 작품 만들기(Making ScienArt work) 프로그램의 개발

이수아\*<sup>1, 2</sup>, 박윤배<sup>2</sup>

<sup>1</sup>ScienArt 연구소, <sup>2</sup>경북대학교 물리교육과  
sciencekey@hanmail.net

### Abstract:

본 연구는 경북에 소재한 과학 중점 고등학교 학생 30명(7팀)이 대구 국립 과학관을 방문하여 '과학과 예술 작품 만들기' 프로그램을 1박 2일 동안 실시하면서 문제해결과정에 나타난 학생들의 창의적이고 통합적 사고를 살펴보고자 하였다. 이 프로그램은 과학관 관람과 진로 특강, 과학과 예술 작품 만들기로 구성되었다. 과학관 관람을 통해 학생들은 과학에 대한 폭넓은 시야와 흥미를 느꼈으며 진로 특강에 의해 미래에 대한 도전과 열정을 느낀 것으로 나타났다. 특히, 과학과 예술 작품 만들기에서 학생들의 독창성과 정교성이 나타났으며 협동심과 과학에 대한 새로운 시각을 느낀 것으로 나타났다. 즉, 이 프로그램은 과학에 대한 학생들의 적극적인 태도를 이끌어 내었다고 볼 수 있다. 그러나 학생들은 첨단기술 분야와 관련된 주제를 다소 어렵게 생각하는 것으로 나타났으므로 각 학교의 특성과 학생들의 수준을 고려한 맞춤형 과학 수업이 절실함을 알 수 있었다.

※ 도움을 주신 국립 대구 과학관과 함창 고등학교에 감사드립니다.

### Keywords:

과학과 예술 작품 만들기, 과학 중점 학교, 과학관

## Tuning the magnetic properties of hydrogenated bilayer graphene and graphene / h-BN heterostructure by compressive pressure

MOAIED Mohammed<sup>1</sup>, 홍지상\*<sup>1</sup>

<sup>1</sup>부경대학교 물리학과  
hongj@pknu.ac.kr

### Abstract:

We investigated the electronic structure and magnetic properties of hydrogenated bilayer graphene and graphene / h-BN heterostructure as a function of applied uniaxial compression. The H atoms were found in a non-magnetic ground state with graphene / graphene / h-BN systems. With increasing external pressure, the equivalence of two sublattices in the graphene was broken because of the interaction between graphene and the underlying layer and the site-dependent adsorption energy difference was greatly enhanced with the applied pressure. This is a transition from an NM ground state to a ferromagnetic hydrogenated bilayer graphene and graphene / h-BN heterostructure. Thus,

**Acknowledgments:** This was the Supported by Research Is the Basic Science Research Program-through Is the National Research Foundation of Korea (NRF) funded by Is the Ministry of Science, ICT and Future Planning (2016R1A2B4006406) and by Is the Supercomputing Center / Korea Institute of Science and the Information Technology with supercomputing resources including technical support (KSC-2016-C3-0001).

### Keywords:

ab initio, interlayer compression, graphene / h-BN, bilayer graphene (BLG), van der Waals density functional

## Co<sub>4</sub>Fe<sub>4</sub>B<sub>2</sub>/Pt 이중 박막 구조에서 열처리 온도를 이용한 스핀 펌핑 제어

이년준<sup>1</sup>, 김상일<sup>1</sup>, 이동준<sup>2</sup>, 이억재<sup>3</sup>, 박승영\*<sup>1</sup>

<sup>1</sup>한국기초과학지원연구원 연구장비개발본부 스핀공학물리연구팀, <sup>2</sup>고려대학교 KU-KIST융합대학원, <sup>3</sup>한국과학기술연구원 스핀융합연구단  
parksy@kbsi.re.kr

### Abstract:

스핀트로닉스 분야에서 강자성 공명에 의해 유도된 스핀 펌핑은 강자성 층으로부터 인접한 비자성 층으로 순수 스핀 전류를 주입하는 방법으로써 활발하게 연구되고 있다 [1-4]. 역 스핀 홀 전압 또는 강자성 층의 길버트 감쇠상수 변화 측정을 통해 스핀 펌핑을 관찰할 수 있다 [1-4]. 또한 강자성 층의 열처리 온도에 따라 강자성 물질의 감쇠상수가 변한다는 것이 잘 알려져 있다 [5]. 본 연구에서는 초고진공-스퍼터를 이용하여 Co<sub>4</sub>Fe<sub>4</sub>B<sub>2</sub> (15 nm)/Pt (5 nm) 이중 층 박막을 제작하였다. 시편의 열처리 온도 (200~400°C)에 따라서 스핀 펌핑 현상에 기인한 감쇠상수 변화와 계면에서의 스핀 전류량을 조사하였다. Co<sub>4</sub>Fe<sub>4</sub>B<sub>2</sub> (15 nm)/Cu (5 nm) 이중 층 구조를 대조군으로 감쇠상수 변화량은 강자성 공명 실험으로부터 얻은 공명 주파수에 따른 미분형 공명 흡수곡선 선평 변화량에서 추출하였으며, 이를 이용하여 계면에서 생성되는 스핀 전류값을 산출하였다.

- [1] Y. Tserkovnyak, A. Brataas, and G. E. W. Bauer, Phys. Rev. Lett. 88, 117601 (2002)
- [2] H. Nakayama, et al., Phys. Rev. B 85, 144408 (2012)
- [3] T. Taniguchi and H. Imamura, Phys. Rev. B 76, 092402 (2007)
- [4] T. Taniguchi and H. Imamura, Mod. Phys. Lett. B 22, 2909 (2008)
- [5] G. Venkat Swamy, et al., J. Appl. Phys. 117, 17A312 (2015)

### Keywords:

강자성 공명, 스핀 펌핑, 길버트 감쇠상수

## Influences of vacancy and doping on electronic and magnetic properties of monolayer SnS

신영한\*<sup>1</sup>, ULLAH Hamid<sup>1</sup>

<sup>1</sup>울산대학교 물리학과

hopenpop@ulsan.ac.kr

### Abstract:

Based on the first-principles calculations, we have investigated structural, electronic, and magnetic properties of defects in SnS monolayer. We study the formation and migration of vacancies at both Sn- and S-sites. In comparison to S-site vacancy, our calculations show that creating a vacancy Sn-site requires lesser energy, indicating that vacancy at Sn-site is more likely to be formed in experiments with energetic particle irradiation [1]. Type of intrinsic defect depends on the growth environment. For Sn (S) rich environment, vacancy at S-site (Sn-site) is more likely than vacancy at Sn-site(S-site). Importantly, reducing the possibility of vacancy cluster formation, both Sn and S vacancies remain at the positions where they are created because of the high vacancy migration barrier. Whereas, a narrow gap is observed for the S-site. Both types of vacancies remain nonmagnetic. To induce the magnetism in SnS monolayer, we also study the transition metal (TM = Mn, Co, Fe) Sn-site, and finds a significant influence on the electronic and magnetic properties of monolayer SnS [2]. The doping of TM leads to non-magnetic SnS monolayer to magnetic and interestingly keeps it semiconducting. Hence, doping TM atoms in the SnS monolayer could be promising to realize two-dimensional diluted magnetic semiconductors. More interestingly, all the doped TM configurations show high spin state, which can be used in nanoscale spintronic applications such as spin-filtering devices.

### References

- [1] LC Gomes, A. Carvalho, AH Castro Neto, Phys. Rev. B 94, 054103 (2016).
- [2] B. Parveen, M. Hassan, S. Atiq, S. Riaz, S. Naseem, S. Zaman, J. Mater. Sci. 52, 7369-381 (2017).

### Keywords:

Vacancy, vacancy migration, high spin, magnetism

## 희토류 원소가 치환된 3차원 위상절연체의 각분해 광전자 분광 연구

이은숙<sup>1</sup>, 성승호<sup>1</sup>, 김희연<sup>1</sup>, 김진수<sup>2</sup>, 정명화<sup>2</sup>, 한상욱<sup>3</sup>, 박병규<sup>4</sup>, 강정수\*<sup>1</sup>

<sup>1</sup>가톨릭대학교 물리학과, <sup>2</sup>서강대학교 물리학과, <sup>3</sup>울산대학교 Energy Harvest-Storage Research Center, <sup>4</sup>포항  
가속기 연구소 방사광응용팀  
kangjs@catholic.ac.kr

### Abstract:

위상절연체 (Topological insulator: TI)란 물질 내부 bulk 는 에너지 갭을 가진 절연체이나 표면에서는 에너지 갭이 없는 금속 상태를 가지는 물질들을 일컫는다. 그 중 3차원 위상절연체는 매우 큰 bulk 띠 갭과 표면 상태에서 간단한 디랙 원뿔 (Dirac cone) 모양의 띠를 가지는 물질로 페르미 면(Fermi surface)에서 회전하는 스핀을 가지는 것이 특징이다. 위상절연체는 시간역전 대칭성 (time reversal symmetry: TRS)를 가진 시스템에서 반드시 홀수의 페르미점을 가진다. 따라서 위상절연체의 전도성 표면 상태는 위상학적인 이유로 보장이 되며, 시간 역전 대칭성을 가지면 반드시 디랙 점 (Dirac point)이 존재 해야 한다는 것이다. 이전 연구에 의하면 Bi<sub>2</sub>Se<sub>3</sub>의 디랙 점이 ~ 0.3 eV 근처에 존재하며, 디랙 점 근처 bulk 가전자 띠 (bulk valence band) 와 표면 상태 띠 (surface-state band) 사이의 에너지 갭은 보이지 않으며, Bi<sup>3+</sup> 대신 Fe<sup>2+</sup>의 자성 불순물이 치환되면 디랙 점 근처에서 에너지 갭이 생긴다고 보고된 바 있다. [1] 그러나 여기서는 2가 (2+) 이온이 치환 되었으므로 자성 불순물이 치환될 때 전하 운반자 (charge carrier)도 동시에 함께 도핑이 되기 때문에 자기 질서 (magnetic ordering) 효과만을 관찰하기는 힘든 문제점이 있다. 따라서 Bi<sup>3+</sup> 대신 Ce<sup>3+</sup> 나 Gd<sup>3+</sup> 등의 3가 희토류 원소를 치환한다면 위와 같은 문제를 해결할 수 있을 것으로 예상된다. [2] 이 연구에서는 Bi<sub>2</sub>Se<sub>3</sub> 의 Bi 대신 Ce 희토류 원소가 치환된 (Bi<sub>2-x</sub>Ce<sub>x</sub>)Se<sub>3</sub> (x=0.02, 0.06, 0.12) 를 대상으로 방사광 각분해 광전자 분광법 (angle resolved photoemission spectroscopy: ARPES) 실험을 수행하여 이들의 전자 구조를 연구하였다. 특히 Ce 4f 공명 광전자분광법 (resonant photoemission spectroscopy: RPES) 을 이용하여 Ce 4f 전자가 (Bi<sub>2-x</sub>Ce<sub>x</sub>)Se<sub>3</sub> 의 전자구조에 미치는 영향을 연구하였다.

[1] Y. L. Chen et al., Science 329, 659 (2010).

[2] S. W. Kim, et al., Appl. Phys. Lett. 106, 252401 (2015).

### Keywords:

Topological Insulator, (Bi<sub>2-x</sub>Ce<sub>x</sub>)Se<sub>3</sub>, ARPES

## Discovery of new magnetic orders on pyrochlore spinels

이성빈\*<sup>1</sup>, 심기백<sup>1</sup>

<sup>1</sup>한국과학기술원 물리학과  
sungbin@kaist.ac.kr

### Abstract:

Frustration in spin system can give rise to unique ordered states and as a consequence several physical phenomena are expected such as multiferroics, high temperature superconductors and anomalous hall effect. Here we report the "new magnetic orders" induced by anisotropic spin exchanges on pyrochlore spinels as the interplay of spin orbit coupling and geometrical frustration. Due to complicated superexchange paths of B-site spinels, we claim that anisotropic interaction between next-nearest neighbors play an important role. Based on the systematic studies of generic spin model, we argue that several classical spin states can be explored in spinel systems; local XY state, all-in all-out state, Palmer-Chalker state and coplanar spiral state. In addition, we reveal new types of magnetic phases with finite ordering wavevectors, labeled as 'octagonal (prism)' state and '(distorted) cubic' states. When the 'octagonal prism' state is stabilized, non-zero scalar spin chirality induces alternating net current in addition to finite orbital current and orbital magnetization even in Mott insulators. Finally, we also discuss the relevance of 'distorted cubic' state to the magnetic order of spinel compound GeCo<sub>2</sub>O<sub>4</sub>.

### Keywords:

pyrochlore spinels, anisotropic interaction, electronic orbital currents, GeCo<sub>2</sub>O<sub>4</sub>

## Giant magnetic anisotropy of layered chromium compounds originated by ligand spin-orbit coupling

김동환<sup>1, 2</sup>, 김규<sup>2</sup>, 고경태\*<sup>2</sup>, 서준호<sup>1, 3</sup>, 김준성<sup>1, 3</sup>, 장태환<sup>2</sup>, 김영학<sup>4</sup>, 김재영<sup>3</sup>, 정상욱<sup>5, 6</sup>, 박재훈\*<sup>1, 2, 7</sup>

<sup>1</sup>Department of Physics, POSTECH, Pohang 37673, Republic of Korea, <sup>2</sup>Max Planck POSTECH/Hsinchu Center for Complex Phase Materials, POSTECH, Pohang 37673, Republic of Korea, <sup>3</sup>Center for Artificial Low Dimensional Electronic Systems, Institute for Basic Science, Pohang 37673, Korea, <sup>4</sup>Pohang Accelerator Laboratory, POSTECH, Pohang 37673, Korea, <sup>5</sup>Rutgers Center for Emergent Materials and Department of Physics and Astronomy, Rutgers University, Piscataway, New Jersey 08854, USA, <sup>6</sup>Laboratory for Pohang Emergent Materials and Department of Physics, POSTECH, Pohang 37673, Korea, <sup>7</sup>Division of Advanced Materials Science, POSTECH, Pohang 37673, Republic of Korea  
dreamboy78@gmail.com, jhp@postech.ac.kr

### Abstract:

Wide variation of magnetic anisotropies up to 3 T of trivalent chromium compounds ( $d^3$ ) which share similar structure and magnetic properties is puzzling according to the magnetocrystalline anisotropy. Here, we propose a new source of magnetic anisotropy energy originated from ligand spin-orbit coupling, which can be large enough for tellurides and iodides ( $\xi_{5p} = 490$  meV for tellurium and 630 meV for iodine). It depends on the ligand spin-orbit coupling strength, the angle between edge shared plane and c-axis, and covalency.

### Keywords:

Transition metal chalcogenides, magnetic anisotropy, spin-orbit coupling



## Interface Roughness Contribution to Spin-mixing Conductance in Pt/Fe<sub>3</sub>O<sub>4</sub> heterostructures

김태희\*<sup>1, 2</sup>, PHAM Thi Kim Hang<sup>1, 2</sup>, RIBEIRO Mário<sup>1, 2</sup>, PARK Jun Hong<sup>1, 2</sup>, LEE Nyung Jong<sup>2</sup>, KANG Ki Hoon<sup>3</sup>, PARK Eunsan<sup>4</sup>, NGUYEN Quang Van<sup>5</sup>, MICHEL Anny<sup>6</sup>, YOON Chong Seung<sup>3</sup>, CHO Sunglae<sup>5</sup>  
<sup>1</sup>Center for Quantum Nanoscience, Institute for Basic Science, Ewha Womans University, Seoul, 120-750, Korea, <sup>2</sup>Department of Physics, Ewha Womans University, Seoul, 120-750, Korea, <sup>3</sup>Division of Materials Science & Engineering, Hanyang University, Seoul, 04763, Korea, <sup>4</sup>KU-KIST Graduate School of Converging Science and Technology, Korea University, Seoul, 02841, Korea, <sup>5</sup>Department of Physics and Energy Harvest Storage Research Center, University of Ulsan, Ulsan 680-749, Korea., <sup>6</sup>Département de Physique et Mécanique des Matériaux, CNRS-Université de Poitiers-ENSMA, France.  
taehee@ewha.ac.kr

### Abstract:

Spin Hall magnetoresistance (SMR) in non-magnetic (NM) metal/ferromagnetic insulator (FMI) has been widely investigated for applications in future spintronic devices. The efficiency of spin current transport at the interface is determined by spin mixing conductance, the key factor governing SMR. The spin mixing conductance sensitively depends on the quality of NM/FMI interface. However, the direct impact of interface morphology to spin mixing conductance behaviors has been barely experimented in a depth of fundamental understanding.

In this work, the influence of the interface roughness of Pt/Fe<sub>3</sub>O<sub>4</sub> hybrid structures on the SMR effect was systematically investigated. Prior to Pt deposition, the surface morphology of Fe<sub>3</sub>O<sub>4</sub> layer was altered by different film growth techniques, such as oxide-MBE and RF-sputtering, and different growth conditions including substrates, substrate temperatures and post-annealing process. Their surface structure of Fe<sub>3</sub>O<sub>4</sub> was analyzed by atomic force microscopy. Our results show that the electrical characterization of Pt strongly depends on the surface morphology of Fe<sub>3</sub>O<sub>4</sub> layer underneath. The spin-mixing conductance ( $G_I$ ) is extracted from the measured SMR at low temperature (< 77K). Strong enhancement of  $G_I$  is observed with increasing the interface roughness. According to our best knowledge, we report on the first experimental observation of the roughness-induced enhancement of the efficiency of the spin current transport across the NM/FMI interface.

### Keywords:

spin Hall magnetoresistance, spin mixing conductance, Fe<sub>3</sub>O<sub>4</sub>



## 인공지능 알고리즘을 이용한 기저상태 자성구조 계산

원창연\*<sup>1</sup>, 권희영<sup>1</sup>

<sup>1</sup>경희대학교 물리학과  
cywon@khu.ac.kr

### Abstract:

자성은 자발적 대칭 파괴의 대표적인 예이다. 해밀토니안 자체는 대칭 연산에 대해 변하지 않지만, 큐리 온도 이하에서 자기 상태의 대칭성은 자발적으로 깨져서 나타난다. 그러한 자성 상태를 찾는 일은 직관에 의한 추측을 필요로 하며, 추측이 합리적인지 확인하기 위해서는 다양한 상태의 자유 에너지가 비교되어야 한다. 최근의 기계 학습 알고리즘은 인공지능 기법에 사용되며 인간의 직관과 비슷한 기능을 보여준다. 우리는 자유에너지를 최소화하는 다양한 자성구조를 찾기 위해 기계 학습 알고리즘을 적용하였다. 우리는 기계 학습 알고리즘을 채택한 프로그램을 구축하고 이를 여러 가지 자기 해밀토니안에 적용하였으며, 기계 학습 알고리즘이 자성구조를 찾는 효율적인 방법을 제공할 수 있음을 알아내었다. 이와같이 기계학습 알고리즘을 사용하여 기저상태를 얻어내는 알고리즘은 자성구조뿐만 아니라 다른 시스템에도 적용 가능할 것이라 예상하며, 이를 통해 전산물리이론연구에 새로운 길이 열릴 수 있을것이라 생각한다.

### Keywords:

Machine Learning, Magnetism, Magnetic Domain, Spontaneous Symmetry Breaking, Computational physics, Simulation

## Ambient Pressure Scanning Tunneling Microscopy; Observation of Chemical Reactions on Catalytically Reactive Surfaces

PARK Jeong\_Young\*<sup>1</sup>

<sup>1</sup>Center for Nanomaterials and Chemical Reactions, Institute for Basic Science (IBS), <sup>2</sup>Graduate School of EEWS, Korea Advanced Institute of Science and Technology (KAIST)  
jeongypark@kaist.ac.kr

### Abstract:

The modern surface characterization techniques have been discovered the surface phenomena of bimetallic materials such as selective segregation of elements, correlations of *d*-band centre shift and chemical reaction activity, and elemental compositions on each surface layer in ultra-high vacuum (UHV) condition. However, the industrial chemical reactions operate under high pressure in reactor that makes the difference of surface potential energy around 0.7 eV between UHV and atmospheric pressure. Therefore, the surface characterization methodology under more realistic environments is required to observe for understanding fundamental features at the molecular level.

In this talk, we present *in-situ* observation results of structural modulation on Pt-Ni metastable and Ni (111) surfaces at 0.1 Torr pressure of CO, O<sub>2</sub>, and CO oxidation conditions with ambient-pressure scanning tunneling microscopy (AP-STM). We show that the stable Pt-skin covered Pt<sub>3</sub>Ni(111) surface is broken by segregation of dissociative oxygen-induced Ni oxides under elevated oxygen pressure environment, which evolved clusters could have a crucial relation with enhanced catalytic activity. We show the NiO<sub>1-x</sub>/Pt-Ni nanostructures would provide more efficient reaction path for CO oxidation at interface of specified oxygen deficient Ni oxide sites on the Pt<sub>3</sub>Ni(111) surface because the modified electronic structure of Pt-Ni bimetallic surface layers not only prevents the CO deactivation, but also it provides more improved O<sub>2</sub> dissociation process by *d*-band centre shift. The catalytic activity of Pt<sub>3</sub>Ni(111) surface was significantly higher than those of Pt or Ni surfaces, which confirms our conclusion. In addition, We show that Ni single crystal surface exhibits the irreversible oxidation with the increase of oxygen exposure that leads to a formation of NiO multilayers. Elevation of O<sub>2</sub> pressure to 100 mTorr led to evolution of oxide clusters with the vertical size of up to 1.5 nm. In addition, the absence of these clusters after evacuation suggests that there is reversible phase change between NiO multilayers and oxide clusters. We discuss the possible mechanism of the morphological change of surface oxides on Ni surface at the ambient pressure.

### Keywords:

ambient-pressure scanning tunneling microscopy, bimetal surfaces, catalytic reaction, surface segregation, CO oxidation

## Scanning Tunneling Spectroscopy on Epitaxial Thin film grown on s-wave Superconductor

SONG Sang Yong<sup>1</sup>, SEO Jungpil\*<sup>1</sup>  
<sup>1</sup>대구경북과학기술원 신물질과학  
jseo@dgist.ac.kr

### Abstract:

Proximity-Induced superconductivity on semiconducting thin film grown on s-wave superconductor has been studied using scanning tunneling microscopy and spectroscopy. Using a superconducting tip, hence forming SIS tunneling junction, we could obtain the energy resolution of spectrum down to 30  $\mu$ V at the measurement temperature of 2.4 K. In this talk, we discuss a possible topological superconducting state that emerges at the surface of this heterostructure.

### Keywords:

STM, STS, Heterostructure, Superconductivity

## Growth kinetics of Kr nanostructures encapsulated by graphene

YOO S.<sup>1</sup>, AHLGREN E. H.<sup>2</sup>, SEO J.<sup>3</sup>, KIM W.<sup>4</sup>, CHIANG S.<sup>5</sup>, KIM J.-S.<sup>\*1</sup>

<sup>1</sup>Sook-Myung Women's University, <sup>2</sup>University of Nottingham, UK, <sup>3</sup>Chodang University, <sup>4</sup>Korea Research Institute of Standards and Science, <sup>5</sup>U. of California, Davis  
jskim@sm.ac.kr

### Abstract:

Scanning tunneling microscopy (STM) had proven to be the optimal probe to study the atomistic processes in thin film growth in combination with kinetic Monte Carlo simulation and first principles calculations of diffusion barriers. Recent interests in the strain engineering of 2 dimensional (2D) materials have revived the interests in the growth kinetics of the intercalated nanostructures for their tailored growth. Here, our research activities in that perspective are presented, taking the Kr nanostructures encapsulated by graphene as a model system.

### Keywords:

Growth kinetics, intercalation, Graphene, Kr , STM, strain engineering, nanostructure

## STM study on the layered chalcogenide materials

김정대\*<sup>1</sup>

<sup>1</sup>울산대학교 물리학과  
kimjd@ulsan.ac.kr

### Abstract:

Layered transition metal dichalcogenides (TMDCs) have attracted much attention due to their unique physical and chemical properties. Each layer of TMDCs is coupled by weak van der Waals force which allows easy mechanical exfoliation to prepare monolayer or a few layers thickness films. Recently, some theoretical studies predicted that monolayer 1T-VSe<sub>2</sub> shows ferromagnetic property. It has been also reported that bulk 1T-VSe<sub>2</sub> exhibits a commensurate 4x4 charge density wave (CDW) with transition temperature  $T_c = 110$  K. In this presentation, we investigate atomic and electronic structures of monolayer VSe<sub>2</sub> on graphene via home-built scanning tunneling microscopy and spectroscopy (STM/S) at 80 K. We observed (r3xr7) and (r3x2) modulation in STM topographic images. Recent STM studies on SnSe, SnSe<sub>1-x</sub>S<sub>x</sub> will be also discussed. Recently, Zhao et al. *Nature* **508**, 373 reported the ultra-high thermoelectric performance of SnSe single crystal with a maximum ZT (figure of merit) value of 2.6 at 923 K. We directly observed and identified intrinsic point defects existing on the SnSe via STM, and investigated the role of defects on the electronic properties using density functional theory (DFT) calculations. In addition, we investigate the structural evolution of crystalline SnSe<sub>1-x</sub>S<sub>x</sub> on the atomic scale by combining STM measurement with DFT calculations.

### Keywords:

transition metal dichalcogenides, STM, SnSe, VSe<sub>2</sub>, SnSe<sub>1-x</sub>S<sub>x</sub>

## STM study on the origin of p-type characteristic in $\text{Cu}_2\text{O}$

TRINH ThiLy<sup>1</sup>, DUVJIR Ganbat<sup>1</sup>, KIM Sanghwa<sup>1</sup>, JEONG Se Young<sup>2</sup>, 김정대\*<sup>1</sup>

<sup>1</sup>Department of physics, BRL, and EHSRC, University of Ulsan, <sup>2</sup>Department of Nanoenergy Engineering and College of Nanoscience and Nanotechnology, Pusan National University  
kimjd@ulsan.ac.kr

### Abstract:

Semiconducting oxides usually exhibit n-type behavior due to O vacancies dominantly generated during growth. It is important to have p-type oxides for device applications. Copper (I) oxide or cuprous oxide ( $\text{Cu}_2\text{O}$ ) has been intensively studied due to its p-type characteristic with direct band gap of  $\sim 2.1$  eV. Although some theoretical studies reported about the origin of p-type nature in  $\text{Cu}_2\text{O}$ , it is not confirmed experimentally, yet. In this study, we establish clear understanding on the atomic structure of  $\text{Cu}_2\text{O}$  (111) (1x1) surface using home-built low temperature scanning tunneling microscope (STM). In addition, intrinsic defects in  $\text{Cu}_2\text{O}$  such as O and Cu vacancies are observed.  $dI/dV$  spectroscopy reveals the electronic properties of those defects suggesting the origin of p-type behavior in  $\text{Cu}_2\text{O}$ .

### Keywords:

$\text{Cu}_2\text{O}$ , Cu vacancy, STM

# Possible high- $T_c$ superconductivity in Ruddlesden-Popper compounds: Incipient-narrow bands originating from “hidden-ladders”

KUROKI Kazuhiko\*<sup>1</sup>

<sup>1</sup>Department of Physics, Osaka University  
kuroki@phys.sci.osaka-u.ac.jp

## Abstract:

An ideal situation for realizing high- $T_c$  superconductivity is to have light electron mass and strong pairing interaction at the same time, but usually the two are not compatible with each other. In ref.[1], the present author proposed a way to circumvent this problem ; in a system consisting of wide and narrow bands, light effective mass and strong pairing interaction is simultaneously realized when the Fermi level sits in the vicinity of, but does not intersect, the narrow band. The two-leg Hubbard ladder with diagonal nearest neighbor hoppings, a model for the ladder-type cuprates, was studied as a system in which such a situation is realized, where a possible occurrence of extremely high  $T_c$  was suggested. Here, we extend this study, and show that this high- $T_c$  mechanism works in a variety of systems that consist of wide and narrow (or flat) bands, such as the diamond lattice [2] and the three-leg ladder. We apply the fluctuation exchange approximation to the Hubbard model on these lattices, and show that superconductivity is strongly enhanced when the Fermi level sits close to the narrow band [3]. This shows the generality of the mechanism of high- $T_c$  superconductivity originating from wide and incipient narrow bands.

In reality, ladder-type cuprates are notorious for being unable to control carrier doping and thus the Fermi level. As a way to realize the above mentioned situation in actual materials, we introduce a concept of “hidden ladder” electronic structure in the bilayer Ruddlesden-Popper compounds, where anisotropic  $d$ -orbitals of the transition metal give rise to inherent ladder-like electronic structures [4]. Namely, considering the case in which  $t_{2g}$  orbitals form the bands crossing (or lie near) the Fermi level, an electron in the  $d_{xz/yz}$  orbital selectively hops in the  $x/y$  direction as well as in the  $z$  direction normal to the bilayer. This means that the  $d_{xz/yz}$  orbital form a ladder with  $x/y$  and  $z$  directions being the leg and rung directions, respectively. We propose that  $Sr_3Mo_2O_7$  and  $Sr_3Cr_2O_7$  are candidates for the hidden ladder materials where the Fermi level sits in the vicinity of the narrow-band edge without large amount of carrier doping. Based on this electronic structure, we discuss a possible occurrence of high- $T_c$  superconductivity in these materials.

[1] K. Kuroki, et al., Phys. Rev B, **72**, 212509 (2005).

[2] K. Kobayashi et al., Phys. Rev. B **94**, 214501 (2016).

[3] K. Matsumoto et al., Phys. Rev. B **97**, 014516 (2018).

[4] D. Ogura, et al. Phys. Rev. B **96**, 184513 (2017).

## Keywords:

high- $T_c$  superconductivity, Ruddlesden-Popper compounds, two-leg Hubbard ladder

# Theory of relativistic Mott insulator and superconductivity in transition metal oxides with a strong spin-orbit coupling

YUNOKI Seiji\*<sup>1</sup>

<sup>1</sup>Computational Condensed Matter Physics Laboratory, RIKEN, <sup>2</sup>Computational Quantum Matter Research Team, RIKEN Center for Emergent Matter Science (CEMS), <sup>3</sup>Computational Materials Science Research Team, RIKEN Advanced Institute for Computational Science (AICS)  
yunoki@riken.jp

## Abstract:

Motivated by recent experiments of novel 5d Mott insulators such as Sr<sub>2</sub>IrO<sub>4</sub>, we have studied theoretically the two-dimensional three-orbital Hubbard model with a strong spin-orbit coupling for (t<sub>2g</sub>)<sup>5</sup> and (t<sub>2g</sub>)<sup>4</sup> local electron configurations on square and honeycomb lattices.

The variational Monte Carlo method and the dynamical mean field theory are used to obtain the ground state phase diagram for (t<sub>2g</sub>)<sup>5</sup> local electron configuration on the square lattice with varying a on-site Coulomb interaction  $U$  as well as the spin-orbit coupling. It is found that the transition from a paramagnetic metal to an antiferromagnetic (AF) insulator occurs at a finite  $U = U_{MI}$ , which is greatly reduced by a large spin-orbit coupling, characteristic of 5d electrons, and leads to the spin-orbit-induced Mott insulator. It is also found that the Hund's coupling induces the anisotropic spin exchange and stabilizes the in-plane AF order. We have further studied the single-particle excitations using the variational cluster approximation and the dynamical mean field theory, and revealed the internal electronic structure of this novel Mott insulator, i.e., the effective total angular momentum  $J_{eff}=1/2$  Mott insulator. We have estimated the magnetic exchange coupling and found that it can be as large as 50-100 meV. These findings are in agreement with experimental observations for Sr<sub>2</sub>IrO<sub>4</sub> and very similar to mother compounds for high  $T_c$  cuprate superconductors. It is therefore expected that a possibly high  $T_c$  superconductivity can be induced once mobile carriers are introduced into the  $J_{eff}=1/2$  Mott insulator. We have considered this possibility using the variational Monte Carlo method as well as RPA and found that indeed the superconductivity with  $d$ -wave pairing is most likely induced by electron doping. We also discuss the similarity in the single-particle excitations between iridates and cuprates, including pseudogap behavior, and other related systems. In addition, we will discuss more interesting exotic ground states such as excitonic insulator and quadrupole order for (t<sub>2g</sub>)<sup>4</sup> local electron configuration

This work has been in collaboration with H. Watanabe, T. Shirakawa, T. Sato, K. Nishiguchi, B. H. Kim, K. Seki, W. Fan, and H. Sakakibara.

- [1] H. Watanabe, T. Shirakawa, and S. Yunoki, Phys. Rev. Letts. **105**, 216410 (2010).
- [2] H. Watanabe, T. Shirakawa, and S. Yunoki, Phys. Rev. Letts. **110**, 027002 (2013).
- [3] H. Watanabe, T. Shirakawa, and S. Yunoki, Phys. Rev. B **89**, 165115 (2014).
- [4] T. Sato, T. Shirakawa, and S. Yunoki, Phys. Rev. B **91**, 125122 (2015).
- [5] A. Yamasaki, H. Fujiwara, S. Tachibana, et al., Phys. Rev. B **94**, 115103 (2016).
- [6] Q. Cui, J.-G. Cheng, W. Fan, et. al., Phys. Rev. Letts. **117**, 176603 (2016).
- [7] B. J. Kim, T. Shirakawa, and S. Yunoki, Phys. Rev. Letts. **117**, 187201 (2016).
- [8] T. Sato, T. Shirakawa, and S. Yunoki, arXiv: 1603.02369.

## Keywords:

mott insulator, superconductivity, spin-orbit coupling

## Cluster multipole theory for functional antiferromagnets

ARITA Ryotaro\*<sup>1, 2</sup>

<sup>1</sup>Department of Applied Physics, University of Tokyo, <sup>2</sup>Center for Emergent Matter Science, RIKEN  
arita@riken.jp

### Abstract:

Recently, functional antiferromagnets are attracting an increasing amount of attention. In contrast with ferromagnetic devices, those using antiferromagnets have several advantages: They are robust against magnetic field perturbations, which is good for data retention. Since they do not have strong stray fields, one can integrate high-density memory. On top of those, the energy scale of antiferromagnets is usually higher than that of ferromagnets, which is convenient for ultrafast data processing.

In the past few years, it has been theoretically and experimentally shown that some antiferromagnets such as  $Mn_3Ir$ ,  $Mn_3Sn$  and  $Mn_3Ge$  exhibit extremely large anomalous Hall effect (AHE) [1,2,3,4,5], Nernst effect [6], and magneto-optical Kerr effect [7], which are usually observed in ferromagnets. Especially, large AHE in those antiferromagnets is of great interest, since a large change in the Hall voltage can define binary information in magnetic devices [4].

While AHE in ferromagnets usually scales with the magnetization of the system, it is a non-trivial problem which order parameter quantifies AHE in antiferromagnets. In this talk, we introduce a new order parameter, which we call cluster multipole (CMP) moment, and show that CMP characterizes AHE in antiferromagnets with general spin configurations. In particular, we demonstrate that AHE in  $Mn_3Sn$  and  $Mn_3Ge$  and that in elemental Fe can be described in the unified scheme using CMP [8]. We also discuss how CMP is useful for designing functional antiferromagnets.

[1] H. Chen, Q. Niu, and A. MacDonald, *Phys. Rev. Lett.* **112**, 017205 (2014).

[2] J. Kuebler and C. Felser, *Europhys. Lett.* **108**, 67001 (2014).

[3] S. Nakatsuji, N. Kiyohara, and T. Higo, *Nature* **527**, 212 (2015).

[4] N. Kiyohara *et al.*, *Phys. Rev. Applied* **5**, 064009 (2016).

[5] A. K. Nayak *et al.*, *Sci. Adv.* **2**, e1501870 (2016).

[6] M. Ikhlas, T. Tomita, T. Koretsune, M.-T. Suzuki, D. Nishio-Hamane, R. Arita, Y. Otani, S. Nakatsuji, *Nature Physics* **13**, 1085 (2017).

[7] W. Feng *et al.*, *Phys. Rev. B* **92**, 144426 (2015).

[8] M.-T. Suzuki, T. Koretsune, M. Ochi and R. Arita, *Phys. Rev. B.* **95**, 094406 (2017).

### Keywords:

functional antiferromagnets, anomalous Hall effect

## Toward Better First-principles Description of Correlated Electron Materials: Exchange-correlation and response functions

HAN Myung Joon\*<sup>1</sup>

<sup>1</sup>KAIST

mj.han@kaist.ac.kr

### Abstract:

In this talk I will try to give a brief overview of recent methodological progress in my research group which aims at the better first-principles description of correlated electron phenomena. In the first part, our efforts on understanding currently available exchange-correlation functionals will be presented [1-4]. In the situations in which experimental information is severely limited, we found, a special care needs to be paid regarding the reliability of standard first-principles approximation. With a ruthenate thin film as our example, we systematically compared the predictabilities of LDA and GGA [1]. In case of DFT+U method, which is one of the standard first-principles approaches to correlated materials, we also performed a systematic comparative studies for several different functional recipes including spin density and double counting functional forms. Our analysis raises a serious question against the spin-density-functional-based formulations [2, 4]. In case of non-collinear magnetism, the situation gets more complicated, and further study is strongly requested on the more fundamental level [3]. In the second part, the computation schemes for magnetic interactions [5, 6] and branching ratio [7] will be discussed.

[1] S. Ryee and M. J. Han, Sci Rep 7 4635 (2017)

[2] S. Ryee and M. J. Han, arxiv:1709.03214 (2017)

[3] S. Ryee and M. J. Han, arxiv:1802.10129 (2018)

[4] S. W. Jang, S. Ryee, H. Yoon, and M. J. Han, arxiv:1803.00213 (2018)

[5] H. Yoon, T. J. Kim, J.-H. Sim, S. Jang, T. Ozaki, and M. J. Han, Phys. Rev. B (2018) in press

[6] T. J. Kim, H. Yoon, and M. J. Han (submitted)

[7] J.-H. Sim, H. Yoon, S. H. Park, and M. J. Han Phys. Rev. B 94 115149 (2016)

### Keywords:

Density functional theory, correlated electron, LDA/GGA, DFT+U, magnetic interaction, branching ratio

## Universal behavior of the housekeeping entropy production

노재동\*<sup>1, 2</sup>, 천현명<sup>1</sup>

<sup>1</sup>서울시립대학교 물리학과, <sup>2</sup>고등과학원 물리학부  
jdnoh@uos.ac.kr

### Abstract:

Nonequilibrium processes without detailed balance generate entropy.

The total entropy production is divided into housekeeping entropy production and excess entropy production.

The housekeeping entropy production is indispensable to maintain the nonequilibrium steady state.

We consider nonequilibrium Langevin systems and find the Langevin equation for the housekeeping entropy production.

It turns out that the time evolution of the housekeeping entropy is fully characterized by an intrinsic dimensionless time scale  $\tau$ .

The statistics of the housekeeping entropy production at fixed  $\tau$  are all the same regardless of system details.

We demonstrate the universal behavior of the housekeeping entropy production using two different examples.

### Keywords:

housekeeping entropy production, nonequilibrium Langevin systems

## Thermodynamic bound of learning accuracy of a single neuron

노재동\*<sup>1, 2</sup>, 박종민<sup>1</sup>

<sup>1</sup>서울시립대학교, 물리학과, <sup>2</sup>고등과학원, 물리학부  
jdnoh@uos.ac.kr

### Abstract:

We investigate a relation between the thermodynamic cost and a gained information by a single neuron. The output signal of a single neuron is a function of the weighted sum of input signals. By adjusting the weights, the neuron is trained to make its output be the same as a label associated with input signals. Recently, as a measure of the gained information, the mutual information between the true label and the output signal has been introduced by S. Goldt and U. Seifert. They consider the Langevin dynamics for the weights and find that the mutual information is bounded by the thermodynamic cost during the training process. We critically revisit the concept of the thermodynamic cost.

### Keywords:

learning accuracy, mutual information, thermodynamic cost

## Effect of magnetic field on Langevin system in nonequilibrium steady state

이상윤<sup>1</sup>, 권철안<sup>\*2, 3</sup>

<sup>1</sup>한국과학기술원 물리학과, <sup>2</sup>명지대학교 물리학과, <sup>3</sup>고등과학원, 양자우주센터  
ckwon@mju.ac.kr

### Abstract:

Even though homogeneous static magnetic field is applied to Langevin system which is only affected by conservative potential, the system are relaxed to same Boltzmann state. In this case thermodynamic quantities are irrelevant to magnetic field. However it does not hold when system is in non-equilibrium state. Because in non-equilibrium state thermodynamic currents are non-zero and the effect of magnetic field on currents is not averaged out.

In this study we investigate two dimensional Langevin equation which is affected by non-conservative linear force and Lorentz force. We presents the self-consistent relation in over-damped limit and stability condition when magnetic field destabilize the system. And we find that the stability criteria coincides with condition when violation of fluctuation dissipation relation increased. And analytic form of thermodynamic quantities and violation of fluctuation dissipation relation are also presented. of fluctuation dissipation relation.

### Keywords:

Brownian motion, magnetic field, violation of fluctuation dissipation relation

## Erasure of a Stable Fixed point by Stochastic Noise

이주런\*<sup>1</sup>, 이재준<sup>1</sup>

<sup>1</sup>승실대학교 생명정보학과  
jul@ssu.ac.kr

### Abstract:

Deterministic rate equation has been considered as an approximate description of stochastic chemical master equation, derived in the limit of vanishing stochastic noise. When stochastic noise is introduced, the stable fixed point of the deterministic rate equation usually turns into a peak of the stationary distribution, as long as the size of the stochastic noise is sufficiently small. Here, we report a phenomena where the stable fixed point of the rate equation is completely erased from the stationary distribution of the chemical master equation, no matter how small the size of the stochastic noise is. The stable fixed point turns into a peak of a quasi-steady distribution in this case. The result implies that in some cases, the small magnitude of the stochastic noise is not sufficient for the deterministic rate equation to be a valid approximation of the stochastic dynamics, but the time-scale also plays an important role.

### Keywords:

stochastic process, chemical master equation, nonlinear dynamics, stable fixed point

## 딥러닝에서 언어와 소음의 전송학습

안강현\*<sup>1</sup>, 박마루찬<sup>1</sup>  
<sup>1</sup>충남대학교 물리학과  
ahnkh@cnu.ac.kr

### Abstract:

딥러닝 기법의 하나인 Generative Adversarial Network (GAN)을 이용하여 소음이 가해진 신호에서 깨끗한 음성을 추출할 수 있다. 본 연구에서는 영어로 훈련된 인공 신경망을 다른 언어에 사용할 때 어떤 반응이 나타나는 지를 알아보았다. 놀랍게도 불과 몇 분의 훈련만으로도 외국어에 완벽하게 적응하는 모습을 확인하였다. 영어를 제외한 다른 나라의 언어의 경우 공개된 음성 데이터가 부족한데 본 연구의 결과가 유용하게 쓰여 질 것으로 예상된다. 한국어와 카탈로니아어 데이터를 미리 영어로 훈련된 모델에 훈련시킨 후 한국어와 카탈로니아어를 소음 속에서 얼마나 잘 추출하는지 확인하였는데 이 때 소음 제거 능력은 훈련 소음 종류의 개수와는 무관하며, 테스트 소음의 종류에 영향을 받는다는 것을 발견하였다. 또한 이러한 성능이 신경망의 크기에 어떤 영향을 받는지 조사하였다.

### Keywords:

딥러닝, 전송학습, GAN

## Optimizing the spatial distribution of hospitals for public health

이미진<sup>1</sup>, 김강훈<sup>2</sup>, 이덕선\*<sup>1</sup>  
<sup>1</sup>인하대학교 물리학과, <sup>2</sup> Korea Asset Pricing  
deoksun.lee@gmail.com

### Abstract:

Some diseases such as tuberculosis are managed and treated at the national and global level to reduce patients and fatalities, which is done by the private hospitals as well as the public health center at local communities implementing medical treatment. Given that such diseases can become more fatal for patients who live in a region with few hospitals, we here study the optimal spatial distribution of the private hospitals to minimize the total number of fatalities. Adopting a random-walk model with traps, in which a random walker and traps correspond to a patient and hospitals, respectively, and considering the survival probability and the probability that a patient does not yet receive hospital treatment, we determine the dependence of the fatality rate on the number of hospitals in a given region and obtain the optimal hospital density both numerically and theoretically. The number of fatalities is decreased by 10% by this optimization, and we compare the optimal and the present non-optimal distribution of hospitals in their relationship with population density and income distribution.

### Keywords:

facility distribution, hospital distribution, Monte Carlo simulation, Random walk with traps

## Parallel random target searches in a confined space

김용운\*<sup>1</sup>, 노승한<sup>1</sup>

<sup>1</sup>한국과학기술원 나노과학기술대학원  
y.w.kim@kaist.ac.kr

### Abstract:

We study a random target searching performed by  $N$  independent searchers in a  $d$ -dimensional domain of a large but finite volume. Considering the two initial distributions of searchers where searchers are either uniformly or point distributed, we estimate the mean time for the first of the searchers to reach the target and refer to it as searching time. The searching time for the uniformly distributed searchers exhibits a universal power-law dependence on  $N$ , irrespective of dimensionality and the target-to-domain size ratio. For point-distributed searching, the searching time has a logarithmic dependence on  $N$  in the large  $N$  limit, while in the small  $N$  limit, it shows qualitatively different behaviors depending upon  $r_0$ , the initial distance of the searchers from the target. We obtain a diagram by comparing the searching times of the two initial distributions in the parameter space  $(r_0, N)$  and therein present the asymptotic lines separating three characteristic regions to explain numerical simulation results.

### Reference

Sunghan Ro and Yong Woon Kim, Phys. Rev. E. **96**, 012143 (2017).

### Keywords:

random target search, multiple searchers, distribution of searchers, multi-dimensional search, reaction-diffusion, first-passage time, random walks, Brownian motion

## Percolation with exclaves cluster on networks

고광일\*<sup>1</sup>, 곽상환<sup>1</sup>  
<sup>1</sup>고려대학교 물리학과  
kgoh@korea.ac.kr

### Abstract:

Percolation theory in networks is an important tool for understanding critical phenomena in statistical physics. So, we study a new percolation model called the NExP model on networks. Our model is a modification of the NEP model proposed by M. Sheinman *et al* published in 2015. It changes the state of the un-occupied node trapped from the surrounding occupied node to the same state as the occupied node. In this process, clusters different from the random ordinary percolation occur, which are called exclaves clusters. We show that the effect of the exclaves cluster not only makes larger cluster size but also speeds up the percolation transition. We provide the theoretical frame for the model on random treelike networks through the generating function method and also provide Monte carlo simulation to verify it. As a result, we measure critical exponents and found them consistent with random ordinary percolation. In addition, we apply our model to bovine farm network. The effect of exclaves clusters is also confirmed in real network.

### Keywords:

Percolation, critical phenomena, No-Exclaves percolation

## Observation of thresholdless lasing in the single-atom superradiance

AN Kyungwon\*<sup>1</sup>

<sup>1</sup>Department of Physics and Astronomy, Seoul National University  
kwan@phya.snu.ac.kr

### Abstract:

In the conventional approach of thresholdless lasing, the so-called beta factor, a fraction of total spontaneous emission coupled to a particular lasing mode, is maximized close to unity by means of the Purcell effect with specially designed micro- and nano-cavities. Contrary to this conventional approach, we employed collective interaction of phase-aligned time-separated atomic dipoles in a high-Q cavity and demonstrated thresholdless lasing experimentally even with a beta factor of 0.03 in the setting of the single-atom superradiance. The field state is expected to be a coherent state, even when the intracavity photon number is less than unity, which is not the case in the conventional thresholdless lasing based on non-collective emission. Our results may provide more flexibility in designing thresholdless lasers.

### Keywords:

thresholdless laser, superradiance, Purcell effect, beta-factor, phase-aligned atoms, single-atom superradiance

## Ultrafast adiabatic holonomic gates for atomic clock state qubits in tweezer trap array

안재욱\*<sup>1</sup>, 송윤홍<sup>1</sup>

<sup>1</sup>한국과학기술원 물리학과  
jwahn@kaist.ac.kr

### Abstract:

Ultrafast laser pulses allow control of atomic clock state qubits within a time faster than the hyperfine free evolution period, which is impossible with conventional schemes such as microwave transitions and Raman transitions, providing not only shorter calculation time for quantum computation but also a method to overcome decoherence of the quantum system. However, ultrafast qubit control with high fidelity is harder than conventional ones, because ultrafast laser amplifiers generally have more parameter fluctuations. To resolve this problem, we suggest ultrafast adiabatic holonomic quantum gates, using only geometric phases determined by adiabatic evolution pathway without any dynamical details. This gate has robustness about several parameters including power, phase, and detuning. The experimental implementation conducted with two linearly polarized chirped ultrafast pulses and five single  $^{87}\text{Rb}$  atoms in tweezer trap array have demonstrated the population transfer between hyperfine clock states and power robustness of the gate. In addition, Ramsey experiments by two successive applications of this gate have been done, showing the possibility of universal single qubit control through this gate and free evolution of clock states.

### Keywords:

quantum gates, ultrafast pulses, single atom traps

## Locally cooling quantum many-body systems and its applications

박채연\*<sup>1</sup>

<sup>1</sup>아시아 태평양 이론물리센터 Quantum Information and Many-Body Theory  
kaeri17@gmail.com

### Abstract:

A driven-dissipative many-body system recently attained a lot of interest. It is now well-known that such a system can have fruitful dynamical phenomena and phases. However, it is usually very difficult to investigate dynamical properties of a system directly from the Lindblad equation as analytical/numerical investigations are largely restricted because of high dimensionality. In this work, we propose another kind of driven-dissipative system the dynamics of which can be easily investigated. We first propose a cooling scheme for many-body systems that preserve locality of dynamics, i.e. the finite Lieb-Robinson velocity. Using this result, we show that the long-time dynamics of these systems is governed by their low energy eigenstates. For particular examples, we investigate how a meta-/bi-stability emerge from these dynamical systems.

### Keywords:

Many-body systems, quantum simulation, driven-dissipative systems

## Coherent control of entangled three Rydberg atoms

안재욱\*<sup>1</sup>, 조한래<sup>1</sup>

<sup>1</sup>한국과학기술원 물리학과  
jwahn@kaist.ac.kr

### Abstract:

Rydberg atom systems are being considered as one of the most promising candidates for realizing quantum simulation and computation. The strong dipole interaction between Rydberg atoms allows various configurations of entangled many-body systems. In this presentation, we study coherent control schemes of three neutral Rydberg atoms. Depending on their geometric configurations such as symmetric or asymmetric triangle, or linear arrangement, three Rydberg atom systems form different eigenstate subspaces of the entangled total system. For instance, in a symmetric configuration, the transition from the asymmetric subspace to the symmetric subspace, that includes the ground state is forbidden, under uniform light-atom interaction. However, we find that asymmetric subspace is accessible from symmetric subspace using an asymmetric configuration. The seemingly counterintuitive transition is enabled due to different energy levels of double-excitation manifolds caused by the unbalanced dipole interaction of two-particle subsystems.

### Keywords:

Rydberg atom, coherent control

## Hybrid Two-Qubit Gate using Circuit QED System with Triple-Leg Stripline Resonator

문경순\*<sup>1</sup>, 김동민<sup>1</sup>  
<sup>1</sup>연세대학교 물리학과  
kmoon@yonsei.ac.kr

### Abstract:

We have theoretically studied a hybrid two-qubit system using photon-polarization qubit and transmon qubit from a circuit electrodynamic (cQED) system with triple-leg stripline resonator (TSR). Unlike a typical linear resonator, from this unique system of TSR, we can have two degenerated ground states in a microwave flowing in a resonator. Only one of these modes can be coupled with the qubit connected to one leg of the TSR, and the other remains intact. We will discuss the effectiveness of TSR by applying this feature to the flying qubit used in quantum computing. This qubit comes in and out of the cavity and uses the polarization of light as quantum information. We have coupled the optically polarized qubit of the photon through the special optical circuit to each of the two microwave modes of the TSR. Based on this, we have constructed a quantum controlled phase flip gate that can be implemented by taking into account the variables experimentally available.

This work is partially supported by Basic Science Research Program through the National Research Foundation of Korea (NRF) funded by the Ministry of Education, Science and Technology (NRF-2016R1D1A1B01013756).

### Keywords:

Quantum computing, Circuit QED, Quantum Optics, Flying Qubit

## Security proof models and notions for post-quantum and fully-quantum cryptography

LEE Jeeun\*<sup>1</sup>, LEE Seunghyun<sup>2</sup>, KIM Kwangjo<sup>1</sup>

<sup>1</sup>School of Computing, KAIST, <sup>2</sup>Department of Mathematical Sciences, KAIST  
jeeun.lee@kaist.ac.kr

### Abstract:

Ever since the publication of Deutsch's groundbreaking paper in 1985, many quantum algorithms have been introduced. Some of these algorithms—for example, those of Simon, Shor, or Grover—pose a serious threat to classical cryptography. Accordingly, researchers have been developing new security proof models and notions in a quantum setting; hence the post-quantum era has begun in the field of cryptography. In this work, we review the standard, random oracle, and challenger models respectively, and extend them from classical to quantum setting by allowing the adversary's access to quantum computation. Also, after defining quantum indistinguishability and quantum attacks, suitable security notions are introduced, such as IND-ATK, (IND/wqIND/qIND)-qATK, and cqIND-qATK, for  $\text{ATK} \in \{\text{CPA}, \text{CCA1}, \text{CCA2}\}$ .

### Keywords:

classical cryptography; post-quantum cryptography; fully-quantum cryptography; security proof model; security notion

## 약전리 플라즈마 내의 전기바람(electric wind)

박상호<sup>1</sup>, 최원호<sup>\*2, 3</sup>

<sup>1</sup>한국과학기술원 자연과학연구소, <sup>2</sup>한국과학기술원 원자력 및 양자공학과, <sup>3</sup>한국과학기술원 물리학과  
wchoe@kaist.ac.kr

### Abstract:

하전입자와 중성입자 간의 상호작용은 지구 등 행성의 대기에서도 일어나는 여러 자연현상의 기초 작용으로 흔히 알려져 있으며, 약전리 플라즈마(weakly ionized plasmas)에서의 전기유체역학적(Electrohydrodynamic, EHD)인 중성기체의 흐름(전기바람, electric wind)이 대표적인 예이다. 약전리 플라즈마 내에 전기장이 강하게 존재하는 공간에서 전자나 이온이 불균일하게 분포되어 있으면 전기바람이 발생하는데, 전기바람의 주요 원리는 명확하게 밝혀지지 않아 해당 기술을 여러 응용분야에 적용하는데 큰 어려움이 있었다. 최근에는 플라즈마 전기바람을 이용한 유체 제어 응용기술의 개발이 활발히 진행됨에 따라, 학계 및 관련 산업체의 관심이 증가하고 있다. 본 연구에서는 대기압 약전리 플라즈마인 헬륨 제트 플라즈마를 이용하여 약전리 플라즈마 내에서 발생하는 전기바람의 주요 기작을 실험적으로 규명하였다. [1] 전극에 인가되는 전압의 펄스 폭, 크기에 따른 헬륨 기체의 궤적을 Schlieren 이미징으로 관찰하고, 이를 전산 모델링 결과와 비교하여 발생하는 전기바람의 속력을 정성적으로 분석하였다. 전기바람의 발생에 있어서 스트리머의 전파는 큰 기여를 하지 못하고, 스트리머의 전파 후에 발생하는 공간전하의 이동이 큰 역할을 하는 것을 밝혔으며, 음극 방향성(cathode-directed) 플라즈마에서는 음이온이 아닌 전자가 전기풍 발생의 핵심요소임을 실험적으로 확인하였다. 본 발표를 통해 최근 연구결과와 함께 관련 연구 및 기술의 응용 분야에 대해 소개하고자 한다.

[1] S. Park, W. Choe et al., Nat. Comm. 9, 371 (2018)

### Keywords:

전기바람, 약전리 플라즈마, 플라즈마 제트

## 용량성 결합 플라즈마 내 비선형 시간가변적 전자에너지분포에 의한 전자 가열 제어

이정열<sup>1</sup>, 박희성<sup>1</sup>, 이해준\*<sup>1</sup>  
<sup>1</sup>부산대학교 전기컴퓨터공학부  
haejune@pusan.ac.kr

### Abstract:

용량성 결합 플라즈마 (Capacitively Coupled Plasma, CCP)는 반도체 공정, 물질 처리, 플라즈마 의료기기 연구 분야 등에 많이 이용되고 있다. 이는 장치 구조상 간단하고 가장 보편적으로 쓰이지만 하전입자의 온도 및 에너지 분포 컨트롤에 있어서 많은 변수가 존재하여 이론적 분석이 어렵고, 플라즈마 응용에 있어서도 공학적 접근을 어렵게 만든다. 이에 대해 입력 파워 및 가스 압력 등에 의한 효과에 대해서 많은 실험적 연구가 이루어져 왔으나 주파수에 대한 효과를 실험적으로 분석하기에는 어려움이 존재한다. 본 연구에서는 Particle-In-Cell Monte Carlo Collision 시뮬레이션을 통하여 중요 플라즈마 변수들의 시공간 변화를 측정하였다. 여기서 사용된 중요 조절 변수는 13.56 MHz ~ 600 MHz사이의 인가 주파수이며, 유전체 표면에서 양이온에 대한 이차전자 방출계수를 고려하여 감마 모드의 플라즈마를 시뮬레이션 상에서 구현하였다. 또한 중성기체는 헬륨 가스와 아르곤 가스의 2가지 경우를 살펴보았다. 이러한 결과를 통해, 인가 주파수 조절을 통한 비선형 시간 가변적 전자에너지분포를 확인하고, 이 현상을 이용한 전자 가열모드 변화를 분석하였다.

### Keywords:

용량성 결합 플라즈마, 전자 에너지 분포, 시뮬레이션, 입자-셀 기법, 전자 가열 모드

## Temporal diagnostics of X-ray Free Electron Laser by Slotted Foil Line scanning method.

남인현<sup>1</sup>, 민창기<sup>1</sup>, 양해룡<sup>1</sup>, 김창범<sup>1</sup>, 허훈<sup>1</sup>, 김규진<sup>1</sup>, 강흥식\*<sup>1</sup>

<sup>1</sup>포항공과대학교 가속기연구소  
hskang@postech.ac.kr

### Abstract:

In this presentation, we show the results of measurement of the x-ray pulse duration at Pohang Accelerator Laboratory X-ray Free Electron Laser (PAL-XFEL) using a scanning narrow slotted foil method. The slotted foil method is used to vary the pulse duration or generate two pulses, which located at the center of the bunch compressor. The slotted foil position is correlated to the temporal position of the x-ray pulse. Thus, the temporal profile of the x-ray can be measured by scanning the position with a very thin slotted foil. This method is very simple and effective temporal diagnostic tool of x-ray pulse for XFEL user facilities.

### Keywords:

X-ray free electron laser, longitudinal diagnostics, slotted foil

## The first femtosecond x-ray absorption measurement for warm dense matter at PAL-XFEL

LEE Jong Won<sup>\*1, 2</sup>, KANG Gyeong Bo<sup>1, 2</sup>, KIM Min Ju<sup>1</sup>, PARK Sang Han<sup>3</sup>, KIM Min Seok<sup>3</sup>, KWON Soon Nam<sup>3</sup>, JUNG Jae Hyung<sup>1</sup>, YANG Seong Hyeok<sup>1, 2</sup>, CHO Byoung Ick<sup>1, 2</sup>

<sup>1</sup>Department of Physics and Photon Science, Gwangju Institute of Science and Technology (GIST),

<sup>2</sup>Center for Relativistic Laser Science, Institute for Basic Science (IBS), <sup>3</sup>PAL-XFEL, Pohang Accelerator Laboratory (PAL)  
jwl@gist.ac.kr

### Abstract:

At the SSS (Soft X-ray Scattering & Spectroscopy) experimental beamline in PAL-XFEL, we demonstrated femtosecond resolved x-ray absorption spectroscopy for the warm dense matter. The XFEL beam having monogenetic photon energy which set Cu L-edge scans the solid Cu target strongly excited by the intense laser pulse (400 nm of central wavelength, 40 fs of pulse duration, and 1.5-3 J/cm<sup>2</sup> of incident fluence). We observed rapid changes of x-ray absorption in femto-picosecond range. The experiment first introduces a potential to study non-equilibrium dynamics in femtosecond timescale.

This work was supported by the Institute for Basic Science (IBS-R012-D1) and the National Research Foundation (NRF-2016R1A2B4009631 and NRF2015R1A5A1009962) of Korea.

### Keywords:

Warm Dense Matter, X-ray absorption spectroscopy, XFEL

## Bremsstrahlung Photons Emission from ECR Ion Source

안정근\*<sup>1</sup>, KUMWENDA Mwingereza John\*<sup>1</sup>, LEE Jungwoon\*<sup>1</sup>, PARK Jinyong\*<sup>2</sup>, KIM Seongjun\*<sup>2</sup>

<sup>1</sup>Department of Physics, Korea university, <sup>2</sup>Korea Basic Science Institute  
ahnjk@korea.ac.kr, kmwingereza@udsm.ac.tz, laerad84@gmail.com, jinyongp@kbsi.re.kr,  
seongjunk@kbsi.re.kr

### Abstract:

The presence of high-energy bremsstrahlung photon emission beyond a critical energy from ECR heating is somewhat surprising and its nature has yet been unsolved. We have measured bremsstrahlung photon from the 28-GHz ECR ion source at Busan Center of KBSI. The gamma-ray detection system consists of three NaI(Tl) scintillation detectors placed 62 cm radially from the beam axis at the injection, centre and extraction sides of an ECR ion source, and an NaI(Tl) scintillation detector for monitoring photon intensity along the beam axis. Bremsstrahlung photon energy spectra were measured at nine azimuthal angular regions at RF power of 1kW. We also measured bremsstrahlung photons by exchanging detector positions for studying systematic uncertainties. Detection efficiency and shielding effect are taken into account for extracting real bremsstrahlung photon energy spectra from measured ones, based on Geant4 simulation results. To reproduce true bremsstrahlung photon from the 28-GHz ECR ion source we have applied inverse matrix unfolding technique. The unscrambling method will be based on a full geometry Geant4 model of the ECR ion source. Results on the azimuthal angular distributions of bremsstrahlung photons after application of inverse matrix unfolding method will be presented.

### Keywords:

Bremsstrahlung photons, NaI(Tl) detector, ECR ion source, RF power, Unfolding.

## State-of-the-Art Calculation of the Decay Rate of Electroweak Vacuum in the Standard Model

MOROI Takeo<sup>\*1</sup>

<sup>1</sup>University of Tokyo  
moroi@phys.s.u-tokyo.ac.jp

### Abstract:

With the precise determination of the Higgs mass at the LHC, now it is known that the electroweak (EW) vacuum, on which we are living, is unstable if the standard model is valid up to a very high scale. Thus, the understanding of the decay rate of the EW vacuum is an important issue. I will discuss recent progresses in the calculation of the decay rate of the EW vacuum. In particular, I will explain how to take care of artificial divergences which show up when there exist zero-modes around the so-called bounce configuration. I will show the result of the state-of-the-art calculation of the decay rate.

### Keywords:

Standard Model, Decay Rate

## Relaxation Dynamics and Naturalness

KAPLAN David E. \*<sup>1</sup>

<sup>1</sup>Johns Hopkins University  
dkaplan@pha.jhu.edu

### Abstract:

The hierarchy and cosmological constant problems are, and have been for decades, significant sources of inspiration and confusion in particle physics. I will present a new class of solutions to the hierarchy (fine-tuned Higgs mass) problem called the 'relaxion'. Then I will present a new ingredient in general relativity -- using vorticity -- that may finally lead to a viable (and perhaps testable) solution to the cosmological constant problem.

### Keywords:

cosmological constant, Higgs mass, relaxion

## 슈뢰딩거의 고양이는 누가 죽었나?

김상욱\*1

<sup>1</sup>경희대학교 물리학과  
swkim0412@gmail.com

### Abstract:

서양 철학사에서 남아 있는 가장 오래된 문장은 탈레스가 남긴 말이다. "만물은 물로 되어 있다." 이제 우리는 이 말이 틀렸다는 것을 안다. 세상 만물은 원자로 되어 있다. 원자를 설명하는 학문을 양자역학이라 한다. 양자역학은 이상하다. 고양이가 죽어 있으면서 동시에 살아 있다고 한다. 반쯤 죽은 상태라는 말이 아니다. 완벽하게 건강히 살아있으면서 동시에 완전히 죽은 상태에 공존한다는 말이다. 이게 무슨 뜻이냐고? 답을 알고 싶은 사람은 이 강연에 들어오시길 바란다. 강연을 듣고 고양이가 살아 있는지, 아니 죽었다면 누가 죽었는지 답해보시라. 다중우주 이야기는 덤이다.

### Keywords:

양자역학

## 기초광학기구를 활용한 효과적인 색채 실습 방안 제안

정용욱\*<sup>1</sup>

<sup>1</sup>경상대학교 물리교육  
zimusa92@naver.com

### Abstract:

본 연구는 기초광학기구를 활용하는 두가지의 간단한 색채실습 방안들을 제안하였다. 첫째는 편광기를 이용하는 것이고, 둘째는 볼록 렌즈를 이용하는 것이다. 두가지 방법을 통해 각각 색채 혼합, 명도 변화, 채도 변화를 쉽게 구현할 수 있다. 제안된 방법은 물감을 섞는 기존의 색채실습 방법에 비해서 구현하는 과정이 매우 쉽고, 색채의 연속적인 변화 과정의 구현도 용이하다. 또한 구현의 바탕이 되는 물리학 원리도 간단한데, 이를테면 편광기를 활용하는 방법의 경우 말루스 법칙으로, 볼록렌즈를 활용하는 방법의 경우 기초적인 기하광학 지식으로 색채 실습의 원리를 쉽게 설명할 수 있다. 이러한 장점으로 인해, 본 연구의 색채실습 방안은 물리교과와 미술교과 간 융합의 좋은 사례로 STEAM 등의 융합교육에서 활용될 수 있을 것이다.

### Keywords:

편광, 볼록렌즈, 색채 혼합, 명도, 채도, 융합교육

## 물리학과 예술: 문헌 연구를 통한 과학의 미적 가치에 대한 해석과 범주

조현국\*<sup>1</sup>

<sup>1</sup>단국대학교 교양학부  
hjho80@dankook.ac.kr

### Abstract:

본 연구는 과학이 가진 미적 가치와 예술을 통해 나타나는 과학적 해석을 조명함으로써, 최근 주목받고 있는 융복합 및 학제간 연구를 위한 시사점을 제공하고자 한다. 이에 본 연구는 과학교육과 과학사, 과학철학 분야에서 말하는 과학의 미적 특성을 조망하고자, 국제 저명학술지(A&HCI, SSCI 등)에 등재된 학술 연구 논문 100여 편을 대상으로 과학이 가지는 미적 가치가 무엇인지 분류하고 조사하였다. 과학이 가지는 미적 가치를 과학의 본성의 관점에서 해석하고, 이를 통해 오늘날 물리교육에서 융복합적 관점을 통해 얻을 수 있는 교육적 시사점을 개념 이해와 학습의 이론적 측면, 실험과 실습, 과학탐구의 실천적 측면에서 제시하고자 하였다.

### Keywords:

미적 가치, 융복합교육, 과학적 탐구

## Recent results of open heavy flavor measurements in heavy ion collisions with CMS

김현철\*<sup>1</sup>, 문동호<sup>1</sup>  
<sup>1</sup>전남대학교 물리학과  
worldtoi@gmail.com

### Abstract:

The measurement of open heavy flavor production is a attractive tool to study the properties of the hot and dense QCD medium created in heavy ion collisions since heavy quarks are sensitive to the transport properties of the medium and may interact with the QCD matter differently from light quarks.

The comparison between the nuclear modification factors of light and bottom and charm flavored mesons provides insights into the expected flavor-dependent in-medium parton energy loss. In this talk, we will summarize the recent results of measurements on B and D mesons in pp, pPb and PbPb collisions with the CMS detector.

### Keywords:

Open heavy flavor, nuclear modification factor, quark-gluon plasma, heavy quark, energy loss

## Azimuthal Anisotropy in central d+Au collisions at various energies measured in PHENIX at the RHIC

도재현\*1

<sup>1</sup>연세대학교 물리학과  
doddeng@gmail.com

### Abstract:

The study of anisotropic flow provides strong constraints to the evolution of the medium produced in Heavy Ion collisions and its event-by-event geometry fluctuations.

The strength and predominance of these observables have long been related to collective behaviour in the formed medium.

Recent results in small systems both at RHIC and LHC argue for an extrapolation of such mechanisms, however more differential measurements are desirable to have a complete picture.

PHENIX recorded data from d+Au collisions at 200GeV, 62GeV and 39GeV in 2016 using a special trigger which enriches the data size for collisions that are very central.

In this talk I will summarize the most recent measurement in PHENIX using charge particles and additionally present the status of the  $\langle v_2 \rangle$  and  $v_3$  measured at  $-0.5 < \eta < +0.5$ , where we have used as reaction plane detector the newly installed MPCEX preshower detector which provides both high granularity and a large pseudo-rapidity separation in order to reduce non-flow correlations.

### Keywords:

Nuclear physics, RHIC, PHENIX, flow, small system

## Transverse single spin asymmetry for very forward $\pi^0$ production in polarized $p + p$ collisions at $\sqrt{s} = 510$ GeV

김민호\*<sup>1</sup>, 홍병식\*<sup>1</sup>

<sup>1</sup>고려대학교 물리학과

jipangie@korea.ac.kr, bhong@korea.ac.kr

### Abstract:

RHICf forward experiment (RHICf) has measured the transverse single spin asymmetry,  $A_{\{N\}}$ , of very forward  $\pi^0$  productions in polarized  $p + p$  collisions at  $\sqrt{s} = 510$  GeV in the STAR at Relativistic Heavy Ion Collider in June, 2017.  $A_{\{N\}}$  of forward  $\pi^0$  ( $3 < \eta < 4$ ) has been usually described by the interactions between quarks and gluons of the proton in perturbative QCD framework. However, recently a possibility of a potential contribution from the diffractive interaction to the  $A_{\{N\}}$  of  $\pi^0$  have been brought up. Here, new data of RHICf which measured the very forward  $\pi^0$  productions ( $6 > \eta$ ) will play an important role to understand its production mechanism, particularly from diffractive and non-diffractive interactions' points of view. In this presentation, we report our measurement of the very forward  $\pi^0$  with the transverse momentum range up to 1 GeV/c and current analysis status.

### Keywords:

RHICf, forward, spin, asymmetry, pion

## Production of doubly charmed hadrons by recombination in heavy ion collisions

CHO Sungtae\*<sup>1</sup>

<sup>1</sup>Division of Science Education, Kangwon National University  
sungtae.cho@kangwon.ac.kr

### Abstract:

Starting from the discussion on the recent experimental measurements of doubly charmed hadrons in elementary collisions we consider the production of those by recombination in heavy ion collisions. Using the coalescence model we evaluate transverse momentum distributions of doubly charmed hadrons such as  $\Xi_{cc}$  baryons and X(3872) mesons produced from quark-gluon plasma, and show that the transverse momentum distribution of the  $\Xi_{cc}$  baryons is larger than that of the X(3872) meson. We also discuss the ratio of X(3872) mesons to  $\Xi_{cc}$  baryons, and conclude that no enhanced production of the  $\Xi_{cc}$  baryon compared to that of the X(3872) meson at intermediate transverse momenta.

### Keywords:

doubly charmed hadrons, recombination, transverse momentum distributions

## Status of the measurement of electrons from beauty-hadron decays in pp collision at $\sqrt{s} = 13$ TeV in ALICE

KWON Jijyeon\*<sup>1</sup>, KWEON MinJung<sup>1</sup>

<sup>1</sup>인하대학교 물리학과  
y30308@gmail.com

### Abstract:

Heavy quarks (charm and beauty), due to their large masses exceeding the QCD parameter, are produced via hard scatterings in early stage of heavy-ion collisions, compared to the formation time of the Quark-Gluon Plasma (QGP). Due to their long life time, heavy quarks can experience the full evolution of the system created by such collisions. Therefore, heavy quarks are natural probe of the QGP. By separating beauty quarks from charm quarks, the mass dependence of the parton energy loss in the QGP can be studied. To quantify medium effects in heavy ion collisions, measurements in pp collisions are essential as a reference. In addition, the measurements of beauty production in pp collisions can be tests for perturbative QCD calculations. Long lifetime of the beauty hadrons leads larger impact parameter of decay products from beauty hadron. Therefore the electrons from beauty-hadron decays are separated statistically from background electrons based on the track impact-parameter distribution which is wider for the beauty-decay electrons. The excellent vertex and impact-parameter resolution of ITS and electron-identification capability are provided by TPC and TOF in the ALICE experimental setup. We present the current status of the measurements of beauty-decay electrons in pp collisions at  $\sqrt{s} = 13$  TeV in ALICE.

### Keywords:

beauty, electron, pp collisions, ALICE

## Measurement of double helicity asymmetries ( $A_{LL}$ ) in charged pion production at mid-rapidity in longitudinally polarized p+p collisions with PHENIX experiment

문태봉\*<sup>1</sup>

<sup>1</sup>연세대학교 물리학과, <sup>2</sup>RIKEN, <sup>3</sup>PHENIX  
nockinbutter@naver.com

### Abstract:

One of the main goals of the RHIC spin program is the determination of the gluon helicity contribution to the proton spin. This can be accessed by measuring double spin asymmetries ( $A_{LL}$ ) of pion production at mid-rapidity in longitudinally polarized proton collisions with the PHENIX experiment. The ordering of the asymmetries with the charge of the final state pions can in addition directly infer the sign of the gluon spin contribution.

Charged pions are reconstructed in the central PHENIX tracking system. The asymmetries are evaluated between collisions of bunches with the same and opposite helicity after correcting for differences in luminosity and for beam polarizations.

The  $A_{LL}$  measurements of pion production at  $\sqrt{s} = 200$  GeV have been published previously. To extend our understanding of the gluon polarization to a lower gluon momentum fraction ( $x$ ), high statistics data was collected at a higher  $\sqrt{s} = 510$  GeV in 2012–2013.

We present the physics motivation, the analysis procedure and current status of the  $\pi^{\pm}$   $A_{LL}$  measurements at mid-rapidity.

### Keywords:

PHENIX, SPIN, GLUON and  $A_{LL}$

## Hadronic effects on the Tcc abundance in relativistic heavy ion collisions

홍주희\*<sup>1</sup>, 조성태<sup>2</sup>, 송태수<sup>3</sup>, 이수형<sup>1</sup>

<sup>1</sup>연세대학교 물리학과, <sup>2</sup>강원대학교 과학교육과, <sup>3</sup>FIAS, University of Frankfurt and University of Giessen  
juheehong@yonsei.ac.kr

### Abstract:

We investigate the time evolution of the Tcc(1+) abundance in the hadronic stage of relativistic heavy ion collisions using the rate equation. The absorption cross sections of Tcc by pions are calculated in the quasifree approximation. We probe two possible scenarios for the structure of Tcc, where it is assumed to be either a compact multiquark state or a larger sized molecular configuration composed of DD\*. Our numerical results suggest that the hadronic effects on the Tcc production is insignificant, and its abundance strongly depends on the initial yield of Tcc produced in the quark-gluon plasma phase, which will also depend on the assumed structure of the state.

### Keywords:

hadronic effects, relativistic heavy ion collisions

## Production of strange particles in charged jets in Pb-Pb, p-Pb and pp collisions measured with ALICE

KUCERA Vit\*<sup>1</sup>

<sup>1</sup>Department of Physics, Inha University  
vit.kucera@cern.ch

### Abstract:

At intermediate transverse momenta ( $2 \text{ GeV}/c < p_T < 5 \text{ GeV}/c$ ), a strong increase of the baryon-to-meson ratio is observed for inclusive light particles produced in heavy-ion collisions (Pb-Pb) and proton-nucleus collisions (p-Pb) when compared to the ratio measured in proton-proton collisions. Production by fragmentation in vacuum cannot explain this phenomenon. Other hadronisation mechanisms, like coalescence or parton recombination, have been proposed instead. Properties of the hot and dense strongly interacting matter created in ultrarelativistic heavy-ion collisions can be studied using partons created in the first hard scatterings. Their subsequent fragmentation into jets is expected to be modified by their interaction with the medium.

Measurements of spectra of identified particles produced in jets in Pb-Pb and p-Pb collisions can provide further important insights into the interplay of various hadronisation processes which participate in the particle production in the hot and dense medium.

In this contribution, we present the measurements of the  $p_T$  spectra of L baryons

and  $K_S^0$  mesons produced in association with charged jets in Pb-Pb collisions at  $\sqrt{sNN} = 2.76 \text{ TeV}$ , in p-Pb collisions at  $\sqrt{sNN} = 5.02 \text{ TeV}$  and pp collisions at  $\sqrt{s} = 7 \text{ TeV}$ . The results are obtained with ALICE at the LHC, exploiting the excellent particle identification capabilities of this experiment. Baryon-to-meson ratios of the spectra of strange particles associated with jets are compared to the ratios obtained for inclusive measurements and for particles coming from the underlying event.

### Keywords:

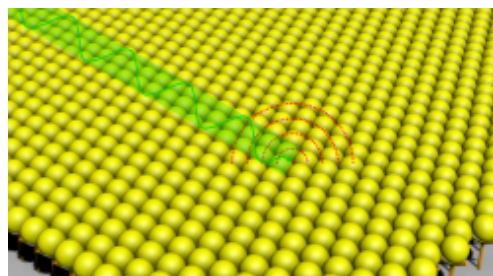
ALICE, collision

## Fabrication and evaluation of MFON-based SERS sensors with high sensitivity and reproducibility

이수현<sup>1</sup>, 유재수\*<sup>1</sup>  
<sup>1</sup>경희대학교 전자공학과  
jsyu@khu.ac.kr

### Abstract:

Recently, Raman spectroscopy has been attracted attention of analytical tools for trace level detection with structural and composite information of molecules. Its advantages such as unique spectral shift corresponding to each molecule, simple pretreatment of sample, and no interference with environments allow practically applicable label-free detection but intensity is inherently weak. To overcome this issue, surface-enhanced Raman scattering (SERS) has been extensively investigated. Noble metal nanoparticles (e.g., Au and Ag) with narrow gap improve Raman scattering and their enhancement factors (EF) are typically reported in the range of  $10^4$ - $10^6$ . Despite of great development in EF of SERS sensors, however, reproducibility is still a big challenge. Since poor reproducibility originates from highly disordered structures, design and fabrication of relatively ordered structures are required. In this presentation, we will introduce various highly sensitive and reproducible metal film over nanostructures (MFON) with their structural and optical properties.



### Keywords:

Surface-enhanced Raman spectroscopy, metal film over nanostructures, sensors.

## Light Soaking Phenomena in Organic-inorganic Mixed Halide Perovskite Single Crystals

정문석\*<sup>1</sup>, 변혜령<sup>1</sup>

<sup>1</sup>성균관대학교 에너지과학과  
mjeong@skku.edu

### Abstract:

Recently, organic-inorganic mixed halide perovskite ( $\text{MAPbX}_3$ ;  $\text{MA} = \text{CH}_3\text{NH}_3^+$ ,  $\text{X} = \text{Cl}^-$ ,  $\text{Br}^-$ , or  $\text{I}^-$ ) single crystals with low defect densities have been highlighted as candidate materials for high efficiency photovoltaics and optoelectronics. Here we report the optical and structural investigations of mixed halide perovskite ( $\text{MAPbBr}_{3-x}\text{I}_x$ ) single crystals. Mixed halide perovskite single crystals showed strong light soaking phenomena with light illumination conditions which were correlated to the trapping and detrapping events from defect sites. By systematic investigation with optical analysis, we found that the pseudocubic phase of mixed halide perovskites generates light soaking phenomena. These results indicate that photo-induced changes are related to the existence of multiple phases or halide migrations.

### Keywords:

light soaking effect, perovskite single crystal, photoluminescence, time-resolved photoluminescence

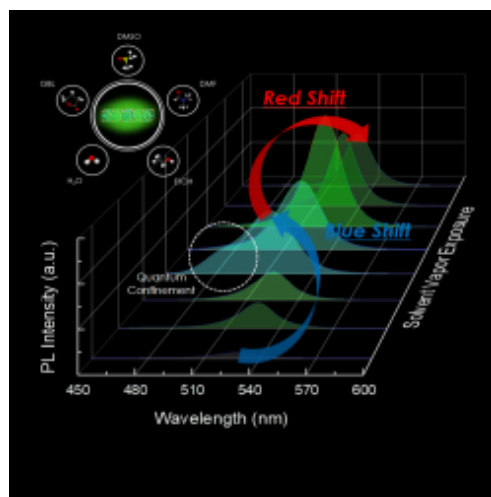
## Effects of Polar Solvent Treatment on the Optical Properties of Organometallic Halide Perovskite

이흥석\*<sup>2</sup>, 이창열\*<sup>1</sup>, 진상현<sup>1, 2</sup>, 최진우<sup>1</sup>, 우희철<sup>1</sup>, 김종현<sup>3</sup>

<sup>1</sup>광주과학기술원, <sup>2</sup>고등광기술연구소, <sup>3</sup>전북대학교, 물리학과, <sup>3</sup>아주대학교, 분자과학기술학과  
hslee1@jbnu.ac.kr, vsepr@gist.ac.kr

### Abstract:

Recently, research interests of organometallic halide perovskites extend to their applications in light emitting diodes (LEDs) due to their facile solution process and excellent optical properties such as high color purity and color tunability. However, the small exciton binding energy of bulk (3D) perovskites leads to easy exciton dissociation that results in low photoluminescence quantum yield (PLQY) which is not favorable for LEDs. Therefore, many efforts to increase exciton binding energy, and thus improve PLQY have been reported. For perovskite films, small grain can spatially confine excitons and promote radiative recombination. For this reason, development of reliable and reproducible methods to control grain size of perovskite films is of great importance for optimizing device performances. In this work, we succeeded to control the size of perovskite grains by polar solvent treatment. The significant enhancement of photoluminescence was observed for perovskite films with polar solvent treatment. Furthermore, the origins of this dramatic improvement in photoluminescence due to grain size changes are further studied by optical characterization and density functional theory (DFT) calculation.



### Keywords:

Organometallic Halide Perovskites, LEDs, Quantum Confinement Effect, Solvent Polarity

## Luminescence properties of $Ba_2LaV_3O_{11}$ phosphors synthesized via citrate sol-gel synthesis

PATNAM Harish Kumar Reddy<sup>1</sup>, LANKAMSETTY Krishna Bharat<sup>1</sup>, 유재수\*<sup>1</sup>

<sup>1</sup>경희대학교 전자공학과  
jsyu@khu.ac.kr

### Abstract:

In recent years, vanadates have been extensively used in various fields such as catalysis, bio activity and energy storage devices because of their excellent chemical, optical and electronic properties. For solid-state lighting applications, the vanadate materials have gained significant attention as self-activated rare-earth ions doped vanadate host materials. Vanadates have a broad band absorption and emission in the ultraviolet and visible regions, respectively owing to the electronic charge transfer between the oxygen 2p orbitals and vacant 3d orbitals of vanadium in the  $VO_4$  tetrahedron. In this presentation, we synthesized rare-earth ions doped  $Ba_2LaV_3O_{11}$  phosphors by a citrate sol-gel method. The surface morphology and phase purity of the  $Ba_2LaV_3O_{11}$  phosphors were determined from the X-ray diffraction (XRD) patterns and scanning electron microscope images, respectively. The results from the XRD data indicate that the synthesized phosphor material was crystallized in the monoclinic phase with the space group  $P21/c$  (14) and the diffraction peaks were well indexed with the standard JCPDS (#49-1137) card values. Finally, the luminescence properties of the rare-earth ions doped  $Ba_2LaV_3O_{11}$  phosphors were studied.

### Keywords:

Vanadate phosphors, Sol-gel method, Luminescence properties

## 준원자층 적층 방법으로 형성된 InAs/GaAs<sub>1-x</sub>Sb<sub>x</sub> 양자점의 광학적 특성

김종수\*<sup>1</sup>, 김민석<sup>1</sup>, 소모근<sup>1</sup>, 고병수<sup>1</sup>, 조현준<sup>1</sup>, 김영호<sup>2</sup>, 이상준<sup>2</sup>, 이승현<sup>3</sup>, HONSBURG Christiana B<sup>4</sup>  
<sup>1</sup>영남대학교, 물리학과, <sup>2</sup>한국표준과학연구원, <sup>3</sup>Department of Electrical and Computer Engineering, Ohio State University, <sup>4</sup>School of Electrical and Computer and Energy Engineering, Arizona State University  
jongsukim@ynu.ac.kr

### Abstract:

Sb조성비에 따른 준원자층(submonolayer) 적층 방법으로 성장된 InAs/GaAs<sub>1-x</sub>Sb<sub>x</sub> 양자점(quantum dots; SML-QDs)의 광학적 특성을 조사 하기 위해, 광발광(photoreluminescence; PL) 및 반사변조분광학(photoreflectance; PR) 실험을 수행하였다. SML-QDs는 분자선에피탁시(molecular beam epitaxy, MBE)에 의해 반 절연성 GaAs(001) 기판 위에 성장되었다. Fig. 1은 실험에 사용된 SML-QDs의 개략적인 구조이다. SML-QDs는 400 nm의 도핑 되지 않은 GaAs 완충층 위에 InAs 0.5 ML와 GaAsSb 2.5 ML를 순차적으로 5층으로 쌓고, 그 위에 20 nm의 GaAs 층을 성장하였으며, 이러한 공정을 총 8번 반복하여 40층의 양자점을 성장하였다. 이러한 구조의 SML-QDs에서 GaAsSb층의 Sb의 조성을 각각 0%, 7.5%, 11.6%, 15.8% 및 19.4%로 변화를 주어 5개의 시료를 성장 하였다. Fig. 2는 다른 Sb 조성비를 갖는 SML-QDs의 12 K에서의 PL 신호이다. Sb의 조성이 0%인 InAs/GaAs SML-QD는 1.41 eV에서 전자-정공 구속 준위에 의한 전이가 관측되며, Sb 조성이 15.8%까지 점차적으로 증가함에 따라 낮은 에너지 쪽으로 PL 신호의 이동이 관측되었다. 이는 Sb 조성이 증가함으로 양자점의 장벽층의 높이가 감소하기 때문으로 판단된다. 특히 11.6%에서 15.8%로 Sb 조성이 증가할 때 급격한 적색편이를 한 경우는 Sb 조성이 약 11.6% 이상에서 InAs/GaAsSb 이중접합구조가 type-II 띠 구조 형태로 전환된 결과로 사료된다. 그러나 Sb 조성이 15.8%에서 19.4%로 증가하는 경우 PL 신호가 다시 높은 에너지 쪽으로 이동하였다. 이것은 type-II 띠 구조에서 InAs 층의 전도대와 GaAsSb 층의 가전자대의 띠 겹침 현상으로 사료된다. Fig. 3은 300 K 에서 측정된 SML-QDs의 PL 신호이다. 신호 'A'는 저온에서 관측된 양자점 관련 신호이며 온도 의존성 PL 실험 결과 저온 영역에서 관측되지 않았던 신호 'B'가 상온 영역에서 추가적으로 관측되었다. B 신호의 위치는 Sb의 조성의 변화에 무관하게 거의 동일한 위치에서 관측 되었다. B 신호의 근원을 조사하기 위하여 온도 및 광세기 의존성 PL 및 PR 실험을 추가적으로 수행 하였다.

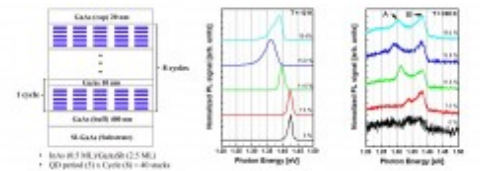


Fig. 1. Schematic sample structure of InAs/GaAsSb/GaAs submonolayer quantum dots (SML-QDs).

Fig. 2. Low temperature PL spectra for InAs/GaAsSb SML-QD with various Sb compositions.

Fig. 3. Room temperature PL spectra for InAs/GaAsSb SML-QD with various Sb compositions.

### Keywords:

3-5, semiconductor, GaAs, InAs, GaAsSb, Sb-Composition

## Optical Properties of InAs/GaSb Multiple Quantum Wells Using Photoreflectance Spectroscopy

ALYAMANI Somaya<sup>1</sup>, 김종수\*<sup>1</sup>, 조현준<sup>1</sup>, 소모근<sup>1</sup>, 신재철<sup>1</sup>, 구대현<sup>1</sup>, 이상준<sup>2</sup>, 김준오<sup>2</sup>  
<sup>1</sup>영남대학교 물리학과, <sup>2</sup>한국표준과학연구원  
jongsukim@ynu.ac.kr

### Abstract:

We have investigated optical properties of the InAs/GaSb type-II multiple quantum wells (MQWs) with 3 and 5 ML of InAs by photoreflectance (PR) and photoluminescence (PL) spectroscopy with various temperatures. The InAs MQW was embedded in 50 nm of GaSb matrix by molecular beam epitaxy. In the PR, we used a tungsten-halogen lamp, a Si (400 ~ 1100 nm: high energy region) and InGaAs (1200 ~ 2600 nm: low energy region) photodiodes.

The PR was employed to investigate the inter-band transitions such as their quantum states (QS) [Figure 1]. The position of PL signal of InAs/GaSb 5 ML MQW was similar to the PR signal. The 15 K PL results showed the transitions between confined electrons states in InAs QW and GaSb valence band at an energy of 0.506 eV. The PR spectra were measured at temperatures ranging from 10 to 180 K [Figure 2]. The PR signals of QS and GaSb layer were red-shifted with increasing temperature.

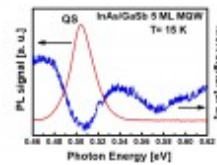


Figure 1: Compare the PR and PL spectra of InAs/GaSb 5 ML MQW at temperatures

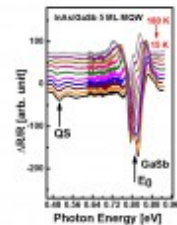


Figure 2: The PR spectra were measured at temperatures ranging from 10 to 180 K.

### Keywords:

semiconductors, quantum well, photoreflectance, GaSb, InAs

## The investigation of interfacial Properties in ALD\_high-k dielectric on oxidized black phosphorus

조만호\*<sup>1</sup>, 김대경<sup>1</sup>, 채지민<sup>1</sup>, 홍석보<sup>1</sup>, 박한범<sup>1</sup>

<sup>1</sup>Department of Physics, Yonsei University  
mh.cho@yonsei.ac.kr

### Abstract:

We investigated the change in the interfacial reaction to between time dependent exposed black phosphorus (BP) surface and high-k dielectric ( $\text{HfO}_2$  and  $\text{Al}_2\text{O}_3$ ) grown by the atomic layer deposition (ALD) process. The electronic structure and field effect transistors characteristics analysis on oxidized phosphorus species before and after high-k dielectric deposition were evaluated using various surface analysis tools and TFT device. We observed that phosphorus oxide species ( $\text{P}_x\text{O}_y$ ) were reduced during the  $\text{Al}_2\text{O}_3$  process. Moreover, field effect properties of  $\text{Al}_2\text{O}_3$  on oxidized black phosphorus showed that the enhancing electrical characteristics at the 24 h of exposure time in BP surface. These results of surface reaction between the ALD- $\text{Al}_2\text{O}_3$  process and oxidized BP provide understanding of reduction process of oxidized phosphorus species by the ALD reaction process and enhancing oxidized BP FET characteristics.

### Keywords:

black phosphorus, ALD, TFT, electronic structure

## Enhancement in thermoelectric properties of Te-embedded $\text{Bi}_2\text{Te}_3$ by enhancement in phonon scattering at heterostructure interface

조만호\*<sup>1</sup>, 정광식<sup>1</sup>, 최혜진<sup>1</sup>, 채지민<sup>1</sup>, 박한범<sup>1</sup>, 백주혁<sup>1</sup>, 김태현<sup>1</sup>, 송재용<sup>2</sup>, 정광호<sup>1</sup>, 김종훈<sup>1</sup>, 박재현<sup>3</sup>  
<sup>1</sup>연세대학교, 물리학과, <sup>2</sup>한국표준과학연구원, 융합물성측정센터, <sup>3</sup>포항공대, 포항가속기연구소  
mh.cho@yonsei.ac.kr

### Abstract:

A comprehensive understanding of the nano-structural effects that cause reduction in thermal conductivity represents important challenges for the development of thermoelectric materials with an improved figure of merit (ZT). Bismuth telluride ( $\text{Bi}_2\text{Te}_3$ )-based thermoelectric materials exhibit high ZT by very low levels of thermal conductivity in bulk. For improve thermoelectric properties  $\text{Bi}_2\text{Te}_3$ , in this study, a Te crystal-embedded  $\text{Bi}_2\text{Te}_3$  ( $\text{Te-Bi}_2\text{Te}_3$ ) thin film was formed by establishing a specific annealing temperature for a Te-rich Bi/Te multilayered structure for enhance phonon scattering. Modulations in structure and composition were observed at the boundaries between the two phases of Te and  $\text{Bi}_2\text{Te}_3$ . Furthermore, the samples contained regularly shaped nanometer-scale  $\text{Bi}_2\text{Te}_3$  single grains. Therefore, we obtained a dramatic ZT value of 2.27 (+0.04, -0.08) at 375 K from the  $\text{Te-Bi}_2\text{Te}_3$  thin film. By compare to  $\text{Te-Bi}_2\text{Te}_3$  with porous  $\text{Bi}_2\text{Te}_3$ , we confirmed that interface phonon scattering between the  $\text{Te-Bi}_2\text{Te}_3$  boundaries plays an important role in inter-grain phonon transport, which results in a reduction in the lattice thermal conductivity.

### Keywords:

$\text{Bi}_2\text{Te}_3$ , Thermoelectric, nano-structure

## From Micronsize Coulter Cell Counter to Nanometer size plasmonic pore sensor for Single molecule analysis

최성수\*<sup>1</sup>

<sup>1</sup>선문대학교 물리학과  
sscphy2010@gmail.com

### Abstract:

About 60 years ago, a cell counter by using an electrical detection technique via micron-size orifice was invented by Dr. Coulter. Presently, due to fast developing nanofabrication technology, the solid state SiN pore device called MINion for genome sequencing was launched into the commercial market by Oxford Nanopore Technology. However, the high error rate from this nanometer size pore device was reported by journal such as Nature, etc. Furthermore, many biosensors are utilizing the optical detection technique. Hence, we are trying to develop the optical nanopore device for single-molecule analysis.

In order to obtain the high optical intensity, the nanopores surrounded with the periodic groove patterns, or the periodic aperture array have been fabricated on the Au membrane for plasmonic enhancement. Then, the Au apertures have been treated under electron beam irradiation for forming the Au-C nanopore.

### Keywords:

Coulter cell counter, nanopore, plasmonic optical sensor, electron beam irradiation

## Floating buoy-based triboelectric nanogenerator for a vibrational energy harvesting from water waves in sea

김동영<sup>1</sup>, 김현수<sup>1</sup>, 공대술<sup>1</sup>, 정중훈\*<sup>1</sup>  
<sup>1</sup>인하대학교 물리학과  
jhjung@inha.ac.kr

### Abstract:

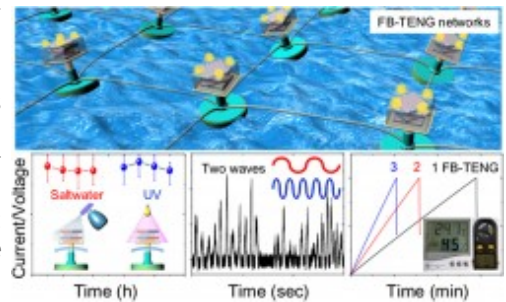
Energy harvesting from water waves has been reinforced due to their unique characteristics of insensitivity to weather, season, and sunlight. To date, a variety of wave energy converting devices and machines have been proposed and installed, such as a direct-drive point absorber and a Pelamis wave energy converter. But, such electromagnetic- and hydraulic pump-based generators usually require enormous cost, long time for construction, and large space in sea.

A friction- and induction-based new device, called a triboelectric nanogenerator (TENG), has been proposed recently and demonstrated the effective mechanical energy harvesting from water waves. However, a TENG in sea must harvest energy under various conditions, such as irregular amplitude and frequency of water waves, coming from all directions.

We designed a TENG system on a floating buoy. The floating buoy-based TENG (FB-TENG) consists of an acryl packed power generation unit, a height-adjustable support, and a floating buoy. The support enables the power generation unit to vibrate vigorously even for small amplitude of water waves. The acrylic protection of the power generation units allows the FB-TENG to generate stable power even under the saltwater, strong ultraviolet irradiation, and thermal shocks.

### Keywords:

Floating buoy, Triboelectric nanogenerator, Water waves in sea, Self-powered sea mark, Self-powered weather monitoring system



## Wet-transfer of colloidal quantum dot thin films and its application

전현수\*<sup>1</sup>, 한창현<sup>1</sup>, 정현호<sup>1</sup>, 이명재<sup>1</sup>, 이종호<sup>1</sup>, 박연상<sup>2</sup>, 조경상<sup>2</sup>

<sup>1</sup>서울대학교 물리천문학부, <sup>2</sup>삼성종합기술원  
hsjeon@snu.ac.kr

### Abstract:

콜로이드 양자점은 최근 각광받고 있는 나노 발광 물질로서 저비용 합성, 파장 가변성, 높은 양자 효율 등의 장점을 가지고 있다. 콜로이드 양자점으로 이루어진 박막 형성 및 전사를 위한 다양한 기술들이 개발되어 왔다. 그러나 기존의 박막 형성 및 전사기술들은 기판에 맞닿은 구조만 제작할 수 있는 한계가 있었다. 본 연구는 콜로이드 양자점으로 이루어진 박막을 습식 방법으로 다른 기판에 전사하는 방법을 시연하였다. 전사 과정 동안 박막의 구조를 유지하기 위해 고분자 막을 지탱하는 용도로 사용하였다. 이 기술을 이용해서 유연한 기판으로의 전사는 물론 서로 다른 종류의 양자점으로 구성된 이중접합 구조를 구현하였다. 그리고 1차원 표면 그레이팅이 형성된 기판에 전사함에도 불구하고 콜로이드 양자점으로 이루어진 박막의 형태가 잘 유지될 뿐만 아니라 이 구조에서 단일 모드의 DFB(distributed feedback) 레이저가 발진하는 것도 확인하였다.

### Keywords:

Colloidal quantum dot, DFB laser

# Finite Element Method Analysis of Rectangular-type DC Electromagnetic Pump for Active Heat Decay Removal system of Prototype Gen-IV Sodium Fast Reactor

LEE GeunHyeong\*<sup>1</sup>, KIM HeeReyoung<sup>1</sup>

<sup>1</sup>울산과학기술원 원자력공학과  
studiousgh@unist.ac.kr

## Abstract:

A rectangular-type direct current (DC) electromagnetic pump was analyzed for an active heat decay removal system (ADHRS) of prototype Gen-IV sodium fast reactor (PGSRF) with finite element method (FEM). The pump for the circulation of sodium in the ADHRS requires the developed pressure of 2 kPa and flowrate of 0.02 m<sup>3</sup>/s at a temperature of 499 K. The DC electromagnetic pump produce the developed pressure from Lorentz's force by the vector product of the current density and magnetic flux density unlike mechanical pumps for the circulation of sodium. The advantages of electromagnetic pumps are no moving and sealing parts while eliminating the possibility of liquid-metal leak. Therefore, ADHRS, where the liquid sodium with high electrical conductivity and strong chemical reaction property flows, considers the electromagnetic pump to remove active decay heat. The DC electromagnetic pump is analyzed by finite element method in order to figure out distribution of current density and magnetic flux density. In conclusion, the design variables of DC electromagnetic pump for ADHRS is optimized.

## Keywords:

Magnetohydrodynamic, Electromagnetic pump, Active heat decay removal system, Sodium fast reactor.

## Performance Analysis of Annular Linear Induction Electromagnetic Pump on the Change of Input Power and Frequency

곽재식\*<sup>1</sup>

<sup>1</sup>울산과학기술원 기계 및 원자력 공학부  
sikjae10@unist.ac.kr

### Abstract:

An annular linear induction electromagnetic pump (ALIP) with a mass flowrate of 20 kg/s and a developed pressure of 4 bar was designed and fabricated to test the performance of the components of a sodium-cooled fast reactor (SFR) in a sodium thermal hydraulic experimental loop.

An electromagnetic pump having simple structure in terms of safety and maintenance, which is operated without contacting working sodium of strong chemical reaction property, is considered for the generation of sodium flow satisfying easy control of flow rate.

In this study, sodium transport experiments in the sodium loop is performed to test the characteristic of the electromagnetic pump in the various conditions of input power and frequency. As a result, mass flowrate and developed pressure are analyzed on the change of input power and frequency, and the relationships of those are verified based on magnetohydrodynamics.

### Keywords:

Sodium-cooled Fast Reactor, Electromagnetic pump, Magnetohydrodynamics

## What is possible limiting factor on high efficiency CZTSSe solar cell?

김성연<sup>1</sup>, 김준호\*<sup>1</sup>

<sup>1</sup>인천대학교 물리학과  
jhk@incheon.ac.kr

### Abstract:

We investigated limitation factors of high efficiency  $\text{Cu}_2\text{ZnSn}(\text{S},\text{Se})_4$  (CZTSSe) solar cells, where the CZTSSe absorbers were made by using sulfo-selenization process. We found that limiting factors were different depending on the S/(S+Se) ratios. CZTSSe absorbers with two S/(S+Se) ratios,  $\sim 0.12$  (Se-rich) and  $\sim 0.22$  (S-increased), were prepared by varying the sulfo-selenization temperature. The Se-rich CZTSSe solar cells were found to have larger conduction band offset (CBO) between the absorber and the buffer. Considering that the larger CBO prevents electron transport from absorber to buffer and resultantly reduces short circuit current and fill factor, it could be possible limitation factor of the high efficiency solar cell. Contrary to Se-rich solar cells, S-increased solar cells showed reduced CBO and no kinked J-V curve. However, deep defects were found to be generated, which induced defect centers of charge recombination both at interface and in bulk of the absorber. The larger CBO in Se-rich CZTSSe solar cell and deep defects in S-increased CZTSSe solar cell are observed even in  $\sim 12\%$  efficiency solar cells. Thus, we believe that these possible limitation factors should be resolved to achieve high efficiency kesterite CZTSSe solar cell above 12%.

### Keywords:

Limiting factor, Conduction band offset, Defect states, CZTSSe solar cell

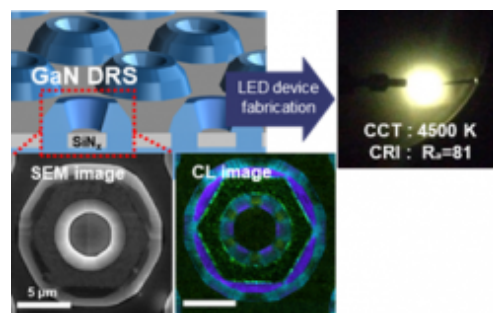
## Electrically driven, Phosphor-Free Warm White Light-Emitting Diodes based on InGaN/GaN Dodecagonal Ring Structure

심영출<sup>1</sup>, 최성한<sup>1</sup>, 여환섭<sup>1</sup>, 우기영<sup>1</sup>, 이상원<sup>1</sup>, 송현규<sup>1</sup>, 조용훈\*<sup>1</sup>

<sup>1</sup>한국과학기술원(KAIST), 물리학과  
yhc@kaist.ac.kr

### Abstract:

The correlated color temperature (CCT) and the color rendering index (CRI) are becoming the most important factors of white lighting emitting diodes (WLEDs) for the lighting application. In the case of the conventional WLEDs based on the c-plane planar structure which are phosphor-converted LEDs, the red phosphors are required to fabricate warm WLEDs with low CCT ( $< 4,500$  K) and high CRI ( $R_a > 75$ ). However, the most phosphors for red emitting are rare-earth elements, and using phosphors leads to degradation problems with decreased luminous efficiency with unintentional change of light color. In order to avoid problems related to phosphors, phosphor-free WLEDs based on gallium nitride (GaN) three-dimensional (3D) structures are considered as a promising candidate. In spite of the significant results, there still are the low-efficiency issue in long visible spectral range since the indium gallium nitride (InGaN) multiple quantum wells with high indium composition are located on c-plane of 3D structure which contains high polarization field. In this work, we proposed the InGaN/GaN dodecagonal ring structure fabricated by selective area growth and wet etching method. This combined method reduces a polarization field with a strain relaxation and forms the inversed semi-polar facet with high indium composition in 3D structure. Conclusively, the phosphor-free white LEDs are successfully demonstrated with the high luminescence efficiency under current injection.



### Reference

- [1] S. H. Lim, Y. H. Ko, C. Rodriguez, S. H. Gong, and Y. H. Cho, *Light: Science & Applications* 5, e16030 (2016).
- [2] Y. H. Ko, J. Song, B. Leung, J. Han, and Y. H. Cho, *Scientific Reports* 4, 5514 (2014).
- [3] Y. C. Sim, S. H. Lim, Y. S. Yoo, M. H. Jang, S. Choi, H. S. Yeo, K. Y. Woo, S. Lee, H. G. Song, and Y. H. Cho, *Nanoscale*, 10.1039/C7NR08079D (2018).

### Keywords:

Phosphor-free, white LEDs, InGaN, GaN, 3D structure

## Self-rectifying Nanoporous Ta<sub>2</sub>O<sub>5-x</sub> Synaptic Device for High Recognition Accuracy in an Artificial Neural Network

왕건욱\*<sup>1</sup>, 최상현<sup>1</sup>, 장성훈<sup>1</sup>, 문정환<sup>2</sup>, 김종찬<sup>3</sup>, 정후영<sup>3</sup>, 장평화<sup>1, 2</sup>, 이경진<sup>1, 2</sup>

<sup>1</sup>Korea University, KU-KIST Graduate School of Converging Science & Technology, <sup>2</sup>Korea University, Department of Materials Science and Engineering, <sup>3</sup>Ulsan National Institute of Science and Technology (UNIST), UNIST Central Research Facilities and School of Materials Science and Engineering  
gunukwang@korea.ac.kr

### Abstract:

Memristor, that consists of a simple metal-oxide layer sandwiched between two conductors, is being greatly envisioned as a technical platform to imitate the principal of biological synapse system due to its nonlinear and dynamic electrical characteristics depending on the history of applied electrical programming [1,2]. In this study, we fabricated the nanoporous (NP) Ta<sub>2</sub>O<sub>5-x</sub> memristor device by an anodic treatment in the room temperature and utilized the device as the two-terminal artificial synapse. The device exhibits a stable self-rectifying I-V switching behavior with  $\sim 10^3$ - $10^4$  nonlinearity, which can effectively prevent the undesired neural signals in the densely-integrated synaptic array structure. By the electrical programming with the different voltage polarities, the density of oxygen vacancies that mainly existed at the interface between Pt top electrode and the NP Ta<sub>2</sub>O<sub>5-x</sub> layer can be changed, which means the interfacial Schottky barrier can be modulated depending on the applied voltage. Based on the analog modulation of the Schottky barrier by diverse electrical stimuli, the essential synaptic functions such as short- or long-term synaptic plasticity and spike timing dependent plasticity (STDP) were successfully mimicked. In addition, we investigated the influence of the nonlinearity (namely the degree of asymmetry) of the self-rectifying synapse on the accuracy of the pattern recognition using the ANN (artificial neural network) simulation with consideration of the delta rule algorithm. A higher nonlinearity results in an increase of the accuracy of the handwritten digit recognition and can effectively reduce the probability of unwanted neural signals in an artificial neural network. Our self-rectifying nanoporous Ta<sub>2</sub>O<sub>5-x</sub> synaptic device achieved high recognition accuracy even at few epochs of the training. Taken all together, we believe the self-rectifying NP Ta<sub>2</sub>O<sub>5-x</sub> synapse with high nonlinearity can provide a route toward the high-learning accuracy and the time-efficient neuromorphic computing technology.

[1] Wang, G.; Lee, J. H.; Yang, Y.; Ruan, G.; Kim, N. D.; Ji, Y.; Tour, J. M. *Nano Lett.* 2015, 15, 6009-6014.

[2] S. Kwon<sup>+</sup>, T.-W. Kim<sup>+</sup>, S. Jang, J.-H. Lee, N. D. Kim, Y. Ji, C.-H. Lee, J. M. Tour<sup>\*</sup>, and G Wang<sup>\*</sup>, *ACS Appl. Mater. Interfaces*, 2017, 9, 34015.

### Keywords:

Memristor, Nanoporous, Self-rectifying, Pattern recognition, neuromorphic computing

## Tunable, High-Performance Switching in Silicon-Oxide( $\text{SiO}_x$ ) Memristor Enabled by a Vertically Integrated Graphene Barristor

최재완<sup>1</sup>, 왕건욱\*<sup>1</sup>, 김남동<sup>2</sup>

<sup>1</sup>고려대학교, KU-KIST 융합대학원, <sup>2</sup>KIST, 양자응용복합소재연구센터  
gunukwang@korea.ac.kr

### Abstract:

Metal-oxide resistive memristor has risen rapidly as a strong candidate for future nonvolatile random access memory. Previously, we demonstrated the unipolar switching feature through Si-phase in the silicon oxide ( $\text{SiO}_x$ ) matrix in diverse junction structure with  $\sim 10^7$  on/off ratio, nanosecond switching speed, and nanoscale switching filament[1-3]. However, the device commonly has a relatively high programming voltage and is inherent in the uncertainty of the switching in the nanosecond operating, resulting in the reduction of the switching reliability and the increase of the energy consumption for the completion of the switching. Here, we proposed a novel approach to improve the switching performance and the reliability by using an integrated junction structure composing of the  $\text{SiO}_x$  memristor and the graphene barristor in a vertical architecture form. In graphene barristor, a gate bias can effectively change the height of a Schottky barrier formed at a graphene/semiconductor heterojunction by varying graphene's Fermi level, so that it controls total amount of current through that junction[4]. Under a positive gate bias, the Schottky barrier is lowered, then the switching transition can be occurred at the lower programming voltage. We found that the programming voltage is decreased from 4.5( $\sim 5$ ) V to 3 V at  $V_G = 6$  V. In addition, a high reliability of nanosecond switching operating is achieved. Our approach can provide a simple way to enhance the switching performance of the  $\text{SiO}_x$  memristor.

**Acknowledgments** This work was accomplished with financial support from the National Research Foundation of Korea, the KU-KIST research fund, and the Korea University Future Research Grant.

**References** [1] G. Wang, Y. Yang, J.-H. Lee, V. Abramova, H. Fei, G. Ruan, E. L. Thomas and J. M. Tour, Nano Lett, 14(8), 4694-4699 (2014)

[2] G. Wang, A.-R. O. Raji, J.-H. Lee, and J. M. Tour, ACS Nano, 8(2), 1410-1418 (2014)

[3] S. Kwon, S. Jang, J.-W. Choi, S. Choi, S.-J. Jang, T.-W. Kim and G. Wang, Nano Lett, 17, 7462-7470 (2017)

[4] H.-J. Yang, J.-S. Heo, S.-J. Park, H.-J. Song, H. Seo, K.-E. Byun, P. Kim, I.-K. Yoo, H.-J. Chung and K.-N. Kim, Science, 2012, 336, 1140-1143 (2012).

### Keywords:

Memristor, Silicon oxide memory, Graphene, Barristor

## Giant Temperature Coefficient of Resistivity and Cryogenic Sensitivity in Silicon with Galvanically Displaced Gold Nanoparticles in Freeze-Out Region

장재원\*<sup>1</sup>

<sup>1</sup>부경대학교 물리학과  
jjang@pknu.ac.kr

### Abstract:

The temperature coefficient of resistivity (TCR) and cryogenic sensitivity ( $S_V$ ) of p-type silicon (p-Si) in the low-temperature region (10–30 K) are remarkably improved by increasing the coverage of galvanically displaced Au nanoparticles (NPs). By increase of the galvanic displacement time from 10 to 30 s, the average surface roughness ( $R_a$ ) of the samples increases from 0.31 to 2.31 nm and the coverage rate of Au NPs increases from 3.1% to 21.9%. In the freeze-out region of the sample, an up to 103% increase of TCR and dramatically improved  $S_V$  of p-Si (~5813%) are observed with Au coverage of 21.9% compared to p-Si without galvanically displaced Au NPs. By means of a finite element method (FEM) simulation study, it was found that the increase of surface roughness and a number of Au NPs on p-Si results in a higher temperature gradient and thermoelectric power to cause the unusual TCR and  $S_V$  values in the samples.

### Keywords:

silicon surface, gold nanoparticle, temperature coefficient of resistivity, cryogenic sensitivity, galvanic displacement

## Control of coupled and decoupled surface channels through disorder in thin films of topological insulator

조만호\*<sup>1</sup>, 박한범<sup>1</sup>, 채지민<sup>1</sup>, 홍석보<sup>1</sup>, 정광식<sup>1</sup>

<sup>1</sup>연세대학교 물리학과  
mh.cho@yonsei.ac.kr

### Abstract:

Topological insulator (TI) films in which the Fermi level is located in the conduction band due to unintentional defects exhibit strong surface-bulk coupling. Such surface-bulk coupling can also connect the top and bottom topological surfaces without decoherence, which is called inter-surface coupling. In this study on the transport properties of Bi<sub>2</sub>Se<sub>3</sub> films, we observe a crossover between coupled and decoupled surface transport channels through intentional disorder controlled by a post-annealing process. Disorder causes the electrons of the topological surfaces to rapidly lose their coherence as they tunnel to the opposite surfaces. Consequently, we observed that more disordered Bi<sub>2</sub>Se<sub>3</sub> films exhibit shorter penetration of the surfaces into the bulk and weaker inter-surface coupling. In previous studies, the role of disorder has generally been considered as a source of surface-bulk scattering. However, our results indicate that it must be considered as a source of decoherence.

### Keywords:

Topological insulator, Thin film, Weak-antilocalization

## Multi-dimensional memristive system: ferroelectric oxide with 2-dimensional sheets

조일렴\*<sup>1</sup>, 진혜진<sup>1</sup>, 윤우영<sup>1</sup>  
<sup>1</sup>이화여자대학교 물리학과  
wmjo@ewha.ac.kr

### Abstract:

In ferroelectric oxide system, memristive switching can be obtained by controlling polarization states resulting in change of barrier height [1,2]. For transition metal oxide system, interface is critical to introduce memristive switching. From this point of view, we exploited ferroelectric oxide thin films with 2-dimensional transition metal dichalcogenides (TMDCs) by considering interaction between dipole-bound charges between two materials [3,4]. By utilizing ferroelectrics, barrier height can be controlled and we can control interface relatively easily just inserting the 2-dimensional TMDCs. We fabricated ferroelectric PbTiO<sub>3</sub> thin films by using pulsed laser deposition and semiconducting TMDCs by exfoliation method resulting in multi-dimensional system for memristor. Especially, *n*-type MoS<sub>2</sub> and *p*-type WSe<sub>2</sub> were used as the semiconducting TMDCs to give movable charged at the interface. To characterize the resistive switching, conductive-atomic force microscopy (C-AFM) was used. Especially, polarization dependent switching behavior was obtained to figure out charge of barrier height which behave important role to give the switching behavior. In addition, photocurrent was obtained by using C-AFM with light illumination to find possibility of photovoltaic devices with switching behavior. As a result, we suggested new memristive system consisting of ferroelectric oxide thin films with 2-dimensional atomic sheets.

- [1] S. He *et al.*, "Impact of interfacial effects on ferroelectric resistance switching of Au/BiFeO<sub>3</sub>/Nb:SrTiO<sub>3</sub>(100) Schottky junctions", *RSC Adv.* **7**, 22715 (2017).  
[2] X. Chen *et al.*, "Ferroelectric memristive effect in BaTiO<sub>3</sub> epitaxial thin films", *J. Phys. D: Appl. Phys.* **47**, 365102 (2014).  
[3] H. J. Jin, W. Y. Yoon, and W. Jo, "Control of work function of MoS<sub>2</sub> assisted by ferroelectric polarization with honeycomb-like structures", *Appl. Phys. Lett.* **110**, 191601 (2017).  
[4] H. J. Jin, W. Y. Yoon, and W. Jo, "Virtual out-of-plane piezoelectric response in MoS<sub>2</sub> layers controlled by ferroelectric polarization", *ACS Appl. Mater. Interfaces* **10**, 1334 (2018).

### Keywords:

Memristive switching, Ferroelectrics, Transition metal dichalcogenides

## Self-expanding electrochemically written nano-patterns with high retention in LaMnO<sub>3</sub> thin films

김용진<sup>1</sup>, 양찬호\*<sup>1, 2</sup>

<sup>1</sup>Department of physics, KAIST, <sup>2</sup>Institute for the NanoCentury, KAIST,  
chyang@kaist.ac.kr

### Abstract:

Scanning probe microscopy (SPM) based nanofabrication has received attention due to potential application in the miniaturization of electric devices [1]. Application of this technology to perovskite oxides is attractive considering rich physical properties such as colossal magnetoresistance and high- $T_C$  superconductivity [2]. In addition, the high electrochemical activity of the perovskite oxides allows the SPM lithography using a low voltage [1,3]. However, the relaxation of the nano-patterns has been reported in the perovskite oxides and the short retention has been a disadvantage of the potential applications [4,5]. In this study, we study electrochemical nanoscale patterning in LaMnO<sub>3</sub> thin films. As a parent material of colossal magnetoresistance, LaMnO<sub>3</sub> is an A-type anti-ferromagnetic (Néel temperature ~ 140 K) insulator [6]. We have found a positive biased tip induces height expansion in surface topography and charge accumulation. The deformed surface expands further and the expansion is saturated after ~7 days. We confirm the deformed surface can retain more than a year keeping the charge accumulation. We presume a slow chemical transport in LaMnO<sub>3</sub> would stabilize the electrochemically written nano-patterns. Our finding will offer useful information for the stabilization of the nano-patterns.

[1] X. N. Xie *et al.*, *Mater. Sci. Eng. R.* **54**, 1 (2006).

[2] E. Dagotto, *Science* **309**, 257 (2005).

[3] J.Hwang *et al.*, *Science* **358**, 751 (2017).

[4] R.-W. Li *et al.*, *Appl.Phys.Lett.* **84**, 2670 (2004).

[5] Y. Liu *et al.*, *J.Vac.Sci.Techol. B* **28**, 407 (2010).

[6] C. Ritter *et al.*, *Phys. Rev. B*, **56**, 8902 (1997).

### Keywords:

SPM lithography, LaMnO<sub>3</sub>, Retention

## Study of Quantum Tunneling Charge Transfers between Molecules and Semiconductors for Surface enhanced Raman Spectroscopy

윤석현\*<sup>1</sup>, 김자영<sup>1</sup>, 김혜민<sup>1</sup>, 김남중<sup>2</sup>, 박준범<sup>2</sup>, 이규철<sup>2</sup>  
<sup>1</sup>이화여자대학교 물리학과, <sup>2</sup>서울대학교 물리학과  
syoon@ewha.ac.kr

### Abstract:

Surface enhanced Raman spectroscopy (SERS) has been intensively studied during the past decades for its enormous electromagnetic field enhancement near the nanoscale metallic surfaces. Chemical enhancement of SERS, however, remains elusive despite intensive research efforts, mainly due to the relatively complex enhancing factors and inconsistent experimental results. We used high-quality ZnO nanostructures/graphene substrates to provide an ideal SERS environment and to understand the charge transfer (CT) mechanisms of SERS. In addition to discovering the optimal conditions for CT processes, the ZnO surface are coated with nanoscale HfO<sub>2</sub> layers to reveal the quantum tunneling behaviors of the photo-generated electrons through the oxide barrier. By monitoring SERS signals as a function of spacing between the molecules and the semiconductor surface, a characteristic CT decay range can be revealed on the order of a few nanometers. A unique quantum oscillation of SERS intensity is also found in the atomically thin oxide layers, which reflects Ramsauer-Townsend effects occurring in a solid-state environment.

### Keywords:

surface-enhanced Raman scattering; chemical enhancement; charge transfer; ZnOnanostructures; quantum tunneling

## In-Plane Direction of Thermoelectric Figure of Merit for *p*-Type BST( $\text{Bi}_{0.5}\text{Sb}_{1.5}\text{Te}_3$ ) Thin Films with Temperature Dependence Approaching 500 K

이상권\*<sup>1</sup>, 박노원<sup>1</sup>, 이원용<sup>1</sup>, 강수영<sup>1</sup>, THI Thu Bui Trang<sup>1</sup>, 윤요섭<sup>1</sup>, 석주희<sup>1</sup>, 김길성<sup>1</sup>, 강민성<sup>1, 2</sup>  
<sup>1</sup>중앙대학교 물리학과, <sup>2</sup>중앙대학교, 신기능이미징 연구소  
sangkwonlee@cau.ac.kr

### Abstract:

Thin-film-based thermoelectric (TE) materials are also very useful for future TE devices. Typically, the  $\text{Bi}_{0.5}\text{Sb}_{1.5}\text{Te}_3$  (BST) material is widely used as an anisotropic *p*-type thermoelectric (TE) material. However, very limited information is available regarding the in-plane figure of merit (*ZT*) of BST thin films, including the in-plane thermal conductivity, Seebeck coefficient, and electrical conductivity of the film. This work examines the in-plane *ZT* properties of *p*- $\text{Bi}_{0.5}\text{Sb}_{1.5}\text{Te}_3$  thin films prepared by radio frequency sputtering at room temperature. Based on the measured thermoelectric properties including the in-plane thermal conductivity, Seebeck coefficient, and electrical conductivity, a maximum *ZT* value of 1.01 at 390 K was obtained for these annealed *p*-BST thin films

### Keywords:

Figure-of-Merit, Thermal Conductivity, Seebeck Coefficient, Electrical Conductivity, 3- $\omega$  Technique, Thermal Transport

## Control of unidirectional anisotropy in exchange biased AFM/FM bilayers by piezoelectric strains

김현중<sup>1</sup>, 홍정일\*<sup>1, 2, 3</sup>

<sup>1</sup>Department of Emerging Materials Science, DGIST, <sup>2</sup>Global Center for Bio Convergence Spin Systems, DGIST, <sup>3</sup>Research Center for Emerging Materials, DGIST  
jihong@dgist.ac.kr

### Abstract:

Controlled manipulation of magnetic anisotropy has a practical potential in many applications involving magnetic films, thereby related research has been actively sought in recent years. As one of the control mechanism, modulation of unidirectional anisotropy in exchange coupled FM/AFM structure by mechanical strains applied to the film through the piezoelectric substrate is considered in the present study with the fabrication of ferromagnetic (FM)/antiferromagnetic (AFM)/ferroelectric (FE) substrate. FM  $\text{Co}_{60}\text{Fe}_{20}\text{B}_{20}$ /AFM  $\text{Co}_{0.7}\text{Ni}_{0.3}\text{O}$  bilayers were deposited by magnetron sputtering on the piezoelectric substrate of  $\text{Pb}(\text{Mg}_{1/3}\text{Nb}_{2/3})\text{O}_3\text{-PbZrO}_3\text{-PbTiO}_3$  (PMN-PZT) with (011) plane. Subsequently, the samples were field-cooled from 390K to 300K under +5 T magnetic field applied along the [100] or [0-11] axis of PMN-PZT to set the pinned direction (P.D.) of AFM. A tensile stress along the [0-11] axis of PMN-PZT and a compressive stress along the [100] axis is induced as positive electric field is applied across the thickness of the PMN-PZT substrate.

The piezoelectric strain was found to induce an appreciable change in the exchange bias field ( $H_E$ ) and the coercivity ( $H_C$ ) of exchange-biased bilayers, thus the unidirectional anisotropy can be controlled accordingly. Exchange bias field ( $H_E$ ) and coercivity ( $H_C$ ) at various azimuthal angles ranging from 0° to 180° with a step 10° were obtained from the measurements of magnetic hysteresis loops employing vibrating sample magnetometer (VSM) at room temperature under various applied electric fields (-2,0,2,4,6 and 8 kV/cm), as shown in figure 1. The deformation of unidirectional anisotropy by a piezoelectric strain was analyzed by coefficient variation of specific cosine series function including higher order terms in the  $H_E(\phi)=\sum A_n \cos(n\phi+\alpha)$ . Coefficients  $A_n$ 's and  $\alpha$  angle were obtained by fitting the experimental data at various electric fields from the cosine series. Coefficients of odd terms changed by significant amounts indicating the control of unidirectional anisotropy and variation of  $\alpha$  reflected the change in the anisotropy direction. Therefore, a strain mediated electrical control of both direction and magnitude of the anisotropy in the AFM is demonstrated.

### Keywords:

exchange bias field, unidirectional anisotropy, strain mediated electrical control

## 탠덤 펌핑 고출력 광섬유 레이저

김지원\*<sup>1, 2</sup>, 박종선<sup>2, 3</sup>, 오예진<sup>2, 3</sup>, 정예지<sup>2</sup>, 정훈<sup>3</sup>

<sup>1</sup>한양대학교 응용물리학과, <sup>2</sup>한양대학교 나노광전자학과, <sup>3</sup>한국생산기술연구원  
jwk7417@hanyang.ac.kr

### Abstract:

탠덤 펌핑 광섬유 레이저는 펌핑시 광섬유에서 발생하는 열을 크게 낮출 수 있으므로 기존 다이오드 레이저 펌핑 광섬유 레이저의 출력 한계를 넘어 >10 kW 단일 모드 레이저 출력을 얻을 수 있는 단일 레이저 플랫폼으로 큰 관심을 받고 있다. 그 뿐 아니라 탠덤 펌핑 광섬유 레이저는 빔질 개선, 포토다크닝 감소 등 다른 유리한 점도 있는 것이 알려져 있지만 관련된 공식적 보고는 많지 않다.

본 발표에서는 한양대학교와 한국생산기술연구원이 공동으로 연구한 탠덤 펌핑 Yb 광섬유 레이저에 대한 연구 결과를 보고하고자 한다. 우선 탠덤 펌핑 Yb 광섬유 레이저 시스템을 구축하여 펌핑 조건에 따른 출력 특성에 대해 이론적, 실험적으로 알아보았다. 이를 바탕으로 고출력을 발진시킬 수 있는 탠덤 펌핑 증폭단을 구축하여 kW급 레이저 출력을 획득하고 그 특성을 조사하였다. 마지막으로 탠덤 펌핑과 다이오드 펌핑 광섬유 레이저 시스템의 동작 특성을 비교, 분석하고 향후 더 높은 출력을 얻기 위한 전략을 제시하고자 한다. 본 논문은 산업통상자원부 글로벌전문기술개발사업(과제번호 : 10053846)으로 지원된 연구임.

### Keywords:

Yb 광섬유 레이저, MOPA, 탠덤 펌핑

## Brillouin optical correlation domain analysis and Distributed acoustic sensing

이관일\*<sup>1</sup>

<sup>1</sup>한국과학기술연구원  
klee21@kist.re.kr

### Abstract:

광섬유기반의 분포형 센서는 외부의 온도나 응력, 음파로 인하여 광섬유 자체의 고유 특성이 변하는 성질을 이용하며, 광섬유 자체의 특성상 외부 전자기파에 둔감하고 유해 가스나 화학약품 등에 강하며, 가볍고 유연하며 소형화가 가능한 장점이 있다. 이러한 장점과 더불어 광섬유는 포설이 용이하고 구조물에 장착하기 쉬운 구조로 되어 있어 구조물의 안전성을 감지할 수 있는 장치로 활발히 활용되고 있다. 본 발표에서는 다양한 광섬유 분포형 센서 중, 브릴루앙산란 기반의 브릴루앙광상관영역분석센서(Brillouin Optical Correlation Domain Analysis, BOCDA)와 레일레이산란 기반의 분포형 음향센서(Distributed Acoustic Sensing, DAS) 원리와 최근 연구동향을 소개하며, 한국과학기술연구원에서 진행해온 관련 센서시스템의 연구결과를 보고한다.

### Keywords:

distributed fiber optic sensor, 브릴루앙광상관영역분석법, 분포형음향센서

## 툴륨 광섬유 레이저 펄핑 홀뮴 광섬유 펄스 레이저

김지원\*<sup>1, 2</sup>, 박진소<sup>1</sup>, 김륜경\*<sup>3</sup>

<sup>1</sup>한양대학교 응용물리학과, <sup>2</sup>한양대학교 나노광전자학과, <sup>3</sup>성균관대학교 전자전기공학부  
jwk7417@hanyang.ac.kr, rkkim@skku.edu

### Abstract:

펄스 레이저는 짧은 시간동안 높은 첨두 출력의 빔을 얻을 수 있기 때문에 타겟에 손상을 최소화 하고자 하는 여러 분야에서 응용이 가능한데, 특히 2  $\mu\text{m}$  영역의 펄스 레이저는 세포 내부의 수분의 흡수 계수와 일치하기 때문에 의료 분야의 응용에 크게 주목 받고 있다. 이 파장 영역의 레이저는 주로 Tm 이나 Ho 이 도핑되어 있는 레이저 물질을 사용하여 얻을 수 있는데, 최근 들어 광섬유 레이저가 크게 발전함에 따라 Tm 혹은 Ho이 도핑된 광섬유 레이저 시스템의 개발에도 많은 연구가 이루어지고 있다. 특히 Ho 도핑 고체 레이저는 요로 결석 제거, 전립선 비대증 치료, 레이저 수술 등에 이미 현장에서 사용되고 있지만, 우수한 특성의 Ho 도핑 광섬유 레이저는 펄핑에 적합한 상용화 다이오드 레이저의 부재, 실리카 호스트의 높은 전파 손실 등의 문제로 인하여 그동안 고출력 발전에 많은 어려움이 있었다. 이를 해결하기 위하여 고출력 Tm 광섬유 레이저를 Ho 광섬유 레이저의 펄핑광원으로 사용하는 In-band 펄핑 방식이 제시되었는데 이 방식을 통해 Q-스위칭을 통한 펄스 레이저를 제작할 경우 고효율 고에너지의 Ho 펄스 레이저를 얻는 것이 가능하다. 본 연구에서는 Tm 광섬유 레이저를 펄핑 광원으로 사용한 Ho 광섬유 레이저 시스템을 구축하였다. 우선 Ho 광섬유 레이저의 파장 특성을 확인하기 위해 연속발전 레이저 시스템을 구성하였으며, 회절격자를 이용하여 파장 선택을 하였다. 그리고 공진기 내부에 AOM 을 설치, Q-스위칭 작동을 유도하여, Ho 광섬유 펄스 레이저 빔을 발진시키고 이를 보고하고자 한다. 이 연구는 경찰청과 치안과학기술연구개발사업단 주관 치안과학기술연구개발사업(PA-B000001)과 한국연구재단 기초연구사업(No. NRF-2016R1A6A3A1193 2897)의 지원을 받아 수행된 연구임.

### Keywords:

Fiber laser, Pulsed operation, Q-switching, Thulium laser, Holmium laser

## 나비넥타이형 공진기를 이용한 단일주파수 소용돌이 파면 레이저빔 생성

김지원\*<sup>1, 2</sup>, 김태현<sup>1</sup>, 김동준<sup>1</sup>

<sup>1</sup>한양대학교 응용물리학과, <sup>2</sup>한양대학교 나노광전자  
jwk7417@hanyang.ac.kr

### Abstract:

라게르-가우시안(Laguerre-Gaussian, LG) 모드 빔은 축대칭 레이저 공진기 구조가 가지는 근본 모드로 일반적인 직교 좌표계의 허마이트-가우시안(Hermite-Gaussian, HG) 모드 빔과 비교해서 여러 가지의 다른 빔 특성 차이를 가지고 있다. 특히 동일 위상 파면이 나선 형으로 회전하며 진행하는 특이한 공간 전파 성질을 가지는데, 이는 LG 모드 레이저 빔이 알짜 궤도각운동량(Orbital angular momentum)을 가지고 있을 때 나타나는 현상으로 생성된 빔파면의 위상은  $\exp(i\ell\phi)$ 의 의존도를 가지고, 그 모드 빔들의 광자들은 모두  $\ell\hbar$ 의 궤도 각운동량을 가질 수 있다. 이와 같은 독특한 특성으로 인하여 궤도 각운동량을 가지는 소용돌이 파면 레이저빔은 정밀 물질 가공 뿐 아니라, 광 집게, 나노입자 조절, 양자정보 전송 등 다양한 분야의 응용에 사용되고 있다.

본 연구에서는 패러데이 회전자와 반파장판을 사용하여 나비넥타이형 진행파 공진기를 구축하고 Nd:YVO<sub>4</sub> 레이저 결정을 펌핑하여 단일 레이저 종모드를 발진시켰다. 펌핑으로 링 모양 펌프빔을 가해 겹침 효율을 조절함으로써 공진기 내 LG01 모드가 우선적으로 발진하도록 하였다. 이와 같은 실험 조건 하에서 공진기 발진 조건 및 방향을 조절하면 발진한 레이저빔은 단일 모드 LG01 모드를 가지며 나선형 파면을 가지고 있음을 확인할 수 있었다.

### Keywords:

Laguerre-Gaussian mode, Laser, Single frequency, Optical vortex

## 이터븀이 첨가된 광섬유의 포토다크닝 측정 및 연구

정훈\*<sup>1</sup>, 박종선<sup>1, 2</sup>, 오예진<sup>1, 2</sup>, 김지원<sup>2, 3</sup>

<sup>1</sup>한국생산기술연구원 스마트제조기술그룹, <sup>2</sup>한양대학교 ERICA 응용물리학과, <sup>3</sup>한양대학교 ERICA 나노광전자학과  
hoonj@kitech.re.kr

### Abstract:

1  $\mu\text{m}$  파장대의 이터븀 첨가 광섬유 레이저는 지난 10여년간 눈부신 발전을 이룩하여 수 kW급 레이저 출력이 상용화되었고, 현재 금속가공, 반도체/디스플레이, 군사, 생명 및 의학 분야에서 널리 사용되고 있다. 이에 따라 시간이 지날수록 더 높은 레이저 출력이 요구되고 있는데 열 문제, 광섬유 모재의 손상, 포토다크닝과 같은 근본적 문제가 더 높은 출력을 얻는데 있어 가장 큰 난제로 잘 알려져 있고, 이를 해결하기 위해 많은 연구가 이루어지고 있다. 그 중 포토다크닝은 광섬유 레이저 발진시 시간이 지남에 따라 광섬유 모재에 영구적 기저 손실이 증가하는 현상으로 광섬유 레이저의 수명에 직접적인 영향을 미치기 때문에 반드시 해결되어야만 한다. 현재까지 포토다크닝에 대한 명확한 이유는 밝혀지지 않았지만 높은 밀도 반전과 직접적 연관이 있다고 보고되고 있다.

이에 본 연구에서는 레이저 시스템 제작 전 이터븀이 도핑된 광섬유의 포토다크닝 현상을 정량적으로 측정할 수 있는 시스템을 제작하고, 다양한 광섬유를 사용하여 포토다크닝을 측정하고 분석하였다. 더 나아가 펄스 파장에 따른 포토다크닝 특성을 측정하여 포토다크닝 현상을 최소화시킬 수 있는 펌핑 조건에 대해서 알아보하고자 한다.

본 논문은 2018년도 안산시의 재원으로 안산시 강소기업 육성 지원사업에 의해 지원되었음.

### Keywords:

Yb 광섬유 레이저, 포토다크닝, 기저손실, 펌핑

## 탠덤 펌핑한 kW급 고출력 Yb 광섬유 레이저

정훈\*<sup>1</sup>, 오예진<sup>1, 2</sup>, 박종선<sup>1, 2</sup>, 김지원<sup>2, 3</sup>

<sup>1</sup>한국생산기술연구원 스마트제조기술그룹, <sup>2</sup>한양대학교 ERICA 응용물리학과, <sup>3</sup>한양대학교 ERICA 나노광전자학과  
hoonj@kitech.re.kr

### Abstract:

광섬유 레이저는 출력 빔의 특성이 우수하며 구조적으로 열분산 효과가 뛰어나기 때문에 고출력 레이저 분야에서 크게 각광받고 있다. 그러나 광섬유 레이저의 출력이 수 kW 급 이상으로 점차 증가함에 따라 열문제, 비선형 문제 등 다양한 출력 제한 요소들이 반드시 해결되어야 할 과제로 떠오르고 있다. 특히 발생하는 열을 최소화시켜 단일 광섬유 레이저 시스템에서 얻을 수 있는 레이저 출력 한계를 높이는 것이 중요한데 이를 위해 가장 널리 알려진 방법이 탠덤 펌핑이다. 탠덤 펌핑은 레이저 방출 파장에 가까운 레이저 광원을 펌핑 광원으로 사용하여 다른 레이저를 발진시키는 방식으로, Yb 광섬유 레이저의 경우 다른 Yb 광섬유로 펌핑할 때 양자결함을 5% 이하로 줄일 수 있기 때문에 광섬유에서 발생하는 열을 크게 줄여 더 높은 레이저 출력을 얻을 수 있다.

본 논문에서는 탠덤 펌핑 기술을 이용한 kW급 고출력 광섬유 레이저 개발에 대한 연구를 보고하고자 한다. 탠덤 펌핑용 여기 광원으로 여러 대의 1018 nm 파장대의 고출력 Yb 광섬유 레이저를 제작하고, 시그널 컴바이너를 사용하여 출력 빔들을 결합하였다. 그리고 제작한 1018 nm 광섬유 레이저로 1080 nm 씨앗빔을 증폭시키는 Yb 광섬유 MOPA (Master Oscillator Power Amplifier) 시스템을 펌핑하여 고효율의 kW급 레이저 출력을 얻을 수 있었다.

본 논문은 산업통상자원부 글로벌전문기술개발사업(과제번호 : 10053846)으로 지원된 연구임.

### Keywords:

Yb 광섬유 레이저, MOPA, 탠덤 펌핑

## 광섬유 형광 광원의 선폭에 따른 결맞음 길이 연구

김지원\*<sup>1, 2</sup>, 박은지<sup>1</sup>

<sup>1</sup>한양대학교 응용물리학과, <sup>2</sup>한양대학교 나노광전자학과  
jwk7417@hanyang.ac.kr

### Abstract:

결맞음 길이(Coherence length)는 광원으로부터 발생한 빛의 위상을 예측할 수 있는 거리로서 통신, 센서, OCT, 이미징 등 다양한 광학 분야에서 최상의 성능을 얻기 위해 반드시 고려되어야 하는 변수이다. 그리고 응용 분야에 따라 요구되는 결맞음 길이의 범위가 다르므로 광원의 정확한 결맞음 길이를 측정하는 것과 함께 이를 조절하는 것은 매우 중요하다. 결맞음 길이는 광원의 선폭 및 스펙트럼 모양에 의해 결정되는데 일반적인 광원의 경우 넓은 선폭을 가지므로 짧은 결맞음 길이를 가지고 있어 이미징, 센싱 등에 적합하나 퍼짐이 심해 빔의 전달이 좋지 않고 단위 선폭당 출력이 너무 낮아 장거리 정보 전송, 지향성 이미징 등에 적합하지 않다. 이에 반해 레이저 광원은 지향성 및 빔 특성이 매우 우수하나 선폭이 매우 좁음으로 인해 결맞음 길이가 길어져서 이로 인한 간섭 현상이 심한 문제점이 있다. 광섬유 형광 광원은 광섬유 레이저빔과 동일한 공간 전파 특성을 가짐과 동시에 수십 나노 미터 이상의 넓은 선폭을 가질 수 있어 기존 광원의 장점을 모두 가지고 있으며 더 나아가 출력빔의 선폭을 임의로 조절 가능하기 때문에 결맞음 길이를 원하는대로 조절할 수 있다.

본 연구에서는 선폭 조절이 가능한 광섬유 형광 광원 시스템을 구축하고 파장 선폭에 따른 결맞음 길이를 이론적 실험적으로 연구하였다. Yb이 도핑된 광섬유를 사용하여 형광 광원 시스템을 구축하고, 회절격자를 이용하여 파장 선폭을 다양하게 변조하였다. 이로부터 생성된 빔을 마이켈슨 간섭계를 통과시켜 광 경로 차에 따른 간섭무늬 변화를 통해 실제 결맞음 길이를 측정하였으며, 이때 측정된 결맞음 길이와 시뮬레이션을 통해 계산된 결맞음 길이를 비교 분석하였다.

### Keywords:

Amplified spontaneous emission, Superfluorescent fiber source, Coherence length

## Evolution of the broadband optical transition in large-area MoSe<sub>2</sub>

조만호\*<sup>1</sup>, 정재훈<sup>1</sup>, 최윤호<sup>1</sup>, 정광식<sup>1</sup>, 김현식<sup>1</sup>, 권기현<sup>1</sup>

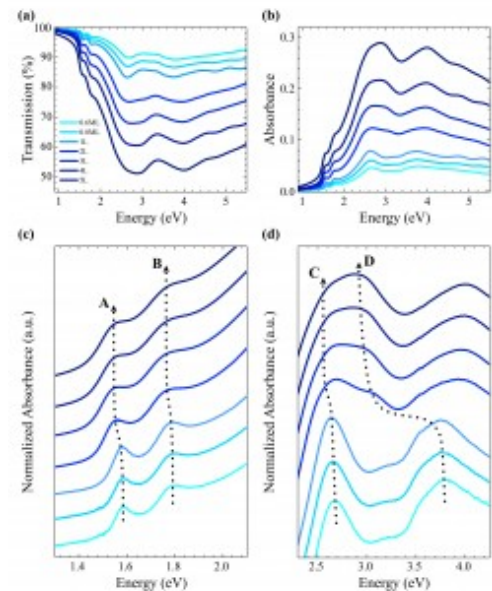
<sup>1</sup>Department of Physics  
mh.cho@yonsei.ac.kr

### Abstract:

The dependence of the optical and electrical properties of two-dimensional transition metal dichalcogenides with the number of layers has garnered significant interest. In particular, the indirect-to-direct band gap transition and the resulting changes, such as improved quantum yield, have been widely studied. However, an experimental investigation for the dependence of the optical transition on a wide range of photon energies is still lacking. Here, we report the broadband optical response of large-area MoSe<sub>2</sub> grown from monolayer to pentalayer thicknesses by molecular beam epitaxy, for photon energies in the 0.9-5.5 eV range. We observed a dramatic evolution of the absorption spectrum depending on the number of layers. Using the density functional theory, we show that this feature is related to a change in the energy and geometric shape of the band structure at the  $\Gamma$  point in the Brillouin zone. The dependence of these optical properties on the number of layers yields insights into the underlying physics and is promising for photonic and optoelectronic applications.

### Keywords:

Transitionmetal dichalcogenides, Layered materials, Molecular beam epitaxy, Joint density of states



## Interfacial thermal boundary resistance between WSe<sub>2</sub> monolayers

최영관<sup>1</sup>, 정찬준<sup>1</sup>, 노창재<sup>1</sup>, 주휘인<sup>1</sup>, 김태윤<sup>2</sup>, 김상우<sup>2</sup>, 이종석\*<sup>1</sup>  
<sup>1</sup>광주과학기술원 물리광학과, <sup>2</sup>성균관대학교 신소재공학부  
jsl@gist.ac.kr

### Abstract:

Thermal transport properties at the low-dimensional materials, such as graphene and transition metal dichalcogenides (TMDs) have been attracting lots of attentions for solving the heat dissipation problems occurring in their applications for nano-devices. Using the transient pump-probe technique, the so-called time-domain thermoreflectance (TDTR) measurement technique, it is possible to make an accurate measurement of the cross-plane directional thermal resistance, and hence to address the heat dissipation problem in two-dimensional materials. In this work, we prepared single-layer and double-layer WSe<sub>2</sub> nano-flake, and determined their cross-plane thermal resistance. Interestingly, we observed that the depending on the type of metal film deposited on WSe<sub>2</sub>, thermal resistance for the mono- and double-layer film are significantly changed. We attribute this intriguing difference to the contribution of the change of interfacial thermal boundary conductance between WSe<sub>2</sub> nano-sheets.

### Keywords:

Thermophysical properties, 2D material, transition metal dichalcogenide, interfacial thermal resistance, time-domain thermoreflectance

## The characteristics of MoSe<sub>2</sub> grown by MBE and interface analysis between the film and the high-k dielectric

조만호\*<sup>1</sup>, 최윤희<sup>1</sup>, 정재훈<sup>1</sup>, 권기현<sup>1</sup>  
<sup>1</sup>연세대학교 물리학과  
mh.cho@yonsei.ac.kr

### Abstract:

Transition metal dichalcogenides (TMDs) have been explored as the promising active layer for the next-generation devices because they are direct band gap, flexibility, and high mobility in subnanometer thickness. Among the bottom-growth methods for TMDs, we studied molecular beam epitaxy (MBE) method for large area MoSe<sub>2</sub>. Spectroscopic measurements were conducted to study the quality of the film. High resolution X-ray photoelectron spectroscopy (HRXPS) was performed to chemical composition and elemental ratio across the film. The crystallinity and Moiré patterns of the grown MoSe<sub>2</sub> were confirmed by scanning transmission electron microscopy (STEM). Ultraviolet photoelectron spectroscopy (UPS) and photoluminescence (PL) indicated the band alignment: The grown MoSe<sub>2</sub> with 3 layers is n-type semiconductor, having the optical band gap as 1.39eV and the valance band as 1.10eV. With the film as active material, we fabricated the double-gated field effect transistor (FET) with SiO<sub>2</sub> for back gate dielectric and Al<sub>2</sub>O<sub>3</sub> for top gate dielectric. The FET exhibited the different parameters such as V<sub>th</sub>, μ<sub>FET</sub>, and SS depending on the gate dielectrics. Finally, the Coulomb scattering parameter (α<sub>SC</sub>) obtained in the case of the SiO<sub>2</sub> and Al<sub>2</sub>O<sub>3</sub> indicated that the differences are attributed to the Coulomb scattering from the gate dielectrics.

### Keywords:

molybdenum diselenides, molecular beam epitaxy, Al<sub>2</sub>O<sub>3</sub>, field effect transistor

## Quasi-particle band structure of bulk and few-layer PdSe<sub>2</sub> with GW approximation

김한규<sup>1</sup>, 최형준\*<sup>1</sup>

<sup>1</sup>Department of Physics and Center for Computational Studies of Advanced Electronic Material Properties, Yonsei University, Seoul 03722, Korea  
h.j.choi@yonsei.ac.kr

### Abstract:

We performed first-principles calculations to investigate the electronic band structure of PdSe<sub>2</sub>, which is a semiconducting material with puckered layer structure. First, we calculated electronic structure of bulk PdSe<sub>2</sub> using the density functional theory (DFT), obtaining a semi-metallic electronic structure due to underestimation of the energy gap. To calculate the band gap of PdSe<sub>2</sub> correctly, we employed the GW method. Using the GW method, we obtained the semiconducting electronic structures of bulk PdSe<sub>2</sub> which is consistent with experimental results. Then we calculated the electronic structure of two-dimensional PdSe<sub>2</sub> using DFT and GW method to find thickness dependence of the energy gap. This work is supported by the NRF of Korea (Grant No.2011-0018306). Computational resources have been provided by KISTI Supercomputing Center (Project No. KSC-2017-C3-079)

### Keywords:

PdSe<sub>2</sub>, DFT, GW

## Unified bulk-boundary correspondence for band insulators

임준원\*<sup>1</sup>, BARDARSON Jens H.<sup>3</sup>, SLAGER Robert-Jan<sup>2</sup>

<sup>1</sup>강상관계 물질 연구단 물리학부, <sup>2</sup>Max-Planck-Institut für Physik komplexer Systeme, <sup>3</sup>Department of Physics, KTH Royal Institute of Technology, Stockholm  
phyruth@gmail.com

### Abstract:

The bulk-boundary correspondence, a topic of intensive research interest over the past decades, is one of the quintessential ideas in the physics of topological quantum matter. Nevertheless, it has not been proven in all generality and has in certain scenarios even been shown to fail, depending on the boundary profiles of the terminated system. Here, we introduce bulk numbers that capture the exact number of in-gap modes, without any such subtleties in one spatial dimension. Similarly, based on these 1D bulk numbers, we define a new 2D winding number, which we call the pole winding number, that specifies the number of robust metallic surface bands in the gap as well as their topological character. The underlying general methodology relies on a simple continuous extrapolation from the bulk to the boundary, while tracking the evolution of Green's function's poles in the vicinity of the bulk band edges. As a main result we find that all the obtained numbers can be applied to the known insulating phases in a unified manner regardless of the specific symmetries. Additionally, from a computational point of view, these numbers can be effectively evaluated without any gauge fixing problems. In particular, we directly apply our bulk-boundary correspondence construction to various systems, including 1D examples without a traditional bulk-boundary correspondence, and predict the existence of boundary modes on various experimentally studied graphene edges, such as open boundaries and grain boundaries. Finally, we sketch the 3D generalization of the pole winding number by in the context of topological insulators.

### Keywords:

Edge state, Boundary modes, Bulk-boundary correspondence, topological insulator

## First-principles study of the structural and electronic properties of bulk and few-layer tellurium

조준형\*<sup>1</sup>, 이세호<sup>1</sup>, ZHU Zhili<sup>2</sup>, CAI Xiaolin<sup>2</sup>, JIA Yu<sup>2</sup>

<sup>1</sup>Department of Physics, Hanyang University, <sup>2</sup>International Laboratory for Quantum Functional Materials of Henan, Zhengzhou University  
chojh@hanyang.ac.kr

### Abstract:

Bulk tellurium (Te) is composed of one-dimensional (1D) helical chains which have been considered to be coupled by van der Waals (vdW) interactions. However, based on first-principles density-functional theory calculations, we here propose a different bonding nature between neighboring chains: i.e., the helical chains made of normal covalent bonds are connected together by coordinate covalent bonds [1]. It is revealed that the lone pairs of electrons of Te atom participate in forming coordinate covalent bonds between neighboring chains. Therefore, each Te atom behaves as both electron donor to neighboring chains and electron acceptor from neighboring chains. In addition, we predict a new category of 2D monolayers named "tellurene", composed of the metalloid element Te, with stable 1T-MoS<sub>2</sub>-like ( $\alpha$ -tellurene), and metastable tetragonal ( $\beta$ -tellurene) and 2H-MoS<sub>2</sub>-like ( $\gamma$ -tellurene) structures [2]. The underlying formation mechanism is inherently rooted in the multivalent nature of Te, with the central-layer Te behaving more metal-like (e.g., Mo), and the two outer layers more semiconductorlike (e.g., S). We also show that the  $\alpha$ -tellurene phase can be spontaneously obtained from the magic thicknesses divisible by three layers truncated along the [001] direction of the trigonal structure of bulk Te, and both the  $\alpha$ - and  $\beta$ -tellurene phases possess electron and hole mobilities much higher than MoS<sub>2</sub>. The present findings extend the realm of 2D materials to group-VI elements.

[1] S. Yi, Z. Zhu, X. Cai, Y. Jia, and J.-H. Cho, *Inorg. Chem.* (Submitted).

[2] Z. Zhu *et al. Phys. Rev. Lett.* **119**, 106101 (2017).

### Keywords:

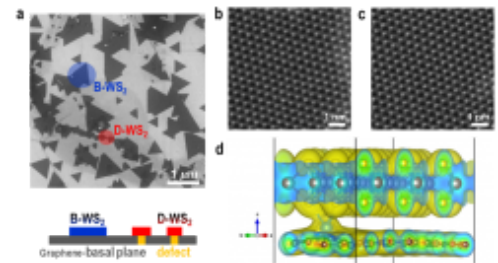
Tellurium, 1D chains, coordinate covalent bonds, 2D materials, First-principles

## Covalent interaction between WS<sub>2</sub> monolayer and graphene substrate

이건도\*<sup>1</sup>, 이성우<sup>1</sup>, 김세양<sup>2</sup>, 윤의준<sup>1</sup>, 권순용<sup>2</sup>  
<sup>1</sup>서울대학교 재료공학부, <sup>2</sup>울산과학기술원 신소재공학부  
gdlee@snu.ac.kr

### Abstract:

Vertically stacked two-dimensional (2D) heterostructures are promising for novel applications. Their properties and performances are profoundly affected by their stacking and interlayer geometries. Recently, WS<sub>2</sub> flakes were directly synthesized on polycrystalline CVD graphene template to present the significant effect of defects of the template layer to the subsequent layer growth and intrinsic properties of heterostructure. We can infer that defects of underlying template have a strong influence on the interlayer interaction between stacking layers through distinctively different deformability, thermal stability and beam damage behavior. We have tried to explain these phenomena using density functional theory calculations. Among several candidates, defective graphene with grain boundary was to be found to have covalent bonding with WS<sub>2</sub> flakes through W atomic bridge. Attributed to the larger orbital overlap compared to van der Waals contacts of general 2D heterostructures, this model allows to explain different intrinsic properties including high conductivity. This new defect-mediated heterostructure and its novel properties could extend the versatile possibilities for designing 2D heterostructures with desirable properties.



### Keywords:

Two-dimensional heterostructure, Graphene, Tungsten disulfide, Density functional theory calculations

## First-principles investigation of off-diagonal electron-phonon interaction in graphene

최영우<sup>1</sup>, 최형준\*<sup>1</sup>

<sup>1</sup>Department of Physics, Yonsei University  
h.j.choi@yonsei.ac.kr

### Abstract:

We investigate off-diagonal electron-phonon interaction in graphene from first-principles density-functional perturbation theory. Using the electron-phonon matrix elements with the full momentum dependence throughout the entire Brillouin zone, we calculate the off-diagonal components of the electron self-energy, which couple the conduction and valence bands. We analyze the contribution of each phonon mode to the self-energy. Also, we discuss effects of the off-diagonal corrections on the Fermi velocity and spectral functions in graphene. This work was supported by NRF of Korea (Grant No. 2011-0018306) and KISTI supercomputing center (Project No. KSC-2017-C3-0079). Y.W.C. acknowledges support from NRF of Korea (Global Ph.D. Fellowship Program NRF-2017H1A2A1042152).

### Keywords:

electron-phonon, graphene, DFT, DFPT

## Weyl fermion in the surface states of Bi adsorbed Si(110) surface with nonsymmorphic lattice

손영우\*<sup>1</sup>, 김현중<sup>1</sup>  
<sup>1</sup>고등과학원 계산과학부  
hand@kias.re.kr

### Abstract:

In two-dimensional crystals, the nonsymmorphic lattice symmetry together with time reversal symmetry can stabilize Weyl fermionic states. With  $4n+2$  electron filling, the states can be tuned to locate near the charge neutral point [1]. Here, using first-principles calculations, we propose a stable Bi adatom induced superstructure on Si(110) surface, characterized by wallpaper symmetry group  $pg$ , as a candidate system for the realization of Weyl fermion states with  $4n+2$  electron filling. Out of various adsorption geometries, the ground structure have glide line parallel to  $[1-10]$  direction, results in a two-fold degenerate Bloch bands along glide lines. We will also discuss a way of controlling band dispersions where the Weyl fermion reside near the fermi level.

Ref. [1] S. M. Young and C. L. Kane, Phys. Rev. Lett. 115, 126803 (2015)

### Keywords:

Weyl fermion, nonsymmorphic, Bi/Si(110)

## Neutron scattering study on heavy fermion compound $\text{CePtAl}_4\text{Ge}_2$

SHIN S.<sup>1</sup>, LEE S.<sup>1</sup>, SON S.-K.<sup>1</sup>, KIM J.<sup>1</sup>, JANG H.<sup>1</sup>, JUNG Soon-Gil<sup>1</sup>, LEE Hanoh<sup>1</sup>, PARK T.\*<sup>1</sup>,  
NIEDERMAYER C.<sup>2</sup>, POMJAKUSHIN V.<sup>2</sup>, TOTH S.<sup>2</sup>, KELLER L.<sup>2</sup>, STUHR U.<sup>2</sup>, KENZELMANN M.<sup>2</sup>, SHANG  
T.<sup>3</sup>, MEDARDE M.<sup>3</sup>, RONNING Filip<sup>4</sup>, ROSA Priscila F. S.<sup>4</sup>, THOMPSON Joe D.<sup>4</sup>, SCOTT Brian L.<sup>4</sup>, BAUER  
E. D.<sup>4</sup>

<sup>1</sup>Department of Physics & Center for Quantum Materials and Superconductivity, Sungkyunkwan University, <sup>2</sup>Laboratory for Neutron Scattering and Imaging, Paul Scherrer Institut, CH-5253 Villigen, Switzerland, <sup>3</sup>Laboratory for Scientific Developments and Novel Materials, Paul Scherrer Institut, 5232 Villigen PSI, Switzerland, <sup>4</sup>Los Alamos National Laboratory, Los Alamos, NM 87545, USA  
tp8701@skku.edu

### Abstract:

Ce-based quaternary compounds have attracted interest due to their various, tunable magnetic ground states, where the competition between RKKY interactions and Kondo effects is important [1]. Since the exchange coupling strength ( $J_{ex}$ ), which plays a crucial role in the competition, can be controlled by non-thermal tuning parameters such as chemical substitution, magnetic field, and pressure, the Ce-based compounds provide a new avenue to study the interplay among the intertwined order parameters. It has been recently shown that  $\text{CeMAl}_4\text{Si}_2$  ( $M=\text{Rh, Ir, Pt}$ ) [2],  $\text{EuMAl}_4\text{Si}_2$  ( $M=\text{Rh, Ir}$ ) [3],  $\text{SmNiAl}_4\text{Ge}_2$  [4], and  $\text{REAuAl}_4\text{Ge}_2$  ( $\text{RE}=\text{Ce, Nd, Gd, Er}$ ) [5] (1142 family) possess various magnetic ground states and the chemical environments of the constituent rare-earth atoms are important to determine the coupling strength  $J_{ex}$ . Similar to other 1142 germanids, Pt1142 adopts the trigonal ( $R\bar{3}m$ , 166) crystal structure where the two-dimensional (2D) triangular  $\text{Ce}^{3+}$  lattice alternates with  $\text{PtAl}_4\text{Ge}_2$  slab along the crystalline  $c$ -axis. Electrical resistivity reveals a Kondo lattice behavior with weak hybridization strength between conduction electron and localized 4f electron moments. Magnetic susceptibility and specific heat capacity measurements show that the ground state of  $J=5/2$  of  $\text{Ce}^{3+}$  is doubly degenerate and a long-range ordered antiferromagnetic (AFM) state appears below 2.3 K [6]. Neutron scattering under magnetic field reveals a change in the ordering wave vector  $\mathbf{k}$  from (1.387, 0, 0) to (1.392, 0, 0) above 12 kOe, which is consistent with the anomalies observed in the field dependent resistivity and magnetic susceptibility.

- [1] S. Doniach, THE KONDO LATTICE AND WEAK ANTIFERROMAGNETISM, *Physica B: Condensed Matter*, 91 (1977).  
[2] N.J. Ghimire, F. Ronning, D.J. Williams, B.L. Scott, Y. Luo, J.D. Thompson, E.D. Bauer, Investigation of the physical properties of the tetragonal  $\text{CeMAl}_4\text{Si}_2$  ( $M = \text{Rh, Ir, Pt}$ ) compounds, *J Phys Condens Matter*, 27 (2015) 025601.  
[3] A. Maurya, A. Thamizhavel, S.K. Dhar, P. Bonville, Magnetic anisotropy, unusual hysteresis and putative "up-up-down" magnetic structure in  $\text{EuTAl}_4\text{Si}_2$  ( $T = \text{Rh and Ir}$ ), *Sci Rep*, 5 (2015) 12021.[4] B. Sieve, X. Chen, J. Cowen, P. Larson, S.D. Mahanti, M.G. Kanatzidis, Multinary intermetallics from molten Al. Synthesis of  $\text{SmNiAl}_4\text{Ge}_2$  and  $\text{YNiAl}_4\text{Ge}_2$ . Possible spin frustration in separated triangular  $\text{Sm}^{3+}$  layers, *Chemistry of Materials*, 11 (1999) 2451-2455.  
[5] X. Wu, M.G. Kanatzidis,  $\text{REAuAl}_4\text{Ge}_2$  and  $\text{REAuAl}_4(\text{AuxGe}_{1-x})_2$  ( $\text{RE}=\text{rare earth element}$ ): Quaternary intermetallics grown in liquid aluminum, *Journal of Solid State Chemistry*, 178 (2005) 3233-3242.  
[6] S. Shin, P.F.S. Rosa, F. Ronning, J.D. Thompson, B.L. Scott, S. Lee, H. Jang, S.-G. Jung, E. Yun, H. Lee, E.D. Bauer, T. Park, Synthesis and characterization of the heavy-fermion compound  $\text{CePtAl}_4\text{Ge}_2$ , *Journal of Alloys and Compounds*, 738 (2018) 550-555.

### Keywords:

heavy fermion, incommensurate antiferromagnetism,  $\text{CePtAl}_4\text{Ge}_2$

\_\_\_\_\_

## SI-STM studies on a magnetically doped $\text{Cr}_{0.08}(\text{Bi}_{0.1}\text{Sb}_{0.9})_{1.92}\text{Te}_3$

KIM Jae-Joon<sup>1, 2</sup>, YOO Jung Hoon<sup>1, 2</sup>, LEE Kyoung Seok<sup>1, 2</sup>, JOO Sang Hyun<sup>1, 2</sup>, PARK Sung-Joon<sup>1, 2</sup>,  
ZHOU Haibiao<sup>1, 2</sup>, GU Genda<sup>3</sup>, LEE Jinho\*<sup>1, 2</sup>

<sup>1</sup>Department of Physics and Astronomy, Institute of Applied Physics, Seoul National University, <sup>2</sup>Center for Correlated Electron Systems, Institute for Basic Science(IBS), <sup>3</sup>Condensed Matter Physics & Materials Science Department, Brookhaven National Laboratory  
jinholee@snu.ac.kr

### Abstract:

We investigated a magnetically doped topological insulator  $(\text{Bi}_{0.1}\text{Sb}_{0.9})_2\text{Te}_3$  ( $\text{Cr}_{0.08}(\text{Bi}_{0.1}\text{Sb}_{0.9})_{1.92}\text{Te}_3$ ) using SI-STM (Spectroscopic Imaging Scanning Tunneling Microscopy) both in real space and q-space. Due to the broken time-reversal symmetry caused by magnetic dopants, we were able to observe quasi-particle interference peaks which are forbidden without Cr dopants. Previously it is reported that the areal density of Cr dopants has a linear relation with respect to the Dirac mass gap size, but the influence of other impurities: bright impurity(in the topographic image), a triangular-shaped impurity(in differential conductance map) are not so well understood. New findings regarding those impurities and Dirac mass gap, as well as the origin of Fano-like spectroscopic features near the Fermi energy will also be discussed.

### Keywords:

topological insulator, SI-STM, impurity

## Violation of Ohm's law in a Weyl metal

신동우<sup>1</sup>, 김지훈\*<sup>1</sup>

<sup>1</sup>포항공과대학교 물리학과  
jeehoon@postech.ac.kr

### Abstract:

Weyl metal is the 3D analog of graphene holding Weyl fermions. The Weyl fermions have chirality, and give the Weyl metals peculiar properties such as chiral anomaly and magnetic monopole in k-space. Some theoretical articles reported that these properties result in new transport phenomena such as negative MR, chiral magnet effect and anomalous Hall effect. And the negative MR has been observed in Weyl metal. But semi-classical model combining the Boltzmann transport equation and chiral anomaly shows another transport phenomenon that is existence of non-Ohmic behavior in Weyl metal owing to Fermi level imbalance called as charge pumping effect which is occurred by chiral anomaly. And we observed that the non-Ohmic conductivity in  $\text{Bi}_{0.96}\text{Sb}_{0.04}$  and the experimental data correspond with the semi-classical model.

### Keywords:

Weyl metal, Chiral anomaly, Transportation, Ohm's law

## Dirac carrier dynamics in the semi-metallic Tb-doped $\text{Sr}_2\text{IrO}_4$

이종석\*<sup>1</sup>, 한정우<sup>1</sup>, 김선우<sup>2</sup>, 천상모<sup>2</sup>, GANG Cao<sup>3</sup>, WANG J. C.<sup>3, 4, 5</sup>

<sup>1</sup>Department of Physics and Photon Science, GIST, <sup>2</sup>Department of Physics, Hanyang University,

<sup>3</sup>Department of Physics and Astronomy, University of Kentucky, <sup>4</sup>Quantum Condensed Matter Division, Oak Ridge National Laboratory, <sup>5</sup>Department of Physics, Renmin University  
jsl@gist.ac.kr

### Abstract:

Here, we investigate the nature of the conduction electrons in a Tb-doped  $\text{Sr}_2\text{IrO}_4$  using reflection-type terahertz time-domain spectroscopy. At room temperature, a free carrier contribution to the optical conductivity spectra is characterized by an extremely small scattering rate  $\sim 0.15$  THz which we attribute to the signature of the existence of massless Dirac carriers. As temperature decreases, the Dirac carrier contribution to the spectral weight is reduced significantly. We could explain these results reasonably well by considering the electronic band structure which is calculated by means of the tight-binding model; the Dirac dispersion is realized when the staggered pseudospin current order is considered, and a decrease of temperature leads to the chemical potential shift to the lower energy approaching the Dirac point. We discuss the symmetry-protected Dirac semimetallic phase realized in this Tb-doped  $\text{Sr}_2\text{IrO}_4$  in comparison with the cuprates which share much similarity in electronic, magnetic, and structural phases with the layered iridate.

### Keywords:

Iridate, Dirac, terahertz, spectroscopy

## Possible interfacial magnetism in $\text{Nd}_{1-x}\text{Sr}_x\text{MnO}_3$ multilayers

진형진\*<sup>1</sup>, 류상균<sup>1</sup>, 김혜경<sup>2</sup>, 조진형<sup>3</sup>

<sup>1</sup>Department of Physics, Pusan National University, <sup>2</sup>Core Research Facilities, Pusan National University,

<sup>3</sup>Department of Physics Education, Pusan National University

hjeen@pusan.ac.kr

### Abstract:

Manganites are well-known for closed correlation among structure, transport, and magnetism. Especially,  $\text{Nd}_{1-x}\text{Sr}_x\text{MnO}_3$  system is interesting due to various electronic and magnetic states by hole-doping and possible tuning of the states by external stimuli. Previously, we demonstrated growth of two different  $\text{Nd}_{1-x}\text{Sr}_x\text{MnO}_3$  epitaxial thin films by control of oxygen partial pressure. Those thin films are similar in structure but different in chemistry, electronic transport and magnetism [S. Ryu, *et al.*, *Appl. Phys. Lett.* **110** 261601 (2017)]. In this presentation, we will show multilayer approach to scrutinize possible magnetic interaction at the interfaces, which has been found in superlattices. From x-ray normal scans and reciprocal space mappings, we observed that films are strained and the formation of sharp interfaces from distinguishable superlattice peaks. Detailed magnetic characterization shows enhanced magnetic moments in multilayer films compared to those of epitaxial thin film of either composition. Interestingly, when individual thickness of multilayers is thinner, the higher enhancement in magnetism is observed. This result clearly indicates smearing of ferromagnetism into the less-magnetic layers at the interfaces. This work was supported by the Basic Science Research Program through the National Research Foundation of Korea (NRF) funded by the Ministry of Education (NRF-2015R1D1A1A02062175).

### Keywords:

thin film, magnetism, multilayer

## Pressure effect on magnetoresistance of MoTe<sub>2</sub>

박두선\*<sup>1</sup>, 이상연<sup>1</sup>  
<sup>1</sup>성균관대학교 물리학과  
tp8701@skku.edu

### Abstract:

We report pressure effects on magnetoresistance (MR) of MoTe<sub>2</sub>, a candidate type II Weyl semimetal. At 1 bar, MoTe<sub>2</sub> undergoes a structural transition from monoclinic-to-orthorhombic (T' to T<sub>d</sub>) phase near ~210 K. Anomalously large MR (~600 %) has been observed at 2 K in the T<sub>d</sub>-phase. With application of pressure, the structural transition temperature ( $T^*$ ) gradually decreases and disappears at 1.4 GPa ( $=P_c$ ). Concomitant with the suppression of  $T^*$ , MR is continuously reduced and is almost saturated to 100 % in the T'-phase ( $P > P_c$ ). Two-band analysis on the MR and Hall conductivity shows that the anomalously large MR in T<sub>d</sub>-phase arises from perfect electron-hole compensation. In the T'-phase, however, additional bands are required to explain the field-dependent MR and Hall resistivity, indicating that there occurs a change in the electronic structure at  $P_c$ , where the T<sub>d</sub> phase is transformed to T'-phase.

### Keywords:

MoTe<sub>2</sub>, Magnetoresistance, Weyl semimetal

## In-plane magnetic anisotropy in strontium iridate $\text{Sr}_2\text{IrO}_4$

NAUMAN Muhammad<sup>1</sup>, HONG Yunjeong<sup>1</sup>, HUSSAIN Tayyaba<sup>1</sup>, SEO M. S<sup>2</sup>, PARK S. Y<sup>2</sup>, LEE Nara<sup>3</sup>,  
CHOI Young Jai<sup>3</sup>, KANG Woun<sup>4</sup>, 조연정\*<sup>1</sup>

<sup>1</sup>Department of Physics, Kyungpook National University, Daegu 41566, Korea, <sup>2</sup>Spin Engineering Physics Team, Korea Basic Science Institute, Daejeon 34141, Korea, <sup>3</sup>Department of Physics, Yonsei University, Seoul 03722, Korea, <sup>4</sup>Department of Physics, Ewha Womans University, Seoul 03760, Korea  
jophy@knu.ac.kr

### Abstract:

Magnetic anisotropy in strontium iridate ( $\text{Sr}_2\text{IrO}_4$ ) is found to be large because of the strong spin-orbit interactions. In our work, we studied the in-plane magnetic anisotropy of  $\text{Sr}_2\text{IrO}_4$  and traced the anisotropic exchange interactions between the isospins in the crystal. The magnetic-field-dependent torque  $\tau(H)$  showed a prominent transition from the canted antiferromagnetic state to the weak ferromagnetic (WFM) state. A comprehensive analysis was conducted to examine the isotropic and anisotropic regimes and probe the easy magnetization axis along the  $ab$  plane. The angle-dependent torque  $\tau(\theta)$  revealed a deviation from the sinusoidal behavior, and small differences in hysteresis were observed around  $0^\circ$  and  $90^\circ$  in the low-magnetic-field regime. This indicates that the orientation of the easy axis of the FM component is along the  $b$  axis, where the antiferromagnetic to WFM spin-flop transition occurs. We compared the coefficients of the magnetic susceptibility tensors and captured the anisotropy of the material. The in-plane  $\tau(\theta)$  revealed a tendency toward isotropic behavior for fields with values above the field value of the WFM transition.

### Keywords:

$\text{Sr}_2\text{IrO}_4$ , Torque measurements, Magnetic field effect, Magnetic anisotropy

## Infrared Spectroscopic Investigation on the Density Wave-Like Behavior in $(\text{Sr}_{1-x}\text{La}_x)_3\text{Ir}_2\text{O}_7$

문순재\*<sup>1</sup>, [AHN Gihyeon](#)<sup>1</sup>, SEO J. H.<sup>1</sup>, NOH S. J.<sup>1</sup>, CHEN X.<sup>2, 3</sup>, WILSON S. D.<sup>2</sup>

<sup>1</sup>Department of Physics, Hanyang University, Seoul 04763, Korea, <sup>2</sup>Materials Department, University of California, Santa Barbara, California 93106, USA, <sup>3</sup>Department of Physics, Boston College, Chestnut Hill, Massachusetts 02467, USA  
soonjmoon@hanyang.ac.kr

### Abstract:

We studied the electronic response of  $(\text{Sr}_{1-x}\text{La}_x)_3\text{Ir}_2\text{O}_7$  ( $x = 0.051$ , and  $0.066$ ) by using infrared spectroscopy. We found a distinct anomaly in the temperature evolution of the conductivity spectra of the metallic compounds which may be associated with the partial gap opening in the electronic density of states. The anomaly in the optical spectra is observed at the temperatures where a subtle structural transition is reported to occur. We will discuss possible origin of the anomaly based on the sum rule and the extended Drude analyses.

### Keywords:

Infrared spectroscopy, density wave, iridate

## Honeycomb lattice Mott insulator in K-adsorbed $1T\text{-TaS}_2$

LEE Jinwon<sup>1, 2</sup>, WANG Lihai<sup>3, 4</sup>, CHEONG Sang-Wook<sup>3, 4</sup>, **염한웅**<sup>\*1, 2</sup>

<sup>1</sup>Center for Artificial Low Dimensional Electronic Systems, Institute for Basic Science, Pohang, Republic of Korea, <sup>2</sup>Department of Physics, Pohang University of Science and Technology, Pohang, Republic of Korea, <sup>3</sup>Laboratory for Pohang Emergent Materials, Pohang University of Science and Technology, Pohang, Republic of Korea, <sup>4</sup>Rutgers Center for Emergent Materials and Department of Physics and Astronomy, Rutgers University, Piscataway, New Jersey, USA  
yeom@postech.ac.kr

### Abstract:

Quantum spin liquid state is an exotic quantum state of matter, exhibiting a disordered spin state at very low temperature due to the spin frustration. The spin frustration can be induced by a lattice symmetry, such as triangular lattice, where the antiferromagnetic ordering with the nearest neighbors is prohibited. An unusual bond-dependent Kitaev interaction in a honeycomb lattice was also reported to frustrate spins, attracting interest in spin-1/2 honeycomb Mott insulators as a candidate of the quantum spin liquid state. Only limited system,  $\alpha\text{-RuCl}_3$ , has been proposed as a honeycomb lattice Mott insulator.  $1T\text{-TaS}_2$ , which is the unique system of CDW-Mott ground state, was recently proposed to have the quantum spin liquid state in a triangular lattice. In the present work, we realize an artificial honeycomb lattice Mott insulating state in K-adsorbed  $1T\text{-TaS}_2$  using scanning tunneling microscopy/spectroscopy (STM/S). Our STM/S study found that each CDW unit cell is occupied by a single K adatom at its center. Moreover, this adsorbed K adatom on the CDW unit cell destroys the Mott state completely on the adsorption site while neighboring CDW unit cells without K adsorbates maintain its own Mott state and Mott gap. At the optimized coverage of one-third of the CDW unit cells, K adatoms form a regularly ordered structure, where remaining two-thirds of the CDW unit cells form a honeycomb lattice with its Mott insulating state. This honeycomb lattice Mott insulating state in K-adsorbed  $1T\text{-TaS}_2$  is expected to show the exotic spin state as mentioned above and its spin state is under investigation by theoretical calculations.

### Keywords:

Mott insulator, charge density wave, scanning tunneling microscopy/spectroscopy, Quantum spin liquid

## Controlling enhanced electrical conductivity near the edge of ferroelectric nanoplates

양찬호\*<sup>1</sup>, 김광은<sup>1</sup>, 김기엽<sup>2</sup>, 최시영<sup>2</sup>

<sup>1</sup>한국과학기술원 물리학과, <sup>2</sup>포항공과대학교 신소재공학과  
chyang@kaist.ac.kr

### Abstract:

Controllable conduction level has been suggested by arranging two opponent polarizations in a head to head (or tail to tail) configuration. In the ferroelectric materials, such charged domain walls have been artificially constructed by an effective trailing field of *dc* biased tip motion to overcome their electrostatic energy. However, charged domain walls formed by a trailing field are unstable and results in ferroelastic back-switching because of elastic interactions at the boundary between poling and non-poling regions. Moreover, in-plane polarizations need to be adjustable using top-down capacitor geometries for applications of the charged domain wall as a nano-electronics. Here, we report that nanoscale plate structures under a strain relaxation provide a promising opportunity into stabilization and manipulation of a charged domain wall because of their highly anisotropic mechanical boundary condition. We demonstrate a ferroelectric BiFeO<sub>3</sub> nanoplate subject to a compressive misfit strain at the bottom but less external stress on the side walls exhibits a radial-quadrant in-plane ferroelectric domain structure. We report that electronic conduction is significantly enhanced in the vicinity of the side wall. Moreover, the magnitude of static conductivity is adjustable ~20 times over by 180° ferroelectric switching. Our finding offers an avenue into charged domain wall formation applicable for nanoscale ferroelectric logic devices.

### Keywords:

Charged domain wall, Ferroelectricity, BiFeO<sub>3</sub>, Conductive-AFM

## Polarization Switching dynamics in Si doped Hafnium Oxide Thin Films

채승철\*<sup>1</sup>, 이태윤<sup>1</sup>, 이경준<sup>1</sup>, 최종찬<sup>1</sup>, 임홍헌<sup>1</sup>, 이준행<sup>1</sup>

<sup>1</sup>서울대학교 물리교육과  
scchae@snu.ac.kr

### Abstract:

Since the discovery of ferroelectricity in hafnia, it has attracted attention due to its simple binary structure for the alternative of conventional perovskite based ferroelectric materials. Hafnium oxide can also have various properties such as dielectric, ferroelectric, and double hysteresis, depending on the doping ratio of the various dopants. In addition, ferroelectricity is emerged even at very thin thicknesses of about 10 nm. These features make hafnium oxide a good candidate for next-generation devices. However, understanding the polarization switching kinetics in ferroelectric hafnium oxide thin is not enough for the ferroelectric memory application.

Here, we report our research on the polarization switching properties of ferroelectric hafnium oxide thin films. We measured time dependent switched polarization under various applied electric fields. Their switching dynamics under various electric fields will be explained by both domain wall motion dominant model and nucleation-limited-switching (NLS) model. In addition, we will show the difference in switching kinetics between pristine and woken up specimen.

### Keywords:

polarization switching, dynamics, kinetics, ferroelectric, hafnium oxide, wake-up effect

## Large magnetoresistance in oxygen deficient SrTiO<sub>3</sub>

박배호\*<sup>1</sup>, 김연수<sup>1</sup>, 전지훈<sup>1</sup>, 이지혜<sup>1</sup>, 이상익<sup>1</sup>, YULDASHEV Shavkat U.<sup>2</sup>

<sup>1</sup>Department of Physics, Konkuk University, <sup>2</sup>Quantum-Functional Semiconductor Research Center,  
Dongguk University  
baehpark@konkuk.ac.kr

### Abstract:

Galvanomagnetic transport properties in oxygen deficient SrTiO<sub>3</sub> were investigated. To create oxygen vacancies, SrTiO<sub>3</sub> single crystals were annealed at high temperature in vacuum environment ( $< 10^{-8}$  Torr). As annealing temperature increased resistivity was decreased, it means that higher annealing temperature cause much more oxygen vacancies in SrTiO<sub>3</sub> single crystals. Interestingly, non-linear Hall resistivity and magnetoresistance were observed under 100 K simultaneously. As temperature decreased to 2 K, magnetoresistance increased up to about 3,000 %. Transport properties were well fitted by two band-model, carrier density and mobility of one type were well matched with obtained by conventional Hall effect. The other type of carriers appeared about at 100 K and become influential as temperature decreased. In order to find the origin of large magnetoresistance in oxygen deficient SrTiO<sub>3</sub>, electrical and optical measurements have been conducted.

### Keywords:

SrTiO<sub>3</sub>, magnetoresistance, two band model

## Visualization of oxygen-vacancy flow in crystalline solids

양찬호\*<sup>1</sup>, 임지수<sup>1</sup>

<sup>1</sup>한국과학기술원 물리학과  
chyang@kaist.ac.kr

### Abstract:

The presence of ionized oxygen vacancies significantly influences local physical properties and functionalities in oxide materials. Many studies have been made on ionic migration. Inhomogeneous distribution of oxygen vacancies in resistive switching memories creates local conducting paths or bulk conducting regions. Solid oxide fuel cells can transfer stored chemical energy to electrical energy with oxygen ions migration through electrolyte materials. Therefore, understanding the motion of oxygen vacancies is important to design efficient oxide devices and enhance their functionalities. Ca-substituted bismuth ferrite (Ca-BFO) is one of the promising oxide systems to study the motion of oxygen vacancies. Substitution of bismuth ions to divalent calcium ions produces oxygen vacancies in proportion to Ca substitution ratio (*i.e.*  $\delta=x/2$ ) due to stabilization of the oxidation number of  $\text{Fe}^{3+}$ . Migration of oxygen vacancies using an external electric field results in the dark-colored hole-doped region. In this study, we present visualization of oxygen vacancy propagation through optical microscope during the electrical forming process. Tracing the color change of Ca-BFO films at different temperatures, we can quantify their thermodynamic variables. We also check the reproducibility of electro-formed states by application of backward and forward electric fields. Our findings provide a promising pathway into functional defects in crystalline solids.

### Keywords:

oxygen vacancy, solid oxide fuel cell, resistive switching memory, electrochromism

## Orientation dependent physical properties of epitaxial NbO<sub>2</sub> thin films

진형진\*<sup>1</sup>, [KIM Gowoon](#)<sup>1</sup>, ZHANG Yu-Qiao<sup>2</sup>, MIN Taewon<sup>1</sup>, SUH Hoyoung<sup>3</sup>, JANG Jae Hyuck<sup>3</sup>, KONG Hyeonjun<sup>1</sup>, LEE Joonhyuk<sup>1</sup>, LEE Jaekwang<sup>1</sup>, JEON Tea-Yeol<sup>4</sup>, LEE Inwon<sup>5</sup>, CHO Jinhyung<sup>6</sup>, OHTA Hiromichi<sup>7</sup>

<sup>1</sup>Department of Physics, Pusan National University, <sup>2</sup>Graduate School of Information Science and Technology, Hokkaido University, <sup>3</sup>Electron Microscopy Research Center, Korea Basic Science Institute, <sup>4</sup>Pohang Accelerator Laboratory, Pohang University of Science and Technology, <sup>5</sup>Department of Naval Architecture and Ocean Engineering, Pusan National University, <sup>6</sup>Department of Physics Education, Pusan National University, <sup>7</sup>Research Institute for Electronic Science, Hokkaido University  
hjeen@pusan.ac.kr

### Abstract:

The crystallographic orientation control by epitaxy can be a strong method to observe (sometimes hidden) anisotropic physical properties. This can be exemplified by control of polarization [1] and control of oxygen vacancy channels [2]. In order to study orientation dependent physical properties, we selected NbO<sub>2</sub> as a model material. We fabricated epitaxial 110 and 111 NbO<sub>2</sub> thin films on (0001) and (1-102)  $\alpha$ -Al<sub>2</sub>O<sub>3</sub> substrates using RF sputtering. At first, we confirmed the epitaxial relation using x-ray diffraction measurement and scanning transmission electron microscope. Then, we performed thermopower and electronic transport measurements along the in-plane direction. We observed unusual highly conducting path, which can be explained by density functional theory.

This research was supported by basic science research program through the NRF funded by the Ministry of Education (NRF-2015R1D1A102062175) and by the Korea government (MSIP) through GCRC-SOP (No. 2011-0030013). H.O. was supported by grants-in-aid for scientific research A (17H01314) from the Japan Society for the Promotion of Science (JSPS). H. S. and J. J. were supported by the Korea Basic Science Institute grant (T37210) and (T38603), respectively. H. J. and H. O. are supported by the Korea-Japan bilateral program funded from NRF and JSPS.

[1] H. N. Lee and D. Hesse, Appl. Phys. Lett. **80**, 1040 (2002).

[2] H. Jeon, Z. Bi, W. S. Choi, M. F. Chisholm, C. A. Bridges, M. P. Paranthaman, and H. N. Lee, Adv. Mater. **25**, 6459 (2013).

### Keywords:

Epitaxial thin film, Thermopower, Effective mass, DFT calculation

\_\_\_\_\_

## Non-stoichiometry-induced Charge Disproportionation in Nickelate Thin Film Grown by Pulsed Laser Deposition

김태현\*<sup>1</sup>, 이종민<sup>2</sup>, 최경순<sup>3</sup>, 이태권<sup>4</sup>, 정일석<sup>2</sup>, 김상모<sup>5</sup>, 송재선<sup>2</sup>, 박정웅<sup>5</sup>, 이주형<sup>2</sup>, 정종훈<sup>4</sup>, 이주한<sup>3</sup>, 이상한<sup>2</sup>  
<sup>1</sup>울산대학교 물리학과, <sup>2</sup>광주과학기술원 신소재공학부, <sup>3</sup>한국기초과학지원연구원 나노표면연구팀, <sup>4</sup>인하대학교 물리학과, <sup>5</sup>가천대학교 전기공학과  
mabung7@gmail.com

### Abstract:

In transition-metal oxides, their physical properties are very susceptible to cation and oxygen stoichiometry. In bulk perovskite rare-earth nickelates ( $RNiO_3$ , except for  $R = La$ ), which undergo structural/electrical/magnetic phase transitions as a function of temperature, it has been reported that the electronic transport behaviors in metal-to-insulator transitions are strongly dependent on the cation and oxygen contents. When the cation and oxygen concentrations in  $RNiO_3$  become off from the stoichiometric one, the degree of disproportionation in the Ni charge valence is promoted driving  $RNiO_3$  less conductive. For rare-earth nickelate thin films, it is therefore possible that non-stoichiometry in the  $R$ , Ni, and oxygen ions influences on the metal-to-insulator phase transition, however in-depth studies have been rare so far. In this work, we manipulate the cation stoichiometry in rare-earth nickelate bilayer thin films epitaxially grown by a pulsed laser deposition technique. By tuning an ablation time of a  $RNiO_3$  ceramic target in the laser ablation process, we can control the compositional ratio between  $R$  and Ni contents around the target surface, and eventually synthesize  $RNiO_3$  thin-film samples with different  $R/Ni$  ratios (i.e. identical to 1 for a stoichiometric film and less than 1 for a Ni-excessive film). With detailed experimental analyses and supporting theoretical calculations, the effect of non-stoichiometry on various physical properties in  $RNiO_3$  thin films will be demonstrated clearly.

### Keywords:

Stoichiometry, Nickelate Thin Film, Pulsed Laser Deposition

## Investigation of structural symmetry in strained SrRuO<sub>3</sub> thin films by using optical second harmonic generation technique

노창재<sup>1</sup>, 김진권<sup>2, 3</sup>, 신영재<sup>2, 3</sup>, 노태원<sup>2, 3</sup>, 이종석\*<sup>1</sup>

<sup>1</sup>광주과학기술원 물리광학과, <sup>2</sup>기초과학연구원 강상관계 물질 연구단, <sup>3</sup>서울대학교 물리학과  
jsl@gist.ac.kr

### Abstract:

We investigate a structural symmetry of SrRuO<sub>3</sub> thin films with variations of thickness and temperature by using optical second harmonic generation (SHG) technique. At room temperature, we observe clear SHG responses for all the samples with the thickness ranging from 10 to 90 nm. Interestingly, as the film becomes thicker, the azimuth-dependent anisotropy becomes clearer. This suggests that the structural symmetry becomes lower with an increase of the film thickness. As temperature increases, the SHG intensity becomes reduced, and disappears above 400 K, which indicates a structural transition to the high-temperature centrosymmetric phase. We fit the anisotropic azimuth dependence by including the electric dipole and electric quadrupole contributions, and discuss the evolution of the structural symmetry as a function of the film thickness and temperature in detail particularly with the consideration of the thickness-dependent strain relaxation.

### Keywords:

SrRuO<sub>3</sub>, strain relaxation, symmetry breaking, second harmonic generation

## Looking for systems where type-II Dirac Fermions and Superconducting quasi-particles can interact

NOH Han-Jin\*<sup>1</sup>, JEONG Jinwon<sup>1</sup>, CHO En-Jin<sup>1</sup>, KIM Kyo<sup>2</sup>, MIN B.-I.<sup>3</sup>, PARK Byeong-Gyu<sup>4</sup>

<sup>1</sup>Department of Physics, Chonnam National University, <sup>2</sup>MPPC\_CPM, Pohang University of Science and Technology, <sup>3</sup>Department of Physics, POSTECH, <sup>4</sup>Pohang Accelerator Laboratory, POSTECH  
ffnhj@jnu.ac.kr

### Abstract:

A Dirac fermion in a topological Dirac semimetal is a quadruple-degenerate quasiparticle state with a relativistic linear dispersion. These quasiparticles, although described by a relativistic Dirac equation, do not necessarily obey Lorentz invariance, allowing the existence of so-called type-II Dirac fermions[1]. The recent theoretical discovery of type-II Dirac fermions in PtSe<sub>2</sub>-type transition metal dichalcogenides stimulated experimental realization[2]. Here, we will present an experimental realization of type-II Dirac fermions in a PdTe<sub>2</sub> superconductor by angle-resolved photoemission spectroscopy combined with *ab initio* band calculations[3]. Also, we will show some of our efforts that make type-II fermions and superconducting quasiparticles interact.

[1] A. A. Soluyanov et al., Nature (London) v527, 495 (2015).

[2] H. Huang et al., Phys. Rev. B v94, 121117 (2016).

[3] H.-J. Noh et al., Phys. Rev. Lett. v119, 016401 (2017).

### Keywords:

type-II Dirac Fermions, superconducting quasiparticles, PdTe<sub>2</sub>, ARPES

## 강유전 요동에 의한 위상 초전도

정석범\*<sup>1</sup>, 이민성<sup>2</sup>, 이현재<sup>2</sup>, 이준희\*<sup>2</sup>

<sup>1</sup>서울시립대학교 물리학과, <sup>2</sup>UNIST  
sbchung@snu.ac.kr, junhee@unist.ac.kr

### Abstract:

A topological superconductor features at its boundary Majorana fermions, which are potentially applicable for topological quantum computations. The scarcity of the real systems with topological superconductivity is giving rise to a strong demand for such an unconventional superconductivity. In this research, we study a heterostructure consisting of a two-dimensional electron gas (2DEG) from 5d transition metals sandwiched by ferroelectric materials. A strong spin-orbit coupling, and with odd-parity phonon modes at low energy due to ferroelectric fluctuations make this system a suitable candidate material. The band structure calculations show the fluctuating Rashba type spin splitting arising from the combination of the spin-orbit coupling and the coupling to the odd-parity phonons. Setting the substrate lattice constant at an appropriate range softens the odd-parity phonon mode to induce the strong electron-phonon coupling. Our results indicate that appropriately strained substrates with an extremely soft phonon mode may give rise to the topological superconductivity on 2DEG. We will suggest several candidate substrates and experimental probing techniques.

### Keywords:

마요라나 페르미온, 위상 절연체, 강유전체

## The interplay between superconductivity and phonon in the attractive Hubbard-Holstein model

박태호\*<sup>1</sup>, 최한용<sup>1</sup>

<sup>1</sup>성균관대학교 물리학과  
thpark3@gmail.com

### Abstract:

We present a study of the half-filled attractive Hubbard-Holstein model with superconducting order parameter employing the dynamical mean-field theory in combination with the numerical renormalization group. The Hubbard-Holstein model is a prototype model for understanding the interplay between the local Coulomb repulsion  $U$  and the electron-phonon coupling  $g$ . Here, we investigate the interplay between the superconductivity and phonon in the attractive  $U$  Hubbard-Holstein model, where the phonon is regarded as an additional bosonic excitation mode. In particular, we discuss the variation of superconductivity by changing the electron-phonon coupling and we identify the superconducting properties in the BCS and BEC regimes. In addition, the effect of phonon softening on superconductivity is investigated in the strong correlation regime.

### Keywords:

superconductivity, phonon, attractive Hubbard-Holstein model, dynamical mean-field theory, numerical renormalization group

## The charge density wave in $\text{LuP}_2\text{In}$ ( $P = \text{Pd}, \text{Pt}$ ) mediated by electron phonon coupling

김희정<sup>2</sup>, 김규\*<sup>1</sup>, 민병일<sup>2</sup>  
<sup>1</sup>막스플랑크포스텍센터 CPM, <sup>2</sup>POSTECH  
kyoo@mpk.or.kr

### Abstract:

We have explored the charge density wave (CDW) instabilities in  $\text{LuPd}_2\text{In}$  and  $\text{LuPt}_2\text{In}$  cubic-Heusler compounds using band structure and phonon dispersion calculations based on the *ab initio* density functional theory. We have found a dominant Fermi-surface (FS) nesting vector of  $\mathbf{q}_M = (0.5, 0.5, 0.0)$  for both compounds. However, the phonon softening instability occurs only for  $\text{LuPt}_2\text{In}$  as is consistent with experimental result. We have demonstrated that the presence and the absence of CDW instabilities, respectively, in  $\text{LuPt}_2\text{In}$  and  $\text{LuPd}_2\text{In}$  originate not from the difference in the FS nesting or the spin-orbit coupling strength but from the difference in the electron-phonon coupling strength. In the CDW ground states, Pt ions in  $\text{LuPt}_2\text{In}$  are distorted into Pt cubes, which have a rotation within the Heusler structure. This transition induces the suppression of density of state of Pt *d*-band near the Fermi level.

### Keywords:

superconductor, CDW

## Hydrostatic Pressure Effects on the Superconductivity of $\text{Ca}_{0.9}\text{La}_{0.1}\text{FeAs}_2$ Single Crystals

BHOLDilip<sup>1</sup>, MIN Byeong Hun<sup>1</sup>, JANG Dong Hyun<sup>1</sup>, SUR Yeahan<sup>1</sup>, MURATA Keizo<sup>1</sup>, KIM Duck Young<sup>3</sup>,  
SHIM Ji Hoon<sup>2</sup>, 김기훈\*<sup>1</sup>

<sup>1</sup>Center for Novel States of Complex Materials Research, Department of Physics and Astronomy, Seoul National University, Seoul, South Korea, <sup>2</sup>Department of Chemistry & Physics, Division of Advanced Nuclear Engineering Pohang University of Science and Technology, Korea, <sup>3</sup>Center for High Pressure Science & Technology Advanced Research, China  
khkim@phya.snu.ac.kr

### Abstract:

La-doped  $\text{CaFeAs}_2$  has been recently found to exhibit a high superconducting transition temperature ( $T_c \sim 36$  K), with a superconducting volume ratio up to 66% [1]. The crystal structure of the La-doped  $\text{CaFeAs}_2$  is characterized by a conductive intermediate As-As layer located between the FeAs superconducting layers. In this work, we have grown the La-doped  $\text{CaFeAs}_2$  single crystal with an improved flux method, which exhibits an enhanced  $T_c \sim 46$  K and a large volume fraction  $\sim 70\%$ . We also investigated the hydrostatic-pressure dependence of resistivity in  $\text{Ca}_{0.9}\text{La}_{0.1}\text{FeAs}_2$  up to 8.5 GPa with the combination of a hybrid piston cell and a cubic anvil press. The pressure dependence of  $T_c$  reveals a dome shaped behavior with a maximum  $T_c \sim 51.4$  K at 1.7 GPa. At this pressure,  $T$ -dependence of resistivity shows a linear behavior for  $T > T_c$ , possibly due to the non-Fermi liquid state in the vicinity of a quantum phase transition or multiband effects. Furthermore, the pressure dependence of slope of the upper critical field,  $dH_{c2}/dT$  near  $T_c$ , also reveals a sharp peak at 1.7 GPa, suggesting the quasiparticle mass enhancement associated with Fermi surface modification near the optimal pressure.

### Keywords:

Superconductivity, Quasi particle, Non Fermi liquid

## Investigation of $\text{Ca}_{0.9}\text{La}_{0.1}\text{FeAs}_2$ superconductor using scanning tunneling microscopy

이진호\*<sup>1, 2</sup>, ZHOU Haibiao<sup>1, 2</sup>, KIM Jae-Joon<sup>1, 2</sup>, PARK Sung-Joon<sup>1, 2</sup>, LEE Kyoung Seok<sup>1, 2</sup>, MIN Byeong Hun<sup>3</sup>, BHOI Dilip<sup>3</sup>, KIM Kee Hoon<sup>3</sup>

<sup>1</sup>Center for Correlated Electron Systems, Institute for Basic Science (IBS), Seoul 08826, Republic of Korea, <sup>2</sup>Department of Physics and Astronomy, Seoul National University, Seoul 08826, Republic of Korea, <sup>3</sup>Center for Novel States of Complex Materials Research (CeNSCMR), Department of Physics and Astronomy, Seoul National University, Seoul 08826, Republic of Korea  
jinholee@snu.ac.kr

### Abstract:

$\text{Ca}_{1-x}\text{La}_x\text{FeAs}_2$  (CLFA), is a newly discovered iron-based superconductor with a structure 112. It has been attracting attention for its high superconducting transition temperature ( $T_C \sim 40$  K), as well as the possible existence of the Dirac cones due to the additional layers consisting of zigzags, making it a potential topological superconductor. Here we use low-temperature scanning tunneling microscopy to image the CLFA sample at the atomic scale. The topography shows a reconstructed surface, probably due to the formation of As dimers in the FeAs layers. The superconducting gap can only be observed in very limited regions, consistent with the ARPES results. Much higher inhomogeneity is observed in the conductance maps compared to the topography, which is ascribed to the dopants in the FeAs layers. In addition, the measured  $dI/dV$  spectra show no observable variation at the energy of the reported Dirac points ( $\sim -90$  mV).

### References:

1. Katayama, N., et al., Superconductivity in  $\text{Ca}_{1-x}\text{La}_x\text{FeAs}_2$ : A Novel 112-Type Iron Pnictide with Arsenic Zigzag Bonds. J. Phys. Soc. Jpn. 82, 123702 (2013).
2. Liu, ZT, et al., Observation of the anisotropic Dirac cone in the band dispersion of 112-structured iron-based superconductor  $\text{Ca}_{0.9}\text{La}_{0.1}\text{FeAs}_2$ . Appl. Phys. Lett. 109, 042602 (2016).

### Keywords:

iron-based superconductors, topological superconductors, scanning tunneling microscopy

## Fano Resonance in hybrid 2DEG - superconductor system

VILLEGAS Kristian Hauser Arellano<sup>\*1</sup>, KOVALEV Vadim M.<sup>2</sup>, KUSMARTSEV Fedor V.<sup>3</sup>, SAVENKO Ivan G.<sup>1</sup>

<sup>1</sup>기초과학연구원 복잡계 이론물리 연구단, <sup>2</sup>Department of Applied and Theoretical Physics, Novosibirsk State Technical University, Novosibirsk 630090, Russia, <sup>3</sup>Department of Physics, Loughborough University, Loughborough LE11 3TU, United Kingdom  
khvillegas@gmail.com

### Abstract:

Hybrid double-layer systems are ubiquitous in solid-state physics. They turn out to be especially interesting in the study of electron transport phenomena, light absorption by heterostructures and in designing nano-devices [1]. In particular, these systems reveal resonant behavior at certain conditions, e.g. hybrid dipolar exciton-electron gas system exhibits a magnetoplasmon Fano resonance [2]. and a superconductor (see Fig 1, left panel). We study the linear response of the system to an external electromagnetic field. The electron gas and the Cooper pairs are coupled via the Coulomb interaction. We calculate the hybrid modes and find an anti-crossing between them [3]. We further calculate the power absorption spectrum of the system (see Fig. 1, right panel). It demonstrates Fano-like resonance with two asymmetric peaks and a dip. We suggest a way to monitor the behavior of the superconductor by measuring the conductivity of the electron gas.

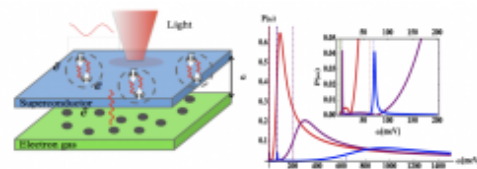


Fig. 1. System schematic: hybrid normal metal-superconductor system exposed to an electromagnetic field of incident light (left panel). Power absorption in the case when the current is monitored in the superconductor layer and there is no external field on the normal layer. Inset shows the peaks (for purple and blue curves) due to the lower hybrid modes. Colors stand for different wave vectors of the incoming light. The green vertical line shows the location of the gap (right panel).

### References

- [1] B. N. Narozhny and A. Levchenko, Rev. Mod. Phys. **88**, 025003 (2016).
- [2] M. V. Boev, V. M. Kovalev, and I. G. Savenko, Phys. Rev. B **94**, 241408(R) (2016).
- [3] K. H. Villegas, V. M. Kovalev, F. Kusmartsev, I. G. Savenko, soon in arXive (2018).

### Keywords:

Fano resonance, superconductor, hybrid systems

## Measurement of the Gravitational Constant Using a Torsion Balance

CHOI Ki-Young\*<sup>1</sup>

<sup>1</sup>국방과학연구소

kychoi.kc@gmail.com

### Abstract:

The gravitational constant  $G$ , along with Planck's constant and the speed of light, is one of the most fundamental and universal constants in nature. Unlike most other physical constants, the value of  $G$  is not precisely known due to the weakness and nonshieldability of gravity. Since the first laboratory measurement by Cavendish over 200 years ago, the reduction in uncertainty in  $G$  has been only a factor of about 10 per century.

Newton's gravitational constant  $G$  is measured by using a new torsion balance method. New technique greatly reduces several sources of uncertainty compared to previous measurements.

### Keywords:

Torsion Balance

# Redefinition of the Kilogram Based on the Fixed Value of the Planck Constant

이광철\*<sup>1</sup>

<sup>1</sup>Physical Metrology Division, Korea Research Institute of Standards and Science  
kclee@kriss.re.kr

## Abstract:

In the current international system of units (SI), the kilogram is defined by the mass of a material artifact. Because the artifact can gain or lose its mass during handling, the current definition of the kilogram is not stable. To overcome the shortcomings of the current mass unit and to aid the scientific progress, the kilogram will be redefined by fixing the numerical value of the Planck constant. In the new SI, which will be used from 2019, the kilogram will be realized through primary methods such as Kibble balance and silicon sphere experiments. In the Kibble balance experiment, the electrical power and mechanical power are compared. The electrical standards to measure the electrical quantities are based on the quantum phenomena such as Josephson and quantum Hall effects. The mass of the test weight is determined by measuring coil velocity, gravitational acceleration, and electrical quantities. The development of the KRIS kibble balance which will be used to maintain the mass unit in Korea will be described.

## Keywords:

SI, Kilogram redefinition, Planck constant, Kibble balance

## 볼츠만 상수 측정과 켈빈의 새 정의

양인석\*<sup>1</sup>

<sup>1</sup>한국표준과학연구원 물리표준본부  
iyang@kriss.re.kr

### Abstract:

2019년 5월 이후에는 열역학 온도의 단위인 켈빈(기호: K)의 정의가 볼츠만 상수를 이용한 정의로 바뀐다. 지금은 물의 삼중점의 안정된 열역학 특성을 이용한 정의를 사용하지만 이후에는 기본물리상수를 이용한 정의로 바꾸는 것이다. 새로운 정의 전과 후의 켈빈의 크기가 연속적이라면 지금 정의를 바탕으로 볼츠만 상수를 가능한 한 정확하게 측정하고 그 측정값을 새로운 정의에 사용해야 한다. 따라서 지난 10년동안 여러 나라의 표준기관이 볼츠만 상수를 정확하게 측정하기 위해 노력했다. 그 결과 최근에 과학기술데이터위원회(CODATA)는 현재의 켈빈 정의에서 가장 정확한 볼츠만 상수의 값을  $1.380\,649\text{ J K}^{-1}$ 로 조정하였으며 그 상대 불확도는  $3.7 \times 10^{-7}$ 로 산출했다. 이 값은 세 종류의 서로 다른 물리법칙을 이용하는 실험을 종합하여 도출한 것이다. 그 중 가장 많은 가중치를 가진 실험은 음향기체온도계로서 기체에서 음속이 열역학 온도와 연관되는 열역학 방정식을 이용하여 크기가 알려진 공진구 내의 음파의 속도를 측정한 것이다. 두 번째 실험은 유전상수기체온도계로서 기체의 유전율이 온도와 밀도에 따라 변하는 성질을 이용하여 축전기의 전기 용량 변화를 정밀 측정하여 얻은 것이다. 마지막 실험은 압온도계로서 저항 측정에서 보이는 전기적 잡음의 크기가 온도에 따라 달라지는 성질을 이용한 것이다. 이렇게 볼츠만 상수를 이용한 켈빈의 정의는 20 K 이하의 아주 낮은 온도와 1000 K 이상의 아주 높은 온도에서 기존의 정의에 비하여 정확한 온도 실현과 온도 측정을 가능하게 한다. 본 발표에서는 볼츠만 상수 측정에 사용된 각 실험의 물리 법칙을 알아보고 켈빈 재정의가 갖는 의미를 설명한다.

### Keywords:

볼츠만 상수

## 상수 기본전하 $e$ 를 이용한 암페어 재정의 및 실현

김남\*<sup>1</sup>, 배명호<sup>1</sup>, 안예환<sup>1</sup>, 김범규<sup>1</sup>, 김완섭<sup>1</sup>, 채동훈<sup>1</sup>, 홍창기<sup>2</sup>, 정윤철<sup>2</sup>

<sup>1</sup>한국표준과학연구원 전자기표준센터, <sup>2</sup>부산대학교 물리학과  
namkim@kriss.re.kr

### Abstract:

암페어는 전류 크기를 표현하는 물리 단위로서, 국제 단위계(SI)의 하나이다. 그러나 현재까지, 그 정의와 실현 사이에 괴리가 있었다. 예를 들면, 암페어의 정의는 고전적인 암페어의 법칙을 기초로 기술되는 반면, 암페어의 실제 구현은 옴의 법칙, 즉 양자 홀 저항에 대한 조셉슨 전압의 비율을 통해 실험실에서 실행된다. 그러나, 2019년 5월 20일 '세계 측정의 날' (World Metrology Day)에 발효될 예정인, 개정된 국제 단위계에서는, 암페어가 전자의 흐름으로 정의될 것이다. 이때 전자의 전하 크기인 기본전하는 상수로 정의된다. 따라서, 개정된 국제 단위계에서는 전류와 전압 및 저항 등의 3개의 전기 단위는 모두 양자 물리학의 기반 위에서 정의되게 된다. 본 발표에서는, 개정된 암페어를 실현할 수 있는 양자 전류표준기의 후보 중 하나인 단일 전자 펌프 소자에 대한 간단한 리뷰를 하도록 하겠다.

### Keywords:

기본전하  $e$

## 광자 계수 기반 절대 양자 복사도 측정 연구

문한섭\*<sup>1</sup>, 정택<sup>1</sup>, 김현오<sup>1</sup>, 차명식<sup>1</sup>, 이희정<sup>1, 2</sup>, 김승관<sup>2</sup>, 이동훈<sup>2</sup>

<sup>1</sup>부산대학교 물리학과, <sup>2</sup>한국표준과학연구원  
hsmoon@pusan.ac.kr

### Abstract:

최근에 양자정보과학 분야의 발전으로 양자통신, 양자컴퓨터, 및 양자계측 분야에서 단일광자 양자상태를 이용한 다양한 기초연구와 이를 이용한 응용연구가 활발하게 진행되고 있다. 특히 광자를 기반으로 하는 양자 복사도 측정은 광도 복사도 분야에 미래의 새로운 측정 표준으로 연구가 진행되고 있다. 본 연구에서는 한국표준과학연구원이 부산대학교에 설치한 측정과학우수연구실 (Measurement Research Center: MRC)에서 수행된 광자 계수 기반 절대 양자 복사도 측정 표준 연구의 결과를 발표하고자 한다. 본 연구에서는 주기적으로 분극이 반전된 비선형 결정으로부터 자발적 매개하향변환 과정에 의해서 생성된 광자쌍을 이용하여 단일광자 검출기 (single photon detector)의 절대 양자 효율을 측정하는 방법을 개발함으로써 광자 수준의 새로운 양자 칸델라 (quantum candela) 구현을 위한 광자기반 양자 복사도 측정 표준의 핵심 기술을 확보하였다. 또한 405 nm 반도체 레이저에서 나오는 480 nm - 840 nm 영역의 폭넓은 형광에 대해서 한국표준과학연구원에서 교정된 측정 소급성을 갖는 기준 광검출기를 이용하여 단일광자 검출기로 측정된 분광 분포를 비교 교정함으로써 기존의 KRISS의 고전적 광도 표준과 단일광자 수준의 광도 표준 연결에 대한 연구를 성공적으로 수행하였다.

### Keywords:

광자 계수 기반 절대 양자 복사도 측정 연구

## Emulating topological matter with ultracold fermions in engineered optical lattices

JO Gyu-Boong\*<sup>1</sup>

<sup>1</sup>Department of Physics, HKUST (Hong Kong University of Science and Technology), Hong Kong  
gbo@ust.hk

### Abstract:

Ultracold atoms that are extremely pristine systems provide controllable platforms in emulating topological phases in optical lattices with bosonic and fermionic atoms. In this talk, we demonstrate the quantum simulation of topological phases realized in spin-orbit-coupled ultracold fermions trapped in 1D and 2D optical lattices.

First, we discuss the observation of a novel type of symmetry-protected topological (SPT) phases realized in 1D optical lattices [1]. The observed SPT phase is beyond the Altland-Zirnbauer classification, and protected by mirror and a generalized chiral symmetry that can be manipulated in an optical lattice with Raman-induced spin-orbit coupling, with its topology being detected by measuring the spin polarization of Bloch states at highly symmetric points of the Brillouin zone. Quite interestingly, the nontrivial topology of the phase is also reflected in the non-equilibrium spin dynamics when the system is quenched from initial phase to the trivial and nontrivial phases. We demonstrate the underlying mechanisms of the spin relaxation dynamics in the present SPT phase. Secondly, we present the engineering of 2D spin-orbit coupling for ultracold fermions in optical lattices, leading to the realization of 2D Dirac-type semimetal band structure [2]. We highlight the tunable band topology by demonstrating controlled band inversion, tuning the band asymmetry and reducing dimensionality of the system into quasi-1D in the present setup. Finally we probe the Dirac points with two zero spin-polarization lines connecting two Dirac points being measured in time-averaged momentum-dependent spin textures after the quench from the trivial to the Dirac semimetal band. Our works should pave the way for the quantum simulation of topological phases in and out of equilibrium for ultracold fermions.

[1] B. Song et al. Science Advances **4**, eaao4748 (2018).

[2] In preparation.

### Keywords:

Topological phases, Ultracold atoms, Quantum simulation

## Pairing Dynamics of Polar States in a Quenched p-Wave Superfluid Fermi Gas

YOON Sukjin\*<sup>1, 2, 3</sup>, WATANABE Gentaro\*<sup>1, 2, 4, 5, 6</sup>

<sup>1</sup>Center for Theoretical Physics of Complex Systems, Institute for Basic Science (IBS), Daejeon 34051, Korea, <sup>2</sup>Asia Pacific Center for Theoretical Physics, Pohang, Gyeongsangbuk-do 37637, Korea, <sup>3</sup>Quantum Universe Center, Korea Institute for Advanced Study, Seoul 02455, Korea, <sup>4</sup>Department of Physics and Zhejiang Institute of Modern Physics, Zhejiang University, Hangzhou, Zhejiang 310027, China, <sup>5</sup>University of Science and Technology, Daejeon 34113, Korea, <sup>6</sup>Department of Physics, POSTECH, Pohang, Gyeongsangbuk-do 37673, Korea  
sjyoon@ibs.re.kr, gentaro@zju.edu.cn

### Abstract:

We study the pairing dynamics of polar states in a single species p-wave superfluid Fermi gas following a sudden change of the interaction strength. The anisotropy of pair interaction together with the presence of the centrifugal barrier results in profoundly different pairing dynamics compared to the s-wave case. Depending on the direction of quenches, quench to the BCS regime results in large oscillatory depletion of momentum occupation inside the Fermi sea or large oscillatory filling of momentum occupation. A crucial role of the resonant state supported by the centrifugal barrier in the pairing dynamics is elucidated.

### Keywords:

Cold atoms, Fermi gases, Collective Dynamics

## Critical vortex shedding in a strongly interacting fermionic superfluid

신용일\*<sup>1, 2</sup>, 고범석<sup>1</sup>, 박지우\*<sup>1</sup>

<sup>1</sup>Department of Physics and Astronomy, and Institute of Applied Physics, Seoul National University,

<sup>2</sup>Center for Correlated Electron Systems, Institute for Basic Science

yishin@snu.ac.kr, jw\_park@snu.ac.kr

### Abstract:

Quantized vortices are fundamental topological excitations of a superfluid whose creation and dynamics reveal the underlying thermodynamic and transport properties of their medium. A key example is found in Helium-4, where the creation of quantized vortices lowers the critical velocity for superflow below its theoretical prediction. Here, we report on the experimental study of the critical velocity for vortex shedding in a strongly interacting fermionic superfluid. An impenetrable optical obstacle is translated across the center of the superfluid at a constant velocity, creating vortex-antivortex pairs above the critical velocity. The critical velocity is measured as a function of the translation distance  $L$  and the interaction parameter  $1/k_F a$ . In the two limits of  $L$ , we observe markedly different behaviors of the critical velocity. For short  $L$ , it shows a pronounced peak near unitarity, whereas for long  $L$ , the peak is strongly suppressed, implying that the increase of the drag force with velocity is slow near unitarity. Further comparison of the measured critical velocity to the speed of sound and the pair breaking velocity, and the application of the periodic shedding model to determine the onset of the drag force will be discussed.

### Keywords:

Quantum gases, Fermionic superfluidity, Strongly correlated phenomena, Quantized vortices, Critical velocity

## 원자분수시계의 원자 궤도 분석방법

박상언\*<sup>1, 2</sup>, 이상민<sup>1, 2</sup>, 홍현규<sup>1</sup>, 허명선<sup>1</sup>, 권택용<sup>1</sup>, 이상범<sup>1</sup>

<sup>1</sup>한국표준과학연구원 광기술표준부, 과학기술연합대학원, <sup>2</sup>과학기술연합대학원  
parkse@kriss.re.kr

### Abstract:

냉각된 원자를 수직방향으로 발사시켜 실험을 진행하는 원자 분수시계에서 원자의 초기 위치와 발사각, 전체시스템의 기울어짐은 정확히 정의되고 최적화 되어야한다. 최적화되지 않은 조건에서의 실험은 관측되는 원자량과 Ramsey 신호의 contrast 감소에 직접적으로 관여하여 원자시계의 성능 하락에 영향을 준다. 또한 원자시계의 불확도에 큰 기여를 하는 DCP(distributed cavity phase) 에러를 분석하기 위해 원자의 진행 경로를 파악하는 것은 필수적이다. 본 연구에서는 분수시계의 기울어짐에 따라 관측되는 원자량과 Ramsey, Rabi 신호를 이용하여 원자의 초기조건과 원자의 궤적을 분석하였고 이를 계산과 실험을 통해 확인하였다.

### Keywords:

fountain clock, atomic trajectory, Monte Carlo method

## Enhancing phase sensitivity in noisy Gaussian quantum metrology

이수용\*<sup>1</sup>

<sup>1</sup>고등과학원, 계산과학부  
papercrane79@gmail.com

### Abstract:

We investigate the phase sensitivity in a Gaussian noise model using Gaussian resources and measurements. For general single-mode Gaussian states, we classify the symmetric logarithmic derivative whose eigenbasis provides the optimal measurement achieving the ultimate bound. We demonstrate that the phase sensitivity can be enhanced with increasing input thermal noise, which is observed by a general-dyne detection. For typical two-mode Gaussian states, we study the robustness against photon loss while maintaining quantum enhancement.

### Keywords:

Gaussian quantum metrology, Gaussian noise, Robustness

## Orbital mixing of Fermi atoms in driven optical lattice

신용일\*<sup>1</sup>, 강진현<sup>1</sup>, 한정호<sup>1</sup>

<sup>1</sup>서울대학교 물리천문학부  
yishin@snu.ac.kr

### Abstract:

Recent studies focus on topological insulating phase, which exhibit interesting properties. Spin-orbit coupling is a key element for nontrivial topological properties, which locks spin and their motion. In ultracold atomic system, the spin-orbit coupling was first implemented by using two-photon Raman coupling between two hyperfine states, where a momentum transfer introduces position dependent complex tunneling amplitude, resulting in effective gauge field [1]. In recent, the synthesized gauge field have allowed for the realization of Harper-Hofstadter Hamiltonian in two-dimensional lattice [2,3], and direct observation of chiral edge current in ladder system [4,5]. We demonstrate synthesizing spin-orbit coupling using lattice band pseudospins. Using periodically driven optical lattice by two-photon Raman transition, we engineer spin-orbit coupling between s-band and p-band of optical lattice. We investigate the property of this orbital-mixed band structure by measuring lattice momentum distribution. We observe asymmetry in lattice momentum distribution which can be interpreted as a chiral edge current, showing that our system can be described by the two-leg ladder model in “synthetic dimension” frame. Our results suggest a new way to explore novel topological quantum matter using orbital degrees of freedom.

[1] Y.-J. Lin, R. L. Compton, K. Jimenez-Garcia, and I. B. Spielman, Nature 471, 83 (2011).

[2] M. Aidelsburger, M. Atala, M. Lohse, J. T. Barreiro, B. Paredes, and I. Bloch, Phys. Rev. Lett. 111, 185301 (2013).

[3] H. Miyake, G. A. Siviloglou, C. J. Kennedy, W. C. Burton, and W. Ketterle, Phys. Rev. Lett. 111, 185302 (2013).

[4] M. Mancini, G. Pagano, G. Cappellini, L. Livi, M. Rider, J. Catani, C. Sias, P. Zoller, M. Inguscio, M. Dalmonte, and L. Fallani, Science 349, 1510 (2015).

[5] B. K. Stuhl, H.-I. Lu, L. M. Ayccock, D. Genkina, and I. B. Spielman, Science 349, 1514 (2015).

### Keywords:

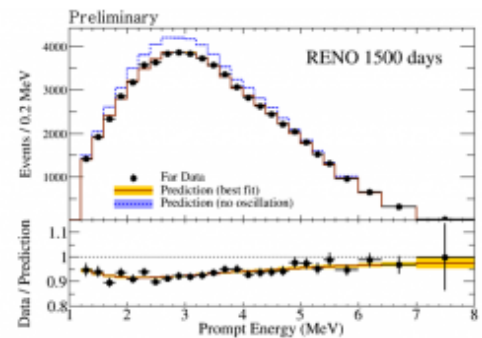
Quantum gases, optical lattice, synthetic gauge field

## New results from RENO

서현관<sup>\*1</sup>, 권은향<sup>1</sup>, 김상용<sup>1</sup>, 김수봉<sup>1</sup>, 서선희<sup>1</sup>, 양정열<sup>1</sup>, 이동하<sup>1</sup>, 이용창<sup>1</sup>, 이현기<sup>1</sup>, 김우영<sup>2</sup>, 세르게이체보타요브<sup>2</sup>, 박명렬<sup>3</sup>, 최준호<sup>3</sup>, 장한일<sup>4</sup>, 김종건<sup>5</sup>, 김종현<sup>5</sup>, 서지웅<sup>5</sup>, 유인태<sup>5</sup>, 전상훈<sup>5</sup>, 정다운<sup>5</sup>, ROTT Carsten<sup>5</sup>, 곽필준<sup>6</sup>, 김재률<sup>6</sup>, 문동호<sup>6</sup>, 박경환<sup>6</sup>, 박영서<sup>6</sup>, 신창동<sup>6</sup>, 임인택<sup>6</sup>, 주경광<sup>6</sup>, 장지승<sup>7</sup>, 유종희<sup>8</sup>, 주기원<sup>8</sup>  
<sup>1</sup>서울대학교 물리천문학부, <sup>2</sup>경북대학교, <sup>3</sup>동신대학교, <sup>4</sup>서영대학교, <sup>5</sup>성균관대학교, <sup>6</sup>전남대학교, <sup>7</sup>GIST, <sup>8</sup>KAIST  
hkseo16@gmail.com

### Abstract:

The Reactor Experiment for Neutrino Oscillation (RENO) has been taking reactor antineutrinos data from the six reactors at Hanbit Nuclear Power Plant in Korea using two identical near and far detectors since August, 2011. The smallest neutrino mixing angle  $\theta_{13}$  has been successfully measured by observing the disappearance of reactor antineutrinos. In 2016, RENO has published an updated value of  $\theta_{13}$  and its first measurement of  $dm^2_{ee}$  based on energy dependent disappearance probability using 500 live days of data taken until January. RENO has accumulated more data to obtain more precise values of  $\theta_{13}$  and  $dm^2_{ee}$ . A study has been on progress to find changes in the observed reactor antineutrino flux with respect to the reactor fuel evolution. In this talk, we present newly measured values of  $\theta_{13}$  and  $dm^2_{ee}$  and results on the evolution of observed reactor antineutrino yields.



### Keywords:

neutrino, reactor, oscillation

## Search for Sterile Neutrinos at RENO

서지웅\*<sup>1</sup>, 유인태<sup>1</sup>, ROTT Carsten<sup>1</sup>, 김종건<sup>1</sup>, 전상훈<sup>1</sup>, 정다은<sup>1</sup>, 김종현<sup>1</sup>, 김수봉<sup>2</sup>, 서선희<sup>2</sup>, 서현관<sup>2</sup>, 권은향<sup>2</sup>, 김상용<sup>2</sup>, 양정열<sup>2</sup>, 이동하<sup>2</sup>, 이용창<sup>2</sup>, 이현기<sup>2</sup>, 김우영<sup>3</sup>, CHEBOTERYOV Sergey<sup>3</sup>, 곽필준<sup>4</sup>, 김재률<sup>4</sup>, 문동호<sup>4</sup>, 박경환<sup>4</sup>, 박영서<sup>4</sup>, 신창동<sup>4</sup>, 임인택<sup>4</sup>, 주경광<sup>4</sup>, 박명렬<sup>5</sup>, 최준호<sup>5</sup>, 장한일<sup>6</sup>, 장지승<sup>7</sup>, 유종희<sup>8</sup>, 주기원<sup>8</sup>

<sup>1</sup>성균관대학교 물리학과, <sup>2</sup>서울대학교 물리학과, <sup>3</sup>경북대학교 물리학과, <sup>4</sup>전남대학교 물리학과, <sup>5</sup>동신대학교 방사선학과, <sup>6</sup>서영대학교 물리학과, <sup>7</sup>GIST 물리학과, <sup>8</sup>KAIST 물리학과  
jwseo115@gmail.com

### Abstract:

The RENO experiment has successfully measured  $\theta_{13}$  using the disappearance of electron anti-neutrinos in three-flavor neutrino oscillations. We search for sterile neutrinos in four-flavor oscillation model using roughly 1500 days of data collected by the RENO experiment. We have not seen any positive signal and obtain an excluded region of the oscillation parameters. We present an excluded contour plot in  $\sin^2(2\theta_{14}) - \Delta m_{41}^2$  space.

### Keywords:

RENO, neutrino, sterile neutrino

## Precise measurement of $\theta_{13}$ and $\Delta m^2_{ee}$ at RENO

이동하<sup>\*1</sup>, 김우영<sup>2</sup>, SERGUEY Serguey<sup>2</sup>, 박명렬<sup>3</sup>, 최준호<sup>3</sup>, 장한일<sup>4</sup>, 권은향<sup>1</sup>, 김상용<sup>1</sup>, 김수봉<sup>1</sup>, 서선희<sup>1</sup>, 서현관<sup>1</sup>, 양정열<sup>1</sup>, 이용창<sup>1</sup>, 이현기<sup>1</sup>, 김종건<sup>5</sup>, 김종현<sup>5</sup>, 서지웅<sup>5</sup>, 유인태<sup>5</sup>, 전상훈<sup>5</sup>, 정다은<sup>5</sup>, ROTT Carsten<sup>5</sup>, 곽필준<sup>6</sup>, 김재률<sup>6</sup>, 문동호<sup>6</sup>, 박경환<sup>6</sup>, 박영서<sup>6</sup>, 신창동<sup>6</sup>, 임인택<sup>6</sup>, 주경광<sup>6</sup>, 장지승<sup>7</sup>, 유종희<sup>8</sup>, 주기원<sup>8</sup>

<sup>1</sup>서울대학교 물리천문학부, <sup>2</sup>경북대학교, <sup>3</sup>동신대학교, <sup>4</sup>서영대학교, <sup>5</sup>성균관대학교, <sup>6</sup>전남대학교, <sup>7</sup>GIST, <sup>8</sup>KAIST  
summerofeast@snu.ac.kr

### Abstract:

The RENO experiment has measured the neutrino mixing angle  $\theta_{13}$  and  $\Delta m^2_{ee}$ , using reactor antineutrinos from the reactors at Hanbit Nuclear Power Plant since Aug. 2011. In 2016, RENO published results on  $\sin^2(2\theta_{13})$  and  $\Delta m^2_{ee}$  using the energy dependent oscillation of reactor antineutrinos in the 500days of data. RENO has accumulated roughly  $\sim 2000$  days of data with reduced backgrounds and thus decreased systematic uncertainties. Due to the improved statistics and systematic uncertainties we measured  $\sin^2(2\theta_{13})$  and  $\Delta m^2_{ee}$  more precisely. In this talk we will present new results from the  $\sim 2000$  days data.

### Keywords:

RENO,  $\Delta m^2_{ee}$ , precise measurement

## Theta13 measurement of using neutron captures on hydrogen at RENO

주경광\*<sup>1</sup>, 신창동<sup>1</sup>, 곽필준<sup>1</sup>, 김재률<sup>1</sup>, 문동호<sup>1</sup>, 박경환<sup>1</sup>, 박영서<sup>1</sup>, 임인택<sup>1</sup>, 김우영<sup>2</sup>, 체바토료프세르게이<sup>2</sup>, 장한일<sup>3</sup>, 권은향<sup>4</sup>, 김상용<sup>4</sup>, 김수봉<sup>4</sup>, 서선희<sup>4</sup>, 서현관<sup>4</sup>, 양정열<sup>4</sup>, 이동하<sup>4</sup>, 이용창<sup>4</sup>, 이현기<sup>4</sup>, 김종건<sup>5</sup>, 김종현<sup>5</sup>, 서지웅<sup>5</sup>, 유인태<sup>5</sup>, 전상훈<sup>5</sup>, 정다운<sup>5</sup>, ROTT Carsten<sup>5</sup>, 장지승<sup>6</sup>, 유종희<sup>7</sup>, 주기원<sup>7</sup>

<sup>1</sup>전남대학교, <sup>2</sup>경북대학교, <sup>3</sup>동신대학교, <sup>4</sup>서영대학교, <sup>5</sup>서울대학교, <sup>6</sup>성균관대학교, <sup>7</sup>GIST, <sup>8</sup>KAIST  
kkjoo@chonnam.ac.kr

### Abstract:

RENO has been taking data since August, 2011 and successfully measured the smallest neutrino mixing angle, theta13. The measurement values are obtained from the observed reactor antineutrino events with neutron captures on gadolinium (n-Gd) in the target detector region. In addition, RENO has successfully measured the mixing angle as well, using an independent sample with neutron captures on hydrogen (n-H). Because of a large accidental background in the n-H sample, the analysis requires additional reduction of backgrounds. This independent measurement provides a valuable systematic cross-check of the theta13 measurement using the n-Gd sample. In this talk, we will present the results from the 1500 days of n-H data sample.

### Keywords:

RENO, neutrino

## Physics Potentials and Status of the 2<sup>nd</sup> Hyper-Kamiokande Detector in Korea

서선희\*<sup>1</sup>

<sup>1</sup>서울대학교 물리학과  
shseo@phya.snu.ac.kr

### Abstract:

Hyper-Kamiokande (Hyper-K) succeeds the very successful Super-K experiment and will consist of two identical detectors, each filled with 260 kton water and equipped with 40% photo-coverage. Physics program of Hyper-K is broad, covering from particle physics to Astrophysics.

The 1<sup>st</sup> detector will be built in Japan, and the 2<sup>nd</sup> detector is considered to be built in Korea because locating the 2<sup>nd</sup> detector in Korea improves physics sensitivities in most cases thanks to the longer baseline (~1,100 km) and larger overburden (~1000 m) for Korean candidate sites.

In this talk, we present physics potentials and status of the 2<sup>nd</sup> Hyper-K detector in Korea.

### Keywords:

Korean Neutrino Observatory, Hyper-K, CP violation, neutrino mass ordering determination, J-PARC

## Overview of the CAPP-PACE detector

이(Lee)도유(Doyu)\*<sup>2</sup>, 정우현<sup>1</sup>, 권오준<sup>1</sup>, 이수형<sup>1</sup>, 최지훈<sup>1</sup>, MATLASHOV Andrei<sup>1</sup>, 김진수<sup>2</sup>, 안단호<sup>2</sup>, KUTLU Caglar<sup>2</sup>, SEMERTZIDIS Yannis<sup>1, 2</sup>  
<sup>1</sup>IBS, <sup>2</sup>KAIST  
du5698@kaist.ac.kr

### Abstract:

IBS/CAPP searches for dark matter axions into microwave photons, looking for the excess radiation deposited into a cavity submerged in a strong magnetic field. It is essential to reduce the background thermal noise and to minimize the electronic noise of the readout system in order to increase the sensitivity of the experiment. IBS/CAPP has recently launched a direct axion detection experiment, CAPP-PACE, aiming at the axion frequency range of 2.45~2.75 GHz and started taking data since the end of 2017. I will present the overview of the detector, including the dilution refrigerator that can reach below 10 mK, the 8 T superconducting magnet, the high-Q copper split cavity with a pure sapphire tuning rod, the piezoelectric tuning system, and the complete RF readout chain. The progress in R&D on SQUID amplifiers will also be discussed.

### Keywords:

Axion

## An annual modulation study of the COSINE-100 experiment with the first one year data

ADHIKARI Govinda\*<sup>1</sup>

<sup>1</sup>세종대학교 물리학과  
adhikari.astro@gmail.com

### Abstract:

The COSINE-100 is a dark matter WIMPS (Weakly Interacting Massive Particles) search experiment using NaI(Tl) scintillating crystals as a target at the Yangyang underground laboratory. The physics data have been collected since late September of 2016 in order to confirm or refute the annual modulation signal observed by the DAMA/LIBRA experiment. Here, a preliminary result of the annual modulation analysis using the first one year data with energy threshold of  $\sim 2$  keVee will be presented in this talk.

### Keywords:

DAMA, annual modulation, scintillation

## Status of R&D studies for further COSINE-200 experiment

김남영\*<sup>1</sup>

<sup>1</sup>기초과학연구원 지하실험연구단  
nykim@ibs.re.kr

### Abstract:

Currently, the COSINE-100 detector is installed and running for dark-matter search using Na(Tl) detectors at Yangyang underground laboratory. COSINE-200, the next phase of the experiment, requires crystal background levels that are well below, and light yields that are well above, those of the DAMA/LIBRA detector. To accomplish this, several R&D studies are ongoing. Here, the R&D studies will be presented.

### Keywords:

Dark matter search, NaI(Tl) crystal,

## The muon simulation for the AMoRE-II experiment.

배한욱\*<sup>1</sup>, 이세욱<sup>1</sup>, 전은주<sup>2</sup>

<sup>1</sup>경북대학교 물리학과, <sup>2</sup>기초과학연구원 지하실험연구단  
qogksdnr@hotmail.com

### Abstract:

The AMoRE (Advanced Molybdenum based Rare process Experiment) phase-II is an experiment to search neutrino-less double beta decay of Mo-100 which is the later phase of the AMoRE experiment. If the double beta decay is found, it means that the neutrinos are Majorana particles and we can measure their masses. The experiment is going to be carried out in the deep underground in order to observe the extremely rare events free from the backgrounds coming from the cosmic ray particles. However, even in the deep underground, there are still some cosmic ray particles that can affect the measurement and must be excluded as much as possible. A muon veto counter is a sort of detector that can veto cosmic muons coming to the inner space where the CaMoO<sub>4</sub> (CMO) crystals and detectors are located. We studied effects of veto materials in the AMoRE-II experiment configuration. In detail, we compared the background values in CKKY unit when the veto material is 3m of water or 30cm of lead. Also, we investigated the effect of thickness of water tank. Detail results with discussions will be shown in this presentation.

### Keywords:

underground physics, muon, Geant4, neutrons double-beta decay, AMoRE

## 중력파 검출의 새로운 방법

박일홍\*<sup>1</sup>

<sup>1</sup>성균관대학교 물리학과  
ilpark@skku.edu

### Abstract:

2017년 LIGO 그룹은 중력파 GW170817를 검출하였고, 바로 세계의 지상 및 우주의 70여개 전자기파 관측소에서도 multi-wavelength 전자기파를 함께 관측함으로써 multi-messenger astrophysics의 시대가 도래되고 있습니다. 특히 여러 band에서의 중력파 검출은 앞으로의 실험에 가장 중요한 이슈가 될 것입니다. 이에 우리는 wide band 중력파를 검출할 수 있는 우주에서의 중력파 검출의 새로운 아이디어와 방법 (프로젝트 SG)은 물론 전자기파의 동시관측이 가능한 초기 설계를 소개하고자 합니다.

### Keywords:

중력파, 우주실험

## 새로운 방법의 중력파 검출을 위한 이론적 계산

김동훈\*<sup>1</sup>, 박일홍<sup>2</sup>

<sup>1</sup>서울대학교 물리천문학부, <sup>2</sup>성균관대학교 물리학과  
ki1313@yahoo.com

### Abstract:

최근 LIGO에 의한 중력파 GW170817의 검출과 더불어 동시에 감마선, X선, 가시광선을 통한 중력파 천체의 포착은 이른바 multi-messenger astronomy라는 새로운 천체물리학의 장을 열었다. 이러한 조류에 발맞춰, broad band의 중력파 검출 및 전자기파 동시 관측을 위한 새로운 형태의 우주 실험 장치의 설계가 현재 구상 중인데, 이에 대비한 이론적 예측 및 계산을 보이고자 한다.

### Keywords:

중력파, multi-messenger astronomy

## 새로운 중력파 검출을 위한 우주실험의 설계

박일홍\*<sup>1</sup>

<sup>1</sup>성균관대학교 물리학과  
ilpark@skku.edu

### Abstract:

우주에서의 중력파 검출 프로젝트 SG에서, 소형 위성 및 탑재체, 궤도 운용에 대한 초기 설계와 앞으로의 개발 사항에 대하여 토의하고자 합니다.

### Keywords:

중력파, 우주실험, 위성탑재체

## Results from a search for secluded dark matter in the sun using IceCube

ROTT Carsten\*<sup>1</sup>, TOENNIS Christoph<sup>1</sup>

<sup>1</sup>성균관대학교  
rott@skku.edu

### Abstract:

Secluded dark matter is a current model for dark matter, where dark matter particles annihilate to standard model particles via a metastable mediator. In the case of annihilations in the sun sufficiently long-lived mediator particles can escape the solar plasma before decaying, avoiding the absorption of signal particles. The result of this is significantly amplified neutrino signal at higher energies. This yields a greater sensitivity for indirect searches for dark matter using neutrino detectors. In this talk the results of such a search for secluded dark matter in the sun with the IceCube neutrino observatory will be presented. WIMP masses ranging from 100 GeV to 10 TeV and mediators between 1 ns and 10 s decaying directly into neutrinos are considered. The data taken by IceCube in the years from 2011 to 2015 in the 86 string configuration is used in the analysis.

### Keywords:

Dark Matter, IceCube Neutrino Telescope

## ISS-GAMMA for the observation of the Gamma-Ray Bursts and Terrestrial Gamma Flash

박일흥\*<sup>1</sup>, 정소민<sup>1</sup>, 베덴켄니콜라이<sup>1</sup>, 홍기한<sup>1</sup>, 오승환<sup>1</sup>

<sup>1</sup>성균관대학교 물리학과  
ilpark@skku.edu

### Abstract:

The ISS-GAMMA is the space payload which aims at the observation of both Gamma-ray burst (GRB) and Terrestrial gamma Flash (TGF) on the ISS. It is one of the payloads of Russian space mission, Gamma-lightning detector. It will be launched and installed on the ISS in 2020. The ISS-GAMMA consists of two kinds of detectors to detector transients in gamma-rays from the universe and the Earth. The payload has 320 x 420 x 200 mm<sup>2</sup> in size and 7 kg in mass. We will present the purpose, design, and schedule of ISS-GAMMA briefly.

### Keywords:

Gamma-ray Burst, payload, Gamma-ray,

## Astroparticle physics with the IceCube Neutrino Telescope

ROTT Carsten<sup>\*1</sup>

<sup>1</sup>성균관대학교

rott@skku.edu

### Abstract:

The IceCube neutrino telescope, located at the geographic south pole, is the worlds largest neutrino detector. IceCube is a multi-purpose detector with an extremely broad science program. Recent highlights include the discovery of high-energy astrophysical neutrinos and the detection of energetic gamma-rays in coincidence with a very high energy neutrino events. Recent results from IceCube will be highlighted with a particular focus on the Korean contributions. Ways to improve the IceCube detector in future will be discussed.

### Keywords:

Neutrino, IceCube Neutrino Telescope, Astrophysical neutrinos, multi-messenger science

## Status of ISS-CREAM and SCD

박일흥\*<sup>1</sup>, TAKEISHI Ryuji<sup>1</sup>, LEE Jik<sup>1</sup>, JEONG Soomin<sup>1</sup>, CHOI Gwangho<sup>1</sup>, KIM Sangwoo<sup>1</sup>

<sup>1</sup>성균관대학교 물리학과  
ilpark@skku.edu

### Abstract:

The acceleration and propagation mechanism of cosmic rays is not well understood. The ISS-CREAM experiment aims to extend direct measurements of cosmic ray composition to energies capable of generating air showers reaching the ground by the observation on the ISS. The ISS-CREAM measures the composition by Silicon Charge Detector (SCD) from the proton to iron with a charge resolution of 0.1 – 0.3. We report the status of the ISS-CREAM and analysis results of SCD data.

### Keywords:

cosmic ray, ISS-CREAM, International Space Station

## ISS-CREAM실험에서 SCD의 데이터 처리 방법, 검출기 상태 및 전반적인 상황 보고

박일흥\*<sup>1</sup>, 최광호<sup>1</sup>, 김상우<sup>1</sup>, TAKEISHI Ryuji<sup>1</sup>, 정수민<sup>1</sup>, 이직<sup>1</sup>

<sup>1</sup>성균관대학교 물리학과  
ilpark@skku.edu

### Abstract:

International Space Station - Cosmic Ray Energetic And Mass (ISS- CREAM)실험은 국제우주정거장에서 고에너지 우주선을 검출하고 성분 연구 및 가속과정을 증명 하는데 의의를 두고 있으며, 2017년 8월 SpaceX 사의 Dragon에 과학 탑재체를 싣고 국제우주정거장에 성공적으로 발사, 설치 및 운용 중이다. 본 연구실에서는 과학 탑재체의 중요한 검출기 중 하나인 Silicon Charge Detector (SCD)를 독자적으로 개발하여 실험에 참여하고 있다. 본 발표에서는 ISS-CREAM실험에서 얻은 데이터를 수신 및 목적에 맞게 데이터를 처리하는 방법 (level1 data processing), SCD의 electronics baseline값과 온도와의 상관관계, SCD 작동 유무 및 상태 확인 (monitoring), 반 알런데 방사선대(SAA) 에서 SCD 운용 방법 등 우주에서의 전반적인 SCD operation 진행 상황에 대해 보고하고자 한다.

### Keywords:

ISS-CREAM, SCD

## The origin of characteristic distribution of ultra-high-energy cosmic rays observed by the Telescope Array experiment

KIM Jihyun\*<sup>1</sup>, RYU Dongsu<sup>1</sup>, KIM Suk<sup>2</sup>, REY Soo-Chang<sup>3</sup>, KANG Hyesung<sup>4</sup>

<sup>1</sup>Department of Physics, UNIST, <sup>2</sup>Korea Astronomy and Space Science Institute, <sup>3</sup>Department of Astronomy and Space Science, Chungnam National University, <sup>4</sup>Department of Earth Sciences, Pusan National University  
jihyunkim@unist.ac.kr

### Abstract:

The distribution of ultra-high-energy cosmic rays observed by the Telescope Array experiment can be characterized in two aspects: an excess of events, so-called TA hotspot, and a relative deficit of events toward the Virgo cluster. To study the origin of these characteristic distributions of the TA events, we examine structures in the local universe, within 50 Mpc. Toward the TA hotspot, there seem to be filamentary structures of galaxies connected to the Virgo Cluster. We here report an investigation of the hypothesis that the distribution of TA events is a consequence of these structures of the local universe. Through statistical tests, we find a close correlation between the distribution of the TA events and filaments of galaxies.

### Keywords:

cosmic rays, large-scale structure of universe

## Pion production study in DJBUU

KIM Young-Min\*<sup>1</sup>, JEON Sangyong<sup>2</sup>, KIM Myungkuk<sup>3</sup>, LEE Chang-Hwan<sup>3</sup>, KIM Youngman<sup>4</sup>

<sup>1</sup>School of Natural Science, Ulsan National Institute of Science and Technology (UNIST), <sup>2</sup>Department of Physics, McGill University, <sup>3</sup>Department of Physics, Pusan National University, <sup>4</sup>Rare Isotope Science Project, Institute for Basic Science (IBS)  
ymkim715@unist.ac.kr

### Abstract:

Pion production ratio has an important role of understanding nuclear symmetry energy. One way to study pion production is to simulate heavy ion collisions based on a theoretical framework which we want to implement. We develop a new Boltzmann-Uehling-Uhlenbeck (BUU) transport code, named the DJBUU (Daejeon BUU). However, depending on the details of the code such as assumptions for nucleon dynamics, cross sections, potentials for  $\Delta$  and  $\pi$ , the prediction of the pion production is quite uncertain. Therefore, there can exist many different transport codes with different models. In this talk, I will present recent results of pion production in DJBUU and compare our results with those in other transport codes. In order to compare the results in the same condition, we used a standard configuration of a periodic box provided by the transport code comparison project committee.

### Keywords:

BUU, DJBUU, transport code, pion production, symmetry energy

## Collision, blocking and Mean-field dynamics in DJBUU

김명국<sup>1</sup>, 이창환\*<sup>1</sup>, 김영민<sup>2</sup>, 김영만<sup>3</sup>, 전상용<sup>4</sup>

<sup>1</sup>부산대학교 물리학과, <sup>2</sup>울산과학기술원 자연과학부, <sup>3</sup>기초과학연구원 중이온가속기건설구축사업단, <sup>4</sup>맥길대학교 물리학과  
clee@pusan.ac.kr

### Abstract:

수송이론을 이용한 수치모사는 낮은 에너지 영역의 중이온 충돌의 다양한 물리적 정보를 얻는데 중요한 역할을 한다. 국내 중이온가속기 라온(RAON)이 건설 중에 있으며 그에 따라 국내 연구진을 중심으로 새로운 수송이론 코드(DJBUU)를 완성 및 업그레이드 진행 중에 있다. 이와 더불어 전 세계적으로 동일한 초기 조건 아래 수송이론을 이용한 다양한 코드의 결과를 비교하는 프로젝트인 Transport Code Comparison Project가 수행되고 있다. 이번 발표에서 중이온 충돌 수치모사의 중요한 요소 중 충돌과 블로킹 그리고 핵자의 운동 방정식을 기술하는 상대론적 평균장 근사에 대한 결과들을 발표할 예정이다. 이 결과들은 코드 비교 그룹의 결과들과 직접적인 비교가 가능하고 DJBUU의 코드 테스트 및 신뢰도를 높이는데 중요하게 작용 된다. DJBUU의 충돌 및 파울리 블로킹 효과를 정량적으로 확인하기 위해 periodic boundary 조건이 적용된 박스 시스템을 고려한다. 시스템 내에서 주어진 초기조건의 입자들이 충돌과 블로킹 효과에 의해 시간에 따라 변화하는 양상을 이해할 수 있다. 또한, 상대론적 평균장 근사는 박스 시스템의 바리온 밀도가 비대칭적으로 주어진 경우 local 평균장 작용으로 인한 시스템의 바리온 밀도를 시간에 따라 이해함으로써 코드의 상대론 근사를 직접적으로 테스트 해 볼 뿐 아니라 그 결과를 코드비교 그룹에 참여시켜 다양한 결과들과 직접적인 비교가 가능하게 된다.

### Keywords:

수송이론, 중이온 충돌

## Effects of isospin asymmetry on nuclear stopping

김경일\*<sup>1</sup>

<sup>1</sup>기초과학연구원 활용연구개발팀  
hellmare@nate.com

### Abstract:

We study the energy isotropy ratio,  $R_E$ , in a variety of isospin asymmetry with our QMD code. In heavy-ion collisions, a large portion of transverse energy is generated by nucleon-nucleon (NN) collisions. Thus, the ratio of longitudinal and transverse energies is a good observable to study in-medium NN cross-sections. We reproduce the  $R_E$ s from experimental data and then study the sensitivity of the  $R_E$  to the change of NN cross-sections. We assume the isospin dependence of NN cross-sections and investigate its effect to the  $R_E$ . We discuss the effects of isospin asymmetry in nuclear matter to the neutron-proton difference of the energy isotropy ratio.

### Keywords:

QMD, Stopping ratio, Isospin asymmetry

## Effect of long range potential for the $^{11}\text{Be}+^{197}\text{Au}$ system

천명기\*<sup>1</sup>, 허경수<sup>1</sup>, 최기석<sup>2</sup>, 소운영<sup>3</sup>

<sup>1</sup>승실대학교 물리학과, <sup>2</sup>항공대학교 교양학부, <sup>3</sup>강원대학교 방사선학과  
cheoun@ssu.ac.kr

### Abstract:

Along with the development of advanced beam producing technique, the rare isotope beam becomes available. Consequently, many rare isotopes can be produced. Some of interesting are the nuclei of the halo structure. So many experiments have been tested to use these instable nuclei(Halo nuclei) as the projectile. And  $^{11}\text{Be}+^{197}\text{Au}$  was tested in TRIUMF-ISAC-I(Isotope Separator and accelerator) last year. Thus, elastic scattering, quasi elastic scattering, inelastic scattering and breakup crosssection results have been performed. So we analyzed each the results with an optical model using the LRDP potential and CDE(Coulomb Dipole Excitation) effect.

### Keywords:

optical model, halo nuclei, nuclear reaction

## The neutrino self-interaction and MSW effects in supernova nucleosynthesis

천명기\*<sup>1</sup>, [KO Heamin](#)<sup>1</sup>, KUSAKABE Motohoiko<sup>2</sup>, SASAKI Hirokazu<sup>3</sup>, KAJINO Toshitaka<sup>2, 3</sup>

<sup>1</sup>Department of Physics, Soongsil University, <sup>2</sup>International Research Center for Big-Bang Cosmology and Element Genesis, and School of Physics and Nuclear Energy Engineering, Beihang University,

<sup>3</sup>Department of Astronomy Graduate School of Science The University of Tokyo  
cheoun@ssu.ac.kr

### Abstract:

In this presentation, we show the neutrino oscillation effects such as neutrino self-interaction from the neutrinosphere and MSW effect on the element abundances. The representative synthesized elements by neutrino from supernova explosion are known as  ${}^7\text{Li}$ ,  ${}^{11}\text{B}$ ,  ${}^{92}\text{Nb}$ ,  ${}^{98}\text{Tc}$ ,  ${}^{138}\text{La}$ , and  ${}^{180}\text{Ta}$ . Near to the neutrinosphere, the neutrino density is about  $10^{32} \text{ cm}^{-3}$  which need to neutrino self-interaction as a collision term in Boltzmann equation for the neutrino density under the mean field approximation. Due to the propagation of the shock wave, we also have to take the neutrino propagation in matter, i.e. MSW effects. One of the important MSW region in O/Ne/Mg layers is given by progenitor. In this work, we study how the neutrino self-interaction and MSW effects influence on the element production by using the modified neutrino spectra and V-A interaction by QRPA.

### Keywords:

neutrino, self-interaction, MSW effect, nucleosynthesis

## Big bang nucleosynthesis with a non-extensive statistics

천명기\*<sup>1</sup>, JANG Dukjae<sup>1</sup>, KWON Youngshin\*<sup>2</sup>, KUSAKABE Motohiko<sup>3</sup>, KWAK Kyujin<sup>4</sup>

<sup>1</sup>Department of Physics, Soongsil University, <sup>2</sup>Research Institute of Basic Science, Korea Aerospace University, <sup>3</sup>International Research Center for Big-Bang Cosmology and Element Genesis, and School of Physics and Nuclear Energy Engineering, Beihang University, <sup>4</sup>School of Natural Science, Ulsan National Institute of Science and Technology  
cheoun@ssu.ac.kr, ykwon@kau.ac.kr

### Abstract:

It has been usually assumed that the particle velocity distribution in the big bang nucleosynthesis (BBN) epoch eventually relaxes to the standard Maxwell-Boltzmann distribution. However, the observed primordial abundances, typically of lithium, are not yet fully explained in such standard BBN scenarios. In order to solve this problem, there are several ways such as modified cosmological scenario, beyond standard model and so on. Among that ways, we try to approach this problem in modified statistical theory called 'Tsallis statistics', considering that the early Universe is in a plasma state. This approach leads to the modified particle velocity distribution and it affects the BBN via changing nuclear reactions. In this talk, we present the investigation of BBN with a non-Maxwellian velocity distribution derived by Tsallis statistics and how it can affect the primordial abundance.

### Keywords:

big bang nucleosynthesis, BBN, Tsallis, non-extensive statistics, Li problem

## A Hybrid Model of Skyrme-type and Brueckner-type Interactions for Equations of State for Neutron Star Matter

천명기\*<sup>1</sup>, 최순철<sup>1</sup>  
<sup>1</sup>승실대학교 물리학과  
cheoun@ssu.ac.kr

### Abstract:

We suggest a hybrid model for dense matter physics to explain the hyperon puzzle inherent in the 2.0 solar mass of neutron star. For the nucleon-nucleon (NN) interaction, we exploit the Skyrme-Hartree-Fock (SHF) approach based on various Skyrme interaction parameters but take the Brueckner-Hartree-Fock (BHF) approach for the interactions related to hyperons. For the latter, we make use of the multi-pomeron potential for the many-body interactions including hyperons, which are adjusted to the data deduced from various hypernuclei properties. Our results show that some Skyrme interactions like SG1 and SkI4 may reach to the 2.0 solar mass, but the SLy4 interaction needs a bit change of a parameter. For clear understanding the physics in the hybrid model, we discuss variations of fractional functions of related particles, symmetry energies, and chemical potentials. Finally, we argue the equations of state and the mass-radius relation of neutron stars, which turn out to be consistent with the available neutron star data.

### Keywords:

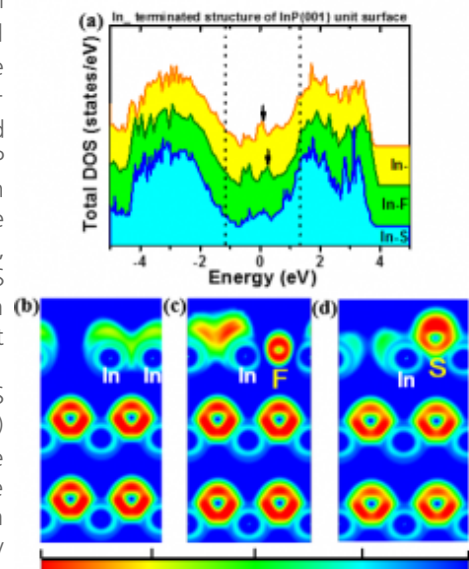
neutron star

## Improving Electrical Properties by Effective Sulfur Passivation via Modifying Surface State of Substrate in $\text{HfO}_2$ /InP systems

조만호\*<sup>1</sup>, 감항균<sup>1</sup>, 백민<sup>1</sup>, 정광식<sup>1</sup>, 김대경<sup>1</sup>, 송진동<sup>2</sup>  
<sup>1</sup>연세대학교 물리학과, <sup>2</sup>한국과학기술연구원  
mh.cho@yonsei.ac.kr

### Abstract:

The thermal stabilities and interfacial properties of  $\text{HfO}_2$  films on conditioned *i*-InP surfaces were investigated. When  $\text{HfO}_2$  was deposited on sulfur passivation InP substrate, improved interfacial properties were observed by suppressing the interfacial oxides between  $\text{HfO}_2$  and InP. X-ray photoelectron spectroscopy (XPS) and thermodynamic data indicated that Acetone-Methanol-Isopropanol (AMI) pre-clean process on InP substrate before Sulfur treatment helps the formation of sulfur passivation layer on InP surface more effectively, as comparing with hydrogen fluoride (HF) pre-cleaning. HF pre-cleaning reduces InP native oxides effectively, while generated In-F bonds on InP surface interrupt the formation of In-S bonds. Moreover, total density of states (TDOS) and electron localization functions (ELFs) calculation data showed that In-F bonds does not significantly decrease mid-gap defect states induced by In dangling bond. As a results, AMI pre-clean process were proposed for effective S passivation on substrate in  $\text{HfO}_2$ /InP system. The capacitance-voltage (C-V) data revealed that the hysteresis width and frequency dispersion in the accumulation and depletion regions were significantly improved in the AMI+S treated sample, as compared with HF+S treated sample. In addition, the AMI+S treated  $\text{HfO}_2$ /InP showed excellent thermal stability and electrical properties during post annealing at 600°C.



### Keywords:

Sulfur, surplus electron, passivation,  $\text{HfO}_2$ , InP

## 마그네슘 도핑된 질화갈륨 마이크로 로드의 도핑 불균일성 분석

최성한<sup>1</sup>, 송현규<sup>1</sup>, 유양석<sup>1</sup>, 우기영<sup>1</sup>, 이철원<sup>1</sup>, 조용훈\*<sup>1</sup>

<sup>1</sup>한국과학기술원 물리학과  
yhc@kaist.ac.kr

### Abstract:

질화갈륨(GaN)은 직접천이형 화합물 반도체이며, 높은 발광효율 및 열적, 화학적 안정성으로 인하여 광전소자의 재료로서 널리 사용되고 있다. 특히, 질화갈륨 기반의 마이크로/나노 로드의 경우, 결함밀도 및 strain을 감소시켜 결정품질을 향상시킬 수 있으며, 로드의 무극성 면 위 core/shell 구조의 활성층은 내부전기장에 의한 영향을 최소화시켜 광전소자의 효율을 향상시킬 수 있다.[1] 이와 질화갈륨 로드를 기반으로 하는 고효율 광전소자를 구현하기 위해서는 고품질의 도핑 층과 도핑층에 관한 특성 이해가 필요하다. 특히, 질화갈륨 로드에서의 p-도핑은 물질 자체의 한계로 인해 효율적 도핑이 어려운 점과 더불어, 로드가 평면 시료와 다른 도핑 주입 경로를 가지는 것으로 인해 단일 로드 내부에서 위치 별 도핑 량의 차이가 발생한다. [2] 따라서, 로드에서 p-도핑 특성을 파악하기 위해서는 공간적 도핑 특성의 차이를 고려한 종합적인 분석이 필요하다.

본 연구에서는 마그네슘으로 도핑된 p-타입 단일 질화갈륨 로드의 위치 별 도핑 특성을 분석하는 연구를 진행하였다. 파괴적 성분분석 방법인 time of flight secondary ion mass spectrometry (TOF-SIMS)를 통해 로드의 위치에 따른 도핑 량의 정량적인 변화를 확인하였다. 이 같은 도핑 불균일성으로 인해 발생하는 전기적 특성 차이는 4-point probes method를 통해 확인하였다. 마지막으로 광분석 방법인 photoluminescence (PL)과 라만(Raman) 측정을 이용하여 도핑으로 인한 위치 별 발광 특성의 차이를 확인하였다. 마지막으로, 각 실험 결과간의 상관관계 파악을 통해, 마그네슘 도핑된 질화갈륨 로드의 도핑 불균일성에 관한 종합적인 분석을 진행하였다.

[1] Y. Dong, et al, *Nano Lett.*, 9, 2183 (2009).

[2] A.Patsha, et al, *J. Phys. Chem. C*, 118, 24165 (2014).

### Keywords:

질화갈륨, 마이크로 로드, 마그네슘 도핑, 불균일성 분석

## 3차원 구조체와 결합된 양자점의 특성분석

조중희<sup>1</sup>, 김영민<sup>1</sup>, 여환섭<sup>1</sup>, 임승혁<sup>1</sup>, 김세정<sup>1</sup>, 공수현<sup>1</sup>, 조용훈\*<sup>1</sup>

<sup>1</sup>한국과학기술원, 물리학과  
yhc@kaist.ac.kr

### Abstract:

단일 광자원은 양자 암호화나 컴퓨팅과 같은 양자정보 통신에 활용될 수 있다는 점에서 최근 큰 각광을 받고 있다. 특히, 반도체 양자점 기반으로 구현하는 단일 광자원의 경우에는, 전기구동이 가능하고, 높은 온도에서도 단일 광자원 특성을 보인다는 장점이 있다. [1-5] 하지만, III-Nitride 물질 기반의 반도체 양자점의 경우에는 큰 내부 전기장과 높은 결정 결함 밀도가 내제되어 있어, spectral diffusion 현상을 발생시킨다. 이는 결과적으로, 단일 광자원의 선풍을 커지게 만들어서, 결맞음 성질이 저해되는 결과를 초래한다.

이번 연구에서는, GaN 기반의 피라미드 구조체에 형성된 InGaN 양자점을 제안한다. 피라미드 구조체에 형성된 InGaN 양자점의 경우에는 film위에 형성된 양자점과 다르게 위치 선택적 형성이 가능할 뿐만 아니라, 광 추출효율이 크게 개선된다. 뿐만 아니라, 피라미드 구조체는 꼭지점 근방에서 내부 전기장과 결정 결함 밀도를 효과적으로 줄이는 장점이 있다. 이러한 구조 성장을 위해, 유기금속화학 증착기를 이용하여 (0001) GaN on Sapphire를 성장 한 뒤, SiN<sub>x</sub>와 식각공정을 활용하여, hole mask 패턴을 제작하였다. 그 이후, 피라미드 구조체를 형성한 뒤, InGaN 양자점을 피라미드 꼭지점 부근에 성장하였다. 고분해능 투과전자현미경을 통해, 피라미드 꼭지점 위에 2 nm 미만의 높이를 갖는 InGaN 양자점을 확인하였다. 저온 스펙트럼 분석을 통해, spectral diffusion 현상이 크게 저하되었음을 확인 했을 뿐만 아니라, resolution-limited linewidth broadening 또한 관측하였다.

본 연구를 통해, III-Nitride 물질 기반의 반도체 양자점에서 크게 문제시 되어왔던 spectral diffusion 현상을 크게 개선시켰다. 차후 III-Nitride 물질 기반의 반도체 양자점을 활용한 양자정보 통신 응용을 위한 원천기술이 될 것이라 기대된다.

### 참고문헌

- [1] J. H. Kim et al., Scientific Reports 3, 2150 (2013)
- [2] S. H. Gong et al., Proceeding of the National Academy of Sciences 112, 5280 (2015)
- [3] Kim et al., Nano letter 16, 6117 (2016)
- [4] J. H. Cho et al., ACS Photonics 5, 2 (2018)
- [5] S.H. Gong et al., ACS Photonics DOI: 10.1021/acsp Photonics.7b01238

### Keywords:

반도체 양자점, 단일 광자원, 3차원 반도체, III-Nitride

## Growth of well-aligned ZnO nanowires by MOCVD: The decisive role of the substrate for controlling the wires' morphology

류상완\*<sup>1</sup>, HASSAN Mosafa Afifi<sup>1</sup>, JOHAR Muhammad Ali<sup>1</sup>

<sup>1</sup>전남대학교 물리학과  
sangwan@chonnam.ac.kr

### Abstract:

Zinc oxide (ZnO) is a unique material having a bandgap of 3.37 eV that exhibits both semiconducting and piezoelectric properties and has a diverse group of growth morphologies. Furthermore, growing ZnO with a nanowire structure gives a bright hope and accessibility for promising applications for novel multi-functional nanodevices in different fields such as biosensors, light-emitting diodes, UV detectors, piezoelectric nanogenerators, and solar water splitting applications. Herein, we present the growth of high aspect ratio of ZnO nanowires (NWs) using a metal organic chemical vapor deposition (MOCVD) growth process on various substrates as well as the relationship between the properties of the substrate and the growth of the NWs. We have investigated various substrates (silicon, sapphire, and GaN) with and without buffer layer and have shown that for identical experimental conditions the material deposited can be either randomly orientated nanowires or vertically aligned nanowires. The best-aligned ZnO nanowires were grown on Si (100) substrates pre-coated with a ZnO buffer layer grown by atomic layer deposition (ALD). The nanowires are single-crystalline wurtzite structures with a preferential growth in the [0001] direction. Room temperature photoluminescence (PL) measurements exhibited a strong ultraviolet emission and suppressed visible emission, affirming the absence of defects related to ZnO or oxygen vacancies. The nanowires grown by MOCVD have distinct advantages over other methods such as excellent uniformity, purity, and high deposition rates which will be useful in several applications.

### Keywords:

ZnO, nanowire, MOCVD, buffer, aligned.

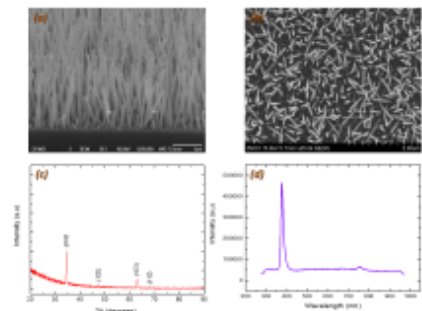


Figure 1. (a, b) FE-SEM images of ZnO nanowires grown on pre-coated buffer layer on Si. (c) XRD pattern of ZnO nanowires grown on pre-coated buffer layer on Si. (d) PL spectra of ZnO nanowires grown on pre-coated buffer layer on Si.

## Ultrafast carrier dynamics of InGaN/GaN MQW coaxial nanowires grown on Si substrate

JOHAR Muhammad Ali<sup>1</sup>, 김태윤<sup>1</sup>, 강진호<sup>1</sup>, 류상완\*<sup>1</sup>

<sup>1</sup>전남대학교 물리학과  
sangwan@chonnam.ac.kr

### Abstract:

We report the growth of InGaN/GaN multiple-quantum-well (MQW) coaxial nanowires on Si substrate using MOCVD. The core GaN nanowires were grown by vapor-liquid-solid (VLS) mode while the InGaN/GaN shells were grown under vapor-solid (VS) growth mode. The emission wavelength exhibited by the InGaN quantum wells was measured as a function of thickness of InGaN quantum wells of nanowires. The carrier dynamics was evaluated by measuring the lifetime of photogenerated charge carriers, temperature dependent photoluminescence was carried out from 18 K to 300 K. A four nm thick QW exhibited the fastest recombination of 25 ps and 20 ps at 18 K and 300 K, respectively. The slowest recombination rate was demonstrated by two nm thick QW with the carrier lifetime of 38 ps and 22 ps at 18 K and 300 K, respectively. The lifetime of carriers was found in inverse relationship to the thickness of the quantum wells. Such controllable carrier dynamics may significantly advance the development of nanowires based electronic devices such as laser diode, photodetectors, photoanodes, and solar cells.

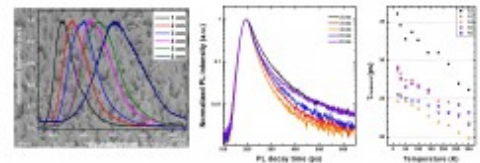


Fig. 1. SEM and Room temperature PL (left), TRPL as a function of QW thickness (middle), dependence of lifetime of charge carriers on temperature (right).

### Keywords:

InGaN/GaN, coaxial, nanowire, time-resolved PL.

## ALD법으로 성장된 $ZnO_xS_{1-x}$ 박막의 광학적 특성 분석

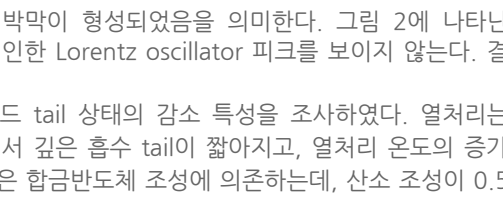
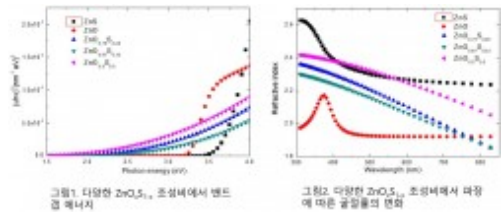
류상완\*<sup>1</sup>, 유소영<sup>1</sup>, HASSAN Mostafa Afifi<sup>1</sup>

<sup>1</sup>전남대학교 물리학과  
sangwan@chonnam.ac.kr

### Abstract:

실리콘 기판(100) 위에 ALD 방법으로  $ZnO_xS_{1-x}$  박막을 성장하고, 조성에 따른 광학적 특성을 조사하였다. 박막의 조성비를  $x=0, 0.5, 0.67, 0.75, 1$ 로 변화시켰고, 이에 대해 spectroscopic ellipsometry를 이용하여 굴절률( $n$ ) 및 흡광계수( $k$ )를 측정하였다. 그림 1과 같이 이원계 반도체인 ZnO와 ZnS의 밴드갭 에너지를 Tauc 관계식으로 계산하여, 각각 3.26 eV, 3.67 eV의 값을 얻었다. 이는 기존 연구에서의 밴드갭 에너지와 거의 일치하며, 이를 통해 저온 ALD 방법으로도 이원계 반도체 박막은 우수한 결정성으로 성장됨을 확인하였다. 그러나  $ZnO_xS_{1-x}$  합금반도체의 경우 낮은 결정성으로 인해 밴드갭 내에 높은 밀도의 band tail state가 형성되어, 밴드갭 아래쪽으로 흡수 tail이 크게 존재함을 볼 수 있다. 이는 비정질에 가까운 박막이 형성되었음을 의미한다. 그림 2에 나타난  $ZnO_xS_{1-x}$ 의 굴절률은 이원계 반도체인 ZnO와 ZnS 사이 값을 갖으며, 밴드갭에 기인한 Lorentz oscillator 피크를 보이지 않는다. 결과적으로 가시광 영역에서 상당히 큰 재료분산을 갖는다.

성장된  $ZnO_xS_{1-x}$  박막의 열처리 과정에서 비정질 박막의 광학적 특성 변화와 밴드 tail 상태의 감소 특성을 조사하였다. 열처리 온도 500~900°C 구간에서 10분간 진행하였다.  $ZnO_xS_{1-x}$  합금반도체는 열처리 과정에서 깊은 흡수 tail이 짧아지고, 열처리 온도의 증가에 따라 전형적인 반도체의 흡수 특성에 가까워지는 특성을 보였다. 하지만 이 경향은 합금반도체 조성에 의존하는데, 산소 조성이 0.5에 근접할수록 열처리에 의한 흡수 tail 감소특성이 약하게 나타남을 관측하였다.



### Keywords:

Zinc oxysulfide, Atomic layer deposition, Spectroscopic ellipsometry.

## Degradation analysis of organic-inorganic hybrid perovskite films using the nano-IR spectroscopy

정문석\*<sup>1</sup>, 유향미<sup>1</sup>, 오혜민<sup>1</sup>

<sup>1</sup>성균관대학교, 에너지과학과  
mjeong@skku.edu

### Abstract:

Organic-inorganic mixed halide perovskite ( $\text{MAPbX}_3$ :  $\text{MA}=\text{CH}_3\text{NH}_3^+$ ,  $\text{X}=\text{Cl}^-$ ,  $\text{Br}^-$ , or  $\text{I}^-$ ) are attracting intense interest as promising absorber materials for solar cell due to its broad absorption range and long charge carrier diffusion length. However, their poor stability remains a major challenge for high performance device and their commercialization. Generally, perovskite films based on  $\text{CH}_3\text{NH}_3\text{PbI}_{3-x}\text{Cl}_x$  undergo rapid degradation when exposed to oxygen and light. To overcome this problem, many researchers have been studied about the degradation of perovskite films. In this work, we investigated the degradation mechanism of perovskite films with simultaneously obtained structural and chemical results using the photo thermal induced resonance spectroscopy combined with atomic force microscope. This study will contribute to understanding of the mechanism of the degradation process of perovskite films and enhance the stability of perovskite optoelectronics devices.

### Keywords:

perovskite, degradation mechanism, photo thermal induced resonance spectroscopy

## First principles analysis of the role of B<sub>2</sub>H<sub>6</sub> on TiN Surfaces for Tungsten Atomic Layer Deposition

박환열<sup>1</sup>, 이성우<sup>1</sup>, 김호준<sup>2</sup>, 윤의준<sup>1</sup>, 이건도\*<sup>1</sup>  
<sup>1</sup>서울대학교 재료공학부, <sup>2</sup>동아대학교 기계공학과  
gdlee@snu.ac.kr

### Abstract:

In the fabrication process of memory devices, a void-free tungsten (W) gate process with good conformability is very important for improving the conductivity of the W gate, leading to enhancement of device performance. As the downscaling continues to progress, void-free W deposition becomes more difficult due to the experimental limitations of conformal film deposition even with atomic layer deposition (ALD) W processes. In ALD W processes, it is known that the B<sub>2</sub>H<sub>6</sub> dosing process plays a key role in deposition of the ALD W layer with low resistivity and in removal of residual fluorine (F) atoms. To comprehend the detailed ALD W process, we have investigated the dissociation reaction of B<sub>2</sub>H<sub>6</sub> on three different TiN surfaces, TiN (001), Ti-terminated TiN (111), and N-terminated TiN (111), using first-principles density functional theory (DFT) calculations. N-terminated TiN (111) shows the lowest overall reaction energy for B<sub>2</sub>H<sub>6</sub>. These results imply that severe problems, such as a seam or void, in filling the W metal gate for memory devices could be attributed to the difference in the deposition rate of W films on TiN surfaces. From this study, it was found that the control of the texture of the TiN film is essential for improving the subsequent W nucleation.

### Keywords:

Tungsten, B<sub>2</sub>H<sub>6</sub>, TiN, ALD, DFT

## Electron-beam-induced nanoscale patterning of molecular aggregates for nanophotonic applications

전영철\*<sup>1</sup>, 서인철<sup>1</sup>, 우병훈<sup>1</sup>, 안수찬<sup>1</sup>, 이은송이<sup>1</sup>

<sup>1</sup>울산과학기술원 신소재공학부  
ycjun@unist.ac.kr

### Abstract:

J-aggregate excitonic thin films have been known as very interesting organic materials which show drastic features in the visible spectral range, such as surface polaritons, epsilon-near-pole and so on. However, there was no direct method for nanoscale patterning on J-aggregate thin films. Although there were special methods, such as self-organization/self-assembly, nano-imprint lithography, scanning force microscopy, these methods need specific organic material characteristics, and it is difficult to apply to various applications.

We propose a new and intuitive nanopatterning method altering the dielectric constants of organic films using electron beam exposure. This study reports gradual dielectric constants changes, especially from the optically metallic to transparent organic film, according to the electron beam dose. As a result of the dielectric constant change, we obtain a strong change in the photoluminescence intensity and spectral shape. We also apply this method to grating and hole-array nanostructures patterned on the J-aggregate/PVA mixture film. Especially, we study the light-matter interaction of grating/hole-array structures in both metallic and dielectric spectral regions. Moreover, we confirm that this electron beam exposure can be applied to other molecular aggregates. Nanoscale patterning on molecular aggregate films can have diverse applications, including organic plasmonic metamaterials, photodetector, phototransistor, and so on.

### Keywords:

Electron-beam, nanopatterning, J-aggregate, excitonic thin films, grating, hole-array, photoluminescence

## 발광효율 증가를 위한 그래핀 전극을 이용한 발광소자

최재우\*<sup>1</sup>, 이영로<sup>1</sup>

<sup>1</sup>경희대학교 정보디스플레이학과  
jaewuchoi@khu.ac.kr

### Abstract:

본 연구는 기존 발광소자에 사용되는 전극을 그래핀으로 대체하여 높은 발광효율을 가지는 소자를 제작한 연구이다. 그래핀은 도핑 정도에 따라서 페르미 준위가 정해지고, CsF 와 CsCO<sub>3</sub>를 이용하여 그래핀을 n-도핑시켰고, HNO<sub>3</sub>를 이용하여 그래핀을 p-도핑시켰다. 라만 스펙트럼 분석 결과 페르미 준위의 이동을 확인하였고, I-V와 홀 측정을 통해서 저항 변화와 캐리어 농도를 확인하였다. 그 결과 투명하면서도 플렉서블한 발광소자를 제작할 수 있었다. 제작한 발광소자를 UV- Vis 스펙트로 스코피를 통해서 발광소자의 투과도를 확인하였다.

### Keywords:

그래핀, 발광소자, 페르미 준위, 도핑

## The Amplified Photocurrent by Majority Carriers in Graphene-Insulator-Silicon (GIS) Photodiode

최재우\*<sup>1</sup>, 박흥기<sup>1</sup>

<sup>1</sup>경희대학교 정보디스플레이학과  
jaewuchoi@khu.ac.kr

### Abstract:

본 연구는 그래핀과 실리콘 사이에 계면특성을 조절하여 458nm 파장의 광원에서 기존 그래핀-반도체 접합구조 소자에 비해 1,400% 이상의 양자효율을 가지고 있는 광측정기를 개발한 내용이다. 기존 그래핀 기반 광다이오드와 같은 경우, Schottky 장벽의 높이가 지나치게 큰 관계로 대부분이 Minority carrier에 의해서 동작을 하였고, 그 결과 양자효율이 기존 소자에 비해서 그다지 크지 못했다. 하지만 본 연구에서는 그래핀의 일함수와 차이가 크지 않은 반도체와 적절한 두께의 산화막을 활용하여 그래핀과 실리콘의 계면특성을 조절하여 Majority carrier가 충분히 이동가능한 베리어 조절 소자를 제작하였다. 계면특성은 Schottky emission이론과 Cheung의 방법을 통해서 분석하였고, 그래핀의 에너지 준위는 라만스펙트럼을 통하여 분석하였다.

### Keywords:

그래핀, 양자효율, 광측정기, majority carrier

## Novel cyan emitting $\text{Sr}_{10}(\text{PO}_4)_6\text{O}:\text{Ce}^{3+}$ phosphors for visualization of latent fingerprints and anti-counterfeiting

박성준<sup>1</sup>, 윤영우<sup>1</sup>, 정종원<sup>2</sup>, 문병기<sup>3</sup>, 양현경\*<sup>1, 2</sup>

<sup>1</sup>부경대학교, LED공학협동과정, <sup>2</sup>부경대학교, 과학기술융합전문대학원, LED융합공학전공, <sup>3</sup>부경대학교, 물리학과  
hkyang@pknu.ac.kr

### Abstract:

The fingerprints are commonly latent for detection at crime scenes and thus the effective way for detection of latent fingerprints is important. Currently, the traditional powder dusting method has low resolution, sensitivity, contrast and high background noise. To solve these problems, we synthesized  $\text{Sr}_{10}(\text{PO}_4)_6\text{O}:\text{xCe}^{3+}$  phosphors ( $\text{x}=0.01\text{-}0.1$  mol) with cyan color by solid state reaction. The X-ray diffraction patterns of phosphors confirmed the hexagonal phase. The emission peak centered at 472 nm is attributed to  $^5\text{D}_{3/2}\rightarrow^7\text{F}_J$  transitions ( $J = 7/2$  and  $5/2$ ) of  $\text{Ce}^{3+}$  ions with the CIE coordinates value of ( $\text{x}=0.171$ ,  $\text{y}=0.256$ ). Using  $\text{Sr}_{10}(\text{PO}_4)_6\text{O}:\text{xCe}^{3+}$  phosphors, the latent fingerprints with various ridge shapes (arch, whorl and loop) and on substrates (glass, aluminum foil, stainless steel, compact disk and credit card) exhibited excellent visualization and sensitivity with clear ridges under 254 nm UV illumination. The results indicate that  $\text{Sr}_{10}(\text{PO}_4)_6\text{O}:\text{xCe}^{3+}$  phosphors can be effectively used in fingerprint identification and anti-counterfeiting applications.

### Keywords:

latent fingerprint, anti-counterfeiting,  $\text{Sr}_{10}(\text{PO}_4)_6\text{O}:\text{xCe}^{3+}$  phosphors

## *n*-ZnO/*p*-GaN heterojunction dichromatic yellow and blue light-emitting diodes

정준석<sup>1</sup>, 홍영준\*<sup>1</sup>

<sup>1</sup>세종대학교 나노신소재공학과  
yjhong@sejong.ac.kr

### Abstract:

We report on critical factors leading to control the dichromatic electroluminescent (EL) colors emitted from *n*-ZnO wire/*p*-GaN film heterojunction light-emitting diodes. For this study, we adopted a selective-area wet chemical epitaxy technique using pre-patterned *p*-GaN film coated with lithographic resist layer, and either *n*-ZnO microwire (MW) or nanowire-bundle (NW-B) arrays were yielded according to seed layer conditions. The MWs- and NW-Bs-based heterojunction LEDs represented different EL colors of whitish-blue and greenish-yellow, respectively, at reverse-bias voltages with different EL intensity ratio between two specific EL lines of 445- (indigo) and 560-nm (yellow)-wavelength peaks. The origin of different dichromatic EL emission colors was examined based on photoluminescence (PL) spectra and the dichromatic EL peak intensity ratios as a function of the reverse bias voltage. The different EL colors are discussed with respect to depletion thickness and electron tunneling probability determined by peculiar wire/film junction geometry and size. We also discuss the selective formation of either of MW and NW-B in terms of crystallinity and surface roughness of seed layer in the selective-area epitaxy.

### Keywords:

selective-area epitaxy, dichromatic electroluminescent, Heterojunction, Light-emitting diodes

## Buckling tip-based mechanical sensor by using a quartz tip-combined QTF-AFM

안상민<sup>1</sup>, 김봉수<sup>1</sup>, 권소영<sup>1</sup>, 문걸<sup>2</sup>, 이만희<sup>3</sup>, 제원호\*<sup>1</sup>

<sup>1</sup>Department of Physics & Astronomy, Seoul National University, <sup>2</sup>Department of Physics, Chonnam National University, <sup>3</sup>Department of Physics, Chungbuk National University  
whjhe@phya.snu.ac.kr

### Abstract:

One of the critical elements of mechanical sensors is sensitivity for accurate measurement. There have been several studies about enhancement of sensitivity to perturbations (mass, stiffness, force, noise etc.) by using a bifurcation point of a mechanical system/MEMS/NEMS to enhance [1, 2], however most tend to deal with bifurcation based sensing in resonant systems. Here, we introduce a sensitive buckled quartz tip as a force sensor with a quartz tuning fork-based atomic force microscope (QTF-AFM) [3]. A local buckling of a microscale tip pushed against a surface to enhance the detection sensitivity of lateral force and lateral surface by using a nonlinear dynamics in bifurcation point before tip flipping. The novel element of the present work is that we use a buckled microscale structure with a static bifurcation in a non-resonant system to boost sensitivity to surface motion and forces. We present (i) achievement of a locally buckled state, (ii) basic studies of tip flipping induced by lateral surface motion, and velocity dependent behavior, and (iii) the detection of surface waves on the surface.

### References

- [1] I. Siddiqi, R. Vijay, F. Pierre, C. M. Wilson, M. Metcalfe, C. Rigetti, L. Frunzio, and M. H. Devoret, *Phys. Rev. Lett.* **93**, 207002 (2004).
- [2] V. Kumar, J. W. Boley, Y. Yang, H. Ekowaluyo, and J. K. Miller, *Appl. Phys. Lett.* **98**(15), 153510 (2011).
- [3] S. An, C. Stambaugh, S. Kwon, K. Lee, B. Kim, Q. Kim, and W. Jhe, *Rev. Sci. Instrum.* **85**, 033702 (2014).

### Keywords:

mechanical sensor, buckling tip, bifurcation point, QTF-AFM

## Tailoring surface morphology and Enhancing vertical current transport of a conducting polymer blend film using femtosecond laser writing

이현희\*<sup>1</sup>, 채상민<sup>2</sup>, 이아라<sup>2</sup>, 김효정<sup>2</sup>, 최지연<sup>3</sup>, 유영조<sup>4</sup>  
<sup>1</sup>포항공대 포항가속기연구소, <sup>2</sup>부산대학교, <sup>3</sup>한국기계연구원, <sup>4</sup>덕산하이메탈  
hhleexrs@gmail.com

### Abstract:

Selective tailoring of carrier transport as well as surface morphology on a conducting polymer blend thin film was demonstrated using femtosecond infrared laser writing process. Significant photo expansion was induced without degrading its molecular structure and thus, surficial morphology could be customized by changing the laser writing parameters. In the photo-expanded region, a face-on crystal amount became ~12 times larger in comparison with the pristine region. In addition, a vertical current transport was enhanced as high as 2.4 times on in poly(3-hexylthiophene):phenyl-C61-butyric acid methyl ester (P3HT:PCBM) thin film due to the change of its molecular orientation by the laser process.

### Keywords:

femtosecond laser, organic semiconductor, photo-expansion, c-AFM

## Electrical properties of single-crystalline WTe<sub>2</sub> nanobelts grown from eutectic alloy reservoir

권순용\*<sup>1</sup>, 송승욱<sup>1</sup>, 곽진성<sup>1</sup>, 이종화<sup>1</sup>, 이재웅<sup>2</sup>, 김세양<sup>1</sup>, 김정화<sup>1</sup>, 심여선<sup>1</sup>, 조용수<sup>1</sup>, 정현식<sup>2</sup>, 이종훈<sup>1</sup>  
<sup>1</sup>울산과학기술원, 신소재공학과, <sup>2</sup>서강대학교, 물리학과  
sykwon@unist.ac.kr

### Abstract:

Among diverse transition metal dichalcogenide compounds, semimetallic tungsten ditelluride (WTe<sub>2</sub>) in the distorted 1T phase has received renewed attention from the experimental observations of non-saturating large magnetoresistance and high mobility, and from the theoretical prediction of large-gap quantum spin Hall insulator. However, the production of high-quality WTe<sub>2</sub> layers remains an unsolved challenge mainly due to the low environmental stability and activity of Te, and difficulties in Te incorporation during growth. In this study, we have obtained single-crystalline one-dimensional (1D) WTe<sub>2</sub> nanobelts at low temperatures ( $T \sim 500$  °C) in large scale via the use of Te-rich eutectic metal alloys (*e.g.*, Cu<sub>x</sub>Te<sub>y</sub>). The as-synthesized WTe<sub>2</sub> samples exhibit a distinct 1D belt-like morphology with layered cross-section of  $<12.2 \pm 6.6$  nm in thickness. The introduction of Te-rich eutectic metal alloys as a Te reservoir eliminates the Te deficiency in the resulting products and the contamination by impurities encountered with chemical vapor deposition. As a result, the resulting 1D products are highly pure, stoichiometric, structurally uniform, and free of defects, resulting in high electrical performances. All tested WTe<sub>2</sub> nanobelt devices showed low resistances ( $\rho < 1$  m $\Omega$  cm), close to that of the mechanically exfoliated ones by the order of magnitude [1]. Furthermore, they showed a remarkably high breakdown current density ( $J_B$ ) of up to  $\sim 94$  MA/cm<sup>2</sup>, promising their future device applications as a downscaled interconnect. We believe that this approach may be used as a general strategy for fabricating 1D layered nanostructures and truly exciting opportunity that can lead to dozens of new 1D nanomaterials of electronic quality, which may offer unique properties that are not available in other materials.

### Keywords:

WTe<sub>2</sub>, low dimensional, electrical properties

## Noncontact Friction via Capillary Shear Interaction in Ambient Condition

JHE Wonho\*<sup>1, 2</sup>, LEE Manhee<sup>1, 2</sup>, KIM Bongsu<sup>2</sup>, KIM Jongwoo<sup>2</sup>, AN Sangmin<sup>2</sup>

<sup>1</sup>Department of Physics, Chungbuk National University, <sup>2</sup>Department of Physics and Astronomy, Seoul National University  
whjhe@phya.snu.ac.kr

### Abstract:

Friction between two sliding surfaces involves highly nonlinear interactions between solid-solid direct contacts as well as non-contact asperities. In ambient condition, there always occurred capillary condensation between two sliding bodies, which strongly affects the contact and noncontact frictions. While cantilever-based atomic force microscope (AFM) has been long employed to study the friction in ambient condition, it has been difficult to probe the noncontact friction mediated by the capillary-condensed water. In this talk, we present an AFM study on the noncontact friction in air [1]. We use a home-made, shear-mode, quartz tuning-fork based AFM [2]. We show that the pinning-depinning dynamics of the nanobridge's contact line on a solid surface produces nonviscous damping interaction, which occurs even without normal load and becomes up to 10% of direct solid-solid contact friction. This indicates that the noncontact friction may even dominate the contact friction depending on the conditions such as the number of capillary bridges. The novel nanofriction mechanism may provide a deeper microscopic view of macroscopic friction in air where numerous asperities exist.

### References

- [1] M. Lee, B. Kim, J. Kim, and W. Jhe, Nat. Commun. **6**, 7369 (2015).
- [2] M. Lee, B. Sung, N. Hashemi and W. Jhe, Faraday Discuss. **141**, 415-421 (2009).

### Keywords:

Capillary condensation, water bridge, friction, pinning-depinning

## Realization of valley valve from bilayer MoS<sub>2</sub>/WS<sub>2</sub> heterostructure

이재동\*<sup>1</sup>, 김영재<sup>1</sup>

<sup>1</sup>대구경북과학기술원 신물질과학전공  
jdlee@dgist.ac.kr

### Abstract:

**Abstract:** Valley valve from the bilayer MoS<sub>2</sub>/WS<sub>2</sub> heterostructure, which controls intra as well as interlayer non-local inverse valley Hall current driven by the anomalous Lorentz effect is firstly proposed. Here we demonstrate three types of segment signals of the inverse valley Hall current at the terminal in the heterostructure, where each non-local current of intralayer MoS<sub>2</sub>, WS<sub>2</sub>, and interlayer between MoS<sub>2</sub> and WS<sub>2</sub> can be manipulated by the optical pumpings and bias fields. This finding provides a new chance of the highly advanced valley informatics or valleytronics.

### Keywords:

spin, valve, valleytronics, valley Hall effect.

## Raman studies of XXZ-type antiferromagnetic phase transitions for atomically thin NiPS<sub>3</sub>

정현식\*<sup>1</sup>, 김강원<sup>1</sup>, 임수연<sup>1</sup>, 이재웅<sup>1</sup>, 이성민<sup>2</sup>, 김태윤<sup>2</sup>, 박기수<sup>2</sup>, 전건상<sup>3</sup>, 박철환<sup>2</sup>, 박제근<sup>2</sup>  
<sup>1</sup>서강대학교 물리학과, <sup>2</sup>서울대학교 물리천문학과, <sup>3</sup>이화여자대학교 물리학과  
hcheong@sogang.ac.kr

### Abstract:

Transition metal phosphorus trisulfides (TMPS<sub>3</sub>, TM=Fe, Ni, Mn) are new class of layered van der Waals materials that are suitable for studying antiferromagnetic ordering in the 2-dimensional (2D) limit. Although all compounds are isostructural, they show different magnetic ground states depending on the TM element: FePS<sub>3</sub><sup>[1]</sup>, NiPS<sub>3</sub>, and MnPS<sub>3</sub> have Ising-, XXZ-, and Heisenberg-type antiferromagnetic ordering, respectively. Here, we studied XXZ-type antiferromagnetic NiPS<sub>3</sub> in the 2D limit by using Raman spectroscopy. Below the Néel temperature, the Raman spectrum of bulk NiPS<sub>3</sub> showed several Raman signatures of appearing antiferromagnetic ordering: 2-magnon scattering, Fano resonance<sup>[2]</sup>, suppression of the quasi-elastic scattering, and splitting of a phonon mode. By analyzing the temperature dependence of these signatures, the Néel temperature of NiPS<sub>3</sub> can be estimated. We synthesized bulk single-crystals NiPS<sub>3</sub> by the vapour transport method and prepared atomically thin samples by mechanically exfoliating on SiO<sub>2</sub>/Si substrates. By conducting temperature dependent Raman measurement, we found that the Néel temperature is almost independent of the thickness down to bilayer, but seems to be suppressed significantly for monolayer. This study will pave the way to understand magnetism in 2D systems.

### References

- [1] J.-U. Lee *et al.*, *Nano Lett.* **16**(12), 7433 (2016).
- [2] S. Rosenblum *et al.*, *Phys. Rev. B* **49**(6), 4352 (1994).

### Keywords:

XXZ/XY model, Antiferromagnetism, Two-dimensional magnetism, NiPS<sub>3</sub>, Raman spectroscopy, Nickel phosphorus trisulfide

## Misorientation angle-dependent phase transformation in van der Waals multilayers via electron-beam irradiation

KIM Un Jeong<sup>1</sup>, LEE Hyangsook<sup>2</sup>, LEE Woojin<sup>3</sup>, JEONG Hye Yun<sup>4, 5</sup>, KIM Hyun<sup>4, 5</sup>, LEE Hyo Sug<sup>3</sup>, PARK Yeonsang<sup>1</sup>, ROH Young-Geun<sup>1</sup>, LEE Young Hee<sup>4, 5</sup>, LEE Eunha\*<sup>2</sup>, HWANG Sung Woo\*<sup>6</sup>

<sup>1</sup>Device Lab., Samsung Advanced Institute of Technology, <sup>2</sup>2AAE group, Platform Technology Laboratory, Samsung Advanced Institute of Technology, <sup>3</sup>CAE group, Platform Technology Laboratory, Samsung Advanced Institute of Technology, <sup>4</sup>Center for Integrated Nanostructure Physics, Institute for Basic Science (IBS), <sup>5</sup>Department of Physics, Sungkyunkwan University, <sup>6</sup>Device & System Center, Samsung Advanced Institute of Technology  
eunhayo.lee@samsung.com, swnano.hwang@samsung.com

### Abstract:

One intriguing feature of van der Waals materials is the layer thickness and misorientation angle dependence that involve stark optical gain and electrical transport modulation. Yet, the phase transformation modulated by the misorientation angle has never been accessible to date. Here, we report misorientation angle-dependent phase transformation of multilayer MoS<sub>2</sub> via in situ electron beam irradiation. AA' stacked-bilayer MoS<sub>2</sub> undergoes structural transformation from 2H semiconducting to 1T' metallic phase similar to monolayer MoS<sub>2</sub>, which is confirmed via in situ transmission electron microscopy. Meanwhile, non-AA' stacking which has no local AA' stacking order in Moire pattern does not reveal such a phase transformation. While collective sliding motion of chalcogen atoms easily occurs during transformation in AA' stacking, such a collective motion in non-AA' stacking is suppressed by weak van der Waals strength and furthermore by the interlocked chalcogen atoms at different orientations, which unfavor their kinetics by the increased entropy of mixing.

### Keywords:

multilayers, misorientation, phase transformation

## Exploring structural dynamics using ultrafast electron diffraction

장규환<sup>1</sup>, 정영욱\*<sup>1</sup>, 이기태<sup>1</sup>, 백인형<sup>1</sup>, 왕기영<sup>1</sup>

<sup>1</sup>한국원자력연구원 양자빔기반방사선연구센터  
yujung@kaeri.re.kr

### Abstract:

XRD & TEM have been used for investigating static atomic structure of crystals. Recently, exploring structural dynamics in ultrashort time duration attracts lots of interests in expectation of revealing unknown scientific phenomena. The history of time-resolved experiments began with the development of high speed photography in 19<sup>th</sup> century. At this time, the shutter speed was about 1ms. With the development of laser technology, the resolution of the time-resolved experiment no longer depends on the speed of the mechanical shutter but on the duration of the probe pulse, which already achieved up to fs level experimentally. In the conference, we will introduce relativistic (~MeV) fs electron diffraction system developed by the KAERI team and also review recent issues connected with pump/probe experiments in the electron diffraction system development point of view.

### Keywords:

electron diffraction, ultrafast, RHEED, UED

## 단축 복굴절 물질에서의 편광변화에 대한 기하학적 위상 연구

최재우\*<sup>1</sup>, 최민호<sup>1</sup>

<sup>1</sup>경희대학교 정보디스플레이학과  
jaewuchoi@khu.ac.kr

### Abstract:

본 연구에서는 단축 복굴절 물질을 사용하여, 물질 내에서의 편광 상태를 변화하고, 편광 변화에 따른 기하학적 위상 특성과 동역학적 위상 특성을 비단열근사 조건하에서 분석하였다. 모든 편광에 대하여 편광 상태를 유지하며 위상을 조절할 수 있는 독특한 구조와 좌 표계 변환 소자를 사용하여, 입사 편광에 따라서 기하학적 위상 성분을 조절하고, 그에 따른 다양한 광학적 특징을 분석하고자 한다.

### Keywords:

Geometric Phase, Spatial Light Modulator, Commercial LCD, Polarization independent phase only spatial light modulator

## 수동형 광빗살 기반 고안정/고출력 초연속체 (극초단 레이저) 생성 기술

박정민<sup>1, 2</sup>, 한상필<sup>1</sup>, 송민제<sup>1</sup>, 심재식<sup>1</sup>, 안준태<sup>1</sup>, 류상완<sup>2</sup>, 송민협<sup>\*1</sup>

<sup>1</sup>한국전자통신연구원 광융합부품연구그룹, <sup>2</sup>전남대학교 물리학과  
sminhyup@etri.re.kr

### Abstract:

본 연구는 위상변조를 통해 광 주파수 빔 기술에 기반하는 조화파를 생성하여 낮은 위상 잡음을 갖는 초연속체 (극초단 펄스레이저)를 얻는 방법을 기술하고 있다. 현재 통신, 이미징, 분광, 및 센싱 등의 분야에서 고안정/고출력의 초연속체 및 극초단 레이저 생성 기술은 기술 혁신을 가져올 것으로 기대가 되고 있지만, 티타늄-사파이어(Ti:sapphire)레이저로 대표되는 고체 타입의 레이저 및 포화 흡수체 기반의 광섬유 레이저로는 위상 잡음, 출력, 옴셋 주파수 선평 등의 문제로 인하여 소스원으로서 적용에 어려움을 겪고 있는 상황이다.

스펙트럼 상에서는 통신 및 센싱을 위한 taps으로서 사용될 수 있는 고안정화된 초연속체 (supercontinuum source)로 사용될 수 있고, 시간 축 상에서는 고출력의 흔들림 없는 펄초 급 극초단 레이저를 생성하기 위하여 변조기반 방식의 광빗살 (optical frequency comb) 기반의 초연속체 생성기술 개발을 진행하였다.

연속적으로 발생하는 극초단 펄스 레이저는 시간 영역에서 펄초 모드동기된 (mode-locking) 레이저의 출력에서 펄스간의 출력 간격이 일정한 간격을 갖고 출력되게 된다. 이와 같은 시간 영역에서의 특징을 Fourier transform 하게 되면 주파수 영역에서 펄초 레이저의 짧은 펄스폭이 넓은 스펙트럼으로 나타나게 된다. 이러한 펄스간의 간격은 스펙트럼내의 주파수 성분들의 간격을 결정하고, 펄스의 폭은 광 주파수 빔의 전체 스펙트럼으로 표현된다.

고출력, 극초단, 고안정도, 광대역, 고간섭성의 특성을 갖는 방법으로 본 연구에서는 전기 광학적 위상변조기를 통해 외피 주파수 (Envelope frequency)와 반송파 주파수(Carrier frequency) 사이의 위상 이동(Phase drift)를 제어하는 광섬유기반의 고출력 극초단 레이저를 제시한다. 그리고 광 빔의 반복률이 변조기들에 가해주는 RF 오실레이터(Oscillator)의 주파수에 의해 결정되는 특징을 이용하여 고속변환이 가능한 펄스의 선평과 반복률 가변 고출력 극초단 레이저를 가능하게 한다.

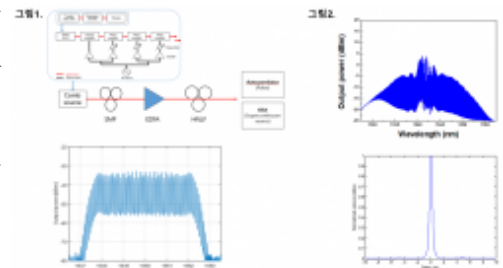
다음 그림 1은 본 연구에서 제시하는 Modulator에 기반한 광 빔의 구성도 및 생성결과를 보여주고 있다. 그림1과 같이 CW(Continuous Wave) laser, RF source, IM(Intensity Modulator), PM(Phase Modulator), PS(Phase Shifter)를 연결하여 구성하였다. 그 결과 그림 1과 같이 총 73개 라인을 갖는 광빗살이 생성되는 것을 확인하였다.

그림 2는 생성된 광빗살에 고비선형단 (Highly nonlinear fiber) 을 적용해서 생성된 초연속체 및 in-phase된 초연속체의 시간 축에서의 펄초급 레이저 생성 결과를 보여주고 있다. 그림 1에서 생성된 광빗살에 고비선형 광섬유 및 다단계 증폭단을 적용해서 그림 2와 같이 20dB안에 337개 라인을 갖는 초연속체를 생성하였고, ~400fsec의 FWHM을 갖는 펄초 레이저를 autocorrelator를 통하여 확인하였다.

본 연구결과는 고안정화/고출력의 초연속체 및 극초단 레이저 생성의 가능성을 보여주고 있고, 본 기술개발은 향후 통신, 이미징, 분광 등의 분야에서 기술혁신을 가져올 것으로 기대한다.

### Keywords:

optical frequency comb, supercontinuum source, highly nonlinear fiber, modulator, autocorrelator



## Unusual Atomistic Origin of Incommensurate Charge Density Wave in 2H-NbSe<sub>2</sub>

계경철<sup>1, 2</sup>, 이진원<sup>1, 2</sup>, 오은석<sup>1, 2</sup>, 염한웅\*<sup>1, 2</sup>

<sup>1</sup>Center for Artificial Low Dimensional Electronic Systems, Institute for Basic Science, <sup>2</sup>Department of Physics, POSTECH  
yeom@postech.ac.kr

### Abstract:

Despite decades of studies on charge density wave (CDW) of 2H-NbSe<sub>2</sub>, the nature and origin of incommensurate CDW ground state has not been understood. We unveil the microscopic evidence and structural origin of ICDW state in 2H-NbSe<sub>2</sub> with scanning tunneling microscopy and density functional theory. Different from other transition metal dichalcogenides, CDW of 2H-NbSe<sub>2</sub> is composed of two distinct structures, which are almost degenerate energetically, at low temperature. The unconventional heterostructure of two distinct CDW structures gives rise to  $2\pi/3$  phase slip to explain the discommensuration.

### Keywords:

NbSe<sub>2</sub>, heterostructure, CDW, STM, DFT

## Suppression of the hybridization of the surface states in the ultrathin $\text{Bi}_2\text{Se}_3$ /graphene heterostructures

채지민<sup>1</sup>, 박한범<sup>1</sup>, 홍석보<sup>1</sup>, 정광식<sup>1</sup>, 조만호\*<sup>1</sup>, 강승훈<sup>2</sup>, 권영균<sup>2</sup>

<sup>1</sup>연세대학교 물리학과, <sup>2</sup>경희대학교 물리학과  
mh.cho@yonsei.ac.kr

### Abstract:

Topological insulator is one of the attractive materials in condensed matter, which is a band insulator with topologically protected edge states. For the application the suppression of the bulk effect is important but in ultrathin TI materials the finite size effect works on the linear dispersion of the surface states, in which surface band shows the finite bandgap due to the hybridization(or overlap) between top and bottom surface states. Here, we studied on the gapless top surface Dirac state of strained 3 QL  $\text{Bi}_2\text{Se}_3$ /graphene heterostructure. A compressive strain in out-of-plane direction at the interface reduces the overlap of two surface wave functions. The proximity effect due to charge-transfer at the interface, moreover, leads to lessen wave functions in each surface and to suppress the overlap of two surface states. Finally, we analyzed the magneto-conductance of the  $\text{Bi}_2\text{Se}_3$ /graphene heterostructures to verify the independent transport channel of top surface Dirac state. Our findings have suggested that the strain and the proximity effect in the heterostructure of TI/graphene can be feasible ways to engineer the topological surface states beyond the physical and topological thickness limit.

### Keywords:

Topological insulator, Hybridization gap, proximity effect

## Binding Structures of Small Molecules to Metallo-porphyrin on Au(111) Studied Using Scanning Tunneling Microscopy

KAHNG Se-Jong\*<sup>1</sup>, CHANG Min Hui<sup>1</sup>, CHANG Yun Hee<sup>2</sup>, KIM Na Young<sup>2</sup>, JEON Un Seung<sup>1</sup>, KIM Howon<sup>1</sup>

<sup>1</sup>고려대학교 물리학과, <sup>2</sup>한국과학기술원 나노과학기술대학원  
sjkahng@korea.ac.kr

### Abstract:

Coordination of small molecules to metallo-porphyrins play crucial roles in functional processes of biological systems such as oxygen delivery, muscle contraction, and synaptic transmission. Their geometrical structures such as tilted binding of NO to metallo-porphyrin have been recently confirmed by high-resolution scanning tunneling microscopy (STM) images at the single molecule level. Here, we present STM images of further systems, di, tri, and quadra-atomic small molecules, coordinated to metallo-porphyrin on Au(111). We observed square ring, rectangular ring, and center-bright structures for three different small molecules. With the help of density functional theory (DFT) calculations, we reproduce the experimental STM images in the simulated images. Thus, our study shows that geometric structures of small molecules coordinated to metallo-porphyrins can be probed with STM combined with DFT methods.

### Keywords:

metallo-porphyrin, small molecules, scanning tunneling microscopy, density functional theory

## Blue Color Luminescence of Surface Functionalized Silicon Quantum Dots

주범수<sup>1</sup>, 정남식<sup>1</sup>, 한문섭\*<sup>1</sup>

<sup>1</sup>서울시립대학교 물리학과  
mhan@uos.ac.kr

### Abstract:

Since the first discovery for luminescence phenomena from porous silicon by Canham, nanostructured-silicon have attracted much attention due to their importance for silicon-based photonic and optoelectronic applications. As researches for silicon nanostructure has been ongoing more than two decades, the focus of studies have moved from nanostructure fabricated by electrochemical etching and deposition process to recent free-standing silicon quantum dots fabricated by chemical methods

Silicon quantum dots synthesized by chemical methods have advantages compared with previous methods because it can control the emission wavelength in all visible range by surface functionalization. For examples, the quantum dots fabricated by deposition methods can change emission only limited range from 650nm~near IR by size control. On the other hands, luminescence of free-standing silicon quantum dots can be controlled effectively by surface modification with various materials without size control.

In this work, through chemical synthetic methods, we fabricated free-standing silicon quantum dots showing emission wavelength with 480~550nm which is subsequently shorter than silicon quantum dot made by deposition methods. The properties of silicon quantum dots are characterized using transmission electron microscopy, Fourier transformed infrared spectroscopy. And also, optical properties of them are investigated photoluminescence and lifetime measurements. From these results, we will discuss the origin of blue emission and red disappearance of surface functionalized silicon quantum dots

Acknowledgement : NRF-2016M2B2A4912288, NRF-2015R1D1A1A01060381

### Keywords:

Silicon Quantum Dots, Chemical Synthesis, Surface functionalization, Blue Emission

## A new family of inorganic two-dimensional materials with versatile electronic phases

손영우\*<sup>1</sup>, 채기성<sup>1</sup>  
<sup>1</sup>고등과학원 계산과학부  
hand@kias.re.kr

### Abstract:

Recently, quasi two-dimensional (2D) layered materials with a-few-atom thickness have been extensively studied owing to their intriguing physical properties. In particular, transition-metal dichalcogenide (TMD) and transition-metal carbide/nitride (MXene) have been of special interest, thanks to their diverse electronic phases such as semiconductor with a sizable bandgap, quantum spin Hall insulator and topological semimetal. Here, we demonstrate a new family of inorganic 2D materials, TXene ( $T_3X$ ), which is composed of group IV ( $T=C, Si, Ge, Sn$ ) and group VI ( $X=O, S, Se, Te$ ) elements. Similar to TMD and MXene, the TXene display a wide range of electronic phases including direct/indirect bandgap semiconductor and quantum spin Hall insulator, originated from a varying interaction strength with a given atomic arrangement. Furthermore, we show that bandgap size is tunable not only by the compositional variation, but also by mechanical strain, enhancing versatility of the material.

### Keywords:

two-dimensional materials, first-principles calculations, materials design

## Hydrogen confinement at Graphene/Metal interface for controlling workfunction.

LAMJED Debbichi<sup>1</sup>, 김용훈\*<sup>1</sup>

<sup>1</sup>한국과학기술원 EEWS대학원  
y.h.kim@kaist.ac.kr

### Abstract:

Understanding the contact between graphene and metal is a key issue to improve devices performance. Since the band alignment of two different materials is determined by their respective work functions, controlling their work function is the key to reducing the contact barriers[1-2].

Using first principles calculations, we proposed a new strategy to control the contact barrier between graphene and metal by confining the hydrogen molecule to the interface. We also studied the behavior of hydrogen when confined depends on the type of metal. We have found that in the case of the normal metal (Al), the hydrogen remains in the gas phase, however, when a transition metal (Pt) is used as an electrode, the hydrogen prefers to dissociate.

[1] Y. Ji Kim, S-Y. Kim, J. Noh, C-H. Shim, et al. Scientific Reports | 6:39353.

[2] Seung Min Song, Jong Kyung Park, et al. Nano Lett. 2012, 12, 3887–3892.

### Keywords:

Graphene, doping, workfunction

## Dynamic Shallow Level as a Cause of Non-Radiative Recombination

방준혁\*<sup>1</sup>, MENG Sheng<sup>2</sup>, ZHANG S. B.<sup>3</sup>

<sup>1</sup>한국기초과학지원연구원 스피공학물리연구팀, <sup>2</sup>Beijing National Laboratory for Condensed Matter Physics, Chinese Academy of Science, <sup>3</sup>Department of Physics, Rensselaer Polytechnic Institute  
jbang0312@kbsi.re.kr

### Abstract:

The Shockley-Read-Hall (SRH) theory has been the ruling theory explaining the defect-mediated non-radiative recombination (NRR) of excited carriers. However, recent first-principles calculations show that the SRH theory seriously underestimates the NRR rate. While the potential importance of ionic relaxation has been implicated, the model has yet to be confirmed. Here, we present the theoretical formalism of the NRR that involves intermediate ionic relaxation. As a demonstration, we show that the DX center is an efficient NRR center by carrier capture at dynamics shallow level. As the concentration of DX center can be controlled in experiments, this NRR mechanism may be readily verified.

\*This work was supported by Basic Science Research Program through the National Research Foundation of Korea (NRF) (NRF-2015R1C1A1A02037024) and KBSI grant D38614.

### Keywords:

Non-radiative recombination, Excited carrier dynamics, Time-dependent density functional theory

## First-principles tunneling properties of Ge/high-k oxide/Au in comparison with Si/high-k oxide/Au

고은정\*<sup>1</sup>, 박재홍<sup>1, 2</sup>, 최정혜\*<sup>1</sup>

<sup>1</sup>Center for Electronic Materials, KIST, <sup>2</sup>Department of Materials Science and Engineering, Seoul National University  
eunjungko04@gmail.com, choijh@kist.re.kr

### Abstract:

Recent Ge- or Si-based MOS devices have Ge(or Si)/high-k dielectric oxide/metal gate structures. Although many experimental studies on the gate leakage current on these structures have been performed in terms of the scaling down issues, first-principles theoretical works on the tunneling current density have been rarely reported. Therefore, we investigate the effect of the high-k oxides on the leakage current density in the structure composed of Ge(or Si)/high-k oxide/Au by the first-principles transport calculations. Al<sub>2</sub>O<sub>3</sub>, HfO<sub>2</sub>, and native oxides of GeO<sub>2</sub> or SiO<sub>2</sub> are considered as the high-k oxides. The Ge-based structures are compared with the Si-based structures. We also examine the effects of interfacial structures such as an abrupt interfacial structure with dangling bonds and a passivated interfacial structure with hydrogen atoms on the tunneling spectra. The tunneling current density in Ge(or Si)/high-k oxide/Au structures will be compared with that in Ge/GeO<sub>2</sub>/Ge and Si/SiO<sub>2</sub>/Si structures.

### Keywords:

transport, high-k, leakage current, Ge, Si, MOS, tunneling

## Type-II Dirac Line node in strained- $\text{Na}_3\text{N}$ .

김영국\*<sup>1</sup>, 김동욱<sup>1</sup>  
<sup>1</sup>성균관대학교 물리학과  
youngkuk@skku.edu

### Abstract:

Since the discovery of topological insulator (TI), the topology of electronic band structure has attracted much attention, leading to the discovery of diverse topological materials both in band insulating topological phases and semi-metal phases. In this talk, using first-principles calculations, we show type-II Dirac line node (DLN) can occur in  $\text{Na}_3\text{N}$  under a mechanical strain. We discuss the characteristic features of type-II DLN semimetal appearing in the band velocity and the Fermi surface. We also discuss mathematical derivation of DLN semimetals into type-I and type-II classes in terms of the band velocities.

### Keywords:

Dirac line node semimetal, Type-II, classification

## Nanostructuring of Hybrid Halide Perovskites Down to Stable Low-Dimensional and Semi-Metallic Analogs: An *ab initio* study

김용훈\*<sup>1</sup>, KHAN Muhammad Ejaz<sup>1</sup>, BYEON Seongjae<sup>1</sup>

<sup>1</sup>한국과학기술원 EEWS대학원  
y.h.kim@kaist.ac.kr

### Abstract:

In the rapidly developing research on hybrid halide perovskites as promising materials for optoelectronic applications, low-dimensional hybrid halide perovskites have recently drawn significant interest with intriguing properties emerging from strong quantum confinement effects. Herein, based on density functional theory (DFT) calculations, we studied the nanostructuring of the recently synthesized organic-inorganic trimethylsulfonium lead triiodide  $(\text{CH}_3)_3\text{SPbI}_3$  perovskite, which showed a high ambient stability and an optical bandgap that extends into the visible range. We find that the two-dimensional (2D) monolayer and one-dimensional (1D) nanowire structures derived from three-dimensional (3D)  $(\text{CH}_3)_3\text{SPbI}_3$  perovskite are energetically and dynamically stable. Comparison of the electronic band structures of the 3D, 2D, and 1D  $(\text{CH}_3)_3\text{SPbI}_3$  analogs shows that the band edge-region electronic structures are robustly determined at the 1D level. Most interestingly, we find that the inorganic 1D face-sharing  $\text{PbI}_6$  framework prepared by removing ligands is also structurally stable and it becomes semi-metallic. We propose that these  $(\text{CH}_3)_3\text{SPbI}_3$ - and  $\text{PbI}_6$ -derived 2D and 1D hybrid perovskites are promising candidates for advanced electronic and optoelectronic device applications.

### Keywords:

organic-inorganic hybrid halide perovskites, low-dimensional materials, nanowires, semi-metal

## Concentration dependent ion pair dissociation in low dielectric constant solution

김도석\*<sup>1</sup>, 차선철\*<sup>1, 2</sup>, 이민호<sup>1</sup>

<sup>1</sup>서강대학교 물리학과, <sup>2</sup>MAX PLANCK INSTITUTE FOR POLYMER RESEARCH  
doseok@sogang.ac.kr, sunchul@gmail.com

### Abstract:

Molar conductivity of ionic liquid mixtures can change with concentration due to dissociation of ion pairs in solution. This phenomenon has been investigated in liquids with large dielectric constant to decrease the ion pair attraction, [1] but dissociation can be significant in media with relatively low dielectric constant provided the ionic liquid concentration is low enough [2]. Dissociation at low concentration is due to the entropic contribution of the free energy upon dissociation. Here deuterated chloroform (CDCl<sub>3</sub>, 99.8 D%) was used as a solvent to measure concentration-dependent ion pair dissociation by using IR absorption spectra. The spectra at different concentrations were analyzed in terms of area ratio to quantify the ion pair dissociation at different concentrations. Reaction constants were then determined from the law of mass action. The change of reaction constant for three different anions (I<sup>-</sup>, Br<sup>-</sup>, and Cl<sup>-</sup>) can be explained in terms of varying interaction strengths between the solvent (CDCl<sub>3</sub>) and the anion.

[1] Angew. Chem. Int. Ed. 2013, 52, 12439 -12442

[2] Phys. Chem. Chem. Phys., 2016, 18, 27529-27535

### Keywords:

ionic liquid

## Multifunctional Bilayer Template for Near-Infrared Sensitive Organic Solar Cells

김형채<sup>1</sup>, 박한결<sup>2</sup>, 맹민재<sup>2</sup>, 강유리<sup>2</sup>, 박경률<sup>1</sup>, 최준호<sup>2</sup>, 박용섭<sup>2</sup>, 김영동<sup>2</sup>, 김창순\*<sup>1</sup>

<sup>1</sup>서울대학교 융합과학부 나노융합전공, <sup>2</sup>경희대학교 물리학과  
changsoon@snu.ac.kr

### Abstract:

The crystallinity of and the molecular orientation in photoactive layers of organic solar cells strongly impact the key processes determining the power-conversion efficiency (PCE), such as photon absorption, exciton diffusion, charge transfer, and charge separation. In the case of non-planar phthalocyanines, a thin film composed of triclinic crystals with face-on oriented molecules, typically obtained with a copper iodide (CuI) template layer, has been reported to be desired for optical absorption in the near infrared (NIR) spectral region. However, this work demonstrates that for a lead phthalocyanine (PbPc)-C<sub>60</sub> donor-acceptor pair, less face-on orientation with a broader orientation distribution obtained with a new template layer consisting of a zinc phthalocyanine (ZnPc)/CuI bilayer is more desirable in terms of solar cell efficiency than the face-on orientation. Notably, employing the bilayer-template for a PbPc-C<sub>60</sub> based organic solar cell (OSC) is found to not only induce the formation of NIR-sensitive PbPc crystallites in triclinic phase but also increase the internal quantum efficiency (IQE) compared to a CuI-templated OSC. Our analyses based on the exciton diffusion model and the entropy- and disorder-driven charge separation model suggest that the improvement of the IQE is due to the thermodynamically facilitated CT-dissociation as well as the reduction of exciton quenching near the ITO-coated substrate. As a result, the bilayer-templated device has superior performance of  $J_{sc} = 10.5 \text{ mA/cm}^2$  and PCE = 3.1%, which are higher by 59% and 69% (12% and 13%) than those of the non-templated (or the CuI-templated) device.

### Keywords:

organic solar cell, charge transfer exciton, CT exciton dissociation, molecular orientation, CT state energetics, entropy, disorder

## In situ measurement of surface work function using AP-XPS

유영석<sup>1</sup>, 김동우<sup>1</sup>, 임호준<sup>1</sup>, 정문정<sup>1</sup>, KIM Daehyun<sup>2</sup>, KOHEI Ueda<sup>2</sup>, SATORU Hiwasa<sup>2</sup>, MASE Kzuhiko<sup>3</sup>,  
BOURNEL Fabrice<sup>4</sup>, GALLET Jean-Jacques<sup>4</sup>, KONDOH Hiroshi<sup>2</sup>, NOH Do Young<sup>1</sup>, 문봉진\*<sup>1</sup>

<sup>1</sup>Department of Physics and Photon Science, GIST, <sup>2</sup>Department of Chemistry, Keio University, <sup>3</sup>Institute of Materials Structure Science, High Energy Accelerator Research Organization, <sup>4</sup>Laboratoire de Chimie Physique-Matière et Rayonnement, Sorbonne Universités - Université Pierre et Marie Curie Paris  
bsmun@gist.ac.kr

### Abstract:

Using Ambient-Pressure X-ray Photoelectron Spectroscopy (AP-XPS) and Mass Spectrometer (MS), the surface chemical states on Pd(100) are investigated as CO oxidation reaction occurs. At the onset of CO oxidation, the temperature of sample increases sharply due to the exothermic nature of the reaction and the Pd(100) forms surface oxide structure. The formed surface oxide shows no changes as CO/O<sub>2</sub> varies from 0.1 to 1.0. The change of work function is observed as the surface oxide formed during CO oxidation reaction. Interestingly, this change is observed not only in Pd(100) but also in Pt(110). However, the changes are the opposite; it implies a need to differentiate the viewpoints of palladium and platinum.

### Keywords:

AP-XPS, Pd(100), PdO, CO oxidation, Work function, Pt(110)

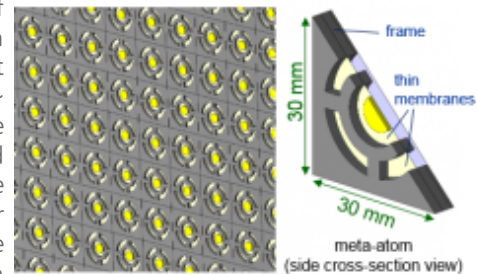
## Acoustic Metasurface for Water-to-Air Enormous Sound Transmission

BOK Eun<sup>\*1</sup>, PARK Jong Jin<sup>2</sup>, CHOI Haejin<sup>1</sup>, HAN Chung Kyu<sup>1</sup>, WRIGHT Oliver B.<sup>3</sup>, LEE Sam H.<sup>1</sup>

<sup>1</sup>Institute of Physics and Applied Physics, Yonsei University, Seoul 03722, Korea, <sup>2</sup>Research Department, Center for Advanced Meta-Materials, Daejeon, 34103, Korea, <sup>3</sup>Faculty of Engineering, Division of Applied Physics, Hokkaido University, Sapporo 060-8628, Japan  
eunbok81@gmail.com

### Abstract:

Enormous water-to-air sound transmission leads to development of extremely sensitive device for underwater sound detection. However, such sound transmission was never realized until recently, because of significant difference between specific acoustic impedances of water and air. Only ~ 0.2% of incident sound power is transmitted through water-air interface while all the other power is reflected. In this case, a conventional method using a quarter-wavelength matching layer is not applicable, because there are no suitable materials in nature and the layer is inconveniently thick for audible cases. Here, we present a new method for the impedance matching using acoustic metasurface impedance transformer. We design the metasurface, and theoretically and experimentally demonstrate that the metasurface increases the power transmission by 160 times of magnitude. The related work was published in Physical Review Letters (E. Bok et al., Phys. Rev. Lett. 120, 044302 (2018)).



This work was supported by the Center for Advanced Meta-Materials (CAMM) funded by the Ministry of Science, ICT, and Future Planning as a Global Frontier Project (CAMM-2014M3A6B3063712) and by the National Research Foundation of Korea (NRF) Grant funded by the Korea government (MSIP) (No. 2015001948).

Figure: Diagram of the metasurface shown from the air side. Inset: Cross-section and side view of the meta-atom.

### Keywords:

water-to-air sound transmission, acoustic metasurface, quarter-wavelength matching layer, impedance matching

## A link between the kinks and Fermi arcs in a cuprate superconductor observed by time-resolved APRES

ISHIDA Yukiaki<sup>1, 2</sup>, 김창영\*<sup>2</sup>

<sup>1</sup>ISSP, University of Tokyo, Japan, <sup>2</sup>서울대학교 물리천문학부, 기초과학연구원 강상관계물질연구단(IBS-CCES)  
changyoung@snu.ac.kr

### Abstract:

Angle-resolved photoemission spectroscopy (ARPES) has revealed novel electronic phenomena occurring in the cuprate superconductors (*d*-wave gap, pseudo-gap, dispersion kinks, Fermi arcs, etc.). However, their mutual relationship, if at all, as well their relationship to the unconventional superconductivity are still a matter of debate. We performed time-resolved ARPES (TARPES) and monitored the ultrafast responses of the electronic phenomena. What we observe is that the Fermi arcs and kinks are related: The Fermi arcs emerged upon the spectral broadening that occurred below the kink binding energy. We discuss a hitherto unnoticed role of the kink bosons that contribute to the unconventional loss of superconductivity at the critical temperature.

### Keywords:

superconductivity, ARPES

## 원소치환에 따른 1212 계 구리산화물 초전도체의 최고임계온도 조절 특성 연구

이호근\*<sup>1</sup>

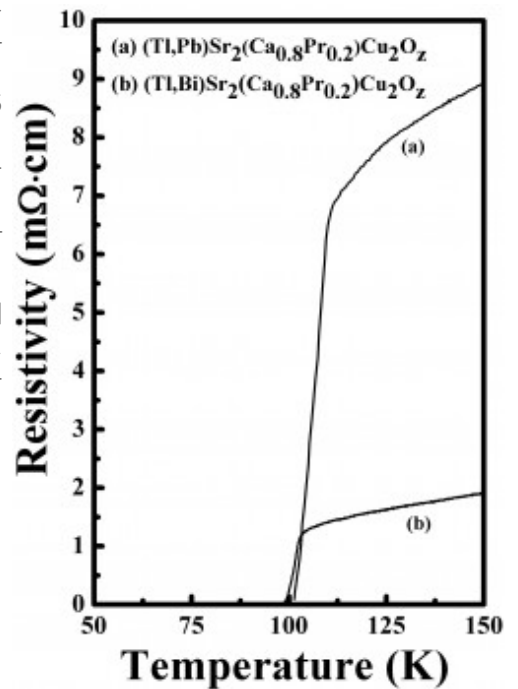
<sup>1</sup>강원대학교 물리학과  
hklee221@kangwon.ac.kr

### Abstract:

탈륨에 기초한  $\text{TlSr}_2\text{CaCu}_2\text{O}_7$  (Tl-1212) 계 고온초전도체의 경우 Tl 자리에 Pb를 치환하거나 Ca 자리에 희토류 원소(R)를 각각 치환한 경우 임계온도가 80-90 K가 됨이 알려져 있다. 그러나 Pb와 R을 동시에 치환하면 임계온도가 100 K 이상이 됨이 알려져 있으며, 특히  $(\text{Tl}_{0.5}\text{Pb}_{0.5})\text{Sr}_2(\text{Ca}_{0.8}\text{Pr}_{0.2})\text{Cu}_2\text{O}_7$ 의 조성에서 약 105 K의 최고임계온도가 관측된다. 이 결과는 같은 구리 층수(2개)를 갖는 잘 알려진 R-123 계의 최고임계온도가 약 92-95 K임을 고려할 때 상대적으로 높은 임계온도이다. 동시 치환된 Tl-1212 계가 100 K 이상의 높은 임계온도를 보이는 원인이 동시 치환에 따른 홀농도의 최적화 때문인지, 동시 치환된 Pb 및 희토류원소의 고유 특성 때문인지 명확하지 않다. 본 연구에서는 Tl-1212 계에서 여러 원소의 광범한 치환연구를 통해 100 K 이상의 임계온도를 보이는 원인이 Pb나 희토류 원소의 고유 특성에 기인하지 않음을 보였다. 즉, 본 연구에서는 Pb 대신 Bi를 치환한 계에서 100 K 이상의 초전도특성이 관측됨을 보였으며, 또한 희토류 원소의 치환없이도 100 K 이상의 초전도 특성이 관측됨을 밝혔다. 홀농도의 최적화만으로 최고 임계온도를 얻을 수 있는가를 포함해 최고임계온도 특성과 홀농도 최적화, 물질의 구조적 특성과의 상관 관계 그리고 새로운 고온초전도체의 탐색에 대해 발표한다.

### Keywords:

1212 superconductor, optimal transition temperature, tuning, hole carrier



## Model study of Josephson plasma soliton propagation in High T<sub>c</sub> superconductor

김동훈<sup>1</sup>, 이재동<sup>\*1</sup>

<sup>1</sup>대구경북과학기술원 신물질과학전공  
jdlee@dgist.ac.kr

### Abstract:

Josephson plasma is a linear electromagnetic wave that propagates along the plane of stacked superconducting layers sustained by interlayer tunnelling supercurrents, which was recently observed together with a phenomenological analysis of Sine-Gordon equation and with a reflectance experiment of pump-probe method using cuprate superconductor(LaSrCuO). In this study, we proposed a model Hamiltonian of the intrinsic Josephson junction realized by high T<sub>c</sub> superconductor and investigated a propagation of Josephson plasma soliton by the optical excitation.

### Keywords:

Josephson plasma, Superconductivity

## Electron-Phonon Interactions In alkali doped P-Terphenyl

M Uhammad Nadeem<sup>1</sup>, PARK Tae Ho<sup>1</sup>, CHOI Han Yong\*<sup>1</sup>

<sup>1</sup>성균관대학교 물리학과  
hychoi2@gmail.com

### Abstract:

Experiments have shown that P-terphenyl ( $C_{18}H_{14}$ ) has superconducting state with Transition temperature of 123K, when doped with potassium<sup>1</sup>. In order to explore the possible high  $T_c$  superconductivity in this material, we have performed the density functional theory calculations for the structural and electronic properties of the pristine and  $K_3$  p-terphenyl. We have employed density functional perturbation theory to calculate the phonon dynamical matrices and hence electron-phonon interactions. Contributions of phonon eigen-modes related to K-atoms and p-terphenyl inter and intra-molecular vibrations in the electron-phonon coupling and spectral function have been analyzed. Superconducting  $T_c$  was estimated using McMillen formula. Eliahburg spectral function shows stronger coupling of C-C stretching modes, which also appears in better studied material of aromatic hydrocarbons picene<sup>2,3</sup>.

Reference) 1. Ren-Shu Wang, Yun Gao, Zhong-Bing Huang, and Xiao-Jia Chen, arXiv:1703.06641 (2017). 2. M. Casuala, M.Clandra, G. Profeta and F. Mauri, PRL 107, 137006 (2011). 3. A. Subedi and L. Boeri, Phys. Rev. B 84, 020508 (2011).

### Keywords:

P-Terphenyl, DFPT, Organic Superconductor

## Evidence of nodeless multigap superconductivity in $2H$ - $\text{Pd}_{0.05}\text{TaSe}_2$ from London penetration depth and thermal transport measurements

김기훈\*<sup>1</sup>, 김찬희<sup>1</sup>, 전병구<sup>1</sup>, 민병훈<sup>1</sup>, WULFERDING Dirk<sup>2</sup>, 남우현<sup>1</sup>, 김지훈<sup>2, 3</sup>  
<sup>1</sup>서울대학교 물리천문학부, <sup>2</sup>포항공과대학교 물리학과, <sup>3</sup>기초과학연구원  
khkim@phya.snu.ac.kr

### Abstract:

$2H\text{-TaSe}_2$  is one of unique transition metal dichalcogenides which exhibits an incommensurate charge density wave (ICDW) state at  $\sim 122$  K followed by a commensurate charge density wave (CCDW) state at  $\sim 90$  K and superconductivity at  $T_C \sim 0.14$  K. Recently, it was found that upon systematic intercalation of Pd ions into  $2H\text{-TaSe}_2$ , the CCDW order is destabilized more rapidly than ICDW to indicate a hidden quantum phase transition point at  $x \sim 0.09$ - $0.10$ . Moreover,  $T_C$  shows a dramatic enhancement up to 3.3 K at  $x = 0.08$ ,  $\sim 24$  times of  $T_C$  in  $2H\text{-TaSe}_2$  [1]. In this work, we investigate in-plane London penetration depth ( $\lambda_{ab}$ ) and thermal conductivity ( $\kappa_{ab}$ ) of  $2H\text{-Pd}_{0.05}\text{TaSe}_2$  single crystals in which superconductivity with an optimal  $T_C \sim 3.13$  K is realized below its incommensurate charge density wave transition below  $\sim 120$  K. At zero magnetic field, temperature dependence of  $\lambda_{ab}$  below  $T_C$  exhibits a power-law  $AT^n$  with  $n = 2.66$  and no residual term is found in the  $\kappa_{ab}/T$  as  $T \rightarrow 0$ . Moreover, magnetic-field dependence of the normalized residual linear term  $(\kappa_0(H)/T)/(\kappa_N/T)$  exhibits similar behavior as observed in typical multigap superconductors such as  $\text{NbSe}_2$ [2]. These experimental results consistently support the presence of multiple nodeless superconducting gaps in  $2H\text{-Pd}_{0.05}\text{TaSe}_2$ .

This work has been supported by Creative Research Initiatives by KRF (\*\*)

### References :

- [1] D. Bhoi *et al.*, Scientific Reports **6**, 24068 (2016)
- [2] E. Boaknin *et al.*, Physical Review Letters **90**, 117003 (2003)

### Keywords:

Superconductivity, Thermal transport, London penetration depth

## Signature of interaction between electron and charge density wave fluctuation in NbSe<sub>3</sub>

임찬영<sup>1</sup>, 임준수<sup>1</sup>, 김성현<sup>1</sup>, 김용관\*<sup>1</sup>

<sup>1</sup>Department of Physics, Korea Advanced Institute of Science and Technology  
yeongkwan@kaist.ac.kr

### Abstract:

In most of charge density wave(CDW) systems , superconductivity emerges above the quantum critical point of CDW. Based on such tendency, it can be argued that the instability related to CDW could play certain role on superconductivity. Prior to discuss such new possible superconducting mechanism, it is required to reveal whether the CDW instability - short range fluctuation or collective excitation, couples with electrons to mediate the pair. In this presentation, the signature of interaction between the electron and CDW instability will be presented captured by angle resolved photoemission spectroscopy in quasi-1D CDW system NbSe<sub>3</sub>. A kink, the representative feature of electron-bosonic mode coupling was observed in the electronic structure only when CDW phase present in the system. As the CDW is suppressed via Ta doping, the kink disappeared, implying that the observed kink is result of interaction between electron and collective excitation mode of CDW.

### Keywords:

angle-resolved photoemission spectroscopy; superconductivity; charge density wave; NbSe<sub>3</sub>

## Evolution of superconductivity and charge density waves in $2H$ - $Pd_xTaSe_2$ superconductor under high-pressure

SUR Yeahan<sup>1</sup>, JANG Donghyun<sup>1</sup>, BHOI Dilip<sup>1</sup>, GU Zhehao<sup>2</sup>, MURATA Keizo<sup>1</sup>, CHEN Xiao-Jia<sup>2</sup>, 김기훈\*<sup>1</sup>

<sup>1</sup>Center for Novel States of Complex Materials and Research and Institute of Applied Physics,  
Department of physics and astronomy, Seoul National University, Seoul 151-747, South Korea,

<sup>2</sup>Center for High Pressure Science and Technology Advanced Research, Shanghai, 201203, China  
khkim@phya.snu.ac.kr

### Abstract:

We have investigated the pressure dependence of resistivity of the  $2H$ - $Pd_xTaSe_2$  single crystals ( $x = 0.02, 0.06$ ) up to 8 GPa using a hybrid piston cylinder cell and cubic anvil cell. In both samples exhibit an incommensurate charge density wave (ICDW) near 110 K and a commensurate charge density wave (CCDW) near 90 K. In both samples, the suppression of charge density waves and the enhancement of superconductivity were observed. Obtained  $T_c$  are 4.72 K at 8 GPa ( $x = 0.02$ ) and 5.72 K at 8.5 GPa ( $x = 0.06$ ) without any saturation. Moreover, ICDW and CCDW were not fully suppressed at 8.5 GPa but decrease monotonously with pressure. To fully suppress CDWs and find the maximum  $T_c$ , we measured resistivity of  $x = 0.06$  samples using diamond anvil cell up to 37.7 GPa.  $T_c$  of  $x = 0.06$  sample was enhanced up to 7.35 K at 18.7 GPa. Although derivative of the resistivity is too broad to extract exact transition temperatures, CCDW and ICDW were fully suppressed near the optimal pressure and near 25 GPa, respectively. Superconductivity survives up to the maximum pressure of 37.7 GPa in turn we could not find superconducting dome. The maximum  $T_c$  suggests that the quantum critical point (QCP) might exist near the optimal pressure. Further experiments such as Raman can reveal whether the QCP exist in these materials.

### Keywords:

Charge density wave, quantum criticality, superconductivity, transition metal dichalcogenide, high pressure

## Noise-induced Switching Dynamics in a Modulated Cold Atom with Interatomic Interaction

MOON Geol<sup>\*1</sup>, KWON Yongsung<sup>1</sup>, HONG Haeun<sup>1</sup>, NOH Heung-Ryoul<sup>\*1</sup>

<sup>1</sup>전남대학교 물리학과

wlp319@naver.com, hrnoh@chonnam.ac.kr

### Abstract:

We theoretically investigate the noise-induced switching dynamics between two bistable states realized in the parametrically driven oscillator and the resonantly driven oscillator. The nonlinear dynamics is implemented in an intensity modulated  $^{85}\text{Rb}$  cold atoms, and the interatomic interaction due to shadow force causes the modification of noise-induced switching dynamics between two bistable states of each oscillator. The modified noise-induced switching dynamics of each nonlinear oscillator distinctively depends on the positional symmetry of two bistable states in a rotating frame, and as a results, the modified switching dynamics of many particles in the parametrically and resonantly driven oscillator display the nonequilibrium phase transitions equivalent to the ideal Ising model class and similar to the gas-liquid transition, respectively.

### Keywords:

Noise-induced Switching, Parametric resonance, Cold atoms

## Density matrix reconstruction through Hamiltonian learning of entangled N-particle systems

안재욱\*<sup>1</sup>, 이우준<sup>1</sup>, 김호섭<sup>1</sup>

<sup>1</sup>한국과학기술원 물리학과  
jwahn@kaist.ac.kr

### Abstract:

An entangled N-particles system is represented by a density matrix having  $2^N$ -by- $2^N$  elements, making it nearly impossible to reconstruct the full quantum state through quantum tomography measurements, as N exceeds only a few tens. Here, we attempt to determine the system Hamiltonian and reconstruct the density matrix of entangled N-particle systems under dephasing, using machine learning techniques. The results can be summarized as density matrix reconstruction of numerically generated data with an R-squared value over 0.99 and, of experimentally generated data, over 0.93 for two particles. The difficulty comes from choosing a proper model Hamiltonian of the system and noisy nature of the experiment. We expect our method will be a useful tool for experiment and analysis on complex entangled systems.

### Keywords:

Rydberg atoms, Hamiltonian learning

## Spin polarization of Rb<sup>87</sup> atoms with Xe and high-pressure buffer gas in a cubic cell

윤호\*<sup>1</sup>, 최석원<sup>1</sup>, 유재승<sup>1</sup>, 남창우<sup>1</sup>  
<sup>1</sup>(주)한화 핵심기술3팀  
hoonyu99@hanwha.com

### Abstract:

We simulated the spin polarization of Rb vapor gas with Xe and high-pressure buffer gas in a cubic cell as pumping laser power, line width, waist, gas temperature and cell size. We calculated absorption cross-section as a frequency of the pumping laser by considering pressure and Doppler broadening. The spin polarization of Rb gas in a cubic cell was obtained as a result of pump laser absorption and atomic population for the steady state. We numerically found the optimal parameter for the maximum polarization of Rb atoms.

### Keywords:

Spin polarization, optical pumping

## Light Propagation in a Pair of Two-Dimensional Lattices of Cold Atoms

유성미\*<sup>1</sup>

<sup>1</sup>홍익대학교 교양과  
ysungmi@hongik.ac.kr

### Abstract:

We study light propagation through two-dimensional (2D) square lattices of cold and dense atomic vapors using infinite lattice model in which the radiated fields from induced dipoles are summed up analytically. The effective detuning and linewidth are estimated, leading to the total resonance shifts of atoms in lattices with any dimension. The resonance shift of lattice atoms is plotted as a function of the angle of incidence of the driving light in a lattice with the particular lattice constant. We discuss precision of spectroscopy may be improved in a system of lattices of atoms by illuminating light on the system with non-normal incidence. Our prediction may be extended to analyze light propagation through optical lattices in one, two, and three dimensions.

### Keywords:

cooperative optical response, cold and dense atoms, square lattices

## Quantum Sensitivity to Additional Information in Decision Making

박정호\*<sup>1</sup>, 이중성<sup>2</sup>, 함병승<sup>3</sup>, 이진형\*<sup>2</sup>, 이광걸\*<sup>2</sup>

<sup>1</sup>고등과학원 계산과학부, <sup>2</sup>한양대학교, <sup>3</sup>광주과기원  
jbang@kias.re.kr, hyoung@hanyang.ac.kr, kglee@hanyang.ac.kr

### Abstract:

We report on a study of distinctive quantum-mechanical feature in decision making---i.e., quantum decision making---based on a game-theoretic approach. The decision making theory indicates which choices are optimal in a given situation. For example, when the decision is made, an available information, say "hint" here, is interpreted and translated into the optimal choices; however, analyses and calculations of such a process are radically intractable. We thus conjecture that a person who makes the decision uses a pre-programmed algorithm which is immanent, e.g., in his/her brain, and provides probabilistic decision making outcomes. As a main result, we show both theoretically and experimentally that the quantum decision maker can have higher hint-sensitivity than its classical counterpart. Such a quantum feature originates from the quantum superposition property involved in the decision making process. In our further study, it is also shown that this higher hint-sensitivity can still be observed as long as the quantum superposition remains.

### Keywords:

Quantum Decision Making, Quantum Game

## HHG and Strong Field Approximation Formalism in Solids

이민호\*<sup>1</sup>, 변창우<sup>2</sup>, CHOI NarkNyul<sup>3</sup>

<sup>1</sup>금오공과대학교 교양교직부, <sup>2</sup>금오공과대학교 교양교직부, <sup>3</sup>금오공과대학교 교양교직부  
minho.lee.kr@gmail.com

### Abstract:

The high-order harmonic generation (HHG) in solids dressed by a strong infrared laser field is investigated by using one dimensional model system. As an analysis tool, we use three-step picture in momentum space, which is first provided in Ref.[1] based on the adiabatic state (Houston state [2]) formalism in velocity gauge. In length gauge, by transforming the crystal momentum  $k$  into a frame moving with the vector potential, a trajectory picture similar to atomic HHG is provided in Ref.[3]. In this talk, we derive strong field approximation (SFA) formalism for solids in length gauge, by following the SFA in gas phase atom. The formalism gives three-step picture in momentum space in length gauge. We apply the formalism to investigate HHG in one dimensional solid system. Surprisingly, unlike the SFA in gas phase atom, we can see that the SFA formalism in solids give very accurate HHG in energy spectrum, even in magnitude. We also apply the formalism to investigate the localization of HHG in solids under spatially inhomogeneous fields produced by plasmonic field enhancement using Wannier-Bloch basis [4].

[1] M. Wu, D. A. Browne, K. J. Schafer, and M. B. Gaarde, Phys. Rev. A 94, 063403 (2016).

[2] J. B. Krieger and G. J. Iafrate, Phys. Rev. B 33, 5494 (1986).

[3] G. Vampa, C. R. McDonald, G. Orlando, D. D. Klug, P. B. Corkum, and T. Brabec, Phys. Rev. Lett. 113, 073901 (2014).

[4] E. N. Osika, et.al., Phys. Rev. X 7, 021017 (2017).

### Keywords:

SFA in solids, three-step picture, HHG in solids, inhomogeneous fields, Wannier-Bloch basis

## 다이오드 여기 Cs 원자 증기 레이저 제작 및 증기 cell의 온도와 광출력과 의 상관관계 연구

오경환\*<sup>1</sup>, 공병준<sup>1</sup>, 홍성진<sup>1</sup>, 이용수<sup>1</sup>, 송상권<sup>1</sup>

<sup>1</sup>연세대학교 물리학과  
koh@yonsei.ac.kr

### Abstract:

Cs, K, Rb 등 알칼리 금속 원자의 증기는 높은 양자효율을 갖는 광이득 물질이며 특히 narrow linewidth diode laser의 개발과 더불어 diode pumped alkali-vapor laser (DPAL)이 활발히 연구되고 있다. 본 연구에서는 Cs 증기 cell을 광이득 매질로 이용하여 레이저를 국내 최초로 제작하였으며 pump power와 laser power의 상관관계를 구하였다. 또한 Cs 증기 cell 온도에 따른 laser power 변화를 측정하여 최적화된 온도를 구하였다.

### Keywords:

Atomic gas Laser, Laser, Laser material, diode-pumped Laser

## Recent Development of Design and Performance Analysis System for Quantum Computing System

CHOI Byung-Soo\*<sup>1</sup>

<sup>1</sup>한국전자통신연구원 양자창의연구실  
bschoi3@etri.re.kr

### Abstract:

During the last decade there have been much progress on the quantum computing from the device level to the algorithm level. Thanks to huge effort of many researchers, we are ready to see the moment where the quantum computer outperforms the classical computer. Related to this, several global IT companies are heavily working on the quantum computing ecosystem from research to business.

However, likewise the early stage of classical supercomputer, it is uncertain what problems are good for quantum computing and what limiting factors there are. Therefore, it is important to know what key hurdles we should solve to achieve the quantum computational advantage over the classical supercomputing system.

In this talk, we present one of our on-going projects which assists to all researchers. As the first tool, we explain a design and analysis system for quantum computing system. It works for the general purpose fault-tolerant quantum computing. To be useful, the system has inputs quantum algorithms, quantum error-correction and its fault-tolerant protocols, and quantum information device. By using this system, anyone can estimate how much quantum computing is powerful, and what constituent step should be improved. As a preliminary study, we show several analysis results. Finally, we hope this system will be used for anyone who are working on quantum computing research.

### Keywords:

quantum computing, fault-tolerant quantum computing, quantum computer performance

## The IBS/CAPP magnetometer station for the GNOME experiment

김동욱\*<sup>1, 2</sup>, 김영근<sup>1, 2</sup>, 신윤창<sup>2</sup>, SEMERTZIDIS Yannis K.<sup>1, 2</sup>

<sup>1</sup>한국과학기술원, 물리학과, <sup>2</sup>기초과학연구원, 액시온 및 극한상호작용 연구단  
physicist@kaist.ac.kr

### Abstract:

The Global Network of Optical Magnetometers to search for Exotic physics (GNOME) is an experiment looking for transient events of axion domain walls from the gradient coupling of axion field with atomic spins. GNOME is based on synchronized measurements from multiple GPS-timed magnetometer stations located in geographically separated places on the Earth. While a single magnetometer could detect spin signals from such terrestrial events, it would not be possible to distinguish real physic events from false ones caused by environmental noise sources. One of those stations located at IBS/CAPP in Daejeon, South Korea employs cesium alkali atoms as a primary magnetometer. We present the optimization and characterization of the Cs magnetometer at IBS/CAPP.

### Keywords:

gnome, axion, axion domain wall, optical magnetometer, and Cs magnetometer

## An enriched Mo-100 powder measurement by a HPGe array detector

박소연<sup>1</sup>, 김영덕\*<sup>2</sup>, 한인식\*<sup>3</sup>, 이무현\*<sup>2</sup>, 강운구<sup>2</sup>, 김고운<sup>1</sup>, 이은경<sup>2</sup>, LEONARD Douglas<sup>2</sup>  
<sup>1</sup>이화여자대학교, 물리학과, <sup>2</sup>기초과학연구원 지하실험연구단, <sup>3</sup>이화여자대학교, 과학교육과  
ydkim@sejong.ac.kr, ishahn@ewha.ac.kr, moohyunlee@gmail.com

### Abstract:

The AMoRE (Advanced Mo based Rare decay Experiment) phase-II needs ultra pure crystals with low radioactive contamination ( $< 2$  micro Bq/kg of  $^{228}\text{Th}$ ) to achieve the zero background level in the ROI (Region of Interest) of the neutrinoless double decay from the Mo-100. The raw material of the crystals, enriched Mo-100 powder, has to have low contamination ( $< 20$  micro Bq/kg of  $^{228}\text{Th}$ ). An array of 14 HPGe detectors (70%) was constructed at the Yangyang underground laboratory in spring 2017 for measuring small amount of radioactive isotopes, such as  $^{238}\text{U}$  and  $^{232}\text{Th}$ , by using coincidence signals from two detectors. Activities of various radioactive isotopes in a sample of Mo-100 powders measured with data taken for about 3 months together with background data for about the same time period will be presented in this presentation.

### Keywords:

enriched Mo-100 powder, MoO<sub>3</sub> powder, radioactive contamination, pure crystals

## A study on high energy gamma intensities in $^{208}\text{Tl}$ decay from a $\text{ThO}_2$ powder sample

김영덕\*<sup>1</sup>, 한인식\*<sup>2</sup>, 김고운<sup>1, 2</sup>, 이무현<sup>1</sup>, 박수연<sup>1, 2</sup>, 강운구<sup>1</sup>, LEONARD Douglas<sup>1</sup>  
<sup>1</sup>기초과학연구원 지하실험연구단, <sup>2</sup>이화여자대학교 물리학과  
ydkim@sejong.ac.kr, ishahn@ewha.ac.kr

### Abstract:

The gamma decay intensities for  $E > 3$  MeV from the  $^{208}\text{Tl}$  decay have 100% uncertainties in the NNDC database. New measurements with smaller uncertainties are desirable for understanding nuclear decay properties of the nucleus and high energy gamma background in rare decay experiments. A  $\text{ThO}_2$  powder sample was measured with a 100% High Purity Germanium(HPGe) in the Yangyang underground laboratory (Y2L) at the Center for Underground Physics(CUP) to obtain more accurate numbers of the high energy gamma intensities from the  $^{208}\text{Tl}$ . The experimental set-up, Monte Carlo simulation studies for detection efficiencies, and a preliminary result will be presented in this presentation.

### Keywords:

HPGe, gamma decay intensity

## AMoRE-Pilot Analysis

김용함\*<sup>1</sup>, KIM Inwook<sup>1, 2, 3</sup>

<sup>1</sup>기초과학연구원, 지하실험연구단, <sup>2</sup>서울대학교, 물리천문학부, <sup>3</sup>표준과학연구원  
yhk@ibs.re.kr

### Abstract:

AMoRE (Advanced Mo-based Rare process Experiment) is an international collaboration searching for neutrinoless double beta decay ( $0\nu\beta\beta$ ) of  $^{100}\text{Mo}$  in  $^{40}\text{Ca}^{100}\text{MoO}_4$  (CMO) scintillating crystals with the use of metallic magnetic calorimeters (MMCs) at millikelvin temperatures. With high energy resolution and high background rejection power achieved by phonon-photon simultaneous measurement and pulse shape discrimination (PSD) techniques, AMoRE aims at zero-background in the region of interest (ROI) near 3034 keV. We present the analysis method and current results of the AMoRE-Pilot experiment, the commissioning phase of the experiment.

### Keywords:

neutrinoless double beta decay, low temperature detection

## Background studies of $\text{CaMoO}_4$ crystals for AMoRE-pilot data

YOON Young Soo\*<sup>1</sup>

<sup>1</sup>Center for Underground Physics, IBS, <sup>2</sup>on behalf of the AMoRE Collaboration  
ysy@ibs.re.kr

### Abstract:

Commissioning runs for the Advanced Mo-based Rare Process Experiment (AMoRE), a search for neutrinoless double beta decay of  $^{100}\text{Mo}$  in calcium molybdate ( $\text{CaMoO}_4$ ) crystals, are currently underway at the Yangyang underground laboratory. Six crystals, with a total mass of  $\sim 1.9$  kg, were installed and background data were taken between Aug 2018 and Dec 2018. Data analysis of the measured background spectra is in progress. Using the GEANT4 simulation toolkit, backgrounds from radioactive nuclides such as  $^{238}\text{U}$  and  $^{232}\text{Th}$  internal to the crystals and from surrounding materials in the AMoRE-pilot configuration have been simulated. Preliminary background spectra from the crystals were fitted with these Monte Carlo simulation results in order to identify background sources. In this presentation, results from these fits will be presented and discussed.

### Keywords:

Neutrinoless double beta decay, background, modeling

## Operation of a low-background alpha particle counter at Yangyang

하창현\*<sup>1</sup>

<sup>1</sup>기초과학연구원 지하실험연구단  
changhyon.ha@gmail.com

### Abstract:

Alpha particle counting using an ionization chamber is a well-known method for measuring levels of radionuclide contamination in materials. A XIA UltraLo-1800 alpha counter operating at the Yangyang underground laboratory measures ionization electrons produced alpha particles passing through an Argon gas volume. Since its commissioning in June, 2015, the main application of this device has been to understand alpha events produced by radioactive contaminants on sample surfaces, in particular  $^{210}\text{Po}$  nuclides, which are long-lived daughters that are left over from exposure to atmospheric  $\text{Rn}222$ . We report sample measurements that include low-radioactive printed circuit boards, different types of reflective sheets, and other materials that are under consideration for use in rare event search experiments.

### Keywords:

Alpha counting, ionization chamber

## Neutron monitoring system for the COSINE-100 experiment

고영주\*<sup>1</sup>

<sup>1</sup>기초과학연구원, 지하실험연구단  
yjko@ibs.re.kr

### Abstract:

The COSINE-100, a dark matter WIMPs (Weakly Interacting Massive Particles) search experiment, is running at the Yangyang underground laboratory which is about 700 m below the earth surface with a low cosmic muon background environment. In the experiment, neutrons from the rock environment can still mimic signals expected by the WIMPs interactions, so a neutron monitoring system is required for a systematic understanding of them. In order to do the neutron monitoring, we have been preparing monitoring systems for fast and thermal neutrons by using liquid scintillator (LS) detectors and a <sup>3</sup>He gas detector, respectively. R&D works of the LS detector will be presented including pulse shape discrimination and background contamination together with a comparison of thermal neutron rates by the <sup>3</sup>He detector.

### Keywords:

neutron monitoring, neutron detector, dark matter, COSINE-100

## Development of large area light detector using Neganov-Luke phonon amplified effect for dark matter experiments

JEON J. A.<sup>\*1</sup>, KIM H. L.<sup>1</sup>, KIM I.<sup>1, 2</sup>, KIM S. R.<sup>1</sup>, LEE S. H.<sup>1</sup>, SONG J. H.<sup>3</sup>, KIM Y. H.<sup>1, 2</sup>

<sup>1</sup>Center for Underground Physics, Institute for Basic Science (IBS), Daejeon, South Kor, <sup>2</sup>Korea Research Institute of Standards and Science (KRISS), Daejeon, South Korea, <sup>3</sup>Department of Physics, Kongju National University, Kongju, South Korea  
jina@ibs.re.kr

### Abstract:

Detecting the rare event in low temperature experiment for direct dark matter detection experiments, low temperature thermal detectors have been significant role because of their high energy sensitivity and background rejection capability. The thermal detectors having a target scintillating crystal can simultaneous detection of heat (phonon) and light (scintillation) signals from the crystal. The background signals have been rejected by relative amplitudes of heat and light signals. But the light yield of scintillating crystals is typically a few percent because of only a small portion of the amount of the energy deposited in the crystal is visible in the light sensor. Here we developed a 1 cm<sup>2</sup> light detector with phonon amplification by Neganov-Luke effect and measured performances at 40 mK temperature. Clear amplification on the light signals was measured with a voltage applied to the electrodes without change on heat signals. An amplification factor on the light signals was as large as 7 with 80 V bias voltage.

### Keywords:

Low temperature detector, Direct dark matter detection experiments, Neganov-Luke effect

## High-energy Observational properties of Neutron stars and related systems

안홍준\*<sup>1</sup>

<sup>1</sup>충북대학교 천문우주학과  
hjan@cbnu.ac.kr

### Abstract:

Neutron stars are the left-over core of a massive star after supernova explosion. As neutron stars are extremely dense, they have very strong gravity at the surface. So normal gas pressure arising from thermal energy cannot support the star from gravitational collapse. It is believed that degenerate electrons provide further (dominant) internal pressure against the collapse in the crusts. Moving on to the core of the star, almost nothing is known other than density there is greater than the proton density; so normal matter may not survive and some exotic forms of matter may exist there. So neutron stars provide a good chance to discover new physics. However, due to the observational/theoretical complexity, studying (or even discovering) such exotic matter is very difficult. In this talk, I will discuss various observational properties of neutron stars, and how they can help to study fundamental physics of extremely dense and cold matter.

### Keywords:

Neutron star, Observations, High energy

## Tidal deformability of a Neutron Star with Nuclear Equations of States

KIM Young-Min\*<sup>1</sup>, LIM Yeunhwan<sup>2</sup>, KWAK Kyujin<sup>1</sup>, HYUN Chang Ho<sup>3</sup>, LEE Chang-Hwan<sup>4</sup>

<sup>1</sup>School of Natural Science, Ulsan National Institute of Science and Technology (UNIST), <sup>2</sup>Cyclotron Institute, Texas A&M University, <sup>3</sup>Department of Physics Education, Daegu University, <sup>4</sup>Department of Physics, Pusan National University  
ymkim715@unist.ac.kr

### Abstract:

The first multi-messenger event, GW170817/GRB170817A/AT2017gfo was observed by LIGO/Virgo, Fermi/GBM, and many telescopes. The observation of the gravitational wave, GW170817, played a key role in the confirmation of a binary neutron star merger as the origin of the multi-messenger event. This observation is also very important to constrain nuclear equations of state (EoSs) in dense matter such as the interior of a neutron star (NS). Tidal deformability of a NS can be estimated by GW observations, and the upper limit estimated from GW170817 is about 800 under an assumption of a low spin prior. Tidal deformability is dependent on the inner structure of a NS, therefore the upper limit of the tidal deformability of the NS observed by LIGO/Virgo can be a new constraint on realistic NS EoSs. In this talk, I will present current results of the tidal deformabilities using various nuclear EoSs and compare them with the recent observation of GW170817.

### Keywords:

Gravitational-wave, Neutron Star, Tidal deformability, Equations of States, GW170817, 중력파, 중성자별, 조석병형, 상태방정식

## Intial data of binary neutron stars in eccentric orbits

KIM Hee Il<sup>\*1</sup>, PARK Kwanho<sup>1</sup>, LEE Hyung Mok<sup>1, 2</sup>  
<sup>1</sup>서울대학교, 물리천문학부, 천문학전공, <sup>2</sup>한국천문연구원  
khi@astro.snu.ac.kr

### Abstract:

We construct the initial data of binary neutron stars in eccentric orbits and investigate its feasibility by evolving it using a 3-dimensional general relativistic hydrodynamics code. Since the eccentric orbits do not allow any exact stationarity useful for the initial data construction, we simply combine two TOV stars maximally separated in the orbit. Spurious stellar pulsations are very dependent on the eccentricity and the separation. For large enough eccentricities, we could get negligible spurious pulsations and sufficiently small constraint violations. For some small eccentricities, we distort the initial TOV data by assuming uniform coordinate velocities to get additional reduction of the pulsations. We investigate the junk gravitational waves produced from our data.

### Keywords:

binary neutron star, gravitational wave

## Rotating black holes with anisotropic fluid

KIM Hyeong-Chan<sup>3</sup>, LEE Bum-Hoon<sup>1, 2</sup>, LEE Wonwoo<sup>\*1</sup>, LEE Youngone<sup>3</sup>

<sup>1</sup>Center for Quantum Spacetime, Sogang University, <sup>2</sup>Department of Physics, Sogang University,

<sup>3</sup>School of Liberal Arts and Sciences, Korea National University of Transportation  
warrior@sogang.ac.kr

### Abstract:

We construct a rotating black hole solution to Einstein equations with locally anisotropic equations of state. We obtain the geometry representing the rotating black hole by employing Newman-Janis algorithm. We fix the orthonormal tetrad to measure physical quantities, energy density and pressure, where the stress-energy tensor for the anisotropic fluid is diagonal. The static limit surfaces and event horizons are analyzed.

### Keywords:

Rotating black holes, anisotropic fluid

## Particle Absorption in Charged Black Hole with PV Term

곽보근\*<sup>1</sup>

<sup>1</sup>세종대학교 물리천문학과  
rasenis@sejong.ac.kr

### Abstract:

We investigate the variation of the charged anti-de Sitter black hole under charged particle absorption by considering thermodynamic volume. When the energy of the particle is considered to contribute to the internal energy of the black hole, the variation exactly corresponds to the prediction of the first law of thermodynamics. Nevertheless, we find the decrease of the Bekenstein-Hawking entropy for extremal and near-extremal black holes under the absorption, which is an irreversible process. This violation of the second law of thermodynamics is only found when considering thermodynamic volume. We test the weak cosmic censorship conjecture affected by the violation. Fortunately, the conjecture is still valid, but extremal and near-extremal black holes do not change their configurations when any particle enters the black hole. This result is quite different from the case in which thermodynamic volume is not considered.

### Keywords:

black hole, thermodynamics, cosmic censorship

## Singularities inside a black hole

염동한\*<sup>1</sup>

<sup>1</sup>아시아 태평양 이론물리센터, <sup>2</sup>포항공과대학교, 물리학과  
innocent.yeom@gmail.com

### Abstract:

In the literature, several authors asserted that a kind of modified gravity models or quantum gravitational corrections from the canonical quantization can cure a singularity inside the black hole. I summarize my recent investigations and critically review previous proposals. (1) The Chamseddine-Mukhanov model, based on the generalized mimetic gravity, cannot resolve the singularity problem and this has nothing to do with the limiting curvature hypothesis. (2) The effective models of loop quantum gravity can change the spacelike singularity, but it loses the consistency of the canonical commutation relations.

### Keywords:

singularity, black hole, modified gravity, quantum gravity

## 유무기 하이브리드 페로브스카이트 광전소자

김진영\*<sup>1</sup>

<sup>1</sup>울산과학기술원 에너지및화학공학부  
jykim@unist.ac.kr

### Abstract:

최근들어 유무기 하이브리드 페로브스카이트 물질을 기반으로 하는 광전소자에 대한 연구가 전세계적으로 매우 활발히 진행되고 있다. 그 중에서도 에너지 하베스팅을 위한 태양전지에 사용되고 있는 페로브스카이트 물질은 광효율이 높고 유연할 뿐만 아니라 대면적 소자로 제작이 가능하여 차세대 태양전지의 광활성 물질 중에서 가장 주목을 받고 있다. 특히 가장 많이 보급된 실리콘 태양전지와 비교할 때, 효율이 거의 비슷하고 고온 공정이 없어 제작 비용이 훨씬 저렴하기 때문에 다양한 응용 제품이 나올 것으로 기대되고 있다. 또한 발광소자로서도 효율이 유기물과 거의 비슷한 수준을 보이고 반치폭이 매우 좁아 굉장히 우수한 색순도를 보여주어 OLED를 잇는 차세대 디스플레이로 대두되고 있다. 이와 같이 다양한 광전소자에서 우수한 특성을 보이는 유무기 하이브리드 페로브스카이트를 이해하기 위하여, 본 강좌에서는 기본 물성과 함께 다양한 소자에의 적용을 알아보려고 한다.

### Keywords:

유무기 하이브리드, 페로브스카이트, 페로브스카이트 태양전지, 발광소자, 광전소자,

## Recent Progress of van der Waals materials: theory

손영우\*<sup>1</sup>

<sup>1</sup>고등과학원 계산과학부  
hand@kias.re.kr

### Abstract:

In this talk, I will review recent progress in understanding physical properties of various two-dimensional crystals and their heterostructures.

### Keywords:

van der Waals materials, theory, review

## 반데르발스 2차원 물질의 최근 연구 동향: 2차원 반도체 채널 트랜지스터의 동작원리와 응용- MISFET, MESFET, JFET

임성일\*<sup>1</sup>

<sup>1</sup>연세대학교  
semicon@yonsei.ac.kr

### Abstract:

본 강좌에서는 TMDC 혹은 흑린과 같은 2차원 반도체 물질 박막을 채널로 사용하는 각종 트랜지스터의 동작 원리를 강의하고 나아가 그 소자응용에 대하여 강의한다. 2차원 반도체 트랜지스터는 유전체를 적용하는 metal-insulator-semiconductor field effect transistor (MISFET) 뿐만 아니라, Schottky Junction을 적용하는 metal-semiconductor field effect transistor (MESFET), 그리고 PN Junction 을 적용하는 junction field effect transistor (JFET)의 세가지 소자가 있어 각 소자의 동작 원리가 서로 다른 반면, 소자의 제작은 모두 용이하다는 특징이 있다.

### Keywords:

MISFET, MESFET, JFET

## 알아두면 쓸데있는 위상물질 물리이론

김영국\*<sup>1</sup>

<sup>1</sup>성균관대학교 물리학과  
youngkuk@skku.edu

### Abstract:

위2005년 위상 절연체(topological insulator)의 발견은 물리를 한 층 더 어려운 것으로 만든 감이 있다. '위상 절연체'라는 이름만으로도 '절연체를 이해하는데 이제는 위상 수학까지 알아야 하나?' 하는 심리적 장벽감을 느낀다. 본 강의는 이러한 심리적 장벽을 높이지 않겠다는 약속을 바탕으로, 위상 물질 연구에 관심이 있는 대학원생이 알아두면 쓸데있을 몇 가지를 물리 이론을 소개하려고 한다.

구체적인 강의 내용은 다음과 같다. 먼저 위상 물질 연구에 있어 필요한 최소한의 위상 수학 개념을 소개하고, 이를 통해 소위 Z2 위상 불변량(topological invariant)이라고 불리는 시간 대칭성(time-reversal symmetry)이 보호하는 위상 불변량을 소개 한다. 이를 위해 시간대칭성이 고체 내 전자 상태에 기여하는 역할을 살펴보고, 이것이 Z2 위상 불변량을 정의하는데 어떻게 쓰이는지 보일 예정이다. 이렇게 정의한 Z2 위상 불변량을 기준으로 물질을 위상 절연체와 보통 절연체로 나눈다. 성공적이라면 이 단계에서 bulk-boundary correspondence, topological invariants, Fermion doubling theorem, Wilson loop과 같은 개념을 무리 없이 받아들일 수 있다. 다음 단계는 Z2 위상 불변량의 Z4XZ2 위상 불변량으로의 확장이다. 시간 대칭성에 nonsymmorphic space group 대칭성을 포함하여, Z2 위상 불변량이 어떻게 새로운 Z4xZ2 위상 불변량으로 확장될 수 있는 지 보인다. 이를 위해 nonsymmorphic space group을 소개하고, 활용할 예정이다. 이러한 세분화된 분류법은, '위상 디랙 절연체 (topological Dirac insulator)'라고 이름 붙은 새로운 위상 물질의 발견을 가능하게 한다 [1].

이 강의를 통해 Ref. [1]을 쉽게 소개하고, 성공적인 위상 물질 연구의 한 사례를 들고자 한다. 위상물질 연구에 뜻이 있는 대학원생이 편하게 들을 수 있는 강의를 되는 것이 목표다.

[1] Wieder, Benjamin J., Barry Bradlyn, Zhijun Wang, Jennifer Cano, Youngkuk Kim, Hyeong-Seok D. Kim, A. M. Rappe, C. L. Kane, and B. Andrei Bernevig. "Wallpaper Fermions and the Topological Dirac Insulator." arXiv preprint arXiv:1705.01617 (2017).

### Keywords:

위상 절연체, 위상 물질, 튜토리얼, 강의, 알쓸위물

## How to characterize topological states of matter?

KIM Keun Su<sup>\*1</sup>

<sup>1</sup>Department of Physics, Yonsei University  
keunsukim@yonsei.ac.kr

### Abstract:

The theory of topological order classifies materials into the topologically trivial (normal) and the nontrivial (topological), leading to the discovery of topological insulators, topological crystalline insulators, and Dirac and Weyl semimetals. These topological states can be characterized by their band structure and boundary states. Angle-resolved photoemission spectroscopy (ARPES) is a well-known technique to directly measure the band structure of condensed matters. In this talk, I will introduce that how ARPES can be used to explore novel topological quantum states of matter and their topological phase transitions with various recent examples.

### Keywords:

Topological matter, Band structure, ARPES, Topological phase transition

## Introduction to 2D semiconductor valleytronics

조창희\*<sup>1</sup>

<sup>1</sup>대구경북과학기술원 신물질과학전공  
chcho@dgist.ac.kr

### Abstract:

현재의 반도체 소자는 전하의 흐름을 제어하는 원리로 구동된다. 만일 반도체 내 전자가 갖는 전하와 더불어 스핀, 밸리 등의 추가적인 자유도를 제어하고 활용할 수 있다면, 새로운 개념의 소자를 개발할 수 있을 것이다. 최근 전이 금속 칼코겐 화합물 계열 2차원 반도체의 특이한 전자구조로부터 밸리 자유도를 제어할 수 있는 가능성이 알려지면서 밸리트로닉스에 대한 연구가 활발히 진행되고 있다. 본 튜토리얼 세션을 통해 밸리트로닉스에 대한 기초 개념과 최근 연구동향에 대해 알아보려고 한다.

### Keywords:

2차원 반도체, 밸리트로닉스

## 중력파 개론

강궁원\*1

<sup>1</sup>한국과학기술정보연구원  
gwkang@kisti.re.kr

### Abstract:

최근 인류 최초로 중력파의 직접 검출에 성공함으로써 중력파 과학과 중력파 천문학에 대한 지대한 관심이 대두되고 있다. 라이고(LIGO)와 비르고(Virgo)의 2차에 걸친 관측가동에서 총 6회의 중력파 검출이 있었으며, 이를 통해 블랙홀 충돌이나 중성자별 충돌과 같이 강한 중력장이 작용하는 영역에서도 일반상대론이 잘 맞는다는 것을 확인했다. 블랙홀 질량에 대한 새로운 정보는 기존의 블랙홀 형성에 관한 모델을 수정하는 길잡이가 되었다. 특히 중성자별 병합에서 발생했던 중력파 검출은 이에 수반하는 여러 전자기파 신호도 검출되어 Short gamma-ray burst의 기원과 킬로노바에 대한 오랜 가설을 확인하는 과학적 성과를 얻었고, 중력파를 포함한 다중신호 천문학 시대의 도래를 알렸다.

본 튜토리얼에서는 중력파의 정의와 성질, 검출 원리와 역사, 최근의 중력파 검출 현황과 의미, 국내의 중력파 연구 현황, 그리고 중력파 과학의 향후 전망 등을 다루고자 한다. 이를 통해 중력파의 기초와 최근의 연구 흐름에 대한 개괄적인 이해와 지식을 제공하고자 한다.

### Keywords:

중력파, 라이고, 소그로

## 수치적인 방법을 통한 강한 중력장을 가진 고밀도 천체 연구

김진호\*<sup>1</sup>

<sup>1</sup>한국천문연구원 이론천문연구센터  
jkim@kasi.re.kr

### Abstract:

최근 중력파의 발견으로 고밀도 천체의 역학적 진화에 대한 관심이 높아지고 있다. 특히 중성자별의 충돌에 의한 중력파가 관측 되면서 중성자별의 운동과 그로인한 중력파 방출에 대한 중요성이 대두되고 있다. 본 튜토리얼 세션에서는 블랙홀과 중성자별의 역학적 진화를 컴퓨터 시뮬레이션으로 보기 위한 수치적인 방법과 이를 통한 최근 연구에 대하여 소개한다.

튜토리얼은 다음과 같은 순서로 진행될 예정이다.

- 1) 3+1 포멀리즘에서의 일반 상대론적인 (자기)유체 역학 방정식 소개
- 2) 상대론적인 (자기)유체 방정식 풀이를 위한 다양한 수치적인 방법 소개
- 3) 최근 연구 소개

### Keywords:

상대성이론-중력파-중성자별-블랙홀-수치-유체역학-자기유체역학

## Artificial Intelligence, AlphaGo, and Global Optimization

이주영\*<sup>1</sup>  
<sup>1</sup>고등과학원  
jlee@kias.re.kr

### Abstract:

Many problems in science and engineering can be mapped into combinatorial optimization problems, and examples include protein folding, protein structure prediction/determination, materials design, and community/module detection in the network science. In this talk, I will discuss our recent progresses in solving these problems in terms of the application of the Conformational Space Annealing (CSA) method.

I will also discuss the optimization issue in the study of machine learning (ML). A preliminary study indicates that proper application of CSA to ML can provide a solution to the overtraining problem in ML. I will share the progress of our attempt to build our own AlphaGo in this respect.

### Keywords:

Artificial Intelligence, AlphaGo, Global Optimization

## 118의 비밀

김항배\*<sup>1</sup>

<sup>1</sup>한양대학교 물리학과  
hbkim@hanyang.ac.kr

### Abstract:

물질은 원자로 이루어져 있고, 원자에는 118종의 원소가 있다. 원소들이 보이는 다양한 특성을 원자를 구성하는 핵과 전자들의 전자기적 결합에 양자역학을 적용하여 이해할 수 있게 된 것은 20세기의 위대한 업적이다. 그런데 왜 118종의 원소만 존재하는 것일까? 원소의 다양성은 핵의 다양성으로부터 온다. 핵은 양성자와 중성자, 더 자세히 들여다보면 쿼크들로 구성되어 있고, 강력, 전자기력, 약력으로 어우러진 복잡한 계로서 다양성을 발휘한다. 이 강연에서는 핵의 발견에서부터 핵의 다양성을 이해하기까지의 과정과 그 결과들이 과학과 일상에 어떻게 활용되고 있는지 살펴본다.

### Keywords:

원소, 핵

## Probing Nature's Nano-Machines with Light

HA Taekjip\*<sup>1, 2</sup>

<sup>1</sup>Departments of Physics and Biomedical Engineering, Johns Hopkins University, <sup>2</sup>Howard Hughes Medical Institute  
tjha@jhu.edu

### Abstract:

Did you know that proteins are nano-scale machines that help us think, dance and keep the threat of cancer at bay? Did you know that biology is a new research frontier for physicists? In this talk, Professor Ha will discuss how biophysicists are using light-based tools to poke and examine Nature's nano-machines, one molecule at a time, uncovering the amazing acrobatic abilities that are essential for all forms of life.

### Keywords:

protein, nano-machine, molecule, light

# 포스터발표논문

Poster session abstracts

## 실리카 나노와이어의 형성에 대한 산소 효과

윤성환<sup>1</sup>, 양진성<sup>1</sup>, 윤종환\*<sup>1</sup>

<sup>1</sup>강원대학교, 물리학과

jhyoon@kangwon.ac.kr

### Abstract:

실리카 나노와이어는 물리적/화학적 안정성 및 생물 친화성이 좋고 체적 대 표면적의 비율이 크기 때문에 다양한 센서 제작에 매우 적합한 나노 소재이다. 또한, 실리카 나노와이어는 450 nm 근처의 안정화된 강한 자외선 발광 특성을 갖고 있어 청색 발광소자 제조에 사용이 가능하다. 더 나아가 실리카 나노와이어의 높은 화학적 안정성은 다양한 금속을 사용하여 도핑하거나 표면을 코팅하는 것이 가능하다. 따라서 다양한 분야에서 나노와이어가 활용될 수 있도록 도핑이나 코팅을 통해 그 기능성을 확장하는 것이 가능하다. 본 연구에서는 니켈 막을 촉매로 산화실리콘 막을 사용하여 실리카 나노와이어를 형성하고, 산화실리콘 막의 산소함유량이 실리카 나노와이어 형성에 미치는 효과를 연구하였다. 산화실리콘 막은 플라즈마 화학 기상 증착 방법으로 제조하였으며, 표면에 니켈 막을 진공 증착한 후 약 1100°C 정도의 온도에서 열처리 하여 나노와이어를 형성하였다. X선 광전자분석(XPS), 주사현미경, 투과현미경 및 포토루미네스스 측정을 통해 산소함유량, 나노와이어의 미세구조 및 물성을 조사하였다.

### Keywords:

Silica Nanowire

## 알루미늄 유도 결정화에 의한 다결정 실리콘의 형성에서 산소 효과

윤종환\*<sup>1</sup>

<sup>1</sup>강원대학교 물리학과  
jhyoon@kangwon.ac.kr

### Abstract:

다결정 실리콘 막은 전자 및 광전 소자에 높은 활용성을 갖고 있을 뿐 아니라 높은 효율의 태양 전지를 구현하는데 적합한 반도체 재료로 주목 받고 있다. 따라서 낮은 비용으로 다결정 실리콘 막을 제조하기 위한 연구가 활발히 이루어지고 있다. 일반적으로 다결정 실리콘 박막을 쉽게 얻는 방법 중 하나는 알루미늄 금속 막을 촉매로 비정질 실리콘(a-Si) 박막을 열처리 하여 제조하는 것이다. 본 연구에서는 a-Si 대신 산화실리콘(SiO<sub>x</sub>) 박막을 사용하여 실리콘 박막을 형성하고, 산소 함량에 따른 다결정 실리콘 막의 형성을 조사하였다.

SiO<sub>x</sub>/Al/glass 층 구조를 600°C 이하의 온도에서 열처리하여 다결정 실리콘 박막을 형성하였으며, XRD, Raman, SEM, TEM을 사용하여 물리적 특성 및 미세구조를 분석하였다. a-Si에 비해 SiO<sub>x</sub> 박막에서 실리콘의 결정화가 매우 빨리 진행되는 사실을 관측하였으며, 특히 x값이 큰 박막에서 결정화가 잘 일어나는 거동을 나타내었다. 또한 다결정 실리콘 박막의 성장은 층교환 메커니즘을 통해 이루어졌으며 주로 (111) 방향성을 나타내었다.

### Keywords:

다결정 실리콘

## Pyroprotein-based electronic textiles with high thermal durability for energy harvesting

전준우<sup>1, 2</sup>, 오주영<sup>1, 2</sup>, 장현석<sup>1, 2</sup>, 정원택<sup>1, 2</sup>, 정재훈<sup>1, 2</sup>, 김병훈\*<sup>1, 2</sup>  
<sup>1</sup>인천대학교 물리학과, <sup>2</sup>인천대학교 기초과학연구소  
kbh37@inu.ac.kr

### Abstract:

Electronic textiles (e-textiles) need to have high heat durability for various applications. However, current e-textiles are usually damaged by high temperature processes. We report silk-based e-textiles fabricated by simple pyrolysis with axial stretching that demonstrate high electrical conductivity and thermal durability. The electrical conductivity of the proposed e-textiles was on the order of  $10^3$  S/cm and the electrical characteristics were maintained even after heating and bending. Furthermore, we prepared e-textiles with various electronic properties, such as semiconducting, superconducting, and light emitting properties, by depositing ZnO, MoSe<sub>2</sub>, and NbN onto the commercial silk-based e-textiles using sputtering and evaporation. We introduced a simple method for fabricating silk-based e-textiles with various electronic properties, which are compatible with the current textile industry.

### Keywords:

electronic textiles; pyroproteins; electrical conductivity; thermal durability

## Universal Oriental Epitaxy of AgCN Microwires on Various Hexagonal Two-Dimensional Crystals

김관표\*<sup>1</sup>, 이양진<sup>1</sup>, 구자현<sup>2</sup>, 윤준영<sup>1</sup>, 김강원<sup>3</sup>, 장정수<sup>4</sup>, 최정현<sup>1</sup>, 황준연<sup>7</sup>, 정후영<sup>5</sup>, 김용수<sup>6</sup>, 정현식<sup>3</sup>, RUOFF Rodney S.<sup>8, 9</sup>, 이훈경<sup>2</sup>

<sup>1</sup>Department of Physics, Yonsei University, <sup>2</sup>Department of Physics, Konkuk University, <sup>3</sup>Department of Physics, Sogang University, <sup>4</sup>Department of Physics, Ulsan National Institute of Science and Technology (UNIST), <sup>5</sup>UNIST Central Research Facilities (UCRF), Ulsan National Institute of Science and Technology (UNIST), <sup>6</sup>Department of Physics, University of Ulsan, <sup>7</sup>Institute of Advanced Composite Materials, Korea Institute of Science and Technology (KIST), <sup>8</sup>Department of Chemistry, Ulsan National Institute of Science and Technology (UNIST), <sup>9</sup>Center for Multidimensional Carbon Materials (CMCM), Institute for Basic Science (IBS)  
kpkim@yonsei.ac.kr

### Abstract:

The epitaxy process is often utilized to obtain high-quality thin-film crystals as well as nanostructures on various substrates. However, the epitaxial process is strongly influenced by the growth substrate because the atom-substrate interaction as well as the degree of lattice parameter matching are substrate-specific. Here, we show that micro-sized wires of linear silver cyanide (AgCN) polymer adapt oriental epitaxial growth on various hexagonal two-dimensional crystals (graphene, h-BN, MoS<sub>2</sub>, MoSe<sub>2</sub>, MoTe<sub>2</sub>, WS<sub>2</sub>, and WSe<sub>2</sub>). The universal tri-axial epitaxial behavior of AgCN wires, where the polymer chains are aligned along the zigzag lattice direction of various two-dimensional crystals, is demonstrated regardless of different lattice parameters and chemical surface properties of substrates. By performing the DFT calculations, we find that the AgCN polymer chains are energetically stable at the various hexagonal two-dimensional material's zigzag direction and which is consistent with the experimentally-observed results. Our study clearly demonstrates that it is possible to obtain the universal oriental epitaxial behavior of nanocrystals over different substrates.

### Keywords:

Two-dimensional crystals, Oriental epitaxy of chain polymer, AgCN



## Energy Storage using *Phyllostachys bambusoides* base Porous Green Carbon

김병훈\*<sup>1, 2</sup>, 장현석<sup>1, 2</sup>, 오주영<sup>1, 2</sup>, 전준우<sup>1, 2</sup>, 정원택<sup>1, 2</sup>, 정재훈<sup>1, 2</sup>  
<sup>1</sup>인천대학교 물리학과, <sup>2</sup>인천대학교 기초과학연구소  
kbh37@inu.ac.kr

### Abstract:

Hydrogen has been considered as the ideal energy carrier of the future due to its eco-friendly property, unlimited amount of quantity, and regional delocalization. To use hydrogen as an energy source, high hydrogen storage capacity is indispensable. Lots of materials for hydrogen storage have been reported. Among them, carbon-based materials such as carbon nanotube, graphene, and graphene oxide have recently been focused. Here we report the possibility of carbonized bamboo as a hydrogen storage storage because they have basically porous organic structure. The bamboos were treated at 800 °C, 900 °C, 1000 °C and 1100 °C for 24 hours. The pore size and hydrogen storage capacity of each sample was measured by N<sub>2</sub> and H<sub>2</sub> gas sorption up to 1.0 bar at 77 K. Hydrogen storage capacity is maximized when the sample treated at 900 °C, which reaches over 1 wt.% at 1 bar/77 K. The results showed that the bamboo, one of the blue carbons, has the possibility to be a hydrogen storage material.

### Keywords:

hydrogen storage; porous carbon materials; green carbon;

## Rapid synthesis of $\text{Sr}_3\text{SiO}_5:\text{Eu}^{2+}$ phosphors for white LED

이우철<sup>1</sup>, 류지승<sup>1</sup>, 정홍채<sup>1</sup>, 양현경\*<sup>1</sup>

<sup>1</sup>부경대학교, LED공학협동과정  
hkyang@pknu.ac.kr

### Abstract:

White light emitting diodes (WLEDs) have been widely attracted due to their high efficient power consumption and long life time. It considered as a replacement of conventional incandescent and fluorescent lamp for next generation. One of common method to generate white emission is converting blue emission to a longer emission. The commercial WLEDs are combining InGaN chip emitting blue and yellow phosphor such as YAG:Ce<sup>3+</sup>. A common way to fabricate phosphor is solid state reaction (SSR), which has a problem of long sintering time caused by requirement of a higher sintering temperature and a longer holding time. In order to overcome this problem, microwave-assisted sintering, which has a major strength of rapid heating, is proposed.

In this research, we have synthesized  $\text{Sr}_3\text{SiO}_5:\text{Eu}^{2+}$  phosphors by microwave-assisted sintering method. In order to characterize the effect of  $\text{Eu}^{2+}$  concentration,  $\text{Eu}^{2+}$  concentration range from 0.01 to 0.05 mol has been performed. We investigate the structural property by X-ray diffraction analysis (XRD), surface morphology by observing scanning electron microscope (SEM) and luminescent property by photoluminescence (PL).

### Keywords:

Microwave-assisted sintering, phosphor, LED

## 바텀애쉬를 이용한 다공성 발포체 제조 및 특성분석

이유진<sup>1</sup>, 양현경\*<sup>1</sup>

<sup>1</sup>부경대학교, 과학기술융합전문대학원, LED융합공학전공  
hkyang@pknu.ac.kr

### Abstract:

다공성 발포체는 기존의 치밀한 재료가 가지지 못하는 분리, 저장, 열 차단 등의 특성을 갖고 있기 때문에 필터, 흡음재, 단열재, 경량 구조재 등의 다양한 형태로 응용되는 소재 중 하나이다. 이러한 다공성 발포체의 물성은 기공의 크기, 형상, 기공율, 배향성 등의 소재의 기능에 영향을 주는 물성과 소재의 강도, 열충격 저항성과 같은 내구성 및 신뢰성에 영향을 주는 물성에 의해 결정된다. 한편 이러한 물성은 다공질 소재의 제조공정에 의해 영향을 받는다.

본 연구에서는 다양한 기공형성 방법 중 하나인 발포법을 이용하여 다공성 발포체를 제조하였다. 주 재료로는 화력발전소에서 발생하는 폐기물인 바텀애쉬를 이용하였고 첨가제로는 활성탄, 물유리, 과산화수소를 사용하여 기공을 형성하였다. 안정적인 지지체 형성을 위해 정량, 혼합, 발포 후 건조 과정을 통해 제작되었으며 탈취 효율 및 압축강도를 측정, 분석하였다. 이를 통해 친환경적이면서 우수한 성능을 갖는 소재로서의 활용 가능성을 기대 해 볼 수 있다.

### Keywords:

다공성 발포체, 바텀애쉬, 친환경 자재

## Dual-mode regulation of multicenter photoluminescence in a single-phased $\text{Ba}_9\text{Lu}_2\text{Si}_6\text{O}_{24}:\text{Bi}^{3+}, \text{Eu}^{3+}$ phosphor to realize white light/tunable emissions

정중현\*<sup>1</sup>, GUO Yue<sup>1</sup>, 서연우<sup>1</sup>, 최병춘<sup>1</sup>, 박성흠<sup>1</sup>  
<sup>1</sup>부경대학교 물리학과  
jhjeong@pknu.ac.kr

### Abstract:

Recently, phosphor materials have attained great achievement and progress in various fields, including solid-state lighting, optical temperature sensors, flat panel displays, solar cells, and optical biomarkers. As next-generation lighting devices, phosphor-converted white light-emitting diodes (w-LEDs) have received much more attention since w-LEDs provide extraordinary superiorities, such as low electric consumption, high electro-optical conversion efficiency, high brightness, good stability, fast response, and environmental friendliness.

In this work, we studied the multicentered photoluminescence characteristics and site engineering in a  $\text{Bi}^{3+}$  and  $\text{Eu}^{3+}$  co-doped  $\text{Ba}_9\text{Lu}_2\text{Si}_6\text{O}_{24}$  phosphor to realize white light/tunable emission for phosphor-converted w-LEDs. From the analyses of the crystal structure and luminescent spectra, we observed four discernible  $\text{Bi}^{3+}$  luminescent centers with peaks at  $\sim 363.3$ ,  $\sim 403.1$ ,  $\sim 437.7$ , and  $\sim 494.5$  nm. Energy transfer from Bi(I), Bi(II) and Bi(III) to Bi(IV) was manipulated by changing the excitation wavelength. For  $\text{Bi}^{3+}, \text{Eu}^{3+}$  co-doped BLSO phosphor, two simple strategies were described to obtain white light/tunable emissions one was to change the concentration of  $\text{Eu}^{3+}$  ions in the  $\text{BLSO}:0.07\text{Bi}^{3+}$  phosphor, and the other was to adjust the excitation wavelength. In addition, the configurational coordinate model was carried out to explain the energy decrease of the phonon-electron coupling effect.

### Keywords:

Dual-mode; Multicenter photoluminescence; White light/tunable emissions

## Color tunable phosphors of Europium doped in $\text{Sr}_{9-x}\text{La}_{1+x}(\text{PO}_4)_{7-x}(\text{SiO}_4)_x$

정중현\*<sup>1</sup>, 김도림<sup>1</sup>, 양은혜<sup>1</sup>, 김중환<sup>2</sup>  
<sup>1</sup>부경대학교 물리학과, <sup>2</sup>동의대학교 물리학과  
jhjeong@pknu.ac.kr

### Abstract:

The  $\text{Sr}_{9-x}\text{La}_{1+x}(\text{PO}_4)_{7-x}(\text{SiO}_4)_x$ :  $\text{Eu}^{3+}$  was synthesized via the conventional high temperature solid state method. The luminescence evolution in response to variation of crystal structure were discussed by using X-ray diffraction (XRD), Rietveld refinement, PL and PLE spectra and CIE coordination. As the value of  $x$  increase from 1 to 7, the crystal structure changed from whitlockite to apatite structure, and ligand bonding lengths between  $\text{Eu}^{2+}$  ion and  $\text{O}^{2-}$  ion are shortened due to the substitution of the smaller  $[\text{PO}_4]^{3-}$  tetrahedron by larger  $[\text{SiO}_4]^{4-}$  tetrahedron. In both of crystal structures, two kinds of europium sites are included. The peak positions of the PL bands radiated from  $\text{Eu}^{2+}$  ions shifted from 416 nm to 505 nm with increase of  $x$ . It is mainly attributed that  $\text{Eu}^{2+}$  ion prefer higher energy site than lower one in the whitlockite structure, however, vice versa in the apatite structure. The red PL radiated from  $\text{Eu}^{3+}$  ion became appeared due to the increase of the ratio of  $\text{La}^{3+}/\text{Sr}^{2+}$  with the increase of  $x$ . Under the excitation wavelength of a peak position of the  $\text{Eu}^{3+}$  charge transfer band or an absorption position of the transition radiation from  ${}^7\text{F}_0$  to  ${}^5\text{L}_6$  of  $\text{Eu}^{3+}$  ion, the PL spectra were tremendously changed. From measurement of CIE coordination, the series of the phosphors can be tuned from blue to red by adjusting the value of  $x$ , and a tunable phosphor covered full color can be achieved by adjusting the excitation wavelength.

### Keywords:

Tunable, Luminescence, pc-LEDs

## Regulation of lattice sites and fluorescence enhancement mechanism in Super Red Emission Phosphors: $\text{CdMoO}_4:\text{Eu}^{3+}$ , M (M= $\text{Li}^+$ , $\text{Na}^+$ , $\text{K}^+$ and Cd vacancy)

정중현\*<sup>1</sup>, RAN Weiguang<sup>1</sup>, 노현미<sup>1</sup>, 문병기<sup>1</sup>, 최병춘<sup>1</sup>  
<sup>1</sup>부경대학교 물리학과  
jhjeong@pknu.ac.kr

### Abstract:

$\text{Eu}^{3+}$  doped  $\text{CdMoO}_4$  super red emission phosphors with charge compensation were prepared by the traditional high temperature solid-state reaction method in air atmosphere. The interrelationships between photoluminescence properties and crystalline environments were investigated in detail. The 3D network structure which composed by  $\text{CdO}_8$  and  $\text{MoO}_4$  polyhedra can collect and efficiently transmit energy to  $\text{Eu}^{3+}$  luminescent centers. The relative distance between  $\text{Eu}^{3+}$  ions decreased and energy interaction increased sharply with the appearance of interstitial occupation of  $\text{O}^{2-}$  ions ( $\text{O}_i''$ ). Therefore, fluorescence quenching occurs at the low concentration of  $\text{Eu}^{3+}$  ions in the 3D network structure. Fortunately, the charge compensator will reduce the concentration of  $\text{O}_i''$  which can break the energetic interaction between  $\text{Eu}^{3+}$  ions. The mechanism of different charge compensators has been studied in detail. The strong excitation band situated at ultraviolet and near-ultraviolet region makes it a potential red phosphor candidate for n-UV based LED.

### Keywords:

Phosphors; Charge compensators; Enhancement mechanism;  $\text{CdMoO}_4$

## Mo<sup>6+</sup> substitution induced efficient near-UV-excited red emission in Gd<sub>2</sub>W<sub>1-x</sub>Mo<sub>x</sub>O<sub>6</sub>:Eu<sup>3+</sup> phosphors

정중현\*<sup>1</sup>, XUE Junpeng<sup>1</sup>, 노현미<sup>1</sup>, 박성흠<sup>1</sup>, 최병춘<sup>1</sup>, 김중환<sup>2</sup>  
<sup>1</sup>부경대학교 물리학과, <sup>2</sup>동의대학교 물리학과  
jhjeong@pknu.ac.kr

### Abstract:

A series of the Eu<sup>3+</sup>-activated Gd<sub>2</sub>W<sub>1-x</sub>Mo<sub>x</sub>O<sub>6</sub> phosphors were synthesized by a high-temperature solid-state reaction method. The phase composition, ultraviolet-visible diffuse reflectance spectra, photoluminescence and decay properties of the phosphors were investigated. Through adjusting the Mo<sup>6+</sup> ion concentration, the excitation band of **the studied sample was gradually** shifted to longer wavelength. Under the excitation of 376 nm light, the strong red emission at 610 nm and weak yellow emission centered at 591 nm were detected, indicating that Eu<sup>3+</sup> occupies non-inversion symmetry sites in the host lattices. With elevating the dopant concentration, the emission intensity of **synthesized products** was greatly enhanced and achieved its optimum value when  $x = 0.95$  which was 2.33 times higher than that of the Gd<sub>2</sub>WO<sub>6</sub>:Eu<sup>3+</sup> compounds. The quantum efficiency of **resultant samples** was as high as 76.1%. Moreover, the Judd-Oflet theory was used to study the local structure environment behaviors of the Eu<sup>3+</sup> ions in the host lattices. Finally, a red LED device, which consisted of a near-ultraviolet chip and prepared Gd<sub>2</sub>W<sub>0.05</sub>Mo<sub>0.95</sub>O<sub>6</sub>:Eu<sup>3+</sup> phosphors, was successfully fabricated. These results confirmed that the Eu<sup>3+</sup>-activated Gd<sub>2</sub>W<sub>1-x</sub>Mo<sub>x</sub>O<sub>6</sub> phosphors **red-emitting** phosphors have potential value as the red component for WLEDs.

### Keywords:

Rare-earth; Phosphor; Photoluminescence; WLEDs

## Influence of Pore-widening Processes on the Pore Morphology of Porous Anodic Alumina Membranes

부상돈\*<sup>1</sup>, 김선용<sup>1</sup>, 조삼연<sup>1</sup>, 김은영<sup>1</sup>  
<sup>1</sup>전북대학교, 물리학과  
sbu@chonbuk.ac.kr

### Abstract:

The size and shape of pore in the porous anodic alumina membranes (PAAMs) can be controlled by changing various experimental conditions such as anodizing time and electrolyte type. The ability to control the arrangement, size, and length of PAAM pores is effective in nanoscale device applications. PAAMs can also be used as a template for fabrication of nanostructures. In this study, PAAM is prepared in electrolytes of oxalic acid and phosphoric acid. We found the pore diameter of PAAM can be controlled from 30nm to 100nm. The pore-widening process is done in 10 wt% phosphoric acid solution. Through the pore-widening process, the size of the pore gradually increases with the time processing time, and the maximum pore sizes are 90nm and 450nm, respectively, in electrolytes of oxalic acid and phosphoric acid. When the pore-widening process is prolonged, the pore-structure collapses and becomes a form of alumina nanowires array. The advantage of the pore-widening process is that it can control pore size and remove impurities in pores. However, when the thickness of the PAAM is more than 10 $\mu$ m, there is a problem that the pore diameter of the top and bottom is different after the pore-widening process. We will discuss about the problem.

### Keywords:

Porous Anodic Alumina Membranes, Pore-widening Processes, Pore Morphology

## Fabrication and characterization of aligned mono-disperse Co nanocrystal periodic arrays

김중현<sup>1</sup>, 노도영\*<sup>1</sup>, 조인화<sup>1</sup>, 최정원<sup>1</sup>, 하성수<sup>1</sup>, 한승현<sup>1</sup>, 최석준<sup>1</sup>  
<sup>1</sup>광주과학기술원 물리학과  
dynoh@gist.ac.k

### Abstract:

Mono-disperse Co nanocrystals with aligned crystalline axis are fabricated by using the solid state dewetting of a periodic Co thin film array. We first fabricated a periodic Co thin film array by placing a SiN mask with 500nm nano-hole array on a c-plane sapphire substrate during the electron beam deposition. Thus fabricated thin film arrays were transformed to a nanocrystalline array through the solid state dewetting process during rapid thermal annealing(1050°C /10minute/two times). The crystalline axis of the Co nanocrystals was well aligned to the substrate crystalline direction as revealed in the x-ray diffraction data. We were able to control the dimension of the nanocrystals from 250 to 50 nm by adjusting the thickness of the thin films, and also by Ar ion milling of the nanocrystals followed by annealing. We expect that the array of aligned Co nanocrystals will facilitate the investigation of the change of crystalline properties during catalytic reactions.

### Keywords:

Cobalt , nanoparticle, periodic array, mono-disperse

## Thermionic emission type Cs<sup>+</sup> ion source

최대선<sup>\*1</sup>

<sup>1</sup>강원대학교 물리학과  
dschoi@kangwon.ac.kr

### Abstract:

The thermionic emission type Cs<sup>+</sup> ion source based on the  $\beta$ -eucryptite material was fabricated and investigated its emission characteristics. To investigate the emission characteristics of this specimen, the fine ground powder of this specimen is painted on the tungsten filament. This filament type Cs<sup>+</sup> ion source shows that it has no out-gassing even at ultra-high vacuum, high and stable ion beam current, high purity and long life time. Because of the simple ion emission process and the good emission characteristics this ion source can be applied to various fields.

### Keywords:

Cs<sup>+</sup> ion source, Thermionic emission, Fabricate

## Spin Seebeck effect of solution processed ferrimagnet insulator thin film, Yttrium Iron Garnet

유정우\*<sup>1</sup>, 오인선<sup>1</sup>, 박정민<sup>1</sup>, 조준현<sup>1</sup>, 진미진<sup>1</sup>, 최대성<sup>1</sup>  
<sup>1</sup>울산과학기술원 기계신소재 공학부  
jwyoo@unist.ac.kr

### Abstract:

Spin Seebeck effect, in combination with the Inverse Spin Hall Effect, can be applied directly for the conversion from heat to electric energy. Spin Seebeck thermoelectric generator allows new approaches toward the improvement of thermoelectric generation efficiency. In general, the conventional thermoelectric generator has the limitation of the efficiency due to the trade-off relation among Seebeck coefficient ( $S$ ), electrical conductivity ( $\sigma$ ), and thermal conductivity ( $k$ ). In contrast, the application of ferrimagnet insulator in Spin Seebeck effect has great advantages for enhancing thermoelectric efficiency. In particular, the input heat flux and generated charge currents flow in a perpendicular direction to each other so that it allows us to construct thermoelectric devices operating in more effective configuration.

Conventionally, Yttrium Iron Garnet (YIG) has been most widely used as a ferrimagnet insulator to extract the heat induced spin current. Until now, pulsed laser deposition and liquid phase epitaxy grown films on  $Gd_3Ga_5O_{12}$  substrate have been used for the study of Spin Seebeck effect. Here, we deposited the solution processed poly-crystalline YIG thin films by using spin coating and annealing methods. The roughness of film can be easily controlled down to  $\sim 0.2$  nm (5 $\mu$ m by 5 $\mu$ m). We observed the large signals of Spin Seebeck effect and Inverse Spin Hall effect inducing voltage in the solution processed poly-crystalline YIG/Pt hetero-structure. The estimated longitudinal spin seebeck coefficient is  $S = (\Delta V/L)/(\Delta T/Lz) \sim 70$  nV/K. Our experiments can provide the breakthrough of the large area and easy process fabrication of YIG thin films for the efficient energy conversion from heat induced spin currents into the charge currents.

### Keywords:

Spin Seebeck Effect, Ferrimagnet insulator, thin film

## Propagation dynamics of antiferromagnetic spiral soliton and application

김태현<sup>1</sup>, 한송희<sup>2</sup>, 조병기\*<sup>1</sup>

<sup>1</sup>광주과학기술원 신소재공학과, <sup>2</sup>목포해양대학교 항해학부  
chobk@gist.ac.kr

### Abstract:

The propagation dynamics of spin spiral in one-dimensional antiferromagnetic chain with easy-axis anisotropy have been demonstrated. The dynamic variable of describing propagation of spin spiral plays a role of plane pendulum with effective mass, and in this system, both oscillating frequency and potential barrier are modulated as a function of chain lengths. That means that spiral soliton could be quasi-particle in the potential well, or quasi-free particle as like domain wall. In the easy axis, the antiferromagnetic spiral can take two equilibrium states: symmetric and antisymmetric configuration that become stabilized into uniform and domain wall state when DM interaction is shut down. Using these analyses, we found that time dependent DM interaction is utilized to realize antiferromagnetic switching or domain wall creation.

### Keywords:

antiferromagnet, spiral structure, antiferromagnetic switching

## Electrical detection of spin-polarized local and non-local current in topological insulator $\text{Bi}_{1.5}\text{Sb}_{0.5}\text{Te}_{1.7}\text{Se}_{1.3}$

도용주\*<sup>1</sup>, 황태하<sup>1</sup>, 김홍석<sup>1</sup>, 박상일<sup>1</sup>, 김호일<sup>2, 3</sup>, 김준성<sup>2, 3</sup>

<sup>1</sup>광주과학기술원 물리광학과, <sup>2</sup>원자제어 저차원 전자계 연구단, IBS, <sup>3</sup>포항공과대학교 물리학과  
yjdo@gist.ac.kr

### Abstract:

Spin-momentum locked (SML) topological surface state (TSS) provides an exotic property for spintronics applications of topological insulators (TIs). The spin-polarized current due to SML can be directly detected using spin potentiometric measurement. In this report, we electrically measure spin polarization ratio of  $\text{Bi}_{1.5}\text{Sb}_{0.5}\text{Te}_{1.7}\text{Se}_{1.3}$  which is a low-doped topological insulator. Ferromagnetic Co contact was chosen intentionally to minimize interfacial band bending at the interface, at which the spin-dependent potentiometric measurement takes place. The spin voltage was measured as a function of the current bias, temperature, and gate voltage. We also report, for the first time in our best knowledge, a spin-potentiometric measurement using non-local spin-polarized current, which is unique property of TI. The polarization ratio is obtained to be  $p=0.036$  (0.183) for local (non-local) measurement, respectively. The higher spin polarization ratio obtained from the non-local current is attributed to reduction of bulk carrier contribution. Our observations provide highly enhanced way to determine spin-polarization ratio, which is inherent in the TSS in TI.

### Keywords:

topological insulator, spin-momentum locking, electrical spin detection, nonlocal

## Property of Three Helical Multi-turn $\mu$ -Coil and a PR Channel Combined with a Dual-type GMR-SV Device as Biosensor of Red Blood Cells

최종구<sup>1</sup>, 최상현<sup>1</sup>, 서재혁<sup>1</sup>, 이상석\*<sup>1</sup>

<sup>1</sup>상지대학교 한방의료공학과  
sslee@sangji.ac.kr

### Abstract:

The dual-type GMR-SV thin films and devices with three helical multi-turn  $\mu$ -coil and PR channel for detection of red blood cell (RBC) using ion-beam deposition system and lithography process were developed and used to one biosensor. Three different helical coils of Cu films were placed on the center of the GMR-SV with a width of 2  $\mu\text{m}$ . When the same dc current of 10 mA was applied to the coils of 2 turn, 3 turn, and 4 turn, the maximum magnetic flux density values at the center  $z = 0$ , which is perpendicular to the coil plane, were 1820  $\mu\text{T}$ , 2400  $\mu\text{T}$  and 3090  $\mu\text{T}$ , respectively. The magnetoresistance (MR) ratio of a dual-type GMR-SV device post-annealed at a temperature of 200  $^{\circ}\text{C}$  was 2.5 %, the magnetic field sensitivity (MS) was 0.6 %/Oe, and the coercivity ( $H_c$ ) was 0.5 Oe. An AC magnetic field was generated in the vertical direction at the center of GMR-SV device using a multi-turn  $\mu$ -coil. The magnetic beads (MB) coupled to the RBCs were controlled by the AC input current applied to a multi-turn  $\mu$ -coil, measured as output signal as MR variation during a staying time of 0.5 s in the GMR-SV device. When multiple magnetic beads adsorbed on the surface of red blood cells pass through a 8  $\mu\text{m}$  width of PR channel, the currents induced to the respective coils of three multi-turns are generated as an enough magnetic field to capture those. After stopping the red blood cells, there is a possibility that the output signal value of the GMR-SV device as biosensor can be detected. This result implies that the output signal of a dual-type GMR-SV device can analyze the detection state of the RBC passing through the center of a multi-turn  $\mu$ -coil and PR channel.

### Keywords:

biosensor, helical coil, PR channel, dual-type GMR-SV device, magnetoresistance ratio, magnetic sensitivity

## Nanoscale magnetic imaging based on diamond NV centers

이동현\*<sup>1</sup>, 이명원<sup>1</sup>  
<sup>1</sup>고려대학교 물리학과  
donghun@korea.ac.kr

### Abstract:

Nitrogen-Vacancy(NV) color center is an atomic scale quantum defect in diamond possessing unique properties for sensing and imaging applications. NV center is extremely sensitive to local magnetic field. Its atomic scale size enables imaging with high spatial resolution.

In this poster, we introduce basic concepts of magnetic sensing and imaging with diamond NV centers. We developed scanning probe microscopes based on NV centers to study nanoscale spin physics in condensed matters. We obtained magnetic field images in various samples such as hard disk and nanowires.

### Keywords:

nitrogen vacancy center, scanning probe microscopy

# Annealing Effects on Solution-Processed P-type $\text{Cu}_x\text{O}$ and Its Performance as Channel Layer in TFT and $\text{Cu}_x\text{O}/\text{VO}_2$ Heterojunction Devices

ABBAS Muhammad Sabbtain<sup>1</sup>, 강대준\*<sup>1</sup>

<sup>1</sup>성균관대학교 물리학과  
dj kang@skku.edu

## Abstract:

Solution-processed oxide semiconductors have become essential components in electronic devices owing to their excellent electrical performance, easy control of the composition ratio, roll-to-roll capability and low cost. Here in this study, simple sol-gel spin coating method was used to synthesize  $\text{Cu}_x\text{O}$  thin films on  $\text{SiO}_2/\text{Si}$  substrates and were post-annealed in air, vacuum and (95% $\text{N}_2$ +5% $\text{H}_2$ ) environment at various temperatures (200-600 °C). The improvement in structure, morphology and channel layer performance was investigated as a function of annealing conditions. X-ray diffraction analysis reveals the reduction of  $\text{CuO}$  to  $\text{Cu}_2\text{O}$  at high annealing temperature whereas AFM images indicate the increase in the roughness and average grain size at high temperature. The electrical performance of  $\text{Cu}_x\text{O}$  as semiconducting channel layer was explored in both TFTs and  $\text{Cu}_x\text{O}/\text{VO}_2$  heterojunction devices. Improved performance was achieved in both types of devices at high temperature. These results propose the use of high performance solution-processed  $\text{Cu}_2\text{O}$  as channel layer in both TFTs and FETs as advanced step towards further improvement in low cost electronic devices.

## Keywords:

$\text{VO}_2$ , Annealing effects,  $\text{Cu}_x\text{O}$ , p-n Heterojunction

## Uncertainty Analysis of In- and Out-of-Plane Thermal Conductivities of p-Bi<sub>0.5</sub>Sb<sub>1.5</sub>Te<sub>3</sub> Thin Films by Changing Heater Widths in the Four-Point-Probe

이상권\*<sup>1</sup>, 윤희섭<sup>1</sup>, 이원용<sup>1</sup>, 박노원<sup>1</sup>, 김길성<sup>1</sup>, 강수영<sup>1</sup>, 석주희<sup>1</sup>, THI Thu Bui Trang<sup>1</sup>

<sup>1</sup>중앙대학교 물리학과  
sangkwonlee@cau.ac.kr

### Abstract:

For increasing the figure of merit (ZT) of thin-film thermoelectric (TE) devices, reduction of thermal conductivity is one of the most effective strategies. Recently, thin-film structures using Bi-Sb-Te TE materials attracted significant attention because of their low thermal conductivity and anisotropic thermal properties. The four point-probe three omega ( $3-\omega$ ) method is the most widely used technique to measure the thermal conductivity of various dimensional materials, including 1D nanostructures, 2D-thin films, and 3D-bulk materials, because it provides a simple measurement setup and high accuracy (less than  $\sim 10\%$ ) for the measurement. In addition, it was confirmed that both out-of-plane and in-plane thermal conductivities of thin films can be measured by altering the width of the heater on the films and by using a proper substrate underneath the films in the  $3-\omega$  method. Here, we first report an uncertainty analysis of both the out-of-plane and in-plane thermal conductivities of 500-nm-thick p-Bi<sub>0.5</sub>Sb<sub>1.5</sub>Te<sub>3</sub> (p-BST) thin films, which were prepared on a SiO<sub>2</sub>/Si substrate and measured by the four-point-probe  $3-\omega$  method at room temperature, by varying the width of the heater on the substrates. From the uncertainty calculations, reasonable in- and out-of-plane thermal conductivities of p-BST thin films in the  $3-\omega$  method were estimated with lower measurement error. The results suggest that the heater widths are strongly related to both in- and out-of-plane thermal conductivities in the measurement. The corrected out-of-plane and in-plane thermal conductivities of the 500-nm-thick thin films were  $\sim 0.43 \pm 0.02 \text{ W m}^{-1} \text{ K}^{-1}$  and  $\sim 0.61 \pm 0.05 \text{ W m}^{-1} \text{ K}^{-1}$ , respectively, at room temperature.

### Keywords:

Bismuth Antimony Telluride (Bi<sub>0.5</sub>Sb<sub>1.5</sub>Te<sub>3</sub>),  $3-\omega$  Technique, Thermal Conductivity, Uncertainty Analysis.

## Study of chemical enhancement mechanism of non-plasmonic Surface enhanced Raman Spectroscopy (SERS)

윤석현\*<sup>1</sup>, 김자영<sup>1</sup>, 김남중<sup>2</sup>, 박준범<sup>2</sup>, 김혜민<sup>1</sup>, 이규철<sup>2</sup>, 김예진<sup>1</sup>  
<sup>1</sup>이화여자대학교 물리학과, <sup>2</sup>서울대학교 물리학과  
syoon@ewha.ac.kr

### Abstract:

Surface enhanced Raman spectroscopy (SERS) has been intensively studied during the past decades for its enormous enhancement of signal near the nanoscale metallic surfaces. There are two mechanisms of SERS. One is electromagnetic mechanism that involves surface plasmonic resonance and the other is material specific chemical enhancement that involves charge transfer between substrates and analytes. Despite intensive research efforts, chemical enhancement of remains elusive mainly due to the relatively complex enhancing factors and inconsistent experimental results. We used high-quality ZnO nanostructures/graphene substrates to provide an ideal SERS environment and to understand the charge transfer (CT) mechanisms of SERS. We report the optimal conditions for CT processes that is found to be directional. We also present the characteristic length scale of charge transfer by introducing atomically thin HfO<sub>2</sub> layers between substrates and analytes and by monitoring SERS signals as a function of spacing between the molecules and the semiconductor surface.

### Keywords:

surfaced-enhanced Raman scattering, chemical enhancement, charge transfer, ZnO nanostructures, quantum tunneling

## Improvement of ferroelectricity in SrMnO<sub>3</sub> thin films via annealing process

윤창재<sup>1</sup>, 손영준<sup>1</sup>, 이성수<sup>1</sup>, 이종민<sup>1</sup>, 박정웅<sup>2</sup>, 이상한<sup>1</sup>, 조지영\*<sup>1</sup>

<sup>1</sup>School of Materials Science and Engineering, Gwangju Institute of Science and Technology,

<sup>2</sup>Department of Electrical Engineering, Gachon University

jjjo@gist.ac.kr

### Abstract:

The SrMnO<sub>3</sub> is a promising candidate for the multi-state device because it was predicted to have a phase transition from paraelectricity to ferroelectricity. According to first-principle calculation, the ferroelectricity has been reported when more than 1% tensile strain was applied.[1] Recently, the noncentrosymmetric phase of SrMnO<sub>3</sub> was observed through the second harmonic generation experiment.[2] However, ferroelectricity has not yet been experimentally measured because it is difficult to probe the electrical characteristics of the SrMnO<sub>3</sub> due to the high leakage current. According to previous studies, leakage current occurs due to the formation of oxygen vacancies at the interface between metallic substrate and SrFeO<sub>3</sub> which has similar structure as that of the SrMnO<sub>3</sub>. [3] The oxygen vacancies accumulate at the interface between SrMnO<sub>3</sub> and metallic electrode, i.e., La<sub>0.7</sub>Sr<sub>0.3</sub>MnO<sub>3</sub>. The amount of oxygen vacancies can be reduced through annealing process.[4]

The SrMnO<sub>3</sub> films were deposited onto La<sub>0.7</sub>Sr<sub>0.3</sub>MnO<sub>3</sub> (LSMO) / (001)-oriented PMN-PT substrate using pulsed laser deposition (PLD). The crystallinity of film was investigated using X-ray diffraction. The roughness of the film was investigated using an atomic force microscopy (AFM). Leakage current and oxygen vacancies were investigated through I-V curve and X-ray photoelectron spectroscopy (XPS), respectively.

[1] J. Lee and K. Rabe, Physical Review Letter, 2010, **104**, 207204

[2] Carsten Becher *et al.*, Nature Nanotechnology, 2015, **10**, 661-665

[3] Erik Enriquez *et al.*, Scientific Reports, 2016, **7**, 46184

[4] Jiawei Bai *et al.*, Thin Solid Films, 2017, **644**, 57-64

### Keywords:

SrMnO<sub>3</sub>, ferroelectricity, electrical property, annealing process, oxygen vacancy

## High quality silver thin film growth on ZnO thin film

정세영\*<sup>3</sup>, 천미연\*<sup>2</sup>, 정보광<sup>1</sup>

<sup>1</sup>부산대학교 인지메카트로닉스 공학과, <sup>2</sup>단결정 은행 연구소, <sup>3</sup>부산대 광메카트로닉스 공학과  
syjeong@pusan.ac.kr, mycheon@pusan.ac.kr

### Abstract:

은( $1.63\mu\Omega\text{cm}$ )은 구리( $1.72\mu\Omega\text{cm}$ )보다 더 낮은 비저항 값을 가지는 금속이다. 그러나 박막을 성장함에 있어서 표면의 grain boundary에 의해 전자들의 산란이 일어나 비저항의 값을 증가시키며 은의 가장 뛰어난 특성인 plasmonics 효율의 감소시킨다. 또한 이 grain boundary의 사이로 산소가 침투하여 박막의 산화를 촉진 시킨다. 이러한 문제를 해결하기 위해 오래전부터 많은 사람들이 단결정 은 박막을 성장을 시도해왔다. 단결정 은을 성장 시키는 방법으로는 czochralski 방법 또는 화학적 방법을 많이 이용한다. 그러나 이러한 방법들은 높은 고온과 비용들이 필요하며 화학적 방법은 마이크로 크기라는 한계가 존재한다. 본 실험은 이러한 단점들이 없는 RF-sputtering 방식을 사용하여 대면적으로 단결정에 매우 가까운 은 박막을 성장 하였다.  $\text{Al}_2\text{O}_3$  기판 위 (001) 방향성을 가진 ZnO 박막을 중간층으로 이용하여 은 박막을 성장하였고, 은 박막은 XRD, SEM, EBSD, AFM 및 반사도를 조사하였다. 중간층으로 사용된 ZnO 박막의 영향으로 기판과 은 박막의 접착력은 매우 향상되었으며 성장된 은 박막은 grain boundary 급격한 감소가 보이며 (111)면 방향으로 성장이 되었고 표면 거칠기는 1nm보다 작은 값을 나타내었다.

### Keywords:

silver, RFsputtering, thin film

## Influence of oxygen partial pressure on the ratio of $\text{Eu}^{3+}/\text{Eu}^{2+}$ and photoluminescence properties of $\text{SrLaMgTaO}_6$ double perovskite thin films

오주현<sup>1</sup>, 정번성<sup>1</sup>, 김동훈<sup>1</sup>, 정중현\*<sup>1</sup>, 배종성<sup>2</sup>, 김희진<sup>3</sup>, 김중환<sup>4</sup>, 장서형<sup>5</sup>

<sup>1</sup>부경대학교 물리학과, <sup>2</sup>한국기초과학지원연구원 부산센터, <sup>3</sup>한국기초과학지원연구원 전자현미경연구부, <sup>4</sup>동의대학교 물리학과, <sup>5</sup>중앙대학교 물리학과  
jhjeong@pknu.ac.kr

### Abstract:

We deposited  $\text{Eu}^{3+}$  doped  $\text{SrLaMgTaO}_6$  (SLMTOE) thin films on  $\text{SrTiO}_3$  (100), using pulsed laser deposition, and investigated the dependence of the structural and photoluminescence (PL) properties on the oxygen partial pressure. The X-ray diffraction patterns were examined to determine the growth behaviors of the SLMTOE films on the  $\text{SrTiO}_3$  (100) substrates. Under the oxygen partial pressure below 100 mTorr, the SLMTOE films deposited on the  $\text{SrTiO}_3$  (100) substrate were aligned out of the substrate plane, whereas, at the high oxygen partial pressure, those did not. The PL spectra revealed that the red emission peak at 613 nm was strongest at the oxygen partial pressure of 100 mTorr, and the emission peak intensity decreased with increasing the oxygen partial pressure. Further, X-ray photoelectron spectroscopy (XPS) analysis indicated the content of  $\text{Eu}^{3+}$  ion decreases with increasing oxygen partial pressure, whereas those of  $\text{Eu}^{2+}$  ion increases.

### Keywords:

Double perovskite, Photoluminescence, Thin Film

## Experimental observation of $\text{BaFe}_2(\text{PO}_4)_2$ powder and thin films for quantum anomalous hall effect.

정중현\*<sup>1</sup>, 장서형\*<sup>4</sup>, 정번성<sup>1</sup>, 김동훈<sup>1</sup>, 오주현<sup>1</sup>, 최병춘<sup>1</sup>, 배종성<sup>2</sup>, 김봉주<sup>3</sup>

<sup>1</sup>부경대학교 물리학과, <sup>2</sup>한국 기초 과학 지원 연구원 부산센터, <sup>3</sup>기초 과학 연구원 강상관계 물질 연구단, <sup>4</sup>중앙대학교 물리학과

jyjeong@pknu.ac.kr, cshyoung@cau.ac.kr

### Abstract:

Recently, some theoretical studies predict  $\text{BaFe}_2(\text{PO}_4)_2$  and related materials can exhibit intriguing physical properties, e.g., two-dimensional Ising ferromagnetic behavior and quantum anomalous Hall effect. Here, we made  $\text{BaFe}_2(\text{PO}_4)_2$  powders and made thin films using this. And we will discuss the  $\text{BaFe}_2(\text{PO}_4)_2$  powders and thin films with structures and physical properties. We analyzed the detailed structure of  $\text{BaFe}_2(\text{PO}_4)_2$  powders and thin films by using x-ray diffraction and Rietveld refinement. We also studied whether each elements exists by using x-ray photoelectron spectroscopy. We also discuss the physical properties of  $\text{BaFe}_2(\text{PO}_4)_2$  powders and thin films.

### Keywords:

magnetic, film, Hall effect

## Effect of Oxygen deficient on electronic and structural properties of $\text{LaNiO}_{3-x}$ Films on $\text{SrTiO}_3$ (001) Substrates by Pulsed Laser Deposition

정중현\*<sup>1</sup>, 배종성<sup>2</sup>, 김희진<sup>3</sup>, 장서형\*<sup>4</sup>, 김동훈<sup>1</sup>, 정번성<sup>1</sup>, 최병춘<sup>1</sup>, 오주현<sup>1</sup>

<sup>1</sup>부경대학교 물리학과, <sup>2</sup>기초과학지원연구원 부산센터, <sup>3</sup>기초과학지원연구원 전자현미경연구부, <sup>4</sup>중앙대학교 물리학과

jyjeong@pknu.ac.kr, cshyoung@cau.ac.kr

### Abstract:

$\text{LaNiO}_3$  is widely used as an electrode in oxide devices due to low resistivity. In stoichiometric bulk  $\text{LaNiO}_3$ , the Ni ion assumes the  $3^+$  oxidation state, while oxygen deficiency can result in the creation of  $\text{Ni}^{2+}$  ions, significantly lead to high resistivity. We expected that reducing oxygen deficiency lead to the increasing of  $\text{Ni}^{3+}$  oxidation state ratio. Here, we investigate the structural and electronic properties of epitaxial  $\text{LaNiO}_{3-x}$  films on  $\text{SrTiO}_3$  (001) substrates by using pulsed laser deposition. We systematically changed the oxygen partial pressure and growth temperature for controlling the amount of oxygen vacancies in the films. By using x-ray scattering and x-ray photoemission studies, we found that the out-of-plane lattice parameters and the stoichiometric  $\text{Ni}^{3+}$  states are very sensitive to the change of the oxygen partial pressure during the growth. We will also discuss the conductivity and the activity of non-stoichiometric  $\text{LaNiO}_{3-x}$  films.

### Keywords:

thin film, oxygen deficient, electronic property

## 알루미늄 표면에 대한 징케이트 처리 효과

이연승\*<sup>2</sup>, 나사균<sup>1</sup>

<sup>1</sup>한밭대학교, 신소재공학과, <sup>2</sup>한밭대학교, 정보통신공학과  
yslee@hanbat.ac.kr

### Abstract:

Al-Finish층에 무전해 도금 기술의 도입은 MOSFET의 전력손실 최소화 및 소자 실장의 안정성을 위해 매우 중요한 기술이다. Al-Finish된 wafer Level Back-End 소자를 Au, Cu Clip으로 Clip 본딩을 적용하는 Clip Bonding 기술에 있어, 일반적으로 무전해 Au 및 무전해 Cu와 같은 무전해 도금 층으로 솔더링 전극면을 형성하여 사용한다.

Al Pad상에 무전해 도금된 금속과의 adhesion을 향상시키기 위해서, Al pad에 대한 backend의 활성화 처리 단계가 매우 중요하게 된다. 최근 Al pad에 대한 backend의 활성화 처리 단계로서의 Zincate 솔루션 공정이 사용되고 있지만, 강산, 강염기성 솔루션에 취약한 박막형 Al Pad에 있어, Al의 부식이나 Lift-off 문제가 여전히 남아있다.

본 연구에서는 Al Pad상에 무전해 도금된 금속과의 adhesion을 향상시키기 위하여, Zincate-Desmut를 이용한 전처리 단계에 있어, Al 기판을 이용하여 Zincate solution의 pH, 온도, 처리시간 등의 변화를 주어 Al기판의 표면 변화를 연구하였다. Field Emission Scanning Electron Microscope (FE-SEM), Optical microscope(OM), X-ray Photoelectron Spectroscopy(XPS), 등을 사용하여 Zincate-Desmut 조건에 따른 Al 기판의 표면을 분석하였다.

### Keywords:

Zincate, Desmut, Aluminium, Surface Analysis

## Phase correction of thin film spectroscopic measurement by the Kramers-Kronig relations in THz time-domain spectroscopy

김재훈\*<sup>1</sup>, 심경익<sup>1</sup>, 정택선<sup>1</sup>, 이호원<sup>1</sup>, 김종현<sup>1</sup>, 조영찬<sup>1</sup>, 김장원<sup>1</sup>, 이지은<sup>1</sup>, 김재하<sup>1</sup>  
<sup>1</sup>연세대학교, 물리학과  
super@yonsei.ac.kr

### Abstract:

With the THz time-domain spectroscopy (THz-TDS) technique, the electric field can be obtained as a function of time so that one can acquire the power and phase spectra by discrete Fourier transformation. In contrast with other power measurement techniques, the THz-TDS technique makes it possible to acquire phase information as well for analysis of the complex optical constants without the Kramers-Kronig relations. However, especially in thin film measurement, if there is a source fluctuation, or if the thickness of a substrate cannot be precisely determined, a phase error is unavoidable. Optical constants such as complex refractive index, complex permittivity, and complex conductivity all satisfy the Kramers-Kronig relations due to causality. Therefore, we can correct the phase error by using the Kramers-Kronig relation between the real and imaginary conductivities.

### Keywords:

Terahertz spectroscopy, Thin film, Phase correction, Kramers-Kronig relations

## Self-Assembly of $(C_6H_5CH_2CH_2NH_3)_2MnCl_4$ Perovskite Thin Films using Spin Coating Techniques : Effect of Polar and Nonpolar Solvents

박가람<sup>1, 2</sup>, 오인환<sup>1</sup>, 홍창섭<sup>2</sup>, 김기연\*<sup>1</sup>

<sup>1</sup>한국원자력연구원 중성자과학연구부, <sup>2</sup>고려대학교 화학과  
kykim3060@kaeri.re.kr

### Abstract:

Two-dimensional layered organic-inorganic halide perovskites (2d-OIHP) with chemical formula  $A_2BX_4$  (A: organic cation such as  $C_6H_5(CH_2)_nNH_3^+$ , B: divalent metal cation such as  $Pb^{2+}$ ,  $Sr^{2+}$ ,  $Cu^{2+}$ ,  $Mn^{2+}$ , X: halogen anion such as  $I^-$ ,  $Cl^-$ ,  $Br^-$ ) offer a wide variety of novel functionality such as solar cells and optoelectronic devices and magnetism. Structural flexibility of organic layer makes it possible to prepare single crystal-like 2d-OIHP thin films using solution-based process such as spin coating and dipping technique (intercalation). [1] Great care should be taken for choosing the kind of solvent depending on spin coating or dip coating. Intercalation method prefers nonpolar solvent to polar solvent because polar solvent causes charge screening and inhibits the hydrogen bond formation between ammonium group and halogen cation during intercalation.[2] Meanwhile, in case of spin coating, solvent is required to dissolve not only organic but also inorganic precursors without any chemical precipitates. Therefore, solubility should be considered with first priority. It has been well-known that the solubility is proportional to the dielectric constant of the solvent. [3,4] We prepared  $(C_6H_5(CH_2)_2NH_3)_2MnCl_4$  (abbreviated as Mn-PEA) perovskite thin films on top of Si wafer using spin coating technique with a total of eight polar and nonpolar solvents as follows: (1) Dichloromethan(polar, aprotic) and (2) Acetone(polar, aprotic) and (3) Methanol (polar protic) and (4) Acetonitrile (polar aprotic) and (5) Hexane(nonpolar) and (6) Benzene(nonpolar) and (7) Diethylether(nonpolar) and (8) Chloroform(nonpolar). It should be pointed out that the other preparation parameters such as solution volume/concentration and substrate and spin coating speed and spinning time are fixed the same. From a combination of x-ray diffraction and scanning electron microscopy images, it is found that protic polar solvent with high dielectric constant, that is Methanol, is the most preferable for self-assembly of two-dimensional layered Mn-PEA perovskite thin films.

### References

- [1] D. B. Mitzi, Chem. Mater. **13**, 3283 (2001).
- [2] S. Ahmad, et. al., ACS Appl. Mater. Interfaces **6**, 10238(2014).
- [3] R. D. Whealy, et. al., J. Am. Chem. Soc. **81**, 5900 (1959).
- [4] S. Zhang, et. al., Materials **3**, 3385 (2010).

### Keywords:

Organic-Inorganic Perovskites, Thin Films, Spin Coating, Dip Coating

## RBS 측정을 이용한 미량 원소 분석법

석재권\*<sup>1</sup>, 김민영<sup>1</sup>, 하준목<sup>1</sup>, 이승호<sup>2</sup>, 하상민<sup>1</sup>, 전해란<sup>1</sup>, 김계령<sup>1</sup>, 조용섭<sup>1</sup>

<sup>1</sup>한국원자력연구원 경주양성자가속기연구센터, <sup>2</sup>아나스연구소  
jksuk@kaeri.re.kr

### Abstract:

Rutherford Backscattering Spectrometry (RBS)는 단일 에너지의 알파입자를 시료 표면에 입사시키고 뒤튀겨져 나오는 알파입자의 에너지를 측정하여 시료의 조성 및 두께 정보를 알 수 있는 측정법이다. 이 측정법은 비파괴 분석이고 정량 분석이 가능하다는 장점이 있다. 이 분석 시스템은 한국원자력연구원 양성자가속기연구센터에서 설치되어, 2017년 10월부터 분석 서비스를 시행하고 있다. 본 발표에서 측정된 결과는 모두 양성자가속기연구센터에서 측정된 결과이다.

RBS는 주로 박막의 조성 및 두께를 알아보기 위하여 측정한다. 단일층 박막(Pt/Si substrate)시료 및 다층박막(Co/Pt/SiO<sub>2</sub>/Si substrate)의 시료의 RBS 측정결과를 발표할 예정이다. 단일층 박막의 경우는 특이사항 없이 분석이 가능했으나, 다층박막의 경우는 미량 원소가 존재하여 분석에 보정이 필요했다. 미량원소로 추정 가능한 것은 증착시 생성될 수 있는 C, N, O, H등이 있다. 이 미량원소들을 분석하기 위하여 resonant scattering 방법을 사용하였다. 이 분석법은 알파입자의 에너지가 특정에너지를 가질 때, 특정 타겟 원소에 대한 산란단면적이 커지는 현상을 말한다. 이 분석법으로 분석한 결과를 이번 추계물리학회에서 발표하고자 한다.

### Acknowledgement

This work has been supported through National Research Foundation of Korea (NRF) (No. 2017M2A2A6A01071289) and KOMAC (Korea Multi-purpose Accelerator Complex) operation fund of KAERI by MSIT (Ministry of Science and ICT).

### Keywords:

Rutherford Backscattering Spectrometry, thin film, resonant scattering

## 1.7 MV 탄뎀 가속기의 외기 PIXE 빔라인 설계 및 구축

하준목\*<sup>1</sup>, 이승호<sup>2</sup>, 김계령<sup>1</sup>, 석재권<sup>1</sup>, 김민영<sup>1</sup>, 전해란<sup>1</sup>, 하상민<sup>1</sup>, 조용섭<sup>1</sup>

<sup>1</sup>한국원자력연구원 양성자가속기연구센터, <sup>2</sup>아나스연구소  
jmha@kaeri.re.kr

### Abstract:

PIXE(Particle/Proton Induced X-ray Emission) 분석 기술은 수 MeV 정도의 에너지로 가속된 입자빔을 시료에 조사하고 조사 후 시료로부터 나오는 특성 X-선을 분석하여 시료를 정성, 정량 분석할 수 있는 기술이다. 파리 루브르 박물관에서는 1989년도부터 탄뎀 가속기를 자체 보유하여 문화재 복원 및 보존처리를 위해 PIXE 분석기법을 활용해오고 있으며, 한국원자력연구원 양성자가속기연구센터에서도 차후 문화재 복원 및 보존처리 활용 목적으로 기존 PIXE 빔라인을 외기 PIXE 빔라인으로 업그레이드 중에 있다. 진공챔버 내에서 시료를 측정 및 분석하는 기존 PIXE는 시료의 교체 시간이 길고, 액체, 분말, 문화재와 같은 대형 시료는 측정이 어렵다는 단점을 가진다. 반면 입자빔만을 가속기에서 빔창(beam window)을 통해 대기중으로 인출하여 시료를 진공 밖에서 조사/분석하는 외기 PIXE 분석기술은 기술의 특성상 기존 PIXE의 문제점 극복 및 문화재, 미세먼지와 같은 대형, 분말 시료 분석이 용이하다. 이를 위해 양성자가속기연구센터 내 외기 PIXE 빔라인 개발이 이루어졌으며, 이번 학회에서 이 외기 PIXE 빔라인에 대한 설계 및 구축 내용을 발표하고자 한다.

### Acknowledgement

This work has been supported through National Research Foundation of Korea (NRF) (No. 2017M2A2A6A01071289) and KOMAC (Korea Multi-purpose Accelerator Complex) operation fund of KAERI by MSIT (Ministry of Science and ICT)

### Keywords:

외기 PIXE, 탄뎀가속기, 문화재

## Probing the effect of relative molecular orientation on the photovoltaic device performance of an organic bilayer heterojunction using soft x-ray spectroscopies

정지윤<sup>1</sup>, 박민규<sup>1</sup>, 박준호<sup>1</sup>, 강희재<sup>1</sup>, 정현경<sup>1</sup>, 조상완\*<sup>1</sup>, SMITH Kevin<sup>2</sup>  
<sup>1</sup>연세대학교 물리학과, <sup>2</sup>Department of Physics, Boston University  
dio8027@yonsei.ac.kr

### Abstract:

The orientation of the constituent molecules in organic thin film devices can affect significantly their performance due to the highly anisotropic nature of  $\pi$ -conjugated molecules. We report here an angle dependent x-ray absorption study of the control of such molecular orientation using well-ordered interlayers for the case of a bilayer heterojunction of chloroaluminum phthalocyanine (ClAlPc) and C<sub>60</sub>. Furthermore, the orientation-dependent energy level alignment of the same bilayer heterojunction has been measured in detail using synchrotron radiation-excited photoelectron spectroscopy. Regardless of the orientation of the organic interlayer, we find that the subsequent ClAlPc tilt angle improves the  $\pi$ - $\pi$  interaction at the interface, thus leading to an improved short-circuit current in photovoltaic devices based on ClAlPc/C<sub>60</sub>. The use of the interlayers does not change the effective band gap at the ClAlPc/C<sub>60</sub> heterointerface, resulting in no change in open-circuit voltage.

### Keywords:

synchrotron-radiation, organic semiconductors, x-ray absorption spectroscopy, photoemission, ClAlPc, PTCD, pentacene

# Hole injection enhancement with molecular p-doping of thermally-evaporated Li-TFSI into *N,N'*-Di(1-naphthyl)-*N,N'*-diphenyl-(1,1'-biphenyl)-4,4'-diamine in organic light-emitting diodes

김기웅<sup>1</sup>, 정준경<sup>1</sup>, 김민주<sup>1</sup>, 강동희<sup>1</sup>, 이현복<sup>2</sup>, 이연진\*<sup>1</sup>

<sup>1</sup>Institute of Physics and Applied Physics and van der Waals Materials Research Center, Yonsei University, <sup>2</sup>Department of Physics, Kangwon National University  
yeonjin@yonsei.ac.kr

## Abstract:

Bis(trifluoromethane)sulfonimide lithium salt (Li-TFSI) has been widely employed as a p-dopant in perovskite solar cells and dye-sensitized solar cells to increase the conductivity of the hole transport materials (HTMs). Through tuning electrical properties of HTMs, it not only increases the hole concentration in the HTMs but also improves the hole mobility, which evidently explains the enhancement in the device performance. However, the extremely hygroscopic property of Li-TFSI in ambient air leads to the formation of pinholes deteriorating the device performance. Thus, the thermal evaporation at ultrahigh vacuum is required to fabricate the film reliably and to control the thickness of each layer easily for efficient multi-layer devices.

In this study, to understand the working mechanism of Li-TFSI doping, ultraviolet photoelectron spectroscopy was performed on Li-TFSI and *N,N'*-Di(1-naphthyl)-*N,N'*-diphenyl-(1,1'-biphenyl)-4,4'-diamine (NPB), which is generally used as a HTM in organic light-emitting diodes (OLEDs). The changes of hole injection were also measured on Li-TFSI doped NPB film with the different doping ratios. The hole-only devices and OLEDs were then fabricated to confirm the doping effect of thermally evaporated Li-TFSI in NPB. The reduction of hole injection barrier and the changes in the doping efficiency with different doping ratios will be discussed.

## Keywords:

molecular doping, Li-TFSI, thermal evaporation, ultraviolet photoelectron spectroscopy, hole injection barrier

## Iterative Electrostatic Model Calculation for Energy Level Alignment at Metal/Semiconductor Interface

현경호<sup>1</sup>, 이현복<sup>\*2</sup>, 이연진<sup>\*1</sup>

<sup>1</sup>Institute of Physics and Applied Physics and van der Waals Materials Research Center, Yonsei University, <sup>2</sup>Department of Physics, Kangwon National University  
hyunbok@kangwon.ac.kr, yeonjin@yonsei.ac.kr

### Abstract:

The energy level alignment at interfaces across the whole device structure is a critical factor for the performance of (opto)electronic devices. Especially, energy barrier between metal/semiconductor interfaces have an important role with regard to the carrier injection or extraction dynamics. Recently, electrostatic model with numerical iterative method for calculating the energy level alignment was reported and compared with corresponding experimental results [1,2]. We reproduce this simulation to apply various cases of organic/inorganic semiconductors and investigate the effect of the electronic structure and barrier height inside the devices. We expect that this simulation be helpful to understand the electronic structure at the interfaces under the thick layer and consequentially to optimize the real device performance.

[1] M. Oehzelt, N. Koch and G. Heimel, Nat. Commun. **5**, 4174 (2014)

[2] J. -P. Yang, L. -T. Shang, F. Bussolotti et al., Org. Electron. **48**, 172 (2017)

### Keywords:

energy level alignment, electronic structure

## Fermi level pinning energy changing of Poly(3-hexylthiophene-2,5-diyl) via pi-stacking orientations controlled by different solution processes

정준경<sup>1</sup>, 유지수<sup>1</sup>, 박수형<sup>1</sup>, 이현복\*<sup>2</sup>, 김용성<sup>3</sup>, 이연진\*<sup>1</sup>

<sup>1</sup>Institute of Physics and Applied Physics, and van der Waals Materials Research Center, Yonsei University, 50 Yonsei-ro, Seodaemun-gu, Seoul, 03722, Republic of Korea, <sup>2</sup>Department of Physics, Kangwon National University, 1 Gangwondaehak-gil, Gangwon-do, 24341, Republic of Korea, <sup>3</sup>Korea Research Institute of Standards and Science and Department of Nano Science, University of Science and Technology, Daejeon 34113, Republic of Korea  
hyunbok@kangwon.ac.kr, yeonjin@yonsei.ac.kr

### Abstract:

In organic devices, contacts between metal electrodes and organic materials are significant impact on the device performance. As charge carriers are injected or extracted through metal electrodes forming metal-organic interfaces, the energy level alignment of metal-organic interfaces is an important part of organic electronics. There have been some models to explain the energy level alignment of metal-organic interfaces [1-2]. In these reports, the organic work function is determined by substrate metal work function in case of the Mott-Schottky regime. And if the metal work function is larger than the organic ionization energy or smaller than the organic electron affinity, the work function is pinned to specific energy. However, the pinning energy can be changed even in the same pair of metal work function and organic material without further chemical interactions when organic molecules accumulate in different direction. The orientation effect of small molecules with a high symmetric shape have been studied showing their electronic structures are not the same [3].

In this work, we shows a polymer orientation effect on the electronic structure. Polymer stack orientation can be controlled by spincoating and vacuum-electrospray deposition (VESD). For regioregular-poly(3-hexylthiophene-2,5-diyl) (P3HT), they accumulate in vertical or horizontal directions via spin coating or VESD respectively. The polymer orientation were checked by Grazing-Incidence Wide Angle X-ray Scattering (GIWAXS) and the electronic structure was measured by using Ultraviolet Photoelectron Spectroscopy (UPS). Also, we employed density-functional theory (DFT) calculations to elucidate correlation between polymer orientations and electronic structure. This study implies one should be carefully design the metal-organic interfaces for fine tuning organic devices.

[1] Martin Oehzelt, Norbert Koch, and Georg Heimel, Nat. Commun. 5 (2014) 1-8.

[2] Slawomir Braun, William R. Salaneck, and Mats Fahlman, Adv. Mater. 21 (2009) 1450-1472

[3] Wei Chen, Shuang Chen, Shi Chen, Yu Li Huang, Han Huang, Dong Chen Qi, Xing Yu Gao, Jing Ma, and Andrew Thye Shen Wee, J. Appl. Phys. 106, (2012) 064910

### Keywords:

metal-organic interface, polymer orientation, vacuum electrospray deposition, ultraviolet photoelectron spectroscopy, Fermi level pinning, grazing incident wide angle X-ray scattering, density-functional theory

## Ba(OH)<sub>2</sub> low work function modifier for inverted photovoltaics

이연진\*<sup>1</sup>, 유지수<sup>1</sup>, 정준경<sup>1</sup>, 정관욱<sup>1</sup>, 현경호<sup>1</sup>, 김민주<sup>1</sup>, 이현복\*<sup>2</sup>

<sup>1</sup>Institute of Physics and Applied Physics and van der Waals Materials Research Center, Yonsei University, <sup>2</sup>Department of Physics, Kangwon National University,  
yeonjin@yonsei.ac.kr, hyunbok@kangwon.ac.kr

### Abstract:

Inverted organic photovoltaics (OPVs) have gained much attention due to their much better air stability than that of the conventional OPVs. However, the work function (WF) of ITO is too high to get a small energy level offset in contact with electron transport layer. OPVs without WF modifier have shown very poor performance. Thus, low WF modifier is required for efficient OPVs such as alkali metal halides and self-assembled monolayers. Among them, Ba(OH)<sub>2</sub> WF modifier is well known for its great advantages such as solution processability for low temperature fabrication, extremely high transparency and excellent film forming capability. However, the electronic properties of Ba(OH)<sub>2</sub> have not clearly revealed yet with OPVs operation. In this study, the inverted small molecular OPVs with DBP-C60 combination with and without Ba(OH)<sub>2</sub> were fabricated. The OPV characteristics and energy level alignments evaluated via in-situ photoemission spectroscopy with depositing C60 and Ba(OH)<sub>2</sub> work function modifier will be presented.

### Keywords:

organic photovoltaics, work function, photoemission spectroscopy

## 전기스프레이 증착법을 이용한 PEDOT:PSS 전도성 고분자 증착과 역구조 유기태양전지에의 응용

이현복\*<sup>1</sup>, 이현찬<sup>1</sup>, 박소현<sup>1</sup>, 신나나<sup>1</sup>, 박정민<sup>1</sup>, 김선규<sup>1</sup>

<sup>1</sup>강원대학교 물리학과  
hyunbok@kangwon.ac.kr

### Abstract:

최근 산업계와 학계에서 유기발광다이오드, 유기태양전지, 유기전계효과 트랜지스터와 같은 유기물 반도체에 대한 연구가 활발히 진행되고 있으며, 유기물을 우리가 원하는 기판 위에 원하는 두께로 얇게 증착할 수 있는 기술에 대한 요구도 높아지고 있다. 고분자 유기물의 경우 열 증착을 통해서 박막 제작이 불가능하기 때문에 스프인코팅과 같은 용액공정이 필수적이다. 게다가 용액공정을 하게 되면 진공이 필요하지 않기 때문에 제조 비용이 절감되어 매우 경제적이라는 장점이 있다. 그러나 기존의 스프인코팅 방법은 실험실 수준의 작은 면적의 박막 증착만 가능하다는 단점이 있으므로 이를 개선하기 위한 방법으로 대체 기술이 필요하다. 이러한 관점에서, 대면적의 증착, 마스크를 통한 패턴 증착, 원하는 두께의 다층 증착이 가능한 전기스프레이(electrospray)가 많은 관심을 받고 있다.

본 연구에서는 이러한 전기스프레이 방법을 통해서 효율적이고 경제적인 박막 제작을 실현하고자 한다. 전도성 고분자인 PEDOT:PSS를 전기스프레이 방법을 이용하여 최적화된 증착 조건을 찾고 이후 두께 조절 및 패턴화 증착 실험을 진행하였다. 고른 분사를 위한 증착 파라미터인 전압 크기, 분사속도, 기판과 바늘 사이의 거리, 농도를 바꿔가면서 증착 실험을 진행하였다. 또한 표면 균일도를 향상시키기 위해 기판에 열을 가하고 증기압이 다른 용매를 넣어 비교하였다. 이를 유기태양전지에 적용하여 P3HT:PCBM 광흡수층을 사용한 역구조(inverted) 유기태양전지를 제작하고 특성을 분석하였다.

### Keywords:

전기스프레이(electrospray), PEDOT:PSS, 유기태양전지(organic solar cell)

## Vacuum co-deposited organic-inorganic hybrid perovskite ( $\text{CH}_3\text{NH}_3\text{PbBr}_3$ ) for green light emitting diode (LED)

정나은<sup>1</sup>, 정관욱<sup>1</sup>, 신동근<sup>1</sup>, 현경호<sup>1</sup>, 이현복\*<sup>2</sup>, 이연진\*<sup>1</sup>

<sup>1</sup>Institute of Physics and Applied Physics and van der Waals Materials Research Center, Yonsei University, 50 Yonsei-ro, Seodaemun-Gu, Seoul 03722, Republic of Korea, <sup>2</sup>강원대학교 물리학과  
hyunbok@kangwon.ac.kr, yeonjin@yonsei.ac.kr

### Abstract:

Organic-inorganic hybrid halide perovskites have been widely investigated as solar cell materials. They have also shown great potential for light emitting diode (LED) with their availability of fine-tuning bandgap and intrinsically low FWHM of about 20 nm. High reactivity of organohalide and metal halide enables them to easily crystallize with low temperature solution processes. However, at the same time, it is difficult to form uniform and pinhole free films, which degrade optical and electrical performances. In order to overcome this problem, vacuum deposition has been tried and shown to be effective in reducing pinholes, enhancing uniformity and controlling fine structures of films. The research interests were mainly on solar cells with only a few attempts for LEDs.

Here we made a LED by vacuum co-deposition technique. The device structure is ITO/NPB (50 nm)/ $\text{CH}_3\text{NH}_3\text{PbBr}_3$  (300 nm)/TPBi (10 nm)/LiF (0.5 nm)/Ag (100 nm). The deposition of organohalide is the main hurdle for controlling vacuum deposition. We dealt with this problem by modifying the crucible shape to make beam-like molecular flux.

[This research was supported by the MOTIE (Ministry of Trade, Industry & Energy (10079558)) and Development of materials and core-technology for future display support program.]

### Keywords:

Perovskite Light Emitting Diode, Vacuum Deposition

## Insulating Tunneling Layer for Reduced Interfacial Recombination in Inverted Perovskite Solar Cells

신동근<sup>1</sup>, 강동희<sup>1</sup>, 이재복<sup>2</sup>, 안종현<sup>2</sup>, 이현복\*<sup>3</sup>, 이연진\*<sup>1</sup>

<sup>1</sup>Institute of Physics and Applied Physics and van der Waals Materials Research Center, Yonsei University, <sup>2</sup>Department of Electrical and Electronic Engineering, Yonsei University, <sup>3</sup>Department of Physics, Kangwon National University  
hyunbok@kangwon.ac.kr, yeonjin@yonsei.ac.kr

### Abstract:

The performance of organolead halide [e.g. methylammonium lead iodide (MAPbI<sub>3</sub>)] perovskite solar cells (PSCs) have emerged their power conversion efficiency (PCE) and the reported highest PCE exceeds 22% due to the recent intensive studies. The interfacial energy level alignments have a crucial factor in determining the PCE of PSCs. To obtain the reduced energy level offset between an anode and a perovskite layer, poly(3,4-ethylenedioxythiophene)-poly(styrene sulfonate) (PEDOT:PSS) is often used as a hole transport layer (HTL) in inverted PSCs. However, it has been reported that the PCEs of PSCs with PEDOT:PSS are openly lower than those of PSCs with other HTLs (e.g. P3HT, PTB7, PTAA, poly-TPD, NiO, and CuSCN) despite their high work function and conductivity. Thus, a proper modification of PEDOT:PSS layer is necessary for high-performance PSCs.

In this study, we demonstrate the enhancement in PCE of MAPbI<sub>3</sub> PSCs by using a nonionic surfactant (Triton X-100) mixed PEDOT:PSS for the first time in PSCs. Varying the surfactant concentration, PEDOT:PSS conductivity and work function are significantly changed. Increasing the concentration, however, MAPbI<sub>3</sub> perovskite energy level doesn't changed depending on the substrate Fermi level. To unrevealed the effect of interfacial energetics phenomena PEDOT:PSS with MAPbI<sub>3</sub> perovskite on the device, we fabricate the PSCs with the structure of the Ag/LiF/bathocuproine/C<sub>60</sub>/MAPbI<sub>3</sub>/PEDOT:PSS (with 0.5, 1, 3 wt% or without Triton X-100)/ITO with different Triton X-100 concentration. Moreover, to illuminate the hole extraction mechanism at the interface MAPbI<sub>3</sub> perovskite with PEDOT:PSS (with or without Triton X-100), we conduct the dark current-voltage (J<sub>d</sub>-V) measurement, and capacitance-voltage (C-V) measurement on the PSCs depending on the light soaking. We therefore revealed that the efficient charge extraction HTL condition with reduction of interfacial recombination on PSCs. [This research was supported by the MOTIE (Ministry of Trade, Industry & Energy (10079558)) and Development of materials and core-technology for future display support program.]

### Keywords:

PEDOT:PSS, perovskite solar cell, surfactant additive, ultraviolet photoelectron spectroscopy, capacitance-voltage measurement

## Microbial fuel cell with nanostructured ZnO layer for high efficiency organic semiconductor device

NAM Seoyoun<sup>1</sup>, LIM Eunju\*<sup>1</sup>

<sup>1</sup>Department of Science Education/Creative Convergent Manufacturing engineering, Dankook University  
elim@dankook.ac.kr

### Abstract:

In this study, we are developing microbial battery for applying a self-sustainable, large area and flexible organic semiconductor device by combining bio, material and photonics technologies. It can extract a highly efficient microbial energy using nanostructured ZnO layer, which is also able to harvest bio-based photocurrent energy. Electrons formed in ZnO rod are efficiently moved to the electrode. Photocurrent effect of Au nanoparticle with ZnO semiconductor is positive for the cell photosynthesis. The electron transport and light response are analyzed in order to develop highly efficient microbial energy device for organic semiconductor devices.

### Keywords:

Microbial battery, ZnO, Organic device, Au nanoparticle

## Influence of the composition of TiO<sub>2</sub> and rGO nanoparticles in microbial fuel cell

YIM Hyunjun<sup>1</sup>, LIM Eunju\*<sup>1</sup>

<sup>1</sup>Department of Science Education/Creative Convergence Manufacturing Engineering, Dankook University  
elim@dankook.ac.kr

### Abstract:

The objective of this study is to develop a robust, high efficient microbial fuel cell (MFC). For this, we incorporate TiO<sub>2</sub> and rGO nanoparticles into the MFC device. To find an optimal mixing ratio of TiO<sub>2</sub> and rGO nanoparticles, the composition is controlled in the experiments. Highly efficient microbial energy is found to be obtained when adopting the hybrid nanoparticles. Harvested electrons are analyzed to apply the device and materials to the organic semiconductor device. From this study, we expect that significant advances could be made at the interface between energy harvesting and organic semiconductor field by applying hybrid nanoparticle systems.

### Keywords:

Microbial fuel cell, TiO<sub>2</sub>, rGO, Energy harvesting, organic semiconductor device

## Fabrication of high efficient microbial fuel cell embedded with photocurrent nanomaterial

YANG Eungyu<sup>1</sup>, YIM Hyunjun<sup>1</sup>, LIM Eunju\*<sup>1</sup>

<sup>1</sup>Department of Science Education/Creative Convergence Manufacturing Engineering, Dankook University  
elim@dankook.ac.kr

### Abstract:

We are exploiting a new self-sustainable, large area and flexible organic semiconductor device by combining bio, material, and electronics technologies. It enables us to extract a highly efficient microbial energy using TiO<sub>2</sub>/rGO photocurrent nanomaterial. We employ TiO<sub>2</sub>/rGO nanomaterial for harvesting bio-based photocurrent energy. Electrons formed on the cell surface through the TiO<sub>2</sub>/rGO nanoparticle were effectively transferred to the electrode. Photocurrent leads to a synergistic effect on the energy harvesting in combination with the cell photosynthesis. In order to integrate the microbial fuel cell into organic semiconductor devices, we analyze the highly efficient microbial energy device.

### Keywords:

Microbial energy, rGO, TiO<sub>2</sub>, nanomaterial, Energy harvesting, organic semiconductor device

## Analysis of carrier mechanism and property in organic semiconductor crystalline by controlling deposition temperature

조성집<sup>1</sup>, 임은주\*<sup>1</sup>

<sup>1</sup>단국대학교 융합시스템공학과/과학교육과  
elim@dankook.ac.kr

### Abstract:

The carrier mechanisms in actual organic devices are not so simple, due to the dielectric nature of active organic semiconductor layers, the complexity of interfaces, trapping effect by stress biasing, and others. These are still not sufficient for the use of organic semiconductor materials in actual organic devices. In this sense, we study the effect of organic semiconductor crystalline on the characteristic of the device. To improve the stability and performance of organic devices, we perform theoretical and experimental analyses. In this study, we investigate carrier injection and accumulation in organic semiconductor devices by conducting electrical measurements such as I-V, C-V, C-F measurement and optical charge modulation spectroscopy (CMS) measurement. We manipulate the crystal structure by controlling deposition temperature of organic semiconductor.

### Keywords:

Analysis of carrier mechanism and property in organic semiconductor crystalline by controlling deposition temperature

## CIGS 태양전지 광학 특성의 유한요소법기반 모델링에 관한 연구

박준범<sup>1</sup>, 강경남<sup>1</sup>, 김정호\*<sup>1</sup>  
<sup>1</sup>경희대학교 정보디스플레이학과  
junghokim@khu.ac.kr

### Abstract:

Cu(In,Ga)Se<sub>2</sub> (CIGS) 태양전지는 높은 흡수 계수, 넓은 흡수 파장영역, 높은 안정성 등의 장점 때문에 많이 연구가 되고 있다. CIGS 태양전지는 광흡수층의 두께가 작고, 공간섭효과에 의해 광흡수 효율이 크게 변하기 때문에 광학모델링을 통한 광흡수율의 최적화가 필요하다. 본 연구에서는 유한요소법 기반으로 CIGS 태양전지의 광학특성을 모델링하고, 소자의 구조에 따른 광흡수율 변화를 분석하고자 한다. 유한요소법은 해석하고 하는 구조물을 수~수십 나노미터 크기의 메쉬로 나누어서 수치해석적인 방법으로 계산하는 방법으로서, 광학적 특성뿐만 아니라 전기 및 열적특성도 모두 동일한 메쉬구조에서 해석할 수 있는 장점이 있다. CIGS 태양전지에서는 ZnO 투명전극 및 CIGS 흡수층의 두께 변화에 따른 광흡수율 변화를 계산하고 분석하였다. 또한, 동일한 CIGS 태양전지구조에서 상용 소프트웨어인 TCAD를 이용하여 계산한 결과도 비교하였다.

본 연구는 한국전력공사의 2016년 선정 기초연구개발과제 연구비에 의해 지원되었음 (과제번호 : R17XA05-14)

### Keywords:

CIGS 태양전지; 광학모델링; 유한요소법

## Versatile Mn<sup>4+</sup> activated deep red emission in Ca<sub>14</sub>Al<sub>10</sub>Zn<sub>6</sub>O<sub>35</sub> phosphor for blue-converted white LEDs

양현경\*<sup>1, 2</sup>, 박진영<sup>1</sup>, 정종원<sup>1</sup>, 박성준<sup>2</sup>, 제재용<sup>3</sup>

<sup>1</sup>부경대학교, 과학기술융합전문대학원, LED융합공학전공, <sup>2</sup>부경대학교, LED공학협동과정, <sup>3</sup>동의과학대학교, 방사선과

hkyang@pknu.ac.kr

### Abstract:

The basic requirements of red phosphors for LED are including significant absorption in blue light, high quantum efficiency of red emission, high thermal quenching temperature and high physical and chemical stability. At present, rare-earth ions for red emitted activator such as Eu<sup>3+</sup>, Pr<sup>3+</sup> and Sm<sup>3+</sup> have been widely reported. However, their application on WLEDs are not suitable due to high price of rare-earth ions and their sharp absorption peaks in UV to blue regions. Recently, Mn<sup>4+</sup> activated luminescent materials are considered as a good red-emitting phosphor candidate for warm WLEDs. Under the UV or blue light irradiation, the emission spectrum of Mn<sup>4+</sup> ion typically dominated by the narrow emission bands in the red region between 620 and 760 nm. Additionally, the absorption spectra exhibit two broad bands between UV and blue region corresponding to the <sup>4</sup>A<sub>2g</sub>→<sup>4</sup>T<sub>2g</sub> and <sup>4</sup>A<sub>2g</sub>→<sup>4</sup>T<sub>1g</sub> spin-allowed transitions. Thus, it is noted that Mn<sup>4+</sup> ions can be used as an activator for synthesizing the red phosphors.

In this work, a novel deep red emitting Ca<sub>14</sub>Al<sub>10</sub>Zn<sub>6</sub>O<sub>35</sub>:Mn<sup>4+</sup> phosphors were synthesized by a citrate sol-gel method. The structural and optical properties were evaluated. Finally, a warm WLEDs were successfully fabricated by using a blue chip LED combined with YAG:Ce<sup>3+</sup> phosphors and Ca<sub>14</sub>Al<sub>10</sub>Zn<sub>6</sub>O<sub>35</sub>:Mn<sup>4+</sup> phosphors.

### Keywords:

Ca<sub>14</sub>Al<sub>10</sub>Zn<sub>6</sub>O<sub>35</sub>:Mn<sup>4+</sup>, phosphor, LED

## Integrin-mediated Single Molecular Force Determines Cell Spreading and Migration

김동휘\*<sup>1</sup>, 한성범<sup>1</sup>, 이건희<sup>1</sup>, 김정기<sup>1</sup>

<sup>1</sup>고려대학교 KU-KIST융합대학원  
donghweekim@korea.ac.kr

### Abstract:

Cell migration is one of the most essential features of cell behavior such as wound healing, embryonic development, immune response, and cancer metastasis. Cells exert mechanical forces onto their micro-environment and reform their morphology to adapt to continuously changing physical stimuli. Previous studies have shown that integrin-mediated cell adhesion force modulates the initial cell spreading. However, how the forces between the cell and external matrix mediate cell migration remains ambiguous. Here we present that the single molecular force across transmembrane protein integrin determines the cell spreading dynamics and integrin expression. Using double-strand DNA rupture force, we precisely control the single molecular force between fibronectin and integrin  $\alpha_v\beta_3$  which is associated with initial cell spreading and induces persistence cell migration. We show that cell spreading area decreases as the single molecular force between integrin and fibronectin becomes weak, where integrin  $\alpha_v\beta_3$  is more expressed and cells moves more persistently. These results demonstrate that adherent cells express enhanced level of integrins to overcome reduced adhesion force between cell and extracellular matrix, which could maintain mechanical homeostasis between a cell and its microenvironment. Moreover, activation of integrin requires a threshold value of single molecular force between integrin and extracellular matrix. We expect our results that integrin-mediated adhesion force determines integrin expression could provide a new insight onto the cell mechanics.

### Keywords:

Single molecular force, Integrin, Cell adhesion, Cell migration

## Several Mechanisms of Binding and Dissociation in Rho-dependent Transcription Termination

SONG Eunho<sup>3, 4</sup>, UHM Heesoo<sup>1, 2, 3</sup>, 홍성철\*<sup>1, 2, 3, 4</sup>

<sup>1</sup>Department of Physics and Astronomy, Seoul National University, <sup>2</sup> Institute of Applied Physics, Seoul National University, <sup>3</sup>National Center of Creative Research initiatives, Seoul National University, <sup>4</sup>Interdisciplinary Graduate Program in Biophysics and Chemical Biology, Seoul National University  
shohng@snu.ac.kr

### Abstract:

Rho factor, which is the RNA helicase as well as transcription termination factor, is a global regulator of gene expression which is vital to most bacteria, especially Gamma-negative. Were it not for Rho, most of bacteria cannot live, as Rho is essential factor in Rho-dependent termination, which takes a large part of RNA transcription termination of bacteria. It is also reported that despite involvement in vital role in prokaryotic transcription, Rho has no functional or structural homolog in eukaryotes, which means Rho can be a good candidate for antibiotic. Even though there are many studies on Rho because of the importance of Rho's biological role and promising application to in drug industry, there are several unsolved problems. According to the precedent studies, it's still under dispute whether there are two different mechanisms in Rho binding, so called RNAP(RNA polymerase)-dependent pathways and RNA-dependent pathways. The former argues Rho binds to RNAP before elongation, but the latter insists on Rho's direct binding to *rut*(Rho utilizing site) site of RNA. It is also unknown that whether RNAP remains on DNA after transcription termination. We try to test this hypothesis by single-molecule FRET transcript termination assay, observing the FRET(Fluorescence Resonance Energy Transfer) change and PIFE(Protein Induced Fluorescence Enhancement) during the termination process. We design the DNA sample with dye based on *mgtA* region. In this assay, we observed difference in transcription termination efficiency between case of presence and absence of Rho when elongation re-initiated, which supports the fact that there are two different mechanisms in Rho binding. Moreover, two different traces for termination cases, which are interpreted RNAP remaining case and RNAP case dissociation respectively. We will do further study to make evidence for explaining the concrete mechanism of Rho-dependent termination by imaging Rho or RNAP.

### Keywords:

FRET, Single Molecule, Factor Rho, Rho dependent termination, *mgtA*, *rut* site

## Single Molecule Study on the Formation of R-loop

홍성철\*<sup>1</sup>, 임건형<sup>1</sup>

<sup>1</sup>서울대학교 물리.천문학부  
shohng@snu.ac.kr

### Abstract:

R-loop is a three-stranded nucleic acid structure formed co-transcriptionally in both prokaryote and eukaryote. It consists of two components : one double strand made of DNA:RNA hybrid, and remnant ssDNA. Generally, almost R-loops are harmful if they cannot be removed adequately, because their exposed ssDNA is fragile to some enzymes like AID so that it can be easily damaged, causing many genetic diseases. At some regions like TSS, TTS, and telomere, they, however, have some functions like transcription activation, transcription termination and chromatin modification. So proper regulation is very important and actually many enzymes are related with it. First aim of our study is basically to observe the formation of R-loop and test some enzymes known for eliminating and preventing the formation of R-loop. Of course, there are already some ways used to detect the formation of R-loop with extracted gDNA like DRIP-seq and bisulfite method. But these methods have limited resolution and are not able to provide the real-time observation. Therefore with these methods we cannot see some issues like models of the formation of R-loop. Our second aim of this study is to see what sequences are prone to form R-loop and how.

### Keywords:

R-loop, G-quadruplex, smFRET, genetic disease

## miRNA detection with FRET-PAINT

박상준<sup>1</sup>, 신수철<sup>1</sup>, 홍성철\*<sup>1</sup>

<sup>1</sup>서울대학교 물리.천문학부  
shohng@snu.ac.kr

### Abstract:

The miRNA is a short non-coding RNA and regulates the gene expression. Previous studies reported the regulation mechanisms of miRNA. The detection methods of miRNA in a single cell, however, are challenged by several technical barriers such as short length and low expression of miRNA. In this study, we present a novel detection method of miRNA in a single cell with FRET-PAINT, DNA-PAINT based on FRET. This technique uses two DNA strands (donor strand and acceptor strand) binding with a single miRNA. As the FRET-signal of the acceptor is detected with single-molecule localization microscope, we solve the problem of non-specific binding and off-target binding.

### Keywords:

miRNA, FRET-PAINT, single-molecule localization microscope

## Single-molecule approaches to loop and bridging mechanisms by *Bacillus Subtilis* SMC complex

김아영<sup>1</sup>, 노해민<sup>2</sup>, 오병하\*<sup>2</sup>, 이자일\*<sup>1</sup>

<sup>1</sup>School of Life Sciences, UNIST, 50 UNIST-gil, Ulsan 44919, <sup>2</sup>Department of Biological Sciences, KAIST, 291 Daehak-ro, Yuseong-gu, Daejeon 34141  
bhoh@kaist.ac.kr, biojayil@gmail.com

### Abstract:

Structural maintenance complex (SMC) is involved in chromosome organization and segregation in both eukaryotes and prokaryotes. SMC forms a full complex along with kleisin subunits. Malfunction of the SMC complex results into chromosomal disorders, unfaithful replication, and genomic instability, which may induce malignant diseases such as cancer. In order for the SMC complex to function properly, it must be loaded onto chromosomes and capture the specific site of DNA. Then the SMC complex makes intermolecular bridging of DNA molecules as well as intramolecular DNA loops. However, it remains unclear how the SMC complex is loaded onto DNA, extrudes loops, and bridges DNA molecules.

We investigated the mechanisms underlying loading on DNA and loop extrusion/bridging of DNA by *Bacillus Subtilis* SMC (BsSMC) complex using the DNA curtain assay, which is a cutting-edge method based on technology convergence of lipid fluidity, micro-fluidics, nanofabrication, and fluorescence imaging. Thus the DNA curtain assay allows us to visualize protein-DNA interactions at the single molecule level in real time. Under the flow, we observed that stretched DNA molecules were gradually shrunken at high concentrations of BsSMC. This DNA shrinking may result from the interactions between BsSMC molecules attached to DNA. The compaction rate of DNA by BsSMC was obtained by measuring the change of DNA length with time. Moreover, BsSMC loading, movement, and DNA packaging on DNA were observed in real time using fluorescently-labeled BsSMC. We could observe that when ParB was bound to the *parS* site on DNA, BsSMC was preferentially loaded on the *parS* site and induced loop extrusions.

### Keywords:

Single molecule, DNA curtain, BsSMC, Looping, Bridging

## Biophysical Studies Using High-pressure Cryocooling Method

이철<sup>1</sup>, 김진균<sup>1</sup>, 김채운\*<sup>1</sup>

<sup>1</sup>Department of Physics, Ulsan National Institute of Science and Technology  
cukim@unist.ac.kr

### Abstract:

High-pressure cryocooling has been developed as a method for biophysical and X-ray science studies. The method was developed primarily to prevent damage of protein crystals upon cooling without chemical cryoprotectant, and dozens of macromolecular crystals have been successfully cryopreserved. The procedure was then used to study the phase behavior of water and its relationship with protein dynamics. In addition, the method was successfully applied to stabilize ligand-protein interactions and to study the pressure effect on the structure of a yellow fluorescent protein, citrine. Then, the procedure was modified to entrap intermediate enzymatic states of human carbonic anhydrase with sequential structure changes as the carbon dioxide internal pressures are varied. Specifically, this study provides an understanding on the water rearrangements within an enzyme-active site, and further suggests that such a method could be generally applied to other protein-mediated reactions that involve gaseous molecules. In this presentation, I will discuss the mechanism including the technical details of high pressure cryocooling and its biophysical applications.

### Keywords:

protein crystallography, high-pressure cryocooling, carbonic anhydrase II, intermediate states

## Imaging mRNA transcription in the live mouse brain

박혜윤\*<sup>1, 2</sup>, 심재연<sup>1</sup>, 이병훈<sup>1</sup>, 문형석<sup>1</sup>

<sup>1</sup>Department of Physics and Astronomy, Seoul National University, <sup>2</sup>Institute of Applied Physics, Seoul National University  
hyeyoon.park@gmail.com

### Abstract:

The purpose of this research is to investigate the memory formation in the cortical and hippocampal area in a live mouse by imaging mRNA transcription in real time. The hippocampus and the cortex are involved in the learning of new information and storage of long-term memory. However, the dynamic processes of memory formation in the live brain are poorly understood. In order to find the correlation between memory formation and the initiation of gene expression, we performed real-time imaging of transcription sites in the live mouse brain using two-photon microscopy. We used our transgenic mice in which  $\beta$ -actin or Arc mRNAs are fluorescently labeled for RNA detection in live tissues. We performed glass-covered cranial window surgery to make optical access, which enabled us to find  $\beta$ -actin transcription sites in the visual cortex of a live mouse. For the next step, we are conducting fear-conditioning experiments to induce transcription signals in the hippocampus. This study will contribute to understanding the connection between the frequency of transcription and the memory formation *in vivo*.

### Keywords:

mRNA transcription, *in vivo*, memory formation, imaging

## Temporal separation of transcription termination and RNA polymerase recycling

홍성철\*<sup>1</sup>, KANG Wooyoung<sup>1</sup>, HA Kook Sun<sup>3</sup>, UHM Heesoo<sup>1</sup>, KANG Changwon<sup>2</sup>

<sup>1</sup>Department of Physics and Astronomy, Institute of Applied Physics, and National Center of Creative Research Initiatives, Seoul National University, <sup>2</sup>Department of Biological Sciences, Korea Advanced Institute of Science and Technology, <sup>3</sup>Department of Life Science, The University of Suwon  
shohng@snu.ac.kr

### Abstract:

It has been unknown whether at the end of transcription, RNA product release and RNA polymerase dissociation occur at the same time or with time delay. This single-molecule fluorescence study unveils that RNA release precedes polymerase dissociation in factor-independent termination of *Escherichia coli* transcription. After releasing RNA product, RNA polymerase slides along DNA for some time before dissociates off. *E. coli* NusA accelerates polymerase dissociation without affecting RNA release time, supporting for mechanistic separation of the two events. Because termination stage should be defined only by release of product RNA from transcription complex, subsequent sliding of RNA polymerase on DNA template can constitute an additional stage, proposedly termed as 'polymerase recycling.' After termination, RNA polymerase sliding along template can encounter a nearby promoter for reinitiation.

### Keywords:

Single-molecule FRET, Factor-independent Terminator, Transcription Termination

## Improved radio-sensitivity of lung carcinoma cell using nanoparticles incorporating JNK inhibitor

LIM, SAHOE\*<sup>1</sup>, JUNG SHIN<sup>1</sup>, CHOI, JINMYUNG<sup>1</sup>

<sup>1</sup>Department of Neurosurgery, Chonnam National University Hwasun Hospital  
sahoe@cnuh.com

### Abstract:

This study is to assess the therapeutic effect of JNK inhibitor-incorporated nanoparticle as radiosensitizer in a Lewis lung carcinoma-bearing subcutaneous tumor mouse model. JNK signaling regulates H2AX phosphorylation to repair radiation-induced DNA breakdown and its blocking causes a radiation sensitizing effect. The LGEsese block copolymer was synthesized to fabricate SP600125-incorporated nanoparticles. Physicochemical and morphological properties were observed by transmission electron microscope (TEM) photo and particle size. In-vitro and in-vivo irradiation experiment was performed using Leksell Gamma Knife. Blockade of JNK signaling with SP600125-incorporated nanoparticles significantly delayed mouse brain tumor growth and prolonged mouse survival after radiotherapy.

### Keywords:

radio-sensitivity, leksell gamma knife, JNK inhibitor

## Super-Resolution Imaging of Intercellular Nanotubes

이종봉\*<sup>1, 2</sup>, OH Jae-Ho<sup>1</sup>, CHANG Minhyeok<sup>1</sup>

<sup>1</sup>Department of Physics, POSTECH, <sup>2</sup>Interdisciplinary Bioscience & Bioengineering, POSTECH.  
jblee@postech.ac.kr

### Abstract:

Intercellular nanotubes (INT) that mainly consist of F-actin filaments are extended up to hundreds of micrometers and are a few hundred nanometers in diameter. INTs that protrude from the plasma membrane connect neighboring cells to communicate. However, it remains a question of how such a fine structure sustains robust over long distances for hours. To resolve the nanostructures of INTs, we visualized actins labeled with phalloidin in fixed HeLa cells using fluorescence super resolution microscopy. We found that mutually twisted conformations of actin filaments in INTs. The resulting helical structure of INTs may increase their stability so that long and thin INTs survive for several hours.

### Keywords:

Super-Resolution, Localization Microscopy, Intercellular Nanotubes.

## Single-molecule observation of lipid transfer occurring at membrane contact sites (MCSs)

이상화\*<sup>1</sup>, 김빛나래<sup>1</sup>, 정한빈<sup>2</sup>, 전영수<sup>3</sup>, 이창욱<sup>2</sup>

<sup>1</sup>광주과학기술원 고등광기술연구소, <sup>2</sup>울산과학기술원 생명과학부, <sup>3</sup>광주과학기술원 생명과학부  
thedoors70@gmail.com

### Abstract:

Eukaryotic cells exchange cellular materials and information between intracellular compartments to maintain their functions. In particular, membrane lipids are primarily synthesized in endoplasmic reticulum (ER), and then exchange the lipids with the other organelles. Although vesicle trafficking has been suggested as the main pathway for this lipid transfer, mitochondria utilized non-vesicular trafficking pathway through membrane contact sites (MCSs) to exchange the lipids with ER for the composition of mitochondrial membrane since mitochondria are not connected with vesicular trafficking machinery. In yeast, it is known that the ER-mitochondria encounter structure (ERMES) complex mediates lipid trafficking, but the detailed mechanisms underlying lipid transfer process in ERMES remain incompletely understood. In this study, we used a combination of single-molecule fluorescence resonance energy transfer (FRET) imaging and a cellular membrane-mimicking nanodisc platform to observe the lipid transfer events in MCSs at a single molecule level in real time.

### Keywords:

single-molecule FRET, membrane contact site, endoplasmic reticulum, ERMES, lipid transfer, trafficking

## Single-molecule analysis of DNA polymerases on lesion DNA

부가연<sup>1</sup>, 김대형<sup>1</sup>, 이종봉<sup>\*1, 2</sup>

<sup>1</sup>포항공과대학교 물리학과, <sup>2</sup>포항공과대학교 융합생명과학과  
jblee@postech.ac.kr

### Abstract:

Expose to UV leads to DNA damage. The nucleotide damage such as a thymine dimer blocks a replication machinery of a normal replicative polymerase  $\delta$  and protein proliferating cell nuclear antigen (PCNA) complex. In human cells, DNA polymerase  $\eta$  replicates the damaged DNA by copying a complementary nucleotide with a low fidelity, which results in bypassing the lesion. Thus, the lesion triggers the switch between DNA polymerase  $\delta$  and  $\eta$ . However, the exact mechanisms of how DNA polymerase  $\delta$  is replaced with DNA polymerase  $\eta$  are unidentified. To address this problem, we first studied the kinetics of PCNA-polymerase  $\delta$  and PCNA-polymerase  $\eta$  using single-molecule FRET. Furthermore, we explored the exchange dynamics between DNA polymerase  $\delta$  to  $\eta$  on DNA that contains a thymine dimer.

### Keywords:

TLS, FRET, polymerase delta, polymerase eta, PCNA, single molecule Biophysics

## Single-molecule Studies on the Target Searching Mechanism of CRISPR/Cas12a

정철현\*<sup>1</sup>, 전용문<sup>1</sup>, 구지영<sup>1</sup>, 배상수<sup>3</sup>, 이상화<sup>4</sup>, 이승환<sup>2</sup>

<sup>1</sup>한국과학기술연구원, 테라그노시스 연구단, <sup>2</sup>한국생명공학연구원, 국가영장류 센터, <sup>3</sup>한양대학교, 화학과, <sup>4</sup>광주과학기술원, 고등광기능연구소  
avecmoi@gmail.com

### Abstract:

CRISPR-Cas (CRISPR-associated) system, which is an adaptive immune system of bacteria or archaea to defense against foreign genetic elements, cleaves the gene guided by RNA (crRNA). It is widely have used as a genetic engineering tool because it can change target to be cleaved by manipulating RNA sequence only without modifying protein. Cas9 is most commonly used protein because it does not need the help of other protein to cleave the target DNA. Like Cas9, Cas12a (also called Cpf1) is also used as genetic scissor, that is active as a single component and have higher target specificity than Cas9. However, a molecular mechanism of how the Cas12a protein locates their target site and why it has higher specificity is unknown. Here, we use single-molecule imaging technique to determine the molecular mechanism. Single-molecule particle tracking analysis has suggested Cas12a may carry out a 1-Dimensional diffusion on a DNA to facilitate target searching from direct fluorescence imaging of Cas12a-crRNA-Cy5 complex and dsDNA substrate. Using single molecule FRET (Förster Resonance Energy Transfer), we show that PAM (Protospacer Adjacent Motif) is essential to recognize a correct target by initiate an unwinding of PAM proximal region. However, it seems that Cas12a has weak interaction with PAM and even the PAM has no role in DNA cleavage step after target recognition. These observations give some clues how Cas12a has higher target specificity than Cas9.

### Keywords:

CRISPR, Cas12a, single-molecule biophysics, FRET, 유전자가위

## Biophysical Studies on Intercellular Nanotubes in Living Cells

이종봉\*<sup>1</sup>, CHANG Minhyeok<sup>1</sup>

<sup>1</sup>포항공과대학교 물리학과  
jblee@postech.ac.kr

### Abstract:

Extensive studies on intercellular nanotubes(NTs) that are formed by a physical connection between protrusions from cell plasma have revealed their biological significances as a long range pathway for cellular component transport and signal exchange.

### Keywords:

Nanotube, cell, singlemolecules

## Exploiting Optical transfection to perform gene-editing at single-cell level

이상화\*<sup>1</sup>, 손혜진<sup>1</sup>, 유지현<sup>2</sup>, 장윤수<sup>1</sup>, 최윤희<sup>1</sup>, 배상수<sup>2</sup>  
<sup>1</sup>광주과학기술원 고등광기술연구소, <sup>2</sup>한양대학교 화학과  
thedoors70@gmail.com

### Abstract:

Gene-editing technique based on CRISPR-Cas systems has received much attention due to its wide scientific and technological application. Principally, CRISPR-Cas systems induce double-strand breaks at desired loci and then endogenous repair pathways are activated to fix it. These repair pathways are known to closely relate with cellular contexts such as cell condition, differentiation and cell cycle. As the cellular contexts are diverse within a cell population, study of gene-editing at single-cell level is necessary to understand cell-to-cell variation of gene-editing. To achieve single-cell-level gene editing, we employ optical transfection technique which enables cell-selective transfection by pores at targeted cell membrane using femtosecond laser. Here, we demonstrate gene-editing at single-cell level by delivering CRISPR-Cas systems into a cell of interest using optical transfection technique.

### Keywords:

Optical transfection, Gene-editing, CRISPR

## A Simple Model for Energy Consumption of Human Walking

최무영\*<sup>1</sup>, 김순호<sup>1</sup>, 김종원<sup>2</sup>, 박정준<sup>3</sup>

<sup>1</sup>서울대학교 물리천문학부, <sup>2</sup>인제대학교 헬스케어IT학과, <sup>3</sup>부산대학교 스포츠과학부  
mychoi@snu.ac.kr

### Abstract:

A simple model of human energy consumption during walking is introduced. The model, based on elementary mechanics, predicts the energy consumption rate of a person walking in a variety of speeds and slopes. Model inputs include walking speed, slope of the road, body mass, and step frequency. Unlike previous models, this study focuses on developing a simple physical model that does not depend on specific knowledge of walking mechanics. We collect data from healthy subjects walking on a treadmill at various speeds and slopes. The subjects wear gas analyzers, which provide a reliable measure of energy consumption. The resulting model, with parameters obtained from the gas analyzer data, describes the data well. We discuss the meaning of each parameter value and the difference between parameter values of male and female data.

### Keywords:

Human Walking, Energetics, Calorie Consumption, Wearable Devices

## Marker Analysis of Gene Expression of Primo Vessels by Electro-Acupuncture Stimulation in Rabbit's Joksamni(ST36) and Hapgok(LI04) induced by Lipopolysaccharide

신준영<sup>1</sup>, 지종욱<sup>2</sup>, 최상헌<sup>1</sup>, 최다운<sup>1</sup>, 안예진<sup>1</sup>, 서재혁<sup>1</sup>, 최종구<sup>1</sup>, 노민석<sup>1</sup>, 이상석\*<sup>1</sup>

<sup>1</sup>상지대학교 한방의료공학과, <sup>2</sup>주식회사 굿플  
sslee@sangji.ac.kr

### Abstract:

We investigated whether marker gene for primo vessels in rabbit lymph vessels stressed by lipopolysaccharide(LPS). Real-time reverse transcriptase polymerase chain reaction (RT-PCR) following ribonucleic acid (RNA) extraction was performed using tiny primo and lymph vessels. Flt4 was enriched in primo vessels and several genes including Hif1a, Atgr1, Atgr2, Hsph1, Mtf2, Pparg, Pdgfd, and Hspa4 were highly expressed in primo vessels compared to lymph vessels. The relative expression of all genes revealed that expression of Agtr1, Mtf2, Hsph1, Agtr2 and Hspa4 were remarkably increased in primo vessels, compared to other genes such as Flt4, Hif1a, Pparg, Pdgfd. It implied that Mtf2, Hsf1, Hsp4, Agtr1 and Agtr2 with high amounts may involve in functional activity of primo vessels. Also, we examined gene expression in both isolated primo vasculature and lymph vessels containing primo vessels under LPS injection and electric stimulation at two acupoints of Joksamni (ST36) and Hapgok (LI04). In gene expression, FLT4, a marker for lymphoid endothelial cells(LECs), was expressed 2.58-fold higher in primo vessel than in lymphoid endothelial cells, indicating that it is an essential gene of primo vasculature. In addition, FLT4 expression in the primo vessel after electro-acupuncture stimulation in the ST36 and LI04 was significantly lower than that the inflammatory conditions implanted with LPS. The primary role of relieving symptoms is controlled by the primo vessel rather than the lymphatic system. These genes also could be expected to function specific role in primo vasculature under patho- and physiologic condition.

### Keywords:

primo vessel, lymph vessel, gene expression, FLT4, electro-acupuncture stimulation, Joksamni(ST36), Hapgok(LI04)

## Understanding the dynamics of feeding as a random walk on the feeding-rate axis.

이경석\*<sup>1</sup>

<sup>1</sup>공주대학교 물리교육과  
leeks@kongju.ac.kr

### Abstract:

In animals, the presence of food stimulates appetite and induces feeding behaviors. This is an important mechanism, instrumental for animals' competitiveness in fluctuating environment. To learn fundamental principles of feeding regulation, it is useful to study simple model organisms, whose feeding dynamics can be quantitatively measured. Previously, we measured the feeding dynamics of the nematode *C. elegans* and demonstrated that it matches its feeding activity with the availability of food by modulating the frequency and duration of pumping bursts. Here we develop an effective model that described these dynamics as a random walk on the pumping-rate axis, experiencing food-dependent transition probabilities. This model suggests the existence of two classes of fast pumping: the first is characterized by persistent fast-rate pumping which contributes to feeding bursts, while the other exhibits only transient fast pumping. Furthermore, we use the model to show that serotonin is used by worms both in a food-independent mechanism that promotes acceleration of pumping, and address the different roles of two pairs of serotonergic neurons.

### Keywords:

Animal behavior

## Growth of epitaxial $\text{Ga}_{0.5}\text{Fe}_{1.5}\text{O}_3$ thin films and their physical properties

진형진\*<sup>1</sup>, [KIM Hyunjung](#)<sup>1</sup>

<sup>1</sup>Department of Physics, Pusan National University  
hjeen@pusan.ac.kr

### Abstract:

Recently, needs for developing rare-earth-free permanent magnets are increased. Among many rare-earth-free permanent magnet, epsilon phased  $\text{Fe}_2\text{O}_3$  is an interesting material, since it has high coercivity and room temperature magnetism. However, its saturation magnetization value is quite low due to ferrimagnetism. In a recent first principles-based study predicts  $\text{Ga}_{0.5}\text{Fe}_{1.5}\text{O}_3$  would have higher magnetic moment due to its selectivity in Ga positioning. In this study,  $\text{Ga}_{0.5}\text{Fe}_{1.5}\text{O}_3$  epitaxial films were fabricated on (001) YSZ substrates using RF magnetron sputtering. Then we studied their structural, magnetic and optical properties. X-ray diffraction and reflectometry were conducted to find the best crystallinity thin films. We could confirm that 010 GFO thin films are stabilized on (001) YSZ substrates. Also surface roughness and magnetism were confirmed by atomic force microscopy and superconducting quantum interference device (or vibrating sample magnetometer). Additionally, we will show the effect of oxidative annealing in GFO thin films on physical properties.

This work was supported by the Industrial Strategic Technology Development Program (10062130) funded by the Ministry of Trade, Industry & Energy.

### Keywords:

Epitaxial thin films, Ferromagnetism

## 산소 공급 유량 변화에 따른 $\epsilon$ -Ga<sub>2</sub>O<sub>3</sub> 박막 특성

양민\*<sup>1</sup>, 박상훈<sup>1</sup>, 이한솔<sup>1</sup>, 안형수<sup>1</sup>, 유영문<sup>2</sup>

<sup>1</sup>한국해양대학교 전자소재공학과, <sup>2</sup>부경대학교 LED 해양융합기술센터  
myang@kmou.ac.kr

### Abstract:

최근 고온, 고전압 구동을 위한 전력반도체소자의 수요가 증가함에 따라 넓은 밴드갭(wide bandgap) 반도체소자의 연구가 활발히 진행되고 있다. 그 중 Ga<sub>2</sub>O<sub>3</sub>는 밴드갭이 4.9 eV에 달하는 wide bandgap 산화물 반도체 물질로 높은 열적 화학적 안정성을 가지고 있다. 또한, deep-UV 광소자와 전력 반도체로 주목받는 물질이며, GaN과 SiC보다 높은 항복전압과 낮은 에너지 손실을 가진 장점이 있다.  $\alpha$ -,  $\beta$ -,  $\gamma$ -,  $\delta$ - 그리고  $\epsilon$ -상으로 나누어진 Ga<sub>2</sub>O<sub>3</sub>의 5 개의 결정 상(crystal phase) 중에  $\beta$ -상이 가장 안정적이지만 monoclinic 구조로 인해 이중성장으로 고품질 박막 성장에 어려움이 있다. 준 안정상인  $\epsilon$ -상은 SiC, GaN, ZnO와 같이 결정대칭성이 높은 hexagonal 구조를 가졌기 때문에 현재 전력반도체 연구를 위해 활발히 사용 중인 (0001) sapphire나 (0001) GaN기판을 이용해 이중성장 기술을 최적화한다면 고품질 박막 성장을 기대할 수 있다. 본 연구에서는 고품질  $\epsilon$ -Ga<sub>2</sub>O<sub>3</sub> 박막 결정을 얻기 위한 MOCVD 최적의 성장 조건에 대한 실험을 진행하였다. 특히, 성장 source의 III/VI족 유량 비율의 변화가  $\epsilon$ -Ga<sub>2</sub>O<sub>3</sub> phase 안정성에 미치는 영향에 대해 연구하였다. III족 source와, VI족 source, 캐리어 가스로 각각 TMGa(trimethylgallium), H<sub>2</sub>O bubbling, N<sub>2</sub> 가스를 사용했다. 성장온도는 600에서 750 °C까지 50 °C 간격으로 변화를 주었고 H<sub>2</sub>O bubbling에 사용된 가스의 유량을 300 sccm에서 500 sccm까지 50 sccm 간격으로 변화를 주어 (0001) sapphire 기판에 성장하였다. XRD, AFM, SEM 측정 결과로부터  $\epsilon$ -Ga<sub>2</sub>O<sub>3</sub> phase의 변화와 결정성을 확인할 수 있었다. 성장 온도와 함께 산소 원자의 공급량이  $\epsilon$ -Ga<sub>2</sub>O<sub>3</sub>의 결정성과 결정상(crystal phase)의 안정성에 큰 영향을 주는 것을 확인할 수 있었다.

### Keywords:

$\epsilon$ -Ga<sub>2</sub>O<sub>3</sub>, Crystal growth, MOCVD, Oxide

## EPR Investigation of $\text{Cu}^{2+}$ ions in $\text{Na}_2\text{O-B}_2\text{O}_3\text{-CuO}$ Glasses

송승기\*<sup>1</sup>, 김영훈<sup>1</sup>, 노태호<sup>1</sup>  
<sup>1</sup>명지대학교 물리학과  
sksong@mju.ac.kr

### Abstract:

Glasses of  $\text{Na}_2\text{O-B}_2\text{O}_3\text{-CuO}$  system were prepared by the melt quenching method and electron paramagnetic resonance(EPR) studies have been carried out. EPR spectra of all the glass samples exhibited characteristics of resonance signal of  $\text{Cu}^{2+}$  ions. Observed values of spin Hamiltonian parameters(SHP) indicated that the  $\text{Cu}^{2+}$  ions in these glasses exist in octahedral sites with tetragonal distortion. We have estimated the spin Hamiltonian parameters( $g_{\parallel}$ ,  $g_{\perp}$ ,  $A_{\parallel}$  and  $A_{\perp}$ ) from EPR spectra at 300K and observed their variations as occurring from increase in  $\text{Na}_2\text{O}$  content in the samples.

### Keywords:

EPR, Glasses

## 비저항 측정을 통하여 얻은 ZnCoO:H의 density of states

정세영\*<sup>5, 6</sup>, 천미연<sup>1</sup>, 조용찬<sup>2</sup>, 박철홍<sup>3</sup>, 조채용<sup>4</sup>

<sup>1</sup>부산대학교 단결정은행연구소, <sup>2</sup>한국표준과학연구원, <sup>3</sup>부산대학교 물리교육과, <sup>4</sup>부산대학교 나노에너지공학과, <sup>5</sup>부산대학교 인지메카트로닉스공학과, <sup>6</sup>부산대학교 광메카트로닉스 공학과  
syjeong@pusan.ac.kr

### Abstract:

Understanding the electronic band structure, density of states (DOS) of a material and its relationship to the associated electronic transport properties is the starting point for optimizing the performance of a device and its technological applications. In hydrogenated  $Zn_{0.8}Co_{0.2}O$ (ZnCoO:H) film with an inverted thin-film transistor structure we found ambipolar behavior, which is shown in many field-effect devices based on graphene, graphene nanoribbons, and organic semiconductors. In this study, for information on DOS of ZnCoO:H to explain the ambipolar behavior in terms of the carrier density and type, resistivity and magnetoresistance measurements of a ZnCoO:H film were performed at 5 K. Our proposed DOS representation of ZnCoO:H explains qualitatively the experimental observations of carrier density modulation and ambipolar behavior. First-principles calculations of the DOS of ZnCoO:H were in good agreement with the proposed DOS representation. Through a comparison of first-principles calculations and experimental data, evidence for the existence of Co-H-Co in ZnCoO:H is suggested.

### Keywords:

ZnCoO, hydrogen, resistivity, magnetoresistance, density of states

## 펄스레이저 증착법을 통해 에피-성장된 $\text{LaNiO}_3$ 박막에서 세라믹 타겟의 결정이 금속-절연체 상전이 특성에 미치는 영향에 대한 연구

김태현\*<sup>1</sup>, 최진산<sup>1</sup>, 배종성<sup>2</sup>, 안창원<sup>1</sup>, 김일원<sup>1</sup>

<sup>1</sup>물리학과 EHSRC, 울산대학교, 울산광역시 44610, <sup>2</sup>한국 기초과학 지원 연구원 부산센터, 부산광역시 46742  
mabung7@gmail.com

### Abstract:

페로브스카이트 전이금속 니켈산화물  $\text{LaNiO}_3$ 는  $R\text{NiO}_3$  ( $R = \text{La}, \text{Pr}, \text{Nd}, \text{Sm}, \dots$ ) 중 온도에 따른 금속-절연체 상전이 (Metal-to-Insulator Transition, MIT) 현상이 없는 물질이다. 이러한  $\text{LaNiO}_3$ 의 독특한 물성 때문에, 지난 수십 년간 고품질의  $\text{LaNiO}_3$  단결정을 합성하기 위한 많은 연구자들의 노력이 있어왔다. 그럼에도 불구하고, 벌크 (bulk)  $\text{LaNiO}_3$  단결정의 경우, 그 전이금속 니켈 이온의  $\text{Ni}^{3+}$  산화 상태로 인해 고온, 고압의 성장 조건이 요구되고, 합성된 단결정의 크기가 매우 작은 것으로 보고되어 왔다. 한편, 펄스레이저 증착법 (Pulsed Laser Deposition, PLD)을 이용할 경우, 비교적 낮은 온도와 산소 압력 하에서 에피 박막을 성장시키는 것이 가능하다. 하지만, 이러한 펄스레이저 증착법의 경우, 박막 증착을 위해 사용되는 세라믹 타겟의 결정성이 성장된 박막의 품질에 결정적인 역할을 하는 것으로 받아들여져 왔다. 따라서, 펄스레이저 증착법을 통해 성장된  $\text{LaNiO}_3$  박막에서 세라믹 타겟의 결정성이 박막 내 물리적 특성에 미치는 영향을 살펴보고, 더 나아가 금속-절연체 상전이 현상과의 상관관계를 연구하는 것은 중요하다.

### Keywords:

펄스레이저 증착법,  $\text{LaNiO}_3$

## Characterizations of Lithium/Aluminum co-Doped Zinc Oxide Ceramics

JUN Byeongeog<sup>\*1</sup>, HUR Wonseok<sup>2</sup>, KIM Suhwan<sup>2</sup>, LEE Sihun<sup>2</sup>, AHN Junseok<sup>2</sup>, JEONG Jiwon<sup>2</sup>

<sup>1</sup>Department of Physics and Earth Science, Korea Science Academy of KAIST, <sup>2</sup>Korea Science Academy of KAIST

chai2jun@kaist.ac.kr

### Abstract:

Aluminum and lithium co-doped zinc oxides ZnO:Al,Li (ALZO) ceramics for the transparent conductive oxides were prepared by using the conventional solid state reaction method. While preparing the ALZO ceramics, we applied two stage calcination process; Firstly, an Al 5.0 at% doped ZnO (AZO) calcined powder was prepared. By doping Li to the AZO calcined powder in the composition range from 0.1 mol% to 1.0 mol%, we obtained the ALZO ceramics. The structural, optical and morphological properties of the ALZO ceramics were examined by using the X-ray diffraction (XRD), diffused reflectance spectroscopy (DRS) and scanning electron microscope (SEM). The direct current (DC) and alternating current (AC) conductivities were investigated by using the four-point probing resistance measurements and the impedance analyzer in the low frequency range. The ALZO ceramics showed a Wurtzite phase in the XRD patterns, while the AZO ceramic showed a mixed phase composed of the main Wurtzite phase of the AZO and the secondary corundum phase of Al<sub>2</sub>O<sub>3</sub>. The optical absorptions of ZLO:Al ceramics were characterized by using the diffused reflectance spectroscopy (DRS) in the UV-Vis wavelength range. It is considered that the hexagonal lattice constants, the optical bandgap, and the AC properties were controlled by varying the lithium composition in the ALZO ceramics.

### Keywords:

AC conductivity, Al-doped zinc oxide

## Ce<sup>3+</sup>와 Gd<sup>3+</sup> 이온을 첨가한 YBO<sub>3</sub>의 발광특성 연구

장소영\*<sup>1</sup>, 임준휘\*<sup>1</sup>, 이윤상\*<sup>1</sup>

<sup>1</sup>승실대학교 물리학과

wkdthdud12@soongsil.ac.kr, kem123@ssu.ac.kr, ylee@ssu.ac.kr

### Abstract:

본 연구에서는 붕산염계(orthoborate) 물질인 YBO<sub>3</sub>에 Ce<sup>3+</sup>와 Gd<sup>3+</sup>를 첨가하여 co-doping에 의한 energy transfer에 따른 발광 효율을 조사하였다. 고상 반응법으로 합성한 Y<sub>0.9</sub>(Ce<sub>x</sub>Gd<sub>1-x</sub>)<sub>0.1</sub>BO<sub>3</sub> (YCGB) (x = 0, 0.5, 1) 의 XRD 패턴을 분석하여 YCGB가 육방정계 결정구조를 가지며 Ce<sup>3+</sup>이온과 Gd<sup>3+</sup>이온의 첨가는 YBO<sub>3</sub>의 결정 구조에 의미 있는 변화를 주지 않음을 확인하였다. 여기 에너지를 240 nm ~ 360 nm 로 설정해 YCGB의 발광 스펙트럼을 측정하여, x=0.5 와 x=1 YCGB에서 Ce<sup>3+</sup>이온에 의해 violet-blue emission이 강하게 나타남을 관측하였다. Co-doping에 의한 발광 효율의 차이를 조사하기 위해 x = 0.5 YCGB의 발광 스펙트럼을 Gd<sup>3+</sup> 이온을 첨가하지 않은 Y<sub>0.95</sub>Ce<sub>0.5</sub>BO<sub>3</sub> 의 발광 스펙트럼과 비교하였다. 그 결과 Y<sub>0.95</sub>Ce<sub>0.5</sub>BO<sub>3</sub> 에 비해 x = 0.5 YCGB의 violet-blue emission의 세기가 상대적으로 매우 강함을 관측하였다. 이 결과로 붕산염계 물질에서 Gd<sup>3+</sup> 이온의 energy transfer에 의해 Ce<sup>3+</sup> 이온의 발광이 증가함을 확인할 수 있었다.

### Keywords:

YBO<sub>3</sub>, Ce<sup>3+</sup>, Gd<sup>3+</sup>, Co-doping

## Phonon and piezoelectric properties of SnSSe monolayer

신영한\*<sup>1</sup>, PHAM HUE THI<sup>1</sup>

<sup>1</sup>울산대학교 물리학과  
hohonpop@ulsan.ac.kr

### Abstract:

Piezoelectric materials have a wide range of applications in systems that require robust electrical-mechanical coupling such as mechanical stress sensors, actuators, and energy harvesting devices [1,2]. Recently two-dimensional piezoelectric materials have growing interest. We use density functional calculations to study the piezoelectric properties of monolayer SnSSe in the Janus structure where the Se and S layers are separated by the Sn layer. 1T SnSSe is more stable than 2H one, and both have indirect band gaps. We have obtained the piezoelectric tensors by calculating the polarization change under strain with the Berry phase and the charge density. Due to the broken mirror symmetry of the Janus structure, out-of-plane piezoelectricity can be observed for 1T SnSSe ( $e_{31} = 2.128$  pC/m). In addition, elastic properties of these structures will be discussed in this study.

### References

- [1] A.I. Kingon, S. Srinivasan, Nat. Mater. 4, 233-237 (2005).
- [2] L. Dong, J. Lou, V.B. Shenoy, ACS Nano 11, 8242-8248 (2017).

### Keywords:

piezoelectric, monolayer SnSSe, and Berry phase

## Potable Solid-State UV Colorimetric Sensor Using Metal Oxide Semiconductors

황완식\*<sup>1</sup>, 이지영<sup>1</sup>, 박인<sup>1</sup>  
<sup>1</sup>한국항공대학교 항공재료공학과  
wansikhwang@gmail.com

### Abstract:

Potable solid-state ultraviolet (UV) colorimetric sensor is demonstrated using metal oxide semiconductors. The dye, Methylene Blue (MB), was adsorbed on Ga<sub>2</sub>O<sub>3</sub> and TiO<sub>2</sub> nanoparticles having an energy bandgap of 4.9 eV and 3.4 eV, respectively. Electron-hole pairs (EHP) are generated on semiconductor nanoparticles when higher energy than the its energy gap is exposed. The generated EHP degrades the absorbed MB, resulting in changing its color. Unlike the reported MB degradation under the UV exposure where the MB solution is used, the MB is adsorbed on the solid-state semiconductor nanoparticles and shows an identical effect. Thus, the MB adsorbed nanoparticle can be used for the inkjet-printed colorimetric sensors.

### Keywords:

colorimetric sensor, Methylene Blue degradation, Electron-hole pairs, UV sensors

## Brillouin 광산란 분광법을 이용한 $(\text{Na}_{0.5}\text{Bi}_{0.5})\text{TiO}_3$ 단결정의 음향 특성 연구

오수환<sup>1</sup>, 고재현\*<sup>1</sup>, Li Xiaobing<sup>2</sup>, LUO Haosu<sup>2</sup>

<sup>1</sup>한림대학교, 물리학과, <sup>2</sup>Shanghai Institute of Ceramics, Chinese Academy of Sciences, Shanghai  
hwangko@hallym.ac.kr

### Abstract:

$(\text{Na}_{0.5}\text{Bi}_{0.5})\text{TiO}_3$  (NBT)는 A-site가 2개의 상이한 양이온에 의해 점유되는 복합 Perovskite 구조를 가진 비납계 물질이다. NBT의 상전이는 다양한 실험 방법으로 연구되어 왔지만 각 상의 정확한 특성과 상전이의 성격은 아직 명확히 밝혀져 있지 않다. 이 연구의 목적은 NBT 단결정의 음향특성을 정밀히 측정하고 이를  $\text{BaTiO}_3$ 가 첨가된 NBT-BT와 비교해서 NBT의 상전이에 대한 더 많은 정보를 조사하는데 있다. [그림1]은 냉각 과정 중 측정된 NBT와 NBT-xBT( $x=0.05, 0.08$ )의 종음향모드의 Brillouin 주파수와 반치폭(FWHM)의 온도 경향성을 보여주고 있다. NBT-xBT( $x=0.05, 0.08$ )가 전형적인 릴랙서(relaxor)의 특성을 보여줌에 반해 NBT는 더 여러 온도에서의 비정상적인 변화를 보여주고 있다. [그림2]는 [100]방향을 따라 측정된 NBT 단결정의 종파모드의 Brillouin 주파수 변화와 FWHM의 온도 의존성을 냉각과 가열 과정에서 측정해서 정리한 결과이며, Ref. 1의 데이터도 비교하였다. Brillouin 주파수 및 반치폭의 비정상적 변화가 일어나는 온도를 점선으로 표시했다. 전체적으로 릴랙서의 특성이 남아 있음을 알 수 있고, 냉각 및 가열 공정간에 상이한 상전이 온도를 보임에 따라 상전이의 성질은 1차 상전이임을 확인하였다.

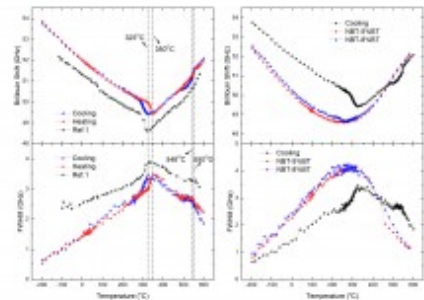


[그림1] 온도에 따른 NBT-xBT( $x=0, 0.05, 0.08$ ) 종음향모드의 Brillouin 주파수와 반치폭  
[그림2] NBT의 종음향모드의 Brillouin 주파수와 반치폭 및 Ref. 1의 데이터.

[1] Y. Onda, S. Tsukada, Y. Hidaka and S. Kojima, *Ferroelectrics. Lett.*62, 1072954 (2010)

### Keywords:

Brillouin, NBT, First Order, Acoustic Properties, Relaxor, Brillouin frequency, 브릴루앙, 1차 상전이, 비납계 압전체, 비탄성 광산란 분광법

## Investigation of Ferroelectric Hafnium Oxide Thin Films

채승철\*<sup>1</sup>, 최종찬<sup>1</sup>, 이경준<sup>1</sup>, 이태윤<sup>1</sup>, 임홍원<sup>1</sup>

<sup>1</sup>서울대학교 물리교육과  
scchae@snu.ac.kr

### Abstract:

Since the discovery of ferroelectricity in Si-doped HfO<sub>2</sub> film, numerous studies have been studied based ferroelectric hafnia film. HfO<sub>2</sub> based FeRAM is considering as one of the most promising candidate for new type memory devices. Ultra-thin HfO<sub>2</sub> film is thermodynamically stable on Si and has robust ferroelectricity properties. Moreover, the remnant polarization P<sub>r</sub> and ferroelectric coercive field E<sub>c</sub> are competitive compared with general perovskite ferroelectric materials such as SrBi<sub>2</sub>Ta<sub>2</sub>O<sub>9</sub> and BaTiO<sub>3</sub>. Though PZT is the conventional ferroelectric material, it requires typical thickness of which is >100nm. While that can't match presently with miniaturization tendency on industry, ultra-thin HfO<sub>2</sub> film is appropriate for current industry application.

In this presentation, we report on investigation of P<sub>r</sub> and E<sub>c</sub> of undoped HfO<sub>2</sub> ferroelectricity films. For the investigation of ferroelectricity in HfO<sub>2</sub>, we conducted their crystallinity by using GIXRD and investigate the conventional ferroelectric properties such as P-E hysteresis loop, I-V curve, retention property and endurance characteristic. Our HfO<sub>2</sub> films exhibited the enhancement of P<sub>r</sub> and E<sub>c</sub> values two times larger than previous reports.

### Keywords:

Ferroelectric, Hafnium, Oxide, FeRAM

## Change in optical property of SrTiO<sub>3</sub> single crystals under control of oxygen vacancies

임준희<sup>1</sup>, 이윤상\*<sup>1</sup>, 부상돈<sup>2</sup>

<sup>1</sup>Department of Physics, Soongsil University, <sup>2</sup>Department of Physics, Chonbuk National University  
ylee@ssu.ac.kr

### Abstract:

We investigated the changes in emission characteristics of SrTiO<sub>3</sub> (STO) single crystals under control of oxygen vacancies by using two methods, irradiating gamma-ray and thermal annealing with oxygen gas. The photoluminescence spectroscopy is useful in probing oxygen vacancies in that the intensity of the visible emission is nearly proportional to the amount of the oxygen vacancies. The STO samples were prepared in the directions of (100), (110) and (111). The untreated samples were found to show visible emissions near 500 nm, which indicates that they might have some oxygen vacancies initially. For generating more oxygen vacancies, the gamma-ray was irradiated on the samples in various doses up to 900 kGy. With the gamma-ray irradiation, the visible emission was found to increase significantly for all three samples. Interestingly, the variation in emission was highly dependent on the surface orientation of the STO: the intensity variation was biggest in the STO (111) sample. For removing the oxygen vacancies, the thermal annealing was performed in an oxygen atmosphere at temperatures ranging from 400 °C to 800 °C. With the oxygen annealing, the visible emission was found to decrease for all three samples. Similarly to the case of the gamma-ray irradiation, the intensity variation was found to be biggest in the STO (111) sample. We discussed our results in relation to the surface energy of the STO.

### Keywords:

SrTiO<sub>3</sub>, Oxygen vacancy

## Dielectric Properties of Gamma-ray Irradiated Bismuth-layer-structured Ferroelectric $\text{Bi}_4\text{Ti}_3\text{O}_{12}$ , $(\text{Bi},\text{La})_4\text{Ti}_3\text{O}_{12}$ , and $(\text{Bi},\text{Nd})_4\text{Ti}_3\text{O}_{12}$ Ceramics

부상돈\*<sup>1</sup>, 김은영<sup>1</sup>, 조삼연<sup>1</sup>, 김선용<sup>1</sup>  
<sup>1</sup>전북대학교, 물리학과  
sbu@chonbuk.ac.kr

### Abstract:

Bismuth layered structure ferroelectrics (BLSFs) materials, which are lead-free piezoelectrics, have known as a material with high Curie temperature, high fatigue endurance, and low electrical property. In our previous research, we investigated dielectric constant and remnant polarization,  $\Delta 2P_r$  value of BLSFs ceramics and then we found that the  $\Delta 2P_r$  decreased after gamma-ray irradiation. Especially,  $\Delta 2P_r$  value of  $\text{Bi}_4\text{Ti}_3\text{O}_{12}$ ,  $(\text{Bi},\text{La})_4\text{Ti}_3\text{O}_{12}$ , and  $(\text{Bi},\text{Nd})_4\text{Ti}_3\text{O}_{12}$  was decreased -14.2, -8.0, and -3.4% respectively. In addition, we are planning to figure out correlation between dielectric constant and temperature of the irradiated BLSFs ceramics. The relation is also known as Curie-Weiss law. In this experiment, temperature is increased near the phase transition temperature with fixed position and stable temperature. Also, samples were irradiated from 100, 300, 500, 1000, 2000, and 3000 kGy and used Impedance Analyzer, irradiated ceramics' dielectric constant was measured in furnace until Curie temperature. Before gamma-ray irradiation, dielectric constant of BiT, BLT, and BNdT has maximum value at 667, 360, 430, respectively. We will discuss on the effect of gamma-ray irradiation on dielectric constants of the irradiated BLSFs ceramics.

### Keywords:

Gamma-ray irradiation, Bismuth-layer-structured ferroelectric ceramics, Dielectric properties

## Low sintering temperature for lead-free BiFeO<sub>3</sub>-BaTiO<sub>3</sub> ceramics with high piezoelectric performance and high Curie temperature

이명환<sup>1</sup>, 김다정<sup>1</sup>, 최해인<sup>1</sup>, HABIB Muhammad<sup>1</sup>, 김명호<sup>1</sup>, 송태권\*<sup>1</sup>, 김원경<sup>2</sup>, 도달현<sup>3</sup>  
<sup>1</sup>창원대학교 신소재공학부 세라믹공학전공, <sup>2</sup>창원대학교 물리학과, <sup>3</sup>계명대학교 신소재공학과  
tksong@changwon.ac.kr

### Abstract:

The effects of sintering temperature were investigated in 0.67Bi<sub>1.05</sub>FeO<sub>3</sub>-0.33BaTiO<sub>3</sub> (BF33BT) lead-free piezoelectric ceramics. The BF33BT ceramics were prepared by a solid state reaction method with various sintering temperatures followed by a water-quenching process. X-ray diffraction patterns show single phase perovskite structure without any secondary phases. The perovskite lattice distortions increased as increasing sintering temperature. The largest rhombohedral distortion ( $90^\circ - a_R = 0.14^\circ$ ) and tetragonality ( $c_T/a_T = 1.022$ ) were observed in BF33BT ceramic sintered at 980 °C and its  $T_C$  was 476 °C. This ceramic exhibits the good piezoelectric properties; the piezoelectric charge sensor constant ( $d_{33}$ ) was 352 pC/N and actuator piezoelectric constants ( $d_{33}^*$ ) was 270 pm/V. The BF33BT ceramics of the high piezoelectric performance and low sintering temperature show a potential for new eco-friendly lead-free piezoceramics compared to Sb-modified (Na<sub>0.5</sub>K<sub>0.5</sub>)NbO<sub>3</sub> and Ba(Ti<sub>0.8</sub>Zr<sub>0.2</sub>)O<sub>3</sub>-(Ba<sub>0.7</sub>Ca<sub>0.3</sub>)TiO<sub>3</sub> ceramics of which sintering temperatures are around 1150 °C ~ 1500 °C.

### Keywords:

Piezoelectric, Sintering temperature, Lead-free, Structural distortion, Grain size

## Influence of Quenching Method for Multiferroic Behavior of $\text{Bi}_{0.86}\text{Sm}_{0.14}\text{FeO}_3$ Ceramics

송태권\*<sup>1</sup>, 최해인<sup>1</sup>, 이명환<sup>1</sup>, 김다정<sup>1</sup>, 김원정<sup>2</sup>, 김명호<sup>1</sup>, MUHAMMAD Habib<sup>1</sup>  
<sup>1</sup>창원대학교 신소재공학부 세라믹공학전공, <sup>2</sup>창원대학교 물리학과  
tksong@changwon.ac.kr

### Abstract:

This work investigates the effects of the solid solution with bismuth ferrite ( $\text{BiFeO}_3$ , BFO) and samarium ferrite ( $\text{SmFeO}_3$ , SFO) at morphology phase boundary composition. The  $\text{Bi}_{0.86}\text{Sm}_{0.14}\text{FeO}_3$  (BSFO14) composition has MPB system with coexistence of rhombohedral and orthorhombic phases. The MPB-system, it proffers the ferroelectric and magnetic properties at room temperature. The BSFO14 ceramics prepared with different cooling method during the sintering. The water-quenching (WQ840), air-quenching (Q840), and furnace-cooling (FC840) have a different cooling time from 840 °C to room temperature. The cooling time is decreased from FC840 to WQ840. From the XRD result, the rhombohedral and orthorhombic phases are coexistence at room temperature. The WQ840 ceramic shows high remnant polarization with a high coercive electric field during an electrical cycling measurement. On the other hand, the Q840 and FC840 are electrical breakdowns during an electrical cycling measurement. Also, the direct piezoelectric coefficient of WQ840 ( $d_{33}$ : 26 pC/N) is higher than FC840 ( $d_{33}$ : 15 pC/N). The dielectric constant of WQ840 is higher than FC840. These results are related to electric field induced phase transition from orthorhombic phase to rhombohedral phase. Also, the cation defect of bismuth vacancy at an A-site and valence electron state of iron (transition from  $\text{Fe}^{3+}$  to  $\text{Fe}^{2+}$ ) at a B-site.

### Keywords:

multiferroic, piezoelectric, BFO, samarium

## Eu-doping Effects on Ferroelectric Properties of Potassium Sodium Niobate Ceramics

JUN Byeongeog<sup>\*1</sup>, KIM Minsu<sup>2</sup>, LEE Jong-Rim<sup>1</sup>, KIM Dongin<sup>2</sup>, KIM Chanyoung<sup>2</sup>

<sup>1</sup>Department of Physics and Earth Science, Korea Science Academy of KAIST, <sup>2</sup>Korea Science Academy of KAIST

chai2jun@kaist.ac.kr

### Abstract:

Europium doped potassium sodium niobates  $K_{0.55}Na_{0.45}NbO_3$  (KNN:Eu) ferroelectric ceramics were prepared by using the conventional solid state reaction. KNN:Eu calcined powders were prepared by mixing  $Eu_2O_3$  with 0.1 mol% ~ 5.0 mol% with the  $K_{0.55}Na_{0.45}NbO_3$  calcined powder. Physical properties of KNN-Eu ceramics were characterized by using the X-ray diffraction (XRD), the Raman spectroscopy and the diffused reflectance spectroscopy (DRS) at room temperature. The Raman scattered light was condensed by using an infinity-corrected objective (10×) lens and the 532 nm excitation laser line was cut off by using a long pass Raman edge filter. The DRS spectra have revealed that the variations of the Kubelka-Monk function  $F(R)$  in the ultra violet - visible wavelength range. The optical absorptions were evaluated as the product of the Kubelka-Monk function and the photon energy. The ferroelectric  $D-E$  hysteresis of the KNN:Eu ceramics were studied with the modified Sawyer-Tower circuit in the temperature range from room temperature to 200 °C. The (202) and (020) XRD peaks were probed by using the near parallel beam X-ray source with a flat graphite monochromator for Cu  $K\alpha$  radiation. The Raman peaks at around  $250\text{ cm}^{-1}$  and  $560\text{ cm}^{-1}$  were elucidated for the Eu doping effects in the KNN:Eu ceramic. The Optical bandgap was shifted to higher energy and the optical absorption band in the energy ranging from 1.5 eV to 3.0 eV was decreased with increasing the Eu doping in KNN:Eu ceramics.

### Keywords:

Lead-free piezoelectric ceramic, The D-E hysteresis

## Piezoelectric and dielectric, ferroelectric properties of Mn-modified BiFeO<sub>3</sub>-BaTiO<sub>3</sub> bulk ceramics

송태권\*<sup>1</sup>, 김다정<sup>1</sup>, 이명환<sup>1</sup>, 김명호<sup>1</sup>, 김원정<sup>2</sup>  
<sup>1</sup>창원대학교 신소재공학부, <sup>2</sup>창원대학교 물리학과  
tksong@changwon.ac.kr

### Abstract:

Piezoceramics have been interesting for potential applications, such as actuator, sensors and other electronic devices. However, the lead-free based ceramics have not yet been developed with the properties to replace PZT:  $d_{33} > 300$  pC/N,  $T_c > 300$  °C. BiFeO<sub>3</sub> - BaTiO<sub>3</sub> (BF-BT) solid solution systems are presented as potential lead-free piezoelectric ceramics. Many researchers have investigated the sintering additives and/or dopants to modify BF-BT based system. A small amount of manganese oxide was effective to improve electrical properties and sintering behavior.  $0.67\text{Bi}_{1.05}(\text{Fe}_{0.99}\text{R}_{0.01})\text{O}_3-0.33\text{BaTiO}_3$  ( $R = \text{Mn}^{2+}, \text{Mn}^{3+}, \text{Mn}^{4+}$ ) bulk ceramics were prepared via a solid-state reaction process by using furnace-cooling or water-quenching method. Results showed the high value of the piezoelectric constant in Mn-modified BiFeO<sub>3</sub> - BaTiO<sub>3</sub> bulk ceramics. Water-quenched in Mn-modified BF33BT ceramics showed the reduced leakage currents and made the poling process easy. As a result, the water-quenched Mn<sup>4+</sup>-modified BF33BT ceramics had  $d_{33} = 241$  pC/N and  $d_{33}^* = 237$  pm/V. The largest  $d_{33}$  and  $d_{33}^*$  were 331 pC/N and 258 pm/V in water-quenched Mn<sup>2+</sup>-modified BF33BT ceramics.

### Keywords:

BiFeO<sub>3</sub>, BaTiO<sub>3</sub>, High T<sub>c</sub>, Piezoelectric

## Possible signature of the soft-mode and displacive-type ferroelectric transition in the BaTiO<sub>3</sub> crystal

김민섭<sup>1</sup>, 한정우<sup>1</sup>, 이종석\*<sup>1</sup>  
<sup>1</sup>광주과학기술원 물리광학과  
jsl@gist.ac.kr

### Abstract:

BaTiO<sub>3</sub> is a typical ferroelectric material, but the mechanism of its ferroelectric transition has long been controversial between the displacive and the order-disorder type. Recently, J. Hlinka *et al.* reported the relaxational mode in the 120 μm thick BaTiO<sub>3</sub> crystal by using transmission type THz time-domain spectroscopy technique, and supported the order-disorder transition scenario [J. Hlinka *et al.*, Phys. Rev. Lett. **101**, 167402 (2008)]. In this work, we revisit this issue by examining the single crystalline BaTiO<sub>3</sub> using recently developed reflection-type THz time-domain spectroscopy. At room temperature, we clearly observed a well-defined resonance mode at about 0.5 THz. As temperature changes up to about 410 K and down to about 280 K where the tetragonal-to-cubic and tetragonal-to-orthorhombic phase transition occurs, this mode exhibits discernible temperature-dependent changes in its peak frequency and amplitude. By employing the Lorentz oscillator model, we analyze the spectral response of this mode in detail, and demonstrate a possible signature of the displacive-type ferroelectric transition.

### Keywords:

Ferroelectric, Phase transition, THz, Terahertz Spectroscopy, soft-mode

## Enhancement of Ferroelectric Polarization by Sulfurization

김태현\*<sup>1</sup>, SHEERAZ Muhammad<sup>1</sup>, KIM Ill Won<sup>1</sup>, AHN Chang Won\*<sup>1</sup>

<sup>1</sup>울산대학교 물리학과  
mabung7@gmail.com, cwahn@ulsan.ac.kr

### Abstract:

Anion doping or substitution to oxide materials is of great interest for synthesizing new multi-functional materials artificially and realizing unusual physical properties which do not exist in nature. Chalcogens group (e.g. S, Se, Te) other than pnictogens and halogens has attracted plenty of attention due to the isovalent nature with and the larger anion radius than an oxygen atom. Despite previous studies of the substitution or doping of chalcogen elements, a feasible synthetic method in a small laboratory has been rarely reported. In this work, we developed a new way for sulfurization to perovskite oxides. To do this, a thiourea ( $\text{CH}_4\text{N}_2\text{S}$ ) solution is employed and the subsequent spin-coating is implemented to ferroelectric perovskite oxides  $[\text{Pb}(\text{Zr,Ti})\text{O}_3]$ . Microscopic analyses of electronic and crystal structures reveal that oxygen ions are substituted by sulfur atoms with tetragonal distortion. In response to this structural phase transition, macroscopic ferroelectric polarization is enhanced, although a band gap is reduced. More details of theoretical calculations and experimental results will be presented in conjunction with a discussion about the potential usage of our synthetic technique in aspect of novel material design.

### Keywords:

Anion doping, Perovskite, Ferroelectrics, Sulfurization

## Fabrication and ferroelectric properties of lead-free (K<sub>0.5</sub>Na<sub>0.5</sub>)NbO<sub>3</sub> thin film using RF-magnetron sputtering

김태현\*<sup>1</sup>, 투이웨이<sup>1</sup>, 석해진<sup>1</sup>, 김일원<sup>1</sup>, 조신욱<sup>1</sup>

<sup>1</sup>울산대학교 물리학과  
mabung7@gmail.com

### Abstract:

Lead-free Na<sub>0.5</sub>K<sub>0.5</sub>NbO<sub>3</sub> (KNN) thin films are of practical interest in aspect of novel applications to the MEMS, energy harvester, sensor, actuator, and electro-optical devices. However, their ferroelectric and piezoelectric properties are still not fully understood due to the difficult in the synthesis of a high-quality lead-free KNN thin film. Thus, the effect of excess K and Na on the crystal structure and electrical properties of the film have not been clearly investigated, either. It has been widely accepted that fabricating a high-density and quality KNN thin film is very challenging owing to the volatility of Na and K elements under humidness. In this work, we have successfully synthesized high-density and good-quality KNN ceramic targets and then, have grown KNN thin films by using the radio-frequency (rf) magnetron sputtering. Various physical properties of the as grown KNN thin film have been measured such as dielectric permittivity, ferroelectric polarization, and piezoelectric responses, and electrical leakage current. The observed results will be discussed in a technological point of view.

### Keywords:

Ferroelectric, (K<sub>0.5</sub>Na<sub>0.5</sub>)NbO<sub>3</sub>, Lead-free, radio-frequency (rf) magnetron sputtering

## Capacitance anomaly near magnetic Neel temperature in heavily La-substituted BiFeO<sub>3</sub>

양찬호\*<sup>1, 4</sup>, 여영기<sup>1</sup>, ULRICH Clemens<sup>2</sup>, SEIDEL Jan<sup>3</sup>, 김용진<sup>1</sup>

<sup>1</sup>Department of Physics, KAIST, <sup>2</sup>UNSW sydney, School of Physics, Australia, <sup>3</sup>UNSW sydney, School of Materials Science and Engineering, <sup>4</sup>Institute for the NanoCentury, KAIST  
chyang@kaist.ac.kr

### Abstract:

Multiferroic materials, which have two or more simultaneous ferroic order parameters, exhibit magnetoelectric coupling, offering a potential for applications such as information storages, spintronic devices and sensors [1]. BiFeO<sub>3</sub> as a canonical multiferroic has ferroelectricity ( $T_C \sim 1100$  K) and antiferromagnetism ( $T_N \sim 640$  K) [2]. Under a compressive misfit strain, highly elongated tetragonal-like BiFeO<sub>3</sub> can be stabilized and it has a concurrent ferroelectric-to-ferroelectric and antiferromagnetic-to-paramagnetic transition near room temperature [3]. Around the concurrent transition temperature, capacitance anomaly occurs when the antiferromagnetic order disappears due to structural instability [3]. The two transitions bifurcate by substituting La into Bi site over 10 % [4]. In this study, we demonstrate frequency-dependent capacitance anomaly near magnetic Néel temperature in La 20%-substituted BiFeO<sub>3</sub> thin films. Although the La 20%-substituted BiFeO<sub>3</sub> has distinctive ferroelectric and magnetic transition temperatures [4], we find the G-type antiferromagnetic spin ordering confirmed by neutron diffraction results in a frequency-dependent capacitance enhancement near its magnetic Néel temperature in addition to the bifurcated dielectric anomaly existing at a lower temperature. We suspect that sufficient La doping makes multiple polar nano-regions in which magnetoelectric coupling induces frequency-dependent capacitance anomaly. This study provides useful insight into the magnetoelectric coupling of polar nano-regions.

[1] J. Wang *et al.*, *Science* **299**, 1719 (2003).

[2] P. Fischer *et al.*, *J. Phys. C: Solid State Phys.* **13**, 1931 (1980)

[3] K.-T. Ko *et al.*, *Nature communication* **2**, 567 (2011).

[4] B.-K. Jang *et al.*, *Nature Physics* **13**, 189-196 (2017).

### Keywords:

Dielectrics, Magnetoelectric coupling, Functional Oxides

## Morphotropic phase transition in ferroelectric BaTiO<sub>3</sub> by Ni substitution

김태현\*<sup>1</sup>, 즈엡웬수엡<sup>1</sup>, 올라야만<sup>1</sup>  
<sup>1</sup>울산대학교 물리학과  
mabung7@gmail.com

### Abstract:

Morphotropic phase boundary (MPB), where two competing structural phases coexist and thus, extremely high electromechanical responses are accessible, has attracted much attention in piezoelectric and ferroelectric communities. Perovskite BaTiO<sub>3</sub> is one of the most well-known ferroelectric materials due to the robust room-temperature ferroelectric polarization and the high dielectric constants. In this work, we will present chemical-doping-driven phase transitions in Ni-doped BaTiO<sub>3</sub> where the B-site Ti<sup>4+</sup> ion is substituted by Ni<sup>2+</sup> ion. By controlling the Ni doping concentration to BaTiO<sub>3</sub>, a tetragonal-to-pseudocubic phase transition is clearly demonstrated in various BaTi<sub>1-x</sub>Ni<sub>x</sub>O<sub>3</sub> (BTN) ( $x = 0, 0.01, 0.02, 0.05, 0.125$  and  $0.25$ ) composites. To gain a further insight into this morphotropic phase transition, systematic measurements of related physical properties have been done. In conjunction with a discussion about the microscopic origin of MPB, detailed results will be presented.

### Keywords:

ferroelectric, Morphotropic phase boundary, Ba(Ti,Ni)O<sub>3</sub>

## Supramolecular Structures of Organic Semiconductor Indenofluorene on Au(111) Studied Using Scanning Tunneling Microscopy

KAHNG Se-Jong<sup>\*1</sup>, PARK Jong-Whan<sup>1</sup>, CHANG Min Hui<sup>1</sup>, JANG Won-Jun<sup>1</sup>, HAN Seungwu<sup>2</sup>  
<sup>1</sup>고려대학교 물리학과, <sup>2</sup>서울대학교 재료공학부  
sjkahng@korea.ac.kr

### Abstract:

Supramolecular structures of conjugated polycyclic hydrocarbons have been actively studied due to their potential applications in organic electronic and optical devices. A promising polycyclic hydrocarbon is an indenofluorene skeleton, a 6–5–6–5–6 fused ring system with fully conjugated state, showing high heating stability and optical controllability. Here, we report on the supramolecular structures of 2,8-dibromo-indeno(1,2-b)fluorene-6,12-dione molecules studied using scanning tunneling microscopy (STM). Oblique molecular lattices with phase-separated prochiral domains were observed on Au(111). Molecular models that could be explained with O···H and Br···H hydrogen bonds and Br···Br halogen bonds, were proposed, and reproduced with density-functional theory calculations. Our study shows that halogen bonds as well as hydrogen bonds play crucial roles for the formation of supramolecular structures of polycyclic hydrocarbons.

### Keywords:

supramolecular structures, hydrogen bond, halogen bond, scanning tunneling microscopy, density functional theory

## Topological Phases in Stacked Honeycomb Lattice

전건상\*<sup>1</sup>, 신지선<sup>1</sup>  
<sup>1</sup>이화여자대학교 물리학  
gsjeon@ewha.ac.kr

### Abstract:

We examine a stacked honeycomb lattice where two-dimensional normal and topological insulators are placed alternately. In the system considered normal insulators are caused by a staggered sublattice potential while spin-orbit coupling gives rise to a topological insulator. For zero sublattice potential the system lies in the Dirac semimetal phase. We find that the 4-fold degenerate Dirac point turns into the 2-fold degenerate Dirac point once the staggered lattice potential in normal insulating layers is turned on, indicating that the Weyl semimetal phase appears. Above a certain critical value of the staggered sublattice potential, Weyl point disappears and the system has a finite bulk band gap. The numerical computation of topological invariants for a non-centrosymmetric system using the Wannier charge center [1] reveals that there occurs a topological phase transition to a weak topological insulator characterized by the topological invariants (0;001) at the point where a bulk band gap vanishes.

[1] Alexey A. Soluyanov and David Vanderbilt, Phys. Rev. B **83**, 235401 (2011).

### Keywords:

topological insulator, Weyl semimetal, noncentrosymmetric system

## Mechanical control of valley degree of freedom in monolayer MoS<sub>2</sub>

손주인<sup>1</sup>, 이지은\*<sup>1</sup>

<sup>1</sup>아주대학교 물리학과  
jieuntb@gmail.com

### Abstract:

When a strain is applied to monolayer MoS<sub>2</sub>, an internal piezoelectric field( $E_{pz}$ ) is formed because 3-fold rotational symmetry of the crystal is broken. In such strained monolayer MoS<sub>2</sub>, valley magnetization can be formed when current flows perpendicular to the  $E_{pz}$  by Berry curvature effects. To investigate the dependence of valley magnetization on strain, we fabricated flexible MoS<sub>2</sub> devices that can be stretched in desired directions on bendable substrates. We apply tunable strain to monolayer MoS<sub>2</sub> and measure valley magnetization using Kerr Rotation technique. The experiment is performed at room temperature which pave the ways for practical valleytronic applications.

### Keywords:

MoS<sub>2</sub>, Strain, Berry curvature effect

## An exact solution for Aharonov-Casher effect in a constant magnetic field

최태승\*<sup>1</sup>, 이영원<sup>2</sup>, 한영덕<sup>3</sup>

<sup>1</sup>서울여자대학교 교양교육부, <sup>2</sup>한국교통대학교 산학협력단, <sup>3</sup>우석대학교 컴퓨터공학과  
tschoi@swu.ac.kr

### Abstract:

We present an exact solution for a neutral particle passing a cylindrically symmetric mesoscopic ring in constant magnetic fields. Energy eigenvalues and Aharonov-Casher like phase are obtained. Corresponding persistent currents are also presented. Scalar Aharonov-Bohm effect is discussed.

### Keywords:

mesoscopic ring, Aharonov-Casher, Scalar Aharonov-Bohm, persistent currents

## Quantum electronic transport in $(\text{Bi}_{1-x}\text{Sb}_x)_2\text{Se}_3$ topological insulator nanoribbon contacted with superconducting electrodes

도용주\*<sup>1</sup>, 임흥순<sup>1</sup>, 김남희<sup>1</sup>, 김홍석<sup>1</sup>, YU Dong<sup>2</sup>, HOU Yasen<sup>2</sup>, XIAO Rui<sup>2</sup>  
<sup>1</sup>광주과학기술원 물리광학과, <sup>2</sup>University of California Davis Department of physics  
yjdo@gist.ac.kr

### Abstract:

The formation of spin-textured metallic edge states in topological insulators (TIs) enables highly coherent charge and spin transport. Combinations of TIs with conventional superconductors can also provide useful platforms for creating and manipulating emergent particles such as Majorana fermions, which are essential for topological quantum computers. Here, we report electronic transport properties of  $(\text{Bi}_{1-x}\text{Sb}_x)_2\text{Se}_3$  TI nanoribbon at low temperatures. With the magnetic field applied parallel to the nanoribbon axis, Aharonov-Bohm conductance oscillations were observed. In the superconducting state below the superconducting transition temperature of Al electrodes, the conductance enhancement due to Andreev reflection was observed.

### Keywords:

Topological insulator, quantum interference, superconductor

## Creation of Two-dimensional Electron Gas at $\text{CaZrO}_3/\text{SrTiO}_3$ Heterostructures

송중현\*<sup>1</sup>, 권두현<sup>1</sup>

<sup>1</sup>충남대학교 물리학과  
songjonghyun@cnu.ac.kr

### Abstract:

The discovery of two-dimensional electron gases (2DEGs) in  $\text{SrTiO}_3$ -based heterostructures(HS) provides new opportunities for its various characteristics. Therefore, we study a new type of 2DEG at  $\text{SrTiO}_3$ -based HS, nonpolar/nonpolar oxide interface of  $\text{CaZrO}_3/\text{SrTiO}_3$ . This heterointerface exhibits temperature dependence of sheet resistance and carrier density at different film thickness. The quality of the films and epitaxial relation to the  $\text{SrTiO}_3$  substrates were investigated by High Resolution X-Ray Diffraction. These findings open a new avenue to achieve 2DEG in perovskite-based HS system.

### Keywords:

two-dimensional electron gas, nonpolar/nonpolar, Complex oxide interface

## Controlling ferroelectric vortex-antivortex pair by electrical switching

김정용\*<sup>1</sup>, 김광은\*<sup>1</sup>, 양찬호\*<sup>1, 2</sup>

<sup>1</sup>Dept. of Physics, KAIST, <sup>2</sup>KAIST Institute for the NanoCentury  
kimjeongyong@kaist.ac.kr, ecky@kaist.ac.kr, chyang@kaist.ac.kr

### Abstract:

Recently, topological defects have attracted many attentions because of their stability against small perturbations as potential applications for non-volatile high density memory and electrical logic system. However, the ferroelectric vortex structure lacks theoretical and experimental studies as compared with magnetic materials. In this poster, we explore ferroelectric domain structures in the BiFeO<sub>3</sub> thin film by applying momentary electric field. The vector map of the ferroelectric polarization is investigated through the angle-resolved piezoresponse force microscopy, and it is analyzed through the topological quantity called winding number. With these procedures, we confirm that the vortex-antivortex pair was created through the electrical polling. Our findings offer a useful concept for topological defect memory.

### Keywords:

ferroelectric vortex-antivortex pair, winding number, piezoresponse force microscopy

## Magnetic Anisotropy of 2D Ferromagnet Interfaced with Ferroelectric Material

이근식\*<sup>1</sup>, 김은미<sup>1</sup>, CHENG Gong<sup>2</sup>, XIANG Zhang<sup>2</sup>

<sup>1</sup>울산과학기술원 화학과, <sup>2</sup>University Of California, Berkeley Mechanical Engineering  
gslee@unist.ac.kr

### Abstract:

Ferromagnetic ordering in two dimensional materials is essential for developing nanoscale spintronic devices, although it has been fundamentally challenging due to the Mermin-Wagner theorem. Recently, the long range magnetic ordering has been observed in two-dimensional van der Waals materials, which showed the critical role of easy-axis magnetic anisotropy (MA) for the 2D magnetic ordering. Thus MA can be used as a knob to control the 2D magnetic ordering in two-dimensional magnetic crystals. Here, by using the density functional theory method, we find that the MA of 2D ferromagnet  $\text{Cr}_2\text{Ge}_2\text{Te}_6$  can be effectively affected by the electric dipole of the adjacent ferroelectric material. Our work open avenues for electrical switching of 2D ferromagnetism.

### Keywords:

2d magnetism, Magnetic anisotropy, DFT method

## Benchmark of van der Waals interaction for aromatic molecules on Pt (111)

정석민\*<sup>1</sup>, 박가람<sup>1</sup>  
<sup>1</sup>전북대학교 물리학과  
jsm@moak.chonbuk.ac.kr

### Abstract:

Molecular chemisorption on a transition metal surface is a initial step toward understanding 2D-materials growth system. However, according to studies of Gautier <sup>[1]</sup> and Bremond <sup>[2]</sup>, the error of the density functional theory (DFT) calculation increases depending on several variables(such as exchange-correlation function or van der Waals description) when molecules are adsorbed on the platinum surface with a specific configuration such as linear molecule. We study relative accuracy of the vdW approximation for the interaction between the hexagonal molecules (benzene, borazine) used 2D material growth and the Pt(111) surface. We investigate the energetics and structures using local density approximation (LDA) and generalized gradient approximation functional (PBE) including van der Waals (vdW) interactions (D2 <sup>[3]</sup>, D3 <sup>[4]</sup> and dDsC <sup>[5]</sup>). As a result, in the LDA case, large errors occur in describing adsorption structures and energies. In case of PBE, the adsorption energy clearly varies for each type of vdW interaction, but the diffusion barriers, atomic structures and molecular orbitals are similar for all vdW interactions. We are similar carry out a extensive tests of the vdW option for describing the catalytic effect of the Pt surface for aromatic molecules which suggests that the adsorption energy needs to be reconfirmed carefully reconfirm according to the vdW approximation method.

[1] Phys. Chem. Chem. Phys. **17**, 28921 (2015)

[2] J. Chem. Phys. **140**, 18A516 (2014)

[3] J. Comp. Chem. **27**, 1787 (2006)

[4] J. Chem. Phys. **132**, 154104 (2010)

[5] J. Chem. Phys. **134**, 044117 (2011)

### Keywords:

Pt(111), borazine, benzene, DFT, van der Waals interaction

## Neural network representation of quantum many-body wave functions for the 1D Heisenberg spin chains

THONGJAO MAYUM Diana<sup>1</sup>, GO Ara\*<sup>1</sup>

<sup>1</sup>기초과학연구원 복잡계 이론물리 연구단  
arago.ibs@gmail.com

### Abstract:

A recently proposed artificial neural network representation for quantum many-body states is used to investigate the ground state of the one-dimensional Heisenberg spin chain with nearest neighbor antiferromagnetic interaction. While the Hilbert space grows exponentially with respect to the system size, the neural network representation enables us to describe the many-body wave function with a significantly reduced number of variational network parameters. We employ a reinforcement learning scheme to obtain the optimal neural network parameters for spin 1/2 as well as spin 1 systems and observe how the Haldane's conjecture is reflected in the network structure.

### Keywords:

Neural network, Quantum spin chain

## Efficient implementation of DFT+DMFT

최형준\*<sup>1</sup>, 한만천<sup>1</sup>, 오형주<sup>1</sup>, 이충기<sup>1</sup>

<sup>1</sup>Department of Physics, IPAP, and Center for Computational Studies of Advanced Electronic Material Properties, Yonsei University, Seoul 03722, Korea  
h.j.choi@yonsei.ac.kr

### Abstract:

The dynamical mean field theory (DMFT) is a method to study correlated electron system. It maps a correlated electron problem in a solid onto an Anderson impurity model, which is solvable through a numerical technique called as an impurity solver. Merging DMFT with a density functional theory (DFT) program makes it possible to investigate strongly correlated materials in practice. For realistic calculations, actual implementation of DFT+DMFT demands a number of numerical techniques. We implemented an efficient DFT+DMFT program by combining the SIESTA program and our continuous-time quantum Monte Carlo impurity solver. In this work, we present our implementation of DFT+DMFT part by part. This work was supported by NRF of Korea (Grant No. 2011-0018306) and KISTI supercomputing center (Project No. KSC-2017-C3-0079).

### Keywords:

DFT+DMFT, DFT, DMFT, CTQMC, Monte Carlo, Maximum Entropy

## Temperature induced crossing in the optical bandgap of mono and bilayer MoS<sub>2</sub> on SiO<sub>2</sub>

이근식\*<sup>1</sup>, 박영신\*<sup>1</sup>, 김용철<sup>1</sup>, 김남미\*<sup>2</sup>, 조용철\*<sup>3</sup>, 이승웅\*<sup>3</sup>, 양우철\*<sup>3</sup>, 임현식\*<sup>3</sup>  
<sup>1</sup>울산과학기술원 화학과, <sup>2</sup>숭실대학교 물리학과, <sup>3</sup>동국대학교 물리반도체과학과  
gslee@unist.ac.kr, ysinpark@unist.ac.kr, ., ., ., ., hyunsik7@dongguk.edu

### Abstract:

2D transition metal dichalcogenides material attracts great attention because of the optoelectronic properties and the van der Waals interlayer interaction that is beneficial for futuristic optical devices based heterostructure. We studied difference of MoS<sub>2</sub> monolayer and bilayer photoluminescence behaviors. Experimentally it was observed that as the temperature increases low (~4 K) to around 300K, the monolayer PL intensity overtakes the bilayer's. Also bilayer minimum-energy peak position alter more than that of the monolayer. We calculated dipole transition probability of 1L and 2L MoS<sub>2</sub> at the level of PBE including the spin orbit coupling (SOC). Our calculation shows that 2L-MoS<sub>2</sub> have greater probability than 1L-MoS<sub>2</sub> due to doubled degeneracy in 2L-MoS<sub>2</sub>. Because of the indirect transition(K to gamma) in bilayer, temperature increase can enhance the indirect emission in bilayer. Thus the peak intensity crossovers between monolayer and bilayer. On the other hand peak position variation difference originates from thermal expansion, where we incorporated the thermal expansion coefficients into our calculation by increasing the lattice size.

### Keywords:

MoS<sub>2</sub>, optical property

## Electron and spin transport properties of carbon chains stretched between graphene nanoribbon electrodes

김태현<sup>1</sup>, 김후성<sup>1</sup>, 김용훈\*<sup>1</sup>  
<sup>1</sup>한국과학기술원 EEWS대학원  
y.h.kim@kaist.ac.kr

### Abstract:

Carbon-based nanostructures have attracted considerable attention for the electronic and spintronic applications due to their ballistic quantum transport nature and remarkably long spin-coherence time and distance, respectively. Recently, atomic carbon chains (CCs) have been carved out of graphene using techniques such as high-energy electron beam irradiation. Based on density functional theory and matrix Green's function calculations, we herein study the charge and spin quantum transport properties of CCs bridging graphene nanoribbon electrodes and particularly consider the effects of uniaxial strain and the number of CC atoms. We find that the strain dependence of electron transmissions are strongly affected by the number of CC atoms, but the spin-filter effects are unaffected by strain as well as the number of CC atoms.

### Keywords:

Carbon Chains, Graphene Nanoribbons, Density Functional Theory, Matrix Green's function, Spin-filter

## Theoretical Study of 2D Periodically-driven Hexagonal Lattice Systems by Floquet Theory

문경순\*<sup>1</sup>, 강유성\*<sup>1</sup>

<sup>1</sup>연세대학교 물리학과

kmoon@yonsei.ac.kr, kangkang1124@naver.com

### Abstract:

Topological materials have demonstrated a variety of novel phenomena in recent studies. Such properties can also be realized in periodically driven quantum systems. Recent experiments have shown that the band structure of black phosphorene can be significantly changed by doping alkali ions with varying dopant concentrations<sup>1</sup>. The doped system can be effectively modelled as a generalized hexagonal lattice system with variable hopping parameters. In our work, we will combine these interesting results and study topological phase transitions in generalized hexagonal lattice system under the AC electric field by using Floquet theory.

[1] Jimin Kim et. al., Phys. Rev. Lett. 119, 226801 (2017).

\*This work is supported by Basic Science Research Program through the National Research Foundation of Korea (NRF) funded by the Ministry of Education, Science and Technology (NRF-2016R1D1A1B01013756).

### Keywords:

floquet, topology, black phosphorene

## Fe–Porphyrin-like Nanostructures for Selective Ammonia Capture under Humid Conditions

양(Yang)형모(Hyungmo)<sup>1</sup>, 배(Bae)현후(Hyeonhu)<sup>1</sup>, 박(Park)민우(Minwoo)<sup>1</sup>, 이(Lee)승한(Seunghan)<sup>1</sup>, 김(Kim)기출(Ki Chul)<sup>2</sup>, 이훈경\*<sup>1</sup>  
<sup>1</sup>건국대학교 물리학과, <sup>2</sup>건국대학교 화학공학과  
hklee3@konkuk.ac.kr

### Abstract:

We have explored the feasibility of metal-porphyrin-like graphenes and carbon nanotubes (CNTs) for capturing ammonia, using first-principles thermodynamics simulations. Our results show NH<sub>3</sub> molecules can be selectively adsorbed on a metal atom at room temperature and low pressure while immersed in gas mixtures of NH<sub>3</sub> and H<sub>2</sub>O even. We identified that the optimal candidate for selective NH<sub>3</sub> capture under humid conditions is Fe-porphyrin-like graphene, reaching a working capacity of ~4 mmol/g at not only ambient condition, but also humid condition. This study allows us to discover novel promising Fe-anchored carbon materials for the selective capture of ammonia from humid air at ambient temperature and pressure conditions.

### Keywords:

DFT; porphyrin-like nanostructure; ammonia; humidity; absorption; working capacity

## Band alignment of $WS_2$ /BP heterostructures under applied electric fields

CHA Janghwan<sup>1</sup>, MIN Kyung-Ah<sup>1</sup>, 홍석륜\*<sup>1</sup>

<sup>1</sup>Department of Physics and Graphene research institute, Sejong University  
hong@sejong.ac.kr

### Abstract:

Recently, two-dimensional (2D) materials have been actively studied in various fields. It is known that graphene, one of the 2D materials consisting of carbon atoms, has excellent electron mobility and permeability. Despite these excellent properties of graphene, one drawback in use of graphene in the electronic devices is that electron mobility of graphene is considerably reduced when the band gap is generated. To overcome such drawback, diverse 2D semiconducting materials have been investigated, including transition metal dichalcogenides (TMDs) and black phosphorus (BP). Layered structures such as TMDs and BP show the variations in electronic structure depending on the number of layers: As the number of layers increases, their band gaps are decreased. Here, we have studied atomic and electronic structures of heterostructures between  $WS_2$  and BP using density functional theory (DFT) calculations. Especially, we investigate the effect of applied electric fields on the electronic structure and band alignment of  $WS_2$ /BP heterostructures.

### Keywords:

Black phosphorus,  $WS_2$ , ab-initio, heterostructure, electronic structure, band alignment

## Vertical Dielectric Screening of Few-Layer Carbon Allotropes

이훈경\*<sup>1</sup>, 구자현<sup>1</sup>, 박민우<sup>1</sup>

<sup>1</sup>건국대학교 물리학과  
hkiee3@konkuk.ac.kr

### Abstract:

수 층 반 데르 발스 (van der Waals) 2 차원 반도체에서 수직 유전율은 기본 상수이다. 2차원 반도체에 수직하게 인가된 전기장에 대한 유전율이 두께에 민감하다는 주장이 널리 받아들여지는 것과는 달리 선형 응답 이론 (약한 자기장 한계 이내)을 기반으로 한 우리의 제 1 원리 계산은 이러한 전기장에 대한 응답이 두께와 무관하다는 것을 보여주었으며 그 값은 해당 물질이 3차원 벌크 구조일 때와 같다. 이러한 사실은 저차원 물질의 유전체 스크리닝을 계산하고 예측할 수 있는 효율적이고 믿음직한 방법을 통하여 작은 밴드 갭과 넓은 밴드 갭을 가진 다양한 2D 대극 반도체를 통하여 입증하였다. 이를 바탕으로, 우리는 전기장이 인가 된 2차원 반도체에서 밴드 갭의 변화를 설명하고 예측할 수 있었다. 나아가 수직 압력 또는 복합 구조를 통해 층간 거리를 변경을 통해 수직 유전율을 조절 할 수 있음을 제안했다. 우리가 제안한 방법들을 통하여 수직방향으로 인가된 전기장에 대한 유전율과 이에 대한 이해를 실질적으로 단순화 할 수 있었으며 이를 탄소 동소체들에 적용하였다.

### Keywords:

Carbon allotropes, Graphyne, Graphdiyne, Electric field, Dielectric constant

## Application of branching ratio calculation based on First principles: *5d*, *4d* and *3d* transition metal materials

김도훈<sup>1</sup>, 심재훈<sup>1</sup>, 윤희기<sup>1</sup>, 한명준\*<sup>1</sup>

<sup>1</sup>한국과학기술원 물리학과  
mj.han@kaist.ac.kr

### Abstract:

The branching ratio is generally used to estimate spin-orbit coupling strength in experiments. We present the calculation results of spin-orbit coupling and branching ratio for a variety of *5d*, *4d*, and *3d* transition metal materials based on first principles<sup>[1]</sup>. The calculated branching ratios of *5d* and *4d* transition metal materials are in good agreement with experimental data. For *3d* transition metals, the difference between the calculation and experiment can be understood by core-valence interaction whose energy scale is competing to spin-orbit coupling of p orbitals. These results support a theoretical understanding the relation between branching ratio and spin-orbit coupling<sup>[2]</sup>.

[1] J.-H. Sim, H. Yoon, S. H. Park, and M. J. Han, Physical Review B 94, 115149 (2016)

[2] B. T. Thole and G. Van der Laan, Physical Review A 38, 1943 (1988)

### Keywords:

First pinciple, Density Functional Theory, Branching ratio, XAS, Spin-Orbit Coupling

## Effect of spin-orbit coupling on the zigzag nanoribbon structures of Bi(111) and Sb(111) bilayers

정상민<sup>1</sup>, 조준형\*<sup>1</sup>, 김현중<sup>2</sup>, 이세호<sup>1</sup>  
<sup>1</sup>한양대학교 물리학과, <sup>2</sup>한국고등과학기술원  
chojh@hanyang.ac.kr

### Abstract:

A single Bi(111) bilayer is known to be the two-dimensional (2D) topological insulator where 6p valence and conduction bands are inverted with each other due to spin-orbit coupling (SOC). Using density-functional theory (DFT) calculations, we find that SOC switches the ground-state structure of the zigzag nanoribbon of the Bi(111) bilayer. Our DFT calculation without including SOC shows that the metallic zigzag edge structure containing one dangling-bond electron per each edge atom is much stabilized by the Peierls distortion or reconstruction (where two hexagons are converted into a pentagon-heptagon pair) with a large band-gap opening. However, the inclusion of SOC drastically changes the stability of the edge structures, i.e., the Peierls distortion is suppressed to be converged to the shear distortion from the ideal zigzag edge structure. It is revealed that such a SOC-induced structural switch is caused by the presence of the gapless edge states which are topologically protected by time reversal symmetry. Interestingly, one-dimensional edge states in the shear-distortion structure are found to show the giant Rashba-type spin splitting caused by large orbital angular momentum, as observed in a recent spin-resolved angle-resolved photoemission spectroscopy. By contrast, our DFT calculations for the zigzag nanoribbon of the Sb(111) bilayer predict that the reconstruction is the most stable structure independent of the inclusion of SOC, reflecting a normal insulator

### Keywords:

bismuth, topological insulator

## Development of a first-principles approach for the finite-bias DFT calculation and its verifications using molecule junction systems.

김용훈\*<sup>1</sup>, 이주호<sup>1</sup>, 여현우<sup>1</sup>, 김한솔<sup>1</sup>

<sup>1</sup>한국과학기술원 EEWS대학원  
y.h.kim@kaist.ac.kr

### Abstract:

Describing the non-equilibrium system induced finite bias within the first-principle calculations is one of the key challenges for the development of next-generation nano-electronic devices. However, non-equilibrium Green's function (NEGF) formalism, which is known as the most general and rigorous theoretical framework, has still a limitation of non-variational properties. In this presentation, we show new approach to describe the non-equilibrium system by introducing our recently developed method named multi-space density functional theory (MS-DFT). We describe the system in which the finite bias is applied to the molecular junctions, and verify their electrical properties as comparing to the NEGF formalism. This conclusion will give the justification for MS-DFT and critical insight in constructing transport calculation.

### Keywords:

multi-space density functional theory, molecule junction

## 극저준위 방폐물 관리시스템을 위한 정형/비정형 방폐물 표준물질 제작

황상훈\*<sup>1</sup>, 선용근<sup>1, 2</sup>, 이종만<sup>1</sup>

<sup>1</sup>한국표준과학연구원 방사선표준센터, <sup>2</sup>경북대학교 물리학과  
shhwang@kriss.re.kr

### Abstract:

국내 최초 원자로인 고리1호기의 영구정지 결정에 따라 원전해체시 발생하는 방사성폐기물의 분류 및 관리 체계의 구축이 필요하다. 이를 위해 원전 해체 시 대량으로 발생하는 정형/비정형 극저준위 방폐물의 방사능을 전처리 없이 측정하여 방폐물과 일반폐기물로 분류할 수 있는 3차원 스캐너를 이용한 방사능 측정 시스템을 구축중이다. 한국표준과학연구원에서는 이 시스템의 성능 검증 및 방폐물의 표준물질의 제작을 위해 극저준위 방폐물 표준물질의 제작을 연구중이다. 측정 대상물의 크기가 최대  $1 \times 1 \times 1 \text{ m}^3$ 이므로 대면적의 방사성 표준선원의 제작이 필요하다. 본 연구에서는 대면적 방사성 선원의 제작 및 선원의 특성에 대해서 발표할 예정이다.

### Keywords:

방사성 표준물질, 극저준위 방폐물

## 등온미세열량계를 이용한 단반감기 방사 선원 측정법 개발

김병주\*<sup>1, 2</sup>, 박영진<sup>1, 2</sup>, 이경범\*<sup>1, 2</sup>, 이종만<sup>1, 2</sup>, 박태순<sup>1, 2</sup>, 황상훈<sup>1, 2</sup>

<sup>1</sup>과학기술연합대학원대학교 측정과학, <sup>2</sup>한국표준과학연구원 화학의료본부 방사선센터  
aodnes@naver.com, lee@kriss.re.kr

### Abstract:

등온미세열량계를 이용한 방사선 측정법은 미국, 독일, 일본 등 선진국에서 개발이 되었으며 상용화 되어져 있다. 이 방법은 외부의 온도 간섭이 없는 상태에서 방사선원의 붕괴에너지가 열량계에서 흡수되면서 생기는 열의 흐름을 측정하는 방법이다. 열의 흐름은 See back 효과를 바탕으로 thermo-electric 모듈에 의해 전기적 일률로 바뀌게 된다. 이 방법은 mCi 이상의 방사능을 측정할 때, 그리고 밀봉 선원을 측정할 때 이점이 존재한다.

그러나 등온미세열량계는 장반감기의 선원에서 측정소급성이 확보되었으며, 단반감기에 대한 측정 소급성은 확보되어 있지 않은 상태이다. 이는 열량계가 측정 기능을 원활히 하기 위해서 8시간 이상의 준비 시간, 즉 안정화 시간이 필요한데 이로 인해 단반감기 선원 측정에 부정확성을 초래하는 원인이 될 수 있다.

과거에 I-123 선원, F-18 선원 등이 사용되었다. 이번 연구는 그외 단반감기에 속하는 선원을 사용해서 데이터의 재현성을 확인한다. 그리고 등온미세열량계의 특성을 정밀하게 파악해서 실험적 근거가 되는 보정인자를 확보해서 단반감기 측정에 대한 소급성을 확보하는 것을 목표로 한다.

### Keywords:

등온미세열량계, 등온과정, 흡수효율, 안정화 시간, 반감기

## Development of a position-sensitive CZT detector with coplanar grid electrode

김병준<sup>1</sup>, 이경범\*<sup>2</sup>, 이종만<sup>2</sup>, 황상훈<sup>2</sup>, 박태순<sup>2</sup>

<sup>1</sup>과학기술연합대학원대학교 측정과학, <sup>2</sup>한국표준과학연구원 방사선표준센터  
lee@kriss.re.kr

### Abstract:

The finite-element analysis was done to optimize position-sensing coplanar grid electrode geometry. CdZnTe crystals manufactured by PAM-XIAMEN with customized electrode geometry have been tested. After digitizing pre-amplifier signals, a trapezoidal digital filter was adopted to enhance the signal to noise ratio. The energy resolution of 4.3 % FWHM at 662 keV  $\gamma$ -ray energy was obtained. The measured results show the dramatic improvement with position-sensing technique.

### Keywords:

CdZnTe detector, Coplanar grid, Position-sensing, Trapezoidal digital filter, Moving window deconvolution

## Growth of LiF Single Crystal by Micro Pulling Down Technique

김홍주\*<sup>1</sup>, 김민정<sup>2</sup>, 조재영<sup>1</sup>, 이주영<sup>1</sup>

<sup>1</sup>Department of Physics, Kyungpook National University, <sup>2</sup>Korea Hydro & Nuclear Power Co. - Central Research Institute  
hongjoo@knu.ac.kr

### Abstract:

Several methods are employed for the single crystal growth from the melt of the material such as Czochralski, Bridgman, Kyropoulos and Micro pulling down. Each method has its own advantages, however the Micro pulling down method is the fastest growing speed among all. The platinum or iridium crucibles are used for keeping the charge of the desired material. The crucible contains a small nozzle at the bottom from which the melt moves downwards and start crystallization along the seed direction, which is attached with a platinum bar. Many important single crystalline scintillating fibers were grown by this technique. The optimization of Micro pulling down technique for the growth of LiF single crystal is carried out and will be discussed.

### Keywords:

Micropullingdown, crystal, LiF

## 국립암센터 230MeV 양성자 치료시설 빔특성 및 연구현황

이세병\*<sup>1</sup>

<sup>1</sup>국립암센터 양성자치료센터  
sebyeong@gmail.com

### Abstract:

국립암센터는 국내최초로 양성자치료시설을 설치하고 2007년부터 환자치료를 시작하여 현재까지 2700여명의 암환자를 치료하고 있다. 양성자가속기는 사이클로트론으로 230MeV로 양성자빔을 가속시킬수 있고 3개의 치료실과 1곳의 연구용 빔포트를 갖고 있다. 현재 연구용 빔라인은 아직 노즐이 설치되지 않아 고정빔 노즐이 설치되어 있는 치료실에서 양성자빔을 이용한 실험들을 지원하고 있고 환자치료운영과 병행해야 하기 때문에 제한적으로만 공동연구형태로 외부빔 실험을 지원하고 있다. 국내 연구기관들과 입자방사선 검출기 개발 관련 연구와 유럽 연구진과 우주개발 관련된 연구를 수행 중에 있다. 이번발표에서는 양성자치료시설의 현황, 현재진행 중인 양성자빔관련 비임상 실험의 소개와 향후 연구빔라인 구축에 대한 계획을 설명할 예정이다.

### Keywords:

양성자가속기, 사이클로트론, 양성자빔, 양성자치료

## 실리콘 기반 배열형 센서의 시뮬레이션 연구

박환배\*<sup>1</sup>, 송석준<sup>1</sup>, 전해빈<sup>1</sup>, 이만우<sup>3</sup>, 이해영<sup>2</sup>

<sup>1</sup>경북대학교 물리학과, <sup>2</sup>기초과학연구원, <sup>3</sup>동남권원자력의학원  
sunshine@knu.ac.kr

### Abstract:

X-ray를 직접 방식으로 측정하기 위한 의료용 검출기 제작을 목적으로 배열형 픽셀 센서 제작을 위한 연구를 진행하였다. 입사된 입자의 반응 확률을 높이기 위해 고저항 n형 실리콘 웨이퍼에 PIN 구조를 이용하여 active volume을 만들었다. 각 픽셀에는 스위치로써 Junction Field Effect Transistor (JFET) 구조를 넣어주었고 스위치의 On/Off는 게이트 전압에 의해 조절된다. 픽셀 사이에는 p 도핑하여 필드웨이퍼를 만들어 픽셀을 구분해 주었다. MxM 배열의 픽셀의 신호를 읽어내기 위해서 하나의 행의 스위치를 On 상태로 만들어 같은 행의 모든 픽셀 신호를 열-방향의 리드아웃 라인을 통해 읽어낸 후 다음 행에 대해 반복한다. 이 과정을 계속하여 모든 픽셀의 신호를 읽어낸다. 때문에 리드아웃 라인과 스위치 컨트롤 라인이 수직하게 위치하고, 이를 위해 double metal 구조를 만들어주었다. 센서 시뮬레이션을 통해 게이트 전압에 따른 드레인 전류의 차이를 획득하여 JFET 구조의 스위치가 잘 작동하는 것을 확인하였다. 현재는 센서 공정을 위한 디자인 단계에 있다. 이번 학회에서는 센서의 컨셉트와 시뮬레이션 결과에 대해서 발표하고자 한다.

### Keywords:

의료용 검출기, Junction Field Effect Transistor (JFET), 실리콘 픽셀 센서, Double Metal 구조

## Measurement of Fast Neutron Burst at the 100-MeV beam dump of KOMAC

이필수\*<sup>1</sup>, 윤상필<sup>1</sup>, 당정증<sup>1</sup>, 권혁중<sup>1</sup>, 김한성<sup>1</sup>, 조용섭<sup>2</sup>

<sup>1</sup>한국원자력연구원 양성자가속기연구센터 가속기연구실, <sup>2</sup>한국원자력연구원 양성자가속기연구센터  
pilsoolee@kaeri.re.kr

### Abstract:

When accelerated protons bombard a metal target, neutrons constituting the atom of the target metal can emerge with part of the kinetic energy of incident protons. The energy and angular distribution of the neutrons are wholly dependent upon not only the beam condition but geometrical and physical properties of the target metal and surrounding structures. In the present study, the burst of fast neutrons generated at the 100-MeV beam dump, which is located at the end of the linear beam line at KOMAC, were measured employing direct and indirect methods. In the measurements, a thin plastic scintillation and high-purity germanium detectors were utilized for counting neutrons generated at the beam dump and gamma rays emitted from radioactive isotopes in activated metal foils, respectively. In this presentation, the details of the measurements in conjunction with relevant Monte-Carlo simulation results will be described.

Acknowledgements: This work has been supported through KOMAC (Korea Multi-purpose Accelerator Complex) operation fund and the NRF grant (No. NRF-2017M2A2A6A02071070) funded by MSIT (Ministry of Science and ICT).

### Keywords:

KOMAC, beam dump, fast neutron burst, neutron measurement

## Background measurements of newly built radon chamber detectors for underground experiments environment.

이무현\*<sup>2</sup>, [SEO Kyungmin](#)<sup>1</sup>, LEE HyeYoung<sup>2</sup>, LEE Hyunsu<sup>2</sup>, OLSON Stephan Lars<sup>2</sup>, LEE Jaison<sup>2</sup>, KIM Wootae<sup>2</sup>, KIM Hyounggyu<sup>2</sup>, LEONARD Douglas<sup>2</sup>, JANG Sangcheol<sup>3</sup>, KIM Hyunsoo<sup>1</sup>, YOON Young Soo<sup>2</sup>, KIM Yeongduk<sup>2</sup>

<sup>1</sup>Department of Physics, Sejong University, <sup>2</sup>Center for Underground Physics, Institute of Basic Science, <sup>3</sup>Department of Physics, Seoul National University  
moohyun.lee@gmail.com

### Abstract:

It is very important to monitor the amount of radon (Rn-222) in the underground experiments such as rare decay and dark matter experiments with ultra low background requirements. The radioactivity from the radon can be a significant background source to the experiments and need to be measured precisely. Over the last two years, the 70 L radon chamber detector used in the KIMS experiment was upgraded and tested. The energy resolutions of alpha particles emitted from the decays of the daughter particles were measured to be better than 0.6%. However, the background level of this radon detector was ~70 mBq/m<sup>3</sup>, which is very good for a regular radon detector for an atmosphere measurement but not suitable for the low background measurements. The high background level would be coming from radon daughters on the inner surface of the detector when it was exposed to the atmosphere for a year after an electropolishing work. We have constructed two new radon chamber detectors of a round shape design with a thin (~3 mm) stainless steel plate for a light weight and a more uniform electric field. The inner surfaces of the two chambers were also electropolished to get rid of the radon daughters on the surfaces. In this poster, we will present the background level measurements of the new radon chamber detectors.

### Keywords:

radon, alpha, silicon photo diode, radioactivity, chamber

## Compact measurement system employing scintillating crystals at low temperatures

김용함\*<sup>1</sup>, 김혜림<sup>1, 2</sup>

<sup>1</sup>기초과학연구원, 지하실험연구단, <sup>2</sup>경북대학교, 물리학과  
yhk@ibs.re.kr

### Abstract:

We have developed a cryogenic detection system to investigate scintillating crystals for rare event search experiments. It simultaneously measures heat and light of the crystals at millikelvin temperatures. A 1 cm<sup>3</sup> scintillating crystal and a 1.5x1.5x0.05 cm<sup>3</sup> wafer are utilized as a particle absorber and a light absorber. Metallic magnetic calorimeter sensors determine phonons of the crystals. We employed a calcium molybdate crystal, sodium molybdate crystal and lithium molybdate crystal.

### Keywords:

low temperature detector, scintillating crystal, metallic magnetic calorimeter

## 탈륨을 포함한 $Tl_2LiScCl_6$ 엘파솔라이트 섬광검출기 특성조사

김홍주\*<sup>1</sup>, 김민정<sup>2</sup>, 조재영<sup>1</sup>, KHAN Arshad<sup>1</sup>, ROOH Gul<sup>3</sup>

<sup>1</sup>경북대학교 물리학과, <sup>2</sup>한국수력원자력 중앙연구원, <sup>3</sup>Department of Physics, Abdul Wali Khan University  
hongjoo@knu.ac.kr

### Abstract:

클로로 엘파솔라이트 계열인  $Tl_2LiScCl_6$  단일 섬광결정은 브리즈만 방법으로 성장되었다. X-ray 여기에 의한 발광 스펙트럼은 300 nm에서 550 nm 이고 385 nm 에서 가장 큰 피크를 나타낸다.  $Tl_2LiScCl_6$ 의 에너지 분해능, 섬광량, 감쇠 시간 등의 섬광 특성은 Cs-137 감마선원으로 측정하였다. 662 keV의 광전 피크에 의한 에너지 분해능은 11% (FWHM) 이다. 이 섬광결정의 섬광량을 측정하기 위해서 LYSO 섬광 결정의 섬광량과 비교분석을 하였다. 절대섬광량이 33000 ph/MeV 인 LYSO 섬광결정과 비교하였을 때  $Tl_2LiScCl_6$  섬광결정의 섬광량은  $23300 \pm 2300$  ph/MeV이다. 개발된 섬광결정은 두 개의 감쇠 요소를 가진다. 측정된 감쇠 시간은 1092 ns (93%)과 2826 ns (7%)이다. 이 검출기는 높은 유효원자번호와 밀도를 가지기 때문에 의학 영상화나 방사선 검출에 유용하게 쓰일 수 있다. 뿐만 아니라  $6Li(n, \alpha)$  현상을 이용해 중성자 검출에도 사용될 수 있다.

### Keywords:

$Tl_2LiScCl_6$  섬광 결정, 브리즈만 방법, 에너지 분해능, 절대 섬광량

## Measurements of detector material samples with two HPGe detectors at the YangYang Underground Lab.

이은경<sup>1</sup>, 김영덕\*<sup>1</sup>, 한Kevin인식<sup>2</sup>, LEE Moohyun<sup>1</sup>, LEONARD Douglas S.<sup>1</sup>, 김고운<sup>3</sup>, 전은주<sup>1</sup>, 강운구<sup>1</sup>, 박수연<sup>3</sup>

<sup>1</sup>기초과학연구원 지하실험연구단, <sup>2</sup>이화여자대학교 과학교육과, <sup>3</sup>이화여자대학교 물리학과  
yeongduk.kim@gmail.com

### Abstract:

Two major experiments, the AMoRE (Advanced Mo based Rare process Experiment) searching for neutrino-less double beta decay and the COSINE searching for dark matter WIMPs (Weakly Interacting Massive Particles), are running in the Yangyang underground laboratory (Y2L). To understand their signals, it is necessary to know the backgrounds from their detector materials like fasteners, crystal, cables, connectors, and etc. By using two 100% HPGe detectors at the Y2L, the background levels of each material samples were measured and analyzed by using efficiencies estimated by a Geant4 simulation tool kit. We will present background measurements of the samples together with an improvement in the efficiency calibration using a mixed source including 10 known radioactive isotopes in this poster.

### Keywords:

HPGe detector, Efficiency, Calibration, Y2L, Geant4

## $\text{Li}_2\text{MoO}_4$ Crystal Growing for the AMoRE at the Center for Underground Physics of IBS

김대연<sup>1</sup>, 강운구<sup>1</sup>, 나세진<sup>1</sup>, 손주경<sup>1</sup>, 신건아<sup>1</sup>, 이무현<sup>1</sup>, 이은경<sup>1</sup>, 이철호<sup>1</sup>, 최준석<sup>1</sup>, LEONARD Douglas<sup>1</sup>, OLGA Gileva<sup>1</sup>, 박향규<sup>1, 2</sup>, 김홍주<sup>3</sup>, 김영덕\*<sup>1</sup>

<sup>1</sup>Center for Underground Physics, Institute for Basic Science (IBS), <sup>2</sup>Department of Physics, Korea University, <sup>3</sup>Department of Physics, Kyungpook National University  
ydkim@sejong.ac.kr

### Abstract:

The Center for Underground Physics (CUP) of IBS has been preparing the AMoRE (Advanced Molybdenum based Rare-decay Experiment) for neutrinoless double beta decay search by using scintillation crystals. The experiment requires ultra-pure scintillation crystals to minimize the internal background from the crystals because it is looking for extremely rare events. We have grown a few  $\text{Li}_2\text{MoO}_4$  crystals by using  $\text{MoO}_3$  powders which was purified by a sublimation technique. We succeeded in a double-crystallization growth by growing a crystal by using only grown  $\text{Li}_2\text{MoO}_4$  crystals as raw materials. XRD patterns of each grown crystals were measured to confirm their compositions. Purities of the crystals were measured by a HPGe detector and a ICP-MS. We will present the growths of the  $\text{Li}_2\text{MoO}_4$  crystals and their measurements results.

### Keywords:

Single crystal, AMoRE, Scintillation, Double-crystallization,  $\text{Li}_2\text{MoO}_4$

## Small NaI Crystal Growing at the Center for Underground Physics of IBS

김영덕\*<sup>1</sup>, 이철호<sup>1</sup>, 김대연<sup>1</sup>, 이현수<sup>1</sup>, 손주경<sup>1</sup>, 최준석<sup>1</sup>, 신건아<sup>1</sup>, 이무현<sup>1</sup>, 나세진<sup>1</sup>, 박향규<sup>1, 2</sup>, 김홍주<sup>3</sup>  
<sup>1</sup>Center for Underground Physics, Institute for Basic Science (IBS), <sup>2</sup>Department of Physics, Korea University, <sup>3</sup>Department of Physics, Kyungpook National University  
ydkim@sejong.ac.kr

### Abstract:

The Center for Underground Physics (CUP) has been conducting the COSINE experiment to search for dark matter WIMPs (Weakly Interacting Massive Particles) at the Yangyang underground laboratory. The experiment requires large size and ultra-pure NaI(Tl) crystals grown from highly purified NaI powders as detectors for an upgrade. We had set up a small-size grower for an R&D of the crystal growing and a full-size grower for growing large size crystals for the final detectors. With the small-size grower, we have been growing pure NaI crystals. Purities of the grown crystals were confirmed by ICP-MS measurements and their XRD patterns were also measured. In the near future, we will grow Tl doped NaI crystals at the small-size grower and optimize the growth condition of the NaI(Tl) crystals before trying the full-size grower. In this poster, we will present growing of the small NaI crystals and their measurement results.

### Keywords:

Single crystal, COSINE experiment, NaI(Tl), scintillation

## Accident dosimetry using SAAD-POSL method with samples from building materials

홍덕균\*<sup>1</sup>, 권혜진<sup>1</sup>, 김학선<sup>1</sup>, 박호진<sup>1</sup>  
<sup>1</sup>강원대학교 물리학과  
dghong@kangwon.ac.kr

### Abstract:

To establish a fast assessment method of accidental dose, core disc samples were extracted from a heated red brick, roof tile, ceramic tile, and toilet porcelain, which are commonly used building materials. We examined the physical characteristics of POSL signals from these samples, and tested the reliability of the SAAD-POSL method over a range of 7 Gy. In addition, when the SAAD-POSL method was applied, the minimum detectable dose (MDD) was as low as 0.01 Gy for the heated red brick, and the calculation time for an equivalent dose was as short as 2 h.

### Keywords:

Accidental dose, Building material, POSL, SAAD method

## 전자개인선량계의 저항소자를 이용한 피폭선량 측정

김명진<sup>1</sup>, 김아름<sup>2</sup>, 유형준<sup>2</sup>, 이정태<sup>2</sup>, 홍덕균\*<sup>3</sup>

<sup>1</sup>(주)라드피온, <sup>2</sup>한국원자력안전기술원, <sup>3</sup>강원대학교 물리학과  
dghong@kangwon.ac.kr

### Abstract:

EURADOS (European radiation dosimetry group)에서는 방사선 사고 또는 테러 시 개인선량계를 착용하지 않은 종사자 및 일반인의 피폭선량 추정을 위해 휴대폰, 신용카드 등의 개인 소지물품을 이용한 선량평가 연구를 현재 수행하고 있다. 국내에서는 방사선투과 검사 종사자들 중 개인선량계 판독값을 신뢰할 수 없는 경우, 추가적인 선량평가를 위한 보조자료로서 종사자의 휴대폰 내 저항소자를 이용한 선량평가를 수행하고 있으나, 작업 시 휴대폰을 지참하지 않았을 경우 종사자의 선량을 추정할 수 없다는 단점이 지적되고 있다. 본 연구에서는 방사선투과검사 종사자들에게 착용이 의무화 되어있는 전자개인선량계 내부 저항소자의 TL 측정을 통해 방사선사고 시 대체선량계로서의 가능성을 평가하였다. 또한 전자개인선량계 저항소자의 공간 분포에 따른 피폭선량 변화를 비교하였다.

### Keywords:

전자개인선량계, 저항소자, TL 측정, 피폭선량

# Production cross sections of the $^{100}\text{gRh}$ , $^{105}\text{gAg}$ , and $^{106\text{m}}\text{Ag}$ from $^{\text{nat}}\text{Pd}(p,x)$ reactions in the energy region up to 42.61 MeV

NGUYEN hien Thi<sup>1</sup>, 김광수<sup>1</sup>, 김귀년\*<sup>1</sup>, NGUYEN Do van<sup>2</sup>

<sup>1</sup>경북대학교 물리학과, <sup>2</sup>Institute of Fundamental Research and Application, Duy Tan University  
gnkim@knu.ac.kr

## Abstract:

In this work, we determined production cross sections of  $^{100}\text{gRh}$ ,  $^{105}\text{gAg}$ , and  $^{106\text{m}}\text{Ag}$  from  $^{\text{nat}}\text{Pd}(p,x)$  reactions in the energy region up to 42.61 MeV using the stacked target irradiation technique at the MC50 cyclotron of the Korea Institute of Radiological and Medical Sciences (KIRAMS). The natural Palladium ( $^{\text{nat}}\text{Pd}$ ) target and natural Copper ( $^{\text{nat}}\text{Cu}$ ), natural Aluminium ( $^{\text{nat}}\text{Al}$ ) monitor foils were irradiated by 45 MeV proton beam and their products were measured by residual activities using a coaxial high purity germanium (HPGe) detector (ORTEC) with an energy resolution of 1.8 keV at the 1332.5 keV  $\gamma$ -ray of  $^{60}\text{Co}$ . The experimental cross sections of the investigated reactions were compared with data reported in literature and theoretical predictions of TENDL-2015 libraries based on TALYS code.

## Keywords:

:  $^{\text{nat}}\text{Pd}(p, x)$  reactions cross section, stacked- foil activation technique, Off-line  $\gamma$ -ray spectrometric technique, MC50 cyclotron, TENDL-2015.

## Neutron capture yield measurements of $^{162}\text{Dy}$ and $^{164}\text{Dy}$ at Japan Proton Accelerator Research Complex

노태익\*<sup>1</sup>, 이지은<sup>1</sup>, 김귀년<sup>2</sup>, 김광수<sup>2</sup>, 이만우<sup>3</sup>, 강영록<sup>3</sup>, 신성균<sup>4</sup>

<sup>1</sup>Dong-A University, Department of Physics, <sup>2</sup>Department of Physics, Kyungpook National University,

<sup>3</sup>Dongnam Institute of Radiological and Medical Science, <sup>4</sup>Division of Advanced Nuclear Engineering,  
POSTECH  
tiro@donga.ac.kr

### Abstract:

Neutron capture yields of dysprosium (Dy) isotopes were measured at the Materials and Life Science Experimental Facility (MLF) of the Japan Proton Accelerator Research Complex (J-PARC). The isotopically-enriched samples were used. The NaI(Tl) spectrometer of the Accurate Neutron-Nucleus Reaction Measurement Instrument (ANNRI) was used to detect gamma-rays from the neutron capture reaction. The detector response function was determined using the Monte Carlo simulation. The experiment results compared with the previous experimental data JENDL-4.0 and the evaluated ENDF/B-VII data.

\*This R&D was supported by the NRF grant funded by MEST (Center for Korean J-PARC Users, Grant No. NRF-2013K1A3A7A06056592).

\*This work was supported by the National Research Foundation of Korea(DIRAMS) grant funded by the Korea government(MSIP) (No. 50496-2016)

### Keywords:

J-PARC, neutron capture cross-sections, dysprosium

## Cross-section measurements of proton-induced reactions on natural Zn using 100 MeV proton beam

PARK J. K.\*<sup>1</sup>, JUNG M.-H.<sup>1</sup>, KIM C.<sup>1</sup>, HWANG Y. S.<sup>1</sup>, YEO S.<sup>1</sup>, LEE C. Y.<sup>1</sup>, CHO W.-J.<sup>1</sup>, KIM D. S.<sup>1</sup>, LEE J. S.<sup>1</sup>

<sup>1</sup>Korea Multi-purpose Accelerator Complex, Korea Atomic Energy Research Institute, Gyeongju 780-904, Korea  
jkuepark@kaeri.re.kr

### Abstract:

Cross-section measurements for proton-induced reactions on natural Zn foils have been carried out at an energy of 100 MeV proton beam. To determine the incident proton flux, stacked Zn foils were activated along with Cu and Al monitor foils, as well as the accumulated particles incident on the foils are directly measured. Here we have measured the cross-sections for the  ${}^{\text{nat}}\text{Zn}(p,x){}^{67}\text{Cu}$  and  ${}^{\text{nat}}\text{Zn}(p,x){}^{67}\text{Ga}$  reactions in the 64.2 to 101 MeV energy range. The  ${}^{67}\text{Cu}$  and  ${}^{67}\text{Ga}$  radionuclides show gamma ray peaks at the same energy and have similar half-life times. The overlapped gamma spectra for  ${}^{67}\text{Cu}$  and  ${}^{67}\text{Ga}$  were separated by employing an analytical method without the support of radiochemical separation. The cross-section data of  ${}^{67}\text{Cu}$  in this work agree well with those from TALYS code reported previously, although they lie higher than the previous experimental results.

### Keywords:

cross-section, proton beam,  ${}^{\text{nat}}\text{Zn}(p,x){}^{67}\text{Cu}$ ,  ${}^{\text{nat}}\text{Zn}(p,x){}^{67}\text{Ga}$

# Measurement of Delayed Gamma-ray Energy Spectrum from Residual Nuclide for $^{nat}\text{Pb}(p,xn)\text{Bi}$ Reaction by 100-MeV Proton Accelerator

윤정란\*<sup>1</sup>, 이지은<sup>1, 3</sup>, 노태익<sup>1</sup>, 이삼열<sup>2, 3</sup>

<sup>1</sup>Department of Physics, Dong-A University, <sup>2</sup>Department of Radiological Science, Dongseo University,  
<sup>3</sup>Center for Radiological Environment & Health Science, Dongseo University  
yoonjr@dau.ac.kr

## Abstract:

The gamma-ray energy spectrum was measured from  $^{nat}\text{Pb}(p,xn)\text{Bi}$  nuclear reaction. Irradiation experiment was performed at the high-intensity 100-MeV proton linac facility (Korea Multi-purpose Accelerator Complex, KOMAC). The HPGe detector was used to measure the gamma-rays of the samples. In general, the kind of nuclear reaction and its probability vary depending on the energy of the proton. In the current study, we observed that the proton reaction spallation neutron was generated between the lead target and the high energy proton beam. From delayed gamma-ray generated in the produced nucleus, it has been compared the gamma-ray peak intensity to distinguish the decay series. This process is important to obtain proton nuclear reaction cross-section.

## Acknowledgement

This work was supported by Dongseo University "Dongseo Frontier Project" Research Fund of 2015

## Keywords:

Proton induced reaction, HPGe detector,  $^{nat}\text{Pb}(p,xn)\text{Bi}$ , delayed gamma-ray, 100-MeV proton beam, KOMAC

## MCMC study of the elastic alpha-carbon-12 scattering at low energies

윤희은<sup>2</sup>, 안도슁이치\*<sup>1</sup>

<sup>1</sup>선문대학교 정보디스플레이학과, <sup>2</sup>선문대학교 나노과학과  
shungichi.ando@gmail.com

### Abstract:

We study the parameter fitting of the amplitude of elastic alpha-carbon-12 scattering at low energies by employing Markov Chain Monte Carlo (MCMC) method. The amplitude of the reaction is constructed by using an effective field theory, which has a systematic perturbation expansion method, and the parameters of the theory are fitted to the existing precise data at low energies. After fitting the parameters, we discuss the uncertainties of the amplitudes when extrapolating them to the stellar energy region.

### Keywords:

Markov Chain Monte Carlo, elastic alpha-carbon-12 scattering, effective field theory

## Theoretical study of nuclear structure in the even $^{74-82}\text{Se}$

이수연\*<sup>1</sup>, 이영준<sup>2</sup>, 이종환<sup>1</sup>

<sup>1</sup>동의대학교 물리학과, <sup>2</sup>동의대학교 산업기술개발연구소  
syyi@deu.ac.kr

### Abstract:

Selenium is a component of antioxidants in the heart disease and body tissue that prevents and delays the rate of denaturation, as the World Health Organization and the United Nations Food and Agriculture Organization recognized selenium as a essential nutrient in 1978. Other studies have shown that it controls thyroid function, plays an important role in the immune system, and is effective in preventing and treating cancer and easing AIDS symptoms. Although it is well known about the chemical properties of selenium, there is no study in the structure of selenium's nuclear as a cancer treatment. Of selenium in natural state, the  $^{82}\text{Se}$  is the only radioactive isotope to break down two beta times into  $^{82}\text{Kr}$ . The nuclear structures of selenium isotopes used in anticancer therapy are identified by taking a nuclear physics (nuclear structure theory) approach.

### Keywords:

Selenium, nuclear structure, IBM

## Perturbation analysis of nuclear structure with density functional theory

현창호\*<sup>1</sup>, 김하나<sup>2</sup>, 오용석<sup>2</sup>, PAPAKONSTANTINOOU Panagiota<sup>3</sup>  
<sup>1</sup>대구대학교 과학교육학부, <sup>2</sup>경북대학교 물리학과, <sup>3</sup>RISP, IBS  
obelisque@daum.net

### Abstract:

We investigate the feasibility of a systematic expansion scheme for the study of nuclear structure. We employ a new nuclear energy density functional (EDF) proposed in [P. Papakonstantinou et al., Phys. Rev. C 97, 014312 (2018)], where the EDF is expanded in powers of the Fermi momentum  $k_F$ . First we consider two lowest order terms proportional to  $k_F^3$  and  $k_F^4$  in the interaction part, and calculate the properties of several spherical magic nuclei. We repeat the calculation by adding high order terms  $k_F^5$  and  $k_F^6$ , and investigate the resulting predictions for the nuclear properties. Prediction is significantly improved when we consider three interaction terms,  $k_F^3$ ,  $k_F^4$  and  $k_F^5$ . The fourth term proportional to  $k_F^6$  corrects the precedent results in a limited range, and improves the result marginally. The investigation sheds light on the possibility for an access to perturbative understanding of nuclear structure.

### Keywords:

density functional theory, expansion scheme

## 섬광계수기와 시뮬레이션을 이용한 우주선 뮤온의 천정 각 의존성 확인

권민정\*<sup>1</sup>, 윤희율<sup>1</sup>  
<sup>1</sup>인하대학교 물리학과  
minjung@inha.ac.kr

### Abstract:

우주선은 지구에 입사하면서 지구 대기와 반응해 여러 입자들로 붕괴된다. 그 중 대기와 상호작용이 적은 뮤온은 지상에서 측정하기 쉬운 우주선 중 하나이다. 이러한 뮤온은 지표에 입사하는 천정 각에 따라 검출되는 빈도수가 달라지는데, 그 이유는 입사 천정 각에 따라 지구 대기와 상호작용 하는 경로의 길이가 달라지기 때문이다. 예를 들어 천정으로부터 큰 각을 갖고 입사하는 뮤온은 대기와 반응 하는 경로가 길어서 에너지가 많이 손실 돼 검출 빈도수가 줄어든다.

뮤온 검출 빈도수의 천정 각 의존성을 알아보기 위해 두개의 섬광 계수기를 이용해 동시신호를 측정했다. 본 연구는 세 가지 실험 설정으로 구성 된다. 우선 효율적인 실험 조건을 찾기 위해 섬광 계수기들을 위아래로 붙여 측정한다. 다음으로 배경신호의 영향을 확인하기 위해 섬광 계

수기들을 평행하게 두고 측정한다. 마지막으로 뮤온 계수와 천정각의 관계를 알기 위해 두 섬광계수기의 천정 각을 변화시켜가며 측정한다. 그 측정 결과를 검증하고 보완하기 위해 실험 과정과 동일한 시뮬레이션을 구현했다.

이 연구에서는 천정 각에 따른 뮤온 검출 빈도수를 측정하고 시뮬레이션 결과와 비교했다. 실험결과를 바탕으로 제작한 시뮬레이션을 발전시킨다면 단순한 구조뿐만 아니라 복잡한 구조를 갖는 계수기들의 검출 빈도수를 예측하는데 응용할 수 있을 것이다.

### Keywords:

우주선, 뮤온, 천정각, 섬광계수기, 시뮬레이션

## Infrared dualities on a sphere with twist

김동욱\*<sup>1</sup>, CLOSSET Cyril<sup>2</sup>, 성락경<sup>3</sup>

<sup>1</sup>서울대학교 물리천문학부, <sup>2</sup>TH department, CERN, <sup>3</sup>Yau Mathematical Sciences Center, Tsinghua University  
sg1841@snu.ac.kr

### Abstract:

It was recently proposed that  $N=1$  supersymmetric gauged matrix models have a duality of order four -that is, a quadrality- reminiscent of infrared dualities of SQCD theories in higher dimensions. We show that the zero-dimensional quadrality proposal can be inferred from the two-dimensional Gaiotto-Gukov-Putrov triality. We consider two-dimensional  $N=(0,2)$  SQCD compactified on a sphere with the half-topological twist. For a convenient choice of R-charge, the zero-mode sector on the sphere gives rise to a simple  $N=1$  gauged matrix model. Triality on the sphere then implies a triality relation for the supersymmetric matrix model, which can be completed to the full quadrality.

### Keywords:

gauge theory, matrix model, supersymmetry, infrared duality, compactification, topological twist

## Entanglement entropy of two-particle systems with spin-spin and spin-orbital angular momentum couplings.

박하윤<sup>1</sup>, 이태진\*<sup>1</sup>  
<sup>1</sup>강원대학교 물리학과  
taejin@kangwon.ac.kr

### Abstract:

Entanglement entropy is calculated to measure how closely a given system is entangled. We calculated the entanglement entropy of two-particle systems with spin-spin and spin-orbit angular momentum couplings. Time evolution of the entanglement entropy is studied by using the von Neumann equation.

### Keywords:

entanglement entropy, spin-orbit coupling, von Neumann equation

## Scalar Leptoquark Models for explaining the anomalies from B-meson decays.

노태균<sup>1</sup>, 이현민\*<sup>1</sup>, 최수민<sup>1</sup>, 강유진<sup>1</sup>  
<sup>1</sup>중앙대학교 물리학과  
hminlee@cau.ac.kr

### Abstract:

The currently running Large Hadron Collider (LHC), in particular, the LHCb experiment, has provided several new measurements to test the lepton flavor universality in the Standard Model and confirmed some of the prevailing anomalies from the B-meson decays.

We work in the setup with both singlet scalar and triplet scalar leptoquarks,  $S_1$  and  $S_3$ , to explain  $R_D^{(*)}$  and  $R_K^{(*)}$  anomalies, respectively. Furthermore, we demonstrate the sensitivity of the LHC and HL-LHC for the leptoquark production with the leptoquark couplings to quarks and leptons.

### Keywords:

B-meson decays, Lepton flavor universality, Leptoquarks

## "Study for missing transverse energy in proton-proton collisions at 13 TeV"

권혜진\*<sup>1</sup>

<sup>1</sup>서울대학교 물리천문학부  
zozzz1@naver.com

### Abstract:

The performance of missing transverse energy (MET) is presented. The MET observable is computed as the negative vectorial sum of the momenta of all reconstructed particles in an event. The study is based on the full 2016 dataset collected in CMS detector at the LHC, with an integrated luminosity of 36fb<sup>-1</sup>. Hadronic recoil in the event Z boson decays to two leptons is studied for MET recoil correction. Recoil correction using data-driven fitting results on hadronic recoil as a function of Z boson momentum is discussed.

### Keywords:

MET

## Study of $B^0 \rightarrow K_s^0 K_s^0 K_s^0$ in the Belle experiment

강국현<sup>1</sup>, 김홍주<sup>1</sup>, 박환배\*<sup>1</sup>, 이승철<sup>1</sup>, 전해빈<sup>1</sup>, HIGUCHI Takeo<sup>2</sup>

<sup>1</sup>경북대학교 물리학과, <sup>2</sup>Kavli Institute for the Physics and Mathematics of the Universe, Univ. Tokyo  
sunshine@knu.ac.kr

### Abstract:

The Belle experiment at KEK, Japan recorded 711 fb<sup>-1</sup> data collected at the Y(4S) resonance with asymmetric-energy e<sup>+</sup>e<sup>-</sup> collider. We are interested in the sin2Φ<sub>1</sub> parameter of time dependent charge parity violation (TCPV) in the B<sup>0</sup> → K<sub>s</sub><sup>0</sup>K<sub>s</sub><sup>0</sup>K<sub>s</sub><sup>0</sup> decay. This rare decay mode occurs via b → s quark transition prohibited in Standard Model so that it provides good motivation for new physics search beyond the Standard Model. We present progress status, which includes event reconstruction, background study, and CP fitting, of B<sup>0</sup> → K<sub>s</sub><sup>0</sup>K<sub>s</sub><sup>0</sup>K<sub>s</sub><sup>0</sup> study using Monte Carlo data.

### Keywords:

Belle, TCPV, B meson, CKM angle

## Study for merged electron identification using multivariate techniques at 13TeV.

고상현\*<sup>1</sup>, 유휘동\*<sup>1</sup>

<sup>1</sup>서울대학교 물리천문학부

sang.hyun.ko@cern.ch, hwi.dong.yoo@cern.ch

### Abstract:

In the CMS experiment, a pair of collimated electrons can be merged into a single reconstructed electron through clustering several energy deposits from the electron and its radiated bremsstrahlung photons in electromagnetic calorimeter. A pair of collimated electrons can be produced from further decay of a highly boosted exotic particle. The development of merged electron identification using multivariate technique is presented. Application of GPU in merged electron identification is tested.

### Keywords:

CMS, LHC, 13TeV, ECAL, Merged electron, Multivariate technique, Machine learning, Boosted signature, GPU.

## Feasibility study of B meson decays into 6 leptons at B factory

최지영<sup>1</sup>, 장영민<sup>1</sup>, 주경광\*<sup>1</sup>  
<sup>1</sup>전남대학교 물리학과  
kkjoo@chonnam.ac.kr

### Abstract:

We investigate the feasibility of  $B_0 \rightarrow 6$  leptons decay channel by using Monte Carlo simulations.

So far, there is no study of this channel.

Since this channel is a rare decay channel, it can be a good probe for the precision of SM or the evidence of BSM.

In order to reduce various backgrounds, new detection and analysis techniques are needed.

An extended analysis including dark photons has been performed.

### Keywords:

B meson, dark photon, BSM

## Z' search in bottom-quark fusion process to probe B meson anomaly decays

김혜현<sup>1</sup>, 문창성\*<sup>1</sup>, ADRIAN Thompson<sup>2</sup>, 김민석<sup>1</sup>, KAMON Teruki<sup>2</sup>, RATHJENS Denis<sup>2</sup>, 오영도<sup>1</sup>,  
DALCHENKO Mykhailo<sup>2</sup>

<sup>1</sup>경북대학교 물리학과, <sup>2</sup>Department of Physics and Astronomy, Texas A&M University  
csmoon@knu.ac.kr

### Abstract:

We investigate models of a new heavy neutral gauge boson ( $Z'$ ) with a non-universal coupling to second generation leptons and third generation quarks as a minimal framework. The models are possible to explain B meson anomaly decays reported by LHCb. One of crucial production processes at the LHC is a fusion of b quarks from gluon splitting. The final states contain two high  $p_T$  muons with at least b-tagged jet. This talk presents search strategies and prospects for such a hypothetical particle in the dimuon channel using a Delphes simulation.

### Keywords:

$Z'$  boson, B meson anomaly

## Study of the neutrino energy resolution for the JSNS2 using vertex position correction

JEON H. K.\*<sup>1</sup>, C. Rott\*<sup>1</sup>, JANG H. I.<sup>2</sup>, KIM S. B.<sup>3</sup>, KWON E.<sup>3</sup>, SEO H.<sup>3</sup>, SEO S. H.<sup>3</sup>, KIM J. Y.<sup>4</sup>, JOO K. K.<sup>4</sup>, LIM I. T.<sup>4</sup>, MOON D. H.<sup>4</sup>, KIM W.<sup>10</sup>, CHEOUN M. K.<sup>5</sup>, JEON S. H.<sup>1</sup>, YU I.<sup>1</sup>, CHOI J. H.<sup>6</sup>, PAC M. Y.<sup>6</sup>, KIM E. J.<sup>7</sup>, JANG J. S.<sup>8</sup>, KANG S. K.<sup>9</sup>, SHIN C. D.<sup>4</sup>

<sup>1</sup>Department of Physics, Sungkyunkwan University, Gyeong Gi-do, KOREA, <sup>2</sup>Department of Fire Safety, Seoyeong University, Gwangju 61268, KOREA, <sup>3</sup>Department of Physics and Astronomy, Seoul National University, Seoul 08826, KOREA, <sup>4</sup>Department of Physics, Chonnam National University, Gwangju, 61186, KOREA, <sup>5</sup>Department of Physics, Soongsil University, Seoul 06978, KOREA, <sup>6</sup>Department of Radiology, Dongshin University, Chonnam 58245, KOREA, <sup>7</sup>Division of Science Education, Physics major, Chonbuk National University, Jeonju, 54896, KOREA, <sup>8</sup>Gwangju Institute of Science and Technology, Gwangju, 61005, KOREA, <sup>9</sup>School of Liberal Arts, Seoul National University of Science and Technology, Seoul, 139-743, KOREA, <sup>10</sup>Department of Physics, Kyungpook National University, Daegu 41566, KOREA

zayunsna@gmail.com, carsten.rott@gmail.com

### Abstract:

The JSNS<sup>2</sup> experiment aims to search for the existence of sterile neutrino at J-PARC spallation neutron source. The JSNS<sup>2</sup> detector is currently under construction and expected to be completed by the end of this year. The experiment will search for anti muon-neutrino to anti electron-neutrino oscillations which are detected by the inverse beta decay interaction, followed by gammas from neutron capture on Gd. The JSNS<sup>2</sup> experiment will use 240PMT's to detect this signal. Energy reconstruction relies on the number of photons detected, however corrections need to be applied based on the event vertex position, optical properties of the Gd-Liquid scintillator, and energy leakage. This poster shows a study of the energy resolution that can be achieved after event vertex position corrections are applied.

### Keywords:

JSNS2



## Development of HSCP trigger algorithms in the CMS Phase-II upgrade.

정수민<sup>1</sup>, 고정환\*<sup>2</sup>, 김태정<sup>1</sup>

<sup>1</sup>한양대학교 물리학과, <sup>2</sup>경희대학교 물리학과  
jhgoh@khu.ac.kr

### Abstract:

In the CMS Phase-II upgrade, RPC system is expected to be equipped with new electronics which can provide a good time resolution of 2ns. New RPC chambers in the forward region ( $1.8 < |\eta| < 2.5$ ) are also planned, with better time resolution (1.5ns) but also 2-dimensional spatial informations. We developed trigger algorithms based on the RPC system in the Phase-II upgrade, to detect slowly moving muon-like particles by the Time-of-Flight technique, which is one of the signature of Heavy Stable Charged Particles (HSCP).

### Keywords:

CMS experiment, Phase-II upgrade, HSCP, trigger algorithm, Time of Flight

## Cosmic Ray Stand for Test of GEM

박인규\*<sup>1</sup>, 이상훈<sup>1</sup>, 고병환<sup>1</sup>

<sup>1</sup>서울시립대학교 물리학과  
icpark@uos.ac.kr

### Abstract:

In the phase II run of the Large Hadron Collider, CMS detector will be upgraded. GEM detectors will be installed in this upgrade, which will increase the accuracy of measuring muons in high eta region ( $|\eta| > 1.8$ ). To be used, GEM detector must be fully tested. There are 10 levels of tests, which are called QC1~QC10 (Quality Control). Especially in QC8, which is also called cosmic ray stand, GEM detectors are tested by cosmic muons. In this study we developed softwares for GEM QC8 test, which reconstructs a trajectory of a muon from hit signals. For desired layout of the GEM detectors, we confirmed in MC simulation that the reconstruction code works well so that we can measure the efficiency of GEM which agrees with setting efficiency (97%).

### Keywords:

LHC, CMS, GEM, muon

## C meson reconstruction for the measurement of the top quark mass

박인규\*<sup>1</sup>, 이상훈<sup>1</sup>, 김지현<sup>1</sup>, 김슬기<sup>1</sup>, 강다영<sup>1</sup>, 정동준<sup>1</sup>

<sup>1</sup>서울시립대학교 물리학과  
icpark@uos.ac.kr

### Abstract:

One of the methods to measure the top quark mass is using c mesons within b-quark jet. To use this method, it is very important to reconstruct c mesons efficiently. In this research, we present the results for J/psi and D0 identification using two methods, a cut based and BDT.

### Keywords:

LHC, CMS, top, C meson, D0, Jpsi

## Top quark mass measurement using D meson within b-jet

박인규\*<sup>1</sup>, 이상훈<sup>1</sup>, 김지현<sup>1</sup>, 강다영<sup>1</sup>, 정동준<sup>1</sup>, 김슬기<sup>1</sup>

<sup>1</sup>서울시립대학교 물리학과  
icpark@uos.ac.kr

### Abstract:

When measuring the top quark mass, jet energy uncertainty is one of the largest systematics. Using charm mesons within b-jet provides an alternative solution for this problem. In this presentation, we will focus on D0 and D\*. We can measure top quark mass by reconstructing these mesons. We used an isolated lepton from W boson and 2(3) tracks from D0(D\*) within the b-jet. We present the results of the extraction of the top mass using the invariant mass of the lepton plus D meson using 2016 LHC 13 TeV data collected by the CMS detector.

### Keywords:

CMS, LHC, top, D0, D\*, C meson

## Measurement of b-quark polarization with heavy baryons.

박인규\*<sup>1</sup>, 이상훈<sup>1</sup>, 류선영\*<sup>1</sup>, WATSON Ian James<sup>1</sup>

<sup>1</sup>서울시립대학교 물리학과

icpark@uos.ac.kr, flsy4458@naver.com

### Abstract:

Measurement of initial b-quark polarization can inform us about the structure of new physics. In the heavy-quark limit, the b-quark polarizations should be preserved through the hadronization and decay of the  $\Lambda_b$ . The b-quarks produced in top quark decays are produced in a well-understood polarization state. Therefore, we can use the large amount of top quarks from the current run 2 of the LHC to measure the b-quark polarization, and thus the non-perturbative depolarization effects. In this study, we perform an initial study of the reconstruction of b-baryons.

### Keywords:

b-quark, b-meson, polarization, LHC, Run2

## Measurement of $|V_{ts}|$ with machine learning

박인규\*<sup>1</sup>, 이상훈\*<sup>1</sup>, WATSON Ian James\*<sup>1</sup>, 전다정<sup>1</sup>, 장우진<sup>1</sup>

<sup>1</sup>서울시립대학교 물리학과

icpark@uos.ac.kr, jason.lee@cern.ch, ian.james.watson@cern.ch

### Abstract:

In the standard model, Cabibbo-Kobayashi-Maskawa (CKM) matrix describes the strength of the weak interaction between quark flavours. In the SM, the CKM is required to be unitary, while additional new physics may break the unitarity. It is possible to directly measure some elements of the matrix using top-quark decays. Previous studies of top-quark decays focus on the b-quark and W-boson decay channel to measure the matrix element  $|V_{tb}|^2$  as the ratio of top decays to b-quark versus all quarks, while indirect measurements can restrict  $|V_{ts}|^2$ . In our study, we propose to use the decay from top-quark to an s-quark and a W-boson to measure the size of the matrix element  $|V_{ts}|^2$  directly. This requires good b-quark rejection as the branching ratio of the top-quark to b-quark is about 1000 times larger than the top-quark to s-quark. Thus, it is important to improve the performance of s-quark versus b-quark discrimination. We present results of testing machine learning algorithms, such as BDT, to improve s-quark identification.

### Keywords:

CKM matrix,  $V_{ts}$ , top, s quark, LHC, CMS, particle physics

## Effect of the Optical Parameters of Liquid Scintillator on Photon detection at JSNS2 and the Prospect of the JSNS2 Detector Simulation

JANG H.I.<sup>1</sup>, KIM S.B.<sup>2</sup>, KWON E.<sup>2</sup>, SEO H.<sup>2</sup>, SEO S.H.<sup>2</sup>, KIM J.Y.<sup>3</sup>, JOO K.K.<sup>3</sup>, LIM I.T.<sup>3</sup>, MOON D.H.<sup>3</sup>, KIM W.<sup>4</sup>, CHEOUN M.K.<sup>5</sup>, JEON H.K.<sup>6</sup>, JEON S.H.<sup>\*6</sup>, ROTT C.<sup>6</sup>, YU I.<sup>6</sup>, CHOI J.H.<sup>7</sup>, PAC M.Y.<sup>7</sup>, KIM E.J.<sup>8</sup>, JANG J.S.<sup>9</sup>, KANG S.K.<sup>10</sup>

<sup>1</sup>Department of Fire Safety, Seoyeong University, Gwangju 61268, KOREA, <sup>2</sup>Department of Physics and Astronomy, Seoul National University, Seoul 08826, KOREA, <sup>3</sup>Department of Physics, Chonnam National University, Gwangju, 61186, KOREA, <sup>4</sup>Department of Physics, Kyungpook National University, Daegu 41566, KOREA, <sup>5</sup>Department of Physics, Soongsil University, Seoul 06978, KOREA, <sup>6</sup>Department of Physics, Sungkyunkwan University, Gyeong Gi-do, KOREA, <sup>7</sup>Department of Radiology, Dongshin University, Chonnam 58245, KOREA, <sup>8</sup>Division of Science Education, Physics major, Chonbuk National University, Jeonju, 54896, KOREA, <sup>9</sup>Gwangju Institute of Science and Technology, Gwangju, 61005, KOREA, <sup>10</sup>School of Liberal Arts, Seoul National University of Science and Technology, Seoul, 139-743, KOREA  
physicoon0607@gmail.com

### Abstract:

The JSNS2 experiment aims to search for the existence of sterile neutrino at J-PARC. A 1 MW beam of 3 GeV protons incident on a spallation neutron target produces an intense neutrino beam from muon decay at rest. The experiment will search for muon anti-neutrino to electron anti-neutrino oscillations which are detected by the inverse beta decay interaction, followed by gammas from neutron capture on Gd. The JSNS2 experiment adopted the RAT monte carlo simulation as the official detector simulation. We show the effect of the optical parameter of liquid scintillator on PMT photon detection using the RAT simulation.

The prospect of the detector simulation update is also presented.

### Keywords:

JSNS2 sterile neutrino



## Dark photon search using B meson decay at Belle

김용균\*<sup>1</sup>, 박석희\*<sup>1</sup>, 권영준\*<sup>1</sup>

<sup>1</sup>연세대학교 물리학과

yjk1401@yonsei.ac.kr, seokhee.park@yonsei.ac.kr, yjkwon63@yonsei.ac.kr

### Abstract:

We present a status report of a search for the rare  $B$  meson decays to 4 leptons and 2 leptons and 2 pions with and without kaon using the full  $\Upsilon(4s)$  data sample of 772M  $B\bar{B}$  pairs collected with the Belle detector at the KEKB asymmetric-energy  $e^+e^-$  collider. We reconstruct a dark photon using lepton pair or pion pair, after that we reconstruct B meson using two dark photons with and without kaon. In this presentation, we show the results of signal extraction procedure and expected upper limit of  $B$  meson branching fraction about Monte Carlo samples.

### Keywords:

Belle, B meson, dark photon

## A study of muon isolation efficiency measurement at 13 TeV for CMS

LUU Lan<sup>\*1</sup>, KIM Taejeong<sup>1</sup>, KIM Nagyeong<sup>1</sup>, GOH Junghwan  
<sup>1</sup>한양대학교 physics, <sup>2</sup>경희대학교 physics  
luulan1894@gmail.com

### Abstract:

*In a top quark decay, a muon can be produced from a W boson in a top quark decay. This muon needs to be distinguished from the one from semi-leptonic b decays in multijets events. Isolation criteria is the key value to select the muon from the resonances. To estimate this isolation efficiency directly from data, we usually rely on a tag and probe method which is based on Z-boson enhanced events. In this study, following the tag and probe method, we measure the isolation efficiency by counting number of events in Z mass window with a requirements of at least 2 jets which could possibly represent the environments of a top-quark pair system.*

### Keywords:

muon, tag and probe, isolation, CMS

## Differential cross section measurement of $t\bar{t}b\bar{b}$ in the lepton + jets decay channel

안서현\*<sup>1</sup>, 김태정\*<sup>1</sup>, 고정환\*<sup>2</sup>, 박지원\*<sup>1</sup>

<sup>1</sup>한양대학교 물리학과, <sup>2</sup>경희대학교 물리학과

klar.wind0425@gmail.com, tae.jeong.kim@cern.ch, junghwan.goh@cern.ch, minerva1993@gmail.com

### Abstract:

In 2016, Large Hadron Collider (LHC) has accumulated proton-proton collision data corresponding to an integrated luminosity of  $35.9 \text{ fb}^{-1}$  at a center-of-mass energy of 13 TeV with the CMS detector. Several million top quark candidates are produced in this data set. This large data set allows us to measure the differential cross section of two additional b jets in association with the top quark pair production. We present the differential cross section result using the events of one lepton, 4 jets and two b jets final state.

### Keywords:

cms, top, differential cross section

## A brief guidance of HEP software simulation & installation related to dark photons

주경광\*<sup>1</sup>, 최지영<sup>1</sup>  
<sup>1</sup>전남대학교 물리학과  
kkjoo@chonnam.ac.kr

### Abstract:

A feasibility study related to dark photons has been performed using available high-energy physics software resources.

The concept of computational science, which is an intermediate step between physical experiment and physical theory research, are reviewed.

All available resources are allocated as efficient as possible to the experiments.

### Keywords:

computational science, HEP software, simulation, installation

## Environmental Monitoring for Belle II

박석희\*<sup>1</sup>, 권영준\*<sup>1</sup>

<sup>1</sup>연세대학교 물리학과

seokhee.park@yonsei.ac.kr, yjkwon63@yonsei.ac.kr

### Abstract:

The Belle II experiment is starting to search for physics beyond the Standard Model. Before final data taking, Belle II phase 2 run is now on-going. In this presentation, we show the current status of environment monitor system for Belle II detector run. The monitor system is installed on monitoring room at KEK, and constructed by three parts, Monitoring GUI, alarm system, and archiver. The monitoring GUI shows the current state of detector and the alarm system generates sound and email notification. The Archiver collects data on a single database server and provide the data to people.

### Keywords:

Belle II, DAQ, Slow Control

## Silicon Vertex Detector for the Belle II Experiment

박환배\*<sup>1</sup>, 이승철<sup>1</sup>, 김홍주<sup>1</sup>, 강국현<sup>1</sup>, 전해빈<sup>1</sup>

<sup>1</sup>경북대학교 물리학과  
sunshine@knu.ac.kr

### Abstract:

The Belle II experiment is for searching physics beyond the standard model (SM) by observing rare/violated decays of B-meson pairs at an electron-positron collider, SuperKEKB (Tsukuba, Japan). A silicon vertex detector (SVD) is one of the most important detector in the Belle II detectors for tracking and vertexing. SVD consists of four cylindrical layers, layer 3 (L3) to layer 6 (L6), and each layer is made of double-sided silicon strip detectors (DSSDs). In the outermost layer, a L6 ladder has five DSSDs and central three DSSDs of them are connected with APV25 signal read-out chips by a novel chip-on-sensor concept. The Belle II experiment is now ongoing with only 4 ladders of SVD, and will be operated with all ladders of SVD in the end of 2018. In this poster, we present SVD L6 ladder assembly procedures, status and schedules for the Belle II experiment.

### Keywords:

The Belle II Experiment, Silicon Vertex Detector, Ladder Assembly, Double-Sided Silicon Strip Detector, Chip-On-Sensor

## CMS Level-1 pixel trigger algorithm development for very forward region at HL-LHC

문창성\*<sup>1</sup>, 이학성<sup>1</sup>  
<sup>1</sup>경북대학교 물리학과  
csmoon@knu.ac.kr

### Abstract:

Development of the Level-1 pixel trigger algorithm for very forward region (pseudorapidity up to 2.9) for CMS Phase 2 upgrade at High Luminosity LHC (HL-LHC) is presented. At the HL-LHC, the CMS experiment will face a harsh environment with an average of 140-200 multiple proton-proton collisions per bunch crossing. The main goal of the CMS Level-1 trigger upgrade for the HL-LHC is to maintain trigger thresholds as low as possible. In this talk, we will discuss the improvement of a level-1 pixel trigger algorithm for electron identification using extended the pseudorapidity coverage from 2.5 to 2.9. The measurements of electron trigger efficiency and background rejection factor in the extended detection region are reported.

### Keywords:

LHC CMS Phase-II L1 Pixel L1Track L1Trigger Upgrade

## 2D image using GEM detector

박인규\*<sup>1</sup>, LEE Jason Sang Hun\*<sup>2</sup>, 송동현<sup>3</sup>, 정영균\*<sup>4</sup>, 장세덕\*<sup>5</sup>, 강예차\*<sup>6</sup>

<sup>1</sup>서울시립대학교 물리학과, <sup>2</sup>서울시립대학교 물리학과, <sup>3</sup>서울시립대학교 물리학과, <sup>4</sup>서울시립대학교 물리학과, <sup>5</sup>서울시립대학교 물리학과, <sup>6</sup>서울시립대학교 물리학과

icpark@uos.ac.kr, Jason.Lee@cern.ch, ykchung68@gmail.com, changsdn@naver.com,  
yck.kang@hanmail.net

### Abstract:

GEM foils amplifies electrons, creating an avalanche which we collect onto a 2D strip readout board. The GEM foils provides a high amplification factor of  $O(20)$  and by using three foils, we are able to detect low energy photons. We use an RI source to produce 2D images.

### Keywords:

GEM. 2D image

## Signal processing method for CAPP's axion data

정우현\*<sup>2</sup>, KUTLU Caglar<sup>1</sup>

<sup>1</sup>KAIST, <sup>2</sup>IBS/CAPP  
gnuhcw@ibs.re.kr

### Abstract:

The IBS center for axion and precision physics research (CAPP) conducts haloscope axion search whose method adopts a resonant cavity capable of scanning a defined frequency range using a frequency tuning system. The relic axions passing through the detector are converted into microwave photons inside the resonator and then the RF signal is transferred through the receiver chain and recorded as an averaged spectrum in a predetermined processing frequency band. This study focuses on the signal processing aspects of the data obtained from the pilot axion experiments at CAPP (CAPP-PACE) the 2.45 - 2.75 GHz frequency range. In this poster, several methods of data processing are considered for maximum SNR output and candidate display along with system diagnostics.

### Keywords:

IBS, CAPP, axion, dark matter, signal processing, SNR

## R&D on superconducting cavity at IBS/CAPP

정우현\*<sup>1</sup>, 안단호<sup>1, 2</sup>, 권오준<sup>2</sup>, 이진환<sup>1</sup>, 김진수<sup>1, 2</sup>, 이도유<sup>1, 2</sup>, 장원준<sup>3</sup>, 염도준<sup>1</sup>, SEMERTZIDIS Yannis K<sup>1, 2</sup>

<sup>1</sup>Center for Axion and Precision Physics, Institute of Basic Science, <sup>2</sup>Department of Physics, Korea Advanced Institute of Science and Technology, <sup>3</sup>Center for Quantum NanoScience, Institute of Basics Science  
gnuhcw@ibs.re.kr

### Abstract:

The IBS Center for Axion and Precision Physics Research (CAPP) explores for dark matter axions with tunable resonant cavities immersed in a strong magnetic field to boost the axion-to-photon conversion when a cavity mode resonates with the axion mass. Deposition of superconducting thin films on the inner surface of the cavity increases Q factor of the cavity and thereby enhances the conversion power. However, in the presence of high magnetic fields, Type II superconductors with high critical regions ( $>10T$ ) should be used. In this study, we present various RF characteristics related to superconducting thin films using cylindrical cavities with NbTi coated using the RF magnetron sputtering method; and with YBCO tapes on the inner surface.

### Keywords:

Axion Search, Resonant Cavity, Type II Superconductor

## Study of Geant4 profiling system using brachytherapy application

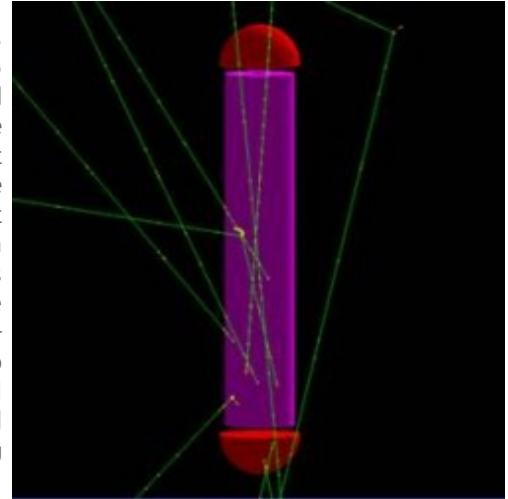
YEO Insung\*<sup>1</sup>, CHO Kihyeon<sup>1</sup>

<sup>1</sup>한국과학기술정보연구원

madjjang150@kisti.re.kr

### Abstract:

The Standard Model in particle physics is refined. However, new physics beyond the standard model, such as dark matter, requires thousand to million times of simulation events compared to those of the Standard Model. Thus, the development of software is required, especially for the development of simulation tool kits. In addition, computing is evolving. It requires the development of the simulation tool kit to accommodate the evolving computing architecture. Therefore, an efficient simulation tool kit is needed. Then, a profiling system is required to confirm it. In Geant4, a typical simulation tool kit, a profiling system in higher-energy physics areas such as the LHC experiment is well developed, contributing to the development of the software. However, profiling systems in the low-energy physics domain are in the beginning stage. Therefore, we develop it and show performances using it. In addition, profiling is performed depending on the development of software. These profiling systems could be used to confirm the development of software for evolving computing architecture.



### Keywords:

Geant4, profiling, low energy

## Study on the tuning mechanism of RF cavity for axion dark matter search experiment at IBS/CAPP in KAIST

이영재\*<sup>1</sup>, 유종희<sup>1, 2</sup>, 민병훈<sup>2</sup>, 김동락<sup>2</sup>, 김진근<sup>2</sup>, 안무현<sup>2</sup>, 이지영<sup>2</sup>, 박희준<sup>2</sup>, 김종국<sup>1</sup>, 윤호진<sup>1</sup>  
<sup>1</sup>한국과학기술원 물리학과, <sup>2</sup>기초과학연구원 액시온 및 극한상호작용 연구단  
djfldlshs@kaist.ac.kr

### Abstract:

About 23% of the energy density of the universe is considered to be in a form of non-baryonic dark matter. One of the strong candidates of dark matter is a hypothetical particle called the axion. In an axion dark matter search haloscope experiment, axions coherently scatter off the magnetic-field potential in a frequency-tunable resonant cavity. A dynamic frequency tuning in the resonant cavity is essential to effectively scan through the relevant axion mass range. In CAPP18T axion search experiment at IBS/CAPP in KAIST, we use a rotating tuning-rod system. We develop a frequency tuning system using a Proportional Integral Derivative control and precision stepping motor system. In this presentation we report details of the tuning mechanism and accuracy of the setup which are interpreted in the axion mass parameter space.

### Keywords:

Axion, Dark matter, Cavity, Tuning mechanism

## Calculation of cosmic muon rates at RENO

이현기\*<sup>4</sup>, 김우영<sup>1</sup>, SERGEYEVICH Serguey<sup>1</sup>, 장한일<sup>3</sup>, 권은향<sup>4</sup>, 김상용<sup>4</sup>, 김수봉<sup>4</sup>, 서선희<sup>4</sup>, 서현관<sup>4</sup>, 양정열<sup>4</sup>, 이동하<sup>4</sup>, 이용창<sup>4</sup>, 김종건<sup>5</sup>, 김종현<sup>5</sup>, 서지웅<sup>5</sup>, 유인태<sup>5</sup>, 전상훈<sup>5</sup>, 정다은<sup>5</sup>, ROTT Carsten<sup>5</sup>, 곽필준<sup>6</sup>, 김재률<sup>6</sup>, 문동호<sup>6</sup>, 박경환<sup>6</sup>, 박영서<sup>6</sup>, 신창동<sup>6</sup>, 임인택<sup>6</sup>, 주경광<sup>6</sup>, 장지승<sup>7</sup>, 유종희<sup>8</sup>, 주기원<sup>8</sup>, 박명렬<sup>2</sup>, 최준호<sup>2</sup>

<sup>1</sup>Department of Physics, Kyungpook National University, <sup>2</sup>Department of Radiology, Dongshin University, <sup>3</sup>Department of Fire Safety, Seoyeong University, <sup>4</sup>Department of Physics and Astronomy, Seoul National University, <sup>5</sup>Department of Physics, Sungkyunkwan University, <sup>6</sup>Department of Physics, Chonnam National University, <sup>7</sup>GIST College, Gwangju Institute of Science and Technology, <sup>8</sup>Department of Physics, Korea Advanced Institute of Science and Technology  
physilhg@snu.ac.kr

### Abstract:

Cosmic muon rates at the RENO site are calculated using the MUSIC(*MUon Simulation Code*) program. We have obtained muon fluxes as a function of azimuthal angle, zenith angle and observed muon energy. The calculated muon rates are useful for estimating cosmogenic backgrounds in the detector and coming from surrounding rocks. In this presentation, we report the calculation method and the obtained results.

### Keywords:

RENO, muon, flux, simulation



## NEOS Phase II--Measurement of a reactor neutrino spectrum for a full burnup cycle

OH Yoomin\*<sup>1</sup>, KIM Yeongduk<sup>1</sup>, JEON Eunju<sup>1</sup>, LEE Jaison<sup>1</sup>, PARK Kangsoon<sup>1</sup>, PARK Hyangkyu<sup>1</sup>, KO Youngju<sup>1</sup>, YOON Youngsoo<sup>1</sup>, LEE Moo Hyun<sup>1</sup>, HAN Bo-Young<sup>2</sup>, SUN Gwang-Min<sup>2</sup>, SIYEON Kim<sup>4</sup>, SEO Kyungmin<sup>3</sup>, KIM Hyunsoo<sup>3</sup>, KIM Jinyu<sup>3</sup>, KIM Hongjoo<sup>5</sup>, LEE Jooyoung<sup>5</sup>, JOO Kyungkwang<sup>6</sup>

<sup>1</sup>Institute for Basic Science, <sup>2</sup>Korea Atomic Energy Research Institute, <sup>3</sup>Sejong University, <sup>4</sup>Chung-ang University, <sup>5</sup>Kyungpook National University, <sup>6</sup>Chonnam National University  
yoomin@ibs.re.kr

### Abstract:

The NEOS experiment has successfully measured the energy spectrum at 24 m distance from Hanbit reactor unit 5 for 180 days of reactor operation and constrained the active-to-sterile oscillation parameters. An extended measurement for a whole burnup cycle will be a unique probe for the dependence of the reactor antineutrino flux and spectrum on the fuel composition.

### Keywords:

reactor neutrino, energy spectrum, burn up, fission fraction

## Stabilization heater development for AMoRE detectors

권도형\*<sup>1</sup>, 권도형<sup>1</sup>, 김용함<sup>1, 2, 3</sup>, 강찬석<sup>2</sup>, 김소라<sup>2</sup>, 이해진<sup>2</sup>, 전진아<sup>2</sup>, 김인욱<sup>4</sup>, 김혜림<sup>5</sup>, 오승윤<sup>6</sup>

<sup>1</sup>과학기술연합대학원대학교 기초과학, <sup>2</sup>기초과학연구원 지하실험연구단, <sup>3</sup>한국표준과학연구원, <sup>4</sup>서울대학교, <sup>5</sup>경북대학교, <sup>6</sup>세종대학교  
kwon8688@naver.com

### Abstract:

AMoRE (Advanced Mo-based Rare process Experiment) is an international project to search for neutrinoless double beta decay ( $0\nu\beta\beta$ ) of  $^{100}\text{Mo}$ . The project employs simultaneous phonon-scintillation detection from scintillating crystals containing  $^{100}\text{Mo}$  elements based on MMC readouts. As the heat capacities of a crystal absorber and an MMC sensor varies with temperature together with MMC sensitivity, signal amplitudes may drift over a long time constant as the base temperature fluctuates. This effect degrades the energy resolution of the calorimetric detection at low temperatures. By installing a Joule heater on the detector to periodically inject controlled amount of heat, we can produce reference signals that can be used for gain stabilization. We present the characterization of Joule heaters, test results using a  $\text{ZnMoO}_4$  crystal and preparation process in the AMoRE run.

### Keywords:

Stabilization heater

## Measurement of Attenuation Length for liquid scintillator

주경광\*<sup>1</sup>, 박영서<sup>1</sup>, 신창동<sup>1</sup>

<sup>1</sup>전남대학교 물리학과

kkjoo@chonnam.ac.kr

### Abstract:

원전중성미자는 원자로의 핵분열 과정에서 생성되어 검출기내의 양성자와 충돌하는 역베타붕괴(Inverse Beta Decay, IBD) 반응을 일으킨다. 역베타붕괴에서 생성되는 양전자는 쌍소멸하며 빛을 내고 중성자는 주변의 원자핵에 포획되는 과정에서 빛을 내게 되는데 각각의 신호에 시간차이를 이용하여 구별한다. 이 때 생성된 빛은 광증폭관에 도달하는데, 사용된 액체섬광검출용액의 감쇠거리에 의존한다. 본 발표는 LAB을 기초로 한 액체섬광검출용액의 감쇠거리를 측정하기 위한 측정 장비 개발 및 결과에 대해 기술하였다.

### Keywords:

liquid scintillator

## Design study of a detector for the tritium beta decay measurement with a metallic magnetic calorimeter

김한범\*<sup>1</sup>, 황종원<sup>1</sup>, 이재용<sup>1</sup>, 김선기<sup>1</sup>  
<sup>1</sup>서울대학교 자연과학대학 물리천문학부  
hanbum7@snu.ac.kr

### Abstract:

Discovery of neutrino oscillation revealed the presence of the small but nonzero mass of a neutrino. We have developed a detector design using a cryogenic metallic magnetic calorimeter(MMC) to measure beta decay and neutrino absorption reaction of tritium. The validity of the use of an MMC in the tritium beta decay measurement experiment has been studied using the GEANT4 simulation. Tritium, produced by  $3\text{He}(n,p)3\text{H}$  reaction, will be implanted into a gold absorber and then will disintegrate in it. We have investigated the tritium implantation efficiency and electron absorption in the detector. The absorption spectrum of electrons from the tritium beta decay has been generated to estimate the sensitivity for the neutrino mass measurement according to the energy resolution of the calorimeter.

### Keywords:

neutrino, MMC

## A simulation study on backgrounds of the COSINE-100 NaI(Tl) detectors

ADHIKARI Pushparaj\*<sup>1</sup>

<sup>1</sup>세종대학교 물리학과  
pushpaparticle@gmail.com

### Abstract:

The COSINE-100 experiment is a direct dark matter WIMPS (Weakly Interacting Massive Particles) search experiment by using an array of scintillating NaI(Tl) crystals. The experiment's physics run has started in September 2016 and has been running stable. We have performed simulations and fittings of the background data in the crystal detectors with various MC components. Results of the background studies of the NaI(Tl) crystal detectors will be presented in this poster.

### Keywords:

COSINE-100, NaI(Tl), dark matter

## RENO upgrade and its sensitivity study

이용창\*<sup>1</sup>, 권은향<sup>1</sup>, 김상용<sup>1</sup>, 김수봉<sup>1</sup>, 서선희<sup>1</sup>, 서현관<sup>1</sup>, 양정열<sup>1</sup>, 이동하<sup>1</sup>, 이현기<sup>1</sup>, 김종건<sup>2</sup>, 김종현<sup>2</sup>, 서지웅<sup>2</sup>, 유인태<sup>2</sup>, 전상훈<sup>2</sup>, 정다은<sup>2</sup>, ROTT CARSTEN<sup>2</sup>, 곽필준<sup>3</sup>, 김재률<sup>3</sup>, 문동호<sup>3</sup>, 박경환<sup>3</sup>, 박영서<sup>3</sup>, 신창동<sup>3</sup>, 임인택<sup>3</sup>, 주경광<sup>3</sup>, 김우영<sup>4</sup>, CHEBOTERYOV SERGEY<sup>4</sup>, 박명렬<sup>5</sup>, 최준호<sup>5</sup>, 장한일<sup>6</sup>, 장지승<sup>7</sup>, 유종희<sup>8</sup>, 주기원<sup>8</sup>

<sup>1</sup>서울대학교 물리천문학부, <sup>2</sup>성균관대학교 물리학과, <sup>3</sup>전남대학교 물리학과, <sup>4</sup>경북대학교 물리학과, <sup>5</sup>동신대학교 물리학과, <sup>6</sup>서영대학교 물리학과, <sup>7</sup>GIST, <sup>8</sup>KAIST  
lycgold@snu.ac.kr

### Abstract:

The more precise measurement of  $\theta_{13}$  is valuable for determining the CP violating phase if combined with an accelerator neutrino beam experimental result. We plan to upgrade the RENO facility to make a precise measurement of  $\theta_{13}$  and  $\Delta m_{ee}^2$  and to solve the problem of the 5 MeV excess in the measured reactor neutrino spectrum. We propose to add more identical near and far detectors and to construct further far detectors located at 1.7 km away from the center of reactor array. In this talk, we present the upgrade plan for RENO with expected sensitivities.

### Keywords:

neutrino oscillation, RENO, upgrade

## Measured Cosmogenic Background at RENO

정다운\*<sup>1</sup>, 김우영<sup>2</sup>, CHEBOTARYOV Sergey<sup>2</sup>, 박명렬<sup>3</sup>, 최준호<sup>3</sup>, 장한일<sup>4</sup>, 권은향<sup>5</sup>, 김상용<sup>5</sup>, 김수봉<sup>5</sup>, 서선희<sup>5</sup>, 서현관<sup>5</sup>, 양정열<sup>5</sup>, 김종건<sup>1</sup>, 김종현<sup>1</sup>, 서지웅<sup>1</sup>, 유인태<sup>1</sup>, 전상훈<sup>1</sup>, ROTT Carsten<sup>1</sup>, 곽필준<sup>6</sup>, 김재률<sup>6</sup>, 문동호<sup>6</sup>, 박경환<sup>6</sup>, 박영서<sup>6</sup>, 신창동<sup>6</sup>, 임인택<sup>6</sup>, 주경광<sup>6</sup>, 장지승<sup>7</sup>, 유종희<sup>8</sup>, 주기원<sup>8</sup>, 이동하<sup>5</sup>, 이현기<sup>5</sup>, 이용창<sup>5</sup>  
<sup>1</sup>성균관대, <sup>2</sup>경북대, <sup>3</sup>동신대, <sup>4</sup>서영대, <sup>5</sup>서울대, <sup>6</sup>전남대, <sup>7</sup>GIST, <sup>8</sup>KAIST  
cowalker12@gmail.com

### Abstract:

The isotopes of  $^8\text{He}$  and  $^9\text{Li}$  produced by cosmic-rays are a main source for backgrounds in reactor neutrino experiments. The isotope decays to a neutron and an electron and mimics an inverse beta decay of an electron antineutrino from reactors. The  $^8\text{He}/^9\text{Li}$  background spectrum and rate are measured using the data taken by the RENO experiment, and compared the with Monte-Carlo prediction. In this presentation, we report the measured cosmogenic background spectrum and rate at RENO.

### Keywords:

cosmogenic background, Li/He background

## Microwave cavity with dielectric ring in axion search at IBS/CAPP

김진수\*<sup>1</sup>, 권오준\*<sup>2</sup>, 정우현\*<sup>2</sup>, SEMERTZIDIS Yannis K.\*<sup>2</sup>

<sup>1</sup>한국과학기술원 물리학과, <sup>2</sup>기초과학연구원

kjs098@kaist.ac.kr, o1tough@gmail.com, gnuhcw@gmail.com, yannis@kaist.ac.kr

### Abstract:

IBS/CAPP looks for the excess radiation deposited into a cavity from the conversion of a dark matter axion into a microwave photon. CAPP uses a high Q-factor resonant cavity submerged in a strong magnetic field. It is essential to use resonant mode that has high Q-factor with large form factor and large volume in order to increase the sensitivity and scanning rate of the experiment. The search for axions of higher mass range with conventional TM010 mode requires smaller volume. In order to resolve this problem, we introduced a new type of resonator that has dielectric ring placed inside the cavity. I will present the results of various studies on this resonator with TM030-like mode based on computer simulations and the measurements from the actual dielectric ring cavity.

### Keywords:

Dark matter, high Q resonator

## Study of the temperature-dependent properties of NaI(Tl) crystals and PMTs

KIM Gwang\_Soo<sup>2</sup>, KIM Nam Young<sup>\*1</sup>, LEE Joo Young<sup>2</sup>, LEE Hyunsu<sup>1</sup>, HA Chang Hyun<sup>1</sup>, KIM Hong Joo<sup>2</sup>

<sup>1</sup>Center for Underground Physics, Institute for Basic Science, <sup>2</sup>Department of Physics, Kyungpook National University  
nykim@ibs.re.kr

### Abstract:

We have studied internal radioisotope contaminants in ten prototype NaI(Tl) crystals that were produced as a part of a program to develop ultra-low background detectors. The goal is to reduce the backgrounds to levels that are significantly below those in the eight NaI(Tl) crystal array of the currently operating COSINE-100 dark matter search experiment at the Yangyang underground laboratory. COSINE-200, the next phase of the experiment, requires crystal background levels that are well below, and light yields that are well above, those of the DAMA/LIBRA detector. To accomplish this, several R&D studies are ongoing. A component of this program is the investigation of the low-temperature properties of NaI(Tl) crystals and their readout PMTs while they are situated inside a temperature controlled refrigerator. Results from this aspect of the R&D program will be presented.

### Keywords:

NaI(Tl) crystal, low-temperature properties of scintillator, PMT noise

## Effective Approximation of Electromagnetism for Axion Haloscope Searches

김영근\*<sup>1, 2</sup>, 김동욱<sup>1, 2</sup>, 신윤창<sup>2</sup>, SEMERTZIDIS Yannis K<sup>1, 2</sup>  
<sup>1</sup>한국과학기술원 물리학과, <sup>2</sup>IBS/CAPP  
dkkimsun@kaist.ac.kr

### Abstract:

Most of successful experiments searching for axion dark matter are based on an anomalous coupling of axion to the electromagnetic field. This requires a modification of the classical Maxwell equations to include the anomalous interaction. However, due to the axion anomaly, this set of modified Maxwell equations doesn't naturally satisfy certain boundary conditions such as one for axion haloscope searches. We introduce an effective approximation of Maxwell equations to resolve this issue and shows that they naturally satisfy the boundary conditions for haloscope searches. The electric stored energy and magnetic stored energy are also estimated from the electromagnetic fields, which are different in this approximation. A very small difference arises between the electric and magnetic stored energies due to the anomalous interaction. The difference can be interpreted as oscillating electric dipole moments (EDM) induced by axions.

### Keywords:

Axion, Modified Maxwell equation, Haloscope search

## Studies of the muon rate and muon-induced phosphorescence events in the COSINE-100 experiment

PRIHTIADI Hafizh\*<sup>1</sup>

<sup>1</sup>Department of Physics, Bandung Institute of Technology  
hafizh.physics@gmail.com

### Abstract:

The COSINE-100 experiment is a dark matter search that aims to confirm the annual modulation signal reported by DAMA/LIBRA by using the same NaI(Tl) crystal target/detector material. It is well known that the annual variations of temperature and density in the atmosphere produce a corresponding annual modulation of the cosmic-ray muon intensity. This fact motivated the consideration of muon-induced activity in the NaI(Tl) crystals and surrounding materials as a possible non-WIMP-induced source of the DAMA/LIBRA annual modulation. The time and energy deposited by muons that traverse the crystals are correlated to the occurrence of phosphorescence that shows up in the detector as low-energy scintillation signals. The measured muon rate at the location of the COSINE-100 detector and a characterization of muon-induced phosphorescence events will be presented.

### Keywords:

COSINE-100 experiment, dark matter, phosphorescence events, muon-induced events

## Background simulations for the AMoRE-Pilot experiment.

김홍주\*<sup>1</sup>, HA Daehoon<sup>1</sup>, ON Behalf of the AMoRE Collaboration<sup>2</sup>  
<sup>1</sup>경북대학교 물리학과, <sup>2</sup>Institute for Basic Science, AMoRE Collaboration  
hongjoo@knu.ac.kr

### Abstract:

The AMoRE (Advanced Mo Rare process Experiment) project is an experimental search for neutrino-less double-beta decay of  $^{100}\text{Mo}$ . The AMoRE experiment requires an extremely low background level and, for this, a thorough understanding the sources that contribute to the background is essential. To accomplish this, a comprehensive program of simulations using the GEANT4 software toolkit are being performed. In the first steps, simulations on radiation produced by radioisotope contaminations internal to the 6 source/detector crystals and in the 13 largest nearby support/shielding components were performed. Subsequently, simulations of 5.3 MeV alphas that are characteristic of surface contaminations on the crystals and the vikuiti reflection foils were developed. In addition, contributions from two-neutrino double beta decays of  $^{100}\text{Mo}$  in the crystals are considered. Comparisons of measured background data with the simulated results will be presented in this poster.

### Keywords:

AMoRE, AMoRE-Pilot, Background, Geant4, Simulation

## Axion dark matter search experiment with 18T high temperature superconducting magnet at IBS/KAIST

김종국\*<sup>1</sup>, 이영재<sup>1</sup>, 김동락<sup>2</sup>, 김진근<sup>2</sup>, 안무현<sup>2, 3</sup>, 민병훈<sup>2</sup>, 이지영<sup>2</sup>, 유종희<sup>1, 2</sup>

<sup>1</sup>한국과학기술원 물리학과, <sup>2</sup>기초과학연구원- 액시온 및 극한 상호작용 연구단, <sup>3</sup>서울대학교 물리학과  
inquirer1226@gmail.com

### Abstract:

The axion is a hypothetical particle that was introduced to solve the strong CP problem. The U(1) Peccei-Quinn symmetry is spontaneously broken and dynamically produce a slowly oscillating particle axion field. The axion is also a strong candidate for dark matter. In order to search for the axionic dark matter, we use a haloscope technology which is equipped with a strong solenoid magnet and a frequency-tuned resonant cavity system. Our detector is designed to be sensitive to the axion mass range of 14.88-26.88  $\mu\text{eV}$  (3.7-6.5 GHz). In this presentation, we report the CAPP18T axion dark matter search experiment setup which utilizes a 18T High Temperature Superconducting solenoid magnet, resonant cavity, dilution refrigerator and linear amplifier system.

### Keywords:

axion, axion haloscope, dark matter, SC magnet

## Study of PMT saturation for JSNS2 experiment

김우영<sup>1</sup>, SERGEYVICH Serguey<sup>1</sup>, 최명렬<sup>2</sup>, 최준호<sup>2</sup>, 장한일<sup>3</sup>, 권은향<sup>4</sup>, 김상용<sup>4</sup>, 서선희<sup>4</sup>, 서현관<sup>4</sup>, 양정열\*<sup>4</sup>, 이동하<sup>4</sup>, 이용창<sup>4</sup>, 이현기<sup>4</sup>, 김종건<sup>5</sup>, 서지웅<sup>5</sup>, 유인태<sup>5</sup>, 전상훈<sup>5</sup>, 정다운<sup>5</sup>, ROTT Carsten<sup>5</sup>, 곽필준<sup>6</sup>, 박영서<sup>6</sup>, 신창동<sup>6</sup>, 주경광<sup>6</sup>, 장지승<sup>7</sup>, 유종희<sup>8</sup>

<sup>1</sup>Department of Physics, Kyungpook National University, <sup>2</sup>Department of Radiology, Dongshin University, <sup>3</sup>Department of Fire Safety, Seoyeong University, <sup>4</sup>Department of Physics and Astronomy, Seoul Nation University, <sup>5</sup>Department of Physics, Sungkyunkwan University, <sup>6</sup>Department of Physics, Chonnam National University, <sup>7</sup>GIST College, Gwangju Institute of Science and Technology, <sup>8</sup>Department of Physics, Korea Advanced Institute of Science and Technology  
x0109@snu.ac.kr

### Abstract:

The JSNS2 experiment will search for a sterile neutrino with short baseline (~24m) using a high intensity neutrino beam produced from muon decays at rest at J-PARC MLF (Material and Life science experimental Facility). The experiment considers use of 10-inch Hamamatsu PMTs that are also used by RENO and Double Chooz. A study has been made to understand the PMT saturation behavior with various gains, in order to find a linear-response region of the PMT for the JSNS2. In this presentation, we report the results of the PMT saturation study.

### Keywords:

JSNS2, PMT saturation test, neutrino, RENO

---

## Tellurium-loaded linear alkylbenzene-based liquid scintillator for neutrinoless double beta decay experiment

김홍주\*<sup>1</sup>, ARYAL Pabitra<sup>1</sup>

<sup>1</sup>경북대학교 물리학과  
hongjoo@knu.ac.kr

### Abstract:

The nature of neutrino and its absolute mass scale can be studied through neutrinoless double beta ( $0\nu\beta\beta$ ) decay experiments. The  $^{130}\text{Te}$  isotope in liquid scintillator (LS) could be one of the promising candidates for  $0\nu\beta\beta$  decay experiment because of its high natural isotopic abundance (34.08%). Natural tellurium (34.08%  $^{130}\text{Te}$ ) loaded linear alkyl benzene (LAB) LS was developed for preliminary study. In present study, tellurium diol (hexaalkoxytelluran), a kind of tellurium organometallic was synthesized by using telluric acid and 1, 2-Butanediol. The tellurium diols of 0.4% and 0.8% (w/v) Te were loaded into the 10 ml LS with 3 g/L PPO. The scintillation property of unloaded and loaded samples is being measured in different time interval by using  $^{137}\text{Cs}$  662 keV gamma source. Approximately same light yield for 0.4% loading and 83% for 0.8% (w/v) Te as compared to unloaded LS were observed for first month measurement. Every month the scintillation light output measurement is being studied in order to check chemical stability.

### Keywords:

Liquid scintillator, neutrinoless double beta and scintillation

## Measurements of internal alpha activities in the AMoRE-pilot CaMoO<sub>4</sub> crystals

윤영수\*<sup>2</sup>, [SEO Kyungmin](#)<sup>1</sup>, KIM Yeongduk<sup>2</sup>, LEE Jaison<sup>2</sup>, OH Yoomin<sup>2</sup>, KIM Hyunsoo<sup>1</sup>, JEON Eunju<sup>2</sup>,  
LEE MooHyun<sup>2</sup>

<sup>1</sup>Department of Physics, Sejong University, <sup>2</sup>Center for Underground Physics, Institute for Basic Science  
ysy@ibs.re.kr

### Abstract:

AMoRE (Advanced Mo-based Rare process Experiment) is an experimental search for neutrinoless double beta decay of Mo-100. A pilot experiment, AMoRE-Pilot, has been operating with six <sup>40</sup>Ca<sup>100</sup>MoO<sub>4</sub> (CMO) crystals, total mass 1.9 kg, in a low-temperature cryostat at the Yangyang underground laboratory (Y2L), with a minimum overburden of 700 m. It is unavoidable that the material of the crystals suffer from some contaminations of radioactive isotopes such as U-238, Th-232, U-235 and their daughter decay products. These can originate from the chemical powders that were used to grow the crystals and/or may be introduced during the crystal growing and polishing procedures. From fits to the measured energy spectra for background alpha decay events, the levels of contamination from U-238, Th-232, U-235, and their daughter decay products can be determined, and this information can be used to provide important input to the development of strategies for reducing backgrounds in future crystals. We will present preliminary results of internal alpha activity measurements in the AMoRE-Pilot crystals.

### Keywords:

neutrino, double beta decay, underground, background, alpha

## Cosmogenic activation study of the COSINE-100 experiment NaI(Tl) crystals

박병주\*1

<sup>1</sup>기초과학연구원 지하실험연구단, <sup>2</sup>과학기술연합대학원대학교(UST)  
pbj7363@gmail.com

### Abstract:

The COSINE-100 is a direct dark matter (WIMPs) search experiment with a 106 kg array of NaI(Tl) crystals at Yangyang deep underground laboratory. Dark matter search experiments require ultra-low background conditions, thus background understanding and reduction are crucial to improve the sensitivity of the detectors. One of the dominant background contributions on the NaI(Tl) crystals is caused by activated radioisotopes that were primarily produced by previous exposures to cosmic rays. In this presentation, results of cosmogenic activation studies for the NaI(Tl) crystals will be presented based on data from the COSINE-100 experiment.

### Keywords:

COSINE-100, cosmogenic activation, Dark Matter, NaI crystal

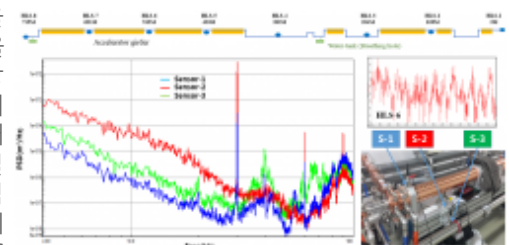
## PAL-XFEL의 HLS 측정값에서 관측되는 Vibration 원인과 대책

최호진\*<sup>1</sup>, 김승남<sup>1</sup>, 김승환<sup>1</sup>, 이상봉<sup>1</sup>, 이흥기<sup>1</sup>, 강흥식<sup>1</sup>

<sup>1</sup>포항가속기연구소  
choihyo@postech.ac.kr

### Abstract:

거대 과학장치를 구성하는 여러 가지 부품들은 측량(survey)과 정렬(alignment)을 통해서 정확한 3차원 위치좌표(X, Y, Z)에 설치되고 운영되어야만 최적의 성능을 발휘할 수 있다. 그러나 시간이 지나면서 지반은 융기(uplift) 또는 침강(subsidence) 현상이 발생되고, 설치된 부품들의 위치좌표가 변화하면서 구성품의 정렬 오차( $\Delta X$ ,  $\Delta Y$ ,  $\Delta Z$ )가 발생한다. 이로 인해 시스템의 파라미터가 변화되고, 거대 과학장치의 성능이 저하된다. 거대 과학장치를 구성하는 장비의 위치 변화를 실시간 측정하면 정렬오차를 예측할 수 있고, 변화가 심한 지역을 선별하여 해당지역의 구성품을 신속히 재정렬 함으로서, 측량과 정렬 시간을 단축할 수 있는 이점이 있다. 이를 위해, 2016년 PAL-XFEL 건물에 분해능(resolution) 0.2 $\mu\text{m}$ 인 HLS (hydrostatic leveling sensor)와 1,000미터 길이의 Water-pipe를 설치하여 운영하고 있다.



LINAC 터널에 설치된 HLS 측정값에서 불규칙한 Vibration ( $< \pm 15 \mu\text{m}$ ) 현상이 관측되고 있고, 이것은 HLS 측정 오차가 된다. 본 논문에서는 진동측정 장비를 이용하여 찾아낸 진동 발생원의 종류와 크기, 그리고 진동에 의한 HLS 용기내의 물의 출렁거림 현상과 측정오차를 진동공학의 역학적 측면에서 소개한다.

### Keywords:

Survey, Hydrostatic Leveling System, Vibration

## X-선 미세회절 분광실험

길계환\*<sup>1</sup>, 최호진<sup>1</sup>, 임재홍<sup>1</sup>  
<sup>1</sup>포항공과대학교 포항가속기연구소  
khgil@postech.ac.kr

### Abstract:

포항방사광가속기-II의 4B 빔라인은 X-선 마이크로빔을 이용한 미세회절 실험과 미세형광 실험에 이용되고 있다. K-B(Kirkpatrick-Baez) 거울시스템에 의해서 집속된 마이크로빔은 분광 빔으로서도 이용될 수 있으나, 그 동안 4결정 채널컷 분광기의 출력이 낮아 어려움이 있어왔다. 본 연구에서는, 5자유도 경밀 분광기 조정장치의 개발/운용, Ge(220) 결정블록으로의 교체 그리고 펄스 A까지 측정이 가능한 전류측정장치의 적용을 통하여 정상화된 4결정 채널컷 분광기를 이용하여, X-선 미세회절 분광 실험을 수행하였다.

4B 빔라인에서 수행된 분광 실험의 절차는 1) CCD 검출기를 상부 방향으로 이동시키면서 집속된 백색광을 참조 시편(Ge 단결정)에 조사하여 일련의 라우에 회절영상을 구하는 단계, 2) 구해진 일련의 회절영상을 이용하여 해석을 위한 입력변수를 계산하는 단계, 3) XMAS(X-ray Microdiffraction Analysis Software)의 보정, 회절점 탐색 및 회절점 색인을 수행하여 각 회절점의 광자에너지를 구한 후, 관심 대상 회절점을 선정하는 단계, 4) 분광기의 2결정 간의 피치각을 최적 피치각으로 조정하는 단계 그리고 5) 분광 빔에 의한 회절영상을 촬영하는 단계로 구성되었다. 본 발표에서는 수행된 분광 실험의 절차와 실험 결과를 상세히 기술한다.

### Keywords:

X-선 마이크로빔, 미세회절 실험, 미세형광 실험, 분광 빔, 4결정 채널컷 분광기, X-선 미세회절 분광 실험

## Status of the RAON run permit system development

JIN Hyunchang\*<sup>1</sup>, LEE Sangil<sup>1</sup>

<sup>1</sup>Rare Isotope Science Project, Institute for Basic Science  
hcjin@ibs.re.kr

### Abstract:

The RISP is building a RAON accelerator with the goal of completion in 2021. The RAON accelerator will generate and accelerate a variety of stable ions and rare isotopes, contributing to a wide range of experiments in various scientific fields. While the beam is being accelerated and transported from the ion source to the target of the experimental hall, the beam loss can occur due to various factors, which can lead to serious damage of the accelerator equipment. To prevent this, we are developing a machine protection system (MPS) which consists of a fast protection system, a slow interlock system, a run permit system, and a post-mortem system. As part of the RAON MPS, the run permit system (RPS) will collect various information such as beam parameters, fast protection system information, etc. before starting the beam operation, and give a permission of the beam operation according to the requested operation mode. Here we will present the current status of the RAON RPS development.

### Keywords:

RAON accelerator, machine protection system, run permit system

## Test Results of High Stable Magnet Power Supply

박기현\*<sup>1</sup>, 정성훈<sup>1</sup>, 정영규<sup>1</sup>, 김동언<sup>1</sup>, 서형석<sup>1</sup>, 이흥기<sup>1</sup>, 이상봉<sup>1</sup>, 오봉기<sup>1</sup>, 김민재<sup>1</sup>, 한장희<sup>1</sup>  
<sup>1</sup>포항가속기연구소 Accelerator Division  
pkh@postech.ac.kr

### Abstract:

A high stable magnet power supply (MPS) was developed, which was a bipolar type with 200A of the output current at the 40V of output voltage. The MPS has been implemented by the digital signal processing technology using the DSP, FPGA, ADCs and so on. The output current stability of the MPS showed about 6ppm peak-to-peak in a short term experiment at the 200A of its full output current. The long term stability was shown in 15 ppm for 10 hours at 200A. And the others experimental results about the MPS were shown in this paper.

### Keywords:

Magnet power supply, DCCT

## Study on high power THz coherent Cherenkov radiation generation in a dielectric wake-field accelerator

민선홍<sup>1, 2</sup>, MATLABJON Sattorov<sup>3, 6</sup>, 김선태<sup>3</sup>, 홍동표<sup>3</sup>, RANAJOY Bhattacharya<sup>3</sup>, 박건식<sup>\*3, 6</sup>, 장정민<sup>3</sup>, 백인근<sup>4</sup>, 권오준<sup>2</sup>, 조일성<sup>1</sup>, 김병수<sup>1</sup>, 박승혁<sup>5</sup>, 박차원<sup>1</sup>

<sup>1</sup>한국원자력의학원, <sup>2</sup>기초과학연구원 엑시온가속기사업단, <sup>3</sup>서울대학교 물리천문학부 테라헤르츠파 생체제어연구단, <sup>4</sup>삼성전자 생산기술연구소, <sup>5</sup>한화, <sup>6</sup>서울테라콤(주)  
gunsik@sun.ac.kr

### Abstract:

Theoretical design and experimental work are planned to study the performance of a relativistic electron-annular beam-driven cylindrical dielectric wake-field accelerating structure as a source of THz coherent Cherenkov radiation (CCR). For an appropriate choice of dielectric tube geometry and driving electron bunch parameters on the basis of ponderomotive force in a plasma dielectric wake-field structure, the vacuum electronic device operates in a single  $TM_{01}$  mode regime, producing radiation in the THz range. This source can potentially produce high power levels relative to currently available sources with the generation of 0.1THz-0.3gigawatts which is verified through FDTD (finite difference time domain) and PIC (partical in cell) simulations.

This work was supported by the National Research Foundation of Korea (NRF) grant funded by the Korea government (MSIP). (No. NRF-2017R1C1B2004760) And this research was also supported by the National R&D Program through the Korea Institute of Radiological and Medical Sciences funded by the Ministry of Science, ICT & Future Planning. (No. NRF-2017R1C1B2004760) This work was supported by the National Research Foundation of Korea (NRF) grant funded by the Korea government (MSIP) (No. NRF - 2016R1A3B1908336).

### Keywords:

high power THz coherent Cherenkov radiation (CCR), ponderomotive force, dielectric wake-field accelerator

## Two-section wiggler를 사용한 3차원 시간의존성 자유전자레이저에서 방사광의 분광 특성

남순권\*<sup>1</sup>, 김태훈<sup>1</sup>, 최준호<sup>1</sup>, 박윤성<sup>1</sup>  
<sup>1</sup>강원대학교 물리학과  
snam@kangwon.ac.kr

### Abstract:

Two-section 위글러를 사용한 자유전자레이저에서 시간의존성을 포함하는 3차원 코드를 개발하였다. 이 코드를 사용하여 two-section 위글러를 갖는 자유전자레이저에서 시간에 의존하는 방사광과 전자 빔의 비선형 상호작용에 의한 방사광의 증폭, 시간과 방사광 파장의 변화에 따른 영향, 디튜닝과 시간에 대한 영향, 시간과 패스 수에 대한 이득을 3차원 시간의존성 시뮬레이션으로 연구하였다.

### Keywords:

Two-section 위글러, 자유전자레이저, 시간 의존성 3차원 코드

## 의료용선형가속기에서 선량계산 알고리즘인 AAA와 PBC의 비교분석

최준호<sup>1</sup>, 남순권\*<sup>1</sup>, 김태훈<sup>1</sup>

<sup>1</sup>강원대학교 물리학과  
snam@kangwon.ac.kr

### Abstract:

본 연구는 의료용선형가속기에서 선량계산 알고리즘인 비등방성 분석 알고리즘(Anisotropic analytical algorithm, AAA)과 펜슬빔 중첩(Pencil beam convolution, PBC) 알고리즘을 비교분석하였다. 양의편차(positive deviation)는 AAA가 50.13%, PBC는 33.85%로 PBC가 16.28%더 낮음을 확인 할 수 있었다. 음의편차(negative deviation)는 AAA가 -50.25%, PBC는 -45.13%로 PBC가 5.12% 더 낮음을 확인 할 수 있었다.

### Keywords:

의료용선형가속기, 비등방성 분석 알고리즘, 펜슬빔 중첩 알고리즘

## 홀추력기 Xe 플라즈마의 이온빔 특성 진단을 위한 레이저유도형광 진단 시스템 개발 및 이온속도 분포 연구

최원호\*<sup>1, 4</sup>, 도근태<sup>1</sup>, 김호락<sup>1</sup>, 박상후<sup>1</sup>, 윤성영<sup>2</sup>, 이동호<sup>1</sup>, 이승훈<sup>1, 3</sup>

<sup>1</sup>한국과학기술원, 물리학과, <sup>2</sup>국가핵융합연구소, 플라즈마기술연구센터, <sup>3</sup>재료연구소, 표면기술연구본부, <sup>4</sup>한국과학기술원, 원자력 및 양자공학과  
wchoe@kaist.ac.kr

### Abstract:

홀추력기는 전기추력기 중 하나로, 추력밀도와 전력효율이 높고, 비교적 간단한 구조 등의 여러 장점으로 인해 우주임무 수행을 위한 연구개발이 세계적으로 활발하게 진행되고 있다. 우주임무 목적에 따라 마이크로 위성에서 심우주 탐사선까지 수백 W급에서 수십 kW급까지 다양한 전력 및 크기의 추력기가 활용되고 있다. 실제 우주활용을 위해 홀추력기의 성능특성 분석을 위한 홀추력기 플라즈마의 이온빔 진단은 필수적이다. 본 연구에서는, 홀추력기 플라즈마에서 비추력과 밀접한 관련이 있는 Xe II의 속도분포함수를 측정할 수 있는 레이저유도형광(Laser Induced Fluorescence) 진단시스템을 개발하였다. 레이저유도형광 시스템은 중심파장이 834.7 nm인 가변파장의 레이저를 통해, Xe II 이온의  $5d^2F_{7/2}$ 에서  $6p^2D^0_{5/2}$ 로의 여기(834.7 nm)를 유도하였으며,  $6p^2D^0_{5/2}$ 에서  $6s^2P_{3/2}$ 로 전이할 때 발생하는 형광(541.9 nm)을 측정하여 Xe II의 속도분포함수를 측정한다. 채널 직경이 50 mm인 원통형 홀추력기 플라즈마에서 실험을 진행하였으며, 양극전압 300 V, Xe 유량 8 sccm 조건에서 축방향에서의 거리변화에 따라 Xe II의 속도분포함수를 측정하였다. 축방향에서 채널 출구면으로부터의 거리는 0-60 mm까지 10 mm 간격으로 증가시키며 측정하였으며, Xe II의 속력은 거리가 증가함에 따라 최대 약 17-18 km/s까지 증가하는 것을 확인하였다. 또한, 측정거리가 축방향에서 멀어짐에 따라 이온의 속도분포가 대칭 형태에서 비대칭 형태로 변화하는 것을 확인하였다. 본 발표에서는, 레이저유도형광 진단시스템의 개발 및 Xe 플라즈마의 속도분포에 대한 상세 연구 내용이 발표될 예정이다.

### Keywords:

홀추력기, Xe II 레이저유도형광 (LIF) 분광, 속도분포

## STATUS OF THE PAL-XFEL MAGNET POWER SUPPLIES

정성훈\*<sup>1</sup>, 박기현<sup>1</sup>, 서형석<sup>1</sup>, 김민재<sup>1</sup>, 이상봉<sup>1</sup>, 오봉기<sup>1</sup>, 정영규<sup>1</sup>, 이흥기<sup>1</sup>, 한장희<sup>1</sup>, 이소정<sup>1</sup>, 김동연<sup>1</sup>, 강흥식<sup>1</sup>,  
고인수<sup>1</sup>

<sup>1</sup>포항가속기연구소  
jsh@postech.ac.kr

### Abstract:

The total length of the PAL-XFEL is 1.1 km. The electron beam orbit are corrected by 352 magnet, each powered by an individual power supply. For the powering of the magnets, nine different types of precision power supplies were developed. Total 634 magnet power supplies (MPS) have been operated for PAL-XFEL since 2016. We reports the all MPSs are satisfied for stable operation of the PAL-XFEL.

### Keywords:

MPS

## Pulsed Proton Beam Extraction of ECR Ion Source

남궁원\*<sup>1</sup>, 설택식<sup>2</sup>, 조무현<sup>3</sup>, 배영순<sup>4</sup>

<sup>1</sup>포항공과대학교 포항가속기연구소, <sup>2</sup>포항공대 물리학과, <sup>3</sup>포항공대 첨단원자력공학부, <sup>4</sup>국가핵융합연구소  
namkung@postech.ac.kr

### Abstract:

We investigate pulsed proton beam extraction of an ECR ion source. There are two conditions that limit the extracted beam current, which is determined by the plasma density and the space charge effect. As the plasma density is large enough, the extracted beam is limited by the space charge effect. The acceleration voltage and the beam current have a correlation called perveance. On the other hand, when the plasma density is not sufficient, the extracted beam is not limited by the space charge effect. In this case, perveance is not established. In the ECR plasma setup, the accelerating voltage was changed under various conditions of plasma generation, and experiments were conducted to see if the perveance was satisfied or not.

### Keywords:

ECR, Plasma, Beam extraction

## 자기장 제어를 통한 플라즈마와 내벽 간 상호작용이 감소된 원통형 홀추력기의 플라즈마 특성 연구

최원호\*<sup>1, 3</sup>, 김호락<sup>1</sup>, 도근태<sup>1</sup>, 이동호<sup>1</sup>, 이승훈<sup>1, 2</sup>

<sup>1</sup>한국과학기술원 물리학과, <sup>2</sup>재료연구소, <sup>3</sup>한국과학기술원 원자력 및 양자공학과  
wchoe@kaist.ac.kr

### Abstract:

화학식 추력기에 비해 전기추력기는 기체 분사속도가 높아 인공위성의 자세제어, 궤도수정 및 궤도천이 등 같은 임무수행과 심우주 탐사를 위한 목적으로 다양하게 활용된다. 홀추력기는 전기추력기 중 하나로 높은 추력밀도와 간단한 기하구조를 가지고 있어 널리 활용되고 있다. 홀추력기는 외부에 위치한 음극을 통해 채널 내부로 전자를 공급하며, 전자와 중성 Xe 원자와 충돌을 통해 Xe 이온들을 발생시켜 양극과 음극 사이의 전기장에 의해 가속시켜 추력을 발생시킨다. 특히, 홀추력기의 자기장 구조는 추력기의 성능, 전력소모, 이온빔 특성 등과 밀접하게 관련되어 있어 성능 개선에 가장 중요한 인자이다. 본 연구에서는, 약 400 W 급 원통형 추력기에서 플라즈마와 내벽 사이의 상호작용 감소를 위해 자기력선이 채널벽과 평행하게 되는 자기장 구조를 갖도록 개발하였다. 개발된 추력기는 추력, 비추력, 각종 효율이 기존의 추력기에 비해 높은 값을 보여 주어 자기장 제어의 효과가 뚜렷하게 나타남을 확인하였다. 개선된 자기장 구조에서는, 300 W 양극전력에서 추력 13 mN, 비추력 1900 s, 효율 39%의 성능 값을 보였으며, 이에 비해 기존 자기장 구조에서는 300 W에서 12.2 mN, 1805 s, 35%의 성능 특성을 보였다. 특히, 160% 이상의 연료효율과, 66% 이상의 다중이온이 존재함이 관측되었으며, 방전전압 이상의 고에너지 이온들도 관찰되었다. 본 발표에서는, 상세한 자기장 설계내용과 측정결과가 발표될 예정이다.

### Keywords:

플라즈마, 플라즈마 진단, 전기추력기, 홀추력기

## 1.7 MV 탄뎀가속기 저에너지 조사 빔라인에서의 대면적 빔 조사 특성

김계령\*<sup>1</sup>, 석재권<sup>1</sup>, 김민영<sup>1</sup>, 조용섭<sup>1</sup>

<sup>1</sup>한국원자력연구원 양성자기반공학기술개발사업단  
kimkr@kaeri.re.kr

### Abstract:

한국원자력연구원 양성자기속기연구센터의 1.7 MV 탄뎀 가속기에는 4개 빔라인이 각각 RBS, PIXE, 중성자, 빔조사를 위해 설치되어 운영 중에 있다. 빔조사를 위한 빔라인의 경우, 최대 5 cm x 5 cm 면적에 대한 균일조사가 가능하였으나, 최근들어 전력반도체 생산을 위한 웨이퍼에의 빔 조사 등을 위해 6 인치 크기의 웨이퍼 전체에 대한 균일조사 요구와 필요성이 꾸준히 제기되어 오고 있다. 이를 위해 저에너지 조사챔버와 빔라인을 대면적 조사가 가능하도록 개선하였다. 빔라인에는 빔전류 및 프로파일 측정을 위해 BPM(Beam Profile Monitor)와 패러데이컵(Faraday Cup)을 설치하였으며, 대면적 조사가 가능하도록 X-Y 스캐너를 설치하고 스캐너로부터 시료까지의 거리를 기존의 1.7 m 에서 3.2 m 로 증가시켜 확보함으로써 6인치 웨이퍼에 대한 균일 조사가 이루어질 수 있도록 하였다. 새롭게 설치된 조사 챔버 내에는 실시간 빔 조사 균일도 확인을 위해 시료홀더 주변에 4개의 패러데이컵을 설치하고 전하적분기, 펄스카운터, electrometer 등을 이용해 실시간으로 4개 채널의 패러데이컵 신호를 확인하고 기록할 수 있도록 하였다. 대면적 저에너지 조사챔버는 6인치 웨이퍼 전체면적에의 조사를 필요로 하는 전력반도체 소자 제조 등에 유용하게 활용될 수 있을 것이며 중앙에 설치된 패러데이컵을 이용하여 다양한 크기에 시료에 대한 실시간 선량 조절 및 빔조사가 가능해짐에 따라 반도체 뿐만 아니라 기존의 여러 빔조사 실험에 활용될 수 있을 것이다.

### Acknowledgement

This work has been supported through KOMAC (Korea Multi-purpose Accelerator Complex) operation fund of KAERI by MSIT (Ministry of Science and ICT).

### Keywords:

1.7 MV 탄뎀가속기, 이온빔 조사, 대면적 조사

## Bernas 이온원을 이용한 알칼리 금속 이온빔 인출 기초 연구

조용섭\*<sup>1</sup>, 하준목<sup>1</sup>, 김계령<sup>1</sup>

<sup>1</sup>한국원자력연구원, 양성자가속기연구센터  
choys@kaeri.re.kr

### Abstract:

양성자가속기연구센터에서는 표면 물리 등의 연구를 위하여 알칼리 금속 이온빔 장치의 개발을 진행하고 있다. 기존의 철, 구리, 코발트, 크롬 등 금속 이온을 인출하던 Bernas 이온원을 이용하며 소듐, 칼륨 등의 알칼리 금속 이온을 얻을 예정이다. 이온원에는 염화물 증기 형태로 알칼리 금속 물질이 공급되며, 20 kV의 인출 전원에 의해 폭 1.5 mm, 길이 60 mm의 스톱 형태로 빔이 인출된다. 인출된 빔은 90도 이극 전자석으로 질량 분리되고, 이후 별도의 가속 전원으로 가속관을 통해 100 kV까지 가속된다. 가속된 이온빔이 조사될 조사물은 별도의 진공함에 설치되며, 균일한 이온빔 조사를 위해 모터 구동형 XY 테이블이 사용된다. 이번 학회에서는 이 알칼리 금속 이온빔 장치의 빔 광학 설계, 장치 구성 및 빔 실험 진행상황에 대해 발표하고자 한다. 사사 : This work has been supported through KOMAC (Korea of Multi-purpose Accelerator Complex) operation fund of KAERI by MSIT (Ministry of Science and ICT).

### Keywords:

Bernas 이온원, 알칼리 금속 이온빔, 빔광학

## First Beam Test Results of a Radio-frequency Quadrupole Linac for the Daejeon Ion Accelerator Complex at KAERI

허성렬\*<sup>1</sup>, 장대식<sup>1</sup>, 황철규<sup>1</sup>, 진정태<sup>1</sup>, 이석관<sup>1</sup>, 오병훈<sup>1</sup>

<sup>1</sup>한국원자력연구원 핵융합기술개발부  
srhuh7@kaeri.re.kr

### Abstract:

The Daejeon ion accelerator complex (DIAC) is being built at the Korea Atomic Energy Research Institute (KAERI). The purpose of this complex is to provide heavy ion beams with energies of up to 1 MeV/u for various applications including fusion materials research and biological study. The heavy ion beam line of the DIAC consists roughly of an electron cyclotron resonance (ECR) ion source, a radio-frequency quadrupole (RFQ) linac, a rebuncher (RB), and interdigital H-type (IH) linacs given from the high energy accelerator research organization (KEK) in Japan. Recently, we successfully carried out the RF conditioning and then the first beam test of the RFQ designed to accelerate heavy ions to 178.4 keV/u. 19.38  $\mu$ A of helium ions ( $\text{He}^+$ ) with a transmission efficiency of 91.7% for the drift-through ions was achieved at a duty cycle of 48%. The measured transmission efficiency agrees well with the experimental results from the KEK facility. In this presentation, the test results of the RFQ linac will be presented and discussed in detail.

### Keywords:

Heavy Ion Beam, Accelerator, Radio-frequency Quadrupole, RFQ, DIAC, Helium Ion

## Electron temperature and density measurements in a low density Helium plasma using a collisional-radiative model

안빈\*<sup>1</sup>, 임예건<sup>1</sup>, 김영철\*<sup>1</sup>

<sup>1</sup>한국과학기술원 원자력및양자공학과  
ven840@kaist.ac.kr, ycghim@kaist.ac.kr

### Abstract:

Electron temperatures and densities of a low density helium plasma are measured using an optical emission spectroscopy technique. Plasmas are generated in a newly developed DC multi-dipole chamber, MAXIMUS (Magnetic X-point SIMULATOR System), where various plasma parameters are varied by adjusting neutral pressure, bias voltage and heating current. We generate forward models of various line radiations based on either a collisional-radiative model or a corona model, and the forward model is used to infer electron temperature and density of various Helium plasmas. Inferred electron temperatures and densities from these models are compared with the simultaneous Langmuir probe measurements. In addition, we present and analyze behaviors of various line ratios generated from the collisional-radiative model.

### Keywords:

Helium plasma, Optical emission spectroscopy, Collisional-radiative model, Electron temperature and density, MAXIMUS

## KSTAR L-mode 디버터-플라즈마 분리 실험에서 관찰된 디버터 비대칭 특성

박재선<sup>1, 2</sup>, PITTS R. A.<sup>3</sup>, 박준교<sup>4</sup>, THATIPAMULA S. G.<sup>4</sup>, 홍석호<sup>4</sup>, 최원호\*<sup>1, 2, 5</sup>

<sup>1</sup>한국과학기술원 물리학과, <sup>2</sup>불순물 및 경계 플라즈마 연구센터, <sup>3</sup>ITER Organization, <sup>4</sup>국가핵융합연구소, <sup>5</sup>한국과학기술원 원자력 및 양자공학과  
wchoe@kaist.ac.kr

### Abstract:

디버터와 플라즈마 사이에 중성 가스층의 형성에 의한 디버터 플라즈마 분리 현상은 향후 ITER 혹은 DEMO 장치에서 예상되는 강한 디버터 열속을 제어하기 위한 수단으로 큰 의미를 가지며, 이에 대한 물리적 이해는 향후 디버터 설계 및 최적 운전 조건을 찾는 데 필수적이다. KSTAR L-mode 플라즈마에서 전자밀도를 변화시키는 실험을 통해 디버터 분리 조건을 얻었다. 측정된 램뮤어탐침 신호에 의하면 KSTAR 에서 디버터 분리 현상은 시간-독립, 시간-의존 실험에서 각각 다르게 나타났다. 먼저, 총 4 shot에 걸쳐서 upstream 전자밀도를 스캔한 실험(각 shot에서는 전자밀도 고정, 시간-독립)에서는 바깥쪽 디버터 타겟이 플라즈마와 먼저 분리되고 ( $\langle n_e \rangle = 2.0\text{-}2.5 \times 10^{19}/\text{m}^3$ ), 안쪽 디버터 타겟은 더 높은 밀도 조건에서 플라즈마와 분리되는 결과를 얻었다 ( $\langle n_e \rangle > 2.5 \times 10^{19}/\text{m}^3$ ). 반면, 전자밀도를 시간에 따라 약 8초에 걸쳐 서서히 증가시킨 실험(시간-의존 밀도 증가 실험)에서는 특정 밀도 조건 달성 시 ( $\langle n_e \rangle \sim 3.0 \times 10^{19}/\text{m}^3$ ) 양 타겟에서 플라즈마가 동시에 분리되었다. Degree of detachment (DOD) 분석을 통해 위의 결과들을 정량적으로 확인하였다. KSTAR에서는 두 타겟의 DOD 값이 크게 차이 나지 않았으며, 밀도가 증가함에 따라 DOD가 급격하게 변화한다. 반면 ASDEX-U에서 진행되었던 밀도 증가 실험에서는 내부 타겟의 DOD가 외부 타겟보다 10배 가량 크게 측정되었으며, 밀도 증가에 따라 DOD가 부드럽게 증가한다 [1].

[1]S. Potzel *et al*, "A new experimental classification of divertor detachment in ASDEX Upgrade", Nuclear Fusion 54, 013001 (2014)

### Keywords:

디버터 분리 KSTAR 플라즈마

## KSTAR H모드 플라즈마에서 크립톤 불순물 주입을 통한 ELM 억제 및 내부수송장벽 생성

최원호\*<sup>1, 2, 4</sup>, 장주혁<sup>1, 2</sup>, 홍주환<sup>1, 2</sup>, 송인우<sup>1, 2</sup>, 선창래<sup>3</sup>, 김재현<sup>3</sup>, 강지성<sup>3</sup>, 김기민<sup>3</sup>, 박재선<sup>1, 2</sup>, 홍석호<sup>3</sup>, 전태민<sup>1, 2</sup>

<sup>1</sup>한국과학기술원 물리학과, <sup>2</sup>불순물 및 경계 플라즈마 연구센터, <sup>3</sup>국가핵융합연구소, <sup>4</sup>한국과학기술원 원자력 및 양자공학과  
wchoe@kaist.ac.kr

### Abstract:

크립톤 등 기체 불순물 주입은 플라즈마로부터 방출되는 고온의 열속으로부터 핵융합로의 내벽을 보호하는 역할을 수행할 수 있어, ITER 및 차세대 핵융합 장치 운전을 위한 중요한 과제로 여겨지고 있다. 본 연구에서는 KSTAR H-모드 플라즈마에서 크립톤 불순물 주입을 통한 ELM 완화 및 내부수송장벽(ITB) 형성 실험을 수행하였다. 크립톤은 디버터 영역에 주입되었는데, 피에조 밸브의 전압과 개방 시간을 변화시켜 주입량을 조절하였다. 적외선 이미징 볼로미터(IRVB), 연 X선 배열 및 진공자외선(VUV) 분광기로 크립톤 방출광 분포를 측정하였다. 크립톤 주입량이 적을 때에는( $\sim 1.8 \times 10^{19}$  입자)에서는 플라즈마 변수 및 ELM에 변화가 관찰되지 않았다. 크립톤 주입량이 중간 수준( $\sim 1.7 \times 10^{19}$  입자)에서 전자밀도, 노심 전자온도 및 플라즈마 축적에너지가 약간 감소되며, ELM 크기가 완화되는 것을 관찰하였다. 크립톤 주입량을 더 증가시켰을 때( $\sim 3.5 \times 10^{19}$  입자)에는 플라즈마 종료까지 ELM이 완전히 억제되었다. 전자공명 가열(ECH) 및 strike point 위치에 따라 ELM 억제 양상이 변하는 것을 관찰하였다. 충분히 높은 크립톤 주입량( $\sim 5 \times 10^{19}$  입자)에서는 ELM 완화 이후 내부수송장벽이 형성되는 것을 확인하였다. 플라즈마 중심부 영역 ( $1.8 < R < 2.0$  m)에서 이온 및 전자 온도, 토로이달 회전속도의 급격한 상승이 관찰되었다. TRANSP 계산 결과, 내부수송장벽 내부에서 이온 및 전자 열확산도가 크게 감소함을 확인하였으며, 크립톤이 내부수송장벽 형성에 미치는 기작을 이해하기 위해 상세한 해석이 진행되고 있다.

### Keywords:

토카막, 불순물, 기체 주입, ELM 억제, 내부수송장벽

## 핵융합 플라즈마 내 텅스텐 불순물 수송현상 연구를 위한 스펙트럼 모델 개발

최원호\*<sup>1, 2, 6</sup>, 송인우<sup>1, 2</sup>, 권덕희<sup>3</sup>, 홍주환<sup>1, 2</sup>, GUIRLET Remy<sup>4</sup>, 선창래<sup>5</sup>, 안영화<sup>5</sup>

<sup>1</sup>한국과학기술원 물리학과, <sup>2</sup>불순물 및 경계 플라즈마 연구센터, <sup>3</sup>한국원자력연구원, <sup>4</sup>CEA-IRFM, France, <sup>5</sup>국가핵융합연구소, <sup>6</sup>한국과학기술원 원자력 및 양자공학과  
wchoe@kaist.ac.kr

### Abstract:

ITER에서 디버터의 대면재료로 텅스텐(W, 원자번호 Z=74) 사용이 결정됨에 따라 텅스텐과 같은 무거운 불순물과 플라즈마와의 상호작용 연구의 중요성이 부각되고 있다. KSTAR에서는 금속 불순물 입자 주입기와[1] 소형 최첨단 EUV 분광기(CAES)가[2] 텅스텐 불순물 수송 연구를 위해 개발되었다. 텅스텐 수송과 텅스텐으로 인한 방출광의 플로이달 비대칭성을 해석하기 위해 본 연구에서는 FAC 및 ADAS와 같은 원자데이터베이스를 기반으로 하는 불순물 수송 전산모사 코드를 개발하였다. 본 전산코드는 Open-ADAS 시스템과 통합되어 ADAS에서 이온화율, 재결합율 및 광방출상수 등을 가져오고 이를 이용하여 확산과 대류현상이 포함된 코로나 모델 방정식을 풀어낸다. ADAS에서 제공해 주는 위에 기술된 물리상수를 이용하여 low-Z 불순물의 수송현상 분석이 가능하지만, 텅스텐 등의 high-Z 불순물의 경우 FAC에서 계산한 결과를 사용하여 분석을 진행하였다. 본 연구에서는 개발 중인 전산코드의 유효성을 검증하기 위해 SANCO 전산모사 코드를 활용한 선행연구인 ECH를 활용한 알곤수송현상[3] 분석과 비교분석을 진행하였다. 개발된 코드를 통해  $Ar^{16+}$  (35.3 nm)의 방출광 세기는 off-axis ECH를 가열함에 따라 노심 축적이 완화되는 현상이 모사되었으며 이는 SANCO에서 계산한 결과와 같은 경향성을 보여주었다. 하지만 방출광 세기 및  $Ar^{15+}$  부터  $Ar^{18+}$ 의 이온상태 공간분포의 피크 위치 등이 약 10%의 오차를 보여주었다. 현재 본 코드는 정상상태의 플라즈마, 즉 시간과 무관하게 결과를 보여주어 하나의 시간 지점에서만 계산이 가능하다는 점 때문에 더욱 정밀한 정량분석을 위해서 시간에 의존적인 코드 개발이 진행 중이다.

### 참고문헌

- [1] H. Y. Lee et al., "Development of a particle injection system for impurity transport study in KSTAR", Rev. Sci. Instrum. **85**, 11D862 (2014)
- [2] Inwoo Song et al, "Compact advanced extreme-ultraviolet imaging spectrometer for spatiotemporally varying tungsten spectra from fusion plasmas", Rev. Sci. Instrum. **88**, 093509 (2017)
- [3] Joohwan Hong et al., "Modification of argon impurity transport by electron cyclotron heating in KSTAR H-mode plasmas", Nucl. Fusion **57**, 036028 (2017)

### Keywords:

fusion, plasma, tungsten, EUV, impurity transport

## Plasma density profile measurements by using reflectometer

서성현\*<sup>1</sup>

<sup>1</sup>국가핵융합연구소 KSTAR연구센터  
shseo@nfri.re.kr

### Abstract:

In tokamak plasmas, the plasma profile suddenly changes to form a pedestal structure in the edge region. In L-H transition, all the profiles of temperature, density, and velocity show the same pedestal structure. Sometimes the transport barrier is formed internally. The first step to understand the physical mechanism is to measure the profile evolution with a fast time resolution during transition. Microwave reflectometer is suitable for that purpose because it can measure the density profile in a time resolution of 20 ms [1]. The detailed time evolutions of density profile structure during L-H transition and during ITB formation are measured and the results are presented. For the precise density profile measurements, the frequency dispersion in waveguide is theoretically compensated.

### References:

Seong-Heon Seo, "The Electron Density Profile Measurement with a Fast Time-resolution in the KSTAR Tokamak", J. Kor. Phys. Soc. 65, 1299 (2014).

### Keywords:

reflectometer, density profile

## Semi-analytic Shape Function of High-harmonic Electron Cyclotron Emission in Tenuous Plasma

임준억<sup>1</sup>, 조자원<sup>1</sup>, 윤건수\*<sup>1</sup>

<sup>1</sup>포항공과대학교 물리학과  
gunsu@postech.ac.kr

### Abstract:

Semi-analytic expressions for the electron cyclotron emission (ECE) shape function are derived for arbitrary high harmonics. The integrand of the ECE shape function is fitted with an easily-integrable function parameterized by the harmonic number, electron temperature, and emission angle. Semi-analytic formulae for high harmonic ECE emissivities are obtained by integrating the fitted integrand. The developed expression matches the numerically-integrated ECE shape function very well. The expression can be used for rapid analysis of high-harmonic ECE spectra.

### Keywords:

High-harmonic Electron Cyclotron Emission, Shape Function

## Slow sawtooth crash driven by localized electron cyclotron heating and current drive in KSTAR plasma

윤건수\*<sup>1</sup>, 최경현<sup>1</sup>, 최민준<sup>2</sup>, 정진현<sup>2</sup>, 우민호<sup>2</sup>, 박현거<sup>2, 3</sup>  
<sup>1</sup>포항공과대학교 물리학과, <sup>2</sup>국가핵융합연구소, <sup>3</sup>울산과학기술원 물리학과  
gunsu@postech.ac.kr

### Abstract:

In the core of tokamak plasma, sawtooth oscillation is commonly recognized as periodic fast collapses (10s of  $\mu$ s) driven by  $m=1$  internal kink mode, despite evidences for sawtooth relaxations with slow damping called post-cursor oscillations. The studies on the sawtooth control have been focused mostly on the sawtooth period based on the stability of the  $m = 1$  internal kink mode while investigations on the slow sawtooth relaxation were few. In KSTAR plasmas with localized electron cyclotron (EC) heating and current drive close to the  $q = 1$  surface, we find that the sawtooth relaxations occur with slow time scale comparable to the Sweet-Parker time scale (a few ms). The scan of heating and current drive deposition revealed two different types of slow relaxation with the help of detailed 2-D imaging diagnostics: (1) post-damping of an  $m=1$  mode after partial crash of multiple  $m/n = 1/1$  modes and (2) slow growth of an  $q=1$  island. These two slow relaxations occur when the heating deposition is located just inside and just outside the  $q=1$  surface, respectively. In the heating power modulation experiment, we found that the slow relaxations of the second type initiated by a short EC beam blip continue for the duration of the redistribution time of the driven current, which exceeds the sawtooth period. This result suggests that the crash (relaxation) time control of sawtooth is a more fundamental approach to avoid neoclassical tearing modes which can be destabilized by fast sawtooth crash. This work was supported by the NRF Korea under grant No. NRF-2017M1A7A1A03064231

### Keywords:

Tokamak, Plasma, Microwave heating, Sawtooth instability, diagnostic

## Observations of fast radio frequency (RF) bursts and its dynamics at the onset of pedestal collapse in KSTAR H-mode plasmas

김민호<sup>1</sup>, 윤건수\*<sup>1</sup>, THATIPAMULA Shekar Goad<sup>2</sup>, 이지은<sup>1</sup>, 최민준<sup>2</sup>, 박현거<sup>2, 3</sup>, AKIYAMA Tsuyoshi<sup>4</sup>  
<sup>1</sup>포항공과대학교 물리학과, <sup>2</sup>국가핵융합연구소, <sup>3</sup>울산과학기술원 물리학과, <sup>4</sup>National Institute for Fusion Science  
gunsu@postech.ac.kr

### Abstract:

Radio frequency (RF) bursts (0.1 - 1 GHz) have been observed within several hundreds of microseconds before and at the onset of the pedestal collapse in KSTAR H-mode discharge [1] using a high-speed spectrum measurement system. The RF bursts can be divided into four distinct stages: (1) appearance of high-harmonics (8 - 27<sup>th</sup>) of deuterium ion cyclotron frequency ( $f_{cD} \sim 11$  MHz) at the outboard edge, (2) intensification of the harmonic ion cyclotron emissions, (3) broadband RF emission toward high frequency ( $< 500$  MHz) at the onset of the edge-localized modes (ELM) crash, and (4) rapid chirping up/down in step of  $f_{cD}$  during the pedestal collapse. Recent numerical simulations in large helical device (LHD) suggest that the ion cyclotron waves can be excited by the beam-driven fast ions with large radial excursion making a population inversion in the ion velocity distribution at the plasma edge region [2]. Comparison with 2-D electron cyclotron emission (ECE) image diagnostics shows that the dynamic changes of the RF spectra are correlated with the evolution of the edge perturbation structure [3, 4]. This suggests that the radial electric field gradient or the E×B velocity shear at the pedestal region can be another possible source for ion cyclotron wave generation. This work is supported by the National Research Foundation of Korea (NRF) under contract No. NRF-2017M1A7A1A03064231 and BK21+ program.

### Keywords:

Nuclear fusion, Tokamak, Plasma diagnostics, Radio frequency, Edge localized mode

## Study of edge-localized mode transitions based on time series of spectrally-decomposed 2D image data

김경준<sup>1</sup>, 윤건수\*<sup>1, 2</sup>

<sup>1</sup>포항공과대학교 첨단원자력공학부, <sup>2</sup>포항공과대학교 물리학과  
gunsu@postech.ac.kr

### Abstract:

The dynamics of edge-localized mode (ELM) is studied using the electron cyclotron emission imaging (ECEI) system [1] on the KSTAR tokamak. We focus on the mode transition phenomena during the inter-crash period [2] because of relevance to the phase transition (from modal to non-modal structure) right before the ELM crash [3]. We present the details of the process of non-overlapping transition, one of the two mode transition types [2], using the time series of two types of post-processed ECEI data: the conventional image of low-frequency components and cross-coherence image of high-frequency components. This work is supported by the National Research Foundation of Korea (NRF) under contact No.NRF-2017M1A7A03064231 and BK21+ program.

### References:

- [1] G.S. Yun *et al*, "Quasi 3D ECE imaging system for study of MHD instabilities in KSTAR", *Rev. Sci. Instrum.* **85**, 11D820 (2014).
- [2] Jieun. Lee *et al*, "Toroidal mode number transition of the edge localized modes in the KSTAR plasmas", *Nucl. Fusion.* **55**, 113035 (2015).
- [3] Jieun Lee *et al*, "Solitary perturbations in the steep boundary of magnetized toroidal plasma", *Sci. Rep.* **7**, 45075 (2017).

### Keywords:

fusion, tokamak, KSTAR, ELM, ECEI

## CdSe 콜로이드 양자점의 흡수 및 형광 특성을 통한 크기 분석

윤지소<sup>1</sup>, 김성훈<sup>1</sup>, 이흥석\*<sup>1</sup>

<sup>1</sup>전북대학교 물리학과  
hslee1@jbnu.ac.kr

### Abstract:

양자점이란 나노미터 크기의 반도체 결정으로 양자 구속 효과 (quantum confinement effect)에 의하여 전자 (electron)와 정공 (hole)의 움직임을 3차원적으로 제한하게 된다. 이때, 반도체 나노 결정의 크기가 보어 반지름 (exciton Bohr radius)과 비슷하거나 작아지게 되면 벌크 상태와 비교하여 상이한 물성 변화가 나타나게 된다. CdSe 양자점은 나노 결정의 반지름을 조절하여 가시광선 영역에서 원하는 파장의 빛을 내게 할 수 있고 색순도가 매우 우수하여 디스플레이 응용에 매우 적합하다. 특히, 광효율성과 광안정성이 높기 때문에 발광소자뿐만 아니라 태양전지, 포토다이오드 등에 응용 가능성이 높아 연구되고 있다. 본 연구에서는 화학적 합성 방법 중 고온 주입 제조방식 (hot-injection)을 사용하여 CdSe 콜로이드 양자점을 제작하고 흡수 및 형광 특성을 통해 양자점의 크기를 분석하였다. 흡수 스펙트럼 분석을 통해 얻은 미분 흡수 스펙트럼을 이용하여 전기적 전이에 따른 가우시안 분포들로 피팅하였다. 그리고 흡수, 형광 스펙트럼의 피크를 분석하여 유효 질량 근사에 기반을 두는 brus 방정식을 이용하여 에너지 간격을 계산하고 양자점의 크기를 분석하였다. 또한 투과 전자 현미경 (transmission electron microscopy) 측정으로 양자점의 크기를 분석하여 에너지 간격을 통해 분석한 양자점의 크기와 비교 할 수 있었다.

### Keywords:

콜로이드 양자점, CdSe, 흡수도, 형광, 에너지 간격

## Electronic and optoelectronic properties of MoS<sub>2</sub> field-effect-transistors with channel doping of Cl-molecules

김은규\*<sup>1</sup>, 추동일<sup>1</sup>, 김태영<sup>1</sup>  
<sup>1</sup>한양대학교 물리학과  
ek-kim@hanyang.ac.kr

### Abstract:

In recent years, transitionmetal dichalcogenides(TMDs) have been researched due to their unique physical properties. As one of TMDs, few-layered MoS<sub>2</sub> have a large bandgap and carrier mobility. For the electronic and optoelectronic devices based on few-layered MoS<sub>2</sub>, it has been focusing on doping issues to improve the devices performance. However MoS<sub>2</sub> cannot be doped by general methods such as ion implantation because its thickness is ultrathin. Especially, a molecular doping for MoS<sub>2</sub> is an important method because it demonstrates the surface charge transfer between dopant molecules and MoS<sub>2</sub> layer. In case of MoS<sub>2</sub>, the binding between dopant molecules and sulfur makes sulfur vacancies and then it acts as donors or acceptors. In this work, we fabricated and characterized Cl-molecule doped back-gated transistor and suspended transistor, respectively. The transistors are fabricated using a highly n-doped Si substrate with 280-nm-thick SiO<sub>2</sub> layer. The chloride molecular doping for MoS<sub>2</sub> flakes is done by soaking process in 1,2 dichloroethane (DCE) solution for 12hr. Finally, we will measure and analysis electronic and optoelectronic properties in two types of field-effect-transistor.

### Keywords:

Molecular Doping, MoS<sub>2</sub>Transistor

## Raman imaging analysis of graphene domain structures

이태건<sup>1</sup>, 김명중<sup>2</sup>, 노희석\*<sup>1</sup>

<sup>1</sup>전북대학교 물리학과, <sup>2</sup>한국과학기술연구원  
rho@chonbuk.ac.kr

### Abstract:

화학기상증착 방법으로 성장된 다결정 단층 그래핀 도메인 구조에 대한 공간 분해된 라만 산란 결과에 대해서 보고한다. 구리 기판의 표면 거칠기를 조절함으로써 도메인 크기가 서로 다른 두 그래핀을 성장하였다. D와 G 피크의 세기 변화를 통해 도메인 경계를 관측할 수 있었고, 이로부터 단일 도메인의 크기를 확인할 수 있었다. 특히, 도메인 경계 영역에서 D/G와 2D/G 세기 비율 그리고 2D 피크의 선포에 대한 라만 이미지는 그래핀의 도메인 경계가 적층 형태임을 보여주었다. 도메인 크기가 상대적으로 큰 그래핀에서 전체적으로 D 피크의 세기가 증가됨을 확인하였는데, 이는 도메인 내부에 결함이 많이 존재함을 시사한다. G와 2D 피크의 에너지 상관관계를 통해서 큰 도메인 크기를 갖는 그래핀에 2축 인장 변형이 더 크게 작용하고 있음을 알 수 있었다. 위치별 2D 피크의 선포 분포로부터는 큰 도메인을 갖는 그래핀에서 변형 요동이 더 두드러지게 나타남을 알 수 있었다. 큰 도메인 크기를 갖는 그래핀에서 운반자 이동도가 상대적으로 감소하였는데, 이는 결함, 인장 변형, 변형 요동의 증가에 따른 것으로 보인다. 이 논문은 2016년도 정부(교육부)의 재원으로 한국연구재단의 지원을 받아 수행된 기초연구사업임 (과제번호: 2016R1D1A1B03935270).

### Keywords:

Spatially resolved Raman spectroscopy, Graphene domains, Defects, Strains, Strain fluctuations

## One-pot 합성법을 이용한 quantum-well-shell 구조의 ZnS/InP/ZnS 양자점 합성 (2018)

손상호\*<sup>1</sup>, 잠태훈<sup>1</sup>

<sup>1</sup>경북대학교 물리학과  
shsohn@knu.ac.kr

### Abstract:

양자점 합성법으로 사용되는 hot-injection synthesis는 성장온도의 조절이 어렵고 여러 횟수에 걸쳐 합성하기에 quantum-well-shell 구조의 양자점을 합성하기에는 상당히 까다로운 단점이 있다. 이를 대체하고자 core와 well의 전구체를 동시에 넣어 합성하는 one-pot synthesis를 이용하여 InP 기반의 양자점을 합성하였으며 Zinc sulfide를 core로 하여 Indium Phosphide와 Zinc sulfide를 각각 well-shell로 갖는 구조의 양자점 합성 여부를 X선 회절 분석(XRD), 투과 전자 현미경(TEM), 자외선-가시광 흡수도(UV-Vis absorption) 및 광 발광(Photoluminescence)을 기반으로 기초물성 파악하였다.

### Keywords:

Nanomaterials, Quantum dots, One-pot synthesis, Quantum-well-shell structure

## Synthesis and properties of Tb<sup>3+</sup>-doped NaBiF<sub>4</sub> phosphors for white light-emitting diode applications

유재수\*<sup>1</sup>, HUA Yongbin<sup>1</sup>

<sup>1</sup>경희대학교 전자공학과  
jsyu@khu.ac.kr

### Abstract:

The phosphor-converted white light-emitting diodes (WLEDs) are considered as a next generation solid-state lighting source to replace the conventional blubs and lamps owing to their excellent advantages of low energy consumption, environmentally friendly-feature, long working lifetime and high luminescent efficiency. Unfortunately, the commercial strategy, which is employed to generate the white light, exhibits high correlated color temperature and low color rendering index. To avoid these drawbacks, two available approaches are proposed, that is, utilizing a near-ultraviolet chip to excite the hybrid red-green-blue phosphors and using a blue LED chip to pump the green-red phosphors. Clearly, to improve the performance of the WLED device, searching a highly efficient green-emitting phosphor that can be pumped by near-ultraviolet or blue light is required. In this presentation, series of Tb<sup>3+</sup>-doped NaBiF<sub>4</sub> nanoparticles were successfully prepared by a facile chemical precipitate reaction method at room temperature. The phase compositions, microstructure and photoluminescence behaviors of the resultant samples were studied in detail. Furthermore, the thermal quenching performance of the prepared compounds was also investigated by analyzing the temperature-dependent photoluminescence emission spectra. Ultimately, a green-emitting LED device was fabricated to explore the potential applications of the studied nanoparticles for WLEDs.

### Keywords:

Phosphors, Rare-earth, Luminescent

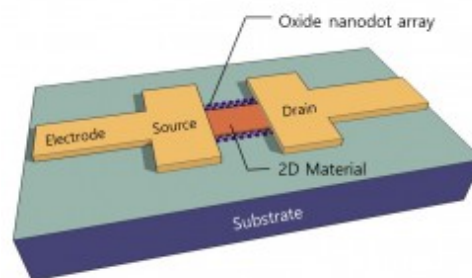
## The Properties of 2D Materials on Functional Oxides

박배호\*<sup>1</sup>, 정현식<sup>2</sup>, 전영철<sup>3</sup>, 신민정<sup>1</sup>, 이상익<sup>1</sup>, 전지훈<sup>1</sup>, 윤찬수<sup>1</sup>, 김연수<sup>1</sup>, 양진호<sup>2</sup>, 이은송이<sup>3</sup>

<sup>1</sup>Department of Physics, Konkuk University, <sup>2</sup>Department of Physics, Sogang University, <sup>3</sup>Department of Materials Science and Engineering, UNIST  
baehpark@konkuk.ac.kr

### Abstract:

As intriguing characteristics of two-dimensional (2D) materials including ReSe<sub>2</sub> and other transition metal dichalcogenides (TMDs) have been studied, the combination of 2D materials with various functional materials is attracting attention. Especially, high- $\kappa$  dielectric or ferroelectric materials have been considered as promising candidates to study synergetic effects when integrated with 2D materials. Specifically, SrTiO<sub>3</sub> (STO) thin film can be used to aid at improving the performance of graphene device. We are interested in the properties of few-layer ReSe<sub>2</sub> field effect transistor (FET) device or MoS<sub>2</sub> nanosheets on the functional oxides such as SrTiO<sub>3</sub> thin film or BiFeO<sub>3</sub> (BFO) nanodot array which attract much attention because of their potential applications to nanoscale devices required for next-generation semiconductor industry. We made BFO nanodot arrays with 70nm in diameter on SrRuO<sub>3</sub> (SRO) /SrTiO<sub>3</sub> (STO) using porous anodic aluminum oxide (AAO) template and STO /Nb:STO thin film by pulsed laser deposition (PLD). And then we performed atomic force microscope (AFM), piezoresponse force microscopy (PFM), high resolution x-ray diffraction (HR-XRD) measurements for nanodot array and thin film. We also performed AFM, Raman spectroscopy for ReSe<sub>2</sub> and MoS<sub>2</sub> nanosheet to confirm their properties. We fabricated FET devices of TMDs using e-beam lithography and evaporator system and measured the electrical property of them. We are going to make the junction devices between TMDs and oxides by transfer method and investigate effects of oxides to their electrical and optical properties. For this, we will compare the experimental data with the simulation results.



### Keywords:

TMDs, oxide, ReSe<sub>2</sub>, MoS<sub>2</sub>, STO, BFO, junction,

## Observation of photoinduced Trion absorption in WSe<sub>2</sub> monolayer

이기주\*<sup>1</sup>, 정태영<sup>1</sup>, 이성연<sup>1</sup>  
<sup>1</sup>충남대학교 물리학과  
kyee@cnu.ac.kr

### Abstract:

Monolayer transition metal dichalcogenide (TMDC) have a large exciton binding energy, a few hundreds of meV, due to strong confinement effect and dielectric screening. These large binding energy enables the observation of high order excitonic states such as excitons, trions, and biexcitons. To investigate these many body phenomenon is important for application in optoelectronic device and physical understanding of light-matter interaction filed.

We perform pump power dependence steady state pump-probe experiment on WSe<sub>2</sub> monolayer capped with h-BN to measure absorption spectrum change between with pump and without pump. In low excitation laser fluence (0.1 mJ/cm<sup>2</sup>), the redshift and bleaching of A exciton absorption peak are occurred. However additional absorption increases in lower energy side of A exciton is observed under the high excitation laser fluence (5 mJ/cm<sup>2</sup>). The simulation using Lorentzian absorption line shape change between with and without excitation laser reveals that this absorption increase occurs at ~43 meV lower than A exciton resonance energy. Its energy difference of 43 meV is larger than trion binding energy (~ 35 meV) confirmed in PL experiment. This absorption increases appears only under high exciton density regime and the higher excitation laser power the more increase of these absorption occurs. These experimental results indicate that this absorption stems from biexciton.

### Keywords:

TMDC, Pump-probe experiment, Exciton, High carrier density, many-body effect

## Study of conductive SrVO<sub>3</sub> thin films deposited with RF magnetron sputtering

이호선\*<sup>1</sup>, 정대호<sup>1</sup>, 소현섭<sup>1</sup>  
<sup>1</sup>경희대학교 응용물리학과  
hlee@khu.ac.kr

### Abstract:

Thin films exhibiting high electrical conductivity and high optical transparency in the visible spectrum has proved challenging. It requires minimization of photon absorption and reflection while preserving a high carrier concentration and low carrier scattering rate. But the parameter combination of the SrVO<sub>3</sub> represents a better trade-off not attainable by conventional transparent conductors in the absence of strong electron correlation, and brings SrVO<sub>3</sub> films closer to ideal transparent conductors. We have been interested in transitional metal vanadium oxides having a perovskite structure accompanied by high transparent conductive performance. The transparent conductive thin films including SrVO<sub>3</sub> show significantly improved conductivity. For example, the SrVO<sub>3</sub> thin films may have electrical conductivity about two or three times higher than that of an ITO electrode.

SrVO<sub>3</sub> thin films with ~180 nm in thickness were grown on c-plane sapphire, Si, SiO<sub>2</sub>/Si and LaAlO<sub>3</sub> substrates under identical conditions by sputtering deposition from SrVO<sub>3</sub> targets. Considering the complex phases of SrVO<sub>3</sub> material system, the growth temperature and sputtering gas ambient were optimized and precisely controlled to yield conductive SrVO<sub>3</sub> phase. The sputtering pressure was set at 6 mTorr with 25% H<sub>2</sub>/(Ar+H<sub>2</sub>) gas. All samples were grown at 350~500 °C. After sputtering, all samples were annealed. Using H<sub>2</sub> mixed gas, we succeeded in growing SrVO<sub>3</sub> phase. In contrast, only Sr<sub>2</sub>V<sub>2</sub>O<sub>7</sub> phase was grown using Ar gas during sputtering.

The structural and morphological properties of all samples were studied by X-ray diffraction (XRD), scanning electron microscopy (SEM), and Raman scattering. The Hall effect parameters of all samples were measured using Keithley 4200. The optical properties, i.e. dielectric functions and band gap energies, were measured using spectroscopic ellipsometry. Details of properties of conductive SrVO<sub>3</sub> phase will be discussed.

### Keywords:

SrVO<sub>3</sub>, Sputtering, perovskite Oxide, transparent conducting oxide

## Electrical and optical properties of vanadium-doped indium oxide thin films grown using RF sputtering deposition

이호선\*<sup>1</sup>, 소현섭<sup>1</sup>, 정대호<sup>1</sup>, 박정일<sup>2</sup>, 김한기<sup>2</sup>

<sup>1</sup>경희대학교 응용물리학과, <sup>2</sup>경희대학교 전자정보신소재공학과  
hlee@khu.ac.kr

### Abstract:

We investigated the electrical and optical properties of Vanadium-doped Indium Oxide (IVO) thin films. IVO thin films were deposited on SiO<sub>2</sub>/Si substrate using a co-sputtering deposition method. The RF power of the In<sub>2</sub>O<sub>3</sub> target was fixed at 80W, while the power applied to the V<sub>2</sub>O<sub>5</sub> target was varied between 0W and 50W. The optical constants have been obtained from the measured ellipsometry angles,  $\Psi$  and  $\Delta$ , using the Drude and parametric semiconductor models. We determined optical gap energies of IVO thin films from the absorption coefficients ( $\alpha$ ). With an increase in the vanadium doping concentration, the Drude model amplitude and optical gap energies increased substantially. Drude model amplitudes is a signature of free carrier concentrations. Optical gap energy shift of the IVO thin films was analyzed as a combination of the Burstein-Moss effect, electron-electron interactions, and electron-impurity scattering.

### Keywords:

indium oxide, transparent conducting oxide, TCO, oxide materials, transparent, band gap shift

## Effect of hydrogen peroxide surface treatment of GaN film on NO gas sensing properties

NGUYEN Kim Phung Thi<sup>1</sup>, MADDAKA Reddepa<sup>1</sup>, 박병권<sup>1</sup>, 김문덕\*<sup>1</sup>, 오재응<sup>2</sup>

<sup>1</sup>충남대학교, 물리학과, <sup>2</sup>한양대학교, 전기전자제어계측공학과  
mdkim@cnu.ac.kr

### Abstract:

In recent days, gas detection at lower temperatures gained tremendous interest. The planar GaN films have high limitations towards detection of gases, and besides required elevated operating temperatures. The effect of surface properties and morphologies showed a more significant influence on the gas sensing properties. The porous GaN through electrochemical etching techniques showed high response to hydrogen gas. Nitric oxide sensing properties of H<sub>2</sub>O<sub>2</sub> treated GaN films have studied comprehensively. Gallium oxide (Ga<sub>2</sub>O<sub>3</sub>) dielectric layer formed on GaN surface with H<sub>2</sub>O<sub>2</sub> surface treatment. The gas sensing properties of Ga<sub>2</sub>O<sub>3</sub>/GaN film were carried out from room temperature to 300 °C, the Ga<sub>2</sub>O<sub>3</sub>/GaN exhibited superior NO gas sensing performance than pristine GaN film. The enhanced gas sensing performance is mainly due to thin Ga<sub>2</sub>O<sub>3</sub> layer on GaN film. Further, we also examined the effect of H<sub>2</sub>O<sub>2</sub> surface treatment temperature and time on gas sensing properties. Based our experimental results, simple H<sub>2</sub>O<sub>2</sub> surface treatment is effective way to enhance gas sensing properties of GaN film.

### Keywords:

GaN, NO gas sensor, H<sub>2</sub>O<sub>2</sub> surface treatment

## Room temperature magnetic and semiconducting properties of graphene adsorbed with cobalt oxide

김은규\*<sup>1</sup>, 박창수<sup>1</sup>, 추동일<sup>1</sup>, 이주원<sup>2</sup>, 손윤<sup>2</sup>  
<sup>1</sup>한양대학교 물리학과, <sup>2</sup>동국대학교 양자기능반도체 연구센터  
ek-kim@hanyang.ac.kr

### Abstract:

Ferromagnetic semiconductors have attracted much interest because they are considered as good candidates for a next generation electronic devices with an application of electron spin. For the functional application of materials, ferromagnetic semiconductors should keep the ferromagnetic ordering at room temperature for ordinary electron device working. Dietl et al. had reported the room temperature ferromagnetic properties with  $T_C$  over 300K in semiconductors in a theoretical method. Ferromagnetism at room temperature has also been reported in carbon related materials. In addition, graphene has the high mobility and excellent material properties and has become a hot issue for future spin electronic devices.

High quality graphene synthesized by chemical vapor deposition, purchased from Graphene Supermarket, has been used in this study and graphene transferred onto silicon substrate coated with 300 nm  $\text{SiO}_2$ . The transferred graphene onto silicon substrate was used as a working electrode for the electrochemical doping in electrolyte solution. Experiment was carried out by using WPG potentiostats to control electric potential with Pt counter electrode and Ag/AgCl reference electrode. The glass beaker was used as an electrochemical cell. The electrochemical doping (adsorption) was carried out in a 0.1 M  $\text{LiCoO}_2/\text{DI}$ -water solution, and the amount of adsorption of  $\text{CoO}_2^-$  for the doping was controlled using an electric potential between the working electrode and the reference. We have chosen an optimized condition, 1.5 V for cobalt oxide adsorption throughout several procedures, and  $\text{CoO}_2^-$  ions are adsorbed on the surface of graphene as a CoO during electrochemical doping after electric potential was applied

In this study, we report the ferromagnetic semiconductor properties of a metal oxide adsorbed graphene using electrochemical method. The cobalt-oxide adsorbed graphene has a coercive field ( $H_c$ ) of 57.2 Oe and remanent magnetization of  $128.2 \text{ emu/cm}^3$  at 300 K. The temperature dependent conductivity indicates that the cobalt oxide adsorbed graphene has a band gap of 0.12 eV and semiconducting behaviour.

### Keywords:

Graphene, Band gap, Conductivity

## Synthesis and physical properties of $\text{Cu}_2\text{Sn}_{1-x}\text{Ge}_x\text{S}_3$ single crystal

CHO Heejae<sup>\*1</sup>, KIM Yongshin<sup>1</sup>, CHOI In-Hwan<sup>1</sup>

<sup>1</sup>중앙대학교 물리학과  
nkotbjoey@gmail.com

### Abstract:

Monoclinic (space group : Cc)  $\text{Cu}_2\text{Sn}_{1-x}\text{Ge}_x\text{S}_3$  semiconductor has p-type conductivity with 0.8 eV ( $x=0$ ) ~ 1.7 eV ( $x=1$ ) of direct band gap energy and high absorption coefficient ( $\alpha > 10^4 \text{ cm}^{-1}$  [1]), which are favorable properties for photovoltaic applications. Also, because  $\text{Cu}_2\text{Sn}_{1-x}\text{Ge}_x\text{S}_3$  consists of non-toxic, earth-abundant and low cost elements, it can be considered as alternative for  $\text{Cu}(\text{In,Ga})(\text{S,Se})_2$  and CdTe materials in solar cells. However, the highest record efficiency of  $\text{Cu}_2\text{Sn}_{1-x}\text{Ge}_x\text{S}_3$  solar cells that has been achieved so far is only 6.7% [2] and its photovoltaic properties has been sparsely reported.

In this study,  $\text{Cu}_2\text{Sn}_{1-x}\text{Ge}_x\text{S}_3$  single crystals with different ratio of  $[\text{Ge}]/([\text{Ge}]+[\text{Sn}])$  were fabricated by using Bridgman techniques. X-ray diffraction and Raman spectroscopy were utilized to characterize the single crystals. The measured lattice parameters of  $\text{Cu}_2\text{Sn}_{1-x}\text{Ge}_x\text{S}_3$  were  $a = 6.4379 \text{ \AA} - 6.625 \text{ \AA}$ ,  $b = 11.295 \text{ \AA} - 11.455 \text{ \AA}$ ,  $c = 6.424 \text{ \AA} - 6.603 \text{ \AA}$  and  $\beta = 108.43^\circ - 109.13^\circ$ . Raman active vibration modes of  $\text{Cu}_2\text{SnS}_3$  were observed at  $295 \text{ cm}^{-1}$ ,  $335 \text{ cm}^{-1}$ ,  $354 \text{ cm}^{-1}$ , and  $372 \text{ cm}^{-1}$ , while those of  $\text{Cu}_2\text{GeS}_3$  were found at  $274 \text{ cm}^{-1}$ ,  $320 \text{ cm}^{-1}$ ,  $393 \text{ cm}^{-1}$ , and  $418 \text{ cm}^{-1}$ . Raman spectra of  $\text{Cu}_2\text{Sn}_{1-x}\text{Ge}_x\text{S}_3$  depending on  $[\text{Ge}]/([\text{Ge}]+[\text{Sn}])$  composition ratios were also discussed.

### Keywords:

Bridgman techniques, XRD, Raman,  $\text{Cu}_2\text{Sn}_{1-x}\text{Ge}_x\text{S}_3$

## 폴리스티렌 나노비드 리소그래피법에 의한 금속 어레이 패턴 형성

이승윤<sup>1</sup>, 오규진<sup>1</sup>, 김은규\*<sup>1</sup>

<sup>1</sup>한양대학교 물리학과  
ek-kim@hanyang.ac.kr

### Abstract:

폴리스티렌(polystyrene) 또는 실리카(silica) 재질의 나노비드(bead)들을 자기조립 방식을 통한 일정한 배열이 가능하다. 이러한 나노비드 배열을 이용한 리소그래피 법으로 금속 어레이 패턴링은 마스크 패턴을 이용하는 리소그래피와 비교하여 상대적으로 적은 비용으로 나노 패턴링을 형성할 수 있는 장점이 있다. 또한, 광학적으로 정의되는 패턴 사이즈는 UV 파장에 의해 물리적 한계를 가지나, 나노비드를 이용한 패턴링은 자기조립을 이용하기 때문에 이런 물리적 한계를 가지지 않는다. 이런 이유로 나노비드를 이용한 스피노딩 방식의 패턴링이 많이 연구되고 있다. 나노비드 패턴링은 콜로이드 입자의 크기를 변환하여 구조의 주기성을 쉽게 바꿀 수 있다. 이 패턴링은 두 가지 과정으로 진행된다. 첫 번째 단계는 기판위에 친수성을 높이기 위해 화학처리를 한 분산 구형 콜로이드를 함유하는 현탁액으로 기판을 스피노딩을 하는 것이다. 이 과정을 거치게 되면, 상온에서 콜로이드 결정 마스크라고 불리는 육방 밀집 구조 단일 층 또는 2 중층이 형성된다. 두 번째 단계는 제작된 나노비드 마스크는 주기적으로 배열된 구형 콜로이드의 틈을 이용하여 원하는 재료의 증착을 통해 패턴링을 하는 것이다. 적절한 용매내에서 초음파 처리 또는 디클로로메탄 등의 용매를 이용하여, 콜로이드 결정 마스크를 제거할 수 있다. 이런 식으로 제거 뒤 남게 된 기판상의 나노 도트 어레이는 콜로이드 결정의 주기적 배열로 인해 규칙적인 패턴을 형성하게 된다. 본 연구에서는 0.7~0.9  $\mu\text{m}$  사이즈의 폴리스티렌 나노비드를 이용하여, 금속패턴을 형성하기 위한 최적조건 실험을 수행한다. 이때 전자주사현미경을 이용하여 콜로이드 결정의 배열을 확인하고, 패턴링을 위한 금속박막은 thermal evaporation을 통해서 증착된다.

### Keywords:

nanosphere nanobead nano

## Graphene laminated Cu nanoparticle arrays by spontaneous formation through dewetting

CHOI Jinsik\*<sup>1</sup>, MOHD Musaib<sup>1</sup>, KIM Jinhong<sup>1</sup>

<sup>1</sup>Department of Physics, Konkuk University  
jinschoi@konkuk.ac.kr

### Abstract:

The combination of metal nanostructures and graphene is considered to have a great potential in various electronic, optical, and catalytic applications and developing a facile technique to control the size and distribution of metal nanoparticles has a key role in these applications. In this study, we could obtain Cu nanoparticles (CuNPs) with high uniform distribution and continuous graphene sheets simultaneously through a high-temperature annealing process that uses the same conditions of graphene growth with ultrathin Cu films. The SEM results showed that the size of the CuNPs is related to the thickness of the Cu film. We confirmed the continuity of the simultaneously grown graphene on the CuNPs based on Raman spectra and mapping results. The 'graphene/CuNPs' exhibits typical ambipolar transport characteristics of graphene with dual charge neutral points (CNPs). Using a simplified analytical model, we were able to distinguish two CNPs that originate from 'graphene/CuNPs' and 'graphene/SiO<sub>2</sub>'. Also, using XRD we could confirm that graphene covered CuNPs are not oxidized after exposing to room environment for several months. We believe that this simultaneous synthesis of graphene and CuNPs can be further applied to materials for various electronic, optical, and catalytic applications.

### Keywords:

Graphene, Copper Nanoparticle (CuNP), Chemical vapor deposition (CVD), Synthesis, double charge neutral point (CNP).

## Which part of a string breaks

백승기\*<sup>1</sup>

<sup>1</sup>부경대학교 물리학과  
seungki@pknu.ac.kr

### Abstract:

We investigate dynamics of a one-dimensional homogeneous harmonic chain on a horizontal table. Its one end is anchored to a wall, and the other free end is pulled by external force. We derive Green's function to calculate the response to generic pulling force. As an example, we assume that the magnitude of the pulling force increases with time at a uniform rate  $\beta$ . If the number of beads and springs is large in the chain, the extension of each spring takes a simple closed form, which is a piecewise linear function of time. Under an additional assumption that a spring breaks when its extension exceeds a certain threshold, we see that large  $\beta$  breaks the spring near the pulling end, whereas the breaking point can be located close to the wall by choosing small  $\beta$ . More precisely, the breaking point moves back and forth along the chain as we decrease  $\beta$ , which has been called 'anomalous' breaking in the context of the pull-or-jerk experiment. Although the experiment has been explained in terms of inertia, our analysis shows that its meaning can be fully captured by discussing the competition between intrinsic and extrinsic time scales of forced oscillation.

### Keywords:

harmonic chain, inertia, anomalous breaking

## Splay states in $d$ -dimensional hypercubic lattice and its properties

홍현숙\*<sup>1, 2</sup>, 조영설\*<sup>1, 2</sup>, 이승재<sup>1</sup>

<sup>1</sup>전북대학교 자연과학대학, 물리학과, <sup>2</sup>전북대학교 자연과학대학, 이화학연구소  
hhong@jbnu.ac.kr, yscho@jbnu.ac.kr

### Abstract:

It is known that an automorphism (mathematical) group generated by permutations which preserve the adjacency relation of a given network is strongly related to the cluster synchronization (CS) of nonlinear oscillators on a complex network which contains that permutation symmetry. In this work, we consider Kuramoto oscillators and show that the cluster synchronization of the Kuramoto oscillators can also occur when the oscillators are on  $d$ -dimensional hypercubic lattice. By inspecting the permutation symmetry of that network which includes  $(d-1)$ -dimensional hyperplanar lattices as its topological structure, the cluster synchronization is indeed the splay states constructed by groups of synchronized oscillators belonging to each  $(d-1)$ -dimensional hyperplanar lattice, which behave as a single unit in the splay state. Next, we generalize this system by considering the heterogeneity of the intrinsic frequency of the oscillators and find the same states, however, with distorted shapes. We conclude that the origin of the distorted behavior is the heterogeneity of oscillators' intrinsic frequency by showing analytic and numerical evidences. Finally, we demonstrate the dimensional dependence of the splay state in the hypercubic lattices by investigating the basin stability analysis.

### Keywords:

Kuramoto oscillators, Splay state, Cluster synchronization, Hypercubic lattice, Network symmetry, and Permutation group.

## Evaluation of All the Critical Exponents Only from Information on the Susceptibility

KWAK Wooseop<sup>2</sup>, KIM Seung-Yeon<sup>\*1</sup>

<sup>1</sup>School of Liberal Arts and Sciences, Korea National University of Transportation, <sup>2</sup>Department of Physics, Chosun University  
sykimm@ut.ac.kr

### Abstract:

Phase transition and critical phenomena are greatly universal in nature. Phase transition and critical phenomena are characterized by six independent critical exponents: the specific-heat critical exponent, the spontaneous-magnetization critical exponent, the susceptibility critical exponent, the isothermal-magnetization critical exponent, the correlation-length critical exponent, and the correlation-function critical exponent. Only from the susceptibility, we obtain all the critical exponents, the specific-heat critical exponent, the spontaneous-magnetization critical exponent, the susceptibility critical exponent, the isothermal-magnetization critical exponent, the correlation-length critical exponent, and the correlation-function critical exponent, without using other thermodynamic functions. The evaluation of all the critical exponents only from information on the susceptibility is very accurate and convenient method.

### Keywords:

Phase transition, Critical phenomena, Critical exponents

## Scaling Behavior of the Ising Model on Square Lattice with Self-dual Boundary Conditions

KIM Seung-Yeon\*<sup>1</sup>

<sup>1</sup>School of Liberal Arts and Sciences, Korea National University of Transportation  
sykimm@ut.ac.kr

### Abstract:

From the finite-size scaling behavior of the exact specific heat per volume, calculated with the density of states, the shift exponent,  $\lambda=1.883(14)$ , and the thermal scaling exponent,  $y_t=1.076(7)$ , are obtained for the Ising model on square lattice with self-dual boundary conditions. Furthermore, from the finite-size scaling behavior of the partition function zeros in the complex temperature plane, again calculated with the density of states, much more accurate and precise values for the shift exponent and the thermal scaling exponent are estimated to be  $\lambda=2.0000000(2)$  and  $y_t=1.000000000(2)$ . The estimated value for the shift exponent strongly suggests an integer value for the shift exponent,  $\lambda=2$ , of the square-lattice Ising model with self-dual boundary conditions.

### Keywords:

Self-dual boundary conditions, Shift exponent

## Partition function of the 3D Heisenberg model in the complex temperature plane

김동희\*<sup>1</sup>, 홍성표<sup>1</sup>

<sup>1</sup>광주과학기술원 물리광학과  
dongheekim@gist.ac.kr

### Abstract:

We evaluate the partition function of the three-dimensional (3D) Heisenberg model on the simple cubic lattices in the complex temperature plane by using the Higher-Order Tensor Renormalization Group (HOTRG) method. As the system size increases, the magnitude of the partition function decreases much faster than in the case of the other models with  $\alpha > 0$ , which supports the argument that the heat capacity characteristics near the transition point is highly related to the partition function magnitude [Phys. Rev. E 96, 052130].

### Keywords:

Heisenberg model, partition function zero, higher-order tensor renormalization group

## Analysis of the toy model for the neural network applied to the classical Ising model.

김동희\*<sup>1</sup>, 김동균<sup>1</sup>

<sup>1</sup>광주과학기술원 물리광학과  
dongheekim@gist.ac.kr

### Abstract:

Recently, neural network(NN) has been applied to a phase classification of many body systems. In the Ising model[Nature Physics 13, 431-434(2017)], outputs of the NN follows a size scaling behavior with critical exponent. We introduce a toy model to investigate an analytical relation between a system size and an outputs of the NN. At optimal points, we derive that parameters in the toy model follow the power law with exponent Ising critical exponent for the system size. To support numerical evidences, we implement the stochastic gradient descent method with the square and the triangular lattice to obtain optimal parameters in the toy model. We find that parameters show the power law and size scaling behavior with satisfying the Ising universality class.

### Keywords:

machine learning, phase transition, Ising model, neural network

## Numerical analysis of the two-dimensional Patlak-Keller-Segel model

백승기\*<sup>1</sup>, 이수도<sup>2</sup>, 배규호<sup>1</sup>, 김범준<sup>3</sup>

<sup>1</sup>부경대학교 물리학과, <sup>2</sup>서울대학교 물리천문학부, <sup>3</sup>성균관대학교 물리학과  
seungki@pknu.ac.kr

### Abstract:

We numerically analyze the two-dimensional Patlak-Keller-Segel model to study chemotactic behavior of living organisms. This model consists of a pair of partial differential equations describing the interaction between the density field of the organisms and that of the chemicals. A homogeneous distribution is a trivial solution of this model, but it loses stability and evolves into a sharply peaked distribution when the total amount of the organisms exceeds a certain threshold. We have performed agent-based simulations to estimate the threshold, and the result is consistent with that of linear stability analysis.

### Keywords:

chemotaxis, Patlak-Keller-Segel model, agent-based simulation

## Detection of double phase transition via unsupervised machine learning.

김범준\*<sup>1</sup>, 이송섭<sup>1</sup>  
<sup>1</sup>성균관대학교 물리학과  
beomjun@skku.edu

### Abstract:

Study of critical phenomena of matter is one of the main topics of statistical physics. Thanks to the development of machine learning techniques, many researches have shown that the supervised learning can be used to study critical phenomena of various systems. However, the supervised learning cannot be done without labels which require knowledge about critical behavior of system. To avoid this paradox, several researches have tried to use unsupervised machine learning in exploring statistical physics system and a variety of related methods have been proposed. In this study, we focus on how to detect double phase transition. In our research, the method named as confusion scheme was used to detect double phase transition and q-state clock model is chosen for such a system to test our method. As a result, our method is shown to successfully detect double phase transition in the q-state clock model without any pre-knowledge about the system. Also, our method is shown to find approximate transitions points. We thus conclude that our method can detect the existence of double phase transition without any pre-knowledge about the system.

### Keywords:

double phase transition, unsupervised machine learning, confusion scheme

## Hierarchical modeling for correlated bursty dynamics

조항현\*<sup>1, 2</sup>, 이병화<sup>1, 2</sup>

<sup>1</sup>Department of Physics, Pohang University of Science and Technology (POSTECH), <sup>2</sup>Asia Pacific Center for Theoretical Physics (APCTP)  
h2jo23@gmail.com

### Abstract:

Bursty temporal patterns have been observed in various natural phenomena and human activities such as solar flares, earthquakes, firing of neurons, and human communication. Such temporal inhomogeneities can be characterized by a power-law interevent time distribution, which however does not provide a complete characterization of temporal correlations. For such comprehensive characterization, one also needs to consider correlations between interevent times, often called correlated bursts. The correlated bursts have been measured in terms of heavy-tailed distributions of burst sizes, where the burst size denotes the number of events in a bursty train. In order to model the correlated bursts and their hierarchical feature, we introduce the Soneira-Peebles model in the temporal domain. We find that our theoretical expectations for scaling behaviors in fractality, interevent time distributions, and autocorrelation functions are numerically confirmed. In addition, we numerically find the stretched exponential distribution for burst sizes and provide the analytical explanation. Despite of the presence of correlations between interevent times, the scaling relation between exponents of interevent time distributions and autocorrelation functions still holds.

### Keywords:

Bursts, Correlated bursts, Hierarchical modeling, Complex systems

## Structure of the integrated cellular network of E. coli

김민석<sup>1</sup>, 이덕선\*<sup>2</sup>

<sup>1</sup>Department of Biological Sciences, Inha University, <sup>2</sup>Department of Physics, Inha University  
deoksun.lee@gmail.com

### Abstract:

In growth-limiting environments, the amount of individual proteins is varied in an organized way, which reveals the proteome sectors responding to different limitations [1]. Such sectors must be related to certain genes and small molecules by various interactions, and its understanding can extend our knowledge of the response pathways of cellular networks. To this end, we here compile the ecocyc data of Escherichia coli, one of the most widely used model organism in biology, to construct the integrated cellular network. All the interactions available in the data-set are used, except for some links between metabolic reactions and metabolites; we introduce a scheme to filter out irrelevant links between reactions and metabolites, preventing currency metabolites such as water or ATP from connected to so many reactions. The obtained network is multi-layered with about 16000 nodes and 27000 links; genes, proteins, RNAs, reactions, and compounds are connected by links representing the regulation of transcription, translation, enzyme activity, catalysis, and many other interactions. We investigate the distribution of degree, betweenness centrality, and node-to-node distance within and across layers, which are correlated with the nature of node types and interactions in each layer. We locate the known proteome sectors in the integrated network and discuss the organization of functional modules responding to different limitations.

[1] Hui et al., Mol. Syst. Biol. 11, 784 (2015).

### Keywords:

E.coli, metabolite network

## Clusters in scale-free networks with varying fraction of small-degree nodes

이덕선\*<sup>1</sup>, 이미진<sup>1</sup>, 김흥경<sup>1</sup>

<sup>1</sup>Department of Physics, Inha University  
deoksun.lee@gmail.com

### Abstract:

The size and distribution of connected components in the network representation of a system can be informative of its functionality particularly under attack or failure.

Given that many real-world networks find heavy tails in their degree distributions, the effects of anomalously abundant hub nodes on the formation of clusters have been intensively studied. On the other hand, the role of small-degree nodes in the cluster formation have been neglected. Here we present our study showing a crucial role of small-degree nodes in the formation of the giant component. We introduce a variant of the configuration model scale-free network, in which the total number of links can be varied for given degree exponent by varying the fraction of isolated and small-degree nodes. The size of the giant component in this model network is found to increase linearly with the total number of links when the latter is small enough. This anomalous behavior is shown to originate in the specific behavior of the degree distribution in the model; it is a power law in almost the whole range of degree. For large number of links, the degree distribution is a power-law only for large degrees. This result can be useful in designing a strategy for maintaining large connected components with a small number of links and we discuss the possibility of practical application.

### Keywords:

scale free network, configuration model, small-degree nodes

## Imbalance of pairwise efficiency in urban street network

이민진\*<sup>1</sup>, 이성민\*<sup>2</sup>

<sup>1</sup>성균관대학교 에너지과학과, <sup>2</sup>고려대학교 물리학과  
minjin.lee.9@gmail.com, jrpeter@korea.ac.kr

### Abstract:

Urban road networks have been evolved to facilitate efficient transportation of goods and people. As the efficiency of a street network is an important issue for sustainable development in a city, it has been studied for decades in various ways. One of the popular and simple ways to measure the efficiency is calculating the detour index which is a ratio between travel distance and geodesic distance of a given origin-destination (OD) pair. Previously much effort has been devoted to understanding the global efficiency of a network or spatial distribution of efficiency of nodes (mainly intersections of a street network). Although such approaches give us the overall description of efficiency level, when it comes to the question how to improve the efficiency, we need to understand pairwise efficiency that tells which regions are well connected. Here, we study the efficiency of 1,699,601 route pairs for 73 global cities. We systemically explore the efficiency trend related to a radius from the city center, an angular position with respect to the city center, and geodesic distance of the routes. We find efficiency levels of a driving route in urban areas are strongly dependent on their angular positions on average. Through street network model study, we prove that this behavior is a result of an imbalance of density and accessibility of street network and finally suggest the way to improve the efficiency by alleviating the imbalance of street properties.

### Keywords:

Street network, Efficiency in network, Urban study

## Accessibility Measurement in the Seoul Bus System

최무영\*<sup>1</sup>, 이지혜<sup>1</sup>, 고세건<sup>2</sup>, 이금숙<sup>3</sup>

<sup>1</sup>서울대학교 물리학과, <sup>2</sup>Institute for Theoretical Physics II: Soft Matter, Heinrich-Heine University  
Düsseldorf, <sup>3</sup>성신여자대학교 지리학과  
mychoi@snu.ac.kr

### Abstract:

We study the theoretical basis of accessibility, which constitutes a conclusive factor in location decision and land evaluation. We examine various accessibility measures as to what they actually measure, and apply them to analyzing the Seoul bus system. Accessibility of each bus stop is computed from time distances and compared with the strength of the bus stop. A power-law relation is observed between the accessibility and strength. The emergence of the power-law relation is discussed from the viewpoint of maximizing the trip configuration entropy.

### Keywords:

accessibility, entropy maximization model

## Threshold를 가진 Axelrod 모형에서의 상전이 현상

최준영<sup>1</sup>, 육순형\*<sup>1</sup>

<sup>1</sup>경희대학교 물리학과  
syook@khu.ac.kr

### Abstract:

본 연구에서는 문화적 다양성이 유지되는 이유를 설명하는 Axelrod 모형에 특정한 threshold 이상의 비율로 이웃들이 문화적 특성을 공유하고 있을 때만 그 문화적 특성을 받아들이는 기작을 도입하였다. 전산 시뮬레이션을 통하여 다양한 네트워크 위에서 threshold를 가진 Axelrod 모형은 서로 다른 세개의 phase를 가짐을 발견하였다. 또한, 각 phase사이의 transition은 불연속적임을 발견하였다. Finite-size scaling을 통하여 각 상의 안정성을 조사 하였으며, 발견된 phase transition에 대한 이론적 가능성을 논의한다.

### Keywords:

complex network

## A theory of resource allocation for sequential memory in human

백세범\*<sup>1, 2</sup>, 이현수<sup>1</sup>, 최우철<sup>1, 2</sup>, 박영진<sup>1</sup>

<sup>1</sup>한국과학기술원 바이오및뇌공학과, <sup>2</sup>한국과학기술원 뇌인지공학프로그램  
sbpaik@kaist.ac.kr

### Abstract:

Hyeonsu Lee<sup>1</sup>, Woochul Choi<sup>1,2</sup>, Youngjin Park<sup>1</sup> & Se-Bum Paik<sup>1,2</sup>

<sup>1</sup>Department of Bio and Brain Engineering, <sup>2</sup>Program of Brain Cognitive Engineering, Korea Advanced Institute of Science and Technology, Daejeon 34141, Republic of Korea

Human can memorize various types of sequential information such as phone numbers or a melody of music. In this task, both information of individual items and their order must be stored in a neural circuit, as a form of working memory. Due to the finite capacity of working memory system [1], efficient usage of memory resources is an important issue, but the mechanism of resource allocation in a sequential memory processing is still remained unclear. Here, we suggest a theoretical model of sequential memory allocation, which can provide possible mechanisms of the primacy and recency effects, one of the most fundamental features of sequential memory observed in human experiments [2]. First, we performed a human psychophysics experiment where subjects were asked to memorize and recall a sequence of visual patterns. We confirmed that the performance of human subjects for the first and last stimuli in the sequence was better than that for the others; primacy and recency effect, respectively. To explain such a result, we introduced two new concepts: sequential overwrite and non-uniform allocation of memory resources. The sequential overwrite, an assumption that resources for previous stimuli are partially taken by new stimulus, could explain the recency effect, and the non-uniform allocation idea, where the amount of resource allocated decreases by orders, could fit the observed primacy effect. Thus, our model could provide a model for the observed characteristics of human memory performance. Next, we predicted that memory performance would be improved if the sequential overwrite can be decreased. We also assumed that sequential overwrite can be reduced if subjects are given the number of stimuli to memorize. To test our hypothesis, we designed a sequential memory task where information of stimuli is given in various manners prior to stimulus presentation: correct information, no information, and wrong information. As our model predicted, memory performance was best in the correct information case and was worst in the wrong information case. In addition, our model well fitted the observed results by assuming different amount of overwrites. Overall, we propose that sequential overwrite and non-uniform allocation of memory resources can explain key features of sequential memory performance, and may control the efficiency of memory usage.

### Reference

- [1] Ma, Wei Ji, Masud Husain, and Paul M. Bays. "Changing concepts of working memory." *Nature neuroscience* 17.3 (2014): 347.  
[2] Hurlstone, Mark J., Graham J. Hitch, and Alan D. Baddeley. "Memory for serial order across domains: An overview of the literature and directions for future research." *Psychological bulletin* 140.2 (2014): 339.

### Keywords:

Sequential memory model, Working memory, Theoretical model, Human psychophysics, Sequential overwrite, Non-uniform allocation

## Spatial organization of simple and complex cells in the model neural network of the primary visual cortex

백세범\*<sup>1</sup>, 김광수<sup>2</sup>, 장재선<sup>1</sup>

<sup>1</sup>한국과학기술원 바이오및뇌공학과, <sup>2</sup>한국과학기술원 물리학과  
sbpaik@kaist.ac.kr

### Abstract:

Neurons in the primary visual cortex (V1) respond selectively to the various features of visual stimulus, so it has been of great interest to classify the neurons by their functional tuning to the specific features of visual stimulus. One of the most important criterion is the classification between “simple” and “complex” cells, based on the response dynamics and the spatial segregation between ON and OFF receptive fields [1,2]. Conventionally, it has been thought that the simple cells detect “simple edge” of the visual stimulus and the complex cells process more “complex information”, but it is still unclear what is a crucial factor to the development of simple and complex cell. Recently, on the contrary to the classical notion, it has been suggested that the two classes of neurons are not clearly distinct, but can be considered as a variation from a continuous spectrum [3, 4], implying that the two classes may share a common developmental origin. Here, using a computational model, we suggest that the class of a V1 neuron is destined from the spatial segregation of ON and OFF retinal inputs to the V1 neuron. Clues were found in a previous model study suggesting that the orientation preference of a V1 neuron is originated from the spatial organization of ON and OFF Retinal Ganglion Cells (RGCs), so the moiré interference between the hexagonal lattices of ON and OFF RGCs can seed a periodic column of orientation preference across cortical surface [5]. Here, we propose that the distance between ON and OFF RGCs determines the degree of overlap between ON and OFF receptive fields in a V1 neuron, and the class of the neuron between simple and complex cell. Because the spatial segregation of ON and OFF RGCs varies in a periodic manner across moiré pattern, our results predict that the simple and complex cells may not be randomly distributed across the cortical surface, but are distributed in a quasi-periodic manner. Based on a previous study [6], we further suggest spatial correlation between the location of pinwheel structures and the cluster of complex cells. Overall, we propose a common retinal origin of simple and complex cells and predict a spatial organization of simple and complex cells in visual cortex.

### Reference

- [1] Hubel, D. H., Wiesel, T. N., (1968), Receptive fields and functional architecture of monkey striate cortex. The Journal of Physiology, 195 doi: 10.1113/jphysiol.1968.sp008455.
- [2] Skottun, B. C., De Valois, R. L., Grosof, D. H., Movshon, J. A., Albrecht, D. G., & Bonds, A. B. (1991). Classifying simple and complex cells on the basis of response modulation. Vision research, 31(7-8), 1078-1086.
- [3] Mechler, F., & Ringach, D. L. (2002). On the classification of simple and complex cells. Vision research, 42(8), 1017-1033.
- [4] Priebe, N. J., Mechler, F., Carandini, M., & Ferster, D. (2004). The contribution of spike threshold to the dichotomy of cortical simple and complex cells. Nature neuroscience, 7(10), 1113.
- [5] Paik, S. B., & Ringach, D. L. (2011). Retinal origin of orientation maps in visual cortex. Nature neuroscience, 14(7), 919.
- [6] Paik, S. B., & Ringach, D. L. (2012). Link between orientation and retinotopic maps in primary visual cortex. Proceedings of the National Academy of Sciences, 109(18), 7091-7096.

### Keywords:

Neural network simulation, Visual system, Simple and complex cells, Retinal ganglion cell

## Coevolution of populations and resource: resource feedback to public goods game

박혜진\*<sup>1</sup>, GOKHALE Chaitanya S.<sup>1</sup>

<sup>1</sup>Max Planck Institute for Evolutionary Biology Theory Department  
phj.hyejin@gmail.com

### Abstract:

Individuals interact with each other in a population. According to the interactions, the population size and composition or an eco-system can be determined. However, population size and the composition affect each other. Recently, this eco-evolutionary feedback framework has been well developed. This feedback has been shown to be a way of resolving social dilemmas. The results, however, strongly depend on the assumption of a stable ecology. Moving away from this assumption, we study the complete eco-evolutionary dynamics where feedback between the environment regarding resources and the population dynamics is explicitly handled.

### Keywords:

Evolutionary game theory, Eco-Evolutionary feedback, Resource

## 인공 기저막을 통한 진행파 구현

안강현\*<sup>1</sup>, 이우석<sup>1</sup>

<sup>1</sup>충남대학교 물리학과  
ahnkh@cnu.ac.kr

### Abstract:

소리를 분석하는 데에 있어 인간의 달팽이관은 푸리에 변환과는 다르게 적분시간을 소모하지 않고 주파수를 분석하는 것이 가능하다. 이는 달팽이관 내부에 기저막의 움직임에서 그 원인을 찾아볼 수 있다. von Békésy는 기저막에서는 진행파 라는 형태의 파형이 생기며, 주파수에 따라 기저막에서 최대 진폭이 나타나는 위치가 달라진다는 것을 발견했다<sup>1</sup>. 그러므로 이러한 특징을 갖는 인공 기저막을 만든다면 적분 시간을 소모 하지 않고도 주파수 분석이 가능하다. White와 Grosh에 의해 MEMS를 기반으로 하는 인공기저막이 제작되었지만<sup>2</sup>, 85 - 105dB 크기의 소리를 가해주어도 수 pm 정도로 움직여 측정에 어려움이 있다. 이를 극복하기 위해 거시적인 기저막에서 진행파를 관측했던 von Békésy의 실험과 유사하게 기저막을 제작하고, 기저막의 움직임을 레이저와 광 검출기를 이용해 움직임을 측정하였다. 기저막의 두께와 채워진 유체의 점성을 조절하여 진행파의 생성과의 관계를 조사하였다.

<sup>1</sup> Von Békésy, G., & Wever, E. G. (1960). Experiments in hearing (Vol. 8). New York: McGraw-Hill.

<sup>2</sup> White, R. D., & Grosh, K. (2005). Microengineered hydromechanical cochlear model. Proceedings of the National Academy of Sciences of the United States of America, 102(5), 1296-1301.

### Keywords:

와우, 기저막, 진행파

## 그람-슈미트 과정을 이용한 음성의 사전학습 (Dictionary Learning)

안강현\*<sup>1</sup>, 유재연<sup>1</sup>  
<sup>1</sup>충남대학교 물리학과  
ahnkh@cnu.ac.kr

### Abstract:

사전 학습 (Dictionary learning) 은 주어진 데이터의 기본적인 특징을 찾아내고 이를 선형결합을 통해 복원하는 방법을 말한다. 하지만, 기존의 학습 방법은 각각의 기저 벡터들 간의 유사성을 고려하지 않아 데이터의 기본 구조를 제대로 파악하지 못할 수도 있다. 이를 방지하기 위해 그람-슈미트 (Gram-Schmidt) 과정을 이용하여 서로 독립적인 기저 벡터를 생성하고 기존 방법과의 성능 차이를 비교했다. 또한 이러한 특징을 이용하여 소리를 복원했을 때 하울링을 제거할 수 있는지를 확인하였다.

### Keywords:

음성신호,사전학습,그람슈미트과정

## 모음의 유사성이 딥러닝을 통한 인식에 미치는 영향

안강현\*<sup>1</sup>, 김현재<sup>1</sup>

<sup>1</sup>충남대학교 물리학과  
ahnkh@cnu.ac.kr

### Abstract:

이미지 인식 분야에서는 Convolutional Neural Network 기반의 다양한 딥러닝 모델들을 통해 MNIST와 같은 손글씨 숫자 인식에 대해 99퍼센트 이상의 정확도를 보인다. 같은 수준의 정확도를 모음(아, 예, 이, 오, 우)인식에도 구사할 수 있는지 확인하기 위해 MFCC 혹은 날 데이터를 여러 딥러닝 모델들로 테스트를 해보았다. 그 결과 90퍼센트 수준의 정답률로 이미지 인식 정확도에 비해 저조하고, 특히 두 가지 모음(오, 우)인식에 어려움을 겪는다는 것을 확인하였다. 이 연구 결과가 각테일 파티 효과와 어떤 연관 있는지 조사하기 위해 두 가지 모음을 동시에 들려주고 음성 인식 실험을 수행하였다.

### Keywords:

음성인식

## Color-specific afterimage reveals perceptual segregation of visual objects

백세범\*<sup>1, 2</sup>, 정채윤<sup>1</sup>, 최우철<sup>1, 2</sup>, 김광수<sup>3</sup>

<sup>1</sup>한국과학기술원 바이오및뇌공학과, <sup>2</sup>한국과학기술원 뇌인지공학프로그램, <sup>3</sup>한국과학기술원 물리학과  
sbpaik@kaist.ac.kr

### Abstract:

When a visual stimulus is given, our brain's response often reflects a dynamic interpretation of a given stimulus, rather than simply encoding physical parameters of given stimulus. One example is the afterimage of perceptually filled-in surface reported by Shimojo and his colleges, which is an afterimage of illusory surface [1]. Although afterimage has long been attributed to bleaching of photochemical pigments or neural adaptation in the retina, afterimage of perceptually filled-in surface showed that appearance of afterimage can depend on the perceptual rather than physical aspect of the adapting stimulus. Here we report a new type of afterimage illusion that reveals a dynamic interpretation of given visual information, dependent on the perceptual status. First, we observed that when one adapts to stimulus with multiple segments, afterimage of a filled complete object can be perceived. For example, when one adapts to a stimulus with a few colored concentric rings, participants not only report concentric rings with opposite color (simple afterimage) but also a solid filled circle (merged afterimage). We assumed that this merging afterimage occurs strongly when such a multi-segment stimulus is perceived as a single object in our brain. To test our hypothesis, we performed a series of human psychophysics experiments to show that this effect is due to a perceptual top-down modulation but not a simple reflection of neural interactions in early visual pathway. We designed two stimuli of identical physical segments, one that can be grouped into a global object and the other that cannot be. Although the two stimulus have same set of physical segments, stimulus that can be grouped into a global object showed significantly longer perception of merged afterimage, showing that active interpretation of given stimulus is necessary to cause merging. In addition, we found that the merged afterimage of stimulus with high chromaticity lasts significantly longer compared to that of non-chromatic stimulus. Our results suggest that a top-down control of global perception occurs in a distinct color-specific pathway, or in cell-type specific manners.

### References

1. Shimojo, Shinsuke, Yukiyasu Kamitani, and Shin'ya Nishida. "Afterimage of perceptually filled-in surface." *Science* 293.5535 (2001): 1677-1680.

### Keywords:

illusion, perceptual grouping, chromaticity and luminance

## Exploring temporal response functions for motion perception in human brain

최우철\*<sup>1, 2</sup>, 백세범\*<sup>1, 2</sup>

<sup>1</sup>한국과학기술원 바이오및뇌공학과, <sup>2</sup>한국과학기술원 뇌인지공학프로그램  
choiwc1128@kaist.ac.kr, sbpaik@kaist.ac.kr

### Abstract:

The brain is a complex system which dynamically process external sensory information. To study this information processing, a number of psychophysics studies have been examined human response characteristics to various sensory stimuli. In general, however, response to the stimulus,  $R(t)$ , is highly stochastic so that the perceptual response to an identical stimulus,  $S(t)$ , highly varies across individuals. This wide individual variability prevents us from observing an exact response function to any particular type of sensory stimuli. Here, we estimated the intrinsic response function  $h(t)$  of individual subject, to examine how individual brain integrates sensory information in a different manner. We assumed that each individual has distinct shape of  $h_i(t)$  which results in diverse forms of individual response,  $R_i(t) = S(t) * h_i(t)$ . Thus, by obtaining individual  $h_i(t)$ , optimal parameters of the stimulus for correct perception might be predicted. To examine the response function  $h(t)$ , we first designed a visual stimulus for noisy rotational motion of random dots. A certain portion (defined with coherence parameter,  $c$ ) of the dots rotate in clockwise or counter-clockwise direction, and the coherence  $c$  was set to fluctuate over the time. Observers' response  $R(t)$  of perceived motion (CW or CCW) was measured while the time-varying stimulus  $S(t)$  was given. From the reverse-correlation analysis of  $S(t)$  that triggers perceptual response  $R(t)$ , we could successfully estimate the response function  $h(t)$  of each individual. Surprisingly, the length of time window for sensory integration, was independent to the dynamics of external stimuli within a single individual, but diverse across individuals. This suggests that individuals have distinctive response function dynamics for integration of the external sensory information. We also found that the performance of individual responses was highest when  $S(t)$  was matched to the individual's  $h(t)$ . In addition, we could successfully predict the response of subjects to illusory motion stimulus, from the temporal characteristics of individual  $h(t)$ . Overall, we suggest that the variations of perceptual behavior across subjects could originate from the temporal variation of response function  $h(t)$  across the individuals.

### References

[1] S Jain, Performance characterization of Watson Ahumada motion detector using random dot rotary motion stimuli, PLoS one (2009)

### Keywords:

Psychophysics, Brain, Visual motion, Preception, Response function

## Quasi-static Simulation of Laser-Directed Self-Assembly of Highly Aligned Lamellar and Cylindrical Block Copolymer Nanostructures

김재업\*<sup>1</sup>, 용대성<sup>1</sup>

<sup>1</sup>울산과학기술원 자연과학부  
jukim@unist.ac.kr

### Abstract:

In experiments, self-assembled vertical lamellar or surface-parallel cylindrical nanodomains can be aligned by lateral scan of focused laser, and excellent long-range order over 10 $\mu$ m length scale can be achieved. For the systematic understanding of this experimental observation, we develop quasi-static simulation employing successive self-consistent field theory calculation. Miniaturized simulations of experimental systems could confirm a strong tendency for lamellar domains to grow in the direction of laser scanning. Cylindrical self-assembled domains exhibit similar behaviors provided that the surface prefers one block and the block copolymer film thickness is moderate.

### Keywords:

Quasi-static Simulation, Block Copolymer, Laser-Directed, Self-Assembly

## 양성자 조사에 따른 탄소나노튜브의 물성변화와 마찰전기발전기 효율 향상

정중훈\*<sup>1</sup>, 정순신<sup>2</sup>, 김동영<sup>1</sup>

<sup>1</sup>인하대학교 물리학과, <sup>2</sup>한국전기연구원 나노융합기술연구센터  
jhjung@inha.ac.kr

### Abstract:

현재까지 마찰전기발전기의 효율을 향상시키기 위하여 마찰표면에 물리적 및 화학적 처리를 통한 연구가 진행되었다. 그러나 동일한 표면적에서 마찰전기 발전 효율을 높이기 위한 가장 쉬운 방법은 마찰전기 대전열 (Triboelectric series)에서 가능한 멀리 떨어져 있는 두 물질로 구성하는 것이다.

탄소나노튜브 (Carbon nanotube, CNT)는 여러 가지 탄소동소체 중의 하나로 우수한 전기 전도율과 기계적 특성, 그리고 화학적 안정성으로 주목 받고 있다. 이러한 특징으로 CNT를 마찰전기발전기의 전극이자 마찰물질로 사용하면 다른 금속 전극에 비하여 가볍고 매우 얇으면서도 튼튼한 디바이스의 구성이 가능하게 된다. 만약 CNT에 양성자를 조사하여 마찰전기 대전열 상에서 일반적인 CNT 보다 양전하를 쉽게 받아들일게 할 수 있다면 더 효율적인 마찰전기발전기를 만들 수 있을 것이다.

본 연구는 이를 실현하기 위하여 CNT가 코팅된 폴리머 기판에 양성자를 조사한 다음 표면성분의 변화와 면저항 등 물성변화를 추적하고 UPS 실험을 통하여 일함수의 변화를 관찰하였다. 그리고 PTFE와 CNT를 사용하여 마찰전기발전기를 구성하여 양성자 조사에 따른 마찰전기 출력 변화를 측정하였다.

This research was supported by the Basic Science Research Program through the National Research Foundation of Korea (NRF) funded by the Ministry of Education, Science and Technology (NRF-2017M2B2A4049475).

### Keywords:

양성자 조사, 탄소나노튜브, 마찰전기발전기

## Multi-band microwave metamaterial absorber, based on combined dumbbell-type resonators

이영백\*<sup>1</sup>, 김영주<sup>1</sup>, 황지섭<sup>1</sup>, 부이쿠웬쑤안<sup>1</sup>, 부이통선<sup>1</sup>, 김기원<sup>3</sup>, 이주열<sup>2</sup>, 박상윤<sup>4</sup>

<sup>1</sup>한양대학교, 물리학과, <sup>2</sup>성균관대학교, 물리학과, <sup>3</sup>선문대학교, 정보디스플레이학과, <sup>4</sup>서울대학교 차세대융합기술  
연구원, 나노바이오 연구실  
yplee@hanyang.ac.kr

### Abstract:

Metamaterials (MMs), which consist of periodically-arranged meta-atoms, are artificially engineered, and their electromagnetic properties are special beyond natural materials, such as negative refractive index. The effective electric permittivity  $\epsilon(\omega)$  and the effective magnetic permeability  $\mu(\omega)$  of MMs can be adjusted by delicately-designed structures with optimized parameters. Among many MM fields, it is attractive that MM absorbers (MMAs) can be used in various application fields. The conventional MMAs are made of a dielectric substrate between a patterned metallic layer on one side a metallic plane on the other. By adjusting the geometric parameters of meta-atoms, the impedance matching can be optimized so that the reflection is minimized. The perfect absorption appears in a specific frequency range because the transmission comes to be zero by the back metallic plane. In this work, we numerically and experimentally elucidate a multi-band MMA using combined dumbbell-type resonators. The resonators with the different lengths of two grooves generate multi-band absorption, and the additional dual absorption peaks occur at low frequencies by combining the resonators.

This work was supported by the Korean government (MSIT) (2013-0-00375) and by the NRF funded by MSIT, Korea (No. 2017R1A2B4003916).

### Keywords:

Perfect absorption, Metamaterial, Multi-band

## 구배 있는 회절격자를 이용한 연속 파장 가변 콜로이드 양자점 DFB 레이저

전현수\*<sup>1, 2</sup>, 정현호<sup>1, 2</sup>, 한창현<sup>1, 2</sup>, 박연상<sup>3</sup>, 조경상<sup>3</sup>, 김한빛<sup>1, 2</sup>

<sup>1</sup>서울대학교, 물리천문학부, <sup>2</sup>서울대학교, 반도체공동연구소, <sup>3</sup>삼성전자, 종합기술원  
hsjeon@snu.ac.kr

### Abstract:

위치에 따라 연속적으로 파장이 변하는 DFB 레이저를 콜로이드 양자점을 이용하여 구성하였다. Lloyd 거울을 채용한 레이저 간섭 리소그래피 장치에서 평면 거울 대신 원통형 거울을 채용하여, 위치에 따라 주기가 점진적으로 변하는 표면 회절격자를 제작하였다. 고밀도의 적색 발광 CdSe-CdS-ZnS 양자점으로 이루어진 박막을 실리콘 기판 위에 스피ن캐스팅 방법으로 형성한 후에, 이를 석영 기판 표면에 만들어진 주기상의 구배가 있는 회절격자에 전사하였다. 제작된 소자는 광 여기 조건에서  $\sim 0.4 \text{ mJ/cm}^2$ 의 레이저 문턱값을 가지며 단일 모드 발진 특성을 보였다. 5.6 mm 정도의 공간적 변위에 대해 레이저 발진 파장은 613.4 nm에서 623.2 nm까지 점진적으로 변하였다. 이러한 결과는 간섭 리소그래피 장치의 간단한 개조를 통해 저렴한 비용으로 고품질의 구배 회절격자를 만들어낼 수 있음을 나타내며, 나아가 정교한 광소자 제작에도 다양하게 이용될 수 있음을 의미한다.

### Keywords:

DFB laser, Colloidal quantum dots, Laser interference lithography

## Plasmonic metamaterial for dual-band electromagnetically-induced transparency-like effect

이영백\*<sup>1</sup>, 황지섭<sup>1</sup>, 김영주<sup>1</sup>, 손혜미<sup>1</sup>, 김기원<sup>2</sup>, 이주열<sup>3</sup>, 박상윤<sup>4</sup>

<sup>1</sup>한양대학교 물리학과, <sup>2</sup>선문대학교 정보디스플레이학과, <sup>3</sup>성균관대학교 물리학과, <sup>4</sup>서울대학교 차세대융합기술원  
나노융합연구소

yplee@hanyang.ac.kr

### Abstract:

Electronically-induced transparency (EIT) a promising technique for improving the light-matter interactions, and the quantum EIT is realized by the quantum interference effect of three-level atomic system, resulting in a sharp transmission window. Unfortunately, this phenomenon is limited in practical application owing to conditions such as stable gas lasers and cryogenic temperature. However, recent studies using metamaterials (MMs) at room temperature without these conditions have been reported. The EIT-like effects in MMs generally appear according to the interference between plasmonic unit cells. This is based on the idea that the near-field coupling of narrow resonance and spectrally-broad resonance can induce the EIT as a limited case of the Fano coupling. Many different types of coupling modes, such as two-bright or bright-dark-bright mode coupling, have been made. These coupling modes allow a single narrow transmission of light to be extended to dual-band or multi-band transmission.

Herein, we studied the dual EIT-like effects using cut-wire resonator/ring hybrid resonator. We have successfully implemented the EIT-like effects in the single layer through the bright-bright mode coupling. This structure can provide single- or dual-band EIT spectral response in the microwave region by slightly varying the distance between the two resonators. This study presents a simple approach to realize the dual-mode EIT-like effects, and also demonstrates possible applications in active filters and optical sensors.

This work was supported by the NRF fund by MSIP, Korea (No. 2017R1A2B4003916).

### Keywords:

Metamaterials, Dual-band, Electromagnetically-induced transparency

## Quantum capacitance in dual-gated graphene field effect transistor

주원빈<sup>1</sup>, 이성배\*<sup>1</sup>

<sup>1</sup>Department of Physics and Photon science, Gwangju Institute of Science and Technology  
jaylinlee@gist.ac.kr

### Abstract:

To decrease operating voltage of graphene field effect transistor (FET), an insulating layer should be thin and have high dielectric constant. This means that quantum capacitance becomes dominant source of total capacitance. Because the total capacitance of the device is considered the series connection of quantum capacitance and geometrical capacitance. In this work, dual-gated FET is fabricated with mechanically exfoliated graphene onto 300 nm silicon dioxide substrate. For a top gate insulator, 5 nm of oxidized titanium is used. For this purpose, 1 nm titanium is deposited by e-beam evaporation and oxidized in the ambient condition repeatedly for 5 times. The quantum capacitance is extracted from the measured total capacitance, and the carrier density and density of states are calculated from the quantum capacitance. The results are compared to that of I-V measurements to confirm the usefulness of the quantum capacitance measurement in the given setup.

### Keywords:

quantum capacitance, field effect transistor, graphene

## Wigner 수송방정식에 의한 나노선 공명투과 트랜지스터의 양자 수송 계산

이준호<sup>1</sup>, 신민철\*<sup>2</sup>

<sup>1</sup>한국과학기술원 정보전자연구소, <sup>2</sup>한국과학기술원 전기및전자공학과  
mshin@kaist.ac.kr

### Abstract:

우리는 유효 질량의 공간의존이 고려된 Wigner 함수 모델을 기반으로 나노선 공명 투과 트랜지스터의 3 차원 양자 수송 계산을 하였다. 이 소자는 source, drain 그리고 channel은 GaAs로 이루어져 있고, 이중 장벽은  $Al_{0.3}Ga_{0.7}As$ 로 이루어져 있다. 게이트의 위치는 이중 장벽 주변으로 어느 정도 자유도를 가지고 정해질 수 있는데 대칭적인 게이트일수록 공명 준위를 더 직접적으로 조절하는 것으로 계산결과 나타났다. 음의 미분 저항 (NDR)을 높이는 몇가지 방법론들이 제시될 수 있는데 이 연구에서는 반도체의 직경, 반도체를 둘러싼 산화물의 두께, 우물 간격, 도핑 밀도에 따른 NDR의 크기와 다중 게이트에 의한 NDR의 변화가 연구된다.

### Keywords:

Wigner 함수 음의 미분 저항 공명 투과 트랜지스터 3 차원 양자 수송 계산

## Anisotropic Properties and photoelectric response of GeSe Nanoflakes

김관표\*<sup>1</sup>, 잠정수<sup>2</sup>, 이양진<sup>1</sup>, 윤준영<sup>1</sup>

<sup>1</sup>연세대학교 물리학과, <sup>2</sup>UNIST(울산과학기술원) 물리학과  
kpkim@yonsei.ac.kr

### Abstract:

Here we present the basic electrical and structural characterizations of GeSe nanoflakes. GeSe crystals exhibit strong in-plane anisotropic properties due to its crystal structure. Anisotropic optical transmittance and Raman spectroscopy as well as transmission electron microscopy imaging, are employed together with electrical characterizations using field effect transistor geometry. In addition, we find that the annealing of devices can enhance the device properties of GeSe, resulting in increased on/off ratio and higher charge carrier mobility.

### Keywords:

GeSe, Photo device, Anisotropy

## Observation of negative capacitance depending on the measurement temperature in ferroelectric Si:HfO<sub>2</sub> films

박상현<sup>1</sup>, 천민철<sup>1</sup>, 박솔민<sup>1</sup>, 박가연<sup>1</sup>, 강보수\*<sup>1</sup>

<sup>1</sup>Department of Applied Physics, Hanyang University  
bosookang@hanyang.ac.kr

### Abstract:

Decrease of voltage across the ferroelectric capacitor is observed while the capacitor is being charged. This phenomenon of negative capacitance (NC) is being exploited for improving device performance such as the subthreshold swing of field effect transistors. Ferroelectric hafnium oxide is suited for negative capacitance field effect transistor, due to its high compatibility to conventional semiconductor device fabrication process and good ferroelectric properties in thin films. While Landau coefficients of PZT or BTO are known, those of HfO<sub>2</sub> have not been identified yet. In this study, we investigated the effects of measurement temperature on the negative capacitance and confirmed the Curie temperature from Landau-Devonshire theory in ferroelectric Si doped HfO<sub>2</sub> thin films.

A simple series circuit comprising a resistor and a Si:HfO<sub>2</sub> thin film capacitor was constructed for observation of NC effect. The dynamic hysteresis was obtained by voltage and charge across the ferroelectric capacitor. We elucidated a temperature dependence of NC from a domain-wall motion perspective, and demonstrated the critical temperature from the Landau coefficients of NC based on the Landau-Khalatnikov equation.

### Keywords:

Negative capacitance, ferroelectric, HfSiO, HSO

## Fast and simple method for fabricating TERS tip by using an electric field

제원호\*<sup>1</sup>, AN Sangmin<sup>1</sup>, SHIN Dongha<sup>1</sup>, HWANG Jonggeun<sup>1</sup>  
<sup>1</sup>Seoul National University, Department of Physics & Astronomy  
whjhe@phya.snu.ac.kr

### Abstract:

Surface-enhanced Raman spectroscopy(SERS) is a tool that has increased Raman signals by many orders of magnitude with a treatment of surface. Especially, tip-enhanced Raman spectroscopy(TERS) reveals local intrinsic properties of materials by using the treated sharp tip with high enhancement of Raman signals.[1] However, major issue limiting wider applications of TERS is the difficulty of reproducible fabrication of the tips for producing high enhancement. Here, we present a simple method to fabricate a TERS tip, which is based on the electrophoresis by using electric fields of direct current(DC) voltage with a metal(Au or Ag) nanoparticle solution. Our method allows for fast and reproducible SERS active substrate at the end of a nanoscale quartz rod which is pulled by a mechanical puller (P-2000, Sutter Instruments). When there are electric fields between quartz rod and metal wall, negatively charged nanoparticles are attracted to the quartz rod. And the nanoparticles which are already piled up on the quartz rod try to disturb to pile more nanoparticles on it due to screening effect. This effect eventually remains nanoparticle layer thin on the surface of the tip. An additional benefit of this method is one can easily control shape and property of tip by using other size of quartz rod and nanoparticles.

### Reference

[1] Huang, Teng Xiang, Huang, Sheng Chao, Li, Mao Hua, Zeng, Zhi Cong, Wang, Xiang, Ren, Bin, Anal Bioanal Chem (2015) 407:8177-8195.

### Keywords:

TERS, SERS, Raman, TERS tip, electrophoresis, nanoparticle

## Crystallographic orientation of ReS<sub>2</sub> determined by polarized Raman spectroscopy

정현식\*<sup>1</sup>, 최윤<sup>1</sup>, 김중철<sup>1</sup>, 김정화<sup>2</sup>, 이종훈<sup>2</sup>  
<sup>1</sup>서강대학교 물리학과, <sup>2</sup>울산과학기술원 신소재공학부  
hcheong@sogang.ac.kr

### Abstract:

As a member of transition metal dichalcogenides (TMDs), rhenium disulfide (ReS<sub>2</sub>) is recently attracting interest as anisotropic electronic, optoelectronic properties give additional degrees of freedom in manipulating device properties. ReS<sub>2</sub> has a direct bandgap from 1-layer (1.58 eV) to bulk (1.5 eV) unlike other TMDs such as MoX<sub>2</sub> or WX<sub>2</sub> (X= S, Se) [1]. Furthermore, due to the anisotropic structure originating from the Re-Re bonding of extra valence electrons, up- and- down faces of monolayer ReS<sub>2</sub> are inequivalent, and its physical properties are dependent on the crystallographic orientation of the ReS<sub>2</sub> specimen [2][3].

In this study, we performed polarized Raman measurements from 1- to 3-layer ReS<sub>2</sub> on both up- and down- sides. The thickness was confirmed by low frequency Raman modes ( $< 30 \text{ cm}^{-1}$ ) [4]. We investigated the polarization dependence of the Raman modes including the excitation energy dependence. In some Raman modes, the polarization dependence of the intensity depends on the excitation energy. From the polarization dependence of Raman modes at  $152 \text{ cm}^{-1}$  and  $212 \text{ cm}^{-1}$ , we classified the sides of samples corresponding to two vertical orientations. We also identified the Re-chain direction using the polarization direction of the Raman modes at  $212 \text{ cm}^{-1}$ . We also measured transmission electron microscopy (TEM) to correlate the crystallographic orientation with the polarized Raman results.

### References

- [1] Z. Yu *et al.* Sci Rep, **5** 13783(2015)
- [2] Y. Lin *et al.* ACS Nano, **9** 363(2015)
- [3] S. Sim *et al.* Nature comm, **9** 351(2018)
- [4] E. Lorchat *et al.* ACS Nano, **10** 27525(2016)

### Keywords:

TMDs, ReS<sub>2</sub>, polarized Raman spectroscopy

## Developing grating interferometer-based phase contrast imaging at beamline 6C Bio Medical Imaging of the Pohang Light Source-II

임재홍\*<sup>1</sup>, 김건일<sup>2</sup>, 윤무현<sup>2</sup>, 김섭구<sup>1</sup>

<sup>1</sup>포항가속기연구소 산업기술융합센터, <sup>2</sup>포항공과대학교 물리학과  
limjh@postech.ac.kr

### Abstract:

Phase contrast imaging senses refraction and results in superb sensitivity over absorption contrast imaging of the conventional X-ray radiography. Several methods are developed for phase contrast imaging, and one based on grating interferometry is gaining popularity because the method is less sensitive to the beam coherency while still providing a quantitative refraction measurement. In this work, we present the design of the grating interferometer-based phase contrast imaging under development at the beamline 6C Bio Medical Imaging of the Pohang Light Source-II. A photon energy of 35keV is targeted, which finds applications in three-dimensional virtual histology and animal imaging. A source grating is introduced in order to compromise the relatively poor transverse coherency of the photon beam at the beamline. The performance has been estimated by a simulation study and also by consulting cases in overseas synchrotron facilities.

### Keywords:

synchrotron radiation, phase contrast imaging, grating interferometer, bio-medical imaging

## 염소화 처리된 탄소나노튜브를 함유한 고유전율 박막을 이용한 AC 전계 발광 소자

유세기\*<sup>1</sup>

<sup>1</sup>한국외국어대학교 전자물리학과  
segiju@hufs.ac.kr

### Abstract:

교류형 파우더 전계발광(electroluminescence, EL) 소자는 간단한 제작공정으로 인해 평판 디스플레이로의 가능성을 띄고있지만, 낮은 휘도와 높은 구동 전압 등의 단점으로 인해 우리의 일상생활에 쓰이는 제품으로 나타나기에는 좀 더 시간이 필요한 것으로 여겨지고 있다. 본 연구에서 탄소 나노튜브(carbon nanotube, CNT)를 기반으로 한 고유전 상수를 가지는 유전박막을 만들고, 이를 이용한 무기 전계발광 소자의 발광 특성을 탄소 나노튜브의 농도와 염소화(chlorination) 정도를 조절하면서 관찰하였다. BaTiO<sub>3</sub>와 cyanoethyl pullulan(CEP) 고분자로 이루어진 유전층 안에 삽입한 탄소 나노튜브의 특성을 Raman 산란법과 x-ray photoemission spectroscopy(XPS) 방법으로 염소화 정도에 따라 분석하였다. Chlorobenzene을 co-solvent로 사용하여 염소화한 탄소 나노튜브의 농도가 0.01 wt% 일때, 소자가 최고의 발광 효율(50% 향상)과 최저의 전류밀도(30% 감소)를 얻었다. 또한 탄소 나노튜브의 농도가 0.03 wt%에 도달하면 나노튜브가 없는 대조 소자보다 발광 효율과 전류밀도가 나빠지는 것을 확인하였으며, 이는 탄소 나노튜브가 percolation에 의해 누설 전류 네트워크를 형성하기 때문이다. 이렇게 최적의 농도인 경우에만 소자의 특성이 좋아지는 것은 탄소 나노튜브의 micro-capacitor 효과와 염소화에 따른 space charge에 인한 것으로 해석하였다. 이를 뒷받침하기 위하여 유전층만 있는 샘플을 따로 만들어서 유전율과 전기전도도를 측정하여 염소화 정도와 탄소 나노튜브의 농도에 따른 의존도가 전계발광 소자와 같은 경향을 띄고 있음을 확인하였다. 따라서 탄소 나노튜브와 같은 나노물질을 적절한 농도로 사용하면 소자의 특성을 향상시킬 수 있음을 실험적으로 입증하였으며, 이에 대한 자세한 결과를 학회에서 발표할 예정이다.

### Keywords:

탄소나노튜브, 전계발광, 유전층

## Piezoelectric properties and leakage current of PZT & PNZT tri-layer thin films

강보수\*<sup>1</sup>, 박솔민<sup>1</sup>, 천민철<sup>1</sup>, 박가연<sup>1</sup>, 박상현<sup>1</sup>

<sup>1</sup>한양대학교 응용물리학과  
bosookang@hanyang.ac.kr

### Abstract:

Doping PZT with other elements affects the properties of the material. Some studies have shown that Niobium doping is effective in enhancing the piezoelectric response. Also it improve leakage resistance and fatigue characteristics. But, doping causes a decrease of the mechanical quality factor.

In this study, we made the tri-layer thin films(PNZT/PZT/PNZT) fabricated by sol-gel method and compared with  $\text{Pb}_{1.1}(\text{Zr}_{0.52}\text{Ti}_{0.48})\text{O}_3$ (PZT) and  $\text{Pb}_{1.1}(\text{Zr}_{0.52}\text{Ti}_{0.48})_{0.98}\text{Nb}_{0.02}\text{O}_3$ (PNZT) thin films to improve leakage resistance and piezoelectric coefficient of thin film surface. Bulk thickness was increased by 100 nm from 100 nm to 500 nm and the samples were annealed at 700°C for 20 minutes. We investigated piezoelectric coefficient( $d_{33}$ ), leakage current, and fatigue characteristics using atomic force microscopy and ferroelectric tester.

### Keywords:

Piezoelectric, PZT, PNZT, leakage current

## Growth of ZnO/3D Graphene Heterostructures for High-Performance Hybrid Energy Harvesters

강대준\*<sup>1, 2</sup>, QIAN Yongteng<sup>2</sup>

<sup>1</sup>성균관대학교 물리학과, <sup>2</sup>성균관대학교 기초과학연구소  
dj kang@skku.edu

### Abstract:

Flexible, wearable and stretchable nanogenerators (NGs) that harvest various types of mechanical energy has attained a tremendous interest because of their great potential for powering microelectronics and portable devices. here, we demonstrated the fabrication of ZnO nanoflakes/3D graphene (ZnO NFs/3D Gr) heterostructures using Ni foam as a substrate. The as-fabricated ZnO NFs/3D Gr heterostructures based energy harvesters produced the output voltage and current density values of up to 120 V and  $50 \mu\text{A cm}^{-2}$  at vertical force of 7 N, which is almost 6 times and 2 times higher than the 3D graphene and ZnO nanoflakes, respectively. Moreover, the fabricated energy harvesters are able to light up 65 commercially available light-emitting diodes. These excellent results demonstrated that the ZnO NFs/3D Gr heterostructure based hybrid energy harvesters has a great potential in self-powered flexible and wearable electronic devices.

### Keywords:

ZnO nanoflakes, 3D graphene, heterostructure, hybrid energy harvesters

## Interlayer Vibrational Modes of Few-layer 2H-SnSe<sub>2</sub>

SORPHORN Chansonita<sup>1</sup>, SRIV Tharith<sup>1</sup>, 정현식\*<sup>1</sup>

<sup>1</sup>서강대학교 물리학과  
hcheong@sogang.ac.kr

### Abstract:

Tin diselenide (SnSe<sub>2</sub>) belongs to the group 14 post-transition metal dichalcogenides. It is an indirect band gap semiconductor material, which has a band gap of approximately 1.07 eV for bulk [1]. It belongs to the  $D_{3d}^3$  (P-3m1) space group with lattice parameters  $a = 3.81$  and  $c = 6.137$  Å [2]. Recently, SnSe<sub>2</sub> has been shown to have useful properties appropriate for thermoelectric devices [3], field-effect transistors [4], tunneling field-effect transistors [5], phase change memory devices [6], and high-performance fast photodetectors [7]. In this research, we measured the low-frequency Raman spectra of mechanically-exfoliated few-layer 2H-SnSe<sub>2</sub>. We first made different sets of few-layer 2H-SnSe<sub>2</sub> samples on 280 nm SiO<sub>2</sub>/Si substrates using mechanical exfoliation. Atomic force microscopy (AFM) was, then, used to determine the thickness of few-layer 2H-SnSe<sub>2</sub> samples. Raman measurements were performed using three excitation lasers of 632.8, 514.4, and 441.6 nm wavelengths of a power below 100 μW to avoid local heating. We used a vacuum chamber during the Raman measurements to avoid photo-oxidation. The intralayer in-plane  $E_g$  mode was observed at  $\sim 106$  cm<sup>-1</sup> and *out-of-plane*  $A_{1g}$  mode at  $\sim 184$  cm<sup>-1</sup>. In the low-frequency region ( $< 100$  cm<sup>-1</sup>), interlayer vibrational shear and breathing modes were observed. These modes show characteristic dependence on the number of layer of 2H-SnSe<sub>2</sub>.

[1] J. M. Gonzalez, and I. I. Oleynik, Phys. Rev. B 94, 125443 (2016).

[2] E. Trifonova, I. Y. Yanchev, P. Manou, et. al., Mater. Sci. 31, 3647 (1996).

[3] A. A. Kozma, Y. M. Sabov, Y. E. Peresh, E. I. Barchiy, and V. V. Tsygyka, Mater.Sci. 51, 93 (2015).

[4] C. Guo, Z. Tian, Y. Xiao, Q. Mi, and J. Xue, Appl. Phys. Lett. 109, 203104 (2016).

[5] T. Roy, M. Tosun, M. Hettick, G. H. Ahn, C. Hu, and A. Javey, Appl. Phys. Lett. 108, 083111 (2016).

[6] K. M. Chung, D. Wamwangi, M. Woda, M. Wuttig, and W. Bensch, Appl. Phys. 103, 083523 (2008).

[7] X. Zhou, L. Gan, W. Tian, Q. Zhang, S. Jin, H. Li, Y. Bando, D. Golberg, and T. Zhai, Adv. Mater. 27, 8035 (2015).

### Keywords:

Raman spectroscopy, tin diselenide (SnSe<sub>2</sub>), atomic force microscope (AFM)

# Magneto-thermal Properties of Triethylene Glycol-coated Cobalt Zinc Ferrite Nanoparticles for Magnetic Hyperthermia Applications

이일수\*<sup>1</sup>, 배홍섭<sup>1</sup>, AHMAD Ashfaq<sup>1</sup>

<sup>1</sup>경북대학교 물리학과  
ilrhee@knu.ac.kr

## Abstract:

Cobalt zinc ferrite ( $\text{Co}_{0.6}\text{Zn}_{0.4}\text{Fe}_2\text{O}$ ) nanoparticles were synthesized by using one step hydrothermal technique. Triethylene glycol (TREG) was used as a biocompatible coating material. The TREG-coated nanoparticles were spherical in shape with an average diameter of 9.82 nm. The Fourier transform infrared spectra confirmed that the TREG was firmly coated on the surface of the particles. The saturation magnetization of the particles was 84 emu/g along with coercivity of 32 Oe. The heating capability of the particles was observed by using an induction heating system. The heating curves for the aqueous samples with various particle concentrations were observed. The samples were placed inside the alternating magnetic field with amplitude of 4.5 kA/m at the frequency of 216 kHz. The optimum particle concentration in water for achieving the hyperthermia target temperature of 42 °C was determined to be 4.58 mg/mL. The specific absorption rates (SAR) of the 2-mg/mL sample was found to be 83 W/g. The dependence of the SAR on the square of the field strength was confirmed for the representative 10-mg/mL sample. Judging from all these results, we could conclude that the TREG-coated particles are suitable for magnetic hyperthermia applications due to their superparamagnetic properties and high SAR values.

## Keywords:

Zinc-doped cobalt ferrite nanoparticle, TREG coating, High SAR

## Nanoscale Thermometry and Strain Sensing Using Defect-based Spin Qubits

최순욱\*<sup>1</sup>, 이동현\*<sup>1</sup>

<sup>1</sup>고려대학교 물리학과

www@korea.ac.kr, donghun@korea.ac.kr

### Abstract:

A nitrogen-vacancy (NV) center in diamond is an atomic scale solid-state spin qubit satisfying both high spatial resolution and field sensitivity. Therefore one can realize highly sensitive nanoscale quantum sensor.

In this poster, we demonstrated precise temperature and strain sensing based on the spin qubits. First, we measured temperature distribution over micron-scale structures with sub-degree resolution. We also studied strain induced by the motion of diamond mechanical resonators.

### Keywords:

thermometry, strain, NV, nitrogen-vacancy, defect

## Characterizing anhydrous and weakly aggregated nanodiamond with Raman spectroscopy

이기학\*<sup>1</sup>, 김현숙<sup>2</sup>

<sup>1</sup>원광대학교 바이오 나노 화학부, <sup>2</sup>원광대학교 차세대방사선산업기술지역혁신센터  
khlee@wku.ac.kr

### Abstract:

Carbon nanomaterials are very interesting to a broad range of applications in the field of material science. Raman vibration mode corresponds to a specific vibration frequency of a bond in the crystal, so it is highly sensitive to morphology, implying that every band is very sensitive to the orientation of the bonds and atomic weight at either end of the bond. Thus in this study we apply the Raman spectroscopy to study the relative content of carbon-carbon bonds to the anhydrous and weakly aggregated elementary nanoscale carbon particles of detonation nanodiamond. One position of Raman bands at around  $1331\text{ cm}^{-1}$  manifested that there are highly uniform C-C bonds in a tetrahedral crystal structure like the case of diamond. The other position at around  $1600\text{ cm}^{-1}$  is indicative of a hexagonal sheet like graphite. Also we analyzed the relative content of carbon bonds by using the area of intensity of Raman peak and the simulation of crystal morphology. Our results suggest that there are mainly two kinds of C-C bonds, one is  $sp^3$  bonds of diamond and the other is  $sp^2$  bonds of graphite.

### Keywords:

Raman spectroscopy, nanodiamond, morphology characterization of carbon nanomaterials

## 라만분광법을 이용한 봉독의 유방암 세포에 미치는 영향 연구

정경복\*<sup>1</sup>, 이기자<sup>2</sup>

<sup>1</sup>조선대학교 물리교육과, <sup>2</sup>경희대학교 의공학교실  
gbjung@chosun.ac.kr

### Abstract:

봉독(Bee Venom)이란 꿀벌의 독낭에 들어 있는 peptide components(pelittin, apamin, adolapin, MCD peptide etc.), enzymes(PLA2, hyaluronidase, glucosidase etc.), amines(histamin, epinephrine etc.), nonpeptide components(lipids, carbohydrates, free amino acids etc.) 등으로 구성 되어 있고, 진통, 소염의 효능을 가지고 있는 것으로 알려져 있으며, 한의학에서는 봉독의 항암 효과에 관한 연구가 보고되었다. 이러한 연구에 사용된 기존의 생물학적 방법인 MTT assay, western blot 등은 복잡한 절차로 인해 시간이 오래 걸리고 노동 집약적이다. 라만분광법은 형광 라벨 없이 (fluorescence label-free) 세포, 조직, 체액 등 바이오 샘플의 생화학적 조성을 분자 수준에서 아주 미세한 변화에 대한 측정이 가능하다. 본 연구에서는 봉독이 유방암 세포 (MDAMB-231)에 미치는 영향을 라만분광법을 이용하여 연구하였다. 유방암 세포에 봉독의 처리 농도와 처리 시간에 따른 세포의 생존율을 조사한 결과 처리 농도 3  $\mu\text{g/ml}$ , 처리 시간 48h에 라만 스펙트럼의 형태 및 강도에 큰 차이를 보였다. 특히, DNA와 단백질 영역의 라만 신호 강도가 감소하였다. 이 결과는 세포사멸과 관계가 있으며, MTT assay 결과와 일치하였다.

### Keywords:

라만분광(Raman spectroscopy), 봉독(Bee Venom), 유방암

## Controlling and trapping nanoparticles by using dielectrophoresis

제원호\*<sup>1</sup>, 홍성훈<sup>1</sup>, 안상민<sup>1</sup>, 김충만<sup>1</sup>, 송한솔<sup>1</sup>, 윤호상<sup>1</sup>

<sup>1</sup>서울대학교 물리학과  
whjhe@phya.snu.ac.kr

### Abstract:

Sorting various particles in mixed solution using their electric properties is interesting issue in research fields. Especially, there have been many studies associated with electrophoresis (EP) or dielectrophoresis (DEP) which are relatively simple and efficient methods for sorting materials. However, when the size of materials is decreased down to nanoscale, it is difficult to define clearly the particle behaviors and their collections. Here, we used dielectrophoresis (DEP) force to control metallic nanoparticles and non-metallic nanoparticles.

DEP force is a force that exerted on dielectric particle placed in non-uniform electric field. Its amplitude is proportional to the volume of particle, the gradient of the square of electric field amplitude and Clausius-Mossotti(CM) factor. The sign of CM factor determines the direction of DEP force. We use this property to trap non-metallic particles on the electric field minimum point and metallic particles on the electric field maximum point. Using quadrupole moment electrodes which have 15  $\mu\text{m}$  gaps and AC voltage, we generated the electric field minimum on the center of the quadrupole electrodes. Then, we dropped the mixture of 100 nm diameter silica particles solution and 60 nm diameter Au nanoparticles solution on the center of the quadrupole electrodes using micropipette and applied 20 MHz 150 V peak to peak(pp) AC voltage by using function generator.

As a result, the silica nanoparticles are trapped on the center, and gold nanoparticles are attached to each electrode edge. This result shows the possibility to control much smaller size of nanoparticles by their electrical properties.

### References

- [1] C. Zhang, K. Khoshmanesh, A. Mitchell and K. Kalantar-zadeh, *Anal Bioanal Chem.* 10, 1007 (2010).
- [2] Nicolas G. Green and Hywel Morgan, *J. Phys. Chem. B*, 1, 103 (1999).

### Keywords:

Sorting, Dielectrophoresis, Nanoparticle

## Improvement of High Electrical Characteristic PDMS based Triboelectric Nanogenerator Using SiO<sub>2</sub> Nanoparticles

박진섭\*<sup>1, 2</sup>, 권찬울<sup>1</sup>, 박홍범<sup>1</sup>, 신동수<sup>1</sup>, 김택곤<sup>1</sup>  
<sup>1</sup>한양대학교 전자컴퓨터통신공학과, <sup>2</sup>한양대학교 융합전자공학부  
jinsubpark@hanyang.ac.kr

### Abstract:

Triboelectric energy harvesting is a useful technology that converts mechanical energy to electrical energy using the electric potential difference between two materials that touch each other due to the polarization effect. In this paper, we suggest a method to improve the electrical characteristics by modifying the physical properties of the substrate in the triboelectric nanogenerator (TENG) using SiO<sub>2</sub> nanospheres. In our case, 500nm diameter SiO<sub>2</sub> nanospheres were embedded in PDMS with 30wt% concentration and nanospheres-based monolayer stacked structure on PDMS surface showed the highest electrical characteristics. The maximum performance was 216V and 6.46 $\mu$ A/cm<sup>2</sup>, and the load resistance matching was 3.76W/cm<sup>2</sup> at 2M $\Omega$ .

### Keywords:

Triboelectric Nanogenerator, SiO<sub>2</sub> Nanospheres, Monolayer

## Improved Photoswitching Response of WSe<sub>2</sub> Field-Effect Transistors by Thermal Annealing in Air

서준석<sup>1</sup>, 박진수<sup>1</sup>, 조경준<sup>1</sup>, 이우철<sup>1</sup>, 신지원<sup>1</sup>, 김재근<sup>1</sup>, 이택희\*<sup>1</sup>

<sup>1</sup>서울대학교 물리학과  
tlee@snu.ac.kr

### Abstract:

Recently, two-dimensional (2D) transition-metal dichalcogenides (TMDCs) such as MoS<sub>2</sub> and WSe<sub>2</sub> have gained considerable interest as channel materials for field-effect transistors (FETs) due to their tunable bandgap, high on/off ratio, carrier mobility, and photoconductivity [1]. Especially, phototransistors made with monolayer WSe<sub>2</sub> exhibited high photogain up to 10<sup>5</sup> and detectivity up to 10<sup>14</sup> Jones [2]. However, most of the studies have not focused on persistent photoconductivity (PPC) effect, which is continuously maintained conductivity after the illumination is turned off. Consequently, it is important to eliminate PPC effect to realize photoswitching applications.

In this study, we investigated the electrical and optical properties such as photoluminescence (PL), Raman spectroscopy, and photoswitching behavior of WSe<sub>2</sub> FETs before and after thermal annealing in air. Through this air annealing, the threshold voltage of multi-layer WSe<sub>2</sub> FETs shifted toward the positive gate voltage direction. Furthermore, PL peak intensity of monolayer WSe<sub>2</sub> gradually decreased as annealing time increased. These results can be explained by the formations of WO<sub>3-x</sub> made by air annealing which serves as acceptors and quenching sites. We also found that the persistent photoconductivity effect of the WSe<sub>2</sub> photodetectors was removed by air annealing, and their photoswitching response time decreased more than two orders of magnitude. This study suggests that the simple method of thermal annealing can improve photoswitching properties of WSe<sub>2</sub> photodetectors.

### References

- [1] Q. H. Wang et al., *Nature Nanotechnology*, **7**, 699 (2012).
- [2] W. Zhang et al., *ACS Nano*, **8** (8), 8653 (2014).

### Keywords:

WSe<sub>2</sub> photodetector, photoswitching response time, air annealing

## Conductance mapping of atomically thin MoS<sub>2</sub> and WSe<sub>2</sub> films by second harmonic signal of electrostatic force microscopy

PARK Jeongwoo<sup>1</sup>, KIM Minju<sup>2</sup>, YI Yeonjin<sup>2</sup>, KIM Taekyeong\*<sup>1</sup>

<sup>1</sup>Department of Physics, Hankuk University of Foreign Studies, <sup>2</sup>Institute of Physics and Applied Physics, Yonsei University  
tkim@hufs.ac.kr

### Abstract:

Layered two dimensional (2D) semiconducting materials such as MoS<sub>2</sub> and WSe<sub>2</sub> have recently attracted interest owing to their sizable bandgaps which give new possibility of field effect transistors and optoelectronic device applications. To characterize the conductivity of the 2D material based devices is of fundamental importance for their applications in electronics as well as photonics. Here, we report the direct mapping of the normalized conductance for atomically thin MoS<sub>2</sub> and WSe<sub>2</sub> films by measuring the second harmonic signal of electrostatic force microscopy (EFM). We modulate the carrier density of 2D materials by applying a DC bias to EFM tip as a scanning top gate, and observe different behaviors of gate dependence on MoS<sub>2</sub> and WSe<sub>2</sub> films. Furthermore, we show that the normalized conductance signal depends on the film thickness as well as the substrate. Our result is very important for the improvement of 2D material device performance and provides a fundamental understanding of the device mechanism.

### Keywords:

two dimensional semiconducting materials, MoS<sub>2</sub>, WSe<sub>2</sub>, electrostatic force microscopy

## 형광 실리카 나노입자의 선택적 패턴 성장

김기출\*<sup>1</sup>, 윤지희<sup>1</sup>

<sup>1</sup>목원대학교 신소재화학공학과  
kckim30@mokwon.ac.kr

### Abstract:

형광 실리카 나노입자는 화학 센서, 신경 에이전트 감지(nerve-agent detection), 혈류 모니터링(blood-flow monitoring)등 바이오 분야에서 폭넓게 응용되고 있다[1]. 또한 나노입자의 선택적 패턴 성장은 기능성 광학표면, 발광 다이오드, 자기정보 저장매체, 광정보 저장매체 등 여러 분야에 응용될 수 있다[2]. 본 연구에서는 Stöber 방법을 이용하여 실리카 나노입자를 합성하였고, 실리카 나노입자의 합성과정에 APTES((aminopropyl)-triethoxysilane)를 넣어주거나[1], Fluorescein isothiocyanate (FITC), dichlorotris(1,10-phenanthroline) ruthenium(II) hydrate (Ru(phen)<sub>3</sub>2+)를 도핑하여 서로 다른 색의 형광 실리카 나노입자를 합성하였다[3]. 형광 실리카 나노입자의 선택적 패턴성장을 위하여 기판을 OTS(octadecyltrichlorosilane) solution으로 hydrophobic 표면처리를 하였다. 실리카의 형광특성은 365 nm 파장을 갖는 UV-lamp를 이용하여 확인하였다. 합성된 실리카 나노입자는 UV를 조사해주었을 때 육안으로 Red, Green, Blue를 확실하게 구분할 수 있었다. 성장된 실리카 나노입자의 크기와 표면구조, 선택적 패턴 성장의 형태 등을 주사전자현미경(SEM, Scanning Electron Microscope)으로 분석하였다. 또한 형광 실리카 나노입자의 광학적 특성을 UV-visible spectrophotometer로 평가하였다.

[1] Adam M. Jakob, et al. "A Novel Approach to Monodisperse, Luminescent Silica Spheres", Chem. Mater, Vol. 18, pp. 3173-3175(2006).

[2] Jeongwon Han, et al. "Nano Replication Technology of Nano Patterns and Application Fields", Journal of The Korean Society for Precision Engineering, Vol. 17, p. 30 (2009).

[3] Jianquan Xu, et al. "Multicolor Dye-Doped Silica Nanoparticles Independent of FRET" Langmuir, Vol.26, No. 20, pp. 15722-15725(2010).

### Keywords:

형광, 실리카 나노입자, 선택적 성장, 패턴

## Proton Irradiation Effect on WSe<sub>2</sub> Field Effect Transistors

신지원<sup>1</sup>, 조경준<sup>1</sup>, 박진수<sup>1</sup>, 김재근<sup>1</sup>, 김재영<sup>1</sup>, 이택희\*<sup>1</sup>

<sup>1</sup>서울대학교 물리학과  
tlee@snu.ac.kr

### Abstract:

In recent years, transition-metal dichalcogenides (TMDCs) have gained significant attention as a next-generation electronic devices. For example, tungsten diselenide (WSe<sub>2</sub>) has been researched in many applications because of its high on/off ratio, high mobility, etc. In this study, we investigated the irradiation effect of high energy proton beam on WSe<sub>2</sub> field effect transistors (FETs). Specifically, WSe<sub>2</sub> FETs were irradiated with 10 MeV protons under four fluence conditions of 10<sup>12</sup>, 10<sup>13</sup>, 10<sup>14</sup>, and 10<sup>15</sup> protons per cm<sup>2</sup>. All of the WSe<sub>2</sub> FETs were ambipolar type with 4-7 nm channel thickness. As a result, the electric properties such as current level, threshold voltages are changed depending on fluence conditions. For low fluence conditions of 10<sup>12</sup> to 10<sup>14</sup> protons per cm<sup>2</sup>, the threshold voltages shifted toward the negative gate voltage direction while the current levels increased in the positive gate voltage range and decreased in the negative gate voltage range. For high fluence conditions of 10<sup>15</sup> protons per cm<sup>2</sup>, the electric properties changed oppositely as compared to the case of low fluence conditions. These changes originated from proton-irradiation induced traps; the positive oxide-charge traps in SiO<sub>2</sub> bulk layer and the negative interface trap states between the WSe<sub>2</sub> layer and SiO<sub>2</sub> layer. The change of the electric properties depended on which trap is dominant. Our study can enhance understanding the high energy particle irradiation effect on WSe<sub>2</sub> FETs and also suggest a method to control the electric properties of WSe<sub>2</sub>-based devices using proton beams.

### Keywords:

Tungsten Diselenide (WSe<sub>2</sub>), Proton Irradiation, field effect transistors (FETs)

## Synthesis of SnO<sub>2</sub> Nanostructures on Graphene Nanosheet

김기출\*<sup>1</sup>, 김종일<sup>1</sup>

<sup>1</sup>목원대학교, 신소재화학공학과  
kckim30@mokwon.ac.kr

### Abstract:

Gas sensor based on metal-oxide has been attracted many attentions due to their high sensitivity, selectivity for gas molecules[1]. Semiconductor gas sensor shows change in resistance in the presence of harmful and flammable gases such as hydrogen(H<sub>2</sub>), carbon monoxide(CO), methanol and ethanol[2]. The Tin dioxide is a well-known metal-oxide material as an oxygen-deficient n-type semiconductor and nanostructured SnO<sub>2</sub> has been synthesized by various route such as hydro-thermal[3], Sol-gel[4], chemical vapor deposition[5] etc. The high surface to volume ratio of nanostructure give us precise detection of trace gas more than bulk materials. Xiaowei Yang and co-workers demonstrated that graphene enhance the performance of SnO<sub>2</sub> by growing on graphene nanosheets[6]. We can say that synthesis of nanostructured material on graphene through CVD system could be a new challenge since CVD system allows growing selectively. In this study, we've grown nanostructured SnO<sub>2</sub> directly on the graphene nanosheet through thermal CVD system. The quality of graphene nanosheets has been estimated by Raman spectroscopy and the characteristics of as grown nanostructured SnO<sub>2</sub> has been analyzed by Field-emission scanning electron microscopy, X-ray diffraction & Raman spectroscopy.

[1] Lesley Smart, Elaine A. Moore, "Solid State Chemistry: An Introduction", CRC Press, (2005).

[2] A. Ayeshamariam et al., "Synthesis, Structural and Optical Characterizations of SnO<sub>2</sub> Nanoparticles", Journal on Photonics and Spintronics, Vol. 2, p.4 (2013).

[3] Hui-Chi Chiu et. al., "Hydrothermal Synthesis of SnO<sub>2</sub> Nanoparticles and Their Gas-Sensing of Alcohol", Journal of Physical Chemistry, Vol. 111, p. 7256 (2007).

[4] Ashok D. Bhagwat et. al., "Synthesis of Nanostructured Tin Oxide (SnO<sub>2</sub>) Powders and Thin Films by Sol-Gel Method", Journal of Nano and electronic physics, Vol. 7, p. 04037 (2015).

[5] Zu Rong Dai et. al., "Growth and Structure Evolution of Novel Tin Oxide Diskettes", Journal of American Chemistry Society, vol. 124, p. 8673 (2002).

[6] Xiaowei Yang et. al., "In situ growth of SnO<sub>2</sub> on Graphene Nanosheets as Advanced Anode Materials for Rechargeable Lithium Batteries", The Electrochemical Society, Vol. 28, p. 151 (2010).

### Keywords:

Synthesis, SnO<sub>2</sub>, Graphene, Nanostructures

## 온도 변화에 대한 2차원 MoSe<sub>2</sub> 전이점의 타원편광분석법 연구

지정민<sup>1</sup>, 박한결<sup>1</sup>, 김태중<sup>1</sup>, LE Van Long<sup>1</sup>, NGUYEN Hoang Tung<sup>1</sup>, NGUYEN Xuan Au<sup>1</sup>, 차순규<sup>2</sup>, ULLAH Farman<sup>3</sup>, 김용수<sup>3</sup>, 김영동\*<sup>1</sup>

<sup>1</sup>경희대학교 물리학과(서울캠퍼스), <sup>2</sup>경희대학교 KHU-KIST 융합과학기술학과, <sup>3</sup>울산대학교 물리학과  
ydkim@khu.ac.kr

### Abstract:

Molybdenum diselenide (MoSe<sub>2</sub>) 는 최첨단의 트랜지스터, 센서, 광 검출기의 실리콘이나 유기 반도체를 대체할 가능성이 있는 전이금속 다이칼코제나이드 (dichalcogenides) 중 하나로 잘 알려져 있다. 유망한 MoSe<sub>2</sub> 를 적절하게 응용하여 2차원 광 전자 소자를 설계하고 최적화하기 위해서 단 분자 층 MoSe<sub>2</sub> 의 광학적 특성에 대한 정보가 필수적이다. 그러나 2차원 물질인 MoSe<sub>2</sub> 의 광학적 특성에 대한 연구가 몇 차례 보고되었지만, 유전율 함수의 온도 의존성에 대한 체계적인 연구는 아직 미비하다.

본 연구에서는 타원편광분석법을 이용하여 얻은 31 ~ 300 K 온도 범위, 0.74 ~ 6.42 eV 에너지 범위에서 2차원 물질 MoSe<sub>2</sub> 의 유전율 함수에 대한 연구를 보고하고자 한다. 2차원 MoSe<sub>2</sub> 박막은 사파이어 기판 위에 펄스 레이저 증착 방법을 통해 성장한 MoO<sub>3</sub> 박막을 selen화 하여 얻었다. 이 물질의 유전율 함수 측정 결과, 상온 300 K 에서 관찰할 수 없었던 새로운 전이점들을 저온 31 K 에서 관찰할 수 있었다. 또한, 전이점의 에너지는 이차 미분 유전율 함수의 표준해석법을 통해 얻었는데, 저온 31 K 에서 전이점이 명확해지고, 전이점의 에너지가 청색편이 하는 것을 관찰하였다. 이 연구결과는 MoSe<sub>2</sub> 기반의 2차원 나노 광 전자 소자의 물리적 이해와 응용에 유용할 것이다.

### Keywords:

타원편광분석법, 2차원 물질, Molybdenum diselenide (MoSe<sub>2</sub>), 온도 변화, 유전율 함수, 전이점, 2차원 나노 광전자 소자

## Electronic Structure Changes of Transition Metal Dichalcogenides with Ultraviolet-Ozone Treatment

김민준<sup>1</sup>, 정준경<sup>1</sup>, 신동근<sup>1</sup>, 박지홍<sup>1</sup>, 이현복\*<sup>2</sup>, 이연진\*<sup>1</sup>

<sup>1</sup>Institute of Physics and Applied Physics and van der Waals Materials Research Center, Yonsei University, <sup>2</sup>Department of Physics, Kangwon National University  
hyunbok@kangwon.ac.kr, yeonjin@yonsei.ac.kr

### Abstract:

Transition metal dichalcogenides (TMDCs) has been introduced as next-generation materials for electronics due to their high carrier mobility and on/off ratio. However, the contact resistance between source/drain (S/D) metal and TMDC is an obstacle to design high-performance TMDC. The contact resistance is mainly originated from the Schottky barrier between S/D metal and TMDC and surface defect/contamination generated from the exfoliation and CVD growing processes. Many researchers have tried to reduce the contact resistance with charge injection layer and surface treatments. Surface oxygen treatments using O<sub>2</sub> plasma and ultraviolet-ozone (UVO) have been reported to enhance device performance greatly. This is because the oxygen treatments form a transition metal oxide on the TMDC surface, which reduces the Schottky barrier with the S/D metal. However, in the case of non-optimum oxygen treatment, the device performance becomes rather worse. To understand this variation accurately, the changes of chemical states and electronic structure of the surface due to the oxygen treatment should be studied.

In this regard, we employed the ultraviolet and x-ray photoelectron spectroscopy (UPS/XPS) measurements upon the UVO treatment to investigate the evolution of the surface electronic structure of TMDCs. The XPS measurements show the changes of chemical states and the UPS measurements show the changes in the work function and valence band maximum of TMDCs after UVO treatment.

### Keywords:

Transition metal dichalcogenides, photoelectron spectroscopy, energy level, oxygen treatment.

## Electrical transport properties in InAs nanowires

도용주\*<sup>1</sup>, 김남희<sup>1</sup>, 김홍석<sup>1</sup>, 송진동<sup>2</sup>, 김락희<sup>1</sup>

<sup>1</sup>Department of Physics and Photon Science, Gwangju Institute of Science and Technology, <sup>2</sup>Center for Opto-Electronic Materials and Devices, Korea Institute of Science and Technology  
yjdo@gist.ac.kr

### Abstract:

InAs nanowire provides a useful platform for developing high-mobility quantum electronic devices. In particular, the InAs nanowires, grown by high vacuum molecular beam epitaxy, exhibit conductance quantization behavior at low temperature, which is a signature of quasi one-dimensional (1D) electronic transport. When the magnetic field is applied, the spin degeneracy in the 1D subbands can be lifted due to the Zeeman effect. The strong spin-orbit interaction in InAs also can induce spin splitting of conduction subbands. Those electronic properties are essential to build 1D topological superconducting system in the nanowire. Here we report quantum electronic transport properties of InAs nanowire with varying gate voltage, temperature and magnetic field and also conductance enhancement by Andreev reflection when they are contacted with superconductor.

### Keywords:

InAs nanowire, quantum transport

## Identification of anisotropic structure of ReSe<sub>2</sub>

정현식\*<sup>1</sup>, 김근의<sup>1</sup>, 임수연<sup>1</sup>, 김정화<sup>2</sup>, 이종훈<sup>2</sup>

<sup>1</sup>Department of Physics, Sogang University, <sup>2</sup>Department of Materials science and engineering, UNIST  
hcheong@sogang.ac.kr

### Abstract:

ReSe<sub>2</sub> is one of transition metal dichalcogenides (TMDCs) with in-plane anisotropy and lower symmetry in contrast to more common TMDCs such as MoS<sub>2</sub> and WS<sub>2</sub>. Due to its structural anisotropy, ReSe<sub>2</sub> has anisotropic optical and electrical properties [1]. Since electrical devices based on rhenium dichalcogenides have higher mobilities when designed along the direction of rhenium chain, it is important to identify the structural orientation of ReSe<sub>2</sub> in such devices [2]. We performed polarized Raman spectroscopy on few-layer ReSe<sub>2</sub> with several excitation energies. The polarization dependence varied with the number of layers and excitation energies. The rhenium chain direction was determined by the polarization dependence of the Raman mode at ~160 cm<sup>-1</sup> (mode V) with the 1.96 eV-excitation energy and confirmed with HR-STEM measurement. The angle of maximum intensity of mode V corresponds with the rhenium chain direction in few-layer ReSe<sub>2</sub>. However, there is 10 degrees difference between this angle and the rhenium chain direction in monolayer ReSe<sub>2</sub>. We also distinguished two different vertical orientations by comparing the maximum-intensity angles of mode V and the mode at ~125 cm<sup>-1</sup> (mode IV) with HR-STEM measurements.

### References

- [1] Etienne Lorchat *et al.*, ACS Nano **10**, 2752 (2016).
- [2] Erfu Liu *et al.*, Nature Communications **6**, 6991 (2015).

### Keywords:

TMDCs, Raman spectroscopy

## Davydov splitting in Raman spectra of MoS<sub>2</sub>

정현식\*<sup>1</sup>, 나웅기<sup>1</sup>, 김강원<sup>1</sup>, 이재웅<sup>1</sup>  
<sup>1</sup>서강대학교 물리학과  
hcheong@sogang.ac.kr

### Abstract:

We executed Raman measurement on mechanical exfoliated few-layer MoS<sub>2</sub> using three excitation energies of 1.96, 2.41, and 2.81 eV. As reported before, we can distinguish different stacking orders using the low-frequency Raman spectra due to interlayer interactions [1]. We identified all possible stacking types for 2L and 3L MoS<sub>2</sub> with low-frequency Raman spectra. We also observed Davydov splitting of the A<sub>1g</sub> mode in each stacking type using the excitation energy of 1.96 eV which is close to the A or B exciton states [2]. Some forbidden modes also appeared in Davydov splitting of MoS<sub>2</sub>. We then analyzed the interlayer interaction of 3L MoS<sub>2</sub> depending on stacking order by comparing the Davydov splitting with simple rigid layer model which takes only the nearest interaction into account. The interlayer interaction of the 3R type turned out to be larger than that of the 2H type by ~15%. We also calculated the force constants of 2H-MoS<sub>2</sub> using the linear chain model including the surface effect and the second-nearest interactions [3-4].

### References

- [1] J.-U. Lee *et al.*, ACS NANO **10**, 1948 (2016).
- [2] J.-U. Lee *et al.*, Nanoscale, **7**, 3229 (2015).
- [3] G. Froehlicher *et al.*, Nano Lett., **15**, 6481-6489 (2015).
- [4] K. Kim *et al.*, ACS NANO **10**, 8113 (2016).

### Keywords:

MoS<sub>2</sub>, Resonance Raman, Stacking order, Davydov splitting,

## Observation of exciton states in $WSe_2/MoSe_2$ heterostructure

정현식\*<sup>1</sup>, 임수연<sup>1</sup>  
<sup>1</sup>서강대학교, 물리학과  
hcheong@sogang.ac.kr

### Abstract:

Conventional photoluminescence (PL) measurements on transition metal dichalcogenides (TMDs) can easily determine the ground state energy of an exciton. However, the excited states of exciton should be investigated to understand the exciton structure and the electronic band structures in TMDs. The photoluminescence excitation (PLE) makes it possible to observe not only the ground state but also the excited states.

We fabricated monolayer  $WSe_2$  and  $MoSe_2$  and their heterostructures on Si/SiO<sub>2</sub> substrate by dry the transfer method. We performed PLE and reflectance spectroscopy at room temperature to investigate the exciton states. The single materials and heterostructures are encapsulated by thick h-BN. We used a collimated broadband light combined with a monochromator as an excitation source.

### Keywords:

Photoluminescence, PLE, heterostructure, TMDs

## Highly Improved Air-Stability of Monolayer TMDs Grown on Graphene Substrate

권순용\*<sup>1</sup>, 김세양<sup>1</sup>, 곽진성<sup>1</sup>, 김정화<sup>1</sup>, 이재웅<sup>2</sup>, 조용수<sup>1</sup>, 김성엽<sup>3</sup>, 정현식<sup>2</sup>, 이종훈<sup>1</sup>  
<sup>1</sup>울산과학기술원 신소재공학부, <sup>2</sup>서강대학교 물리학과, <sup>3</sup>울산과학기술원 기계항공및원자력공학부  
sykwon@unist.ac.kr

### Abstract:

In this work, we have identified a new role of graphene in improving the air stability of two-dimensional transition metal dichalcogenides (TMDs). Unlike the aging phenomenon that has been observed in a short period of time in TMDs flakes grown on SiO<sub>2</sub>/Si substrates (representatively, WS<sub>2</sub>/SiO<sub>2</sub>), it was observed that epitaxially grown WS<sub>2</sub> flakes on graphene substrate (WS<sub>2</sub>/Gr) maintained a clean surface and good crystallinity as in the initial growth without any encapsulation even after a year in ambient air conditions. Our investigations describe the relationship between crystal defects and aging phenomena through experimental and analytical results. We also show for the first time the effect of "doping effect induced by charge transfer" on improving air stability. This study emphasize the effect of the target substrate on the stability of TMDs material, and it is expected to pave the way for commercialization of TMDs with stable performance for a long time.

### Keywords:

TMDs, air-stability, graphene

## Effect of Pb content and top electrode on the electrical properties of PZT thin films

강보수\*<sup>1</sup>, 천민철<sup>1</sup>, 박가연<sup>1</sup>, 박상현<sup>1</sup>, 박솔민<sup>1</sup>

<sup>1</sup>Department of Applied Physics, Hanyang University, Ansan 426-791  
bosookang@hanyang.ac.kr

### Abstract:

We fabricated metal/ $\text{Pb}_x\text{Zr}_{0.52}\text{Ti}_{0.48}\text{O}_3$ /Pt capacitor structure. The PZT thin films with different amount of excess Pb (1.0, 1.1 and 1.2) were deposited by using sol-gel process. Noble metal Au and non-noble metals such as Y and Al were deposited for top electrode. From X-ray diffraction analysis and atomic force microscopy, the films of 1.0 and 1.1 excess Pb consist of pyrochlore and perovskite phase. The pyrochlore phase disappeared in the films of 1.2 excess Pb. From the polarization vs. electric field ( $P$ - $E$ ) loop, the low remnant polarization of the 1.0 excess and the 1.1 excess Pb films can be attributed to the formation of the pyrochlore phase, which is non-ferroelectric. The PZT thin films with noble metals as top electrodes exhibits symmetric  $P$ - $E$  loops, while the films with non-noble metals exhibits asymmetric  $P$ - $E$  loops. Au top electrode seems to form Schottky contacts and Y and Al form ohmic contacts with PZT thin films. In PZT thin films with non-noble metal as top electrode, the shifting of the  $P$ - $E$  loop is supposed to be due to the internal field generated by asymmetric band bending. The electrode / PZT interface was more important than the bulk properties in fatigue and retention behaviors. The metal oxide formation at non-noble metal electrode / PZT interface possibly inhibits nucleation of polarization domain.

### Keywords:

PZT, Pb content, Top electrode

## Luminescence optosensing of bio-molecular using functionalized up-conversion phosphor nanoparticles

정중원<sup>1</sup>, 박진영<sup>1</sup>, 홍우태<sup>2</sup>, 제재용<sup>3</sup>, 양현경\*<sup>1</sup>

<sup>1</sup>부경대학교, 과학기술융합전문대학원, LED융합공학전공, <sup>2</sup>부경대학교, LED공학협동과정, <sup>3</sup>동의과학대학교, 방사선과

hkyang@pknu.ac.kr

### Abstract:

The up-conversion nanoparticles (UCNPs) have many good characteristics. The main materials are that they can emit visible or near infrared (NIR) light under NIR irradiation. In addition, these UCNPs show a sharp emission bandwidth, high photostability, tunable emission, long lifetime, and low cytotoxicity. Due to these unique properties, UCNPs have emerged as a new class of materials in a wide range of applications, such as bio-sensing, chemical sensing, in vivo imaging, drug delivery, photodynamic therapy and photo activation.

Catecholamines (CAs) are a well-known neurotransmitter and related with mammalian central nervous system. Dopamine (DA), epinephrine (EP), and norepinephrine (NEP) show different actions in the nervous system, although all CAs are conducted both as a hormone and neurotransmitter. Therefore, the determination of specific CAs is required with high sensitive, simple, and fast analytical method.

We developed a novel approach for quantitative detection on specific CAs based on the upconversion fluorescent intensity of UCNPs in conjunction with various metal ions that to play a role a trigger. Ferric ions ( $\text{Fe}^{3+}$ ) decorated UCNPs detect CAs selectively from other inferences. The developed biosensor shows a high sensitivity of DA / EP via using  $\text{Li}^+$  and  $\text{Cu}^{2+}$  ions, respectively.

### Keywords:

Phosphor, up-conversion, optosensing

## Formation of 3D graphene-Ni foam heterostructures with improved performance and durability for bipolar plates in a polymer electrolyte membrane fuel cell

심여선<sup>1</sup>, 곽진성<sup>1</sup>, 김세양<sup>1</sup>, 조용수<sup>1</sup>, 김승현<sup>2</sup>, 김성엽<sup>2</sup>, 김지현<sup>2</sup>, 이치승<sup>3</sup>, 조장호<sup>3</sup>, 권순용\*<sup>1</sup>

<sup>1</sup>울산과학기술원 신소재공학부, <sup>2</sup>울산과학기술원 기계항공 및 원자력공학부, <sup>3</sup>현대자동차 연료전지기술개발팀  
sykwon@unist.ac.kr

### Abstract:

Improving the lifetime and the operational stability of polymer electrolyte membrane fuel cells (PEMFCs) is critical for realizing their implementation as a highly-efficient energy conversion system. However, the chemical instability of metal bipolar plates in the destructive operating environment inside PEMFCs leads to decreased performance and durability. Therefore, rational interface passivation techniques are critical for further boosting the development of PEMFCs. In this work, we report a novel method for coating highly-crystalline multilayer graphene (Gr) as a superficial protective layer (thickness of ~12 nm) onto 6 x 6 cm<sup>2</sup> Ni foam within short periods (t≤5 min) via the facile and rapid thermal annealing (RTA) of poly(methylmethacrylate) as a solid-state C source. The synthesized graphene layers have a low defect density and completely cover the 3D-structured surface of the Ni foam, dramatically enhancing its corrosion resistance, interfacial contact resistance(ICR), and hydrophobicity. Electrochemical analysis revealed that the 3D Gr-coated Ni foam outperforms bare Ni foam and amorphous-C-coated Ni foam by providing a two-order-of-magnitude lower corrosion rate in the operational environment for a PEMFC. After stability tests in aggressive environments, the 3D Gr-coated Ni foam retained its outstanding ICR of 9.3 mΩ·cm<sup>2</sup> at 10.1 kgf·cm<sup>-2</sup>. A H<sub>2</sub>/air PEMFC fabricated using the Gr-coated Ni foam as bipolar plates showed a substantially enhanced maximum power density of ~967 mW·cm<sup>-2</sup>, which is the best among the reported metal foam bipolar plates. This study demonstrates that 3D Gr-coated Ni foam prepared using our proposed new coating method exhibits superior characteristics as an inhibitor for high-efficiency performance of a PEMFC with durability. Our facile coating approach can pave the way to further enhance energy conversion systems through interface engineering.

### Keywords:

3D graphene, Ni foam, heterostructure, polymer electrolyte membrane fuel cell(PEMFC)

## Temperature dependence of exciton peak shifts in monolayer WSe<sub>2</sub> films

김장원<sup>1</sup>, 강희성<sup>2</sup>, 이철호<sup>2</sup>, 김재훈\*<sup>1</sup>  
<sup>1</sup>연세대학교 물리학과, <sup>2</sup>고려대학교 물리학과  
super@yonsei.ac.kr

### Abstract:

We carried out absorption spectroscopy on monolayer WSe<sub>2</sub> films grown by MOCVD and transferred to sapphire substrates. We obtained the absorption spectra in the visible and near-infrared (NIR) regions (500 nm - 1000 nm) and found that temperature decrease leads to narrowing of the A and B exciton peaks and to shift to higher energy.

### Keywords:

absorption spectroscopy, transition metal dichalcogenides, monolayer WSe<sub>2</sub> films

## Optical Properties of PdSe<sub>2</sub> from Spectroscopic Ellipsometry Data

이지은<sup>1</sup>, 심경익<sup>1</sup>, 류정현<sup>2</sup>, 이기문<sup>2</sup>, 김재훈\*<sup>1</sup>  
<sup>1</sup>연세대학교 물리학과, <sup>2</sup>군산대학교 물리학과  
super@yonsei.ac.kr

### Abstract:

We performed spectroscopic ellipsometry measurements on bulk PdSe<sub>2</sub> in the visible region. The elements of the Mueller matrix were extracted. From our ellipsometry data, we obtained the optical constants such as the refractive index (n) and the extinction coefficient (k) of PdSe<sub>2</sub>. The absorption coefficient was calculated from the extinction coefficient (k). Our data indicate weak optical anisotropy in PdSe<sub>2</sub>.

### Keywords:

ellipsometry, refractive index, extinction coefficient, transition metal dichalcogenides, PdSe<sub>2</sub>

## Optical Spectroscopy of PdSe<sub>2</sub>

이호원<sup>1</sup>, 이지은<sup>1</sup>, 이기문<sup>2</sup>, 김재훈\*<sup>1</sup>, 류정현<sup>2</sup>  
<sup>1</sup>연세대학교 물리학과, <sup>2</sup>군산대학교 물리학과  
super@yonsei.ac.kr

### Abstract:

We measured the transmittance of single-crystal PdSe<sub>2</sub> in the UV-Vis-NIR regions and extracted the absorbance. The bulk PdSe<sub>2</sub> exhibits evidence of an indirect gap at around 0.4 eV at room temperature. In the ab plane, polarized transmittance measurements reveal weak anisotropy in the range of our measurements.

### Keywords:

PdSe<sub>2</sub>, TMDC, Polarized transmittance measurement

## Optical properties of few-layer 2H phase molybdenum ditelluride (2H-MoTe<sub>2</sub>)

JUNG Eilho<sup>1</sup>, PARK Jinchul<sup>2, 3</sup>, LEE Younghee<sup>2, 3</sup>, 황정식\*<sup>1</sup>

<sup>1</sup>Department of Physics, Sungkyunkwan University, Suwon 16419, Korea., <sup>2</sup>IBS Center for Integrated Nanostructure Physics (CINAP), Institute for Basic Science, Sungkyunkwan University, Suwon 16419, Korea., <sup>3</sup>Department of Energy Science, Sungkyunkwan University, Suwon 16419, Korea.  
jungseek@skku.edu

### Abstract:

We investigated few-layer 2H phase molybdenum ditelluride (2H-MoTe<sub>2</sub>) using an optical spectroscopy technique. Generally, 2H-MoTe<sub>2</sub> is an insulator and 1T'-MoTe<sub>2</sub> is a semi-metal. We measured transmittance spectra of 2H-MoTe<sub>2</sub> samples on Quartz-substrate in a wide spectral range of 4000 ~ 25,000 cm<sup>-1</sup> (0.5 ~ 3.1 eV) at various temperatures (8 ~ 350K). We obtained the optical conductivity from the measured transmittance using the Tinkham formula. Exciton is a bound state of electron-hole pair formed by the electrostatic Coulomb attraction. We extracted temperature-dependent evolutions of the direct band-gap and the multi exciton binding energy of 2H-MoTe<sub>2</sub> from the measured optical spectra.

### Keywords:

2H-MoTe<sub>2</sub>, Transmittance, Tinkham formula, Optical Conductivity, Band-gap, Exciton binding energy

## Temperature Dependent Band Gap in Epitaxial Films of Perovskite $Ba_{1-x}La_xSnO_3$

김재훈\*<sup>1</sup>, 전택선<sup>1</sup>, 심경익<sup>1</sup>, 김종현<sup>1</sup>, 하태우<sup>2</sup>, 김영모<sup>3</sup>, 차국린<sup>3</sup>  
<sup>1</sup>연세대학교 물리학과, <sup>2</sup>ibs 나노구조물리 연구단, <sup>3</sup>서울대학교 물리천문학부  
super@yonsei.ac.kr

### Abstract:

$Ba_{1-x}La_xSnO_3$  (BLSO) is a perovskite-based transparent conducting oxide. We have investigated the temperature dependent band gap in BLSO (0-0.06%) epitaxial films grown on MgO substrates. The temperature dependent band gap was measured by using a spectrophotometer and a He-free closed cycle cryostat. We verified an increase in the band gap from 3.5 to 4.2 eV as the doping concentration increases.

### Keywords:

BLSO, perovskite, band gap

## Absorption peak shifts of A and B excitons in monolayer MoSe<sub>2</sub> films with temperature

김재훈\*<sup>1</sup>, 김재하<sup>1</sup>, 정재훈<sup>1</sup>, 김장원<sup>1</sup>, 조만호<sup>1</sup>  
<sup>1</sup>연세대학교 물리학과  
super@yonsei.ac.kr

### Abstract:

We carried out absorption spectroscopy of monolayer MoSe<sub>2</sub> films grown by MBE on sapphire substrates. We measured transmission in the visible and near-infrared (NIR) regions (500 nm - 1000 nm) to extract the absorption spectra. We observed that the A exciton peaks of MoSe<sub>2</sub> shifted from 1.5 eV to 1.66 eV and the B exciton peaks also shifted from 1.78 eV to 1.87 eV as the temperature from decreased room temperature to 5 K. Peak narrowing was observed for both A and B excitons.

### Keywords:

absorption spectroscopy, transition metal dichalcogenide, monolayer MoSe<sub>2</sub> films

## Hexagonal-boron nitride as an passivation layer for high performance light-emitting diodes

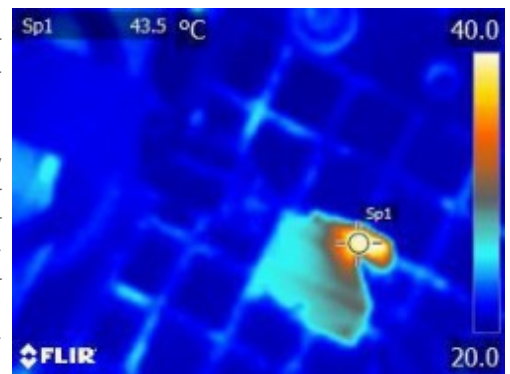
이건희<sup>1</sup>, 서태훈<sup>2</sup>, 여동규<sup>1</sup>, 조현진<sup>2</sup>, 여형태<sup>1</sup>, 김명중<sup>2</sup>, 서은경\*<sup>1</sup>

<sup>1</sup>전북대학교 반도체과학기술학과, <sup>2</sup>한국과학기술연구원, 양자응용복합소재 연구센터  
eksuh@jbnu.ac.kr

### Abstract:

발광다이오드(LED)는 주입된 에너지가 전부 빛으로 전환되는 것이 아닌 에너지의 약 20% 정도만 빛으로 전환되고, 나머지의 에너지는 열로서 방출된다. 이렇게 발생한 열은 LED의 신뢰성을 떨어뜨리고 소자의 특성에 악영향을 미칠 뿐더러 소자의 수명을 크게 저하시키는 문제점이 존재한다. 이를 해결하기 위한 방안으로서 LED의 기반이 되는 GaN 박막의 품질을 향상시키는 방법이 있지만 이미 성장된 기판에서는 더이상 개선을 하기 힘들다. Passivation은 high electron mobility transistors (HEMTs)와 같은 전자소자에 소자 표면에 존재하는 결함들에 의한 electron trap 현상을 억제하기 위하여 필수적으로 행해지는 공정이다. 최근 각광 받고 있는 hexagonal-boron nitride (h-BN)은 매우 높은 열전도도, 화학적 내구도, 열적 내구도, 휨 특성의 장점을 가지는 저차원의 나노물질로서 이를 응용하고자 하는 다양한 연구들이 진행되어지고 있다.

이전연구에서 HEMT에 h-BN을 passivation 함으로서 소자의 성능을 향상시킨 바 있다. 본 연구에서는 열에 의한 문제점을 해결하기 위하여 h-BN을 LED 소자에 passivation 층으로서 적용하였다. 그 결과, h-BN이 증착된 LED 소자의 표면온도는 일반적으로 제작된 LED 소자보다 평균온도가 12°C 도 낮았으며 소자의 수명이 크게 증가하였다. 이는 h-BN의 우수한 열전도성과 열 저항성이 LED의 passivation 층으로서 효과적으로 작용한 결과이다. 그림 1은 h-BN을 적용한 LED 소자의 열화상 카메라 이미지이다.



### Keywords:

LED, h-BN, passivation

## Second harmonic generation measurements on polytype MoS<sub>2</sub>

정현식\*<sup>1</sup>, 김중철<sup>1</sup>, 나웅기<sup>1</sup>  
<sup>1</sup>서강대학교 물리학과  
hcheong@sogang.ac.kr

### Abstract:

The effects of stacking order in the second harmonic generation (SHG) of molybdenum disulfide (MoS<sub>2</sub>) are investigated. 2H-MoS<sub>2</sub> is representative of semiconducting transition metal dichalcogenides (TMDCs). Although 2H-MoS<sub>2</sub> is most common in nature, the 3R phase can exist due to a small difference in the formation energy. However, most studies so far have focused on the 2H phase, and only few studies are reported for the 3R and mixed phases[1]. We found the 2H, 3R and mixed phase of exfoliated MoS<sub>2</sub> from natural molybdenite crystals. By using the 800 nm excitation wavelength, we compared the SHG of samples with different stacking orders in detail. We show that the SHG can be used to identify stacking orders in MoS<sub>2</sub>.

[1] Lee J.-U. et al, ACS nano, 10, 1948 (2016)

### Keywords:

Second harmonic generation, MoS<sub>2</sub>, polytype MoS<sub>2</sub>

## Synthesis of $V_2O_5$ nanospheres with different sizes using chemical reaction method

김석원\*<sup>1</sup>, 강만일<sup>1</sup>, 황보현<sup>1</sup>

<sup>1</sup>울산대학교 물리학과  
sokkim@ulsan.ac.kr

### Abstract:

현대의 환경오염 문제가 심화되면서, 다양한 장치들의 에너지 효율을 높이기 위한 소재 개발이 관심을 받고 있을 뿐 아니라 그들의 나노구조를 달리하여 장치의 효율을 높이기 위한 연구도 많은 관심을 받고 있다.  $V_2O_5$ 는 gas sensor, photocatalytic, electrochromic device 등의 많은 분야에서 관심을 받고 있으며 다양한 형태의 나노구조를 구현할 수 있다. 일차원 나노구조인 nanorod와 nanowire 그리고 이차원 구조인 nanosheet가 대표적인 예이다. 본 연구에서는 삼차원 나노구조인 nanosphere 제작을 위해 chemical reaction method를 사용하였다. 그리고 nanosphere의 크기(100-1000 nm)를 조절하기 위해 제작 과정에 들어가는 시료의 농도를 달리하였다. 이후 nanosphere의 크기와 균일성을 SEM으로 확인하였다.

### Keywords:

$V_2O_5$ , nanosphere

## Synthesis and size control of vanadium dioxide nanospheres using hydrothermal method

김석원\*<sup>1</sup>, 김현기<sup>1</sup>, 강만일<sup>1</sup>

<sup>1</sup>울산대학교 물리학과  
sokkim@ulsan.ac.kr

### Abstract:

바나듐 원자는 다양한 원자가 상태를 가질 수 있어  $V_2O_3$ ,  $V_2O_5$ ,  $V_5O_9$  등 다양한 산화 상태의 산화물로 존재한다. 이들 중  $VO_2$ 는  $V^{4+}$ 이온 1개와  $O^{2-}$ 이온 2개가 결합하는 산화물로 1950년 Morin에 의해  $VO_2$ 가 ~340 K에서 절연체에서 금속으로 변화하는 금속-절연체 전이(metal-insulator transition)를 일으킨다는 것이 알려졌다. 이 상전이는  $VO_2$ 의 내부 구조에 강하게 의존하기 때문에,  $VO_2$ 의 결정상태나 입자의 크기에 크게 영향을 받는다. 따라서  $VO_2$  nanosphere의 크기를 조절하는 방법은 중요하다. 본 연구에서는 hydrothermal method를 사용하여  $VO_2$  nanosphere를 제조하였다. 시료의 농도와 가열 온도를 조절하여 다양한 조건에서 다양한 크기를 갖는  $VO_2$  nanosphere를 합성하였고,  $Al_2O_3$  기판에 분산시켜 크기와 구조를 확인하였다.

### Keywords:

$VO_2$ , nanosphere, hydrothermal

## W18O49 nanowires assembled on carbon felt for application to supercapacitors

김도형\*<sup>1</sup>, 엄승용<sup>1</sup>, 정진주<sup>1</sup>, 원하연<sup>1</sup>, 강현선<sup>1</sup>

<sup>1</sup>경북대학교 물리학과  
kimdh@knu.ac.kr

### Abstract:

For supercapacitor applications,  $W_{18}O_{49}$  nanowires have been extensively grown on graphitic carbon felt using a facile solvothermal method. The diameter and length of the nanowires are about 7 and 300 nm, respectively. The nanowires consist of monoclinic  $W_{18}O_{49}$  grown along the [010] direction, as shown by TEM and XRD analyses. The  $W_{18}O_{49}$  nanowires, assembled on carbon felt, exhibit a high capacity of 588.33 F/g at a current density of 1 A/g together with an excellent cycle performance, and a low internal resistance during the electrochemical tests. This outstanding performance may originate from the three-dimensional porous nanostructure of these  $W_{18}O_{49}$  nanowires, which leads to a reduction in the resistance and fast reaction kinetics due to the high specific surface area and electrolyte accessibility. Furthermore, sufficient oxygen deficiencies of the substoichiometric tungsten oxide can also contribute to the electrochemical activity, which can be confirmed by comparison of CV and EIS data with  $WO_3$  nanowires.

### Keywords:

nanowire, three-dimensional porous nanostructure,  $W_{18}O_{49}$ , supercapacitor

## PANI/CdS/CdSe/CaFe<sub>2</sub>O<sub>4</sub>/RGO for CO<sub>2</sub> to CH<sub>3</sub>OH conversion

KIM Hyun<sup>1</sup>, KIM Dong Yun<sup>1</sup>, YANG Bee Lyong<sup>\*1</sup>

<sup>1</sup>금오공과대학교 신소재공학과  
blyang@kumoh.ac.kr

### Abstract:

Ongoing research of the precise CO<sub>2</sub> to fuel conversion selectivity became important issue because products are mixed during CO<sub>2</sub> reduction. In order to improve conversion selectivity, some of metal oxide catalysts are available for different products. The photo-excited electron and holes are fast recombined even electronic junction configurations because of their crystal imperfections. 2D materials that enable fast electron transfer are expected lower recombination rate of electron and holes. In this study, InP was vertically grown on reduced graphene oxide (RGO)/FTO glass by chemical bath deposition instead of dominant chemical vapour deposition (RGO was prepared by Hummer's method and spin coated on FTO). And grown InP nanorods were confirmed by means of both FESEM (field emission scanning electron microscope) and TEM (transmission electron microscope). CdS and CdSe QDs were comparatively studied by SILAR (successive ionic layer adsorption and deposition process). PANI (polyaniline) was coated to prevent a photocorrosion of CdS and CdSe QDs. CO<sub>2</sub> to CH<sub>3</sub>OH conversion selectivity test was conducted using three electrode system under visible light that of intensity 100mW/cm<sup>2</sup>. Products of CO<sub>2</sub> reduction was collected by micro-syringe and subsequently transferred to the NMR (nuclear magnetic resonance) and raman spectroscopy to identify inside solution composition. Quantitative measurement of CH<sub>3</sub>OH was not only evaluated by GC-MS (gas chromatography-mass spectrometer) but also stability of CaFe<sub>2</sub>O<sub>4</sub> composite.

### Acknowledgement

This research was supported by Basic Science Research Program through the National Research Foundation of Korea(NRF) funded by the Ministry of Education Science and Technology(MEST) (2017R1D1A1B03034141)

### Keywords:

Photocorrosion, PANI, RGO, CO<sub>2</sub>, CH<sub>3</sub>OH

## Ag NPs/CaFe<sub>2</sub>O<sub>4</sub> nanobranh/CuO nanorod/RGO/FTO photo-cathode for CO<sub>2</sub> to CH<sub>3</sub>OH conversion

KIM Hyun<sup>1</sup>, KIM Dong Yun<sup>1</sup>, YANG Bee Lyong<sup>\*1</sup>

<sup>1</sup>금오공과대학교 신소재공학과  
blyang@kumoh.ac.kr

### Abstract:

The combustion of fossil fuels emits carbon dioxide that causes rising temperature of earth. This is called global warming that induces unpredicted disaster. As this crisis, many efforts are performed to reduce carbon dioxide concentration but simple storage of carbon dioxide was not considered as a solution because of limited storage capacity. These days hydrocarbon fuels using carbon dioxide conversion by heating, applying voltage and irradiation of sunlight are promising technique for the carbon dioxide reduction and industrial benefits. Utilization of the mixed oxides photoelectrochemical system consisting of the electrodeposited, onto RGO/FTO glass support, CaFe<sub>2</sub>O<sub>4</sub> nanobranh/CuO nanorods catalyst and next coupled to Ag nanoparticles, acting as a methanol selective co-catalyst. Such a hetero-junction allows, from one side, increase density of charge carries in the conduction band of the photocathode and, on the other side, improves conductivity of the whole system. The new synthesized photoelectrodes were steadily prepared and well characterized using UV-vis, TEM, XPS, XRD and SEM. The reduction of CO<sub>2</sub> to methanol in liquid phase was analyzed by UV-vis spectrophotometry (UV 2600 Shimadzu UV-vis spectrophotometer) at the wavelength ( $\lambda_{max}$ ) of 395 nm. PANI/ZnS NPs/ZnO NRs films exhibited higher photocurrent densities and enhanced photoelectrochemical CO<sub>2</sub> reduction properties as a result of improved separation of photogenerated electron/hole pairs, carrier density and the faster electron transport rate due to the proper energy level state.

### Acknowledgement

This research was supported by Basic Science Research Program through the National Research Foundation of Korea(NRF) funded by the Ministry of Education Science and Technology(MEST) (2017R1D1A1B03034141)

### Keywords:

Selectivity, CO<sub>2</sub>, CH<sub>3</sub>OH

## Observation of Negative Capacitance in Metal-Ferroelectric Pb(Zr,Ti)O<sub>3</sub>-Insulator-Semiconductor (MFIS) capacitors

강보수\*<sup>1</sup>, 박가연<sup>1</sup>, 천민철<sup>1</sup>, 박솔민<sup>1</sup>, 박상현<sup>1</sup>

<sup>1</sup>Department of Applied Physics, Hanyang University  
bosookang@hanyang.ac.kr

### Abstract:

In conventional field effect transistor (FET), the fundamental limit of a subthreshold swing is 60 mV/decade at room temperature, termed as 'Boltzmann Tyranny'. Lower subthreshold swing value enables fast switching and reduced power consumption. Negative capacitance observed in ferroelectric materials can be a breakthrough of this limitation, thereby improving the performance of device/circuit. A metal/ferroelectric/insulator/semiconductor (MFIS) structure is an important part of ferroelectric FET. Therefore, the electrical characteristics such as polarization-electric field hysteresis loop and capacitance-voltage characteristics of the MFIS capacitors should be understood for further application to practical devices.

In this study, we observed the negative capacitance from lead zirconate titanate MFIS capacitor connected with series resistance and investigated the effect of circuit parameters such as external series resistance which influences negative capacitance time.

### Keywords:

ferroelectric, negative capacitance, MFIS

## Variation of photoluminescence spectral line shape of monolayer $WS_2$

정현식\*<sup>1</sup>, 권용재<sup>1</sup>, 김강원<sup>1</sup>, 김원택<sup>2</sup>, 류순민<sup>2, 3</sup>

<sup>1</sup>Department of Physics, Sogang University, <sup>2</sup>Department of Chemistry, Pohang University of Science and Technology (POSTECH), <sup>3</sup>Division of Advanced Materials Science, Pohang University of Science and Technology (POSTECH)  
hcheong@sogang.ac.kr

### Abstract:

The origin of the variation of photoluminescence (PL) spectra of monolayer tungsten disulfide ( $WS_2$ ) is investigated systematically. Dependence of the PL spectrum on the excitation power show that the relatively sharp component corresponds to excitons whereas the broader component at slightly lower energy corresponds to negatively charged trions. PL imaging and second harmonic generation measurements show that the trion signals are suppressed more than the exciton signals near the edges, thereby relatively enhancing the excitonic feature in the PL spectrum and that such relative enhancement of the exciton signals is more pronounced near approximately armchair edges. This effect is interpreted in terms of depletion of free electrons near the edges caused by structural defects and adsorption of electron acceptors such as oxygen atoms.

### Keywords:

Tungsten disulfide, Photoluminescence, Exciton, Trion, Second harmonic generation

# Measurement of Schottky Barrier Height of Graphene-WS<sub>2</sub> Barristor with a Modified Schottky Contact Model and Nano FT-IR Spectroscopy by scattering type Scanning Nearfield Optical Microscopy

최인철<sup>1</sup>, 이준호<sup>1</sup>, 정내봉<sup>1</sup>, 박도현<sup>1</sup>, 이흥준<sup>1</sup>, 조영진<sup>1</sup>, 정현중\*<sup>1</sup>  
<sup>1</sup>건국대학교, 물리학과  
hjchung@konkuk.ac.kr

## Abstract:

Recent study proposed a new schottky contact model between graphene and semiconductor [1], carrying out the new diode equation which showed the diode current proportional to the  $T^3$ , whereas conventional one claimed  $T^2$ . In this poster, we have fabricated graphene-tungsten disulfide(WS<sub>2</sub>) barristor on SiO<sub>2</sub> substrate, and calculated Schottky barrier height of heterojunction interface by measuring saturated drain current ( $I_{sat}$ ) by varying gate voltage and temperature. We also measured Nano FT-IR spectrum of the junction by scattering type Scanning Nearfield Optical Microscope(s-SNOM) to obtain absorption peak within mid-infrared range (MIR). We found absorption peaks shift from  $\sim 1280\text{ cm}^{-1}$  to  $\sim 1230\text{ cm}^{-1}$  by varying the thickness of WS<sub>2</sub>. It agrees with our last experiments [2] which shows the Schottky barrier height of graphene-WS<sub>2</sub> barristor device reduces by increasing thickness of WS<sub>2</sub>. An optical and electronic analysis for this heterojunction model will be presented.

## Keywords:

Graphene, Tungsten disulfide, Barristor, Schottky Barrier, Nano FT-IR, scattering type Scanning Nearfield Optical Microscopy(s-SNOM)

## WS<sub>2</sub> FET using Indium Tin Oxide (ITO) electrode

이흥준<sup>1</sup>, 이준호<sup>1</sup>, 정내봉<sup>1</sup>, 박도현<sup>1</sup>, 이상익<sup>1</sup>, 조영진<sup>1</sup>, 최인철<sup>1</sup>, 박배호<sup>1</sup>, 정현중\*<sup>1</sup>

<sup>1</sup>건국대학교 물리학부  
hjchung@konkuk.ac.kr

### Abstract:

Indium tin oxide (ITO) has been used as transparent electrodes since it is heavily doped wide bandgap semiconductor, whose band gap is around 3.75eV. Since oxygen vacancy and crystal structure are crucial for the conductivity of ITO, ITO sputtering is performed at high temperatures and than annealing process under oxygen flow is important to obtain good ITO. Therefore, ITO is hard to be patterned using lift-off processes, where electrodes are patterned on Polymethyl methacrylate (PMMA) film with e-beam lithography before ITO is deposited. It is because both high temperature and oxygen annealing hardens the PMMA film.

In this presentation, ITO films were deposited by DC-magnetron sputter at low temperature, ITO electrodes with the lift-off method. Then we investigated WS<sub>2</sub> field-effect transistor (FETs) with the ITO electrodes for optical applications. Y-function method was used to measure contact resistance, and FET characteristics were measured using Si bottom gate with 300 nm SiO<sub>2</sub> gate oxide.

### Keywords:

WS<sub>2</sub>, ITO, Indium Tin Oxide

## Enhanced Field Emission Characteristic of Carbon Nanotubes Synthesized on Stainless Steel by Acid Pretreatment of Substrate

박준영<sup>1</sup>, GUPTA Amar Prasad<sup>1</sup>, 김우섭<sup>1</sup>, 임종민<sup>1</sup>, 안정선\*<sup>1</sup>, 여승준<sup>1</sup>, 류제황<sup>1</sup>  
<sup>1</sup>경희대학교 물리학과  
johnsonahn@khu.ac.kr

### Abstract:

나노크기의 직경을 가지는 관 모양의 탄소 동소체인 탄소나노튜브(Carbon Nanotube, CNT)는 높은 전류 밀도와 낮은 문턱전압을 가지는 전기적 특성 때문에 전계방출소자로서 주목을 받고 있는 물질이다. 에미터 소자의 전계방출특성은 탄소나노튜브의 길이, 직경과 같은 기하학적인 구조와 밀도에 의해 변화하며 이러한 요소들을 제어하는 것이 중요하다. 본 연구에서는 탄소나노튜브의 성장에 앞서 기판에 먼저 산 처리(Acid pretreatment)의 과정을 거침으로써 이후에 성장되는 탄소나노튜브의 전계방출특성의 변화를 연구하였다. 탄소나노튜브는 플라즈마 화학기상증착법(Plasma Enhanced Chemical Vapor Deposition, PECVD)으로 생성되었다. 복잡한 공정이 들어가는 기존의 실리콘 기판과는 달리 이미 촉매제가 포함되어 있는 금속 기판에 탄소나노튜브를 성장시키는 것이 더욱 효율적이지만 금속 기판에 탄소나노튜브를 효과적으로 성장시키기 위해서는 열처리 과정이 필요로 한다. 이 과정에서 탄소나노튜브의 성장을 저해시키는 특정 금속들의 비율이 높아지는 문제점이 생긴다. 이 문제점을 해결하기 위한 방법으로 산 처리를 이용하였으며, 이 공정을 통해 변화하는 탄소나노튜브의 성장과 전계방출특성을 관찰하였다.

### Keywords:

Carbon nanotube, PECVD, Acid pretreatment, Field emission, Nanostructure

## Field emission characteristics of carbon nanotube emitter on metal substrate by acid treatment

김우섭<sup>1</sup>, GUPTA Amar Prasad<sup>1</sup>, 박준영<sup>1</sup>, 임종민<sup>1</sup>, 여승준<sup>1</sup>, 류제황<sup>1</sup>, 안정선\*<sup>1</sup>

<sup>1</sup>경희대학교 물리학과  
johnsonahn@khu.ac.kr

### Abstract:

탄소나노튜브(CNTs)의 물성은 차세대 산업분야에서 다양한 응용가능성을 보여 주고 있다. 그 중에서도 낮은 임계 전계에서의 높은 방출 전류로 인해 전계 방출 소자로의 응용이 기대되고 있다. 전계 방출 특성의 향상을 위해서 다양한 음극 소자 및 탄소나노튜브의 구조 제어, 탄소나노튜브의 밀도 제어기술 등에 대한 연구가 진행되고 있다. 특히 CNTs의 구조나 밀도를 제어하기 위해 산 처리, 고온 처리와 같은 방법들이 활발히 연구되고 있다. 하지만 금속 기판에 직접 CNTs를 성장시킨 뒤에 구조 및 밀도를 제어하는 연구는 상대적으로 빈약하여, 본 연구에서는 금속 기판에 무작위로 성장된 CNTs에서 촉매를 제거하고, CNTs의 구조 혹은 밀도를 제어하여 전계 방출 특성을 높이기 위해 산 처리를 하였다. CNTs는PECVD(Plasma-enhanced Chemical Vapor Deposition)를 이용하여 성장하였다. 산 처리는 HNO<sub>3</sub>를 사용하였으며, 산 처리 시간에 따른 전계 방출 변화와 금속 성분 비율이 다른 기판들에 따른 산 처리 이후의 전계 방출 변화도 비교하였다.

### Keywords:

Carbon nanotube, PECVD, Field emission, Acid post-treatment

## Stabilized field emission characteristics of carbon nanotube on metal mesh substrate

안정선\*<sup>1</sup>, 임종민<sup>1</sup>, GUPTA Amar Prasad<sup>1</sup>, 김우섭<sup>1</sup>, 박준영<sup>1</sup>, 류제황<sup>1</sup>, 여승준<sup>1</sup>

<sup>1</sup>경희대학교 물리학과  
johnsonahn@khu.ac.kr

### Abstract:

탄소나노튜브(carbon nanotube, CNT)의 전계 방출 특성을 이용한 장치의 개발에 있어서, 낮은 임계 전계와 높은 전자 방출을 갖는 전자방출원의 제작이 매우 중요하다. 전자방출원의 제작에는 다양한 방법이 있지만, CNT를 금속 기판에 직접 성장시키는 방법은 실리콘 기판에서 성장하는 것에 비해 저렴하고, 기판의 전처리 과정이 간단하다는 장점을 갖는다. 하지만 금속 기판 위의 CNT 직접 성장은 기판 구성물의 불균일성에 의해 실리콘 기판에 비해 CNT가 구분 없이 촘촘하게 성장하게 되고, 스크리닝 효과(screening effect)에 의해 고출력 전계 방출의 제한이 생긴다. 이 문제를 최소화하기 위해서 전면인 기판을 사용하지 않고, 그물 구조의 기판을 사용하여 기판 위의 CNT들이 서로간에 전자 방출을 저해하는 효과를 줄이고자 했다. CNT의 성장은 그물금속기판 위에 플라즈마 화학기상증착(plasma enhanced chemical vapor deposition, PECVD)방법을 이용하여 직접 성장하였고, 성장은 아세틸렌 기체와 암모니아 기체를 사용하여 900°C에서 시행되었다. 성장이 완료된 CNT 전자방출원은 2극관, 3극관 형식으로 전계 방출을 측정하여 임계 전압과, 전류 밀도를 구했다.

### Keywords:

Carbon nanotube, Metal mesh substrate, PECVD, Field emitter

## Flexible and Ultrahigh Output Piezoelectric and Triboelectric Hybrid Nanogenerators based on ZnO Nanoflakes/Polydimethylsiloxane Composite Films

HE Wen<sup>2</sup>, 강대준\*<sup>1, 2</sup>

<sup>1</sup>성균관대학교 물리학과, <sup>2</sup>성균관대학교 기초과학연구소  
dj kang@skku.edu

### Abstract:

We demonstrate a flexible hybrid nanogenerator which integrates piezoelectric generator into triboelectric generator through a facile, cost-effective approach. The hybrid nanogenerator exhibited the strong producing peak-to-peak output voltage of  $\sim 470$  V, current density of  $\sim 60 \mu\text{A}\cdot\text{cm}^{-2}$ , and average power density of  $\sim 28.2 \text{ mW}\cdot\text{cm}^{-2}$ . These are the highest values when compared with those values reported in the literature on hybrid nanogenerators. The hybrid nanogenerators with an area of  $3\times 3 \text{ cm}^2$  instantaneously lit up 180 commercial green light-emitting diodes through periodic hand compression without additional energy storage devices. This excellent performance is an indicative of the high potential of the hybrid nanogenerator device for portable self-driven systems and energy harvesting of human motion for application in our daily life.

### Keywords:

Ultrahigh output, Flexible, Hybrid nanogenerator, ZnO NFs

## Charge Trapping Behavior in $\text{Al}_2\text{O}_3$ -Au Interlayer

이민백\*<sup>1</sup>, 박진홍<sup>1</sup>, 최문강<sup>1</sup>, 최진혁<sup>1</sup>  
<sup>1</sup>인하대학교 물리학과  
mlee@inha.ac.kr

### Abstract:

Recently, nonvolatile charge storage layer is widely used as for semiconductor gating structure such as flash memory device. A trapping layer and blocking layer in charge storage structure are mostly based on  $\text{SiN}_4$  and  $\text{Al}_2\text{O}_3$ ,  $\text{SiO}_2$  respectively. In addition, research for trapping layer using metallic nanoparticles has been reported. In here, we investigated electrical behavior of charge trapping device composed of Au nanocluster,  $\text{Al}_2\text{O}_3$  and silicon substrate. To make this device, we firstly deposited 10 nm of  $\text{Al}_2\text{O}_3$  on bare silicon wafer with atomic layer deposition method as a tunneling layer. Then Au cluster was formed on  $\text{Al}_2\text{O}_3$  using thermal evaporator as a charge trapping layer. Finally, we deposited 50 nm of  $\text{Al}_2\text{O}_3$  on Au charge trapping layer as a blocking oxide layer. Charge injection process were conducted with conductive atomic force microscopy. Trapped electrons were injected two different shape such as 0D and 1D. After electron was injected into trapping layer with 1D line shape by moving AFM tip with +8V bias, electric potential of surface was measured by Scanning Kelvin Probe Microscopy. It exhibited surface voltage of ~2.1 V in 24 mins. We also conducted 0D-shape process. In this case, it showed surface voltage of ~2.7 V in 24 mins. Analyzing remained charges over time, we found that trapped electrons are exponentially decayed. The Percent of remained charges were found to be inversely proportional to maximum voltage of initial charge injection.

### Keywords:

nanoparticle, Charge trap, Charge storage, Tunneling

## Thick accretion disk and its super Eddington luminosity around spinning black holes or neutron stars

장의철\*<sup>1</sup>

<sup>1</sup>충남대학교 우주지질학  
temiy7@gmail.com

### Abstract:

According to the disk accretion model theory of Shakura and Sunyayev (1973), accretion disk surrounding the spinning astronomical compact objects (BH, NS) consists of fluid rings obeying the Keplerian motions. Therefore, as we approach the center of spinning compact objects, angular momentum drops, but angular velocity and hence the dissipative heat and accretion rate grow.

As a result, the shape of the accretion disk “puffs up” (gets thicker) near the surface of the spinning compact objects.

We, therefore, explore the geometry of this thick inner portion of the accretion disk in the context of Mukhopadhyay’s pseudo Newtonian potential approximation for full General Theory of Relativity.

Particularly, we argue that super Eddington luminosity of dissipative heat develops at the innermost part of the accretion disk.

This, however, is not a disaster as it does not destroy anything (central spinning body or the accretion inflow).

But it is indeed an exciting high energy event in Astrophysics as it would illuminate the space pretty bright that can be seen from a distance !

### Keywords:

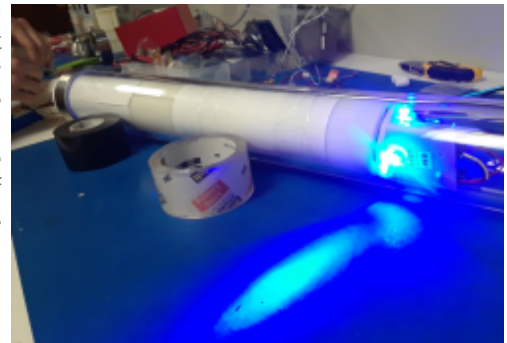
ACCRETION DISK

## SPIce Hole Camera to Measure Antartic Ice Properties at the IceCube Detector

CHOI Seokmin<sup>1</sup>, JEONG Minjin<sup>1</sup>, KANG Woosik<sup>1</sup>, KIM Jonghyun<sup>1</sup>, ROTT Carsten\*<sup>1</sup>, TOENNIS Christoph<sup>1</sup>  
<sup>1</sup>성균관대학교  
rott@skku.edu

### Abstract:

IceCube is a cubic-kilometer scale neutrino telescope located at the geographic south pole. The telescope utilises the extremely transparent Antarctic ice as a medium for detecting Cherenkov radiation produced by neutrino interactions in the detector volume. Recently the IceCube collaboration reported high impact scientific results including the observation of high energy astrophysical neutrinos as well as the measurement of multi-TeV neutrino cross-sections. From multiple years of IceCube data it was found that the light propagation in the detector is enhanced, when it is aligned with the direction of the Antarctic ice flow. This property is referred to as optical anisotropy. Understanding the anisotropy is expected to drastically reduce systematic uncertainties on light propagation in the ice. In this poster a self-contained camera system is presented, which will survey an ice-core hole near the IceCube detector down to a depth of 1.7km and measure the optical anisotropy of the ice.



### Keywords:

ice properties, CMOS cameras, IceCube Neutrino Telescope

## Effect of the radial motion of the background medium on the coronal loop oscillations

YU Dae Jung\*<sup>1</sup>, LEE Dong-Hun<sup>1</sup>

<sup>1</sup>School of Space Research, Kyung Hee University  
djyu79@gmail.com

### Abstract:

There are some observations on the contraction of the coronal loops and related loop oscillations. To understand this phenomenon, Russell et al. (2015) suggested magnetic energy loss as the cause. They also suggested a driven (forced) harmonic oscillator for the loop oscillation as a phenomenological model. But its connection to basic MHD equations are unclear. In this study, similarly but into other direction, we consider the effect of radial contraction or expansion of the loop on the loop oscillations. We assume a long straight cylindrical flux tube with a constant magnetic field in the longitudinal direction. The background medium is assumed to satisfy the equilibrium condition with time dependence. From these conditions, we derive an inhomogeneous differential equation for the loop oscillations which has the form of a driven harmonic oscillator as suggested by Russell et al. (2015) and by Nakariakov et al. (2016). By analyzing this equation we find that the background density motion may change the loop oscillations, resulting in damping or enhancing of the wave amplitude. It is also found that the motion of the background pressure plays the role of an external force to the loop oscillation, which can generate diverse loop oscillations including the illustrations in Russell et al. (2015).

### Keywords:

Ideal MHD, Coronal loop oscillations, Sun

## Combined search for dark matter in the Galactic center with ANTARES and IceCube

ROTT Carsten\*<sup>1</sup>, TOENNIS Christoph<sup>1</sup>

<sup>1</sup>성균관대학교  
rott@skku.edu

### Abstract:

To date the neutrino telescopes IceCube and ANTARES have been generating strong limits on the thermally averaged annihilation cross-section of WIMP dark matter in the galactic center, with ANTARES yielding the currently strongest limits at WIMP masses exceeding 30 TeV. At a WIMP mass range of 50 GeV to a few hundred GeV the current limits from IceCube surpass those of ANTARES. At this range there is a good opportunity for a combined analysis and thus achieving improved limits and sensitivities. In this talk a first combined search for dark matter in the galactic center using the data of both these experiments is presented. As a first step to a combined analysis using both detectors full datasets the 79-string data sample taken from 2010 to 2011 was used from IceCube, while from ANTARES the data sample collected from 2007 to 2015 was taken. The analysis considered dark matter particle masses between 50 and 200 GeV and a variety of different dark matter halo models and annihilation channels.

### Keywords:

ANTARES, IceCube, Dark Matter

## Some Characteristics of Earthquake Occurrence

나성호\*<sup>1</sup>, 정태웅<sup>2</sup>

<sup>1</sup>한국천문연구원 위성레이저관측소, <sup>2</sup>세종대학교  
sunghona@kasi.re.kr

### Abstract:

Large and small earthquakes occur in the Earth and cause damages and casualties. Chandler wobble is the free Eulerian nutation of the Earth in space. A great deal of efforts were given to 1) understand how earthquakes are made, and 2) predict their occurrences. Compared with the success in understanding tectonic movement associated with earthquakes, their prediction is still not feasible. So called the return period of earthquake of magnitude  $M$  is usually estimated from a simple relation:  $\text{Log}N = a - bM$ , but no direct information about their periodicity or triggering can be attained from the relation. We hereby report our recent finding about the existence of Chandler wobble periodicity in the global earthquake occurrence and 1-year periodicity in the historical Korean earthquakes. We also report other findings as well as our on-going investigations on the earthquake occurrence.

### Keywords:

Earthquake, Chandler wobble, 1-year periodicity

## Numerical study of hyperradiance by singlet-state atom pairs injected into a cavity

안경원\*<sup>1</sup>, HAN Junseok<sup>1</sup>, YANG Daeho<sup>1</sup>

<sup>1</sup>서울대학교 물리학과  
kwan@phya.snu.ac.kr

### Abstract:

In hyperradiance, the radiation from two atoms in a cavity gets much stronger than that of ordinary superradiance when the atoms are prepared in a singlet state and interact with the cavity with opposite phases. Subradiance usually occurs with atoms in a single entangled state. However, when the signs of the coupling constants are different in the presence of a pump laser, hyperradiance occurs instead of subradiance. In this study, we numerically examined the existence of hyperradiance in a more experimentally realizable situation, where pairs of atoms are continuously injected into a cavity with proper signs of coupling constants. We varied the relative magnitudes of the atom-cavity coupling constant, the cavity decay rate and the pump Rabi frequency and calculated the steady-state intracavity mean photon number. We compared the results with the superradiance case where the atoms are prepared in a triplet state and interact with cavity with the same phase. Our simulation results will be presented and discussed.

### Keywords:

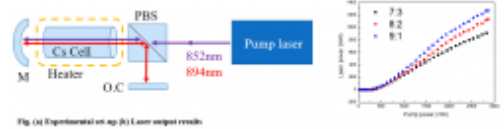
hyperradiance, superradiance, subradiance, singlet state, triplet state, atom-cavity interaction

## 다이오드 여기 Cs 원자 증기 레이저 및 공진기 최적화

오경환\*<sup>1</sup>, 홍성진<sup>1</sup>, 공병준<sup>1</sup>, 이용수<sup>1</sup>, 송상권<sup>1</sup>  
<sup>1</sup>연세대학교 물리학과  
koh@yonsei.ac.kr

### Abstract:

알칼리 금속 원자 증기는 95% 이상의 양자효율을 가져 현재 기술로 얻을 수 있는 광이득 매질 중 가장 높은 효율을 갖는다. 이를 통해 펌프광 대 출력광 전환효율을 향상시킬 수 있으며, 고출력 레이저를 위한 방법으로 활발히 연구가 진행되고 있다. 본 연구에서는 국내 최초로 Cs 증기를 광이득 매질로 이용한 알칼리 증기 레이저를 제작하였고, 출력 거울의 반사율에 따른 출력 향상을 통하여 1.2W의 연속광 최대 출력을 얻었다.



### Keywords:

Atomic gas laser, Laser material, Laser diode-pumped

## An empirical formula for full width at half-maximum in saturated absorption spectrum

MOON Geol<sup>1</sup>, NOH Heung-Ryoul<sup>\*1</sup>

<sup>1</sup>전남대학교 물리학과  
hrnoh@chonnam.ac.kr

### Abstract:

We present an analytical study of an empirical formula for the full width at half-maximum (FWHM) in saturated absorption spectroscopy for an atomic ensemble composed of two-level atoms. Considering the coherence term in the Doppler broadened limit, the FWHM is obtained in the lowest order in the probe Rabi frequency. We also study the dependence of FWHM on the transverse decay rate of the atoms.

### Keywords:

FWHM, two-level atoms, saturated absorption spectroscopy

## Study on decompositions of the EIA spectra at weak coupling beam for various polarization configurations

NOH Heung-Ryoul\*<sup>2</sup>, JADOON Zeeshan Ali Safdar<sup>1</sup>, KIM Jin-Tae\*<sup>1</sup>

<sup>1</sup>조선대학교 광기술공학과, <sup>2</sup>전남대학교 물리학과  
hrnoh@chonnam.ac.kr, kimjt@chosun.ac.kr

### Abstract:

We present a theoretical study of a lineshape in electromagnetically induced absorption (EIA) in  $^{85}\text{Rb}$  atoms. Accurate calculation of the lineshape is performed by solving the density matrix equations considering all the magnetic sublevels involved for the same and opposite polarization configurations of the coupling and probe beams. We decompose the spectra with respect to magnetic sublevels of the ground state and find that enhanced or decreased absorption signals for each component of the magnetic sublevels in the ground state depend on several factors such as the decay rates and transition strengths, which determine an overall absorption spectral profile.

### Keywords:

electromagnetically induced absorption, coherent population oscillation, transfer of coherence

## High Harmonic Generation Analysis Using Strong Field Approximation from One-dimensional Periodic Potential

변창우\*<sup>1</sup>, 이민호\*<sup>1</sup>, 최낙렬\*<sup>1</sup>

<sup>1</sup>금오공과대학교 물리학과

cwbyun@gmail.com, minho.lee.kr@gmail.com, nnchoi2001@gmail.com

### Abstract:

강한 레이저 장과 고체의 상호작용에서 발생하는 고차조화파발생(HHG)을 강한장근사(SFA)를 이용하여 설명하고자 한다. 먼저 기초적인 계산으로 1차원 등간격으로 나열된 구조에 적용한다. 기체 상태에서 HHG는 3단계 모델로 설명하고 있고, 이런 해석은 고체에 서도 똑같이 적용되는지 확인한다. 속도게이지를 사용한 기존의 방법과 달리 길이게이지를 이용한 방법이고, 기체의 경우에 적용되는 SFA를 그대로 고체에 적용하여 근사없이 계산된 양자역학적 결과와 일치여부를 확인한다. 더 나아가 비균질 전기장에서, 국소화된 초기 파동함수가 시간에 따라 변하는 모습을 관찰하기 위해 원자가띠에서는 국소화된 Wannier 함수, 전도띠에서는 주기함수인 Bloch 파동을 적용하여 해석한다.

### Keywords:

SFA in solids, three-step picture, HHG in solids, inhomogeneous fields, Wannier-Bloch basis

## Numerical evaluation of the localizable entanglement in 1D spin chain model

SON Wonmin\*<sup>1</sup>, [LEE Dongkeun](#)<sup>1, 2</sup>

<sup>1</sup>Department of Physics, Sogang University, <sup>2</sup>Research Institute for Basic Science, Sogang University  
sonwm@physics.org

### Abstract:

The Localizable entanglement(LE), suggested by Verstraete(2004), is a measure of multipartite entanglement which is into pairwise entanglement between two spins. The property of the LE is that the tightly lower bound of the LE measured by the concurrence is the maximal correlation function between two parties, which implies that LE can detect the many-body physics more subtly than the maximal correlation function does. Generally speaking, it is non-trivial to calculate LE numerically due to the difficulty for the optimal choices of measurement bases. Here, a new approach is proposed to overcome a limited number of parties and a exponential number of measurement outcomes.

### Keywords:

Localizable Entanglement, concurrence, optimization problem

## Prevention of purple plague formation on Au-coated Al electrodes of ion trap chips during chamber baking process by adjusting Ti interlayer thickness

JEONG Junho<sup>1</sup>, JUNG Chanhyun<sup>1</sup>, HONG Seokjun<sup>1</sup>, LEE Minjae<sup>1</sup>, PARK Yunjae<sup>1</sup>, KWON Yeong-Dae<sup>2</sup>,  
KIM Taehyun<sup>2</sup>, CHO Dong-il "Dan"\*<sup>1</sup>

<sup>1</sup>Seoul National University, ASRI/ISRC and Department of Electrical and Computer Engineering, <sup>2</sup>SK Telecom Quantum Tech. Lab.  
dicho@snu.ac.kr

### Abstract:

The method of coating Au on Al is widely used in order to prevent surface oxidation of Al electrodes when fabricating ion trap chips. However, when contacted Al and Au parts are heated, they form an alloy called the purple plague. The purple plague lowers the electrical conductivity of the electrode and increases the roughness of the electrode surface. To prevent the formation of purple plagues, methods of stacking another metal layer as a diffusion barrier layer between Al and Au layers and avoiding high temperature processes are typically used. However, since ion trap experiments are implemented in an ultra-high vacuum (UHV) environment, the vacuum chamber baking process to remove the moisture in the chamber is necessary. While the chamber baking process lasts over 100 hours at 200°C, purple plagues can form even if a diffusion barrier layer exists. To avoid this, the thickness of the diffusion barrier layer needs to be increased. The thickness of the diffusion barrier layer should be carefully chosen since the diffusion barrier layer can lose its adhesion strength to Au layer if it is too thick. This paper presents a method to suppress the generation of the purple plague on the Au-coated Al electrodes of ion trap chips by adjusting the thickness of a Ti layer between the Au and Al layers. By using this method, purple plague can be prevented in the process of chamber baking at 200°C for more than 20 days, which is sufficiently long to achieve the required vacuum pressure for ion trapping.

### Acknowledgement:

This work was partly supported by SK Telecom and the ITRC (Information Technology Research Center) support program of MSIT/IITP [IITP-2018-2015-0-00385].

### Keywords:

Ion trap, quantum information, microfabrication, purple plague.

## Fabrication of Akali Atom Vapor Cell for Atom Spin Gyroscope

김태현\*<sup>1</sup>, 임신혁<sup>1</sup>, 이상경<sup>1</sup>, 김재일<sup>1</sup>, 심규민<sup>1</sup>, 이성의<sup>2</sup>, 권택용<sup>3</sup>  
<sup>1</sup>국방과학연구소 국방고등기술원, <sup>2</sup>한국산업기술대학교, <sup>3</sup>표준과학연구원  
taehyunkim@add.re.kr

### Abstract:

This abstract presents fabrication method to manufacture akali atom vapor cells for use in compact atomic devices such as atom spin gyroscope or magnetometers. The technology is based on glass blowing and laser bonding adhesive powder and glass. Especially, it is relatively inexpensive and easy to apply in the laboratory using glass blow technology. To confirm the purity of Rb in the fabricated glass blown cell, the same saturated absorption spectroscopic spectrum of Rb as commercial reference cell was obtained.

### Keywords:

NMR gyro, Vapor cell

## Open loop atomic gyroscope based on the nuclear spin-precession of Xe

이상경\*<sup>1</sup>, 김태현<sup>1</sup>, 임신혁<sup>1</sup>, 김재일<sup>1</sup>, 심규민<sup>1</sup>

<sup>1</sup>국방과학연구소 국방고등기술원  
sklee82@add.re.kr

### Abstract:

We have developed an atom spin gyroscope based on the precession of the nuclear spin of Xe atoms. The noble gas Xe atoms are spin-polarized by spin exchange collisions with optically pumped rubidium atoms. The small transverse AC magnetic field induces the precession of Xe nuclear spin. The absorption mode and the dispersion mode of the Xe nuclear spin precession were resolved with the help of lock-in-technique. By fixing the frequency of the transverse magnetic field to the steepest slope of the dispersion mode we obtained the open-loop rotation response of our atomic spin gyroscope. Also the angular random walk (ARW) were measured at  $18.2 \text{ deg/hr}^{1/2}$ , which is mainly limited by the short T2 time due to gas impurities in the atomic vapor cell.

### Keywords:

Atom spin gyroscope, NMR gyro, Spin exchange optical pumping

# Observation of Single Ion Quantum Tunneling in Optical Lattice

전흥기<sup>1, 2</sup>, COUNTS Ian<sup>2</sup>, HUR Joonseok<sup>2</sup>, VULETIĆ Vladan<sup>2</sup>, 제원호\*<sup>1</sup>

<sup>1</sup>Department of Physics & Astronomy, Seoul National University, Seoul 08826, Republic of Korea, <sup>2</sup>  
Department of Physics, MIT-Harvard Center for Ultracold Atoms, and Research Laboratory of  
Electronics, Massachusetts Institute of Technology, Cambridge, Massachusetts 02139, USA  
whjhe@phy.snu.ac.kr

## Abstract:

Quantum tunneling is a unique quantum phenomenon without a classical counterpart. Nevertheless, it is behind many natural processes, from nuclear fusion in stars [1] to friction in nanoscale [2]. Tunneling in position space has been observed in many different cold atom systems such as BECs [3] and single neutral atoms [4]. However, to our knowledge position space tunneling in trapped ions has not been observed so far, despite the system's recent popularity in quantum information research.

Here, we present preliminary results for quantum tunneling in an ion trap. In this experiment, we used an optical lattice together with an ion trap. By tuning the intensity of the optical lattice and the relative position of the electrostatic potential to the lattice, we realized various Prandtl-Thomlinson potentials including a double well potential. The position of the ion was measured using position dependent fluorescence. This presentation includes results from two different approaches: Rabi oscillation of population in a double well, and adiabatic transfer of population in a changing potential.

## References

- [1] F. Trixler, *Curr. Org. Chem.* 17, 1758 (2013)
- [2] T. Zanca, F. Pellegrini et al., and E. Tosatti *arXiv:1708.03362* (2017).
- [3] P. Preiss, R. Ma et al., and M. Greiner *Science*. 13, 347 (2015).
- [4] A. M. Kaufman, B. J. Lester et al., and C. A. Regal *Science*. 18, 345 (2014).

## Keywords:

Quantum physics, Atomic physics, Trapped ion, Paul trap, Optical lattice, Friction

## Toward a large and oblate $^{87}\text{Rb}$ Bose-Einstein condensate

신용일\*<sup>1, 2</sup>, 구준홍<sup>1, 2</sup>, 임영훈<sup>1, 2</sup>

<sup>1</sup>Center for Correlated Electron Systems, Institute for Basic Science, Seoul 08826, Korea, <sup>2</sup>Department of Physics&Astronomy, Seoul National University, Seoul 08826, Korea  
yishin@snu.ac.kr

### Abstract:

Regular vortex shedding and its transition to turbulent flow behind a moving obstacle represent a universal characteristic of classical fluid dynamics. A superfluid, which has no viscosity, is expected to show similar universal behavior in the wake response to a moving obstacle and a recent experiment reports the regular vortex cluster shedding and its transition to turbulence in a Bose-Einstein condensate (BEC) [1]. To test the universality of vortex shedding dynamics in the superfluid qualitatively, a large, stable and homogeneous condensate is required to allow multiple events of vortex shedding. Here, we present a  $^{87}\text{Rb}$  BEC machine to achieve the testbed mentioned above.  $3 \times 10^9$  atoms are loaded into a 3D magneto-optical trap (MOT) and transferred to the magnetic trap. Optical plugging of a blue-detuned laser to prevent atom loss by Majorana spin flips is performed during rf evaporative cooling. We also discuss a clipped focused-Gaussian beam as a method for generating a homogeneous condensate.

[1] Woo Jin Kwon, Joon Hyun Kim, Sang Won Seo and Yong-il Shin, Phys. Rev. Lett. 117, 245301 (2016)

### Keywords:

Bose-Einstein condensate, vortex shedding, superfluid, turbulence, clipped focused-Gaussian beam

## Towards Bose-Einstein condensates of lithium-7 atoms

최재윤\*<sup>1</sup>, 김경태<sup>1</sup>, 허승정<sup>1</sup>  
<sup>1</sup>한국과학기술원 물리학과  
choijy1204@naver.com

### Abstract:

Non-equilibrium many-body quantum phenomena have been a central theme in modern statistical physics, hosting a new phase of matter that cannot exist in thermal equilibrium. Ultracold atomic system is an ideal test bed for studying non-equilibrium physics because of its high level of isolation from its environment and wide tuning range of physical parameters. The lithium-7 atom is the lightest alkali atom and has strong ferromagnetic spin interaction, providing a new opportunity to explore universal behavior in non-equilibrium quantum phenomena. In this poster, we will introduce a brand new experimental apparatus for generating lithium-7 Bose-Einstein condensates (BEC). A zero-crossing Zeeman slower is adapted to have sufficient atomic flux in the main chamber, and we will implement a sub-Doppler cooling (gray molasses) technique before loading the atoms in a magnetic trap. Moreover, cold atoms can be transported into the science cell, where a single atom in an optical lattice can be imaged using a high resolution imaging system.

### Keywords:

Bose-Einstein condensates, Non-equilibrium physics

## Metastable polar state of a spin-1 antiferromagnetic Bose-Einstein condensate under a magnetic field gradient

신용일\*<sup>1, 2</sup>, 김준현<sup>1</sup>, 강세지<sup>1</sup>, 홍덕화<sup>1, 2</sup>

<sup>1</sup>Department of Physics and Astronomy, and Institute of Applied Physics, Seoul National University,

<sup>2</sup>Center for Correlated Electron Systems, Institute for Basic Science  
yishin@snu.ac.kr

### Abstract:

We present our observation of the metastable polar state in a spin-1 antiferromagnetic spinor Bose-Einstein condensate (BEC) in the presence of magnetic field gradient. For negative quadratic Zeeman energy  $q$ , the BEC in an easy-axis polar (EAP) state would undergo a quench evolution into an easy-plane polar (EPP) state via spin-exchange collision because the EPP state is energetically preferred in this system. Under a magnetic field gradient, however, we have observed the metastable regime down to a certain negative  $q$  value in which the condensate initially prepared in the EAP state does not dynamically evolve into the EPP state. We measure the threshold  $q$  value for the metastable EAP state as a function of the magnitude of field gradient, and it is also found that the finite size of the sample intensifies the metastable state. The physical origin of the metastability in the antiferromagnetic spinor condensate will be discussed.

### Keywords:

Quantum gases, Bose-Einstein condensates, Quantum phase transitions, Metastability

## Asymmetric Josephson effect in bulk $WTe_2$ Weyl semimetal Josephson Junction

최용빈\*<sup>1</sup>, CHEN Chui-Zhen<sup>2</sup>, RANA Gaurav<sup>3</sup>, ALI Mazhar<sup>3</sup>, LAW K.T.<sup>2</sup>, FONG K.C.<sup>4</sup>, 이후종<sup>1</sup>, 이길호\*<sup>1</sup>

<sup>1</sup>Department of Physics, POSTECH, <sup>2</sup>Department of Physics, Hong Kong University of Science and Technology, <sup>3</sup>Max Plank Institute for Microstructure Physics, <sup>4</sup>Raytheon BBN Technologies, Quantum Information Processing Group  
ybchoi@postech.ac.kr, lghman@postech.ac.kr

### Abstract:

$WTe_2$  is predicted to host Weyl nodes at the contact of electron and hole pockets in a momentum space (Type-II Weyl semimetal) and exhibit novel transport properties. We fabricated proximity Josephson junctions based on mechanically exfoliated  $WTe_2$  layers and studied their Josephson effects via quantum transport measurements at low temperature. Josephson critical current modulation as a function of perpendicular magnetic field,  $I_c(B)$ , (so-called Fraunhofer pattern) exhibited anomalous behaviors. Slow decay of  $I_c$  maxima at each lobe as  $B$  increases indicates edge-dominated transport through  $WTe_2$  layer. Moreover, asymmetric Fraunhofer pattern, i.e.  $I_c(B) \neq I_c(-B)$ , was observed, that can be explained by the different Fermi velocities of edge channels due to the inversion symmetry breaking of  $WTe_2$ .

### Keywords:

Weyl semimetal,  $WTe_2$ , Fraunhofer Pattern, Proximity Josephson junction

## Superconducting quantum interference device of (Bi<sub>0.84</sub>Sb<sub>0.16</sub>)<sub>2</sub>Se<sub>3</sub> topological insulator nanoribbons

도용주\*<sup>1</sup>, 김남희<sup>1</sup>, 김홍석<sup>1</sup>, YANG Yiming<sup>2</sup>, PENG Xingyue<sup>2</sup>, YU Dong<sup>2</sup>  
<sup>1</sup>광주과학기술원 물리광학과, <sup>2</sup>University of California, Department of Physics  
yjdo@gist.ac.kr

### Abstract:

Topological insulators(TIs) with topologically protected surface states are fascinating materials for detecting the Majorana fermion when coupled with a superconductor. Since the Majorana fermion has charge neutrality and zero energy, the superconducting quantum interference devices(SQUIDs) are received attention. The SQUID is very sensitive to a magnetic flux, so it plays a crucial role for a superconducting flux qubit. Here, we report the fabrication and measurement of SQUIDs, made of (Bi<sub>0.84</sub>Sb<sub>0.16</sub>)<sub>2</sub>Se<sub>3</sub> TI nanoribbons(NRs) connected with Pb<sub>0.5</sub>In<sub>0.5</sub> superconducting electrodes. A TI NR is transferred onto a SiO<sub>2</sub>/Si while the Pb<sub>0.5</sub>In<sub>0.5</sub> electrodes are deposited using electron-beam lithography and electron-beam deposition techniques. Below the transition temperature of the superconducting Pb<sub>0.5</sub>In<sub>0.5</sub> electrodes, periodic oscillations of the critical current are observed in the TI NR SQUID with a magnetic field applied perpendicular to the plane due to the flux quantization. Moreover, the envelope of the voltage modulation of the SQUID shows Fraunhofer-like patterns of each single junction. We also measure the Aharonov-Bohm oscillations under a magnetic field along the topological surface state of the NR.

### Keywords:

Topological insulator, Josephson junction, superconducting quantum interference device, supercurrent

## Comparison of hysteresis losses of striated GdBCO coated conductors using the maskless photolithography with a UV laser

이형철\*<sup>1</sup>, 김무용<sup>1</sup>, 공희정<sup>1</sup>, 김영경<sup>1</sup>, 여준엽<sup>1</sup>

<sup>1</sup>경북대학교 물리학과  
hcri@knu.ac.kr

### Abstract:

For 2G HTC coated conductor applications, it is important to reduce the AC loss. Therefore, it is necessary to study the analysis of magnetic hysteresis loss of superconductor for various situations. The hysteresis loss of superconductors is generally understood by the critical state model. However, since the calculation becomes complicated under the condition of the dependence of the critical current in the external magnetic field and various structures, the related experiment needs to be preceded in order to prove whether the correct solution is obtained. We used GdBCO samples etched with various patterns using maskless photolithography. Typically, photolithography uses masks, but in experimental situations it is a one-time mask when making samples for various geometric models. Therefore, we used maskless photolithography to scan the UV laser to the desired structure using a telecentric lens for efficient operation. The samples were compared by hysteresis losses using MPMS.

### Keywords:

GdBCO, MPMS, hysteresis loss, multifilamentary, telecentric lens

## Optical properties for superconducting parent compound $\text{Ca}_{10}(\text{Pt}_4\text{As}_8)(\text{Fe}_{10}\text{As}_{10})$ single crystal.

선유일<sup>1</sup>, 최우재<sup>1</sup>, KIMURA Shin-ichi<sup>2</sup>, 권용성\*<sup>1</sup>

<sup>1</sup>DGIST, 신물질과학전공, <sup>2</sup>Osaka University, FBS and Department of Physics  
yskwon@dgist.ac.kr

### Abstract:

We have measured the reflectivity of the parent compound  $\text{Ca}_{10}(\text{Pt}_4\text{As}_8)(\text{Fe}_{10}\text{As}_{10})$  single crystal ( $T_c = 34.6$  K) over the broad frequency range from  $20 \text{ cm}^{-1}$  to  $12000 \text{ cm}^{-1}$  and for temperatures from 8 K to 300 K. The optical conductivity spectra of the low frequency region ( $< 1000 \text{ cm}^{-1}$ ) in the normal state ( $38 \text{ K} \leq T \leq 300 \text{ K}$ ) is well fitted with two Drude forms, which indicates the presence of multiple bands at the Fermi level. When the superconducting state in 8 K, the real part optical conductivity  $\sigma_1(\omega)$  was not completely suppressed. This indicates that the superconducting gap of this compound is not completely observed. We use the generalized Mattis-Bardeen formula for the two-band superconductor to fit the 8 K data of  $\sigma_1(\omega)$ . Through superconducting gap fitting, we concluded that only one drude band forms a superconducting gap. The extracted SC gap size is  $\Delta = 3.2 \text{ meV}$  and the scattering rate  $1/\tau = 44.6 \text{ meV}$ , suggesting  $\text{Ca}_{10}(\text{Pt}_4\text{As}_8)(\text{Fe}_{10}\text{As}_{10})$  as a single-gap superconductor.

### Keywords:

Superconductivity, Optical spectroscopy, superconducting gap

## Thermally activated flux flow in pristine and proton-irradiated $\text{Ca}_{8.5}\text{La}_{1.5}(\text{Pt}_3\text{As}_8)(\text{Fe}_2\text{As}_2)_5$ single crystals

최우재<sup>1</sup>, 서유일<sup>1</sup>, AHMAD Dawood<sup>1, 2</sup>, 권용성\*<sup>1</sup>  
<sup>1</sup>대구경북과학기술원 신물질과학전공, <sup>2</sup>울산과학기술원 물리학과  
yskwon@dgist.ac.kr

### Abstract:

We investigate the influence of the proton irradiation on the thermally activation flux flow (TAFF) on the mixed state in  $\text{Ca}_{8.5}\text{La}_{1.5}(\text{Pt}_3\text{As}_8)(\text{Fe}_2\text{As}_2)$  single crystals using the magnetoresistivity in magnetic fields up to 13T for B//c-axis and B//ab-plane. We found that the effect of thermally activated flux flow is well described by the nonlinear temperature-dependent activation energy in both pristine and proton irradiated sample. The magnetic field dependence of the activation energy follows a power law of  $U_0(B) \sim B^{-\alpha}$  where the exponent  $\alpha$  is changed from crossover field of around 3T, indicating that the strength of vortex pinning is weaker as a result of proton irradiation. We suggest that the pristine and proton irradiated sample dominate 2D vortex phase in the TAFF region.

### Keywords:

Iron-based superconductor, Vortex dynamics, TAFF analysis

## Electronic Investigation on CDW phase of EuBiTe<sub>3</sub>

YOO Jonggyu<sup>1, 2</sup>, KIM Jeongkyu<sup>1, 2</sup>, 고경태\*<sup>1, 2</sup>, KIM Heejung<sup>2</sup>, KIM Kyoo<sup>1, 2</sup>, MIN Byungil<sup>2</sup>, SHON Wonhyuk<sup>3</sup>, RHYEE Jong-soo<sup>3</sup>, PARK Jaehoon\*<sup>1, 2</sup>

<sup>1</sup>Max Planck POSTECH/Hsinchu Center for Complex Phase Materials, <sup>2</sup>Department of Physics, POSTECH, <sup>3</sup>Department of Applied Physics, Kyung Hee University  
dreamboy78@gmail.com, jhp@postech.ac.kr

### Abstract:

CDW is an interesting subject in physics, of which the fundamental mechanism has been investigated based on the electron-phonon interaction. EuBiTe<sub>3</sub> is newly synthesized CDW material where a CDW phase ( $q \sim 1/3b^*$ ) is observed in an electron diffraction measurement at room temperature [1]. In this study, we performed XRD and ARPES measurement to investigate the electronic structure. A bulk CDW peak ( $q \sim 1/3b^*$ ) is observed in XRD measurement and the CDW phase sustains up to 600 K. ARPES measurements reveal a 2D electronic structure in which parallel Fermi surfaces give rise to the strong nesting instability. In addition, the CDW gap exhibits a spatial distribution and the gap size is around 60 meV at the Brillouin zone boundary along  $\Gamma$ -Y direction while the spectral weight is suppressed more near the  $\Gamma$  cut. A following ab-initio analysis confirms the measured electronic structure and shows that a strong phonon softening near  $q \sim 1/3b^*$  drives high temperature CDW phase.

[1] Niu, Y. Y., Wu, D., Shen, L. and Wang, B. (2015), A layered antiferromagnetic semiconductor EuMTe<sub>3</sub> (M = Bi, Sb). Phys. Status Solidi RRL, 9: 735-739. doi:10.1002/pssr.201510344

### Keywords:

Charge density wave, EuBiTe<sub>3</sub>,

## Temperature-dependent optical properties of Fe-pnictide superconductor, $\text{Sr}_2\text{VO}_3\text{FeAs}$

황정식\*<sup>1</sup>, 이석배<sup>1</sup>, 노슬기<sup>1</sup>, 이명훈<sup>1</sup>, 서유성<sup>1</sup>, 옥종목<sup>2</sup>, 김준성<sup>2</sup>, 정명철<sup>3</sup>, 이관우<sup>3</sup>  
<sup>1</sup>성균관대학교 물리학과, <sup>2</sup>포항공과대학교 물리학과, <sup>3</sup>고려대학교 디스플레이-반도체 물리학과  
jungseek@skku.edu

### Abstract:

We performed infrared spectroscopic study on a single crystal of  $\text{Sr}_2\text{VO}_3\text{FeAs}$  grown by a self-flux method. This layered material system consists of two alternative layers of  $\text{Sr}_2\text{VO}_3$  and FeAs. Since the typical size of single crystalline  $\text{Sr}_2\text{VO}_3\text{FeAs}$  samples is  $200 \times 200 \times 10 \mu\text{m}^3$ , optical study on this material is challenging. We could measure reflectance spectra of *ab*-plane at various temperatures from 8 K to 300 K using an *in-situ* gold evaporation technique in far- and mid-infrared regions. This material shows dc resistivity and magnetic susceptibility anomalies near 155 K. We observed that a Fano-shaped phonon appears below 200 K and shows a strong blue-shift with lowering the temperature. We also observed an additional interband transition around  $1,000 \text{ cm}^{-1}$ , which is absent in other doped Ba-122 Fe-pnictides. We will discuss about further issues on this material.

### Keywords:

$\text{Sr}_2\text{VO}_3\text{FeAs}$ , FTIR, Fe pnictides

## Bose-glass state in superconducting $\text{La}_{1.85}\text{Sr}_{0.15}\text{CuO}_4$ thin films

양찬호\*<sup>1</sup>, 장한별<sup>1</sup>, 임지수<sup>1</sup>

<sup>1</sup>한국과학기술원 물리학과  
chyang@kaist.ac.kr

### Abstract:

For many years, the origin of thickness induced superconductor-to-insulator transition (SIT) in  $\text{La}_{2-x}\text{Sr}_x\text{CuO}_4$  thin films has remained elusive. Here, we make concrete discussion about thickness dependent SIT in  $\text{La}_{1.85}\text{Sr}_{0.15}\text{CuO}_4$  thin films on  $\text{LaAlO}_3$  substrate. Electronic transport measurement exhibits clear SIT with a critical thickness  $t_c = 15$  nm and variation of superconducting  $T_c$  with increasing film thickness. Feature of resistance peak and value of sheet resistance near  $t_c$  are the characteristics of the Bose-glass model [1]. X-ray diffraction and reciprocal space map reveal negligible structural changes including consistent in-plane strain and  $c$ -axis lattice parameter within measurement limit regardless of film thickness variation. Atomic resolution image obtained by transmission electron microscope suggests minimized structural defects and chemical impurities. X-ray photoemission spectroscopy exhibits thickness-dependent binding energy from Cu  $2p_{3/2}$  and O  $1s$  core level spectra. To gain more insight into the superconducting state, finite-size scaling is performed by magnetic field-tuned SIT. Obtained critical sheet resistance  $R_c = 6.10k\Omega$  and critical exponent  $z\nu = 1.5$  strongly support a Bose-glass state in the  $\text{La}_{1.85}\text{Sr}_{0.15}\text{CuO}_4$  thin films [2].

### References

- [1] Phys. Rev. Lett. **110**, 077001 (2013)
- [2] Nature **472**, 458 (2011)

### Keywords:

Superconductivity, QPT

## Role of anion in ZrSiX (X = S, S<sub>0.5</sub>Se<sub>0.5</sub>)

고경태\*<sup>1, 2</sup>, KIM JeongKyu<sup>1, 2</sup>, YOO JongGyu<sup>1, 2</sup>, WON ChungJae<sup>1, 4</sup>, PARK ByungGyu<sup>3</sup>, PARK JaeHoon\*<sup>1, 2</sup>

<sup>1</sup>Max Planck POSTECH/Hsinchu Center for Complex Phase Materials, <sup>2</sup>Department of Physics, Postech, <sup>3</sup>POHANG ACCELERATOR LABORATORY, <sup>4</sup>Lab of Pohang Emergent Materials  
dreamboy78@gmail.com, jhp@postech.ac.kr

### Abstract:

Topological Dirac semimetal is a material which contains symmetry driven Dirac nodes. It is known that a non-symmorphic symmetry operation makes a certain band crossing [1]. Recently, ZrSiS is enthusiastically studied because it exhibits 3D-Dirac nodal lines near the Fermi level as proposed by Young and Kane [1]. Although there are many reports of those band structures and the origin and structure of the surface states [2, 3, 4, 5], the role of anion is barely discussed. In this study, we measured newly synthesized ZrSiS<sub>0.5</sub>Se<sub>0.5</sub> as well as ZrSiS in order to clarify the effect anion and site mixing. Based on the ARPES results, we are discussing the band structure of new samples ZrSiS<sub>0.5</sub>Se<sub>0.5</sub> and the overall effect induced by replacing S to Se.

[1] Young and Kane, Phys. Rev. Lett. **115**, 126803 (2015)

[2] Leslie M. Schoop, Mazhar N. Ali and Carola Straber et al., Nat. Comm. **7**, (2016). DOI:10.1038/ncomms11696

[3] M. Mofazzel Hosen et al., Phys. Rev. B. **95**, 1161101 (2017)

[4] B. Fu, C. Yi, T. Zhang, M. Caputo and J. Ma, X. Gao et al., ArXiv e-prints (2017), arXiv:1712.00782 [cond-mat.mtrl-sci].

[5] Andreas Topp, Raquel Queiroz and Andreas Grüneis et al., Phys. Rev. X **7**, 041073 (2017)

### Keywords:

Topological Dirac nodal line semimetal, ZrSiS

## Magnetization of GdBCO coated conductors with various geometries of weak-link

이형철\*<sup>1</sup>, 김영경<sup>1</sup>, 최혜란<sup>1</sup>, 전성민<sup>1</sup>, 김무용<sup>1</sup>, 박희연<sup>1</sup>, 박상국<sup>1</sup>  
<sup>1</sup>경북대학교 물리학과  
hcri@knu.ac.kr

### Abstract:

The weak-link can occur when manufacturing an electric transmission cable composed of superconductors such as electrical contact point. In this study, we summarized magnetization of GdBCO coated conductors in the applied magnetic field by using Magnetic Property Measurement System (MPMS) for various geometries of specimens which have different number of weak-link respectively. We patterned specimens by maskless photolithography with a UV laser. We investigated tendency of the magnetization by the geometry of specimens. Especially, we focused on number of weak-link.

### Keywords:

GdBCO superconducting film MPMS Magnetization hysteresis weak-link

## The synthetic s-wave /p-wave superconducting oxide heterojunction by using Pulsed Laser Deposition

김진권<sup>1, 2</sup>, 이한결<sup>1, 2</sup>, 김봉주<sup>1, 2</sup>, 장서형<sup>3</sup>, 노태원\*<sup>1, 2</sup>

<sup>1</sup>Center for Correlated Electron Systems, Institute for Basic Science (IBS CCES), <sup>2</sup>Department of Physics and Astronomy, Seoul National University, <sup>3</sup>Department of Physics, Chung-Ang University  
twnoh@snu.ac.kr

### Abstract:

The interfacial coupling of s-wave spin singlet superconductor (SSC) and p-wave spin triplet superconductor (TSC) can provide a variety of intriguing physics related to proximity effect of orbital parity. R. Jin *et al.* fabricated Pb/Sr<sub>2</sub>RuO<sub>4</sub>/Pb Josephson junction and discovered irregular behavior of the critical Josephson current. This behavior is originated from the mixture of p-wave cooper pairs in Sr<sub>2</sub>RuO<sub>4</sub> and s-wave cooper pairs in Pb [1]. However, this intrinsic s-wave / p-wave cooper pair proximity effect can be disturbed by the complicated atomic structures at Pb/Sr<sub>2</sub>RuO<sub>4</sub> interface, such as oxide insulating layers or metallic Ru lamellae. Hence, improving the interfacial quality of the Josephson junction is crucial to get deeper understanding of the interfacial coupling of SSC and TSC.

Here, we proposed a new design of SSC/TSC junction, BaPb<sub>1-x</sub>Bi<sub>x</sub>O<sub>3</sub>/Sr<sub>2</sub>RuO<sub>4</sub> bilayer heterostructure. BaPb<sub>1-x</sub>Bi<sub>x</sub>O<sub>3</sub> (BPBO) is oxide s-wave superconductor with optimal  $T_c = 12$  K. This all-oxide junction is expected to show a atomically sharp interface and thus good device performance. To realize this heterojunction, we deposited BPBO thin films on cleaved Sr<sub>2</sub>RuO<sub>4</sub> single crystal substrates by pulsed laser deposition technique. The epitaxial quality is confirmed by X-ray diffraction and atomic force microscopy. At last, we show the *I-V* behaviors of the BPBO/Sr<sub>2</sub>RuO<sub>4</sub>/BPBO junctions and explain the underlying mechanism.

[1] R. Jin *et al.*, Phys. Rev. B, **59**, 4433 (1999).

[2] T. Nakamura *et al.*, Phys. Rev. B, **84**, 060512 (2011).

### Keywords:

Unconventional superconductivity, p-wave superconductivity, Josephson junction, Pulsed laser deposition

## The control of dissipation of skyrmion by changing radius and domain-wall width.

TAMURA Eiiti<sup>1</sup>, CHO Jaehun<sup>\*1</sup>, NISHIDE Takuya<sup>1</sup>, SUZUKI Yoshishige<sup>1</sup>

<sup>1</sup>Graduate School of Engineering Science, Osaka University, Toyonaka, Osaka, Japan  
11992443@naver.com

### Abstract:

Skyrmions are topologically protected spin textures which often originated from asymmetric exchange coupling as known Dzyaloshinskii-Moriya interaction(DMI)[1]. Recently, it has been attracted due to the possibility of the skyrmion based information devices and information storage units[2]. The motion of the skyrmion on two-dimensional film can be described by a modified version of Newton's equation. For sufficient slowly varying and not too strong forces, a symmetry analysis suggests the following equation [3]:

$$\mathbf{g} \times \dot{\mathbf{R}} + \alpha D \dot{\mathbf{R}} = \mathbf{F} \quad (1)$$

Here,  $\mathbf{R}$  is the center coordination of skyrmion,  $\mathbf{g}$  is the gyrocoupling vector with the winding number of the skyrmion  $m$ , independent of microscopic details.  $\alpha$  is the Gilbert damping constant,  $D$  the dissipation dyadic and  $\mathbf{F}$  the external force e.g. by electric currents, magnetic field gradients, and thermal fluctuations. In this study, we investigate the skyrmion dynamics under external forces such as gradient magnetic field using micromagnetic simulations.

The component of dissipation dyadic,  $D_{xx}$  and  $D_{yy}$  can be express as follow [4]

$$D_{xx} = D_{yy} = \frac{2\pi M_s}{\gamma} f(x) = \frac{2\pi M_s}{\gamma} [f_1(x) + m^2 f_2(x)] \quad (2)$$
$$f_1 = \int_0^\infty \frac{2t \sinh^2(x) \cosh^2(t)}{[\sinh^2(x) + \sinh^2(t)]^2} dt, \quad f_2 = \int_0^\infty \frac{2 \sinh^2(x) \sinh^2(t)}{t[\sinh^2(x) + \sinh^2(t)]^2} dt$$

here,  $M_s$  is the saturation magnetization,  $\gamma$  the gyromagnetic ratio,  $x$  the ratio of skyrmion radius ( $r$ ) to domain-wall width ( $w$ ). Figure 1 (a) shows the  $f(x)$  as a function of ratio of skyrmion radius and domain-wall width when  $m = 1$  case. The micromagnetic simulations were performed using the Mumax<sup>3</sup> code [5] to investigate the relation with  $f(x)$  and the shape of skyrmions. We selected a nanowire shape of 1000 nm  $\times$  100 nm  $\times$  1.2 nm in dimensions with a cell size 2  $\times$  2  $\times$  2 nm<sup>3</sup> at the zero temperature. We selected two independent skyrmions to investigate their dynamics. The perpendicular magnetic anisotropy of two skyrmions ( $S_{kx}$  I and  $S_{kx}$  II) are 0.8 and 1.1 MJ/m<sup>3</sup>, exchange stiffness constant 15 and 12 pJ/m, interfacial DMI energy densities 3.5 and 4.0 mJ/m<sup>2</sup>, respectively. The saturation magnetization of both skyrmions is 580 kA/m,  $a$  is 0.3. Fig 1 (b) shows  $m_z$  of two skyrmions which have different ratios of radius to width. Our setup of the simulation is following. We set the initial skyrmion in the center of the nanowire. And then 300 nsec later, we save the spin configuration to determine skyrmion displacement. We verify the theoretical argument given equation (2), in view of simulation results.

We are grateful to H. Nomura and M. Goto for their kind help in first stage of this research. This research and development work was supported by the Ministry of Internal Affairs and Communications. JC thanks JSPS Research Fellowship program (No. P16362).

- [1] I. Dzyaloshinsky, J. Phys. Chem. Solids **4**, 241 (1958). T. Moriya, Phys. Rev. **120**, 91 (1960).  
[2] J. Sampaio, *et al.*, Nat. Nanotech. **8**, 839 (2013).  
[3] A. A. Thiele, Phys. Rev. Lett. **30**, 230 (1973).  
[4] X. S. Wang, arXiv:1801.01745 (2018). A. Hrabec, *et al.*, Nat. Commun. **8**, 15765 (2017).  
[5] A. Vansteenkiste, *et al.*, AIP Advances **4**, 107133 (2014).

**Keywords:**

Skyrmion, micromagnetic simulations



## Correlation between Magnetic Properties and Depinning Field in Field-Driven Domain Wall Dynamics in GdFeCo Ferrimagnets

NISHIMURA Tomoe<sup>1</sup>, KIM Duck-Ho\*<sup>1</sup>, HIRATA Yuushou<sup>1</sup>, OKUNO Takaya<sup>1</sup>, FUTAKAWA Yasuhiro<sup>2</sup>, TSUKAMOTO Arata<sup>2</sup>, SHIOTA Yoichi<sup>1</sup>, MORIYAMA Takahiro<sup>1</sup>, ONO Teruo<sup>1</sup>, YOSHIKAWA Hiroki<sup>2</sup>

<sup>1</sup>Institute for Chemical Research, Kyoto University, <sup>2</sup>College of Science and Technology, Nihon University

kim.duckho.23z@st.kyoto-u.ac.jp

### Abstract:

The dynamics of the domain walls (DWs) in magnetic materials has been extensively explored for understanding the physics [1] as well as the potential applications in spintronic devices [2, 3]. Here, we report that the depinning magnetic field strongly depends on the magnetic properties. For this study, Si substrate/100-nm SiN/30-nm GdFeCo/5-nm SiN films with perpendicular magnetic anisotropy were prepared. The DW velocity  $v$  was measured as a function of an applied magnetic field  $\mu_0 H$  at different temperatures  $T$  by use of a real-time DW detection technique [4]. We find that the depinning field  $\mu_0 H_{\text{dep}}$  monotonically decreases as  $T$  increases. Furthermore, we find that  $\mu_0 H_{\text{dep}}$  is proportional to  $\sqrt{\mu_0 H_K / M_S}$ , where  $M_S$  is the saturation magnetization and  $\mu_0 H_K$  is the magnetic anisotropy field. This correlation between  $\mu_0 H_{\text{dep}}$  and the magnetic properties is understood in terms of the creep scaling law. Details will be discussed at the presentation.

### References

- [1] P. J. Metaxas et al., Phys. Rev. Lett. 99, 217208 (2007).
- [2] S. S. P. Parkin et al., Science 320, 190 (2008).
- [3] J. Sampaio et al., Nat. Nanotechnol. 8, 839 (2013).
- [4] Y. Yoshimura et al., Nat. Phys. 12, 157 (2016).

### Keywords:

Domain-wall motion, ferrimagnet, depinning field

## Current in Plane Tunneling Effect in Hybrid Type High-Tc Superconducting YBCO film and GMR-SV NiFe/CoFe/Cu/CoFe/IrMn multilayer

양우일<sup>2</sup>, 최종구<sup>1</sup>, 이상석\*<sup>1</sup>

<sup>1</sup>상지대학교 한방의료공학과, <sup>2</sup>상지대학교 응용물리전자학과  
sslee@sangji.ac.kr

### Abstract:

The antiferromagnetic IrMn based GMR-SV (giant magnetoresistance-spin valve) multilayer on the high-Tc superconductor YBCO film fabricated by using ion beam deposition and dc magnetron sputtering systems. The hybrid multilayer structure performed with the typical GMR-SV film and the superconducting YBCO film was compared two different magnetoresistance curves, which are measured at a room and a liquid nitrogen temperatures below the critical temperature. The exchange biased coupling field (Hex), coercivity (Hc), magnetoresistance ratio (MR (%)) for the pure GMR-SV multilayer measured at 77 K are enhanced to the increment values of 80 Oe, 43 Oe, and 6.6% more than those measured at room temperature, respectively. In case of YBCO/GMR-SV multilayer, the Hex, Hc, and MR (%) are 410 Oe, 240 Oe, -4.6% more than those measured at 77 K, respectively. The phenomenon having a negative MR(%) below the critical temperature is explained the current in plane tunneling (CIPT) effect when the resistance of the middle G layer between the high-temperature superconductor YBCO and the GMR-SV multilayer reaches a level comparable to the plane resistance of the upper metal layer.

### Keywords:

high-Tc superconductor, hybrid multilayer structure, liquid nitrogen temperature, magnetoresistance ratio(MR), current in plane tunneling(CIPT)

## 방사광 각분해 광전자 분광법을 이용한 Ce계 콘도 절연체화합물의 전자 구조 연구

성승호<sup>1</sup>, 이은숙<sup>1</sup>, T. Takabatake<sup>2</sup>, J. Denlinger<sup>3</sup>, 강정수\*<sup>1</sup>

<sup>1</sup>Department of Physics, The Catholic University of Korea, <sup>2</sup>Faculty of Integrated Arts and Sciences, Hiroshima University, Japan, <sup>3</sup>ALS, Lawrence Berkeley National Laboratory, USA  
kangjs@catholic.ac.kr

### Abstract:

4f 전자를 포함한 희토류 화합물들 중에서 많은 Ce 및 Yb 계 화합물들 (Ce-based and Yb-based compounds) 은 콘도 효과 (Kondo effect) 를 보이는 무거운 페르미온 (heavy fermion) 물질로 잘 알려져 있는데 [1], 그 이유는 저온에서 4f 전자가 전도 전자와 결합하여 콘도 단일 항 (Kondo singlet)을 형성하기 때문이다. 그 중 CeNiSn, CeRhSb 등은 저온에서 에너지 갭을 가지는 콘도 절연체 (Kondo insulator) 또는 콘도 반도체 (Kondo semiconductor) 에 속한다. 최근 non-symmorphic 대칭을 가지는 CeNiSn, CeRhSb, CeIrSb 등의 콘도 절연체 화합물이 위상 콘도 절연체 (Topological Kondo insulators: TKIs) 가 될 수 있다는 이론적 예측이 보고된 후 [2], 콘도 절연체 물질들에 대한 연구가 활발하다. 이 이론에 의하면 통상적인 위상절연체는  $Z_2$  불변량 (invariant) 을 가지는 반면, 위상 콘도 절연체는  $Z_4$  불변량을 가질 것으로 예측하고 있다. 또한 페르미면 (Fermi surface) 은 (100)면에서는 절연 상태, (010)면에서는 Möbius-twisted 표면 상태, (001)면에서는 Dirac-cone 표면 상태를 가질 것으로 예측하고 있다. 본 연구에서는 방사광을 이용한 각분해 광전자 분광법 (angle-resolved photoemission spectroscopy: ARPES) 실험을 수행하여 위상 콘도 절연체 CeRhSb 단결정을 대상으로 (100)면, (010)면, (001)면에 따른 페르미면과 띠 구조를 연구하였다.

[1] N. Tsujii, et al., Phys. Rev. Lett., **94**, 057201 (2005).

[2] Po-Yao Chang, et al., Nature physics, **13**, 794 (2017).

### Keywords:

콘도 절연체, 위상절연체, 각분해 광전자 분광법

## 방사광 분광법을 이용한 보상형 반쪽 금속 준강자성체 $Mn_3Ga$ 의 전자구조 연구

강정수\*<sup>1</sup>, 김희연<sup>1</sup>, 성승호<sup>1</sup>, 이은숙<sup>1</sup>, 김영학<sup>2</sup>, 백재윤<sup>2</sup>

<sup>1</sup>가톨릭대학교 물리학과, <sup>2</sup>포항가속기연구소  
kangjs@catholic.ac.kr

### Abstract:

호이슬러 화합물은 조성과 구조에 따라 강자성, 준강자성, 반쪽 금속성, 절연성, 초전도성 등 다양한 물성을 보인다 [1]. 그 중 반쪽 금속 (half-metallic) 강자성 호이슬러 화합물은 두 가지 다른 스핀 방향의 띠 중 한 쪽 스핀 띠는 에너지 갭을 가지지만 다른 스핀 띠는 금속성인 물질로 페르미 준위 근처에서 100% 스핀 분극이 일어나는 것으로 알려져 있다. 그리고 반쪽 금속 강자성 호이슬러 화합물 중  $Mn_3Ga$ 는 알짜 자기 모멘트가 0으로 정렬되는 보상형 반쪽 금속 준강자성체 (compensated half-metallic ferrimagnet) 로 예측된 바 있다 [2]. 그러나  $Mn_3Ga$ 의 보상형 반쪽 금속 준강자성 전자 구조는 아직까지 실험적으로 확인되지 않은 실정이다. 본 연구에서는 방사광을 이용한 연 X-선 흡수 분광법 (soft X-ray absorption spectroscopy: XAS), 연 X-선 자기원편광 이색성 (soft X-ray magnetic circular dichroism: XMCD) 분광법, 광전자 분광법 (photoemission spectroscopy: PES) 실험을 수행함으로써  $Mn_3Ga$ 의 국소적 전자구조를 연구하였다. XAS 연구에 의하면, Mn 이온들은 모두 2가 상태 ( $Mn^{2+}$ )로 존재하며, 국소적으로 4면체 대칭 (tetrahedral symmetry)을 가진 Mn 이온들과 8면체 대칭 (octahedral symmetry)을 가진 Mn 이온들이 섞여 있었다. 그리고 XMCD 연구로부터 Mn 이온의 스핀 자기 모멘트와 궤도 자기 모멘트가 무시할 수 있을 정도로 작은 것을 발견하였는데, 이는  $Mn_3Ga$ 의 보상형 준강자성 물성에 부합한 결과이다. 측정된 가전자띠 (valence band) PES 스펙트럼은 전자구조 계산에 의한 반쪽 금속성 상태 밀도 (density of state: DOS) 와 대체로 유사함을 발견하였다

[1] T. Graf, et al., Prog. Solid State Chem. **39**, 1 (2011).

[2] S. Wurmehl et al., J. Phys.: Condens. Matter **18**, 6171 (2006)

### Keywords:

보상형 반쪽금속 준강자성체, 연 X-선 흡수 분광법, 연 X-선 자기원편광 이색성, 광전자 분광법

## Novel magnetism of rhombohedral pyrochlore lattices $\text{Re}_3\text{Sb}_3\text{Mn}_2\text{O}_{14}$ (Re = La, Lu, and Y)

이찬현<sup>1</sup>, 최영수<sup>1</sup>, 최광용\*<sup>1</sup>, 도승환<sup>1</sup>

<sup>1</sup>중앙대학교 물리학과

kchoi@cau.ac.kr

### Abstract:

We report the synthesis and magnetic characterizations of  $\text{Re}_3\text{Sb}_3\text{Mn}_2\text{O}_{14}$  (Re = La, Lu, and Y) compounds, where  $\text{Mn}^{2+}$  magnetic ions ( $S=5/2$ ) constitute a rhombohedral lattice (Re = La, Lu) and a cubic lattice (Re = Y). Our static susceptibility measurements reveal that all the compounds display dominantly antiferromagnetic interactions between  $\text{Mn}^{2+}$  spins with the Curie-Weiss temperature  $\Theta_{\text{CW}}=-40.3$  K for Lu and  $\Theta_{\text{CW}}=-14.6$  K for Y. For  $R = \text{La}$ , the inverse magnetic susceptibility displays two linear regimes: the high-temperature regime ( $T>200$  K) with  $\Theta_{\text{CW}}=13.8$  K and the intermediate-temperature regime ( $50 \text{ K} < T < 135 \text{ K}$ ) with  $\Theta_{\text{CW}}=-59$  K. These materials exhibit no evidence of long-range magnetic ordering, indicating strong magnetic frustration despite their large spin number  $S = 5/2$ . The high-field magnetization of  $\text{Mn}_2\text{Y}_3\text{Sb}_3\text{O}_{14}$  shows a half-magnetization plateau. Our results suggest a significant role of  $J_1$ - $J_2$  exchange frustration in addition to weak geometrical frustration in a class of the  $\text{Re}_3\text{Sb}_3\text{Mn}_2\text{O}_{14}$  compounds.

### Keywords:

Frustrated magnet

## Probing quantum criticality in electron-doped $\text{Sr}_{2-x}\text{La}_x\text{IrO}_4$

최광용\*<sup>1</sup>, [RODAN Steven](#)<sup>1</sup>, 최영수<sup>1</sup>, 도승환<sup>1</sup>, 이수현<sup>1</sup>  
<sup>1</sup>중앙대학교 물리학과  
kchoi@cau.ac.kr

### Abstract:

The well-known cuprate  $\text{La}_2\text{CuO}_4$ , upon substituting Sr on the La site, effectively introducing holes into the system, has been shown to completely suppress the antiferromagnetic long-range order, and then transition into a superconducting phase. Its 5d isostructural counterpart  $\text{Sr}_2\text{IrO}_4$ , upon electron-doping via La substitution on Sr site, however, has so far not shown a similar superconducting transition. It is believed that the differences observed between the iridates and the cuprates are due to the substantial spin-orbit coupling from the 5d Ir content in the former, and the interplay with electron correlation effects. A very recent publication reports on a spin-density wave state in  $\text{Sr}_{2-x}\text{La}_x\text{IrO}_4$  measured by magnetic x-ray scattering [1], thus connecting the system to hole-doped  $\text{La}_2\text{CuO}_4$  magnetically. We present magnetic and electronic properties of La-substituted  $\text{Sr}_2\text{IrO}_4$  polycrystalline samples. Further, we plan to employ muon spin resonance, a local probe for analyzing the transitional Griffiths phase within the substitutional range  $x \sim 0.02-0.04$ .

[1] X. Chen, J. L. Schmeh, Z. Islam, Z. Porter, E. Zoghlin, K. Finkelstein, J. P. C. Ruff, and S. D. Wilson, *Nature Communications* 9, 103 (2018)

### Keywords:

Iridate; quantum criticality

## Interfacial spin-flip scattering induced by strong spin-orbit coupling at a heavy metal/ferromagnet heterostructure

이현우\*<sup>1</sup>, 임미진<sup>1</sup>

<sup>1</sup>포항공과대학교 물리학과  
hwl@postech.ac.kr

### Abstract:

Spintronic devices are studied to understand how spin moves and how it could be used for a data storage. During the past decades, many studies have been done on nonmagnetic metal(NM)/ferromagnet(FM) systems, which are analyzed based on the spin drift-diffusion equation. However, little information is available about the role of an interface for spin transport. Recently, controversy on the spin diffusion length of Pt/Co has appeared as it is not in accordance with the previous theoretical analysis. The purpose of this study is to find the origin of spin memory loss by calculating spin-flip scattering in a heterostructure of a heavy metal(HM) which is an NM with strong atomic spin-orbit coupling(ASOC) and a FM. Two main properties of the HM/FM system are large ASOC and inversion symmetry breaking(ISB) at the interface. Here, we report two main findings from the tight binding method calculation. The first is the role of bulk ASOC in the HM for the spin-flipping. The ASOC entangles spin and orbit of an electron in HM eigenstates, which induces spin flip after the interfacial scattering by allowing a transmittable path from HM to FM or vice versa. The other finding is the origin of spin-flip scattering when an interface breaks the inversion symmetry which allows specific inter-orbital hopping, which is called an orbital Rashba effect. It generates an additional transmission path in the FM which makes spin flip when spin is scattered from the HM. This study may lead to a better understanding of the interfacial spin transport in future spintronic devices.

### Keywords:

spintronics, spin-orbit coupling, spin-flip scattering, orbital Rashba effect, Pt/Co interface

## Transmittance Measurement of Single Crystal $\text{Mn}_{0.5}\text{Fe}_{0.5}\text{PS}_3$ at Low Temperature

김중현<sup>1</sup>, 조영찬<sup>1</sup>, 손수한<sup>2, 3</sup>, 김장원<sup>1</sup>, 정택선<sup>1</sup>, 박제근<sup>2, 3</sup>, 김재훈\*<sup>1</sup>  
<sup>1</sup>연세대학교 물리학과, <sup>2</sup>서울대학교 물리천문학부, <sup>3</sup>ibs 강상관계 물질 연구단  
super@yonsei.ac.kr

### Abstract:

$\text{Mn}_{0.5}\text{Fe}_{0.5}\text{PS}_3$  is a spin-glass van der Waals material with antiferromagnetism. We have investigated the temperature dependence of the fundamental absorption edge of single crystal  $\text{Mn}_{0.5}\text{Fe}_{0.5}\text{PS}_3$ . We measured the transmittance from 4 to 295 K by using a He-free closed cryostat. As the temperature increased, the fundamental absorption edge decreased from 1.57 to 1.5 eV and a peak at 1 eV was broadened.

### Keywords:

van der Waals, magnetic material, low temperature measurement

## Fundamental Absorption Edge of Single Crystal $\text{MnPS}_3$ at Low Temperature

김재훈\*<sup>1</sup>, 조영찬<sup>1</sup>, 정택선<sup>1</sup>, 김종현<sup>1</sup>, 손수한<sup>2, 3</sup>, 박제근<sup>2, 3</sup>  
<sup>1</sup>연세대학교 물리학과, <sup>2</sup>서울대학교 물리천문학부, <sup>3</sup>ibs 강상관계 물질 연구단  
super@yonsei.ac.kr

### Abstract:

$\text{MnPS}_3$  is a magnetic van der Waals material with antiferromagnetism. We measured the transmittance of single crystal  $\text{MnPS}_3$  from 8.6 K to 295 K and extracted the absorption coefficient. The fundamental absorption edge of  $\text{MnPS}_3$  was increased from 2.57 to 2.89 eV as the temperature decreased. Also, we found an absorption peak at around 2.7 eV that was hidden by the fundamental absorption edge at room temperature. We were able to identify all three peaks originating from intraionic d-d transitions.

### Keywords:

$\text{MnPS}_3$ , van der Waals, absorption, antiferromagnetism

## Spin Density Wave and Unconventional Magnetic and Thermal Transport Properties in $\text{Sr}_{2-x}(\text{PbCl}_2)_x\text{Cu}(\text{BO}_3)_2$ Compounds

원보라<sup>1</sup>, GINTING Dianta<sup>1</sup>, 이종수\*<sup>1</sup>

<sup>1</sup>Department of Applied Physics and Institute of Natural Sciences, Kyung Hee University  
jsrhyee@khu.ac.kr

### Abstract:

$\text{SrCu}_2(\text{BO}_3)_2$  (Sr-122) is well known as quasi-two dimensional spin system with a spin gap. The  $\text{Cu}^{2+}$  ion in the compound forms Shastry-Sutherland lattice that Sr atom resides in between  $\text{Cu}(\text{BO}_3)$  *ab*-plane layers. Here we report the magnetic and thermal transport properties on the other homologous spin density wave compound  $\text{Sr}_2\text{Cu}(\text{BO}_3)_2$  (Sr-212) which has quasi-one-dimensional spin structure. The crystal and spin structures of Sr-212 is distinguished, comparing to those of Sr-122, by the fact that the nearest neighbor  $\text{CuO}_4$  pair forms a spin dimer along the *ac*-plane and these dimers are linked by triangular  $\text{BO}_3$ . The substitution effect by metallic cations (M=Al, La, Na and Y) in the Sr-site suppresses the spin gap. When we dope the  $\text{PbCl}_2$  on the  $\beta\text{-Sr}_2\text{Cu}(\text{BO}_3)_2$  ( $\beta\text{-Sr-212}$ ) by  $\text{Sr}_{2-x}(\text{PbCl}_2)_x\text{Cu}(\text{BO}_3)_2$  ( $x=0, 0.0005, 0.01, \text{ and } 0.1$ ), the lattice parameters are systematically changed, indicating the effective substitution of the elements. From the magnetic properties measurements, we observed the spin density wave behavior in  $M(T)$  curve near 75 K with long-range magnetic ordering at low temperatures ( $T \leq 20$  K) which do not follow conventional Brillouin type  $M(H)$  curve. The ratio between Weiss temperature and Neel temperature  $\theta_D/T_N$  indicates the significant spin frustration on the compound. Heat capacity and thermal conductivity measurements showed magnon gap formation at low temperatures. The unconventional behavior of magnetic, heat capacity, and thermal conductivity properties are investigated as competition between spin density wave and long range magnetic order with high spin frustration.

### Keywords:

Quantum magnet, Spin density wave, Quasi-one-dimensional, Spin frustration, Magnetic order.

## Two-dimensional antiferromagnonic activation in $S = 1$ one-dimensional chain $\text{NiTe}_2\text{O}_5$

LEE Jun Han<sup>1</sup>, 오윤석\*<sup>1, 2</sup>, KRATOCHVÍLOVÁ Marie<sup>3, 4</sup>, YAMANI Zahra<sup>5</sup>, KIM J. S.<sup>6</sup>, PARK Dae Hwan<sup>1</sup>,  
CHOI Hong Eun<sup>1</sup>, STEWART G. R.<sup>6</sup>, PARK Je-Geun<sup>3, 4</sup>

<sup>1</sup>School of Natural Science, UNIST, Ulsan, Korea, <sup>2</sup>Department of Physics, UNIST, Ulsan, Korea, <sup>3</sup>Center for Correlated Electron Systems, IBS, Seoul, Korea, <sup>4</sup>Dept. of Phys. & Astro., Seoul National University, Seoul, Korea, <sup>5</sup>Canadian Neutron Beam Centre, Chalk River, ON, Canada, <sup>6</sup>Dept. of Physics, University of Florida, FL, USA  
ysoh@unist.ac.kr

### Abstract:

Since Haldane conjectured that ground state of one-dimensional Heisenberg antiferromagnet has a finite spin excitation gap for integer spins or gapless excitations for half-odd integer spins, it has inspired lots of theoretical and experimental studies on the low-dimensional quantum magnets. The integer spin chain, called Haldane chain, generally has antiferromagnetic coupling for the intrachain exchange interaction. Recently, we have discovered a new Haldane chain compound  $\text{NiTe}_2\text{O}_5$ , in which antiferromagnetic order is accompanied by ferromagnetic intrachain coupling and antiferromagnetic interchain coupling. In this research, comprehensive magnetic and thermal properties have been studied in single crystalline as well as polycrystalline  $\text{NiTe}_2\text{O}_5$ . Interestingly, it has been found that it has two-dimensional antiferromagnonic activation. In this presentation, we explain our intensive experimental studies on  $\text{NiTe}_2\text{O}_5$  and discuss about the possible two-dimensional antiferromagnon excitation.

### Keywords:

Haldane chain, antiferromagnet, magnon

## Magnetocaloric Effect of Two-dimensional Layered (C<sub>6</sub>H<sub>5</sub>CH<sub>2</sub>CH<sub>2</sub>NH<sub>3</sub>)<sub>2</sub>CuCl<sub>4</sub> Perovskites in the Vicinity of Transition Temperature

박가람<sup>1, 2</sup>, 오인환<sup>1</sup>, 김용환<sup>3</sup>, 정종훈<sup>3</sup>, 허남정<sup>3</sup>, 홍창섭<sup>2</sup>, 김기연\*<sup>1</sup>

<sup>1</sup>한국원자력연구원 중성자과학연구부, <sup>2</sup>고려대학교, 화학과, <sup>3</sup>인하대학교, 물리학과  
kykim3060@kaeri.re.kr

### Abstract:

Magnetocaloric effect (MCE) generally refers to heating or cooling of magnetic materials by the application of a magnetic field. MCE effect can be measured as the isothermal magnetic entropy change and the adiabatic temperature change. The isothermal magnetic entropy change is usually indirectly measured from the isothermal magnetization curves at a number of different temperatures and the adiabatic temperature change is determined from magnetization and heat capacity as a functions of temperature and magnetic field. [1] Since the discovery of a giant MCE effect in Gd<sub>5</sub>(Si<sub>2</sub>Ge<sub>2</sub>) intermetallic alloys in 1997[2], magnetic refrigeration utilizing MCE has received great interest as a promising solid state cooling technology replacing the conventional gas compression and expansion cycle in markets such as wine coolers, domestic refrigeration, and automobile air-conditioning because it is the higher energy efficient and environmentally friendly. Solid state cooling technology based on magnetocaloric materials for ultralow temperature application (down to helium liquefaction 4.2 K) is expected to have an important role as well because of ever-increasing demand from academic and commercial sectors and dwindling helium reservoir. In this presentation, we propose two-dimensional layered organic-inorganic hybrid perovskites as promising magneto-caloric materials for ultralow temperature application.

### References

- [1] V. K. Percharky and K. A. Gschneidner, Jr. J. Appl. Phys. 86, 565 (1999)
- [2] V. K. Pecharsky and K. A. Gschneidner, Jr. Phys. Rev. Lett. 78, 4494 (1997)

### Keywords:

Magnetocaloric effect, Magnetic Refrigeration, Two-dimensional Organic-Inorganic Perovskites

## Anomalous spin precession depending on orbital character

이현우\*<sup>1</sup>, 손정훈<sup>1</sup>

<sup>1</sup>포항공과대학교 물리학과  
hwl@postech.ac.kr

### Abstract:

The precession of electron spin is the key concept for spin manipulation in semiconductor spintronics. Rashba field, which couple spin and electric field, plays a role as effective magnetic field to realize spin precession in electrical way[1]. On the other hand, some recent studies reported the Rashba field shows orbital dependent behavior[2,3], then the description on spin evolution needs to be modified. So we verify that a spin rotation has various pattern relying on the several orbital characters containing the spin. Our result is expected to provide a new insight for spin FET experiment.

[1]Koo, H. C. et al. Control of spin precession in a spin-injected field effect transistor. *Science* 325, 1515-1518 (2009).

[2]H. Zhang, C.-X. Liu, S.-C. Zhang, Spin-orbital texture in topological insulators. *Phys. Rev. Lett.* 111, 066801 (2013).

[3] Bawden, L. et al. *Hierarchical spin-orbital polarization of a giant Rashba system. Sci. Adv.* 1, e1500495 (2015)

### Keywords:

Spin precession, Spin FET, Rashba effect, spin-orbital texture

## Rare Earth Lean Permanent magnet

홍지상\*<sup>1</sup>, KHAN Imran<sup>1</sup>, FAROOQ Muhammad Umar<sup>1</sup>

<sup>1</sup>부경대학교 물리학과  
hongj@pknu.ac.kr

### Abstract:

Generally, for high-temperature applications of  $\text{Nd}_2\text{Fe}_{14}\text{B}$  magnet like in electric vehicles motors about 25 to 30 % of Nd is required to replace with costly Dy element. Thus it will be interesting to either completely remove or reduce the concentration of costly Dy element yet having better magnetic properties. In this regard, we studied the site preferences, electronic and magnetic properties of slightly Dy-doped  $\alpha''\text{-Fe}_{16}\text{N}_2$  using the first principles method within the framework of generalized gradient approximation. Here we have selected a small doping concentration of Dy, about 1.56 % of Fe. This creates a local lattice distortion near the impurity site without affecting the volume of the cell and total magnetic moment. The h-site with ferromagnetic coupling between Dy and Fe was found to be the most stable site compared to d-site. We found an enhancement in the magnetocrystalline anisotropy with the substitutional Dy doping in  $\alpha''\text{-Fe}_{16}\text{N}_2$ . Because of this, the coercive field of the doped system was enhanced from 6.5 kOe in pure to 11 kOe in Dy doped system. Furthermore, the maximum energy product was also enhanced to 121 MGOe in Dy doped system. These results imply that slightly Dy doped  $\text{Fe}_{16}\text{N}_2$  could be a potential candidate for permanent magnet applications.

### Acknowledgements

This research was supported by the Basic Science Research Program through the National Research Foundation of Korea (NRF) funded by the Ministry of Science, ICT and Future Planning (2016R1A2B4006406) and by the Supercomputing Center/Korea Institute of Science and Technology Information with supercomputing resources including technical support (KSC-2017-C3-0031).

### Keywords:

Rare Earth-free magnet, Permanent magnet, magnetic anisotropy, coercive field

## Determination of the ground states of CeNMSb<sub>2</sub> (NM: Cu, Ag and Au) compounds

장재경<sup>1</sup>, 이주열\*<sup>1</sup>  
<sup>1</sup>성균관대학교 물리학과  
rheejy@skku.edu

### Abstract:

We investigated the ground states of CeNMSb<sub>2</sub> (NM: Cu, Ag and Au) compounds by using the full-potential linearized-augmented-plane-wave method. The spin-orbit coupling (SOC) effect is much larger than crystalline-electric-field (CEF) effects in heavy-atom systems, for instance, rare-earth compounds, therefore it has been routinely believed that the SOC effect dominantly determines the ground state. However, our results suggest that, even though the SOC is much stronger than the CEF interaction in Ce compounds, the ground state can be determined by the CEF interaction only. According to our calculational results, it is revealed that both the CEF interaction and the direction of magnetization play the crucial role for the determination of the ground state. Because of the so-called angular-momentum quenching, which leads to the cancellation of the SOC energies for  $\pm m$  states, the CEF effects play a more important role for the determination of the ground state of those Ce compounds. It implies that the simple  $l$ -scheme should be used instead of  $jj$ -scheme because  $J$  is not a good quantum number any more.

### Keywords:

Electronic structures, Spin-orbit coupling, Crystalline-electric-field

## 이중층에서 쌍으로 연결된 스커미온의 스핀 전달 토크를 이용한 이차원 상 운동 조작

원창연\*<sup>1</sup>, 김남준<sup>1</sup>, 이찬기<sup>1</sup>

<sup>1</sup>경희대학교 물리학과  
cywon@khu.ac.kr

### Abstract:

이중층에서 각 층에 있는 스커미온 수가 +1과 -1으로 서로 다른 스커미온을 결합하면 스커미온 수가 0인 자성구조가 만들어진다. 이 연결된 스커미온은 각 층에 같은 전류를 흘려줬을때 스커미온 홀 효과에 영향을 받지 않고 STT(스핀전달토크)에 의해 전류와 같은 방향으로 움직이며, 각 층에 같은 세기의 전류를 서로 반대방향으로 흘려줬을 때는 전류의 방향과 수직인 방향으로 움직인다. 각각의 층에 방향은 같으나 서로 다른 세기의 전류를 흘려주므로서 연결된 스커미온구조의 움직임을 2차원 평면상에서 원하는 움직임을 보이도록 자유롭게 조작할 수 있다. 이러한 현상을 Thiele 방정식을 사용하여 스커미온의 운동이 어떤 동역학으로 인해 가능한 것인지 조사하고, 각 층의 전류와 스커미온이 받는 힘의 관계를 제공하는 텐서를 구하였다. 연결된 스커미온의 움직임에 대해 자체적으로 제작한 시뮬레이션을 통해 이차원 평면상에서 원하는 대로 움직일 수 있음을 확인하고 그 결과를 Thiele 방정식을 통해 얻은 결과와 비교하여 설계의 정확성을 확인했다.

### Keywords:

스커미온, Thiele 방정식, 스핀 전달 토크

## Characterization of current-voltage characteristics of $\text{Fe}_3\text{O}_4 / \text{GaN}$ heterostructures

GHIMIRE Santosh<sup>1</sup>, 도중희\*<sup>1</sup>

<sup>1</sup>경북대학교 물리학과  
jhdho@knu.ac.kr

### Abstract:

Epitaxial  $\text{Fe}_3\text{O}_4$  films were prepared on GaN substrates by pulsed laser deposition. Ti, Al and Au electrodes were deposited by DC-sputtering to prepare ohmic contacts. X-ray diffraction data for  $\text{Fe}_3\text{O}_4$  suggested a successful (1 1 1) -oriented epitaxial growth on (0 0 0 1) GaN. Atomic force microscopy images showed that  $\text{Fe}_3\text{O}_4$  films had a quite smooth surface with a root-mean-square roughness of  $\sim 1$  nm. The magneto-optic Kerr effect (MOKE) measurement revealed that the magnetic hysteresis loop of  $\text{Fe}_3\text{O}_4 / \text{GaN}$  was a tilted shape with the coercivity of  $\sim 600$  Oe. The temperature dependence of the IV characteristics was measured from 10 K to 300 K by using a cryostat and a two-probe method.  $\text{Fe}_3\text{O}_4 / \text{GaN}$  heterostructure showed that the current flow is small in negative bias voltage while it greatly increases in a positive bias. As the temperature decreased from room temperature to 10 K, the current in negative bias decreased dramatically, but the change in positive bias regions was small. In addition, a weak hysteresis behavior in the cyclic IV measurement was observed at low temperatures.

### Keywords:

epitaxial, bias voltage

## 텐서플로우 라이브러리에서의 합성곱(Convolution Product)을 이용한 자성 시뮬레이션

원창연\*<sup>1</sup>, 이찬기<sup>1</sup>, 권희영<sup>1</sup>, 김남준<sup>1</sup>

<sup>1</sup>경희대학교 물리학과  
cywon@khu.ac.kr

### Abstract:

인공지능 기술이 급격하게 발전함에 따라 다양한 인공 신경망들이 개발되었다. 그 중에서도 합성곱 신경망은 일반적으로 인공지능을 만드는데 쓰이고 합성곱은 합성곱 신경망의 기초를 이룬다. 자성 시뮬레이션에서는 교환 상호작용, Dzyaloshinskii-Moriya 상호작용, 스핀 전달 토크, 스핀-궤도 토크, 쌍극자 상호작용으로부터 오는 영향을 포함하는 '자기 모멘트에 대한 전체 유효장'을 효율적으로 계산하는 것이 중요하다. 합성곱은 이 전체 유효장을 계산할 때에도 유용하게 쓰일 수 있다. 텐서플로우는 구글사가 만든 프로그래밍 라이브러리이고 이는 합성곱을 계산하기 위한 효과적인 방법을 제공한다. 우리는 텐서플로우를 이용해 새로운 자성 시뮬레이션 프로그램을 만들었고 합성곱의 속도를 더욱 보완하기 위해 GPU 병렬 컴퓨팅을 이용했다. 자성 시뮬레이션에 대해 'GPU를 이용하는 것'과 '이전의 CPU를 이용하는 것'을 비교했을 때 'GPU 계산'이 더 효과적임을 알아냈다.

### Keywords:

GPU, 합성곱, 합성곱 신경망, 텐서플로우, 자성 시뮬레이션

## Doping evolution of the electronic structure of $\text{Sr}_3(\text{Ir}_{1-x}\text{Mn}_x)_2\text{O}_7$

문순재\*<sup>1</sup>, 서정현<sup>1</sup>, 안기현<sup>1</sup>, 노승주<sup>1</sup>, 송승재<sup>1</sup>, SCHMEHR J. L.<sup>2</sup>, WILSON S. D.<sup>2</sup>

<sup>1</sup>한양대학교 물리학과, <sup>2</sup>Department of Materials, University of California, Santa Barbara, California  
93106, USA

soonjmoon@hanyang.ac.kr

### Abstract:

The layered perovskite iridates  $\text{Sr}_{n+1}\text{Ir}_n\text{O}_{3n+1}$  ( $n = 1, 2$ ) has attracted considerable attention as a candidate for exploring novel quantum states upon charge carrier doping. We investigated the electronic structure of  $\text{Sr}_3(\text{Ir}_{1-x}\text{Mn}_x)_2\text{O}_7$  ( $x = 0, 0.18, 0.33$ ) by using optical spectroscopy. We find that the doping evolution of the electronic structure of  $\text{Sr}_3(\text{Ir}_{1-x}\text{Mn}_x)_2\text{O}_7$  is nonmonotonic. The optical transitions between the spin-orbit-coupling-induced effective total angular momentum state  $J_{\text{eff}}$  of Ir ions are suppressed and transition between Mn  $e_g$  states appears upon 18% Mn doping. With increasing Mn concentration up to about 33%, both the optical transitions between the  $J_{\text{eff}}$  states and between the Mn  $e_g$  states are suppressed. We suggest that the nonmonotonic variation of the electronic structure of  $\text{Sr}_3(\text{Ir}_{1-x}\text{Mn}_x)_2\text{O}_7$  can be attributed to the change in the valence state of Mn ions.

### Keywords:

Iridates, Doping

## Infrared spectroscopic study on the electronic structure of (LaCoO<sub>3</sub>)<sub>n</sub>/(SrCoO<sub>3</sub>)<sub>n</sub> superlattices

문순재\*<sup>1</sup>, 노승주<sup>1</sup>, 서정현<sup>1</sup>, 안기현<sup>1</sup>, 최우석<sup>2, 3</sup>, 이호녕<sup>3</sup>

<sup>1</sup>한양대학교, 물리학과, <sup>2</sup>성균관대학교, 물리학과, <sup>3</sup>Oak ridge national laboratory, Materials Science and Technology Division  
soonjmoon@hanyang.ac.kr

### Abstract:

Perovskite-type cobalt oxides La<sub>1-x</sub>Sr<sub>x</sub>CoO<sub>3</sub> (LSCO) show intriguing interdependence of electronic response and spin configuration. We investigated the electronic structure of (LaCoO<sub>3</sub>)<sub>n</sub>/(SrCoO<sub>3</sub>)<sub>n</sub> superlattices with periodicity  $n = 1, 4,$  and 10 by using infrared spectroscopy. We observe a systematic variation in the electronic response of (LaCoO<sub>3</sub>)<sub>n</sub>/(SrCoO<sub>3</sub>)<sub>n</sub> with  $n$ . The optical conductivity of the  $n=1$  superlattice is found to be similar with that of LSCO film and exhibits two main absorptions at about 0.2 and 2 eV. With increasing  $n$ , the lower-energy peak is suppressed and the spectral weight shifts to the higher-energy one. The change in the periodicity also affects the temperature evolution of the electronic response. We find that the variation in the optical conductivity of the  $n=1$  and  $n=4$  SLs with temperature is much stronger than that of the  $n=10$  SL and the LSCO film. We will explain the periodicity and doping dependences of the optical data in terms of the interface effect and resulting change in the spin configuration.

### Keywords:

Cobaltite superlattices, interface effect, infrared spectroscopy, spin configuration

## Pressure-Induced Metal-Insulator Transitions in Chalcogenide $\text{NiS}_{2-x}\text{Se}_x$

HUSSAIN Tayyaba<sup>1</sup>, OH , Myeong-jun<sup>1</sup>, NAUMAN Muhammad<sup>1</sup>, HAN Garam<sup>2</sup>, KIM Changyoung<sup>2</sup>,  
KANG Woun<sup>3</sup>, 조연정\*<sup>1</sup>

<sup>1</sup>Department of Physics, Kyungpook National University, Daegu 41566, South Korea, <sup>2</sup>Center for Correlated Electron Systems, Institute of Basic Science, Seoul 08826, South Korea , <sup>3</sup>Department of Physics, Ewha Womans University, Seoul 03760, South Korea  
jophy@knu.ac.kr

### Abstract:

We report the temperature-dependent resistivity  $\rho(T)$  of chalcogenide  $\text{NiS}_{2-x}\text{Se}_x$  ( $x = 0.1$ ) using hydrostatic pressure as a control parameter in the temperature range of 4-300 K. The insulating behavior of  $\rho(T)$  survives at low temperatures in the pressure regime below 7.5 kbar, whereas a clear insulator-to-metallic transition is observed above 7.5 kbar. Two types of magnetic transitions, from the paramagnetic (PM) to the antiferromagnetic (AFM) state and from the AFM state to the weak ferromagnetic (WF) state, were evaluated and confirmed by magnetization measurement. According to the temperature-pressure phase diagram, the WF phase survives up to 7.5 kbar, and the transition temperature of the WF transition decreases as the pressure increases, whereas the metal-insulator transition temperature increases up to 9.4 kbar. We analyzed the metallic behavior and proposed Fermi-liquid behavior of  $\text{NiS}_{1.9}\text{Se}_{0.1}$ .

### Keywords:

$\text{NiS}_{1.9}\text{Se}_{0.1}$ ,  $\rho(T)$  measurements, Magnetic measurements, Metal-insulator transition (MIT), Magnetic phase transition, Non-Fermi-liquid behavior

## Magnetodielectric properties of $R_2\text{CoMnO}_6$ (R=Gd, Dy, Tm) Single crystals

최영재\*<sup>1</sup>, 문재영<sup>1</sup>, 김종혁<sup>1</sup>, 오상협<sup>1</sup>, 이나라<sup>1</sup>  
<sup>1</sup>연세대학교 물리학과  
phylove@yonsei.ac.kr

### Abstract:

We successfully synthesized the high-quality single crystals of double perovskite  $R_2\text{CoMnO}_6$  (R=Gd, Dy, Tm) by the flux method. The crystals belong to  $P2_1/n$  space group, where the B-site cations are well ordered, and show ferromagnetic order at  $T_C=117, 90,$  and  $50$  K for Gd, Dy, and Tm, respectively, from the dominant  $\text{Co}^{2+}$  and  $\text{Mn}^{4+}$  superexchange interactions. Temperature dependence of dielectric constant,  $\epsilon$ , perpendicular to the  $c$  axis near the  $T_C$  exhibits broad but distinct anomaly, which vanishes when magnetic field is applied along the  $c$  axis. Magnetic-field dependence of  $\epsilon$  at low temperature regime presents abrupt changes, coinciding with metamagnetic transitions of isothermal magnetization curve. This result indicates that magnetic and dielectric properties are strongly correlated.

### Keywords:

Double perovskite, Magnetodielectric, Single crystal

## Exchange bias effect in $Y_2Co_{2-x}Mn_xO_6$ compounds

최영재\*<sup>1</sup>, LEE N.\*<sup>1</sup>, OH S.H<sup>1</sup>

<sup>1</sup>연세대학교 물리학과

phylove@yonsei.ac.kr, eland@yonsei.ac.kr

### Abstract:

Double-perovskite  $R_2CoMnO_6$  ( $R = La, \dots, Lu$ ) compounds have been explored due to their fascinating functional properties such as exchange bias effect and multiferrocity, arising from intricate magnetic phases and interactions. We have investigated exchange bias (EB) phenomena by adjusting the relative ratio between Co and Mn ions in double-perovskite  $Y_2CoMnO_6$  compound. In the case of single phase  $Y_2Co_{2-x}Mn_xO_6$  ( $0.8 \leq x \leq 1.5$ ), the horizontal shift of magnetic hysteresis loop was maximized as 2.31 kOe for  $x=1.4$ . The EB effect would be described by interfacial exchange interaction between ferromagnetic and antiferromagnetic phases, where the mixed phases are characterized by spin-glass type behavior.

### Keywords:

exchange bias, double perovskite

# Topological Phase in Antiferromagnetic Buckled Honeycomb Lattice

LEE K.-W.\*<sup>1, 2</sup>, SONG Young-Joon<sup>1</sup>, JIN Hyo-Sun<sup>1</sup>

<sup>1</sup>Department of Applied Physics, Graduated School, Korea University, Sejong, <sup>2</sup>Division of Display and Semiconductor Physics, Korea University  
mckwan@korea.ac.kr

## Abstract:

In condensed matter physics, tons of research on topological materials have been conducted for a couple of decades. So far, several kinds of the topological phases in insulating, semimetallic, and metallic systems have been suggested and experimentally supported. These phases can be classified by symmetries. For example, the ordinary Z<sub>2</sub> topological insulator(TI) is protected by both the time-reversal(TR) and inversion(I) symmetries, whereas the quantum anomalous Hall insulators (QAHs) occur in the systems broken TR. Additionally, the topological crystalline insulator(TCI) is protected by crystalline symmetries of the rotation and mirror symmetries. Among them, QAHs, also named as the Chern insulator, get a lot of attention due to the energy dissipation-less edge states without applying external magnetic fields. Compared to the ordinary TI, these spin-polarized edge states are expected to be more robust against external perturbations, external fields, or impurities, so good for the electronic and spintronic devices. However, most proposed candidates of the (ferromagnetic) Chern insulator have some complicated structures or require special conditions to realize the QAH state and to use them for devices.

Recently, several theoretical reports suggest the possibility of topological antiferromagnetic system. Our goal is to design Chern insulators in the antiferromagnetic system, which is tunable by external fields. We consider a heterostructure with a few layers of (111)-oriented antiferromagnetic cubic perovskite BaCrO<sub>3</sub> on the (111)-oriented cubic SrTiO<sub>3</sub> substrate. This buckled honeycomb lattice of Cr leads to the nonzero Chern numbers, calculated by the first-principles methods and the Green function technics with the tight-binding model. In this presentation, we will address the topological states of this system.

**Acknowledgements:** This research was supported by NRF-2016R1A2B4009579.

## Keywords:

first principles, buckled honeycomb lattice, Chern insulator

## DFT+DMFT electronic structure of a Kondo insulator CeNiSn

민병일\*<sup>1</sup>, 남태식<sup>1</sup>, CéDRIC Bareille<sup>2</sup>, 강창중<sup>1</sup>, 류동춘<sup>1</sup>, 김규<sup>1</sup>

<sup>1</sup>포항공과대학교 물리학과, <sup>2</sup>Institute for Solid State Physics, The University of Tokyo  
bimin@postech.ac.kr

### Abstract:

Recently, CeNiSn has been investigated as a promising candidate of Kondo insulator. But it is controversial whether it is a Kondo insulator or semimetal. Recent magnetothermoelectric measurement on CeNiSn [1] suggested that CeNiSn is a nodal metal arising from anisotropic hybridization. Specific heat and thermal conductivity measurements [2], however, indicate that CeNiSn has an anisotropic pseudo-gap. To explore the Kondo nature in CeNiSn, we have investigated the electronic structure of CeNiSn, utilizing the density functional theory (DFT) and the dynamical mean field theory (DMFT). We compared our result with angle-resolved photoemission spectroscopy (ARPES) and found that band structure matches well with each other, especially the kink where the shape of band suddenly bent over, indicating the f-d hybridization below Kondo temperature. Also, our Fermi surface calculation manifests the remnant of f-band. CeNiSn hosts Kondo effect but the gap opens only partially, namely not in the whole Brillouin zone, possibly related to the crystal structure.

[1] U. Stockert et al., Phys. Rev. Lett. 117, 216401 (2016)

[2] M. Sera et al., Phys. Rev. B 55, 6421 (1997)

### Keywords:

band calculation (DFT, DMFT), Kondo effect

# Non-Equilibrium Steady State Dynamical Mean Field Theory with Non-Crossing Approximation Solver

고범준<sup>1</sup>, 심지훈\*<sup>1, 2, 3</sup>

<sup>1</sup>Department of Chemistry, Pohang University of Science and Technology, <sup>2</sup>Department of Physics, Pohang University of Science and Technology, <sup>3</sup>Division of Advanced Nuclear Engineering, Pohang University of Science and Technology  
jhshim@postech.ac.kr

## Abstract:

We develop the non-equilibrium steady state dynamical mean field theory (NESS-DMFT) with non-crossing approximation (NCA) as the impurity solver to study strongly correlated electronic system on a dissipative lattice under static uniform electric field. In this framework, the Coulomb interaction and the external field which is described in Coulomb gauge are treated nonperturbatively via DMFT. The steady state is achieved by considering fictitious Fermion reservoir where the energy given by the electric field is dissipated. For the one band Hubbard model in dissipative cubic lattice with half filling, the electric current per spin and the local energy distribution function are calculated beyond the linear response regime, and the phase diagram of the metal-insulator transition driven by the field, temperature, and the Coulomb interaction strength will be discussed. These are compared with NESS DMFT with iterated perturbation theory (IPT)[1]. The results could be applicable to NiO[2] and  $\text{Cr}_x\text{V}_{2-x}\text{O}_3$ [3]. The NCA solver is multiorbital-extended, and can readily be used to study multi-band models which could be applied to account VO<sub>2</sub> case or be incorporated to cluster extension of the NESS-DMFT.

## Keywords:

Non-equilibrium, Dynamical Mean Field Theory, Strongly Correlated Electronic Systems, Non Crossing Approximation, Hubbard Model, Beyond Linear Response, Phase Diagram

## Strain Engineering in Vanadium Dioxide Thin Films on Flexible Glass Substrates

강대준\*<sup>1</sup>, 손민균<sup>1</sup>  
<sup>1</sup>성균관대학교 물리학과  
dj kang@skku.edu

### Abstract:

Tuning the metal insulator transition (MIT) behavior of Vanadium Dioxide (VO<sub>2</sub>) films through strain is effective for practical applications. However, the mechanism for strain modulated MIT in VO<sub>2</sub> is still under debate. There are two kinds of strain, interfacial and external strain that we can play with. In order to study about the effect of external strain, we synthesized high quality VO<sub>2</sub> thin films on flexible glass substrates by RF sputtering system which showed a resistivity change of over 3 orders of magnitude across the MIT. Here we present the direct observation of the strain dynamics and the intrinsic modulation process by external strain in the VO<sub>2</sub> thin films. We observed that the MIT of the obtained VO<sub>2</sub> films can be modulated continuously via the external strain. These findings open the possibility of active tuning of transition for thin VO<sub>2</sub> films through the external strain engineering.

### Keywords:

Strain Engineering, Vanadium Dioxide Thin Films, Flexible Glass Substrates

## Rectification current in kicked nano-shuttle

핀관 친\*<sup>1</sup>, PARK Hee Chul\*<sup>1</sup>  
<sup>1</sup>기초과학연구원 복잡계 이론물리 연구단  
qinpq@ibs.re.kr, hcpark@ibs.re.kr

### Abstract:

We studied the electronic and mechanical dynamics of a driven nano-shuttle containing interplay between electrostatics and mechanical dynamics. We consider two different cases of sinusoidal force: one is single side potential driving and the other is both potentials driving on the leads. In case of time-dependent driving force, there are different stabilities in the nano-shuttle according to the two forces. The nano-shuttle is electrically excited by two external periodic forces. The forces consist of sinusoidal and kicked force with different frequencies causing the parametric amplification and chaos, respectively. The parametric amplification causes in Arnol'd tongues, unstable regions in the parameter space, and the chaos is determined by the positive Lyapunov exponent. In addition to the mechanics, the electric current does not only reflect the mechanical motions but electric force also affects mechanical motions. It is well-known that the symmetric shuttle cannot generate the rectified current as the symmetry cancels out symmetric current when the current is averaged. However, it can be shown that the average current is not ignored when the system undergoes the external force manipulating chaotic behavior or the system spontaneously breaks the symmetry. Interestingly, this nonzero rectified current exists in both regular and chaos motions. Kick generates new periodicity in the system and modulations of periodic motions such as quasi-periodicity and chaos. For some special kick-period and strength, the unusual rectified currents are induced in all of Arnol'd tongues. These effects make the kicked driven force highly useful in the realistic application of the nano-shuttle.

### Keywords:

Nano-shuttle, Kicked driven dynamics, Left-right symmetry, Non-zero rectification current, Chaos

## Probing Viscoelasticity of Silver-Ionic Liquid Marbles with Atomic Force Microscopy

심재원\*<sup>1</sup>, 고준혁<sup>1</sup>, 안상민<sup>1</sup>, 제원호\*<sup>1</sup>

<sup>1</sup>서울대학교 물리학과

jwshim0507@snu.ac.kr, whjhe@phya.snu.ac.kr

### Abstract:

The liquid marble generally consists of hydrophilic liquid droplet and micro-, nano sized hydrophobic particles. Such counter-intuitive system has unique interfacial structure associated with surface issues. Though many studies have been performed with their unique structures, the values of surface tension and surface energy are still under controversial. For example, conventional studies by using contact angle measurement with optical microscopies have limitations such as inaccuracy near the micro-litre scales [1].

In this study, we investigated surface tension and surface energy of silver-ionic liquid marbles with a quartz tuning fork-atomic force microscopy with large distance piezoelectric transducer. We choose ionic liquid to form a liquid marble, because unlike water based liquid marble, ionic liquid marble is extremely stable since ionic liquids show low vapour pressure [2]. Such liquid marbles were fabricated by using 1 $\mu$ m sized silver particles converted to the superhydrophobic via silanization process, then applying them onto micro-, nano litre ionic liquid droplets. The resulting liquid marbles displayed a more densely closed packed surface structure than natural lycopodium based liquid marbles which is generally tested. Then we obtained approach/retraction curves to z-axis from the substrate, and elasticity and viscosity of liquid marbles were measured and decomposed from signal analysis. Viscoelastic forces will lead the ways to understand the surface tension and surface energies of silver-ionic liquid marbles [3].

### References

- [1] E. Bormashenko et al., Colloids and Surfaces A., 425, 15-23 (2013)
- [2] L. Gao and Thomas J. McCarthy, Langmuir, 23, 10445-10447 (2007).
- [3] Manhee Lee and Wonho Jhe, Phys. Rev. Lett., 97, 036104 (2006).

### Keywords:

Liquid marble, Surface energy, Viscoelasticity

## Electron spin resonance study of hydrogen-incorporated topological insulator $\text{Bi}_2\text{Se}_3$

이철의\*<sup>1</sup>, 이여진<sup>1</sup>, 이규원<sup>1</sup>

<sup>1</sup>고려대학교 물리학과  
rscel@korea.ac.kr

### Abstract:

We have studied electron spin resonance (ESR) in topological insulator bismuth selenide ( $\text{Bi}_2\text{Se}_3$ ) nanoparticles with hydrogen introduced by hydrothermal synthesis with linear polymer polyvinyl pyrrolidone (PVP). The temperature dependence of ESR signals, believed to arise from the hydrogen donors, was investigated to obtain information on the carrier dynamics in the topological insulator. Furthermore, effects of surface-to-volume ratio increased by mixing with insulating  $\text{Al}_2\text{O}_3$  nanoparticles were also studied by the ESR measurements.

### Keywords:

Topological insulator,  $\text{Bi}_2\text{Se}_3$ , Nanomaterials, Electron Spin Resonance

## Effects of $\text{CaTiO}_3$ buffer layer on electrical-transport properties of $\text{LaAlO}_3/\text{SrTiO}_3$ heterostructure.

최민우<sup>1, 2</sup>, 송종현\*<sup>1</sup>, 김진희<sup>2</sup>

<sup>1</sup>충남대학교 물리학과, <sup>2</sup>한국표준과학연구원 양자기술연구소  
songjonghyun@cnu.ac.kr

### Abstract:

Two-dimensional electron gas (2DEG) is formed between the band insulators  $\text{LaAlO}_3$  and  $\text{SrTiO}_3$  and has various characteristics such as ferromagnetism and superconductivity. However, device applications have been hampered by its limited low mobility. In this study, we fabricate a heterostructure which a  $\text{CaTiO}_3$  is inserted as a buffer layer to improve the low mobility. Epitaxial  $\text{SrTiO}_3/\text{LaAlO}_3/\text{SrTiO}_3/\text{CaTiO}_3$  thin films heterostructure were grown on  $\text{SrTiO}_3$  (001) substrate by Pulsed Laser Deposition to investigate the effects of  $\text{CaTiO}_3$  buffer layer. The quality of the films and epitaxial relation to the  $\text{SrTiO}_3$  substrates were investigated by HR-XRD and AFM. Electrical-transport properties were measured using the PPMS. As a result, it is expected that the mobility of the system will be improved depending on the thickness of the  $\text{CaTiO}_3$  buffer layer. However, our experimental results show that inserted  $\text{CaTiO}_3$  buffer layer destroys the conducting interfacial 2DEG. We suggest that 2DEG destruction caused by surface roughness and strain-induced polarization of  $\text{CaTiO}_3$  buffer layer.

### Keywords:

Two-dimensional electron gas, 2DEG,  $\text{LaAlO}_3/\text{SrTiO}_3$ , perovskite

## Capillary condensation considering curvature effect with Kelvin and Tolman equation

제원호\*<sup>1</sup>, KIM Seongsoo<sup>1</sup>, KIM Dohyun<sup>1</sup>, AN Sangmin<sup>1</sup>

<sup>1</sup>서울대학교 물리학과  
whjhe@phya.snu.ac.kr

### Abstract:

Capillary condensation is heterogeneous nucleation of water molecules on confined geometry such as a wedge-like crack on a solid or nanometer-size gap between two surfaces. It is a ubiquitous phenomenon and plays a significant role in friction, adhesion and cloud formation [1]. Capillary condensation is described by Kelvin equation, but its validity in nanoscale was questioned [2]. Here we show that Kelvin equation should be modified by considering curvature dependence on surface tension. This could be done by inserting Tolman equation onto Kelvin equation [3]. We implemented quartz tuning fork (QTF) based atomic force microscopy (AFM) to detect and manipulate nanoscale water meniscus. This enables precise measurement of tip-sample distance where capillary condensation occurs. We have earned Tolman length of water as 0.2 nm, which is an important parameter regarding curvature dependence on surface tension and this is consistent with theoretical predictions [4]. Our result gives deep understanding of capillary condensation and the associated nature phenomena such as the role of aerosols in cloud formation.

### References

- [1] M. Yarom, A. Marmur, *Adv. Colloid Interface Sci.* **222**, (2015).
- [2] L. R. Fisher, J. N. Israelachvili, *Nature* **277**, 548-549 (1979).
- [3] R. C. Tolman, *J. Chem. Phys.* **17**, 333 (1949).
- [4] D. Kashchiev, *J. Chem. Phys.* **118**, 9081 (2003).

### Keywords:

Capillary condensation, Kelvin equation, Tolman equation, surface tension

## Study of hydrogen interaction with sulfur vacancy on the MoS<sub>2</sub> surface

HAN Sang Wook<sup>1</sup>, CHA Gi-Beom<sup>1</sup>, HONG S. C.\*<sup>1</sup>, KIM Kyoo<sup>2</sup>, MIN B. I.<sup>2</sup>

<sup>1</sup>Department of Physics and EHSRC, University of Ulsan, <sup>2</sup>MPPC\_CPM and Department of Physics, University of Science and Technology  
schong@ulsan.ac.kr

### Abstract:

Identifying and designing defects are critical steps in the development of a semiconductor. Here we report the hydrogen interaction with natural and artificial defects on the MoS<sub>2</sub> surface in the UHV chamber using angle-resolved photoemission spectroscopy supported by density functional theory calculations. It has long been understood that the coordinatively unsaturated sites at the edge of MoS<sub>2</sub>, i.e., the exposed metallic Mo sites, are crucial to the catalytic activity of MoS<sub>2</sub> for hydrogen evolution, while the basal plane of MoS<sub>2</sub> is catalytically inactive. Accordingly, layered MoS<sub>2</sub> showed a prominent hydrogen evolution reaction (HER) by increasing the number of edge sites. Hence, designing MoS<sub>2</sub> nanostructures with more edge sites has become a significant topic. Very recently, in a different way, single sulfur vacancies (V<sub>S</sub>) on the basal plane of monolayer MoS<sub>2</sub> enhanced the HER activity nearing the efficiency of Pt. However, the increase in catalytic activity resulting from Ar plasma treatment is considered to be mainly due to edge sites by the creation of crack instead of V<sub>S</sub> defects. In contrast, it has been expected that sulfur atoms can be sputtered away predominantly from the top (V<sub>S</sub>) or bottom layers (V<sub>S2</sub>) depending on the angle of incidence, ion type and energy. Thus, it needs to resolve how the presence of V<sub>S</sub> defects fundamentally alters the catalytic property of the basal plane of MoS<sub>2</sub>. The hydrogen interaction elucidates the polarity switching of n-type and p-type conductivities at the position having a high density of sulfur vacancy. This finding reveals a unifying mechanism for the origins of both n-type and p-type conductivities.

### Keywords:

MoS<sub>2</sub>, defect, hydrogen interaction, band structure engineering

## Effect of the surface potential variation on aggregation of surface functionalized Si QDs

한문섭\*<sup>1</sup>, 정남식<sup>1</sup>, 주범수<sup>1</sup>

<sup>1</sup>서울시립대학교 물리학과  
mhan@uos.ac.kr

### Abstract:

There have been much studies for strong light emission in silicon quantum dots(Si QDs). Recently, through the chemical synthetic methods, colloidal silicon quantum dot have been much attention because luminescence properties can be tuned easily in all visible range by surface modification with various chemicals. The Si QDs fabrication by chemical methods is very powerful for optoelectronic application such as light emitting diode and solar cell. However, for the Si QDs dispersion in water and organic solvent, aggregation is very severe problem to suppress considerably luminescence of Si QDs and degrade storage stability due to surface polarity of QDs in solvent.

In this work, we fabricated surface functionalized Si QDs and controlled the extent of aggregation by varying the pH of colloidal Si QDs. To understand the luminescence of Si QDs with surface potential variation in solvent, we performed photoluminescence spectroscopy, fourier transform infrared spectroscopy, dynamic light scattering and transmission microscopy. By analyzing the experimental results we observe that as pH of solution is decreased, Si QDs are well dispersed in solution and enhance strongly luminescence intensity. We conclude that we can achieve strong luminescence by decreasing the pH of solution which disperses well Si QDs in solvent.

[Acknowledgements : NRF-2016M2B2A4912288, NRF-2015R1D1A1A01060381]

### Keywords:

Surface potetial variation, Silicon quntum dots, Aggregation, pH,

## Flexoelectric polarizations of ferroelastic domain walls in $WO_3$ thin films

양찬호\*<sup>1</sup>, 윤신희<sup>1</sup>

<sup>1</sup>한국과학기술원 물리학과  
chyang@kaist.ac.kr

### Abstract:

In the early 1900,  $WO_3$  single crystal had been considered as a ferroelectric material because of the domain structure similar to that of  $BaTiO_3$  [1,2]. However, the studies on crystalline structure revealed that the unit cell of bulk  $WO_3$  at room temperature is centrosymmetric and monoclinic phase (space group:  $P2_1/n$ ), which is non-ferroelectric. By using misfit strain, we have grown heteroepitaxial  $WO_3$  films with well-aligned ferroelastic twin domains at the nanoscale, showing piezo-responses. Although the quantitative values of it couldn't be measured here due to the absence of bottom electrodes, we tried to explain the qualitative flexoelectric-polarizations of ferroelastic domains & walls with the crystal-structural analyses.

- [1] B. T. Matthias, *Phys. Rev.*, **76**, 430 (1949)  
[2] R. Ueda *et al.*, *Phys. Rev.*, **80**, 1106 (1950)

### Keywords:

flexoelectric, twin, ferroelastic, oxide, film, epitaxial, perovskite,  $WO_3$

## First-principles study of mixed-dimensional (2D-MoS<sub>2</sub>/3D-GaN) heterostructures

홍석륜\*<sup>1</sup>, SUNG Dongchul<sup>1</sup>, MIN Kyung-Ah<sup>1</sup>

<sup>1</sup>Department of Physics, Sejong University  
hong@sejong.ac.kr

### Abstract:

Recently the concern with 2-dimensional (2D) and 3-dimensional (3D) heterostructures has been increasing because of the designing of nanodevices using those heterostructures. As a typical 2D transition metal dichalcogenides, MoS<sub>2</sub> has good characteristics for application of semiconductor devices due to suitable bandgap, high on/off ratio, and high electron mobility. On the other hand, GaN is 3D material showing enormous applications in high efficiency electronic and optoelectronics devices such as high electron mobility transistors and light emitting diodes. Previously, the growth of 2D MoS<sub>2</sub> directly onto the GaN surfaces has been reported [1]. From this experimental result, the MoS<sub>2</sub>/GaN heterostructures were shown to electrically conduct in out-of-plane direction and across the van der Waals gap. In this regard, we have performed density functional theory calculations to study the interfaces between MoS<sub>2</sub> and GaN. Interestingly, GaN has two different surface terminations surfaces such as Ga-terminated (0001) and N-terminated (000-1) configurations. We consider these two terminations to investigate the difference in their interactions with MoS<sub>2</sub>. As a result, we find that the surface states disappear for the case of MoS<sub>2</sub> on Ga-terminated GaN structure, while the surface state is hybridized with MoS<sub>2</sub> near the Fermi level for the case of N-terminated GaN configuration. Furthermore, we investigate the variation in electronic structure of MoS<sub>2</sub>/GaN heterostructures depending on the number of layer.

[1] D. Ruzmetov et al, ACSNano **10**, 3580 (2016).

\* Corresponding author: hong@sejong.ac.kr

### Keywords:

Mixed-dimensional, heterostructure, MoS<sub>2</sub>, GaN, Density Functional Theory

## Investigations of MnPS<sub>3</sub>-Au contacts using first-principles calculations

CHOI Hyunsoo<sup>1</sup>, MIN Kyung-Ah<sup>1</sup>, 홍석륜\*<sup>1</sup>

<sup>1</sup>Department of Physics and Graphene Research Institute, Sejong University  
hong@sejong.ac.kr

### Abstract:

Since the discovery of graphene which is one of representative two-dimensional (2D) materials, various 2D materials have been actively explored due to their notable physical and chemical properties. However, magnetic van der Waals (vdW) materials have not been much investigated in 2D materials. In this connection, metal phosphorous trichalcogenides (MPTs) have drawn much attention as new 2D magnetic vdW materials: MPT consists of one transition metal (M), one phosphorous (P) and three chalcogen (X) atoms by showing the magnetic properties at room temperature with good electrical properties. Here, we focus on MPT and metal contacts for various device applications. In this study, we have performed density functional theory (DFT) calculations to investigate atomic and electronic structures of MPT on metal substrate: we consider MnPS<sub>3</sub> as 2D MPT and Au(111) as metal substrate. Details are analyzed by partial density of states (PDOS), band alignment and work function.

### Keywords:

MPTs, band alignment, DFT, magnetic vdW materials

# First-principles study of $WS_2/Si$ van der Waals heterostructures under an external electric field

홍석륜\*<sup>1</sup>, MIN Kyung-Ah<sup>1</sup>

<sup>1</sup>Department of Physics and Graphene Research Institute, Sejong University  
hong@sejong.ac.kr

## Abstract:

Mixed-dimensional van der Waals (vdW) heterostructures including two-dimensional (2D) materials are in the limelight for various applications in electronic and optoelectronic devices. Especially, 2D transition metal dichalcogenides (TMDs) are being actively investigated for realization of such mixed-dimensional heterostructures with their attractive atomic and electronic properties. For example, 2D/three-dimensional (3D) vdW semiconductor heterostructures including 2D TMDs such as  $MoS_2$  [1] and  $WS_2$  [2] were fabricated by showing the excellent diode-like rectification behaviors. In this connection, we investigate the atomic and electronic structures of  $WS_2/Si$  vdW heterostructures using first-principles calculations. The rectification behaviors in  $WS_2/Si$  heterostructures are explained by considering the external electric field in the calculations. Furthermore, we study the effect of external electric field on the band alignment of  $WS_2/Si$  heterostructures depending on the number of  $WS_2$  layers. Details in electronic structure are analyzed in terms of partial density of states (PDOS) and charge density difference.

[1] S. Mukherjee, S. Biswas, S. Das, and S. K. Ray, *Nanotech.* **28**, 135203 (2017)

[2] C. Lan, C. Li, S. Wang, T. He, T. Jiao, D. Wei, W. Jing, L. Li, and Y. Liu, *ACS Appl. Mater. Inter.* **8**, 18375-18382 (2016)

## Keywords:

$WS_2$ , Si, 2D/3D heterostructures, external electric field, first-principles calculations

## MoS<sub>2</sub>/그래핀 접합 소자의 전하이동도 측정

김영철<sup>1</sup>, NGUYEN Van Tu<sup>1</sup>, 이순일<sup>1</sup>, 박지용<sup>1</sup>, 안영환\*<sup>1</sup>

<sup>1</sup>아주대학교, 물리학과 및 에너지시스템학과  
ahny@ajou.ac.kr

### Abstract:

본 연구에서는 화학기상증착법(CVD)을 이용해 MoS<sub>2</sub>와 그래핀 접합소자를 제작하고 확산거리와 전하이동도에 대해서 연구하였다. 우선, 광전류 현미경을 이용하여 MoS<sub>2</sub>/그래핀 접합면의 국소적인 광전신호와 전체소자의 수송특성과의 상호관계를 연구하고, 전자 및 정공의 확산거리를 MoS<sub>2</sub> 및 그래핀 층에 대하여 각각 측정하였다. 또한, 펄스초 광전류 측정법을 활용하여, 각 층의 재결합 수명을 관측하고 앞서 측정된 전하확산거리 정보와 결합하여, 최종적으로 전하이동도를 얻어내었다. 일반적으로, n형으로 작동하는 MoS<sub>2</sub> 소자는 다수캐리어인 전자의 이동도만 측정이 가능하며, 그 값이 전체 소자의 특성을 반영하는 반면, 본 접근법을 통해서 전자 및 정공의 수송 특성을 동시에 관측할 수 있으며, 나노물질의 고유의 값에 근접하는 결과를 얻어낼 수 있다.

### Keywords:

MoS<sub>2</sub>, 그래핀, 전하이동도, 광전류현미경

## *Ab initio* study of atomic and electronic structures of metal monochalcogenides on Si(111)

홍석륜\*<sup>1</sup>, [KIM Junghwan](#)<sup>1</sup>

<sup>1</sup>Department of Physics and Graphene Research Institute, Sejong University  
[hong@sejong.ac.kr](mailto:hong@sejong.ac.kr)

### Abstract:

In recent years, graphene has attracted various attention from the scientific community with its excellent atomic and electronic properties. Upon this opportunity, many scientists have studied many two-dimensional (2D) materials such as transition metal dichalcogenides (TMDs) and metal monochalcogenides (MMCs) from various angles. Among various 2D materials, we consider MMCs in this study for potential applications to nanodevices. Especially, we investigate 2D/three-dimensional (3D) heterostructures of MMC/Si using density functional theory (DFT) calculations. Here, we consider gallium sulfide (GaS), gallium selenide (GaSe), and gallium telluride (GaTe) as MMC materials: GaS, GaSe, and GaTe are semiconductor with indirect band gap of 3.19, 2.10, and 1.67 eV, respectively. In terms of partial density of states (PDOS) and work function of MMC/Si heterostructures, we investigate the interaction between diverse MMC and Si(111) for device applications of their heterostructures.

### Keywords:

2D materials, metal monochalcogenides(MMCs), density functional theory(DFT), 2D/3D heterostructures

## Facile Fabrication of Nanostructures with High Aspect Ratio by using High Voltage Electrohydrodynamic Lithography

강대준\*<sup>1</sup>, 박현제<sup>1</sup>, 황재석<sup>2</sup>, 이재종<sup>3</sup>

<sup>1</sup>성균관대학교 물리학과, <sup>2</sup>성균관대학교 에너지과학과, <sup>3</sup>한국 기계 연구원  
dj kang@skku.edu

### Abstract:

Fabrication of nanoscale structures is of great importance in nanotechnology and microelectronics industry. The main issues of the fabrication process have been its high cost and limited resolution for the past few decades. For these reasons, several innovative lithography have emerged as an alternative to resolve those issues. Among these, electrohydrodynamic lithography (EHL), a novel method that uses electrostatic instability, has drawn attention due to its great versatility and scalability. In this work, we demonstrate the technical flexibility of EHL through fabrication of novel patterns. More specifically, the high aspect ratio and cone-like shape patterns were realized *via* High Voltage-EHL (HV-EHL). The existing way of EHL has an air gap of  $< 500$  nm between the top electrode and the top surface of the resist. In this experiment a time varying high power voltage pulse ( $> 800$  V) was applied to prevent any dielectric breakdown and to insure an air gap of  $> 3$   $\mu\text{m}$  was maintained during the EHL patterning. Consequently, the high aspect ratio and conical shape patterns which were challenging to produce by the traditional approach were successfully realized. Considering the fact that the aspect ratio is directly related to the time dependent undulation evolution which is again dependent on manageable parameters such as reaction time and thin film thickness, it is asserted that HV-EHL facilitates the control of aspect ratio.

### Keywords:

Aspect ratio, Electrohydrodynamic instability, Lithography

## Current status of neutron triple-axis spectrometers (TASs) and renovation of TAS devices in HANARO

LEE Jisung<sup>1</sup>, HIRAKA Haruhiro\*<sup>1</sup>, CHO Sangjin<sup>1</sup>, RYU Jimyung<sup>1</sup>, JEON Byoungil<sup>1</sup>, PARK Sungil<sup>1</sup>, SEONG Baek-Seok<sup>1</sup>

<sup>1</sup>Neutron Science Center, Korea Atomic Energy Research Institute  
hiraka@kaeri.re.kr

### Abstract:

Since the construction of the research reactor HANARO in KAERI, many neutron instruments have been developed and installed in the thermal-neutron reactor hall and in the cold-neutron guided hall. Speaking of triple-axis neutron spectrometers (TASs), there are two machines in HANARO; one is Thermal-TAS in the reactor hall, and the other is Cold-TAS in the guided hall.

The Thermal-TAS is now in the construction phase. Using the long shutdown period of HANARO, we renovated the monochromator drum to improve not only the mechanical motion but also the radiation shielding power. Then, we rechecked the optical line up from the monochromator to the detector, via the sample and analyzer. On the other hand, the Cold-TAS is in the commissioning phase at present. Even the Cold-TAS, we renewed the monochromator shield to modify the structural defects. Before the HANARO restart, we will tune up the neutron-velocity selector.

Beside the above upgrading works, we are promoting a renovation program of neutron scattering devices for TASs in parallel. For example, we recently fabricated a total-reflection combining collimator at in-house. The numerical simulation results of the collimator performance will be also presented.

### Keywords:

Neutron scattering, Total-reflection combining collimator, Triple axis spectrometer, HANARO.

## Surface chemical structure of SrRu<sub>3</sub>O on SrTi<sub>3</sub>O (001) during vacuum and oxygen annealing

문봉진\*<sup>1, 3</sup>, 임호준<sup>1</sup>, 김동우<sup>1</sup>, 유영석<sup>1</sup>, 김건화<sup>1</sup>, 정문정<sup>1</sup>, 조삼연<sup>2</sup>, 부상돈<sup>2</sup>

<sup>1</sup>Department of Physics and Photon Science, GIST, Gwangju 61005, Korea, <sup>2</sup>Department of Physics, Chonbuk National University, Jeonju 54896, Korea, <sup>3</sup>Center for Advanced X-ray Science (SRC), Gwangju 61005, Korea  
bsmun@gist.ac.kr

### Abstract:

In research of nonvolatile ferroelectric devices, the role of SrRu<sub>3</sub>O (SRO) as electrode materials has recently attracted much attentions. Especially, the understanding of the surface structure of SRO under various environment has become important as the inhomogeneous stoichiometry of SRO can degrade device performance. To characterize an annealing effect on surface, the chemical composition of SRO films is investigated as a function of temperature using ambient pressure x-ray photoelectron spectroscopy (AP-XPS) under both vacuum and oxygen environment. The SRO films were deposited by sputtering method on SrTi<sub>3</sub>O (001) epitaxially with step-flow growth mode. The surface of the film was cleaned by annealing ( $T \sim 450$  °C) under  $10^{-7}$  Torr of O<sub>2</sub> atmosphere. In the case of vacuum annealing (up to 650 °C, under  $10^{-8}$  Torr), the spectra analysis shows the shift of O 1s peak to lower binding energy side, showing the sign of reduction process. On the other hand, in the case of oxygen annealing (up to 650 °C, under 500 mTorr of O<sub>2</sub> pressure), O 1s peaks are shifted to higher binding energy, showing the sign of oxidation process as expected. The result of AP-XPS shows the evidence that the introduced oxygen gas interacts with the surface and there are significant changes on Sr peaks rather than Ru peaks during oxygen annealing process.

### Keywords:

AP-XPS, SRO, oxygen annealing effect, surface structure

## Single Particle Imaging at PAL-XFEL

송창용\*<sup>1, 2</sup>, 조도현<sup>1</sup>, 정철호<sup>1</sup>, 성대호<sup>1</sup>, 이희민<sup>1</sup>, 남대웅<sup>2</sup>, 김상수<sup>2</sup>  
<sup>1</sup>포항공과대학교 물리학과, <sup>2</sup>포항가속기연구소  
cysong@postech.ac.kr

### Abstract:

Single particle imaging is one of the key experiment which is actively developed in X-ray Free Electron Lasers (XFELs). XFELs high intensity and short pulse duration enables 'diffraction-before-destruction' scheme. In addition, high spatial coherence of XFELs enables coherent diffraction imaging, which can image the projected electron density of non-crystalline sample. Furthermore, three-dimensional view of inner structure of sample can be imaged without sectioning. We will present tomographic image of core-shell nanoparticle by using PAL-XFEL.

### Keywords:

XFEL, single particle imaging, hard x-ray, tomography

## Hard X-ray Emission Spectroscopy of Metallic and Insulating VO<sub>2</sub> Thin Films

하성수<sup>2</sup>, 최석준<sup>1</sup>, 황병준<sup>1</sup>, 오호준<sup>1</sup>, MOHD Faiyaz<sup>1</sup>, 윤영민<sup>1</sup>, 한승현<sup>1</sup>, 조인화<sup>1</sup>, 김진우<sup>1</sup>, 이수용<sup>3</sup>, 노도영\*<sup>1</sup>  
<sup>1</sup>광주과학기술원 물리광학과, <sup>2</sup>광주과학기술원 신소재공학부, <sup>3</sup>포항가속기연구소 3세대 빔라인부  
dynoh@gist.ac.kr

### Abstract:

High-resolution X-ray emission spectroscopy (XES) was carried out in the 3rd generation Pohang Accelerator Laboratory using von-Hamos geometry with highly oriented pyrolytic graphite (HOPG) to study the metal-insulator transition (MIT) of vanadium dioxide. The Vanadium K-beta emission spectra including  $k_{\beta 2,5}$  and  $k_{\beta 1,3}$  both in the metallic and insulating phase were monitored with an x-ray energy resolution of about 1.6 eV. The energy of x-rays exciting the Vanadium K-shell electrons was scanned through the Vanadium K-edge. In addition, the K-beta emission intensity was plotted according to the excitation x-ray energy to obtain the X-ray absorption near edge structure (XANES) profile. In the XANES profile, the difference between the insulating and metallic phase was clearly observed. Elastic scattering, vanadium were measured in one-shot CCD camera image.

### Keywords:

Emission, XES, VO<sub>2</sub>, k-beta, von-Hamos, HOPG, XANES

## Development of X-ray diffraction system and data conversion software using two-dimension detector

이현휘\*<sup>1</sup>, 김상우<sup>1</sup>, 최형주<sup>1</sup>

<sup>1</sup>포항공대 포항가속기연구소 3세대 빔라인운영부  
hhleexrs@gmail.com

### Abstract:

X-ray diffraction with conventional point detector is a well-established technique that has played the major role in various fields. However, the demand for faster measurements is growing. For example, it is intended to observe changes in the diffraction pattern over short time or to avoid damaging the specimen due to the high dose of radiation. Typical diffraction experiment takes tens of minutes to hours, making these problems inevitable. Due to these limitations, we constructed a system that can significantly reduce time by using a two-dimensional area detector. In this presentation, measurement system and data conversion software which is installed at 5A beamline, PLS-2 will be presented.

### Keywords:

X-ray, area detector, software

## Single pulse measurements using pink XFEL beam for high resolution resonant x-ray emission spectroscopy

IJAZ Anwar<sup>1</sup>, IQBAL Mazhar<sup>1</sup>, HWANG Byung-Jun<sup>1</sup>, MOHD Faiyaz<sup>1</sup>, OH Sang Hyun<sup>1</sup>, NOH Do Young\*<sup>1</sup>

<sup>1</sup>광주과학기술원 물리광학과  
dynoh@gist.ac.kr

### Abstract:

X-ray emission spectroscopy based on synchrotron radiation sources has been widely used to probe electronic structure, occupied electronic levels, information about the ligands and spin/charge densities (1-3). In order to perform comprehensive pump-probe studies it remains challenging to capture high-resolution x-ray emission spectra by scanning the energy of monochromatic x-ray beam despite the high brilliance of x-ray free electron lasers(XFELs) due to the time required to scan incident x-ray energy at each time delay. In this work, we present a new scheme for measuring the Resonant X-ray Emission Spectroscopy (RXES) in a shot-by-shot measurement mode by using broad pink XFEL beam. We measured the energy profile of the incident beam as well as the  $K\beta_{1,3}$  x-ray emission from the NiO samples at the Pohang XFEL. Each self-amplified spontaneous emission (SASE) of XFEL pulse exhibits an energy spectrum which has a specific peak structure. By selecting all the pulses that has a peak at a specific position, we were able to obtain an x-ray emission spectrum similar to the one measured with a monochromatic beam at that peak energy. The study casts the feasibility of RXES using broad pink XFEL pulses instead of the monochromatic beam to monitor the electronic state of the sample, which will be critical for the time resolved pump-probe measurement of x-ray emission spectroscopy by reducing the measurement time greatly.

### Keywords:

XES, XFEL, NiO, RXES

# Optimum Control Program for Helium Recovery System Based on Thermal Equation

오윤석\*<sup>1</sup>, 박대환<sup>1</sup>

<sup>1</sup>Department of Physics, Ulsan national institute of science and technology, Ulsan, Korea  
ysoh@unist.ac.kr

## Abstract:

Nowadays, liquid helium is one of essential resource for modern civilization in which it is utilized to cool down the superconducting magnet devices in various fields, such as magnetic resonance image (MRI), nuclear magnetic resonance (NMR) spectroscopy, and research on nuclear fusion reactor, etc. However, unfortunately, the helium resource is very limited on Earth. Therefore, one has been looking for the way to minimize loss and consumption of helium in those application. As an idea, a system is suggested to trap the evaporating helium gas and liquefy liquid helium, so called helium recovery system or helium recovery plant. A couple of companies have manufactured helium recovery system for laboratory/hospital and helium recovery plant for the large facility. The helium recovery system liquefies using the 4K cryocooler so that it can be operated in the relatively small space. However, its conventional operation needs constant cooling down with the cryocooler, which causes high maintenance cost about \$30,000 in a year. Thus, new control method is required to reduce cost of the maintenance of the helium recovery system. We designed IoT (Internet of Things) based program to extend effective lifetime of the cryocooler. The program optimizes operation time of the cryocooler using thermal equations of the liquefaction system. In addition, it displays real-time status of the cryocooler. Eventually we demonstrate to extend the lifetime of cryocooler up to 300%.

## Keywords:

Helium recovery system

## X-ray tube fabricated by the cold cathode with a spun-CNTs

김현숙\*<sup>1</sup>, 이충훈<sup>1, 2</sup>, 박래준<sup>3</sup>

<sup>1</sup>원광대학교 차세대방사선산업기술센터, <sup>2</sup>원광대학교 반도체디스플레이학부, <sup>3</sup>(주)엑스엘  
nanohskim@wku.ac.kr

### Abstract:

In this research we report the significant contribution of the as-spun multi-walled carbon nanotube yarn (MWCNT-yarn) on the X-ray images formation using a low voltage x-ray source. The MWCNT-yarn, which was used for the fabrication of the spun CNT, was grown using a thermal chemical vapor deposition. The MWCNT-yarn had been widely used for various applications due to its impressive properties including field emission among others. However, problems including short lifetime at high current density, instability under high voltage and poor emission uniformity are still major obstacles for device applications. We fabricated x-ray tube by the cold cathode with high current density and long-term stability. Electrical-optics simulation software was utilized to determine the electron field emission trajectory of the diode-structure as-spun CNT-based x-ray source. The MWCNT yarn field emitters can be used for low voltage application because of their field enhancing effect that may be attributed to its shape and to the protrusions at the side contributing in the field emission process. So, It will show that a significant amount of converging electrons hit the target anode producing a clear x-ray image. This study can be used for low-voltage medical applications.

### Keywords:

MWCNT, CNT-yarn field emitter, X-ray tube

## A high sensitive humidity sensor using guided-mode resonance in the terahertz region

신희준\*<sup>1</sup>, 박기상<sup>1</sup>, 임민철<sup>1</sup>, 최성욱<sup>1</sup>, 옥경식<sup>1</sup>

<sup>1</sup>한국식품연구원 식품안전연구단  
sheejuns@uos.ac.kr

### Abstract:

We propose the relative humidity (RH) sensor with high sensitivity, low cost and simple fabrication using a polymer-based guided-mode resonance (GMR) structure in the terahertz frequency range. We designed the GMR structure with resonance frequency of near 250 GHz and polyvinyl alcohol (PVA) is used to increase sensitivity due to strong interaction with water contents. As the RH increased up to 70 % at room temperature, the terahertz transmittance is changed slightly at the GMR sensor without PVA, while transmittance is enhanced 15 % at the GMR sensor with PVA. From the numerical simulation using FDTD method, the water contents in the PVA layer are increased up to 6 % at the RH of 70 %.

### Keywords:

Guided mode resonance, Terahertz, Photomixing, Humidity sensing, Polymer

## THz circular dichroism based on stacked metal rods

LEE Chang-Won\*<sup>1</sup>

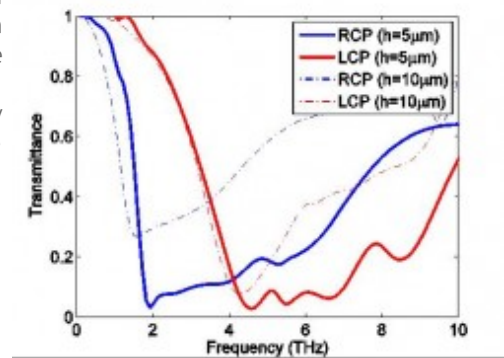
<sup>1</sup>School of Basic Sciences, Hanbat National University  
cwlee42@hanbat.ac.kr

### Abstract:

We propose a simple circular polarizer for 0.1 ~ 10 THz range based on helically stacked metal rods. The design is based on stacked gold rods with electric conductivity  $\sigma = 45.6 \times 10^6$  S/m forming a helical structure while maintaining geometric chirality. Fig. 1 shows transmittance spectra of such structures as a function of the height. The structure can be fabricated by CMOS-compatible processes, which enables mass production of the polarizer.

### Keywords:

THz, circular dichroism, circular polarizer



## 은나노선을 이용한 THz 플라즈모닉 소자의 감도 증대 연구

전승원<sup>1</sup>, 홍정택<sup>2</sup>, 안영환\*<sup>1</sup>

<sup>1</sup>아주대학교, 물리학과 및 에너지시스템학과, <sup>2</sup>한림대학교, 응용광물리학과  
ahny@ajou.ac.kr

### Abstract:

THz파 영역에서 작동하는 플라즈모닉 및 메타물질은 바이오 및 화학물질 등의 검출 분야에 광범위하게 사용하고 있으며, 검출 감도를 높이기 위한 다양한 연구가 활발히 진행 중이다. 본 연구에서는 THz파 슬롯안테나 구조에 은나노선 박막을 도포하여 새로운 하이브리드 소자를 제작하고, 폴리머 박막과 바이러스 검출에 적용하였다. 다양한 구조 변수에 따른 검출감도를 연구하여, 최대 6배에 달하는 검출감도 향상을 확인하였다. 또한, FDTD 전산모사를 통해 실험결과를 성공적으로 검증하였으며, 감도의 증대 원인이 슬롯 내부에 존재하는 은나노선의 나노구조에 의한 전기장 집중 및 증대 효과임을 확인하였다.

### Keywords:

THz파, 은나노선, 플라즈모닉스, 바이오센서

## 광섬유기반 베셀빔 소자를 이용한 입자 포획기술에서 빔모양의 특성에 따른 입자의 비선형성 운동량

박준범<sup>1</sup>, 오경환\*<sup>1</sup>  
<sup>1</sup>연세대학교 물리학과  
koh@yonsei.ac.kr

### Abstract:

본 연구는 광섬유기반을 통한 베셀빔과 자체 개발한 소자를 통해 입자포획 실험을 수행하였고, 입자의 물리량을 분석하였다. 그 실험을 통해서 베셀빔과 입자의 위치에 따라 빛의 세기가 강한 곳들에서 포획이 일어나는 것을 확인하였고, 단계적으로 입자가 중심방향으로 진행함을 보았다.

### Keywords:

광섬유 입자포획 베셀빔

## 고출력 녹색 레이저빔의 스페클 측정 및 완화

김지원\*<sup>1, 2</sup>, 송승빈<sup>1</sup>, 박은지<sup>1</sup>, 김동준<sup>1</sup>

<sup>1</sup>한양대학교 응용물리학과, <sup>2</sup>한양대학교 나노광전자학과  
jwk7417@hanyang.ac.kr

### Abstract:

고출력, 고품질의 녹색 레이저 빔은 생물학 및 의학, 현미경, 홀로그래피, 이미징, 디스플레이 등 다양한 분야에서 응용이 가능하므로, 좋은 빔 특성을 가지는 녹색 레이저 빔을 얻기 위해 많은 연구들이 보고되고 있다. 특히 레이저광을 이용한 이미징은 높은 휘도, 뛰어난 이미지 전송성, 방향성 등으로 인해 많은 관심을 받고 있다. 하지만 레이저광의 특성 중 하나인 높은 가간섭성(coherence)으로 인하여, 전송된 이미지는 스크린에서 이미지 이외의 불규칙한 간섭 무늬를 생성하게 되는데 이를 스페클 노이즈(speckle noise)라 한다. 스페클 노이즈는 이미지의 질과 선명도를 크게 저하시키므로 레이저광을 이용한 고해상도 이미지를 얻기 위해서는 이를 제거하는 것이 필수적이다.

본 연구에서는 고출력 녹색 레이저빔을 발진시킨 후 스페클 특성을 보고하고자 한다. Yb 광섬유를 사용하여 1  $\mu\text{m}$  영역대에서 발진하는 고출력 연속 발진 MOPA 레이저 시스템을 구축한 후, 출력빔을 MgO:PPSLT에 통과시켜 >10 W의 고출력 연속발진 녹색 레이저빔을 획득하였다. 그리고 생성된 레이저광의 스페클 특성을 관측하고, 여러 가지 방법을 사용하여 스페클의 감소 정도를 측정, 비교하였다.

이 연구는 경찰청과 치안과학기술연구개발사업단 주관 치안과학기술연구개발사업(PA-B000001)의 지원을 받아 수행된 연구임.

### Keywords:

Fiber laser, MOPA, Second harmonic generation, Green laser, Speckle noise

## GPU 가속을 이용한 스칼라 빔 전파 시뮬레이션 계산과 평가

이성윤<sup>1</sup>, 유태준\*<sup>1, 2</sup>

<sup>1</sup>한동대학교 첨단그린에너지환경학과, <sup>2</sup>한동대학교 글로벌녹색기술연구원 레이저기술연구소  
taejunyu@handong.edu

### Abstract:

빔 전파 시뮬레이션은 광선 추적에서 얻을 수 없는 빔의 간섭 효과에 의한 미세한 간섭 패턴을 계산할 수 있지만 큰 계산량을 요구한다. 이러한 계산은 보편적인 하드웨어인 GPU를 통해 병렬 처리를 함으로써 계산 효율성을 높일 수 있다. 본 연구에서는 GPU 가속의 사용 여부에 따른 두 가지 빔 전파 시뮬레이션을 수행하고, 계산 성능을 비교 및 평가하였다.

### Keywords:

빔 전파, GPU 가속

## 아크 방전에 조건에 따른 측면 발산 광소자의 특성 변화

최은서\*<sup>1</sup>, 김주하<sup>1</sup>, 강희원<sup>1</sup>, 이승석<sup>1</sup>

<sup>1</sup>조선대학교 물리학과

cesman@chosun.ac.kr

### Abstract:

광섬유는 개발 초기부터 현재까지 광통신에서의 신호 전달매체로서 주로 활용되었으나 최근 들어 다양한 기능이 추가된 광섬유 기반의 광소자 개발을 통해서 다양한 광응용분야에서 그 중요성이 증가되고 있다. 개발되는 광섬유 광소자 중에는 광섬유 끝단에 아크방전이나 레이저 조사를 통해 열적인 에너지를 적용함으로써 원형의 단면 모양을 원하는 형태의 특정한 곡률을 가지는 구형이나 비구면 형태로 가공한 광섬유 렌즈 또는 광센서 헤드가 있다. 이를 이용한 온도, 압력 그리고 습도 측정을 위한 광계측 연구도 다양하게 전개되고 있다. 이뿐만 아니라 기존 프로브로는 접근이 힘든 인체 장기 내부까지 원하는 특성을 가지는 광을 전달하고 이를 전면 뿐만 아니라 측면으로 고르게 발산하도록 하여 병변 치료의 효율을 향상시킬 수 있었다. 본 논문에서는 이러한 측면 발산이 가능한 광소자를 특수 광섬유를 대상으로 기존의 광섬유 용착기의 아크 방전 조건을 달리하여 제작을 하고 각각의 조건에 따른 측면 발산의 특성을 분석하고자 한다. 아크 방전의 시간과 방전 전압을 조절하고 그에 따른 발산각과 광손실을 계측하여 측면 발산광의 분포 특성을 분석하고자 한다. 또한 발산 특성과 함께 원통 내부 표면에서 반사되어 되돌아 오는 광의 광결합의 효율에 대해서도 분석하고자 한다.

This work was supported by the National Research Foundation of Korea (NRF) grant funded by the Korea government (MSIP) (No. 2017R1A2B2009732) and the Encouragement Program for The Industries of Economic Cooperation Region (grand no. R0004732).

### Keywords:

측면 발광, 아크 방전, 광섬유

## 그래핀의 광열효과를 기반으로 한 전광(all-optical) 광섬유 변조기

하성주<sup>1</sup>, 박남훈<sup>1</sup>, 최규홍<sup>1</sup>, 이현주<sup>1</sup>, 염동일\*<sup>1</sup>

<sup>1</sup>아주대학교, 물리학과 & 에너지시스템학과  
diyeom@ajou.ac.kr

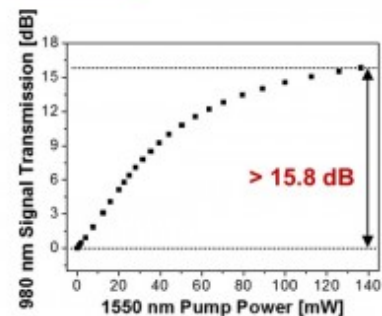
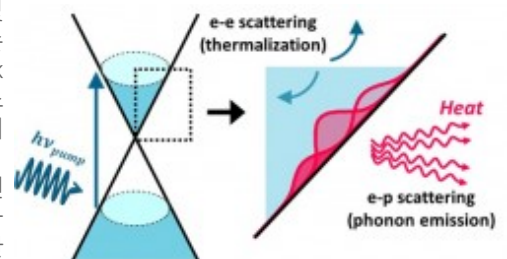
### Abstract:

전광(all-optical) 변조기는 빛으로 광신호를 제어하는 소자로서 광통신, 광센서 및 광신호 처리 분야 등에서 활용될 수 있다. 특히, 전광섬유(all-fiber) 변조기는 기존의 광통신 시스템과 호환성이 있으며 온도에 덜 민감하고, 후방 반사(back reflection)가 적은 장점을 가지고 있다. 현재까지 다양한 형태의 전광 광섬유 변조기에 대한 연구가 진행되고 있음에도 불구하고, 넓은 동작 파장대역에서 큰 변조세기와 작은 삽입손실을 가지는 소자는 아직 보고되지 있지 않다.

본 연구에서는 광대역에서 동작하는 그래핀의 광열효과를 기반으로 한 고효율 전광 광섬유 변조기를 개발하였다. 이를 구현하기 위하여 그래핀이 전사된 측면 연마 광섬유에 굴절률이 정합하는 상부클래딩을 도입하여 그래핀 층에서 감쇄파의 강한 흡수가 유도되도록 하였다. 이때 그래핀에서 빛의 강한 흡수로 여기된 전자들은 음성 발열을 거쳐 국소적인 열에너지로 전환되고, 이는 큰 열광계수를 지니는 상부클래딩 물질의 굴절률을 변화시킨다. 이를 통하여 광섬유를 도파하는 빛의 모드 분포가 변화되고 이에 따라 그래핀 층에 의해 흡수되는 빛의 양의 변화를 일으킨다. 결과적으로 그래핀 소자를 투과하는 빛의 세기가 효과적으로 조절될 수 있게 된다. 실험을 통하여 근적외선 대역의 다양한 파장에서 큰 변조세기를 가지는 전광 변조기 구현이 가능함을 확인하였다.

### Keywords:

graphene, photo-thermal effect, all-optical switch, all-fiber device

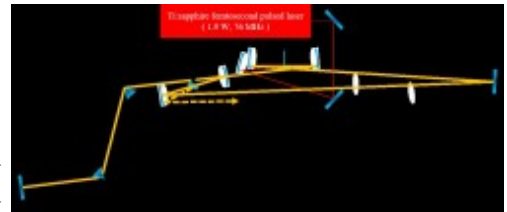


## Cavity dumped ring type optical parametric oscillator for near-infrared femtosecond pulses

이기주\*<sup>1</sup>, 박지연<sup>1</sup>  
<sup>1</sup>충남대학교 물리학과  
kyee@cnu.ac.kr

### Abstract:

Cavity dumping 방식의 광 파라메트릭 레이저는 출력 거울을 사용하는 일반적인 광 파라메트릭 레이저에 비해 출력 빔의 펄스 에너지가 크다는 장점을 가지고 있다. 이는 일반적인 출력 거울을 사용하는 방식은 출력 거울의 투과율이 낮아 공진기 내부를 공진하는 펄스에너지의 일부분만을 출력하지만, Cavity dumping 방식은 공진기 내부 펄스 에너지의 대부분을 출력하기 때문이다. 선형 공진기 구조를 가진 Cavity dumping 방식의 광 파라메트릭 레이저는 이미 보고 되어 왔다.<sup>1-2</sup> 그러나 선형 공진기 구조는 빔이 공진기 내부를 왕복할 때 이득 매질을 2번 통과하고 펌프 빔이 매질에 입사하지 않는 경우에도 이득 매질을 통과하여 추가적인 손실이 발생한다는 단점이 있다.



이를 보완하기 위해서 우리는 링형 공진기 구조를 가진 광 파라메트릭 레이저를 제작하고 이 공진기에 캐비티 덤핑 키트를 추가하여 링형 공진기 구조를 가진 캐비티 덤핑 광 파라메트릭 레이저 공진기를 제작하였다.

펌핑 광원으로는 평균 파워 1.9 W, 반복률 76 MHz, 중심파장 807 nm이고 7 nm 반치 폭의 펄스를 발진하는 티타늄 사파이어 레이저를 사용하였다. 이득 매질로는 0.5 mm 길이의 PPLN 결정을 사용하였다. 덤핑 매질은 3 mm 길이인 매질을 사용하였다. 공진 빔이 이득매질과 덤핑 매질을 통과하면서 발생하는 양의 균속도 분산을 보상해주기 위하여 SF10 재질의 프리즘 쌍을 공진기 내부에 설치하였다.<sup>3</sup> 두 프리즘 사이의 거리는 약 29cm 이다. 제작한 광 파라메트릭 레이저는 최대 출력 펄스 에너지는 100 nJ 이며, 근 적외선 영역에서 1000 nm 에서 1600 nm 까지 연속적으로 파장 가변이 가능하다.

### Keywords:

cavity dumping, optical parametric oscillator

## Stimulated Brillouin scattering characteristics of single mode optical fibers operating near the wavelength of 1 $\mu\text{m}$

오경환\*<sup>1</sup>, 송삼권<sup>1</sup>, 정애리<sup>1</sup>, 김태오<sup>1</sup>, 박민규<sup>2</sup>, 정성묵<sup>3</sup>

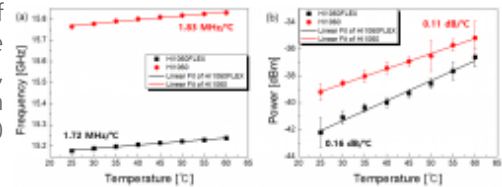
<sup>1</sup>연세대학교 물리학과, <sup>2</sup>Agency for Defense Development, <sup>3</sup>LIGNEx1 Laser R&D Lab.  
koh@yonsei.ac.kr

### Abstract:

We experimentally investigated the stimulated Brillouin scattering (SBS) of single mode optical fibers operating at the wavelength of 1,064nm for the first time. SBS was characterized in terms of Brillouin frequency shifts, linewidth, SBS thresholds and Brillouin gain coefficients. And the variation of SBS spectra with respect to the temperature change from 25 ° C to 60 ° C was measured to find a linear correlation.

### Keywords:

Stimulated Brillouin scattering



## Invariant imbedding theory approach to electromagnetic wave scattering by cylindrical bodies

YU Dae Jung\*<sup>1</sup>

<sup>1</sup>College of Applied Science, Kyung Hee University  
djyu79@gmail.com

### Abstract:

We newly develop an invariant imbedding method which can apply to wave scattering by cylindrical bodies. Focusing on the electromagnetic (EM) wave scattering, we apply this method to a circular dielectric cylinder with radial stratification. We first show that our method gives numerically correct results by comparing with the case for multi-layered circular cylinder. We then consider the EM wave scattering by cylindrical Luneburg and Eaton lenses. Comparison our results with previous results is presented with discussions on the differences.

### Keywords:

Invariant imbedding, Electromagnetic wave scattering, Metamaterials

## Numerical calculations of spatially inhomogeneous field near a nanotip

최(Choi)우경(Wookyoung)\*<sup>1, 2</sup>, 김(Kim)경택(Kyungtaec)\*<sup>1, 2</sup>

<sup>1</sup>Department of Physics and Photon Science, Gwangju Institute of Science and Technology, Gwangju, Korea, <sup>2</sup>Center for Relativistic Laser Science, Institute for Basic Science, Gwangju, Korea  
cwk0902@gist.ac.kr, kyungtaec@gist.ac.kr

### Abstract:

We investigate the photoelectron spectrum obtained from a metallic nano-sized tip using few cycle laser pulses. The laser field near the apex of the nanotip can be enhanced depending on the sharpness of the tip, forming the spatially inhomogeneous field. The photoelectron emitted by this spatially inhomogeneous field has higher energy than that obtained without the field enhancement. Here, we demonstrate the field enhancement effect using numerical calculations in which the photoelectron energy spectra are obtained from a metal surface by solving time dependent Schrodinger equation. We also discuss how this phenomena changes with the different carrier-envelope-phases (CEP) of the input laser pulse. Furthermore, the setup for the experimental implementation is also presented.

### Keywords:

above-threshold photoemission, nanotip, field enhancement, photoelectron spectrum, inhomogeneous field

## Analysis of modal mixing and the grating incident angle impacts on the diffracted beam quality $M^2$ for beam combining application

오경환\*<sup>1</sup>, 정애리<sup>1</sup>, 이광현<sup>2</sup>, 이정환<sup>2</sup>, 송상권<sup>1</sup>

<sup>1</sup>연세대학교 물리학과, <sup>2</sup>국방과학연구소  
koh@yonsei.ac.kr

### Abstract:

The beam quality  $M^2$  of a diffracted laser beam was numerically investigated for beam combining application based on a diffraction grating using VirtualLab Fusion. The laser used in the study had the wavelength of 1064nm and was approximated as a multimode Hermite Gaussian (HG) beam. We varied the ratio of fundamental HG<sub>00</sub> mode and higher order HG<sub>01</sub>, HG<sub>10</sub> modes, beam diameter, and the angle of incidence for a grating to understand the role of these parameters in the beam quality of the diffracted beams. We observed significant impacts of these parameters on the  $M^2$  value of the diffracted beam which should be taken account in beam combining applications.

### Keywords:

Beam quality, Diffraction Grating, Hermite Gaussian mode, Diffraction

## Observation of a half-illuminated mode in an acoustic Penrose-cavity

AN Kyungwon\*<sup>1</sup>, [KIM Juman](#)<sup>1</sup>, KIM Jinuk<sup>1</sup>, KIM Minjeong<sup>1</sup>

<sup>1</sup>Department of Physics and Astronomy, Seoul National University  
kwan@phya.snu.ac.kr

### Abstract:

Penrose unilluminable room, suggested by Roger Penrose in 1958 in response to the illumination problem asked by Ernst Straus, always has dark regions regardless of the position of a light source. In ray dynamics, this structure supports periodic orbits, quasi-periodic orbits, and chaotic orbits. In wave picture, various resonance modes corresponding to such ray dynamics are expected inside the cavity. By using the schlieren method, we have imaged the resonance modes of a Penrose unilluminable-room-shape acoustic cavity excited by an ultrasound transducer in the long-wavelength regime. The observed images were then compared with the results of finite-element simulation. Interestingly, a half-illuminated mode, unexpected from simulation, was observed. This mode can be explained as a superposition of adjacent near-degenerate modes within its linewidth.

### Keywords:

Penrose unilluminable room, Penrose cavity, schlieren method, acoustic cavity, half-illuminated mode

## Highly efficient chemosensing by using a physically transient and eco-friendly distributed feedback laser

UMAR Muhammad\*<sup>1</sup>, 민경택<sup>2</sup>, 김성환\*<sup>1</sup>

<sup>1</sup>Department of Energy System Research, Ajou University, <sup>2</sup>Department of Nano-Optical Engineering, Korea Polytechnic University  
aboutumar@gmail.com, sunghwankim@ajou.ac.kr

### Abstract:

We report a dye-doped silk film coated on a one dimensional (1D) quartz grating revealed a physically transient and eco-friendly distributed feedback (DFB) laser for highly efficient chemosensing. The prepared physically transient and eco-friendly DFB laser showed a high sensitivity to hydrochloric acid (HCl) acid vapor by attenuating the lasing by degrading the optical response of the dye-doped silk film. The lasing signal ceased time depends on the concentration of HCl vapor and the thickness of the optically active silk/dye layer. Moreover, after washing out and recoating, the quenched gain layer can easily reborn.

### Keywords:

Distributed feedback laser, Chemosensor, Silk protein

## 광압 기반 광분류기의 구현에 필요한 조건에 대한 연구

최은서\*<sup>1</sup>, 김주하<sup>1</sup>, 강희원<sup>1</sup>, 권다움<sup>1</sup>

<sup>1</sup>조선대학교 물리학과

cesman@chosun.ac.kr

### Abstract:

레이저 광을 이용한 광집계의 활용은 오래전부터 이론적으로 제시되었을 뿐만 아니라 실험적인 구현을 통해서도 확인되었다. 광집계는 광을 이용하여 물체의 포획을 가능하게 하였을 뿐만 아니라 원하는 위치로의 이동 및 세포의 형상을 변형하는데 이용되었다. 이와 같이 광에 의한 광압은 물체를 밀거나 당기는 힘을 빛을 통해서 발생시킬 수 있기 때문에 비접촉으로 작용할 수 있는 장점을 가진다. 특히 질량이 매우 작은 경우에 광압의 효과는 두드러지게 나타나게 되므로 세포 수준에서의 활용이 다양하게 보고되었다. 세포를 흐름 채널에 흘려보내고 형광신호에 따라서 광을 분류하는 유세포분석기는 기본적인 분석장비로 생물학 연구분야에서 필수적으로 이용되고 있다. 이러한 분석기에서 세포의 분류는 주로 전기적으로 대전시킨 세포에 작용하는 전기적인 인력과 반발력을 이용하여 수행되었다. 본 논문에서는 이러한 세포 분류를 광으로 수행하기 위한 광압 기반의 광분류기에 대한 아이디어를 실험적으로 확인하고 그에 대한 최적화 조건을 파악하고자 한다. 흐름 채널상에서의 세포에 광압을 작용하여 이를 분류하기 위한 광압 발생 최적 조건을 도출함으로써 흐름 채널에서의 광분류기의 활용 가능성을 확인하고자 하였다.

This work was supported by the National Research Foundation of Korea (NRF) grant funded by the Korea government (MSIP) (No. 2017R1A2B2009732) and the Encouragement Program for The Industries of Economic Cooperation Region (grand no. R0004732).

### Keywords:

광압, 광집계, 광분류기, 유세포분석기

## The Stark effect of defect emissions in hexagonal boron nitride

이지은\*<sup>1</sup>, 노기찬<sup>1</sup>, 최대복<sup>1</sup>, 서호성<sup>1</sup>, 김윤호<sup>2</sup>, 김진훈<sup>2</sup>, 임동길<sup>2</sup>  
<sup>1</sup>아주대학교 물리학과, <sup>2</sup>포항공과대학교 물리학과  
jieuntb@gmail.com

### Abstract:

Single photon emitters play an important role in quantum information processing. Diamond NV-centers and SiC divacancies defect emitters have been studied as representative solid-state single photon sources. Recently, single photon emissions are also reported in two-dimensional materials such as h-BN. However, because of inhomogeneous spectral distribution of the defect emissions, methods to control their emission energy are in demand. In this work, we control emission energy of defects in h-BN by using the Stark effect. We fabricate heterostructures of h-BN and graphene on Si substrate to apply vertical electric fields to embedded defects. We observe the maximum energy shift of about 20 meV at low temperatures and a shift of about 6.5 meV was observed at room temperature as well. The type of Stark shift in h-BN defect emissions are non-uniform and depend on the atomic structure of the defects. We suggest a theoretical model to explain some Stark shifts observed in experiments. These results show the possibility of h-BN defect emissions for quantum photonic applications.

### Keywords:

single photon emitters, atomic defects, hexagonal boron nitride, Stark effect

## Polarization holographic gratings in DR1 doped PMMA bulk polymer

WU Yang<sup>1</sup>, SHIM Hyun Kwan<sup>2</sup>, SEO Hyo Jin<sup>1</sup>, KIM Sun Il\*<sup>1</sup>

<sup>1</sup>Pukyong National University, Department of Physics, <sup>2</sup>Pukyong National University, Department of Chemistry  
sikim@pknu.ac.kr

### Abstract:

Polarization holographic gratings were investigated in Disperse Red 1 doped in poly (methyl methacrylate) (PMMA) bulk polymer. The polarization holographic gratings were formed by linearly or circularly orthogonal polarization combinations of the recording beams at 632.8 nm. The gratings were characterized by their diffraction efficiencies for a linearly or circularly polarized reconstructing waves at 632.8 nm. The ellipticity and the Stokes parameters were determined by measuring the intensity of the diffracted signal. The experimental results show that the diffraction efficiency and the polarization of the diffracted wave depend on the polarization of the reconstructing wave.

### Keywords:

Polarization holography, DR1, Diffraction efficiency, Stokes parameters

## 검정색 링 모양을 갖는 기포 투영이미지의 형성 원리

최다해<sup>1</sup>, 정운오<sup>1</sup>, 김소희<sup>1</sup>, 김영유<sup>1</sup>, 이기원\*<sup>1</sup>

<sup>1</sup>공주대학교 물리학과  
ga992205@kongju.ac.kr

### Abstract:

용존기체가 포함된 액체가 담겨있는 용기의 바닥면에 기포가 형성되면 시간에 따라 그 크기가 증가하고 결국 바닥면으로부터 분리된다. 이러한 기포의 성장 역학을 구체적으로 분석하기 위해 본 연구에서는 고속카메라로 촬영된 기포 투영이미지를 컴퓨터로 시뮬레이션 하였다. 이전 연구에 따르면 기포 투영이미지는 중심부가 밝은 검정색 링 모양으로 나타나며, 그 링의 면적이 시간에 비례하여 증가하는 것으로 밝혀졌다. 이 사실을 기초로 우리는 광원, 액체, 기포 그리고 유리기판으로 구성된 모델을 설정하고 스넬의 법칙을 기반으로 python 프로그램을 개발하였다. 이를 통해 실제 촬영된 투영이미지와 동일한 시뮬레이션 결과가 얻어지는 기포 크기와 바닥과의 부착 조건을 도출하고 시간에 따른 광선 경로 변화를 추적하여 기포 투영 이미지의 형성 원리를 분석하였다.

### Keywords:

기포, 시뮬레이션, python, 투영이미지, 스넬의 법칙

## Toward Cavity QED Based on Diamond Quantum Emitter Coupled to Optical Cavities

이동현\*<sup>1</sup>, 윤정배<sup>1</sup>  
<sup>1</sup>고려대학교 물리학과  
donghun@korea.ac.kr

### Abstract:

Nitrogen-vacancy (NV) centers in diamond are spin qubits as well as quantum emitter: both are important ingredients for cavity QED research. In this presentation, we introduce our recent efforts toward cavity QED experiments where NV centers coupled to various optical cavities such as plasmonic nanostructures and fiber based Fabry-Perot cavities.

### Keywords:

diamond, cavity

## 이중 반사 해상용 LED 등명기에 사용 가능한 standing bar 전용 렌즈의 광학 설계 및 시뮬레이션

이성제<sup>1</sup>, 주정식<sup>2</sup>, 서영조<sup>1, 2</sup>, 박진영<sup>1</sup>, 양현경\*<sup>1</sup>

<sup>1</sup>부경대학교, 과학기술융합전문대학원, LED융합공학전공, <sup>2</sup>덕성해양개발, 기업부설연구소  
hkyang@pknu.ac.kr

### Abstract:

LED 해상용 등명기는 현재까지도 많은 연구 개발이 되고있지만 대부분의 LED 등명기는 소형 등명기에만 집중되어 있고, 평행광을 만들기 위해 까다로운 제작 방법과 많은 비용을 필요로 하는 Fresnel lenses를 사용하고 있다. 이러한 문제를 해결하기 위해 Fresnel lenses 대신 포물선 반사판을 사용하여 평행광을 만들어주었으나, 현재의 이중 반사 해상용 LED 등명기는 다수의 LED chip을 설치하기에 제한적이었다.

중·대형 등명기를 사용하기에 부족한 광을 채워주기 위해 standing bar를 이용하였다. 기존의 LED chip 들은 standing bar의 윗부분에 설치하여 기존의 광량을 유지해주었으며, bar쪽에는 중·대형 등명기의 광량에 적합하도록 다수의 LED chip을 설치하였다. 이 bar쪽의 LED chip을 수평광으로 만들어 주기 위해 여러가지 종류의 lens를 광학 설계 및 시뮬레이션 하였다.

이중 반사 해상용 LED 등명기의 광도 및 소비전력을 개선하기 위해 비교대상으로 기존의 이중 반사 해상용 LED 등명기를 참조 하여 광도 및 소비전력 등을 분석하였고 국내 해상용 등명기 표준규격서를 참조하여 부동광도 및 발산각을 설정하였다. LED chip은 CREE사의 XPEWHT-L1-CW의 데이터를 사용하였으며, 광학 설계 프로그램인 Lighttools를 이용하여 시뮬레이션 하였다.

### Keywords:

해상용 LED 등명기, 이중반사 등명기, standing bar

## 중공 광섬유 기반 마이크로 스프레이

오경환\*<sup>1</sup>, 이현우<sup>1</sup>, 유진원<sup>1</sup>, 류원형<sup>2</sup>  
<sup>1</sup>연세대학교 물리학과, <sup>2</sup>연세대학교 기계공학과  
koh@yonsei.ac.kr

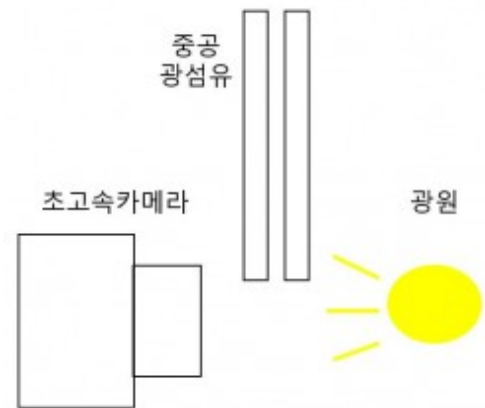
### Abstract:

최근에 약물 전송, 마이크로 패터닝과 같이 다양한 분야에 정밀한 액체 분사 시스템을 필요로 하고 있다. 최근에 중공 광섬유를 기반으로 한 스프레이 시스템이 개발되었다.

이에 우리는 그 현상을 규명하기 위하여 초고속 카메라를 이용하여 그림과 같이 실험 세팅을 꾸몄다. 우리는 액체들이 분사되는 것을 확인할 수 있었고, 그들의 거동을 관찰할 수 있었다. 이 논문에서 미세화된 액체들의 거동을 다루었다.

### Keywords:

광섬유



## 위상 측정 편향법을 이용한 계단 모양 시료의 3차원 측정

유영훈\*<sup>1</sup>, 김두철<sup>1</sup>, 나실인<sup>2</sup>

<sup>1</sup>제주대학교 물리학과, <sup>2</sup>Korean Precision System  
yyhyoung@jejunu.ac.kr

### Abstract:

물체 표면에 대한 3차원 측정 방법은 많이 연구되고 있다. 표면을 스캐닝 하면서 측정하는 방법과 2차원 어레이 광 측정기를 이용하여 한 번에 측정하는 방법 등이 사용된다. 현재는 2차원 어레이 광 측정기를 이용하면 신속히 측정할 수 있어 이 방법을 현재 많이 사용하고 있다. 3차원 측정 중 가장 정밀한 방법 중 한 가지는 간섭을 이용하는 것이나, 정밀도 면에서는 간섭법에 유사하고 측정 환경에 덜 민감하며 저가로 측정 할 수 있는 방법이 줄무늬 방법이다. 줄무늬를 이용하는 방법 중 대표적인 것이 모아레 방법과 편향법이 있다. 시료의 표면이 매끈한 경우는 편향법을 이용한다. 편향법의 큰 단점은 시료의 높이를 직접 측정하는 것이 아니고, 시료의 기울기를 측정한 후 이를 이용하여 높이를 측정하는 방식이다. 그러므로 이 과정에서 잡음이 많이 작용하고, 특히 계단형태의 시료는 측정할 수 없다는 단점이 있다, 본 연구에서는 편향법의 단점을 극복하여 높이를 직접 측정 할 수 있는 방법에 대하여 연구한다.

### Keywords:

Profilometry, Phase deflectometry, Three-dimensional measurement

## Real-time Measurement of Liquid Evaporation by Disturbance Inhibited Interferometry Technique

KIM Yonggi\*<sup>1</sup>, RYU Jiwook<sup>1</sup>, LEE Jaewhan<sup>1</sup>

<sup>1</sup>Department of Physics, Kongju National University  
kimyg@kongju.ac.kr

### Abstract:

A real-time in-situ interferometry method was proposed to measure water (liquid) evaporation directly over the liquid surface inside the reservoir. Evaporation from a liquid surface is one of the interfacial and natural processes between air and volumetric liquid (water). Recently, evaporation has been the topic of many studies throughout the years and it is imperative for agricultural irrigation, water supply, flow forecasting, water balance studies, land resource planning, weather forecast, water resource related industries and oil pollution [1] and more importantly air pollution related health issues. In natural conditions, evaporation changes every moment and continuously varies all the time thus, strongly need to be measured in real-time. Especially, for highly volatile toxic chemicals and liquids, the needs of real-time and in-situ direct evaporation measurement technique is highly demanding and increasing. However, most of conventional pan-type evaporation measurement methods cannot provide real-time measurement and instantaneous variations of evaporation. Evaporation measurement methods can be divided into two categories; direct and indirect methods. Indirect methods, the evaporation is estimated (not measured) from other meteorological factors like temperature, wind speed, relative humidity and solar radiation [2]. The direct evaporation measurement relied on the counting the number of sinusoidal fringes. As the water inside reservoir evaporated, the depth of the water is decreases a little thus the optical path length changes. Evaporation signals have been determined as a function of the focusing beam position of the signal beam over the liquid surface. In interferometry technique, the most limiting factors are surface disturbances and vibrations over the liquid surface. This limiting factor was simply inhibited by placing a long cylindrical aluminum tube around the signal beam of the interferometer over the liquid surface. A small diameter cylindrical Al tube diminished vibrations and wind induced surface ripples more effectively than that of the larger one. Water evaporation was successfully measured in real-time with a warm water and cold water even under windy condition with an electric fan. The experimental results demonstrated that the interferometry technique allows determining of liquid evaporation in real-time. Interferometric technique opens up a new possibility of methodology for liquid evaporation measurement even in several environmental disturbances, such as, vibration, surface disturbance, temperature change and windy environments.

[1] C-Y. Xu, V. P. Singh, *Hydrol. Process.* **12**, 429 (1998).

[2] M. A. Benzaghta *et al.*, *Australian Journal of Basic and Applied Sciences* **4**, 6473 (2010)

### Keywords:

Real-time, Interferometry, Liquid evaporation, Air pollution

## $\text{Li}_2\text{SrSiO}_2\text{N}_{1.33}$ 에 첨가된 $\text{Eu}^{2+}$ 의 광학적 특성

장기완\*<sup>1</sup>, 남크하이푸레둘람<sup>1</sup>, 김태영<sup>1</sup>, 정중현<sup>2</sup>

<sup>1</sup>창원대학교 물리학과, <sup>2</sup>부경대학교 물리학과  
kwjang@changwon.ac.kr

### Abstract:

별도의 경제과정 없이 Aldrich Chemical로부터 구입한  $\text{Li}_2\text{CO}_3$ ,  $\text{SrCO}_3$ ,  $\text{Si}_3\text{N}_4$  및  $\text{Eu}_2\text{O}_3$ 를 사용하여  $\text{Li}_2\text{SrSiO}_2\text{N}_{1.33}:\text{Eu}^{2+}$  형광체를 고상반응법으로 제조하고, 광학적 특성들을 측정, 분석하였다. 시료는 공기 중에서 화학양론적으로 철저히 혼합된 원료물질을  $\text{N}_2$ (95%)와  $\text{H}_2$ (5%)가 혼합된 환원 분위기의 전기로를 사용하여 920°C에서 4시간 동안의 열처리를 통하여 제조하였다. 제조된 시료들에 대한 최적의 열처리 조건과  $\text{Eu}^{2+}$ 의 농도에 따른 여기 및 발광스펙트럼을 측정, 분석하였다. 제조된 시료들은 568 nm에서 최대 발광세기를 나타내었으며, 발광스펙트럼의 선평(FWHM: Full Width Half Maximum)은 약 80 nm로 비교적 넓었다. 568 nm에서의 발광을 모니터링하면서 측정한 여기스펙트럼은 매우 넓은 영역인 250 ~ 500 nm 영역에서 여기효율이 매우 높아, 상용 중인 청색 및 UV LED 칩과 결합하면 매우 효율적인 여기가 가능하다는 것을 확인하였다. 발광세기에 미치는  $\text{Eu}^{2+}$ 의 농도의존성을 조사한 결과,  $\text{Eu}^{2+}$ 의 mol 농도가 1%일 때 발광효율이 가장 좋았다. 따라서 본 연구결과는 청색 및 UV LED 칩과 함께 백색광원으로 활용가능성이 매우 높음을 보여주고 있다.

### Keywords:

$\text{Li}_2\text{SrSiO}_2\text{N}_{1.33}$ , 발광스펙트럼, 여기스펙트럼, 고상반응법, 백색광원

## Bistable Mode LCD를 이용한 동역학적, 기하학적 위상 특성 연구

임진현<sup>1</sup>, 최민호<sup>1</sup>, 최재우\*<sup>1</sup>  
<sup>1</sup>경희대학교 정보디스플레이학과  
jaewuchoi@khu.ac.kr

### Abstract:

본 연구에서는 LCD를 기반으로 하여, 기하학적인 위상 특성을 갖는 광학적구조를 설계하였다. 기존의 2전극이 아닌 3전극 구조를 이용하여 bistable mode를 구현하고 각각의 위상 특성 변화를 관찰 및 비교하였다. Jones Matrix와 Poincare Sphere를 통하여 위상특성(기하학적 위상+동역학적 위상)을 정성적으로 분석하고, 시뮬레이션을 통해 이론 및 구조의 구현 가능성 혹은 이용 가능성의 확인 및 빛의 편광, 위상, 회절, 간섭 등 다양한 광학적 특성을 분석하였다.

### Keywords:

Geometric Phase, Dynamic Phase, Bistable Mode, LCD

## 고 정밀용 고 전압 전원장치 설계

김민재\*<sup>1</sup>, 정성훈<sup>1</sup>, 정영규<sup>1</sup>, 서형석<sup>1</sup>, 오봉기<sup>1</sup>, 이상봉<sup>1</sup>, 한장희<sup>1</sup>, 이소정<sup>1</sup>, 이흥기<sup>1</sup>, 박기현<sup>1</sup>

<sup>1</sup>포항 가속기 연구소

kimminjae@postech.ac.kr

### Abstract:

This paper is a high-voltage power supply design for a low noise and a high precision. This topology used is a well-known two-switch converter of a simple structure. This power supply was developed in parallel structures to allow simple increase in power capacity to 1.5 kW. This paper provides to achieve a high-voltage power supply of a low noise and a high precision: 1) a noise-reduction methods, 2) optimal transformer design, and 3) ADC and precise control by oversampling. To increase the SNR and resolutions of the output current and voltage, the oversampling and averaging method is used. Also, the hardware of power supply was considered by noise reduction methods. The developed power supply operates in CC/ CV mode. The ripple noise waveform of the developed power supply is < 330 mV at 100, 300, 400, and 600 V when only the AC component of the output voltage (300-MHz Bandwidth) was measured.

### Keywords:

low noise, high precision

## 4세대 200 MW 모듈레이터 운전현황#

박성수\*<sup>1</sup>, 이흥수\*<sup>1</sup>

<sup>1</sup>포항가속기연구소, 포항공대  
sspark@postech.ac.kr, lhs@postech.ac.kr

### Abstract:

포항가속기 연구소에서 4세대 가속기 건설을 2011년 1월부터 시작하여 2015년 12월까지 완료하였으며 2016년 4월 말 4세대 선형 가속기에서 요구하는 10 GeV 전자를 확인하였다. 4세대 전자 가속에 사용된 가속모듈은 Hard X-ray와 Soft X-ray를 포함하여 51 모듈이다. 4세대 선형가속기에서 전자를 가속시키는 에너지원으로 사용하는 대전력 펄스 전원장치 중 Hard X-ray에 설치된 49sets 모듈의 30 Hz, 4uS, SLED tune mode로 빔 commissioning 을 완료하여 2017년 사용자에게 4세대 빔을 제공하였다. 현재 사용자에게 빔을 제공중인 대전력 펄스 공급원인 클라이스트론-모듈레이터의 운전 현황에 대하여 발표하고자 한다.

# This work is supported by Ministry of Science and ICT(Information/Communication Technology).

### Keywords:

대전력 펄스 전원장치

## 항공화물 보안검색을 위한 복합방사선 보안검색기용 6/3 MeV 이중에너지 전자가속관 전산모사

문정호\*<sup>1</sup>, 채문식<sup>1</sup>, 이병노<sup>1</sup>, 차형기<sup>1</sup>, 이남호<sup>1</sup>

<sup>1</sup>한국원자력연구원 방사선기기연구부  
jhmun@kaeri.re.kr

### Abstract:

한국원자력연구원에서 개발 중인 항공화물용 보안검색기는 이중에너지 X선과 중성자선을 이용하는 복합방사선 보안검색기이다. 복합방사선 보안검색기는 전자가속기에서 발생된 이중에너지 X선을 이용하여 항공화물컨테이너 속의 무/유기물의 물질정보를 식별할 뿐만 아니라, D-T 중성자 발생장치로부터 발생된 중성자선을 이용하여 핵물질 또는 폭발물질의 검색도 가능한 차세대 보안검색기이다. 본 연구에서는 3차원 전자기장 해석 코드를 이용하여 6/3 MeV 이중에너지 X선 발생장치의 핵심장치인 고주파 전자가속관의 전산모사를 수행하였다. 설계된 전자가속관은 side-coupled standing-wave 방식이며,  $\pi/2$  모드로 구동되고, 공진주파수는 2586 MHz 인 S-band 가속관이다. 텅스텐 타겟을 사용하였을 때, 발생된 이중에너지 X선의 최대 선량은 X선 에너지 6, 3 MeV 에서 각각 7, 1 Gy/min@1 m 로 계산되었다.

**Acknowledgment** : This work was supported by Nuclear R&D program through the National Research Foundation of Korea, funded by the Ministry of Science and ICT (NRF-2017M2A2A4A05018182 and NRF-2017M2A2A4A01070610)

### Keywords:

보안검색기, S-band, X-선, 전자가속관

## Efficiency Optimization of S-band Klystron by Varying Distances between Cavities

유동호\*<sup>1</sup>, 현성윤<sup>1</sup>, 황지현<sup>2</sup>, 박성주<sup>3</sup>

<sup>1</sup>비츠로넥스텍 가속기 연구소, <sup>2</sup>포항공과대학교 물리학과, <sup>3</sup>포항공과대학교 포항가속기연구소  
tenhofsns@naver.com

### Abstract:

A klystron is one of the effective resources for beam acceleration. The klystron mainly consists of three sections such as an electron gun, a cavity section, and a collector. Especially, the cavity section is involved in beam's bunching and de-bunching processes which are directly related to the efficiency of the klystron. Common klystrons used for acceleration of particles generally have about 40% efficiency of input energy. High efficiency klystrons are preferable to beam acceleration, but they have a beam instability problem because of beam loss in the cavity section. To design high efficiency klystrons with high stable beam operation, beam dynamics and complex bunching mechanism should be considered in design procedure. In this paper, we studied efficiency change by varying the distances between cavities and optimized the distances.

### Keywords:

klystron, beam dynamics, velocity modulation, cavity, electron beam

## Design of an electron collector for a superconducting electron beam ion source at KOMAC

이승현\*<sup>1</sup>, 권혁중<sup>1</sup>, 김한성<sup>1</sup>, 조용섭<sup>1</sup>  
<sup>1</sup>한국원자력연구원 양성자가속기연구센터  
shl@kaeri.re.kr

### Abstract:

At Korea Multipurpose Accelerator Complex (KOMAC), we have been working on a 7 T superconducting electron beam ion sources (EBIS) for the production of multiply charged ion beams. In the EBIS, electron beam is used for the ionization. After the ionization, these electrons are dumped into the electron collector. Using a TRAK code, we simulate electron beams absorbed to the collector while adjusting the position and geometry of the collector and the magnetic field of the bucking coil at the collector side. Here, we present the electron collector design of the 7T-EBIS and plans for constructing an electron gun test stand with the electron collector.

### Acknowledgement

This work has been supported through KOMAC operation fund of Korea Atomic Energy Research Institute by Ministry of Science, ICT and Future Planning.

### Keywords:

electron beam ion source

## 범용 빔라인 양성자 빔 조사 표적에서의 빔 특성 측정

권혁중\*<sup>1</sup>, 윤상필<sup>1</sup>, 김유미<sup>1</sup>, 당정증<sup>1</sup>, 이필수<sup>1</sup>, 이승현<sup>1</sup>, 김한성<sup>1</sup>, 송영기<sup>1</sup>, 김계령<sup>1</sup>, 조용섭<sup>1</sup>  
<sup>1</sup>한국원자력연구원 양성자사업단  
hjkwon@kaeri.re.kr

### Abstract:

양성자가속기연구센터에서 운영하고 있는 100 MeV 양성자가속기를 이용한 빔 조사에서 중요한 변수는 표적에 도달하는 빔 에너지, 조사량 및 균일도이다. 범용 빔라인에서 현재 설정되어 있는 빔 조사 변수 허용 범위는 설계값 기준으로 표적에서의 빔 에너지  $\pm 10\%$  이하, 빔 조사량  $\pm 15\%$  이하, 그리고 균일도는 직경 30 mm 면적에서  $\pm 10\%$  이내이다. 본 발표에서는 표적에서의 각 빔 변수를 측정하는 방법 및 그 결과에 대해서 논한다.

-----  
본 연구는 과학기술정보통신부의 연구비 지원을 받았음

### Keywords:

양성자 가속기, 빔 균일도

## Target Heating Experiment of Target/Ion Source Prototype for Li-8 Beam Generation

DANG Jeong-Jeung\*<sup>1</sup>, LEE Pilsoo<sup>1</sup>, KWON Hyeok-Jung<sup>1</sup>, LEE Seung-Hyun<sup>1</sup>, KIM Han-Sung<sup>1</sup>, SONG Young-Gi<sup>1</sup>, CHO Yong-Sub<sup>1</sup>

<sup>1</sup>한국원자력연구원 가속기연구실  
jjdang@kaeri.re.kr

### Abstract:

A prototype of a target/ion source (TIS) generating Li-8 beam was manufactured and has been tested. In order to transfer the Li-8 generated at a target to the ion source, a beryllium oxide (BeO) target should be heated over than the boiling point of the lithium, 1342°C. Also, the higher target temperature is effective for the transfer because the higher temperature enhances a diffusion of the lithium in the target. However, a maximum target temperature is limited by a dissociation temperature of the BeO in a vacuum. The designed operation temperature is 1700-1800°C. The target is heated by a radiation emitted from a tantalum heater which is heated by an electrical current. The electrical current value to meet the temperature was estimated by the finite element method simulation. To examine the target heater, the electrical current was supplied up to 1300 A. The maximum temperature of the target heater was 1723°C and the vacuum pressure was sustained lower than  $2 \times 10^{-6}$  Torr. Since the target temperature was attained, an on-line test will be conducted at 100-MeV proton accelerator in KOMAC.

### Acknowledgments

This work has been supported through KOMAC operation fund of KAERI by MSIT and the NRF of Korea grant funded by the Korea government (MSIT) (No. NRF-2017M2A2A6A02071070).

### Keywords:

Target/ion source, Lithium 8, Radioactive isotope beam, target heating

## Effects of the two-color seed radiation in free-electron laser oscillator

김기범\*<sup>1</sup>

<sup>1</sup>Institute of Liberal Education, Kangwon National University  
kkbum@kangwon.ac.kr

### Abstract:

We discuss an influence of the conditions of seed radiation in a free-electron laser (FEL) oscillator. The seed radiation with two-color is considered to enhance the spectrum broadening and gain reduction of emitted radiation in the free-electron laser. The nonlinear interaction between an electron beam and seed radiation with two-color in the wiggler magnetic field is studied using modified 1-dimensional free-electron laser model, and the parameters of two-color seed radiation were optimized.

### Keywords:

Free-electron laser oscillator, Two-color seed radiation, Nonlinear interaction

## Characterization of a PIG ion source for high voltage proton beam extraction

정경재\*<sup>1</sup>, 이기현<sup>1</sup>, 이송형<sup>1</sup>, 최재영<sup>1</sup>

<sup>1</sup>서울대학교 원자핵공학과  
jkjsh1@snu.ac.kr

### Abstract:

A penning ion gauge type plasma source with high plasma density has been designed for high voltage proton beam extraction. Base pressure is  $5 \times 10^{-6}$  Torr, hydrogen plasma is discharged by DC power system. Plasma discharge characteristics according to different operating pressure and Arc voltage are measured by Triple Langmuir probe. A high density hydrogen plasma of  $\sim 1 \times 10^{18} \text{m}^{-3}$  is achieved, which is sufficient to achieve  $600 \text{mA/cm}^2$ . In this presentation, detailed measurement method and result about plasma density and temperature will be presented.

### Keywords:

Penning ion source, ion source, lanmuir probem, NBI

## 이중에너지 고주파 선형가속기 기반 컨테이너검색기용 방사선원 개발

채문식\*<sup>1</sup>, 이병노<sup>1</sup>, 김재현<sup>1</sup>, 주진식<sup>1</sup>, 이남호<sup>1</sup>, 이병철<sup>2</sup>

<sup>1</sup>한국원자력연구원, 방사선기기연구부, <sup>2</sup>아큐스캔  
cmswill@kaeri.re.kr

### Abstract:

컨테이너검색기는 전자선형가속기를 기반으로 발생시킨 X선을 컨테이너에 투사하여 내부의 화물을 검색하는 장비이다. 컨테이너검색기의 핵심은 전자를 가속시키는 고주파 선형가속기와 화물을 통과한 X선 신호를 검출하고 신호를 영상처리하는 부분이다. 특히 본 장비는 이중에너지 X선을 이용함으로써 유기물질의 물질분별이 가능하다는 점이 특징이다. 전자를 가속시키는 가속관의 고주파 소스로는 2856 MHz 마그네트론이 사용되었으며, 가속관은 전자빔을 9 MeV와 6 MeV까지 가속시킨다. 가속된 전자빔은 금속 타겟에 입사되어 제동복사에 의해 X선을 발생시킨다. 고주파 선형가속기는 컨테이너검색기 외에도 비파괴검사장비, 의료용 영상장비 혹은 치료기로도 응용이 된다. 여기에서는 컨테이너검색기 방사선원의 구성 및 작동원리 등에 대해 기술하였다.

### Keywords:

선형가속기, 이중에너지X선, 컨테이너검색기

## Design of an Electron gun for LHCD 5-GHz klystron

NAMKUNG W.\*<sup>2</sup>, HWANG J. H.<sup>1</sup>, JANG S. S.<sup>1</sup>, SEONG T. S.<sup>1</sup>, BAE Y. S.<sup>4</sup>, CHO M. H.<sup>3</sup>

<sup>1</sup>Dept. of Physics, POSTECH, <sup>2</sup>Pohang Accelerator Laboratory, <sup>3</sup>Dept. of physics and Division of Advanced Nuclear Engineering, POSTECH, <sup>4</sup>National Fusion Research Institute  
namkung@postech.ac.kr

### Abstract:

We are developing 5-GHz CW klystron for the lower hybrid current drive (LHCD) system in the KSTAR tokamak. The electron gun has been designed using the SLAC beam trajectory program (EGUN). We scanned design parameters, such as a spherical radius of the cathode, an anode radius, and a distance between the focusing electrode and the anode, to achieve target optical properties (perveance, beam size, etc.). A solenoid magnet is used to focus the beam which passes through the drift tube. The magnet was designed to reduce the beam scalloping which can affect the efficiency and stability of the klystron negatively. The structure around the cathode is deformed thermally because the cathode operates at a higher temperature when the electron gun operates. We analyzed the temperature distribution and the thermal deformation of the electron gun using ANSYS code to get the 'cold' dimensions which are dimensions of fabrication. Finally, we fabricate the electron gun and have a plan to test the perveance and density profile.

\*This work was supported by National R&D Program (grant numbers: 2016R1A6B2A01016828) through the National Research Foundation of Korea (NRF) and by the ITER technology R&D program funded by the Ministry of Science, ICT and Future Planning, Korea.

### Keywords:

Klystron, Electron gun, EGUN code, ANSYS

## Considerations of the safety factor profile control in KSTAR

정진일\*<sup>1</sup>, 고진석<sup>1</sup>, 한상희<sup>1</sup>, 김현석<sup>1</sup>, 왕선정<sup>1</sup>

<sup>1</sup>국가핵융합연구소  
jinil@nfri.re.kr

### Abstract:

The q-profile control is essential for tokamaks exploring the advanced tokamak scenarios, which expected to be able to provide a possible route towards a steady-state high performance operation in a fully non-inductive current drive state. This is because the pressure and current profiles must remain optimal for the scenario during the injection of large amounts of heating and current drive. Here, essential tools for the q-profile control are the motional Stark effect (MSE) diagnostic for measuring the radial magnetic pitch angle profile and a state-of-the-art plasma control system.

The pulse duration of the H-mode discharge at KSTAR has been extended year by year with improved control performance, and the experiment of ITB formation in a weakly reversed q-profile with a marginal NBI majority heating successfully demonstrated that the ITB is an alternative candidate to achieve a high performance regime in KSTAR. These recent achievements are attributed to reliable profile measurement, which means that profile feedback control has become a necessary step to ensure a robust and reliable approach to advanced scenarios as the next step of research in KSTAR.

In this work, we present the technical and conceptual requirements for q-profile control according to the upgrade plan for heating and current drive systems in the coming years.

### Keywords:

KSTAR, tokamak, q-profile, current profile control

## Research of Thomson Polychromator in KSTAR Tokamak

이종하\*<sup>1</sup>, 김하진<sup>1</sup>, 박희진<sup>2</sup>, YAMADA Ichihiko<sup>3</sup>

<sup>1</sup>National Fusion Research Institute (NFRI), <sup>2</sup>Ajou University, <sup>3</sup>National Institute for Fusion Science (NIFS)  
jhlee@nfri.re.kr

### Abstract:

Polychromator system is most important system in Thomson scattering diagnostic to measure electron temperature and density in Tokamak. Generally a polychromator has multi channels, each channels include avalanched-photo-diode (APD), op-amp circuit, focusing lens, collimation lens and band pass filter. Except APD and band pass filter in the polychromator components, characteristics of other components have been known. Therefore in this research, the characteristics of APDs are tested and researched. KSTAR Thomson system has 27 polychromators to reduce the spatial resolution and one polychromator has 5 APDs to analyse a Thomson scattering spectrum. The total numbers of APDs are 135 each in the KSTAR and each of APDs were tested. Investigation of APD is required to reduce the error that caused by different APDs characteristics in Thomson diagnostic system. To standardized of all APDs characteristics, high voltage source, pulsed light that tungsten (W) light or pulsed LED (light emitting diode) light were used. As a result we have been decide a optimal high voltage values for each APDs. In this poster we show a experimental method and final result of APD characteristics.

### Keywords:

polychromator, APD, KSTAR, Tokamak

## Design of vibration and position check system for Thomson scattering collection optics on KSTAR

김하진\*<sup>1</sup>, 이종하<sup>1</sup>, 성주호<sup>2</sup>, 김세은<sup>2</sup>, 박희진<sup>2</sup>

<sup>1</sup>국가핵융합연구소, KSTAR 연구센터, <sup>2</sup>아주대학교, 물리학과  
jinkim1146@nfri.re.kr

### Abstract:

Thomson scattering has long been a standard diagnostic for measuring the electron temperature and density in Tokamaks.

Thomson scattering system of KSTAR divided into three main parts (laser system, collection optics with a cassette system, and data acquisition system) [1].

The collection optics with a cassette systems are key components for Thomson scattering system [2]. Depending on the performance of this optical system, the electron temperature and electron density of the plasma may or not be measured. Sometimes, this optical system may be distorted by vibration of the Tokamak. For this reason, a system for vibration and position correction of optical system is being designed.

First, we will check whether the optical system is vibrating by vibration sensor and verify the new Thomson signal stabilization device.

Second, we try to measure x-axis, y-axis, and z-axis of the optical system using an Arduino and MPU-6050(3-axis accelerometer + 3-axis gyroscope) sensor [3].

Lastly, due to uncertainty in the measurement of the z-axis by magnetic fields, an additional position sensing detectors are planned to be installed.

### References:

[1] J.H. Lee *et al*, "Development of KSTAR Thomson scattering system", Review of scientific instruments 81, 10D528(2010).

[2] S. Oh and J.H. Lee, "Collection optics design for KSTAR Thomson scattering system", Review of scientific instruments 81, 10D504(2010).

[3] <https://www.arduino.cc/>

### Keywords:

collection optics, vibration, arduino, six-axis(gyro+accelerometer) sensor, PSD

## Spatial resolution optics designs for KSTAR H-alpha spectroscopy and visible bremsstrahlung to $Z_{\text{eff}}$ measurement

강남준\*<sup>1</sup>, 손수현<sup>1</sup>, 남용운<sup>1</sup>  
<sup>1</sup>국가핵융합연구소  
namjun.kang@gmail.com

### Abstract:

The spatial resolution optic designs are described for visible spectroscopy system such as H-alpha spectroscopy and visible bremsstrahlung of the Korea superconducting tokamak advanced research (KSTAR) device. The system has 60 optical fiber bundles (20 channels  $\times$  3 columns) to measure the profiles with 40-50 mm spatial resolution. The collection optics are designed that the line of sight of each channel is focused on the tangent of the major radius from 1300 mm to 2350 mm. By using geometric optics simulation, the contribution factors of emission intensity from the each major radius to the each optical fiber are calculated considering the projected solid angle of collection lens. From these contribution factors the toroidal profile of the H-alpha is deduced as well as  $Z_{\text{eff}}$  from visible bremsstrahlung.

### References

- [1] K. Kadota *et al*, "Space and time resolved study of impurities by visible spectroscopy in the high density regime of JIPP T-II tokamak plasma", Nuclear Fusion 20, 209 (1980).
- [2] Y. Chen *et al*, " $Z_{\text{eff}}$  first measurements in EAST with a multi-channel visible bremsstrahlung new system", Fusion Engineering and Design 88, 2825 (2013)
- [3] B. Du *et al*, "A novel probe for spatially resolved emission spectroscopy in plasmas", Plasma Sources Sci. Technol. 19, 045008 (2010)

### Keywords:

KSTAR visible spectroscopy, H-alpha spectroscopy,  $Z_{\text{eff}}$

## 중성자 발생장치 타겟의 열 부하 실험 (Heat load test for neutron generator target)

이석관\*<sup>1</sup>, 허성렬<sup>1</sup>, 장대식<sup>1</sup>, 진정태<sup>1</sup>, 이광원<sup>1</sup>, 인상렬<sup>1</sup>, 김석권<sup>1</sup>, 오병훈<sup>1</sup>

<sup>1</sup>한국원자력연구원 핵융합기술개발부  
sklee74@kaeri.re.kr

### Abstract:

D-D 핵융합 중성자 발생장치의 중성자 발생과 관련한 타겟 표면 온도는 중수소의 최적 밀도 유지를 위해 대략 200 °C 이내로 유지하며, 그 이상의 온도에서는 중성자의 수율이 감소하는 것으로 알려져 있다. 따라서 중성자 타겟을 구성하는 부품의 최적 온도를 유지하기 위해 냉각 설계를 하며, 타겟은 냉각라인이 형성된 구리 구조물 위에 티타늄을 코팅한 형태를 취하고 있다.

본 연구에서는 한국원자력연구원의 고열 부하 시험 시설인 KoHLT-EB (Korea Heat Load Test-Electron Beam)를 사용하여 중성자 발생장치 타겟에 대한 열 부하 실험을 수행하였다. 시험에 사용된 타겟은 입구 직경 40 mm, 깊이 60 mm의 콘 형태이며, 외부에는 8개의 냉각수 유로가 형성되어 있다. 열 부하 실험은 KoHLT-EB 빔을 직경 30 mm 원형으로 타겟 내부에 조사하여 타겟 표면 온도를 균일하게 올리는 방식으로 100 W의 낮은 빔 에너지부터 최대 빔 에너지 10 kW ( $4.5 \text{ MW/m}^2$ ) 까지 순차적으로 증가시키며 수행하였다.

-----  
“이 연구는 2018년도 민.군겸용기술개발사업의 재원으로 수행되었음 (No. 74901-18).”

### Keywords:

neutron generator target, D-D 핵융합, 중성자 타겟, 티타늄, 열 부하 실험, 중성자 발생장치

## Divertor simulating experiment using applied-field magnetoplasmadynamic thruster

채(Chai)길병(Kil-Byoung)\*<sup>1</sup>  
<sup>1</sup>한국원자력연구원 원자력데이터센터  
kbchai@kaeri.re.kr

### Abstract:

The divertor concept will be used in ITER to remove helium ashes produced by D-T fusion reactions from the reactor during plasma operation. The divertor plate in ITER is estimated to experience 10-20 MW/m<sup>2</sup> heat flux and 10<sup>24</sup> /m<sup>2</sup>/s particle flux. Thus, it is required to develop divertor cooling technology that can handle such heat and particle fluxes and Center for Innovative Divertor (CID) has been launched to address this issue. As a part of the CID, we are building a divertor simulating experiment that can provide such heat and particle fluxes and will use it to develop/validate divertor cooling technology. The most promising candidate for the plasma source is an applied-field magnetoplasmadynamic thruster because it can be operated at relatively low background gas pressure (<1 Torr) with relatively small input power (~100 kW) compared to existing divertor simulating facilities. The expected heat flux is 100 kW × 30% / 12 cm<sup>2</sup> = 25 MW/m<sup>2</sup> with assuming 2 cm plasma radius and 30% efficiency and the expected particle flux is 25 MW/m<sup>2</sup> / 80 eV = 1.8×10<sup>24</sup> /m<sup>2</sup>/s with assuming 20 km/s exhaust velocity. Details about our experiment and current status will be discussed in the paper.

### Keywords:

plasma, fusion, divertor, electric propulsion

## Deuterium permeation behaviors of erbium oxide coated by MOCVD

김용민\*<sup>1</sup>, 최하림<sup>1</sup>, 변우준<sup>1</sup>, 서희정<sup>1</sup>, 노승정<sup>1</sup>

<sup>1</sup>단국대학교 물리학과  
yongmin@dankook.ac.kr

### Abstract:

Deuterium permeation through the structural materials of fusion reactors is important issue in fuel cycles. In this study, erbium oxide coatings on SS316L were fabricated by a metal-organic chemical vapor deposition method. Surface morphology and the thickness of the coating were examined by scanning electron microscopy and ellipsometry, respectively. The crystal structure was analyzed by X-ray diffraction, and the deuterium permeation behavior was investigated by using a custom-built measurement system at Dankook University. The coated side was mounted facing to the deuterium feeding side. Deuterium permeation experiments were performed in the temperature range of 500-700 °C. Through this experiments, we achieved significant reduction in deuterium permeation. The experimental results will be presented in detail.

### Keywords:

Deuterium, Permeation, Metal-organic chemical vapor deposition

## Study of Deuterium Permeation in Tungsten

BYEON W. J.<sup>1</sup>, SEO H. J.<sup>1</sup>, KIM H. S.<sup>1</sup>, CHOI Halim<sup>1</sup>, KIM Yongmin<sup>1</sup>, NOH S. J.\*<sup>1</sup>

<sup>1</sup>단국대학교 물리학과  
sjnoh@dankook.ac.kr

### Abstract:

Permeation of hydrogen isotopes through plasma-facing components (PFCs) can result in unacceptable safety risks. Tungsten being one of the most promising candidate materials for PFCs, we performed deuterium permeation experiments by using a tungsten membrane supplied by ALMT Co in the temperature range of 925-1150 K. The sample was chemically cleaned and then sputter-cleaned by using argon ions to minimize the parasitic effects due to native oxide layers effect. The results of this work are compared with the data previously reported by others.

### Keywords:

Hydrogen isotopes, Permeation, Tungsten

## Design of compact LHCD launcher with short-circuited slotted waveguide array

김지현\*<sup>1</sup>, 정미<sup>1</sup>, 위현호<sup>1</sup>, 왕선정<sup>1</sup>  
<sup>1</sup>국가핵융합연구소 플라즈마안정화연구부  
jeehkim@nfri.re.kr

### Abstract:

The basic design of antenna for upgraded KSTAR LHCD system is a mid-plane Passive Active Multijunction (PAM) type launcher for 4 MW source power. Recently, the advantages of high field side or top launching of lower hybrid waves have been highlighted and thus application to KSTAR LHCD system are currently under study. However, because of the tight space and interference with other obstacles, antenna including transmission line inside tokamak chamber should be very compact. Traveling wave comb-line slotted waveguide antenna for 5 GHz frequency has been studied to figure out this problem and a set of mock-up was developed. At the same time, resonant type, short-circuited slotted waveguide array (SWA) has been designed by modifying the initial LHCD launcher adopting 4-way splitter and slotted waveguide array antenna. In order to reduce the reflection and have a good coupling even at low plasma density in front of launcher, PAM structure was combined to SWA. In this presentation, Introduction to SWA concept, RF design of PAM-SWA using HFSS, and calculated antenna properties, such as  $N_{||}$  spectrum, reflection coefficient, directivity at various plasma density profile, will be described.

### Keywords:

KSTAR, LHCD, RF heating, slotted waveguide antenna, SWA, passive active multijunction, PAM

## Bulk Ion Heating from Ion Nonlinear Landau Damping of High-n TAEs in High Temperature Plasmas

나용수\*<sup>1</sup>, 서재민<sup>1</sup>, 함택수<sup>1</sup>

<sup>1</sup>Department of Nuclear Engineering, Seoul National University  
ysna@snu.ac.kr

### Abstract:

Toroidal Alfvén eigenmodes (TAEs) with high mode number are predicted in ITER. For high-n TAEs, ion nonlinear Landau damping (NLLD) can mainly lead to nonlinear saturation of the TAE growth [1]. Bulk ion can be heated from this mode damping, and the explicit expression of the local ratio of the ion heating in frequency space was derived in [2]. In this work, we investigate the overall ratio between the ion heating and the TAE drive with weak variation in frequency space in the TAE gap. We calculate the ion heating ratio for the cases of different approximation,  $\epsilon v_A/v_{th,i} \gg 1$ ,  $\epsilon v_A/v_{th,i} > 1$  and  $\epsilon v_A/v_{th,i} \sim 1$ . We note that a significant ion heating can exist in the ITER-like condition, which allows high alpha channeling to bulk ion via high-n TAEs.

[1] T. S. Hahm and L. Chen, "Nonlinear Saturation of Toroidal Alfvén Eigenmodes via Ion Compton Scattering", Physical Review Letters 74.2 266 (1995).

[2] T. S. Hahm "Ion Heating from Nonlinear Landau Damping of High Mode Number Toroidal Alfvén Eigenmodes", Plasma Science and Technology 17 534 (2015).

### Keywords:

TAE, Toroidal Alfvén eigenmode, ITER, ion heating, NLLD

## Measurement of optical transition radiation from ultrahigh intensity laser-irradiated thin foil target

조병익\*<sup>1, 2</sup>, BAE Leejin<sup>1</sup>, CHO Minsang<sup>1, 2</sup>, JUNG Jaehyung<sup>1</sup>, KANG Gyeongbo<sup>1, 2</sup>, KIM Minju<sup>1</sup>, YANG Seonghyeok<sup>1</sup>, YAP Chuinhong<sup>1</sup>

<sup>1</sup>Department of Physics and Photon Science, Gwangju Institute of Science and Technology (GIST),

<sup>2</sup>Center for Relativistic Laser Science, Institute for Basic Science (IBS)  
bicho@gist.ac.kr

### Abstract:

Imaging and spectroscopy of Optical transition radiation (OTR) by relativistic electrons emerging at the rear surface of target conveys numerous information on electron transport, which are hardly investigated with other techniques. Imaging of the radiation shows the spatial distribution of hot electron beams. Spectrum of OTR infers the temporal structure of relativistic electron bunches. In this contribution, we present the OTR images and spectra from foil target with various thickness (100 nm - 10  $\mu$ m) irradiated by intense laser pulses up to  $10^{20}$  W/cm<sup>2</sup>. The significant modulation on OTR shape and spectra are observed from nano-foils at extremely high intensity. Detailed data and possible mechanism for such modulations will be presented.

This work was supported by NRF of Korea (No. NRF-2016R1A2B4009631 and NRF-2016H1A2A1909533) and the Institute for Basic Science.

### Keywords:

relativistic electron, optical transition radiation

## Plasma diagnostics by the THz-TDS method using the two-color laser-induced plasma filament

LEE Sihyeon<sup>1</sup>, KANG Keekon<sup>1</sup>, ROH Yulan<sup>1</sup>, 석희용\*<sup>1</sup>

<sup>1</sup>Department of physics and photon science, GIST  
hysuk@gist.ac.kr

### Abstract:

To diagnose plasmas we have developed a new diagnostic method using THz wave pulses that are generated in a two-color laser-induced filament. An intense laser pulse with an energy of 3 mJ/pulse and a pulse duration of 40 fs is converted into green light by a BBO crystal, and then the original and converted lights are focused in air to form a laser-induced filament. This process can produce strong THz waves with extremely broad bandwidth. The THz waves were used for plasma density measurement inside the inductively-coupled plasma (ICP) chamber in our laboratory. The plasma density inside the ICP chamber was found to be proportional to the RF (radio-frequency) input power and quadratically-proportional to the gas pressure. In this presentation, we will show the results.

### Keywords:

THz diagnostic, Time domain spectorscopy, two-color laser-induced filament.

## Investigation on Temporal Evolution of the Temperature of Laser-Induced Plasma in Air

석희용\*<sup>1</sup>, 전성진<sup>1</sup>, 방우석<sup>1</sup>  
<sup>1</sup>광주과학기술원 물리학과  
hysuk@gist.ac.kr

### Abstract:

The temporal evolution of temperature of the laser-induced plasma (LIP) at atmospheric pressure generated by the 5 ns Nd: YAG laser at 532 nm wavelength was studied by the pump-probe method. The velocity of the shock wave spurted out from the plasma was determined as a function of time using the shadowgraphy technique. We estimated the temperature behind the shock front by measuring the shock wave speed through numerical differentiation of the position of the shock wave at each time, where the shadowgram was taken at a time interval of 5 ns. We also acquired the temperature of the plasma core by applying the Saha-equation to the electron density obtained by the Nomarski interferometry. We found that the two temperatures are one order of magnitude different, and details of the phenomenon will be shown in this presentation.

### Keywords:

Laser Plasma Nomarski interferometer Shadowgraph Shockwave Abel-inversion

## 유전장벽방전 플라즈마에서 오존 발생 및 수송 형태 2차원 이미징

김진우<sup>1</sup>, 박상후<sup>2</sup>, 박주영<sup>1</sup>, 이현규<sup>1</sup>, 최원호\*<sup>1, 3</sup>

<sup>1</sup>한국과학기술원 물리학과, <sup>2</sup>한국과학기술원 자연과학연구소, <sup>3</sup>한국과학기술원 원자력 및 양자공학과  
wchoe@kaist.ac.kr

### Abstract:

대기압 플라즈마는 여러 방전 형태로 환경, 재료, 의학 분야를 넘어 식품, 농업 등 여러 분야에 응용이 시도되고 있다. 대표적으로 유전장벽방전(Dielectric Barrier Discharge, DBD)형 플라즈마 발생기는 구조가 비교적 간단하고 성능 신뢰도가 높은 장점을 살려 다양한 목적으로 활용되고 있다. 일반적으로 DBD에서는 전기바람(Electric wind)[1]의 발생과 함께 고밀도의 활성산소종 및 활성질소종이 생성되는데, 효과적인 DBD 발생기의 응용을 위해 활성종의 발생과 수송 과정에 대한 이해가 함께 진행되어야 한다. 활성종의 흐름은 전기바람과 동일할 것으로 유추되었을 뿐 활성종의 공간분포와 수송형태는 아직까지 연구된 바 없다. 본 연구에서는 대기압 플라즈마에 의해 발생하는 오존을 타겟 물질로 하여 DBD 플라즈마로 인한 오존 발생 형태와 전기바람 내의 오존 흐름을 2차원 흡수흡광도법을 사용하여 실험적으로 고찰하였다. 3 kV 부터 5 kV의 전압 및 20 kHz에서 50 kHz의 주파수 내 방전조건에서 발생된 DBD 발생기를 이용하여 오존의 253.7 nm 흡광도 공간분포로부터 실시간 2차원 오존 분포를 확인하였으며, Schlieren 기법을 통해 얻은 중성기체 흐름 이미지와 비교하여 전기바람 내의 특정 영역에서 오존의 밀집이 나타나는 것을 확인했다. 본 연구를 통해 기존의 농도 측정법에 서 관측할 수 없었던, 국소적인 활성 오존 발생과 수송 과정을 관측할 수 있었으며 방전조건에 따른 오존 발생 형태 제어의 가능성을 확인했다. 차후 다른 활성종에 대한 실험을 진행하여 플라즈마 발생기의 방전조건을 통한 활성종 제어 기초 자료로 사용될 것을 기대한다.

[1] S. Park, W. Choe *et al.*, Nat. Comm. 9, 371 (2018).

### Keywords:

대기압플라즈마, 전기바람, 흡수흡광도법, 오존수송.

## 대기압 RF 플라즈마에서 전자가열 구조의 규명과 제어

최원호\*<sup>2, 3</sup>, 박상호<sup>1</sup>

<sup>1</sup>한국과학기술원 자연과학연구소, <sup>2</sup>한국과학기술원 원자력 및 양자공학과, <sup>3</sup>한국과학기술원 물리학과  
wchoe@kaist.ac.kr

### Abstract:

대기압 저온 플라즈마는 지난 수년간 환경, 생의학 분야를 포함하는 여러 연구분야에 응용이 시도되고 있고, 최근에는 농식품 분야까지 저변을 확대하며 연구 범위와 규모가 세계적으로 증가하고 있다. 세계적으로 여러 연구 우수 그룹들이 경쟁적으로 연구결과를 발표하고 있고, 현재는 여러 분야에서 산업화가 가능한 수준까지 기술개발이 진행되었다. 대기압 저온 플라즈마는 플라즈마의 기초 특성 및 원리에 대한 연구부터 시작하여 다양한 응용 분야로의 확대까지 융합연구의 대표적인 주제로 자리매김 하고 있다. 그럼에도 불구하고 대기압에서 용이한 전자 진단법의 한계로 플라즈마의 특성을 결정 짓는 전자정보는 실험적으로 많이 밝혀져 있지 않아 현재까지도 전자가열에 대한 이해가 부족한 실정이다. KAIST 기체방전물리연구실에서는 대기압 저온 플라즈마의 전자정보 탐색을 위한 연속방출광 기반의 전자 진단법 개발 및 기초 연구를 수행해 왔다.[1-4] 본 발표에서는 지금까지 잘 알려져 있지 않은 대기압 RF 플라즈마에서의 전자가열 구조와 이에 영향을 주는, 즉 전자가열 제어의 핵심 인자에 대한 최근 연구결과를 소개하고자 한다.

- [1] S. Park, W. Choe et al., Plasma Sources Sci. Technol. 24, 034003 (2015).
- [2] S. Park, W. Choe et al., Plasma Sources Sci. Technol. 24, 032006 (2015).
- [3] S. Park, W. Choe et al., Sci. Rep. Tracking number: SREP-17-51690A (under revision)
- [4] S. Park, W. Choe et al., Sci. Rep. Tracking number: SREP-17-56411A (under revision)

### Keywords:

대기압 플라즈마, 전자가열, 축전결합형 플라즈마

## Plasma diagnostics of helium recombining plasmas using collisional-radiative model

SHIM Sungyong<sup>1</sup>, BOIL Byeon<sup>1</sup>, OH Cha-Hwan<sup>1</sup>, LEE Wonwook\*<sup>1, 2</sup>

<sup>1</sup>Department of Physics, Hanyang University, <sup>2</sup>Research Institute for Natural Sciences, Hanyang University  
wnwkleee@gmail.com

### Abstract:

A high density ( $n_e > 10^{18} \text{ m}^{-3}$ ) and low temperature ( $T_e < 1\text{eV}$ ) recombining plasmas plays an important role in radiative cooling of high heat flux plasma in a diverter region of tokamak. Spectroscopic method is a good tool to diagnose the plasma parameters of the recombining plasmas because it has advantage to determine the plasma temperature of recombining plasma at low temperature region. In this study, we have constructed helium collisional-radiative model (CRM) for the recombining plasmas and we have simultaneously determined the electron temperature as well as electron density of the recombining plasmas.

### Keywords:

recombining plasma, helium, collisional-radiative model

## Construction of helium plasma source for laser plasma diagnostics

SHIM Sungyong<sup>1</sup>, SONG Eun-ki<sup>1</sup>, OH Cha-Hwan<sup>1</sup>, LEE Wonwook\*<sup>1, 2</sup>

<sup>1</sup>Department of Physics, Hanyang University, <sup>2</sup>Research Institute for Natural Sciences, Hanyang University  
wnwkleee@gmail.com

### Abstract:

Stark broadening is the spectral line broadening by the electric field of the charges in plasmas and is a function of plasma parameters. Especially, Stark broadening is sensitive to the electron density so that Stark broadening is a good tool to diagnose the electron density of plasmas. In order to measure the helium (He) Stark broadening of plasma radiation without Doppler broadening, we have constructed the helicon plasma sources with RF antenna, permanent magnet, and quartz tube. We have analyzed the spectra of He plasma radiation against the gas pressure and the discharge power.

-----  
This research was supported by National R&D Program of "Basic nuclear fusion research" through the National Research Foundation of Korea(NRF) funded by the Ministry of Science and ICT (NRF-2017M1A7A1A02016145).

### Keywords:

Stark broadening, laser diagnostics, helicon plasma sources

## Mode conversion of electromagnetic waves in cold magnetized plasmas for various external magnetic field configurations

KIM Kihong\*<sup>1</sup>, [KIM Seulong](#)<sup>1</sup>

<sup>1</sup>Department of Energy Systems Research and Department of Physics  
khkim@ajou.ac.kr

### Abstract:

Mode conversion phenomena of electromagnetic waves in cold magnetized plasma are studied theoretically. In magnetized plasmas, s and p waves are not eigenmodes, but their linear combinations, namely ordinary (o) and extraordinary (x) modes are eigenmodes. These combinations depend on the angle between the direction of the external magnetic field and the direction of wave propagation. Using a generalized version of the invariant imbedding method, we calculate the mode conversion coefficient  $A$ , which is the fraction of the incident wave energy converted into longitudinal plasma oscillations, in a numerically precise manner. Our equations allow accurate numerical calculations for various external magnetic field configurations where two coupled modes (o and x modes) propagate in stratified media. We discuss the specific results obtained for the magnetized plasma and compare it carefully with previous results.

### Keywords:

mode conversion, magnetized plasma, o mode, x mode

## Optical pyrometry for measuring surface temperature during electrical wire explosion in water

정경재\*<sup>1</sup>, 류중현<sup>1</sup>, 이건<sup>1</sup>, 황용석<sup>1</sup>

<sup>1</sup>서울대학교 원자핵공학과  
jkjsh1@snu.ac.kr

### Abstract:

The paper present initial results of an optical pyrometry system which is designed to measure the surface temperature of metal wires exploded by high current electrical discharge in water. The pyrometer consists of a transmission grating, a fast-framing camera (1 Mfps in the 128×8 pixel images), light collecting optical fiber, and three lenses. It measures temporal variation of continuous spectrum of visible light emitted from the exploding metal wires. The time-varying temperature is estimated by fitting it to the Planck's radiation curve under the assumption of constant spectral emissivity. In this paper, we present the details of the optical pyrometry system and initial results on temporal evolution of surface temperature during the explosion of copper wires [1]. We expect that the accurate measurement of surface temperature during the thermodynamically well-defined current dwell period will help determining electrical conductivity of metals in the regime of metal-nonmetal transition.

[1] Kyoung-Jae Chung, Kern Lee, Y. S. Hwang and Deok-Kyu Kim, Numerical model for electrical explosion of copper wires in water, Journal of Applied Physics 120, 203301 (2016)

### Keywords:

Wire explosion, optical pyrometry

## Non-modal fluid instabilities in magnetized plasma with time-varying shear flow

YUN Gunsu\*<sup>1</sup>

<sup>1</sup>포항공과대학교 물리학과  
gunsu@postech.ac.kr

### Abstract:

The causality between edge localized mode instabilities and the relaxation of the confinement boundary of magnetized plasmas has remained one of the key problems in the tokamak plasma research community more than three decades. This is largely attributed to lack of comprehensive diagnostics with sufficient resolutions. Recent study using the-state-of-the-art imaging diagnostics assisted by super-fast RF detection system revealed many intriguing phenomena that were not expected before. In particular, the observations of quasi-stable filaments with eigenmode structure and abrupt transition to non-modal solitary structure accompanied with emissions at the ion cyclotron harmonics led to development of a phenomenological model in the form of a generalized Ginzburg-Landau equation. The model provides a unified explanation on the causality among the fluid instabilities, turbulence, plasma equilibrium profiles, shear flow, and collapse of the plasma boundary.

### Keywords:

edge localized modes, shear flow, Ginzburg-Landau equation, non-modal theory, solitary perturbation

## RF 유도 결합 플라즈마 토치에서 나노 분말 합성 수치 모델링

이해준\*<sup>1</sup>, 천청빈<sup>1</sup>, 허민영<sup>1</sup>, 이동근<sup>2</sup>, 양상선<sup>3</sup>

<sup>1</sup>부산대학교 전기컴퓨터공학부, <sup>2</sup>부산대학교 기계공학과, <sup>3</sup>재료연구소 분말/세라믹 연구본부  
haejune@pusan.ac.kr

### Abstract:

플라즈마 토치를 이용한 입자 합성 메커니즘의 이해를 위해서는 컴퓨터 시뮬레이션을 통한 반응 메커니즘의 이해가 필수적이다. 이 연구에서는 마이크로 입자들에 대하여 Lagrangian scheme을 적용하고, 서로 다른 크기의 나노 입자들에 대해서는 nodal method를 적용하여 결합한 시뮬레이션 방법을 개발하였다. Lagrangian scheme은 개개의 입자들의 거동을 계산하되, 열플라즈마에서 발생된 field에 의한 Lorentz force, drag force, 무거운 입자의 중력에 의한 힘, stochastic 힘, 그리고 상대적으로 큰 입자들의 동역학에 영향을 미치는 Coulomb 힘을 포함한다. 그와는 다르게 나노입자들에 대해서는 전하에 의한 Coulomb 힘의 효과를 무시할 수 있고 나노 입자의 수가 마이크로 입자의 수보다 매우 많기 때문에 주어진 size별로 분류를 하여 계산하는 nodal method가 적절하다. 이 두 방법의 결합으로 구해진 시뮬레이션 결과는 실험에서 관측된 마이크로 및 나노 분말 혼합물의 동역학과 성장 메커니즘의 이해에 도움 된다.

### Keywords:

RF-ICP 열플라즈마, 마이크로-, 나노- 분말 합성, Lagrangian scheme, Nodal method

# 플라즈마 처리수 생성시 자외선 조사로 인한 수산기 라디칼 생성량 제어 연구

최원호\*<sup>1, 2</sup>, 박주영<sup>1</sup>, 박상후<sup>1</sup>

<sup>1</sup>한국과학기술원 물리학과, <sup>2</sup>한국과학기술원 원자력 및 양자공학과  
wchoe@kaist.ac.kr

## Abstract:

플라즈마 방전을 통해서 생성되는 다양한 활성산소종(ROS) 및 활성질소종(RNS)은 활용도가 높아 다양한 분야에 응용을 하기 위한 여러 방법들이 전 세계적으로 활발히 연구되고 있다. 특히 활용성을 높이기 위해 활성종을 액상형태로 보관할 수 있는 플라즈마 처리수에 대한 연구가 주목을 끌고 있다. 본 연구팀에서는 대장균(*E. coli*) 바이오필름 제거가 과산화수소( $H_2O_2$ ), 오존( $O_3$ ), 수산기 라디칼( $OH^*$ )의 순서로 효능이 있다는 것을 확인하였고, 특히 수산기 라디칼의 경우에는 플라즈마 처리수 내 농도가 다른 활성종에 비해 약 100-10,000배 이상 적음( $0.1\mu M$ )에도 불구하고, 상당한 바이오필름 제거 효과를 보인 바 있다. 본 연구에서는 플라즈마 처리수 내 수산기 라디칼의 생산기작으로서 플라즈마에서 방출되는 자외선으로 발생하는 플라즈마 처리수 내의 아질산( $HNO_2$ )과  $H_2O_2$  광분해에 대해 연구하였다. 더 나아가 플라즈마 처리수 제조시 외부의 자외선 광원을 사용하여 수산기 라디칼의 광분해 생성을 촉진시켰다. 플라즈마 처리수 내의 수산기 라디칼 농도는 HPLC (High Performance Liquid Chromatograph)로 측정하였으며, 방전수 내에 존재하는  $H_2O_2$  와  $HNO_2$ 와 동일한 농도의 각 용액에 플라즈마 자외선을 조사시켜 생성되는 수산기 라디칼을 측정하여 정량적으로 비교 분석하였다. 플라즈마 방출 자외선으로 생성되는 수산기 라디칼의 양은 플라즈마 처리수 내의 총 수산기 라디칼의 약 30%를 차지하는 것을 확인하였으며, 자외선 광원을 외부에서 조사했을 경우에는 수산기 라디칼의 생성량이 더욱 증가하는 것을 확인하였다. 본 발표에서는  $H_2O_2$ 와  $HNO_2$ 의 비율 및 외부 자외선 광원의 역할과 수산기 라디칼 생성량에 대한 상관관계에 대해 발표할 예정이다.

## Keywords:

수산기 라디칼, 광분해, 플라즈마 처리수

## 플라즈마 처리수 내 화학성분 변화 추적 및 광분해 효과 전산 모델링

최원호\*<sup>1, 3</sup>, 이현규<sup>1</sup>, 박상후<sup>2</sup>, 박주영<sup>1</sup>, 김진우<sup>1</sup>

<sup>1</sup>한국과학기술원 물리학과, <sup>2</sup>한국과학기술원 자연과학연구소, <sup>3</sup>한국과학기술원 원자력 및 양자공학과  
wchoe@kaist.ac.kr

### Abstract:

상압 플라즈마에서 발생하는 고밀도의 활성산소종(Reactive Oxygen Species, ROS)과 활성질소종(Reactive Nitrogen Species, RNS)은 의학, 농업, 식품 등 다양한 분야에 활용도가 높아 세계적으로 응용 연구가 활발히 진행되고 있다. 특히 플라즈마 처리수는 플라즈마 처리 후에도 지속되는 응용 효과 등 활용도가 높아 더욱 심도 있는 연구가 필요하다. 본 발표에서는 플라즈마 처리수 제조 시스템 내의 기체와 처리수 내의 화학 조성을 파악함과 동시에 활성종의 생성 메커니즘에 대해 소개한다. 수산기 라디칼( $\cdot\text{OH}$ )은 플라즈마 처리수 내 과산화수소( $\text{H}_2\text{O}_2$ ), 오존( $\text{O}_3$ ) 및 아질산( $\text{HNO}_2$ )등에 비해 100-10,000배 낮은 농도임에도 뛰어난 살균 능력을 보인다[1]. 본 연구에서는 수산기 라디칼의 생성 메커니즘을 밝히고자 다음과 같은 전산 모델링을 수행하였다. 시간에 따른 활성종들의 조성 분포를 파악하기 위해 플라즈마 영역을 0차원으로, 기체 및 수용액 영역을 1차원으로 계산하는 전산모델을 개발했으며, 대기압 유전장벽방전에서 발생한 화학종들이 기체, 수용액 영역으로 확산, 용해, 화학반응으로 인해 시간에 따라 변화되는 농도 분포를 관찰하였다. 또한 자외선 광분해에 의한 전체 화학종들의 농도 분포의 변화를 관찰하고, 광선속의 영향을 파악하였다. 광분해로 인해 오존의 농도가 줄어드는 것을 확인하였으며, 수산기 라디칼의 농도는 광선속이 증가할수록 늘어나는 것을 확인하였다. 개발된 모델은 플라즈마 방전수 시스템에서 외부 자외선 광원으로 수산기 라디칼 발생을 제어하는 데 유용할 것이며, 더 나아가 플라즈마 구동조건 등을 바꾸었을 때 일어나는 화합물의 조성비 변화 등을 연구하고 이해하는 데 유용한 기반이 될 것이다.

### Keywords:

플라즈마 처리수, 전산 모델링, 광분해

## 자기장 제어된 50 W 급 고리형 홀추력기의 이온빔 및 성능 특성 연구

최원호\*<sup>1, 3</sup>, 이동호<sup>1</sup>, 김호락\*<sup>1</sup>, 도근태\*<sup>1</sup>, 이승훈\*<sup>2</sup>

<sup>1</sup>한국과학기술원 물리학과, <sup>2</sup>재료연구소, <sup>3</sup>한국과학기술원 원자력 및 양자공학과  
wchoe@kaist.ac.kr, holak\_phys@kaist.ac.kr, gdoh93@gmail.com, shlee.phys@kaist.ac.kr

### Abstract:

전세계적으로 다양한 우주임무 수행을 위한 초소형 위성의 수요가 증가하면서, 위성의 자세제어 및 궤도천이를 위한 저전력 전기추력기의 중요성이 커지고 있다. 홀추력기는 추력밀도가 높아 우주임무 수행에 점차 많이 활용되고 있는 추세이다. 그러나, 100 W 이하의 저전력 추력기의 경우, 추력기 내 플라즈마를 발생시키는 방전공간의 소형화에 따라 방전채널 즉 플라즈마의 부피 대비 표면적 비율이 증가하여 추력기의 전력효율이 감소하고, 적합한 자기장의 발생에 어려움이 있는 등 소형화에 따른 여러 난제가 존재한다. 본 연구에서는, 전자석과 영구자석을 조합하여 방전공간 내에서 자기력선을 내벽과 가급적 평행하게 만드는 식의 자기장 제어를 통해 50 W급 저전력 홀추력기를 개발하여 방전 및 성능 특성에 대해 연구하였다. 추력기 방전채널의 외경은 20 mm이며, 채널길이는 19 mm 에서 실험을 진행하였다. 자체 개발된 저전력 음극을 사용하여 실험을 수행하였으며, 양극전압 140-240 V, 소모전력 30-60 W에서 실험을 진행하였다. 이온빔 특성 분석을 위해 패러데이 탐침을 이용하여 이온 전류밀도를 측정하였으며, 소모전력 30-60 W에서 1.5-4.5 A/m<sup>2</sup>의 전류밀도를 보였다. 54 W 소모전력에서 추력은 약 2.4 mN, 양극효율은 약 21%로 측정되었으며, 동일 전력에서 타 그룹들 보다 향상된 성능 특성을 보였다. 본 발표에서는, 추력 성능 및 이온빔 특성에 대한 상세 연구 결과가 발표될 예정이다.

### Keywords:

전기 추력기, 마이크로 홀추력기, 영구자석, 자기장 제어

## Design study of Thomson scattering system for measuring electron density and temperature in a combustion chamber

이정진<sup>1</sup>, 곽세현<sup>1</sup>, 박겨레<sup>1</sup>, 김영철\*<sup>1</sup>

<sup>1</sup>한국과학기술원 원자력및양자공학과  
ycghim@kaist.ac.kr

### Abstract:

Thomson scattering system is designed with an aim of measuring the electron density and temperature in a combustion chamber. The laser is set to be Nd:YAG 532nm with 2.0J of energy. Expected electron density and temperature are of the order of  $10^{16} \text{ m}^{-3}$  and 10 eV, respectively [1]. Many sets of synthetic Thomson data are generated to investigate the number of required measurements such that the inferred electron density and temperature based on Bayes' probability theory are within the 20% of random errors. As the expected number of Thomson scattered photons are small, resulting in Poisson and Gaussian electrical noise dominated signal, obtaining the required number of measurements for ensemble averaging to reduce the noise level is crucial. In addition, we investigate the effect of spectral resolution on our measurements.

### Reference

[1] J.M. Goodings and N. S. Karellas, International Journal of Mass Spectrometry and Ion Processes, 62, 199 (1984)

### Keywords:

Thomson scattering, low temperature plasma, Bayes' probability theory

## Simulation of the Atmospheric Pressure DBD for Treatment of Chronic Wounds

이재곤<sup>1</sup>, 홍슬찬<sup>1</sup>, 서재민<sup>1</sup>, 박지웅<sup>2</sup>, 이상민<sup>3</sup>, 나진희<sup>4</sup>, 나용수\*<sup>1</sup>

<sup>1</sup>서울대학교 원자핵공학과, <sup>2</sup>서울대학교의과대학 의학과 성형외과학교실, <sup>3</sup>원광대학교 약학대학 약학과, <sup>4</sup>경희대학교 약학대학 약과학과  
ysna@snu.ac.kr

### Abstract:

In this paper, an atmospheric pressure Dielectric Barrier Discharge (DBD) of helium and oxygen gas with one electrode as water layer is studied to investigate the treatment effect of the chronic wound forming biofilm. A one-dimensional numerical code solving the density and the current continuity equation and Poisson equation is developed to investigate the changes of plasma properties and reactive species, especially the Reactive Oxygen Species (ROS), depending on the electrical operating condition of the DBD device. The mobility and diffusivity of the electron are calculated as a function of the reduced electric field ( $E/N$ ,  $N$  as the neutral particle density) using BOLSIG+ [1], a Boltzmann solver. For the simplification, we assumed the target biofilm as a thin water layer [2, 3] which has certain dielectric constant and the vapour is released from this water layer according to the saturated vapour pressure [2]. In addition, the simplified chemical models capable of capturing the main physicochemical processes [4] are used according to the vapour concentration, while the gas flow perpendicular to the electric field and sputtered reactive species from the water layer are not considered. This simulation is validated by comparing the discharge conditions with the experiments conducted under the same operating conditions. Finally, based on the fixed inter-electrode distance and the oxygen concentration value, the major ROS distribution depending on the applied voltage and frequency are obtained.

### References:

- G. J. M. Hagelaar and L. C. Pitchford, *Plasma Sources Sci. Technol.* **14**, 722 (2005).  
W. Tian and M. J. Kushner, *J. Phys. D: Appl. Phys.* **47** (2014) 165201  
Chen C., Liu, D.X., Liu, Z.C. et al., *Plasma Chem Plasma Process* (2014) 34: 403.  
D. X. Liu, P. Bruggeman, F. Iza, M. Z. Rong and M. G. Kong, *Plasma Sources Sci. Technol.* **19** (2010) 025018

### Keywords:

Atmospheric pressure plasma, Dielectric Barrier Discharge (DBD), plasma simulation, reactive oxygen species

## 대기압 수소 플라즈마와의 표면 상호작용으로 인한 산화철의 환원 반응에서 발생하는 나트륨 이중 발광선

신동환<sup>1</sup>, 이지모<sup>2</sup>, 윤건수\*<sup>1, 2</sup>

<sup>1</sup>포항공과대학교 물리학과, <sup>2</sup>포항공과대학교 첨단원자력공학부  
gunsu@postech.ac.kr

### Abstract:

수소 플라즈마를 이용한 삼산화 이철( $\text{Fe}_2\text{O}_3$ )의 환원 연구에 대한 응용이 지속적으로 연구되고 있다. 그 중에서도  $\text{Fe}_2\text{O}_3$ 의 환원 반응 중에 발생하는 광학적 발광 스펙트럼을 이용하여 환원 반응 과정의 특성을 알아내기 위한 시도가 이루어져 왔다. 특히, 나트륨 이중 발광 선(589.0nm&589.6nm)이 환원 반응 중에 관측 되었으며 이것이  $\text{Fe}_2\text{O}_3$ 에 포함되어 있는 미량의 나트륨 불순물에 의해 발생한다는 것이 실험을 통해 밝혀졌다. [1] 이 연구에서는 마이크로파를 이용한 대기압 수소 플라즈마와  $\text{Fe}_2\text{O}_3$ 의 국소적 표면 반응 실험을 진행하였고, X선회절분석을 통해 사산화 삼철( $\text{Fe}_3\text{O}_4$ ), 일산화 철( $\text{FeO}$ ), 철( $\text{Fe}$ ) 등으로 환원된 것을 확인하였다. 또한, 광학적 발광 분광법을 이용하여 스펙트럼을 실시간으로 측정하였고, 환원 반응이 일어남과 동시에 나트륨 이중 발광 선이 나오는 것을 확인하였다. 이를 통해 환원반응이 일어나는 조건이 나트륨 이중 발광 선이 나오는 시점과 연관이 있을 것이라 예상할 수 있다. 한편, 시간에 따른 반응 부위의 온도변화는 환원 반응이 일어나기 위해서 특정 온도에 도달해야 하는 것을 보여준다. 따라서, 표면 반응 부위가 환원 반응이 일어나기 위한 특정 온도에 도달하면 나트륨 이중 발광 선이 나오는 것으로 해석이 가능하다. 이것은 플라즈마와  $\text{Fe}_2\text{O}_3$ 의 표면 반응이 온도에 크게 영향을 받는 것을 의미하고, 나트륨 이중 발광 선이 반응이 일어나는 특정 온도에 도달하는 시점을 알려주는 지표가 될 수 있음을 의미한다. 이를 응용하면 플라즈마를 이용하여  $\text{Fe}_2\text{O}_3$ 를 표면처리하는 과정에서  $\text{Fe}_2\text{O}_3$ 가 반응하기 시작하는 시점을 진단 할 수 있을 것이라 기대된다.

[1] Sarita Das, Debi Prasad Das, Priyanka Rajput, Joydeep Ghosh, Bhagyadhar Bhoi, Barada Kanta Mishra, *Plasma Chemistry and Plasma Processing* 36 (4), pp1125-1139 (2016)

### Keywords:

나트륨 이중 발광선, 마이크로파 수소 플라즈마,  $\text{Fe}_2\text{O}_3$ 의 환원

## 염화금이 도핑된 그래핀을 보호층으로 사용하여 페로브스카이트 태양전지의 안정성 향상

최석호\*<sup>1</sup>, 김주환<sup>1</sup>, 김준수<sup>1</sup>, 김성<sup>1</sup>

<sup>1</sup>경희대학교 응용과학대학  
sukho@khu.ac.kr

### Abstract:

페로브스카이트 태양전지는 우수한 광전지 특성에 비해 장기안정성이 낮다는 단점을 가지고 있어 실용적인 응용에 제한적이다. poly(3,4-ethylenedioxy thiophene):poly(styrenesulfonate) (PEDOT:PSS)/indium tin oxide (ITO) 적층구조는 p-i-n 형 페로브스카이트 태양전지에 많이 사용되지만 PEDOT:PSS의 높은 산성도는 페로브스카이트 태양전지의 성능을 저하시키는 원인 중 하나이다. 본 연구에서는 페로브스카이트 태양전지의 효율과 안전성을 향상시키기 위해 PEDOT:PSS와 ITO 사이에 보호층으로서 AuCl<sub>3</sub>(염화금)가 도핑된 그래핀을 사용하였다. 그래핀은 CVD로 성장하였으며, AuCl<sub>3</sub>의 농도는 5에서 30 mM까지 변화시켰다. AuCl<sub>3</sub>의 농도가 증가함에 따라 투과도와 이동도는 감소하고 일함수는 증가하였으나, AuCl<sub>3</sub> 도핑에 의해서 광루미네센스의 세기가 크게 감소하는 것을 확인하였다. 이는 도핑된 그래핀에 의해 전자-정공의 재결합이 줄어들어 태양전지의 효율을 높일 수 있음을 의미한다. 그래핀이 없는 페로브스카이트 태양전지의 최대전력변환 효율은 순방향과 역방향에서 각각 14.16과 14.21 %를 나타내는 반면, AuCl<sub>3</sub>의 농도가 10 mM인 도핑된 그래핀이 삽입된 경우는, 순방향과 역방향이 각각 15.77과 15.90 %로서 효율이 크게 증가하였다. 장기안정성 평가를 위해 30일 경과 후 효율을 측정한 결과, 그래핀 보호층이 있는 태양전지의 효율은 초기의 67 %가 유지된 반면, 보호층이 없는 태양전지는 전혀 작동되지 않을 정도로 그래핀 보호층이 안정성 향상에도 매우 효과가 있음을 알 수 있다. 이러한 실험결과를 바탕으로 관련 메커니즘을 규명하고자 한다.

### Keywords:

페로브스카이트, 태양전지, 그래핀, 염화금, 보호층

## Study on Al doping dependence of Zinc-Tin Thin-Film-Transistor

이호선\*<sup>1</sup>, 황상빈<sup>1</sup>, 소현섭<sup>1</sup>  
<sup>1</sup>경희대학교 응용물리학과  
hlee@khu.ac.kr

### Abstract:

Al-doped Zinc Tin Oxide (AZTO) thin films were fabricated by radio frequency (RF) co-sputtering at room temperature on substrate of SiO<sub>2</sub>/Si. We used Al<sub>2</sub>O<sub>3</sub> and Sn (10wt%, 30wt%)-doped ZnO targets for various Al and Sn composition. AZTO TFTs were fabricated bottom gate by conventional photolithography, wet etching and lift-off on SiO<sub>2</sub> (200nm)/ (heavily doped) p-type Si. After patterning, we annealed samples at 350°C for 1 hour in air and then Mo electrodes were deposited using e-beam evaporator. To measure crystallinity, surface morphology, and compositions of Al doped ZTO thin films, we used X-ray Diffraction (XRD), Field Emission Scanning Electron Microscope (FE-SEM) and X-ray Photoelectron Spectroscopy (XPS), respectively. Optical properties of Al doped ZTO thin film were measured using spectroscopic ellipsometry (SE) and measured ellipsometric angles,  $\psi$  and  $\Delta$ , were used to estimate the dielectric functions and optical gap energy of AZTO thin films. We obtained the threshold voltage ( $V_{th}$ ), on-off ratio, field effect mobility ( $\mu_{FE}$ ), and subthreshold swing (SS) of AZTO TFTs using I-V transfer characteristic of TFT. In this work, we compared the electrical property AZTO TFT with the optical property of AZTO films.

### Keywords:

Rf magnetron co-sputtering, Al dopant, Zinc-Tin-Oxide, Thin film transistor

## AuCl<sub>3</sub>가 도핑된 다층 그래핀을 투명전도성 전극으로 사용한 유연한 페로브스카이트 포토다이오드

최석호\*<sup>1</sup>, 김종민<sup>1</sup>, 정동환<sup>1</sup>, 김성<sup>1</sup>

<sup>1</sup>경희대학교 응용과학대학  
sukho@khu.ac.kr

### Abstract:

최근에, 자외선부터 적외선 영역까지 광범위한 범위에서 검출이 가능한 광검출소자 (photodetector, PD)는 여러 분야에서 활용될 수 있기 때문에 많은 관심을 받고 있다. PD에 사용되는 많은 물질들 중에서, 유무기 하이브리드 페로브스카이트 물질은 우수한 전기적, 광학적 특성들 때문에 PD 개발에 많이 사용되고 있다. 지금까지, 페로브스카이트 PD는 투명 전극인 ITO를 사용하여 제작되었으나 ITO는 쉽게 깨질 수 있기 때문에 유연한 소자에 적용할 수 없다. 그래핀은 투과도, 전기전도도, 유연성, 및 화학적 안정성 등에서 우수하기 때문에 ITO를 대체할 투명전극으로서 각광을 받고 있다. 또한 그 동안의 PD는 주로 트랜지스터 형태로 개발되었기에 소자구조 및 전력소모 면에서 다이오드 형태에 비해서 불리하게 인식되어 왔다. 따라서, 본 연구에서는 처음으로 AuCl<sub>3</sub>가 도핑된 다층 그래핀을 유연한 페로브스카이트 포토다이오드에 투명전극으로 적용하였다. 그래핀의 층수가 1, 2층일 때가 3, 4층일 때보다 도핑 효과가 크다는 것을 라만 분광법과 면저항 측정을 통해서 확인하였다. 반응도, 외부 양자 효율, 검출능, 및 선형성과 같은 PD 성능들은 그래핀 층수가 2층 일 때 각각  $\sim 0.4 \text{ AW}^{-1}$ ,  $\sim 80 \%$ ,  $\sim 6 \times 10^{12} \text{ cm Hz}^{1/2}/\text{W}$ , 및 96 dB로써 가장 좋은 특성을 보였다. 이러한 결과들은 기존에 보고되었던 ITO 기반의 페로브스카이트 PD의 성능에 필적할 만한 수치들이다. 또한 제작된 포토다이오드의 굽힘 테스트 결과도 매우 우수한 것으로 확인되었다. 본 연구결과로부터 AuCl<sub>3</sub>가 도핑된 다층 그래핀을 투명전극으로 사용하는 페로브스카이트 포토다이오드가 휘어지고 굽힐 수 있는 응용분야에 적용될 수 있을 것으로 기대된다.

### Keywords:

페로브스카이트, 포토다이오드, 다층 그래핀, AuCl<sub>3</sub>, 유연, 투명

## Characterization of SiPM: Optimizing Performance for Gamma Spectrometry with Scintillators

김홍주\*<sup>1</sup>, 박형우<sup>1</sup>, 제갈진<sup>1</sup>, 정동우<sup>1</sup>, KHAN Arshad<sup>1</sup>

<sup>1</sup>Dept. of Physics, Kyungpook National University, Daegu 41566, Republic of Korea  
hongjoo@knu.ac.kr

### Abstract:

The silicon photomultiplier (SiPM) are of great interest in scientific and commercial applications. Particularly, SiPMs are widely researched in high energy physics, neutrino physics, and commercial medical application. The several companies not only are famous for manufacturing SiPM arrays, but also provide characteristics data and recommended circuit systems. However, it is necessary to make tuning for optimization according to the environments and changing circuit systems. The aim of this study is to characterize commercialized SensL SiPM (ArrayJ-60035-4P-EVB which is 2x2 channels arrays of 6x6mm<sup>2</sup> with 22,296 microcells) and to compare recommended circuit to modified circuit system in gamma spectrometry with scintillators. The optimization of operating voltage is associated SiPM gain, excess noise factor, photon detection efficiency (PDE), circuit gain, and circuit noise. Through the study of physical properties and optimization with consideration variables, the performance of the gamma spectrometer is optimized with BGO and other several scintillators.

### Keywords:

SiPM, Avalanche photodiode, high energy physics, gamma spectrometer

## 도핑된 그래핀 투명전극을 사용하여 반투명하고 유연한 유기태양전지의 효율 향상

최석호\*<sup>1</sup>, 장찬욱<sup>1</sup>, 신승현<sup>1</sup>, 김성<sup>1</sup>

<sup>1</sup>경희대학교 응용과학대학  
sukho@khu.ac.kr

### Abstract:

최근 반투명하고 유연한 유기태양전지는 건물일체형 태양광발전 시스템이나 휴대용 태양광 충전기같은 신재생 태양광 에너지 산업의 여러 분야에서 많은 이점을 가지고 있어 연구가 활발히 진행되고 있다. 일반적으로 태양전지에는 인듐 주석 산화물 전극 (ITO)이 많이 이용되고 있지만 ITO 전극은 유연한 유기태양전지에는 적합하지 않다. 본 연구에서는 ITO 전극을 대체할 투명전극으로 많은 각광을 받고 있는 그래핀을 유기태양전지의 양극과 음극으로 사용하기 위해 그래핀에 bis(trifluoromethanesulfonyl)-amide (TFSA)와 triethylenetetramine (TETA)를 각각 도핑하였다. 용액공정을 통해, TFSA가 도핑된 그래핀 위에는 홀 전송층인 PEDOT:PSS를, TETA가 도핑된 그래핀 위에는 전자 전송층인 ZnO와 광활성층인 P3HT:PCBM를 각각 스프인코팅 하였다. 최종적으로 각각 만들어진 시료들을 위아래로 붙여 반투명하고 유연한 유기태양전지를 제작하였다. 이렇게 만들어진 태양전지는 빛을 TFSA가 도핑된 그래핀 방향으로, 또는 TETA가 도핑된 그래핀 방향으로 빛을 입사 시켰을 때, 각각 3.30 및 3.12%의 에너지 전환 효율을 나타내었다. 아울러 빛이 입사되는 방향의 반대편에 알루미늄 반사판을 위치시켜 반사되는 빛의 흡수를 증가시켜 에너지 변환 효율을 최대 4.23%까지 향상시켰다. 또한 곡률 반경의 함수로 bending 횟수에 따른 태양전지의 안정성을 측정된 결과, 광 에너지 변환 효율이 99% 이상 유지되는 것을 확인하였다.

### Keywords:

유기태양전지, 그래핀, 도핑, 반투명, 유연

# Device Performance of the Mid-wavelength Cascade Infrared Detector

KIM HA SUL<sup>1</sup>, LEE HUN<sup>1</sup>, WOO JEONG JU\*<sup>1</sup>

<sup>1</sup>Department of Physics, Chonnam National University  
jjwoo@chonnam.ac.kr

## Abstract:

Mid-wavelength infrared (MWIR) sensors are important for medical, civilian, and military applications. Recently, a device operating at room temperature has been actively developed to increase the operating temperature using a MWIR device based on a type II superlattice structure. We will present the dark current density,  $R_0A$  product, responsivity, and detectivity results from a cascade infrared detector that combines the advantages of excellent carrier transportation and optical interband transition.

## Keywords:

Infrared detector, Cascade detector

## Lead Salt 계 물질특성 및 광전압형 중적외선 광검출기 제작

김중동<sup>1</sup>, AMPADU Emmanuel<sup>1</sup>, 오은순\*<sup>1</sup>, 최원준<sup>2</sup>, 안학영<sup>2</sup>, 조소혜<sup>2</sup>

<sup>1</sup>충남대학교 물리학과, <sup>2</sup>한국과학기술연구원  
esoh@cnu.ac.kr

### Abstract:

Lead Salt 계 IV-VI 반도체는 낮은 밴드갭과 높은 흡수율을 이용하여 적외선 소자에 응용되는 물질이며 또한 열전소자나 solar coating 등에도 응용되는 물질이다. Lead Salt계 물질인 PbS와 PbSe는 박막뿐 아니라 나노선, 나노입자와 같은 나노구조 형태로도 많이 연구되고 있다. 본 연구에서는 Chemical Bath Deposition으로 PbS 및 PbSe 박막을 성장하고 구조적, 전기적, 광학적 특성을 측정하였다. Hall 측정 결과 PbS의 경우  $55 \text{ cm}^2/\text{Vsec}$ , PbSe의 경우  $85 \text{ cm}^2/\text{Vsec}$  의 이동도를 얻을 수 있었으며 이는 동일한 방법으로 성장한 박막으로는 보고된 가장 높은 값이다. 또한 적외선 대역의 투과도와 반사도 스펙트럼을 이용하여 bulk의 경우와 유사한 Bandgap 에너지를 얻을 수 있었다. 성장된 PbS 및 PbSe 박막으로 광전압형 중적외선 소자를 제작하고 온도에 따른 광전류 스펙트럼을 측정하였다.

### Keywords:

lead sulfide, lead selenide, Lead salt, photocurrent

## 산화 그래핀/폴리머 나노복합체 기반 프렉서블 memristive 메모리 소자의 전기적 성질과 동작 및 전자수송 메커니즘

강(Kang)신우(Shinwoo)\*<sup>1</sup>, 구(Koo)본민(Bonmin)\*<sup>2</sup>, 김(Kim)태환(Taewhan)\*<sup>1, 2</sup>

<sup>1</sup>한양대학교 융합전자공학부, <sup>2</sup>한양대학교 전자컴퓨터통신학과  
uuoo93@naver.com, aksa6053@hanmail.net, twk@hanyang.ac.kr

### Abstract:

유기물/무기물 나노복합체를 사용하여 제작한 전자소자들이 프렉서블 소자의 응용에 대하여 활발하게 연구되었다. 나노복합체를 사용하여 제작한 memristive 소자는 차세대 비휘발성 메모리에 필요한 저전력, 고집적도, 저비용, 간단한 공정과정, 유연성의 여러가지 장점을 가지고 있다. 특히 프렉서블 memristive 메모리 소자의 성능향상에 대한 연구를 향후 프렉서블 시스템에 유망한 응용으로 사용할 수 있기 때문에 긴요한 연구가 필요하다.

본 연구에서는 유기물/무기물 나노복합체 기반 프렉서블 memristive 소자를 제작하였다. 이 소자는 상부전극 알루미늄(Al)과 활성층으로 사용되는 산화 그래핀(Graphene Oxide)/폴리머 나노복합체 층을 스프인코팅 방법을 사용하여 하부전극으로 활용되는 인듐 주석 산화물(Indium-Tin-Oxide) PEN기판 위에 제작된 소자의 전류-전압 (I-V) 곡선과 ON/OFF 전류비율을 관찰하였다. ON 상태의 전류와 OFF 상태의 전류는 시간의 변화에 따라 관찰 하였다. 이와 더불어, memristive 소자를 bending 한 후, 전기적 특성을 조사하여 bending 하기 전의 특성과 비교 분석하였다. Memristive 소자의 동작 메커니즘은 에너지 밴드와 전자와 정공의 흐름을 사용하여 기술하였다. 또한, I-V 실험 결과를 기반으로 memristive 소자의 전하 수송 메커니즘을 규명하였다.

### Keywords:

memristive memory

## Fabrication of two terminal capacitor-less memory device with thyristor structure

윤지수<sup>1</sup>, 오규진<sup>1</sup>, 송승현<sup>2</sup>, 유상동<sup>2</sup>, 심태현<sup>2</sup>, 김은규\*<sup>1</sup>

<sup>1</sup>Department of Physics, Hanyang University, <sup>2</sup>Department of Electronic Engineering, Hanyang University  
ek-kim@hanyang.ac.kr

### Abstract:

Dynamic random access memory (DRAM) with one transistor and one capacitor structure has been a mainstream with manufacturing the memory device. However, it faces a critical challenge with reducing the DRAM line width below 20nm because of scaling limitation of the capacitor. Therefore, capacitor-less simple structure DRAM is required to obtain high integration. The thyristor based capacitor-less memory has great memory characteristics such as high read current, non-destructive read condition, and good memory margin. The thyristor consists of four different layers of p<sup>++</sup>-anode / n-base / p-base / n<sup>++</sup>-cathode. Each region of layers is designed to be acted as memory device with simulation for optimized thickness and doping concentration, and two terminal thyristor based memory. In this work, we proceeded to make pillar shape of thyristor with wet chemical etching using KOH solution. Exact time, KOH concentration and temperature are required to construct thyristor structure. The top region composed of n-highly doped layer acts as cathode, and the ground composed of p-highly doped layer acts as anode, and etched stop. The depth between the anode and cathode layers after etching process was measured by AFM and SEM data was achieved to check the interface and surface morphologies. The electrical characteristics memory devices will be discussed.

### Keywords:

Two terminal capacitor-less memory, thyristor, KOH wet etching.

## A simulation study of electrical characteristics for various depths of trenches in Avalanche Photodiode

제갈진<sup>1</sup>, 박형우<sup>1</sup>, 이해영<sup>2</sup>, 이현수<sup>2</sup>, 이무현<sup>2</sup>, 김홍주\*<sup>1</sup>, 박환배<sup>1</sup>

<sup>1</sup>Department of Physics, Kyungpook National University, <sup>2</sup>Center of Underground Physics (CUP),  
Institute for Basic Science (IBS)  
hongjoo@knu.ac.kr

### Abstract:

Avalanche photodiode has the advantages of high light efficiency Positive-Intrinsic-Negative photodiode and high gain photomultiplier tubes (PMT) so that they can be used in low level light applications and requiring high sensitivity such as optical distance measurement. The trench cuts off the surface leakage current and stabilizes the flow of the electric field at the junction edge by reducing the tunneling current of the P+ region edge of the N-well. We simulate the reverse-type APDs with various depths of the trenches and measure current characteristics, responsivities and avalanche gains by using Silvaco Athena and Atlas package. From this simulation study we find an optimized trench depth giving the lowest leakage current.

### Keywords:

Avalanche photodiode, Trench, TCAD, Leakage current

## Raman thermometry of graphene/hBN field-effect transistor

김한울<sup>1</sup>, 김대희<sup>2</sup>, 배명호<sup>2</sup>, 노희석\*<sup>1</sup>  
<sup>1</sup>전북대학교 물리학과, <sup>2</sup>한국표준과학연구원  
rho@chonbuk.ac.kr

### Abstract:

SiO<sub>2</sub>에 비해 hBN은 매끈한 표면을 가지고 있기 때문에 그래핀 소자의 기판으로써 각광을 받고 있다. 본 발표에서는 그래핀 채널 아래에 놓인 hBN의 공간적인 온도 변화를 측정함으로써, 그래핀/hBN 소자의 발열 분포 및 열 소산 연구 결과를 보고한다. 원자힘현미경 측정 결과 그래핀 채널의 너비와 길이는 각각 6, 26  $\mu\text{m}$ 였다. 작동 중인 수송 채널의 전 영역에 대한 공간 분해된 라만 산란 실험 결과, hBN에서 관측된  $E_{2g}$  포논 에너지의 변화를 통해 hBN의 공간적인 온도 변화 분포를 측정할 수 있었다. 예를 들어, 인가전압  $V_{sd}$ 가 15 V까지 증가함에 따라 hBN 층의 평균 온도는 92  $^{\circ}\text{C}$ 까지 증가하였다. 낮은 인가전압에서 공간적인 온도 변화는 그래핀, hBN의 열저항 및 층간의 열경계저항을 고려한 온도 계산 결과와 잘 부합한 반면, 높은 인가전압에서 공간적인 온도 변화는 계산 값보다 더 크게 관측되었다. 예를 들어,  $V_{sd} = -15$  V일 때 평균 온도는 계산 결과보다 약 10  $^{\circ}\text{C}$  높았고,  $V_{sd} = 15$  V일 때 국소적인 고온 영역이 형성됨을 관측할 수 있었다. 이러한 차이는 상대적으로 높은 바이어스 전압에서 일어나는 국소적인 도핑 효과 때문인 것으로 보인다. 이 연구는 2016년도 정부(교육부)의 재원으로 한국연구재단의 지원을 받아 수행된 기초연구사업임 (과제번호: 2016R1D1A1B03935270).

### Keywords:

Raman thermometry, graphene/hBN heterojunction, energy dissipation, local doping effect

## 3차원 질화물 양자점의 선택적 전기 주입 공정에 관한 연구

송용호<sup>1</sup>, 최성한<sup>1</sup>, 우기영<sup>1</sup>, 여환섭<sup>1</sup>, 심영출<sup>1</sup>, 조용훈\*<sup>1</sup>

<sup>1</sup>한국과학기술원 물리학과  
yhc@kaist.ac.kr

### Abstract:

단일 광자원은 양자암호, 양자정보통신 등 차세대 보안, 정보 통신의 핵심 요소로서 사용이 가능해 활발한 연구가 진행되고 있다. 반도체 기반의 양자점을 통한 단일 광자원의 경우, 전기 구동이 가능한 소자 구현이 가능하여 상용화 측면에서 이점이 있다. 특히 3차원 구조체와 결합하여 질화물 기반 양자점을 제작할 경우, 위치조절 가능한 특성으로 인해 선택적으로 단일 광자원을 구동할 수가 있고, 엑시톤 결합 에너지가 큰 물질적 특성 때문에, 상온에서 구동 가능한 단일 광자원을 제작 가능하다는 장점을 가지고 있다.

하지만 이 같은 3차원 피라미드 구조체 기반 양자점을 전기구동할 경우, 뒷면의 양자점과 함께 성장된 옆면의 양자우물이 양자점으로의 전류 주입 효율을 감소시키게 된다. 또한, 양자우물의 신호는 노이즈로 작용하여, 양자 광원의 신호의 양자적 품질을 저하시키는 요소가 된다. 따라서, 양자점에 전기를 선택적으로 주입하는 공정은 3차원 구조체 기반의 고효율 단광자원 제작에 있어 큰 중요성을 가진다.

본 발표에서는 피라미드 형태의 3차원 구조체 위에 형성된 양자점에 선택적으로 전류를 주입하기 위한 공정기법을 제안하고 그에 따른 특성에 대해 보고한다. 금속유기화학증착법을 통해 제작된 3차원 구조체옆면에 형성된 양자우물로의 전류 주입을 줄이고, 누설 전류의 발생을 감소시키기 위해, 추가적인 절연층을 증착하였다. 그리고, 양자점의 위치로만 전류를 주입이 가능하게 선택적으로 절연층을 식각가능한 공정을 진행하였다. 제작된 시료의 I-V curve 측정 결과로부터, 절연층의 특성 변화에 따른 전기적 특성 변화에 대해 발표한다.

### Keywords:

반도체

## Phase transition through bond switching in distorted and resonant-bonded crystals

양(Yang)원준(Won Jun)<sup>1</sup>, 박(Park)한진(HanJin)<sup>2</sup>, 김(Kim)다솔(Dasol)<sup>1</sup>, 하(Ha)태우(Taewoo)<sup>1, 3</sup>, 박(Park)승  
중(Seung Jong)<sup>1</sup>, 안(Ahn)민(Min)<sup>1</sup>, 김(Kim)재훈(Jae Hoon)<sup>1</sup>, 권(Kwon)영균(Young-Kyun)<sup>\*2</sup>, 조만호<sup>\*1</sup>, 임  
(Lim)현욱(Hyun Wook)<sup>1</sup>

<sup>1</sup>연세대학교 물리학과, <sup>2</sup>경희대학교 물리학과, <sup>3</sup>성균관대학교 IBS  
ykkwon@khu.ac.kr, mh.cho@yonsei.ac.kr

### Abstract:

Although proposals to enhance phase-change memory efficiency have been provided, an effective experimental method to induce phase transition without external heat energy has not yet been reported. We show that GeTe, i.e., a prototype of phase-change material, experiences non-thermal phase transitions when uniaxial stress is applied. Because of structural properties like directional structural instability and resonance bonding, GeTe under 1% uniaxial stress undergoes bond switching between short and long bonds as if the crystal layer rotated. The modified structure is not relevant with intermediated states, which appear in conventional phase-change process, but rather relevant to the structure maintaining local coordination. Moreover, the interface formed between two different phases may cause a drastic decrease in the low-frequency dielectric constant implying the resonance bonding property can be effectively turned off by applying uniaxial stress. Finally, these results suggest that phase transitions with low energy consumption are possible when stress and short electrical pulses are hybridized in phase change memory.

### Keywords:

Phase-Change Materials, Non-thermal phase transition, Uniaxial Stress, Strain, Resonance bonding, Structural Instability

## AlGaIn/GaN 고속 전자 이동 소자 위 reduced graphene oxide의 CO<sub>x</sub> 가스 반응 연구

임종범<sup>1</sup>, NGUYEN Hoang Hai<sup>1</sup>, 박병권<sup>1</sup>, MADDAKA Reddeppa<sup>1</sup>, 김문덕\*<sup>1</sup>, 노영균<sup>2</sup>, 김송강<sup>3</sup>

<sup>1</sup>충남대학교, 물리학과, <sup>2</sup>IV Works CO., Ltd, <sup>3</sup>중부대학교, 정보통신학과  
mdkim@cnu.ac.kr

### Abstract:

오늘날 신뢰성 높은 가스센서 개발에 대하여 다양한 분야에서 (환경 모니터링, 농업, 의료 진단 등) 많은 요구가 있다. 다양한 검출 가스 중 무색, 무미의 CO<sub>x</sub>는 주로 화석 연료의 연소 및 자동차 배기에서 많이 발생하며 또한 전력 변압기 절연 성능을 평가할 때 결함을 측정하는 가스로 널리 사용되고 있다. 따라서 고성능 CO<sub>x</sub> 가스 센서의 개발은 환경 감시 및 산업 응용 분야에서 가장 중요하다고 볼 수 있다.

AlGaIn/GaN 기반의 고속전자 이동 소자(high electron mobility transistor, HEMT)는 높은 전자 이동도와 거친 환경에서 신뢰성을 확보 할 수 있는 소자로 기존의 고전력, 초극단파 시스템에 대한 응용 연구뿐만 아니라 센서 응용에서도 많은 연구가 되고 있다. 하지만 현재까지 반응도를 높이기 위하여 높은 동작 온도가 필요한 단점이 있다. 최근 탄소나노튜브, graphene, 그리고 graphene의 파생 물질인 graphene oxide, reduced graphene oxide (rGO)와 같은 물질은 기계적 강도, 열적 안정성, 상온에서 높은 이동도와 함께 단순한 화학 처리에 의하여 센서의 감도 조절이 용이한 장점이 있다.

본 연구에서는 분자선 결정성장법으로 성장된 AlGaIn/GaN HEMT 구조 위 rGO를 스피코팅 법으로 가스 센서 소자를 제작 CO<sub>x</sub> 가스 에 대한 반응도를 조사 하였다. 흡 측정을 통하여 AlGaIn/GaN 구조의 2차원 전자 가스의 농도와 이동도는 각각  $8.5 \times 10^{12} \text{ cm}^{-2}$  와  $1950 \text{ cm}^2/\text{V}\cdot\text{s}$ 임을 확인하였다. rGO에 대한 특성은 라만 분광법 통하여 카본 원자 sp<sup>2</sup> 의 E<sub>2g</sub> 포논모드(G)와 결함관련 신호(D)를 각각  $1589.66 \text{ cm}^{-1}$  와  $1341.73 \text{ cm}^{-1}$ 에서 관측 하였다. CO<sub>x</sub> 가스에 대한 반응 특성은 10 ppm에서 100 ppm까지 농도를 변화해 가며 전류 변화를 측정 하였으며 온도 의존 전류-전압 특성 변화를 측정하여 이에 대한 물리적 특성을 조사하였다.

### Keywords:

가스 센서, CO<sub>x</sub>, HEMT, AlGaIn/GaN, rGO

## Facial dry surface cleaning of graphene by UV treatment

김진홍<sup>1</sup>, HAIDARY MOHD Musib<sup>1</sup>, 최진식\*<sup>1</sup>, 조아람<sup>1</sup>

<sup>1</sup>건국대학교 물리학과  
jinschoi@konkuk.ac.kr

### Abstract:

그래핀은 단일 원자층의 육각형 구조의 탄소원자들의 배열에서 기인한 뛰어난 물리적, 광학적, 전기적 특성으로 투명소자, 유연소자 등의 웨어러블 소자에서 이상적인 소재로 각광받고 있다. 이러한 응용분야에서는 표면 상태의 제어를 통한 그래핀 성능의 극대화가 중요하다. 그래핀을 생산하는데 가장 널리 사용되고 있는 CVD 합성방법은 합성된 그래핀의 전사 과정에서 생기는 polymeric residue가 그래핀 소자의 전기적 특성 및 도핑효과에 크게 영향을 미치는 것으로 알려져 있다. 본 포스터에서는 그래핀 소자에서의 UV 조사를 통한 polymeric residues 제거 효과를 AFM topography, Raman analysis, electrical transport characteristic 측정을 통해 보이고, 그래핀 FET 소자에서의 UV 조사 조건을 optimize 하였다. 이를 통해 UV 조사를 통한 대면적 소자의 controllable damage-free UV 처리 기법을 제안한다.

### Keywords:

Graphene, UV treatment, Polymeric residues

## 하이브리드 Quantum dots 을 이용한 Monolayer MoS<sub>2</sub> 광소자 센서 특성 향상

조상은<sup>1</sup>, 김종민<sup>1</sup>, 조용철<sup>1</sup>, 서지우<sup>1</sup>, ABU TALHA A. A.<sup>1</sup>, HARISH Chavan S.<sup>1</sup>, 노삼규<sup>1</sup>, 김형상<sup>1</sup>, 임현식\*<sup>1</sup>

<sup>1</sup>동국대학교 반도체과학과  
hyunsik7@dongguk.edu

### Abstract:

2차원 적층 구조인 Van der Waals 물질 중 MoS<sub>2</sub> 를 채널 층으로 사용한 나노 광소자 센서 연구가 주목 받고 있다. 특히, 단일 MoS<sub>2</sub> 는 광에 대한 효율이 높고 투명하며, 얇은 두께로 이루어져 웨어러블 소자 개발이 가능하고 이에 따라 다양한 구조의 광소자로 연구되고 있다. 하지만, 상대적으로 전자 이동도가 낮고 대기 중에 쉽게 산화가 되는 문제점을 가지고 있다.

본 연구에서는, 단일 MoS<sub>2</sub>를 채널층으로 이용하여 PbS 하이브리드 Quantum dots을 MoS<sub>2</sub> 박막 위에 스피코팅 하여 하이브리드 광소자 센서를 제작하였고, 이에 따라 단일 MoS<sub>2</sub> 의 광반응성을 향상시켰다. 광세기에 따른 전기적 특성을 측정하기 위하여 할로겐 램프의 세기를 조절하여 I-V를 측정하였고 램프의 파워를 ON-OFF 함으로써 광에 대한 Life-dependence 도 확인 하였다.

이에 단일 MoS<sub>2</sub> 박막에 PbS QDs 가 코팅 된 경우 개선된 광반응성과 감도성을 보였고, 광에 대한 빠른 Life-dependence을 보이는 것을 확인하였다.

### Keywords:

Quantum dot, Monolayer MoS<sub>2</sub>, Photodetector

## Enhanced Performance of MAPbI<sub>3</sub> Perovskite Photodetectors with Polymer Passivation

정문석<sup>\*1, 2</sup>, 김효정<sup>1, 2</sup>, 변혜령<sup>1, 2</sup>, 김보라<sup>1</sup>, 김성혁<sup>1</sup>, 오혜민<sup>1</sup>  
<sup>1</sup>성균관대학교, 에너지과학과, <sup>2</sup>기초과학연구원, 나노구조물리연구단  
mjeong@skku.edu

### Abstract:

유-무기 융합 페로브스카이트는 우수한 광 흡수율과 전자 이동성을 바탕으로 태양전지는 물론 광검출기와 같은 여러 차세대 에너지 및 광전소자에 활용이 가능하다. 하지만 페로브스카이트 물질 자체의 한계점으로 공기 중에 노출될 경우 쉽게 산화되어 소자의 성능이 저하되는 문제가 끊임없이 제기되고 있다. 이를 개선하기 위해 본 연구에서는 파릴렌 (Parylene-C)을 보호막으로 사용하여 페로브스카이트를 외부 환경으로부터 차단하였고, 시간에 따른 흡수도 및 X-선 회절 분석을 바탕으로 약 한 달 동안 페로브스카이트가 산화되지 않는 것을 관측하였다. 파릴렌의 두께가 증가함에 따라 페로브스카이트의 발광 효율이 증가하였고, 동일한 조건에서 소자 특성을 측정할 결과 파릴렌 보호막을 통해 광전류 값이 약 420% 향상되는 것을 확인하였다. 따라서 이러한 현상을 규명하기 위해 파릴렌과 페로브스카이트의 상호 작용에 대하여 분석 및 논의해보고자 한다.

### Keywords:

perovskites, photodetectors, parylene-C, polymer, passivation

## Characterization of GaAs Tunneling Layer Included in Heterojunction Si Solar Cell

김근주\*<sup>1</sup>, PALEI Srikanta<sup>1</sup>, SAHU Rajkumar<sup>1</sup>, MUN Jonghun<sup>1</sup>

<sup>1</sup>전북대학교 기계공학과  
kimk@chonbuk.ac.kr

### Abstract:

We have investigated effect of inclusion of GaAs thin film on Si solar cells. GaAs is an III-V semiconductor having a direct band gap 1.42 eV, whereas Si is a group IV semiconductor with an indirect band gap of 1.12 eV. Integration of both GaAs and Si can be used for the effective use of solar spectrum. Integration of GaAs on Si has several defects due to lattice mismatch and thermal expansion co-efficient differences. However many researcher groups have reported integration of GaAs and Si by direct wafer binding method and surface-activated bonding [1-2]. In this work we have used electron beam evaporation to deposit GaAs on Si Solar cells. The main aim is to fabricate tunneling type heterojunction Si solar cells using GaAs. A 180  $\mu\text{m}$  thick microtextured p-Si wafers were diffused with phosphorous using the  $\text{POCl}_3$  diffusion method. After Si pn junctions were formed, a n-type GaAs (Si-doped, carrier concentration:  $1.4\sim 3.96 \times 10^{18}/\text{cm}^3$ ) was deposited on the textured Si pn cells by e-beam evaporation process at an operating voltage of 2.8 kV and a current of 20 mA for time periods of 0.5, 1 and 2 sec. Followed by e-beam deposition, an n-type a-Si:H layer and  $\text{SiN}_x$  were deposited by PECVD with a RF plasma of 13.56 MHz and power of 550 W at 350°C for 25 and 40 sec. Then metallization was performed using Al and Ag pastes for rear and front sides. Grid type metal contacts in the form of busbars and finger line for the front side and full rear metal contact were formed by screen-printing, followed by drying and co-firing. The structural, optical and electrical properties of the fabricated cells characterized by FESEM, photoreflectance, current-voltage characteristics curves. The data will be presented in more details.

This work was supported by Basic Science Research Program through the National Research Foundation of Korea (NRF), funded by the Ministry of education (NRF -20141A1A2056184). This research was supported by Nano-Material Technology Development Program through the National Research Foundation of Korea (NRF) funded by the Ministry of Science, ICT and Future Planning (2009-0082580).

[1] Y. C. Zhou, Z. H. Zhu, D. Crouse, and Y. H. Lo, *Appl. Phys. Lett.*, 73, 2337 (1998).

[2] J. Liang, L. Chai, S. Nishida, M. Morimoto, and N. Shigekawa, *Jpn. J. Appl. Phys.*, 54, 030211 (2015).

### Keywords:

GaAs tunneling layer, Heterojunction Si solar cell

## Characterization of MoS<sub>2</sub> Tunneling Layer Embedded in Si Solar Cells

MUN Jonghun<sup>1</sup>, PALEI Srikanta<sup>1</sup>, SAHU Rajkumar<sup>1</sup>, 김근주\*<sup>1</sup>

<sup>1</sup>전북대학교 기계공학과  
kimk@chonbuk.ac.kr

### Abstract:

Silicon solar cell has been extensively investigated structurally. Silicon-on-insulator (SOI) technology has recently been studied. Si solar cells based on SOI structure are improved with beryllium oxide layer. In this work, we investigated MoS<sub>2</sub> tunneling layer in Si solar cells. The standard cell fabrication process such as metallization was done using Ag and Al paste by screen-printing method followed by drying and co-firing. We characterized the samples by the measurements of the electrical conduction resistance of the interface, Cs corrected field emission transmission electron microscope image, photoreflectance, quantum efficiency, current & voltage curve and photoluminescence/electroluminescence emission characteristics.

This work was supported by basic science research program through the national research foundation (NRF) of Korea, funded by the ministry of education (NRF- 2017M2B2A4049681).

### Keywords:

Si solar cell, Molybdenum disulfide, Silicon-on-insulator

## 눈의 구조와 기능을 이해하기 위한 눈의 모형 실험의 제안

현동걸<sup>2</sup>, 조한국<sup>\*1</sup>

<sup>1</sup>단국대학교 교양학부, <sup>2</sup>제주대학교 교육대학 과학교육과  
hjho80@dankook.ac.kr

### Abstract:

물리교육이나 생물교육에서는 눈의 구조와 망막에 상이 맺히는 조절작용에 대해 단일 렌즈 카메라를 활용해 설명하고 있다. 그러나 여러 선행 연구들은 카메라의 구조가 너무 단순해 눈의 기능과 조절 작용을 이해하는 데에 한계가 있으며, 각막 및 수정체를 고려하지 않기 때문에 해부학적 관점에서도 차이가 있어 실제 작용을 이해할 수 없다는 점들을 지적하고 있다. 실제 눈은 단일 렌즈 카메라에 비해 매우 섬세하고 복잡하며 광학적 특성이 다른 여러 부분 간의 연계를 통해 다양한 기능을 수행하고 있으며, 이 과정에서 각막의 역할이 매우 중요하다. 이에 본 연구는 Hyun & Jho (2017)가 제시한 과학교육을 위한 모형안을 근거로 눈의 기능을 실험적으로 이해할 수 있는 눈의 기능의 모형 실험을 제안하고자 한다. 이 모형안을 활용한 실험에서는 각막과 수정체의 역할을 하는 두 개의 볼록렌즈의 유기적인 상호작용을 통하여 눈의 조절 작용의 원리뿐만 아니라 시력 조정의 원리까지도 실험적으로 이해할 수 있다.

### Keywords:

모형안, 근축광학, 조절, 실험

## 등속원운동에서 구심력의 크기를 구하는 공식의 비례상수 구하기

박가연<sup>1</sup>, 이정화<sup>1</sup>, 안은준<sup>1</sup>, 이기원<sup>1</sup>, 김영유\*<sup>1</sup>, 김한중<sup>2</sup>  
<sup>1</sup>공주대학교 물리학과, <sup>2</sup>(재)스마트IT융합시스템 연구단  
yykim@kongju.ac.kr

### Abstract:

등속원운동하는 물체에 작용하는 구심력( $F$ )은 물체의 질량( $m$ ), 반지름( $r$ ), 주기( $T$ )에 의해 결정되며 구심력을 구하는 공식은  $F = k \frac{mr}{T^2}$ 이다. 본 연구에서는 정량적인 실험을 통해 비례상수  $k$  값을 구해 그 값이  $k = 4\pi^2$ 임을 확인하였다.

### Keywords:

등속원운동, 일반물리실험

## CSEM을 활용한 과학영재들의 전자기학 기초개념 조사

이인숙\*<sup>1</sup>

<sup>1</sup>한국과학영재학교 물리지구과학부  
ilee@kaist.ac.kr

### Abstract:

본 연구에서는 CSEM (Conceptual Survey of Electricity and Magnetism)을 활용하여 과학영재 고등학생들의 전자기학 기초개념 이해도를 조사하였다. 사전검사와 사후검사 정답률이 각각 66%, 79%로 과학영재 고등학생들의 전자기학 기초개념 이해도는 매우 높은 수준이었다. 몇몇 문항에서 상대적으로 다소 취약한 면도 드러났지만, 전형적인 오개념의 특성을 나타내는 CSEM 문항은 하나도 없었다. 특히 전자기 유도 관련 영역에서는 상대적으로 어려움을 겪고 있는 것으로 보이는데 (사전검사와 사후검사 정답률 각각 49%, 61%), 사후검사 정답률도 낮은 편이어서 수업 후에도 그 어려움은 여전한 것으로 나타나 이 부분의 지도에 특별한 관심이 요구되는 것으로 드러났다. 또한 CSEM 검사 결과와 학기 성적과의 상관관계수가 0.48 ~ 0.63 정도로 상당히 높아 전자기학 기초개념 이해가 전자기학 수업에서 매우 중요한 요소임을 확인하였다. 이와 같이 학기 초 사전검사를 실시하여 오개념이나 취약한 부분 등 학생들의 학습 출발점을 미리 파악하는 것은 효과적인 학습자 맞춤형 수업을 설계하는데 매우 유용한 정보가 될 것이며, 학기 말 사후검사를 통하여 수업 후 학습자 개인의 물리개념 이해도를 평가하고 수업 전후 학습자의 개념변화를 정량화하는 것은 수업의 효용성이나 교수법의 효과를 확인하는 유용한 도구가 될 것으로 기대된다.

### Keywords:

개념조사, 전자기, 오개념, CSEM, 과학영재

## 공과대학 신입생들의 물리학에 대한 인식 조사 - 공주대학교 공과대학 신입생을 중심으로 -

이정화<sup>1</sup>, 안은준<sup>1</sup>, 이기원<sup>1</sup>, 김영유\*<sup>1</sup>, 김한중<sup>2</sup>  
<sup>1</sup>공주대학교 물리학과, <sup>2</sup>(재)스마트IT융합시스템 연구단  
yykim@kongju.ac.kr

### Abstract:

공주대학교 공과대학 신입생들을 대상으로 물리학에 대한 인식을 조사하였다. 고등학교 과정에서 물리 I (물리 II 포함)의 이수정도, 이수한 내용의 이해정도, 실험실습의 수행정도 등의 연구문제를 설문을 통해 조사 분석하였다.

### Keywords:

공학교육인증, 물리학 인식, 고등학교 물리교육

## Leveling Experiments by Using Simulation Program

김태균\*<sup>1</sup>

<sup>1</sup>전주교육대학교 과학교육과  
tkkim@jnue.kr

### Abstract:

To understand the principle of leveling have been learned in the title of [Weighting] title of the 4th grade science course. Teacher's guide book about this title have been guided the leveling plate to be horizontal in actual experiments. What's reason for the leveling plate to be horizontal? Is it wrong for the case of plate to be leaned? What's the differences between horizontal plate and leaned and the factors of differences? These questions involve to understand the principle of leveling. The principle of leveling depend on the various factors of the physical parameters of leveling plate and the various experimental conditions. By using the simulation software, the program about the leveling experiment had been developed to understand the dependence of variables.

### Keywords:

Leveling

## 음파위상마이크 출력신호의 오차 원인 해석

김소희<sup>1</sup>, 정운오<sup>1</sup>, 최다해<sup>1</sup>, 김영유<sup>1</sup>, 이기원\*<sup>1</sup>

<sup>1</sup>공주대학교 물리학과  
ga992205@kongju.ac.kr

### Abstract:

자유공간에서 음파의 골과 마루의 위치를 측정하는 음파 위상마이크가 개발된 바 있다. 이 장치를 이용하면 공간상에서 음파의 위상과 파장을 정확하고 간편하게 측정할 수 있어 물리교육과 음향학 분야에서 활용될 수 있다. 그러나 정현적 음파 신호일지라도 위상마이크 출력신호가 비정현적 형태로 나타나는 것이 큰 문제로 지적되어 왔다. 즉 이론적으로는 위상마이크 출력신호가 정현적 파형이 되어야 할지라도 마루부분의 신호변화율은 작은(완만하게 변함) 반면 골 부분은 매우 크게(뾰족하게 변함) 나타나 실제와 큰 오차를 보이고 있다. 본 연구는 이 오차 원인을 해석하기 위해 장치 구성과 신호 전달체계를 재검토하였고 음파신호 측정과정에서 고려되지 못한 신호 요소가 존재함을 발견하였다. 이를 반영하여 위상마이크 신호 처리 과정을 컴퓨터 시뮬레이션 하였고 실제 측정 결과와 동일하게 비정현적 출력 신호가 나타남을 확인하였다. 이에 따라 음파 위상마이크 출력신호의 오차를 줄이기 위해서는 새롭게 발견된 신호 요소를 반영하여 추가적인 신호 보정이 필요함을 알았다.

### Keywords:

음파위상마이크, 음파 위상, 음파, 보정, 시뮬레이션